REPORT UAG-96

# WORLD DATA CENTER A
# for
# Solar-Terrestrial Physics

## SOLAR-GEOPHYSICAL ACTIVITY REPORTS FOR STIP INTERVAL XV 12-21 February 1984 Ground Level Event AND STIP INTERVAL XVI 20 April-4 May 1984 Forbush Decrease

July 1987

## NATIONAL GEOPHYSICAL DATA CENTER

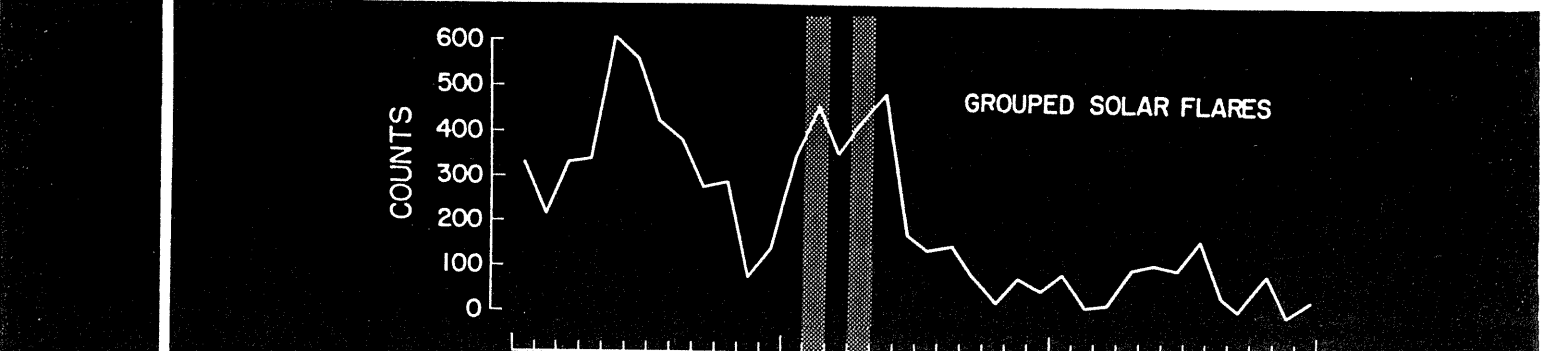

# WORLD DATA CENTER A

National Academy of Sciences
2101 Constitution Avenue, NW
Washington, DC 20418 USA

---

World Data Center A consists of the Coordination Office and the following eight Subcenters:

**COORDINATION OFFICE**
World Data Center A
National Academy of Sciences
2101 Constitution Avenue, NW
Washington, DC 20418 USA
[Telephone: (202) 334-3368]

**GLACIOLOGY** (Snow and Ice)
World Data Center A: Glaciology
(Snow and Ice)
Cooperative Inst. for Research in
Environmental Sciences
University of Colorado
Boulder, Colorado 80309 USA
Telephone: (303) 492-5171

**MARINE GEOLOGY AND GEOPHYSICS**
(Gravity, Magnetics, Bathymetry, Seismic Profiles, Marine Sediment, and Rock Analyses):
World Data Center A for Marine
Geology and Geophysics
NOAA, E/GC3
325 Broadway
Boulder, Colorado 80303-3328 USA
Telephone: (303) 497-6487

**METEOROLOGY** (and Nuclear Radiation)
World Data Center A: Meteorology
National Climatic Data Center
NOAA, E/CC
Federal Building
Asheville, North Carolina 28801 USA
Telephone: (704) 259-0682

**OCEANOGRAPHY**
World Data Center A: Oceanography
National Oceanographic Data Center
NOAA, E/OC
1825 Connecticut Avenue, NW
Universal Building, Room 406
Washington, DC 20235 USA
Telephone: (202) 673-5594

**ROCKETS AND SATELLITES**
World Data Center A: Rockets and
Satellites
NASA/Goddard Space Flight Center
Code 630.2
Greenbelt, Maryland 20771 USA
Telephone: (301) 286-7354

**ROTATION OF THE EARTH**
World Data Center A: Rotation
of the Earth
U.S. Naval Observatory
Washington, DC 20392-5100 USA
Telephone: (202) 653-1529 or 1527

**SEISMOLOGY**
World Data Center A: Seismology
U.S. Geological Survey
Branch of Global Seismology
and Geomagnetism
Box 25046, Mail Stop 967
Denver Federal Center
Denver, Colorado 80225 USA
Telephone: (303) 236-1500

**SOLAR-TERRESTRIAL PHYSICS** (Solar and Interplanetary Phenomena, Ionospheric Phenomena, Flare-Associated Events, Geomagnetic Variations, Aurora, Cosmic Rays, Airglow):
World Data Center A
for Solar-Terrestrial Physics
NOAA, E/GC2
325 Broadway
Boulder, Colorado 80303-3328 USA
Telephone: (303) 497-6324

**SOLID-EARTH GEOPHYSICS** (Seismicity, Earthquake Strong Motion, Tsunamis, Gravimetry, Earth Tides, Recent Movements of the Earth's Crust, Magnetic Measurements, Paleomagnetism and Archeomagnetism, Volcanology, Geothermics):
World Data Center A
for Solid-Earth Geophysics
NOAA, E/GC1
325 Broadway
Boulder, Colorado 80303-3328 USA
Telephone: (303) 497-6521

World Data Centers conduct international exchange of geophysical observations in accordance with the principles set forth by the International Council of Scientific Unions. WDC-A is established in the United States under the auspices of the National Academy of Sciences. Communications regarding data interchange matters in general and World Data Center A as a whole should be addressed to World Data Center A, Coordination Office (see address above). Inquiries and communications concerning data in specific disciplines should be addressed to the appropriate subcenter listed above.

**UNITED STATES DEPARTMENT OF COMMERCE**
**National Oceanic and Atmospheric Administration**
NATIONAL ENVIRONMENTAL SATELLITE, DATA, AND INFORMATION SERVICE

NATIONAL GEOPHYSICAL DATA CENTER
325 Broadway
Boulder, Colorado 80303

August 26, 1987

Dear Colleague,

The enclosed errata sheet is a correction for a table and graph published in *Report UAG-96: SOLAR-GEOPHYSICAL ACTIVITY REPORTS FOR STIP INTERVAL XV (12-21 February 1984 Ground Level Event) AND STIP INTERVAL XVI (20 April - 4 May 1984 Forbush Decrease).* An incorrectly labeled monthly table of "Hourly Equatorial DST Values (Provisional)" was used on page "xx" of the introductory overview article although the discussion in the overview was based on the correct Dst values published by NASA and in *Solar-Geophysical Data Reports* for April 1984.

Uncirculated copies of UAG-96 at the National Geophysical Data Center (NGDC) will have the correction sheet inserted; however, many copies were mailed before discovery of the mistake. We request everyone having copies of UAG-96 to please check page "xx" and insert the enclosed correction page as needed.

Thank you for your cooperation.

Sincerely yours,

Joe H. Allen

Joe H. Allen

TELEPHONE (303) 497-6215; FTS 320-6215 TELEX 592811 NOAA MASC BDR

NASA/GODDARD SPACE FLIGHT CENTER

## HOURLY EQUATORIAL DST VALUES(PROVISIONAL)

APRIL 1984

| DAY | UNIT=NT 1 | 2 | 3 | 4 | 5 | 6 | 7 | 8 | 9 | 10 | 11 | 12 | 13 | 14 | 15 | 16 | 17 | 18 | 19 | 20 | 21 | 22 | 23 | U.T. 24 |
|---|---|---|---|---|---|---|---|---|---|---|---|---|---|---|---|---|---|---|---|---|---|---|---|---|
| 1 | -46 | -46 | -48 | -52 | -62 | -63 | -53 | -52 | -52 | -52 | -56 | -50 | -46 | -42 | -40 | -41 | -46 | -44 | -36 | -30 | -30 | -26 | -24 | -23 |
| 2 | -26 | -31 | -27 | -25 | -25 | -23 | -19 | -24 | -42 | -49 | -59 | -38 | -33 | -38 | -50 | -51 | -43 | -44 | -46 | -48 | -41 | -33 | -31 | -36 |
| 3 | -61 | -83 | -59 | -53 | -63 | -60 | -55 | -55 | -58 | -54 | -50 | -47 | -40 | -42 | -48 | -48 | -40 | -39 | -41 | -46 | -42 | -49 | -47 | -55 |
| 4 | -56 | -62 | -59 | -64 | -59 | -54 | -54 | -61 | -63 | -56 | -45 | -35 | -35 | -41 | -28 | -25 | -18 | -42 | -62 | -86 | -94 | -85 | -106 | -110 |
| 5 | -102 | -102 | -89 | -89 | -84 | -75 | -76 | -75 | -69 | -74 | -76 | -73 | -63 | -64 | -68 | -73 | -77 | -74 | -82 | -90 | -87 | -89 | -79 | -78 |
| 6 | -80 | -71 | -67 | -68 | -61 | -58 | -56 | -56 | -58 | -60 | -60 | -51 | -45 | -46 | -45 | -43 | -40 | -40 | -41 | -39 | -36 | -33 | -33 | -30 |
| 7 | -27 | -28 | -23 | -15 | -10 | -13 | -16 | -18 | -12 | -29 | -47 | -58 | -38 | -32 | -35 | -42 | -41 | -39 | -33 | -24 | -29 | -28 | -34 | -33 |
| 8 | -39 | -45 | -46 | -59 | -59 | -58 | -71 | -83 | -97 | -95 | -77 | -66 | -70 | -66 | -58 | -60 | -49 | -52 | -44 | -40 | -50 | -56 | -65 | -84 |
| 9 | -91 | -96 | -86 | -93 | -86 | -79 | -66 | -56 | -44 | -39 | -38 | -40 | -41 | -35 | -33 | -33 | -29 | -18 | -16 | -18 | -13 | -15 | -14 | -12 |
| 10 | -13 | -15 | -20 | -16 | -14 | -15 | -13 | -16 | -15 | -21 | -24 | -20 | -19 | -18 | -18 | -19 | -17 | -17 | -17 | -14 | -9 | -10 | -13 | -13 |
| 11 | -20 | -34 | -32 | -26 | -23 | -21 | -20 | -24 | -25 | -23 | -18 | -18 | -17 | -16 | -16 | -23 | -22 | -22 | -23 | -21 | -18 | -13 | -9 | -8 |
| 12 | -13 | -15 | -16 | -14 | -19 | -16 | -18 | -16 | -11 | -10 | -6 | -3 | 2 | 3 | 2 | -10 | -19 | -12 | -6 | -7 | -3 | -3 | -21 | -34 |
| 13 | -36 | -28 | -24 | -33 | -30 | -22 | -18 | -17 | -10 | -7 | -4 | -1 | -5 | -4 | -5 | -3 | -2 | -5 | -3 | 0 | 1 | -2 | -1 | 1 |
| 14 | -2 | -4 | -1 | -3 | 0 | 4 | 7 | 6 | 7 | 7 | 9 | 10 | 16 | 17 | 9 | -7 | -6 | -6 | 1 | -3 | -1 | 8 | 12 | -1 |
| 15 | -9 | -4 | -4 | -6 | -8 | -11 | -12 | -15 | -15 | -10 | -8 | -10 | -11 | -7 | -5 | -3 | -3 | -3 | -3 | -4 | -3 | 0 | 4 | 8 |
| 16 | 4 | 2 | 4 | 4 | 5 | 6 | 10 | 8 | 9 | 10 | 11 | 13 | 14 | 13 | 17 | 16 | 18 | 18 | 17 | 13 | 6 | -1 | -4 | -2 |
| 17 | -4 | -5 | -7 | -6 | -5 | -1 | 2 | 3 | 1 | 0 | 1 | 5 | 7 | 9 | 14 | 27 | 24 | 27 | 31 | 30 | 26 | 22 | 29 | 34 |
| 18 | 35 | 38 | 31 | 22 | 12 | 13 | 9 | 5 | 7 | 7 | 9 | 9 | 13 | 13 | 9 | 5 | 6 | 14 | 17 | 19 | 27 | 30 | 31 | 34 |
| 19 | 29 | 28 | 30 | 29 | 29 | 29 | 32 | 45 | 51 | 42 | 36 | 37 | 41 | 47 | 41 | 31 | 29 | 28 | 29 | 33 | 33 | 22 | 26 | 19 |
| 20 | 5 | 3 | 7 | 7 | 4 | -4 | -14 | -8 | -4 | -5 | -1 | -3 | -2 | 3 | 6 | 5 | 5 | 5 | 6 | 6 | 4 | 8 | 9 | 6 |
| 21 | 2 | 0 | 3 | 4 | 5 | 4 | 6 | 1 | 2 | -2 | 0 | -2 | -1 | 4 | 1 | 0 | 0 | 3 | 5 | 3 | 3 | 3 | 4 | 5 |
| 22 | 3 | -1 | -1 | 3 | 5 | 4 | 2 | 3 | 1 | 1 | 2 | 0 | 1 | 3 | 3 | 4 | 6 | 4 | 5 | 5 | 5 | 8 | 10 | 10 |
| 23 | 6 | 4 | 5 | 6 | 8 | 10 | 14 | 14 | 16 | 18 | 19 | 21 | 19 | 17 | 18 | 19 | 15 | 9 | 4 | 5 | 5 | 2 | 1 | -6 |
| 24 | -2 | 4 | 7 | 7 | 8 | 3 | 0 | 4 | 2 | 1 | -1 | -3 | -5 | -3 | -4 | -5 | -3 | -2 | -1 | 2 | 3 | 3 | 4 | 4 |
| 25 | 10 | 12 | 18 | 25 | 35 | 38 | 43 | 44 | 34 | 40 | 36 | 31 | 22 | 7 | -16 | -37 | -47 | -55 | -51 | -56 | -71 | -70 | -61 | -63 |
| 26 | -76 | -81 | -83 | -89 | -88 | -79 | -84 | -75 | -66 | -72 | -68 | -64 | -55 | -57 | -57 | -47 | -58 | -68 | -73 | -75 | -78 | -61 | -66 | -81 |
| 27 | -91 | -87 | -78 | -75 | -67 | -62 | -60 | -61 | -65 | -61 | -55 | -47 | -44 | -42 | -46 | -47 | -46 | -49 | -49 | -48 | -43 | -33 | -30 | -30 |
| 28 | -32 | -32 | -33 | -33 | -32 | -36 | -32 | -35 | -41 | -48 | -45 | -32 | -35 | -38 | -39 | -39 | -36 | -36 | -30 | -28 | -33 | -28 | -20 | -17 |
| 29 | -17 | -17 | -14 | -13 | -17 | -22 | -19 | -24 | -25 | -24 | -25 | -26 | -30 | -35 | -37 | -38 | -34 | -34 | -32 | -28 | -31 | -34 | -32 | -27 |
| 30 | -24 | -21 | -18 | -16 | -22 | -32 | -30 | -25 | -22 | -27 | -30 | -33 | -33 | -32 | -33 | -35 | -34 | -34 | -28 | -23 | -20 | -30 | -35 | -43 |

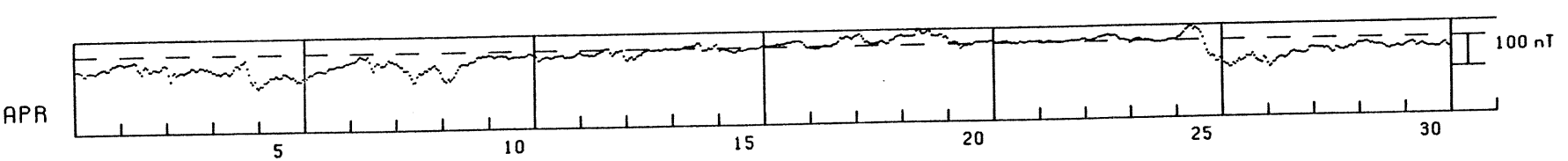


Replacement for page "xx".

# WORLD DATA CENTER A
# for
# Solar-Terrestrial Physics

REPORT UAG-96

# SOLAR-GEOPHYSICAL ACTIVITY REPORTS FOR STIP INTERVAL XV 12-21 February 1984 Ground Level Event AND STIP INTERVAL XVI 20 April-4 May 1984 Forbush Decrease


compiled by

Helen E. Coffey and Joe H. Allen
WDC-A for Solar-Terrestrial Physics
NOAA, National Geophysical Data Center
Boulder, Colorado 80303 USA


July 1987

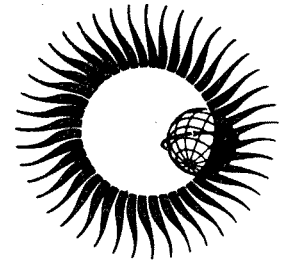


Published by World Data Center A for
Solar-Terrestrial Physics, NOAA
National Geophysical Data Center
Boulder, Colorado

and printed by

U.S. DEPARTMENT OF COMMERCE
NATIONAL OCEANIC AND ATMOSPHERIC ADMINISTRATION
NATIONAL ENVIRONMENTAL SATELLITE, DATA, AND INFORMATION SERVICE
National Geophysical Data Center
Boulder, CO 80303 USA

## FOREWORD

One of the projects under the various programs for cooperation in solar-terrestrial sciences since the International Geophysical Year has been the selection, through international mechanisms, of intervals for special study, chosen on the basis of scientifically significant events or conditions. These "Retrospective World Intervals" were originally selected by the International Ursigram and World Days Service (IUWDS) and announced through suitable solar-terrestrial physics periodicals. Since 1975 the designation of a Retrospective World Interval has been the responsibility of the SCOSTEP Committee on Monitoring the Sun-Earth Environment (MONSEE). The selected intervals are then announced by the requesting group or organization, or by one of the World Data Centers.

Retrospective World Intervals are traditionally selected for specifically disturbed or quiet conditions. Solar-geophysical conditions that have been considered for selecting disturbed periods have included the following:

(1) Magnetic storms with high $A_p$ values.
(2) The occurrence of large cosmic ray Forbush decreases.
(3) The occurrence of ground-level cosmic ray increases.
(4) The occurrence of significant polar-cap absorption events.
(5) Periods of ionospheric F-region disturbances.

Solar-geophysical conditions that have been considered for selecting quiet periods have included the following:

(1) A period when the $A_p$ index is less than 5 and the C index less than 0.2 at the same time on at least one day in the interval.
(2) A period isolated in time from a severe disturbance or in an interesting time relationship with surrounding disturbances.
(3) A period when the ionospheric F region is relatively quiet.

These selection criteria are not intended to be restrictive but are intended to provide guidelines in the designation of Retrospective World Intervals. At times, such as in August 1972, solar activity and the resulting geophysical disturbances are so significant that the period becomes a "self-declared" Retrospective World Interval. At other times, a period of special interest to a selected group of scientists has warranted the designation of Retrospective World Interval.

At the XXVth COSPAR General Assembly held in Graz, Austria, in June 1984, members of SCOSTEP's Study of Travelling Interplanetary Phenomena (STIP) program recommended two intervals for special study. The first interval, designated STIP Interval XV, included the ground-level relativistic solar particle event of 16 February 1984. The second interval, designated STIP Interval XIV, included the events associated with the major solar X-ray flare on 24 April 1984.

The STIP community then requested MONSEE to designate these two periods as Retrospective World Intervals (RWI) and to arrange, if possible, for the publication of an appropriate report containing scientific data that could be used by researchers analyzing these interesting periods. The MONSEE Steering Committee was able to arrange for financial support to make it possible for World Data Center A for Solar-Terrestrial Physics in Boulder, Colorado, to prepare and publish these data in a special issue of the UAG series. A letter was sent to all recipients of **Solar-Geophysical Data** requesting the submission of data reports suitable for this publication. It was emphasized that contributions to the UAG Report were to be data presentations and not analyses which properly belong in scientific journals. Contributors were requested to confine their reports to the following time periods:

**Event of Interest: 16 February relativistic solar particle event.**

| Period of Time | Data of Interest |
|---|---|
| 6-11 February 1984 | Data pertaining only to solar region No. 4408 (i.e., the assumed source region of the flare but behind the West limb of the Sun). |
| 12-21 February 1984 | Solar-terrestrial phenomena giving pre-event conditions, event data, and post-event conditions: related solar activity, interplanetary data, magnetospheric/ionospheric parameters, and geomagnetic variations. |
| 26 February - 5 March | Data on the return of the solar active region. |

**Event of Interest: 24 April solar flare (onset 2355 UT).**

| Period of Time | Data of Interest |
|---|---|
| 20 April - 4 May 1984 | Solar observations related to region No. 4474; flare and post-flare conditions in the interplanetary medium, magnetoshere/ionosphere, and related geomagnetic variations. |

This publication of the Solar-Geophysical Activity Reports for STIP Interval XV (12-21 February 1984 Ground-Level Event) and for STIP Interval XVI (20 April-4 May 1984 Forbush Decrease) contains 62 papers presenting data for these intervals. This is a truly international effort as can be seen by the list of 202 contributors from 13 different countries. In addition to the 62 data reports there are six papers summarizing the data from different disciplines. We sincerely thank Joe H. Allen, Helen Coffey, J. Hruska, Richard Thompson and Daniel C. Wilkinson for their efforts in preparing these overviews.

This UAG report has not been divided into two event sections since many of the papers contain data for both events. In general the individual sections have been arranged in the following manner: papers on the February event, papers on both the February and April events, and papers on the April event. Care should be taken in using the discipline oriented table of contents to ascertain the limits of data contained in each report since some reports contain data covering two disciplines. For example the paper on the auroral zone geophysical phenomena associated with the major solar proton events on 16 February and 24 April by Brunelli et al. (in the ionospheric section of the report) also contains cosmic radiation data.

The advantage of a report such as this is that data from many solar-terrestrial disciplines are collected and printed in one publication rather than being scattered throughout the literature in various publications. In addition, data not commonly published in scientific journals or even in routine data publications are included. Unfortunately it was not possible to include all data contributions primarily because of their nature and the extensive amounts of data contained in each report. These submissions are listed in section 6 of the Table of Contents and are available from the World Data Center. In addition, some of the data sets contained in the appropriate issues of **Solar-Geophysical Data** have not been repeated in this report.

The difficulties of assembling these papers into a common format cannot be fully appreciated until one has attempted to do a similar compilation. Papers are received in all types of formats and styles. Occasionally mistakes have been noted and the author must be contacted regarding the necessary corrections which are usually made by the compilers. Page restraints make it necessary to condense the many tables and figures into as few pages as possible but still retain the legibility and important aspects of the paper. On behalf of the MONSEE Committee and the entire solar-terrestrial research community, I sincerely thank Helen E. Coffey and Joe H. Allen for their painstaking work in producing this UAG report, and Carol Weathers for retyping most of the manuscripts. In addition I thank all the members of the community who contributed data for publication. Finally I would like to remind all users of data in this report to remember to cite the author and report number in any publication using these data. This is essential for establishing the usefulness of such reports whenever needed for administrative reasons.

M. A. Shea, Chairman
Monitoring Sun-Earth Environment Committee

## TABLE OF CONTENTS


Page

SOLAR-GEOPHYSICAL ACTIVITY REPORTS FOR STIP INTERVAL XV 12-21 February 1984 Ground-Level Event AND STIP INTERVAL XVI 20 April-4 May 1984 Forbush Decrease

Overview of Solar-Terrrestrial Physics Phenomena for STIP Interval XV (12-21 February 1984) and STIP Interval XVI (20 April - 4 May 1984). . . . . ix-xxi

1. SOLAR OPTICAL REPORTS. . . . . 1- 47
2. SOLAR RADIO EVENTS . . . . . 48- 99
3. SPACECRAFT OBSERVATIONS. . . . . 100-152
4. COSMIC RAY OBSERVATIONS. . . . . 153-241
5. IONOSPHERE . . . . . 243-325
6. GEOMAGNETISM . . . . . 326-387
7. REFERENCE PAPERS (list)
8. AUTHOR INDEX . . . . . 388-389

## TABLE OF CONTENTS


Page

OVERVIEW of SOLAR-TERRESTRIAL PHYSICS PHENOMENA for STIP INTERVAL XV (12-21 February 1984) and STIP INTERVAL XVI (20 April - 4 May 1984). . . . . ix
(M.A. Shea)

1. SOLAR OPTICAL REPORTS

"Summary of the Solar Optical Observations of the Active Regions Which Produced the Solar-Terrestrial Events of 16 February and 24 April 1984". . . . . 1
(Helen Coffey)
"A White-Light Flare of 24-25 April 1984". . . . . 4
(Eijiro Hiei, Tadashi Natori, Masahide Miyazawa, Kisuke Yamaguchi and Makoto Irie)
"Real-Time Solar Optical and Radio Observations of the 24-25 April 1984 Solar Flare from the U.S. Air Force Air Weather Service Solar Observatories". . . . . 10
(Gary D. Wells)
"Photospheric and H-Alpha Observations of the Region 4474 in the Period between 20 April and 4 May 1984 at Nijmegen" . . . . . 24
(H.A.M. Balster and I. Atanasijevic)
"Solar Observations for the Periods 6-11 February, 26 February - 5 March, and 20 April - 4 May 1984 Made by the A.L.P.O. Solar Section" . . . . . 35
(Richard E. Hill)

2. SOLAR RADIO EVENTS

"Summary of the Solar Radio Events during the 16 February and 24 April 1984 Solar-Terrestrial Events". . 48
(J. Hruska)
"U-shaped Type II Burst Connected with the Flare on 16 February 1984 and Preceding Activity" . . . . . 49
(I.M. Chertok, V.V. Fomichev, A.A. Gnezdilov, R.V. Gorgutsa and A.K. Markeev)
"The Proton Flare of 16 February 1984 Radiopolarimetric Aspect at Meter Wavelengths" . . . . . 52
(P. Zlobec, M. Nonino, M. Messerotti, M. Comari and L. Fornasari)
"RSTN Observations of the 16 February 1984 Cosmic Ray Flare" . . . . . 55
(E.W. Cliver, L.C. Gentile and G.D. Wells)
"Radio Burst Activity in Active Regions 4408 and 4474" . . . . . 58
(H. Aurass, A. Bohme, A. Kruger and J. Kurths)
"East-West Solar Scans for 7 February - 1 March 1984". . . . . 62
(V.M. Bogod, A.N. Korzhavin, N.G. Peterova, V.A. Shatilov and S.M. Vatrushin)
"East-West Solar Scans for 15-17 February and 23-25 April 1984 from the Large Pulkovo Array" . . . . . 78
(V.E. Abramov-Maksimov, S.M. Vatrushin and N.G. Peterova)
"Microwave Activities of Active Region AR4474" . . . . . 81
(S. Enome, K. Shibasaki and M. Nishio)
"Meter Radio Emission and Proton Flare of 24-25 April 1984". . . . . 88
(G.P. Chernov, I.M. Chertok, V.V. Fomichev, A.A. Gnezdilov, R.V. Gorgutsa and A.K. Markeev)
"Strong Rise and Fall Phenomena Recorded at Metric Wavelengths during 25 and 26 April 1984". . . . . 97
(M. Nonino, M. Messerotti, P. Zlobec, M. Comari and L. Fornasari)

3. SPACECRAFT OBSERVATIONS

"Summary of the Spacecraft Observations for the 16 February and 24 April 1984 Solar Events". . . . . .100
(Daniel C. Wilkinson)
"X-ray and Low Energy Gamma-Ray Observations of the 16 February 1984 Solar Flare". . . . . .101
(S.R. Kane, R.W. Klebesadel, E.E. Fenimore, and J.G. Laros)
"Measurements of the >1 Mev Proton Fluxes in February and April 1984 (STIP Intervals 12 to 21 February and 20 April to 5 May) on Board Venera-15,16 Space Probes". . . . . .103
(E.A. Chuchkov, S.I. Ermakov, N.N. Kontor, N.V. Pereslegina and V.I. Tulupov)
"Solar Proton Onset Times and Spectra for 16 February 1984 As Observed by the GOES Spacecraft" . . . . .106
(F.A. Hanser and B. Sellers)
"The Solar Proton Event of 16 February 1984: DMSP Observations at Low Altitude Over the Earth's Polar Caps" . . . . . .117
(J.B. Blake and W.A. Kolasinski)
"DMSP/F7 Dosimeter Measurements during the Solar Particle Events of 16 February and 24-28 April 1984". .123
(M.S. Gussenhoven, E.G. Mullen, M.R. Oberhardt and D.H. Brautigam)
"Energetic Electron and Ion Fluxes at Geostationary Orbit: 6-11 February and 20 April-1 May 1984" . . .132
(D.N. Baker, P.R. Higbie, R.D. Belian, R. Robinson and K. Sofaly)
"Meteor Satellite Observations of Solar Cosmic Rays for February and April 1984" . . . . . .140
(S.I. Avdyushin, N.K. Pereyaslova, M.N. Nazarova and I.E. Petrenko)
"Total Solar Irradiance Variations in February and April 1984" . . . . . .146
(H. Lee Kyle, John R. Hickey and Eugene R. Major)
"The Solar Protons in the Earth's Magnetosphere As Observed on Board Cosmos-1490 and 1520 from 24 April to 1 May 1984". . . . . .150
(L.A. Darchieva, T.A. Ivanova, T.N. Lukina, T.I. Morozova, N.N. Pavlov, I.A. Rubinshtein, E.N. Sosnovetz and L.V. Tverskaya)
"Measurement of the Fluxes of Nuclei CNO with Energies 10-20 Mev/Amu in April 1984 (STIP-Interval 20.04-04.05 1984) on Board the Satellite "Cosmos-1549". . . . . .152
(V.V. Bobrovskaya, N.L. Grigorov, D.A. Zhuravlev, M.A. Kondratyeva, R.A. Nymmik, Ch.A. Tretyakova, N.V. Alekseyev, P.V. Vakulov and V.P. Sechinov)

4. COSMIC RAY OBSERVATIONS

Page

"Summary of the Cosmic Ray Intensity during the Solar-Terrestrial Events of 16 February and 24-28 April 1984" . . . . . .153
(M.A. Shea)
"Asymptotic Directions for Selected Cosmic Ray Stations Calculated Using the International Geomagnetic Reference Field for 1980" . . . . . .155
(M.A. Shea, D.F. Smart and L.C. Gentile)
"Australian Neutron Monitor Data for the 16 February 1984 Event" . . . . . .173
(A.G. Fenton, K.B. Fenton and J.E. Humble)
"Relativistic Solar Cosmic Rays on 16 February 1984" . . . . . .184
(M.A. Pomerantz, J.W. Bieber and C.H. Tsao)
"Turku Double Neutron Monitor Data for the 16 February 1984 Event" . . . . . .192
(Jarmo Torsti)
"Neutron Monitor Observations at Mt. Washington and Durham During the Ground Level Event of 16 February 1984". . . . . .207
(J.A. Lockwood and J. LaBonte)
"The Response of the Neutron Monitors at Jungfraujoch, Kerguelen and Terre Adelie to the 16 February 1984 Relativistic Solar Particle Event" . . . . . .211
(H. Debrunner, E. Fluckiger, F. Golliez, M. Schubnell, G. Sebor, J.-P. Legrand, G. Casarrubios, D. Fouassier, P. Kossa, M. Lambrecht, C. Mottais and A. Zuntini)
"Solar Cosmic Ray Flare on 16 February 1984 Recorded by the Siberian and Far East Neutron Monitor Stations" . . . . . .221
(N.P. Chirkov, A.T. Filippov, A.M. Novikov, A.V. Sergeev, V.K. Korotkov, and V.L. Yanchukovsky)
"The 16 February 1984 Event Registered by the Rome Neutron Monitor". . . . . .223
(N. Iucci, M. Parisi, C. Signorini, M. Storini, G. Villoresi and N.L. Zangrilli)
"The Solar Flare of 16 February 1984 as Recorded at SANAE, Hermanus, Potchefstroom and Tsumeb" . . . . .226
(P.H. Stoker)
"Stratospheric Measurements of Solar Protons in February and April 1984" . . . . . .228
(G.A. Basilevskaya, Yu.I. Stozhkov and T.N. Charakhchyan)
"February-May 1984 Cosmic Ray Events Observed in Yakutsk". . . . . .230
(G.V. Skripin, G.V. Shafer, A.N. Prikhodko, N.M. Belomestnova and S.V. Kholtosunova)
"Cosmic Ray Variations at Alma Ata During the Solar Events in February and April 1984" . . . . . .233
(V.P. Antonova and A.G. Zusmanovich)
"Galactic Cosmic Rays During the Period 20 April-4 May 1984" . . . . . .236
(Martin A. Pomerantz)
"Cosmic Ray Variations in April and May 1984 according to the Novosibirsk Neutron Component Data and Neutron Multiplicity of Local Generation" . . . . . .237
(V.L. Yanchukovsky and R.Z. Khisamov)
"Cosmic Ray Observations at Khabarovsk During the Disturbed Periods in February and April 1984". . . . .238
(S.F. Rezaeva and A.P. Sidorenko)
"Cosmic Ray Intensity Variations from the ASK-1 Ionization Chamber at Tixie Bay during the February, April and May 1984 Solar Events". . . . . .240
(V.I. Ipatyev, A.M. Novikov and G.V. Shafer)

5. IONOSPHERE

"The 16 February and 24 April 1984 Solar-Terrestrial Events: The Ionospheric Observations". . . . . .243
(Richard Thompson)
"SPA's Observed at Inubo During February 6 - March 5, 1984". . . . . .244
(Mitsuo Ohshio, Akira Ohtani and Yoshiko Terajima)
"SWF's and SES's detected at Hiraiso during the period from February 6 to March 6, 1984" . . . . . .250
(H. Mori, C. Nemoto, T. Ishii and C. Ouchi)
"Ionospheric Activity Observed by Vertical Sounding at Japanese Stations During February 6-March 6, 1984" . . . . . .252
(Tokuji Koizumi and Mitsuo Ohshio)
"Solar flare effects on HF Doppler measurements during February 7-11, 1984". . . . . .258
(S. Kainuma, T. Kikuchi, A. Suzuki and Y. Echizenya)
"Sudden phase anomaly due to solar protons on February 16, 1984" . . . . . .262
(H. Sugiuchi, A. Ohtani and T. Kikuchi)
"VLF Propagation Observations During the GLE of 16 February 1984". . . . . .265
(A. Klekociuk)
"Polar Cap Absorption (PCA) Events in February and April-May 1984 by Riometer Data at the Soviet Arctic and Antarctic Stations". . . . . .269
(V.A. Ulyev and A.V. Shirochkov)
"Daily Ionospheric Indices During February and April 1984" . . . . . .276
(P.J. Wilkinson)
"Auroral Zone Geophysical Phenomena Associated With the Major Solar Proton Events on 16 February and 24 April 1984". . . . . .279
(B.E. Brunelli, G.P. Beloglazova, N.I. Fedorova, V.Ya. Gorelov, V.P. Kozelov, R.S. Kukushkina, L.L. Lazutin, N.V. Shulgina, G.F. Totunova, E.V. Vashenyuk and N.V. Volkov)

TABLE OF CONTENTS continued

5. IONOSPHERE continued — Page

"The Phenomena in the Ionosphere on 16 February and 24 April 1984 Observed at Sverdlovsk (Arty) Station (N56°26' E58°34')". . . . . .288
(V.A. Belyaev, M.V. Levin and V.F. Zakharchenko)
"Ionospheric Parameters and Geomagnetic Variations in February and April 1984 from Novosibirsk Data" . .289
(V.V. Kuznetsov, V.T. Levadny, I.I. Nesterova, N.I. Izrayleva, I.V. Pavlova and V.V. Plotkin)
"Standard Ionospheric Observations at Khabarovsk in February and April 1984" . . . . . .293
(V.S. Maksimov, N.D. Pogorelova and T.F. Kudiakova)
"Sudden Ionospheric Disturbances Associated with the Region 4474 as Recorded at Nijmegen". . . . . .303
(I. Atanasijevic and H.A.M. Balster)
"Comprehensive Results of Various Solar-Ionospheric Observations made by Radio Research Laboratory, Japan on April 24-27, 1984" . . . . . .312
(M. Ohshio, K. Ohbu, H. Kumagai, A. Ohtani, H. Mori, T. Ishii, T. Koizumi, S. Kainuma, A. Suzuki, T. Kikuchi, H. Minakoshi and I. Nishimuta)

6. GEOMAGNETISM

"The 16 February and 24 April 1984 Solar-Terrestrial Events: The Geomagnetic Observations". . . . . .326
(J.H. Allen)
"Riometer and Magnetometer Data from South Pole for 16 February 1984". . . . . .327
(S. Krishnaswamy, T.J. Rosenberg, C.G. Maclennan and L.J. Lanzerotti)
"Scandinavian and North American Geomagnetic Variations for the February and April 1984 Active Intervals". . . . . .330
(J.H. Allen, L.D. Morris, C. Sucksdorff and H. Nevanlina)
"Observations of the Geomagnetic Field at Kola Peninsula Stations" . . . . . .355
(G.A. Loginov)
"Magnetic Field and Cosmic Rays Data During 12-21 February and 20 April - 4 May 1984 at Sverdlovsk (Arty) Station" . . . . . .363
(V.A. Belyaev, L.N. Ivanova, V.A. Shapiro and B.L. Shirman)
"The Amplitude and Spectral Characteristics of Mid-latitude Geomagnetic Pulsations Pc2-4". . . . . .367
(T.B. Rusakova)
"Time Variations of the Geomagnetic Field Measured at Tixie Observatory During February, April and May 1984" . . . . . .369
(N.E. Molochushkin and A.M. Novikov)
"Geomagnetic Storms and Pulsations in Yakutsk" . . . . . .378
(A.A. Danilov, A.V. Sobolev and S.I. Solovyev)
"Low Latitude and Equatorial Geomagnetic Field Variations Observed during 25 and 27 April 1984". . . . .381
(G.K. Mukherjee and G.K. Rangarajan)
"Geomagnetic Variations in the Japanese Area". . . . . .383
(Akira Harada, Masayuki Kuwashima and Tetsuya Uwai)

6. REFERENCE PAPERS

EDITOR'S NOTE: These reports were sent for inclusion in this UAG Report. However, due to their nature and our space constraints, we are only able to reference them here. Copies are available from World Data Center A for Solar-Terrestrial Physics, NOAA E/GC2, 325 Broadway, Boulder, CO 80303 USA at the cost of copying. Please contact us for further information.

Ionospheric Data Sweden, February 1984, April 1984, and May 1984 issues, from Dr. Bo Thelin, Kiruna Geophysical Institute, P.O. Box 704, S-981 27 Kiruna, Sweden.

"Tucuman Ionospheric Sounding Data (hourly tables): 12-21 February 1984; 20 April - 4 May 1984 (All Parameters)", by Dr. Jose R. Manzano, Universidad Nacional de Tucuman, Facultad de Ciencias Exactas Y Tecnologia, Instituto de Fisica, Laboratorio de Ionosfera, Avda. Independencia 1800, 4000 Tucuman, Argentina.

Kiruna Geophysical Data, Data Summary 84/1-3 January-March 1984, and Data Summary 84/4-6 April-June 1984, from Dr. Bo Thelin, Kiruna Geophysical Institute, P.O. Box 704, S-981 27 Kiruna, Sweden.

"Tucuman H,Z,D Geomagnetic Components (hourly tables) for: February, April and May 1984" by Dr. Jose R. Manzano, Universidad Nacional de Tucuman, Facultad de Ciencias Exactas Y Tecnologia, Instituto de Fisica, Laboratorio de Ionosfera, Avda. Independencia 1800, 4000 Tucuman, Argentina.

7. AUTHOR INDEX. . . . . .388

# Overview of Solar-Terrestrial Physics Phenomena for STIP Interval XV (12-21 February 1984) and STIP Interval XVI (20 April - 4 May 1984)

M. A. Shea
Air Force Geophysics Laboratory
Hanscom AFB, Bedford, Massachusetts 01731, U.S.A.

ABSTRACT

A summary of the significant solar-terrestrial events that occurred during STIP Interval XV (12 - 21 February 1984) and STIP Interval XVI (20 April - 4 May 1984) is presented. The first period was highlighted by a large relativistic solar particle event recorded at the earth on 16 February 1984. These particles were associated with a flare on the invisible hemisphere of the sun. The second period was highlighted by a major X-ray flare on 24 April 1984 with an associated geomagnetic disturbance on 25-26 April. This flare was associated with the release of solar neutrons - only the third time such an identification has been made.

## Introduction

Two significant and vastly different solar particle events occurred in February and April 1984 during the decline of solar cycle 21. As shown in Figure 1, these events occurred when the monthly mean (Wolf) sunspot number was well above the smoothed "Zurich" sunspot number which is determined by two 12-month means (see McKinnon, 1987); the total number of solar flares was also high for both of these months. What made these events significant was their vastly different pre-event solar activity and their subsequent terrestrial effects.

The relativistic solar proton event on 16 February could not be associated with any specific activity on the visible solar disk and has been attributed to active region number 4408 on the invisible hemisphere of the sun. The particle event was short-lived, had a hard spectrum, and, as typical for flares behind the limb, was not associated with a geomagnetic disturbance. The second event, in active region number 4474, started at the

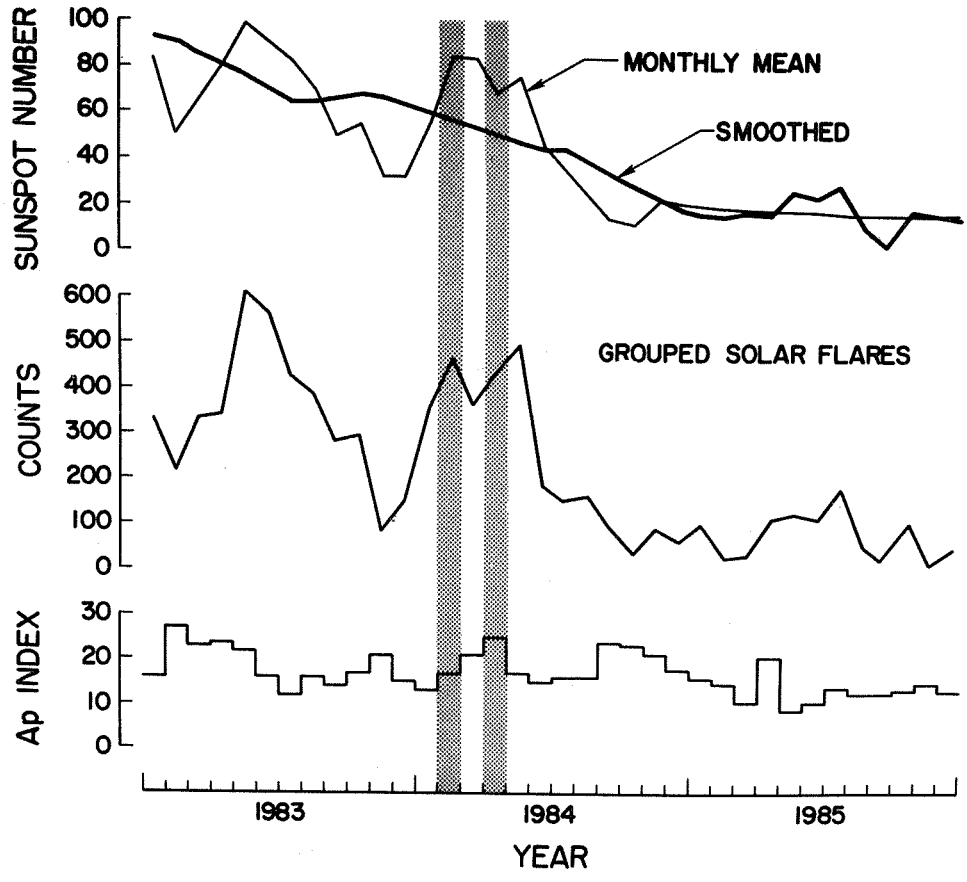


Figure 1. Smoothed sunspot number during the decline of solar cycle 21 and monthly mean (Wolf) sunspot number during February and April 1984. The total number of flares for each month is also shown as well as the monthly average geomagnetic activity index, $A_p$.

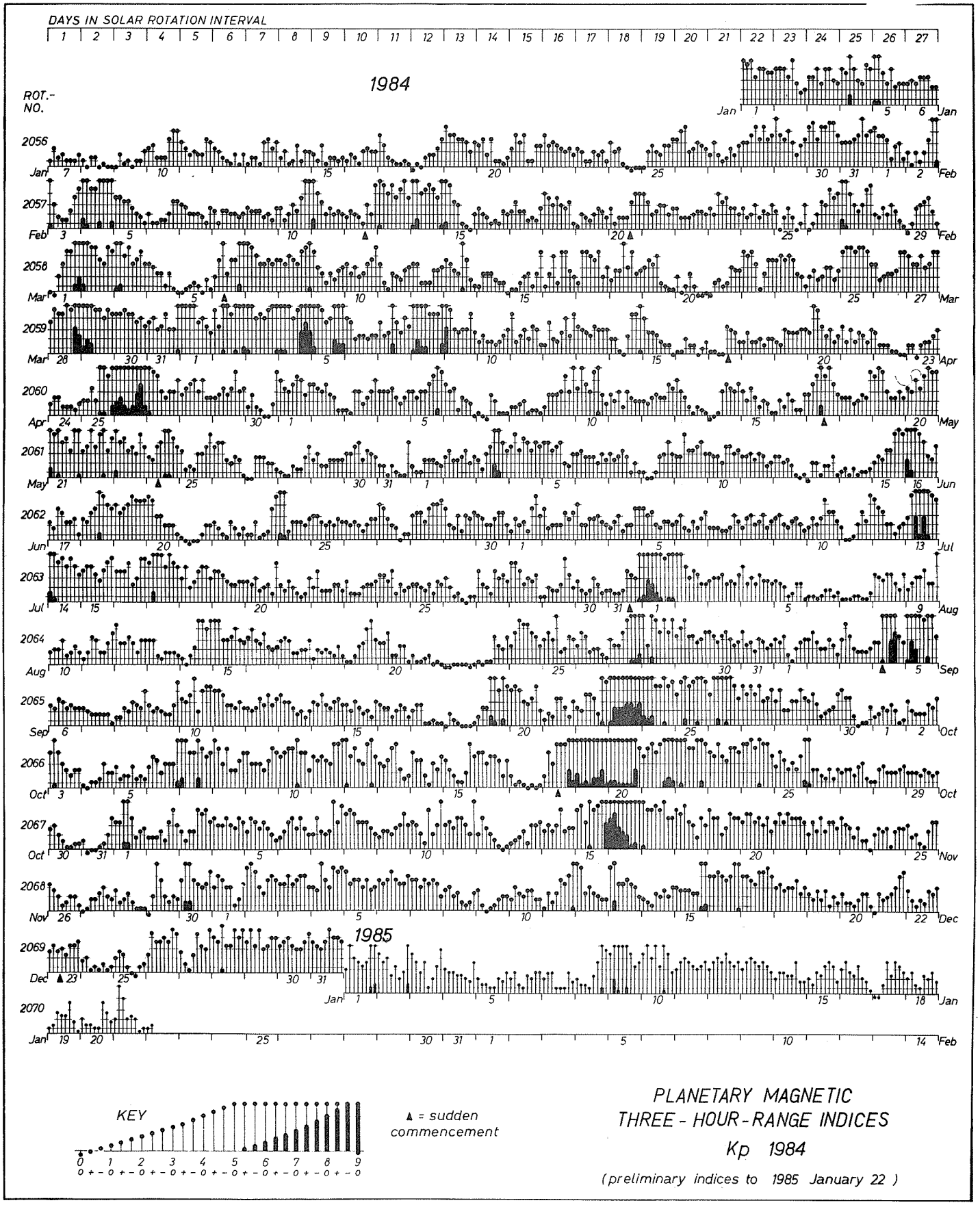


Figure 2. Planetary magnetic three-hour-range indices, $K_p$, for 1984.

end of the UT day on 24 April. This was a major X-ray flare on the eastern hemisphere of the solar disk which produced an entire array of solar emissions resulting in major terrestrial effects ranging from a sudden ionospheric disturbance to strong geomagnetic activity - one of the three largest events of 1984 as indicated by the prolonged period of enhanced $K_p$ values shown in Figure 2.

From an inspection of the H-alpha synoptic charts from early January through mid-June 1984, we note that active region 4408 was located in the southern hemisphere of the sun at Carrington longitude of approximately 340° (see the middle section of Figure 3). Active region 4474 was also located at this same position three solar rotations later (see the middle section of Figure 4). Examination of the solar features from Carrington rotation 1744 through 1749 (Figures 3 and 4) shows a fairly complex structure at this solar location. A coronal hole is located just north of active region 4408 in February. This hole is considerably enlarged by the next rotation, becomes slightly smaller during rotation 1747 and practically disappears by rotation 1748. Both active regions 4408 and 4474 are in close proximity to this coronal hole. It should be noted that although regions 4408 and 4474 are located at approximately the same Carrington coordinates, region 4408, which returned on the solar disk on 28 February as region 4427 disappeared six days later. Thus active region 4474 is not considered to be a long term continuation of region 4408 as seen from chromospheric visible light features.

In the following sections, a brief overview of each of these events is given. Details of many of the various observations are presented in the individual papers published in this UAG data report.

Event of 16 February 1984

Solar activity during the first half of February 1984 was primarily confined to active regions 4408, 4410, and 4413 located at Carrington longitudes of approximately 340°, 305°, and 255° respectively. Active region 4413 produced 91 flares on its transit across the disk; regions 4408 and 4410 produced 32 and 30 flares respectively. Both regions 4408 and 4413 had magnetically complex delta sunspot configurations; region 4408 had a more complex beta configuration than region 4410. Active region 4408 first appeared on the disk on 31 January 1984; however, 7 February was the first date that flares were reported from this region. From 7 February through 13 February when the region rotated over the western hemisphere, 22% of the reported flares and 24% of the X-ray events were associated with this region as illustrated in Figure 5. The sun was relatively quiet from 12 to 21 February with 11 flares of importance 1, none of which were produced by active region 4408. Geomagnetic activity, slightly disturbed on 14 February, was very quiet from 15-21 February as illustrated in Figure 6. Thus, on the morning of 16 February active region 4413 was the only region of importance on the visible disk; regions 4408 and 4410 were approximately 40° and 10° behind the west limb, respectively.

The solar particle event of 16 February came as a complete surprise. Forecasters at the various forecast centers were experiencing very quiet conditions when suddenly ground-based neutron monitors and satellite detectors indicated a major particle event in progress. Although the sun was being monitored by optical and radio sensors, the absence of an optical flare observation coupled with relatively weak solar radio noise and a small increase in the 0.5-4 Angstrom X-ray channel on GOES all indicated that the associated flare was on the invisible hemisphere of the sun. Subsequent analysis of the X-ray observations from ICE (located approximately 3° from the sun-earth line) and PVO (located about 16° behind the west limb of the sun) placed the flare far behind the solar limb. The rapid and very intense X-ray observations by the PVO indicated the flare was in full view of this spacecraft while the considerably smaller increases observed by the ICE and GOES detectors indicated the chromospheric part of the X-ray source was occulted from the line of sight of these spacecraft. Since solar active region 4410 had just rotated over the west limb, region 4408 was selected as the most likely source of this particle event.

This flare accelerated protons to relativistic energies with major increases recorded by ground-based neutron monitors. This was the seventh and largest increase recorded by neutron monitors from a solar flare on the invisible hemisphere, and was the second largest ground-level event of the 21st solar cycle. At 0900 UT the Goose Bay, Canada neutron monitor has an asymptotic cone viewing along the nominal interplanetary field direction and would be expected to record the earliest onset time and largest increase for a sea level location. The increase of particles at Goose Bay was very abrupt with an onset between 0905 and 0907 UT. Since the X-ray onset at PVO was 0857.5 UT and at GOES at 0859 UT, a particle onset of $0906 \pm 1$ UT at the earth is indicative of an extremely rapid transit of relativistic particles onto the magnetic field lines connecting the earth with the sun. The high energy proton flux was extremely anisotropic as shown by the neutron monitor measurements at two comparable stations, Goose Bay and Inuvik, Canada. As illustrated in Figure 7, the Goose Bay detector recorded a 42% increase between 0905 and 0910 UT while the Inuvik monitor remained at background level. In the next five-minute period, the Goose Bay monitor recorded a 94% increase with a 1.5% increase detected at Inuvik. Cosmic ray increases at locations such as Jungfraujoch and Hermanus with geomagnetic cutoff rigidities of 4.63 and 4.55 GV (Shea et al., 1983), respectively, indicate that protons with rigidities greater than 5.0 GV were present. The ground-level event was over very quickly with most stations recording intensities near background within three hours.

A polar cap absorption event was also recorded at several stations. The riometer at the South Pole recorded an onset at 0920 UT with a maximum absorption of approximately 5 db about an hour later. Although the absorption decreased to 1 db by 1400 UT it remained above background through the remainder of the day. Particle increases were also recorded on spacecraft as discussed in several papers in this UAG report. The proton and alpha particle fluxes recorded by sensors on IMP 8 are shown in Figures 8 and 9. The flux maximized either on the 16th or 17th depending upon the energy of the channel. The flux then decayed until the onset of another particle event on the 18th. The geomagnetic activity was relatively low between 16 and 19 February with a sudden commencement recorded at 1556 UT on 20 February, presumably associated with the particle producing flare two days previously. The Dst values for the entire month of February are listed in Table 1.

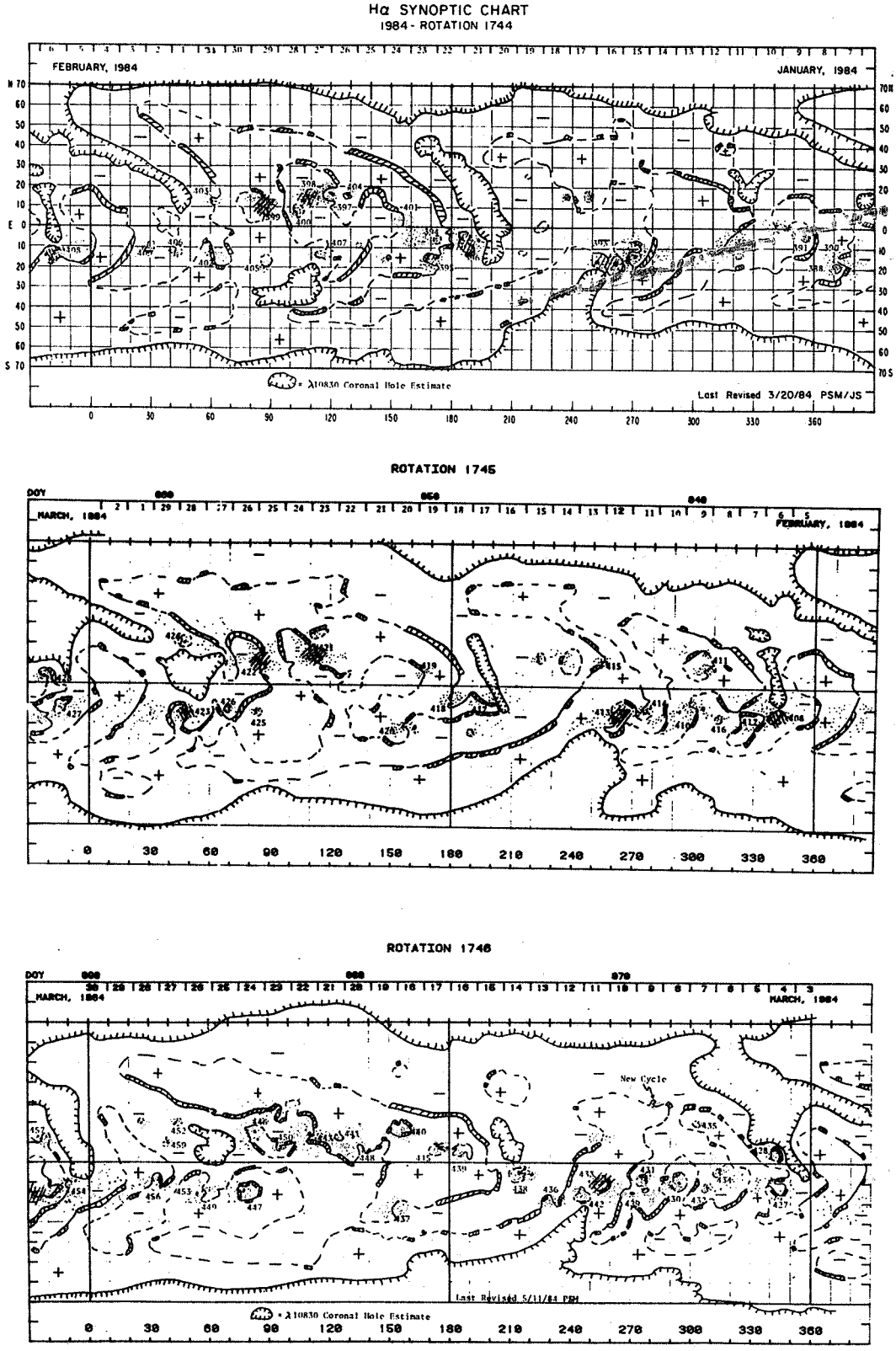


Figure 3. H-alpha synoptic charts for solar rotations 1744, 1745, and 1746 (7 January - 30 March 1984). These charts of the entire solar surface display solar activity in context with large-scale patterns of magnetic fields outlined by neutral lines (polarity inversion lines) inferred from H-alpha solar images. The H-alpha structures and their corresponding symbols are as follows: filaments (cross-hatched), major sunspots (large dots), bright H-alpha plage (closely spaced lines), faint H-alpha plage (stipple), distinct neutral lines (solid lines), estimated neutral lines (dashed lines) and boundaries of coronal holes observed in lambda 10830 (lines bordered with ticks directed toward center of coronal hole). (Figures courtesy of P. S. McIntosh, NOAA, Boulder, Colorado)

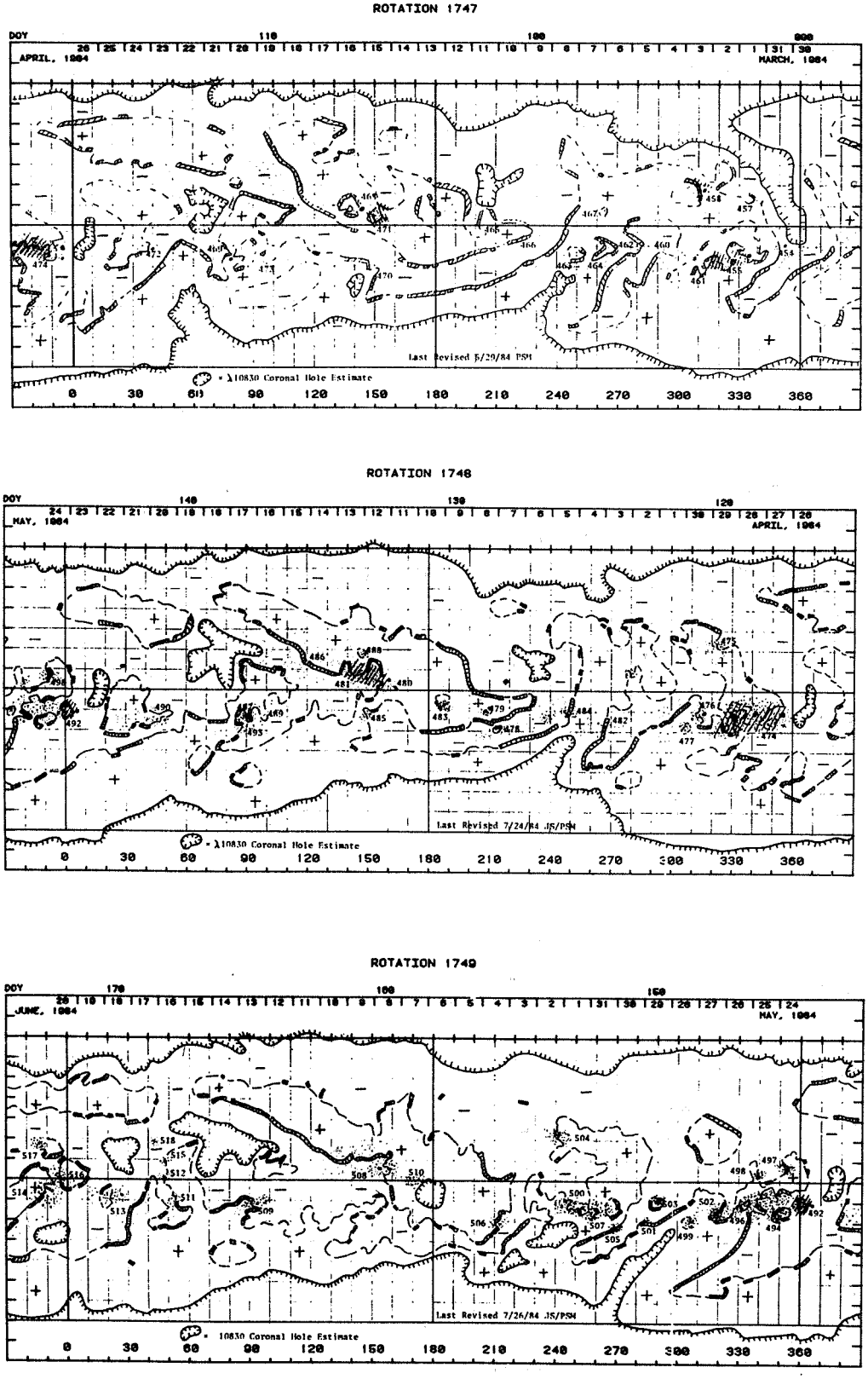


Figure 4. H-alpha synoptic charts for solar rotations 1747, 1748, and 1749 (30 March - 20 June 1984). These charts of the entire solar surface display solar activity in context with large-scale patterns of magnetic fields outlined by neutral lines (polarity inversion lines) inferred from H-alpha solar images. The H-alpha structures and their corresponding symbols are as follows: filaments (cross-hatched), major sunspots (large dots), bright H-alpha plage (closely spaced lines), faint H-alpha plage (stipple), distinct neutral lines (solid lines), estimated neutral lines (dashed lines) and boundaries of coronal holes observed in lambda 10830 (lines bordered with ticks directed toward center of coronal hole). (Figures courtesy of P. S. McIntosh, NOAA, Boulder, Colorado)

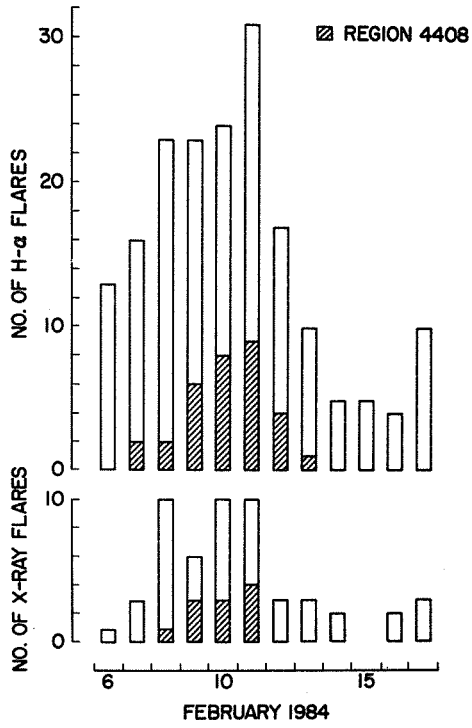


Figure 5. Total number of H-alpha and X-ray flares, 6-17 February 1984. The number of flares associated with active region 4408 is indicated by the shaded area.

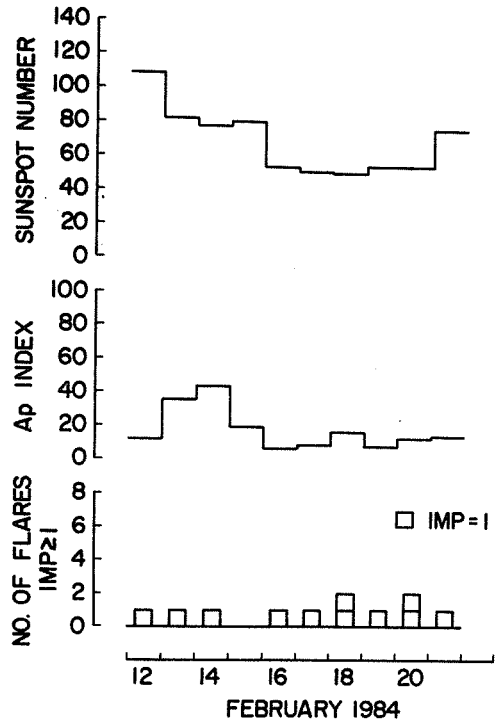


Figure 6. Daily (Wolf) sunspot number, daily magnetic index, $A_p$, and total number of flares with H-alpha importance equal or greater than 1 for 12-21 February 1984.

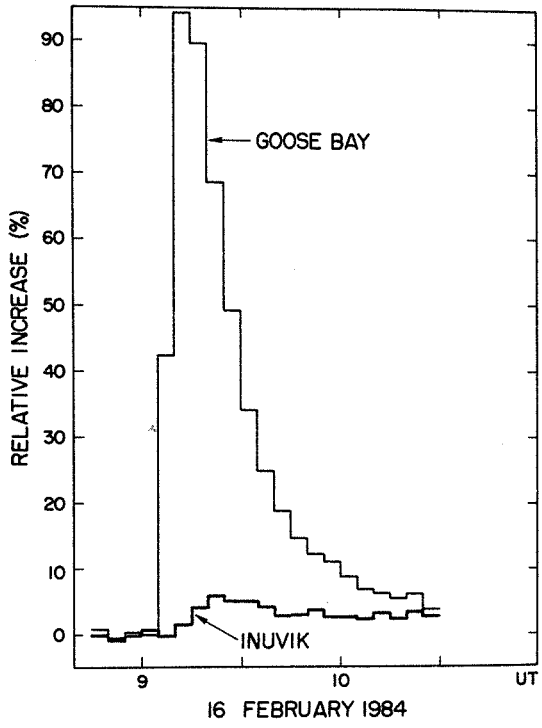


Figure 7. Relative increase in cosmic ray intensity as measured by the Goose Bay (geographic coordinates: 53.33 N,299.58E) and Inuvik (geographic coordinates: 68.35 N, 226.27 E) neutron monitors during the relativistic solar cosmic ray event on 16 February 1984.

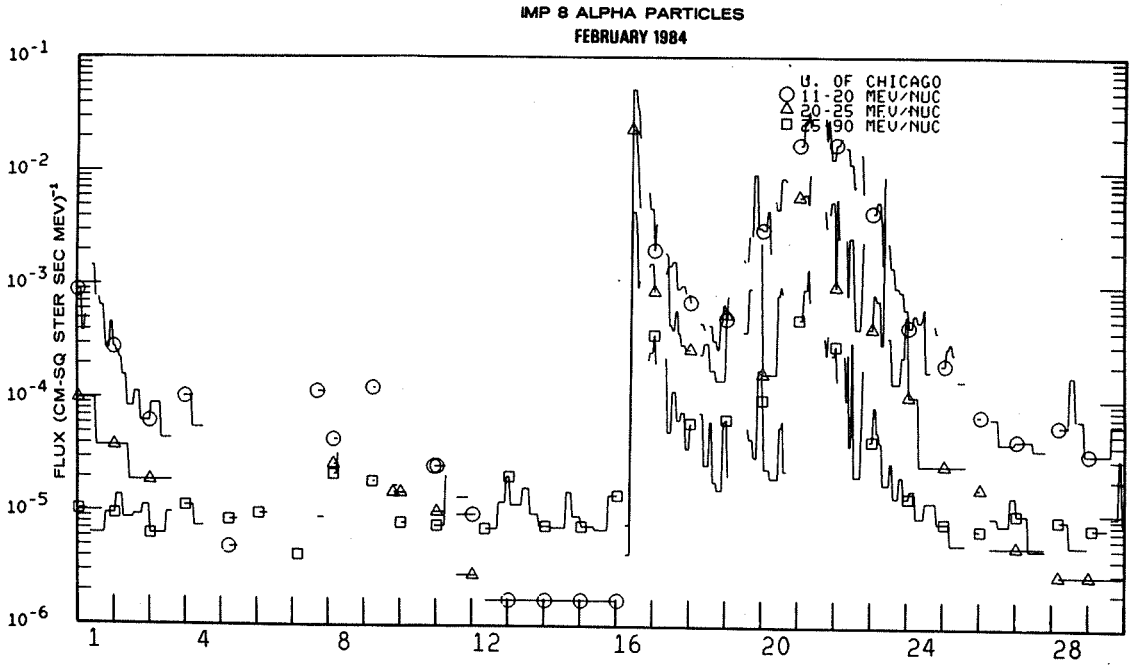


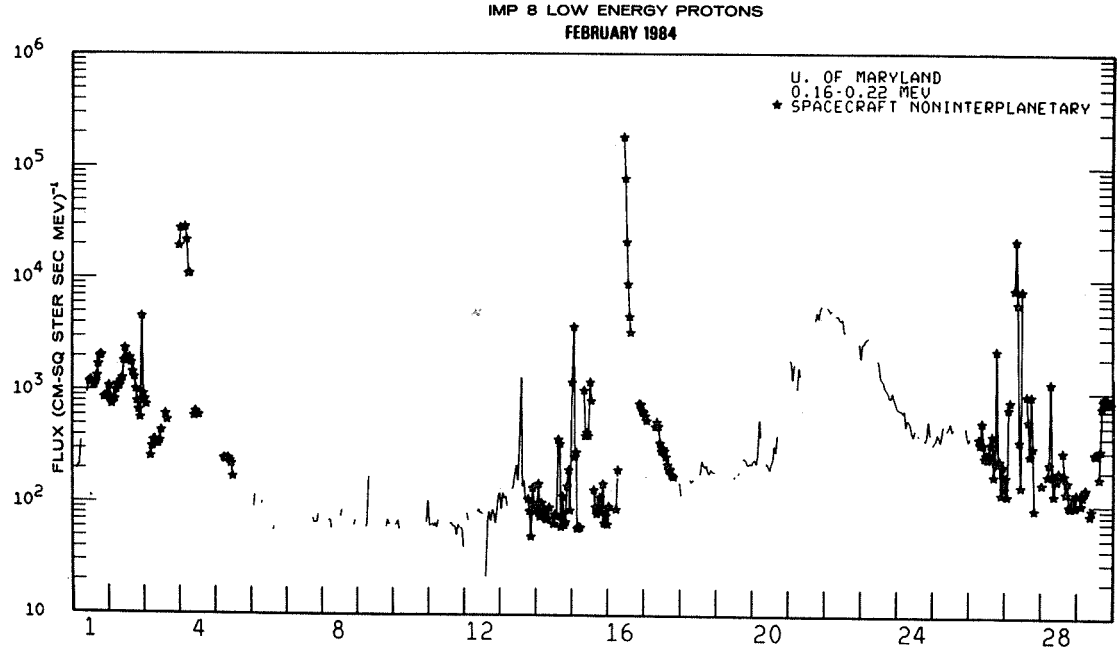


Figure 8. Alpha particle and low energy proton flux measured on IMP 8 during February 1984.

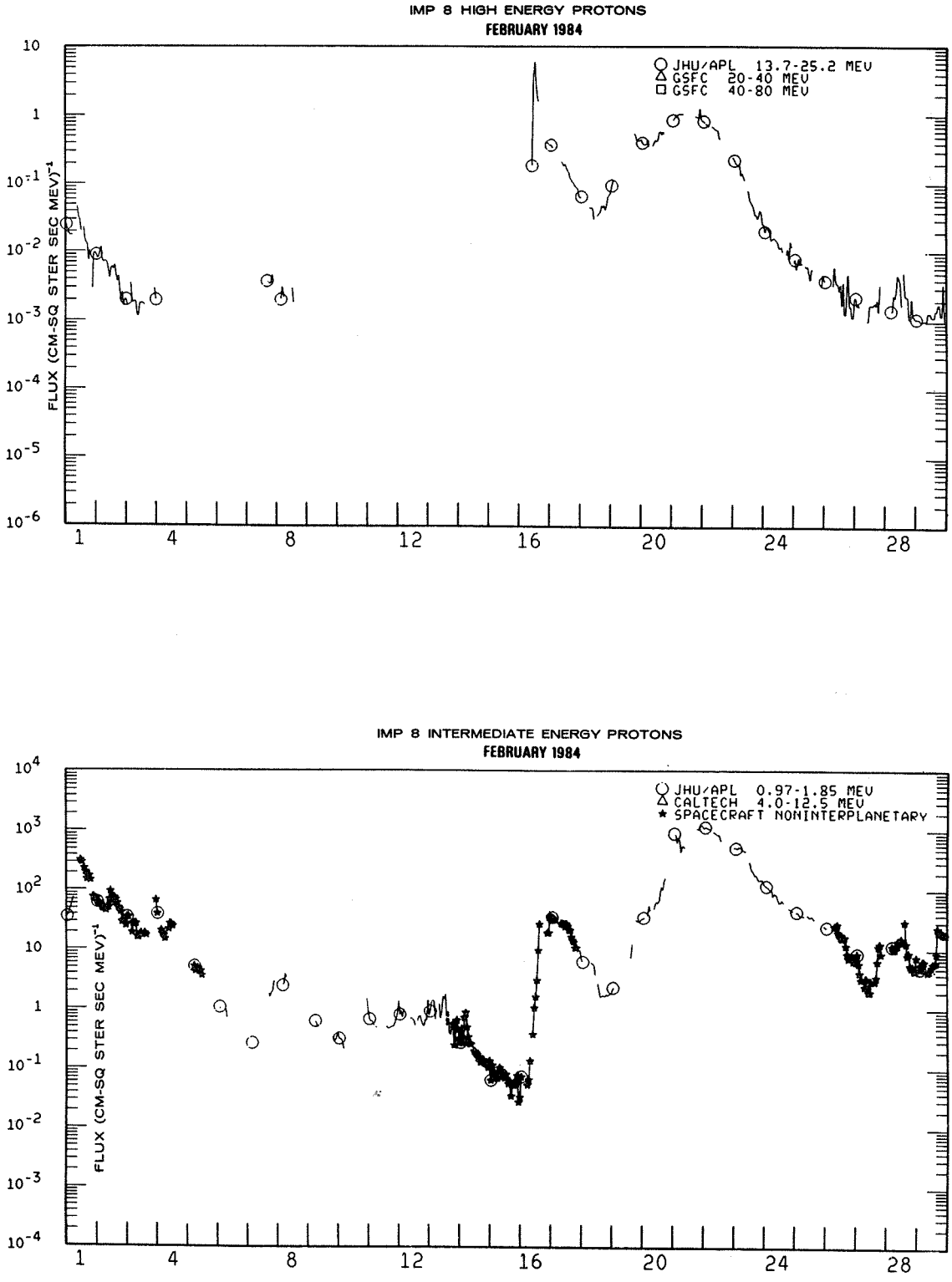


Figure 9. Intermediate and high energy proton flux measured on IMP 8 during February 1984.

NASA GODDARD SPACE FLIGHT CENTER

HOURLY EQUATORIAL DST VALUES (PROVISIONAL)

FEBRUARY 1984

| UNIT=NT | 1 | 2 | 3 | 4 | 5 | 6 | 7 | 8 | 9 | 10 | 11 | 12 | 13 | 14 | 15 | 16 | 17 | 18 | 19 | 20 | 21 | 22 | 23 | U.T. 24 |
|---|---|---|---|---|---|---|---|---|---|---|---|---|---|---|---|---|---|---|---|---|---|---|---|---|
| DAY | | | | | | | | | | | | | | | | | | | | | | | | |
| 1 | -12 | -11 | -7 | -9 | -10 | -13 | -14 | -19 | -15 | -9 | -10 | -10 | -8 | -11 | -13 | -11 | -11 | -13 | -14 | -15 | -13 | -11 | -6 | -3 |
| 2 | 0 | 5 | 7 | 4 | -2 | -4 | 3 | 2 | 2 | 3 | 2 | 0 | -2 | -4 | -5 | -5 | -8 | -13 | -23 | -22 | -27 | -25 | -16 | -30 |
| 3 | -42 | -49 | -45 | -38 | -36 | -38 | -35 | -30 | -29 | -28 | -29 | -25 | -23 | -23 | -23 | -17 | -15 | -17 | -16 | -25 | -29 | -41 | -49 | -56 |
| 4 | -52 | -56 | -61 | -66 | -74 | -80 | -78 | -66 | -58 | -50 | -48 | -58 | -72 | -79 | -81 | -75 | -64 | -62 | -71 | -86 | -86 | -90 | -60 | -59 |
| 5 | -60 | -53 | -47 | -45 | -50 | -47 | -40 | -42 | -50 | -53 | -58 | -56 | -45 | -41 | -44 | -45 | -46 | -43 | -38 | -37 | -38 | -34 | -27 | -25 |
| 6 | -25 | -24 | -22 | -22 | -22 | -19 | -15 | -12 | -11 | -13 | -16 | -18 | -19 | -20 | -17 | -16 | -14 | -14 | -17 | -27 | -35 | -35 | -27 | -25 |
| 7 | -28 | -27 | -24 | -21 | -23 | -26 | -21 | -21 | -24 | -21 | -18 | -19 | -17 | -17 | -15 | -12 | -16 | -17 | -17 | -12 | -10 | -13 | -15 | -18 |
| 8 | -17 | -19 | -19 | -17 | -15 | -12 | -10 | -10 | -17 | -13 | -10 | -10 | -13 | -14 | -14 | -11 | -8 | -6 | -8 | -12 | -13 | -12 | -10 | -12 |
| 9 | -16 | -19 | -14 | -9 | -6 | -6 | -6 | -10 | -9 | -9 | -7 | -11 | -8 | -7 | -5 | -1 | -1 | -4 | -8 | -11 | -10 | -11 | -5 | -4 |
| 10 | -2 | 1 | 2 | -2 | -2 | 0 | 4 | 3 | 2 | 1 | -5 | -5 | -8 | -12 | -13 | -15 | -22 | -31 | -40 | -38 | -43 | -54 | -47 | -43 |
| 11 | -44 | -42 | -35 | -32 | -32 | -34 | -40 | -44 | -41 | -40 | -43 | -43 | -41 | -40 | -38 | -36 | -31 | -28 | -24 | -24 | -27 | -30 | -27 | -27 |
| 12 | -25 | -20 | -20 | -17 | -16 | -14 | -11 | -14 | -10 | -7 | -11 | -14 | -19 | -20 | -19 | -11 | -11 | -11 | -6 | -4 | -5 | -17 | -23 | -29 |
| 13 | -29 | -30 | -34 | -37 | -37 | -36 | -41 | -34 | -30 | -34 | -36 | -36 | -35 | -38 | -42 | -45 | -50 | -58 | -44 | -52 | -55 | -46 | -45 | -52 |
| 14 | -52 | -51 | -52 | -60 | -62 | -64 | -48 | -41 | -36 | -34 | -39 | -38 | -29 | -32 | -21 | -25 | -29 | -24 | -24 | -23 | -37 | -34 | -25 | -31 |
| 15 | -38 | -31 | -27 | -36 | -47 | -51 | -44 | -39 | -38 | -35 | -34 | -28 | -23 | -21 | -17 | -15 | -17 | -20 | -21 | -22 | -22 | -19 | -15 | -12 |
| 16 | -11 | -8 | -11 | -14 | -17 | -19 | -19 | -18 | -16 | -17 | -18 | -17 | -16 | -15 | -13 | -11 | -11 | -11 | -10 | -10 | -7 | -4 | -2 | -3 |
| 17 | -1 | -1 | 2 | -1 | -11 | -16 | -13 | -6 | -3 | -1 | -2 | -4 | -6 | -3 | 0 | 2 | -2 | -3 | -5 | -5 | -5 | 0 | 9 | 12 |
| 18 | -7 | -10 | -12 | -15 | -25 | -32 | -24 | -20 | -16 | -19 | -16 | -9 | -8 | -8 | -8 | -14 | -15 | -13 | -11 | -13 | -13 | -10 | -4 | -3 |
| 19 | -1 | 0 | 1 | -2 | -4 | -2 | 1 | -1 | 0 | 2 | 4 | 4 | 3 | -1 | -6 | -7 | -4 | 0 | -1 | 1 | 3 | 3 | 4 | 0 |
| 20 | 2 | 8 | 10 | 9 | 7 | 10 | 5 | 5 | 12 | 14 | 13 | 16 | 17 | 20 | 20 | 23 | 39 | 38 | 35 | 18 | 5 | -1 | -13 | -8 |
| 21 | -6 | -18 | -21 | -20 | -16 | -14 | -16 | -16 | -19 | -16 | -14 | -15 | -14 | -17 | -12 | -9 | -4 | -1 | 2 | 0 | -7 | -15 | -12 | -8 |
| 22 | -6 | -7 | -11 | -12 | -12 | -13 | -11 | -8 | -6 | -8 | -10 | -11 | -10 | -7 | -6 | -6 | -7 | -8 | -7 | -4 | -5 | -6 | -5 | -1 |
| 23 | 3 | 2 | 2 | 3 | 2 | -2 | -8 | -12 | -8 | 1 | 0 | -5 | -8 | -16 | -12 | -6 | -2 | -1 | -1 | -7 | -6 | -2 | 0 | 1 |
| 24 | 2 | 5 | 7 | 3 | 3 | 2 | 5 | 4 | 2 | 7 | 5 | 3 | 7 | 9 | 9 | 5 | -1 | -5 | -9 | -9 | -6 | -6 | -6 | -7 |
| 25 | -2 | -1 | 0 | 0 | 3 | 4 | 5 | 5 | 0 | -10 | -8 | -7 | -3 | -1 | 0 | 1 | 1 | 0 | 0 | 0 | 1 | 2 | -9 | -6 |
| 26 | -6 | -3 | 0 | 2 | 1 | 0 | -4 | -2 | 2 | 11 | 14 | 3 | 3 | -3 | -10 | -10 | -9 | -21 | -24 | -28 | -21 | -16 | -4 | -1 |
| 27 | 9 | 16 | -10 | -28 | -27 | -27 | -34 | -39 | -40 | -28 | -24 | -29 | -28 | -30 | -23 | -21 | -8 | -5 | -5 | -20 | -40 | -38 | -29 | -22 |
| 28 | -19 | -13 | -5 | 1 | -2 | -4 | -3 | -4 | -10 | -12 | -13 | -9 | -3 | -4 | -6 | -6 | -3 | -5 | -5 | -9 | -5 | -2 | 4 | 4 |
| 29 | 5 | 6 | 5 | 7 | 7 | 4 | 5 | 5 | -3 | -9 | -14 | -6 | -4 | -7 | -11 | -15 | -6 | 1 | 3 | 0 | -3 | -6 | -5 | -6 |

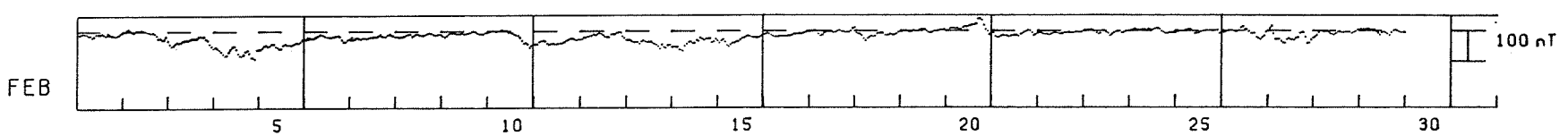

Event of 24-25 April 1984

In contrast to the relatively quiet disk passage of active region 4408 which produced the particle event on 16 February, region 4474 came over the east limb of the sun on 20 April and immediately gave notice of its potential as a major region of activity. On its passage across the solar disk this region produced 64% of the flares and 78% of the X-ray events as illustrated in Figure 10. Of the 170 flares in this region, there were 28 flares of importance 1, 4 flares of importance 2, and one flare of importance 3. This region also produced 66 X-ray events as follows: 44 class C, 20 class M and 2 class X. Although other regions contributed to the total number of major flares shown in Figure 11, region 4474 clearly dominated the solar activity and related terrestrial effects between 20 April and 4 May.

At 0259 UT on 24 April region 4474 produced a 2N flare with a class X1 X-ray event. Throughout the day this region remained active until at 2356 UT a white light flare (3B, X13) was observed located at S11, E45. This flare, shown in Figure 12, was associated with a major ionospheric disturbance on the sunlit hemisphere resulting in severely degraded HF communication links for two hours. The measurements of the associated gamma rays indicated the release of solar neutrons (Chupp, private communication), and indeed, the identification of decay protons from solar neutrons was observed by the ISEE-3 spacecraft (Evenson et al., 1985). In addition, a careful examination of the ground-based neutron monitor data recorded in Japan suggests the detection of secondaries generated by the >400 MeV solar neutrons incident at the top of the earth's atmosphere (Shea et al., 1987). The extremely limited particle measurements on IMP 8 (Solar-Geophysical Data, 1986) indicate a major increase with onset prior to approximately 12 UT on 25 April. A proton event recorded on the GOES synchronous orbit spacecraft had a maximum intensity of 2500 particles $cm^{-2}$ $sec^{-1}$ $ster^{-1}$ greater than 10 MeV at 1430 UT on 26 April. Satellite and balloon measurements indicated a soft proton spectrum. Dosimeter measurements on the DMSP spacecraft under 2 gm $cm^{-2}$ of absorber recorded approximately 0.1 rad per polar pass during the maximum of this event. In spite of the differences in spectrum and maximum particle energy between the event on 16 February and 25 April, this dosimeter recorded approximately the same dosage under 2 gm $cm^{-2}$ absorber during the maximum of each event (Gussenhoven, et al., 1987).

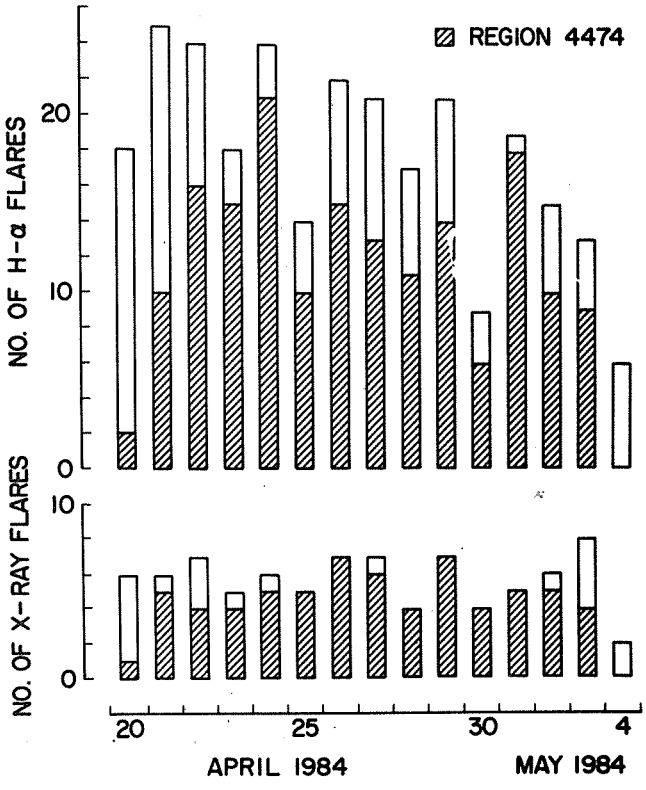


Figure 10. Total number of H-alpha and X-ray flares, 20 April - 4 May 1984. The number of flares associated with active region 4474 is indicated by the shaded area.

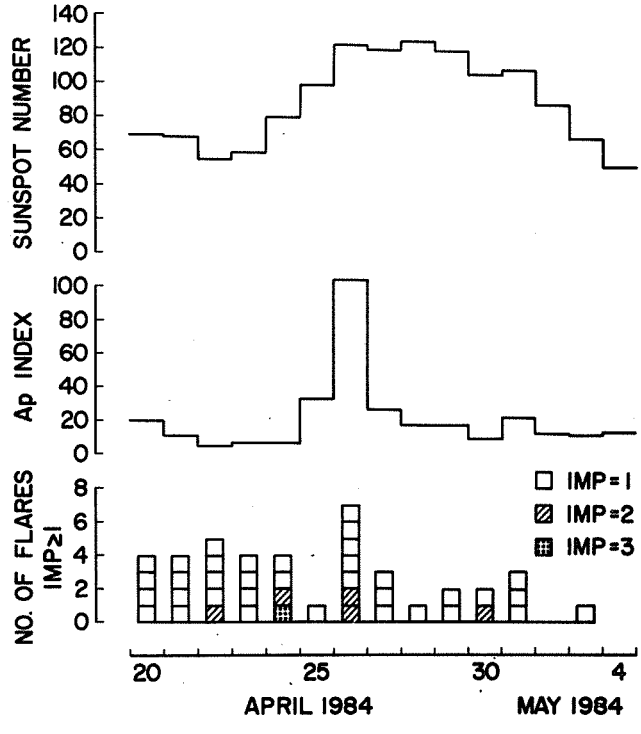


Figure 11. Daily (Wolf) sunspot number, daily magnetic index, $A_p$, and total number of flares with H-alpha importance equal or greater than 1 for 20 April - 4 May 1984.

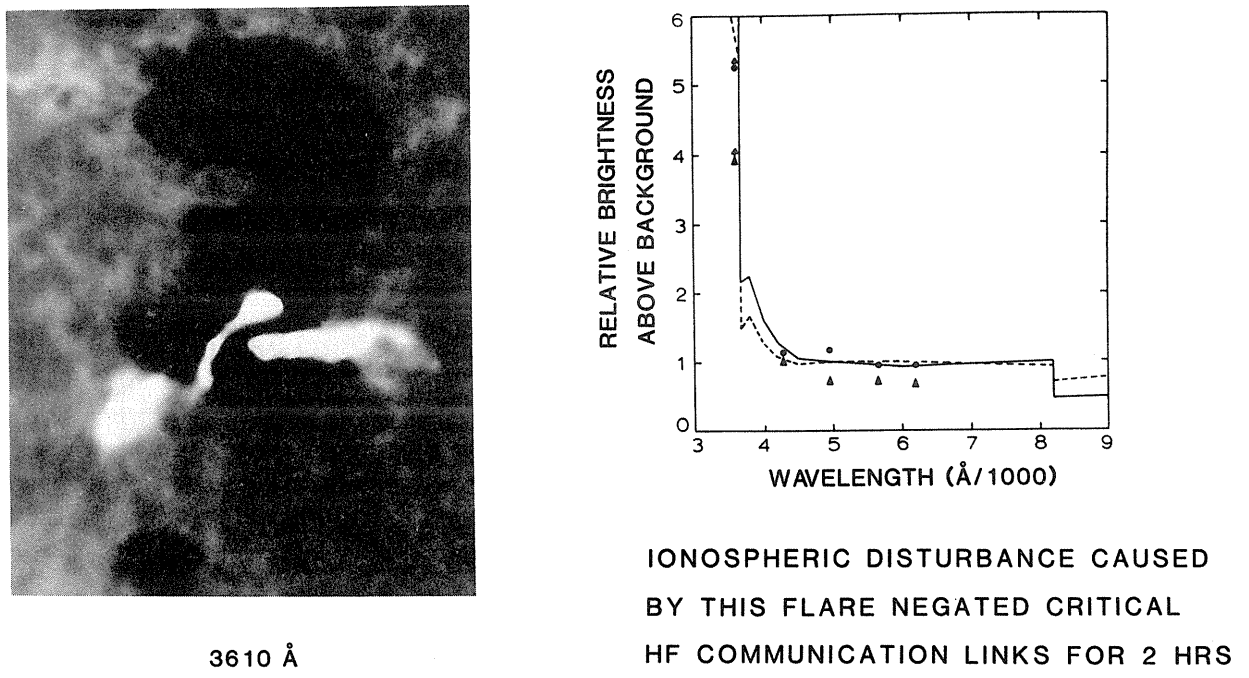


Figure 12. Photograph of the white light flare with onset at 2345 UT on 24 April 1984. The photograph was taken at 0001 UT on 25 April. (Photograph courtesy of National Solar Observatory, U.S.A.)

A 1N solar flare at 0243 UT from region 4472, and a 2B flare at 0420 UT from region 4468 on 22 April, plus continued activity from region 4474 on 22 and 23 April possibly all contributed to relatively disturbed geomagnetic conditions commencing around 00 UT on 25 April as indicated by the Dst values in Table 2. Limited interplanetary magnetic field measurements (Couzens and King, 1986) available between 09 and 18 UT on 24 April show the magnitude of the interplanetary magnetic field slightly above average; when data coverage resumed at 10 UT on 25 April the magnitude of the interplanetary magnetic field had increased by a factor of two (from 7.8 to 15.9 nT). The interplanetary magnetic field turns southward around 13 UT on 25 April with extremely disturbed geomagnetic conditions for approximately 40 hours (see Figure 2 and Table 2). A sudden commencement was initially reported at College, Honolulu, Sitka and Gnangara around 00 UT on 25 April (Solar-Geophysical Data, 1984); however, subsequent examination of the Honolulu magnetogram which showed a 50 nT increase in the H-component indicates that the perturbations recorded may have been a solar flare effect (sfe) instead of a sudden commencement (Sugiura, private communication). The arrival at the earth of an interplanetary shock associated with the 2356 UT flare on 24 April cannot be uniquely identified in the geomagnetic records because of the major disturbance in progress during 25 and 26 April. From the neutron monitor measurements of the galactic cosmic ray intensity we find a small decrease in intensity of approximately one percent at high latitude stations during the afternoon of 25 April followed by a slow recovery until 17 UT on 26 April at which time a rapid Forbush decrease of approximately 5% was recorded for the next few hours. The Dst values, slowly recovering prior to 17 UT indicate an additional perturbation to the geomagnetic field for the next few hours. These data suggest that the interplanetary shock associated with the 2356 UT flare of 24 April might have arrived at the earth around 17 UT on 26 April with a transit time of 41 hours.

## Concluding Remarks

The solar activity and related terrestrial effects on 16 February and 24-26 April 1984 were two different types of events during the decline of solar cycle 21 which should provide enough interest in the solar-terrestrial research community to warrant numerous and detailed analyses. Although there are extensive ground-based measurements, the sparsity of particle and plasma measurements in the interplanetary medium for this period is typical of our severely degraded state of interplanetary monitoring. Thus, it will be extremely difficult, and perhaps impossible, to do the many detailed scientific analyses that would have been possible ten years ago when the critical interplanetary parameters were being routinely measured. Nevertheless, these events have essentially "something for everyone" in the community, and it is anticipated that the data contained in this UAG report will provide a stimulus for both creative and exciting research results that might not have been contemplated prior to the publication of this data compilation.

NASA/GODDARD SPACE FLIGHT CENTER

## HOURLY EQUATORIAL DST VALUES(PROVISIONAL)

APRIL 1984

UNIT=NT

| DAY | 1 | 2 | 3 | 4 | 5 | 6 | 7 | 8 | 9 | 10 | 11 | 12 | 13 | 14 | 15 | 16 | 17 | 18 | 19 | 20 | 21 | 22 | 23 | U.T. 24 |
|---|---|---|---|---|---|---|---|---|---|---|---|---|---|---|---|---|---|---|---|---|---|---|---|---|
| 1 | -1 | 4 | 9 | 12 | 9 | 7 | 9 | 12 | 12 | 1 | 3 | 7 | 6 | 2 | -23 | -41 | -41 | -37 | -32 | -29 | -26 | -26 | -22 | -19 |
| 2 | -22 | -21 | -20 | -17 | -22 | -19 | -17 | -17 | -13 | -8 | -8 | -10 | -14 | -15 | -18 | -22 | -21 | -24 | -23 | -21 | -23 | -21 | -16 | -10 |
| 3 | -10 | -15 | -7 | -7 | -7 | -7 | -9 | -8 | -6 | -5 | -9 | -9 | -9 | -13 | -18 | -16 | -16 | -17 | -17 | -20 | -20 | -17 | -12 | -9 |
| 4 | -15 | -16 | -14 | -14 | -15 | -21 | -20 | -17 | -13 | -16 | -14 | -10 | -12 | -13 | -16 | -20 | -26 | -25 | -21 | -20 | -19 | -15 | -11 | -9 |
| 5 | -13 | -14 | -11 | -11 | -11 | -12 | -11 | -10 | -11 | -12 | -13 | -11 | -13 | -9 | -11 | -9 | -10 | -10 | -7 | -8 | -10 | -14 | -15 | -12 |
| 6 | -11 | -9 | -7 | -5 | -5 | -5 | -6 | -6 | -7 | -10 | -12 | -9 | -7 | -4 | -2 | 0 | 1 | 1 | 0 | -4 | -6 | -4 | 1 | 4 |
| 7 | 3 | 6 | 8 | 6 | 4 | -2 | -9 | -11 | -20 | -19 | -13 | -8 | -6 | -7 | -11 | -11 | -11 | -13 | -10 | -7 | -9 | -8 | -7 | -6 |
| 8 | -7 | -5 | -4 | -5 | -3 | -2 | -1 | 0 | -1 | -1 | -3 | 0 | 1 | 3 | 4 | -1 | -1 | 4 | -1 | -5 | -9 | -24 | -37 | -32 |
| 9 | -28 | -16 | -12 | -11 | -9 | -17 | -22 | -23 | -18 | -28 | -29 | -17 | -22 | -36 | -37 | -56 | -62 | -49 | -35 | -29 | -30 | -31 | -30 | -25 |
| 10 | -22 | -19 | -19 | -20 | -17 | -18 | -22 | -27 | -27 | -26 | -20 | -24 | -19 | -15 | -24 | -26 | -22 | -25 | -25 | -20 | -13 | -12 | -13 | -11 |
| 11 | -14 | -18 | -18 | -19 | -24 | -27 | -24 | -23 | -24 | -23 | -20 | -17 | -20 | -22 | -20 | -19 | -22 | -21 | -17 | -15 | -13 | -11 | -9 | -9 |
| 12 | -11 | -10 | -6 | -5 | -5 | -5 | -5 | -1 | -2 | -4 | -5 | -7 | -2 | -5 | -6 | -11 | -14 | -16 | -17 | -12 | -9 | -10 | -11 | -10 |
| 13 | -12 | -14 | -14 | -9 | -1 | 4 | 4 | 6 | 7 | 5 | 5 | 6 | 3 | 2 | 2 | 7 | 9 | 11 | 13 | 7 | 1 | -3 | -1 | 1 |
| 14 | 3 | -5 | -6 | -10 | -19 | -18 | -18 | -19 | -15 | -15 | -13 | -11 | -14 | -12 | -10 | -7 | -5 | -4 | -5 | -7 | -9 | -8 | -4 | -3 |
| 15 | -4 | -6 | -6 | -7 | -9 | -6 | -3 | -3 | -3 | -1 | 0 | -1 | -6 | -5 | -6 | -4 | 0 | 1 | 1 | 3 | 4 | 6 | 8 | 5 |
| 16 | 5 | 7 | 9 | 8 | 9 | 13 | 17 | 19 | 19 | 18 | 11 | 1 | 2 | 2 | 3 | 3 | 0 | -2 | 4 | 6 | 6 | 5 | -2 | -3 |
| 17 | -3 | -6 | -6 | -4 | 0 | 0 | 0 | 1 | 0 | 2 | 5 | 5 | 6 | 7 | 7 | 8 | 5 | 2 | 0 | -1 | 0 | 0 | -2 | -5 |
| 18 | -4 | -5 | -5 | -4 | -3 | -2 | -2 | -3 | 2 | 5 | 6 | 6 | 5 | 5 | 5 | 4 | 5 | 9 | 12 | 14 | 13 | 12 | 12 | 16 |
| 19 | 21 | 23 | 18 | 11 | 5 | 0 | 1 | -1 | -9 | -12 | -14 | -12 | -12 | -16 | -16 | -23 | -33 | -45 | -50 | -47 | -58 | -55 | -49 | -48 |
| 20 | -54 | -56 | -45 | -32 | -38 | -43 | -20 | -7 | -48 | -61 | -50 | -46 | -44 | -47 | -49 | -48 | -46 | -49 | -50 | -55 | -63 | -90 | -114 | -123 |
| 21 | -126 | -117 | -104 | -107 | -128 | -146 | -158 | -156 | -133 | -119 | -113 | -103 | -97 | -98 | -105 | -112 | -106 | -97 | -96 | -94 | -86 | -78 | -77 | -72 |
| 22 | -70 | -59 | -54 | -46 | -47 | -48 | -46 | -44 | -47 | -54 | -50 | -47 | -50 | -51 | -49 | -48 | -47 | -42 | -35 | -31 | -29 | -29 | -30 | -33 |
| 23 | -34 | -33 | -36 | -35 | -35 | -33 | -33 | -31 | -32 | -34 | -31 | -27 | -26 | -25 | -30 | -30 | -35 | -42 | -39 | -36 | -31 | -29 | -29 | -29 |
| 24 | -30 | -32 | -29 | -28 | -27 | -31 | -43 | -48 | -45 | -40 | -39 | -39 | -42 | -40 | -38 | -35 | -34 | -31 | -28 | -27 | -27 | -26 | -26 | -23 |
| 25 | -24 | -20 | -22 | -29 | -25 | -22 | -23 | -27 | -27 | -24 | -25 | -30 | -37 | -38 | -36 | -32 | -31 | -33 | -35 | -33 | -30 | -29 | -29 | -28 |
| 26 | -30 | -32 | -15 | -23 | -19 | -19 | -22 | -26 | -33 | -37 | -23 | -11 | -5 | -5 | -12 | -22 | -19 | -22 | -26 | -18 | -20 | -37 | -35 | -36 |
| 27 | -35 | -31 | -32 | -42 | -50 | -54 | -51 | -46 | -45 | -48 | -35 | -38 | -48 | -44 | -45 | -41 | -37 | -35 | -35 | -36 | -42 | -41 | -28 | -34 |
| 28 | -30 | -49 | -60 | -68 | -64 | -57 | -68 | -86 | -95 | -95 | -99 | -89 | -76 | -78 | -78 | -72 | -67 | -64 | -61 | -63 | -57 | -51 | -45 | -41 |
| 29 | -46 | -47 | -45 | -45 | -63 | -65 | -53 | -48 | -45 | -47 | -44 | -41 | -39 | -44 | -48 | -43 | -43 | -43 | -39 | -38 | -37 | -34 | -29 | -27 |
| 30 | -27 | -24 | -24 | -23 | -19 | -15 | -14 | -11 | -13 | 4 | 19 | 30 | 5 | -59 | -68 | -64 | -55 | -64 | -63 | -65 | -53 | -59 | -57 | -53 |

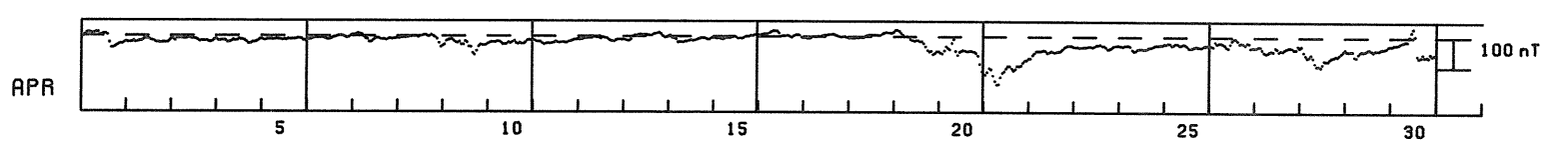


XX

REFERENCES


| | | |
|---|---|---|
| COFFEY, HELEN E., Editor | 1984 | Solar-Geophysical Data, I, No. 478, U. S. Department of Commerce (Boulder, Colorado, 80303) 116-117. |
| COFFEY, HELEN E., Editor | 1986 | Solar-Geophysical Data, II, No. 505, U. S. Department of Commerce (Boulder, Colorado, 80303) 46-49. |
| COUZENS, D. A. and J. H. KING | 1986 | Interplanetary medium data book - Supplement 3A, 1977-1985, NSSDC 86-05a, NASA, Washington, D. C. |
| EVENSON, P., R. KROEGER, and P. MEYER | 1985 | Further observations of protons resulting from the decay of neutrons ejected by solar flares, 19th International Cosmic Ray Conference, Conference Papers, 4, 130, NASA CP-2376. |
| GUSSENHOVEN, M. S., E. G. MULLEN, R. C. FILZ, D. H. BRAUTIGAM, and F. A. HANSER | 1987 | New low-altitude dose measurements, IEEE Trans. Nuclear Sci., NS-34, 676. |
| McKINNON, J. A. | 1987 | Sunspot Numbers: 1610-1985, UAG-95, U. S. Department of Commerce (Boulder, Colorado, 80303). |
| SHEA, M. A., D. F. SMART, and E. O. FLÜCKIGER | 1987 | Possible neutron monitor response to solar neutrons in April 1984, 20th International Cosmic Ray Conference, Conference Papers, (in press). |
| SHEA, M. A., D. F. SMART, and L. C. GENTILE | 1983 | Vertical cutoff rigidities for selected cosmic ray stations for Epoch 1980.0, 18th International Cosmic Ray Conference, Conference Papers, 3, 411. |

# Summary of the Solar Optical Observations of the Active Regions Which Produced the Solar-Terrestrial Events of 16 February and 24 April 1984

by

Helen Coffey
World Data Center A for Solar-Terrestrial Physics
NOAA/NESDIS/NGDC E/GC2
325 Broadway
Boulder, Colorado 80303 U.S.A.

## ABSTRACT

Because the 16 February 1984 Ground Level Event (GLE) is thought to be caused by a solar flare event that occurred behind the West limb of the Sun, there are no direct solar optical observations of a responsible solar flare. We present some summary data derived from **Solar-Geophysical Data** (SGD) to indicate the state of the Sun's activity just prior to the GLE. A summary of the contributed papers on the 24-25 April 1984 solar optical event is given.

## 16 February 1984 Event

On 16 February 1984 the optical solar disk showed no flare activity when suddenly ground-based solar radio monitors recorded fixed frequency bursts beginning at 0858 UT, peaking at 0900 UT at 6000 solar flux units on frequencies around 100-200 MHz. Type II and IV solar radio spectral events lasted from 0858.3-1002 UT. For a discussion on the geometry of the event and the apparent occultation of the radio event by the solar disk, see Chertok et al. in the Solar Radio section of this UAG Report. A satellite proton event at Earth began around 0906 UT, with a maximum flux around 1005 UT of about 700 particles/cm$^2$-s-ster in the greater than 10 Mev channel. The Venera satellite located off the West limb of the Sun also recorded a strong proton event (see Chuchkov et al. in the Satellite section of this UAG Report).

Because no optical solar events occurred, we surmise that a flare occurred in AR4408 which rotated off the visible solar disk early on 13 February. AR4410 rotated off the visible disk late on 15 February. AR4413 was still visible on the solar disk and was relatively quiet by 16 February. Table 1 gives the flaring activity for 1-18 February.

Table 1. Number of Observed Solar Flares During the 1-18 February 1984 Period

| Date Feb 84 | Sunspot Number | Total Number of Flares | AR4408 Number of Subflares/Flares | | AR4413 Number of Subflares/Flares | | AR4410 Number of Subflares/Flares | |
|---|---|---|---|---|---|---|---|---|
| | Note: AR4408 first appeared on the disk on 31 January at S12 E82. | | | | | | | |
| 1 | 110 | 24 | | | | | | |
| 2 | 82 | 19 | | | | | | |
| 3 | 67 | 12 | | | | | | |
| 4 | 61 | 5 | | | | | | |
| 5 | 66 | 3 | | | | | 2 | |
| 6 | 76 | 13 | 1 | | 4 | | 4 | 2(1F,1B) |
| 7 | 79 | 16 | 2 | | 7 | | 5 | |
| 8 | 94 | 22 | 2 | | 11 | 1(1N) | 4 | 1(1B) |
| 9 | 115 | 23 | 6 | | 12 | | 4 | |
| 10 | 123 | 24 | 7 | 1(2B) | 11 | | 3 | |
| 11 | 118 | 29 | 9 | | 16 | 1(1B) | 3 | |
| 12 | 108 | 17 | 4 | | 9 | 1(1B) | 1 | |
| 13 | 82 | 10 | 1 | | 7 | | 1 | |
| 14 | 77 | 5 | | | 2 | | 2 | |
| 15 | 80 | 5 | | | 4 | | 1 | |
| 16 | 53 | 4 | | | 3 | 1(1N) | | |
| 17 | 51 | 10 | | | 4 | | | |
| 18 | 50 | 17 | | | 1 | | | |
| | | | -- | - | -- | - | -- | - |
| | | Total: | 32 | 1 | 91 | 4 | 30 | 3 |

The Active Regions 4413 and 4408 both had magnetically complex delta sunspot configurations. AR4413 was 3 times more active than AR4408. AR4410 had the less complex beta configuration, though it produced as many flares as AR4408. However, AR4408 showed stronger X-ray flaring activity (Patrick McIntosh, private communication). Figure 1 shows a time lapse of the 3 regions as they crossed the disk.

The 16 February flare occurred in either AR4410 or AR4408, with AR4408 more likely because of its complexity. AR4408 returned on 28 February as AR4427, a relative quiet group. It produced 11 subflares and two 1B flares before disappearing on 6 March. AR4413 returned on 3 March as AR4429. It produced 13 subflares and two 1N flares, then stopped flaring 5 days before it rotated off the disk again. And AR4410 apparently died out, though a new group AR4430 developed in its longitude on 4 March at E57.

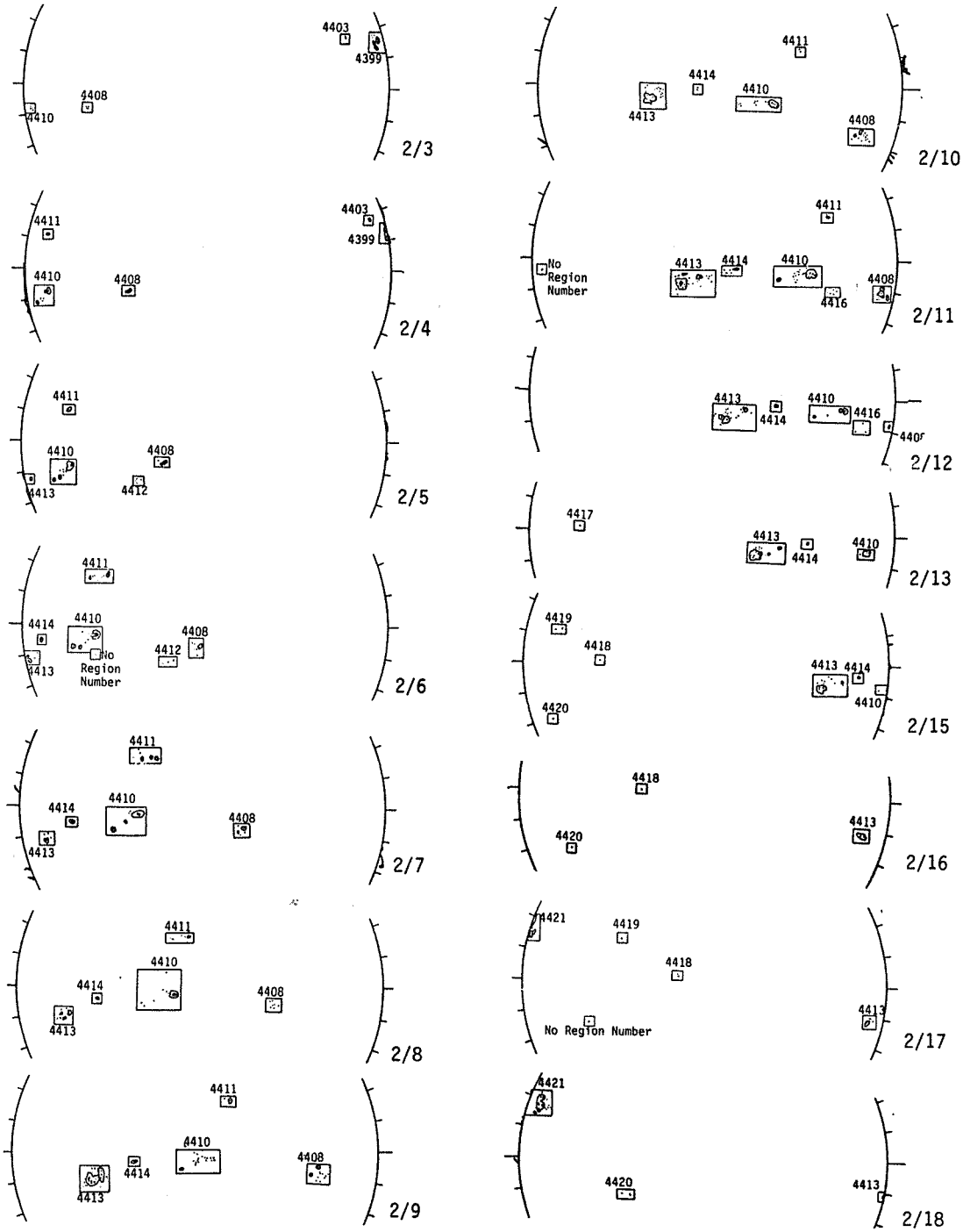


Fig. 1. Active Regions 4408, 4410 and 4413 as they transited the solar disk during the period 3 -18 February 1984.

Note that AR4421, which was about 180 degrees behind the AR4408 and AR4413 conglomerate, produced a 1N/X2.3 event on 17 February at 2226 UT when it was first seen at N17 E81. This caused a satellite proton event beginning on 19 February, slowly rising to a maximum on 21 February. AR4421 produced 96 subflares and 14 greater than or equal to 1F flares during its disk passage. Excellent photographs of AR4421 appear in the paper by Hill.

## 20 April - 4 May 1984 Period

The largest solar flare since December 1982 occurred on 24 April 1984 at 2356 UT. This X13/3B flare originated in Active Region 4474 at S11 E45, producing significant solar radio bursts and a Type IV event (SGD, 1984a, 1985).

Hiei et al. present the Tokyo Astronomical Observatory observations on the white light flare, correlating the white light brightenings with their observed H-alpha strands and the hard X-ray flux data from the SMM satellite. They analyze the motions within the flaring region.

Wells presents USAF Solar Observing Optical Network (SOON) site images of the flaring region on 24-25 April 1984, along with the Radio Solar Telescope Network (RSTN) solar radio burst graphs. The RSTN data have detailed 1 second data for 2358 UT 24 April - 0013 UT 25 April 1984 at eight frequencies: 245, 410, 610, 1415, 2695, 4995, 8800 and 15400 MHz. Also graphed are 20 second averaged data for 1330 UT 24 April - 0400 UT 25 April. Wells summarizes SGD information for the flares and sunspot region for the period 21 April - 5 May 1984. He discusses the events occurring in Active Region 4474 while crossing the Sun's disk, gives detailed information on the solar optical observations of the 3B flare on 24-25 April 1984 and summarizes the solar radio observations 2330 UT 24 April - 0400 UT 25 April 1984.

Balster and Atanasijevic present white light and H-alpha photographs from Nijmegen, The Netherlands, showing the development of Active Region 4474 23 April - 2 May 1984. Detailed H-alpha filtergrams 25-27 April show the change in the structure between 25 and 26 April. Sunspot drawings are also included.

Hill presents some excellent photos taken by amateur observers which show the development of some of the active regions on the Sun during the periods 21-28 February and 25-29 April 1984.

# A White-Light Flare of 24-25 April 1984

by

Eijiro Hiei, Tadashi Natori,
Masahide Miyazawa, Kisuke Yamaguchi, and Makoto Irie
Tokyo Astronomical Observatory, Mitaka, Tokyo 181, Japan

## ABSTRACT

White light brightenings appeared at 4 minutes after the start time of the H-alpha flare of 24-25 April 1984. The time correlation between the white light brightenings and the hard X-ray flux is good. The bright patches moved in the same direction as the movement of the H-alpha strands of the flare.

## Introduction

The white light flare was observed at the Tokyo Astronomical Observatory, the Big Bear Solar Observatory, the Radio Observatories at Nobeyama and Toyokawa, and HXRBS/XRP on board SMM. The start time of the flare in H-alpha was 2356:30 UT on 24 April 1984 and its maximum phase was 2359 UT on 24 April. The flare was very active and classified as 3B and X13. At the Tokyo Astronomical Observatory the sunspot was photographed with a 10 cm telescope from 2303:38 UT on 24 April, during the white light brightening, until 0058:44 UT on 25 April. A total of 19 frames were taken with a Y-filter at an exposure time of 1/200 seconds. The Fuji process sheet film was used and the pictures were photographed with an effective wavelength of 5050A. The H-alpha observation of the flare was made with a 14 cm flare patrol (SECASI) and recorded on the 35 mm film and video tape.

The time change of the brightness of the white light flare and its relation to the hard X-ray flux are discussed here.

## Time Change of the White Light Brightening

There appeared four bright regions as seen in Figure 1. Bright patches A and B were in the north polarity region of the magnetic field, and patches C and D in the south polarity region (see Figure 2 also). The patches A, B and C were above umbra/penumbra, while the patch D appeared on the photosphere near the sunspot and was quite diffuse. The patch D might be the same phenomenon as the white light wave reported by Machado and Rust (1974).

The intensity and position of these bright patches rapidly changed with time. The patches moved continuously with decreasing intensity and then jumped to a slightly different position. This suggests that the energy deposition to the bright patches was made during a short time, and then another energy deposition occurred at a different position. The direction of the movement of the bright patches was the same as that of the two ribbon strands of the H-alpha flare, which suggests that there is a relationship between H-alpha and white light brightenings.

The time profile of the brightness for each bright patch is shown in Figure 2. The hard X-ray flux at 500 keV of HXRBS data (Dennis, 1985) is also shown in Figure 3. It is noted here that the peak brightness of the patches appears almost simultaneously with the spiky peaks of the hard X-ray flux. Figure 4 shows the correlation between the hard X-ray flux and the brightness of the patches. The peak in hard X-ray flux and the maximum brightness of the patches appeared almost simultaneously as shown in Figure 4, but the time progress is different, that is, the brightness of the patches is stronger at the later phase than at the earlier one, even though the flux of hard X-ray is weaker. The energy deposition to the bright patches seems to be more efficient at a later phase.

The duration of the white light brightening is one minute or less, which suggests that the energy release would be made during less than one minute at the original location of the flare energy.

The magnetic field of the flaring region on 24 April 1984 (Hagyard, 1985) shows that the azimuth of the transverse component of the magnetic field is almost parallel to the neutral line, which suggests that the magnetic field at the location of the white light brightening was quite sheared, but we do not know how the sheared field changed during the flare.

The penumbra at the northwest edge of the sunspot group disappeared in an hour after the occurrence of the flare. The disappearance of the penumbra after the white-light flare was also observed in the events of 10 September 1974 (Tanaka, 1978; and Hiei, 1982) and 15 December 1982 (Hiei, 1985).

The energy deposited to the bright patch B and to all patches are estimated as shown in Table 1. Here we estimate it from the increased intensity under the assumption that the energy spectrum of the white light flare is effectively flat for a 3000A bandwidth.

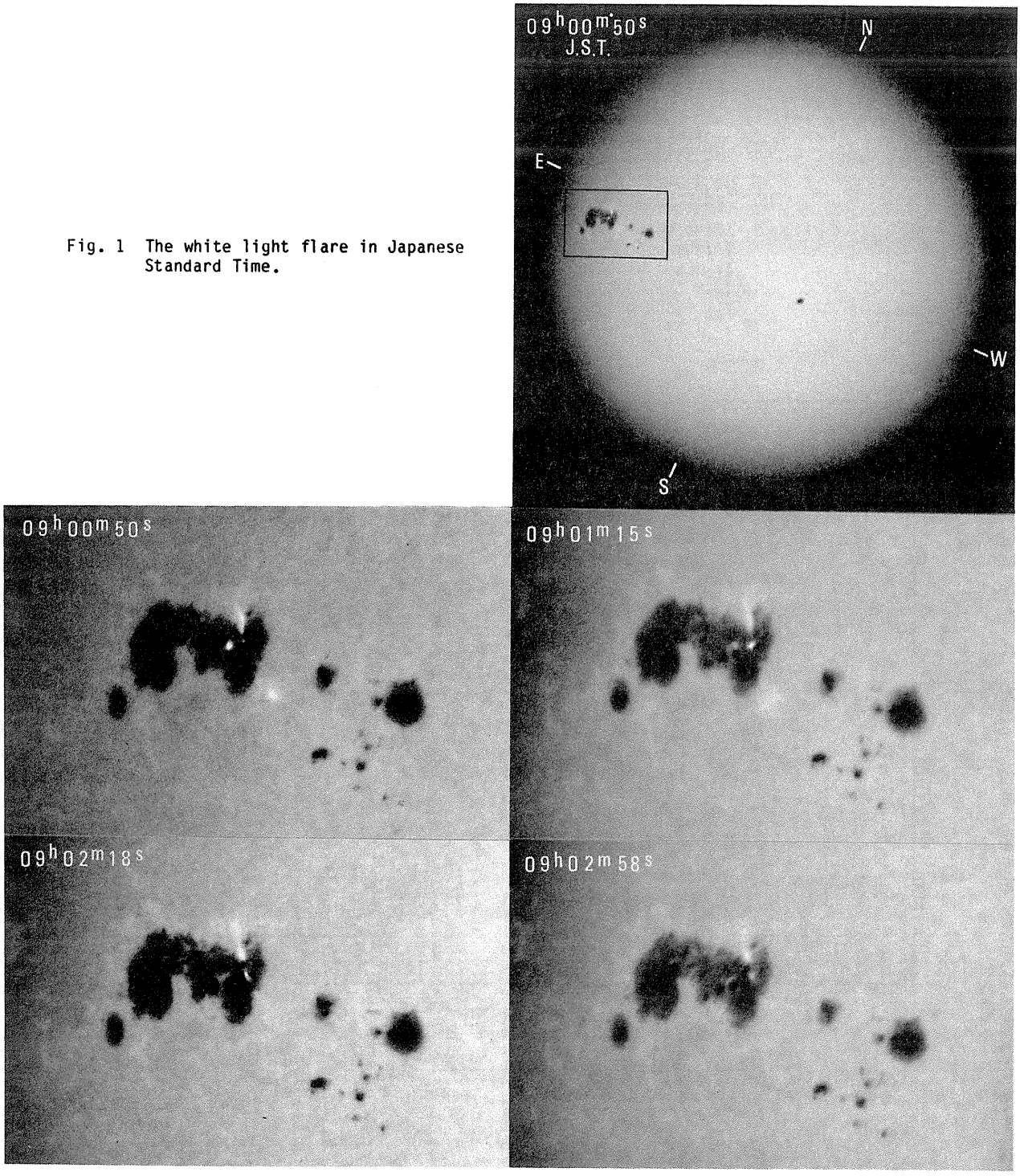


Fig. 1 The white light flare in Japanese Standard Time.

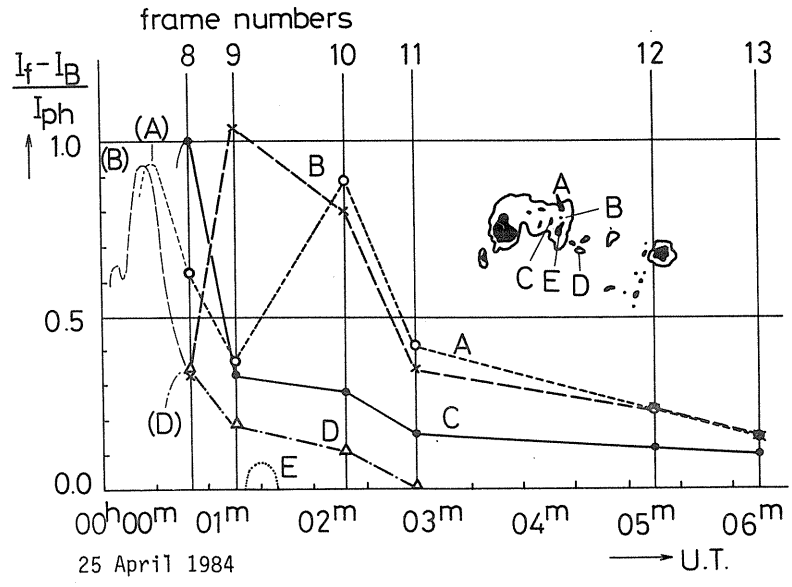


Fig. 2 Light curve of the white light flare for the individual bright patches of A, B, C, and D.
$I_f$ = the brightness of the bright patch;
$I_B$ = the background brightness before the flare; and
$I_{ph}$ = the brightness of the photosphere near the flare.

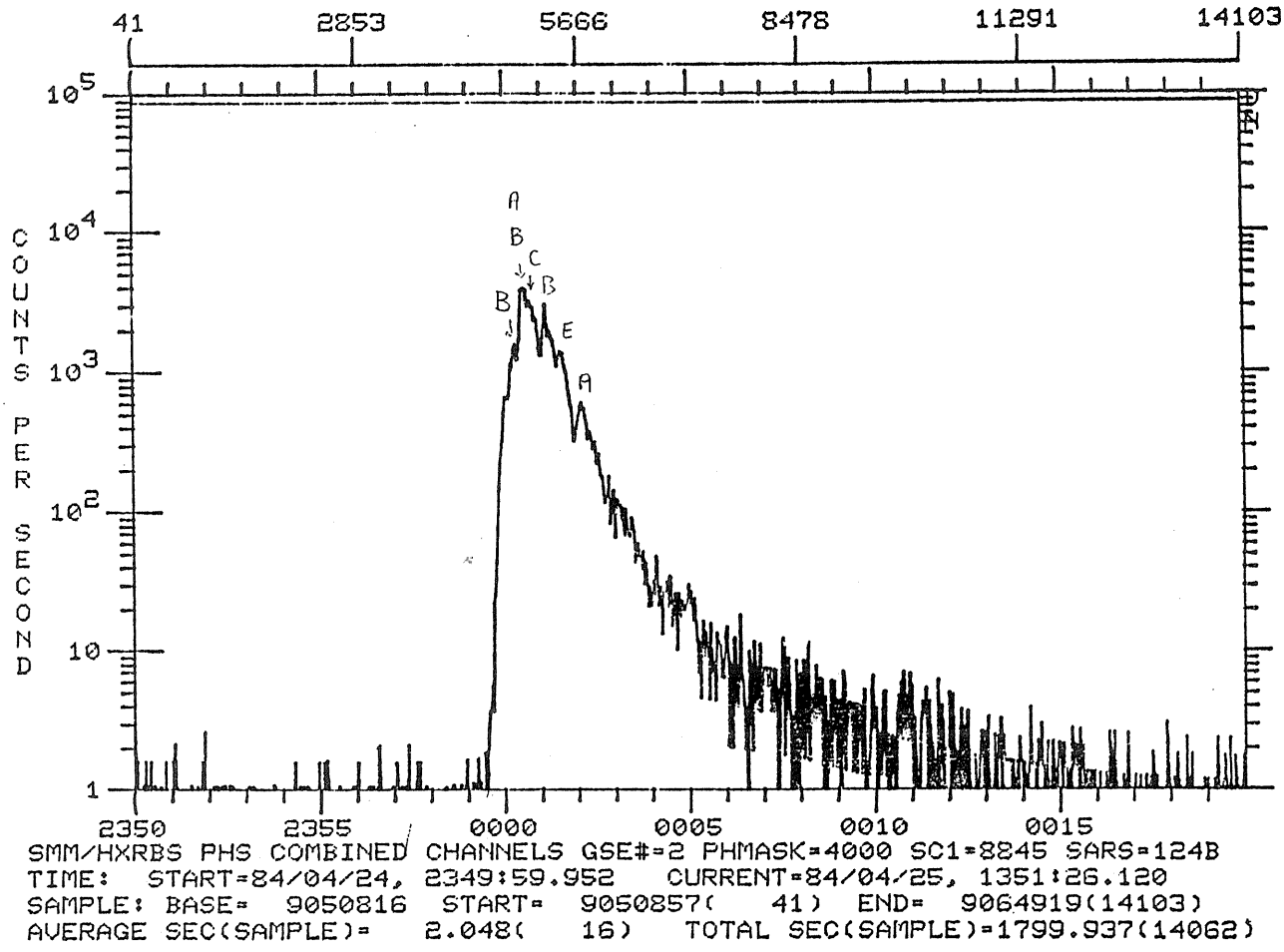


Fig. 3 Time profile of the hard X-ray flux (HXRBS) at 500 keV.

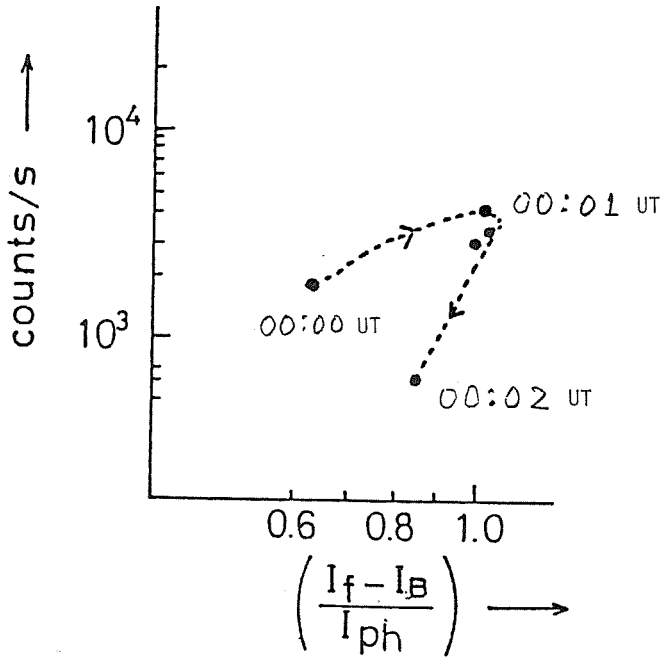


Fig. 4. Correlation between the hard X-ray and the increased intensity of the white light flare. The arrow shows the progress with time.

The opacity of the white light brightening can be estimated if a bright region appears over an umbra and a penumbra, and its source function above the umbra and penumbra is the same. The observed brightness distribution above the umbra and penumbra would be similar to those underneath if its optical depth is thin. It is flat if the optical depth is thick. The brightness distribution of the bright patch B is shown in Figure 5. If we assume that the source function of the bright patch above the umbra and penumbra is the same at these two consecutive times, the bright region would be optically thick. The radiation temperature, then, would be inferred from its brightness, which is about 6800K. At this temperature both the contribution from free-bound and $H^-$ emission is about the same as at 3600A, but $H^-$ is dominating the visible region if the bright region is assumed in LTE.

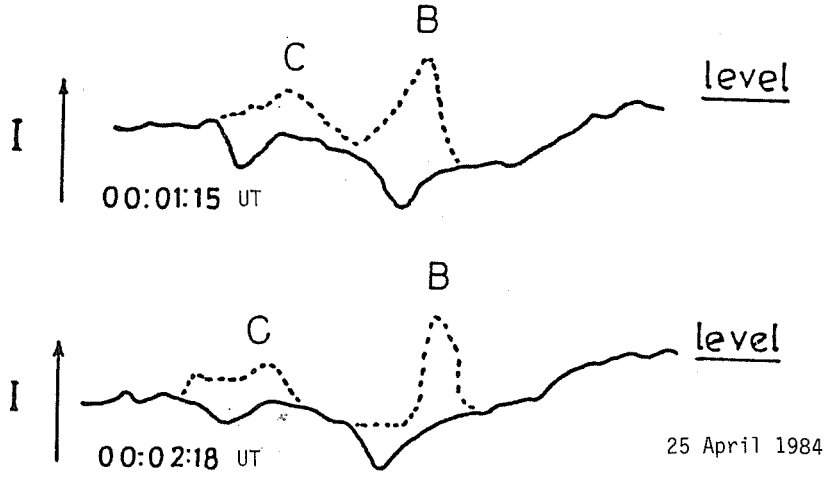


Fig. 5. Microphotometer tracings: The thick line shows the background umbra and penumbra. The dotted line shows the white light flare of patches B and C. The photospheric intensity near the flare is shown as "level".

A flare wave travelled from the flare as shown in Figures 6 and 7. The velocity is 1300 km/s at its earlier phase and 660 km/s at the later one. In order to estimate the onset time of the flare wave, the travelling curve was extrapolated to the onset point of the white light brightening. Then the onset time is inferred to be at 2358:40±20s. The peaks of hard X-ray flux (HXRBS) at 40 keV occurred at 2358 UT and 0000 UT and the inferred onset time of the flare wave was at the increasing phase of the X-ray flux. If the onset time was assumed at the peaks of the hard X-ray flux, then the onset point of the flare wave should be considered at $10^5$ km north or south from the onset point of the H-alpha flare, which seems improbable. If the velocity of the travelling wave is assumed to be as rapid as, say, 4000 km/s, it would be probable for the flare wave to start from 0000 UT at the onset point of the H-alpha flare.

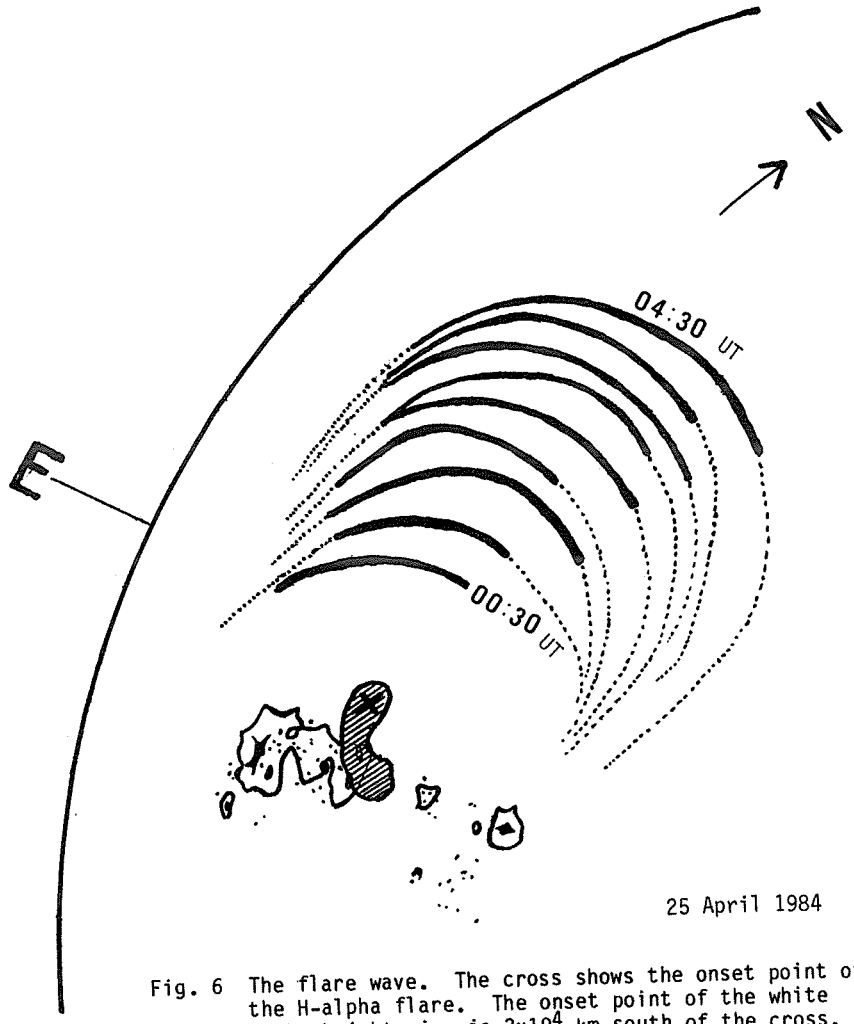


Fig. 6 The flare wave. The cross shows the onset point of the H-alpha flare. The onset point of the white light brightening is $3 \times 10^4$ km south of the cross.

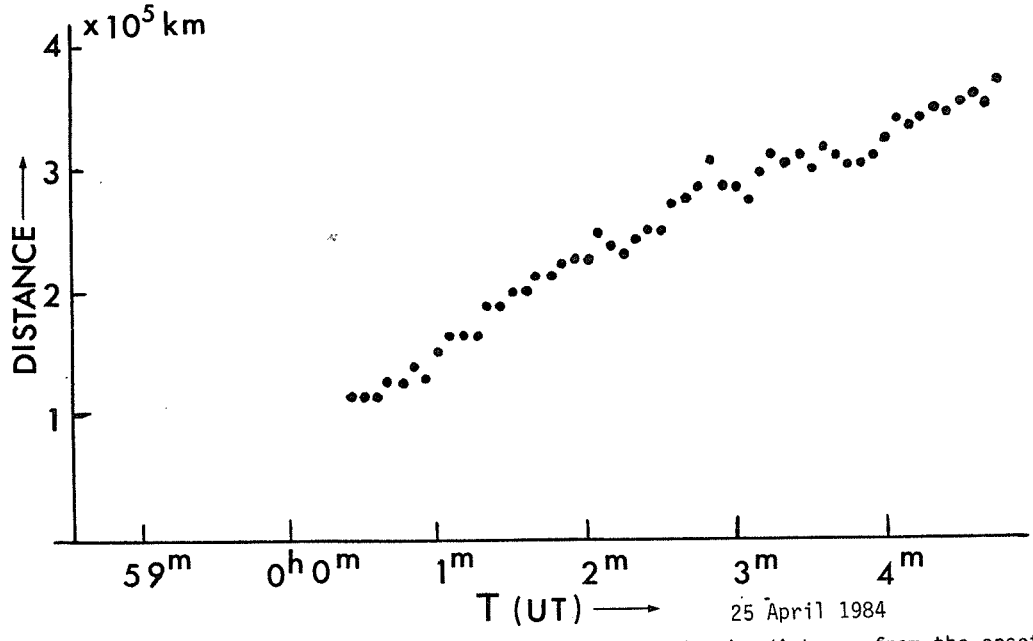


Fig. 7 The movement of the flare wave. The y-axis is the distance from the onset point of the H-alpha flare.

TABLE 1. Energy Deposition

| Event | erg/s-cm-ster-A | erg/s | erg |
|---|---|---|---|
| 10 September 1974 | $8 \times 10^{9}$ | $10^{27}$ | $7 \times 10^{29}$ |
| 15 December 1982 | $3.5 \times 10^{10}$ | $3.5 \times 10^{26}$ | $6 \times 10^{28}$ |
| 25 April 1984 (Patch B) | $1.2 \times 10^{11}$ | $4 \times 10^{27}$ | $6 \times 10^{29}$ |
| 25 April 1984 (Total) | | | $10^{31}$ |

**Acknowledgements**

The authors wish to thank Dr. B.R. Dennis for the HXRBS data and Dr. Hagyard for the map of the magnetic field.

## REFERENCES

DENNIS, B.R. 1985 Private communication.

HAGYARD, M.J. 1985 Private communication.

HIEI, E. 1982 **Solar Physics, 80, 113.**

HIEI, E. 1985 In preparation.

MACHADO, M.E. and D. RUST 1974 **Solar Physics, 38, 499.**

TANAKA, K. 1978 **Solar Physics, 58, 149.**

# Real-Time Solar Optical and Radio Observations of the 24-25 April 1984 Solar Flare From the U.S. Air Force Air Weather Service Solar Observatories

by

Gary D. Wells, Captain, USAF
HQ AFELM NOAA/OL NOA1
325 Broadway
Boulder, Colorado 80303 U.S.A.

## Introduction

The US Air Force's Air Weather Service operates the only worldwide network of fully automated instruments to routinely monitor the sun's activity at optical, radio, and other selected wavelengths. The optical network, i.e., the Solar Observing Optical Network (SOON), consists of solar telescopes at Holloman AFB, NM; Palehua, HI; Learmonth, Australia; and Ramey, Puerto Rico. Manual telescopes are supported at Athens, Greece and Manila, Philippines. The radio network, designated as the Radio Solar Telescope Network (RSTN), operate dish-shaped antennae at Sagamore Hill, MA; Palehua, HI; and Learmonth, Australia. Site preparations are underway at San Vito, Italy, for another SOON and RSTN system. Data from these systems are archived at the National Geophysical Data Center, Solar-Terrestrial Physics Division, NOAA E/GC2, Boulder, Colorado 80303 U.S.A.

On 24 and 25 April 1984, these systems recorded one of the largest flares in the last six years as determined by the peak 1-8 A X-ray emission. The flare occurred in Region 4474 at S12 E43. The peak of the H-alpha flare as observed by Holloman was 3B at 0001 UT on 25 April. This paper presents the optical observations recorded at Holloman, the fixed frequency radio burst observations from Learmonth, and comments from the observer at Holloman concerning activity in Region 4474 immediately preceding and during the flare. A brief summary of the equipment and activity for Region 4474 will also be presented.

## Equipment

The SOON system was designed by Dr. Richard Dunn of the Sacramento Peak Solar Observatory. This network provides objective, automated flare reporting by combining a 10 inch refractor, a Hewlett Packard (HP) 2100A or HP21MXE computer, a Xerox MD51 analog-to-digital converter, and a videometer. The videometer electronically samples specified areas of the solar disk, computes brightness levels for each of a maximum of 125,000 pixels for each region, and determines the areal extent for each of 64 brightness levels. The computer compares this image to previous images to determine whether a flare is in progress and if so, its magnitude. The birefringent filter can be tuned to H-alpha (6563A) or B2 (5172A) and can be tuned 1.0 A off center. The telescope resolution is 3/4 arc sec. The system also produces solar magnetograms, tachograms, and 35-mm film patrol (Air Weather Service Pamphlet (AWSP) 105-60).

The RSTN system consists of a 3 ft, an 8 ft, and a 28 ft dish, as well as a swept frequency interferometer. This system monitors eight discrete frequencies (245, 410, 610, 1415, 2695, 4995, 8800, and 15,400 MHz) and sweep frequencies from 25 to 75 MHz. The half power beamwidths for each frequency from 245 to 15,400 MHz are 10.09, 6.0, 4.068, 6.115, 3.187, 1.72, 0.976, and 1.49 respectively. The RSTN system also provides automated patrol of the sun using an HP computer, a Dicke-switched radiometer, and a Phoenix Model 8000 analog to digital converter with a 132 dB dynamic range. These digitally recorded data have a temporal resolution of one second (AWSP 105-61).

## Event Summary for Region 4474

Region 4474 (Mt. Wilson Region 24029/24030) rotated onto the solar disk on 21 April 1984 (SGD, Jun 84). This was the region's second transit of the disk. It was previously Region 4455 (Mt. Wilson Region 24008) (SGD, May and Jun 84). While still on the east limb, Region 4474 was given a beta magnetic classification and a DSO spot classification by Holloman. However, by 23 April, Holloman classified it as a beta-gamma-delta, FKC group with an area of 2600 millionths of the solar hemisphere and 42 spots. The region exited the disk on 5 May (SGD, May 84); but during its passage, it accounted for 178 optical flares of size subflare or greater and 101 X-ray bursts of class C or greater (See Table 1). This was an increase of 96% in optical flares and 237% in X-ray bursts from its previous rotation. The 24th of April was the most active day for this region in terms of flare events and the 27th was the most active in terms of total X-ray bursts. However, the largest number of X level X-ray bursts occurred on the 24th (SGD, May 84). Holloman reported a maximum area of 2980 millionths of the solar hemisphere for the spot group on 24 April and a maximum of 99 spots on 28 April (SGD,Jun 84). See Tables 2-5 for a comparison of the sunspot region history among the four SOON sites.

Table 1. Summary of Activity for Region 4474
(from SGD Part I, Apr and May issues)

| 1984 Mo. | Day | X-RAYS C | M | X | FLARES 0 | 1 | 2 | 3 | 4 |
|---|---|---|---|---|---|---|---|---|---|
| 04 | 21 | 4 | 4 | 1 | 8 | 0 | 0 | 0 | 0 |
| 04 | 22 | 4 | 2 | 0 | 16 | 1 | 1 | 0 | 0 |
| 04 | 23 | 4 | 4 | 0 | 14 | 6 | 1 | 0 | 0 |
| 04 | 24 | 4 | 2 | 2 | 17 | 3 | 1 | 1 | 0 |
| 04 | 25 | 6 | 1 | 0 | 8 | 1 | 0 | 0 | 0 |
| 04 | 26 | 5 | 4 | 0 | 9 | 3 | 2 | 0 | 0 |
| 04 | 27 | 6 | 4 | 0 | 10 | 2 | 0 | 0 | 0 |
| 04 | 28 | 7 | 0 | 0 | 11 | 0 | 1 | 0 | 0 |
| 04 | 29 | 7 | 2 | 0 | 19 | 3 | 0 | 0 | 0 |
| 04 | 30 | 6 | 3 | 0 | 7 | 0 | 0 | 0 | 0 |
| 05 | 01 | 5 | 1 | 0 | 11 | 0 | 1 | 0 | 0 |
| 05 | 02 | 5 | 1 | 0 | 11 | 1 | 0 | 0 | 0 |
| 05 | 03 | 4 | 0 | 0 | 5 | 2 | 0 | 0 | 0 |
| 05 | 04 | 1 | 1 | 0 | 0 | 0 | 0 | 0 | 0 |
| 05 | 05 | 0 | 1 | 0 | 2 | 0 | 0 | 0 | 0 |
| | | 68 | 30 | 3 | 148 | 22 | 7 | 1 | 0 |

Total H-alpha flares = 178
Total X-ray flares = 101

| Totals from previous rotation (region 4455) | | | | | | | | | |
|---|---|---|---|---|---|---|---|---|---|
| | 25 | 5 | 0 | 87 | 4 | 0 | 0 | 0 |

Total H-alpha flares = 91
Total X-ray flares = 30

Table 2. Palehua Sunspot Region 4474 Summary

| 1984 Mo. | Day | Time (UT) | Magnetic Class | Spot Class | Corrected Area (10-6 hemi) | Spot Count | Long. Extent (deg) |
|---|---|---|---|---|---|---|---|
| 04 | 21 | --- | --- | --- | --- | --- | --- |
| 04 | 22 | --- | --- | --- | --- | --- | --- |
| 04 | 23 | --- | --- | --- | --- | --- | --- |
| 04 | 24 | --- | --- | --- | --- | --- | --- |
| 04 | 25 | --- | --- | --- | --- | --- | --- |
| 04 | 26 | 1740 | BGD | FKC | 2870 | 88 | 28 |
| 04 | 27 | 1905 | BGD | FKI | 2360 | 94 | 27 |
| 04 | 28 | 1720 | BGD | FKI | 2400 | 95 | 28 |
| 04 | 29 | 1742 | BGD | FKI | 2080 | 83 | 27 |
| 04 | 30 | --- | --- | --- | --- | --- | --- |
| 05 | 01 | 1835 | BGD | FKI | 1800 | 45 | 27 |
| 05 | 02 | 1900 | BGD | FKI | 1510 | 39 | 26 |
| 05 | 03 | --- | --- | --- | --- | --- | --- |
| 05 | 04 | 1659 | BG | FKO | 440 | 11 | 18 |

Table 3. Holloman Sunspot Region 4474 Summary

| 1984 Mo. | Day | Time (UT) | Magnetic Class | Spot Class | Corrected Area (10-6 hemi) | Spot Count | Long. Extent (deg) |
|---|---|---|---|---|---|---|---|
| 04 | 21 | 1429 | B | DSO | 130 | 3 | 5 |
| 04 | 22 | 1419 | BD | FKO | 1060 | 12 | 22 |
| 04 | 23 | 1522 | BGD | FKC | 2600 | 42 | 26 |
| 04 | 24 | 1507 | BGD | FKC | 2980 | 60 | 29 |
| 04 | 25 | 1434 | BGD | FKI | 2180 | 74 | 26 |
| 04 | 26 | 1428 | BGD | FKC | 2720 | 51 | 29 |
| 04 | 27 | 1517 | BGD | FKI | 2270 | 67 | 27 |
| 04 | 28 | 1324 | BGD | FKI | 2530 | 99 | 27 |
| 04 | 29 | 1537 | BGD | FKI | 2130 | 83 | 29 |
| 04 | 30 | --- | --- | --- | --- | --- | --- |
| 05 | 01 | 1530 | BGD | FKI | 2100 | 48 | 26 |
| 05 | 02 | 1429 | BGD | FKI | 1880 | 62 | 27 |
| 05 | 03 | 1414 | BGD | FKI | 1390 | 29 | 26 |
| 05 | 04 | 1415 | BG | FKO | 610 | 10 | 20 |

Table 4. Learmonth Sunspot Region 4474 Summary

| 1984 Mo. | Day | Time (UT) | Magnetic Class | Spot Class | Corrected Area (10-6 hemi) | Spot Count | Long. Extent (deg) |
|---|---|---|---|---|---|---|---|
| 04 | 21 | --- | --- | --- | --- | --- | --- |
| 04 | 22 | 0059 | B | EHO | 490 | 8 | 12 |
| 04 | 23 | 0045 | B | FKI | 1500 | 25 | 24 |
| 04 | 24 | 0130 | BGD | FKI | 2120 | 39 | 25 |
| 04 | 25 | 0145 | BGD | FKI | 2080 | 60 | 27 |
| 04 | 26 | 0113 | BGD | FKI | 2230 | 51 | 27 |
| 04 | 27 | 0017 | BGD | FKI | 4460 | 75 | 28 |
| 04 | 28 | 0325 | BGD | FKI | 2370 | 85 | 28 |
| 04 | 29 | 0327 | BGD | FKI | 3210 | 67 | 29 |
| 04 | 30 | --- | --- | --- | --- | --- | --- |
| 05 | 01 | 0203 | BGD | FKI | 1960 | 43 | 25 |
| 05 | 02 | 0215 | BGD | FKI | 1060 | 34 | 28 |
| 05 | 03 | 0025 | BGD | FKI | 680 | 28 | 25 |
| 05 | 04 | 0044 | BGD | FKI | 510 | 16 | 18 |

Table 5. Ramey Sunspot Region 4474 Summary

| 1984 Mo. | Day | Time (UT) | Magnetic Class | Spot Class | Corrected Area (10-6 hemi) | Spot Count | Long. Extent (deg) |
|---|---|---|---|---|---|---|---|
| 04 | 21 | 1339 | B | CAO | 160 | 6 | 6 |
| 04 | 22 | 1140 | BG | FKO | 1130 | 18 | 24 |
| 04 | 23 | 1255 | BG | FKO | 1350 | 20 | 25 |
| 04 | 24 | 1125 | BGD | FKO | 2110 | 42 | 29 |
| 04 | 25 | 1235 | BGD | FKO | 2060 | 82 | 32 |
| 04 | 26 | 1235 | BGD | FKI | 2840 | 99 | 27 |
| 04 | 27 | --- | --- | --- | --- | --- | --- |
| 04 | 28 | 1425 | BGD | FKI | 2440 | 94 | 27 |
| 04 | 29 | 1230 | BGD | FKI | 2280 | 99 | 30 |
| 04 | 30 | --- | --- | --- | --- | --- | --- |
| 05 | 01 | 1422 | BGD | FKI | 2330 | 68 | 28 |
| 05 | 02 | 1249 | BGD | FKI | 1690 | 60 | 30 |
| 05 | 03 | 1230 | BGD | FKO | 1280 | 27 | 28 |
| 05 | 04 | 1245 | BGD | FKO | 630 | 13 | 18 |

## Optical Observations of the 3B Flare on 24-25 April 1984

Prior to the 3B flare which began near 2356 UT on 24 April (Figure 1), the solar analyst at Holloman reported nearly continuous flares and flare intensity fluctuations occurring primarily in the middle and eastern portions of Region 4474. An active dark filament system was reported throughout the middle of the region, and dark surging was in progress in the eastern portion of the region. Kinks in the inversion line and magnetic shear were present over the locale of previous flares. The flare began at 2356 UT over the delta configuration in the middle of the region, as normal intensity point brightenings on either side of the active inversion line. These point brightenings were less than 20 millionths of the solar disk in area. The region reached sub-brilliant by 2356 UT and 1B by 2358 UT with an uncorrected area of 185 millionths (216 millionths corrected) (Figure 2). By 25 April at 0000 UT, the flare reached 2B with an uncorrected area of 493 millionths (577 millionths corrected) (Figures 3 and 4), and by 0001 UT the flare was upgraded to a 3B with an uncorrected area of 1281 millionths (1498 millionths corrected). The flare was accompanied by parallel ribbons and dark surging. The solar analyst at Holloman reported brilliant streaks over the flare area which were flowing northward on the white light board, and a dark surge of 42 degrees in extent flowing eastward and southeastward towards the limb. Loops formed over the northern end of the flare at 0030 UT (Figure 5) and persisted until Holloman went off patrol at 0135 UT. The original flare points became a large rectangle from northeast to southwest. The flare produced a secondary 3B maximum at 0043 UT with an uncorrected area of 1146 millionths (1340 millionths corrected). The flare attained 20 percent umbral coverage and ended near 0243 UT on 25 April (SGD, Apr 1984).

## Radio Observations From 2330 UT on 24 April to 0400 UT on 25 April

Plots of the solar radio emissions as recorded by Learmonth Solar Observatory are shown in Figures 6-13. To normalize the plots, quiet sun values (17.0, 35.0, 78.0, 109.0, 156.0, 181.0, 300.0, 540.0 SFU's) were subtracted from the raw values for each frequency from 245 to 15400 MHz, respectively. The first plot for each frequency is the 20-second averaged data for the entire period. The second plot is 1-second data starting at 2358 UT on 24 April and ending 0013 UT on 25 April. Bursts of at least 10,000 SFU's occurred at all eight discrete frequencies and bursts exceeding 100,000 SFU's were recorded at 245, 410, and 610 MHz. The burst began near 2359 UT on 24 April, and solar radio emissions remained elevated above background levels for several hours afterwards. The peak recorded burst was 315,000 SFU's at 410 MHz at 0000 UT on 25 April. The 2695 MHz channel approached saturation from 0001.2 UT to 0001.5 UT and from 0001.9 UT to 0002 UT on 25 April at around 38,000 SFU's (saturation is 50,000 SFU's).

## Acknowledgements

The author wishes to thank Mr. Ed Cliver, AFGL, for converting the RSTN data to an ASCII format; MSgt Klumb, HQ 4 Weather Wing, for technical information concerning the SOON and RSTN systems; the people at the AWS Solar Observatories without whom this report would be impossible; and Ms. Helen Coffey, Ms. Bonnie Hausman, and Mr. Herb Kroehl for their editorial comments.

## REFERENCES

| | | |
|---|---|---|
| AWSP 105-60 | 1981 | **"Solar Optical Observing,"** 1 October 1981. |
| AWSP 105-61 | 1982 | **"Solar Radio Observing,"** 1 April 1982. |
| SGD | 1984 | **Solar-Geophysical Data,** 476 Part I, April 1984, U.S. Department of Commerce (Boulder, Colorado, USA 80303). |
| SGD | 1984 | **Solar-Geophysical Data,** 477 Part I, May 1984, U.S. Department of Commerce (Boulder, Colorado, USA 80303). |
| SGD | 1984 | **Solar-Geophysical Data,** 478 Part I, June 1984, U.S. Department of Commerce (Boulder, Colorado, USA 80303). |

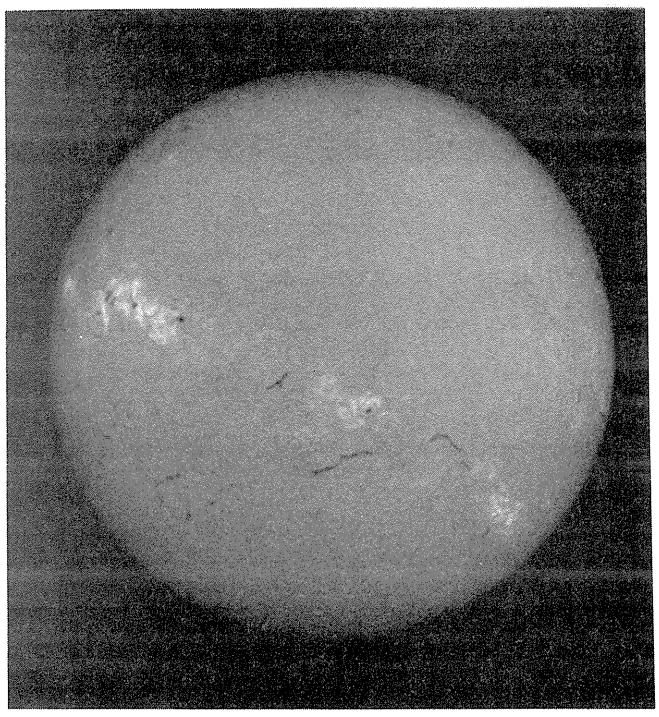

Fig. 1. Region 4474 on 24 April 1984 at 2301:01 UT as observed by Holloman. Photo is not corrected for P angle.

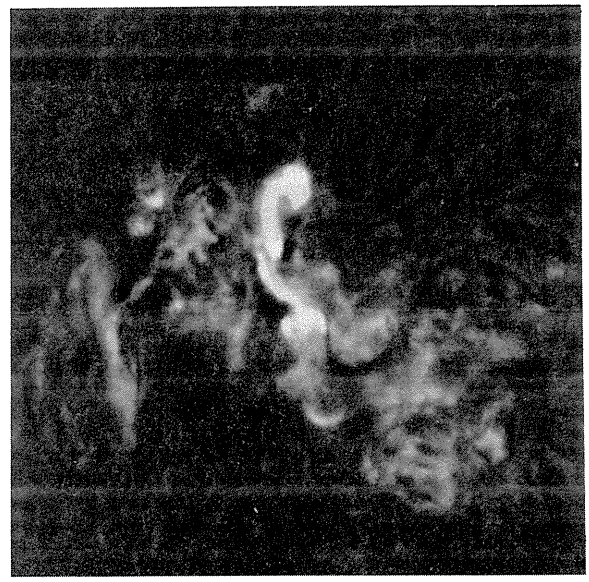

Fig. 2. This large scale image of the Active Region 4474 shows the solar flare at 2359:30 UT 24 April 1984 as observed at Holloman.

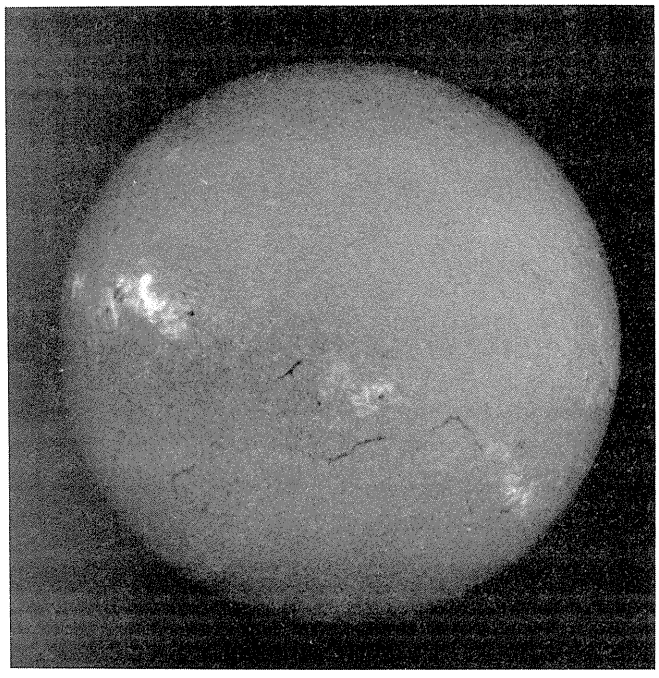

Fig. 3. This disk photo at 0000 UT 25 April 1984 gives an indication of the magnitude of the event.

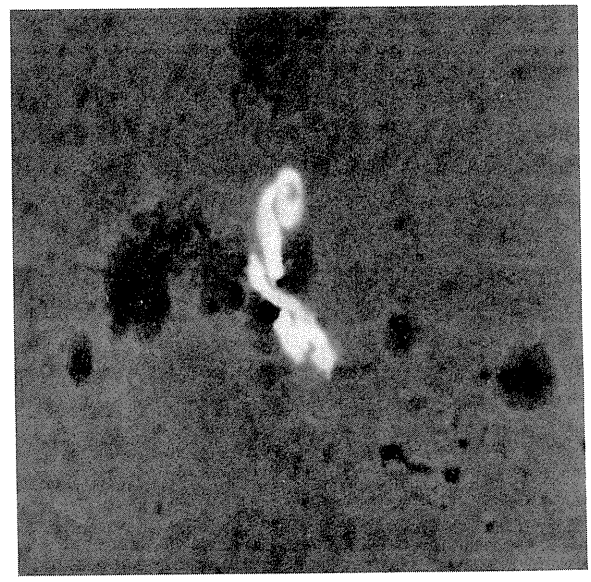

Fig. 4. This large scale off-band image of the solar flare was taken at 0000:32 UT on 25 April 1984.

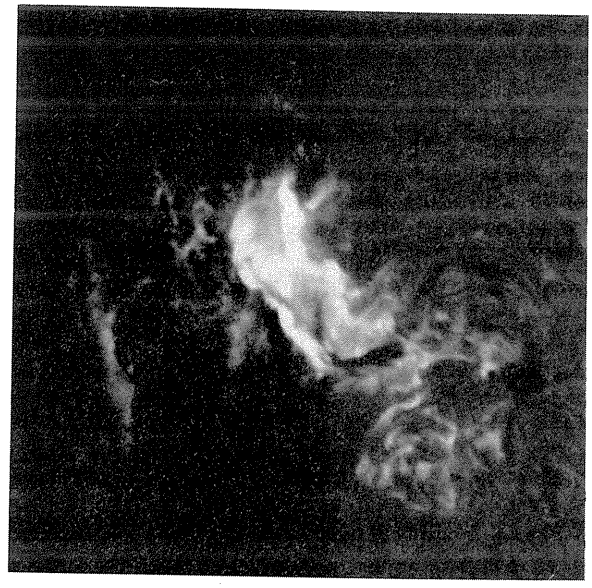

Fig. 5. This large scale H-alpha image shows the parallel ribbons evident at 0032:30 UT on 25 April 1984.

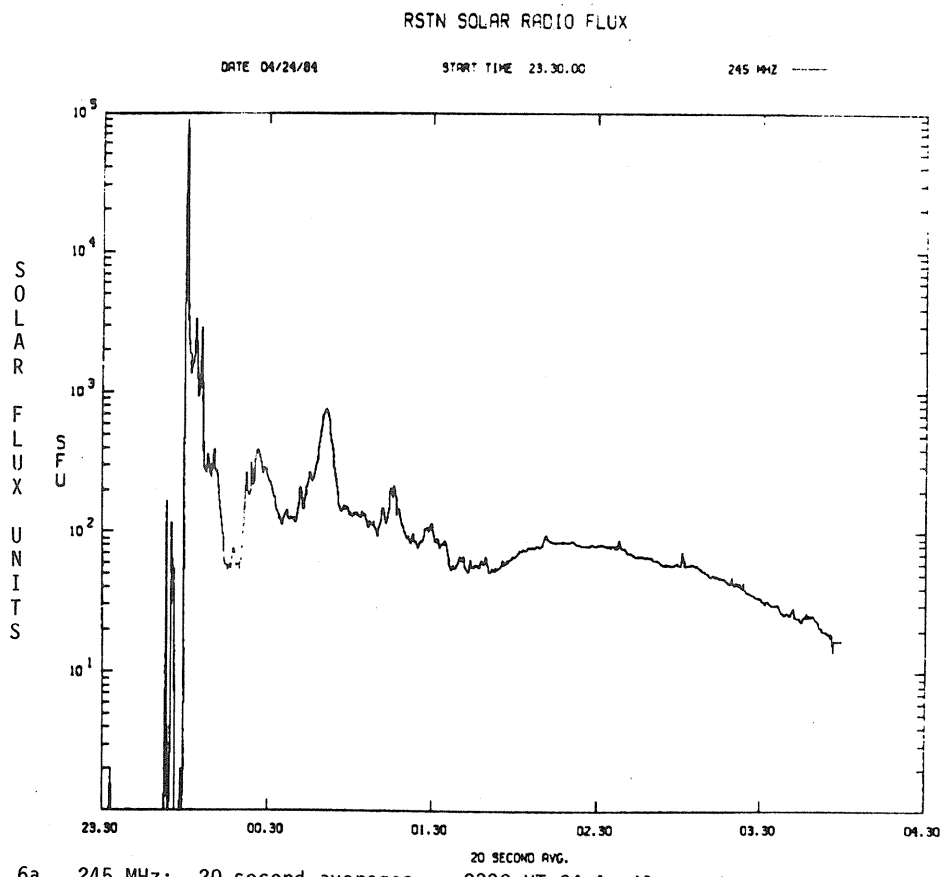


Fig. 6a. 245 MHz: 20 second averages -- 2330 UT 24 April to 0400 UT 25 April 1984.

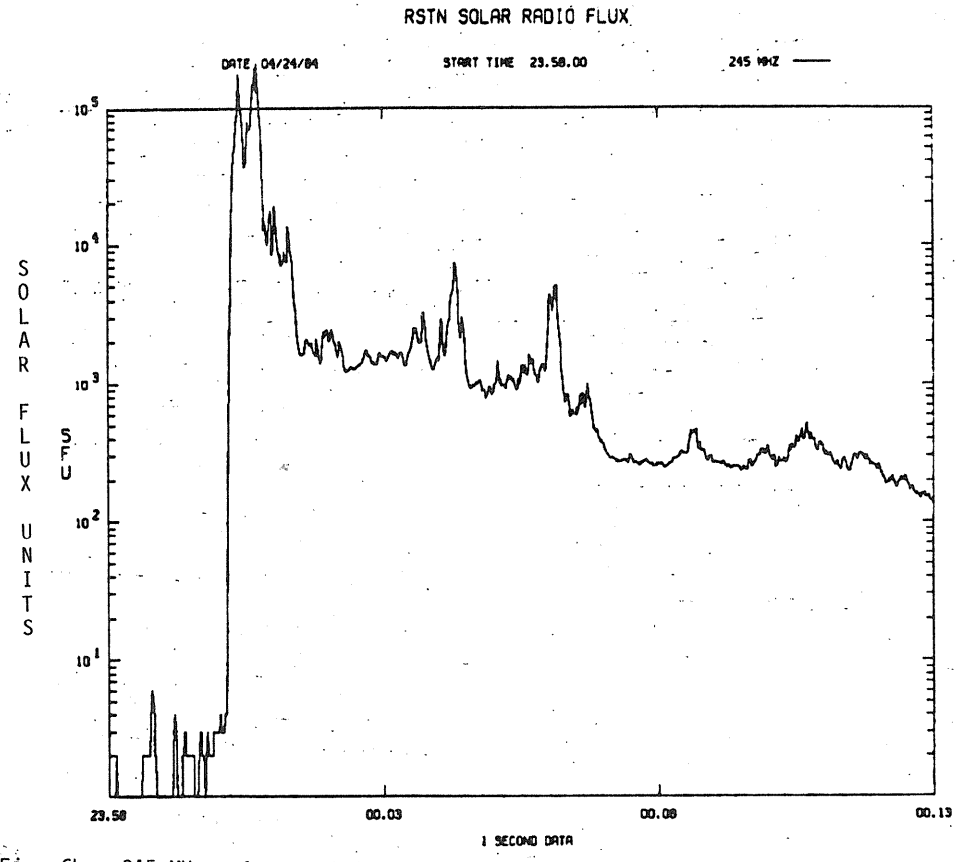


Fig. 6b. 245 MHz: 1-second data -- 2358 UT 24 April to 0013 UT 25 April 1984.

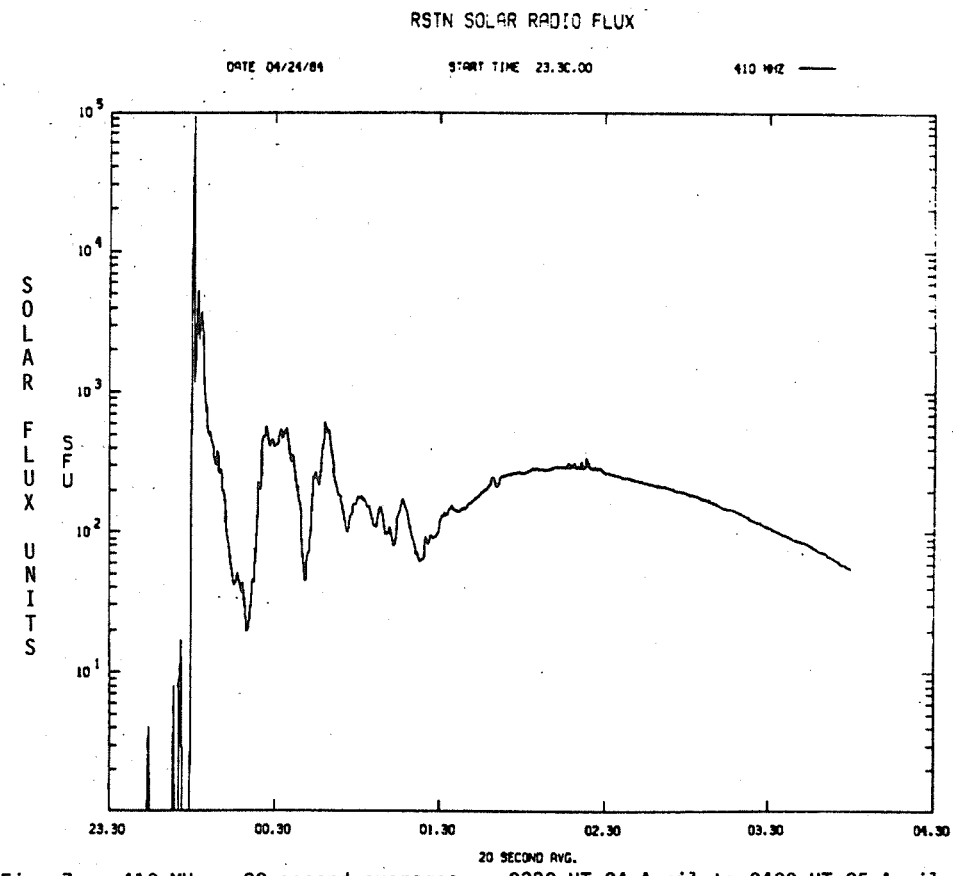


Fig. 7a. 410 MHz: 20-second averages -- 2330 UT 24 April to 0400 UT 25 April 1984.

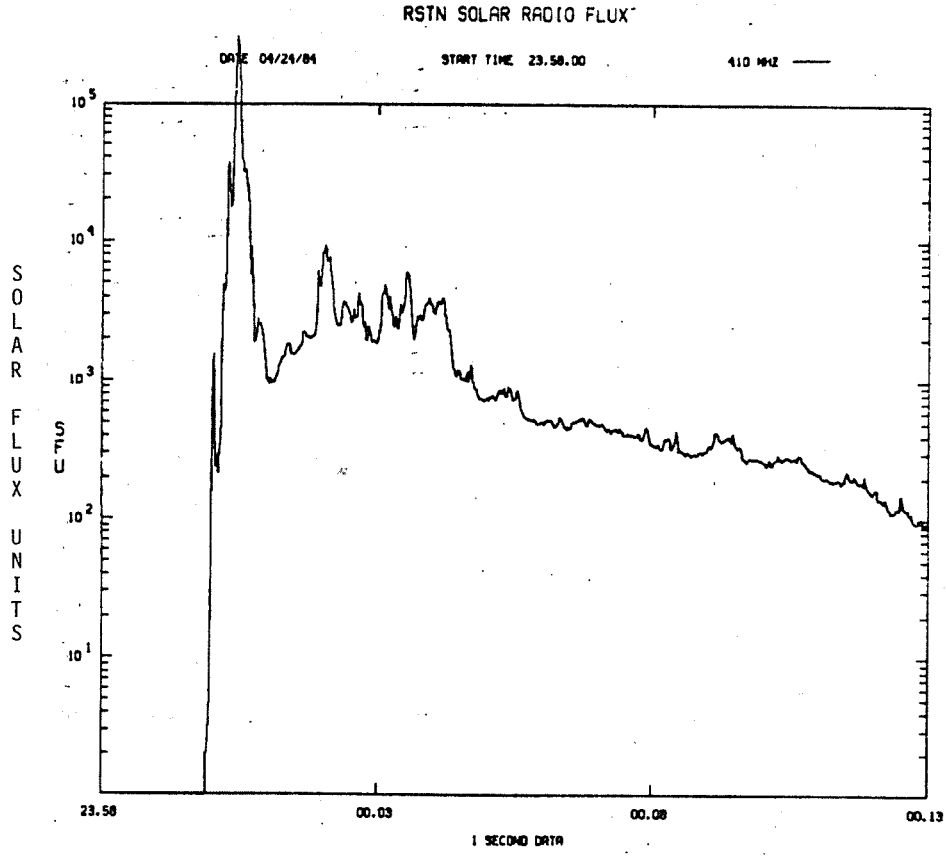


Fig. 7b. 410 MHz: 1-second data -- 2358 UT 24 April to 0013 UT 25 April 1984.

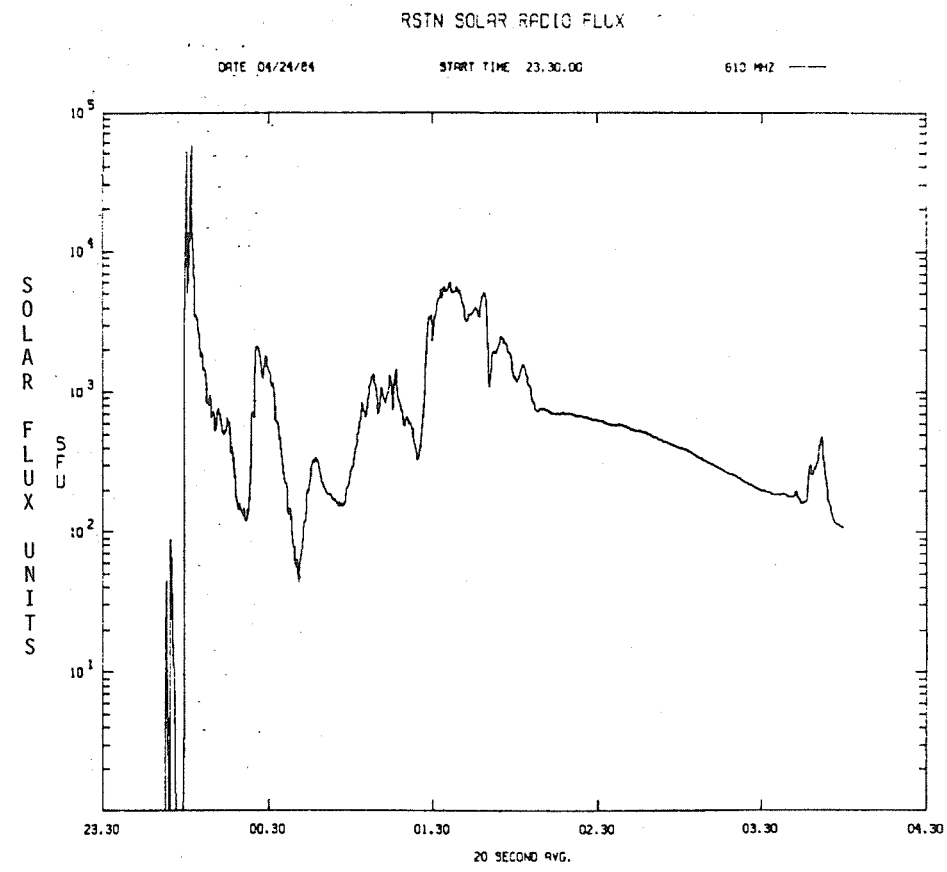


Fig. 8a. 610 MHz: 20-second averages -- 2330 UT 24 April to 0400 UT 25 April 1984.

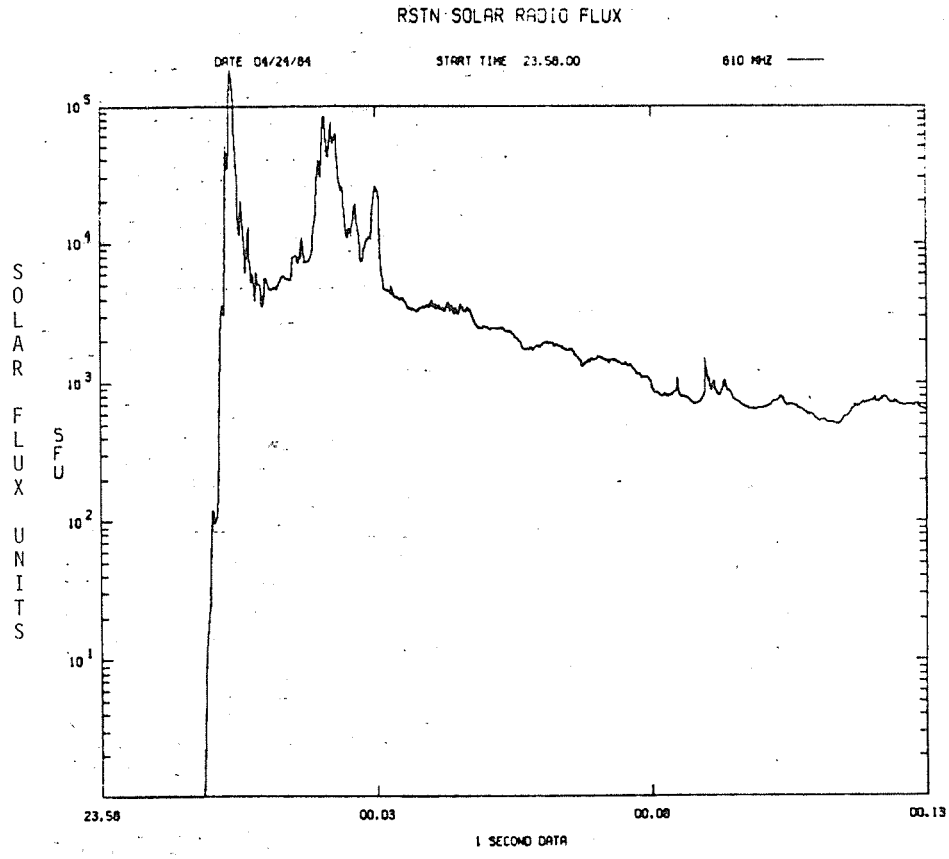


Fig. 8b. 610 MHz: 1-second data -- 2358 UT 24 April to 0013 UT 25 April 1984.

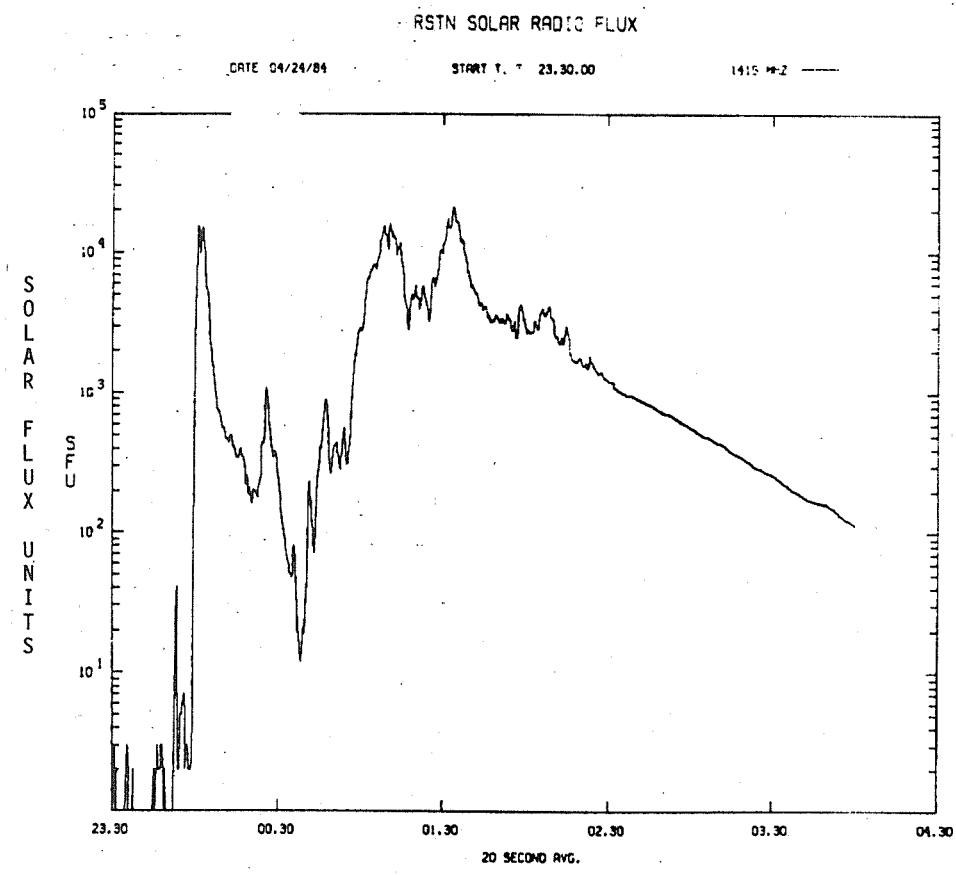


Fig. 9a. 1415 MHz: 20-second averages -- 2330 UT 24 April to 0400 UT 25 April 1984.

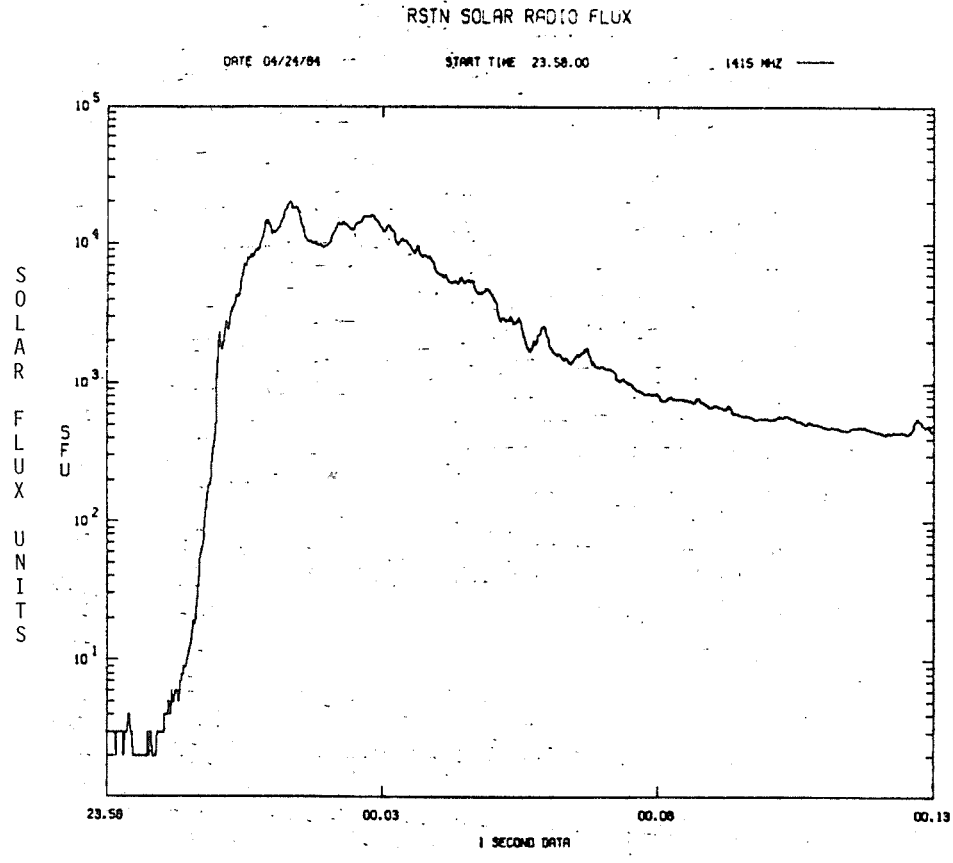


Fig. 9b. 1415 MHz: 1-second data -- 2358 UT 24 April to 0013 UT 25 April 1984.

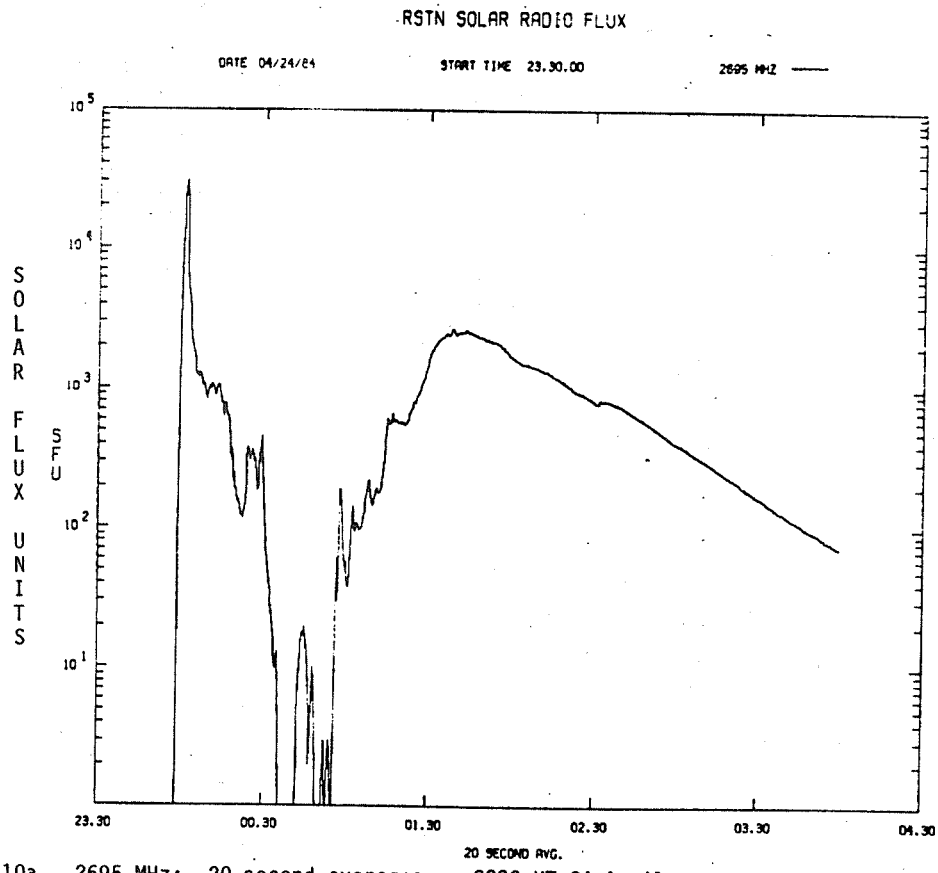


Fig. 10a. 2695 MHz: 20-second averages -- 2330 UT 24 April to 0400 UT 25 April 1984.

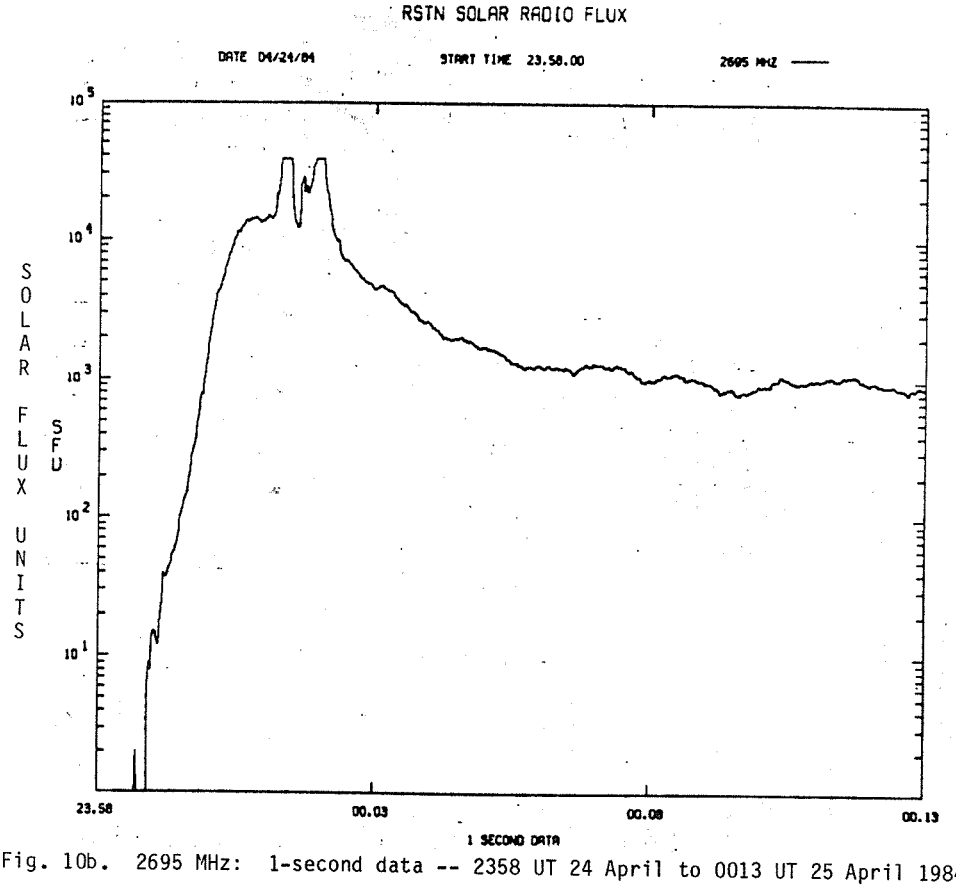


Fig. 10b. 2695 MHz: 1-second data -- 2358 UT 24 April to 0013 UT 25 April 1984.

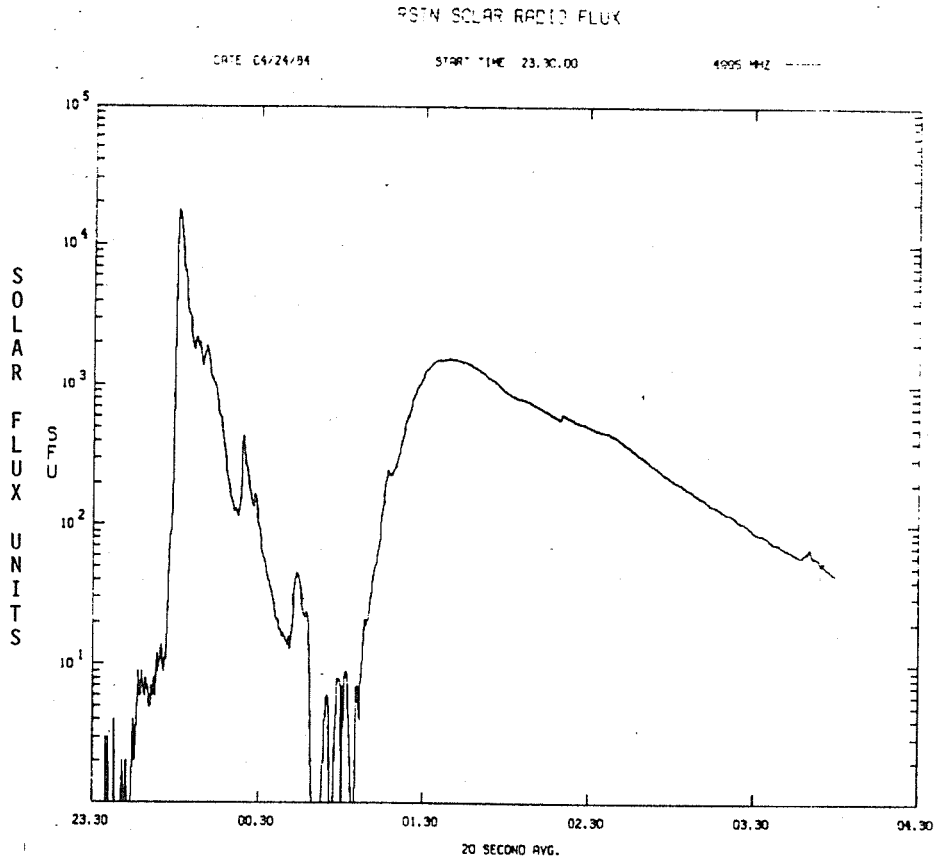


Fig. 11a. 4995 MHz: 20-second averages -- 2330 UT 24 April to 0400 UT 25 April 1984.

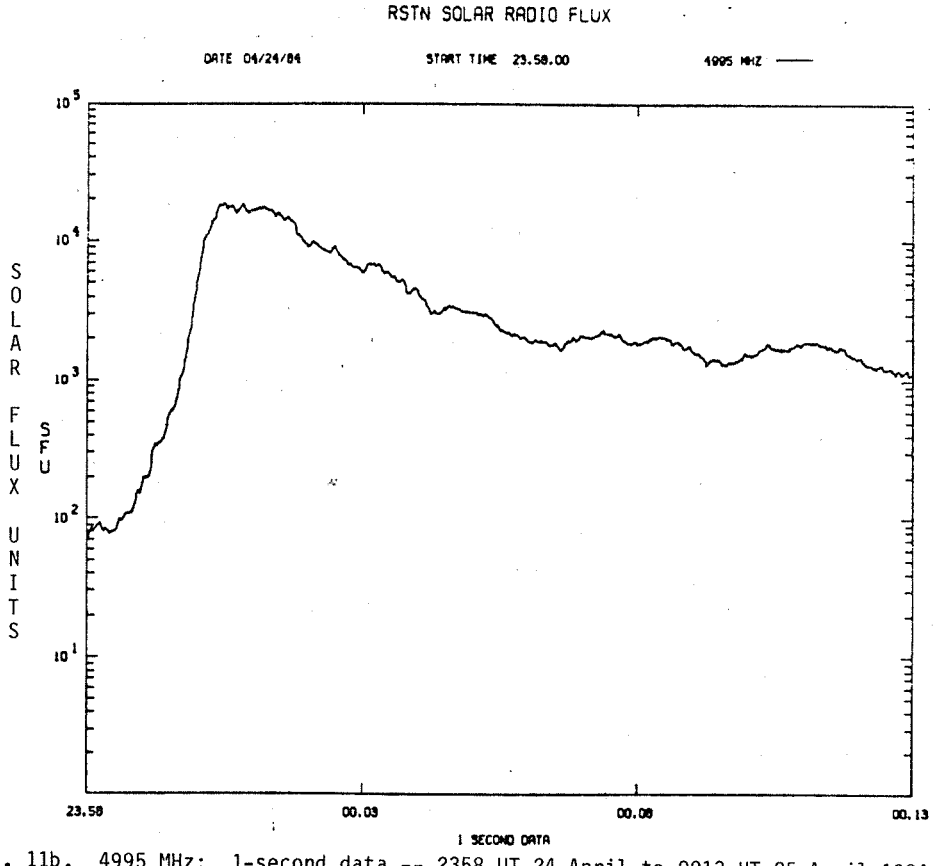


Fig. 11b. 4995 MHz: 1-second data -- 2358 UT 24 April to 0013 UT 25 April 1984.

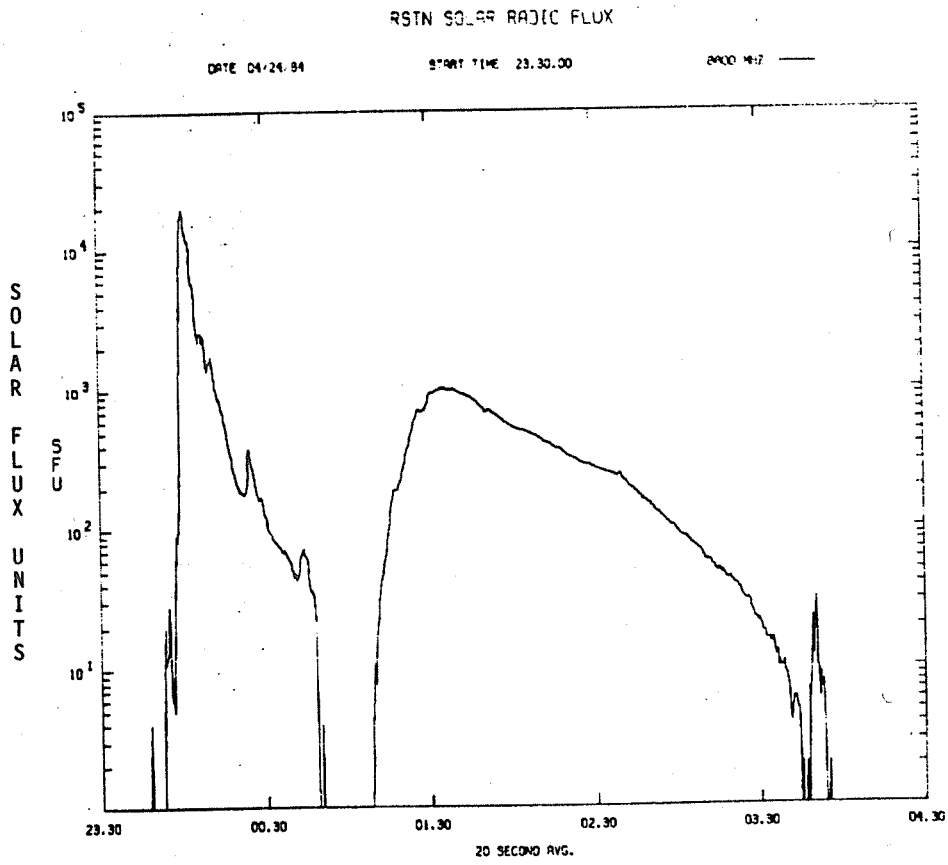


Fig. 12a. 8800 MHz: 20-second averages -- 2330 UT 24 April to 0400 UT 25 April 1984.

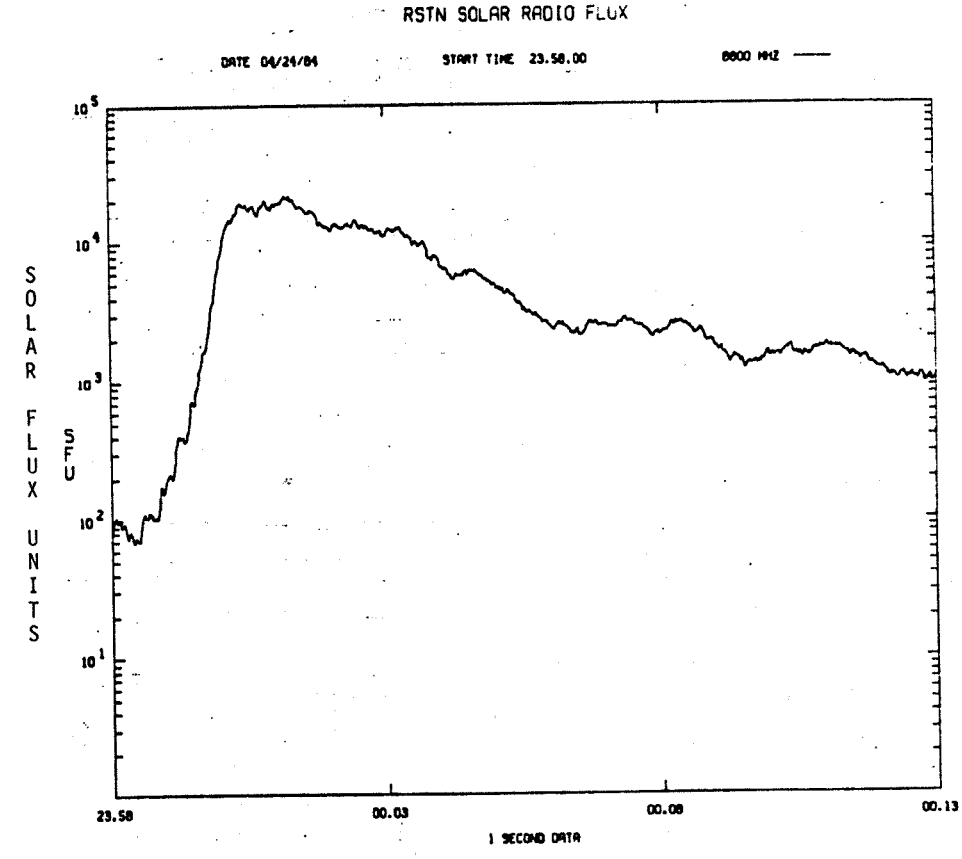


Fig. 12b. 8800 MHz: 1-second data -- 2358 UT 24 April to 0013 UT 25 April 1984.

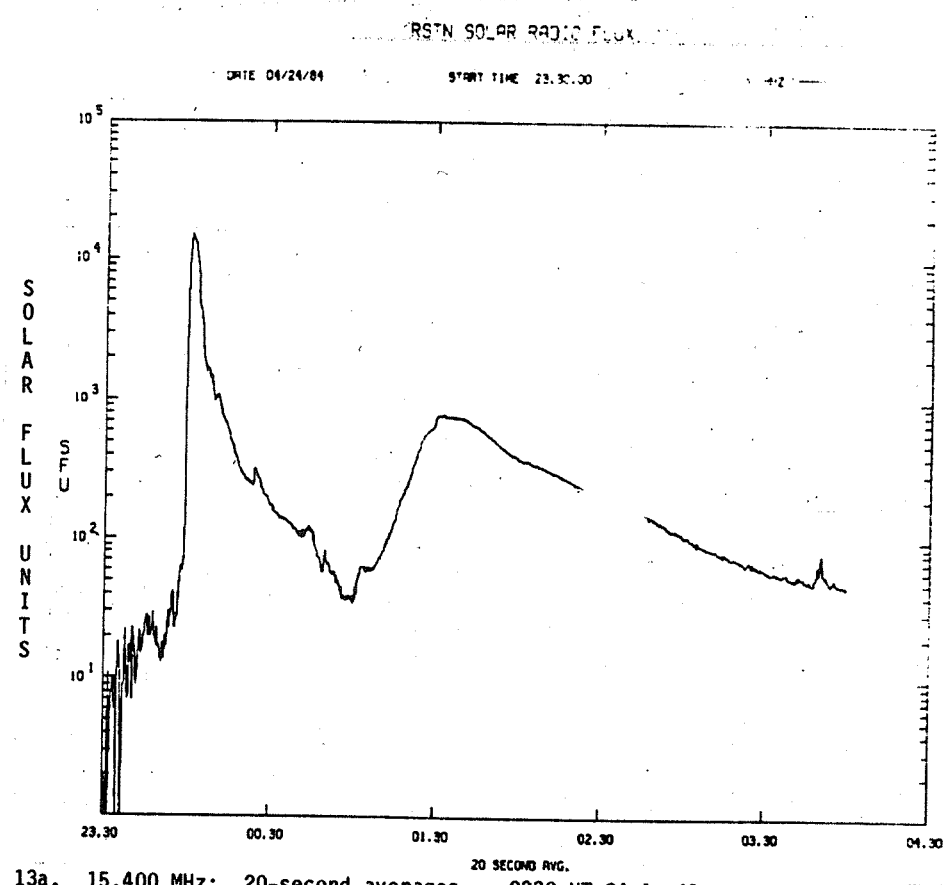


Fig. 13a. 15,400 MHz: 20-second averages -- 2330 UT 24 April to 0400 UT 25 April 1984.

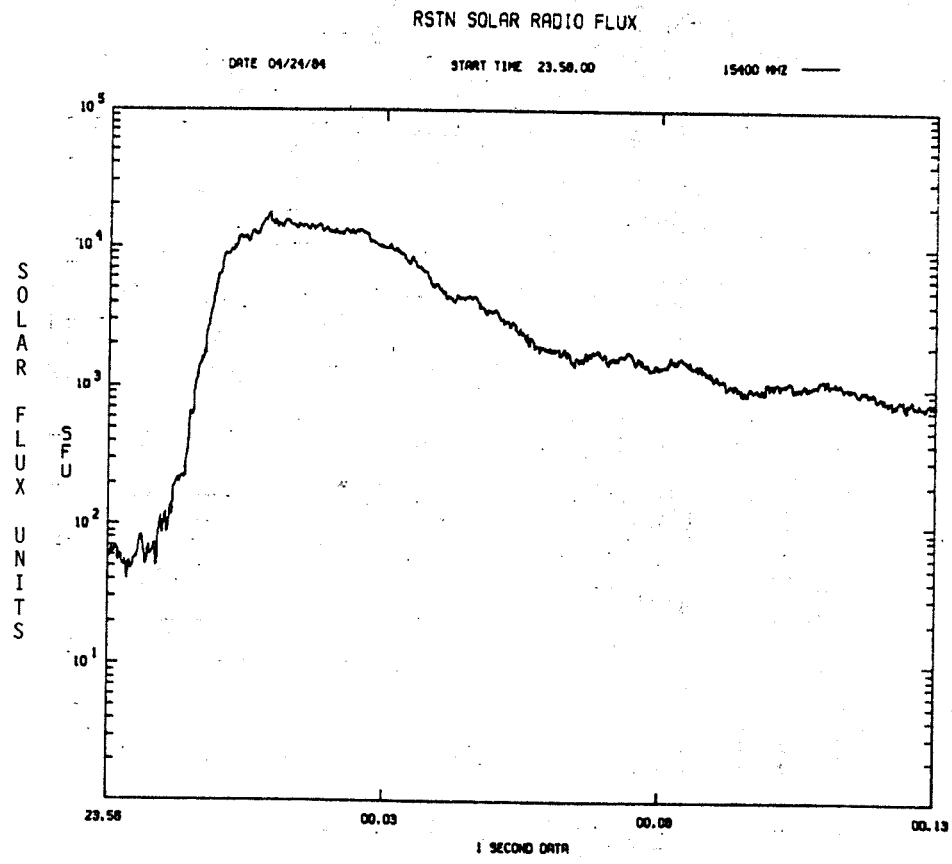


Fig. 13b. 15,400 MHz: 1-second data -- 2358 UT 24 April to 0013 UT 25 April 1984.

# Photospheric and H-Alpha Observations of the Region 4474 in the Period between 20 April and 4 May 1984 at Nijmegen

by

H.A.M. Balster and I. Atanasijevic
Astronomical Institute, Faculty of Sciences
Nijmegen, The Netherlands

Regular solar observations (Wolf number and sunspot charts) have been made at the Astronomical Institute, Faculty of Sciences, Nijmegen, the Netherlands at about noon (UT) since 1 May 1977 (refracting telescope, 20 cm/200 cm, aperture stepped down to 7 cm). Use is made of a Herschel prism and an 80 x ocular with a yellow-green filter. The diameter of the original charts is 15 cm. Data on observed sunspots (Wolf number and modified Zurich classification) are sent to the Sunspot Index Data Center, Brussels, Belgium.

From 12 May 1980 onward these observations are supplemented by photographs of the chromosphere using a 0.6A H-alpha Day-star filter (University model). Moreover, with the filter at ambient temperature, narrow-band exposures of the photosphere are obtained just outside the H-alpha line. The filtergrams covering the whole disk are made at the telescope's prime focus. For detailed filtergrams a 2 x converter is used. All photographs are made on Kodak TP 2415 film.

During the period from 20 April to 4 May 1984 complete observations were made on 23, 24, 25, 26, 27 April and 2 May. Due to adverse weather conditions, observations on 20 April were restricted to sunspot counting and preparation of a chart. Observations were impossible on 21, 22, 28, 29, 30 April and 1, 3 and 4 May.

**Notes about Region 4474**

- The region 4474 was not visible on 20 April at 1040 UT.
- On 23 April at 0852 UT a prominence was observed on the limb above region 4474.
- Note the two very bright patches indicated by arrows on the detailed filtergram on 27 April.
- Note, also, on the detailed filtergrams, the change in the structure of the region which took place between 25 and 26 April.

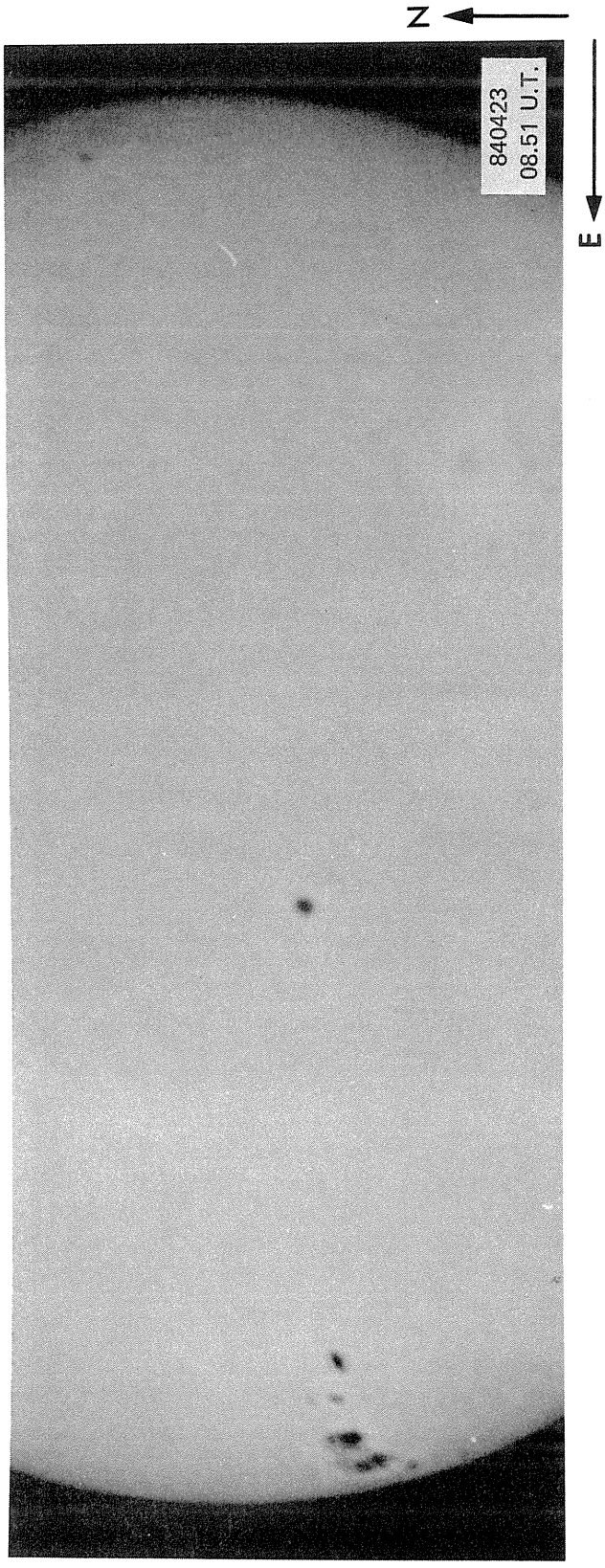
Z
E
840423
08.51 U.T.

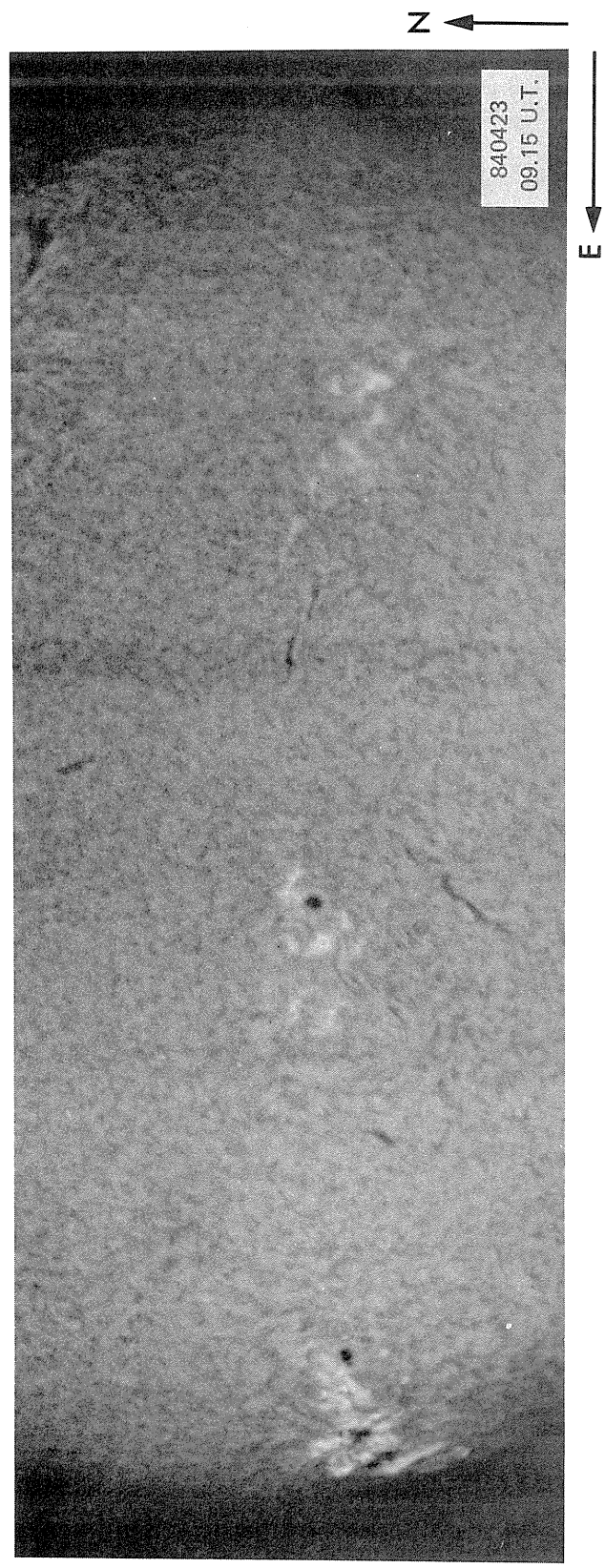
Z
E
840423
09.15 U.T.

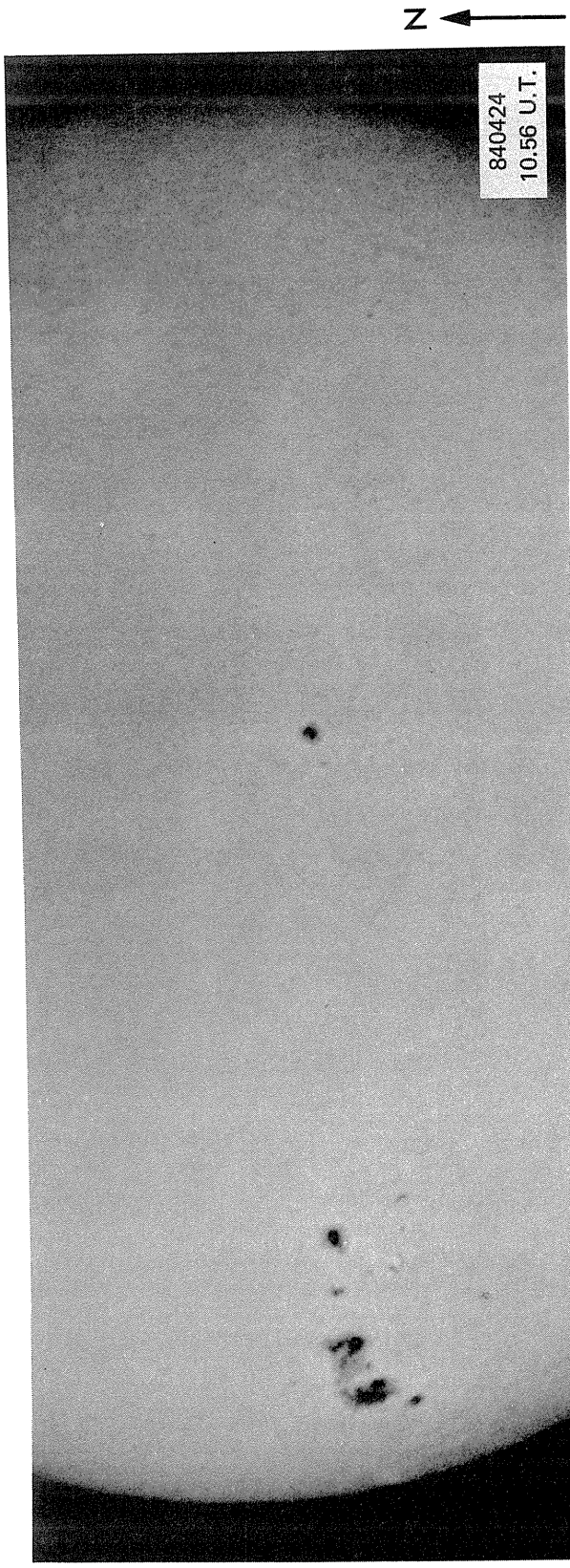
N
E
840424
10.56 U.T.

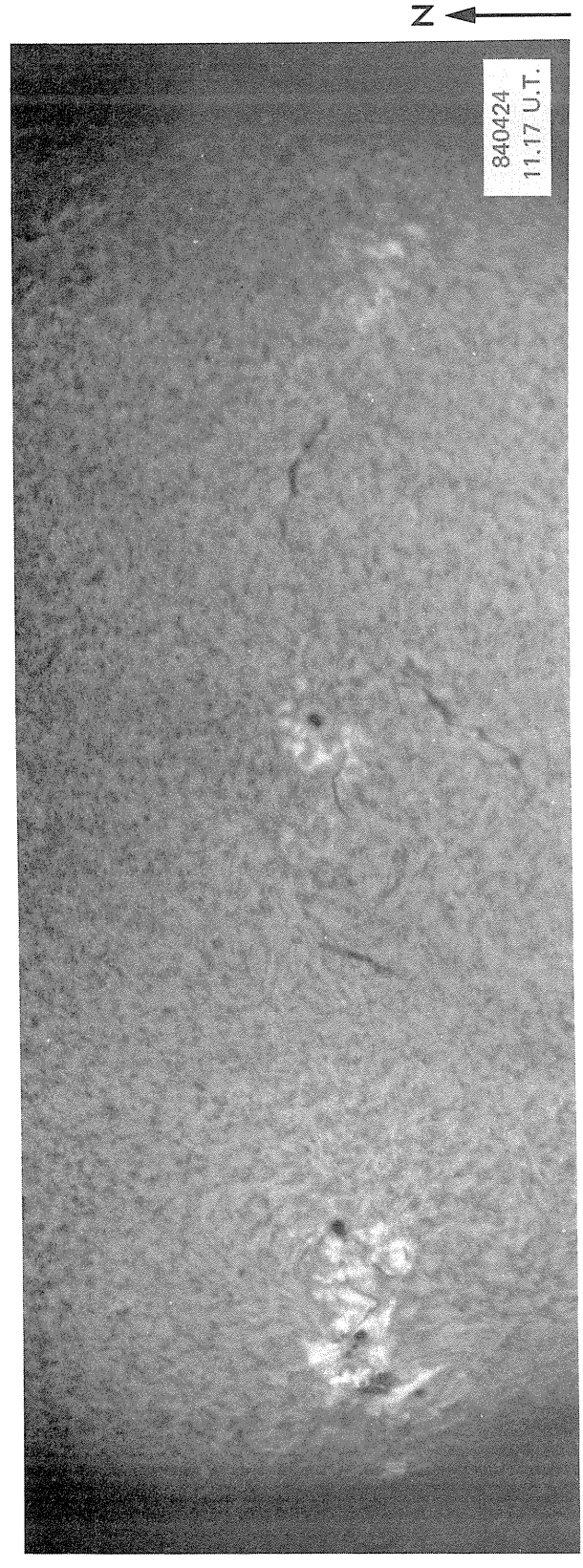
N
E
840424
11.17 U.T.

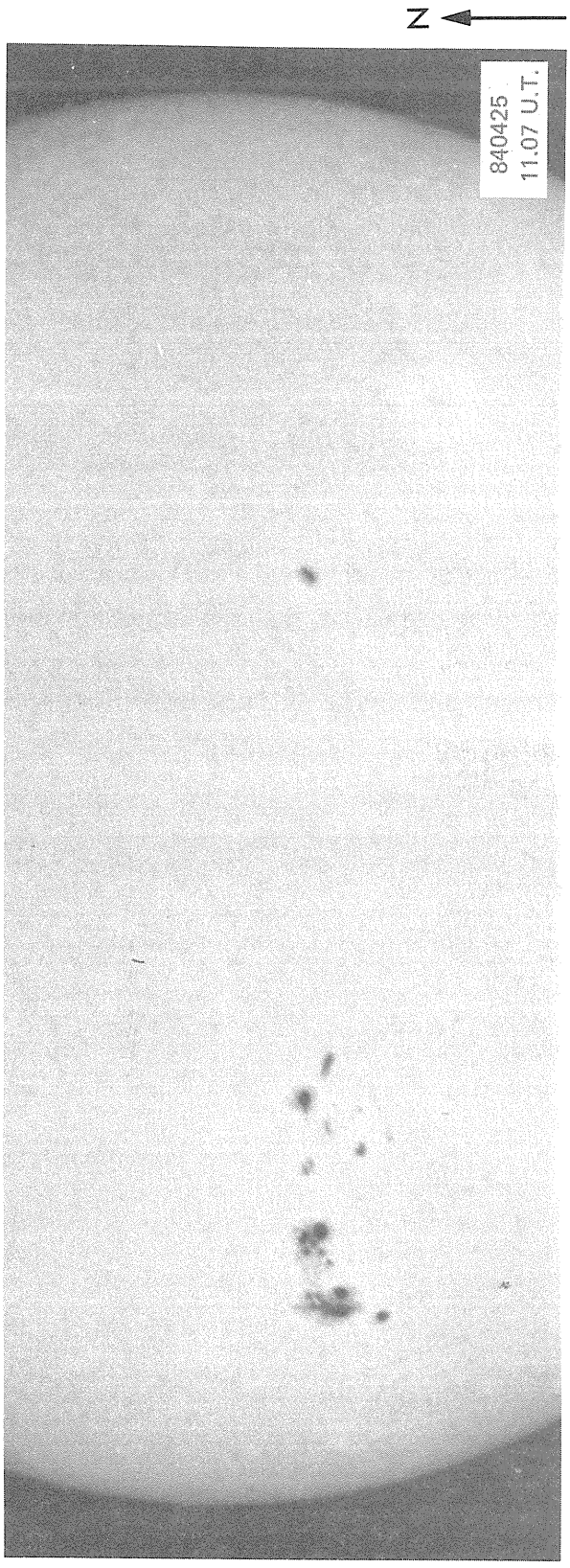
N
E
840425
11.07 U.T.

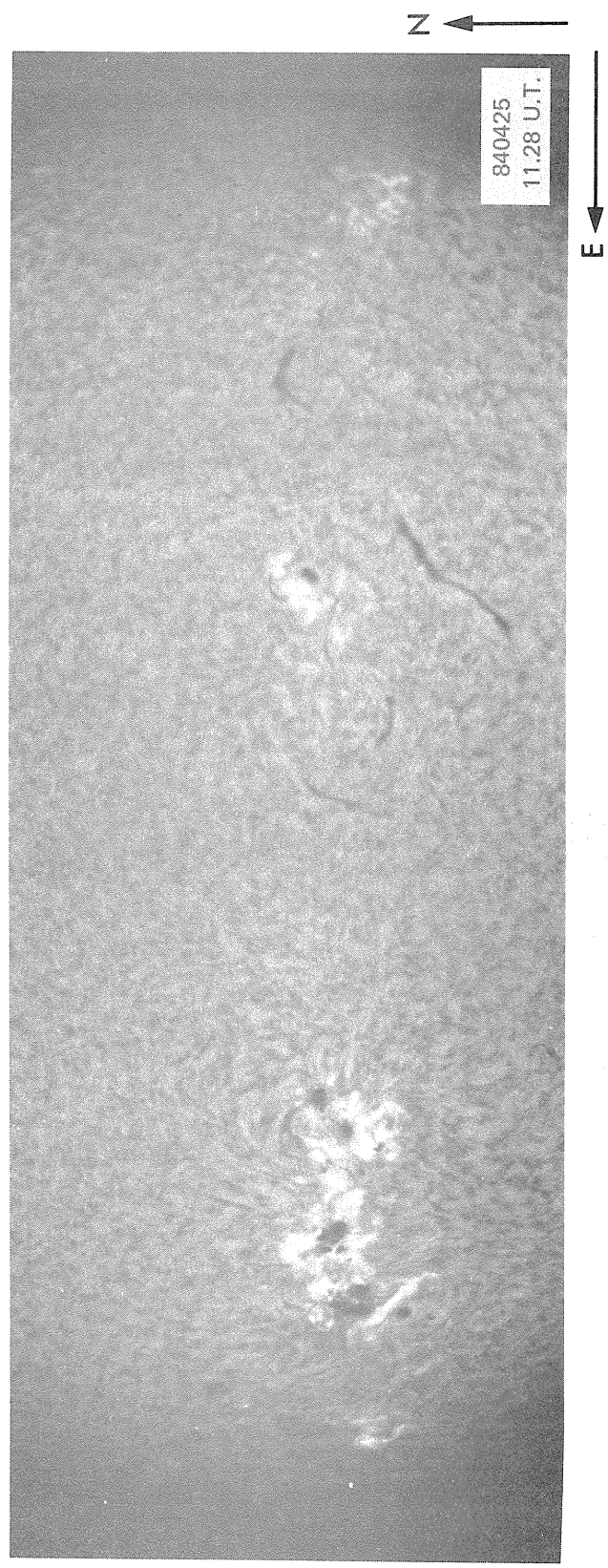
N
E
840425
11.28 U.T.

N
E
840426
10.57 U.T.


N
E
840426
11.19 U.T.

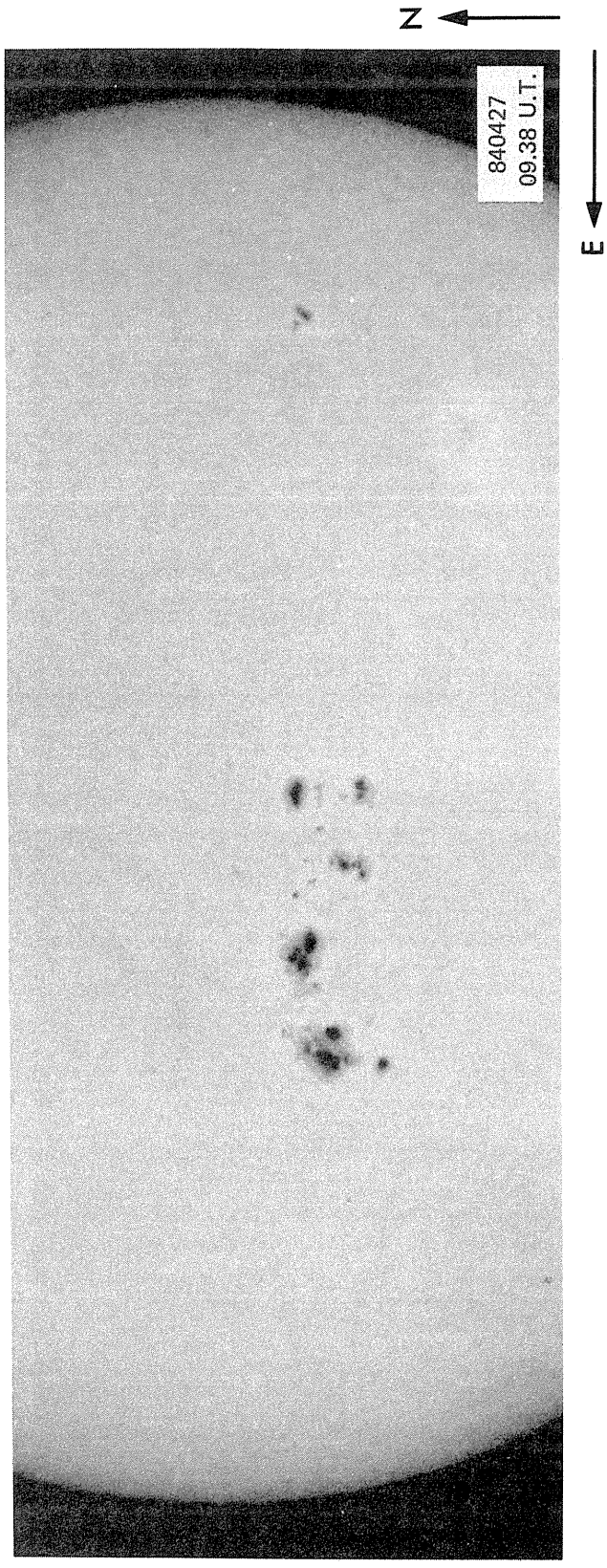
N
E
840427
09.38 U.T.

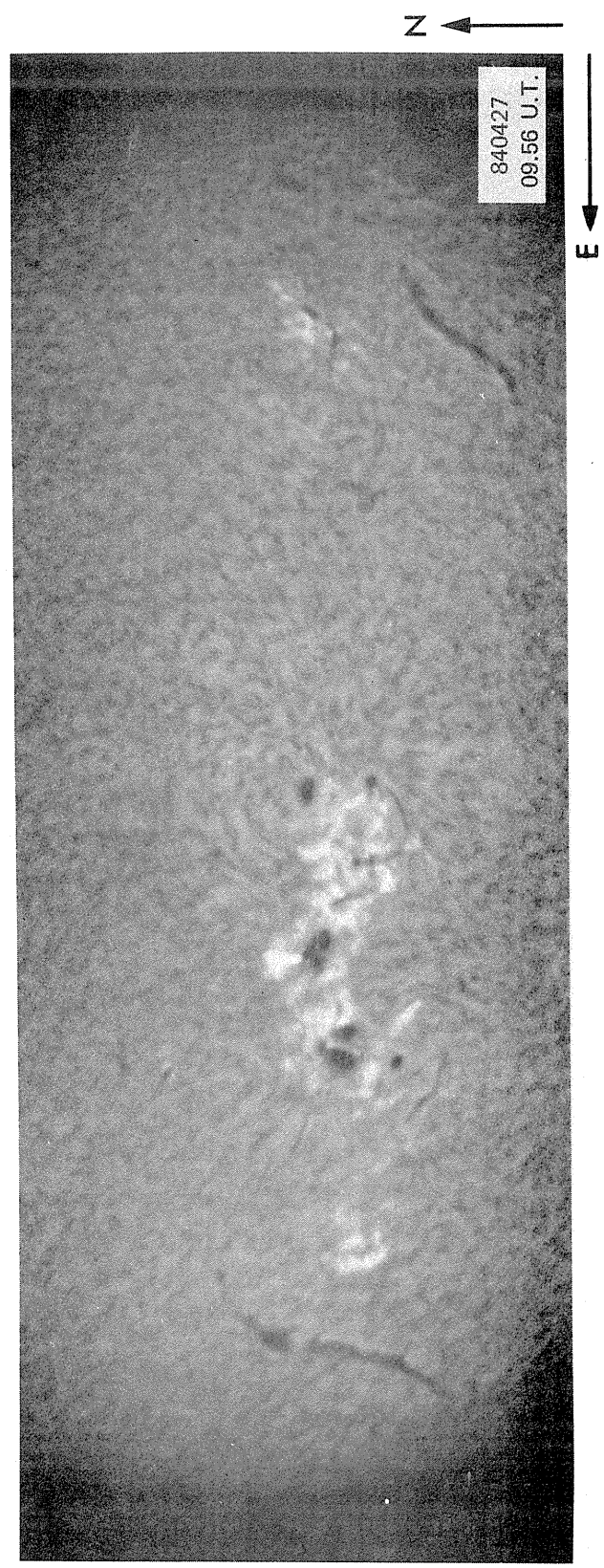
N
E
840427
09.56 U.T.

840502
11.02 U.T.
N
E


840502
11.21 U.T.
N
E

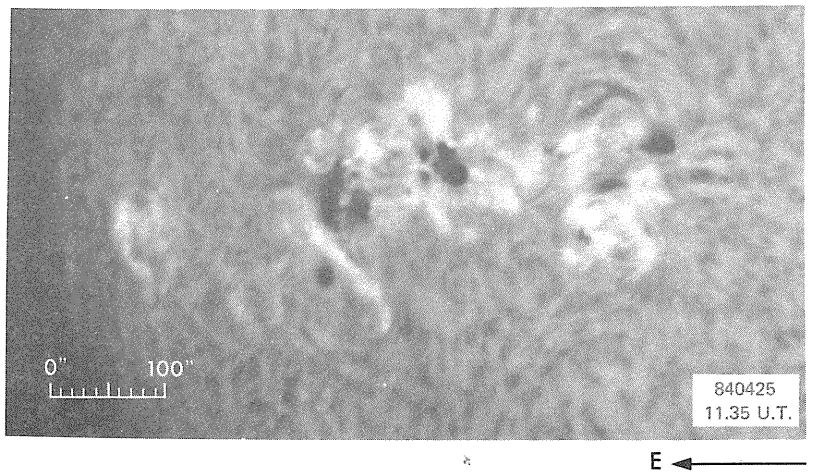
0"
100"
840425
11.35 U.T.
N
E

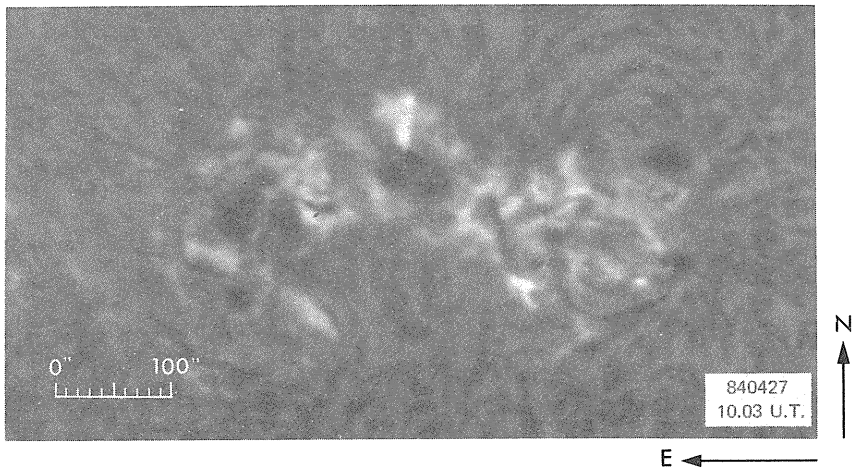
0"
100"
840427
10.03 U.T.
N
E

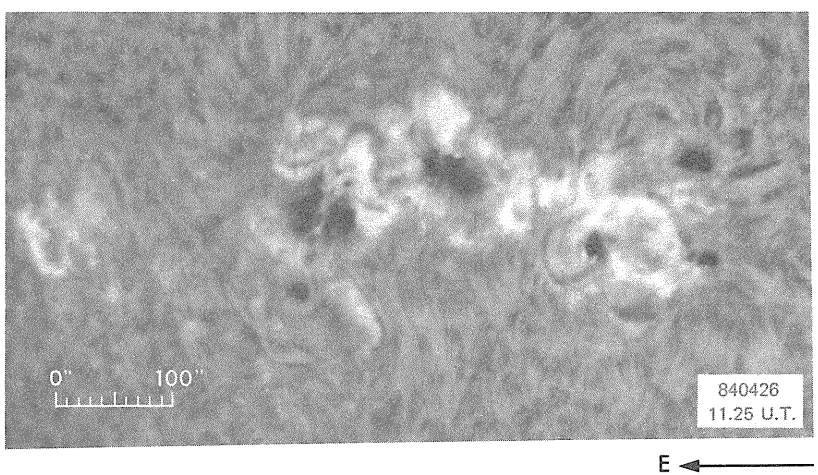
0"
100"
840426
11.25 U.T.
N
E

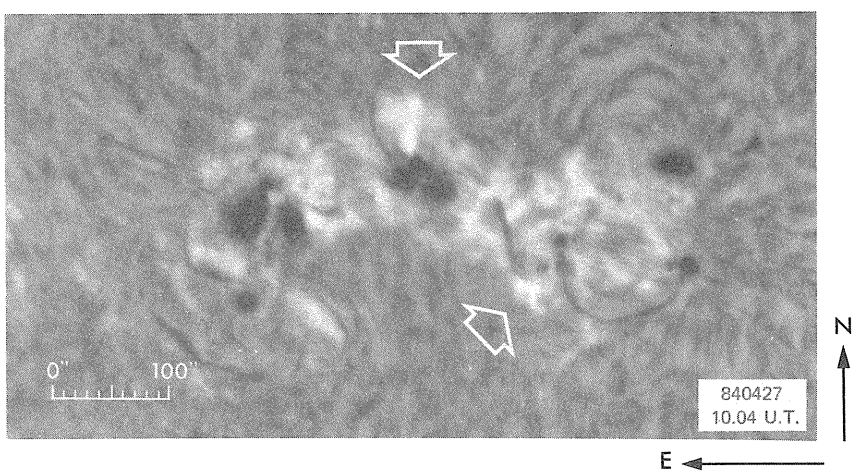
0"
100"
840427
10.04 U.T.
N
E

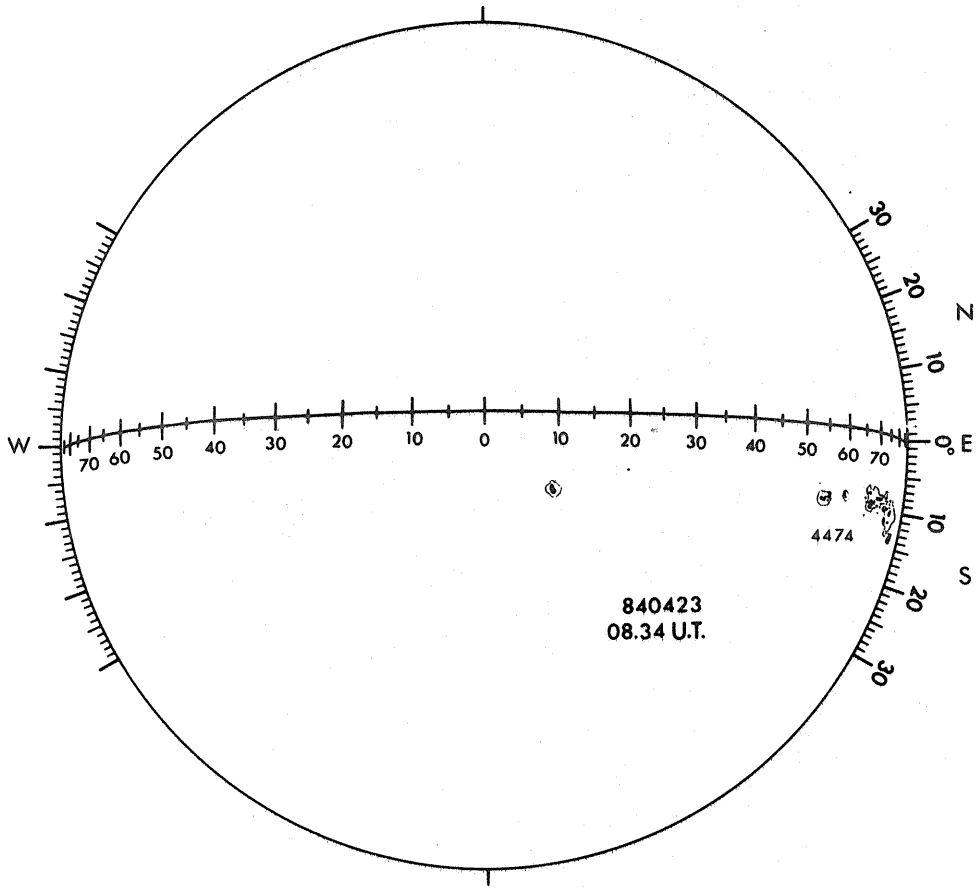
W
70 60 50 40 30 20 10 0 10 20 30 40 50 60 70
0°
E
N
S
10
20
30
4474
840423
08.34 U.T.

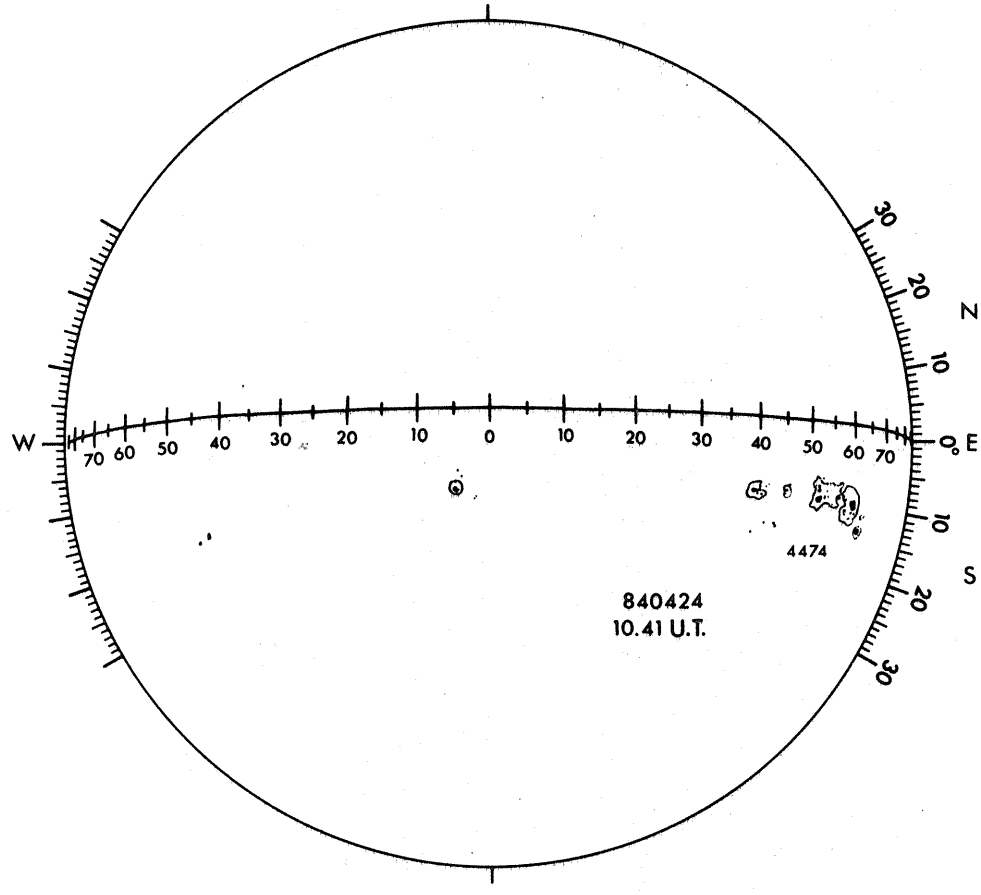
W
70 60 50 40 30 20 10 0 10 20 30 40 50 60 70
0°
E
N
S
10
20
30
4474
840424
10.41 U.T.

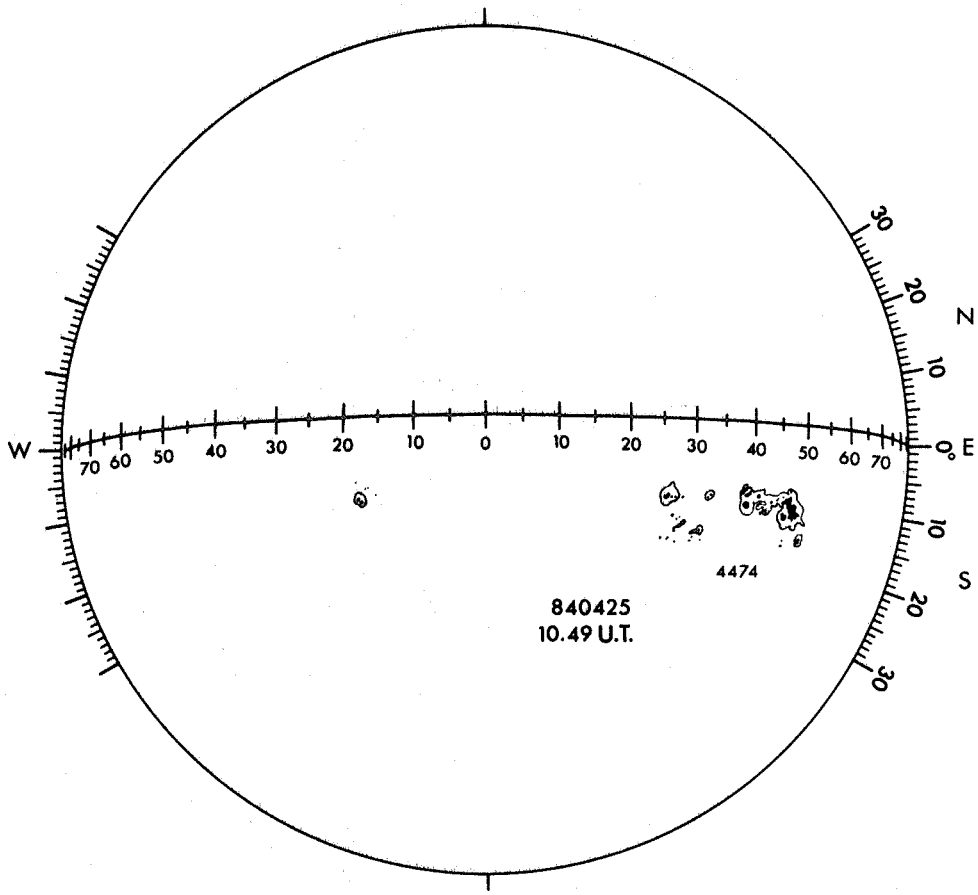
W
70 60 50 40 30 20 10 0 10 20 30 40 50 60 70
0°
E
N
S
10
20
30
4474
840425
10.49 U.T.

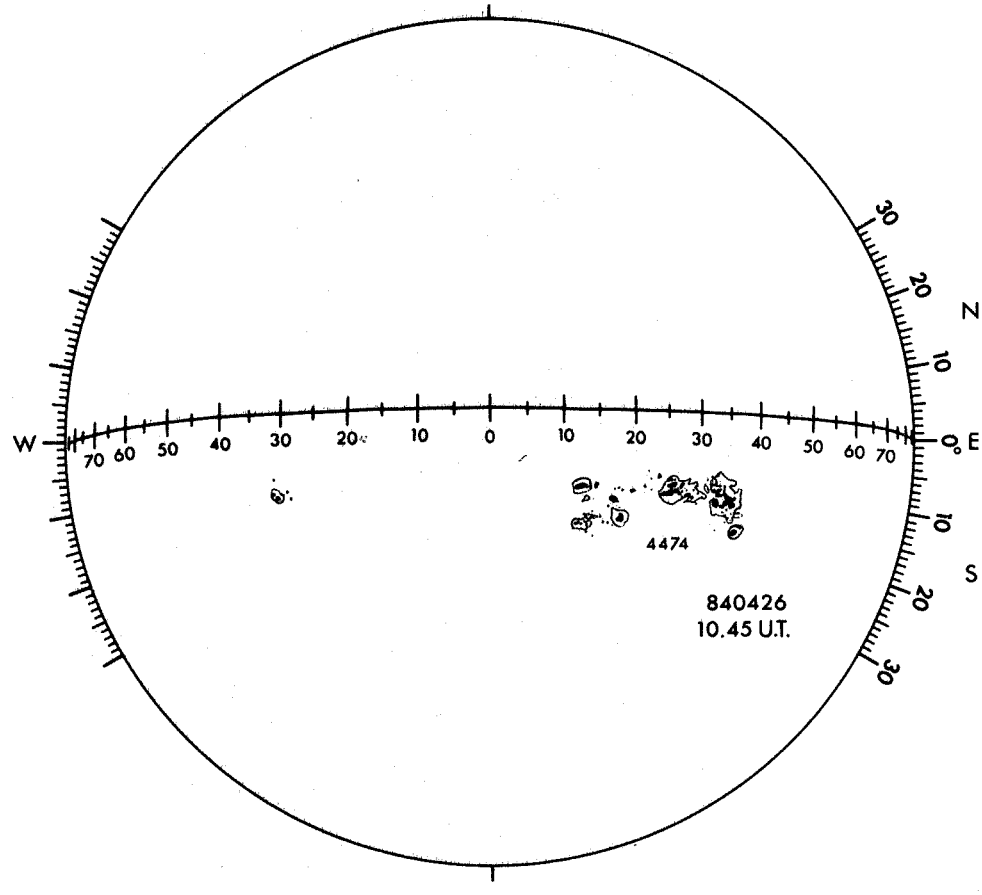
W
70 60 50 40 30 20 10 0 10 20 30 40 50 60 70
0°
E
N
S
10
20
30
4474
840426
10.45 U.T.

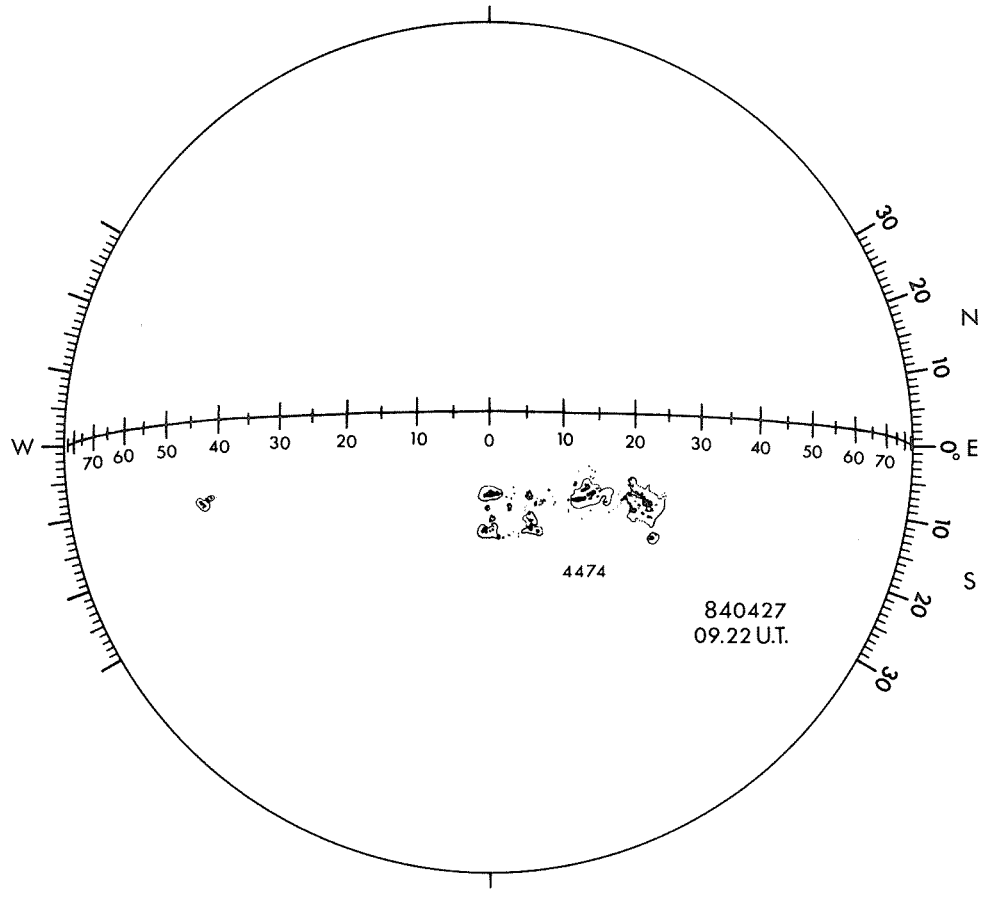
W
70 60 50 40 30 20 10 0 10 20 30 40 50 60 70
0°
E
N
S
10
20
30
4474
840427
09.22 U.T.

# Solar Observations for the Periods 6-11 February, 26 February - 5 March, and 20 April - 4 May 1984 Made by the A.L.P.O. Solar Section

by

Richard E. Hill
ALPO Solar Section, 4632 E. 14th Street
Tucson, Arizona 85711, USA

## Introduction

The Association of Lunar and Planetary Observers Solar Section (ALPO Solar Section) is a worldwide network of amateur solar astronomers who observe the Sun, producing drawings and photographs in both white-light and monochromatic light. All observations are then collected and made available to the professional community at no charge. The Solar Section was established in 1982 by the ALPO to observe and study solar activity. Summaries of these observations and studies are published regularly (Hill, 1985).

Every 28 days the Solar Section publishes the most recently received observational data in its regular publication, **The Rotation Report.** Researchers may obtain copies at no charge from Richard E. Hill. A catalog of all data on hand, now approximately 2000 observations back to Carrington Rotation 1721, will be published before the end of 1986. Researchers interested in obtaining this catalog should also contact Richard E. Hill.

The Solar Section observers also are available for observing programs and can be alerted to sudden events in a matter of minutes. Researchers who have need of such a network for data requests, searches, and alerts should contact Richard E. Hill.

## Observations

Table 1 lists all the observers who contributed data for the reporting periods requested. The data consist largely of photographs with a few drawings. All of the photographs were taken on Kodak Technical Pan Film 2415 (formerly SO-115).

TABLE 1. Observers Contributing to This Report

| Observer | Location | Instrument | Effective Aperture (cm) |
|---|---|---|---|
| Blackburn, N. | Kansas City, Missouri, USA | 15 cm, rfr. | 7.5 |
| Dragesco, J. | Benin, W. Africa | 35.5 cm, cat. | 12 |
| Hill, R. | Tucson, Arizona, USA | 20 cm, cat. | 10 |
| Jahn, J. | W. Germany | 5 cm, rfr. | 5 |
| Maxson, P. | Phoenix, Arizona, USA | 20 cm, cat. | 15 |
| | | 40 cm, rfl. | 15 |
| Tatum, R. | Richmond, Virginia, USA | 17.8 cm, rfr. | 8.9 |
| Timerson, B. | Newark, New York, USA | 32 cm, rfl. | 10 |
| Young, S. | Long Beach, California, USA | 20 cm, cat. | 7.5 |

There are 68 observations, 17 of which (25%) are H-alpha. As Table 2 shows, the quality of the observations ranges from 10 arc seconds for the poorest to arc second resolutions for the best. The high resolution white-light photographs by Dragesco, and the H-alpha photographs by Tatum (with a 0.7 Angstrom filter) are the highest quality available.

Table 2. Data List for 6 February through 3 May 1984

| Carrington Rotation | NOAA Region | Obs. Type | Resolution Arcsec | Mo Day UT | FORMAT Film | Print | Notes |
|---|---|---|---|---|---|---|---|
| 1745 | Whole disk | white light | 5 | 02 06 1839 | 35mm | 8"x10" | |
| 1745 | Whole disk | white light | 3 | 02 06 2009 | 35mm | 5"x8" | 18 cm disk |
| 1745 | Whole disk | white light | 5 | 02 10 1804 | 35mm | 5"x8" | 18 cm disk |
| 1745 | Whole disk | white light | 5-7 | 02 10 2114 | 35mm | 8"x10" | vignetting |
| 1745 | Whole disk | white light | 7-10 | 02 11 1715 | 35mm | 8"x10" | mottled print |
| 1745 | 4410, 4413 4414, 4416 | H-alpha | 3 | 02 12 1721 | 35mm | 5"x7" | |
| 1745 | 4408, 4410 4413, 4414 4416 | H-alpha | 2 | 02 12 1723 | 35mm | 5"x7" | |
| 1745 | Whole disk | H-alpha | 5-7 | 02 12 1727 | 35mm | 8"x10" | |
| 1745 | Whole disk | white light | 3-7 | 02 12 1745 | 35mm | 8"x10" | mottled print |
| 1745 | 4408, 4410 4411, 4416 | H-alpha | 2-3 | 02 12 1750 | 35mm | 5"x7" | |
| 1745 | 4408, 4410 4411 | H-alpha | 3 | 02 12 1812 | 35mm | 5"x7" | |
| 1745 | Whole disk | white light | 5 | 02 16 2045 | 35mm | 8"x10" | |
| 1745 | Whole disk | white light | 10 | 02 17 2109 | 35mm | 8"x10" | |
| 1745 | Whole disk | white light | 5 | 02 18 2000 | 35mm | 8"x10" | |
| 1745 | Whole disk | white light | 7 | 02 19 2015 | 35mm | 8"x10" | |
| 1745 | Whole disk | white light | 7 | 02 20 1835 | 35mm | 8"x10" | |
| 1745 | 4421, 4422 | white light | 5 | 02 21 1715 | 35mm | 8"x10" | image is 5"x7" |
| 1745 | Whole disk | white light | 5 | 02 26 0831 | 35mm | 5"x7" | 9 cm disk |
| 1745 | Whole disk | H-alpha | 5 | 02 26 1457 | 35mm | 8"x10" | |
| 1745 | 4421, 4422 | H-alpha | 2-3 | 02 26 1533 | 35mm | 5"x7" | |
| 1745 | Whole disk | white light | 5-7 | 02 26 1720 | 35mm | 8"x10" | |
| 1745 | 4421 | white light | 3-5 | 02 29 1542 | drawing | | |
| 1745 | 4422 | white light | 3-5 | 02 29 1544 | drawing | | |
| 1745 | 4423 | white light | 3-5 | 02 29 1546 | drawing | | |
| 1745 | 4422 | white light | 3-5 | 03 01 2347 | drawing | | |
| 1745 | 4423 | white light | 3-5 | 03 01 2349 | drawing | | |
| 1745 | Whole disk | white light | 7 | 03 02 2145 | 35mm | 8"x10" | mottled print |
| 1747 | Whole disk | H-alpha | 5 | 04 20 1522 | 35mm | 8"x10" | |
| 1747 | 4468, 4471 | H-alpha | 2-3 | 04 20 1541 | 35mm | 5"x7" | |
| 1747 | Whole disk | white light | 7-10 | 04 20 1825 | 35mm | 8"x10" | |
| 1747 | Whole disk | white light | 5 | 04 21 1905 | 35mm | 8"x10" | |
| 1747 | Whole disk | white light | 7 | 04 21 1930 | 35mm | 8"x10" | |
| 1747 | Whole disk | white light | 10 | 04 21 2325 | drawing | | |
| 1747 | 4474 | white light | 5 | 04 21 2342 | drawing | | |
| 1747 | Whole disk | white light | 10 | 04 22 1705 | 35mm | 8"x10" | |
| 1747 | Whole disk | white light | 10 | 04 22 2350 | drawing | | |
| 1747 | 4474 | white light | 5 | 04 23 0002 | drawing | | |
| 1747 | Whole disk | white light | 10 | 04 23 1148 | 60mm | 8"x3" | mottled print |
| 1747 | Whole disk | white light | 10 | 04 23 1910 | drawing | | |
| 1747 | 4474 | white light | 5 | 04 23 1923 | drawing | | |
| 1747 | 4474-4477 | H-alpha | 3 | 04 25 1541 | 35mm | 5"x7" | |
| 1747 | Whole disk | H-alpha | 3 | 04 25 1632 | 35mm | 8"x10" | |
| 1747 | 4474, 4476 4477 | H-alpha | 3 | 04 25 1921 | 35mm | 5"x7" | |
| 1748 | Whole disk | H-alpha | 3 | 04 27 1245 | 35mm | 8"x10" | |
| 1748 | 4474, 4476 4477 | H-alpha | 2-3 | 04 27 1329 | 35mm | 5"x7" | flare |
| 1748 | Whole disk | white light | 3-5 | 04 27 1949 | 35mm | 8"x10" | |
| 1748 | 4474, 4476 4477 | white light | 5 | 04 27 1952 | 35mm | 8"x10" | |
| 1758 | 4474, 4476 4477 | H-alpha | 2 | 04 29 1547 | 35mm | 5"x7" | |
| 1748 | East Limb | H-alpha | 3-5 | 04 29 1551 | 35mm | 5"x7" | prom. PA=250° |
| 1748 | Whole disk | H-alpha | 3 | 04 29 1558 | 35mm | 8"x10" | |
| 1748 | Whole disk | white light | 3 | 04 29 1655 | 35mm | 8"x10" | |
| 1748 | Whole disk | white light | 3-5 | 04 29 1701 | 35mm | 8"x10" | |
| 1748 | 4476 | white light | 2 | 05 03 1836 | 35mm | 5"x7" | |

The following assembled sequences of photographs of individual regions have resolutions of about 1 arcsec clearly showing granulation. All are from Carrington Rotation 1745:

NOAA Region 4423

| Day | Time |
|---|---|
| 1984 Feb 24 | 1207 UT |
| Feb 25 | 1129 UT |
| Feb 26 | 0940 UT |
| Feb 27 | 1222 UT |
| Feb 28 | 0938 UT |
| Feb 29 | 1111 UT |

NOAA Region 4421-2

| Day | Time |
|---|---|
| 1984 Feb 21 | 0832 UT |
| Feb 23 | 1139 UT |
| Feb 24 | 1205 UT |
| Feb 27 | 1225 UT |
| Feb 28 | 0940 UT |

NOAA Region 4421

| Day | Time |
|---|---|
| 1984 Feb 23 | 1139 UT |
| Feb 24 | 1206 UT |
| Feb 25 | 1131 UT |
| Feb 28 | 0940 UT |

The data in this report are available at no charge. We request that the specific observer and the Solar Section of the ALPO be acknowledged in some manner for any data used.

## REFERENCES


HILL, R.E. 1983 "Burning Bridges", **The Journal of the Assoc. of Lunar and Planetary Observers (JALPO), Vol. 30,** No. 1-2, Jun. 1983, pp. 36-40.

HILL, R.E. 1984 "Observations of the May 30, 1984 Annular Solar Eclipse", **The JALPO, Vol. 30,** NO. 11-12, Nov. 1984, pp. 248-252.

HILL, R.E. 1985 "ALPOSS Solar Observations for Rotations 1732-1734", **The JALPO, Vol. 31,** No. 1-2, Feb. 1985, pp. 16-20.

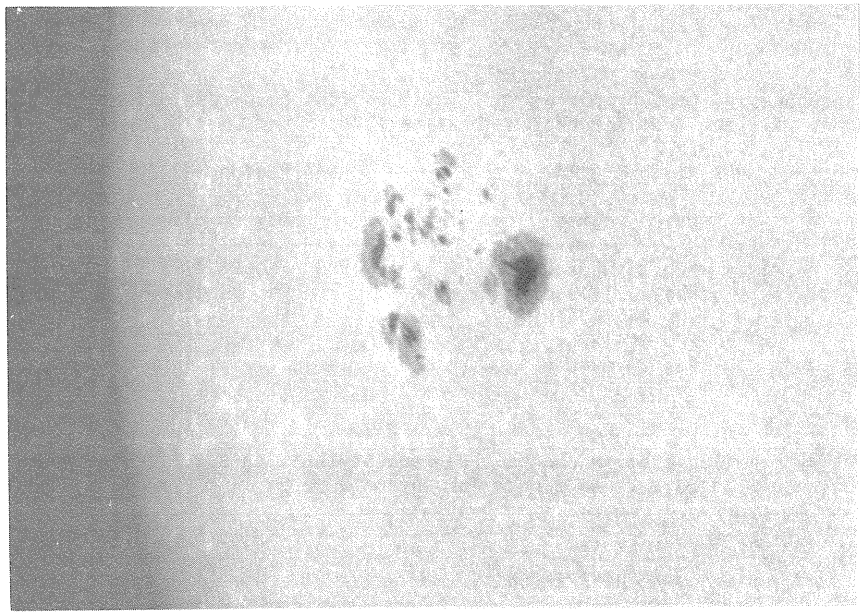

N
E

White Light Active
Region 4423

24 February 1984
1207 UT

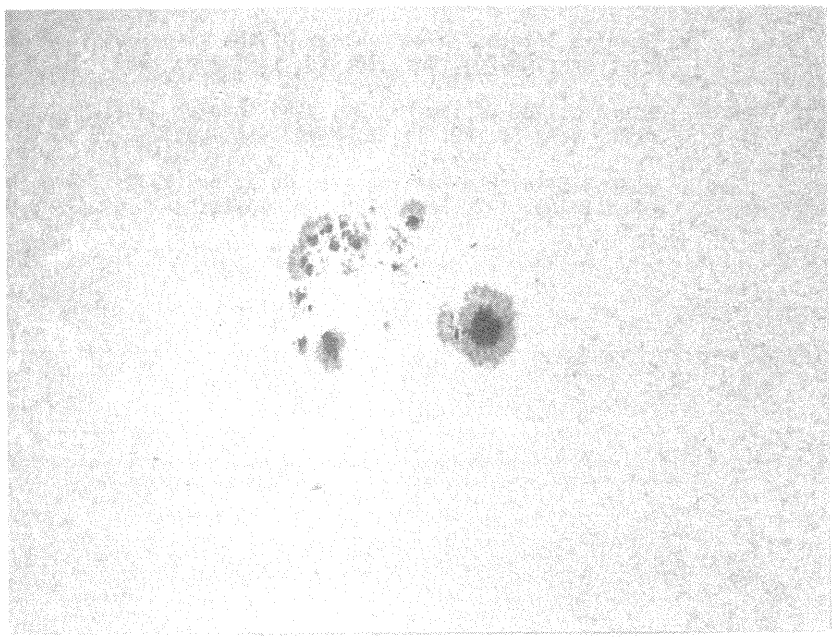

25 February 1984
1129 UT

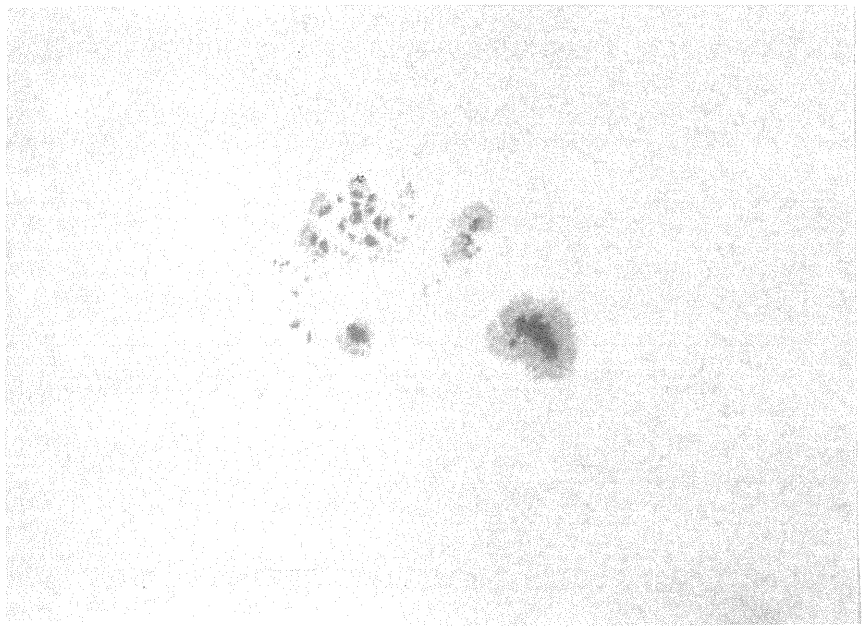

26 February 1984
0940 UT

by J. Dragesco

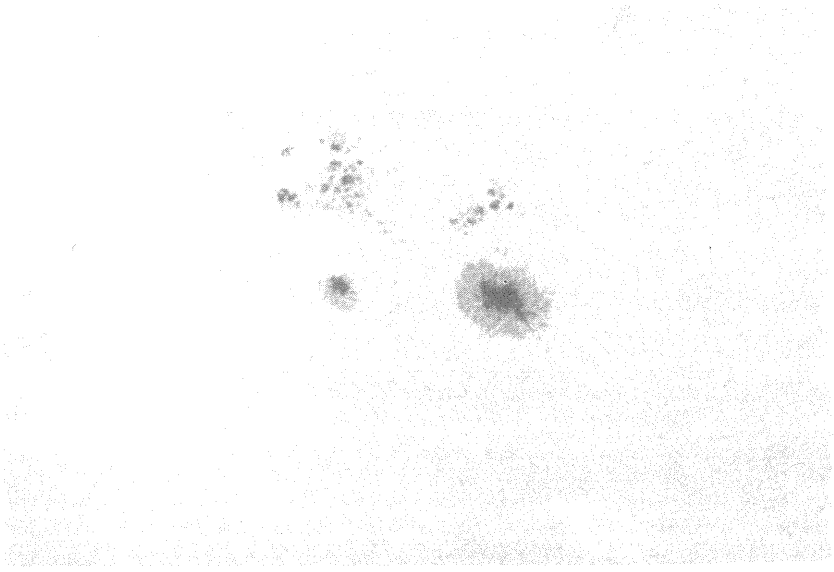

N
E

White Light Active
Region 4423

27 February 1984
1222 UT

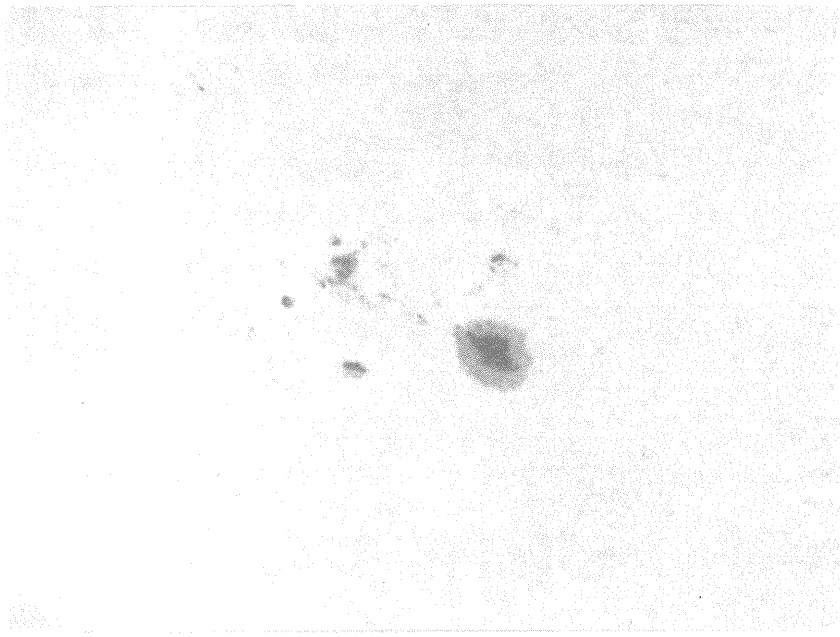

28 February 1984
0938 UT

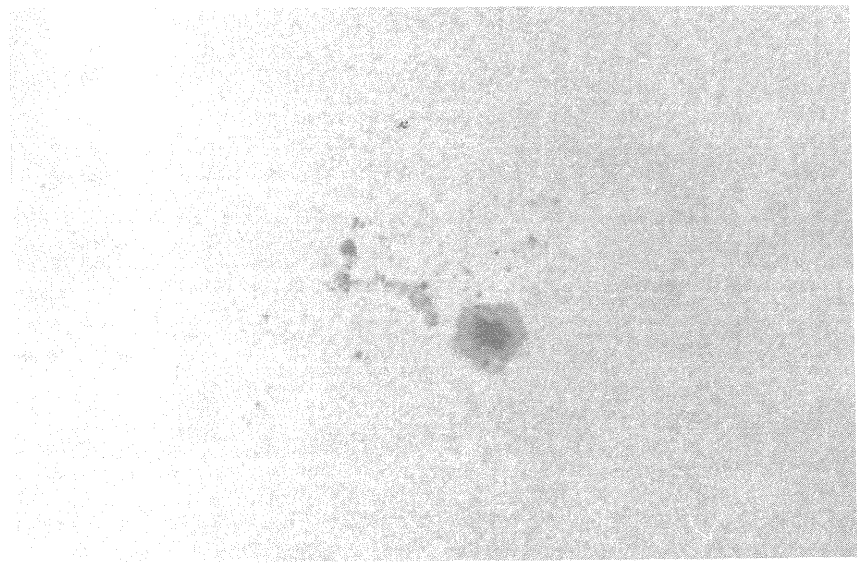

29 February 1984
1111 UT

by J. Dragesco

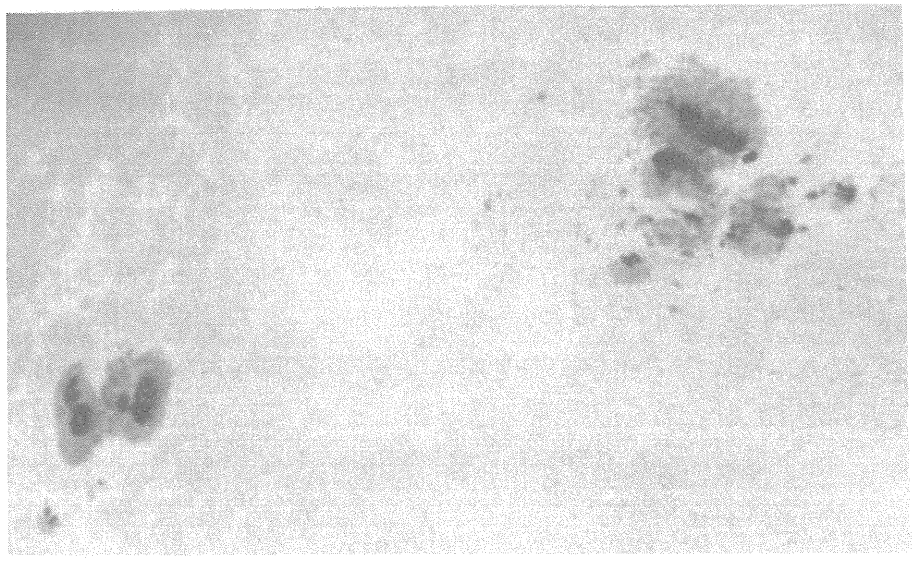

N
E

White Light Active
Regions 4421/4422

21 February 1984
0832 UT

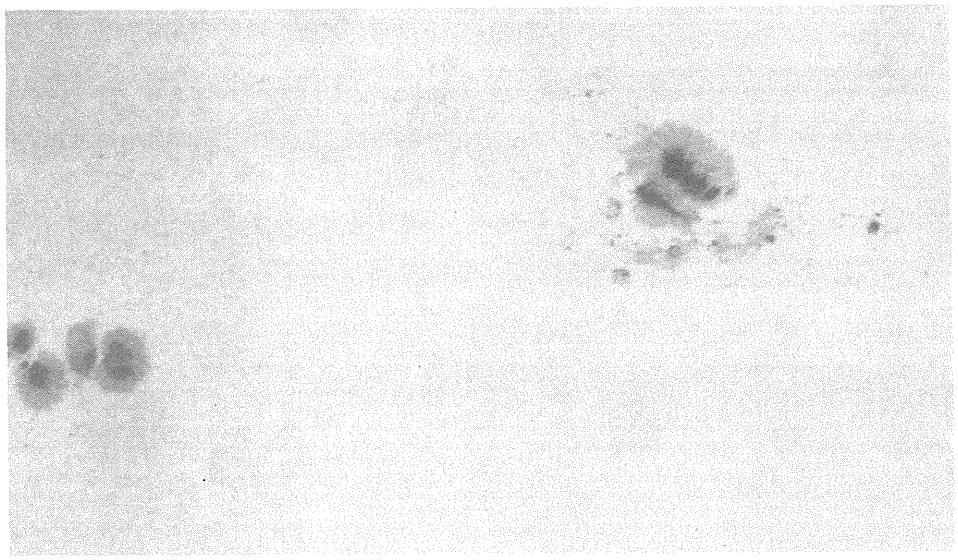

23 February 1984
1139 UT

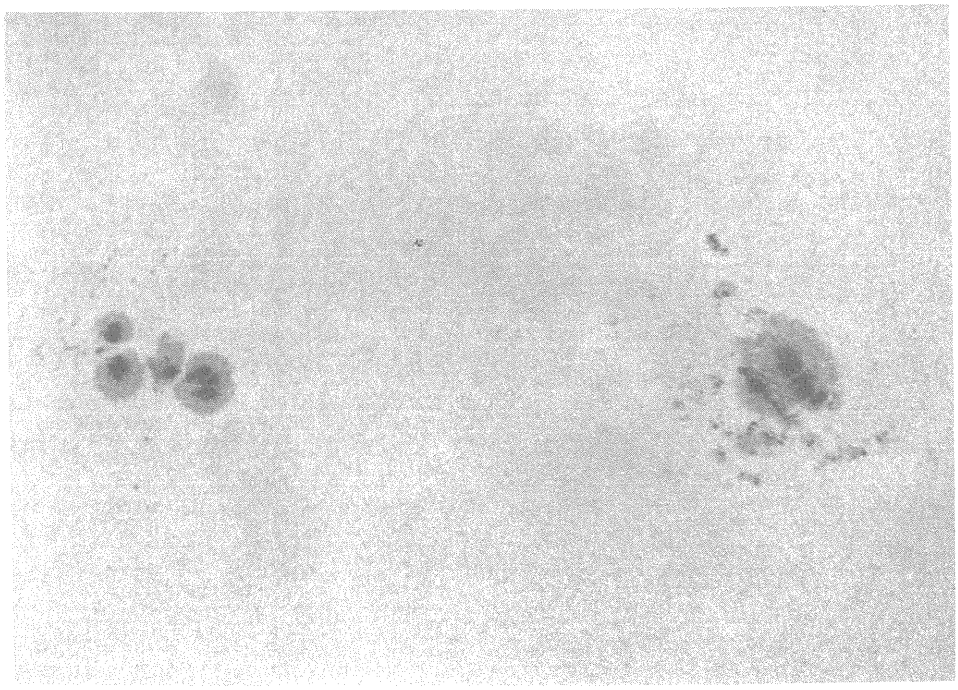

24 February 1984
1205 UT

by J. Dragesco

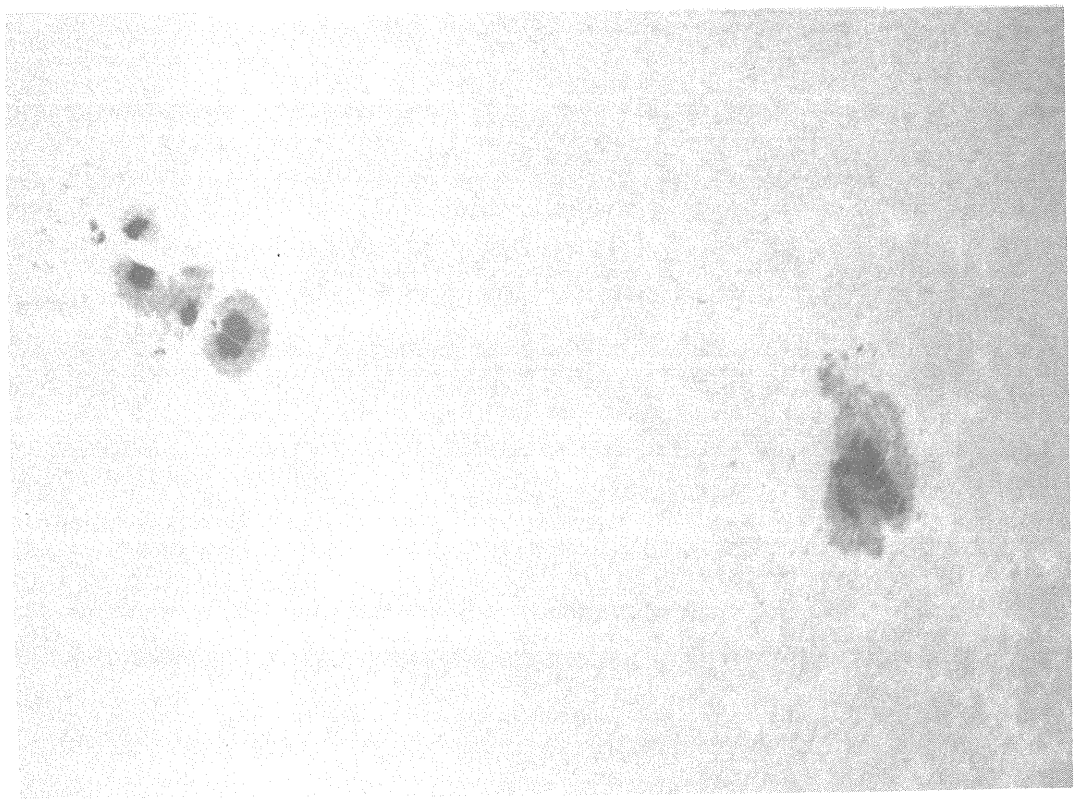


White Light Active
Regions 4421/4422

27 February 1984
1225 UT

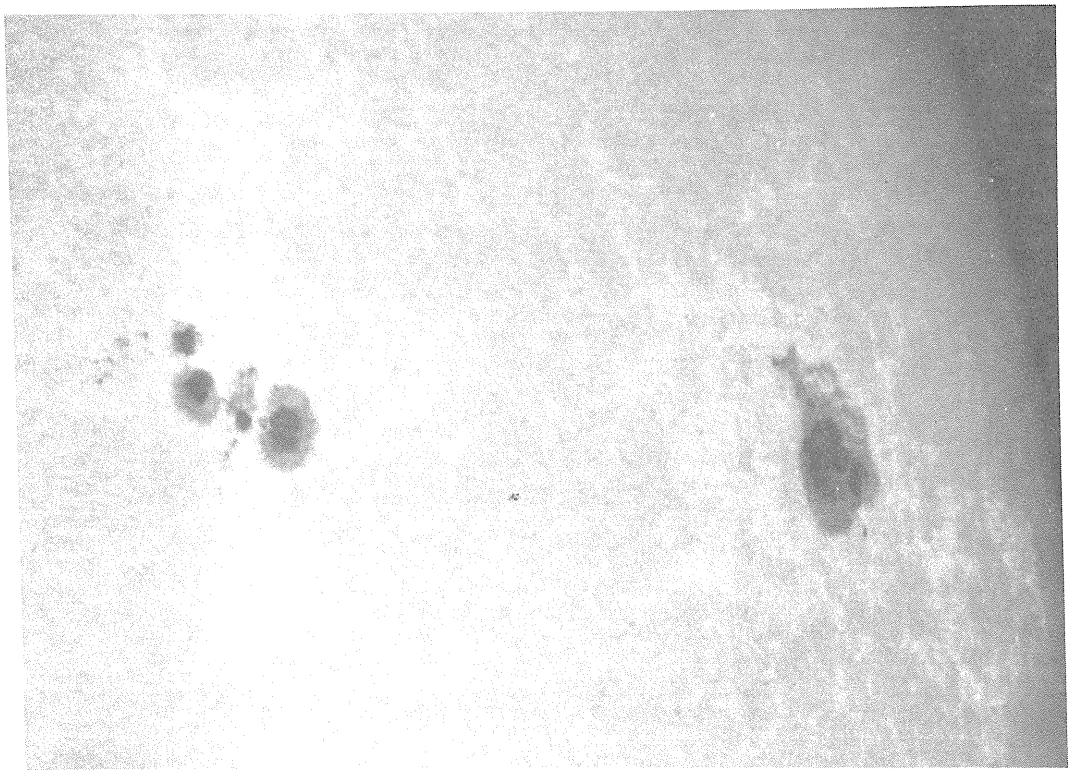

28 February 1984
0940 UT

by J. Dragesco

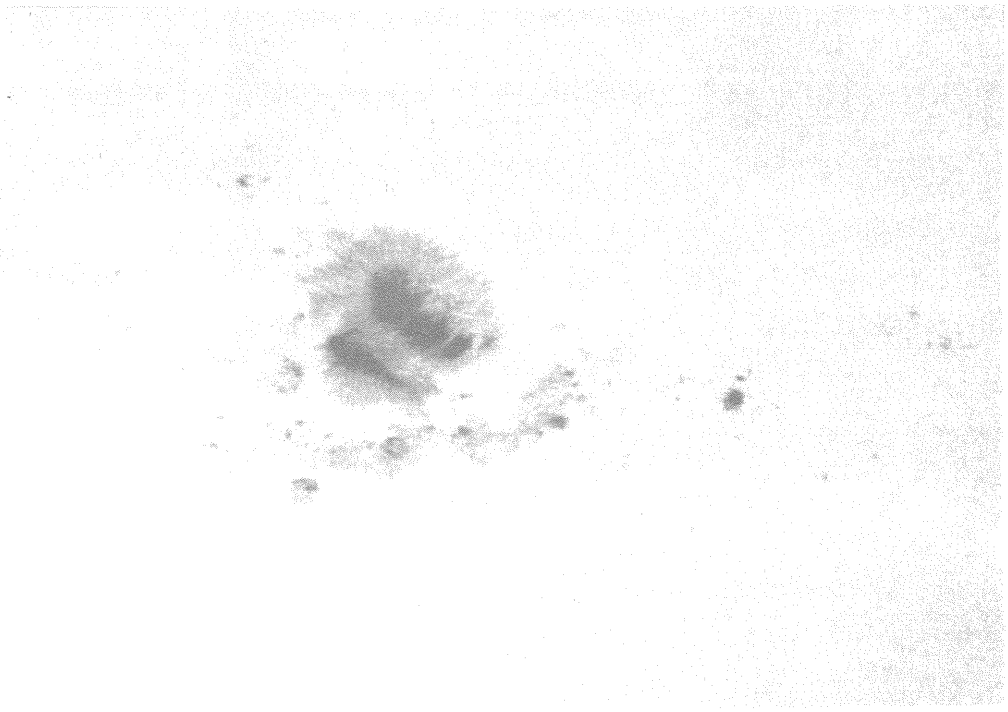


White Light Active
Region 4421

23 February 1984
1139 UT

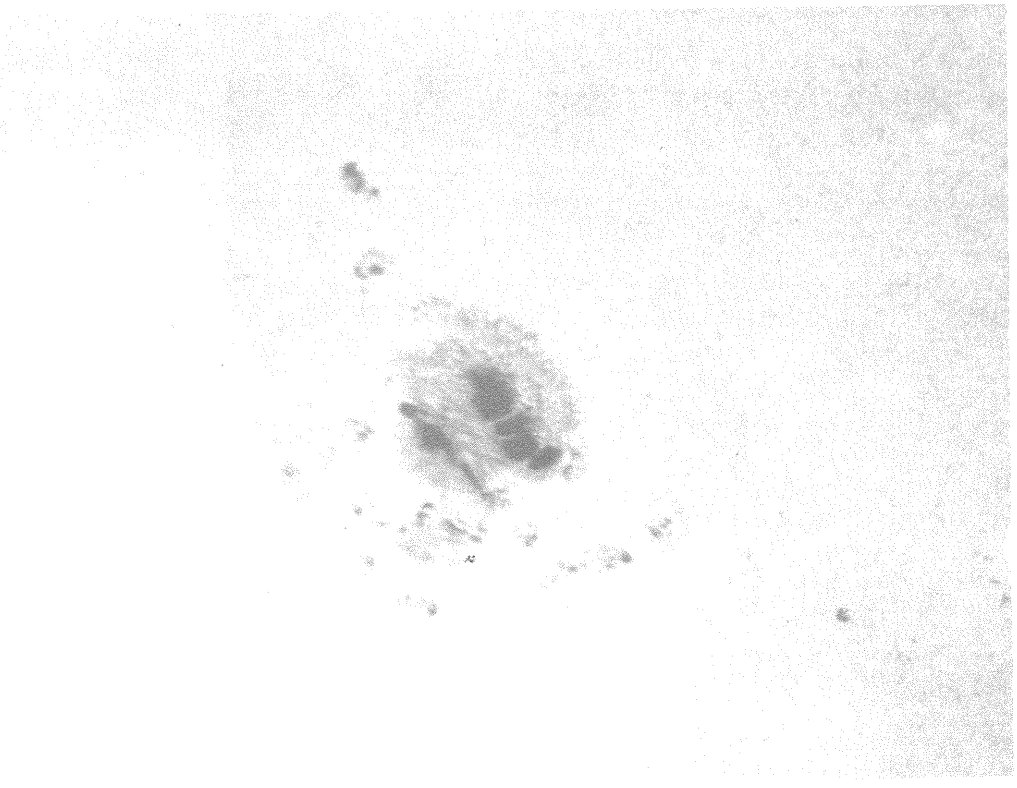

24 February 1984
1206 UT

by J. Dragesco

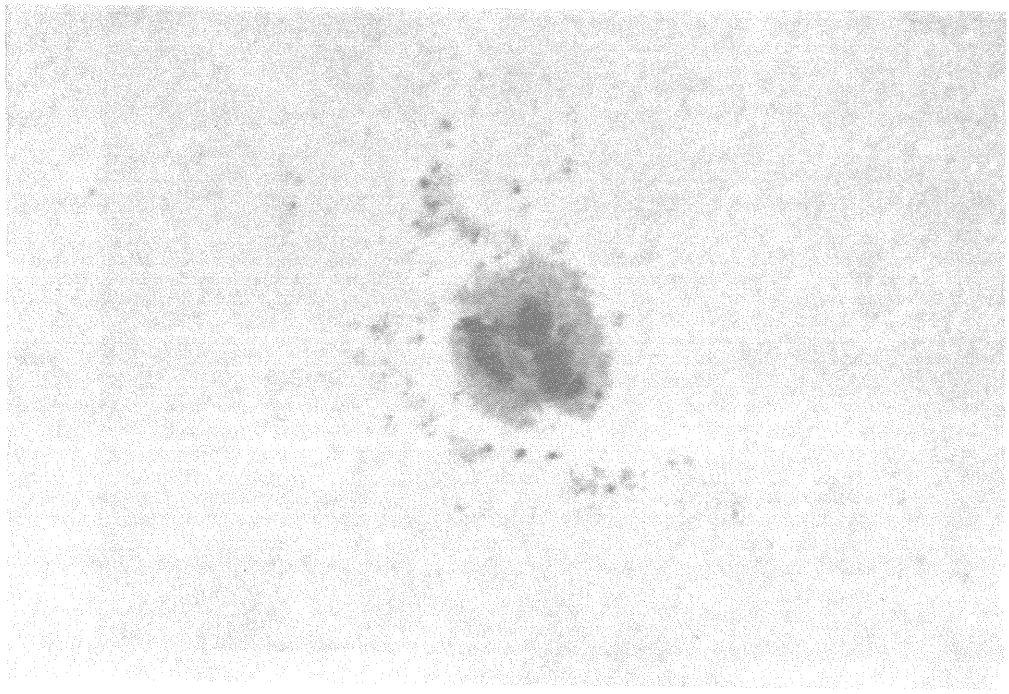

N
E

White Light Active
Region 4421

25 February 1984
1131 UT

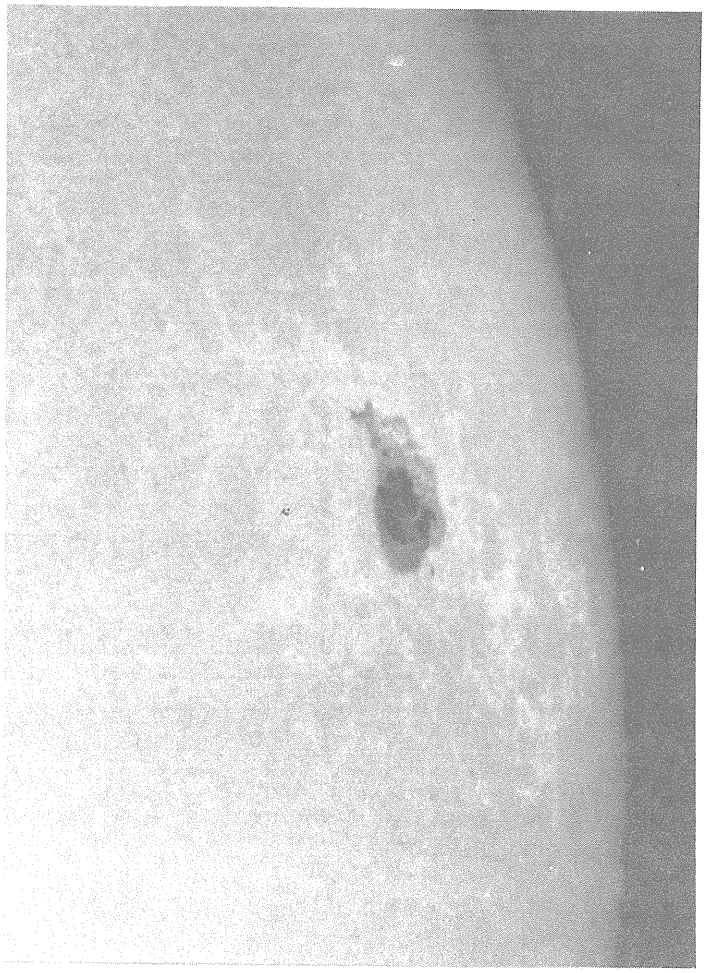

28 February 1984
0940 UT

by J. Dragesco

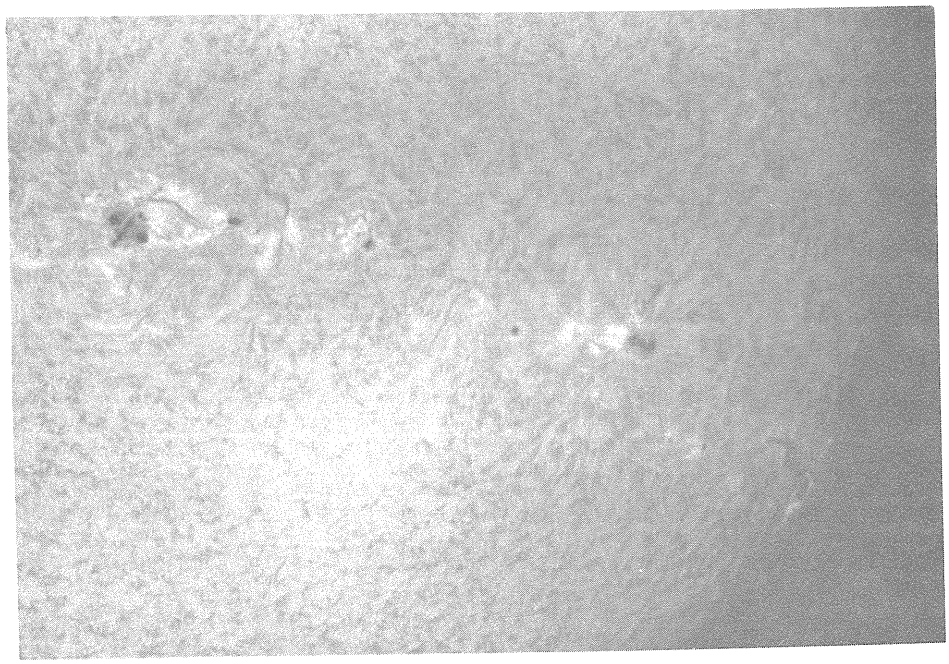


H-alpha photo 1723 UT on 12 February 1984, S12 285° longitude, showing Active Regions 4408, 4410, 4413, 4414, and 4416 (photo by R. Tatum).

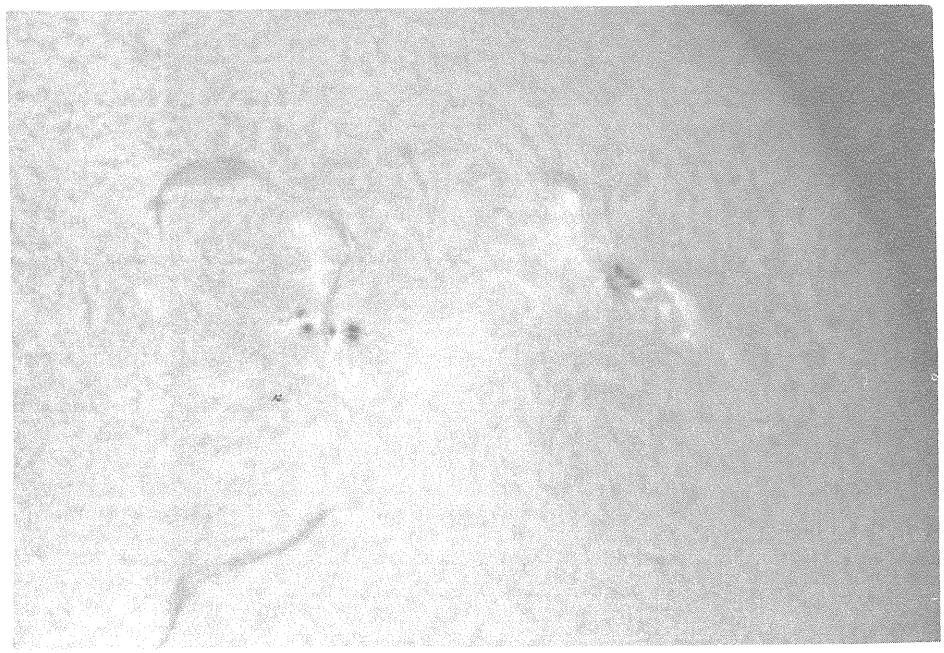

H-alpha photo 1533 UT on 26 February 1984, N11 100° longitude, showing Active Regions 4421 and 4422 (photo by R. Tatum).

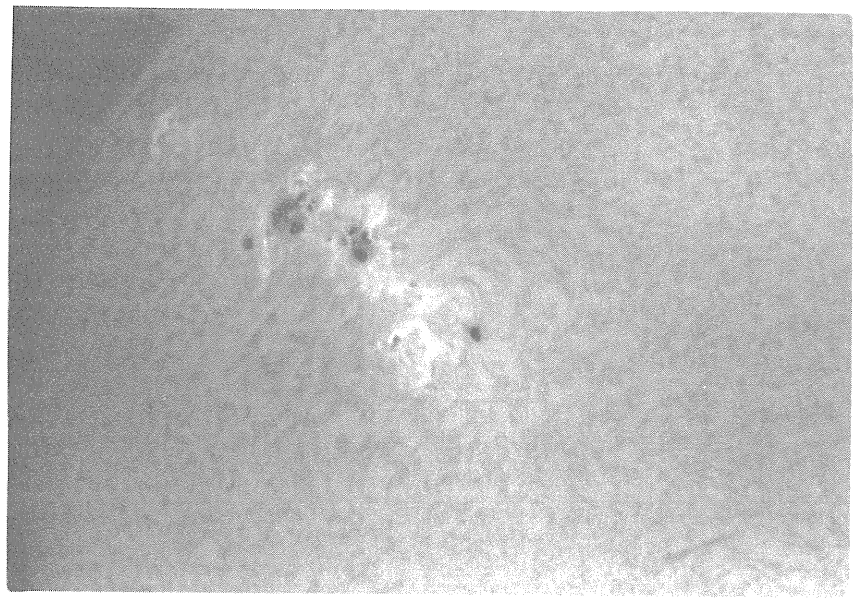

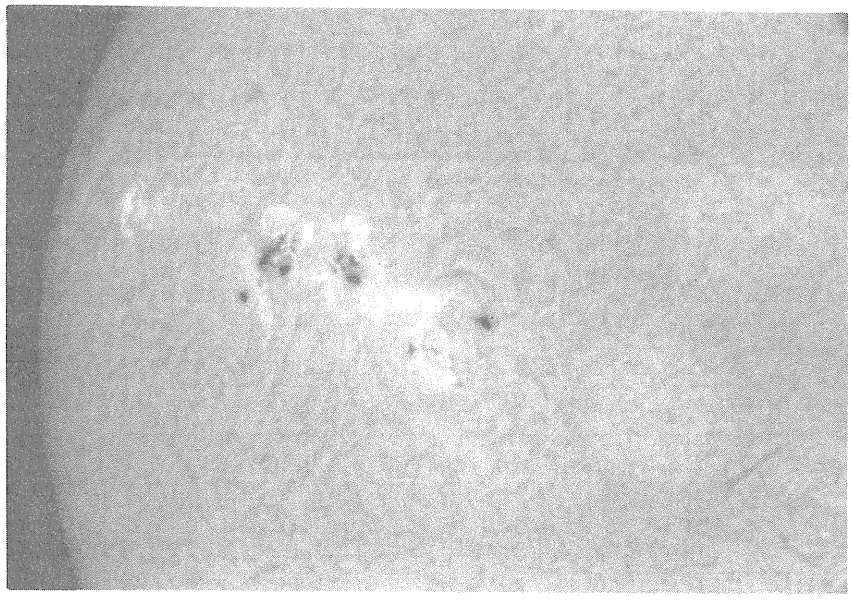

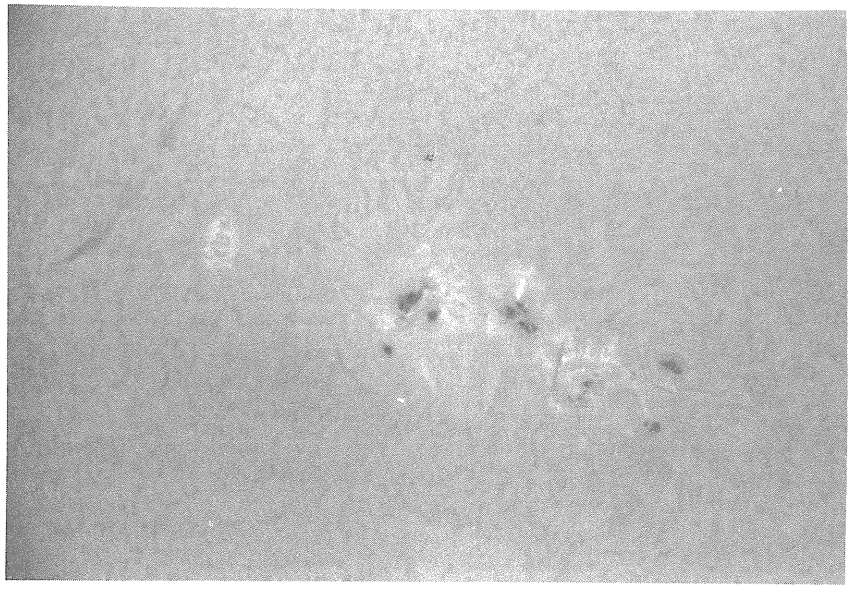

H-alpha photos showing Active Regions 4474, 4476, and 4477.

25 April 1984
1541 UT

25 April 1984
1921 UT

S10 350°longitude

27 April 1984
1329 UT

S10 343°longitude

by R. Tatum

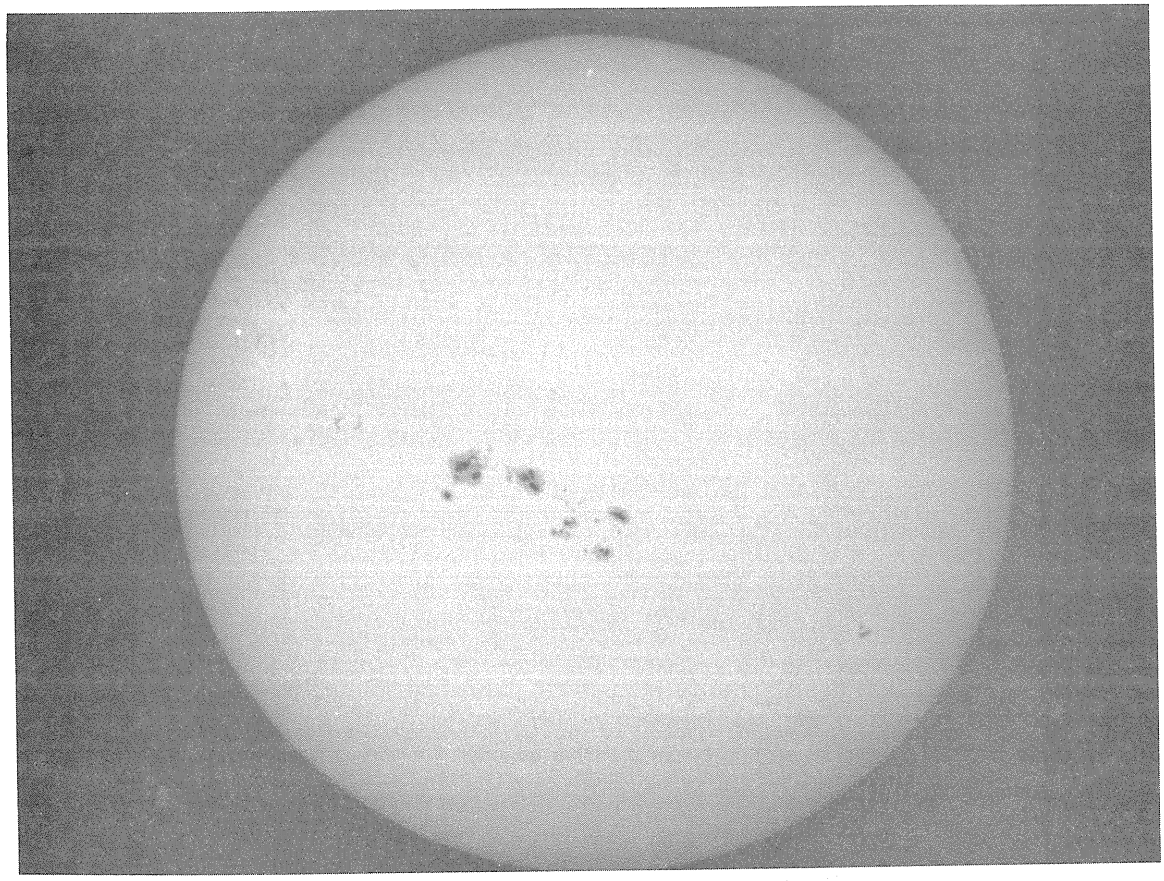

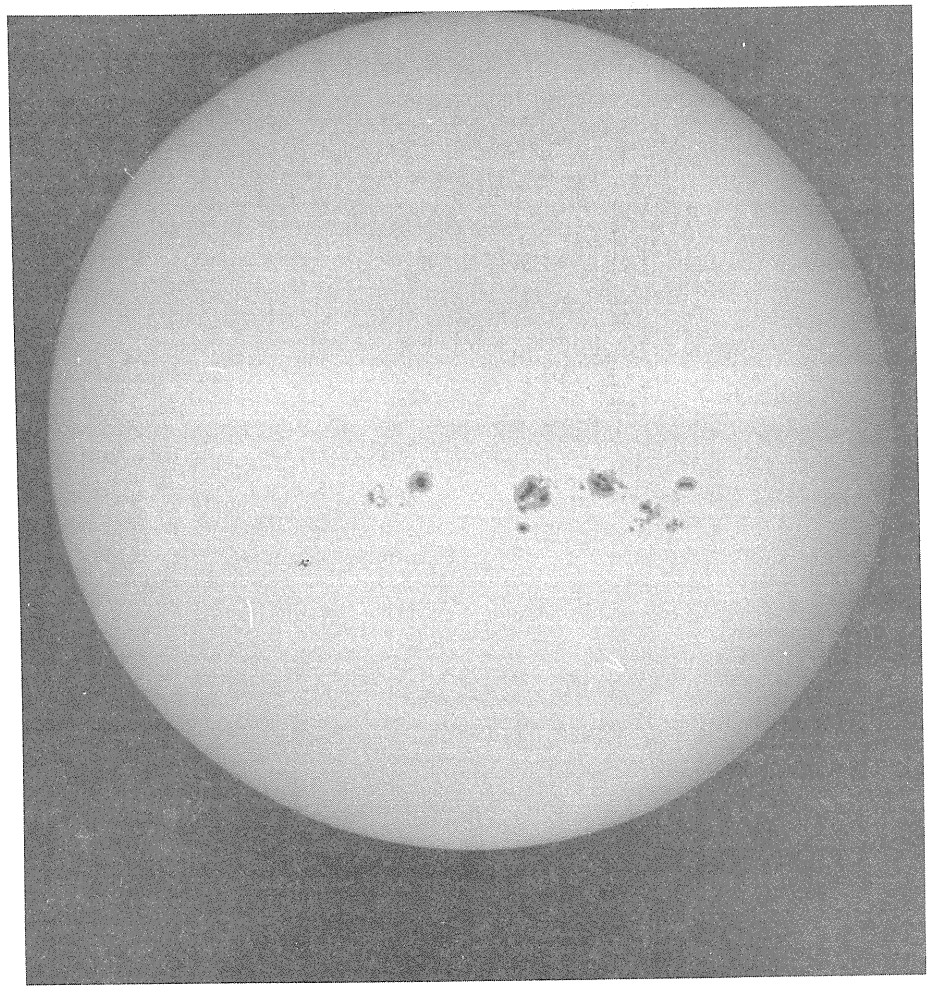

White Light
Whole Disk

Top photo is
27 April 1984.

Side photo is
29 April 1984
(angle
corrected).

by B. Timerson

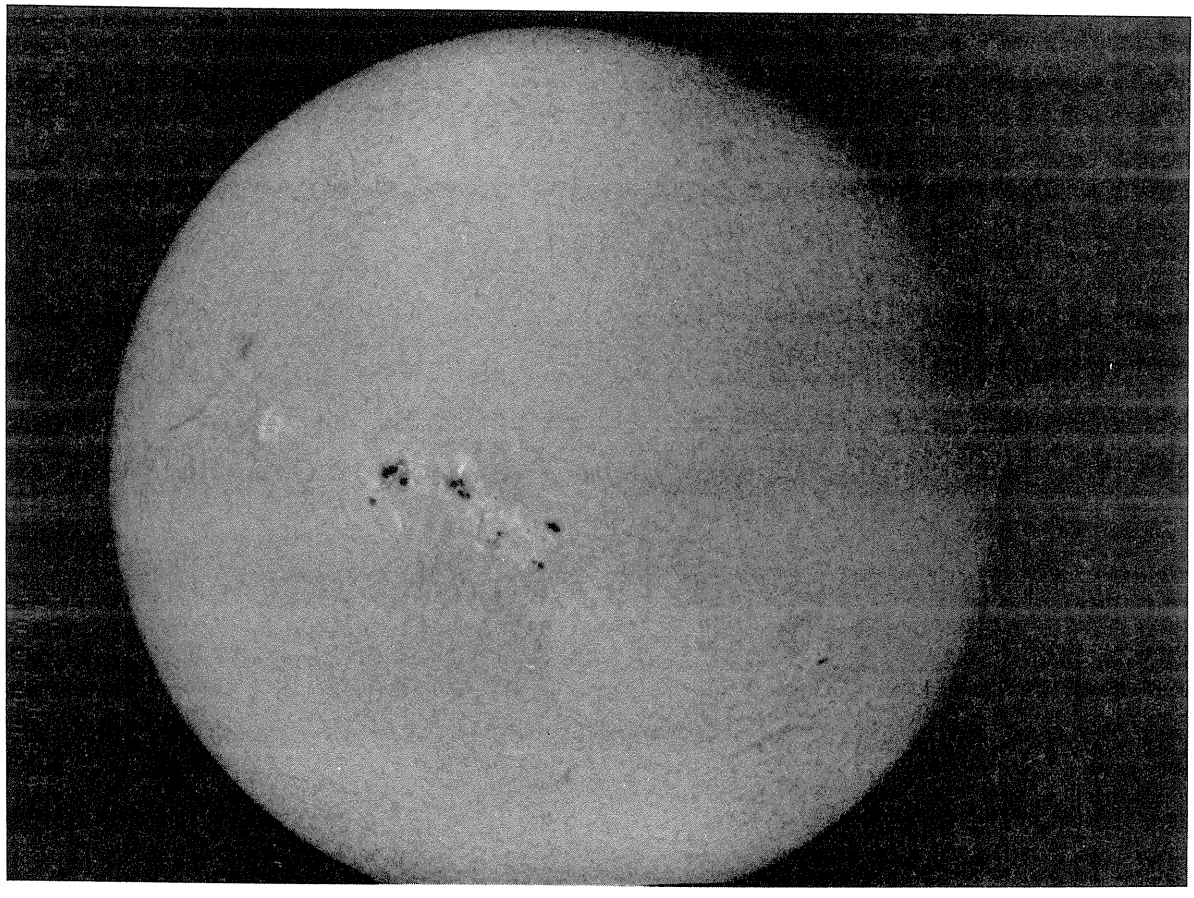

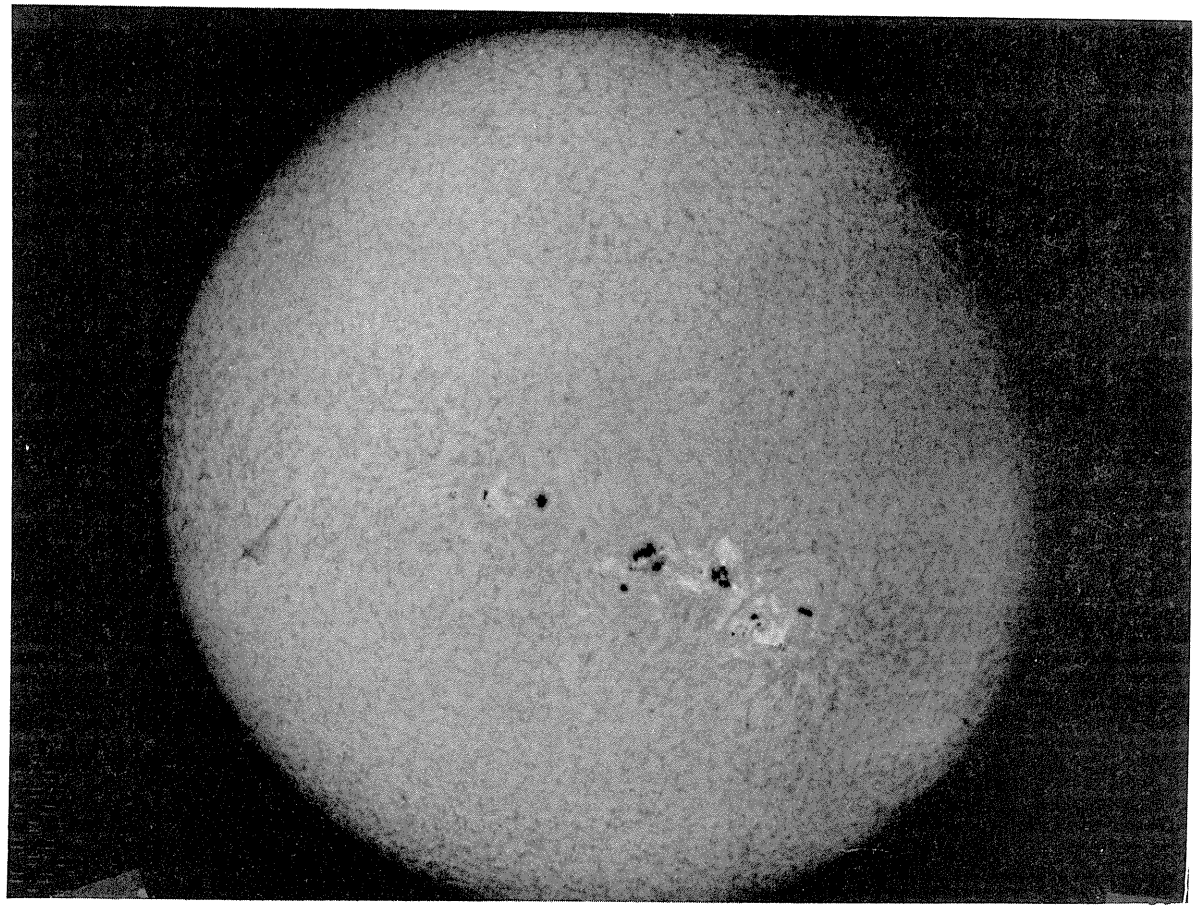

H-alpha whole disk photos: Top photo is 27 April 1984. Bottom photo is 29 April 1984.
(photos by R. Tatum)

# Summary of the Solar Radio Events during the 16 February and 24 April 1984 Solar-Terrestrial Events

by

J. Hruska
Energy, Mines and Resources, Ottawa, Canada

## Solar Radio Observations in February 1984

The most interesting solar radio events recorded on 16 February were the Type II and Type IV bursts which originated in the Active Region 4408, located behind the western limb of the solar disk. The special characteristics of these solar radio emissions are disussed by H. Aurass et al., I.M. Chertok et al., E.W. Cliver et al., and P. Zlobec et al. East-West solar scans on various frequencies for the same period from the Pulkovo Astronomical Observatory are provided by V.A. Abramov-Maksimov at al. and from the Ratan Astronomical Observatory by V.M. Bogod et al.

The solar radio observations during the period from 8 to 15 February are summarized by I.M. Chertok et al. They also discuss the unusual dynamic spectrum of the Type II bursts and its possible origin from the shock wave propagation along curved trajectory.

In the detailed analysis of the onsets of these bursts at different frequencies, H. Aurass et al. noted the delays at higher frequencies and an impulsive time profile at all frequencies, despite the weakness of the microwave emission.

P. Zlobec et al. investigated the polarization of these bursts at metric wavelengths. The Type IV burst was unpolarized and the Type II burst had, as expected, zero polarization, but the spiky structures at the top of enhancement were polarized.

E.W. Cliver et al. provide the flux density profiles and instantaneous flux density spectra for eight fixed frequencies logarithmically spaced from 245 to 15400 MHz. They determined precisely the onset of the microwave burst.

## Solar Radio Observations in April 1984

The solar radio events correlated with the Active Region 4474 visible on the solar disk during 20 April to 3 May 1984 and with the proton flare on 24-25 April are discussed by H. Aurass et al., G.P. Chernov et al., M. Nonino et al. and by S. Enome et al. East-West solar scans on 23 mm, 32 mm and 44 mm for 23-25 April 1984 from the Pulkovo Astronomical Observatory are provided by V.E. Abramov-Maksimov et al. and solar scans on 3 cm and 8 cm for April and May 1984 from Toyokawa Observatory are provided by S. Enome et al.

A list of radio bursts and their parameters originating in AR 4474, examples of the time profiles of microwave of bursts on 27-30 April and a list of types of coronal mass ejections (SGD) during the investigated period were prepared by H. Aurass et al.

The characteristics of the noise storms and of the Type III bursts during the period 20 April to 2 May 1984 the fine structures of bursts on 26 April, estimates of the proton flux parameters by radio data, and the difference between the calculated and observed value of PCA are presented by G.P. Chernov et al.

A detailed description and examples of enhancements and polarization at metric wavelengths on 25 and 26 April 1984 is given by M. Nonino et al.

The microwave activities associated with the AR 4474 are analyzed by S. Enome et al. The authors discuss the temporal coincidences among the absorption at 9.4 GHz and 3.75 GHz, the decimeter wave emission at 1 GHz and 2 GHz, and the simultaneous optical observation of an ejecton of dark matter in the H-alpha at the Hida Observatory. They consider that there could be a physical link between the absorption and the decimeter-wave burst via the dark matter, but more similar events are necessary for further investigation.

# U-shaped Type II Burst Connected with the Flare on 16 February 1984 and Preceding Activity

by

I.M. Chertok, V.V. Fomichev, A.A. Gnezdilov
R.V. Gorgutsa and A.K. Markeev
IZMIRAN, Troitsk, Moscow Region, USSR

Observations of solar radio emission at IZMIRAN in 1984 February were recorded with the 169, 204 and 3000 MHz radiometers and with the radiospectrographs at 45-90 and 90-180 MHz. We describe the general characteristics of the active period and the 16 February 1984 flare.

## Type I Noise Storm

In the period before the 16 February 1984 flare, the Type I noise storm was the dominant type of the meter range activity. Shown in Figures 1b and 1c are the variations of the number of Type I bursts per hour and the flux density of the continuum and burst components of the storm at 204 MHz for 7-16 February. Both components developed analogously, displaying a number of amplifications on 8, 9, 11, 12 and 14 February. Note that in this noise storm the burst component was prevalent for all days with the exception of 7 February. The average amplitude of the Type I bursts for three-hour intervals was about two times the flux density of the continuum background.

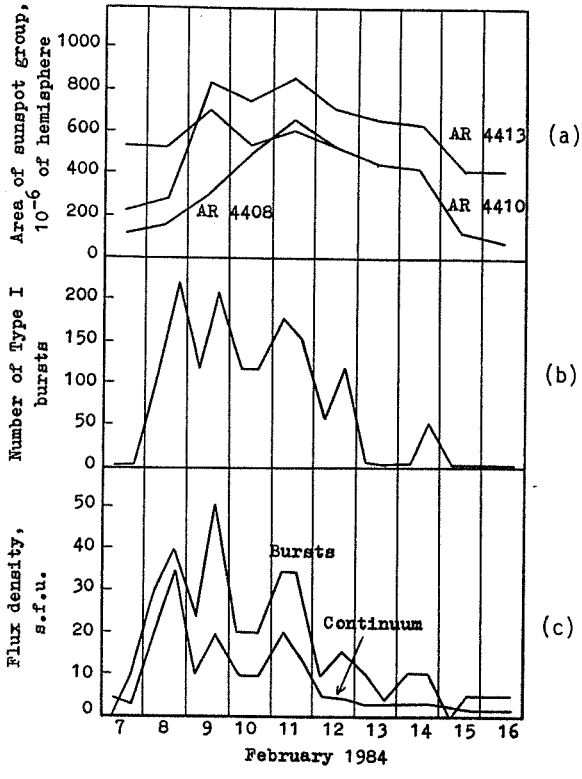


Figure 1. Variations of the sunspot group areas and the noise storm characteristics at 204 MHz during 7-16 February 1984.

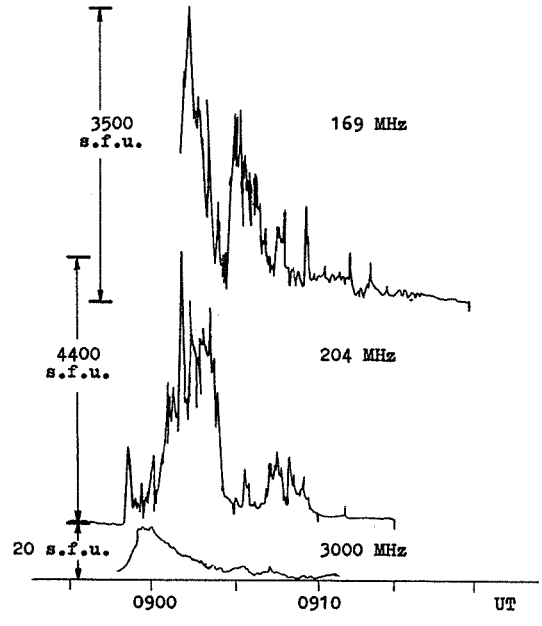


Figure 2. Radio burst observed on 16 February 1984 at IZMIRAN

In Figure 1a the variation of the total area of three of the largest sunspot groups in the NOAA Active Regions (AR) 4408, 4410 and 4413 is shown for the same period. Comparing these, we can see that the noise storm development cannot be connected with the evolution of any single active region and obviously all of these sunspot groups contributed to the radio emission during different periods. This conclusion is confirmed by the Nancay interferometric observations at 169 MHz (SGD, 1984).

## The 16 February Flare

The 16 February event was the most significant one during the period 7-16 February 1984. It was initiated by the flare in the AR 4408 behind the solar limb and included bursts with unusual properties in the microwave and meter ranges.

**Microwave burst.** The Active Region 4408 on 16 February was at longitude $\sim$ W140. Nevertheless, a weak microwave burst was observed in connection with the flare under consideration. The time-intensity

profile of the burst at 3000 MHz is shown in Figure 2. The burst began about 0815:18 UT simultaneously with a group of Type III bursts, had small time duration $\tau \sim 5$ min and weak flux density $S \sim 20$ solar flux units (s.f.u.).

The event was accompanied by a solar cosmic ray ground level event (GLE). The solar flares giving rise to the GLEs have, as a rule, the radio flux density $S \geq 1000\text{-}2000$ s.f.u. at frequencies $f \geq 3000$ MHz. Hence, if the observed microwave burst was generated in the behind the limb AR 4408 the recorded intensity was about 1-2 percent of the flux density which should be observed if such a flare took place on the visible disk. The geometry shows that the main part of the 3000 MHz radio emission was occulted. The upper part of the source extended up to rather large heights $h \geq (0.4\text{-}0.5)R_{\odot}$, thus emitting only 1-2 percent of the total flux density. This seems most probable.

It is possible that the observed weak microwave burst was connected with a more compact and low-situated source and was observed in the rays partially reflected and scattered on plasma inhomogenities located higher in the corona.

One more alternative explanation is the existence of a connection between the behind the limb AR 4408 and 4413 situated on the visible part of the disk (W50-60). The distance between these regions was about $10^{11}$ cm. A part of the electrons (1-2 percent) accelerated in the flare in AR 4408 could reach in approximately 10 seconds the AR 4413 and cause the weak microwave burst there. No restraints in the altitude of the centimeter source are placed in this case. However, a corresponding optical flare was not recorded in this region.

**Type II burst.** In the meter range the event began almost simultaneously with the centimeter burst and consisted of Type III burst groups followed by the Type II and IV bursts with total duration of about 21.5 minutes in the range 45-180 MHz (Figure 3). Observing the radio emission from the far behind the limb flare indicates the weak directivity of the bursts mentioned above. In the case of the Type III bursts with the quasi-radial propagation of the electron streams, the angle between the line-of-sight and the stream velocity was about 135-140 degrees. Such a situation is hardly possible if the Type III bursts were generated at the fundamental mode. However, for the emission at the second harmonic of the plasma frequency, the directivity diagram has lobes to the solar surface that allows observation of the emission from the behind-the-limb source. The diffuse character of the dynamic spectrum of the Type III bursts is also seen on the harmonic.

The main peculiarity of the event is the unusual dynamic spectrum of the Type II burst. Figure 3 shows the range 45-90 MHz consisting of three separate diffuse components: 0900-0903:54 UT, 0904:30-0910:48 UT and 0916:42-0921:42 UT. The two initial components have the inverted U-shaped form of the dynamic spectrum. The third one has no visible drift. In all three components elements of the herringbone structure are present. Analyzing the data in the broader frequency range 45-180 MHz shows that the U-shaped components shown in Figure 3 should be attributed to the fundamental emission. For the ascending branch of the first component one can estimate the shock wave velocity in the corona from the drift of the high-frequency edge using the 2xNewkirk model of the density distribution. This velocity is V about 3000 km/s. Estimating the disturbance velocity at lower altitudes by the time delay between the Type II radio burst start relative to the beginning of the centimeter burst gives the same value.

As a whole the Type II burst dynamic spectrum under consideration is analogous to the 28 March 1980 burst described by Markeev et al. (1983). Its origin may be caused by the shock wave propagation along a curved trajectory (McLean and Nelson, 1977). Because AR 4408 was located far behind the limb, the Type II radio burst was probably excited by the shock wave propagating in the direction of the observer, i.e., to the visible part of the solar disk. Perhaps the large-scale coronal structures connecting the distant active regions were a wave duct for the shock in this case.

The outlined character of the shock wave propagation could influence the solar cosmic ray escape and propagation conditions. This situation took place, for example, in the 30 March 1969 event described by Palmer and Smerd (1972).

## REFERENCES


MARKEEV, A.K., V.V. FOMICHEV, I.M. CHERTOK, A. BHATNAGAR, R.M. JAIN, R.M. SHELKE and R.V. BHONSLE (1983). "U-shaped type II solar radio bursts associated with the 1980 March 28 flare," **Bull. Astron. Soc. India, 11**, No. 4, 318-326.

McLEAN, D.J. and G.J. NELSON (1977). "Recent data on type III solar radio bursts," **Izv. VUZov. Radiofisika, 20**, No. 9, 1359-1368.

PALMER, I.D. and S.F. SMERD (1972). "Evidence for a two-component injection of cosmic rays from the solar flare of 1969, March 30," **Solar Phys., 26**, No. 2, 460-467.

SGD (1984). **Solar-Geophysical Data**, 475 Part 1, 476 Part 1, 480 Part II, U.S. Department of Commerce (Boulder, Colorado, USA, 80303).

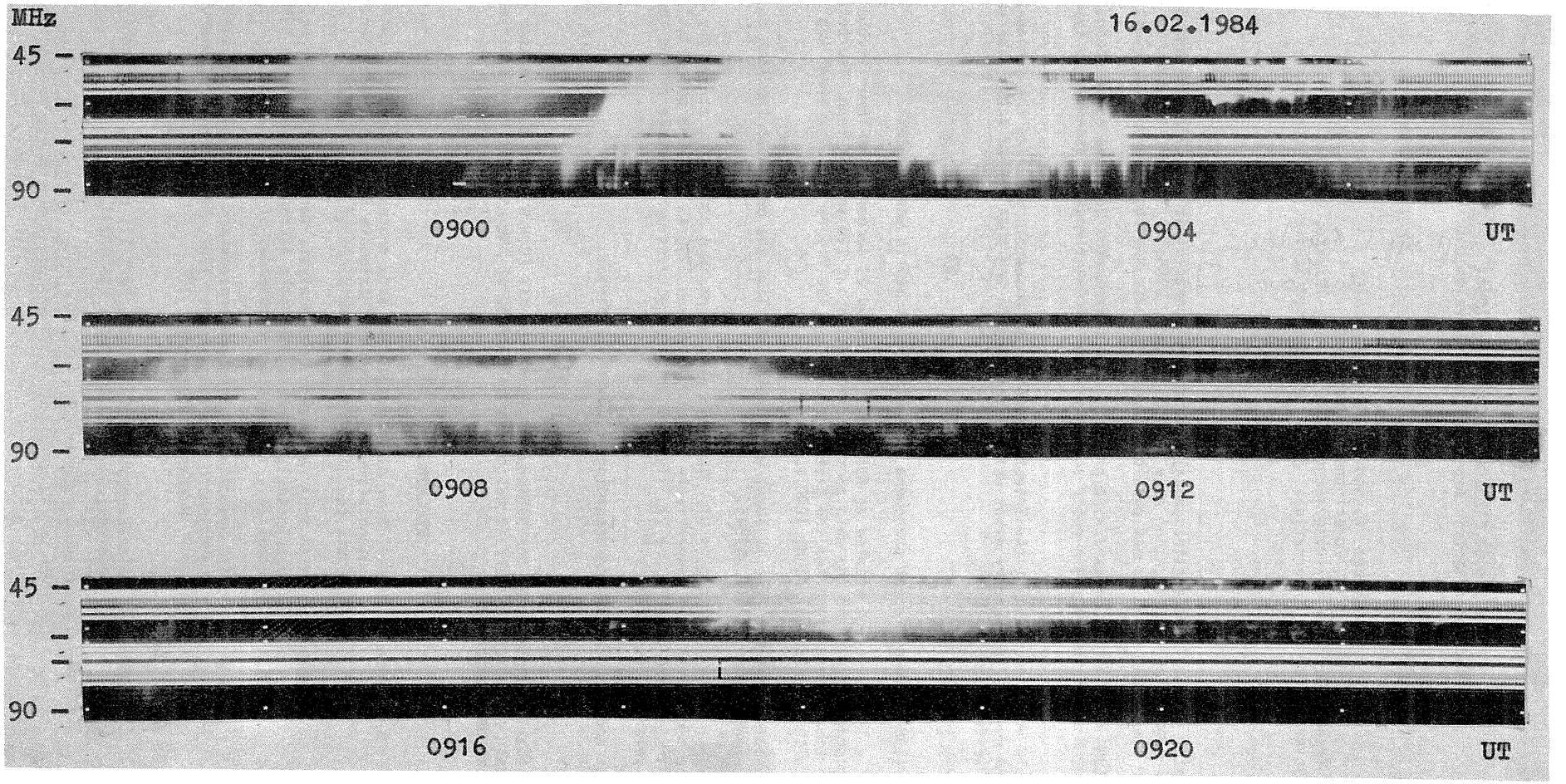


Fig. 3. Dynamic spectrum of the U-shaped burst on 16 February 1984 in the range 45-90 MHz recorded at IZMIRAN.

# The Proton Flare of 16 February 1984
# Radiopolarimetric Aspect at Meter Wavelengths

by

P. Zlobec, M. Nonino, M. Messerotti*
M. Comari and L. Fornasari
Trieste Astronomical Observatory, via Tiepolo, Trieste, Italy
*also associated with the International School of Advanced Studies, Trieste, Italy

## Introduction

The radiopolarimeter of the Trieste Astronomical Observatory operating at 237, 327, 408 and 606 MHz has a rather good time resolution (digitization rate 50 Hz) (Comari, 1985a). The antenna beam is larger than the Sun's angular dimension, so it is not possible to discriminate the region producing events.

During February 1984 many active regions were present. The polarimeter detected noise storms, particularly active during 8 and 9 February and other activity at metric wavelengths (essentially Type III bursts).

The most remarkable event recorded at the Trieste Astronomical Observatory during the period 6 February - 5 March 1984 was the 16 February event which originated in the NOAA Region 4408. The source region was behind the western limb.

## Data Description

According to SGD (1984) two different phenomena were visible at metric wavelengths:

1. At 0858:09 UT a Type IV event started at 606 MHz. It lasted 26 seconds. At lower frequencies the beginning was a few seconds delayed and the main part duration was about 100 seconds long. The polarization was zero for the whole time interval and for the given frequencies (see Figure 1). The event was stronger at higher frequencies with a maximum of about 1000 s.f.u.

It is worthwhile noting that the Type IV burst was unpolarized like the ones near the limb during the 14 and 18 August 1979 events (Kane et al., 1984).

2. The Type II burst started at 0900:23 UT. The main maximum reached 800 s.f.u. at 327 MHz and 3000 s.f.u. at 237 MHz. The two maxima were respectively at 0900:37 UT and 0900:47 UT. The polarization was, as usual for Type II bursts, zero (see Figure 2). Typical spiky structures were visible at the top of enhancements and were polarized (see Figure 3).

The data reduction and plots were made according to Comari (1985b).

## Acknowledgements

This work was partially supported by the National Research Council (C.N.R.) and the Ministry of Education (M.P.I.). Data reduction was carried out on the VAX 11/750 of the Astronet Pole of Trieste at the Trieste Astronomical Observatory.

## REFERENCES

| | | |
|---|---|---|
| COMARI, M. | 1985a | "Real time digitization and data processing for a six channel radiopolarimeter", **Convegno Nazionale Astronet**, Rome, March 1985, G. Sedmak ed., in press under auspices of the S.A.It. |
| COMARI, M. | 1985b | "High time resolution data analysis for a multichannel solar radio polarimeter", **Convegno Nazionale Astronet**, Rome, March 1985, G. Sedmak ed., in press under auspices of the S.A.It. |
| KANE, S.R., M.K. BIRD, V. DOMINGO, et al. | 1984 | **STIP Symposium on Solar/Interplanetary Intervals - Proceedings** of the Maynooth Symposium, August 1982, M.A. Shea, D.F. Smart, S.M.P. McKenna-Lawlor, eds., 175. |
| SGD | 1984 | **Solar-Geophysical Data**, 480, Part II, 57, U.S. Department of Commerce, Boulder, Colorado, USA 80303. |

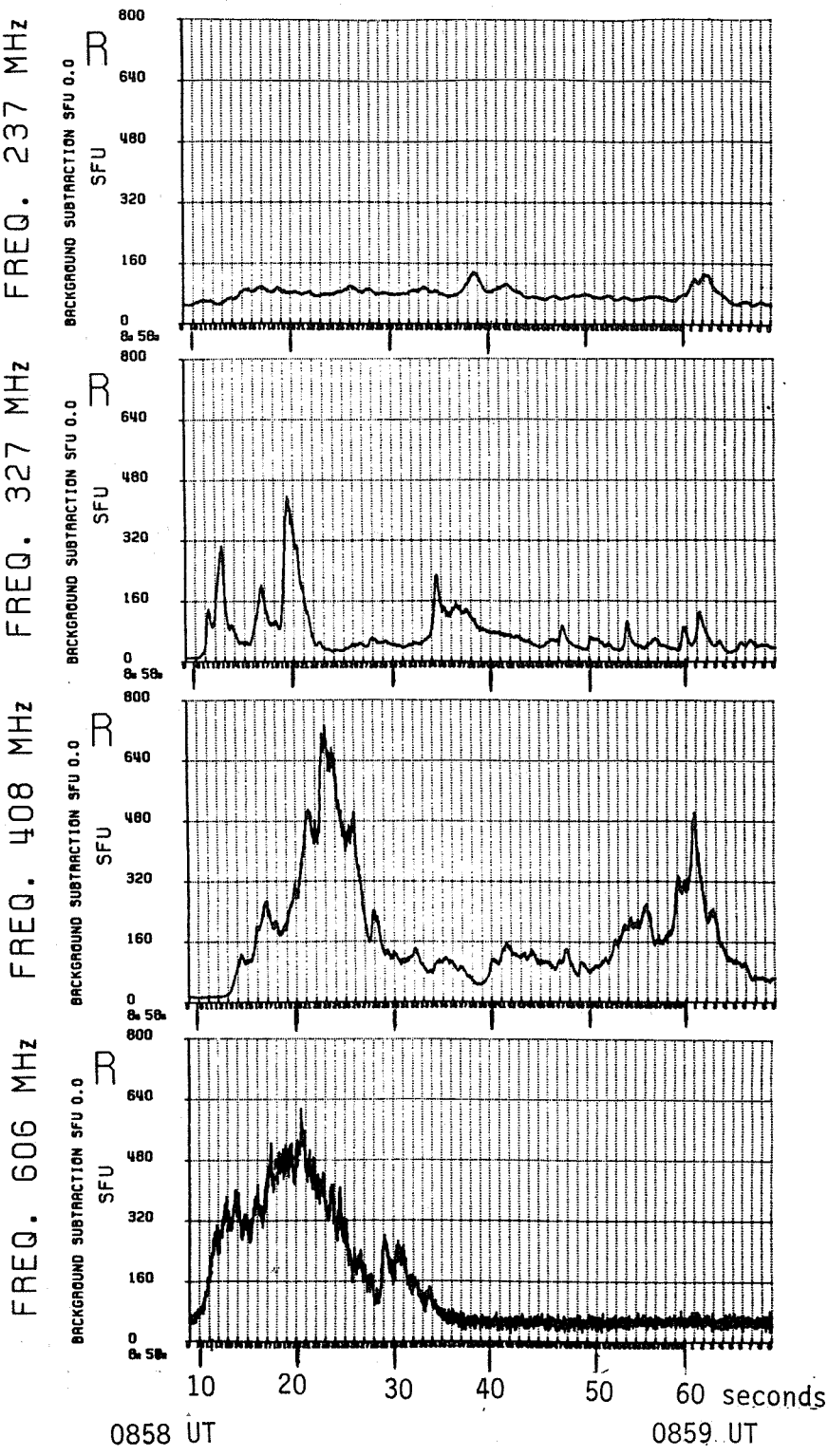


Fig. 1. First minute of the Type IV burst evolution at four frequencies. Starting time 0858:09 UT. The polarization is zero. Only the right circularly polarized flux density is given.

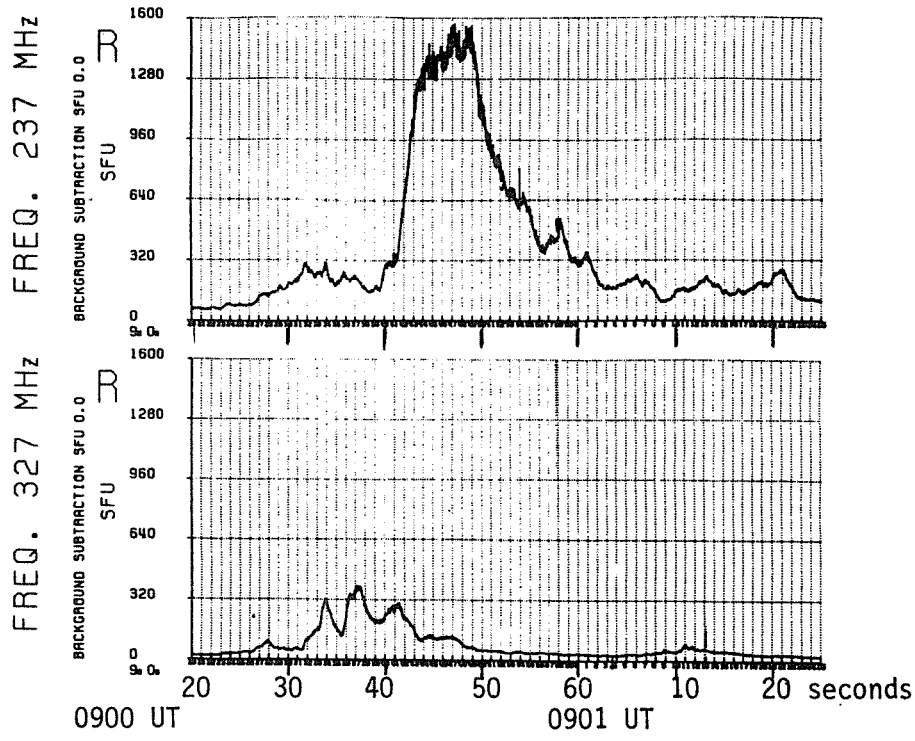


Fig. 2. The Type II burst at 237 MHz and 327 MHz. The polarization is zero. Only the right circularly polarized flux density is given. Start at 0900:20 UT, duration 65 seconds.

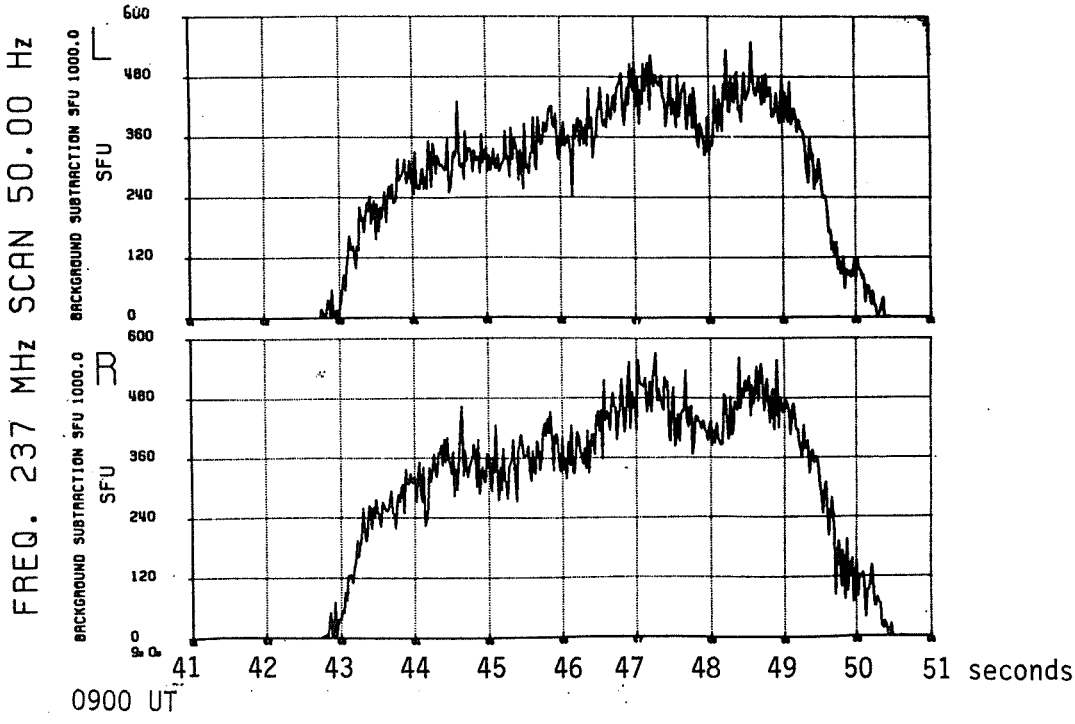


Fig. 3. Details of the spiky structure of the Type II burst at 237 MHz. The flux density of 1000 s.f.u. is subtracted. Starting time 0900:41 UT, duration 10 seconds.

# RSTN Observations of the 16 February 1984 Cosmic Ray Flare

by

E.W. Cliver
Air Force Geophysics Laboratory
Hanscom AFB, Massachusetts 01731, USA

L.C. Gentile
Emmanuel College
Boston, Massachusetts 02115, USA

and

G.D. Wells
OL NOA1, Hq AFELM
NOAA/NGDC E/GC2
325 Broadway
Boulder, Colorado 80303, USA

## Radio Solar Telescope Network

The Radio Solar Telescope Network (RSTN) is operated by the Air Weather Service of the U.S. Air Force. RSTN stations are located at Sagamore Hill (Massachusetts), Palehua (Hawaii), and Learmonth (Australia). A fourth site at San Vito (Italy) will begin making observations in 1986. The RSTN stations monitor the quiet and disturbed Sun at eight fixed frequencies logarithmically spaced from 245 - 15400 MHz. The radiometer patrols are operated from sunrise to sunset. Data are stored on magnetic tape with 1 second time resolution and archived at the World Data Center A in Boulder for dissemination to the scientific community. The Palehua site became operational in July 1980, followed by Learmonth in August 1980, and Sagamore Hill in October 1981. Thus digitized radiometer observations of the Sun are available for a significant fraction of the maximum phase of solar cycle 21.

## The Microwave Burst Associated with the 16 February 1984 Cosmic Ray Flare

RSTN observations from Learmonth Solar Observatory are presented in Figure 1. The background (quiet-sun-flux) value was subtracted from the radiometer output at each frequency and every third second of the resulting burst data was plotted. The background was determined from a 60 second average from 0830 to 0831 UT. Note that the flux density scale is compressed for the three lowest frequencies in comparison with frequencies $\geq$ 1415 MHz. The bursts at 245 and 606 MHz exceeded 1000 s.f.u. and are truncated on the plot. The maximum flux (3876 s.f.u) at 245 MHz occurred at 0901.8 UT and the peak-flux-density (1374 s.f.u) at 606 MHz occurred at 0858.4 UT.

Because the background flux at the lower frequencies was constant for $\geq$10 minutes before the event, the burst onset times can be determined quite precisely:

| Frequency MHz | Start Time UT |
|---|---|
| 245 | 0858:14 (-2,+1 s) |
| 410 | 0858:14 (-3,+1 s) |
| 606 | 0858:11 ($\pm$1 s) |

The earliest possible onset at any frequency was at 2695 MHz where a small (about 2 s.f.u) gradual increase occurs at 0858:05 UT.

In Figure 2 we plot instantaneous spectra for several times during the principal phase of the event. Figures 2(a-c) are for the first three minutes of the event, respectively, with a spectrum taken every 10 seconds. In Figure 2(d), six spectra are plotted at one minute intervals beginning at 0902 UT. The relatively low values of $f_{max}$ (frequency of greatest emission) for the times plotted are consistent with the burst originating beyond the solar limb (higher frequencies occulted) as indicated by observations at other wavelengths.

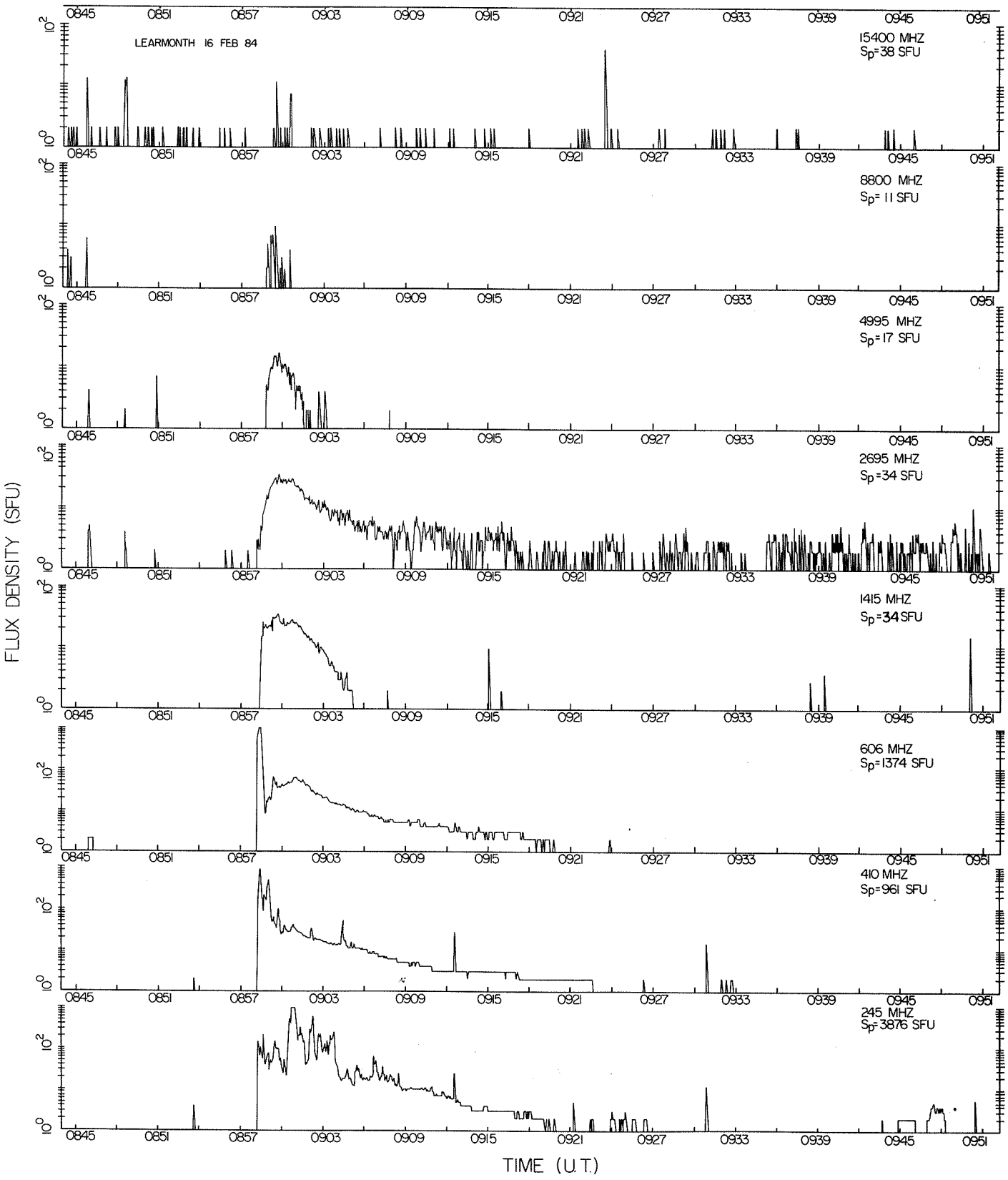


Fig. 1. Flux-density profiles of the microwave burst associated with the 16 February 1984 cosmic ray flare.

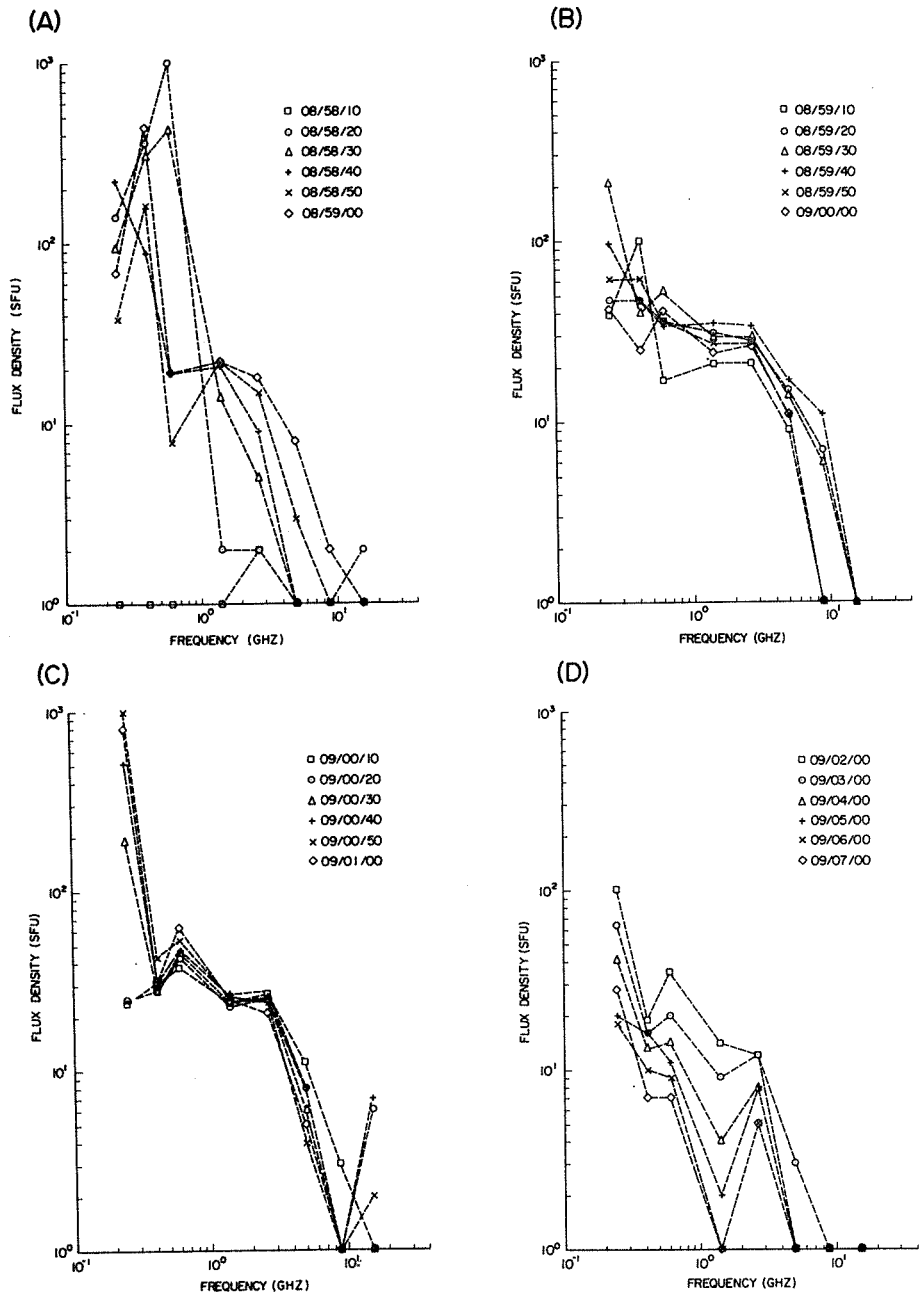


Fig. 2. Instantaneous flux-density spectra for several times during the 16 February solar event.

# Radio Burst Activity in Active Regions 4408 and 4474

by

H. Aurass, A. Bohme, A. Kruger, and J. Kurths
Akademie der Wissenschaften der DDR
Zentralinstitut fur Astrophysik
DDR-1500 Potsdam
German Democratic Republic

## Introduction

This report summarizes observations of the Tremsdorf Observatory of Solar Radio Astronomy. The observations comprise solar flux measurements at selected single frequencies in the cm-dm and m-Dm ranges. The main information available concerns the burst observation on 16 February 1984 as well as a number of microwave burst Type III bursts and noise storm observations during the second period of interest at the end of April 1984.

## Event of 16 February 1984

A remarkable solar radio burst was observed on 16 February 1984 at about 0858 UT. The detailed starting times at different observing frequencies are listed in Table 1. The burst characteristics and the missing association with any flare event on the visible solar disk (SGD) support the assumption that this burst was related to a behind-the-limb event.

Table 1. Starting Times of the 16 February 1984 Event

| Frequency MHz | Start UT |
|---|---|
| 9,500 | 0858.8 |
| 3,000 | 0858.5 |
| 2,000 | 0858.5 |
| 1,470 | 0858.0 |
| 778 | 0858.2 |
| 234 | 0858.4 |
| 113 | 0858.4 |
| 64 | 0858.5 |
| 40 | 0858.5 |
| 30 | 0858.5 |

Exhibiting a Type II/IVmA-like emission, the event is well detectable at meter waves but distorted by calibration in our records. Compatible with the assumed large central meridian distance, the degree of polarization is rather low.

The time profiles of the event at microwaves are shown in Figure 1. According to the suggested source origin behind the solar limb, the microwave emission is rather weak but nonetheless exhibits an impulsive time profile at all observed frequencies. It is interesting that contrary to the normal behavior, the starting times are delayed at higher frequencies (cf. Table 1). This may be connected with a delayed arrival of sufficient high particle energies at those heights not obsured by the limb and producing a detectable emission at higher harmonics of the gyrofrequency.

## Radio Burst and Noise Storm Activity during the Period 20 April - 4 May 1984

During the last ten days of April 1984 a total of 19 radio bursts were observed at Tremsdorf. These were related to the Active Region 4474 as evidenced by flare coincidence (SGD, ZIAP Solar Data). Information about these events is given in Table 2. Most of the events are relatively small (impulsive and gradual) microwave and/or Type III bursts. Some examples of microwave time profiles are shown in Figures 2-4 (events on 27, 29 and 30 April respectively). These show the development of the gradual components. Remarkable post burst increases are one characteristic feature of a number of these bursts. The three events shown in Figures 2-4 are restricted to the microwave range.

Solar noise storm emission was observed during 20 April to 3 May 1984. Daily flux mean values are given in Table 3 for five observing frequencies. The highest flux values were observed in the morning hours on 25 April at 40 MHz. Greatest daily means of flux density at 113 MHz were reported on 26 April. This date is also characterized by a number of broadband radio bursts and coronal mass ejections (SGD). Fluctuations of the noise storms and Type IV bursts were continuously recorded with high-time resolution (sampling rate 0.0625 seconds). An example of such pulsations on 26 April at 234 MHz is shown in Figure 5 where periods of < 1 second are clearly marked.

Table 2. List of Radio Bursts from AR 4474, April 1984

| Day | Frequency Range MHz | Start UT | End UT | SGD Type | Maximum Frequency MHz | Maximum Time UT | Maximum Flux s.f.u. | SGD H-alpha Flares Lat. | SGD H-alpha Flares CMD | SGD H-alpha Flares Opt. Imp. | Remarks |
|---|---|---|---|---|---|---|---|---|---|---|---|
| 21 | 9500 - 30 | 0725.3 | 0732.5 | 3 | 9500 | 0725.5 | 25 | S13 | E80 | 1B | |
| | | | | 4 | 113 | 0725.7 | 600 | | | | |
| 22 | 2000 -1470 | 0703.5 | 0707.5 | 40 | 1470 | 0705.1 | 10 | S12 | E83 | SN | |
| | 2000 - 30 | 1340.0 | 1352.0 | 42 | 1470 | 1341.0 | 13 | S09 | E63 | SB | |
| | | | | 4 | 234 | 1340.8 | 190 | | | | III |
| 23 | 9500 | 1131.5 | 1155.0 | 29 | 9500 | 1132.0 | 14 | S07 | E65 | SF | |
| | 9500 - 775 | 1338.5 | 3555.5 | 4 | 1470 | 1352.6 | 50 | S07 | E51 | SN | |
| 24 | 113 - 40 | 1446.1 | 1447.4 | 4 | 113 | 1446.5 | 700 | S11 | E52 | SF | III |
| 25 | 3000 - 75 | 1226.0 | 1232.0 | 4 | 1470 | 1227.9 | 24 | S11 | E36 | SN | |
| | 9500 - 30 | 1403.0 | 1414.0 | 4 | 9500 | 1405.4 | 280 | S09 | E46 | SN | |
| | | | | 4 | 113 | 1404.8 | 350 | | | | III |
| | 9500 - 30 | 1456.0 | 1509U | 46 | 1470 | 1501.0 | 485 | S11 | E45 | SB | |
| | | | | 4 | 113 | 1456.6 | 9000 | | | | III/V |
| 26 | 9500 - 30 | 0655.0 | 0815.0 | 46 | 1470 | 0659.3 | 107 | S11 | E27 | 1B | Associated mass ejection, |
| | | | | 41 | 113 | 0655.6 | 3800 | S12 | E39 | SB | dm-fine structures, III/V |
| | 9500 - 30 | 0852.0 | 0925.0 | 32 | 9500 | 0857.5 | 280 | S09 | E34 | 1B | |
| | | | | 47 | 234 | 0903.9 | 36000 | | | | III/V, mass |
| | 9500 -1470 | 1241.0 | 1440.0 | 21 | 3000 | 1255.0 | 64U | S14 | E14 | SB | ejection |
| 27 | 234 - 30 | 0534.5 | 0545.6 | 42 | 234 | 0544.0 | 220000 | S08 | E15 | 1B | III |
| | 9500 - 775 | 0725.0 | 0734.0 | 20 | 3000 | 0728.7 | 11 | S11 | E25 | SF | Mass ejection? |
| | 9500 - 775 | 1400.0 | 1451D | 46 | 1470 | 1407.3 | 133 | S14 | E16 | SB | Figure 2 |
| 28 | 3000 - 775 | 0855.5 | 0856.7 | 3 | 3000 | 0856.0 | 13 | S12 | W14 | SB | |
| 29 | 9500 - 775 | 0650.0 | 0820.0 | 21 | 9500 | 0720.0 | 20 | S12 | E08 | SF | Figure 3 |
| | | | | | | | | S15 | W01 | 1N | |
| | 234 - 113 | 1121.0 | 1130.0 | 42 | 113 | 1123.0 | 1000 | S13 | W30 | SN | III |
| 30 | 9500 - 775 | 1120.0 | 1403.0 | 45 | 9500 | 1153.5 | 111 | S13 | W40 | 2B | Figure 4 |

TABLE 3. Daily Mean Noise Storm Flux Values for 25 April - 3 May 1984

| | FREQUENCY | | | | | | | | | |
|---|---|---|---|---|---|---|---|---|---|---|
| | 234 MHz | | 113 MHz | | 64 MHz | | 40 MHz | | 30 MHz | |
| Day | Flux s.f.u. | Time UT | Flux s.f.u. | Time UT | Flux s.f.u. | Time UT | Flux s.f.u. | Time UT | Flux s.f.u. | Time UT |
| April | | | | | | | | | | |
| 25 | 15 | 1530 | 15 | 1530 | 30 | 1100 | 827 | 1100 | 87 | 1300 |
| 26 | 30 | 1500 | 134 | 1500 | 86 | 1500 | 445 | 1500 | 52 | 1300 |
| 27 | 33 | 1500 | 55 | 1500 | 48 | 1400 | 188 | 0800 | 15 | 1100 |
| 28 | 25 | 1430 | 66 | 1430 | disturbances | | 143 | 1430 | 19 | 1430 |
| 29 | 21 | 1430 | 14 | 1430 | 41 | 0900 | 80 | 1000 | - | - |
| 30 | 25 | 1500 | 20 | 1500 | - | - | - | - | - | - |
| May | | | | | | | | | | |
| 01 | 15 | 1430 | 36 | 1430 | 43 | 1430 | 543 | 1430 | - | - |
| 02 | 09 | 1500 | 12 | 1500 | - | - | - | - | - | - |
| 03 | 08 | 1500 | 4 | 1500 | - | - | - | - | - | - |

Remarks: The mean values are computed starting with 0600 UT and ending with the time given in the "Time" column.

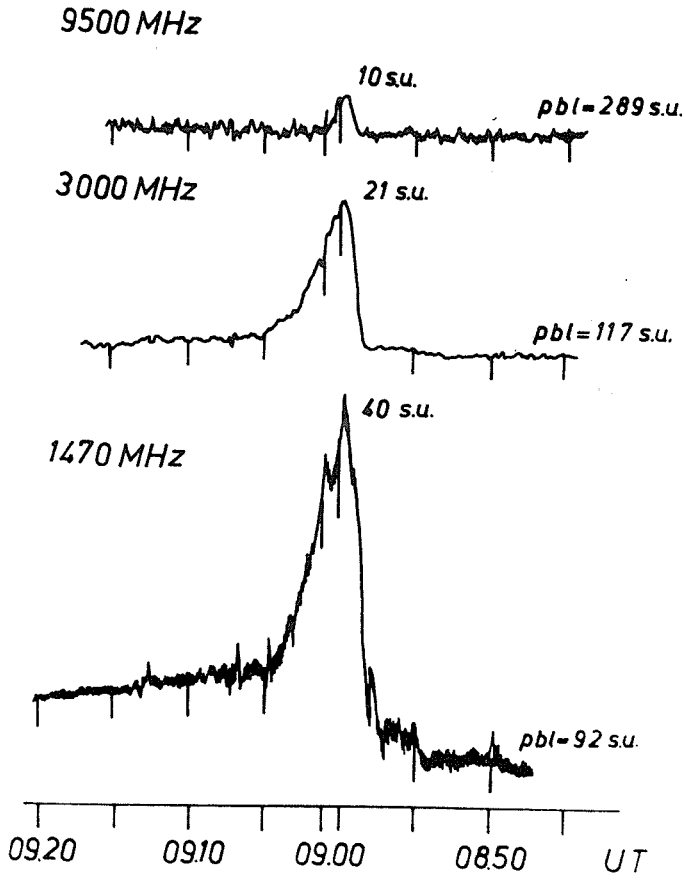


Fig. 1. This shows the microwave time profiles of the event of 16 February 1984.

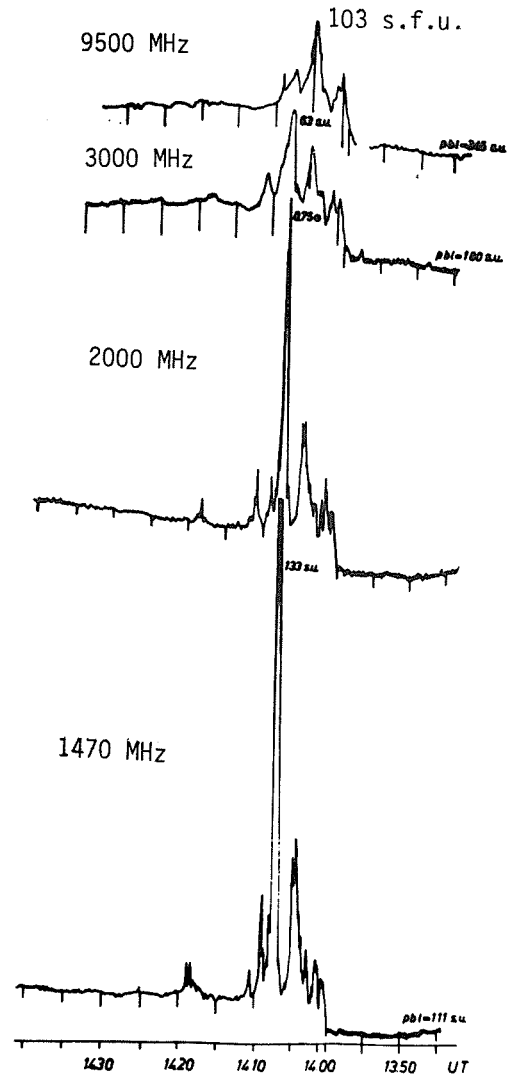


Fig. 2. This shows the time profiles of a microwave burst on 27 April 1984.

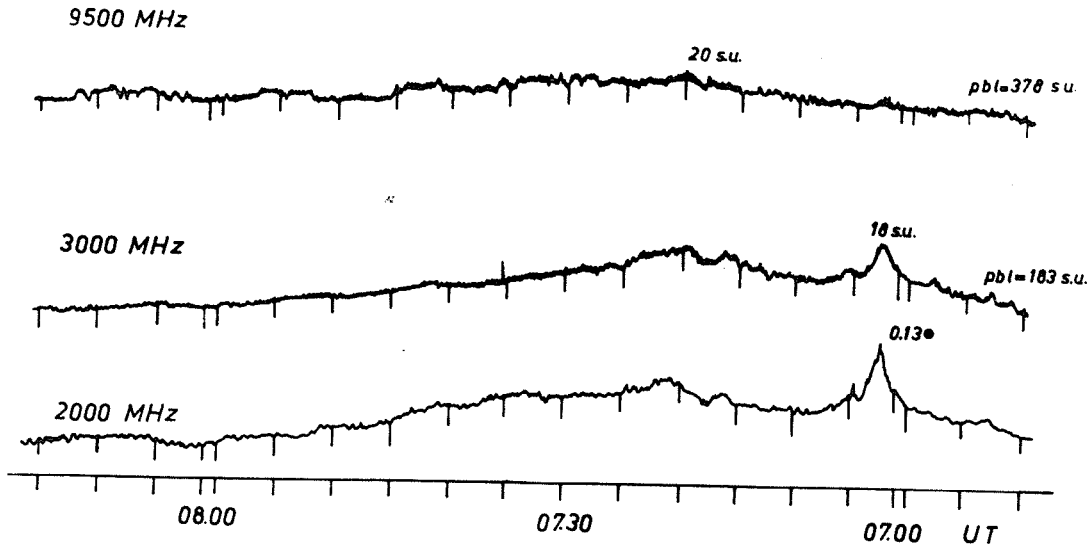


Fig. 3. This shows the time profiles of a microwave burst on 29 April 1984.

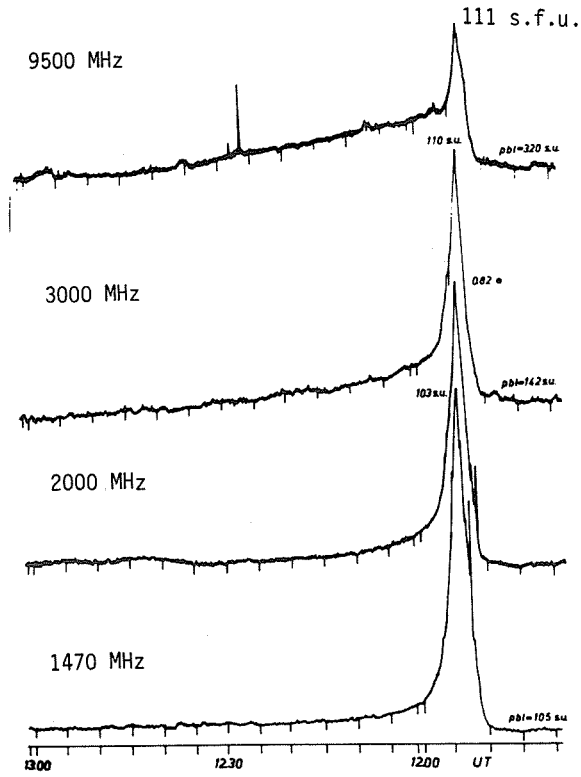


Fig. 4. This shows the time profiles of a microwave burst on 30 April 1984.

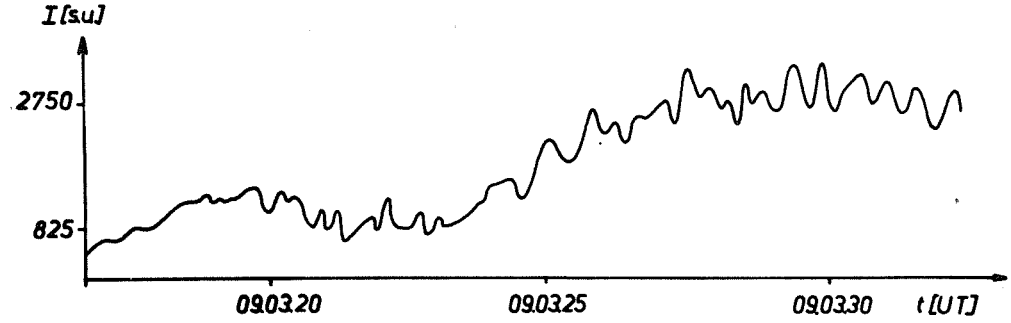


Fig. 5. This is part of a high speed recording showing the solar radio pulsations at 234 MHz on 26 April 1984.

## REFERENCES


| | | |
|---|---|---|
| SGD | 1984 | **Solar-Geophysical Data**, 477, Part I and 482, Part II, U.S. Department of Commerce (Boulder, Colorado, U.S.A. 80303). |
| ZIAP Solar Data | 1984 | **Solar Data**, Zentralinstitut fur Astrophysik (Potsdam, G.D.R.). |

# East-West Solar Scans for 7 February - 1 March 1984 from Zelenchukskaya, North Caucasus, USSR

by

V.M. Bogod, A.N. Korzhavin, N.G. Peterova, V.A. Shatilov
Special Astrophysical Observatory, Leningrad, USSR
and
S.M. Vatrushin
Main Astronomical Obervatory, Pulkovo, Leningrad, USSR

## Explanation of Data

Observatory: SAO AC USSR, RATAN-600

Coordinates: N43.8 E-2.8h

FAN BEAM

| Wavelength cm | E-W resolution second of arc | N-S resolution minutes of arc | Shift from focus point |
|---|---|---|---|
| 2.0 | 20 | 12.5 | 1.38 |
| 2.3 | 23 | 14.4 | -2.26 |
| 2.7 | 27 | 16.9 | 2.32 |
| 3.2 | 33 | 20.0 | -2.78 |
| 4.0 | 41 | 25.0 | 2.58 |
| 20.7 | 210 | 129.0 | -1.60 |
| 31.6 | 321 | 197.0 | -1.05 |

The diagram of the antenna was centered at the center of the solar disk.

The scans at all wavelengths were shifted to the common central meridian. No correction for aberration distortion has been made.

K = correction factor for the scale of I and V Stokes parameters for each day.

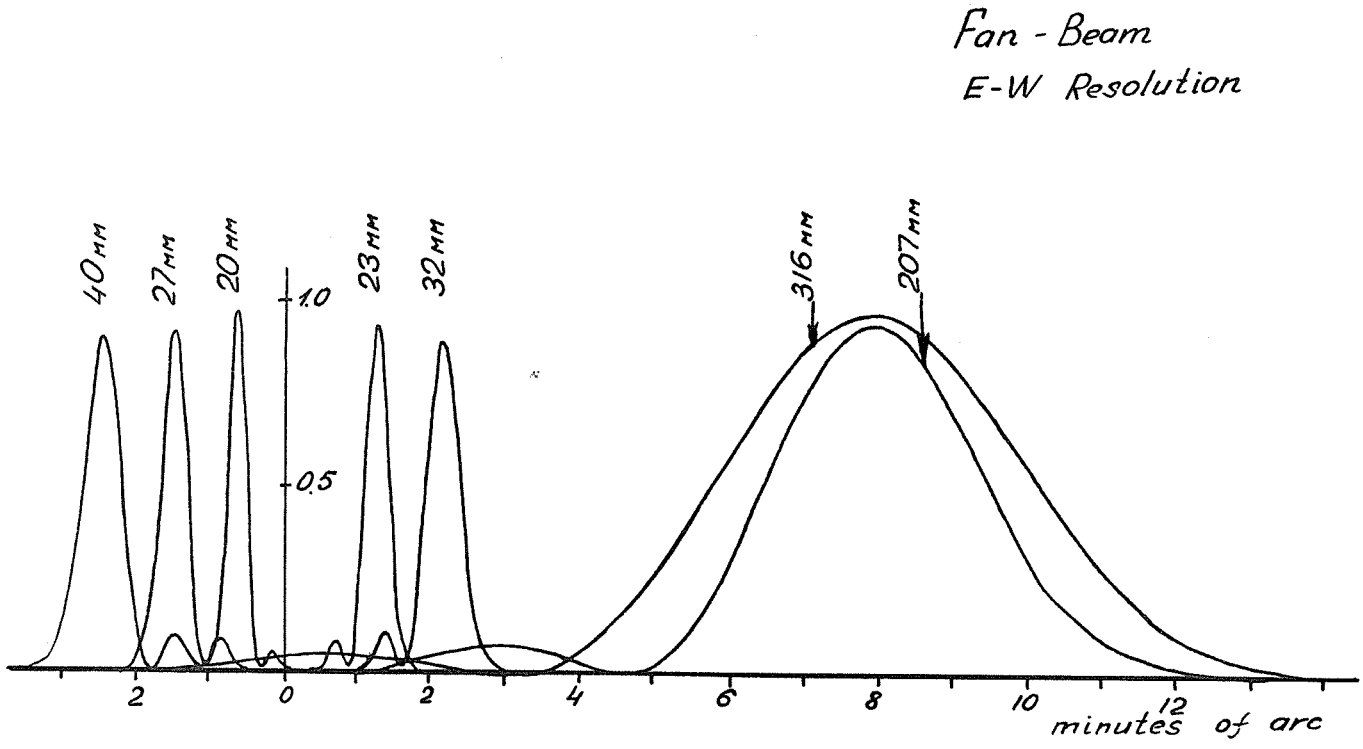


Diagram patterns and their relative position.

# EAST-WEST SOLAR SCANS

Zelenchukskaya, USSR

7 FEBRUARY - 1 MARCH 1984

20 mm
Fan-Beam with 20 seconds of arc
E-W Resolution

## With Polarization Plot Superposed

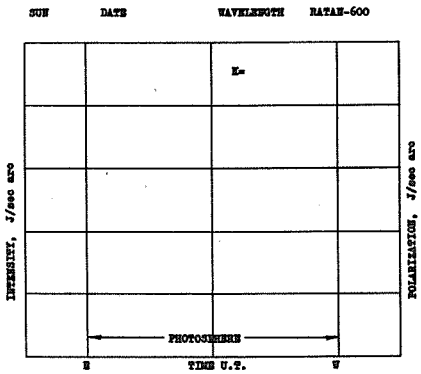


E

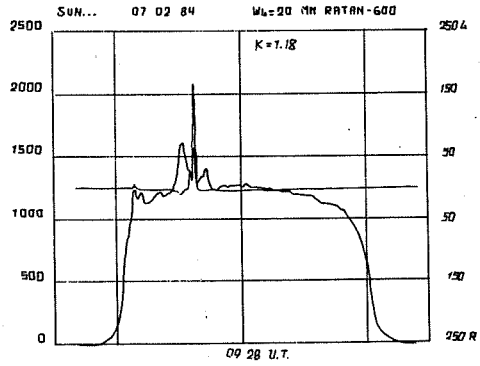


E

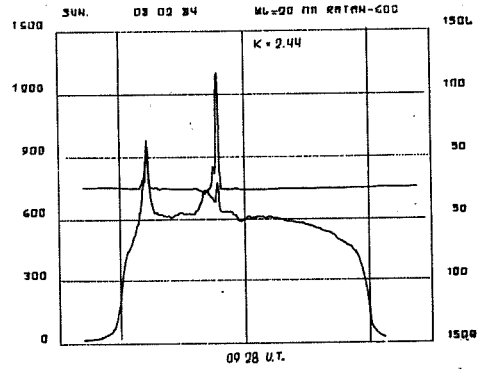


E

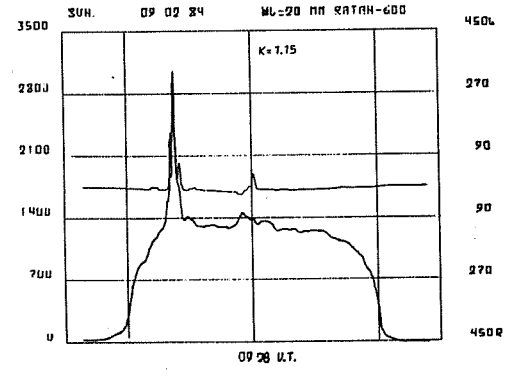


E

## Without Polarization Plot

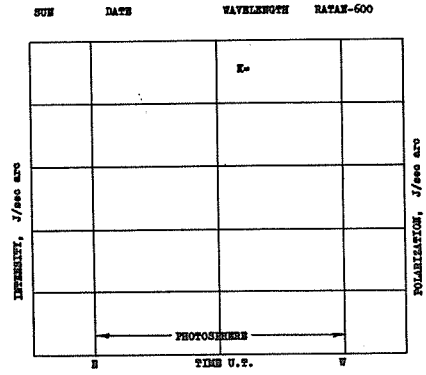


W

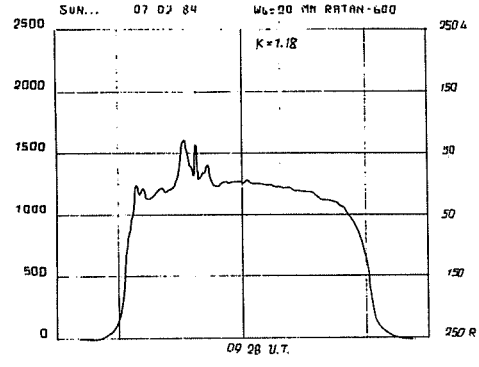


W

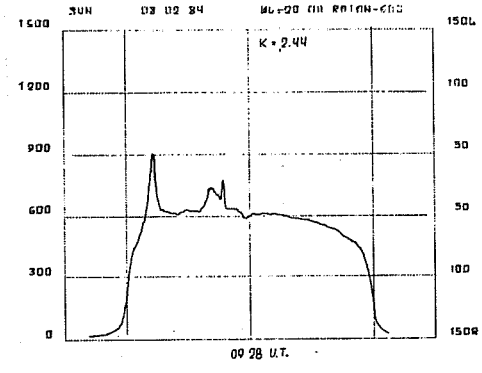


W

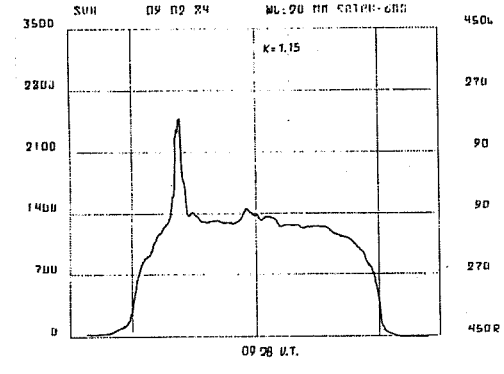


W

# EAST-WEST SOLAR SCANS

Zelenchukskaya, USSR

7 FEBRUARY - 1 MARCH 1984

20 mm
Fan-Beam with 20 seconds of arc
E-W Resolution

With Polarization Plot Superposed

Without Polarization Plot

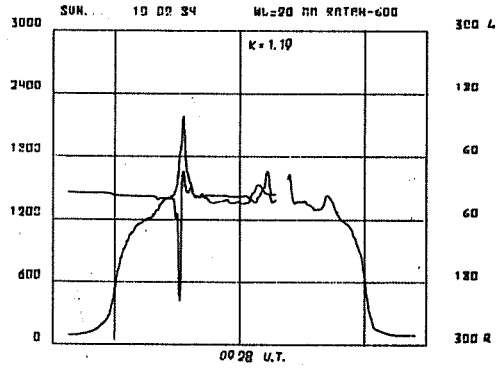


E

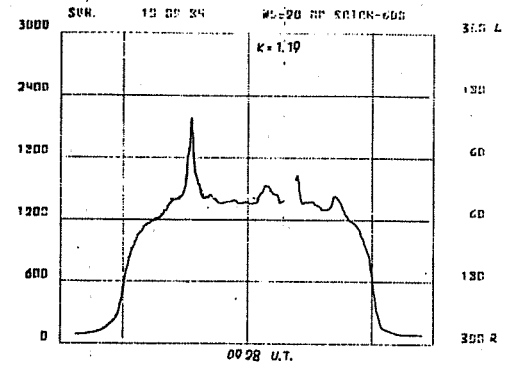


W

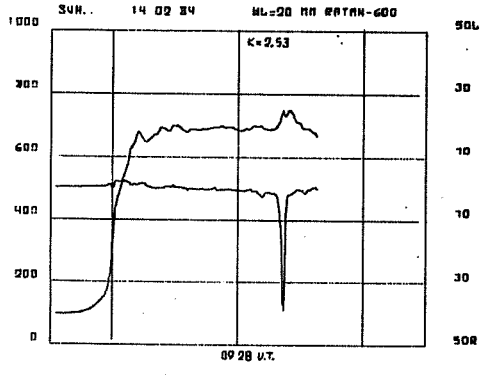


E

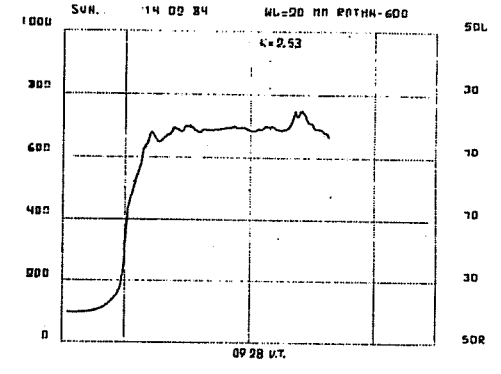


W

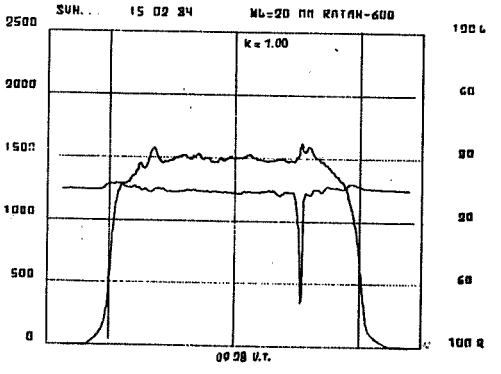


E

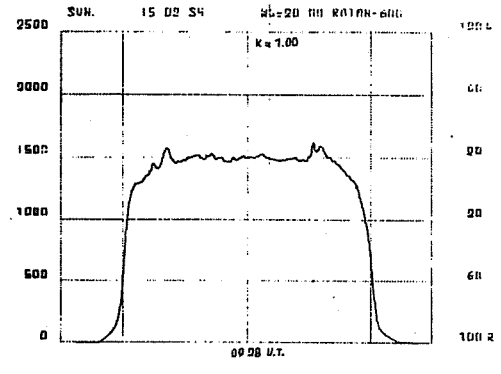


W

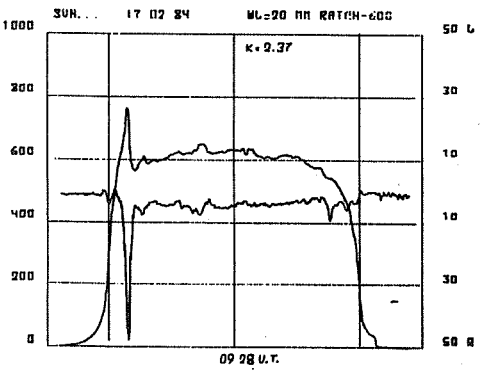


E

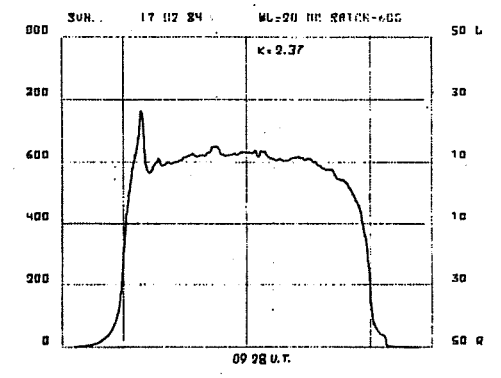


W

# EAST-WEST SOLAR SCANS

Zelenchukskaya, USSR

7 FEBRUARY - 1 MARCH 1984

20 mm
Fan-Beam with 20 seconds of arc
E-W Resolution

With Polarization Plot Superposed

Without Polarization Plot

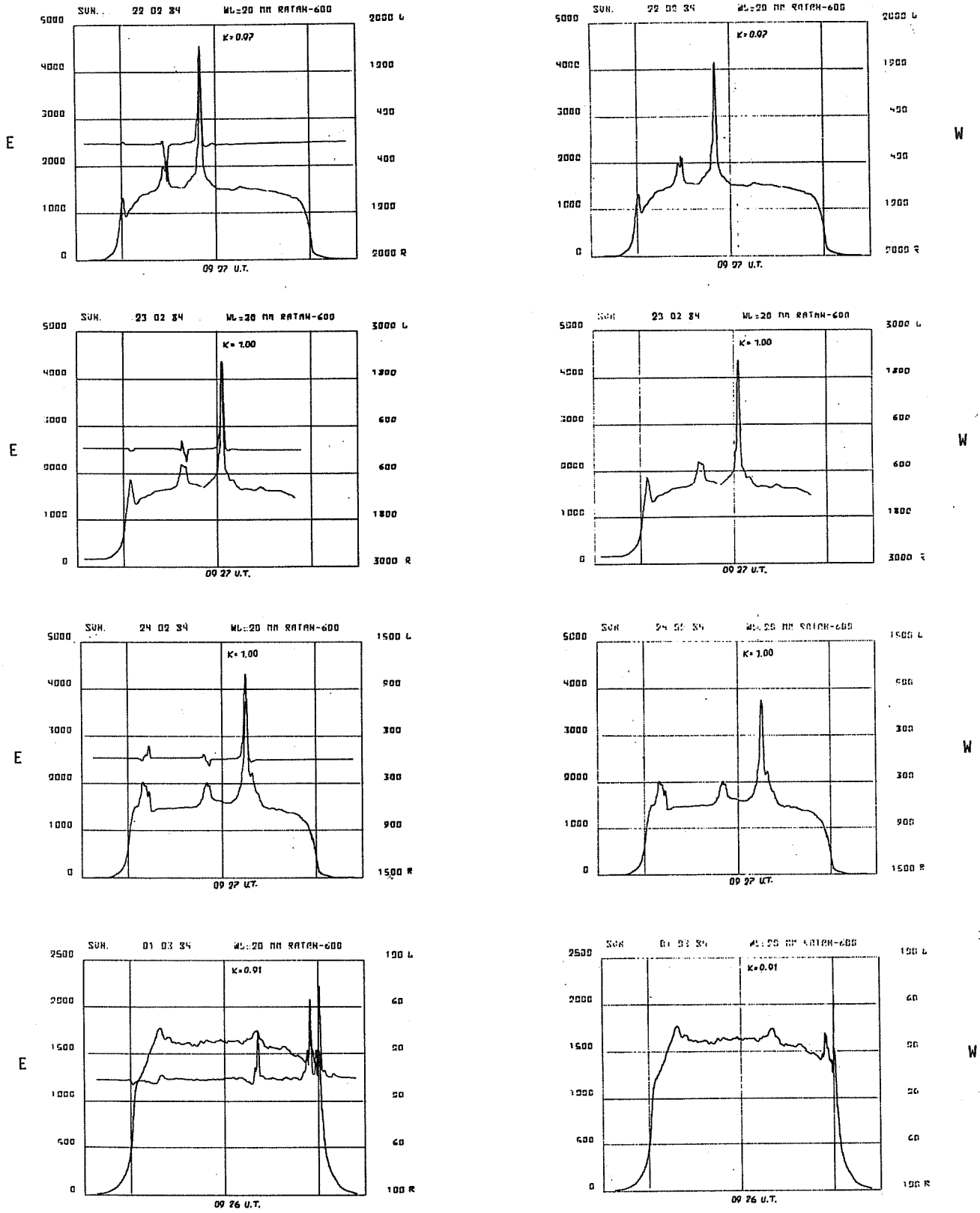

# EAST-WEST SOLAR SCANS

Zelenchukskaya, USSR

7 FEBRUARY - 1 MARCH 1984

23 mm
Fan-Beam with 23 seconds of arc
E-W Resolution

With Polarization Plot Superposed

Without Polarization Plot

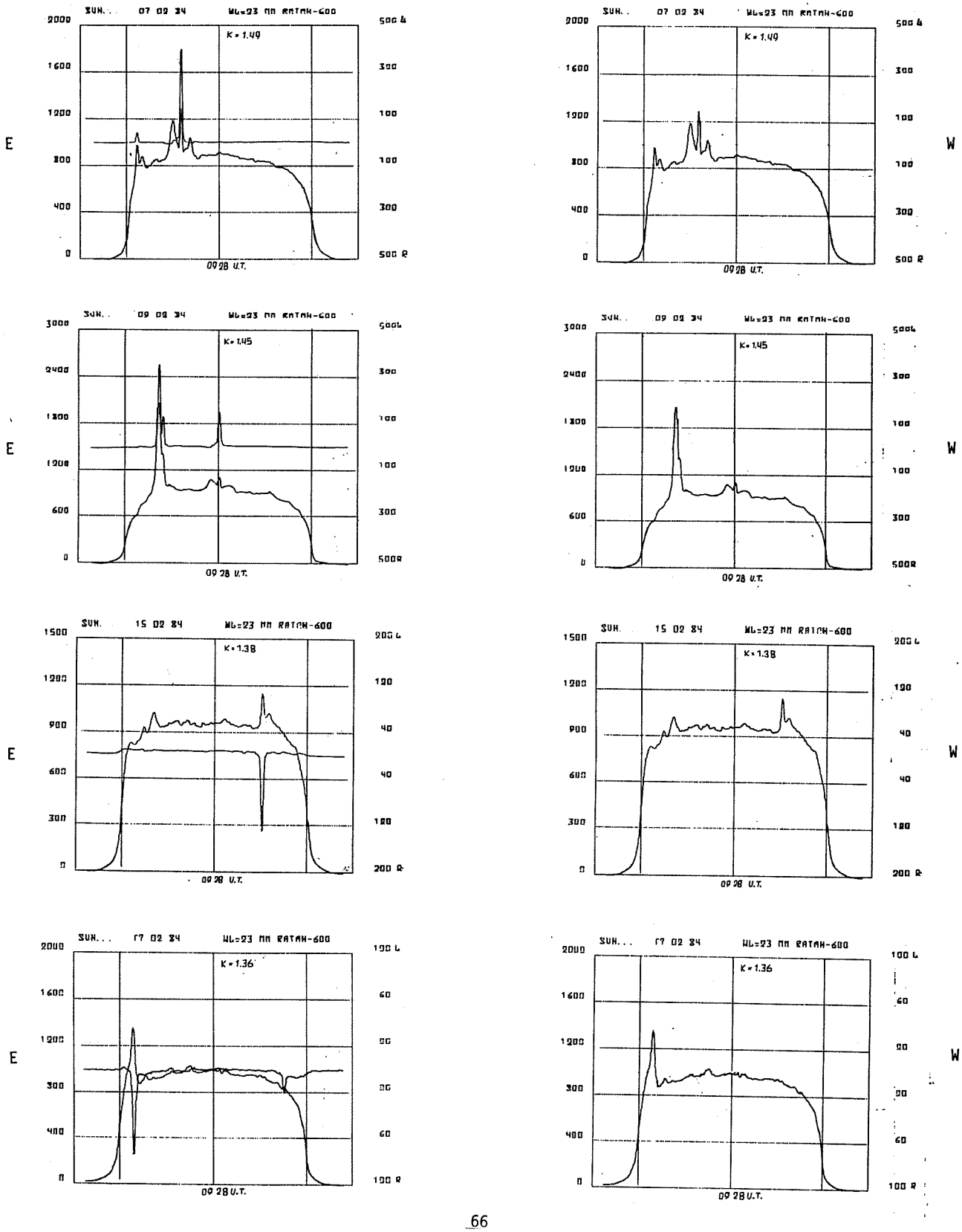

# EAST-WEST SOLAR SCANS

Zelenchukskaya, USSR

7 FEBRUARY - 1 MARCH 1984

23 mm
Fan-Beam with 23 seconds of arc
E-W Resolution

With Polarization Plot Superposed

Without Polarization Plot

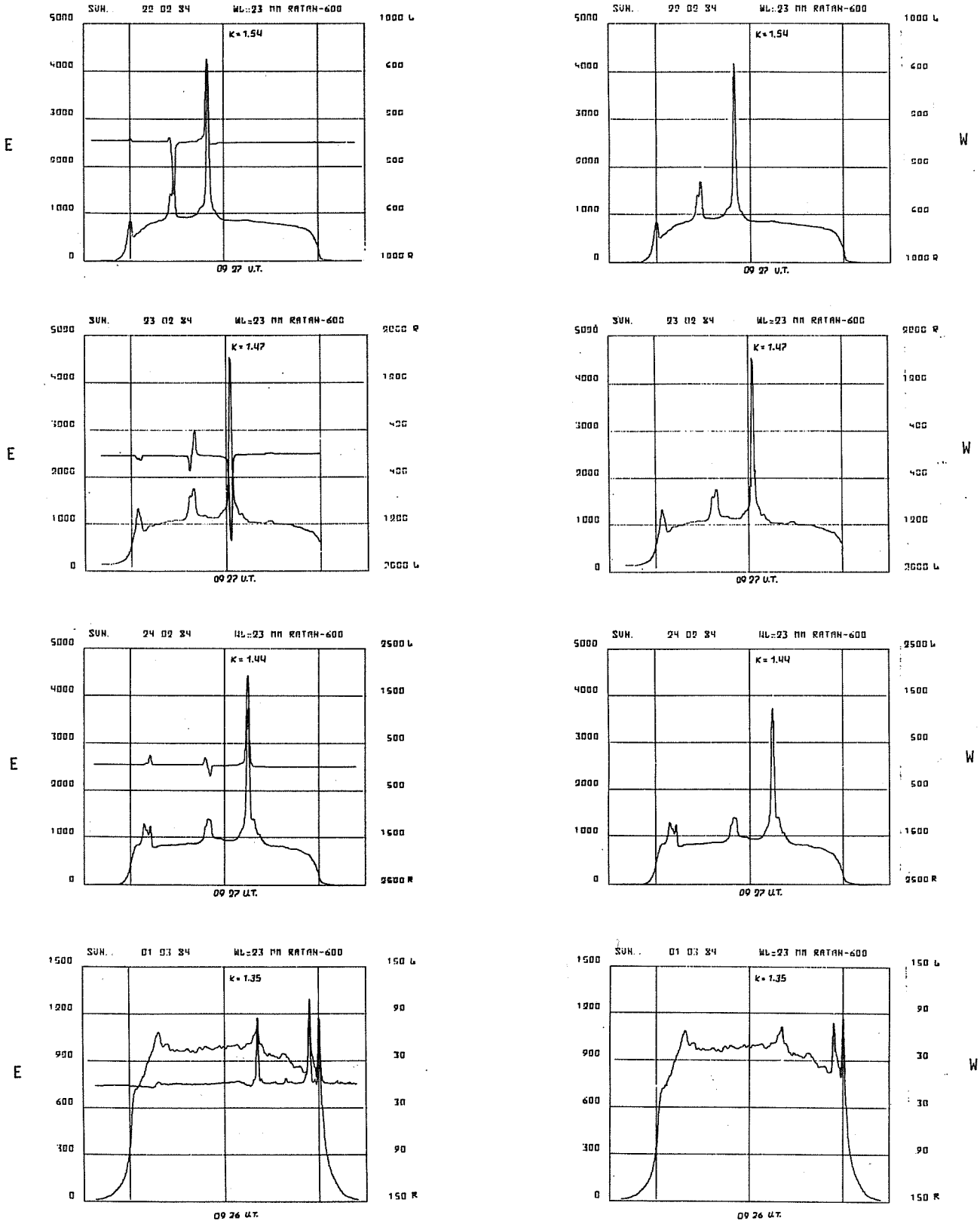

# EAST-WEST SOLAR SCANS

Zelenchukskaya, USSR

7 FEBRUARY - 1 MARCH 1984

27 mm
Fan-Beam with 27 seconds of arc
E-W Resolution

With Polarization Plot Superposed

Without Polarization Plot

E

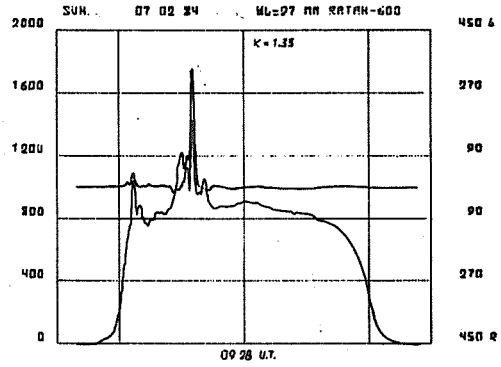


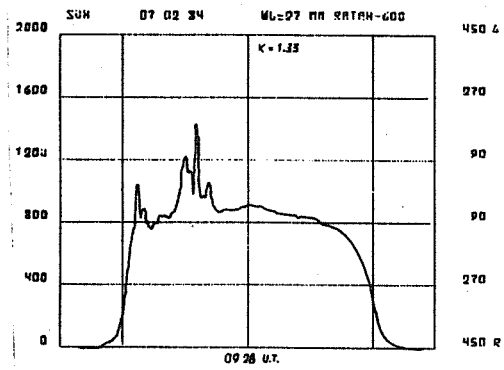


W

E

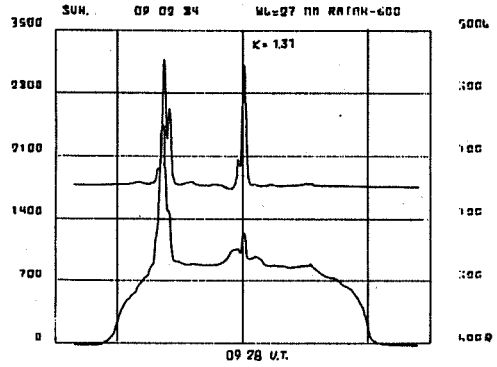


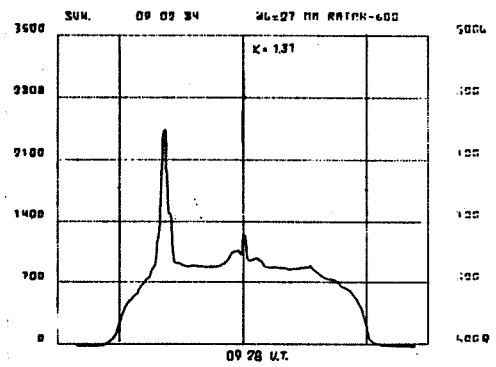


W

E

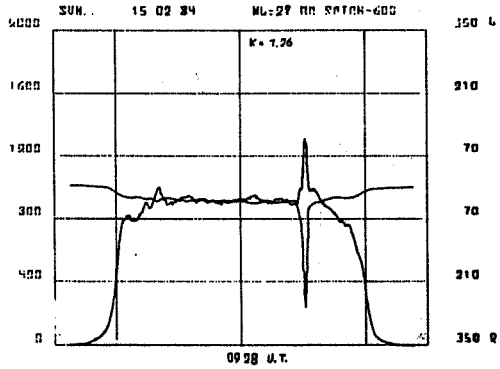


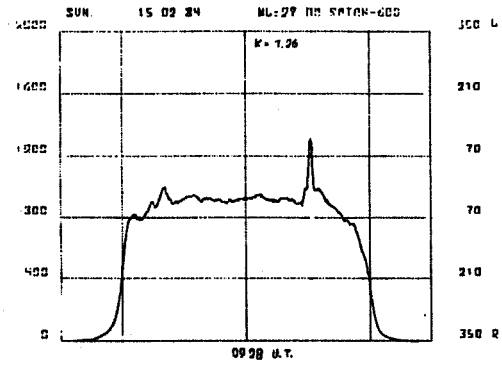


W

E

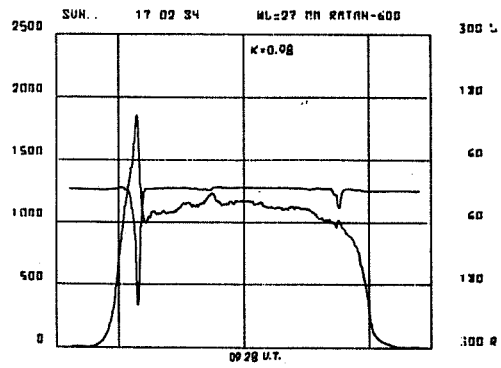


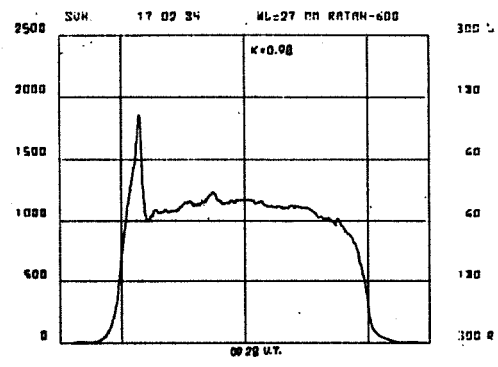


W

# EAST-WEST SOLAR SCANS

Zelenchukskaya, USSR | 7 FEBRUARY – 1 MARCH 1984 | 27 mm Fan-Beam with 27 seconds of arc E-W Resolution

With Polarization Plot Superposed

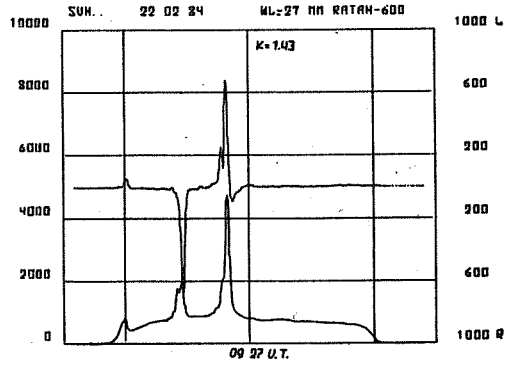


E

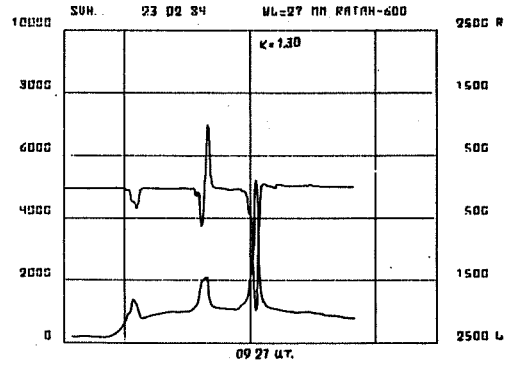


E

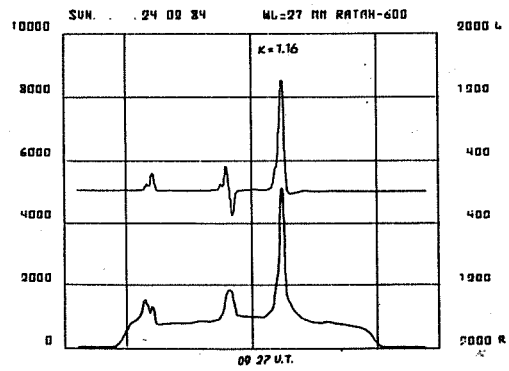


E

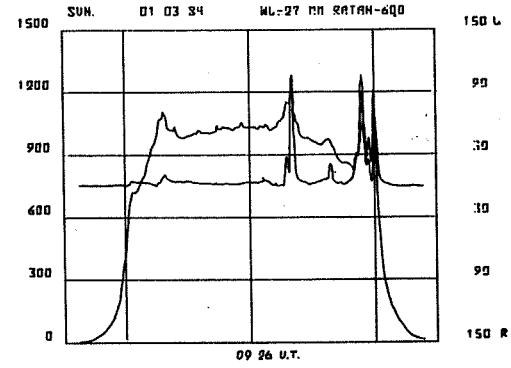


E

Without Polarization Plot

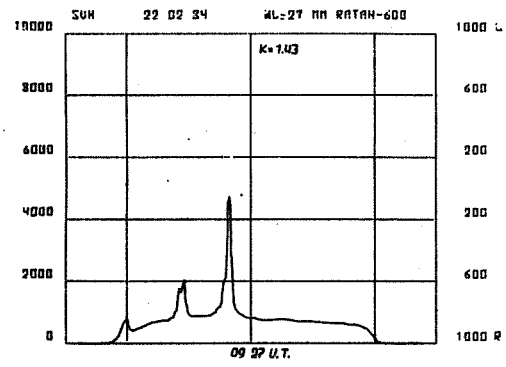


W

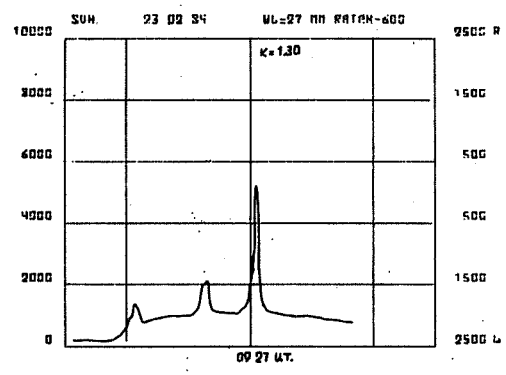


W

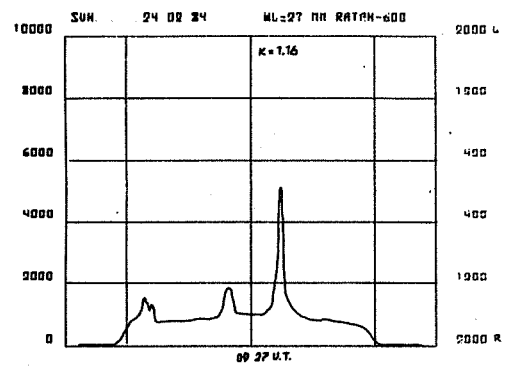


W

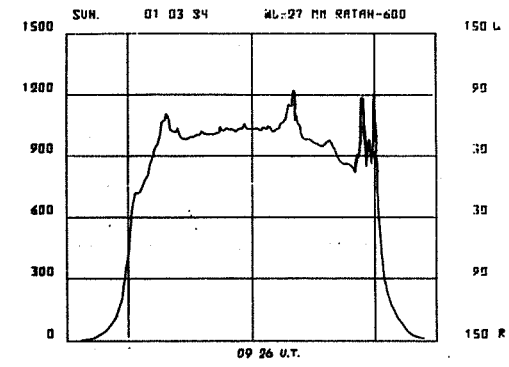


W

# EAST-WEST SOLAR SCANS

Zelenchukskaya, USSR

7 FEBRUARY - 1 MARCH 1984

32 mm
Fan-Beam with 23 seconds of arc
E-W Resolution

With Polarization Plot Superposed

Without Polarization Plot

E

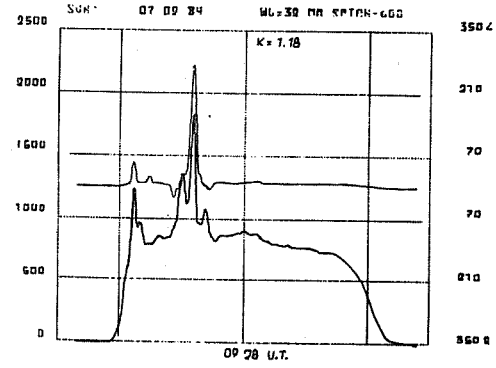


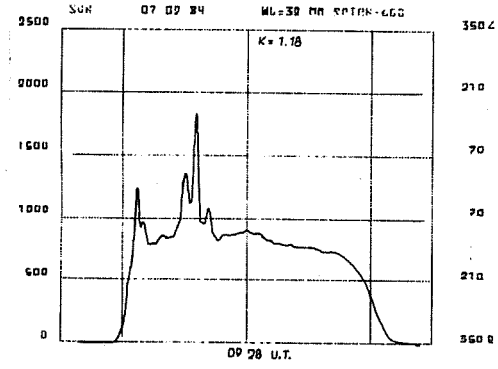


W

E

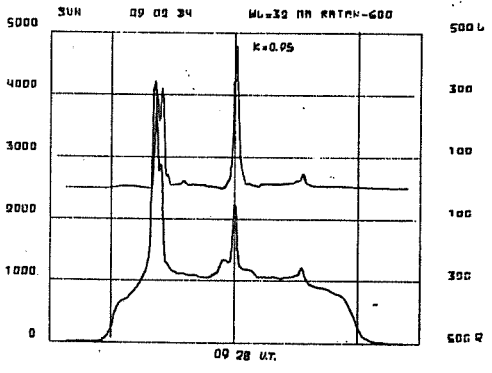


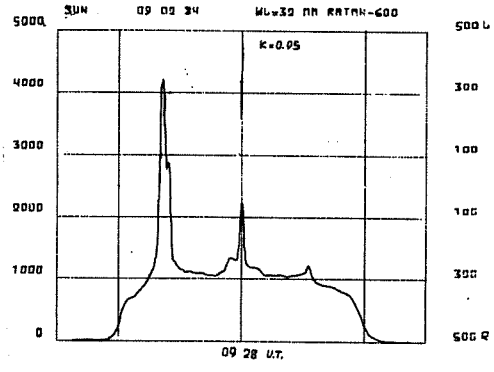


W

E

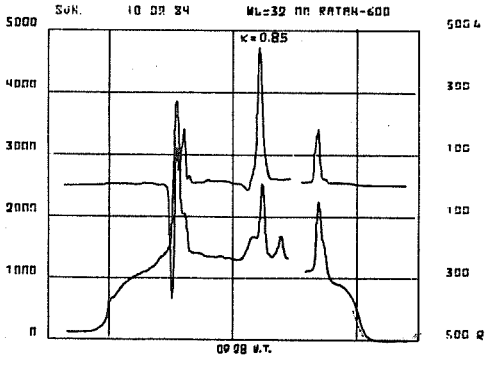


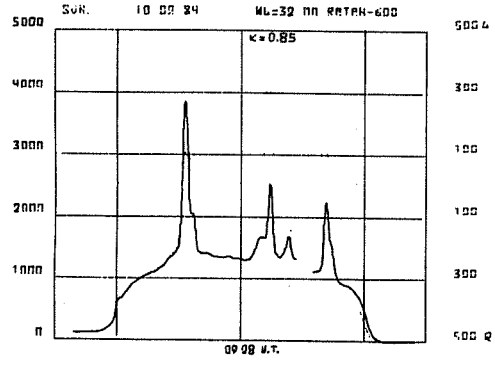


W

E

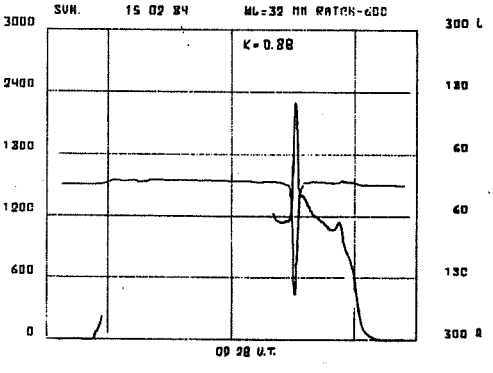


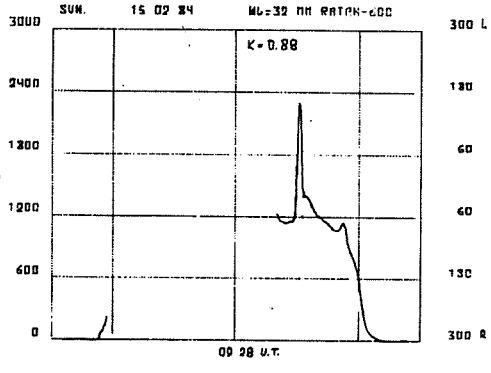


W

# EAST-WEST SOLAR SCANS

Zelenchukskaya, USSR

7 FEBRUARY - 1 MARCH 1984

32 mm
Fan-Beam with 23 seconds of arc
E-W Resolution

With Polarization Plot Superposed

Without Polarization Plot

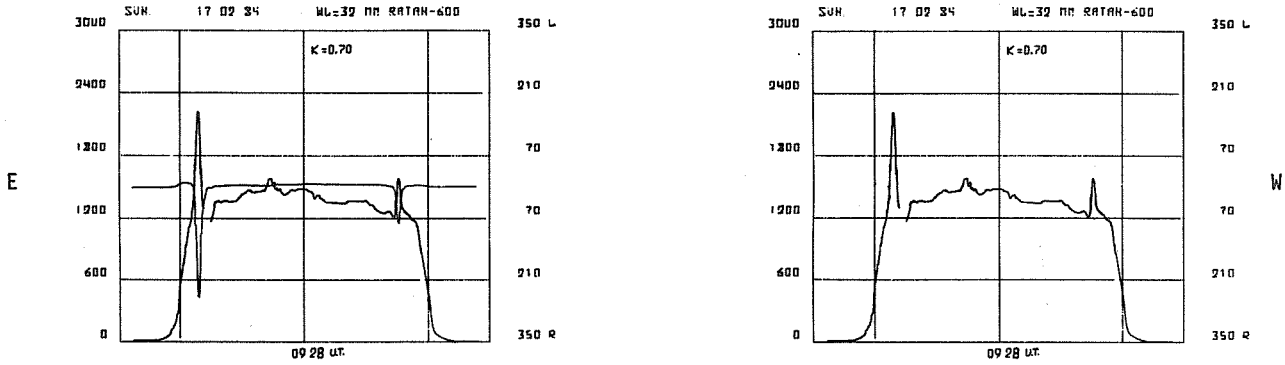


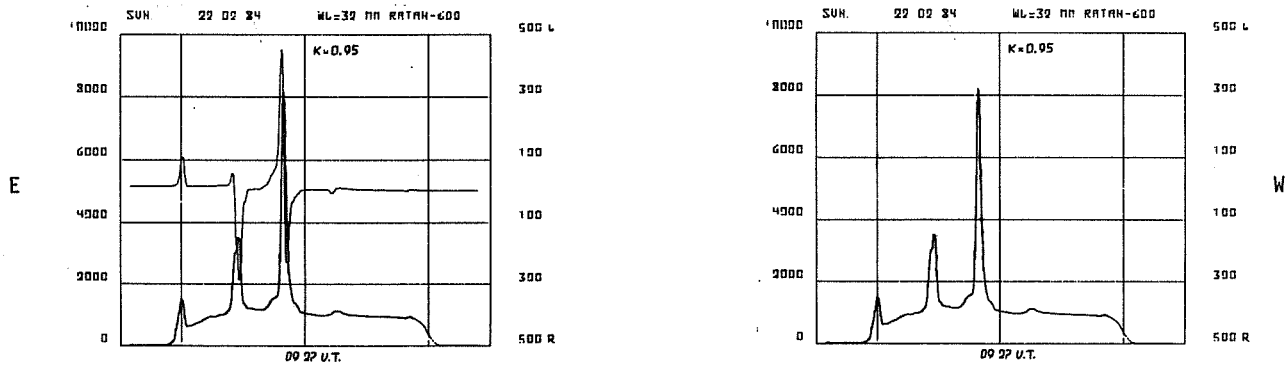


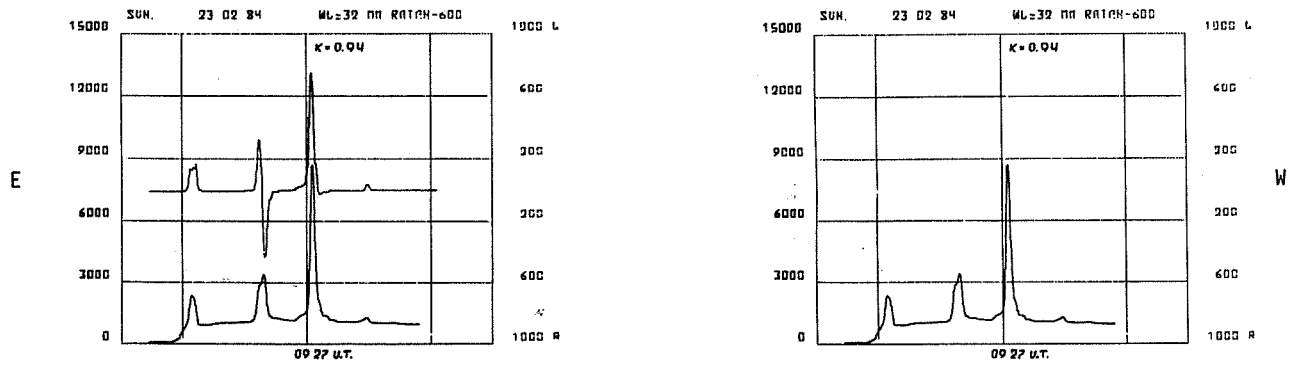


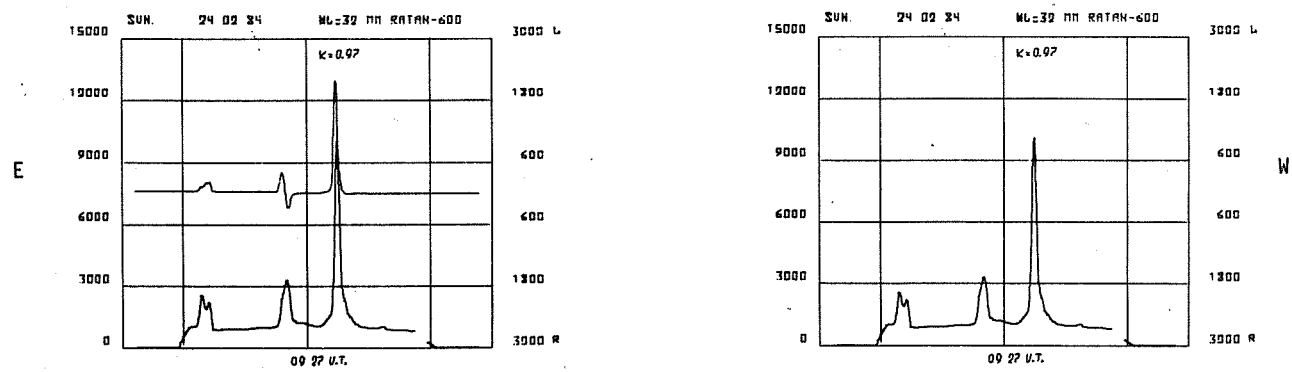

# EAST-WEST SOLAR SCANS

Zelenchukskaya, USSR

7 FEBRUARY - 1 MARCH 1984

40 mm
Fan-Beam with 41 seconds of arc
E-W Resolution

With Polarization Plot Superposed

Without Polarization Plot

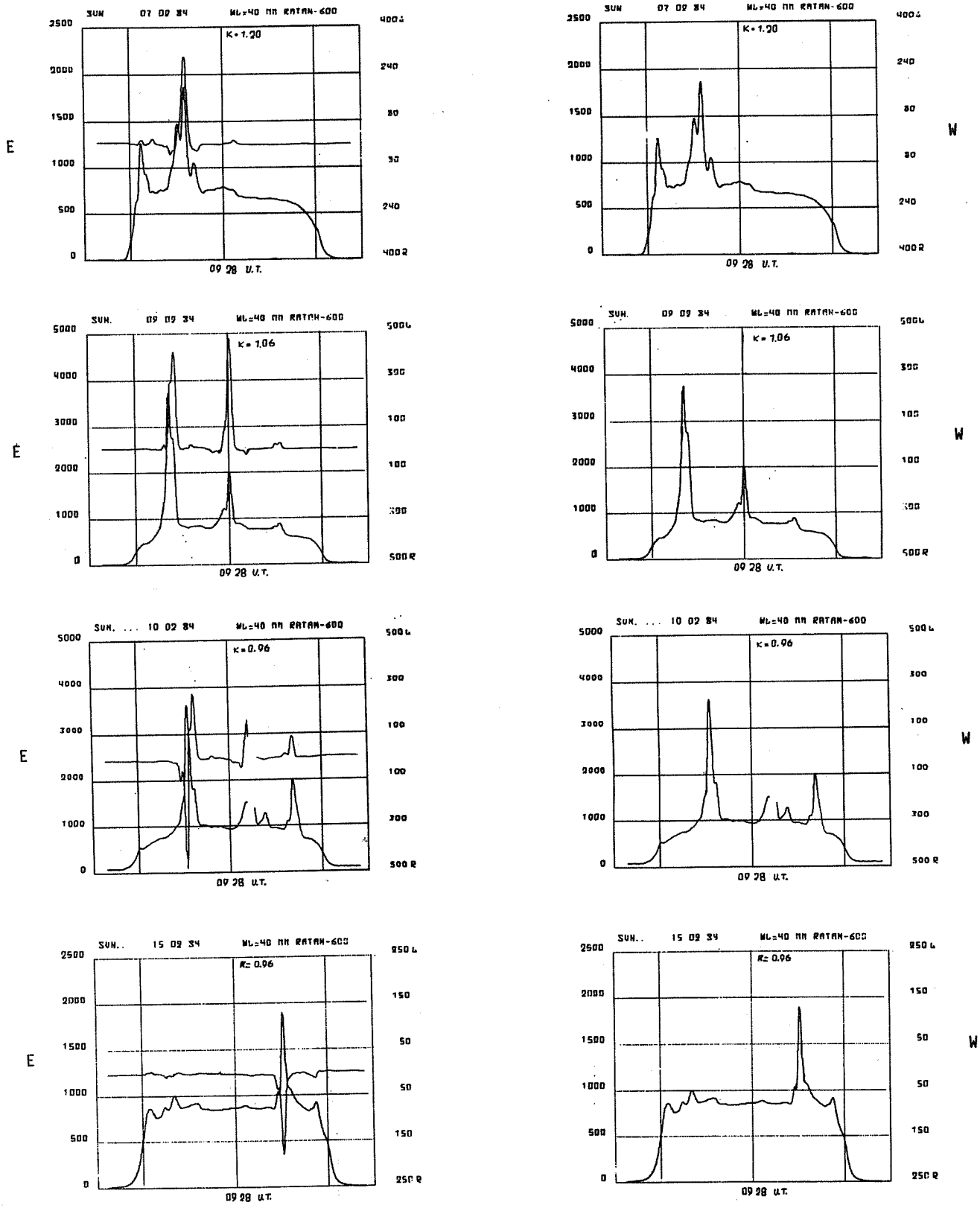

# EAST-WEST SOLAR SCANS

Zelenchukskaya, USSR

7 FEBRUARY - 1 MARCH 1984

40 mm
Fan-Beam with 41 seconds of arc
E-W Resolution

With Polarization Plot Superposed

Without Polarization Plot

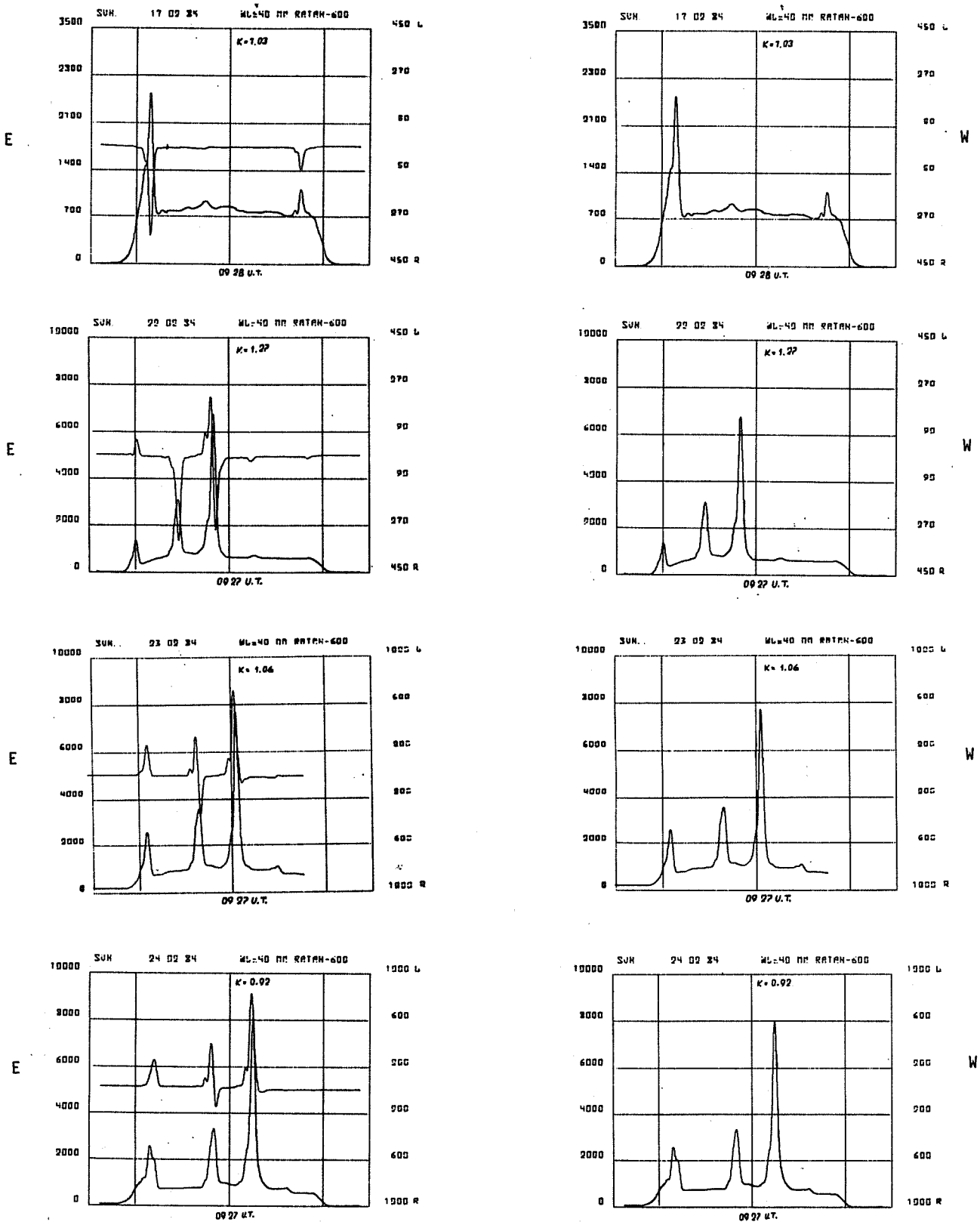

# EAST-WEST SOLAR SCANS

Zelenchukskaya, USSR

7 FEBRUARY - 1 MARCH 1984

207 mm
Fan-Beam with 210 seconds of arc
E-W Resolution

With Polarization Plot Superposed

Without Polarization Plot

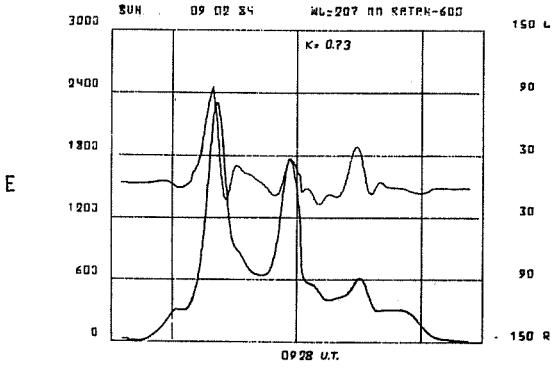


E

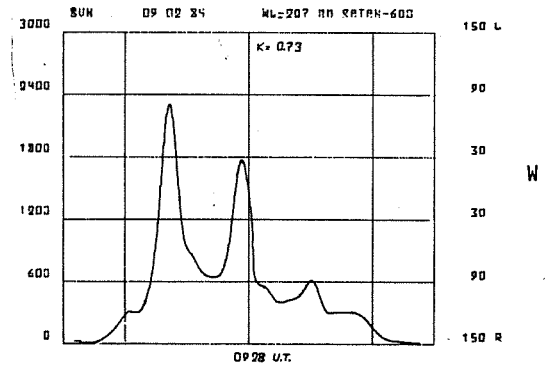


W

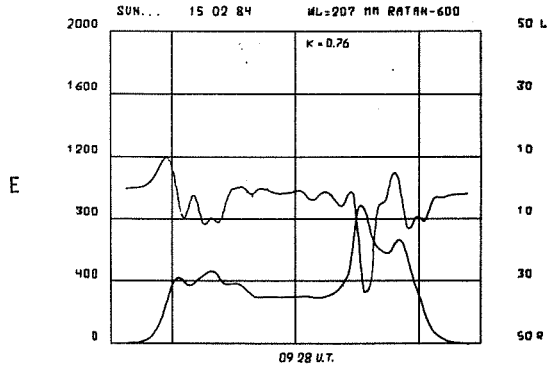


E

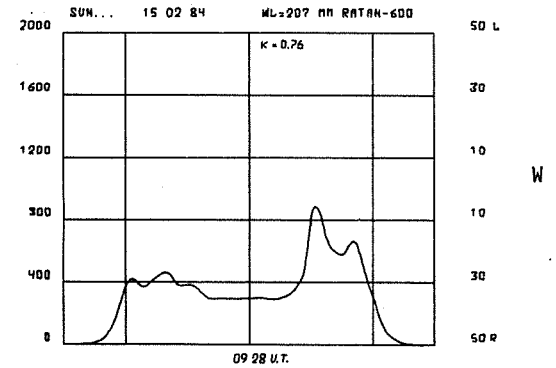


W

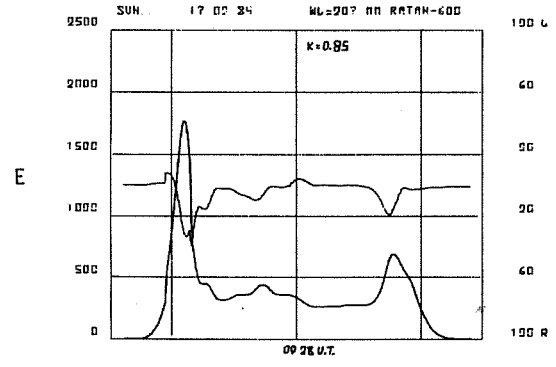


E

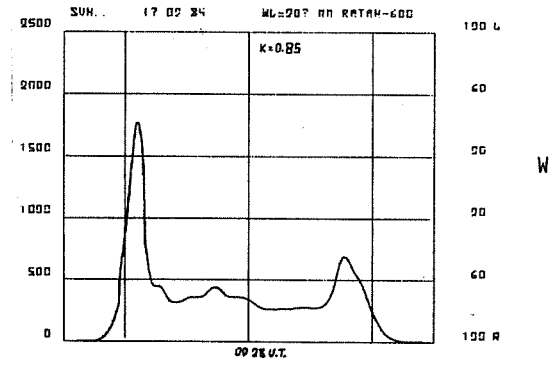


W

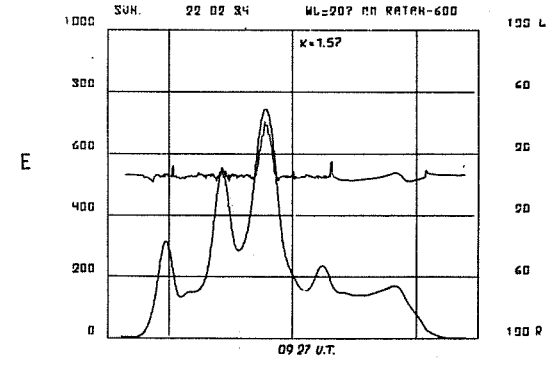


E

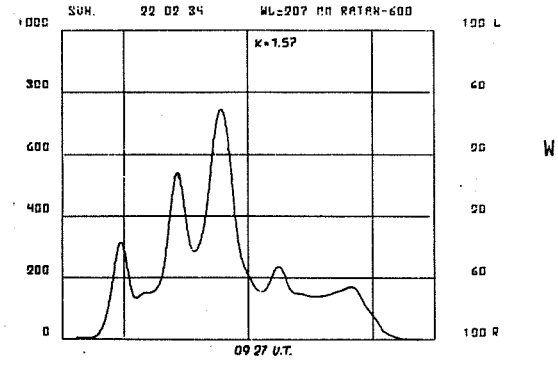


W

# EAST-WEST SOLAR SCANS

Zelenchukskaya, USSR

7 FEBRUARY - 1 MARCH 1984

207 mm
Fan-Beam with 210 seconds of arc
E-W Resolution

With Polarization Plot Superposed

Without Polarization Plot

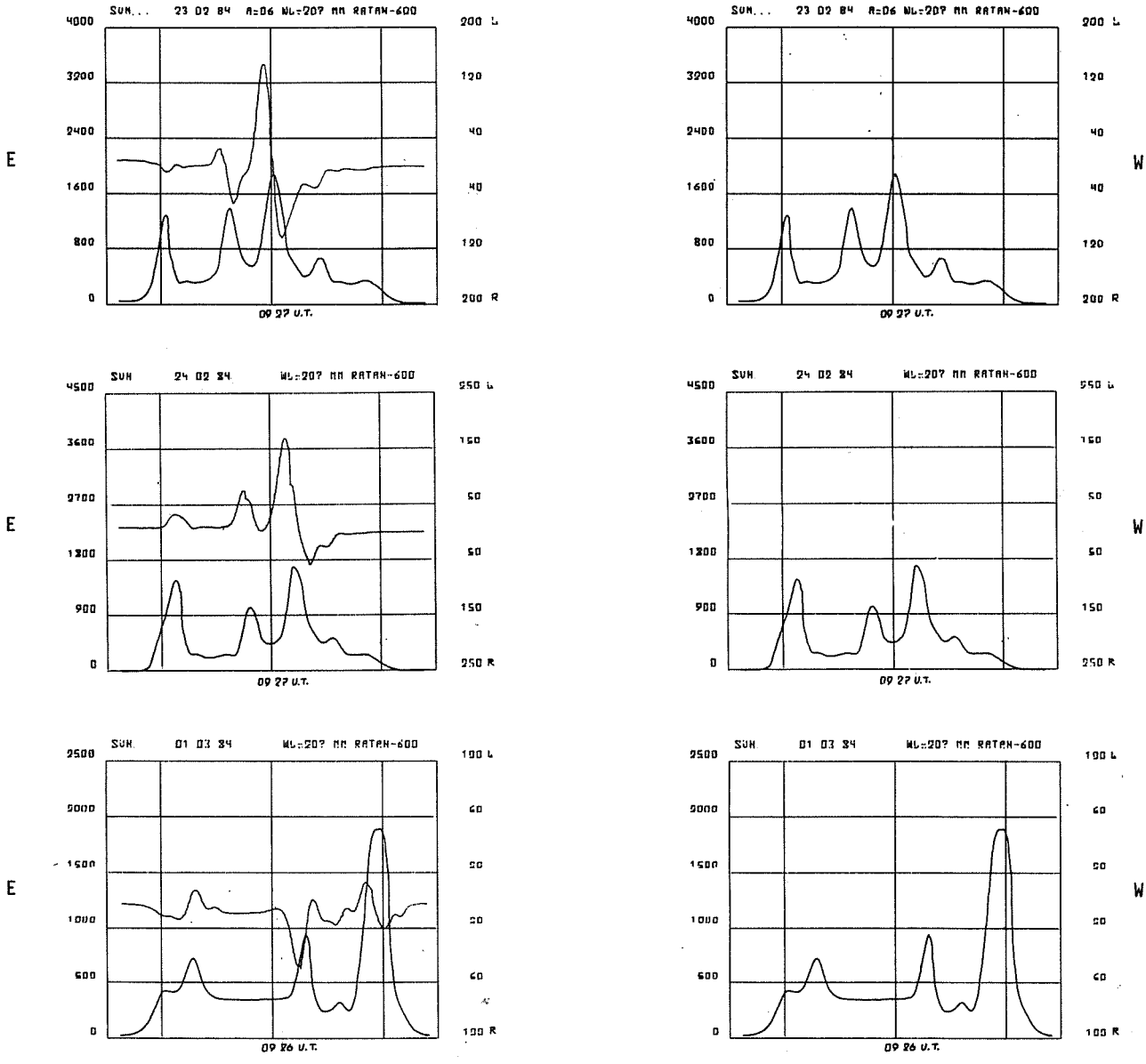

# EAST-WEST SOLAR SCANS

Zelenchukskaya, USSR

7 FEBRUARY - 1 MARCH 1984

316 mm
Fan-Beam with 321 seconds of arc
E-W Resolution

With Polarization Plot Superposed

Without Polarization Plot

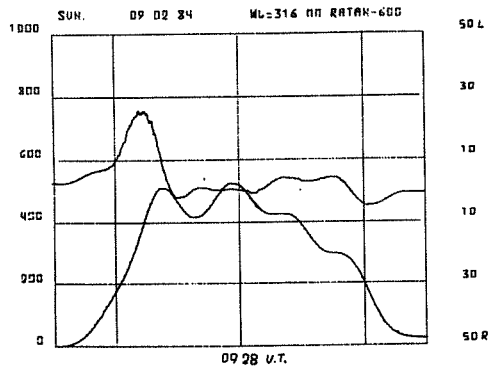


E

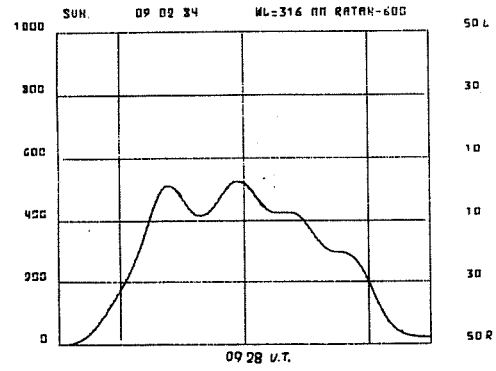


W

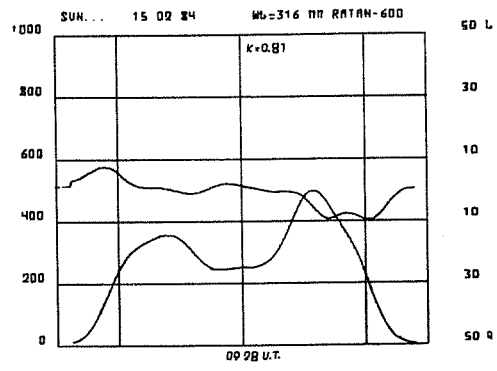


E

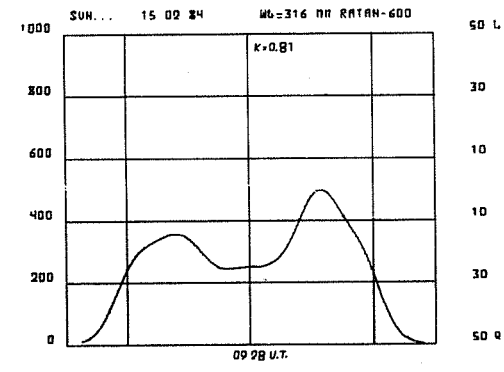


W

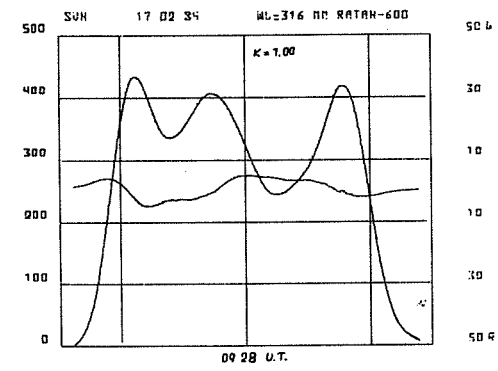


E

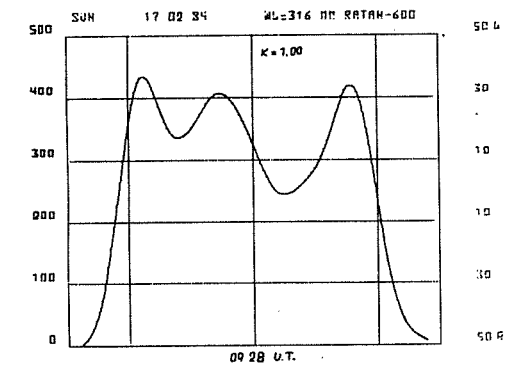


W

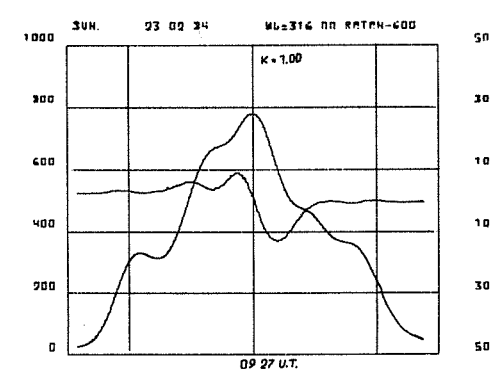


E

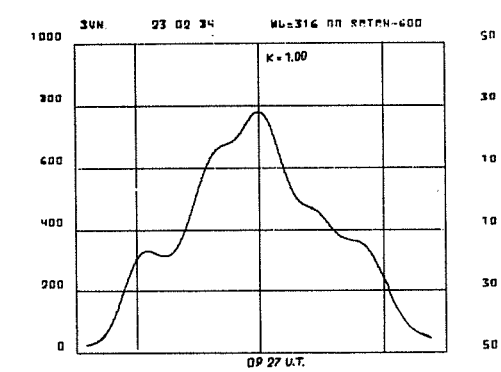


W

# EAST-WEST SOLAR SCANS

Zelenchukskaya, USSR

7 FEBRUARY - 1 MARCH 1984

316 mm
Fan-Beam with 321 seconds of arc
E-W Resolution

With Polarization Plot Superposed

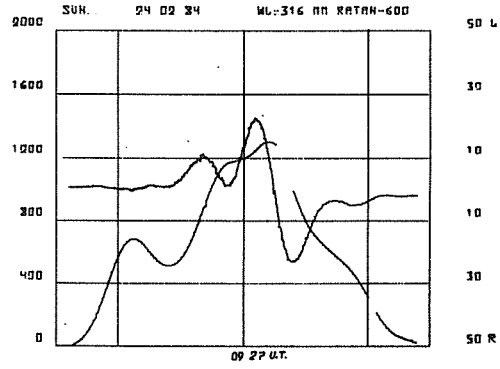


E

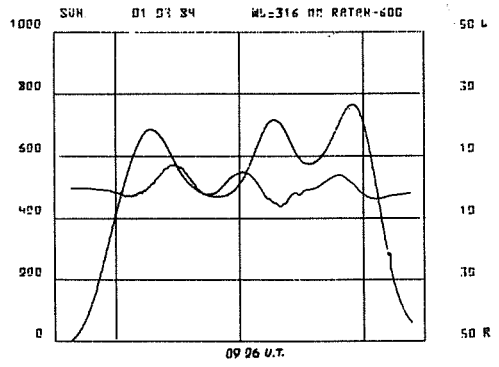


E

Without Polarization Plot

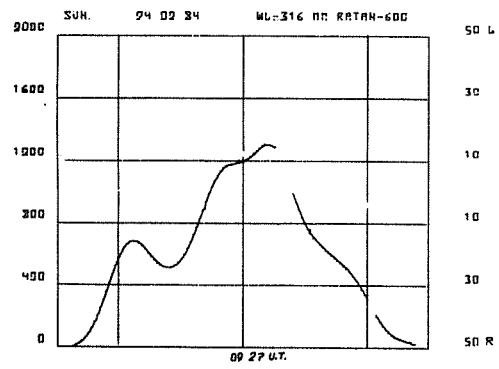


W

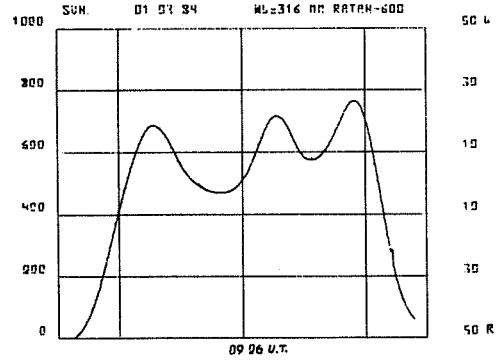


W

# East-West Solar Scans for 15-17 February and 23-25 April 1984 from the Large Pulkovo Array

by

V.E. Abramov-Maksimov and S.M. Vatrushin
Main Astronomical Observatory, Pulkovo, Leningrad, USSR
and
N.G. Peterova
Special Astrophysical Observatory, Pulkovo, Leningrad, USSR

## Explanation of Data

Observatory: Pulkovo, BPR (Large Pulkovo Radiotelescope)

Coordinates: N59.8 E-2.0h

| | FAN BEAM | | | | |
|---|---|---|---|---|---|
| Wavelength cm | E-W resolution minutes of arc | | N-S resolution minutes of arc | | Shift from focus point |
| | Feb. | April | Feb. | April | |
| 2.3 | 0.9 | 0.8 | 15 | 7 | 0.70 |
| 3.2 | 1.3 | 1.2 | 21 | 10 | -0.72 |
| 4.4 | 1.8 | 1.6 | 29 | 14 | 1.54 |

The diagram of the antenna was centered at the center of the solar disk.

The scans at all wavelengths were shifted to the common central meridian. No correction for aberration distortion has been made.

The Intensity is given in °K of antenna temperature.

# EAST-WEST SOLAR SCANS

Pulkovo, USSR

FEBRUARY 1984

23 mm
Fan-Beam with 0.9 minutes of arc
E-W resolution

15

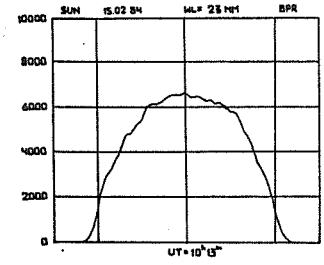


1013 UT

16

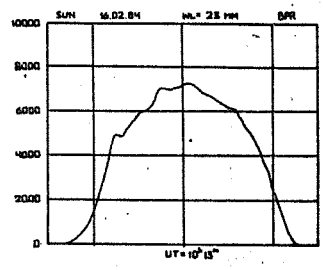


1013 UT

17

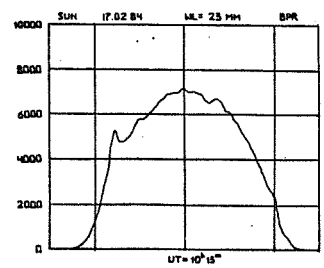


1013 UT

E W

44 mm
Fan-Beam with 1.8 minutes of arc
E-W Resolution

15

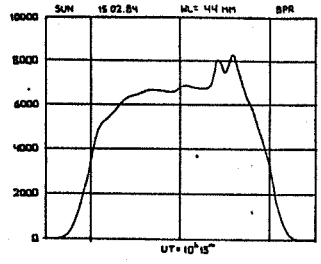


1013 UT

16

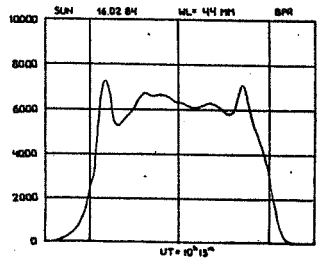


1013 UT

17

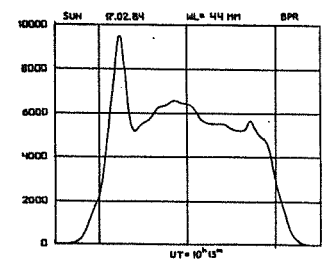


1013 UT

E W

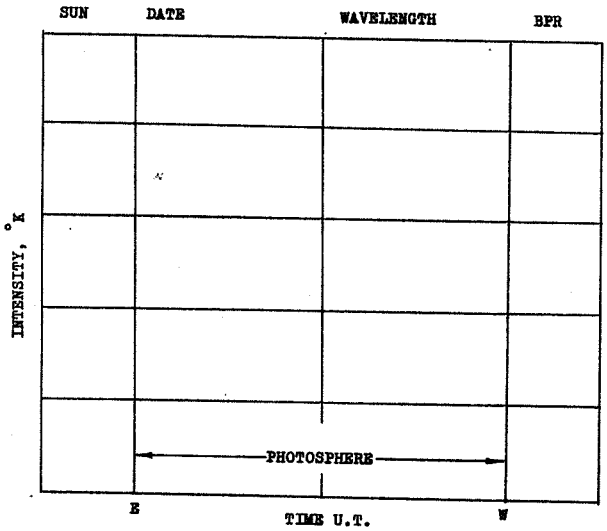


SAMPLE GRID

# EAST-WEST SOLAR SCANS

Pulkovo, USSR

APRIL 1984

**23 mm**
Fan-Beam with 0.8 minutes of arc
E-W resolution

23

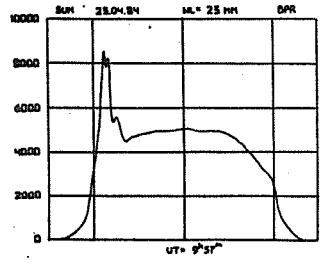


0957 UT

24

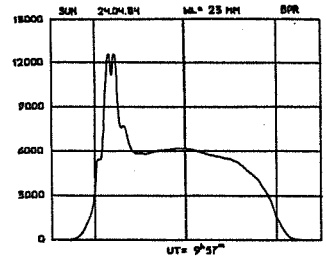


0957 UT

25

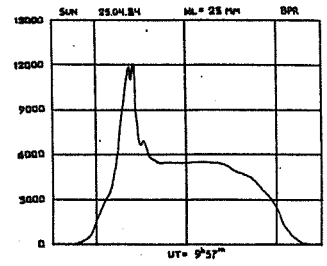


0957 UT

E W

**32 mm**
Fan-Beam with 1.2 minutes of arc
E-W Resolution

23

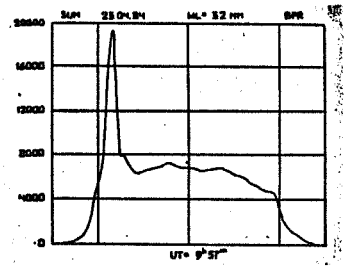


0957 UT

24

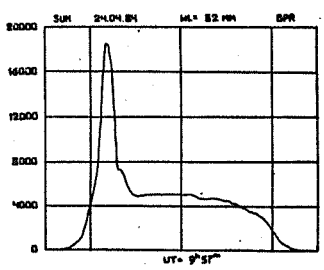


0957 UT

25

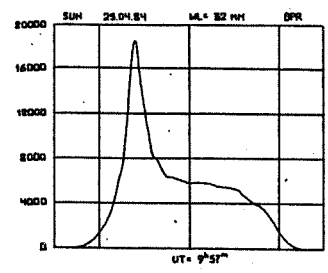


0957 UT

E W

**44 mm**
Fan-Beam with 1.6 minutes of arc
E-W resolution

23

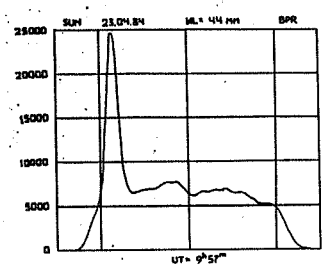


0957 UT

24

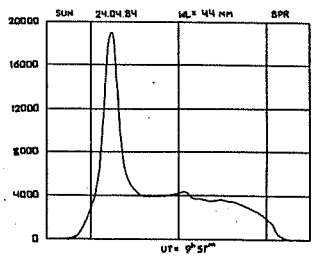


0957 UT

25

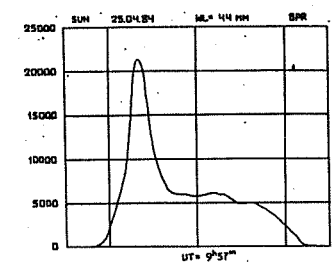


0957 UT

E W

# Microwave Activities of Active Region AR 4474

by

S. Enome, K. Shibasaki and M. Nishio
Toyokawa Observatory, Nagoya University
Toyokawa 442, Japan

## Introduction

This report describes activities of Active Region (AR) 4474 observed at Toyokawa in microwave range with radiopolarimeters at 9.4, 3.75, 2, and 1 GHz (Torii et al., 1979), and with radio interferometer-heliographs at wavelengths 8 and 3 cm (Tanaka and Kakinuma, 1965; Tanaka et al., 1969). Parameters of relevant instruments are briefly summarized below.

Table 1. Parameters of Antennas and Receivers

| | Frequency (GHz) | Antenna Diameter (m) | Integration Time (s) |
|---|---|---|---|
| Polarimeter | 9.4 | 0.8 | 0.5 |
| | 3.75 | 1.5 | 0.5 |
| | 2.0 | 2.0 | 0.5 |
| | 1.0 | 3.0 | 0.5 |
| | | | Half Power Beam Width (arcmin) |
| Interferometer | 9.4 | 2.0 | 1.1 |
| | 3.75 | 3.0 | 1.1 |

## Development of S-component associated with AR 4474

The slowly-varying component of solar microwave emission was first recognized on 20 April 1984 on the east limb associated with the solar active region AR 4474. The digital data of 20 April were not available due to the malfunction of the data acquisition minicomputer. The S-component became very intense on 23 April with flux densities well above 20 solar flux units (1 s.f.u. = $10^{22}$ $Wm^{-2}Hz^{-1}$) at wavelengths 8 and 3 cm for more than two weeks until it disappeared beyond the west limb of the Sun as is illustrated in the one-dimensional drift scans of Figures 1a, 1b, 1c and 1d. The flux ratio of 3 cm over 8 cm of the S-component stayed close to one during these intense periods, which is known to be a good measure to produce a proton flare from the relevant active region (Tanaka and Kakinuma, 1964; Tanaka and Enome, 1975). The active region was spatially compact until 25 April, which may be partly due to the effect of foreshortening, but later as it passed disk center, it changed into disintegrated sub-regions, as seen in Figures 1a, 1b, 1c, and 1d.

## The 24/25 April 1984 Event

During the course of passage across the solar disk AR 4474 produced many microwave bursts, among which the burst starting 2356 UT on 24 April is the largest of all with maximum flux of 20500 s.f.u. at 9.4 GHz at 0001.1 UT on 25 April. The time profile of this burst is composed of an impulsive first phase and a gradual second phase, which may be also described as impulsive and extended. The duration of the first phase was about 50 minutes and that of the second phase was as long as five hours as shown in Figures 2a, 2b, 2c, and 2d.

Microwave spectrum of the impulsive first phase has a maximum of 4100 s.f.u. at 2 GHz, which is more intense than those flux densities at 9.4, 3.75, and 1 GHz by factors of 2, 3, and 3 respectively. The first phase time profile at 1 GHz shows two enhancements in a large time-scale feature separated by about 3 minutes, while others show single temporal enhancements. The maximum time at 3.75 GHz is advanced relative to those at other frequencies by about 30 to 40 seconds. The spectrum of the second gradual phase increases toward lower frequencies with an abrupt jump at 1 GHz, about 90 percent of which may be attributed to a spiky decimeter-wave burst component with a remarkably high degree of circular polarization. Contamination or superposition of the second gradual phase is also slightly affected at 2 GHz by a spiky decimeter-wave burst. If these contaminations are properly subtracted from the observed time profiles, the gradual component has a maximum in spectrum around 2 GHz. The sense of circular polarization is left-hand for the gradual second component at frequencies 9.4 to 1 GHz. The polarization is inconsistent with the observed maximum, if the spectral peak is explained in terms of magneto-bremsstrahlung self-absorption with a simple source structure, since theory predicts a polarization reversal with respect to frequency across the spectral peak.

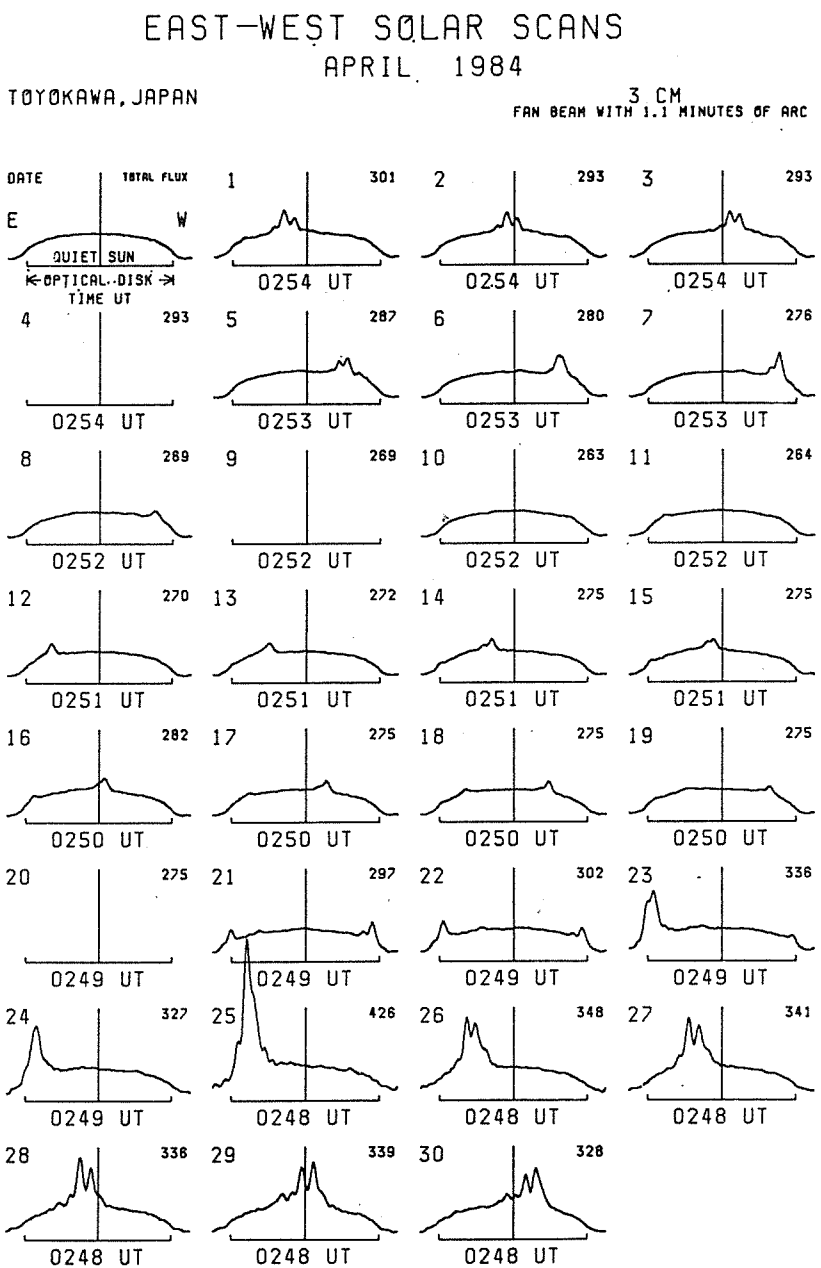


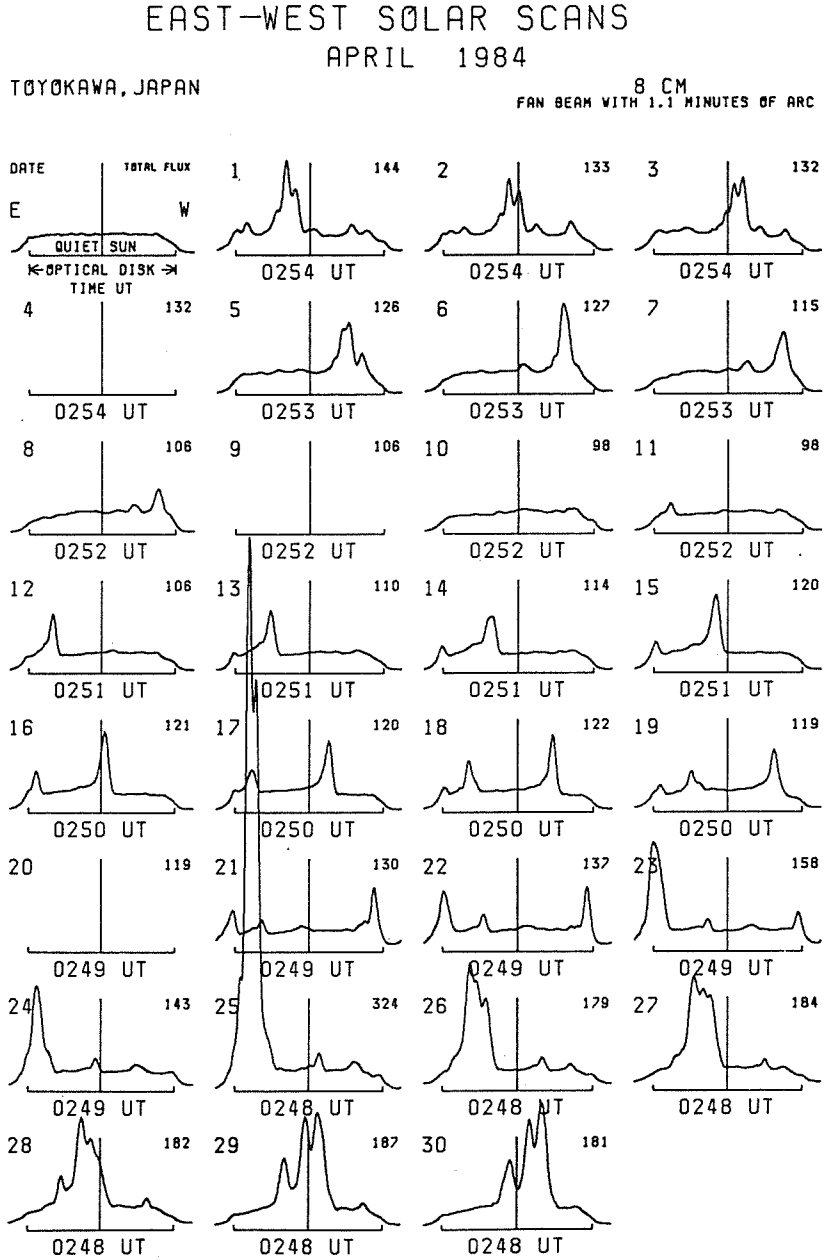


Figs. 1a and 1b. Drift curves of the Sun in one dimension observed at local noon with the 3 cm and 8 cm interferometers at Toyokawa during April 1984.

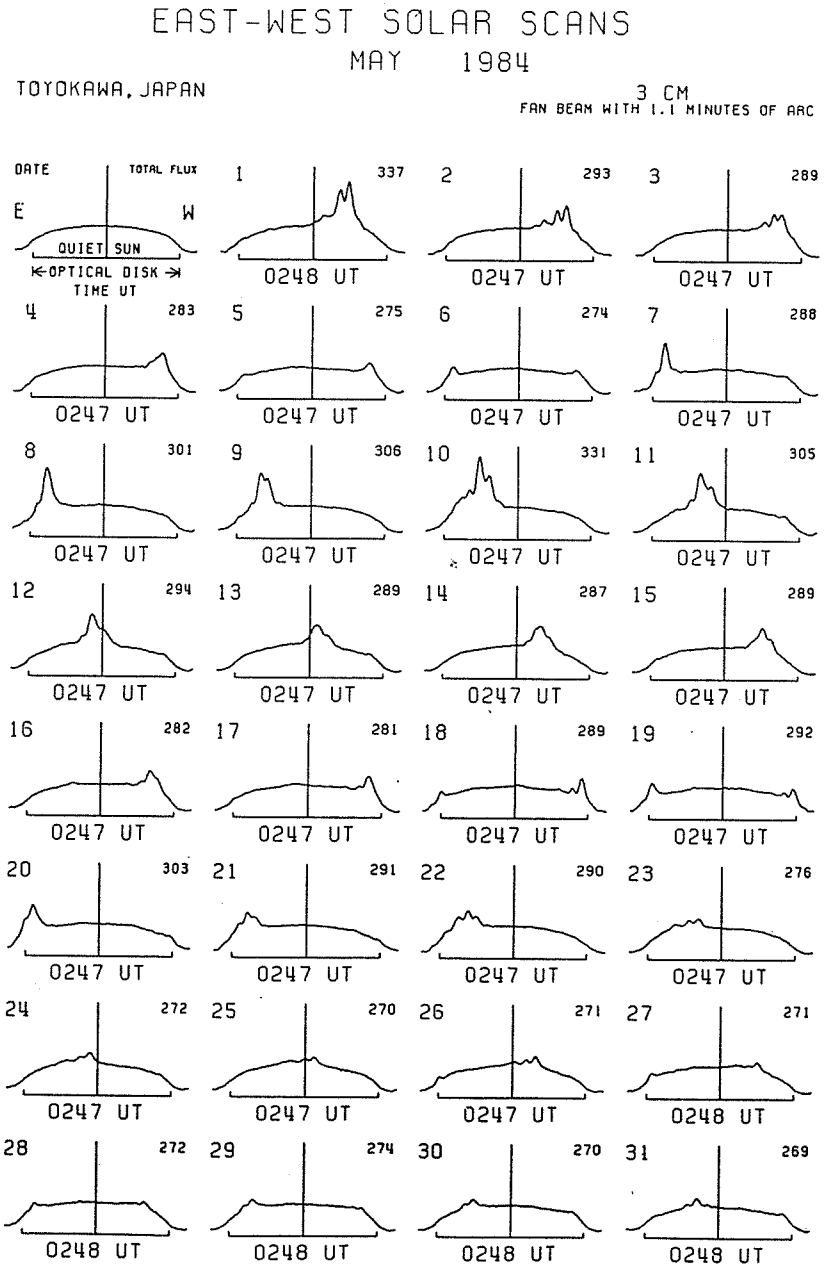


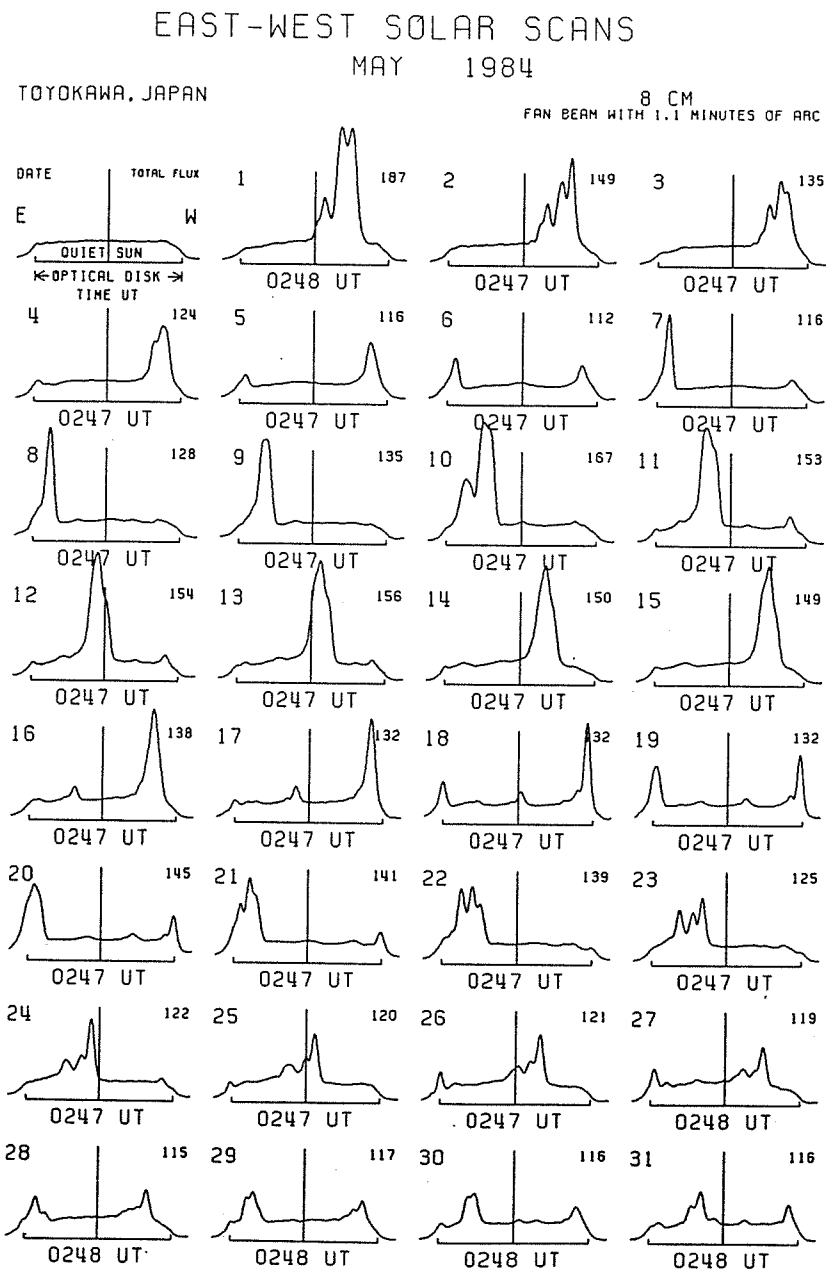


Figs. 1c and 1d. Drift curves of the Sun at 3 cm and 8 cm for May 1984.

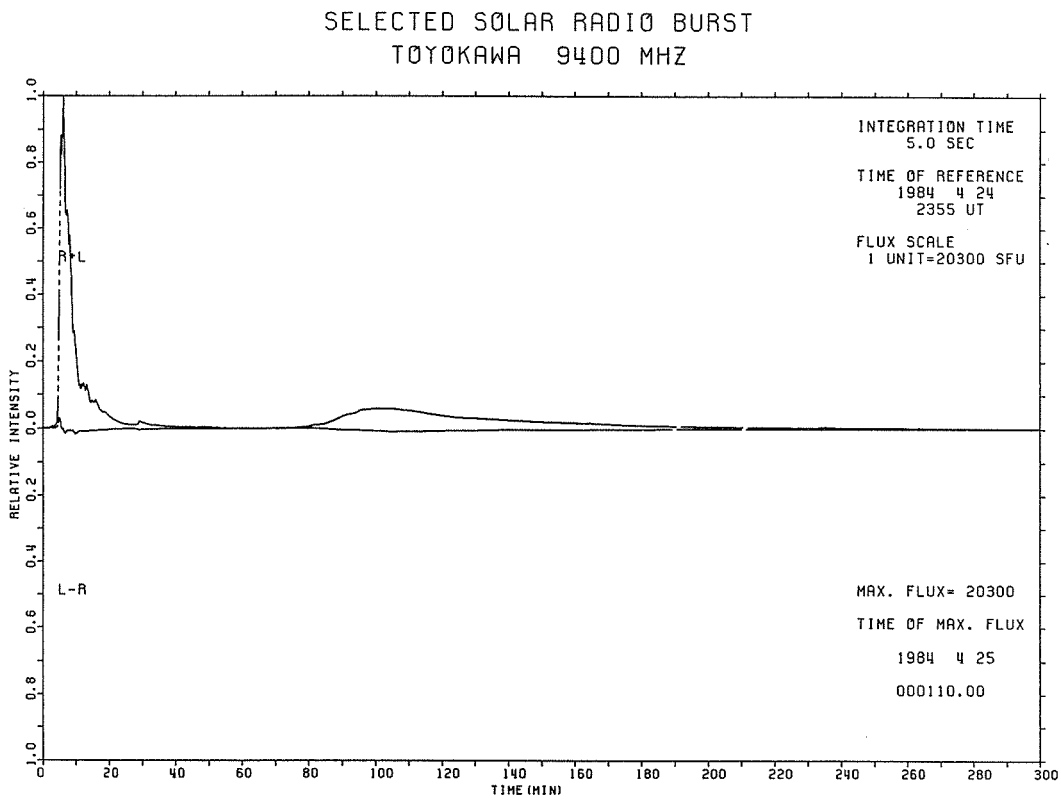


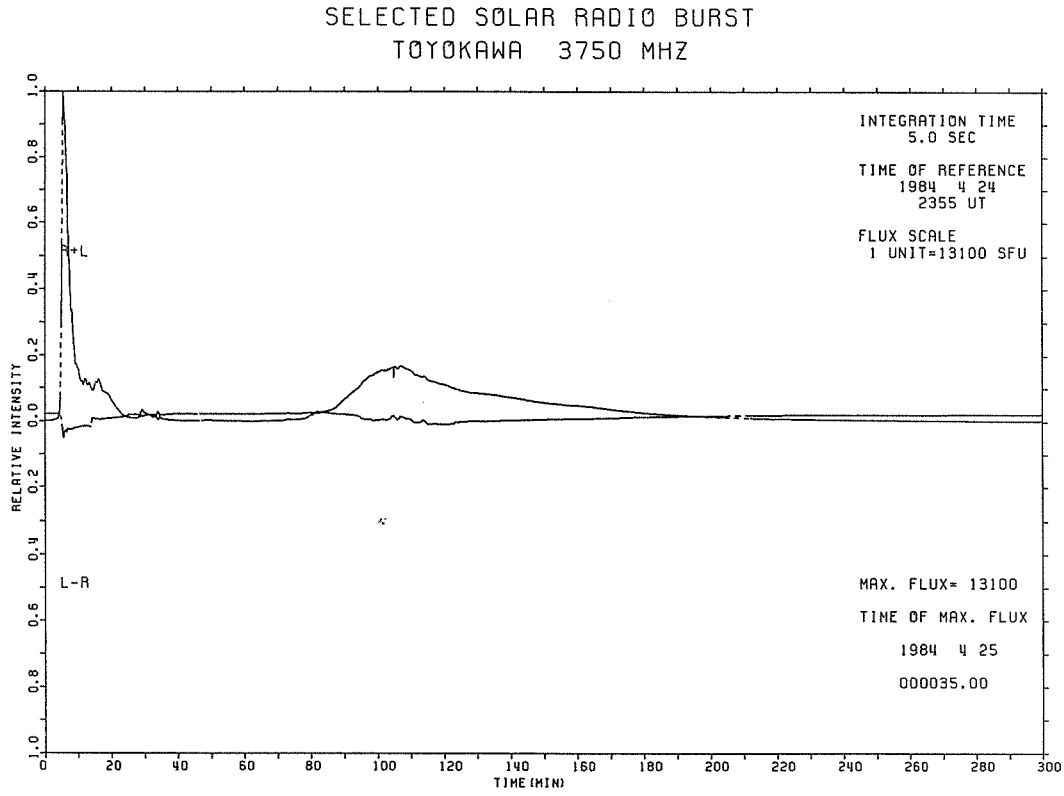


Figs. 2a and 2b. Time profiles of the burst of 24/25 April 1984, at 9.4 and 3.75 GHz in 0.5 second integration time for 300 minute duration with starting time of 2355 UT, 24 April 1984. The upper half of each frame is for intensity display, and the lower half for polarization display, where the sense is indicated either left-right (L-R) or right-left (R-L) in the downward direction. (Continue to Figures 2c and 2d.)

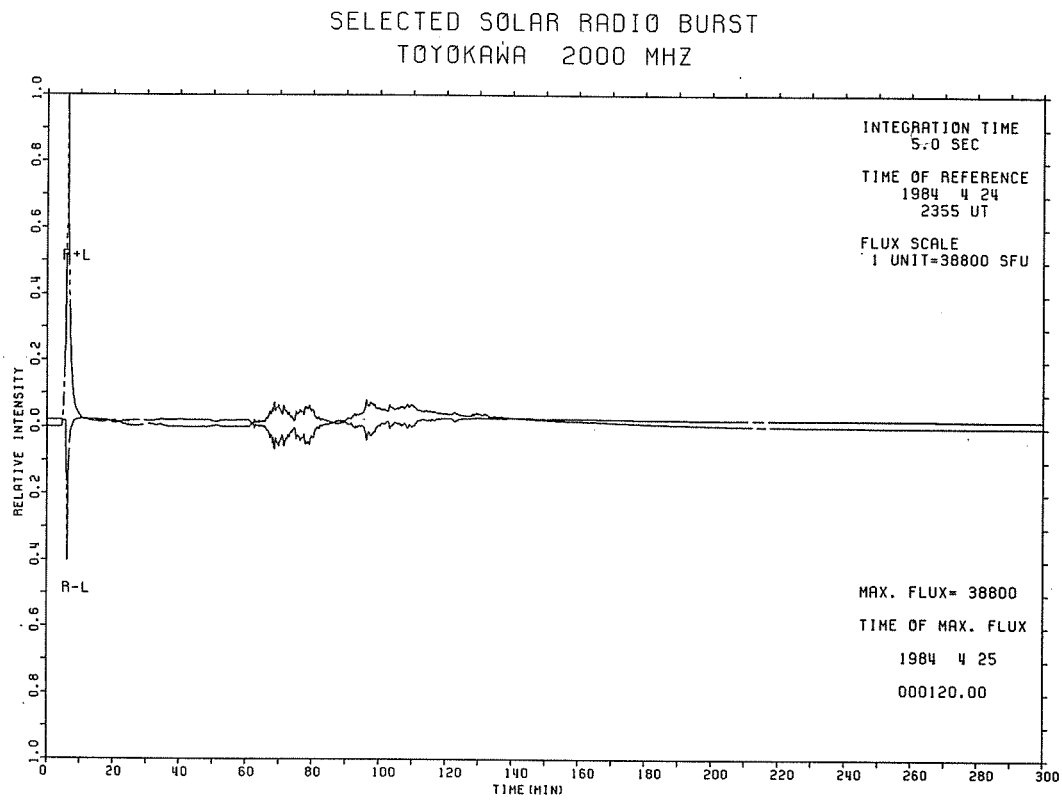


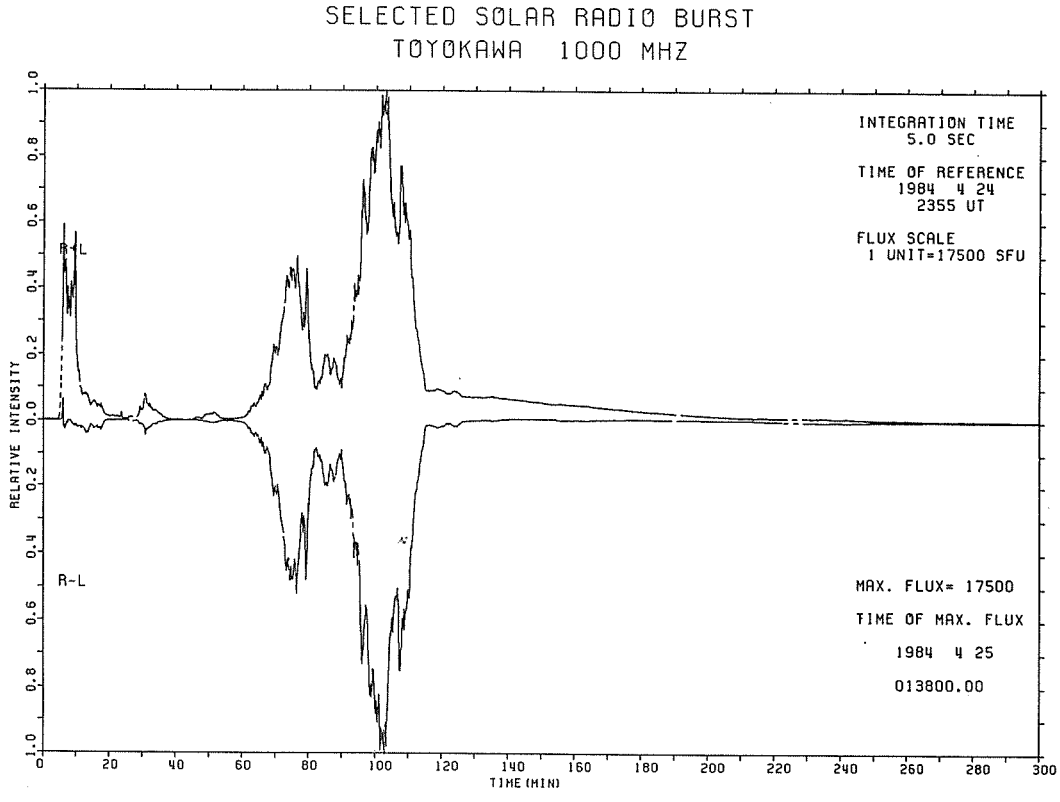


Figs. 2c and 2d. Time profiles of the burst of 24/25 April 1984, at 2 and 1 GHz in 0.5 second integration time for 300 minute duration with a starting time of 2355 UT, 24 April 1984 (continued from Figures 2a and 2b). The maximum flux or time of maximum flux indicated in each frame should not be referenced especially for the impulsive first phase, since they are measured with an integration time of 0.5 seconds and tabulated in the **Solar-Geophysical Data** (SGD).

Between the impulsive first phase and gradual second phase there was an absorption at 9.4 and 3.75 GHz and also associated with it in time there were spiky decimeter-wave emissions at 2 and 1 GHz. The absorption is caused by an occultation of the S-component emission by an overlying cold matter which is illustrated in Figure 3, where drift curves of the relevant S-component displayed in time sequence are overlayed on the sunspot sketch drawn at the Tokyo Atronomical Observatory. Drift scan observations at 8 cm started around 0045 UT. The AR 4474 corresponds to the Tokyo Astronomical Observatory (TAO) AR 133, AR 134, and AR 136. The drift curve of beam # -42 at 0048 UT shows two humps, which corresponds in position to TAO AR 134 and the eastern part of TAO AR 133. The enhancement, which coincides with the main sunspot of AR 4474 began to reduce its brightness in the drift scan of # -41, and it kept low in brightness until 0100 UT, and then it gradually grew into the eastern component of the gradual second phase. The other hump, which did not show a decrease in brightness, also grew into the other component of the gradual second phase. The polarization records indicate that the eastern component of the gradual second phase is right-hand circularly polarized, which implies radiations are emitted in an N or minus polarity region. The TAO AR 134 was a well known delta configuration with north polarity of the northern half side and south polarity with the southern half side of the main sunspot. Combining these two sets of data, it is natural to deduce that the eastern component of the gradual second phase originated from the northern side of the TAO AR 134. Optical observations conducted at Hida Observatory of Kyoto University caught an ejection of dark matter in H-alpha $\pm$ 0.5 or 0.8 angstrom starting at 0029 UT with a possible maximum area of coverage at 0059 UT. The ejection originated somewhere between the TAO AR 133 and 136, directed toward the east to cover the TAO AR 134 of the main sunspot of AR 4474 (private communication from Dr. H. Kurokawa, Hida Observatory). These optical observations are in good agreement with our radio observations with respect to time and space.

Temporal coincidence is already mentioned as above between the absorption and the decimeter-wave burst. The spatial relation, on the other hand, is not in the observational sense possible to handle, since we do not have direct spatial data at the decimeter wavelength range. It is, however, possible to deduce that the decimeter wave source, observed during the course of the absorption, was higher in height than the occulting dark matter, and therefore than the S-component at 8 and 3 cm. It is tempting to imagine possible physical links between the absorption and the decimeter-wave burst via the dark matter, but we will refrain from going further, because this is possibly the first case to observe three subjects simultaneously, and we will need further investigations into observational data for similar events.

## REFERENCES


TANAKA, H. 1964 "The Relation between the Spectrum of Slowly-Varying Component of Solar Radio Emission and Solar Proton Event," **Rep. Iono. Space Res. Japan, 18, 132.**

TANAKA, H. and T. KAKINUMA 1965 "Improvement of the High-Resolution Interferometer at 9.4 Gc/s," **Proc. Res. Inst. Atmospherics, Nagoya University, 12, 27.**

TANAKA, H., T. KAKINUMA, S. ENOME, C. TORII, Y. TSUKIJI S. KOBAYASHI, M. ISHIGURO, and M. ARISAWA 1969 "A High-Resolution Quick-Scan Interferometer for Solar Studies at 3.75 GHz," **Proc. Res. Inst. Atmospherics, Nagoya University, 16, 113.**

TANAKA, H. and S. ENOME 1975 "The Microwave Structure of Coronal Condensations and Its Relation to Proton Flares," **Solar Phys., 40, 123.**

TORII, C., Y. TSUKIJI, S. KOBAYASHI, N. YOSHIMI, H. TANAKA, and S. ENOME 1979 "Full-Automatic Radiopolarimeters for Solar Patrol at Microwave Frequencies," **Proc. Res. Inst. Atmospherics, Nagoya University, 26, 129.**

SGD 1984a **Solar-Geophysical Data, 482, Part II, Oct. 1984, U.S. Department of Commerce, Boulder, Colorado, USA 80303.**

SGD 1984b **Solar-Geophysical Data, 483, Part II, Nov. 1984, U.S. Department of Commerce, Boulder, Colorado, USA 80303.**

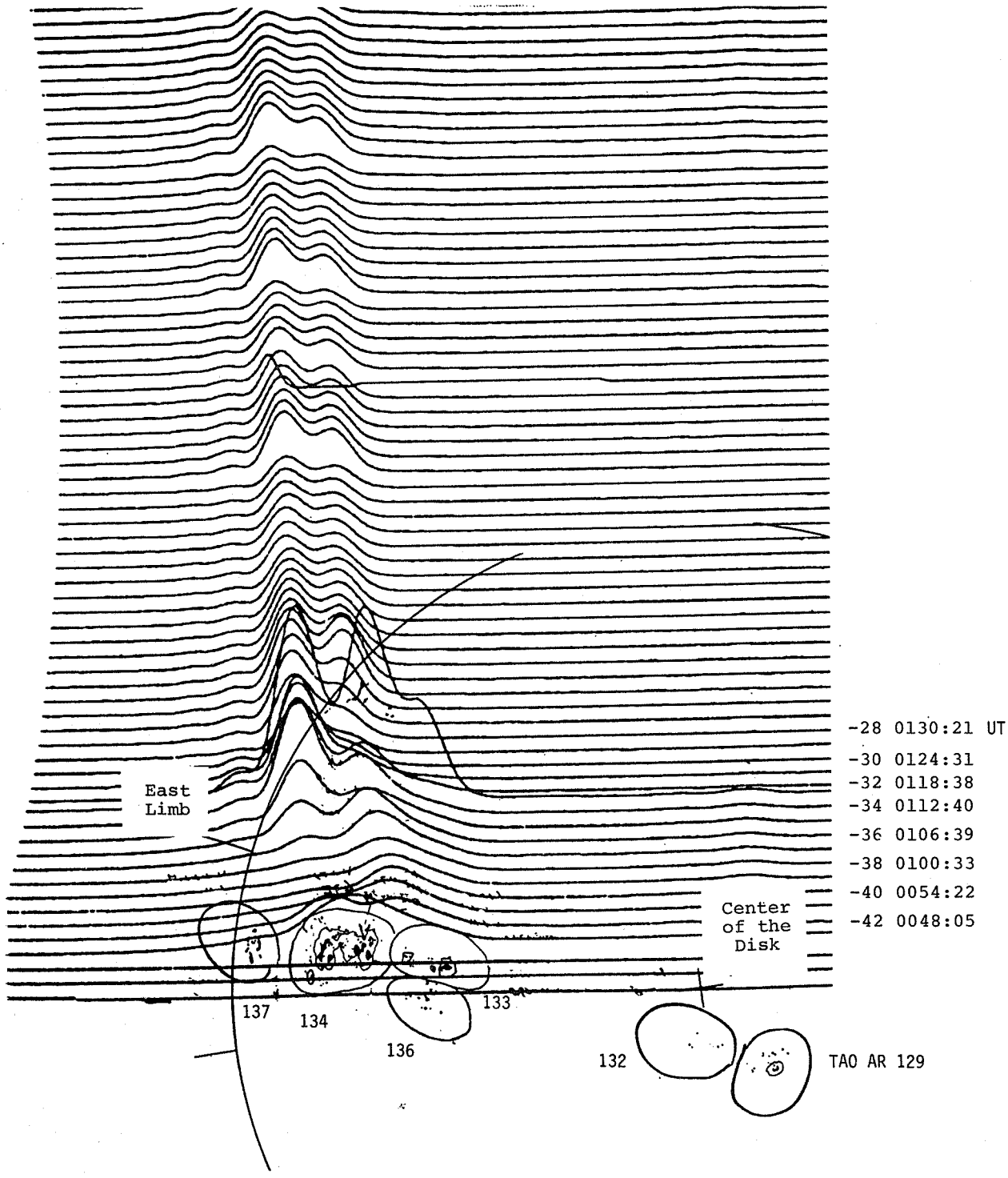


Fig. 3. Drift curves of the Sun at 3.75 GHz for the absorption and the gradual second phase are displayed in time sequence, which are superposed on the sunspot sketch observed at Tokyo Astronomical Observatory. East and west are toward the left and right of the figure, and the scanning point is in the horizontal direction of the figure, for which purpose the sunspot sketch is reversed and tilted properly. The scanning beam number and the time of each two scans are indicated on the right-hand side of the corresponding drift curve. Negative beam number indicates negative hour angle or before local noon.

## Meter Radio Emission and Proton Flare of 24-25 April 1984

by

G.P. Chernov, I.M. Chertok, V.V. Fomichev,
A.A. Gnezdilov, R.V. Gorgutsa, and A.K. Markeev
IZMIRAN, Troitsk, Moscow Region, USSR

Enhanced activity at the end of April was mainly caused by the NOAA Active Region (AR) 4474. According to the NOAA **Solar-Geophysical Data** (SGD), almost all flares took place in this region. The observations reported below were carried out with two identical 45-90 MHz spectrographs at IZMIRAN and Kislovodsk, separated by a distance of about 1500 km in order to exclude ionospheric effects, as well as with spectrographs in the ranges 90-180 MHz and 200-245 MHz and with radiometers at the three fixed frequencies 169, 204 and 3000 MHz. We considered only the radio bursts associated with the flares in AR 4474.

During the period of 20 April - 2 May 1984 no large events occurred during our daily observational interval 0600-1200 UT. However, this active period is very interesting because a number of small flares were accompanied by radio bursts with various fine structure. Different types of radio bursts were observed on the background of a relatively weak noise storm.

### Noise Storm of 20 April - 2 May 1984

We analyzed the noise storm at 204 MHz (see Figure 1). The development of the noise storm correlates mainly with the variations of the area of the AR 4474. The Nancay interferometric observations at 169 MHz also confirm the association of this noise storm with the AR 4474 (SGD, 1984). The influence of the proton flare on 24-25 April is insignificant because the expected increase of the noise storm immediately after the flare was not observed. Also, in the period 29 April - 1 May the two-component source of the noise storm (continuum and burst) was observed, one of which was connected with AR 4476.

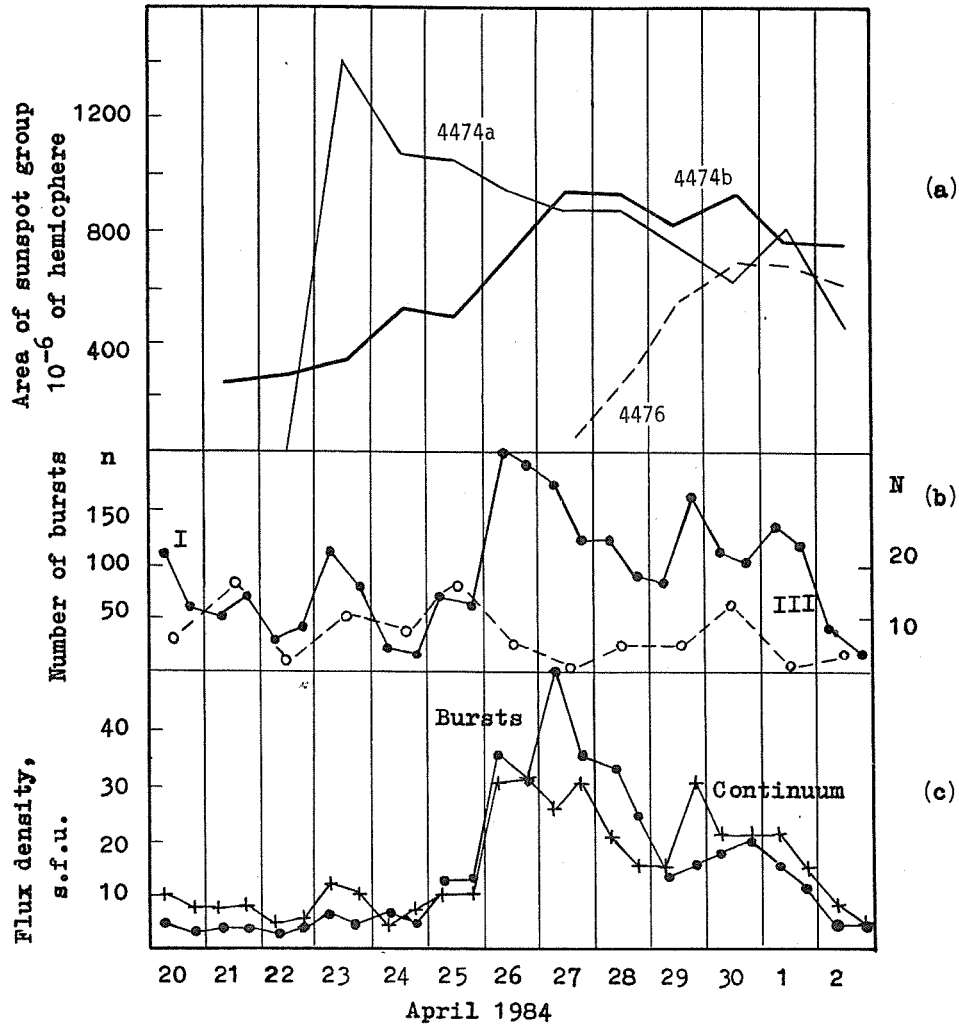


Fig. 1. This shows the variations of the sunspot group areas of the largest active regions (1a) and characteristics of the noise storm (1b and 1c) in April 1984. In Figure 1b the hourly number of Type I bursts (n) and the daily number of Type III groups (N) are given.

The flux densities of the continuum and the burst components of the noise storm are comparable (about 30-40 s.f.u.) (Figure 1c).

## Type III Bursts

The number of Type III burst groups was the greatest on 21 and 23 April (Figure 1b) when the number of Type I bursts also increased. However, beginning on 26 April the number of Type III burst groups decreased although the noise storm intensified. One can hypothesize that many Type III bursts were generated in other active regions.

The peculiarity of the Type III bursts on 21 and 24 April was the different final frequencies (J-type bursts, sharp stops of the emission at a certain frequency).

In Figure 2a and 2b the dynamic spectra of some groups of Type IIIb bursts recorded simultaneously at IZMIRAN and Kislovodsk are shown. One can see the coincidence of the main details of these spectra. Enlarged fragments of the dynamic spectra with the Type III bursts are shown in Figure 3. Note that the parameters of stria-elements of these bursts differ from the known ones (De la Noe and Boischot, 1972). The first burst on 23 April at 0916:48 UT is an isolated one and consists of the strips and blobs of diffuse form. Time duration of small details on the forward edge of the burst is about 0.2 seconds and increases with the decreasing of frequency. Some strips in the frequency range 50-52 MHz have the reverse drift of about 0.5 MHz/s. The second burst at 0917:12 UT contains also the diffuse elements with positive frequency drift.

The burst at 0841:18 UT on 25 April has an unusual form and composition. Its leading edge has an irregular drift. On the high frequency side, the burst consists of numerous short-lived blobs (about 0.2 seconds) and strips with the direct drift of about -0.2 MHz/s, particularly split pairs and triple bursts. Stria bursts show longer duration and less drifting at low frequencies.

## Continuum bursts with Fine Structure on 26 April

A very interesting Type III, V burst group with a fine structure was observed at 0659 UT on 26 April (Figure 2c). The event began with a group of the usual Type III bursts in the frequency range 180-90 MHz. At the time, the emission at low frequencies had diffuse dynamic spectrum. Then in a small time interval the continuum burst began which may be attributed either to the Type V or IV bursts. On the high frequency part (200-242 MHz) the burst has the form of pulsations in emission and absorption with the time scale of seconds, and with the very high frequency drift in the range 240-230 MHz which cannot be measured (Figure 4). At lower frequencies the drift of the pulsations becomes measureable, $df/dt \sim -200$ MHz/s at 220 MHz. In the range 180-220 MHz the frequency drift of the pulsations decreases gradually from $df/dt \sim -180$ to -0.5 MHz/s. The pulsations turn into arch strips similar to the zebra structure with frequency distance between the emission bands of about 1.5 MHz at 150 MHz. The flux density of the pulsations was about 2000 s.f.u. at 204 MHz and 1000 s.f.u. at 169 MHz (Figure 5).

In the range 90-45 MHz these pulsations are not continued, and the dynamic spectrum has a blob structure. At the frequencies 72-84 MHz some drifting filaments with the bandwidth of 2 MHz and with drift $df/dt$ = about -0.75 MHz/s are also present. At the frequencies 66-48 MHz the burst consists of a set of slow drifting strips. Analogous structures in this range have been observed before in Type V bursts (Akinyan, et al., 1976; Gnezdilov et al., 1981).

Thus in this event the continuous transition of the pulsations into the zebra pattern is observed for the first time. Spike bursts with a duration of 0.2-0.3 seconds and without the frequency drift are also observed in this burst.

On 26 April after the 1B flare at 0853-0930 UT (S09 E34) one more continuum burst of a short-time duration was observed (Figure 5b). From 0903-0906 UT this burst revealed the whole set of fine structure characteristic of Type IV bursts (Figure 6): seconds duration pulsations (0903:27-0903:37 UT), fiber bursts (0904:27-0904:41 UT) and zebra pattern (0903:43-0906:00 UT). Minimum time of duration of the pulsations was 0.1-0.2 seconds. Fiber bursts at 0904:30 UT and zebra pattern at 0905:55 UT had the unusually narrow bandwidth of emission lines of about 0.5 MHz. During 0905:30-0906:00 UT another zebra pattern with the usual bandwidth of about 2-2.5 MHz is also present.

Both bursts in the meter range at 0700 and 0900 UT were accompanied by weak microwave emission (Figure 5).

## Diagnostics of the 24-25 April Flare

The 3B/X13 flare of 24-25 April with a maximum at about 25 April 0001 UT and coordinates S12 E43 was the largest event during the disk passage of the Active Region 4474. It is interesting to compare the radio burst parameters with the proton flux ones near the Earth from this flare. Here such comparison is made on the basis of the quantitative proton flare diagnostics technique developed in IZMIRAN (see Akinyan et al., 1980).

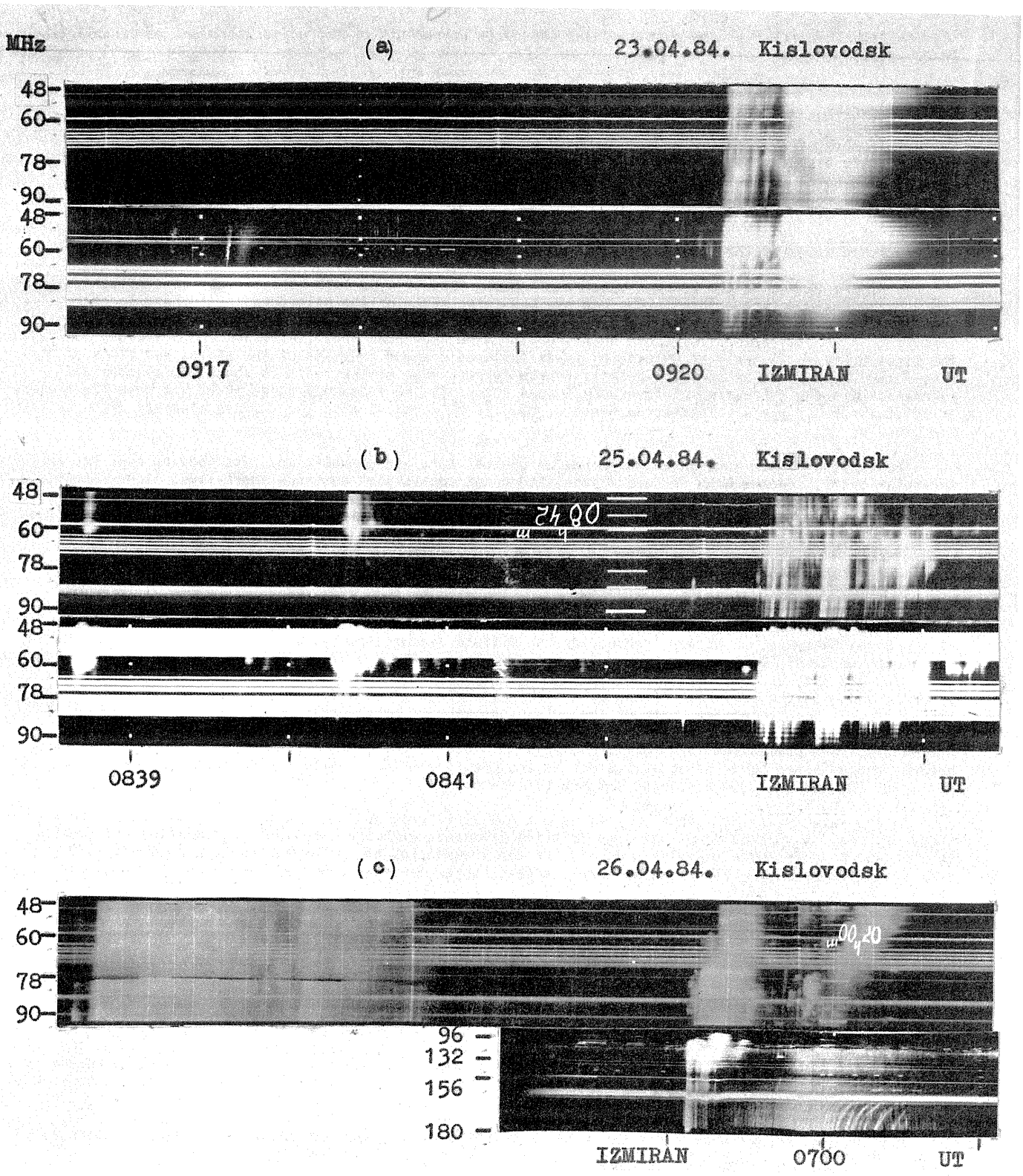


Figure 2. This shows the general form of the dynamic spectra recorded at IZMIRAN (bottom panel) and Kislovodsk (top panel) for the time periods:
(a) 23 April 1984 at 0916-0922 UT;
(b) 25 April 1984 at 0838-0844 UT;
and (c) 26 April 1984 at 0655-0700 UT.

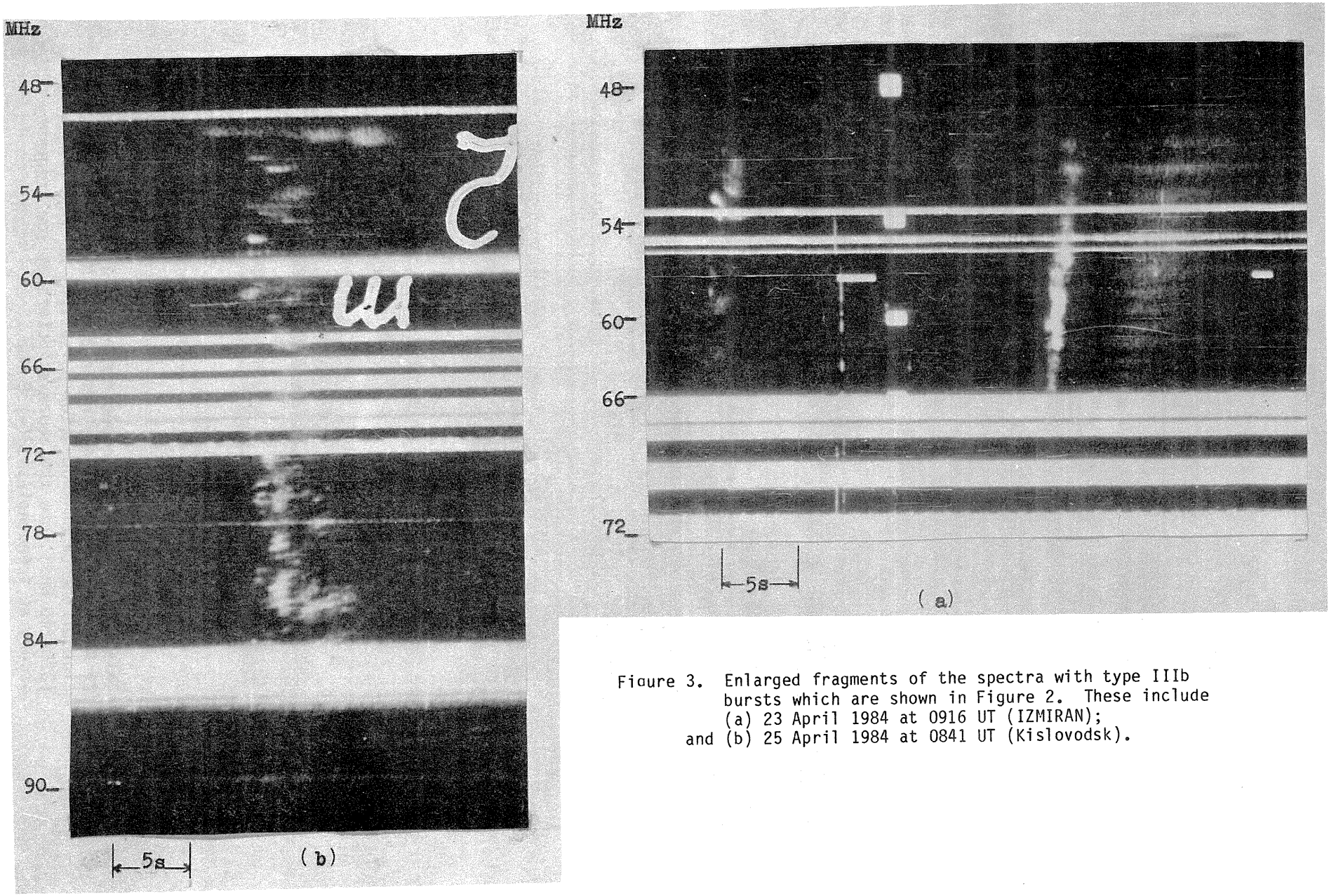


Figure 3. Enlarged fragments of the spectra with type IIIb bursts which are shown in Figure 2. These include (a) 23 April 1984 at 0916 UT (IZMIRAN); and (b) 25 April 1984 at 0841 UT (Kislovodsk).

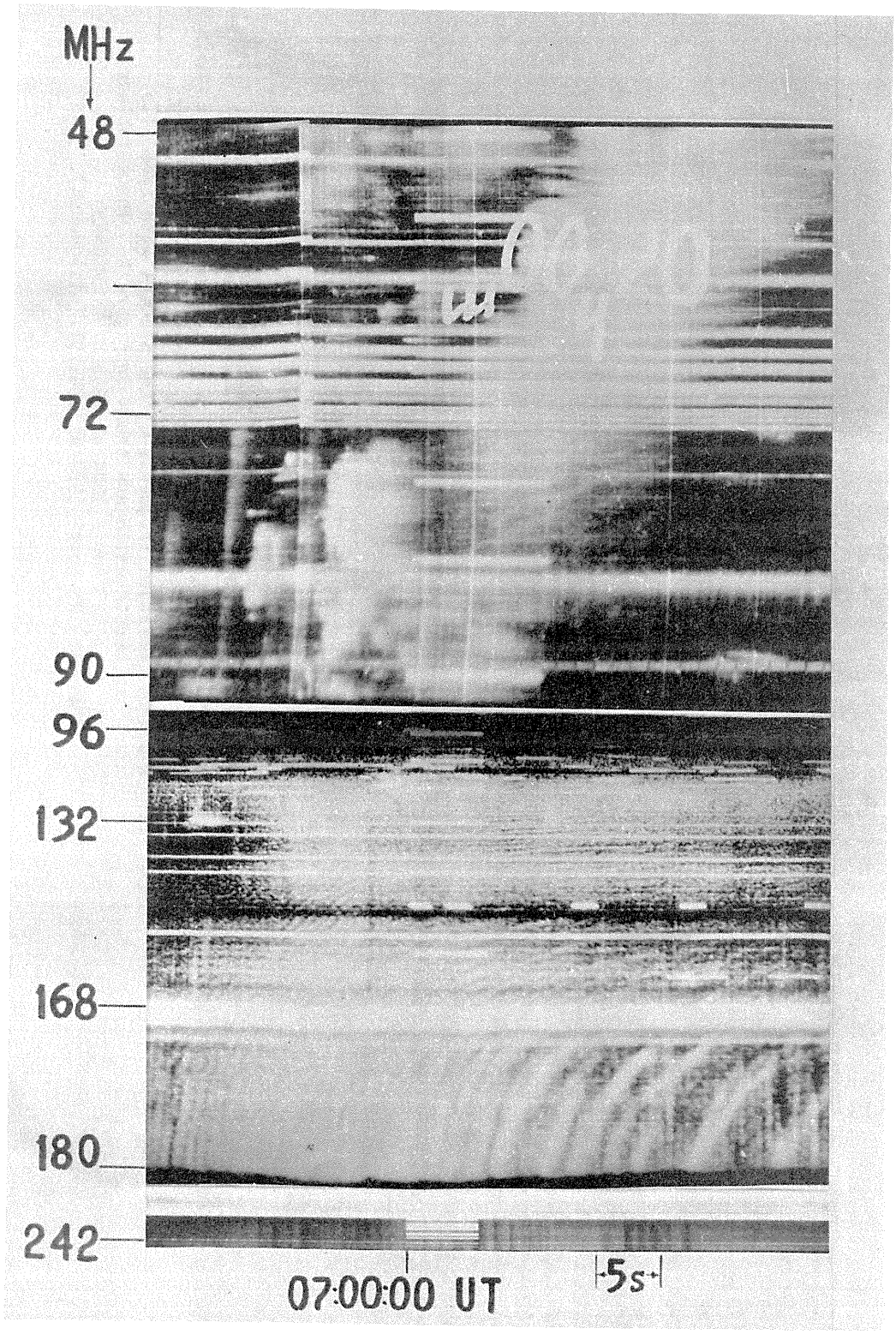


Figure 4. This shows the dynamic spectrum of the Type V burst on 26 April in the frequency range 240-45 MHz. The transition of the seconds duration pulsations at high frequency (220-240 MHz) into the zebra structure at low frequency occurs at frequencies 120-130 MHz.

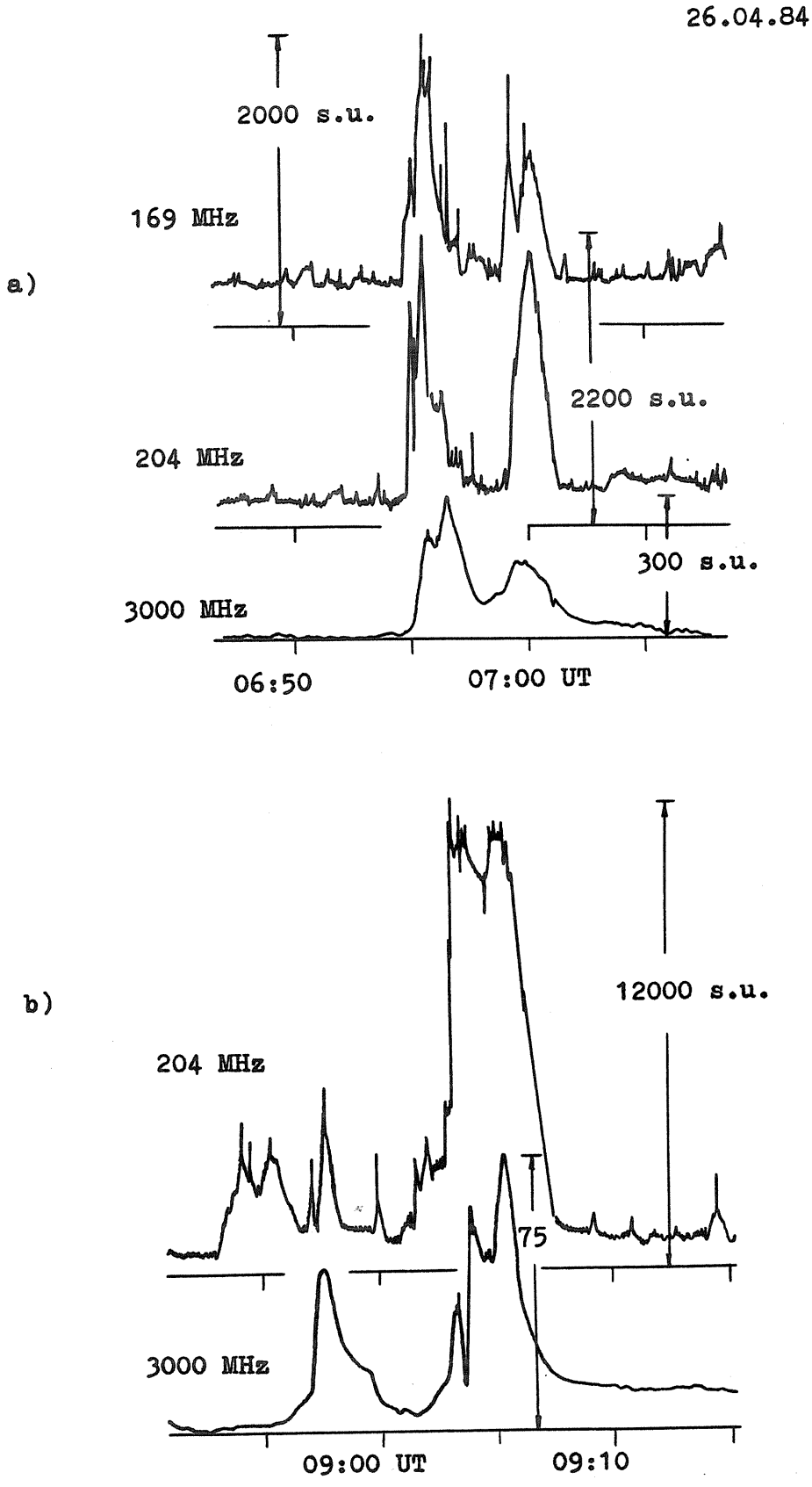


Figure 5. Time intensity profiles of bursts on 26 April: (a) at 169, 204 and 3000 MHz for the period 0650-0700 UT; and (b) at 204 and 3000 MHz for the period 0900-0910 UT.

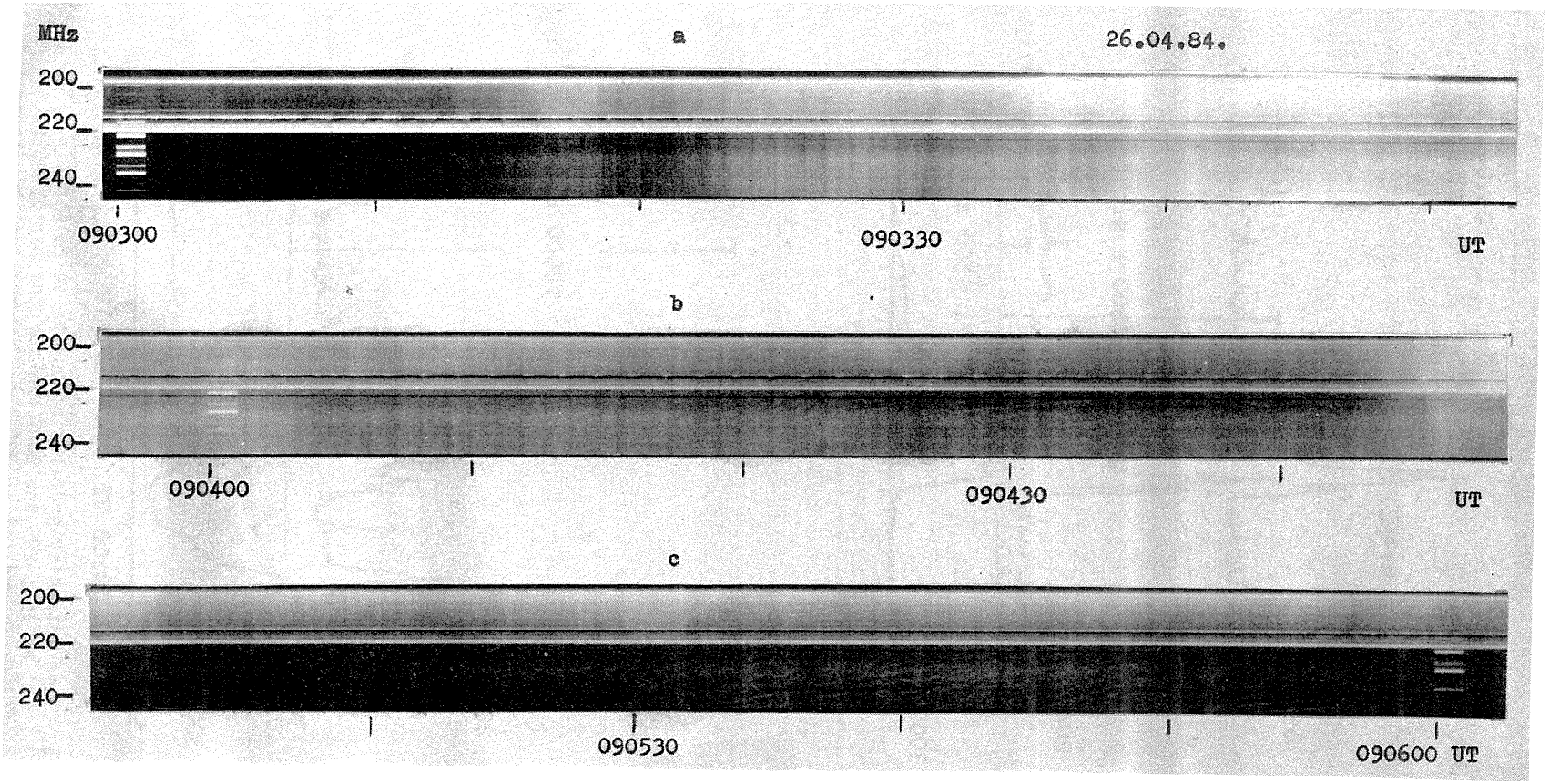


Figure 6. This shows the fine structure of the Type IV burst on 26 April from about 0903 to 0906 UT: (a) seconds duration pulsations; (b) filaments and zebra structure; and (c) continuation of zebra structure.

Judging by the NOAA Solar-Geophysical Data the flare was accompanied by the very intensive radio emission with proton characteristics. The maximum flux density S in the range from millimeter up to meter wavelengths was about tens of thousands of s.f.u. The frequency spectrum of the burst (Figure 7) reveals the flux increase from 3.75 GHz to 9.4 GHz. In the microwave range the main burst component had a comparatively short duration. At 9.4 GHz the burst duration on the level of $0.5 \times S_{max}$ was $d_9$ = about 3.2 minutes. At 2.7 GHz the burst consisted of an intensive pedestal with S = about 12000 s.f.u. and $d_3$ = about 2.5 minutes, on the background of which two powerful (S = about 55000 s.f.u.), but very short (the whole duration is $\tau \leq 1.3$ minutes) impulses were observed. Moreover the spectral maximum of the impulses seems to be in the decimeter range.

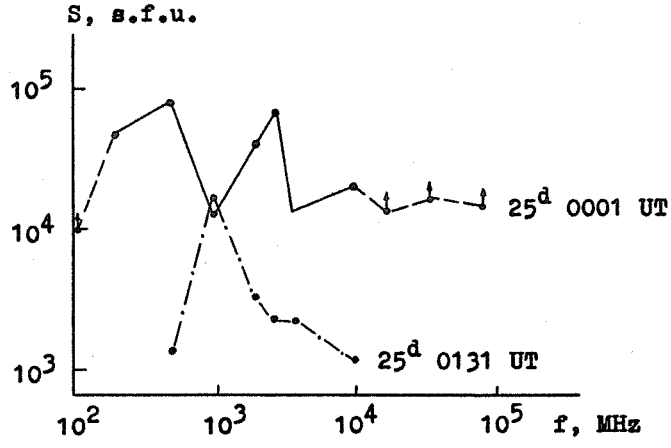


Fig. 7. Frequency spectrum of the peak flux densities of the radio burst accompanying the 24-25 April flare.

Therefore, in the diagnostics, the flux density of the pedestal S = about 12000 s.f.u. is used as an initial $S_3$ parameter (flux density at 3 GHz) and the presence of the impulses is taken into account in calculations of the integral characteristics of the burst. For the other initial parameters the following values are used: peak flux densities at 9 and 15.4 GHz $S_9$ = about 20500 s.f.u., $S_{15}$ = about 13500 s.f.u.; integral fluxes of the increasing phase R and total integral fluxes P of the burst at 3 and 9 GHz (in $10^{-19}$ $Wm^{-2}Hz^{-1}$) are $R_3$ = about 1800, $R_9$ = about 1155, $P_3$ = about 3640, $P_9$ = about 5000. The meter radio emission component is classified as an intensive one.

Shown in Figure 8a are time-intensity profiles of the >10, >30 and >60 MeV protons near the Earth calculated using the initial radio parameters given above. The general character of the profiles is typical for East limb proton events and corresponds sufficiently well to the in situ observations including the time of maximum 26 April 1400-1500 UT. The maximum calculated intensity of the proton flux, in particular for E > 10 MeV, is $J_c$ = about 1215 $cm^{-2}s^{-1}sr^{-1}$, i.e., it is the order of magnitude of the observed intensity $J_0$ = about 2500 $cm^{-2}s^{-1}sr^{-1}$. The energy spectrum of the protons based on the calculated proton intensity for E >10, 30 and 60 MeV (Figure 8b) is characterized by the index $\gamma$ = about 3.2. Approximately the same value of $\gamma$ is obtained from the independent estimates of the spectral index by a ratio of the peak radio burst flux density at 9 and 15.4 GHz, i.e., $S_9/S_{15}$ (Chertok, 1982).

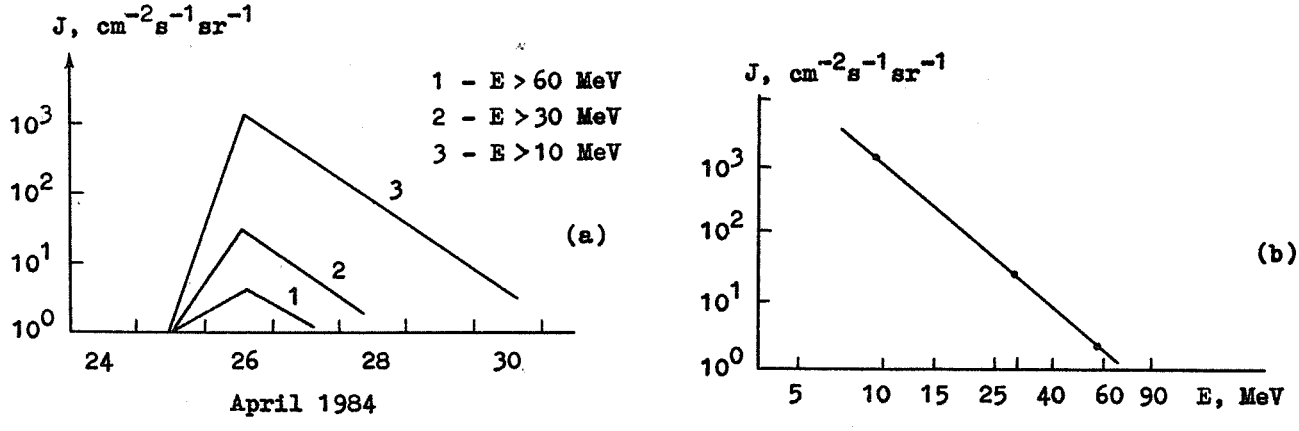


Fig. 8. This shows the (a) calculated time-intensity profiles and (b) energy spectra of protons near the Earth from the 24-25 April flare.

Thus the estimates of the proton parameters using the radio burst data from this flare give, on the whole, satisfactory results. However, note that the sufficiently large calculated values of the proton intensity from this flare were obtained mainly because of the high radio burst flux density at 3 GHz ($S_3$-parameter). The contribution of the other parameters is not large. The computed values of the proton flux close to the observed ones could be obtained under the condition that the protons arrived at the Earth without the normal heliolongitude attenuation. Moreover, using the same radio parameters and with strong heliolongitude attenuation corresponding to the intensive meter component, the calculated value of the PCA absorption ($A_C$ = about 1.2 dB) is much lower than the observed one ($A_O$ = about 17 dB). A PCA value close to the observed one could be obtained from the given parameters of the radio burst if the flare took place on the west half of the solar disk.

Therefore despite the fact that although the formal estimates of the proton flux parameters by radio data give positive results, the proton flux from the flare arrived at Earth without a strong dependence on solar longitude. It is possible also that the rather large proton flux and PCA observed after this East limb flare were caused by the bulk of protons arriving at the Earth together with the flare plasma cloud, which resulted in the strong geomagnetic storm with a sudden commencement on about 26 April at 1400 UT.

## REFERENCES


AKINYAN, S.T. S.A. AMIANTOV A.A. GNEZDILOV, A.M. KARACHUN, V.A. KOVALEV, O.S. KOROLEV, A.K. MARKEEV, V.V. FOMICHEV, C.P. CHERNOV and I.M. CHERTOK — 1976 — "Fine structure of solar radio bursts in July 1974", **Fizika Solnechnoi Aktivnosti"**, Ed. by M.I. Mogilevskii, IZMIRAN, Moscow, 64-80.

AKINYAN, S.T. I.M. CHERTOK and V.V. FOMICHEV — 1980 — "Quantitative forecasts of solar protons based on solar flare radio data", **Solar-Terrestrial Predictions Proceedings", Vol. 3**, Ed. by R.F. Donnelly, NOAA, Boulder, CO, D-14-D-26.

CHERTOK,I.M. — 1982 — "Estimations of proton energy spectral index by data on solar microwave radio bursts", **Geomagn. i Aeronomia, 22**, No. 2, 182-186.

DE LA NOE, J. and A. BOISCHOT — 1972 — "The type IIIb burst: precursor of decametre type III radio burst", **Astron. and Astrophys., 20**, No. 1, 55-62.

GNEZDILOV, A.A. V.A. KOVALEV A.K. MARKEEV V.V. FOMICHEV G.P. CHERNOV and I.M. CHERTOK — 1981 — "The peculiarities of an energy release in the large flares by radio bursts data during August-November 1979", **Solar Maximum Year, Vol. 2**, Ed. by V.N. Obridko, IZMIRAN, Moscow, 59-66.

SGD — 1984 — **Solar-Geophysical Data"** 477 Part I, 478 Part I, 482 Part II, U.S. Department of Commerce (Boulder, Colorado, USA 80303).

# Strong Rise and Fall Phenomena Recorded at Metric Wavelengths during 25 and 26 April 1984

by

M. Nonino, M. Messerotti*, P. Zlobec,
M. Comari and L. Fornasari
Trieste Astronomical Observatory, Via Tiepolo, Trieste, Italy
*also associated with the International School for Advanced Studies, Trieste, Italy

## Introduction

The active region NOAA 4474 was the prominent one during its presence on the Sun's visible hemisphere from 20 April to 5 May 1984. At metric wavelengths the radiopolarimeter of the Trieste Astronomical Observatory detected noise storm activity at 237 MHz from 25 April to 2 May 1984 with very strong activity during 27-29 April. Type I bursts were usually right-hand polarized up to 28 April. Afterwards they changed polarization for three days. During 2 May the low noise storm again became right-hand polarized. This is not exceptional because the very complex active region included strong magnetic fields of both polarities. Many Type III bursts were produced in this active region. In this paper some "rise and fall" phenomena recorded at the Trieste Astronomical Observatory during 25 and 26 April are described. The polarimetric channels were operating at 237, 327, 408 and 610 MHz. Data digitization (50 Hz) and reduction are described in Comari (1985a, 1985b).

## Data Description

**25 April** - An enhancement (1400 s.f.u.) with fine structures was present at 610 MHz from 1227.2 to 1228.2 UT. It was strongly Right(R)-hand polarized as was the fine structures that were superimposed on it. Almost simultaneously (1227.7-1228.3 UT) short bursts (typical duration 0.2 seconds) strongly R polarized were present at 408, 327 and 237 MHz. They were most numerous at 408 MHz.

Another still stronger enhancement (500 s.f.u.) followed at 610 MHz (1228.6-1229.7 UT) with almost the same characteristics; it was accompanied by totally R polarized bursts that were present from 1228.9 up to 1229.8 at 327 MHz. Their intensity and duration were larger (duration 0.6 seconds) than in the previous enhancement. Similar bursts were seen at 408 MHz for a very short time interval (1228.8-1229.0 UT).

At 237 MHz a strongly R polarized enhancement with fine structures started at 1404.7 UT. It lasted about three minutes. The maximum at 1405.3 UT reached 350 s.f.u. Simultaneously, similar, but lower enhancements were present at 327, 408 and 610 MHz. At such frequencies the polarization was correspondingly lower and lower. This might be explained by a change in the cyclotron frequency-plasma frequency ratio.

At 1457.0 UT a large band R polarized enhancement started at 610 MHz. Two maxima were clearly visible (at 1457.5 UT with 2400 s.f.u., and at 1458.0 UT with 5000 s.f.u.). At other frequencies the flux density amount was lower. The enhancements at 610 MHz vary considerably. In a tenth of a second, flux can change 1000 s.f.u. or more (see Figure 1).

The next large band strongly R polarized enhancement started at 1500.3 UT with a duration of 80 seconds. The higher flux density value was at 327 MHz (about 5000 s.f.u. at 1500.8 UT). Absorption was visible at 327 and 408 MHz.

**26 April** - The first recorded large band enhancement showing fine structures started at 0655.6 UT and lasted about 80 seconds. The event was strongly R polarized and its evolution presented a maximum of 350 s.f.u. at 237 MHz.

A few minutes later another large band enhancement developed (start at 0659.2 UT; duration 2 minutes). It was strongly R polarized and evolved mainly at 237 MHz up to 2000 s.f.u. At this frequency sudden reductions are clearly visible (see Figure 2).

At 0903.0 UT a strong large band R polarized enhancement started and lasted 4 minutes. At 237 MHz the event peaked at 0903.7 UT with 12000 s.f.u., while at 327 MHz the value of 2200 s.f.u. was reached.

## Acknowledgements

This work was partially supported by the National Research Council (C.N.R.) and the Ministry of Education (M.P.I.). Data reduction was carried out on the VAX 11/750 of the Astronet Pole of Trieste at the Trieste Astronomical Observatory.

## REFERENCES

COMARI, M. 1985a "Real time digitization and data processing for a six channel radiopolarimeter," **Convegno Nazionale Astronet**, Rome, March 1985, G. Sedmak ed., in press under auspices of the S.A.It.

COMARI, M. 1985b "High time resolution data analysis for a multichannel solar radio polarimeter," **Convegno Nazionale Astronet**, Rome, March 1985, G. Sedmak ed., in press under the auspices of the S.A.It.

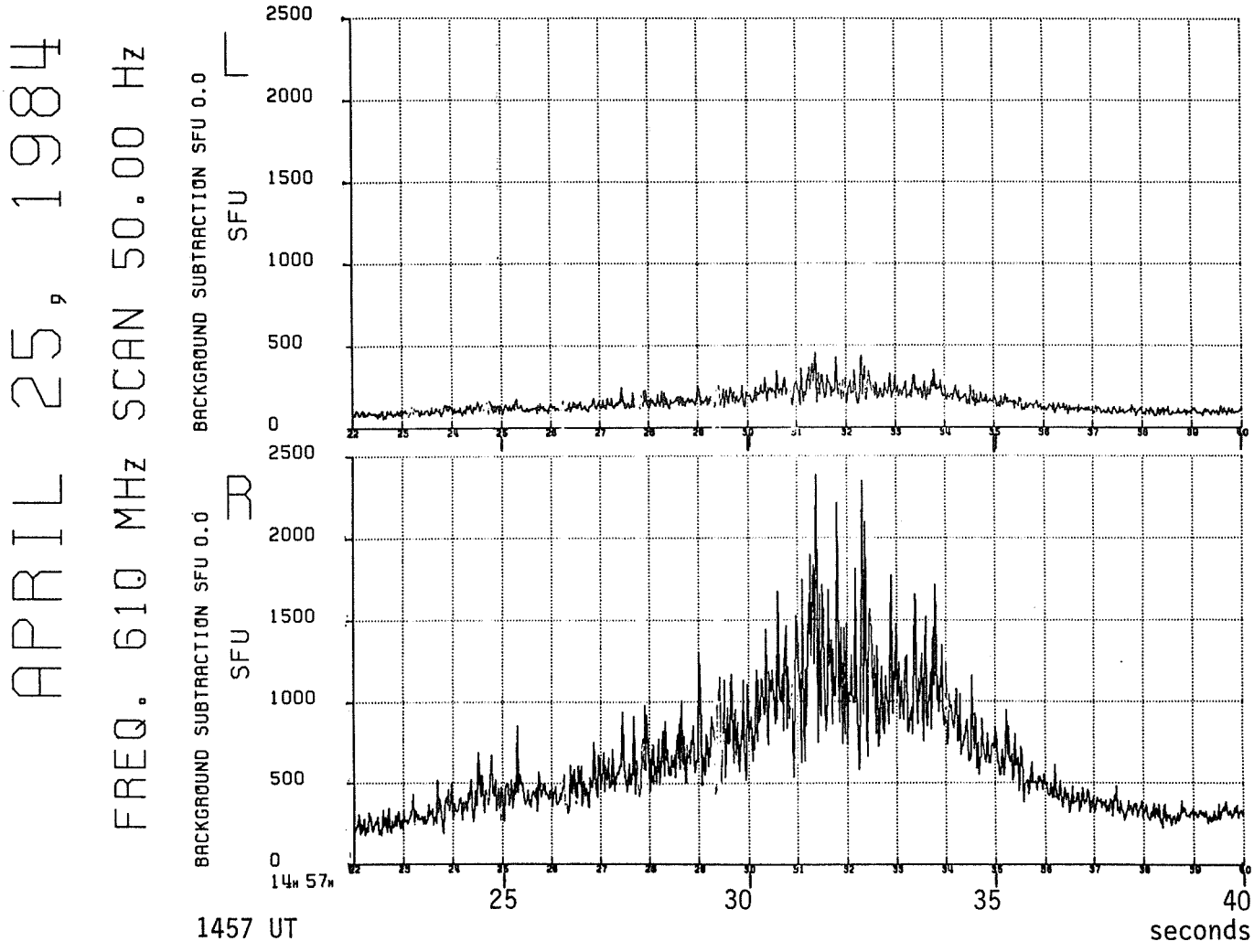


Fig. 1. Strong right-hand polarized enhancement at 610 MHz. Start 1457.22 UT, duration 18 seconds. Note the remarkable amount of short duration bursts of the flux density.

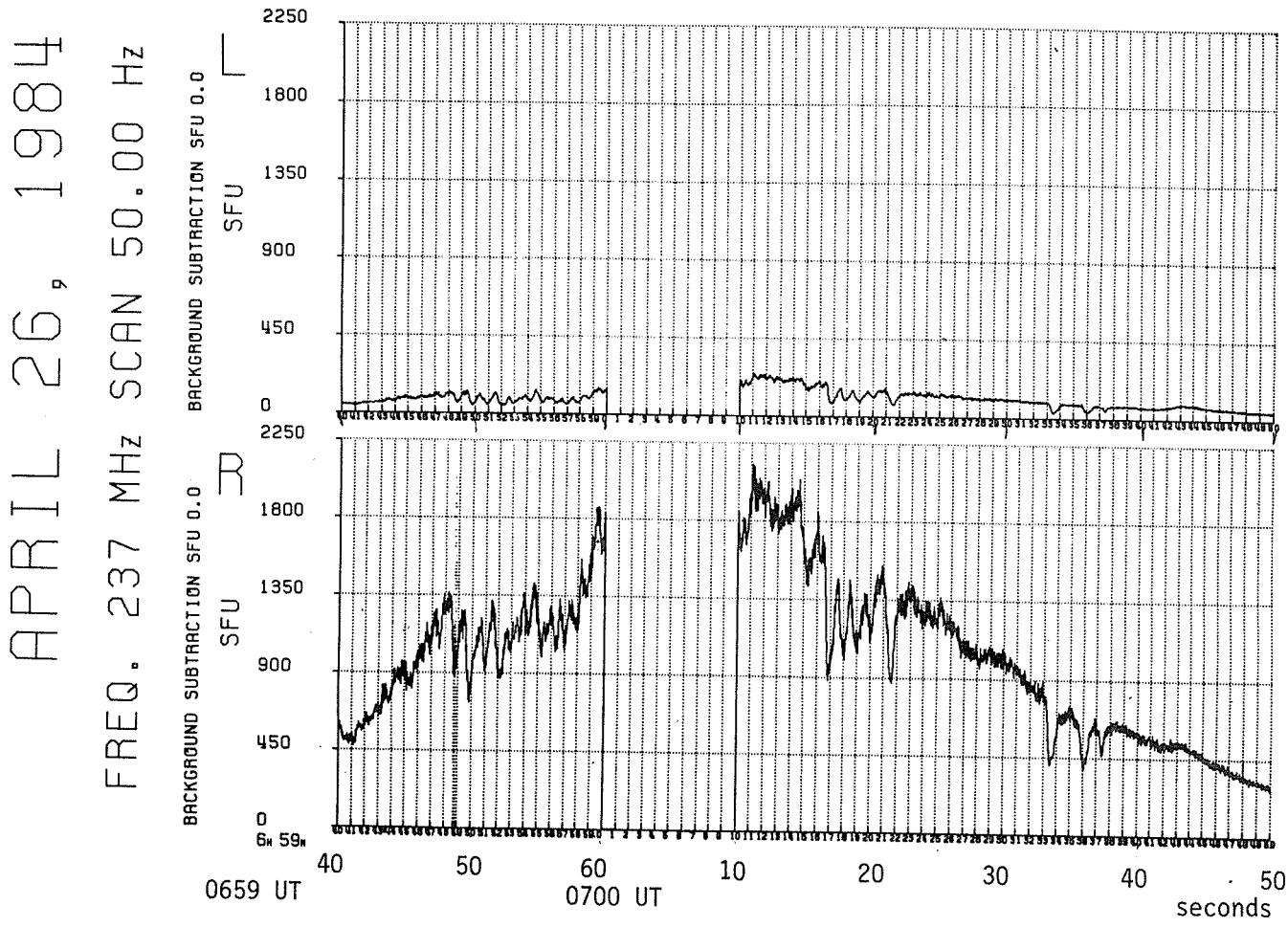


Fig. 2. Strongly right-hand polarized enhancement at 237 MHz. Sudden decreases are clearly visible. Starting time 0659:40 UT, duration 70 seconds. The gap is due to a time marker.

# Summary of the Spacecraft Observations for the 16 February and 24 April 1984 Solar Events

by

Daniel C. Wilkinson
World Data Center A for Solar-Terrestrial Physics
NOAA National Geophysical Data Center E/GC2
Boulder, CO 80303, USA

The spacecraft contributions to this UAG Report range from Carbon and Oxygen Nuclei flux measurements in low Earth orbit (400 km) to Solar Proton flux measurements made at Venus. Most of the 10 reports describe the enhancement of solar proton fluxes measured at polar or geostationary orbits. Others report fluctuations in the trapped electron and ion flux at geostationary altitude and observations of the normalized total solar irradiance.

The 16 February event is characterized by a sharp rise in proton flux near Earth at 0906 UT that peaks at about 1000 UT. This proton enhancement is followed by two lesser proton flux increases on 18 and 20 February.

The 24 April event is associated with a proton flux enhancement that started 25 April 0544 UT and peaked 26 April 1348 UT.

| Authors | Spacecraft | Interval 1984 | Observation Type | Orbit |
|---|---|---|---|---|
| Avdyushin et al. | METEOR | 16 Feb-26 Feb | Solar Proton Fluxes | Alt=700-1000 km, Inclination=81 deg |
| | METEOR | 22 Apr-30 Apr | Solar Proton Fluxes | Alt=700-1000 km, Inclination=81 deg |
| Baker et al. | 1977-007 | 6 Feb-11 Feb | Electron and Ion Fluxes | Geostationary, E70 |
| | 1982-019 | 6 Feb-11 Feb | Electron and Ion Fluxes | Geostationary, W70 |
| | 1981-025 | 6 Feb-11 Feb | Electron and Ion Fluxes | Geostationary, W135 |
| | 1984-037 | 6 Feb-11 Feb | Electron and Ion Fluxes | Geostationary, W40 |
| | 1977-007 | 20 Apr- 1 May | Electron and Ion Fluxes | Geostationary, E70 |
| | 1982-019 | 20 Apr- 1 May | Electron and Ion Fluxes | Geostationary, W70 |
| | 1981-025 | 20 Apr- 1 May | Electron and Ion Fluxes | Geostationary, W135 |
| | 1984-037 | 20 Apr- 1 May | Electron and Ion Fluxes | Geostationary, W40 |
| Blake et al. | DMSP-F6 | 16 Feb | Solar Particle Fluxes | Alt=840 km, Inclination = 99 deg |
| Bobrovskaya et al. | COSMOS-1549 | 19 Apr- 3 May | Carbon and Oxygen Nuclei | Alt=400 km, Inclination=72.9 deg |
| Chuchkov et al. | VENERA-15 | 12 Feb-21 Feb | Solar Proton Fluxes | Venus, Alt=1,000-70,000 km |
| | VENERA-16 | 12 Feb-21 Feb | Solar Proton Fluxes | Venus, Alt=1,000-70,000 km |
| | VENERA-15 | 20 Apr- 5 May | Solar Proton Fluxes | Venus, Alt=1,000-70,000 km |
| | VENERA-16 | 20 Apr- 5 May | Solar Proton Fluxes | Venus, Alt=1,000-70,000 km |
| Darchieva et al. | COSMOS-1490 | 24 Apr- 1 May | Solar Proton Fluxes | Alt=19,000 km, Inclination=65 deg |
| | COSMOS-1520 | 24 Apr- 1 May | Solar Proton Fluxes | Alt=19,000 km, Inclination=65 deg |
| Gussenhoven et al. | DMSP-F7 | 16 Feb | Electron and Proton Flux/Dose | Alt=840 km, Inclination=98.7 deg |
| | DMSP-F7 | 24 Apr-1 May | Electron and Proton Flux/Dose | Alt=840 km, Inclination=98.7 deg |
| Hanser et al. | GOES-5 | 16 Feb | Solar Proton Fluxes | Geostationary, W75 |
| | GOES-6 | 16 Feb | Solar Proton Fluxes | Geostationary, W136 |
| Kane | Pioneer 12 | 16 Feb | Solar X-ray and Gamma Ray Fluxes | Venus |
| | ICE | 16 Feb | Solar X-ray and Particle Fluxes | Earth-Sun line, Alt=0.05AU |
| | GOES-6 | 16 Feb | Solar X-ray Fluxes | Geostationary, W136 |
| Kyle et al. | NIMBUS-7 | Nov '83-Nov '84 | Solar Irradiance | Alt=950 km, Inclination=99.2 deg |

# X-Ray and Low Energy Gamma-Ray Observations of the 16 February 1984 Solar Flare

by

S.R. Kane
Space Sciences Laboratory
University of California, Berkeley, California USA

and

R.W. Klebesadel, E.E. Fenimore, and J.G. Laros
Los Alamos National Laboratory
Los Alamos, New Mexico

The 16 February 1984 (0900 UT) flare was very energetic and produced a variety of emissions. A preliminary summary of the X-ray, gamma-ray, radio and energetic particle observations has been presented earlier (Kane, 1985; Kane and Urbarz, 1986). Here we present only a brief description of the X-ray and gamma-ray continuum measurements. Implications of these observations with respect to the propagation and confinement of energetic electrons in the corona and the chromosphere have been discussed elsewhere (Kane et al., 1987a).

The X-ray and low energy gamma-ray observations were made with instruments aboard the ICE (International Cometary Explorer, formerly ISEE-3) and PVO (Pioneer Venus Orbiter) spacecraft. The characteristics of the two instruments relevant to solar flare measurements have been described elsewhere (Kane et al., 1982; 1987b). The X-ray and low energy gamma-ray continuum spectrometer on ICE consists of two detectors: a xenon-filled proportional counter covering 4.8-14 keV X-rays in 6 energy channels and a NaI(Tl) scintillator covering 26 keV-3.2 MeV photons in 12 energy channels. The time resolution is 0.5-4 seconds depending on photon energy. The PVO gamma-ray burst detector consists of CsI scintillators and covers 0.1-2 MeV photons in 4 energy channels. The time resolution is 0.5-8 seconds depending on the telemetry rate.

The 16 February 1984 (0900 UT) flare was probably located about 40° behind the West limb of the Sun. At the time of the flare, ICE was about 3 degrees away from the Sun-Earth line and about 0.05 AU away from the Earth in the sunward direction. The optical flare was thus completely occulted from the view of the ICE instrument. On the other hand, the PVO spacecraft, which was orbiting the planet Venus, was located about 16° behind the West limb of the Sun. The flare was therefore in full view of the PVO instrument.

Figure 1 shows the PVO and ICE observations. The soft X-ray measurements by GOES satellite are also presented for comparison. The PVO instrument detected a very intense burst of 100 keV-2 MeV photons beginning at about 0857 UT. The burst profile has considerable structure and appears to be related primarily to the impulsive phase of the flare. The impulsive hard X-ray burst and the gradual soft X-ray burst associated with such an intense gamma-ray are also expected to be very intense. However the ICE and GOES observations show that the impulsive hard X-ray burst was very weak and the gradual soft X-ray burst was undetectable, indicating that the very bright parts of these sources were occulted from the view of the near-Earth instruments. This is consistent with the location of the flare being far behind the solar limb. It is interesting to note that the impulsive X-ray emission, as seen from the Earth, could be detected down to about 8 Angstroms in this flare. Also, the ICE instrument detected the onset of high energy particles as early as about 0904:30 UT. This indicates that, at the Sun, these particles were injected promptly at the foot of the spiral interplanetary magnetic field line passing through the Earth.

## Acknowledgments

The research at Berkeley was supported by the National Aeronautics and Space Administration under grants NAS5-376 and NAG2-393. The work at the Los Alamos National Laboratory was performed under the auspices of the U.S. Department of Energy and was supported by NASA Contract A-47981P.

## REFERENCES

KANE, S.R. 1985 "Observations of the behind-the-limb flare on 16 February 1984 (about 0900 UT)," STIP Symposium on Retrospective Analysis and Future Coordinated Intervals, Les Diablaret, June 10-12, Switzerland.

KANE, S.R., E.E. FENIMORE, R.W. KLEBESADEL, J.G. LAROS 1982 "Spatial structure of the >100 keV X-ray sources in solar flares", Ap. J. Letters, 254, L53.

KANE, S.R. and H.W. URBARZ 1986 "A preliminary summary of the observations of the 16 February 1984 solar flare," STIP Symposium on Retrospective Analyses, eds. M.A. Shea and D.F. Smart.

KANE, S.R., R.W. KLEBESADEL, E.E.FENIMORE, J.G. LAROS 1987a "Impulsive hard X-ray source in the high corona", in preparation.

KANE, S.R., R.W. KLEBESADEL, E.E. FENIMORE, J.G. LAROS 1987b "Directivity of 100 keV-1 MeV photon sources in solar flares", submitted to Ap. J.

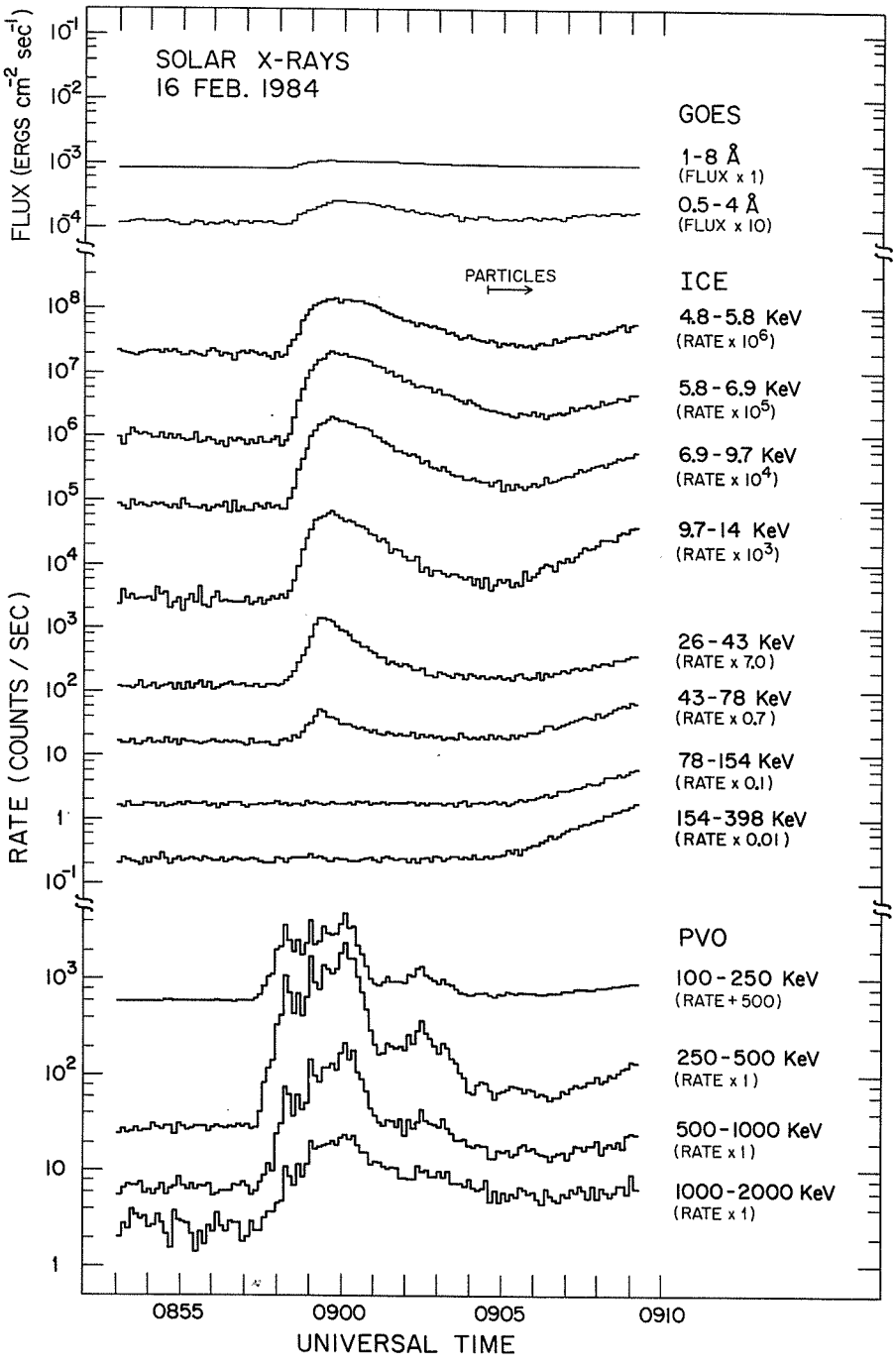


Fig. 1. The hard X-ray and low energy gamma-ray continuum observations of the 16 February 1984 solar flare made with the ICE and PVO spacecraft. The soft X-ray observations made with the GOES satellite are also shown. Note the intense photon flux observed by PVO. The flare was in full view of the PVO which was located behind the West limb of the Sun. However the chromospheric part of the X-ray source was occulted from the line-of-sight of ICE and GOES, resulting in a relatively small X-ray flux observed by these instruments. Also note the prompt onset of energetic particles in the vicinity of the Earth detected by the ICE instrument.

# Measurements of the >1 MeV Proton Fluxes in February and April 1984 (STIP Intervals 12 to 21 February and 20 April to 5 May) on Board Venera-15,16 Space Probes

by

E.A. Chuchkov, S.I. Ermakov, N.N. Kontor, N.V. Pereslegina and V.I. Tulupov
Institute of Nuclear Physics, Moscow State University
Moscow 119899, USSR

The cosmic ray intensity data were obtained in February-April 1984 from the Venera-15 and 16 space probes using the KS-18-6V instrument designed at the Institute of Nuclear Physics of the Moscow State University.

During February to April 1984, Venera-15 and 16 were orbiting Venus. The parameters of their orbits were approximately: maximum altitude above the planet surface was about 70,000 km, the minimum altitude was about 1000 km, the orbit inclination was 89°, the orbiting period was 24 hours. Within the period presented, the Earth-Sun-Venus angle varied in practice linearly from 97° (on 1 February 1984) to 150° (on 30 April 1984).

## Detectors

Cosmic rays were detected on board Venera-15 and 16 with the SBM-20 gas discharge counters and the surface barrier (SBD) and diffusive-drifted (DDD) silicon detectors.

Two SBM-20 counters were sealed in containers on board the space probes. One of the counters was shielded by approximately 1 g/cm$^2$ aluminum and another by approximately 5 g/cm$^2$ (approximately 1 g/cm$^2$ of aluminum and approximately 4 g/cm$^2$ of brass) of matter within an approximate 3 steradian angle on the sunward side. On the other sides the counters were shielded by about 100 g/cm$^2$ of matter. Such a shielding corresponds to the detection of the >30 MeV protons and >2 MeV electrons by the first counter, and of the >60 MeV protons and >3 MeV electrons by the second counter on the sides with the minimum shielding. The geometric factor of the counters was 13 cm$^2$sr for the 30-100 MeV protons. The >500 MeV protons were detected on the sides with the maximum shielding and the geometric factor for such protons was 54 cm$^2$sr in free space. As the space probes were orbiting around Venus, the geometric screening of the space by the planet varied. The appropriate correction for this effect has been introduced into the data presented.

The measurement characteristics of the crystal detctors (two detectors on either space probe) whose data were obtained in February-April 1984 are presented in the following table.

| Space Probe | Type of Detector | Thickness of Sensitive Layer (mcm) | Detected Particle Energy Range (MeV) Protons | Alpha Particles |
|---|---|---|---|---|
| Venera-15 | SBD | 72 | 1.4 - 6 | 3.6 - 130 |
| | | | ----- | 6.6 - 18.5 |
| | DDD | 360 | 1.25- 55 | 3.5 -1000 |
| | | | 5.3 - 7.6 | 6.6 - 125 |
| Venera-16 | SBD | 85 | 1.3 - 8.5 | 3.5 - 190 |
| | | | ----- | 6.6 - 22 |
| | DDD | 460 | 1.3 - 70 | 3.5 -1000 |
| | | | 5.2 - 9.6 | 6.6 - 170 |

The crystal detectors were oriented in the anti-solar direction. Their geometric factors were 0.11 cm$^2$sr. The detector inlet blind angle was $\pm$ 15° and the detector axes made angles of 0° $\pm$20° with the anti-solar direction in the course of the measurements.

The information from the detectors corresponded to the particle numbers recorded during the intervals between two consecutive telemetric data communication periods (the intervals were predominately 4 hours).

## Data Presentation

The data are presented as the intensity (cm$^2$ s sr)$^{-1}$ versus time (UT) plots for the channels of the crystal counters (on logarithmic scale) (four upper plots) and the counting rate (cts/s) versus time plots for the gas discharge counters (two lower plots).

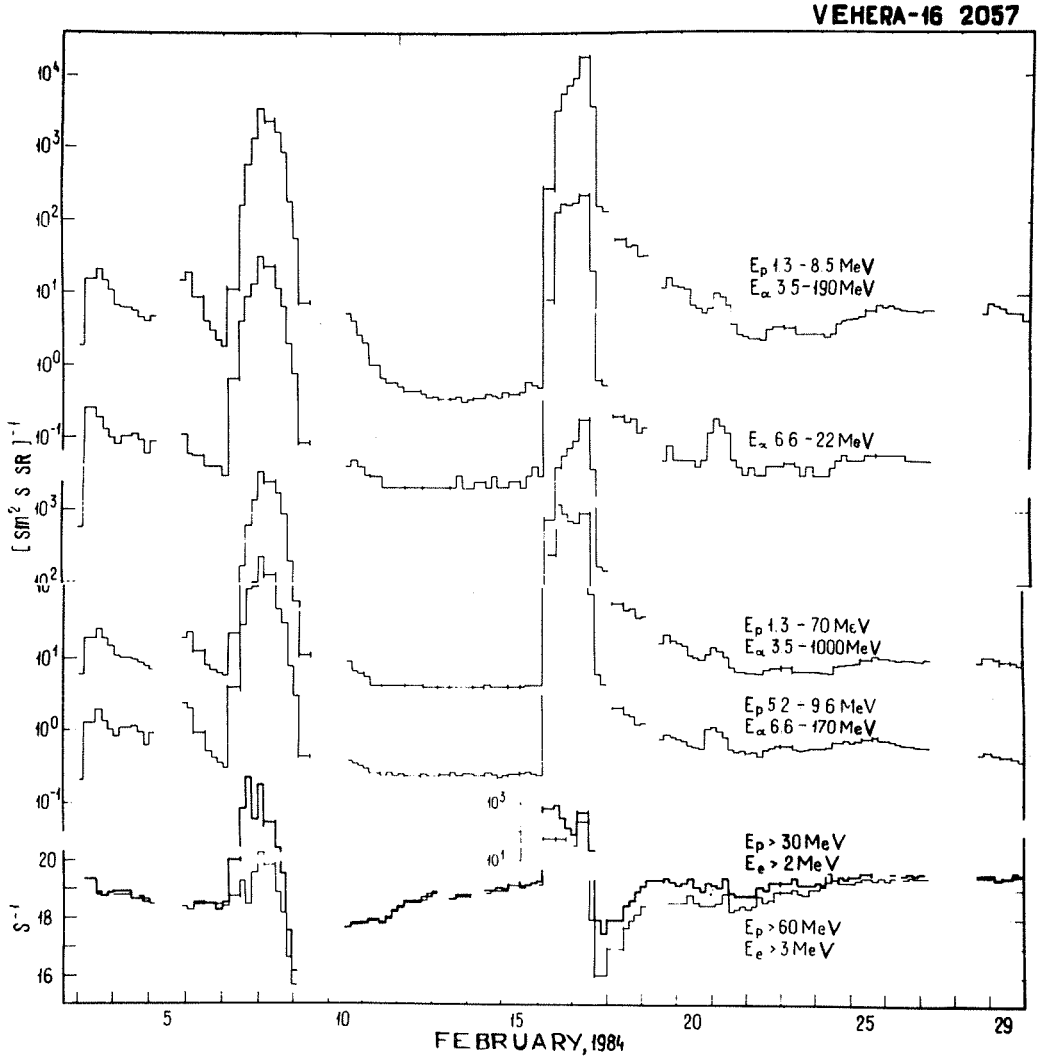


Fig. 1. Intensity $(cm^2\ s\ sr)^{-1}$ versus time (UT) plot of Venera data for February 1984. The four upper plots are the channels of the crystal counters on a logarithmic scale. The two lower plots are the counting rates (cts/s) for the gas discharge counters.

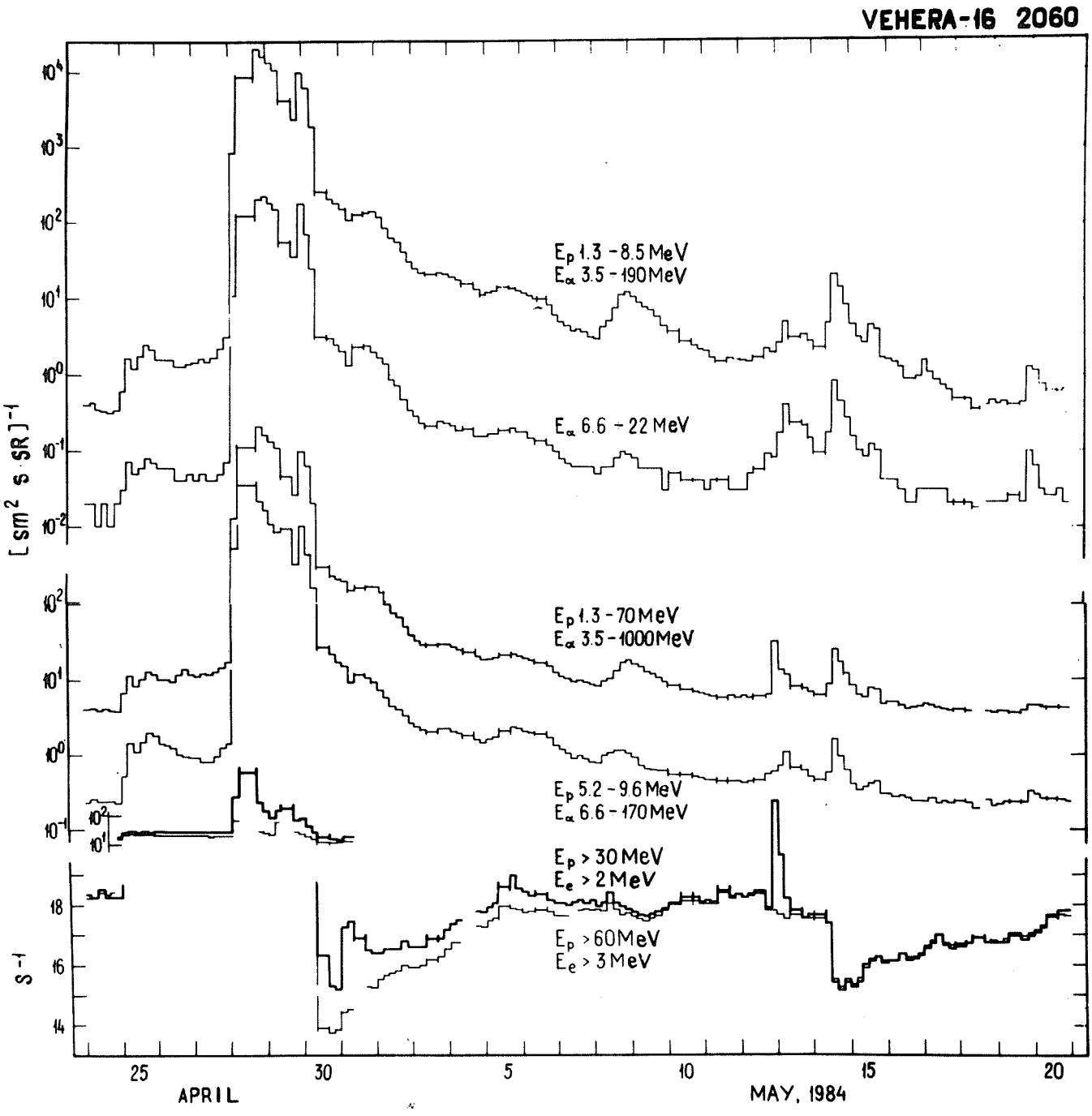


Fig. 2. Intensity (cm$^2$ s sr)$^{-1}$ versus time (UT) plot of Venera data for April-May 1984. The four upper plots are the channels of the crystal counters on a logarithmic scale. The two lower plots are the counting rates (cts/s) for the gas discharge counters.

# Solar Proton Onset Times and Spectra for 16 February 1984 As Observed By the GOES Spacecraft

by

F.A. Hanser and B. Sellers
Panametrics, Inc.
Waltham, Massachusetts, USA

The GOES spacecraft, operated by NOAA, include an Energetic Particle Sensor (EPS) and High Energy Proton and Alpha Detector (HEPAD), which measure protons from 0.6 MeV to greater than 1000 MeV in eleven channels. For February 1984, data are available from GOES-5 at W75 longitude and GOES-6 at W136 longitude. A plot showing all of the GOES-6 proton data for 16 February 1984 (day 47) was given in SESC PRF 442 (NOAA-USAF Space Environment Services Center, 1984). In this report we present more detail on the proton onset time of the 16 February 1984 event and provide proton spectra for several times during the event.

With reference to Table 1, the EPS consists of two detection units, a telescope using two solid state detectors for P1, P2 and P3, and a Dome unit using three moderator/solid state detector sets for P4, P5, P6 and P7. The Dome unit also has an electron channel E1 which detects electron above 2 MeV, but is sensitive to protons. The EPS response to protons below 150 MeV was extensively calibrated (Reports PANA-GOESP-CR2, 1979; and PANA-GOESP-CR3, 1980).

Table 1. GOES 6 EPS and HEPAD Proton Channels

| Channel Designation | Primary Proton Energy Range (MeV) | Maximum Detected Proton Energy (MeV) | Detection Unit |
|---|---|---|---|
| P1 | 0.6 - 4.2 | --- | Telescope |
| P2 | 4.2 - 8.7 | --- | Telescope |
| P3 | 8.7 - 14.5 | --- | Telescope |
| P4 | 15 - 44 | 150 | Dome |
| P5 | 39 - 82 | 190 | Dome |
| P6 | 84 - 200 | 300 | Dome |
| P7 | 110 - 500 | 900 | Dome |
| P8 | 355 - 430 | --- | HEPAD |
| P9 | 430 - 505 | --- | HEPAD |
| P10 | 505 - 685 | --- | HEPAD |
| P11 | > 685 | --- | HEPAD |
| E1 | 32 - 500 | 800 | Dome |

The HEPAD is a two solid state detector/Cerenkov radiator assembly (Rinehart, 1978). The in-orbit HEPAD proton energy ranges depend on the Cerenkov photomultiplier gain, but can be determined from an experimental calibration curve (Report PANA-SEM-5, 1983) and the in-orbit gain data obtained from an alpha lamp in the HEPAD (Report PANA-SEM-6, 1983). The HEPAD provides four proton channels P8, P9, P10, and P11.

The proton channel energies for the EPS and the GOES-6 HEPAD are given in Table 1, along with the maximum detected energies for the Dome channels (from Report PANA-GOESP-CR3, 1980). In February 1984 the GOES-5 HEPAD had a failed lowest threshold circuit for the Cerenkov radiator which eliminated all direct channel data, although a coincidence output from the two solid state detectors (the S5 output) could be used to detect high energy protons.

The 16 February 1984 solar proton event had an onset time of 0906 UT at the Earth. At this time GOES-6 was near local midnight while GOES-5 was near 0400 LT. The details of the main portion of the event are shown in the plots of GOES-6 data in Figure 1. This plot shows two minute averages every four minutes at the event rise, and every eight minutes at later times. Plots of the single counts (some are two-count sums) are shown in Figures 2, 3 and 4, where the event start times are obtained by the intersection of an eye-fit curve to the event data and the pre-event background level. The listed start times are rounded to 10 seconds and corrected to the actual accumulation time of the data. Start times are estimated to be accurate to $\pm$ 50 seconds.

In Figure 5 the start times are plotted against $1/\beta_{max}$ (= $c/v_{max}$)for the Dome channels P4, P5, P6 and P7, and for the HEPAD channels S5 (solid state detector coincidence) and P11 (GOES-6 only). The dispersion for the 16 February 1984 event onset is small, being much less than that expected for simultaneous emission from the Sun and straight line propagation to the Earth ($1.50 \times 10^{11}$ m). In contrast, GOES-5 data for the 7 December 1982 event is in good agreement with straight line transmission from the Sun and is shown primarily to illustrate the validity of GOES ESP/HEPAD data for obtaining such dispersion curves.

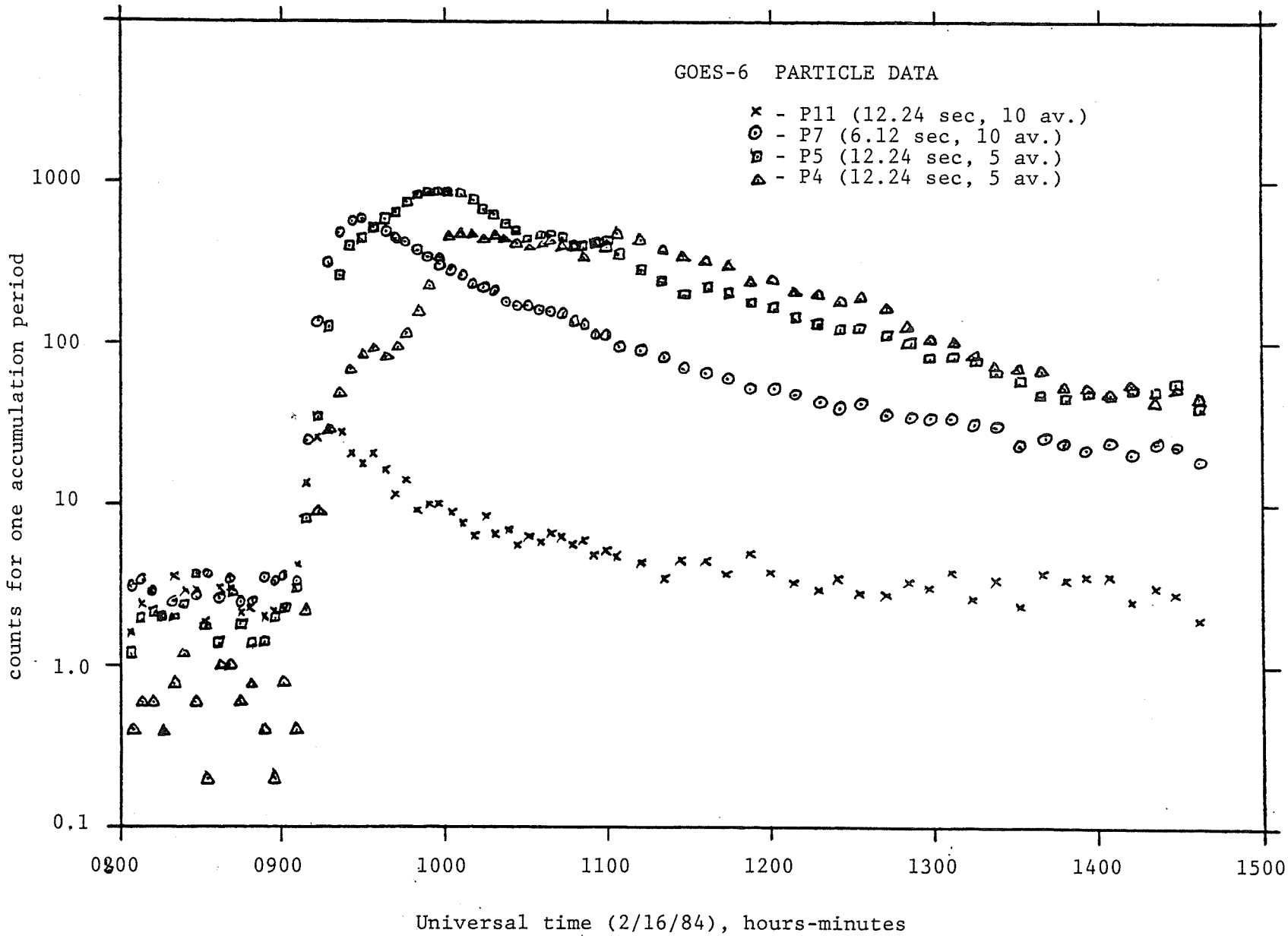


Fig. 1. Plot of some of the GOES-6 particle data for 16 February 1984. Shown are two minute averages plotted every four minutes at the start of the event, and every eight minutes during decay.

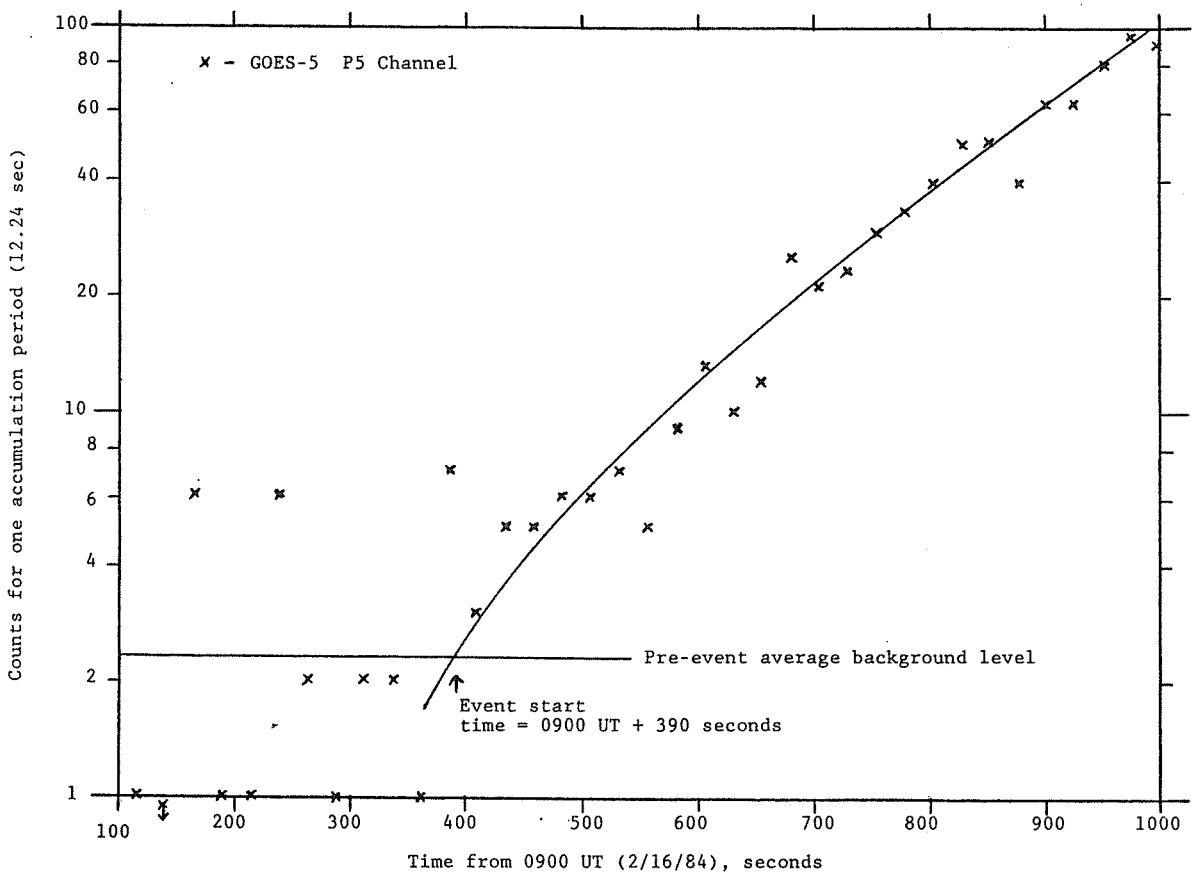


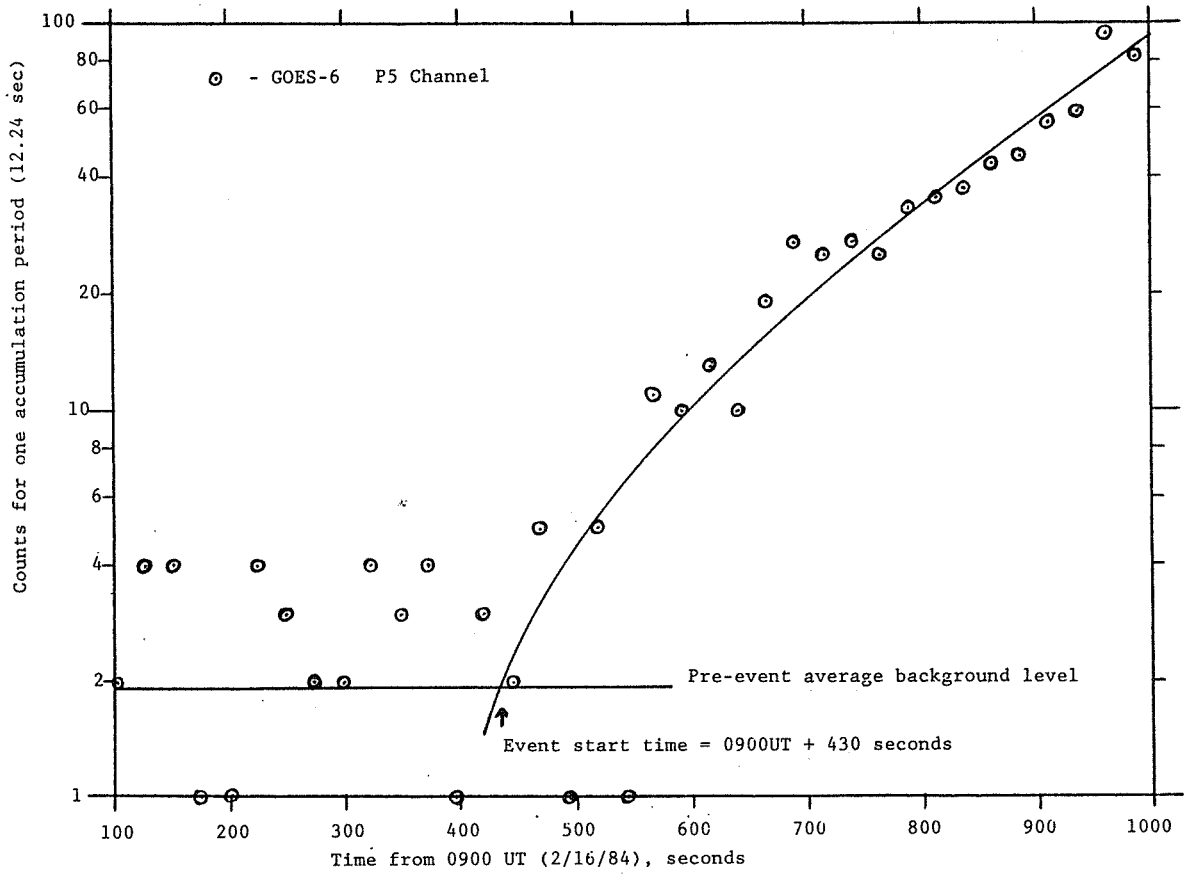


Fig. 2. Plots of the GOES-5 and GOES-6 P5 channels at event onset.

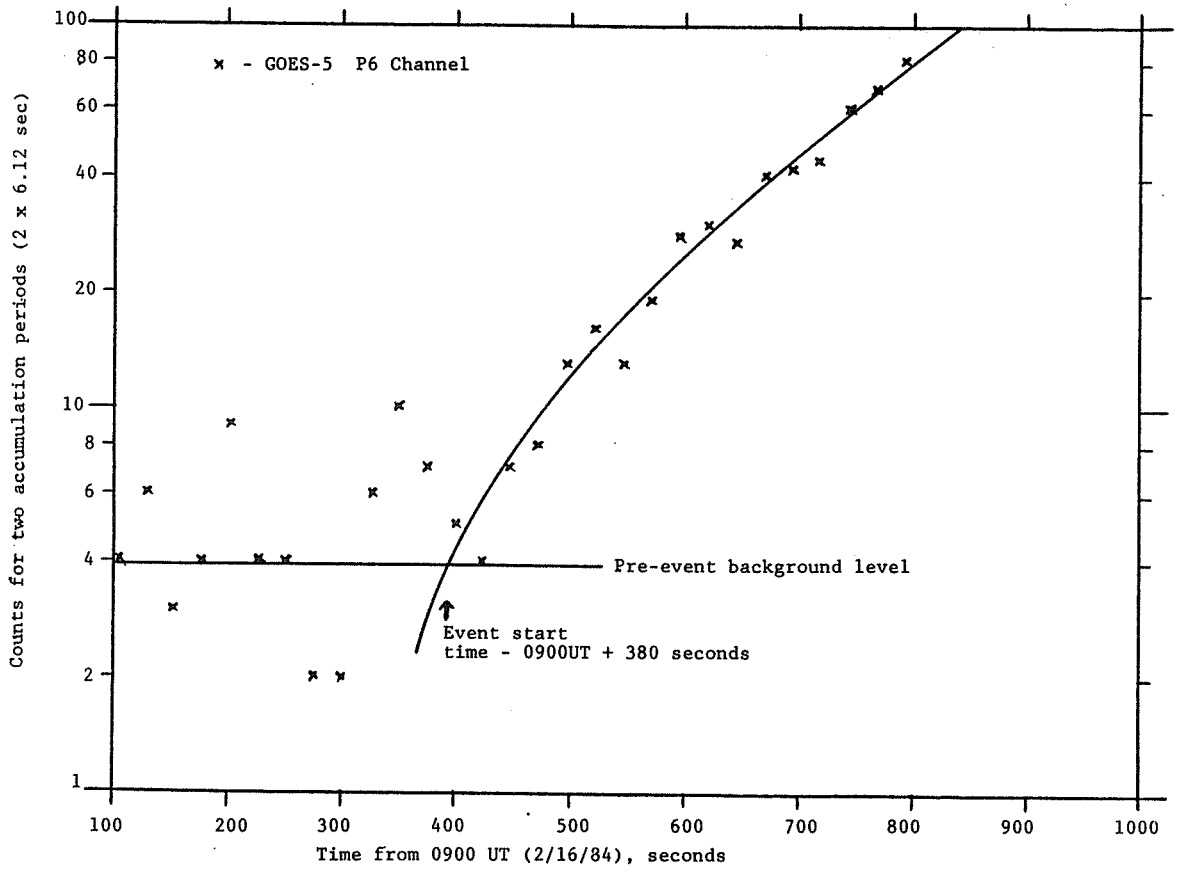


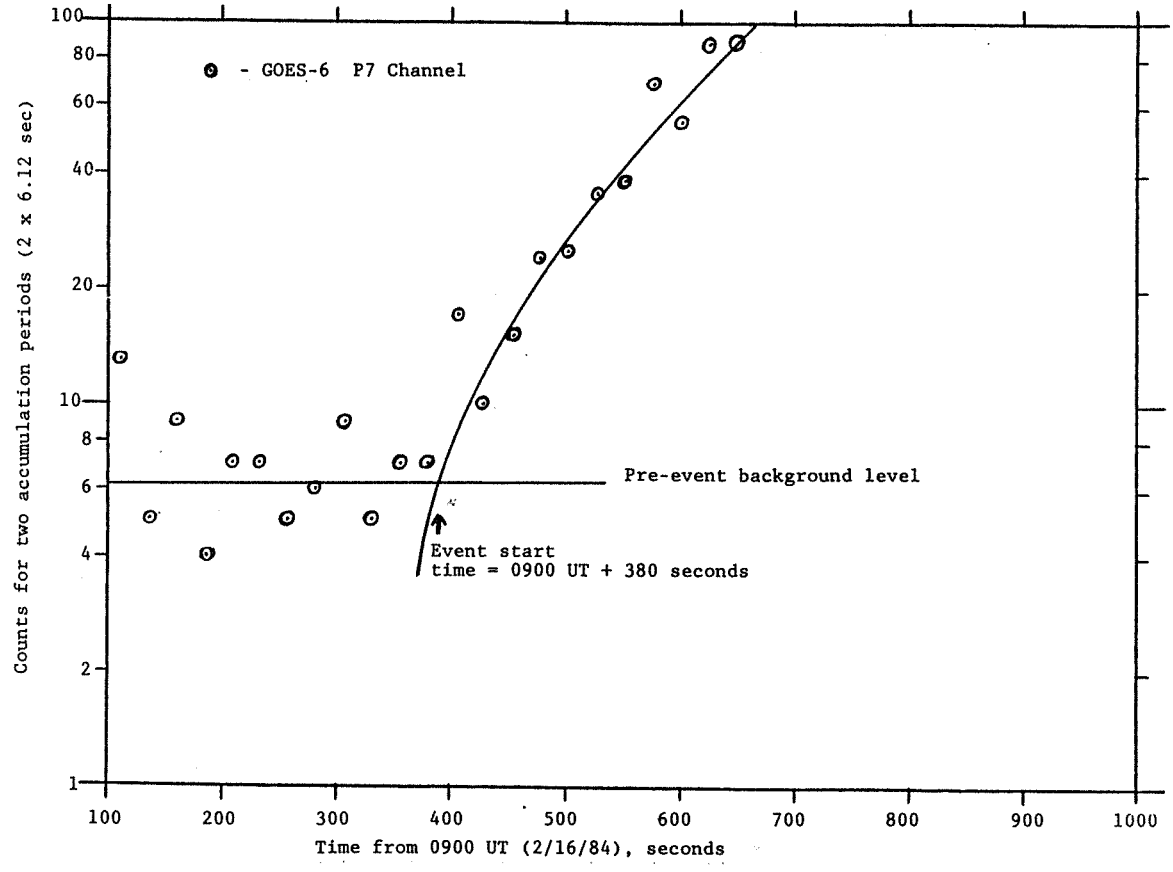


Fig. 3. Plots of the GOES-5 P6 channel and the GOES-6 P7 channel at event onset.

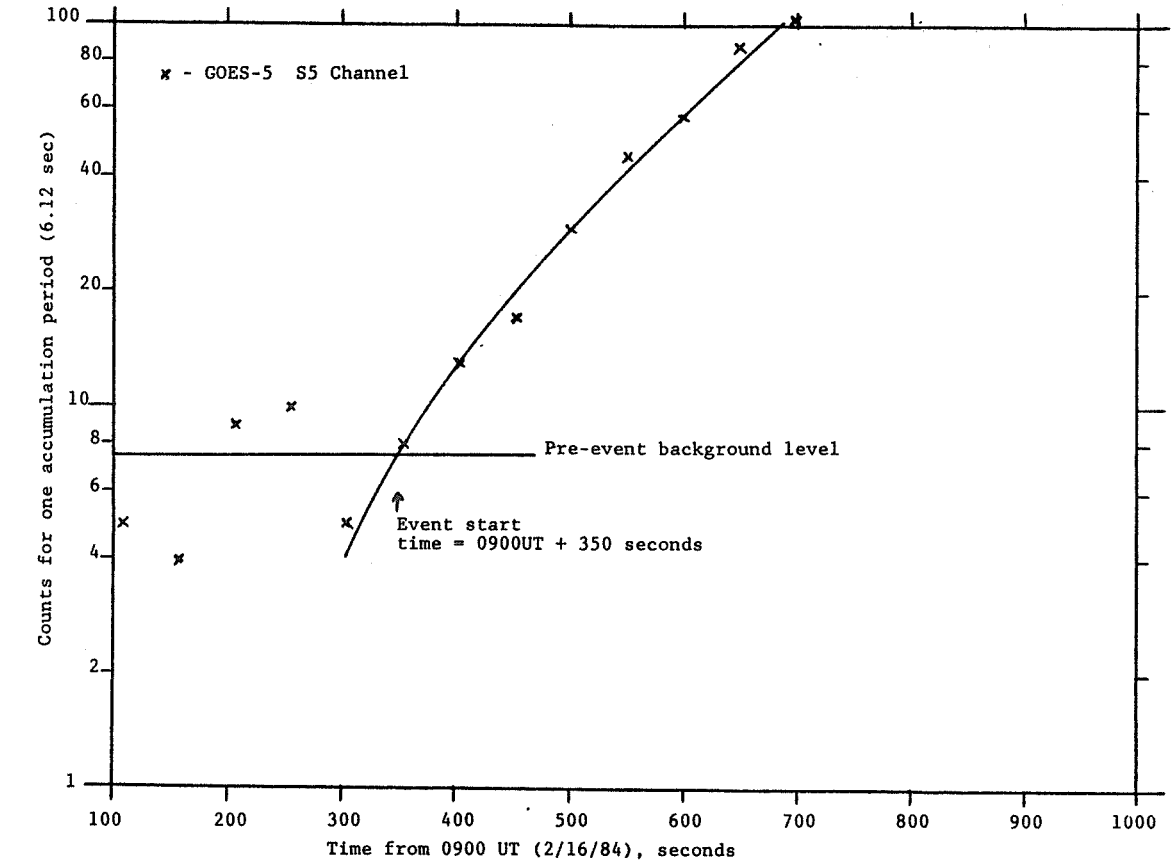


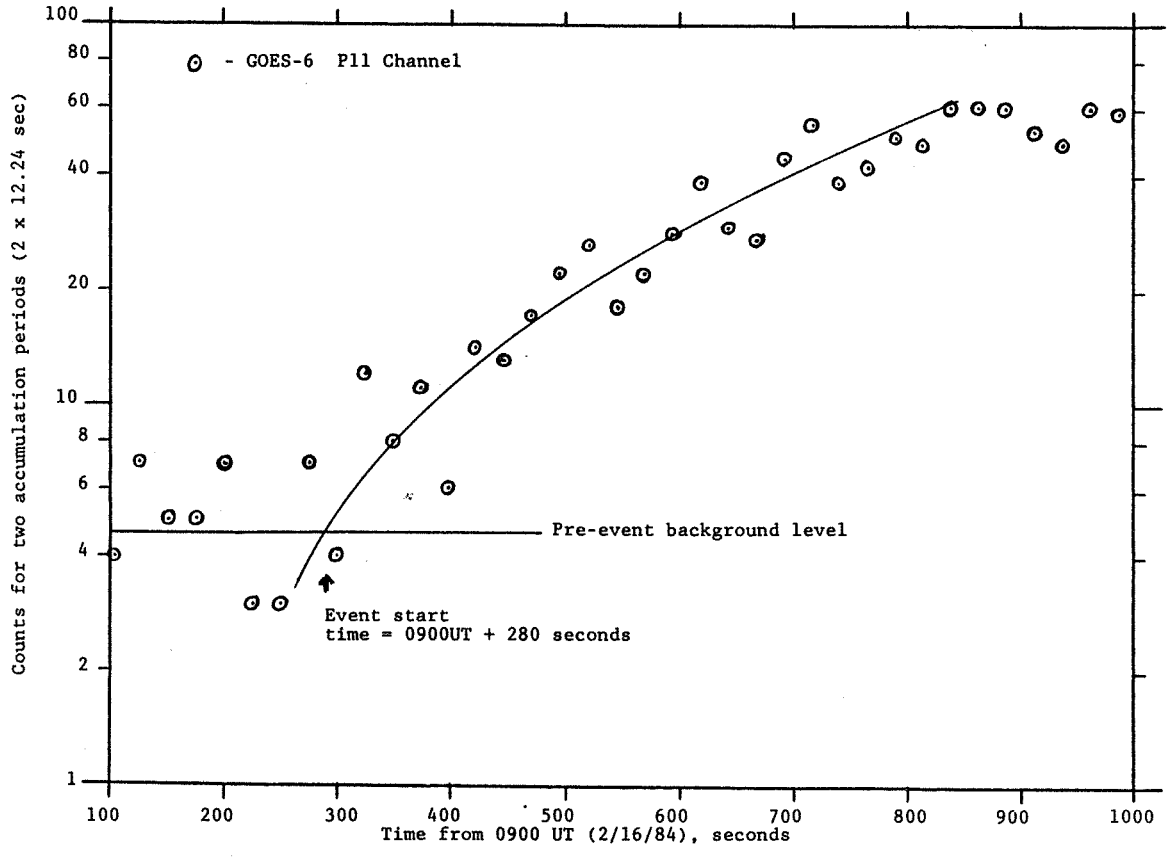


Fig. 4. Plots of the GOES-5 S5 (HEPAD) channel and the GOES-6 P11 channel at event onset.

The remaining Figures 6-14 show the GOES-5 and GOES-6 proton spectra at various times during the event. The telescope channels used only the primary proton energy range and geometric factor to calculate the proton flux. The Dome channels used the entire channel response, including the out-of-aperture response to high energy protons, as given in Report PANA-GOESP-CR3 (1980). Because of the wide energy ranges of the Dome channels a second correction was made for the spectral slope, based on the ratios of adjacent channel fluxes. The HEPAD channels P8 and P9 require some correction for rear entry high energy protons (Report PANA-SEM-5, 1983), but this is only significant during periods of low (cosmic ray background) fluxes. THe highest energy HEPAD channel (P11) is a threshold channel, and the normal cosmic ray background spectral shape was used to derive a factor to give the spectral intensity at 1000 MeV, where that channel is plotted.

Figure 6 shows the proton spectra before the event onset, and illustrates the normal geosynchronous spectrum. P1 is usually quite variable because of geomagnetic effects. Figure 7 shows the proton spectra at 0924 UT, shortly after P11 has peaked and just before the P7 peak. At this time the lower energy protons are still increasing in intensity. The spectra in Figure 8 for 0944 UT are at the start of the second rise in the P4 flux. Figure 9 shows the spectra at 1027 UT, shortly after P4 and P5 have peaked, while Figure 10 shows the spectra at 1100 UT, near the second P4 peak and just before P4 begins a near exponential decay. The 1152 UT spectra in Figure 11 are during the Decay portion of the event when the highest energy proton fluxes (P11) are approaching the pre-event background level.

The spectra in Figure 12 are for 2058 UT on 17 February when P11 is at the pre-event background level, and shows a power law spectrum over the entire range of three decades in proton energy. The final two sets of spectra are for 1620 UT and 1950 UT on 18 February near the end of the event. The highest energy protons, P6 and above, are at pre-event background levels, while the lower energy protons still have a slight enhancement.

## Acknowledgments

The GOES particle data are available from NOAA/NESDIS/E/GC2, 325 Broadway, Boulder, Colorado 80303, USA. We would like to thank R.N. Grubb, Dr. H.H. Sauer, and L. Matheson of the NOAA Space Environment Laboratory for assistance with the data. We would also like to thank Dr. J.B. Blake of the Aerospace Corp. for useful suggestions and comments. The EPS and HEPAD instruments on the present GOES spacecraft were calibrated by Panametrics, Inc., Waltham, Masssachusetts under subcontract to Hughes Aircraft Company, El Segundo, California, and under NOAA contract No. NA84RAC05108.

## REFERENCES

NOAA-USAF Space Environment Services Center 1984 Preliminary Report and Forecast of Solar Geophysical Data, SESC PRF 442, 21 February 1984.

Report PANA-GOESP-CR2 (Panametrics, Inc.) 1979 "GOES D,E,F Progress Report, Energetic Particle Sensor Telescope Calibration Work," prepared for Hughes Aircraft Co. under P.O.'s #T8-779416-LY5 and #08-779413-LBG, November 16, 1979 (unpublished).

Report PANA-GOESP-CR3 (Panametrics, Inc.) 1980 "GOES D,E,F Progress Report, Energetic Particle Sensor Dome Calibration Work," prepared for Hughes Aircraft Co. under P.O. #08-779413-LBG, August 26, 1980 (unpublished).

Report PANA-SEM-5 (Panametrics, Inc.) 1983 "GOES-D, -E, and -F HEPAD's, Report on Ground-Based Tests and on In-Orbit Operations for GOES-D and -E," May 2, 1983 (unpublished).

Report PANA-SEM-6 (Panametrics, Inc.) 1983 "Determination of the Operating H.V. Step of the HEPAD S/N 3 In-Orbit on the GOES-F (-6) Satellite," August 26, 1983 (unpublished).

RINEHART, M.C. 1978 "Cerenkov Counter for Spacecraft Application," **Nucl. Instrum. Methods, 154**, 303-316 (1978)

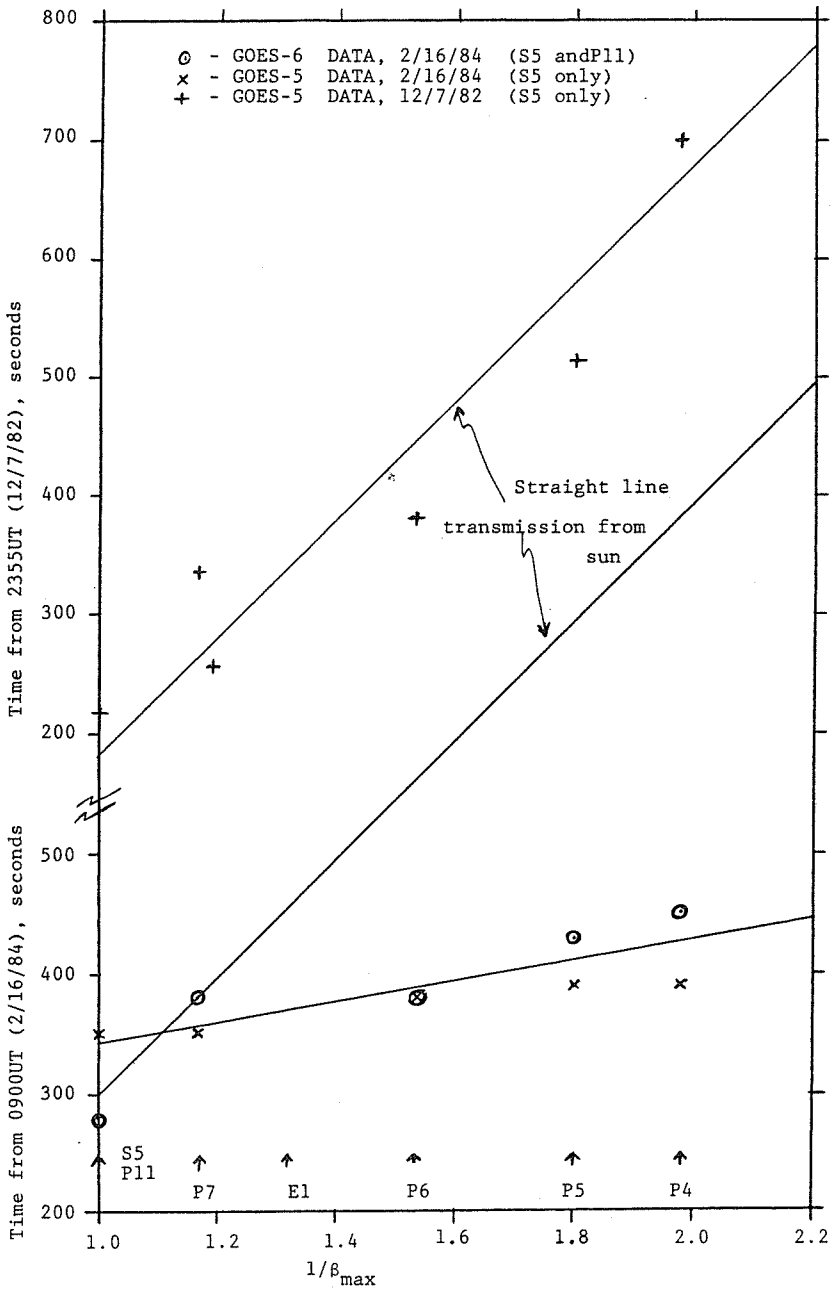


Fig. 5. Channel start time plotted against 1/ max for the Dome and HEPAD channels.

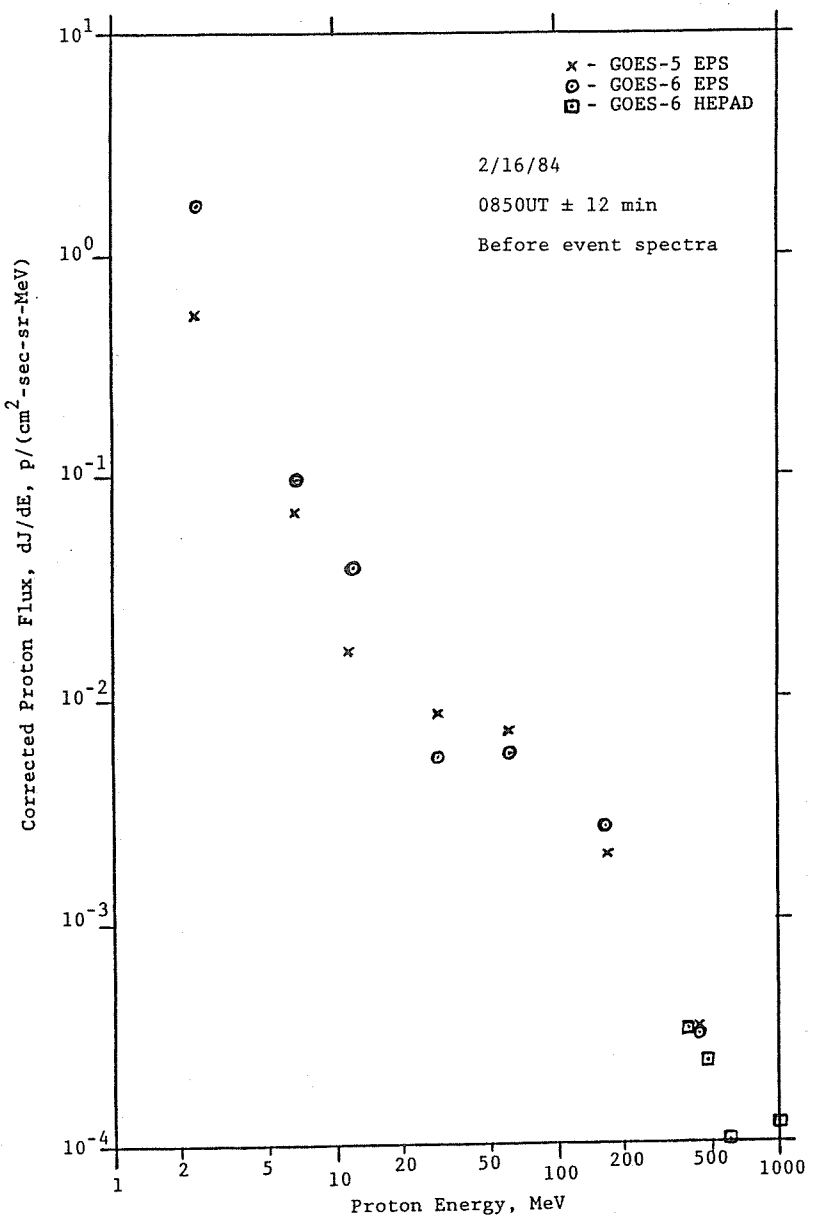


Fig. 6. GOES proton spectra before the start of the 16 February 1984 solar proton event.

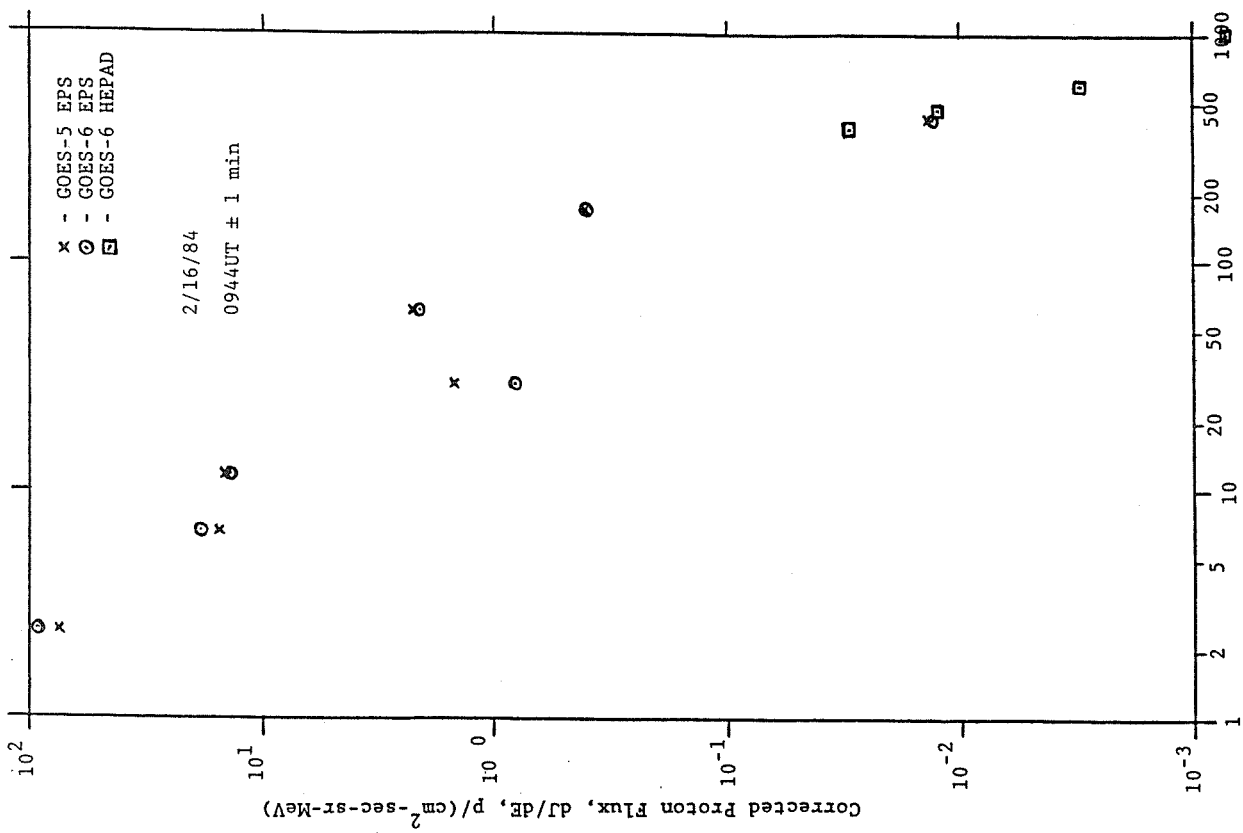


Fig. 8. Proton spectra at 0944 UT, at the start of the second rise in the P4 flux.

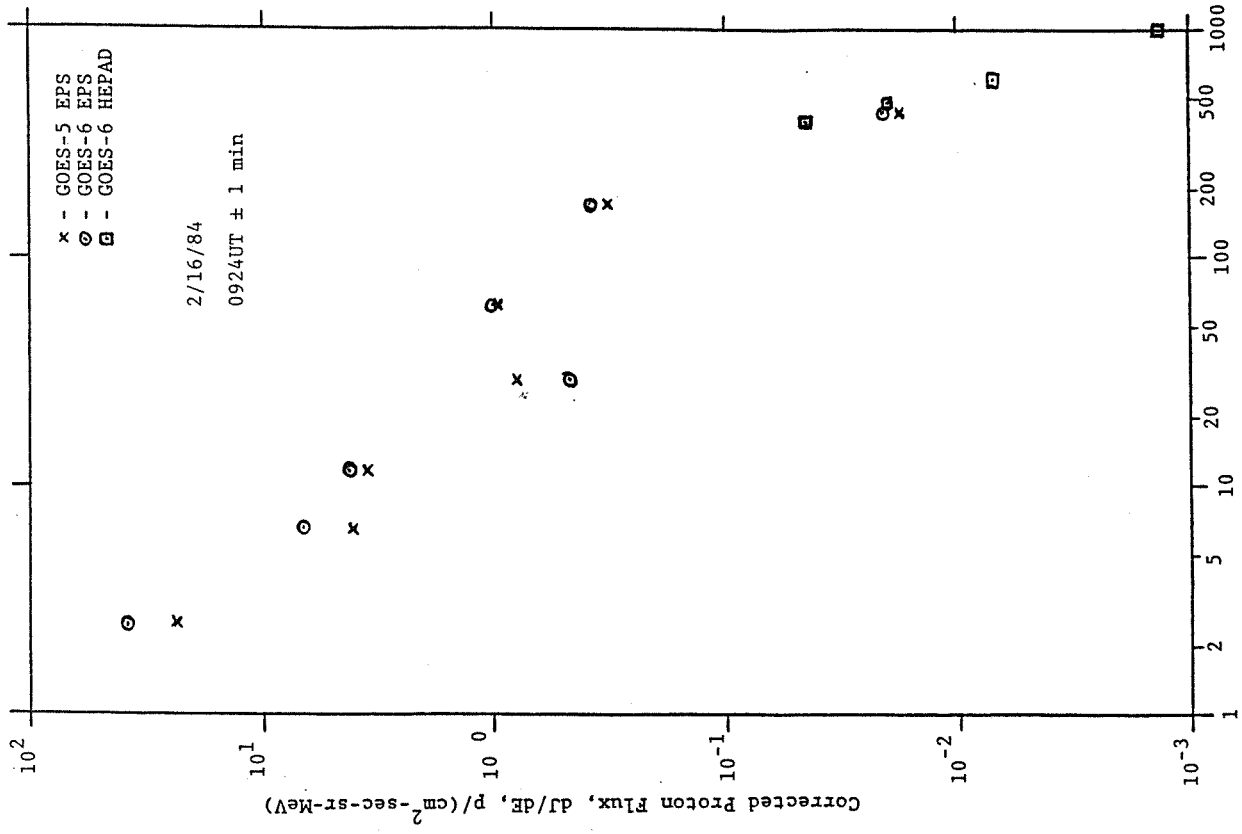


Fig. 7. Proton spectra at 0924 UT, after the P11 peak and before the P7 peak.

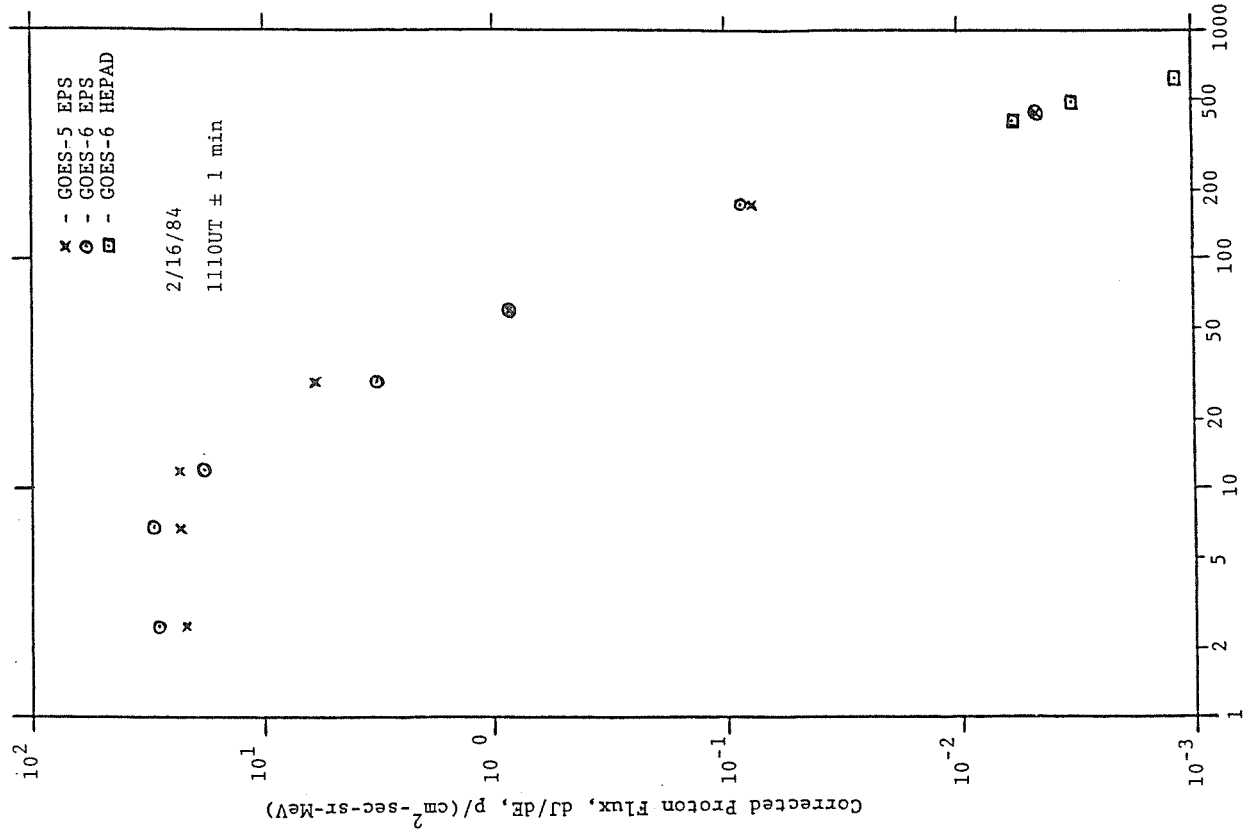


Fig. 10. Proton spectra at 1100 UT, near the second P4 peak and just before P4 begins a near exponential decay.

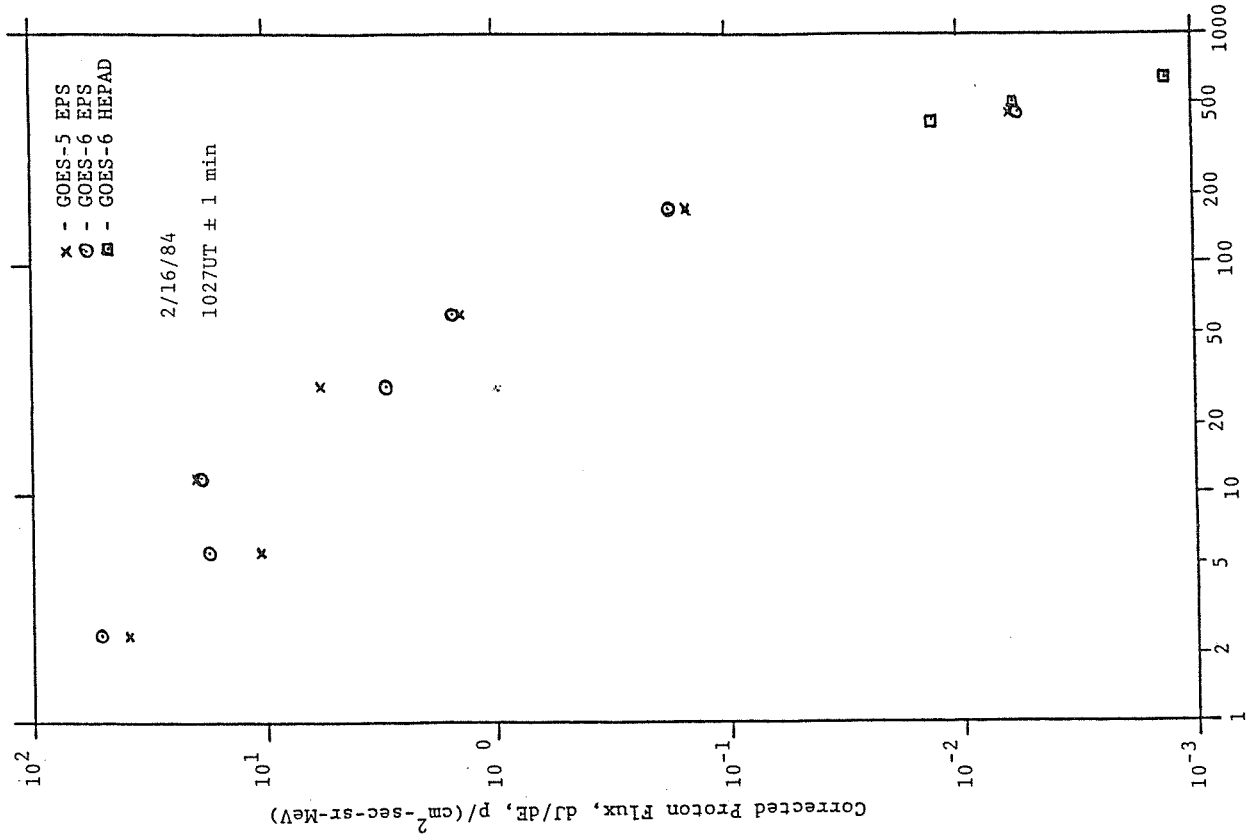


Fig. 9. Proton spectra at 1027 UT, shortly after P4 and P5 have peaked.

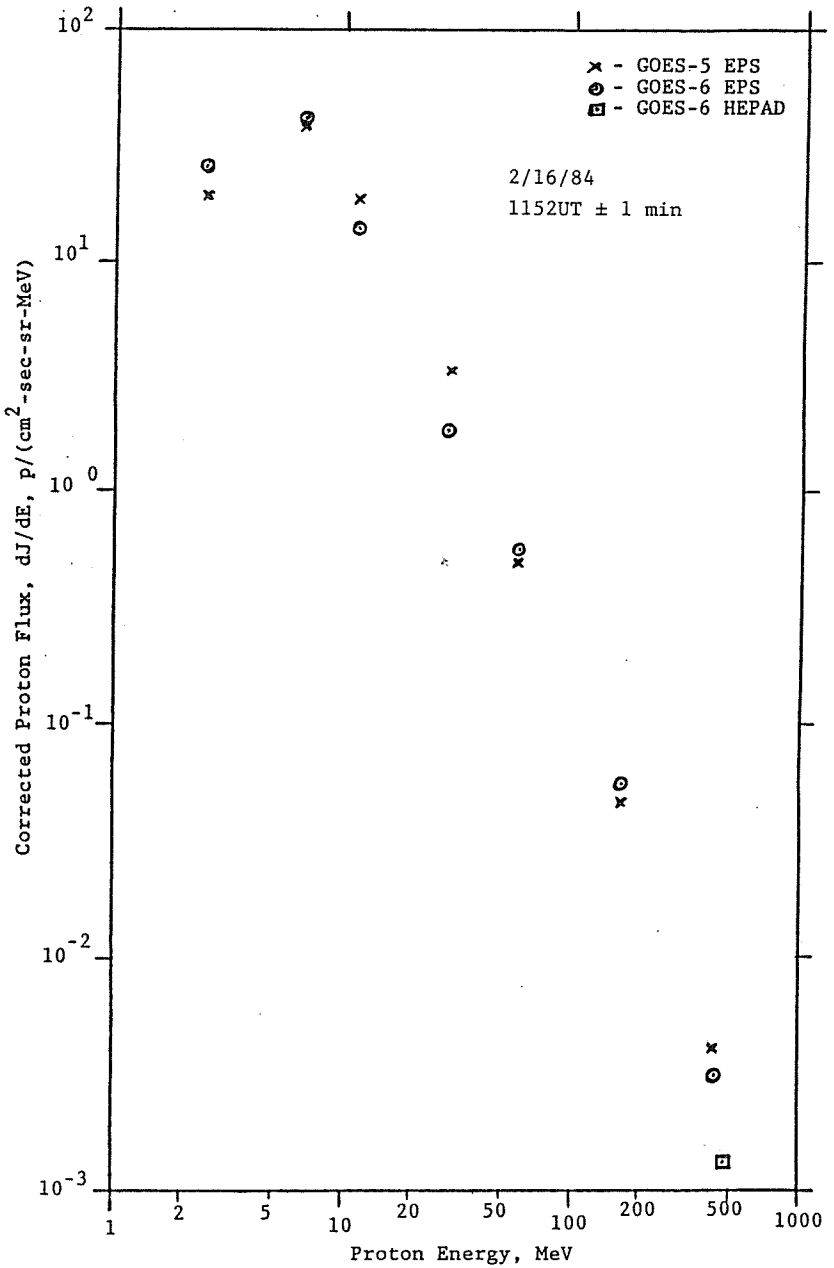


Fig. 11. Proton spectra at 1152 UT, during the event decay phase when P11 (not plotted) is near the pre-event background level.

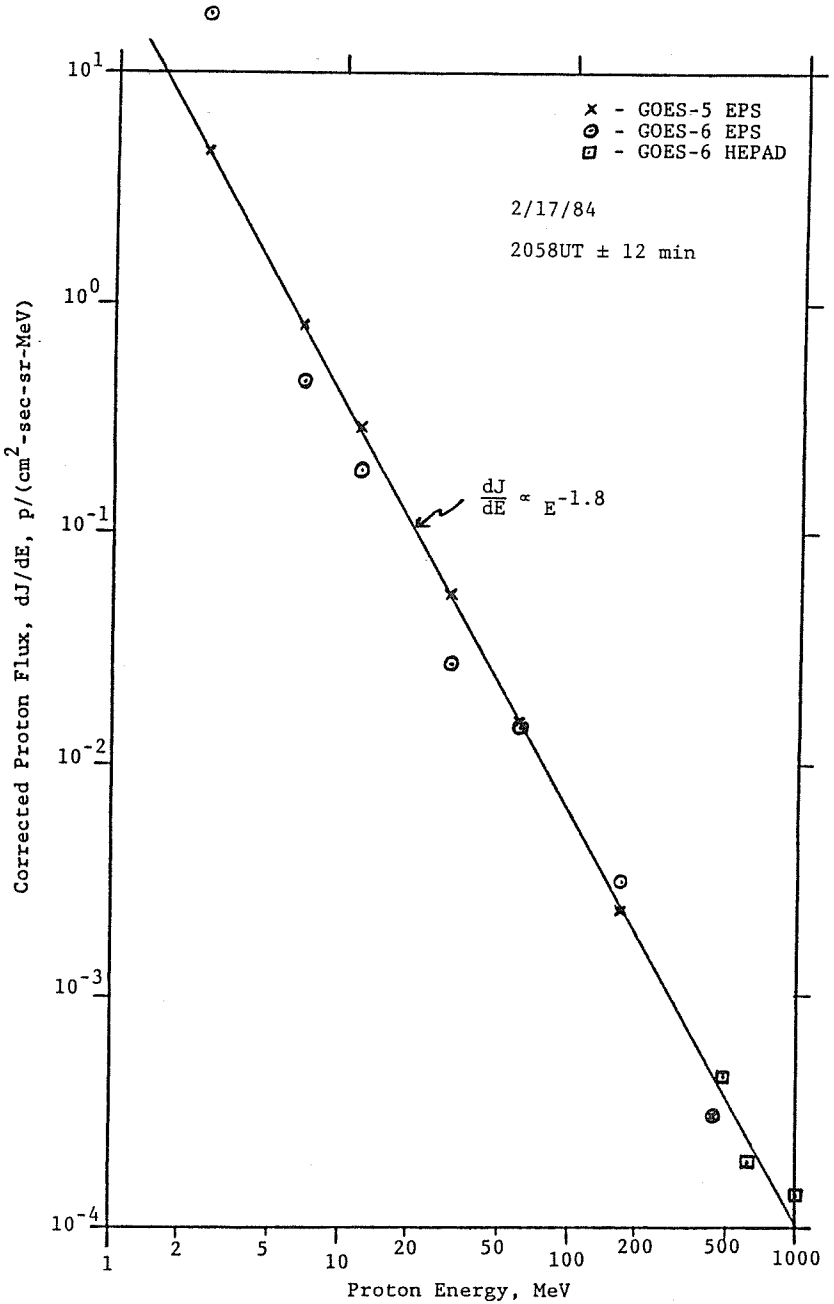


Fig. 12. Proton spectra at 2058 UT on 17 February 1984 showing a power law spectrum over three decades of proton energy.

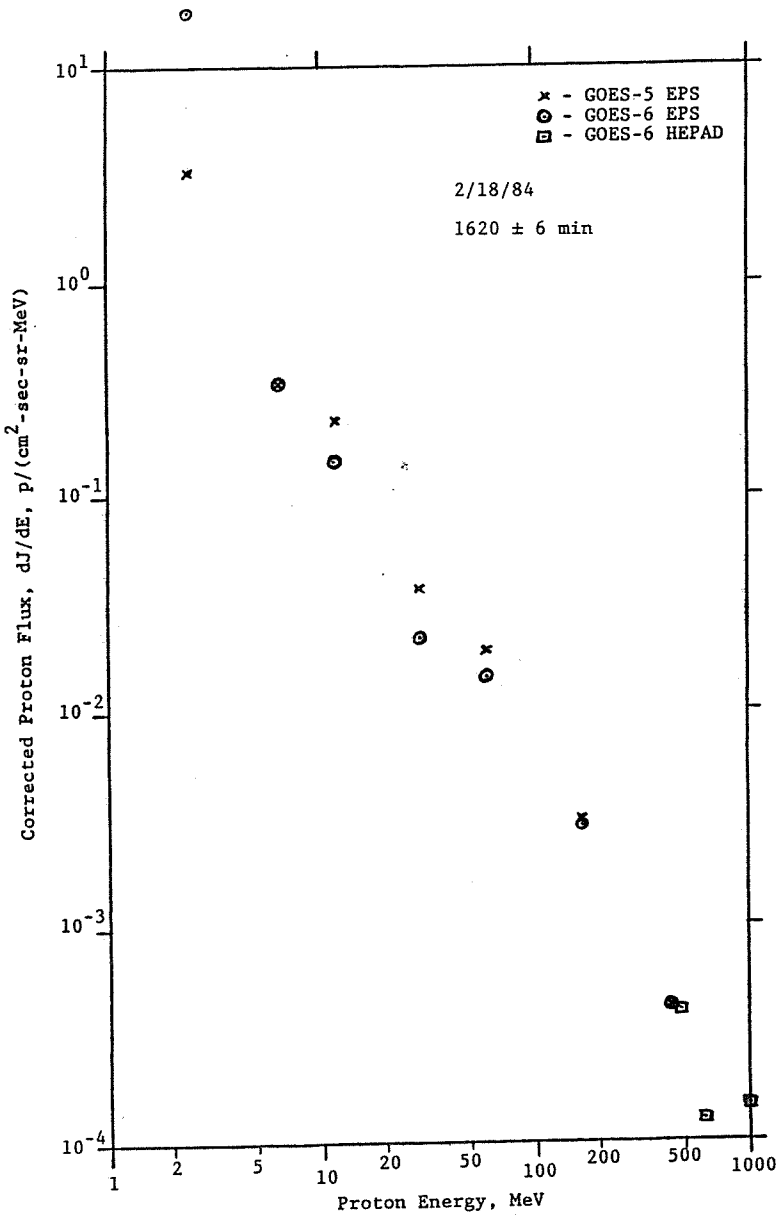


Fig. 13. Proton spectra at 1620 UT on 18 February 1984 near the end of the solar proton event.

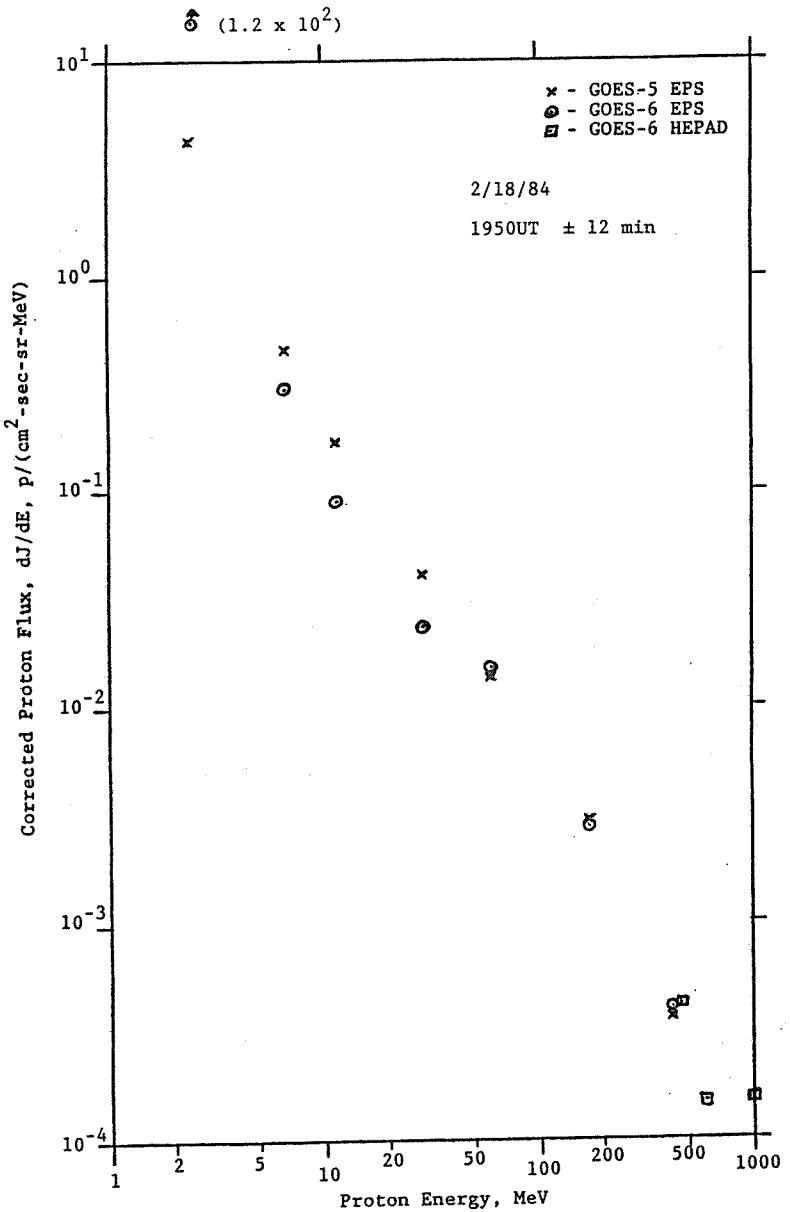


Fig. 14. Proton spectra at 1950 UT on 18 February 1984 near the end of the solar proton event.

# The Solar Proton Event of 16 February 1984: DMSP Observations at Low Altitude Over the Earth's Polar Caps

by

J.B. Blake and W.A. Kolasinski
Space Sciences Laboratory
The Aerospace Corporation
Los Angeles, California 90009 USA

## Introduction

Low altitude polar orbiters were used extensively during the early years of the study of energetic particles emitted by the Sun. For many research purposes polar orbiters are much less desirable platforms than satellites located outside of the magnetosphere because the data coverage is only of the order of 30 percent - the time spent in the polar regions. However, polar orbiters do permit study of the configuration of the magnetosphere. Solar particles, as they move from the interplanetary medium to low altitude over the Earth's polar caps, serve as probes of the distant geomagnetic field configuration and its connection with the interplanetary field. This area of research was reviewed by Morfill and Scholer (1973) and Scholer (1975).

It happens that interplanetary field-aligned anisotropies lead to latitudinal intensity variations in polar cap particle fluxes (Morfill and Scholer, 1973). Unfortunately for such studies, solar particle angular distributions in the vicinity of the Earth are frequently isotropic or nearly so. However the 16 February 1984 solar particle event was very interesting in this regard because the interplanetary fluxes were strongly anisotropic and remained so throughout the intense part of the event (Bieber et al., 1985). As a result, the polar cap fluxes showed substantial latitudinal structure.

In this report observations of the solar particle intensity structure are presented as seen by the Space Sciences Laboratory X-ray imager flown aboard the DMSP-F6 satellite.

## Satellite and Instrumentation

The DMSP-F6 satellite was in a near-polar (i=99°) orbit at an altitude of about 840 km. Continuous data were acquired from the X-ray imager; all polar cap traversals during the event are available.

The X-ray imager had as its prime mission the study of auroral morphology on a global scale by observation of the bremsstrahlung resulting from auroral electrons striking the upper atmosphere. The imager is described by Mizera et al. (1985) and in much more detail in a report by Kolasinski and Mizera (1984).

Part of the sensor complement consisted of three CdTe detectors, surrounded over the upper hemisphere by plastic scintillators viewed by photomultiplier tubes. The purpose of the scintillator/photomultiplier assemblies (SPAs) was to allow vetoing of penetrating particles such as galactic cosmic rays.

The geometric factor and energy threshold of the SPAs are broad because of the irregular configuration of the scintillators and surrounding instrument mass. In addition, the imager was mounted on the earthward side of the satellite which is three-axis stabilized; thus there was massive and irregular shielding in the zenith hemisphere. Finally, the SPAs were part of a scanning system and thus their aspect with respect to the geomagnetic field varied. The SPAs were sensitive to penetrating electrons, to bremsstrahlung generated by radiation belt electrons striking the instrument and the satellite, to trapped energetic protons, and to solar and galactic particles. Therefore the response of the SPAs on-orbit was complex and to a large degree indeterminate. However, by studying the response of the other detectors comprising the imager system, it is possible to determine where the SPA response was dominated by solar particles and to determine the solar particle cutoff. Such a study would take a significant amount of effort and has not been done for this report.

## Observations

Data from a single SPA for an entire orbit prior to the onset of the solar particle event at Earth on 16 February 1984 are shown in Figure 1. The fine structure in the count rate, especially noticeable in the outer-zone electron peak centered at 32236 seconds (0857 UT), is due to the scanning motion of the detector head containing the SPA. In Figure 1 the dominant contributors to the SPA count rate are the outer-zone trapped electrons, inner-zone trapped protons, or galactic cosmic rays, depending upon the orbital position of the satellite. Various locations are labeled in the plot. This plot clearly illustrates the lack of selectivity in the SPA response which was discussed above. Note that the two polar plateaus are featureless except for the fine structure due to statistics and the scanning motion, and that they show the same average count rate. In the time interval between 29640 seconds (0813 UT) and 31100 seconds (0838 UT) the latitudinal dependence of the count rate due to galactic cosmic rays can be seen. These data show directly the geomagnetic cutoff for the galactic cosmic rays.

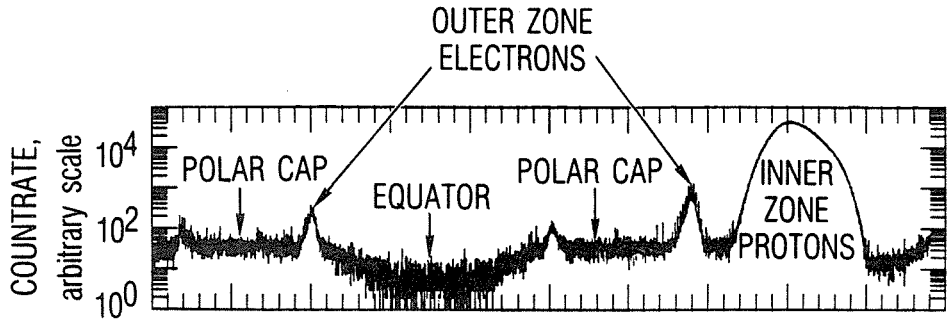


| | | | | | |
|---|---|---|---|---|---|
| UT (sec) | 28033 | 29269 | 30505 | 31741 | 32977 |
| LAT (deg) | 40.94 | 64.01 | −8.03 | −77.65 | −25.72 |
| LON (deg) | 329.99 | 170.75 | 146.05 | 97.54 | 321.20 |
| hr min sec | 0747:12 | 0807:48 | 0828:24 | 0848:00 | 0909:36 UT |

16 February 1984

Fig. 1. An entire orbit of data on 16 February 1984 from a scintillator/photomultiplier asssemblies (SPA) just prior to the first appearance of the solar particles. The "spiky" character of the data at times is only partly due to statistical fluctuations; the scanning motion of the SPA causes count rate variations.

The SPA data from repeated polar-cap traverses of the DMSP-F6 satellite are shown in Figures 2-8 for the time interval between 28000 seconds (0746 UT) to 84500 seconds (2328 UT). This time interval covers the period of relatively high proton fluxes at the Earth determined from GOES-6 data. In Figures 2-8, the average count rates in 10 second intervals are plotted as a function of invariant latitude, lambda (defined as arccos $1/\sqrt{L}$).

Plots of data subsequent to the particle event onset (Figures 2-8) show substantial latitudinal structure. The fluxes over the two polar caps differ markedly from each other, and the latitudinal structure was time dependent. Note that the count rate due to outer zone electrons "rides" on top of the count rate due to the solar particles. The solar particle cutoff is below 60° whereas the electron peak is around 62°. The evolution of the polar cap profile as the day progressed, from highly structured to featureless, can be seen clearly.

The authors would be happy to supply further and more detailed data on this event upon request.

**Acknowledgments**

This work was supported at The Aerospace Corporation by the United States Air Force Space Division under contract F04701-85-C-0086.

REFERENCES

BIEHER, J.W. P.A. EVENSON and M.A. POMERANTZ 1985 **Proceedings of the 9th International Cosmic Ray Conference, La Jolla, 4, 335.**

KOLASINSKI, W.A. and P.F. MIZERA 1984 **Aerospace Corporation Report SD-TR-84-82.**

MIZERA, P.F. D.J. GORNEY and J.L. ROEDER 1985 **J. Spacecraft and Rockets, in press.**

MORFILL, G. and M. SCHOLER 1973 **Space Sci. Rev., 15, 267.**

SCHOLER, M. 1975 **Space Sci. Rev., 17, 3.**

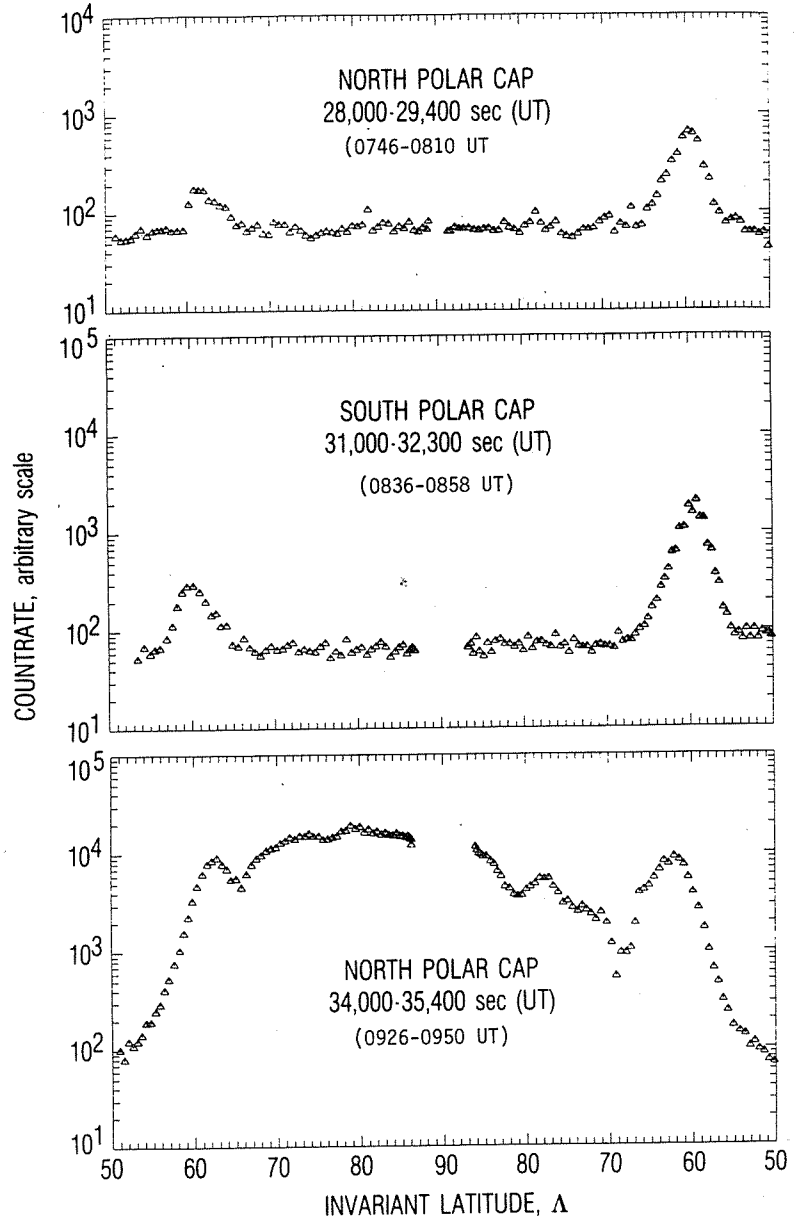


Fig. 2. Three polar cap passes are plotted for times between 28,000 seconds (0746 UT) and 35,400 seconds (0950 UT) 16 February 1984. The count rate is plotted as a function of invariant latitude (defined as arccos 1 $\sqrt{L}$). A gap near 90° arises because the satellite does not cross directly over the magnetic poles.

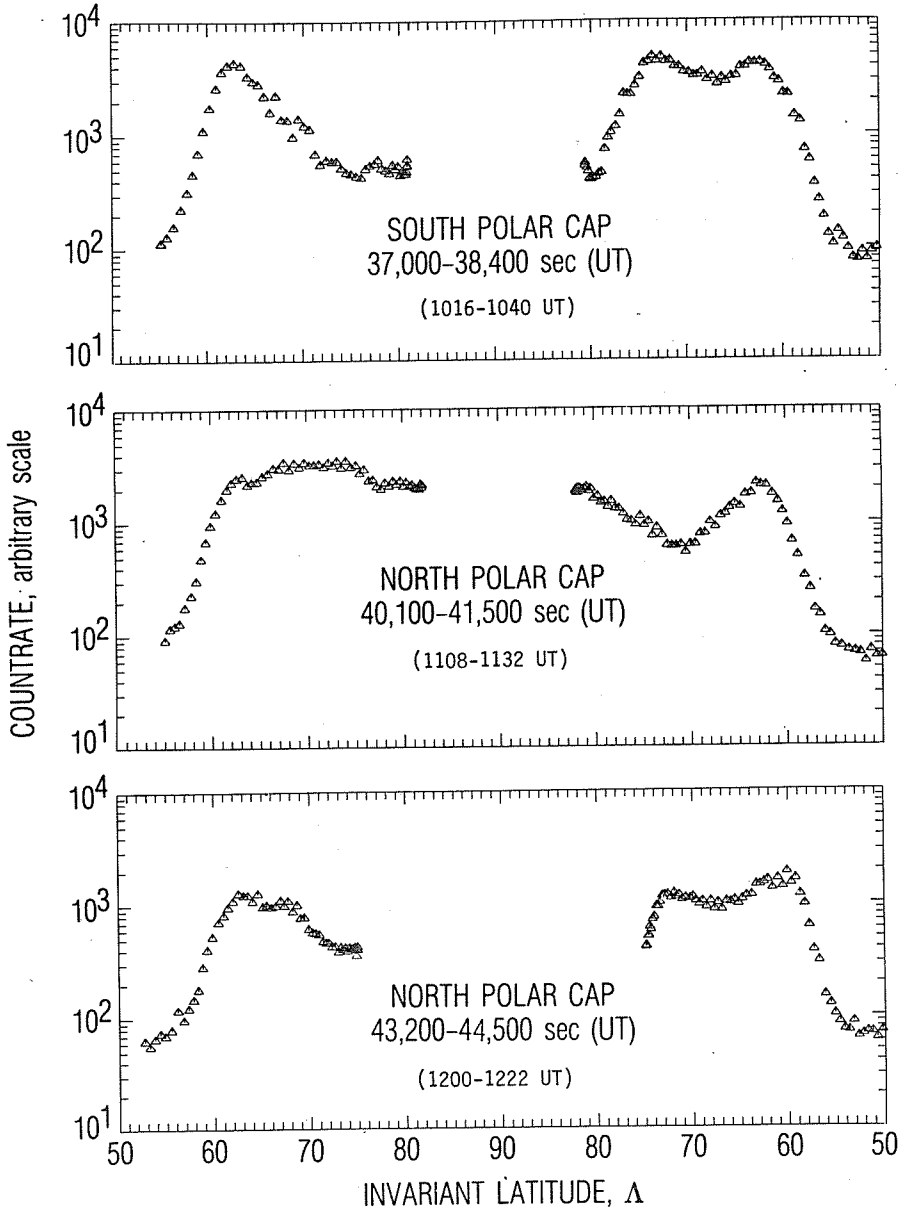


Fig. 3. Three polar cap passes are plotted for times between 37,000 seconds (1016 UT) and 44,500 seconds (1222 UT) 16 February 1984. The count rate is plotted as a function of invariant latitude (defined as arccos 1 $\sqrt{L}$). A gap near 90° arises because the satellite does not cross directly over the magnetic poles.

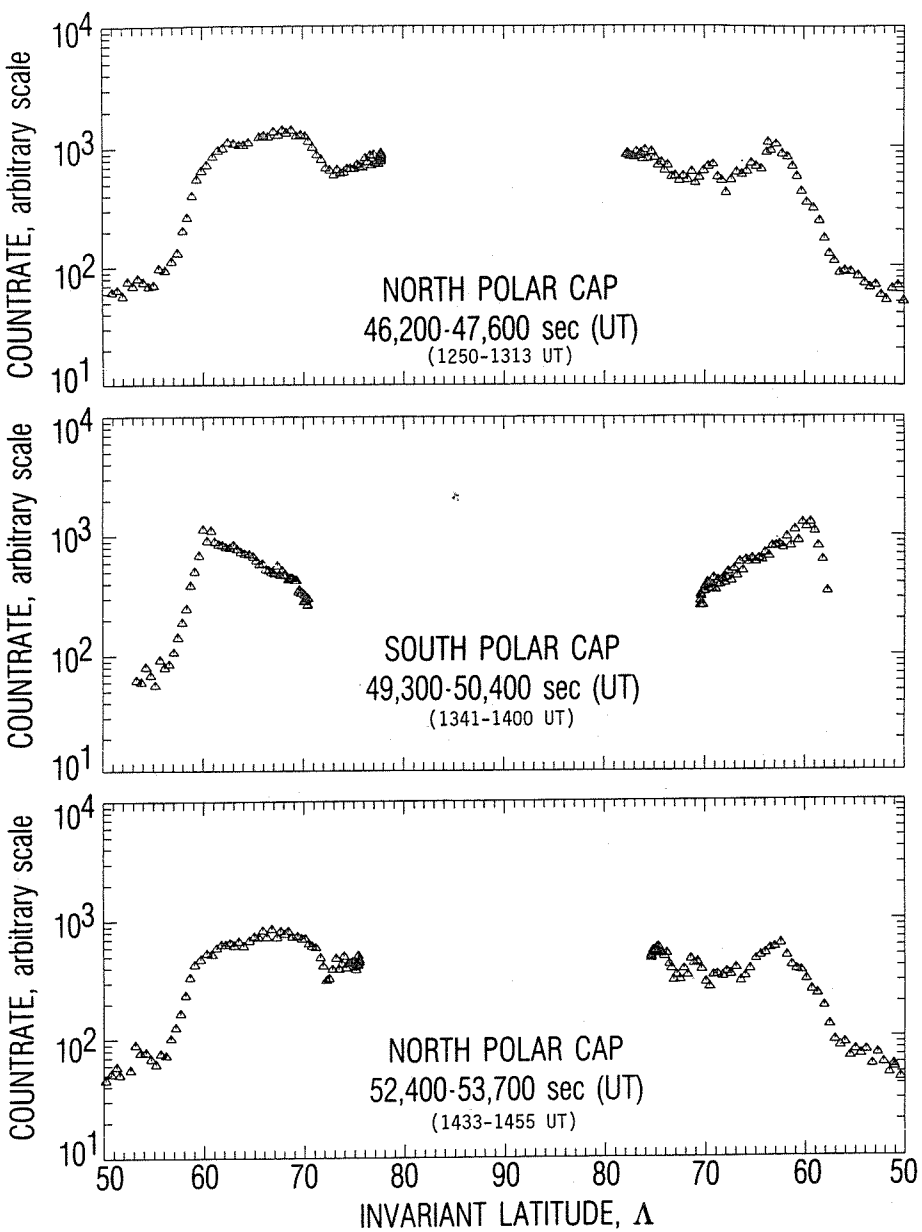


Fig. 4. Three polar cap passes are plotted for times between 46,200 seconds (1249 UT) and 53,700 seconds (1455 UT) 16 February 1984. The count rate is plotted as a function of invariant latitude (defined as arccos $1/\sqrt{L}$). A gap near 90° arises because the satellite does not cross directly over the magnetic poles.

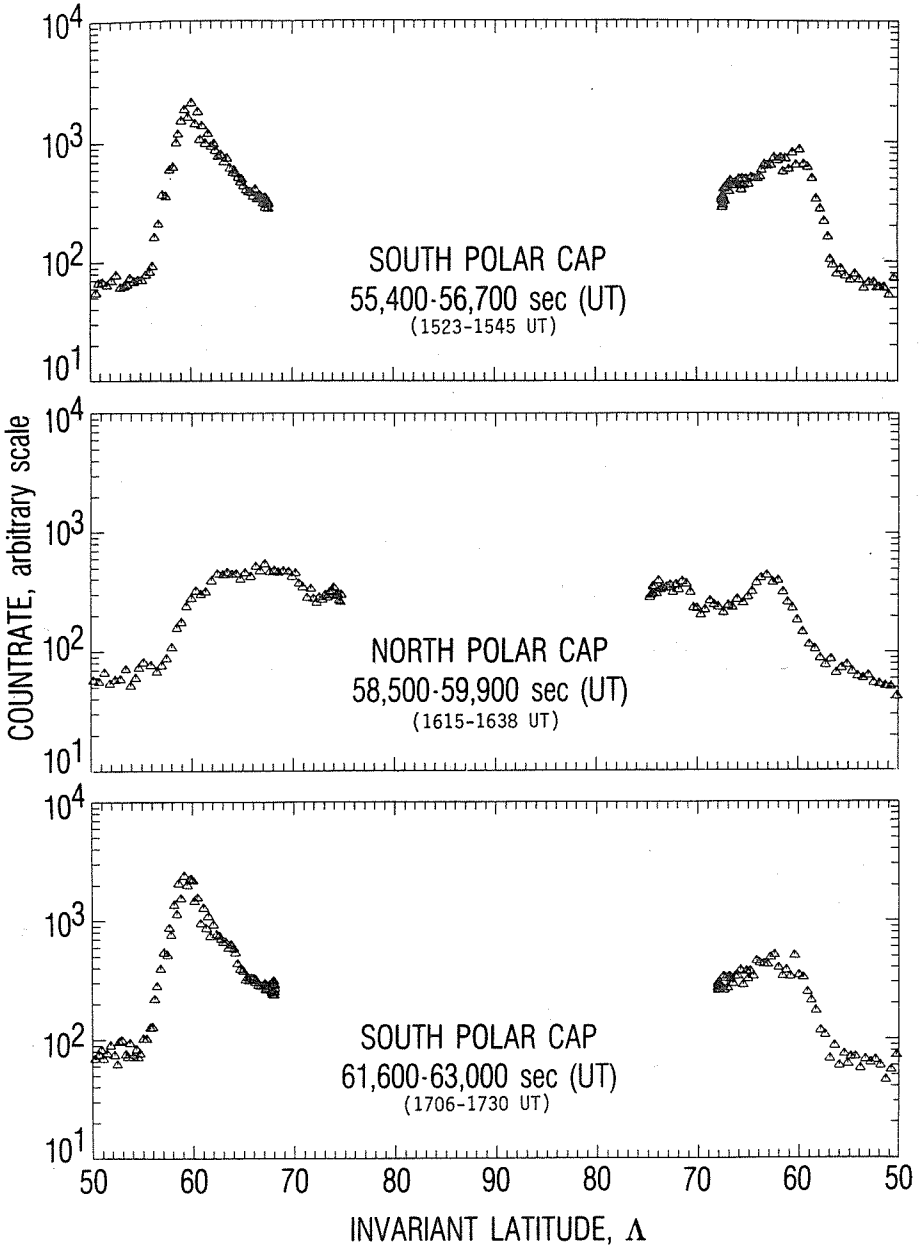


Fig. 5. Three polar cap passes are plotted for times between 55,400 seconds (1523 UT) and 63,000 seconds (1730 UT) 16 February 1984. The count rate is plotted as a function of invariant latitude (defined as arccos $1/\sqrt{L}$). A gap near 90° arises because the satellite does not cross directly over the magnetic poles.

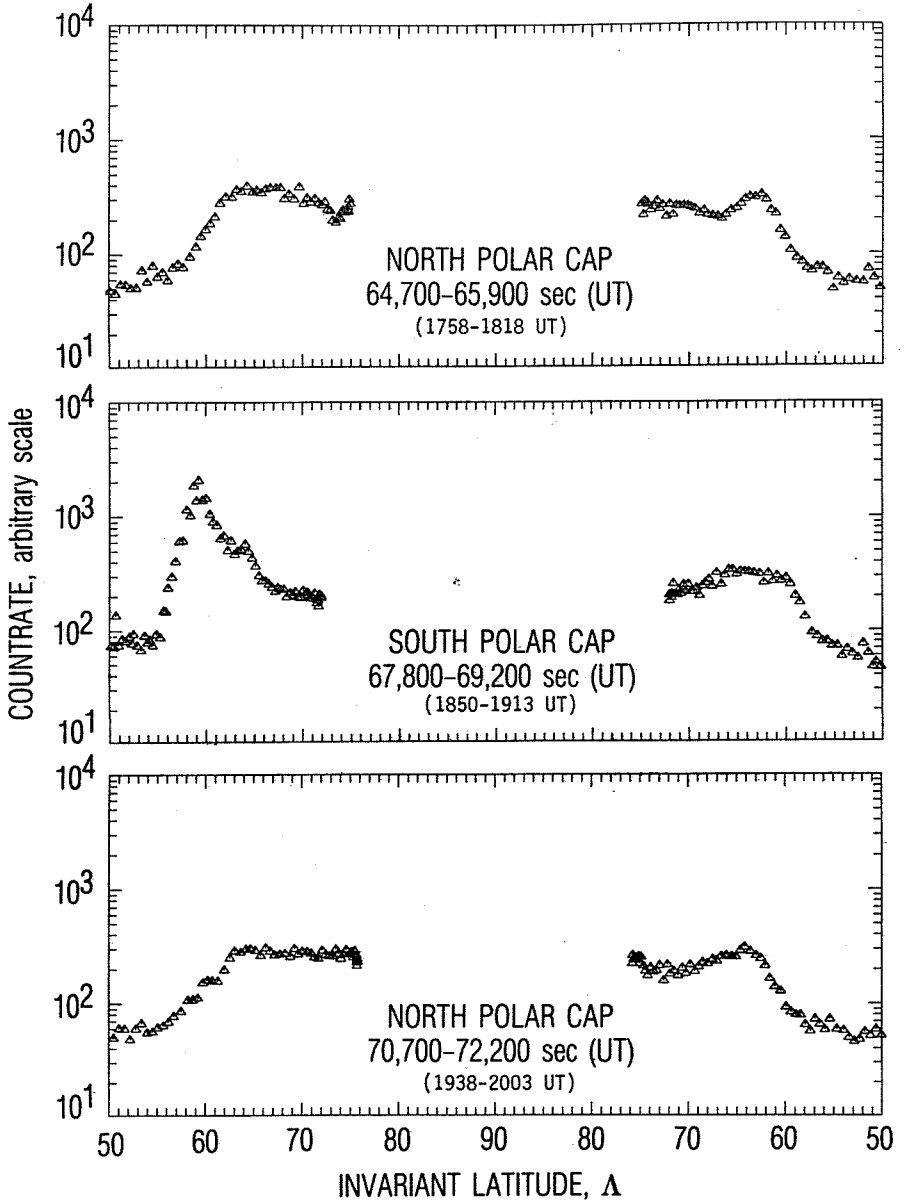


Fig. 6. Three polar cap passes are plotted for times between 64,700 seconds (1758 UT) and 72,200 seconds (2003 UT) 16 February 1984. The count rate is plotted as a function of invariant latitude (defined as arccos $1/\sqrt{L}$). A gap near 90° arises because the satellite does not cross directly over the magnetic poles.

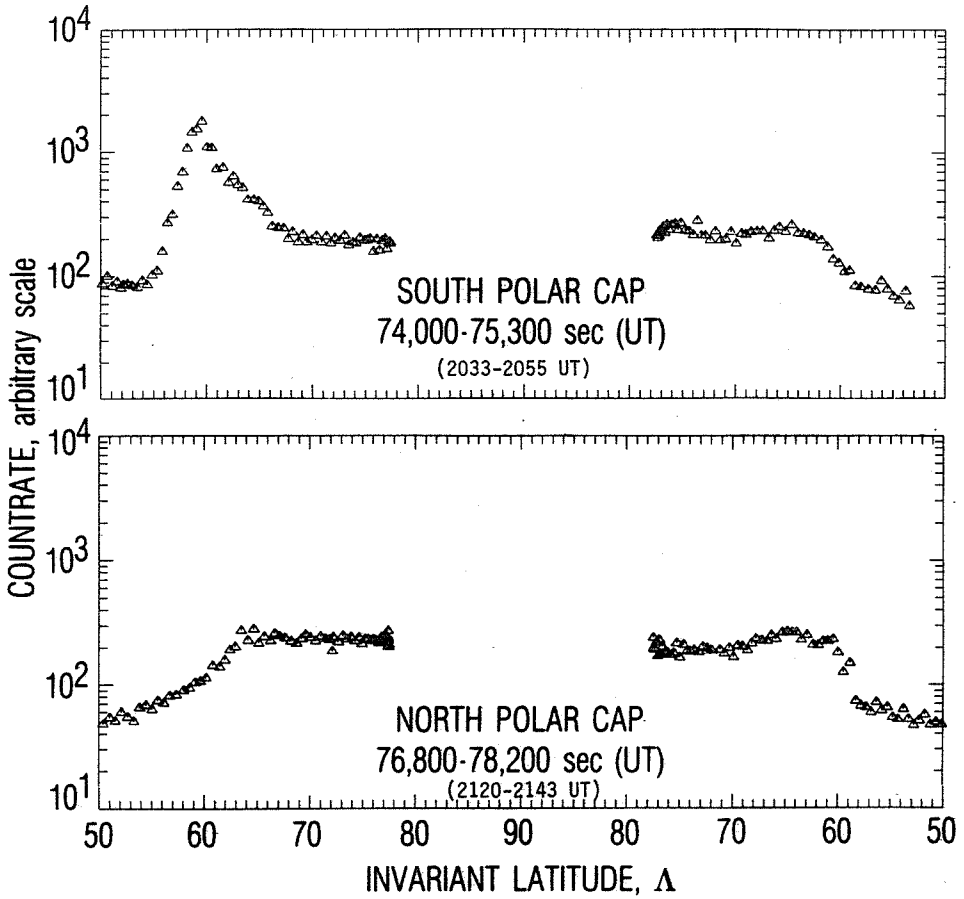


Fig. 7. Two polar cap passes are plotted for times between 74,000 seconds (2033 UT) and 78,200 seconds (2143 UT) 16 February 1984. The count rate is plotted as a function of invariant latitude (defined as arccos $1/\sqrt{L}$). A gap near 90° arises because the satellite does not cross directly over the magnetic poles.

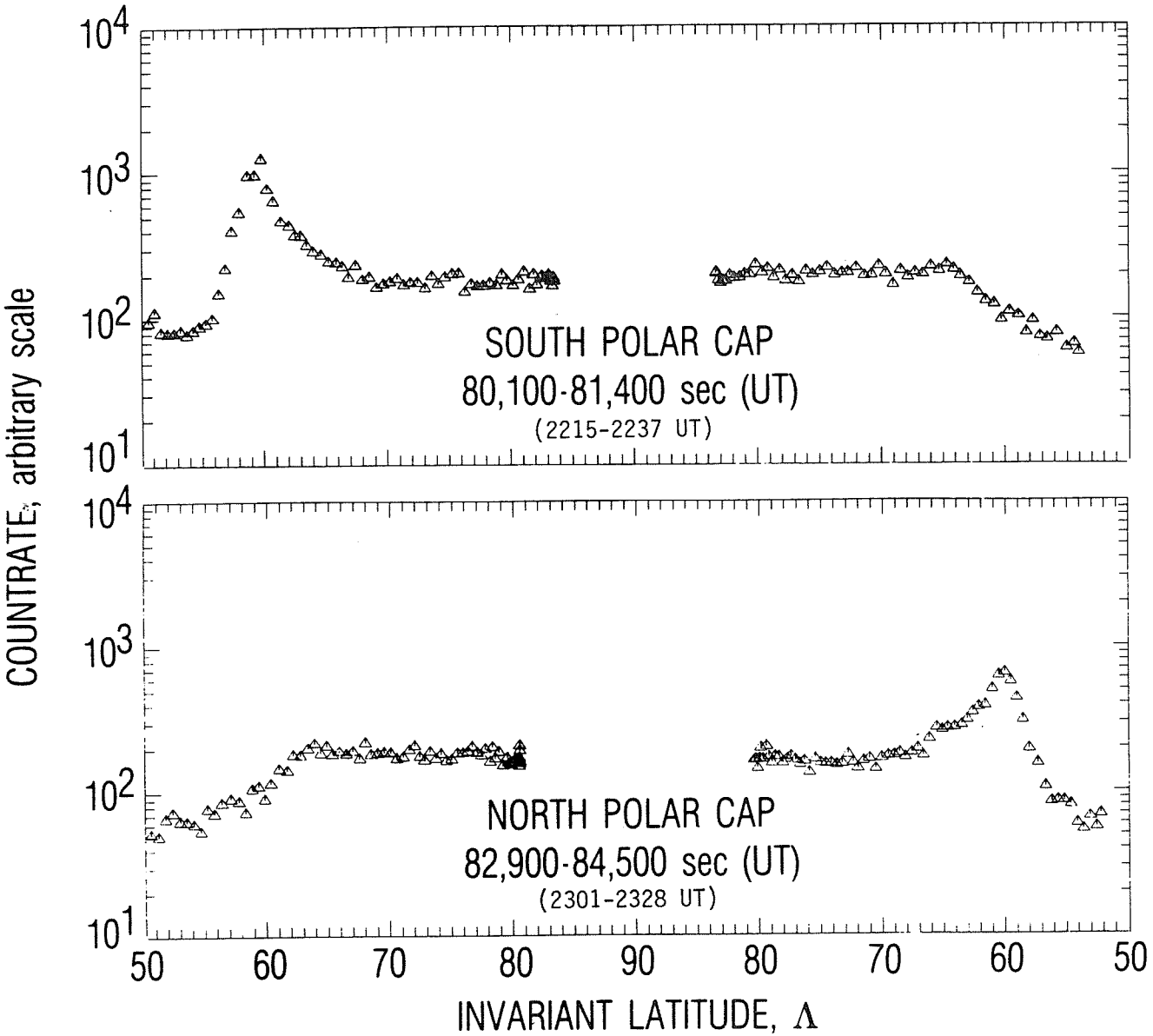


Fig. 8. Two polar cap passes are plotted for times between 80,100 seconds (2215 UT) and 84,500 seconds (2328 UT) 16 February 1984. The count rate is plotted as a function of invariant latitude (defined as arccos $1/\sqrt{L}$). A gap near 90° arises because the satellite does not cross directly over the magnetic poles.

# DMSP/F7 DOSIMETER MEASUREMENTS DURING THE SOLAR PARTICLE EVENTS OF 16 FEBRUARY AND 24-28 APRIL 1984

M. S. Gussenhoven, E. G. Mullen, M. R. Oberhardt and D. H. Brautigam
Air Force Geophysics Laboratory
Hanscom AFB, MA 01731

**ABSTRACT**

The dosimeter onboard the low altitude polar orbiting DMSP/F7 satellite provides information on the electron and proton dose, the high energy electron and proton flux, and the number of nuclear star events in its detectors. Data representative of the instrument's capabilities are presented in this report for the solar particle events of 16 February and 26 April 1984.

## I. INTRODUCTION

In this report we present an overview of the measurements made by the dosimeter on the DMSP/F7 satellite during the solar particle events occurring on 16 February 1984 and 24-28 April 1984. The dosimeter returns information on electron and proton dose, electron and proton flux, and nuclear star events, all with 4 second time resolution and in 4 integral energy steps. It is our intention here to show the versatility of the instrument, not to present extensive analysis. The data is easily accessed and can be provided for detailed studies. A calibration and data usage report has been prepared and will be supplied on request (Gussenhoven et al., 1986).

DMSP/F7 is a three-axis stabilized satellite in a sun-synchronous orbit whose orbital plane is the 1030-2230 local time meridian. The spacecraft altitude is 840 km, its period is 101 minutes, and its inclination is 98.7°. Figure 1 schematically illustrates the three high energy particle populations encountered by the DMSP satellite. The stable inner zone proton belt (cross-hatching) reaches low altitudes in the region of the South Atlantic Anomaly (SAA) due to the Earth's offset dipole. The SAA is limited in longitude and latitude, and as the Earth rotates underneath the satellite, approximately 10 of 14 of the daily orbits encounter portions of the SAA. The outer zone electrons (dotted region) occur in two high latitude rings, one in each hemisphere. The outer zone fluxes are highly variable. The polar caps (horizontal lines) are regions of direct entry for high energy particles. The first two populations are always encountered, the third detected only during solar proton events such as occurred on 16 February 1984 and 24-28 April 1984.

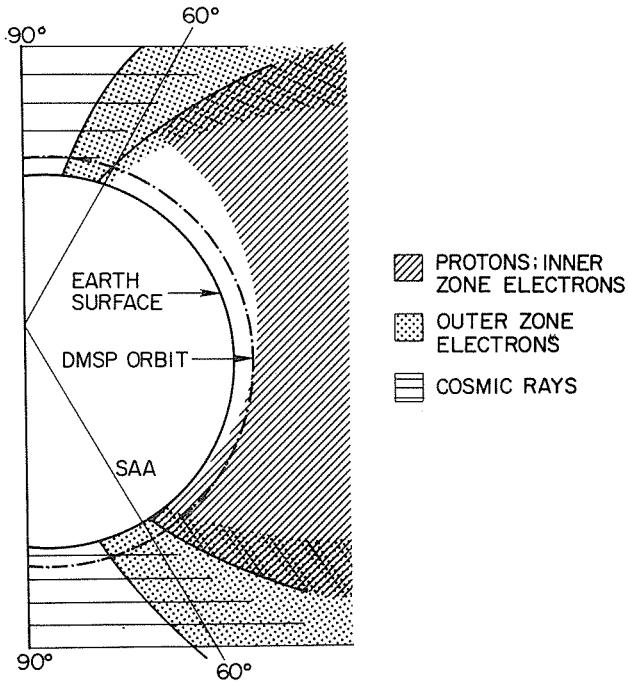


Figure 1. Schematic of the three high energy populations measured by the DMSP satellite emphasizing the effects of the Earth's offset dipole. The populations are solar cosmic rays accessing the caps; outer zone electrons in a high latitude ring, and the proton radiation belts reaching low altitudes in the South Atlantic Anomaly.

## II. DESCRIPTION OF THE SSJ* DOSIMETER

The DMSP/F7 dosimeter measures the radiation dose from both electrons and protons occurring behind four different thicknesses of aluminum shielding. Additionally, information is provided on the differential and integral fluxes of electrons and protons at energies above the thresholds defined by the shields, and on the number of nuclear star events in each detector. The basic measurement technique is the determination of the amount of energy deposited in a simple solid-state detector from particles with sufficient energy to penetrate the shielding. For electrons, the energy penetration thresholds are 1, 2.5, 5 and 10 MeV for increasing dome thickness; and for protons, 20, 35, 51 and 75 MeV. For each detector-shielding combination, the energy deposited in the detector is counted in three ranges every 4 seconds.

Energy depositions in the range between 50 keV and 1 MeV give the low linear energy transfer (LOLET) dose; depositions between 1 MeV and 10 MeV give the high linear energy transfer (HILET) dose; energy depositions above 75 MeV in detector 3 and above 40 MeV in detectors 1, 2, and 4 are counted as very high linear energy transfer (VHLET) events. The LOLET dose is derived primarily from electrons, high energy protons (above approximately 100 MeV incident), and bremsstrahlung. The HILET dose comes primarily from protons below about 100 MeV incident. The VHLET dose results from nuclear interactions (star events) initiated by high energy protons, from heavier cosmic rays, and from protons that traverse sufficiently long path lengths in the detectors. The dose is proportional to the total energy deposition in the detector. The integral flux is proportional to the number of energy depositions counted. Thus, five separate outputs are obtained from each of the four hemispherically shielded detectors: LOLET dose, LOLET flux, HILET dose, HILET flux, and VHLET flux.

During quiet times when there are no high energy solar protons present the high energy proton fluxes measured by DMSP/F7 dosimeter are confined to the SAA. A survey of the satellite's daily encounters of the SAA is shown in Figure 2. Here the average flux count rates for protons >75 MeV are plotted as a function of universal time (UT) in hours for 9 November 1984. The averaging interval is one minute. Each spike in the count rate indicates the crossing of a portion of the SAA as the Earth rotates underneath the DMSP orbit. Between each crossing, the satellite passes over the two polar caps and the equatorial region opposite the SAA; during these intervals, only background counts are detected. Similar spatial distributions occur for the lower energy flux counts and the dose counts.

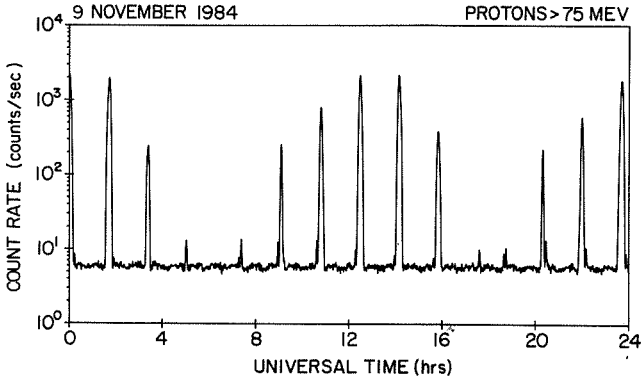


Figure 2. Proton flux counts for energies greater than 75 MeV, measured by DMSP throughout 9 November 1984 when no solar event was in progress. The spikes occur during successive crossings of the South Atlantic Anomaly.

In the following, data from 16 February and from 26 April, during peak flux observations, will be presented side by side. We present event surveys; average spectra; dose per pass and dose per event; and a star count survey.

## III. 16 FEBRUARY and 24-28 APRIL 1984 STORMS

### A. Survey of the events

One minute averages of the flux counts for >75 MeV protons are plotted for 16 February and 26 April in Figures 3a and 3b, respectively. The data presentation format is the same as in Figure 2. Polar cap fluxes lie in between the regularly occurring spikes of the SAA crossings. Figure 3a shows that the onset of the 16 February event is very sharp at ~0900 UT

(32400 s) reaching peak values within one-half an orbit. Following this, there is a steady exponential decay in the precipitation that continues throughout the 17th (not shown). The fluxes fall by an order of magnitude within 4 hours. Significant spatial and/or temporal variations are particularly large at the commencement of the event.

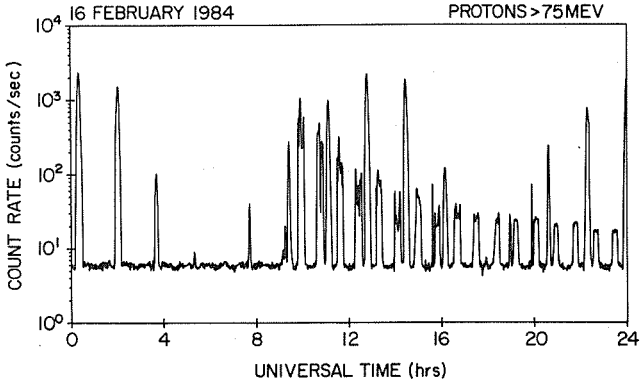


Figure 3a. Proton flux counts for energies greater than 75 MeV measured by DMSP on 16 February 1984.

At the beginning of 26 April there are already significant solar proton fluxes in the caps (Figure 3b). This event had a much slower buildup and decay compared to the 16 February event. In addition, the variations across each cap are weaker, and the peak flux in the >75 MeV proton channel is less by a factor of 2. However, we will show that because of the strength and duration of the April event the total dose accumulated over the event was more than an order of magnitude greater than for the 16 February event.

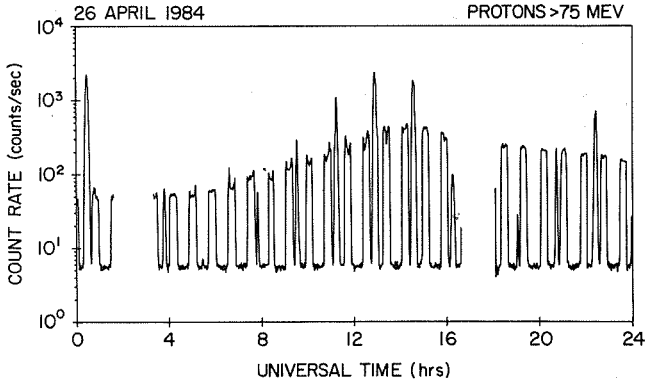


Figure 3b. Proton flux counts for energies greater than 75 MeV measured by DMSP on 26 April 1984.

Figures 4a and b show flux counts for the four electron (E1-E4) and four proton (P1-P4) channels for successive north and south polar crossings at the peak of the 16 February and 26 April events, respectively. Each plot covers one complete orbit in which the satellite moves poleward from the equator in the northern hemisphere; crosses the north polar cap from pre-noon to pre-midnight; proceeds downward past the equator to the southern polar cap which it crosses pre-midnight to pre-noon; moves upward through the SAA to the equator.

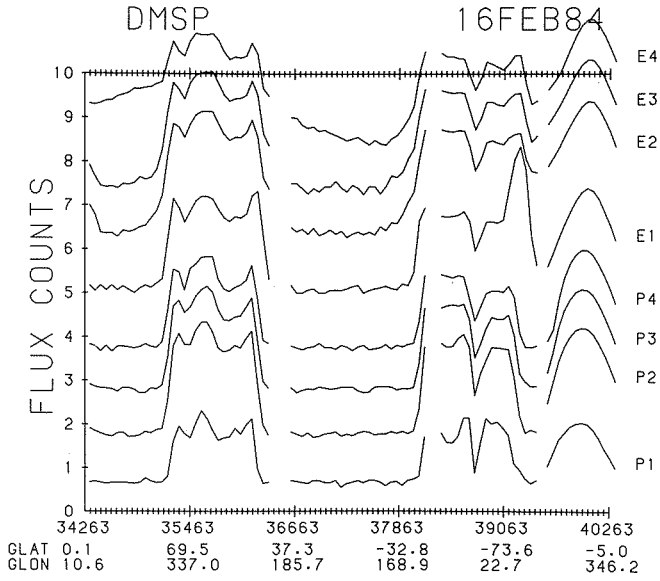


Figure 4a. Full orbit plot of the flux counts (one minute averages) in the four HILET (P1-P4) and four LOLET (E1-E4) channels at the peak of the 16 February event.

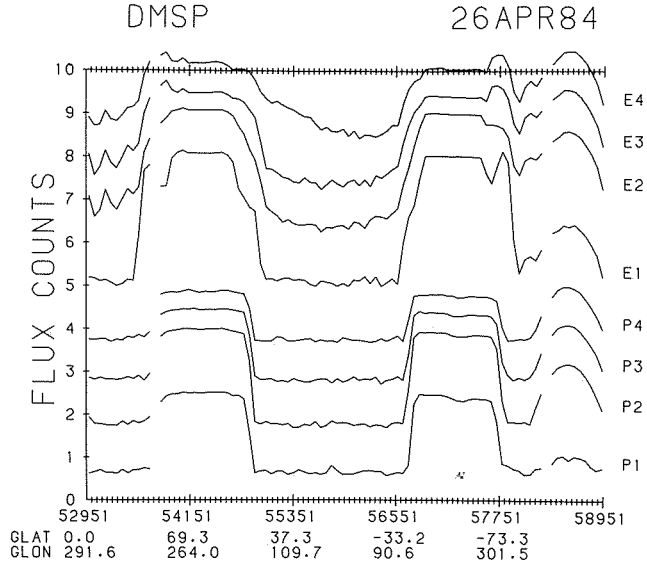


Figure 4b. Full orbit plot of the flux counts (one minute averages) in the four HILET (P1-P4) and four LOLET (E1-E4) channels at the peak of the 26 April event.

The paths of the two polar crossings on 16 February are shown in a different format in Figure 5. Here the satellite track is plotted in corrected geomagnetic latitude (MLAT)-magnetic local time (MLT) coordinates. The length of the black lines vertical to the track represents the count rate in the lowest energy proton channel (>20 MeV). These plots show a) the low latitude cutoffs (<60° MLAT) of the solar particles; b) that the particles fill both the regions normally occupied by the outer zone electrons and the polar cap; c) that relatively deep troughs occur in the flux levels which are located differently in the northern and southern hemispheres, but are near the magnetospheric cusp. Because the variations in electron and proton fluxes are similar in the 16 February event, it is very likely the case that the "electron" count rates are a combination of electron and >100 MeV protons.

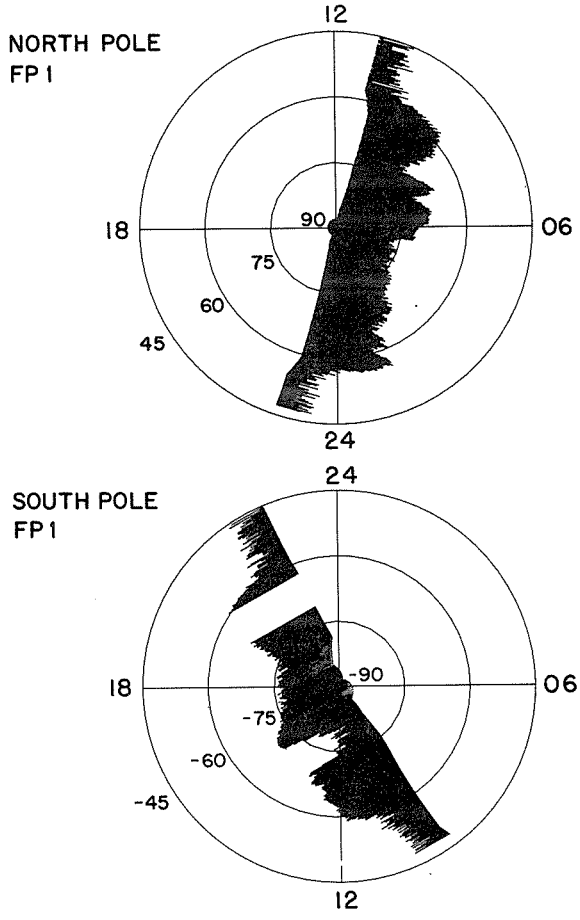


Figure 5. Polar plots of the >20 MeV protons during the peak of the 16 February event. The coordinates are corrected geomagnetic latitude and geomagnetic local time.

B. Power Law Spectra

Since the LOLET flux counts contain contributions from >100 MeV protons as well as electrons, only the HILET flux counts are used to find an average power law spectrum for protons to represent each flare. The method for converting from flux counts to flux is detailed in Gussenhoven et al. (1986). For the 16 February data, at the peak of the proton flux the optimal spectral fit for the counts averaged across the polar cap is:

16 February (peak): $j(E) = 86(\pm 2) \times \{20/E\}^{1.8}$ p/cm$^2$-s-MeV,

where E is in MeV. Under the assumption of complete particle isotropy in the upward hemisphere at DMSP altitudes and integrating from 10 MeV to infinity, the directional integral flux from the equation above is 298 p/cm$^2$-s-sr. The average spectrum for 17 February, using the cap data for the entire day is:

17 February: $j(E) = 0.85\ (\pm 0.05) \times \{20/E\}^{2.7}$ p/cm$^2$-s-MeV.

Because the solar event in April is so slowly varying we list the spectra determined by averaging the cap data for each day from 25 - 28 April. They are:

| | | |
|---|---|---|
| 24 April: | Background levels | |
| 25 April: | $j(E) = 5.6(\pm 0.4) \times \{20/E\}^{3.0}$ | p/cm$^2$-s-MeV |
| 26 April: | $j(E) = 116\ (\pm 4.0) \times \{20/E\}^{3.8}$ | p/cm$^2$-s-MeV |
| 27 April: | $j(E) = 6.8\ (\pm 0.4) \times \{20/E\}^{4.3}$ | p/cm$^2$-s-MeV |
| 28 April: | $j(E) = 18\ (\pm 2.0) \times \{20/E\}^{4.0}$ | p/cm$^2$-s-MeV |

The error listed is the error in the fitting procedure and does not include the instrument's inherent uncertainties. From the power law fits to the flux counts we draw the following conclusions: a) Throughout the February event the spectra were much harder than any of those

occurring in the April event. b) The February event softened in time. c) The April event softened over the first three days, then increased in intensity and became slightly harder.

C. Dose measurements

Figures 6a and b are survey plots of the dose counts for the same time periods of Figures 4a and b, respectively. These counts are easily converted to dose. Figures 7a and 7b are the depth-dose spectra for single polar cap crossings during the peaks of the two events. The time intervals were approximately the same for these polar cap crossings (21.3 min on 16 February, and 19.2 min on 26 April). In each plot, the LOLET (electron) dose, the HILET (proton) dose, and their sum are plotted separately for each of the four dome shielding thicknesses as a function of that aluminum shielding thickness (in mass per unit area).

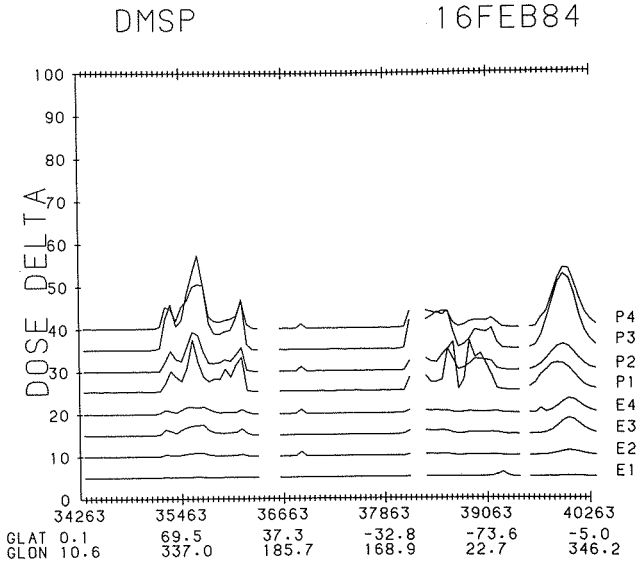


Figure 6a. Full orbit plot of the average dose counts at the peak of the 16 February event

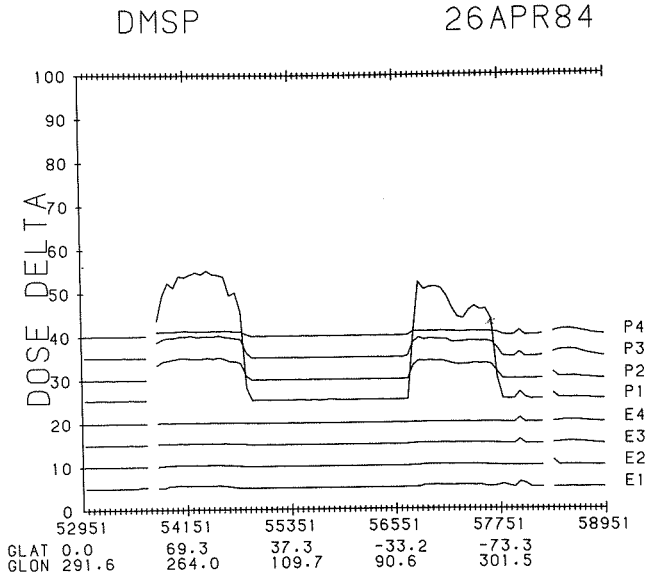


Figure 6b. Full orbit plot of the average dose counts at the peak of the 26 April event.

The depth-dose spectrum for the peak flux on 16 February, Figure 7a, shows that the total dose behind the minimum shielding is 0.2 rads for this particular polar pass. The dose source is mainly protons, the LOLET contribution being less than 25% of the total. The dose falls slowly with increased shielding, indicating that the particle spectrum is very hard. Shielding attenuates the dose and by 5.91 gm/cm$^2$ the total dose is reduced to 0.05 rads

during this polar cap crossing. Since this event decays quickly (Figure 3a), the maximum dose behind the minimum shielding is less than 2 rads over a period of less than one day.

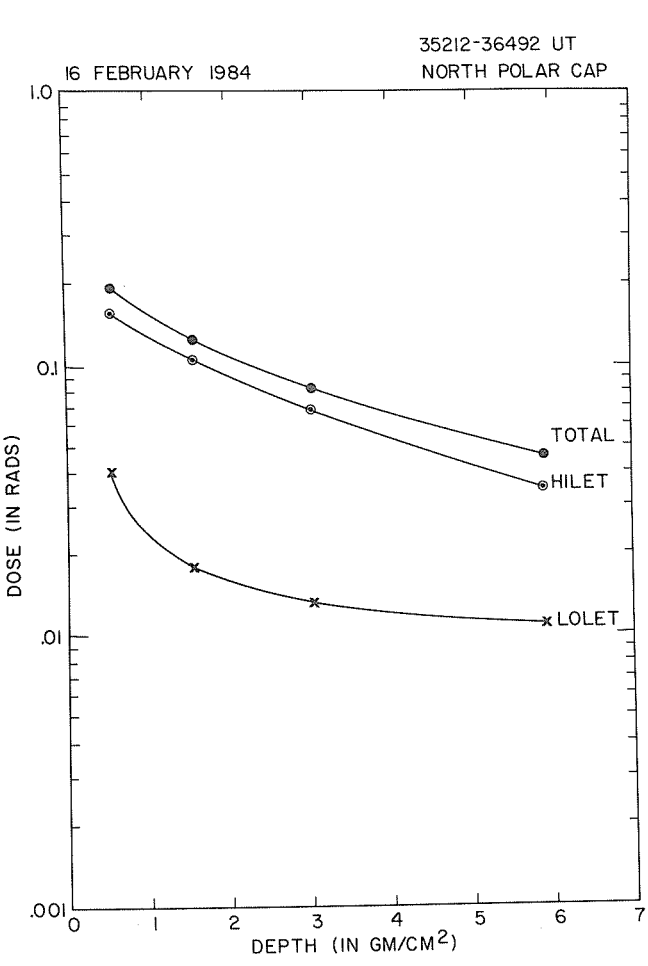


Figure 7a

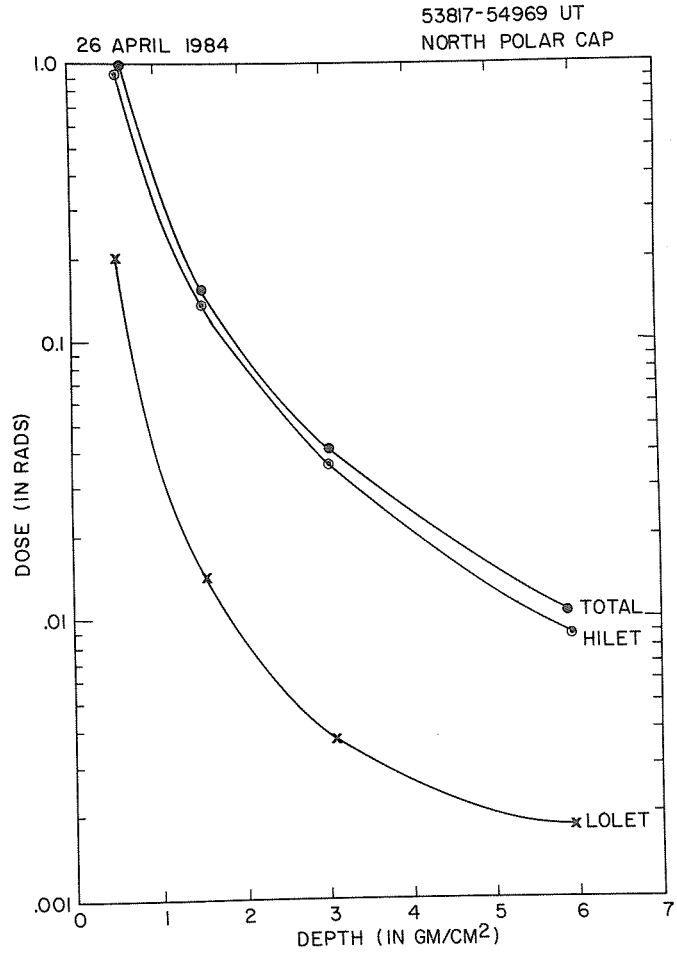


Figure 7b

Figure 7. Depth-dose spectrum for a crossing of the north polar cap at the peak of the particle event a) on 16 February and b) on 26 April.

The depth-dose profile across the northern polar cap for the peak of the solar flare flux on 26 April is shown in Figure 7b. More than 83% of the total dose in Figure 7b comes from protons. The spectrum is considerably softer than that at the peak of the 16 February event. However, the dose is much more intense at low shielding values. For 0.55 gm/cm$^2$ aluminum shielding, 1.2 rads are received in the course of a polar pass. This falls by two orders of magnitude to 0.012 rads at maximum shielding (5.91 gm/cm$^2$) where the dose is approximately an order of magnitude less than that encountered during the peak of the 16 February solar particle flux. Shielding remains effective throughout the spectrum. The dose for each polar crossing remained high for the first five days of this event. The dose per polar pass, normalized to 1000 s (16.7 min), received behind minimum shielding is plotted as a function of time in Figure 8. Although the dose per 1000 seconds interval peaks sharply at ~ 14 UT on 26 April, the slow decay of energetic particles gives a total dose for the first three days of the event of greater than 25 rads for a shielding of 0.55 gm/cm$^2$ of aluminum. This is more than an order of magnitude larger than accumulated during the 16 February event. One can also use the data in Figure 8 (interpolating through the data gap on 26 April) to estimate that for a fixed position in the cap, at 840 km, more than 70 rads would be received in the first three days of the event behind 0.55 gm/cm$^2$ aluminum.

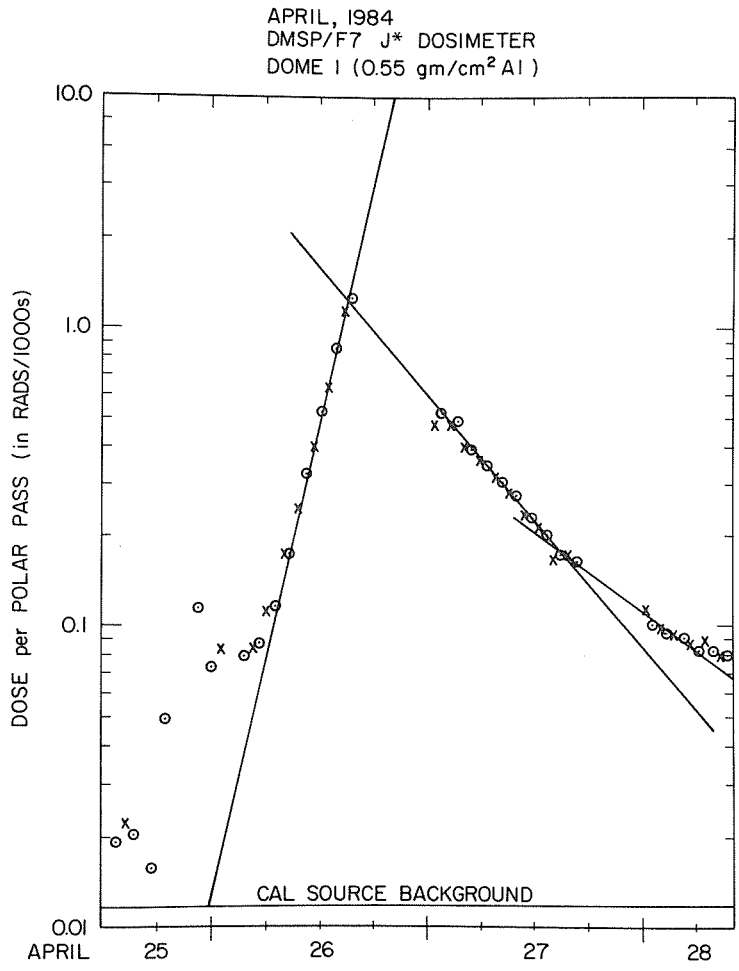


Figure 8. Dose per polar pass plotted as a function of time for the April 1984 solar particle event.

**IV STAR COUNTS**

'Star counts' as defined in this document refers to counts of very high energy loss events in one of the detectors. The 'star' description originally comes from the array of emulsion tracks observed when a high energy proton interacts with a nucleus producing secondaries and a recoiling fragment. To be measured as star counts by the dosimeter, the minimum energy levels for each channel must be met as described in Section II. This energy deposition can be accomplished in one of four ways: directly, by energy deposition from a high-Z particle (e.g. cosmic ray) traversing the detector area; indirectly, by a high energy proton interacting with a nucleus within the detector and producing energetic recoil fragments; indirectly, by a high energy proton interacting with a nucleus outside, but near the detector and a high energy nuclear fragment or secondary depositing the energy in the detector; or directly, in channels 2 and 4 only, by a proton depositing the threshold energy over a long path length.

During large solar particle events in the polar regions, solar protons and cosmic ray particles can produce high level count rates. Separation of the star count component of these rates according to sources is non-trivial, but can be attempted under certain circumstances by detailed analysis of the detector response with particle simulation codes using proton flux spectra obtained from the HILET channels.

Table 1 gives the daily average of star channel count rates for the 4 detectors in counts per second times $10^{-4}$ for the periods 15-17 February 1984 and 24-30 April 1984. Also given are the 1985 average count rates for comparison as a normal background level and the differences from the 1985 averages for the days of interest. The count rates were determined only from the polar regions: between 40° and 90° North Latitude and 55° and 90° South Latitude. Data equatorward of 55° South Latitude were excluded from the table to prevent contamination from the SAA. It is evident from the table that from a star count (single event upset) point of view, April 26 had the highest average count rates. However, from a spectral hardness point of view, the February event was much harder in protons and contained

a much higher proportion of high energy heavy particles. Therefore, unless a spacecraft contained electronic components sensitive to approximately 60 MeV protons or below, the February event would be considered a harsher environment for creating spacecraft anomalies.

Table 1. Star Count Rates

Count Rates (counts/sec x $10^{-4}$)

| CHANNEL | 1985 Ave. | Feb 84 15 | 16 | 17 | 24 | 25 | 26 | Apr 84 27 | 28 | 29 | 30 |
|---|---|---|---|---|---|---|---|---|---|---|---|
| 1 | 1.6 | 0.6 | 12.0 | 1.8 | 1.3 | 9.6 | 83.0 | 26.0 | 9.6 | 7.9 | 2.2 |
| 2 | 27.0 | 28.0 | 170.0 | 38.0 | 27.0 | 87.0 | 500.0 | 190.0 | 91.0 | 38.0 | 27.0 |
| 3 | 11.0 | 12.0 | 14.0 | 8.8 | 12.0 | 9.6 | 18.0 | 12.0 | 8.5 | 7.1 | 10.0 |
| 4 | 24.0 | 22.0 | 53.0 | 26.0 | 20.0 | 25.0 | 62.0 | 29.0 | 22.0 | 18.0 | 19.0 |

Differences from 1985 Averages

| | | | | | | | | | | | |
|---|---|---|---|---|---|---|---|---|---|---|---|
| 1 | | -- | 10.0 | -- | -- | 8.0 | 81.0 | 24.0 | 8.0 | 6.0 | -- |
| 2 | | -- | 143.0 | -- | -- | 60.0 | 473.0 | 163.0 | 64.0 | -- | -- |
| 3 | | -- | 3.0 | -- | -- | -- | 7.0 | --- | -- | -- | -- |
| 4 | | -- | 29.0 | -- | -- | -- | 38.0 | --- | -- | -- | -- |

**REFERENCES**


GUSSENHOVEN, M.S., R.C. FILZ, K.A. LYNCH, E.G. MULLEN, and F.A. HANSER 1986 Space Radiation Dosimeter SSJ* for the Block 5D/Flight 7 DMSP Satellite: Space Calibration and Data Presentation, Air Force Geophysics Laboratory, Hanscom AFB, MA, AFGL-TR-86-0065, March, 1986.

# Energetic Electron and Ion Fluxes at Geostationary Orbit: 6-11 February and 20 April - 1 May 1984

by

D.N. Baker, P.R. Higbie, R.D. Belian, R. Robinson, and K. Sofaly
Los Alamos National Laboratory
Los Alamos, New Mexico, 87545 USA

## Abstract

We present a summary of geostationary orbit energetic electron fluxes in the energy range 30 keV to 2 MeV and energetic ion fluxes in the energy range about 100 keV to about 100 MeV for periods in early 1984. The first interval extends from 6 February through 11 February 1984 and the second interval extends from 20 April through 1 May 1984. Data are given for four geographic spacecraft locations: about E70, about W40, about W70 and about W135. The first interval is characterized by weak-to-moderate geomagnetic activity with many substorm events. The second interval is characterized by intense particle increases including >100 MeV solar flare protons at 6.6 $R_E$.

## Introduction

The geostationary orbit is a region of considerable human activity in space. At this location, 6.6 $R_E$ (42000 km) from the center of the Earth, a spacecraft remains fixed above a given point on the Earth's geographic equator because the satellite completes one revolution as the Earth rotates once each day. This orbit is therefore very useful for many applications to weather, communication, and military needs where it is desirable for a spacecraft to maintain a constant position relative to particular geographic locations or land masses.

Scientifically 6.6 $R_E$ is also a very interesting position within the terrestrial magnetosphere. The geostationary orbit is at the outer edge of the terrestrial trapped radiation region (outer radiation zone) and is also at the inner edge of the magnetotail plasma sheet. From a geostationary spacecraft platform, scientific instrumentation can thus probe the highly dynamic outer magnetosphere and can assess both the trapped (Van Allen) radiation environment and the strongly (substorm) modulated plasma sheet.

The Los Alamos National Laboratory has provided energetic particle sensors for a whole series of geostationary satellites. Each of these energetic particle instruments, consisting of several subsystems, is called the Charged Particle Analyzer (CPA) experiment. The CPA provides an environmental monitoring function for the joint Department of Energy/Department of Defense satellite of which the CPA is part and, also, the CPA provides a global assessment of magnetospheric conditions in a variety of ways.

The CPA instruments have been described in some detail in prior published reports (Higbie et al., 1978; Baker et al., 1979). Each CPA consists of separate electron and proton sensor systems. The electron detectors are designated LoE (low energy electron) and HiE (high energy electron). LoE consists of a fan of five separate detector-collimator units at 0°, $\pm$30°, and $\pm$60° to the spacecraft equatorial plane. The spacecraft rotate with a 10 second period about an axis that points continually toward the center of the Earth. Thus complete (over the unit sphere), continuous pitch angle measurements of the electron distribution are made by LoE every 10 seconds for essentially all magnetic field orientations. Each LoE sensor-collimator unit has a geometric factor of $3.6 \times 10^{-3}$ $cm^2$sr and is sensitive to electrons of energy between 30 and 300 keV (in 6 channels). The basic CPA sampling rate is 8 milliseconds, so that each energy channel of each sensor is sampled 40 times per 10 second spacecraft rotation (i.e., 1200 total samples per rotation).

The HiE subsystem consists of a single detector-collimator unit that is pointed radially outward in the spacecraft equatorial (0°) plane. The HiE geometric factor is $1.8 \times 10^{-2}$ $cm^2$sr and its range of sensitivity is between 0.2 MeV and about 2 MeV. Since a single collimator unit (half-angle of acceptance about 4°) is used in HiE, only a relatively narrow band of the unit sphere is sampled as the spacecraft rotates. For normal, approximately dipolar magnetic field orientations nearly all pitch angles would be sampled by HiE, but for non-dipolar (tail-like) magnetic field configurations often encountered near midnight at 6.6 $R_E$, very limited pitch angle sampling can result.

The energetic proton measurement of 6.6 $R_E$ is made by two separate CPA particle telescope systems: LoP and HiP. LoP is a single thin (about 40 microns) surface barrier solid state detector in front of an anticoincidence scintillator element. A sweep magnet is part of the LoP collimation system and eliminates about <0.5 MeV electrons from entering the LoP sensors. LoP has a geometric factor of $3.9 \times 10^{-3}$ $cm^2$sr and measures ions (which we identify as primarily protons) in the range of about 100 to about 600 keV (10 channels). The HiP is a four-element telescope consisting of three solid state detectors encased in the fourth sensor element, a plastic anticoincidence scintillator cup. HiP also has a strong sweeping magnet to eliminate contamination by about <1.0 MeV electrons. The high-energy proton telescope measures protons between 0.4 and about 200 MeV in 16 quasi-logarithmic differential energy channels with a geometric factor of $4.4 \times 10^{-2}$ cm sr (about $8 \times 10^{-2}$ $cm^2$sr for E >25 MeV).

Energetic electron and ion data at the geostationary orbit have proven to be useful in a variety of magnetospheric studies (e.g., Baker and Fritz, 1984). Data products from the Los Alamos instruments onboard a series of geostationary spacecraft have been previously described (Baker et al., 1981; 1982).

In this report we summarize Los Alamos particle measurements for two intervals of substantial interest to the international scientific community. During each interval we present data from three different spacecraft geographic positions.

## 6-11 February 1984 Interval

Figures 1-3 show data acquired from 6 through 11 February 1984. The data are shown in the form of hourly flux averages. The upper two panels of each figure show integral electron fluxes, while the lower two panels of each figure show energetic ion fluxes which we ascribe mainly to magnetospheric protons.

Table 1 summarizes the energetic electron energy channels pertinent to all spacecraft discussed here. The "low-energy" electrons in Figures 1-3 consist of 30-300 keV particles while the "high-energy" electrons range from 200 keV to 2 MeV. The flux units employed are: electrons $(cm^2\ s\ sr)^{-1}$.

Table 1. Los Alamos Geostationary Orbit Electron Channels

| Channel Designation | Energy Range | Channel Designation | Energy Range |
|---|---|---|---|
| LoE 1 | 30-300 keV | HiE 1 | 0.2-2.0 MeV |
| 2 | 45-300 | 2 | 0.3-2.0 |
| 3 | 65-300 | 3 | 0.4-2.0 |
| 4 | 95-300 | 4 | 0.6-2.0 |
| 5 | 140-300 | 5 | 0.9-2.0 |
| 6 | 200-300 | 6 | 1.4-2.0 |

The proton channels for each of the spacecraft employed here are generally similar in energy range, but they differ somewhat from satellite to satellite. For the sake of completeness, we show the proton energy channels separately for each spacecraft in Table 2.

Table 2. Energetic Proton Channels for Four Spacecraft (S/C)

| Channel Designation | S/C 1977-007 Energy Range | S/C 1982-019 Energy Range | S/C 1981-025 Energy Range | S/C 1984-037 Energy Range |
|---|---|---|---|---|
| LoP-1 | 145-560 keV | 92-600 keV | 107-750 keV | 70-560 keV |
| -2 | 160-560 | 108-600 | 133-750 | 83-560 |
| -3 | 175-560 | 128-600 | 157-750 | 100-560 |
| -4 | 190-560 | 150-600 | 197-750 | 130-560 |
| -5 | 215-560 | 195-600 | 236-750 | 160-560 |
| -6 | 245-560 | 229-600 | 295-750 | 190-560 |
| -7 | 290-560 | 254-600 | 340-750 | 235-560 |
| -8 | 340-560 | 318-600 | 420-750 | 290-560 |
| -9 | 400-560 | 377-600 | 500-750 | 350-560 |
| LoP-10 | 480-560 keV | 462-600 keV | 610-750 keV | 450-560 keV |
| HiP-1 | 0.45-0.54 MeV | 0.37-0.52 MeV | 0.40-0.47 MeV | 0.38-0.49 MeV |
| -2 | 0.54-0.68 | 0.52-0.64 | 0.47-0.62 | 0.49-0.68 |
| -3 | 0.68-0.83 | 0.64-0.80 | 0.62-0.78 | 0.68-0.87 |
| -4 | 0.83-1.1 | 0.8-1.0 | 0.78-1.0 | 0.87-1.05 |
| -5 | 1.1-1.4 | 1.0-1.3 | 1.0-1.3 | 1.05-1.45 |
| -6 | 1.4-1.8 | 1.3-1.7 | 1.3-1.7 | 1.45-1.8 |
| -7 | 1.8-2.2 | 1.7-2.2 | 1.7-2.1 | 1.8-2.3 |
| -8 | 2.8.4.8 | 2.7-4.4 | 2.6-4.4 | 2.9-4.8 |
| -9 | 4.8-9.0 | 4.4-8.3 | 4.4-8.0 | 4.8-9.0 |
| -10 | 9-14 | 8.3-13 | 8-12 | 9-14 |
| -11 | 14-25 | 13-24 | 12-24 | 14-24 |
| -12 | 25-38 | 24-41 | 24-43 | 24-39 |
| -13 | 38-61 | 41-64 | 43-68 | 39-60 |
| -14 | 61-92 | 64-100 | 68-110 | 60-90 |
| -15 | 92-144 | 100-160 | 110-160 | 90-145 |
| HiP-16 | 144-210 MeV | 160-230 MeV | 160-210 MeV | 145-200 MeV |

Figure 1 shows data for spacecraft (S/C) 1977-007. The satellite was located at about E70 geographic longitude throughout the study interval. We see from the top panel of Figure 1 that there were several small substorm "injection" events throughout this period. These substorm flux increases were commonly seen most prominently around the beginning of each day and the effect was largest in 30-100 keV electron energy channels (Channels LoE 1-4). (We note that S/C 1977-007 reached local midnight at about 1900 UT each day; the flux increases were thus largest at, or just after, local midnight).

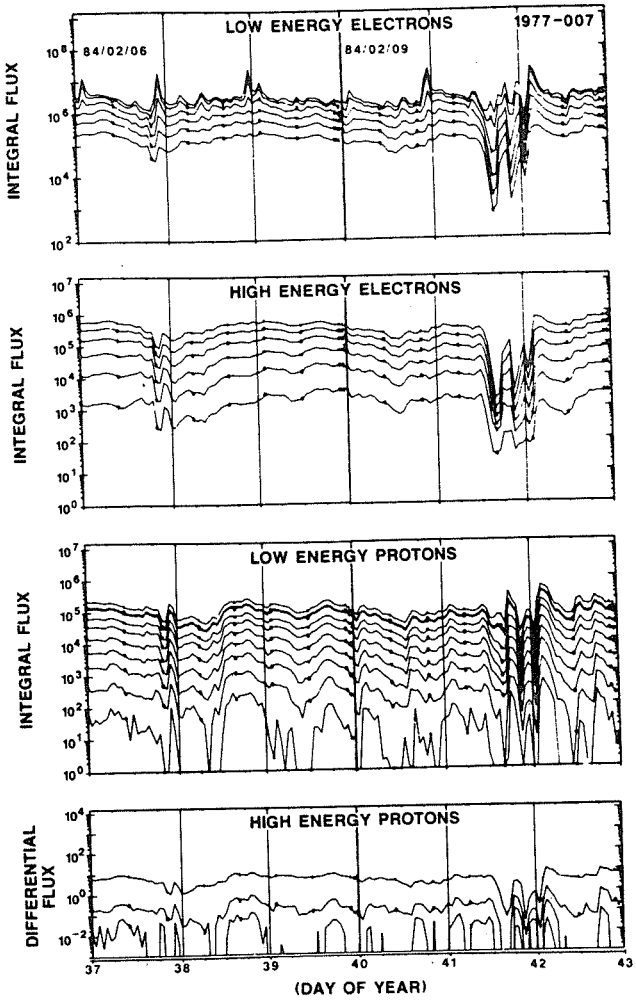


Fig. 1. Hourly averages of energetic electrons and protons for the period 6-11 February 1984 as measured by instruments on board S/C 1977-007 at geostationary orbit (about E70 geographic longitude). Electron energy levels are given in Table 1 and proton energy channels are given in Table 2.

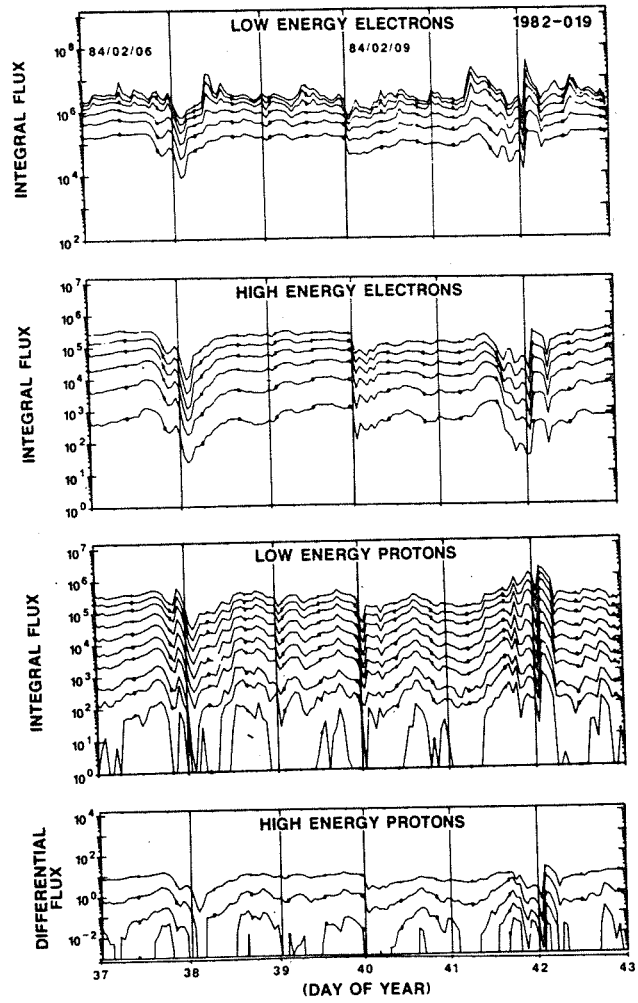


Fig. 2. Same as Figure 1 but for S/C 1982-019 which was located at about W70 geographic longitude.

Large increases in the ≥100 keV proton fluxes were not very evident in most of the substorm events. Exceptions to this rule were seen (weakly) late on Day 37 (6 Feb 84) and on Day 41 and 42 (10-11 Feb 84). This latter interval was notable in that there were very large flux dropouts and strong flux recoveries in all energy channels (both electrons and protons) over a very broad range of local time and UT.

In the higher proton energy ranges there were relatively evident daily flux modulations. On the whole, however, there were no major proton increases above about 500 keV throughout this period.

Figure 2 shows data for S/C 1982-019. This satellite was located at about W70 geographic longitude during the 6-11 February interval. The format of Figure 2 is entirely analogous to that of Figure 1.

As for S/C 1977-007, Figure 2 shows that there were several relatively small substorm events in the S/C 1982-019 data throughout the 6-11 February interval. The S/C reached local midnight at about 0430 UT each day and the largest low-energy electron fluctuations tended to occur between about 0500 and about 1000 UT daily (i.e. in the postmidnight sector). The two dominant intervals of disturbance were seen on Days 37-38 and Days 41-42. These were periods of large flux dropouts and strong flux recoveries, including energetic proton enhancements. These general intervals of large disturbance match those seen at S/C 1977-007.

Figure 3 shows data for S/C 1981-025 which was at a geographic longitude of W135. At this position, the S/C reached local midnight at about 0900 UT each day.

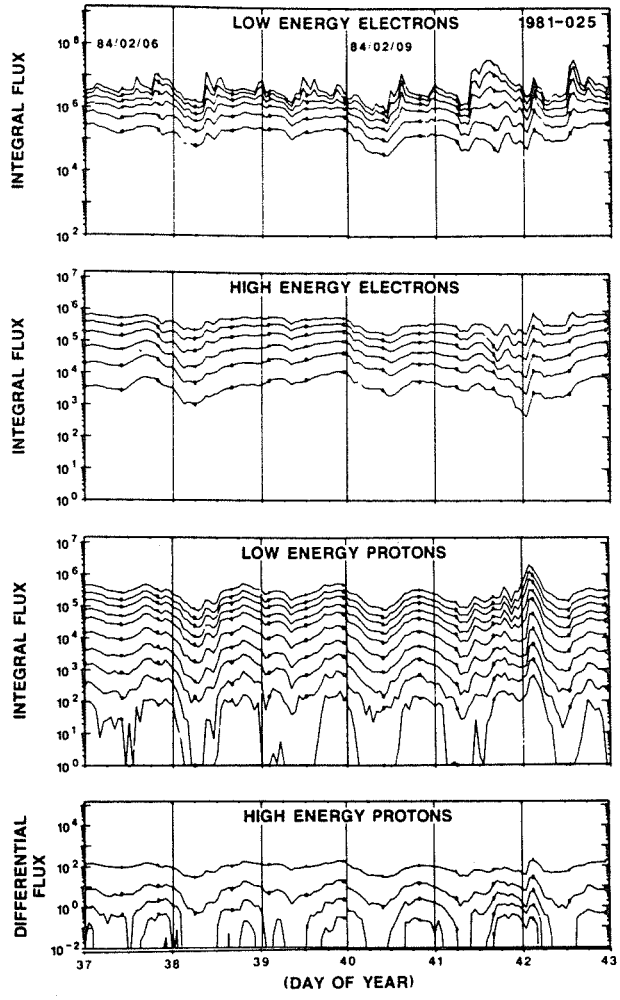


Fig. 3. Same as Figure 1 but for S/C 1981-025 which was located at about W135 geographic longitude.

The data of Figure 3 show relatively prominent low-energy electron flux variations on almost every day. These tended to be largest around 0900-1200 UT. Thus, we see relatively strong substorm effects nearly every day at this S/C location and these effects seem to extend in energy up to well over 100 keV. Similar to the other two spacecraft (Figures 1-2), the largest electron effects and the most prominent variations in the proton fluxes tended to be on Days 37-38 and Days 41-42.

As in the data for S/C 1977-007 and S/C 1982-019, there is little evidence in Figure 3 for any major increase in proton fluxes above about 500 keV. There is, however, a relatively prominent diurnal proton flux modulation.

## 20 April - 1 May 1984 Interval

Figure 4 summarizes data for S/C 1977-007 from 20 April through 1 May 1984 (Day 111-Day 122). The format is the same as in Figure 1. Again, the satellite was located at about E70 geographic longitude, thus reaching local midnight at about 1900 UT each day.

As in the February interval of Figure 1, we tended to see numerous substorm disturbances, primarily in the low-energy electron channels. These occurred most often when the S/C was in the postmidnight region. Prior to Day 116 (25 April) it was relatively rare to see a strong effect in the higher energy electron or in the proton channels.

Late on 25 April (Day 116), and for the remainder of the interval shown here, we see that there was a very strong increase in all particle flux levels. This was true both for electrons and for protons. Note that the flux enhancements extended to very high energies: proton intensities were elevated at energies as high as 150 MeV on 26 April 1984 (Day 117).

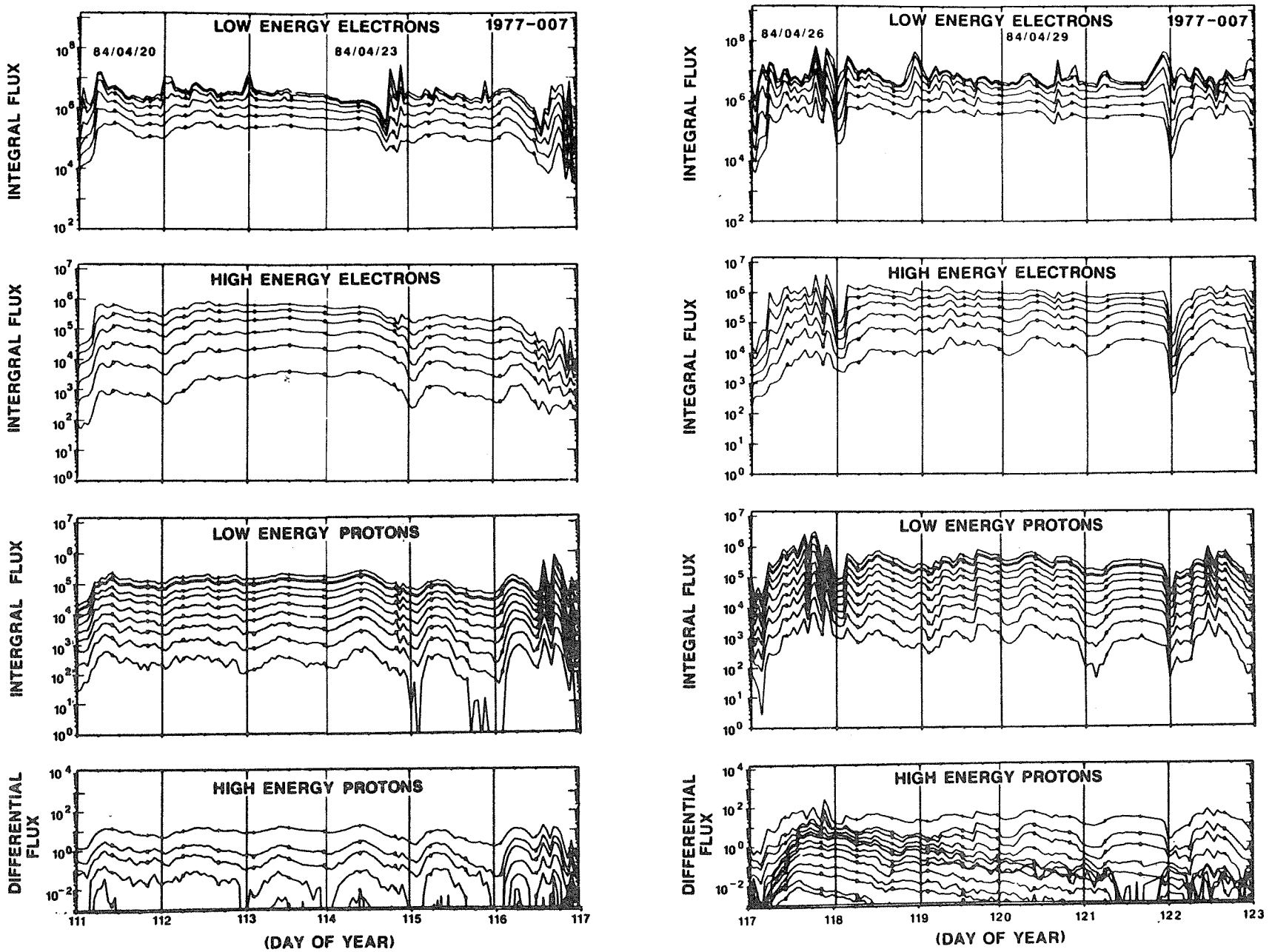


Fig. 4. Hourly averages of energetic electrons and protons for the period 20 April through 1 May 1984, as measured by instruments on board S/C 1977-007 at geostationary orbit (about E70 geographic longitude). Electron energy levels are given in Table 1 and proton energy channels are given in Table 2.

The disturbance commencing on 25 April (Day 116) was a major geomagnetic storm. The daily Kp value ( Kp) reached $51^+$ on 26 April (Coffey, 1984). The greatly increased high-energy proton fluxes resulted from solar flare activity during this interval. The flare proton intensities decayed away at 6.6 $R_E$ with a somewhat energy-dependent time constant. There appeared to be a re-intensification of activity on 1 May (Day 122) as is evident in Figure 4.

Figure 5 shows data for the 20 April - 1 May period (Day 111 - Day 122) for S/C 1982-019. Prior to this time, the satellite had been repositioned to about W40 geographic longitude. Thus, in this location the S/C reached local midnight at about 0230 UT each day.

The same general pattern of activity is evident in Figure 5 as was seen for S/C 1977-007 in Figure 4. There was relatively weak substorm activity with moderate injection events prior to 25 April 1984 (Day 116). Strong storm disturbances commenced on 25 April with intense substorm activity and major energetic proton enhancements persisting throughout the 26 April - 1 May period. Larger and more evident substorm events were identifiable each day from 27 April (Day 118) through 1 May (Day 122) and these episodes were seen most clearly in the LoE data each day at about 0230 UT (i.e., at local midnight).

Note in Figure 5 that the high-energy proton behavior at S/C 1982-019 was nearly identical in character to that seen at S/C 1977-007. This included the renewed activity on 1 May. The high-energy proton decay pattern was very similar at the two locations.

At the W135 geographic position, there were two spacecraft in operation: S/C 1981-025 and S/C 1984-037. During the second half of the interval under investigation here, data from S/C 1983-037 were used to supplant those from S/C 1981-025. Figure 6 shows the combined available data. Virtually all of the features that we have remarked upon in Figures 4 and 5 were also seen at the W135 position. In particular the high-energy protons exhibited the same decay and re-intensification pattern noted previously.

## Summary

We have presented energetic particle data from several geostationary orbit platforms for two intervals in early 1984. The first interval (6-11 February) was characterized by relatively moderate disturbance levels with no major increases in the highest energy proton channels. In contrast, the second interval (20 April - 1 May) encompassed a major geomagnetic storm interval with strong particle injection events and a major increase in protons with energies $\geq$100 MeV.

## Acknowledgments

This work was done under the auspices of the U.S. Department of Energy.

## REFERENCES

BAKER, D.N. and T.A. FRITZ 1984 "Hot plasma and energetic particles in the earth's outer magnetosphere: New understandings during the IMS, **Proceedings of the Symposium on the Achievements of the IMS**, ESA Spec. Pub. 217, p. 85.

BAKER, D.N., R.D. BELIAN, P.R. HIGBIE and E.W. HONES, JR. 1979 "High energy magnetospheric protons and their dependence on geomagnetic and interplanetary conditions," **J. Geophys. Res.**, 84, 7138.

BAKER, D.N., P.R. HIGBIE, R.D. BELIAN, W.P. AIELLO, E.W. HONES, JR., E.R. TECH, M.F. HALBIG, J.B. PAYNE, R. ROBINSON, and S. KEDGE 1981 "The Los Alamos geostationary orbit synoptic data set: A compilation of energetic particle data," **Los Alamos National Laboratory Report LA-8843** August 1981b.

BAKER, D.N. P.R. HIGBIE, R.D. BELIAN, E.W. HONES and R.W. KLEBESADEL 1982 "The Los Alamos synchronous orbit data set," **The IMS Source Book**, (C.T. Russell and D.J. Southwood Eds.), p. 82, American Geophys. Union, Washington, DC.

COFFEY, H.E. 1984 "Geomagnetic and solar data," **J. Geophys. Res.**, 89, 6853.

HIGBIE, P.R., R.D. BELIAN and D.N. BAKER 1978 "High-resolution particle measurements at 6.6 $R_E$, 1, Electron micropulsations, **J. Geophys. Res.**, 83, 4851.

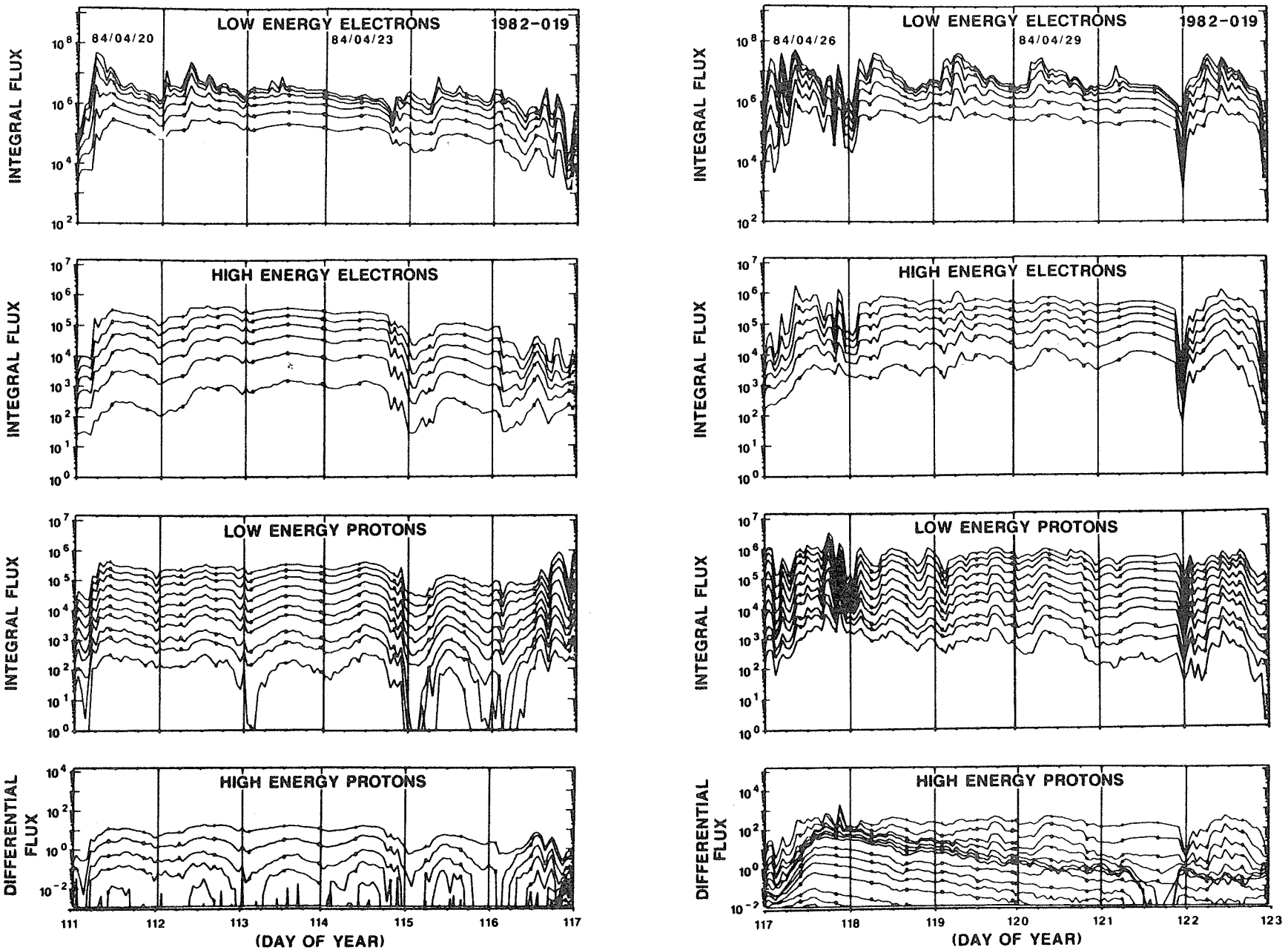


Fig. 5. Same as Figure 2 for the interval 20 April through 1 May 1984. During this period S/C 1982-019 was located at about W40 longitude.

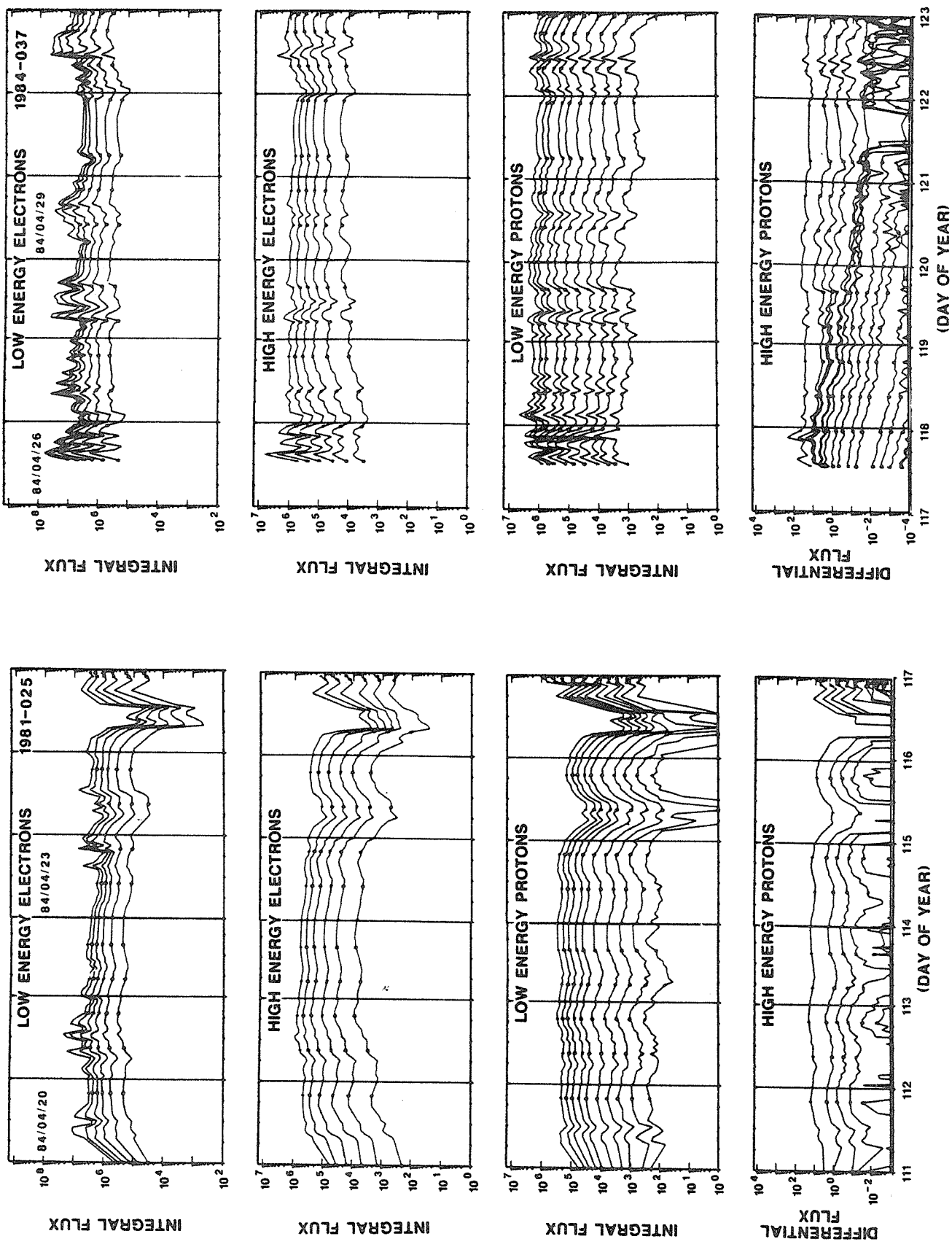


Fig. 6. Similar to Figure 3 but combining S/C 1981-025 and S/C 1984-037 for 20 April through 1 May 1984. Spacecraft are located at about W135 geographic longitude.

# Meteor Satellite Observations of Solar Cosmic Rays for February and April 1984

by

S.I. Avdyushin, N.K. Pereyaslova,
M.N. Nazarova and I.E. Petrenko
Fedorov Institute of Applied Geophysics
Goscomhydromet, Moscow, USSR

## Introduction

Solar cosmic rays and the proton component of galactic cosmic rays are measured on a regular basis by Meteor satellites since 1969 (Avdyushin et al., 1983; Pereyaslova, 1982; Pereyaslova et al., 1983; Avdyushin, 1984). Meteor satellites have a nearly circular orbit with altitude 700-1000 km and inclination angle 81-82°. The radiometric complex of equipment installed on Meteor incorporates detectors of gas discharge, scintillation and Cerenkov counters (Avdyushin, 1984; Avdyushin et al., 1970). The detectors record protons of solar and galactic cosmic rays with energies in the integral channels $E_p$ >5, 15, 25, 30, 40, 90, 600 MeV in the Earth's magnetosphere polar zones, in the region of open fieldlines of the geomagnetic field.

We study the spatial-temporal and spectral characteristics of the solar cosmic rays and their relation to heliogeophysical phenomena (Pereyaslova, 1982; Pereyaslova et al., 1983).

In February - May 1984 cosmic rays were measured from two Meteor satellites with analogous equipment.

## Observations

On 16 February intensive proton fluxes of solar cosmic rays were recorded in the Earth's magnetosphere polar zones throughout the measured range of energies $E_p$ >5-600 MeV (Kosmicheskie dannye, 1984) (Figure 1). The onset of the solar proton event was noted at >0600 UT for all energy ranges. Fluxes increased drastically to maximum, recorded between 0600 and 1400 UT on 16 February. Meteor data at 1400 UT shows that the proton flux with $E_p$ >5 MeV was $1.1 \times 10^2 cm^{-2}s^{-1}sr^{-1}$. The spectrum in the event maximum was hard. The spectrum index was $\gamma_m = 1.4$ ($J(E) \sim E^{-\gamma}$).

A new complex increase of proton fluxes begins with the first event when proton fluxes decrease: on 18 February in the energy range $E_p$ >5-90 MeV, and then in the range 5-90 MeV with several maxima on 19, 20 and 21 February.

Table 1 presents data on the proton fluxes and the spectrum at the event maxima on 16-26 February.

Table 1. Radiation Characterisics of the Events in February 1984.

| Date | Proton Energy $E_p$ MeV | Onset of Event UT | Time of Maximum UT | Proton Flux at Maximum $J_m$ ($cm^{-2}s^{-1}sr^{-1}$) | Spectrum Index at Maximum $\gamma_m$ |
|---|---|---|---|---|---|
| 16 Feb | > 5 | >0546 | <1418 | >110 | 1.4 |
| | > 15 | >0546 | <1418 | > 29 | |
| | > 25 | >0546 | <1418 | > 8.4 | |
| | > 40 | >0546 | <1418 | > 5.7 | |
| | > 90 | >0546 | <1418 | > 2.0 | |
| | >600 | >0546 | <1418 | > 0.04 | |
| 18 Feb | > 5 | 0324 | 2019 | 6.1 | 1.5 |
| | > 15 | 0324 | 1839 | 1.7 | |
| | > 25 | 0324 | 1518 | .54 | |
| | > 40 | 0324 | 1518 | .36 | |
| | > 90 | 0324 | 1518 | .085 | |
| 20 Feb | > 5 | 1256 | 1232* | 93 | 2.5 |
| | > 15 | 1256 | 2118 | 10 | |
| | > 25 | 1256 | 2118 | 1.8 | |
| | > 40 | 1256 | 2118 | 74 | |

* = 1232 UT on 21 February 1984.

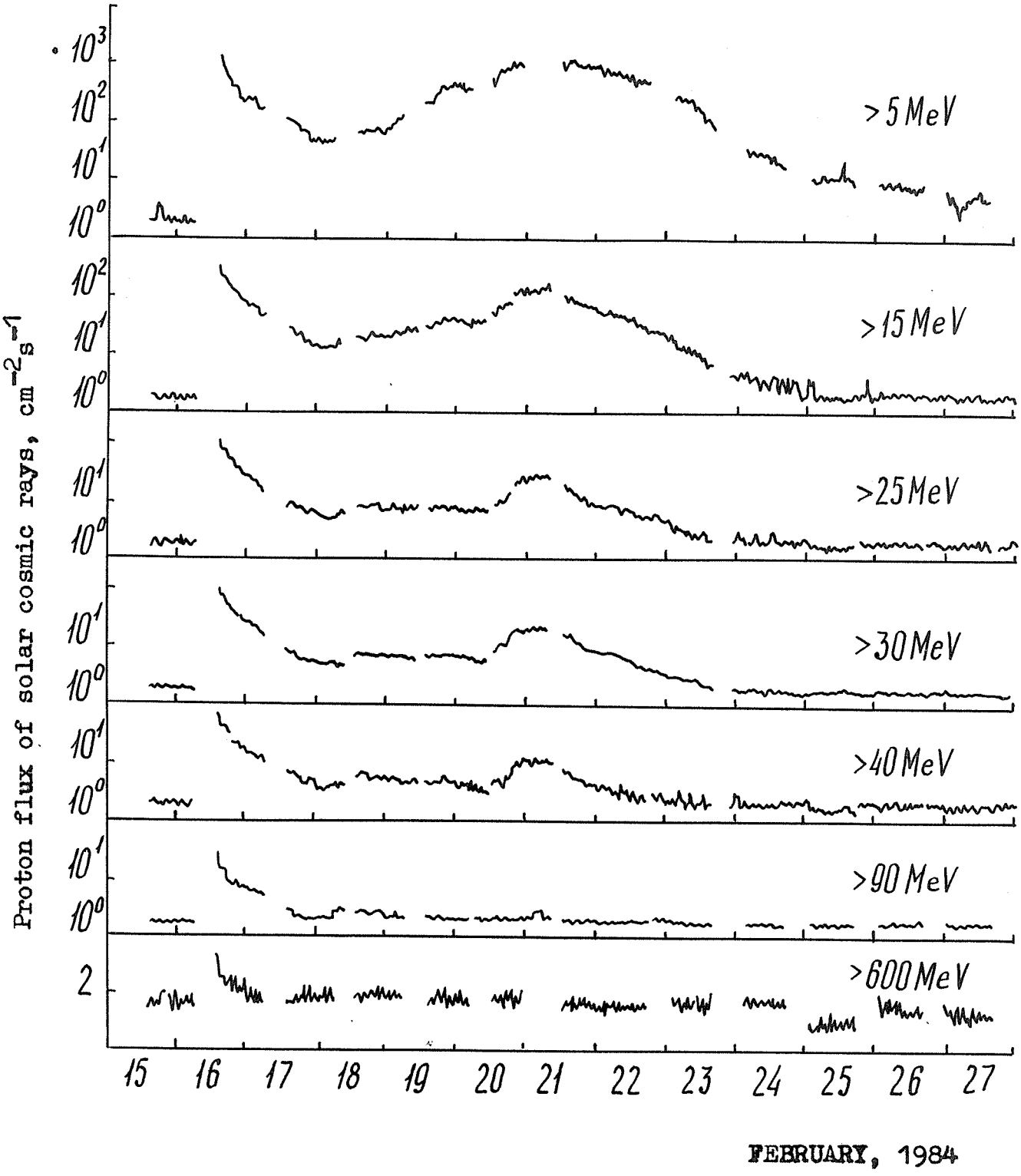


Fig. 1. Proton fluxes in the solar proton events of 16 - 26 February 1984 from the Meteor satellites.

A decrease of proton fluxes is observed in the second half of 21 February. Proton fluxes with $E_p$ >15-40 MeV decreased practically to the background level from 23 to 25 February. Proton fluxes with $E_p$ >5 MeV were decreasing slowly until 1 March.

The 16 February event was caused by the post-limb flare at S14 W130, X-ray class C6, observed at 0858 UT from high intensity radio bursts of Type II and IV. The 18-29 February complex event results fom high flare activity of NOAA/USAF Active Region 4421 with a 2B/X2 flare (N16 E82) recorded at 2224 UT on 17 February, a 1N flare - on 21 February, a 1N/M2 flare - on 22 February, a 2B/M2 flare - on 24 February, a 2N/C1 flare - on 25 February, and 1N and 1B/M2 flares - on 27 February. The latter two were accompanied by radio bursts in various frequency ranges (**Solar-Geophysical Data**, 1984).

The storms were recorded in the Earth's magnetic field: on 20-21 February with a sudden onset at 1554 UT on 20 February resulting from the 17 February 2B/X2 flare, and on 26-27 February - recurrent with a gradual onset.

The solar proton event on 16 February was recorded from the neutron monitor ground-based measurements. The increase amplitude at 0915 UT was about 7% from Moscow station data.

An intensive solar proton event was observed at Meteor from 25 April to 4 May (Figure 2). The full proton flux with $E_p$ >30 MeV reached $I = 1.2 \times 10^8 cm^{-2}$ in this event. The flux at the maximum was $J_m = 10^2 \ cm^{-2}s^{-1}sr^{-1}$. The spectrum index at the maximum (in the power presentation) was $\gamma_m = 3.5$ for the energies $E_p$ >10-90 MeV.

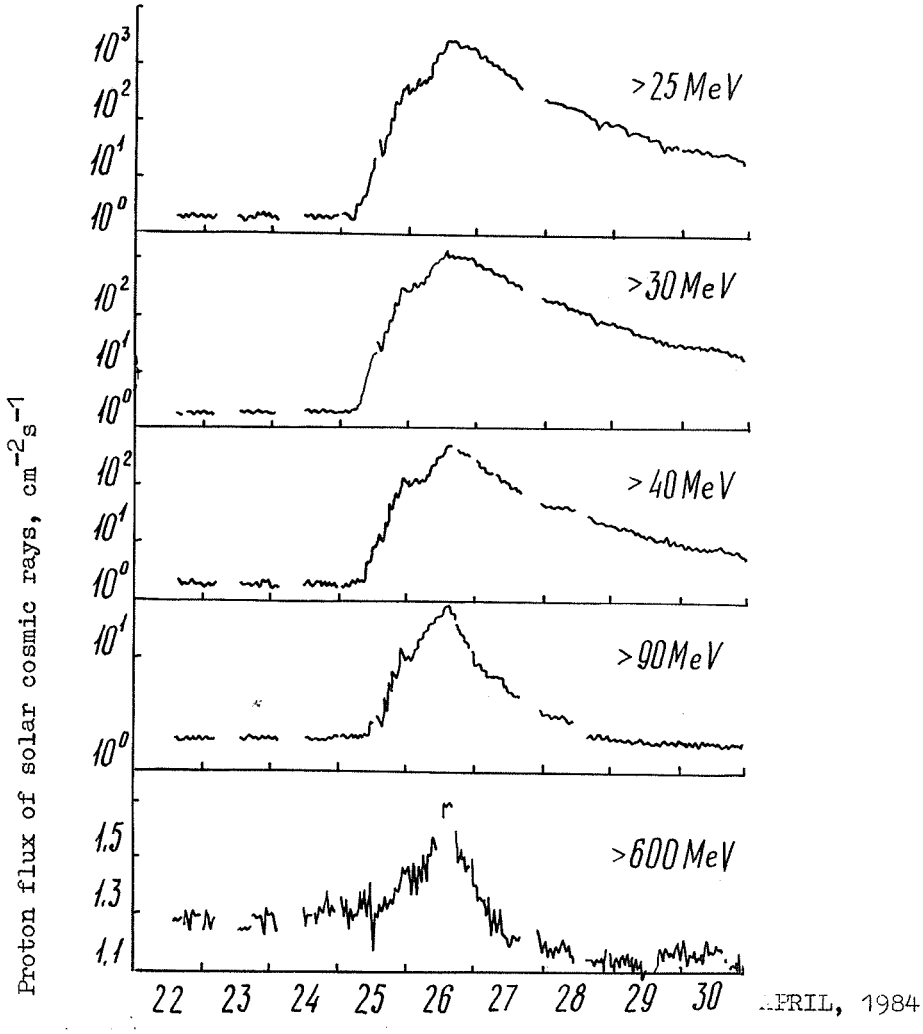


Figure 2. Proton fluxes in the solar event in April 1984 from the Meteor satellites.

The principal maximum in the temporal distribution of solar proton fluxes is related to the powerful impulsive 3B/X13 flare (S11 E43) which started at 2356 UT on 24 April in the active region on the solar Eastern Hemisphere and lasted for 156 minutes. The flare was accompanied by a Type IV radio burst and a meter range burst. At frequency 245 MHz the flux exceeded 220,000 units. A two-ribbon flare was observed. The active region NOAA/USAF 4474 appears on the disk on 21 April and produced a great number of flares while crossing the disk (**Solar-Geophysical Data**, 1984).

Only ten solar proton events comparable to the $E_p$ >30 MeV proton flux integral intensity were recorded during the last two solar activity cycles. The above event was unique in its absorption in the polar cap (17 dB).

Concerning the temporal distribution, in addition to the principal maximum, two short maxima are observed at the flux increase phase. The first at 1332 UT on 25 April was related to the 1B/M7 flare with helio-coordinates S10 E63 that occurred in the same active region as the flare at 1621 UT on 23 April. The second maximum at the flux increase stage may be due to the input of particles generated in the 2B/X1 flare at helio-coordinates S10 E57. The onset time is 0259 UT on 24 April.

Substantial variations of proton fluxes occur at the increase phase. They are evidently related to the interplanetary medium disturbance, change of the sector sign and interplanetary magnetic field irregularities. There is a possibility that the 2B/X13 flare was a source of the proton fluxes of the event under consideration. And a two-maximum structure on the temporal profile during the increase is determined by a complex configuration of the active region photospheric magnetic field.

Table 2 presents data on the maximum fluxes and spectrum hardness in the solar proton events on 25-26 April.

Table 2. Radiation Characteristics of the Solar Proton Event in April and May 1984

| Date | Proton Energy $E_p$ MeV | Onset of Event UT | Time of Maximum UT | Proton Flux at Maximum $J_m$ ($cm^{-2}s^{-1}sr^{-1}$) | Spectrum Index at Maximum $\gamma_m$ |
|---|---|---|---|---|---|
| 25 Apr | > 5 | 0520 | 1429 | 120 | 2.9 |
| | > 15 | 0520 | 1429 | 23 | |
| | > 25 | 0544 | 1332 | 3.3 | |
| | > 30 | 0544 | 1332 | 2.5 | |
| | > 40 | 0544 | 1332 | 1.0 | |
| | > 90 | 0544 | 1332 | 0.1 | |
| 25 Apr | > 25 | | 2259 | 31 | 2.6 |
| | > 30 | | 2259 | 22 | |
| | > 40 | | 2259 | 11 | |
| | > 90 | | 2259 | 0.9 | |
| | >600 | | 2259 | 0.01 | |
| 26 Apr | > 25 | | 1348 | 210 | 3.5 |
| | > 30 | | 1348 | 96 | |
| | > 40 | | 1348 | 44 | |
| | > 90 | | 1348 | 2.1 | |
| | >600 | | 1348 | 0.03 | |

The event started to develop at the background of a recurrent magnetic storm enhanced by flare activity and continued throughout the proton event.

By the neutron monitor (Apatity) readings a Forbush decrease began at 1500-1600 UT on 26 April. Its maximum depth was about 8.5 percent on 27-28 April with fluctuations near the above level for 30 hours. Then a slow recovery began. At 0935 UT (Kerguelen station) and at 1449 UT (College station) on 26 April an SC was recorded and a prominent variation appeared in the proton temporal profile: a smooth configuration of the profile changed, which is characteristic of events caused by Eastern Hemisphere flares.

Figure 3 presents proton integral spectra at the increase stage and during maximum. Data on proton fluxes from two Meteor satellites, as well as data from the NOAA service, were used. It is evident that for the time considered, the spectra measured from Meteor coincide, and the available NOAA data on proton fluxes with $E_p$ >10 MeV fall on the spectral curves from Meteor. Spectrum indices of the first two maxima have close values: $\gamma_m 1 = 2.9$ and $\gamma_m 2 = 2.6$. During the principal maximum the spectrum is softer ($\gamma_m = 3.5$) which is evidently determined by the shock wave coming to the Earth.

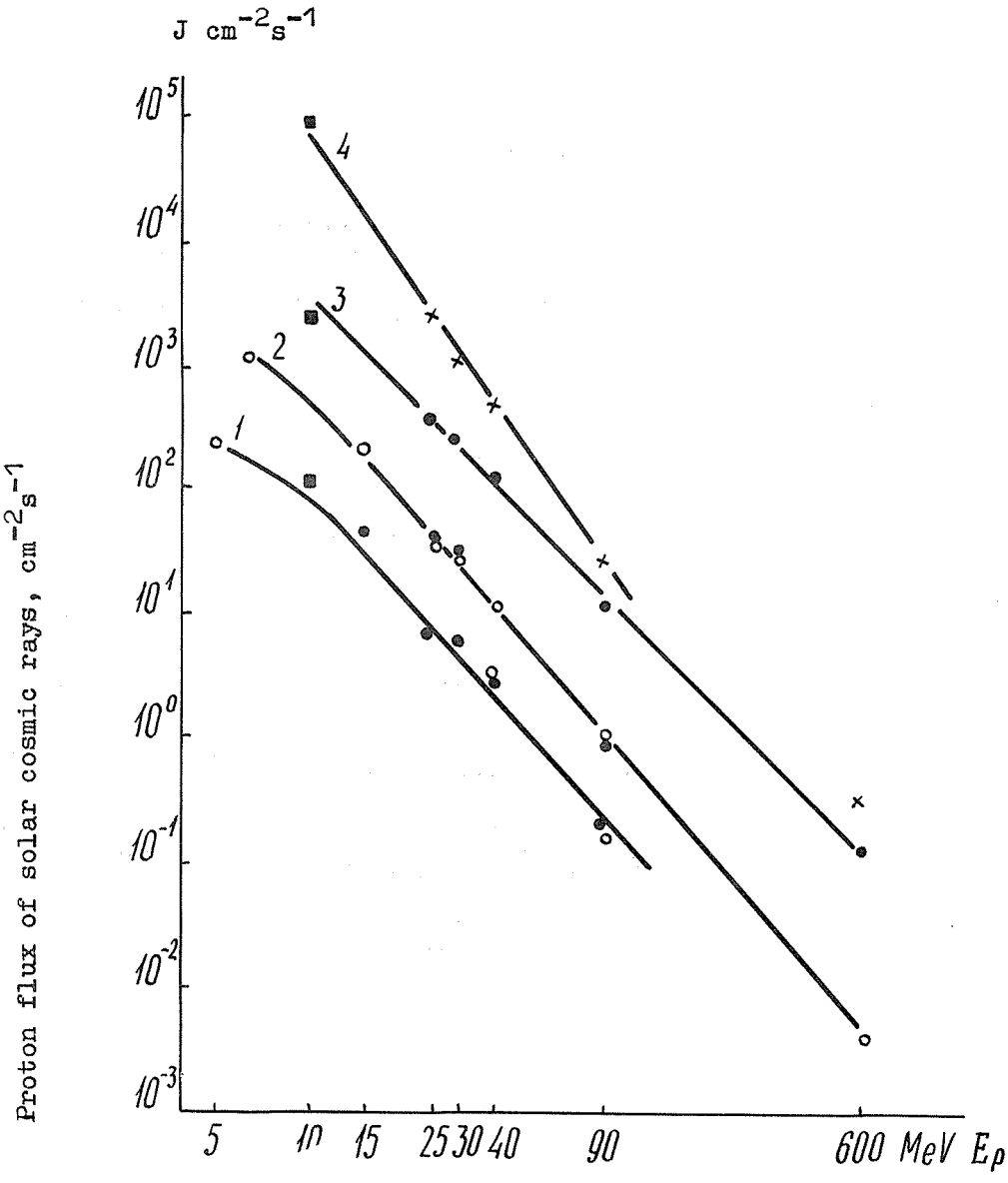


Fig. 3. Integral spectra of solar cosmic ray protons for the event on 25 April 1984.

1) 1003 UT; 2) 1332 UT; 3) 2259 UT; 4) 1348 UT on 26 April.
■ = data from NOAA; . and x = data from Meteor No. 8;
o = data from Meteor No. 10.

The spectrum dynamics of the event under observation were studied. The spectrum hardness rather gradually decreases with time. The spectrum index increases from approximately 2.0 to about 6. Prominent spectrum variations were noted at the onset of the event and during maxima.

Throughout the event the asymmetry of proton fluxes was observed. Its sign was changing. The asymmetry amplitude is calculated by the formula $A=(J_N-J_S)/(J_N+J_S)100\%$, where $J_N$ and $J_S$ are averaged values of solar cosmic ray proton fluxes in the northern and southern polar zones. The northern-southern asymmetry for proton fluxes with $E_p$ >25 MeV is observed at the onset of the event. The amplitude is A = +8%. Southern polar zone fluxes exceed those in the northern polar zone for protons with $E_p$ >40 MeV and $E_p$ >90 MeV; amplitudes are A = -15% and A = -2%, respectively. The asymmetry is southern-northern in the maximum of the events. Amplitudes are -16%, -14%, -7%, -2% for $E_p$ >25, 40, 90, 600 MeV, respectively. The amplitude value varied significantly at the increase stage and at the decrease, in the period of $\gamma$'s greatest change.

The experimental data presented suggest that, as a rule, during the solar activity decreasing phase, powerful proton flares are recorded. They are accompanied by a complex of heliogeophysical phenomena including electromagnetic bursts, intensive proton fluxes of solar cosmic rays, geomagnetic disturbances, etc.

## REFERENCES


AVDYUSHIN, S.I. R.M. KOGAN, YU.M. KULAGIN, G.A. KOROTAEV, Z.A. KORNILOVA, YU.YA. KURILENKO and I.S. YUDKEVICH — 1970 — "Detektirovanie ioniziruyushchikh izlucheniy na ISZ Meteor. Voprosy perekhoda k fizicheskim kharakteristikam potokov registriruemykh chastits", - V sb.: **Voprosy radiatsionnoy kosmofiziki**, Obninsk: Gidrometeoizdat. Trudy IPG, vyp. 1, s. 15-31.

AVDYUSHIN, S.I., and N.K. PEREYASLOVA — 1983 — "Variatsii kosmicheskikh luchei po nablyudeniyam na ISZ Meteor v period 1969-1981" gg. - **Izvestiya AN SSSR, ser. fiz., t. 47**, No. 9, s. 1805-1809.

AVDYUSHIN, S.I. YU.M. KULAGIN, M.N. NAZAROVA, N.K. PEREYASLOVA, I.E. PETRENKO and P.M. SVIDSKIY — 1984 — "Registratsiya solnechnykh kosmicheskikh luchei cherenkovskimi detektorami na sisteme ISZ Meteor", - **Izvestiya AN SSSR, ser. fiz., t. 48**, No. II, s. 2254-2258.

Kosmicheskie dannye — 1984 — **Kosmicheskie dannye**, Mesyachnyi obzor, Moskva, Nauka.

PEREYASLOVA, N.K. — 1982 — "Solnechye protony v magnitosfere Zemli", V sb.: **Energichnye chastitsy v magnitosfere Zemli**, Apatity, s. 3-25.

PEREYASLOVA, N.K. M.N. NAZAROVA and I.E. PETRENKO — 1983 — "Issledovanie kharakteristik solnechnogo kosmicheskogo izlucheniya na sputnikakh Meteor", - **Kosmicheskaya biologiya i aviakosmicheskaya meditsina, t. 17**, No. 3, s. 13-18.

SGD — 1984 — **Solar-Geophysical Data**, Nos. 475, 476, P.I; Nos. 477, 478, P.I, US Department of Commerce (Boulder, Colorado 80303 USA).

# Total Solar Irradiance Variations in February and April 1984

by

H. Lee Kyle
NASA Goddard Space Flight Center
Greenbelt, Maryland 20770 USA

John R. Hickey
The Eppley Laboratory, Inc.
Newport, Rhode Island 02840 USA

and

Eugene R. Major
Research and Data Systems Corp.
Lanham, Maryland 20706 USA

Normalized total solar irradiance (solar constant) measurements by the Nimbus-7 Earth Radiation Budget (ERB) Solar Channel 10c for the 16 February and 24 April 1984 solar events are discussed. We briefly review the operations mode of our solar sensor and then discuss the measurements near 16 February and 24 April in the context of the Nimbus-7 ERB data Year 6 (1 November 1983 - 31 October 1984) results.

The Nimbus-7 ERB Channel 10c is a Hickey-Freidan (HF) electrically self-calibrating total solar irradiance cavity radiometer. Further details concerning Channel 10c and the Nimbus-7 ERB experiment and resultant data sets are given by Hickey et al. (1980), Hickey and Alton (1983), Jacbowitz et al. (1984), and Kyle et al. (1985). The Nimbus-7 is a polar orbiting satellite with the ERB solar sensors facing forward along the velocity vector. The sampling frequency is one measurement period of about three minutes out of every 104 minute orbit. This takes place as the satellite traverses the terminator near the southern extent of its orbit. The sensor acquires signals every second. The central 48 seconds are averaged to obtain a mean orbital measurement. In addition, the sensor establishes a radiometric reference by viewing deep space both before and after the solar measurement time. During the periodic electrical calibration sequences, the cavity also views deep space to assure that the radiometric transfer correction terms can be properly applied. There is also a six step voltage calibration of the electronics which is independent of the sensor itself. Neither the electrical calibration of the sensor nor the voltage calibration of the electronics have shown deviations beyond the resolution limits of the respective measurement parameters. Because of the limitation of the overall data system, resolution is limited by the analog to digital conversion of one part in 2047 referred to full scale. The noise level of the sensor is well below the threshold so that the $\pm.5$ count (roughly 0.384 W/m$^2$) constitutes the maximum error for a single independent reading. For the data presented here, the on-Sun signal is averaged over 48 such readings. The space reference values are also averaged over an equal period. The Nimbus operating schedule generally restricts ERB to three days of measurement out of every four. At turn-on, a thermal transient situation prevails which raises the uncertainty (by tenths of a percent) above that for the remainder of the three day period. Those orbits are eliminated from the data reported here.

The Nimbus-7 available power goes through an annual cycle with maximum power in the winter and minimum power in the summer. By 1984 two of the original Nimbus-7 experiments were terminated. This allowed the ERB experiment to operate continuously during the winter months, but on 17 April it went back to the three days on/one day off cycle for the next six months.

The Nimbus-7 ERB began taking useful data on 16 November 1978 and seven years of data have been received to date. At present, six years of data are processed and in the public archive, while the seventh year is still being processed. The ERB data year is defined to start on 1 November and end on 31 October.

Figure 1a is a plot of the normalized ERB Channel 10c daily averaged total solar irradiance measurements for data Year 6. The measurements are normalized to an Earth-Sun distance of one astronomical unit. Missing data days are indicated by breaks in the line. The mean value for Year 6 was 1370.16 W/m$^2$ compared to the six year mean of 1370 W/m$^2$. There has been a slow decline in the yearly means since meaurements started in 1978. We have not yet established if any of this decline should be attributed to shifts in the instrument. Willson (1984) reports that the ACRIM I sensor on the Solar Maximum Mission satellite also indicates a slight decline in the mean solar irradiance over the period February 1980 to the present.

The two most prominent features in the graph in Figure 1a are the two deep minima of 1367.6 W/m$^2$ and 1367.1 W/m$^2$ on day 88 (27 January 1984) and day 178 (27 April) respectively. Figure 1b is a plot of the Zurich Daily sunspot numbers for comparison. Irradiance minima tend to occur during periods when large sunspot areas face the Earth, but the relationship is complex and is discussed by Schatten et al. (1985) and other authors. Note that the solar event on 16 February occurred when the daily irradiance value of 1370.6 W/m$^2$ was slightly above the annual mean. However, there is considerable structure in the graph in February. Figure 2 is a plot of ERB Channel 10c orbital averages for a 16-day period centered on ERB day 108 (16 February). It shows the structure in more detail.

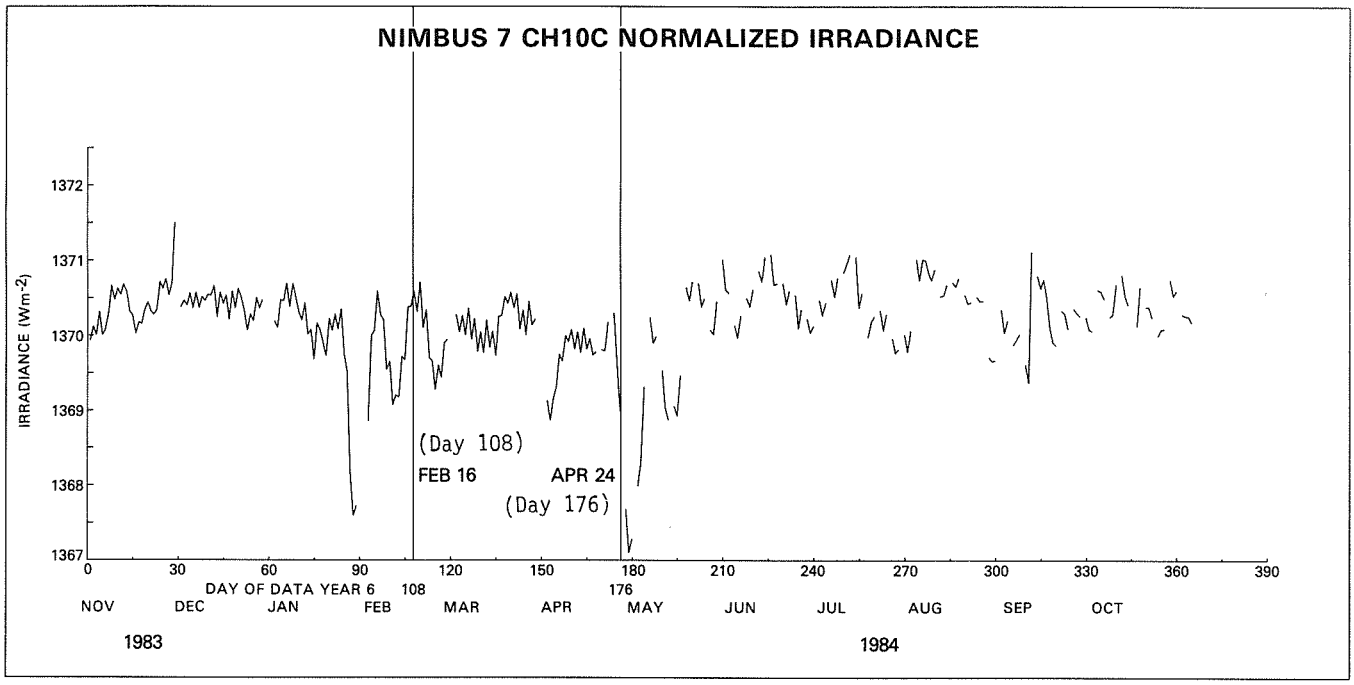


Fig. 1a. Nimbus-7 ERB Channel 10c daily averaged total solar irradiance measurements for the ERB data Year 6 (1 November 1983 - 31 October 1984). The measurements are normalized to an Earth-Sun distance of one astronomical unit.

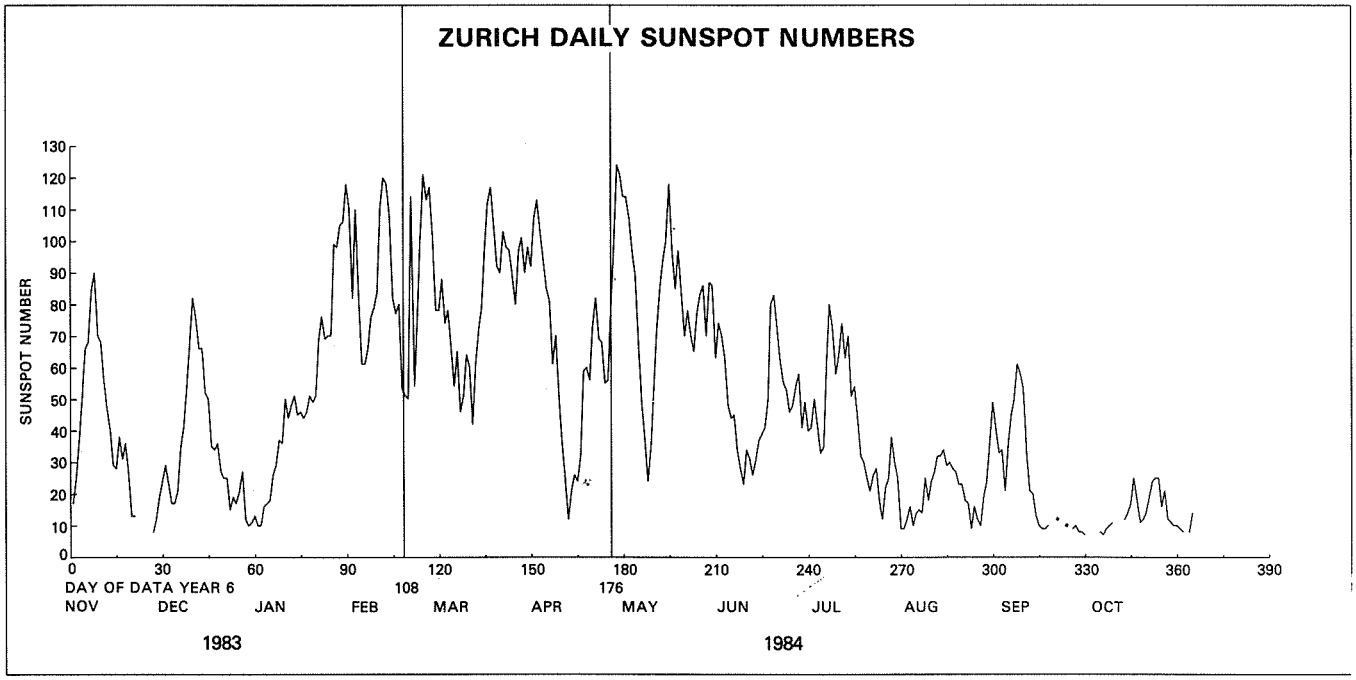


Fig. 1b. Zurich daily sunspot numbers are plotted for the ERB Year 6. Note the solar irradiance minima on days 88 and 178 match peaks in the sunspot number. It is obvious, however, that the sunspot number is not a perfect predictor of variations in the solar irradiance.

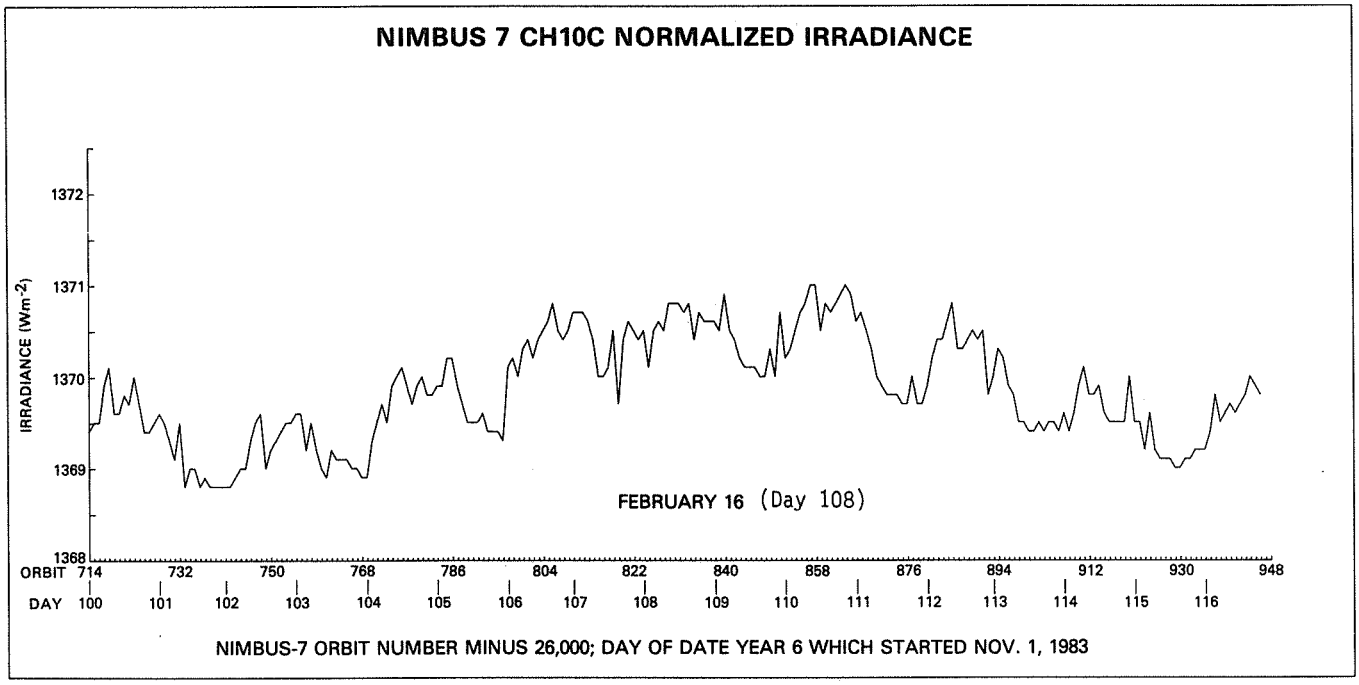


Fig. 2. Plot of average orbital total solar irradiance measurements for a 16-day period centered on 16 February 1984. There are nearly 14 orbits per day.

In contrast, the 24 April (ERB day 176) solar event occurred as the total irradiance was approaching a deep minimum. Figure 3 is a plot of orbital averages for a 16-day period centered on day 176. Unfortunately, the ERB instrument was back on its three-days-on/one-off cycle at this time. Because of the temperature transients problem after turn on, mentioned earlier, only about ten orbits from the first on-days are included in the graph.

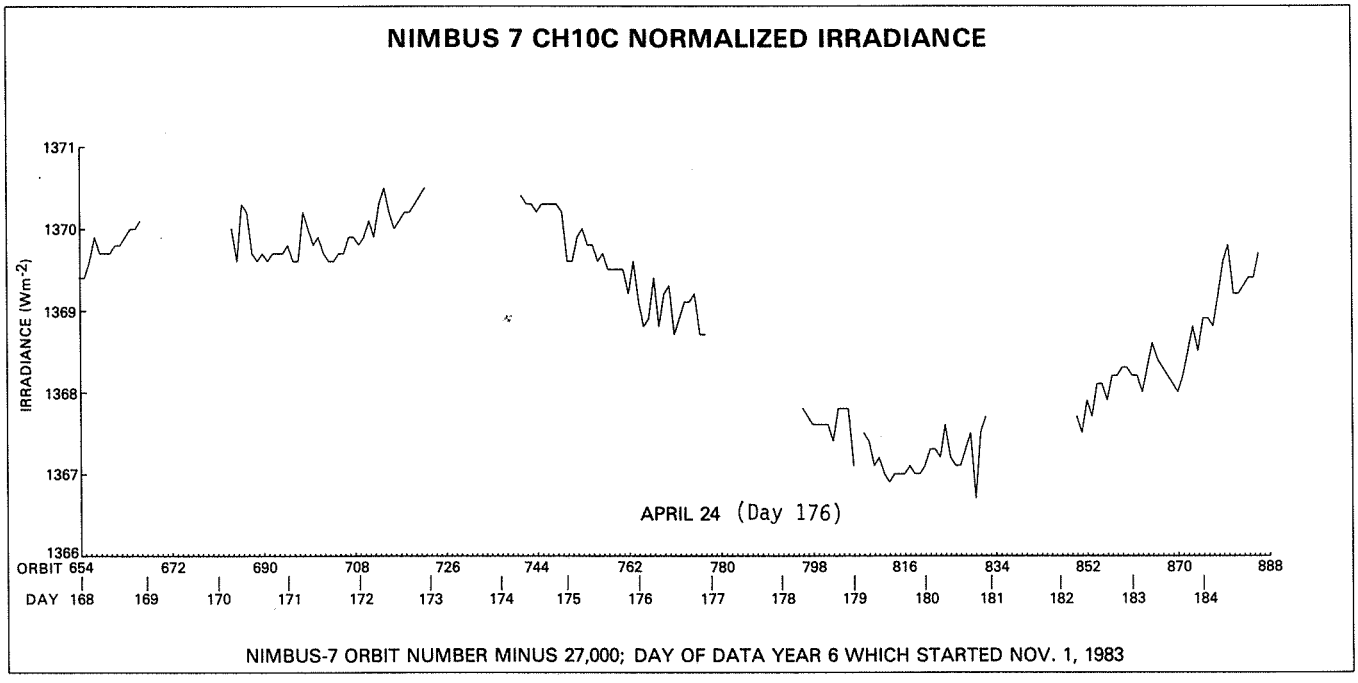


Fig. 3. Plot of average orbital solar irradiance measurements for a 16-day period centered on 24 April 1984. The gaps in the line indicate missing data.

For those wishing to study the Nimbus-7 ERB solar data in more detail, a single 6-year ERB Solar Analysis Tape is available. It contains both orbital and daily averages and can be obtained from:

National Space Sciences Data Center
Request Coordinator, Code 633
NASA Goddard Space Flight Center
Greenbelt, Maryland 20771 USA
Phone: (301) 344-6695

## REFERENCES


HICKEY, J.R., L.L. STOWE, H.JACBOWITZ, P. PELLIGRINO, R.H. MASCHHOFF, F. HOUSE and T.H. VONDER HAAR — 1980 — "Initial Solar Irradiance Determination from Nimbus-7 Cavity Radiometer Measurements", **Science, 208,** p. 281-283.

HICKEY, J.R. and B.M. ALTON — 1983 — "Extraterrestrial Solar Irradiance-Results from the ERB Experiment of Nimbus-7", **5th Conference on Atmospheric Radiation, AMS,** Baltimore, MD, October 31 - November 4, 1983, p. 444-447.

JACBOWITZ, H., H.V. SOULE, H.L. KYLE, F.B. HOUSE and the Nimbus-7 ERB Experiment Team — 1984 — "The Earth Radiation Budget (ERB) Experiment; An Overview", J. **Geophys. Res., 89,,** p. 5021-5038.

KYLE, H.L., P.E. ARDANUY, and E.J. HURLEY — 1985 — "The Status of the Nimbus-7 Earth Radiation Budget Data Set", **Bull. Amer. Meteor. Soc.,** In Press (November 1985).

SCHATTEN, K.H., A.S. ENDAL, G. CHAPMAN and J. HICKEY — 1985 — "The Importance of Improved Facular Observations in Understanding Solar Constant Variations", **Astrophys. J., 294,** p. 689-696.

WILLSON, R.C. — 1984 — "Measurements of Solar Total Irradiance and its Variability", **Space Science Reviews, 38,** p. 203-242.

# The Solar Protons in the Earth's Magnetosphere As Observed on Board Cosmos-1490 and 1520 From 24 April to 1 May 1984

by

L.A. Darchieva, T.A. Ivanova, T.N. Lukina, T.I. Morozova,
N.N. Pavlov, I.A. Rubinshtein, E.N. Sosnovetz and L.V. Tverskaya
Institute of Nuclear Physics, Moscow State University
Moscow 119899, USSR

This communication presents the experimental data obtained by observing the solar cosmic ray protons in the polar caps of the Earth's magnetosphere in April-May 1984 on board Cosmos-1490 and 1520 using the instruments designed at the Institute of Nuclear Physics of the Moscow State University.

The two satellites were circular orbiting at about 19,000 km altitude, at approximately 65° to the plane of the geographic equator. The orbiting period of the satellites was about 11 hours 15 minutes. The satellites were oriented along the radius vector from the Earth's center.

The 1.2-2.3 MeV (Cosmos-1490) and 2.3-3.7 MeV (Cosmos-1520) proton fluxes were measured with silicon junction detectors of about $10^{-1}$ $cm^2sr$ geometric factor. The thickness of the detectors was about 30 mcm of silicon on Cosmos-1490 and about 115 mcm of silicon on Cosmos-1520. The inlet windows of the detectors were screened against the direct solar light by about 7 mcm thick Aluminum foil. The >30 MeV proton fluxes were measured by both satellites with SI-3BG gas discharge counters of about 0.05 $cm^2$ effective area under lead shielding. The particle detection angle was about 2 pi steradians. In addition, the 2.7-100 MeV (Cosmos-1490) and 4-60 MeV (Cosmos-1520) alpha particles may have contributed to the silicon junction detector counting rates. The gas discharge counters could also detect the >2 MeV electrons.

The satellites traversed the southern or northern polar caps, where the solar cosmic ray fluxes were detected, in each about 6 hours and were within either cap for about 3 hours. The data averaging time was about 30 minutes for most of the passes and 1 minute for the remaining passes.

Figure 1a presents the temporal behavior of the approximately 1 MeV solar cosmic ray proton fluxes in the polar caps as a function of Universal Time. The light lines in Figure 1a and 1b show the Cosmos-1490 data, and the dark lines are the Cosmos-1520 data. The approximately 1 MeV proton background was detected before 0900 UT on 25 April. The maximum 1.2-2.3 MeV solar proton flux of about 6 x $10^3$ $cm^{-2}s^{-1}$ was observed from 2300 UT on 26 April to 0200 UT on 27 April. About the same maximum flux of the 2.3-3.7 MeV solar protons were detected from 2000 to 2300 UT on 26 April.

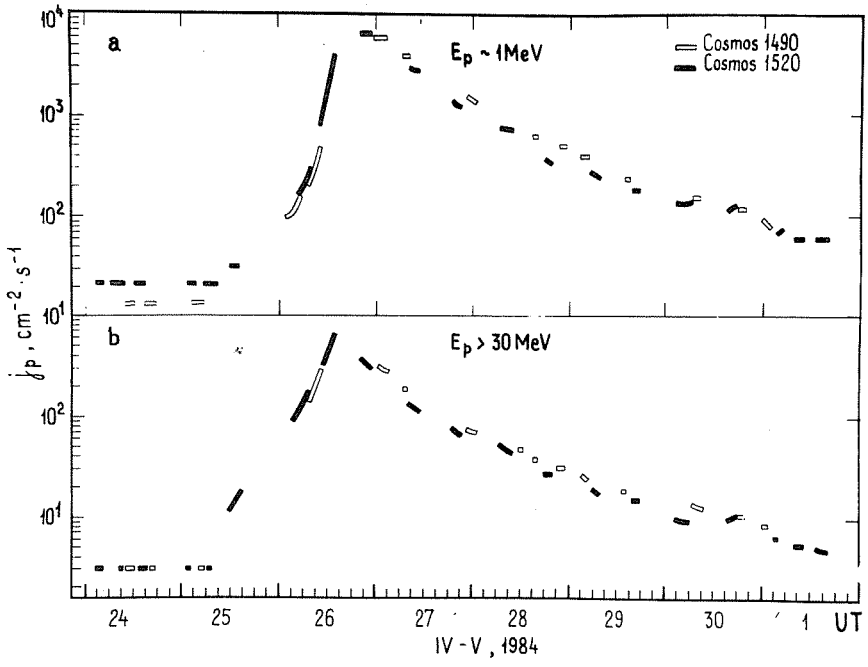


Fig. 1. The approximately 1 MeV (a) and >30 MeV (b) solar cosmic ray proton fluxes in the polar caps from Cosmos-1490 (light lines) and Cosmos-1520 (dark lines) for the period 24 April - 1 May 1984.

Figure 1b presents the temporal behavior of the >30 MeV solar cosmic ray proton fluxes detected in the polar caps by the gas discharge counters on both satellites. The >30 MeV proton flux increase began at 0700-1100 UT on 25 April. The maximum intensity of the >30 MeV protons was detected at 1300 UT on 26 April and was about 7.5 x $10^2 cm^{-2} s^{-1}$. By about 1500 UT on 1 May the approximately 1 MeV and >30 MeV solar proton fluxes in the polar caps had decreased by two orders of magnitude, but failed to reach the background level.

The analysis of the approximately 1 MeV solar proton flux profiles in the polar caps has made it possible to trace the dynamics of the boundaries of the proton penetrations to the Earth's magnetosphere at various local times. A penetration boundary is the invariant latitude from which a decrease is observed in the proton fluxes from their mean level in the polar caps and auroral zones.

Figure 2 shows the temporal behavior of the boundaries of the approximately 1 MeV solar cosmic ray proton penetrations to the Earth's magnetosphere inferred from the data of the two satellites. Plotted as the ordinate is the invariant latitude in degrees, and as the abscissa the Universal Time. The errors at the dots characterize the accuracy in finding the position of the penetration boundary which is determined by the high averaging time (about 30 minutes). The light and dark dots are, respectively, the Cosmos-1490 and 1520 data. Cosmos-1490 traversed the boundary at the dawn and night hours of MLT and Cosmos-1520 at early dusk and dawn hours of MLT. The minimum value (approximately 61°) of the invariant boundary latitude was recorded at approximately 0000 UT on 26 April. The boundary was found to shift to about the same latitude at the dawn, dusk and night hours.

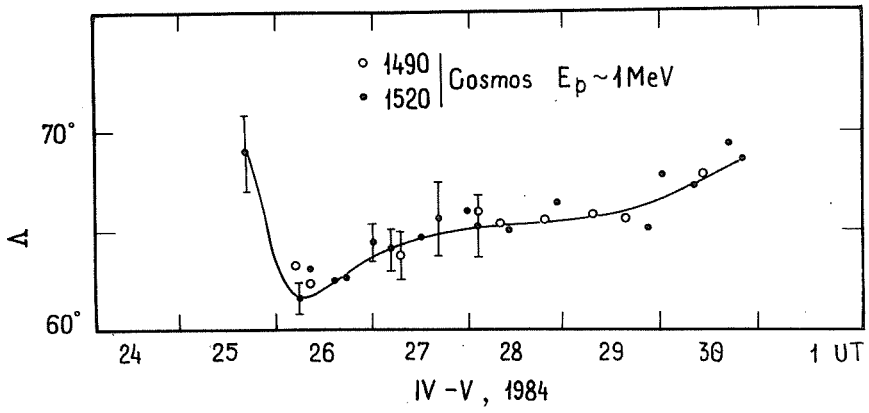


Fig. 2. Plot of the time behavior of the penetration boundary of the approximately 1 MeV solar cosmic ray protons. The light dots are Cosmos-1490 data. The dark dots are Cosmos-1520 data. The error bars are due to the 30 minute averaging of the data.

# Measurement of the Fluxes of Nuclei CNO with Energies 10-20 MeV/Amu in April 1984 (STIP Interval 20.04-04.05 1984) on Board the Satellite "Cosmos-1549"

by

V.V. Bobrovskaya, N.L. Grigorov, D.A. Zhuravlev, M.A. Kondratyeva, R.A. Nymmik, Ch.A. Tretyakova, N.V. Alekseyev, P.V. Vakulov and V.P. Sechinov
Institute of Nuclear Physics
Moscow State University
Moscow, USSR

## Introduction

Data on the spectrum of the middle nucleus group (CNO) obtained during the exposure of a stack of dielectric track detectors (DTD) in April 1984 on board the satellite "Cosmos-1549" are reported. These DTDs were made in the Scientific Institute of Nuclear Physics of Moscow State University and named by M.V. Iomonosov.

## Parameters of the Orbit of the Satellite

During the period 19 April to 3 May 1984 the detectors were exposed on board the satellite Cosmos-1549 at an altitude of approximately 400 km with an inclination of 72.9°, and a period of about 90 minutes.

## Detectors

During this period the nuclei were recorded in a "DTD" stack consisting of 8 sheets; 4 sheets of cellulose nitrate (each 100 mkm thick) and 4 sheets of triacetate (each 135 mkm thick). The stack area was 5 x 5 $cm^2$. The stack was wrapped with two aluminized mylar layers (each 5 mkm thick). The charges of nuclei observed were determined from the etched cone length on a nucleus track versus residual range. The energies of the nuclei were determined from the total lengths.

## Representation of the Data

The data obtained in the cellulose nitrate sheets are represented by a differential energy spectrum of both carbon and oxygen nuclei. The intensity J of nuclei is given in $(cm^2 \text{ ster} \times \text{MeV/Amu})^{-1}$. The energy E is in MeV-Amu.

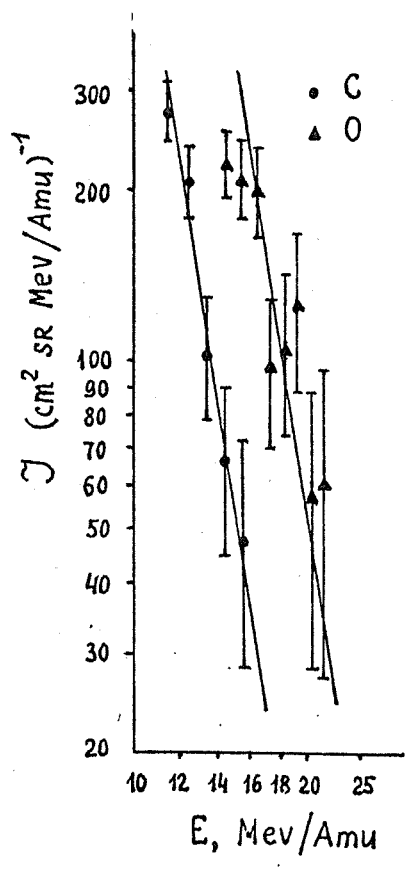


Fig. 1. Differential energy spectrum of Carbon and Oxygen nuclei.

# Summary of the Cosmic Ray Intensity during the Solar-Terrestrial Events of 16 February and 24-28 April 1984

by

M.A. Shea
Air Force Geophysics Laboratory
Hanscom AFB, Bedford, Massachusetts 01731, USA

## ABSTRACT

A brief summary is presented of the ground-level solar cosmic ray event on 16 February 1984 and of the Forbush decrease in cosmic ray intensity associated with the flare of 24 April and subsequent geomagnetic disturbance on 26-28 April 1984.

## Introduction

Two significant solar-terrestrial events occurred during February and April 1984. The event on 16 February was a moderate relativistic solar particle event detected by many ground-based neutron monitors around the world. The events on 24-28 April were initiated by a flare on 24 April followed two days later by a geomagnetic disturbance which generated a Forbush decrease of approximately 5 percent. This paper presents an overview of the cosmic ray intensity data as included in this UAG report.

## Event on 16 February 1984

One of the largest ground-level solar cosmic ray events of the 21st solar cycle occurred on 16 February 1984. This event was particularly significant inasmuch as the associated flare was apparently behind the West limb of the Sun. In this respect this was the largest increase recorded by neutron monitors from a solar flare on the invisible hemisphere.*

The event was characterized by a rapid increase in cosmic ray intensity with the onset in the interval 0905-0910 UT as recorded at several stations, and with maximum intensity recorded between 0910 and 0920 UT. The event was anisotropic as evidenced by the variations in the magnitude of the relative increase detected at equivalent stations. For example, the largest increase recorded by a sea-level neutron monitor with a vertical cutoff rigidity of approximately 1.2 GV was at Sanae, Antarctica, with a measured increase of 67% between 0910 and 0920 UT. Increases from some equivalent stations were 11% at Kerguelen Island and 4% at Tixie Bay, USSR. Anisotropies were also present in the deep polar cap with an increase of 20% at Thule, Greenland, 12% at McMurdo, Antarctica, and 6.5% at Terre Adelie, Antarctica. An increase of 210% was recorded at 0912-0914 UT at the South Pole; however, this station is located at approximately 3000 meters elevation and responds to solar particles with much lower energies than stations located at sea level. Another unusual feature of this event was the duration. In general the increase was over within two hours.

Data from 26 neutron monitors are presented in the cosmic radiation section of this report. It is interesting to note that stations are recording the cosmic ray intensity in much smaller time intervals than previously. For example the detector at Jungfraujoch reported one minute time intervals during the increase, while 30-second data were reported from Turku, Finland and South Pole, Antarctica. In addition to the data contained in this report, hourly cosmic ray intensity data for 16 February for Kiel, Federal Republic of Germany, Thule, Greenland, Alert and Deep River, Canada are plotted in **Solar-Geophysical Data** (1984a).

## Events Between 24 and 28 April 1984

A major flare occurred at approximately 2356 UT on 24 April (**Solar-Geophysical Data**, 1985). In addition to being a major X-ray flare (Class X13) this event, as recorded by the SMM gamma ray experiment, had the characteristic signature of the detection of solar neutrons at the Earth's orbit (Chupp, private communication). A proton event with particles greater than 10 MeV was recorded on a synchronous altitude satellite with an onset at 1330 UT on 25 April. The maximum intensity of 2500 particles/cm$^2$-s-ster greater than 10 MeV was recorded at 1430 UT on 26 April. Stratospheric balloon measurements at Mirny, Antarctica and Murmansk, USSR, on 26 and 27 April indicated that this event had a very soft spectrum. No relativistic solar protons associated with this flare were reported by ground-based neutron monitor measurements.

*Previous ground-level cosmic ray events from flares on the invisible hemisphere (as seen from the Earth) occurred on 20 November 1960 (8%), 28 January 1967 (two events, 2% and 21%), 30 March 1969 (9%), 1 September 1971 (16%), and 24 September 1977 (6%) (Cliver et al., 1982).

The geomagnetic field, relatively quiet prior to the flare, becomes disturbed early on 25 April with a major disturbance commencing late on 25 April and lasting until early on 27 April. The cosmic radiation intensity decreased approximately one percent at high latitude neutron monitor stations during the afternoon of 25 April. A slow recovery was in progress from approximately 0000 UT until 1700 UT on 26 April at which time a rapid Forbush decrease of approximately 5% was recorded for the next few hours at these same high latitude stations. This rapid decrease lasted until the end of the day after which the cosmic ray intensity experienced a more gradual decrease for the next 24 hours. Examples of this decrease are shown by the hourly cosmic radiation intensity data plotted for six neutron monitors in **Solar-Geophysical Data** (1984b). The approximate total decrease for these stations are as follows: Thule, Greenland, 8%; Alert, Canada, 8%; Deep River, Canada, 10%; Kiel, Federal Republic of Germany, 8%; and Toyko, Japan (an equatorial station) 5%. Data on the Forbush decrease as measured by neutron monitors and ionization chambers are presented in this UAG Report. In general the Forbush decreases as recorded by the neutron monitors are similar with slightly smaller decreases for the mid-latitude sea-level detectors.

## REFERENCES


CLIVER, E.W., S.W. KAHLER M.A. SHEA and D.F. SMART — 1982 — "Injection onsets of approximately 2 GeV protons, approximately 1 MeV electrons and approximately 100 keV electrons in solar cosmic ray flares", **Astrophys. J., 260**, 362.

SGD — 1984a — **Solar-Geophysical Data**, I, No. 476, U.S. Department of Commerce (Boulder, Colorado, 80303) 102-104.

SGD — 1984b — **Solar-Geophysical Data**, I, No. 479, U.S. Department of Commerce (Boulder, Colorado, 80303) 88-89.

SGD — 1985 — **Solar-Geophysical Data**, II, No. 494, U.S. Department of Commerce (Boulder, Colorado, 80303) 110.

# ASYMPTOTIC DIRECTIONS FOR SELECTED COSMIC RAY STATIONS CALCULATED USING THE INTERNATIONAL GEOMAGNETIC REFERENCE FIELD FOR 1980

M. A. Shea and D. F. Smart
Air Force Geophysics Laboratory
Hanscom AFB, Bedford, Massachusetts 01731, U.S.A.

L. C. Gentile
Physics Research Division, Emmanuel College
400 The Fenway
Boston, Massachusetts 02115, U.S.A.

ABSTRACT

Asymptotic directions for high energy solar particles are given for selected cosmic ray stations. These values have been calculated employing the International Geomagnetic Reference Field model for Epoch 1980.0.

The emission of relativistic cosmic rays from the sun is a relatively rare event providing a unique opportunity to study the propagation of these particles through the interplanetary medium. The solar particle event of 16 February 1984 was one of the significant relativistic proton events of the 21st solar cycle as detected by neutron monitors at various locations on the earth. Relativistic solar proton events are of immense interest to cosmic ray physicists, and this "ground-level event" was of special interest since the associated flare was apparently behind the western limb of the solar disk as viewed from the earth.

In order to utilize the cosmic ray intensity data from the world-wide network of neutron monitors for detailed analyses of solar particle propagation it is necessary to know the direction of particle motion in the interplanetary magnetic field near the earth. Consequently the concept of asymptotic directions of approach has been developed over the years by many researchers such as Malmfors (1945), Brunberg (1953, 1956), and McCracken (1962). The asymptotic direction of approach defines the direction of a velocity vector in geocentric coordinates such that the direction of this vector is parallel to a radial from the earth's center.

Since the general equation of particle motion in the geomagnetic field does not have a solution in closed form, even in the simple dipole approximation, it is necessary to perform detailed and extensive numerical calculations of cosmic ray trajectories in a mathematical model of the earth's magnetic field to determine the direction, in interplanetary space, from which the particles come to be ultimately detected at a specific point on the earth. The trajectory-tracing procedure, described by McCracken et al. (1968) is generally regarded as the most accurate method of obtaining asymptotic directions for cosmic ray nuclei. For the calculations in this report we have used the Gill (1951) modification of the Runge-Kutta integration method as adopted by McCracken et al. (1965) to trace cosmic ray trajectories through a model of the geomagnetic field. These trajectories were calculated in the following manner. For each station the differential equation describing the motion

$$\ddot{\bar{r}} = (q/m)\dot{\bar{r}} \times \bar{B}$$

of a charged particle of mass M and charge q in a mathematical model of the geomagnetic field was solved at selected rigidities by using the numerical integration technique.

The trajectory-tracing calculations were initiated in the vertical direction 20 km above the surface of an oblate earth where the minimum (polar) radius of the earth is 6356.7747 km, and the eccentricity is $6.73966 \times 10^{-3}$. Calculations were continued to a distance of 25 earth radii where the asymptotic directions of approach were computed. These calculations were made using the International Geomagnetic Reference Field for Epoch 1980.0 (Peddie, 1982). This model, a series of solid spherical harmonics of degree and order 10, was used to describe the quiescent internal geomagnetic field. The effects of the external currents on the magnetosphere were not included in these calculations. For cosmic ray trajectories with rigidities far above the cutoff rigidity, the computed asymptotic directions of approach at the position of the magnetopause obtained using a magnetospheric field model and those calculated using only an internal field are similar. At rigidities within 2 GV of the cutoff rigidity for high polar latitude stations, significant differences occur between the asymptotic directions computed using only internal fields and those computed using magnetospheric models (Gall, et al., 1969).

The following tables contain the asymptotic directions of approach for selected neutron monitors, many of which detected an increase during the relativistic solar particle event of 16 February 1984. Asymptotic longitudes between 180 and 360 degrees for rigidity values at the top of each table indicate that the particle does not cross the Greenwich meridian as it travels from interplanetary space to the detection location. Asymptotic longitude values greater than 360 degrees are indicative of a large longitudinal drift of the particle as it traverses the magnetic cavity. The notation "R" means a reentrant orbit, and hence access from the interplanetary

medium is forbidden. The station name, geographic coordinates and effective vertical cutoff rigidity, in GV, (also calculated using the 1980.0 geomagnetic field model; see Shea et al., 1983) are given at the top of each table. The rigidity values begin at 20.00 GV progressing downward to a rigidity value near the first discontinuity in asymptotic longitude (Flückiger et al., 1983) or to the atmospheric cutoff ($\sim$ 0.9 GV). Increments of 0.01 GV were used throughout the penumbra down to the lower cutoff rigidity. (See Cooke et al., 1985, for definitions of the cosmic ray terms.)

The tables are limited to the vertical direction; in our research utilizing asymptotic directions of approach for solar cosmic ray event studies, we have found that the asymptotic directions of vertically incident particles are a reasonable approximation to the entire asymptotic cone of acceptance (Shea et al., 1979). The tables are organized in the following manner. The values for the polar stations (i.e., those stations where the geomagnetic cutoff rigidity is significantly less than the atmospheric cutoff rigidity) are presented in alphabetical order by station name. These tables are then followed by tables for stations having higher geomagnetic cutoff rigidities which are presented in order of increasing cutoff rigidity.

ACKNOWLEDGMENTS

L. C. Gentile acknowledges support from the U. S. Air Force Geophysics Laboratory under Contract No. F19628-82-K-0039.

REFERENCES

BRUNBERG, ERNST-ÅKE 1953 Experimental determination of electron orbits in the field of a magnetic dipole, Part I, Tellus, V, 135.

BRUNBERG, E.-Å. 1956 Cosmic rays in the terrestrial magnetic dipole field, Tellus, VIII, 2.

COOKE, D. J., J. E. HUMBLE, M. A. SHEA, D. F. SMART, N. LUND, I. L. RASMUSSEN, B. BYRNAK, P. GORET, and N. PETROU 1985 Re-evaluation of cosmic ray cutoff terminology, 19th International Cosmic Ray Conference, Conference Papers, 5, 328.

FLÜCKIGER, E. O., D. F. SMART, and M. A. SHEA 1983 The effect of local perturbations of the geomagnetic field on cosmic ray cutoff rigidities at Jungfraujoch and Kiel, J. Geophys. Res., 88, 6961.

GALL, RUTH, J. JIMÉNEZ, and A. OROZCO 1969 Directions of approach of cosmic rays for high latitude stations, J. Geophys. Res., 74, 3529.

GILL, S. 1951 A process for the step-by-step integration of differential equations in an automatic digital computing machine, Proc. Cambridge Phil. Soc., 47, 96.

MALMFORS, KARL GUSTAV 1945 Determination of orbits in the field of a magnetic dipole with applications to the theory of the diurnal variation of cosmic radiation. Arkiv Math., Astron., Fys., 32A, No. 8, 1.

McCRACKEN, K. G. 1962 The cosmic-ray flare effect. 1. Some new methods of analysis, J. Geophys. Res., 67, 423.

McCRACKEN, K. G., U. R. RAO, B. C. FOWLER, M. A. SHEA, and D. F. SMART 1965 Cosmic Ray Tables (Asymptotic Directions, Variational Coefficients and Cutoff Rigidities), IQSY Instruction Manual, No. 10.

McCRACKEN, K. G., U. R. RAO, B. C. FOWLER, M. A. SHEA, and D. F. SMART 1968 Cosmic rays (asymptotic directions, etc.) Annals of the IQSY, Vol. 1, Geophysical Measurements: Techniques, Observational Schedules and Treatment of Data, Edited by C. M. Minnis, Chapter 14, The MIT Press, Cambridge Massachusetts, 198.

PEDDIE, NORMAN W. 1982 International Geomagnetic Reference Field: the third generation, J. Geomag. Geoelectr., 34, 309.

SHEA, M. A., D. F. SMART, P. J. TANSKANEN, and J. E. HUMBLE 1979 Neutron monitor response to non-vertical arrival directions during GLE's, 16th International Cosmic Ray Conference, Conference Papers, 12, 249.

SHEA, M. A., D. F. SMART, and L. C. GENTILE 1983 Vertical cutoff rigidities for selected cosmic ray stations for Epoch 1980.0, 18th International Cosmic Ray Conference, Conference Papers, 3, 411, 1983.

ALERT, CANADA

| | |
|---|---|
| GEOGRAPHIC LATITUDE | 82.50 |
| GEOGRAPHIC LONGITUDE | 297.67 |
| EFFECTIVE VERTICAL CUTOFF RIGIDITY | 0.00 |

| RIGIDITY (GV) | ASYMPTOTIC LAT | ASYMPTOTIC LONG |
|---|---|---|
| 20.00 | 83.47 | 336.47 |
| 15.00 | 82.39 | 337.30 |
| 10.00 | 82.15 | 330.70 |
| 9.00 | 82.55 | 330.26 |
| 8.00 | 83.05 | 332.59 |
| 7.00 | 83.26 | 339.06 |
| 6.00 | 82.66 | 344.86 |
| 5.00 | 82.09 | 342.50 |
| 4.00 | 82.81 | 346.51 |
| 3.00 | 82.24 | 348.58 |
| 2.00 | 81.77 | 358.79 |
| 1.50 | 81.52 | .53 |
| 1.40 | 81.35 | 3.95 |
| 1.30 | 81.22 | 2.79 |
| 1.20 | 81.02 | 5.98 |
| 1.10 | 81.09 | 6.49 |
| 1.00 | 80.84 | 7.03 |
| .90 | 80.62 | 8.61 |

APATITY, USSR

| | |
|---|---|
| GEOGRAPHIC LATITUDE | 67.55 |
| GEOGRAPHIC LONGITUDE | 33.33 |
| EFFECTIVE VERTICAL CUTOFF RIGIDITY | .61 |

| RIGIDITY (GV) | ASYMPTOTIC LAT | ASYMPTOTIC LONG |
|---|---|---|
| 20.00 | 46.12 | 70.53 |
| 15.00 | 40.36 | 68.82 |
| 10.00 | 36.49 | 67.04 |
| 9.00 | 36.06 | 68.11 |
| 8.00 | 34.96 | 70.37 |
| 7.00 | 32.10 | 73.43 |
| 6.00 | 26.90 | 75.51 |
| 5.00 | 22.25 | 75.16 |
| 4.00 | 20.22 | 78.24 |
| 3.00 | 11.43 | 82.44 |
| 2.00 | 1.80 | 93.52 |
| 1.50 | -7.23 | 106.41 |
| 1.40 | -7.62 | 109.23 |
| 1.30 | -9.96 | 115.44 |
| 1.20 | -10.34 | 120.42 |
| 1.10 | -11.52 | 129.92 |
| 1.00 | -10.55 | 140.32 |
| .90 | -6.82 | 155.05 |

DUMONT DURVILLE, ANTARCTICA

| | |
|---|---|
| GEOGRAPHIC LATITUDE | -66.67 |
| GEOGRAPHIC LONGITUDE | 140.02 |
| EFFECTIVE VERTICAL CUTOFF RIGIDITY | 0.00 |

| RIGIDITY (GV) | ASYMPTOTIC LAT | ASYMPTOTIC LONG |
|---|---|---|
| 20.00 | -67.32 | 154.21 |
| 15.00 | -66.42 | 158.30 |
| 10.00 | -64.08 | 162.23 |
| 9.00 | -63.48 | 162.70 |
| 8.00 | -62.91 | 163.16 |
| 7.00 | -62.38 | 163.91 |
| 6.00 | -61.67 | 165.27 |
| 5.00 | -60.41 | 166.70 |
| 4.00 | -59.09 | 167.55 |
| 3.00 | -57.08 | 169.25 |
| 2.00 | -54.20 | 171.46 |
| 1.50 | -51.86 | 172.62 |
| 1.40 | -51.27 | 173.07 |
| 1.30 | -50.62 | 173.25 |
| 1.20 | -49.88 | 173.71 |
| 1.10 | -49.16 | 174.05 |
| 1.00 | -48.28 | 174.39 |
| .90 | -47.28 | 174.82 |

GOOSE BAY, CANADA

| | |
|---|---|
| GEOGRAPHIC LATITUDE | 53.33 |
| GEOGRAPHIC LONGITUDE | 299.58 |
| EFFECTIVE VERTICAL CUTOFF RIGIDITY | .61 |

| RIGIDITY (GV) | ASYMPTOTIC LAT | ASYMPTOTIC LONG |
|---|---|---|
| 20.00 | 33.84 | 340.41 |
| 15.00 | 25.23 | 340.72 |
| 10.00 | 18.14 | 337.71 |
| 9.00 | 17.97 | 337.62 |
| 8.00 | 17.94 | 338.74 |
| 7.00 | 16.72 | 341.67 |
| 6.00 | 12.20 | 345.52 |
| 5.00 | 5.56 | 347.06 |
| 4.00 | 3.88 | 348.48 |
| 3.00 | -5.05 | 355.59 |
| 2.00 | -11.97 | 8.02 |
| 1.50 | -17.57 | 25.45 |
| 1.40 | -17.38 | 29.06 |
| 1.30 | -17.19 | 35.78 |
| 1.20 | -15.83 | 42.52 |
| 1.10 | -13.15 | 53.02 |
| 1.00 | -7.83 | 63.33 |
| .90 | 2.59 | 79.11 |

INUVIK, CANADA

| | |
|---|---|
| GEOGRAPHIC LATITUDE | 68.35 |
| GEOGRAPHIC LONGITUDE | 226.27 |
| EFFECTIVE VERTICAL CUTOFF RIGIDITY | .16 |

| RIGIDITY (GV) | ASYMPTOTIC LAT | ASYMPTOTIC LONG |
|---|---|---|
| 20.00 | 48.62 | 239.40 |
| 15.00 | 44.91 | 235.90 |
| 10.00 | 42.56 | 232.86 |
| 9.00 | 41.99 | 233.40 |
| 8.00 | 40.71 | 234.47 |
| 7.00 | 38.19 | 235.30 |
| 6.00 | 34.73 | 234.46 |
| 5.00 | 32.61 | 232.49 |
| 4.00 | 30.09 | 233.98 |
| 3.00 | 25.23 | 232.76 |
| 2.00 | 16.71 | 233.92 |
| 1.50 | 11.10 | 233.97 |
| 1.40 | 9.24 | 234.88 |
| 1.30 | 7.51 | 234.53 |
| 1.20 | 5.38 | 235.52 |
| 1.10 | 3.71 | 235.74 |
| 1.00 | .94 | 236.18 |
| .90 | -2.00 | 237.09 |

MAWSON, ANTARCTICA

| | |
|---|---|
| GEOGRAPHIC LATITUDE | -67.60 |
| GEOGRAPHIC LONGITUDE | 62.88 |
| EFFECTIVE VERTICAL CUTOFF RIGIDITY | .20 |

| RIGIDITY (GV) | ASYMPTOTIC LAT | ASYMPTOTIC LONG |
|---|---|---|
| 20.00 | -39.23 | 60.02 |
| 15.00 | -36.22 | 53.31 |
| 10.00 | -38.62 | 47.45 |
| 9.00 | -39.63 | 48.69 |
| 8.00 | -39.49 | 51.62 |
| 7.00 | -36.61 | 55.02 |
| 6.00 | -30.72 | 55.38 |
| 5.00 | -26.77 | 50.93 |
| 4.00 | -28.19 | 51.96 |
| 3.00 | -19.76 | 50.93 |
| 2.00 | -14.41 | 53.30 |
| 1.50 | -5.58 | 55.20 |
| 1.40 | -4.72 | 53.96 |
| 1.30 | -3.26 | 56.10 |
| 1.20 | -.57 | 55.20 |
| 1.10 | 2.03 | 57.37 |
| 1.00 | 3.29 | 57.89 |
| .90 | 6.33 | 58.80 |

MCMURDO, ANTARCTICA

| | |
|---|---|
| GEOGRAPHIC LATITUDE | -77.85 |
| GEOGRAPHIC LONGITUDE | 166.72 |
| EFFECTIVE VERTICAL CUTOFF RIGIDITY | 0.00 |

| RIGIDITY (GV) | ASYMPTOTIC LAT | ASYMPTOTIC LONG |
|---|---|---|
| 20.00 | -85.01 | 305.51 |
| 15.00 | -80.76 | 290.64 |
| 10.00 | -77.72 | 270.79 |
| 9.00 | -77.94 | 268.57 |
| 8.00 | -78.31 | 269.96 |
| 7.00 | -77.90 | 275.98 |
| 6.00 | -75.60 | 279.85 |
| 5.00 | -73.31 | 274.64 |
| 4.00 | -73.40 | 276.06 |
| 3.00 | -70.44 | 274.33 |
| 2.00 | -66.58 | 277.72 |
| 1.50 | -64.43 | 276.43 |
| 1.40 | -63.32 | 277.85 |
| 1.30 | -62.90 | 276.54 |
| 1.20 | -61.64 | 277.62 |
| 1.10 | -61.27 | 277.80 |
| 1.00 | -60.32 | 277.33 |
| .90 | -59.17 | 277.53 |

MIRNY, ANTARCTICA

| | |
|---|---|
| GEOGRAPHIC LATITUDE | -66.55 |
| GEOGRAPHIC LONGITUDE | 93.00 |
| EFFECTIVE VERTICAL CUTOFF RIGIDITY | .03 |

| RIGIDITY (GV) | ASYMPTOTIC LAT | ASYMPTOTIC LONG |
|---|---|---|
| 20.00 | -50.26 | 83.77 |
| 15.00 | -50.36 | 79.07 |
| 10.00 | -52.82 | 79.88 |
| 9.00 | -52.37 | 82.21 |
| 8.00 | -50.62 | 84.39 |
| 7.00 | -47.61 | 84.60 |
| 6.00 | -45.12 | 81.71 |
| 5.00 | -45.84 | 79.59 |
| 4.00 | -43.34 | 83.13 |
| 3.00 | -41.59 | 81.09 |
| 2.00 | -35.24 | 80.86 |
| 1.50 | -33.22 | 80.44 |
| 1.40 | -31.15 | 80.90 |
| 1.30 | -31.17 | 80.06 |
| 1.20 | -29.06 | 80.53 |
| 1.10 | -28.76 | 80.80 |
| 1.00 | -27.57 | 80.18 |
| .90 | -25.99 | 80.13 |

NORILSK, USSR

GEOGRAPHIC LATITUDE 69.26
GEOGRAPHIC LONGITUDE 88.05
EFFECTIVE VERTICAL CUTOFF RIGIDITY .59

| RIGIDITY (GV) | ASYMPTOTIC LAT | LONG |
|---|---|---|
| 20.00 | 49.27 | 123.06 |
| 15.00 | 43.88 | 122.04 |
| 10.00 | 38.75 | 121.10 |
| 9.00 | 37.58 | 121.87 |
| 8.00 | 35.77 | 123.26 |
| 7.00 | 32.69 | 124.89 |
| 6.00 | 28.32 | 125.74 |
| 5.00 | 24.55 | 125.75 |
| 4.00 | 20.45 | 128.72 |
| 3.00 | 12.72 | 131.66 |
| 2.00 | .32 | 141.05 |
| 1.50 | -8.58 | 151.45 |
| 1.40 | -10.54 | 155.34 |
| 1.30 | -12.95 | 160.00 |
| 1.20 | -14.71 | 165.87 |
| 1.10 | -16.04 | 173.28 |
| 1.00 | -16.66 | 184.38 |
| .90 | -14.48 | 199.51 |

SOUTH POLE, ANTARCTICA

GEOGRAPHIC LATITUDE -89.98
GEOGRAPHIC LONGITUDE 0.00
EFFECTIVE VERTICAL CUTOFF RIGIDITY .09

| RIGIDITY (GV) | ASYMPTOTIC LAT | LONG |
|---|---|---|
| 20.00 | -62.81 | 7.69 |
| 15.00 | -58.46 | 355.67 |
| 10.00 | -58.25 | 341.56 |
| 9.00 | -59.33 | 341.14 |
| 8.00 | -60.03 | 343.40 |
| 7.00 | -58.76 | 347.63 |
| 6.00 | -54.49 | 348.69 |
| 5.00 | -50.93 | 343.00 |
| 4.00 | -51.97 | 343.10 |
| 3.00 | -46.09 | 340.74 |
| 2.00 | -41.41 | 342.73 |
| 1.50 | -35.14 | 341.23 |
| 1.40 | -35.55 | 341.40 |
| 1.30 | -32.69 | 341.86 |
| 1.20 | -32.67 | 341.55 |
| 1.10 | -29.82 | 341.13 |
| 1.00 | -27.81 | 342.04 |
| .90 | -25.80 | 342.30 |

THULE, GREENLAND

GEOGRAPHIC LATITUDE 76.55
GEOGRAPHIC LONGITUDE 291.16
EFFECTIVE VERTICAL CUTOFF RIGIDITY 0.00

| RIGIDITY (GV) | ASYMPTOTIC LAT | LONG |
|---|---|---|
| 20.00 | 74.19 | 322.60 |
| 15.00 | 71.97 | 322.54 |
| 10.00 | 70.46 | 317.47 |
| 9.00 | 70.68 | 316.75 |
| 8.00 | 71.04 | 317.30 |
| 7.00 | 71.06 | 319.68 |
| 6.00 | 70.07 | 322.19 |
| 5.00 | 68.74 | 320.93 |
| 4.00 | 69.04 | 321.15 |
| 3.00 | 67.53 | 321.44 |
| 2.00 | 66.19 | 324.17 |
| 1.50 | 64.98 | 323.81 |
| 1.40 | 64.83 | 324.89 |
| 1.30 | 64.30 | 324.31 |
| 1.20 | 64.08 | 325.30 |
| 1.10 | 63.84 | 324.92 |
| 1.00 | 63.26 | 324.98 |
| .90 | 62.79 | 325.25 |

TIXIE BAY, USSR

GEOGRAPHIC LATITUDE 71.55
GEOGRAPHIC LONGITUDE 128.90
EFFECTIVE VERTICAL CUTOFF RIGIDITY .45

| RIGIDITY (GV) | ASYMPTOTIC LAT | LONG |
|---|---|---|
| 20.00 | 49.97 | 164.80 |
| 15.00 | 43.69 | 162.35 |
| 10.00 | 38.39 | 158.53 |
| 9.00 | 37.69 | 158.66 |
| 8.00 | 36.58 | 159.68 |
| 7.00 | 34.14 | 161.34 |
| 6.00 | 29.71 | 162.30 |
| 5.00 | 25.27 | 161.45 |
| 4.00 | 22.12 | 163.06 |
| 3.00 | 14.13 | 164.66 |
| 2.00 | 2.51 | 170.92 |
| 1.50 | -7.19 | 177.41 |
| 1.40 | -9.11 | 179.93 |
| 1.30 | -12.33 | 182.89 |
| 1.20 | -14.58 | 186.61 |
| 1.10 | -17.43 | 191.28 |
| 1.00 | -20.60 | 198.39 |
| .90 | -22.84 | 208.08 |

OULU, FINLAND

| | |
|---|---|
| GEOGRAPHIC LATITUDE | 65.00 |
| GEOGRAPHIC LONGITUDE | 25.42 |
| EFFECTIVE VERTICAL CUTOFF RIGIDITY | .78 |

| RIGIDITY (GV) | ASYMPTOTIC LAT | LONG |
|---|---|---|
| 20.00 | 41.67 | 64.45 |
| 15.00 | 34.89 | 63.05 |
| 10.00 | 30.11 | 61.01 |
| 9.00 | 29.77 | 61.92 |
| 8.00 | 28.92 | 64.15 |
| 7.00 | 26.28 | 67.64 |
| 6.00 | 20.68 | 70.79 |
| 5.00 | 14.77 | 71.45 |
| 4.00 | 12.86 | 74.48 |
| 3.00 | 2.92 | 81.76 |
| 2.00 | -5.66 | 97.55 |
| 1.50 | -11.28 | 120.35 |
| 1.40 | -10.28 | 126.18 |
| 1.30 | -9.38 | 135.56 |
| 1.20 | -5.43 | 147.16 |
| 1.10 | .84 | 164.84 |
| 1.00 | 10.81 | 190.37 |
| .99 | 12.22 | 195.78 |
| .98 | 13.63 | 202.30 |
| .97 | 14.63 | 209.86 |
| .96 | 14.72 | 218.19 |
| .95 | 13.51 | 226.83 |
| .94 | 10.90 | 235.42 |
| .93 | 6.90 | 244.16 |
| .92 | .98 | 254.30 |
| .91 | -9.07 | 269.36 |
| .90 | -26.38 | 308.05 |

SANAE, ANTARCTICA

| | |
|---|---|
| GEOGRAPHIC LATITUDE | -70.30 |
| GEOGRAPHIC LONGITUDE | 357.65 |
| EFFECTIVE VERTICAL CUTOFF RIGIDITY | .86 |

| RIGIDITY (GV) | ASYMPTOTIC LAT | LONG |
|---|---|---|
| 20.00 | -32.81 | 23.67 |
| 15.00 | -23.07 | 18.39 |
| 10.00 | -15.44 | 8.37 |
| 9.00 | -15.81 | 6.68 |
| 8.00 | -17.09 | 6.33 |
| 7.00 | -18.09 | 8.60 |
| 6.00 | -15.21 | 13.78 |
| 5.00 | -4.59 | 17.55 |
| 4.00 | 3.92 | 15.47 |
| 3.00 | 9.81 | 24.24 |
| 2.00 | 26.15 | 42.64 |
| 1.50 | 28.18 | 72.71 |
| 1.40 | 25.49 | 77.51 |
| 1.30 | 21.66 | 94.17 |
| 1.20 | 9.94 | 110.05 |
| 1.10 | -4.98 | 138.63 |
| 1.09 | -8.30 | 145.90 |
| 1.08 | -11.06 | 154.63 |
| 1.07 | -12.46 | 164.88 |
| 1.06 | -11.76 | 176.37 |
| 1.05 | -8.71 | 188.58 |
| 1.04 | -3.84 | 201.22 |
| 1.03 | 1.90 | 214.96 |
| 1.02 | 7.47 | 232.72 |
| 1.01 | 7.47 | 265.84 |
| 1.00 | 9.46 | 396.19 |
| .99 | 10.19 | 476.48 |
| .98 | -4.73 | 423.09 |
| .97 | -23.04 | 286.36 |
| .96 | R | R |
| .95 | -2.73 | 543.37 |
| .94 | -17.52 | 687.48 |
| .93 | -11.32 | 627.72 |
| .92 | -15.31 | 661.86 |
| .91 | -3.86 | 309.19 |
| .90 | 5.52 | 408.70 |

CALGARY, CANADA

GEOGRAPHIC LATITUDE 51.08
GEOGRAPHIC LONGITUDE 245.91
EFFECTIVE VERTICAL CUTOFF RIGIDITY 1.10

| RIGIDITY (GV) | ASYMPTOTIC LAT | ASYMPTOTIC LONG |
|---|---|---|
| 20.00 | 20.21 | 270.62 |
| 15.00 | 12.22 | 268.78 |
| 10.00 | 6.19 | 266.39 |
| 9.00 | 5.54 | 267.19 |
| 8.00 | 4.23 | 269.17 |
| 7.00 | .82 | 272.29 |
| 6.00 | -5.85 | 275.24 |
| 5.00 | -12.71 | 276.39 |
| 4.00 | -15.60 | 280.84 |
| 3.00 | -26.51 | 292.33 |
| 2.00 | -30.45 | 323.88 |
| 1.90 | -29.60 | 332.03 |
| 1.80 | -26.81 | 339.52 |
| 1.70 | -23.23 | 344.75 |
| 1.60 | -18.37 | 353.71 |
| 1.50 | -7.31 | 6.63 |
| 1.40 | 4.05 | 17.83 |
| 1.30 | 24.69 | 53.10 |
| 1.29 | 26.24 | 61.25 |
| 1.28 | 26.51 | 70.83 |
| 1.27 | 24.86 | 81.75 |
| 1.26 | 20.66 | 93.88 |
| 1.25 | 13.28 | 107.48 |
| 1.24 | 2.08 | 124.66 |
| 1.23 | -11.08 | 156.36 |
| 1.22 | -21.01 | 265.47 |
| 1.21 | -2.23 | 252.23 |
| 1.20 | 8.71 | 155.34 |
| 1.19 | -1.74 | 230.16 |
| 1.18 | 10.54 | 212.90 |
| 1.17 | -7.10 | 674.87 |
| 1.16 | R | R |
| 1.15 | 4.81 | 557.47 |
| 1.14 | 3.38 | 577.67 |
| 1.13 | -10.55 | 239.73 |
| 1.12 | R | R |
| 1.11 | -10.72 | 280.37 |
| 1.10 | R | R |
| 1.09 | -3.58 | 1047.00 |
| 1.08 | 5.01 | 1990.47 |
| 1.07 | .22 | 2539.59 |
| 1.06 | R | R |

KERGUELEN ISLAND

GEOGRAPHIC LATITUDE -49.35
GEOGRAPHIC LONGITUDE 70.22
EFFECTIVE VERTICAL CUTOFF RIGIDITY 1.14

| RIGIDITY (GV) | ASYMPTOTIC LAT | ASYMPTOTIC LONG |
|---|---|---|
| 20.00 | -15.00 | 85.81 |
| 15.00 | -8.18 | 83.66 |
| 10.00 | -4.78 | 81.53 |
| 9.00 | -4.89 | 82.50 |
| 8.00 | -4.33 | 84.85 |
| 7.00 | -1.38 | 88.72 |
| 6.00 | 5.86 | 92.96 |
| 5.00 | 14.84 | 95.24 |
| 4.00 | 16.42 | 97.97 |
| 3.00 | 28.09 | 114.48 |
| 2.00 | 27.31 | 147.80 |
| 1.90 | 25.63 | 152.29 |
| 1.80 | 22.93 | 161.94 |
| 1.70 | 15.74 | 173.88 |
| 1.60 | 7.74 | 181.42 |
| 1.50 | .47 | 191.74 |
| 1.40 | -20.98 | 226.61 |
| 1.39 | -22.70 | 233.19 |
| 1.38 | -23.64 | 240.55 |
| 1.37 | -23.57 | 248.58 |
| 1.36 | -22.32 | 257.13 |
| 1.35 | -19.82 | 266.06 |
| 1.34 | -16.10 | 275.41 |
| 1.33 | -11.15 | 285.57 |
| 1.32 | -4.94 | 297.61 |
| 1.31 | 2.46 | 314.53 |
| 1.30 | 7.61 | 347.74 |
| 1.29 | -1.14 | 140.25 |
| 1.28 | -2.53 | 399.95 |
| 1.27 | -.69 | 305.46 |
| 1.26 | 10.65 | 65.19 |
| 1.25 | 13.26 | 40.43 |
| 1.24 | 11.96 | 187.17 |
| 1.23 | -4.77 | 226.97 |
| 1.22 | 2.29 | 547.82 |
| 1.21 | 2.68 | 420.56 |
| 1.20 | 17.61 | 57.66 |
| 1.19 | -.30 | 140.83 |
| 1.18 | -14.85 | 331.07 |
| 1.17 | -8.49 | 4.01 |
| 1.16 | -4.59 | 606.26 |
| 1.15 | -7.66 | 657.47 |
| 1.14 | R | R |
| 1.13 | R | R |
| 1.12 | R | R |
| 1.11 | R | R |
| 1.10 | R | R |
| 1.09 | 10.16 | 2955.82 |
| 1.08 | R | R |

DEEP RIVER, CANADA

GEOGRAPHIC LATITUDE 46.10
GEOGRAPHIC LONGITUDE 282.50
EFFECTIVE VERTICAL
CUTOFF RIGIDITY 1.15

| RIGIDITY (GV) | ASYMPTOTIC LAT | LONG |
|---|---|---|
| 20.00 | 21.26 | 320.23 |
| 15.00 | 11.79 | 321.06 |
| 10.00 | 3.49 | 319.43 |
| 9.00 | 2.98 | 319.71 |
| 8.00 | 2.55 | 321.22 |
| 7.00 | .82 | 324.68 |
| 6.00 | -4.34 | 329.78 |
| 5.00 | -11.84 | 334.00 |
| 4.00 | -14.07 | 338.03 |
| 3.00 | -21.83 | 354.22 |
| 2.00 | -17.50 | 25.11 |
| 1.90 | -15.15 | 32.06 |
| 1.80 | -10.53 | 40.99 |
| 1.70 | -4.40 | 47.80 |
| 1.60 | 1.36 | 55.09 |
| 1.50 | 13.68 | 72.13 |
| 1.40 | 27.22 | 101.24 |
| 1.35 | 26.28 | 123.71 |
| 1.34 | 24.50 | 130.71 |
| 1.33 | 21.26 | 139.29 |
| 1.32 | 15.45 | 150.04 |
| 1.31 | 4.98 | 164.56 |
| 1.30 | -13.28 | 191.64 |
| 1.29 | -7.08 | 289.30 |
| 1.28 | -8.64 | 305.19 |
| 1.27 | -23.38 | 345.51 |
| 1.26 | 6.16 | 210.02 |
| 1.25 | 16.57 | 531.77 |
| 1.24 | R | R |
| 1.23 | -5.16 | 265.80 |
| 1.22 | 2.06 | 353.59 |
| 1.21 | 3.61 | 244.37 |
| 1.20 | -1.24 | 299.72 |
| 1.19 | 10.01 | 434.61 |
| 1.18 | R | R |
| 1.17 | -14.46 | 1381.16 |
| 1.16 | R | R |
| 1.15 | -6.78 | 261.21 |
| 1.14 | 19.71 | 824.11 |
| 1.13 | R | R |
| 1.12 | 5.45 | 1101.80 |
| 1.11 | R | R |
| 1.10 | R | R |
| 1.09 | 8.34 | 778.52 |
| 1.08 | R | R |

MT. WASHINGTON, USA

GEOGRAPHIC LATITUDE 44.30
GEOGRAPHIC LONGITUDE 288.70
EFFECTIVE VERTICAL CUTOFF RIGIDITY 1.43

| RIGIDITY (GV) | ASYMPTOTIC LAT | ASYMPTOTIC LONG | RIGIDITY (GV) | ASYMPTOTIC LAT | ASYMPTOTIC LONG |
|---|---|---|---|---|---|
| 20.00 | 18.98 | 330.53 | 1.34 | R | R |
| 15.00 | 8.46 | 332.49 | 1.33 | R | R |
| 10.00 | -1.15 | 332.02 | 1.32 | R | R |
| 9.00 | -1.66 | 332.35 | 1.31 | R | R |
| 8.00 | -1.84 | 333.90 | 1.30 | -10.82 | 4320.08 |
| 7.00 | -3.01 | 337.74 | 1.29 | R | R |
| 6.00 | -7.72 | 344.36 | | | |
| 5.00 | -15.55 | 351.86 | | | |
| 4.00 | -17.29 | 357.92 | | | |
| 3.00 | -20.13 | 21.94 | | | |
| 2.00 | 5.47 | 67.11 | | | |
| 1.90 | 11.93 | 77.89 | | | |
| 1.80 | 23.96 | 102.60 | | | |
| 1.70 | 13.24 | 160.31 | | | |
| 1.69 | 6.88 | 168.41 | | | |
| 1.68 | -1.08 | 178.00 | | | |
| 1.67 | -10.58 | 191.19 | | | |
| 1.66 | -19.56 | 214.40 | | | |
| 1.65 | -6.23 | 272.84 | | | |
| 1.64 | 6.57 | 464.20 | | | |
| 1.63 | -21.73 | 288.15 | | | |
| 1.62 | -19.31 | 678.12 | | | |
| 1.61 | 5.33 | 218.55 | | | |
| 1.60 | 3.57 | 278.20 | | | |
| 1.59 | 16.38 | 756.30 | | | |
| 1.58 | -5.71 | 346.77 | | | |
| 1.57 | 10.71 | 599.68 | | | |
| 1.56 | -.92 | 444.44 | | | |
| 1.55 | -3.94 | 276.40 | | | |
| 1.54 | R | R | | | |
| 1.53 | R | R | | | |
| 1.52 | R | R | | | |
| 1.51 | -17.36 | 328.67 | | | |
| 1.50 | -5.53 | 657.17 | | | |
| 1.49 | 3.84 | 227.15 | | | |
| 1.48 | -6.84 | 361.34 | | | |
| 1.47 | 3.90 | 234.96 | | | |
| 1.46 | 4.40 | 569.49 | | | |
| 1.45 | 3.11 | 820.14 | | | |
| 1.44 | 14.18 | 1894.45 | | | |
| 1.43 | -13.62 | 1034.44 | | | |
| 1.42 | R | R | | | |
| 1.41 | -.03 | 2312.85 | | | |
| 1.40 | R | R | | | |
| 1.39 | R | R | | | |
| 1.38 | R | R | | | |
| 1.37 | .67 | 7072.60 | | | |
| 1.36 | R | R | | | |
| 1.35 | R | R | | | |

DURHAM, USA

GEOGRAPHIC LATITUDE 43.10
GEOGRAPHIC LONGITUDE 289.16
EFFECTIVE VERTICAL
CUTOFF RIGIDITY 1.61

| RIGIDITY (GV) | ASYMPTOTIC LAT | ASYMPTOTIC LONG | RIGIDITY (GV) | ASYMPTOTIC LAT | ASYMPTOTIC LONG |
|---|---|---|---|---|---|
| 20.00 | 17.11 | 332.16 | 1.57 | R | R |
| 15.00 | 6.16 | 334.64 | 1.56 | R | R |
| 10.00 | -4.01 | 334.94 | 1.55 | R | R |
| 9.00 | -4.56 | 335.39 | 1.54 | R | R |
| 8.00 | -4.66 | 337.04 | 1.53 | R | R |
| 7.00 | -5.64 | 341.11 | 1.52 | R | R |
| 6.00 | -10.08 | 348.54 | 1.51 | R | R |
| 5.00 | -17.69 | 358.06 | 1.50 | R | R |
| 4.00 | -18.74 | 5.87 | 1.49 | R | R |
| 3.00 | -16.89 | 34.45 | 1.48 | 5.76 | 6894.11 |
| 2.50 | -7.26 | 50.28 | 1.47 | -12.72 | 3859.97 |
| 2.40 | -3.46 | 57.63 | 1.46 | R | R |
| 2.30 | 3.00 | 67.32 | 1.45 | R | R |
| 2.20 | 12.18 | 78.75 | 1.44 | R | R |
| 2.10 | 20.87 | 91.77 | 1.43 | R | R |
| 2.00 | 25.70 | 108.27 | 1.42 | R | R |
| 1.90 | 21.72 | 143.92 | 1.41 | 3.58 | 4497.73 |
| 1.89 | 19.00 | 150.44 | 1.40 | R | R |
| 1.88 | 14.98 | 158.02 | | | |
| 1.87 | 9.04 | 167.13 | | | |
| 1.86 | .20 | 179.07 | | | |
| 1.85 | -12.51 | 198.69 | | | |
| 1.84 | -15.22 | 256.85 | | | |
| 1.83 | R | R | | | |
| 1.82 | -8.46 | 401.84 | | | |
| 1.81 | -6.58 | 243.05 | | | |
| 1.80 | 6.09 | 234.56 | | | |
| 1.79 | 19.98 | 395.80 | | | |
| 1.78 | 5.34 | 347.76 | | | |
| 1.77 | R | R | | | |
| 1.76 | R | R | | | |
| 1.75 | R | R | | | |
| 1.74 | -14.48 | 290.98 | | | |
| 1.73 | -7.27 | 275.79 | | | |
| 1.72 | -14.76 | 291.51 | | | |
| 1.71 | -15.06 | 250.99 | | | |
| 1.70 | 8.42 | 209.09 | | | |
| 1.69 | -19.41 | 329.77 | | | |
| 1.68 | 1.18 | 499.09 | | | |
| 1.67 | 19.37 | 427.41 | | | |
| 1.66 | 5.57 | 223.06 | | | |
| 1.65 | 4.83 | 207.77 | | | |
| 1.64 | 17.05 | 460.20 | | | |
| 1.63 | 8.47 | 850.89 | | | |
| 1.62 | -14.18 | 1724.96 | | | |
| 1.61 | -7.84 | 638.53 | | | |
| 1.60 | R | R | | | |
| 1.59 | R | R | | | |
| 1.58 | -.24 | 3002.36 | | | |

MT. WELLINGTON, AUSTRALIA

GEOGRAPHIC LATITUDE -42.92
GEOGRAPHIC LONGITUDE 147.24
EFFECTIVE VERTICAL CUTOFF RIGIDITY 1.80

| RIGIDITY (GV) | ASYMPTOTIC LAT | ASYMPTOTIC LONG | RIGIDITY (GV) | ASYMPTOTIC LAT | ASYMPTOTIC LONG |
|---|---|---|---|---|---|
| 20.00 | -17.63 | 189.08 | 1.79 | -8.54 | 274.32 |
| 15.00 | -7.95 | 191.06 | 1.78 | R | R |
| 10.00 | -1.02 | 192.77 | 1.77 | R | R |
| 9.00 | -.74 | 194.51 | 1.76 | -1.73 | 222.66 |
| 8.00 | .03 | 197.98 | 1.75 | -14.92 | 287.74 |
| 7.00 | 2.98 | 203.80 | 1.74 | 1.04 | 1993.54 |
| 6.00 | 9.21 | 211.59 | 1.73 | R | R |
| 5.00 | 14.02 | 219.11 | 1.72 | R | R |
| 4.00 | 13.46 | 230.60 | 1.71 | 9.93 | 1122.75 |
| 3.00 | 7.98 | 259.84 | 1.70 | R | R |
| 2.90 | 6.30 | 262.92 | 1.69 | R | R |
| 2.80 | 4.39 | 267.22 | 1.68 | R | R |
| 2.70 | 1.76 | 273.32 | 1.67 | R | R |
| 2.60 | -2.46 | 281.48 | 1.66 | -7.26 | 3447.92 |
| 2.50 | -9.00 | 291.61 | 1.65 | R | R |
| 2.40 | -17.00 | 303.68 | | | |
| 2.30 | -23.37 | 318.24 | | | |
| 2.20 | -25.12 | 338.00 | | | |
| 2.10 | -9.51 | 18.19 | | | |
| 2.09 | -3.69 | 25.46 | | | |
| 2.08 | 4.39 | 34.69 | | | |
| 2.07 | 15.60 | 48.55 | | | |
| 2.06 | 27.70 | 79.01 | | | |
| 2.05 | -1.39 | 229.32 | | | |
| 2.04 | 12.42 | 150.14 | | | |
| 2.03 | 3.29 | 98.03 | | | |
| 2.02 | -5.82 | 197.31 | | | |
| 2.01 | 25.48 | 472.61 | | | |
| 2.00 | -6.40 | 331.43 | | | |
| 1.99 | 2.19 | 532.52 | | | |
| 1.98 | R | R | | | |
| 1.97 | R | R | | | |
| 1.96 | R | R | | | |
| 1.95 | 1.51 | 223.81 | | | |
| 1.94 | -9.22 | 231.92 | | | |
| 1.93 | 5.46 | 1527.98 | | | |
| 1.92 | 6.60 | 503.76 | | | |
| 1.91 | 8.20 | 391.61 | | | |
| 1.90 | 9.27 | 168.68 | | | |
| 1.89 | -4.77 | 210.73 | | | |
| 1.88 | R | R | | | |
| 1.87 | 9.40 | 93.82 | | | |
| 1.86 | 2.35 | 158.41 | | | |
| 1.85 | R | R | | | |
| 1.84 | -8.36 | 1041.62 | | | |
| 1.83 | 7.31 | 134.65 | | | |
| 1.82 | -2.54 | 722.80 | | | |
| 1.81 | -8.19 | 705.53 | | | |
| 1.80 | R | R | | | |

NEWARK, USA

GEOGRAPHIC LATITUDE 39.68
GEOGRAPHIC LONGITUDE 284.25
EFFECTIVE VERTICAL CUTOFF RIGIDITY 2.10

| RIGIDITY (GV) | ASYMPTOTIC LAT | ASYMPTOTIC LONG |
|---|---|---|
| 20.00 | 11.11 | 328.11 |
| 15.00 | -.59 | 331.65 |
| 10.00 | -11.69 | 334.10 |
| 9.00 | -12.31 | 335.01 |
| 8.00 | -12.33 | 337.15 |
| 7.00 | -12.93 | 342.05 |
| 6.00 | -16.54 | 351.77 |
| 5.00 | -22.03 | 7.11 |
| 4.00 | -18.52 | 20.70 |
| 3.00 | 4.60 | 62.58 |
| 2.90 | 11.01 | 69.38 |
| 2.80 | 17.00 | 76.79 |
| 2.70 | 21.86 | 85.62 |
| 2.60 | 25.42 | 98.09 |
| 2.50 | 25.96 | 120.74 |
| 2.40 | -4.20 | 178.90 |
| 2.39 | -14.15 | 196.94 |
| 2.38 | -16.83 | 239.68 |
| 2.37 | .92 | 342.90 |
| 2.36 | -23.31 | 285.84 |
| 2.35 | -12.66 | 327.95 |
| 2.34 | -7.03 | 211.14 |
| 2.33 | -23.08 | 627.29 |
| 2.32 | -10.37 | 296.96 |
| 2.31 | -12.76 | 310.18 |
| 2.30 | -5.23 | 570.94 |
| 2.29 | R | R |
| 2.28 | R | R |
| 2.27 | R | R |
| 2.26 | 6.71 | 246.03 |
| 2.25 | -8.92 | 360.78 |
| 2.24 | -6.60 | 271.98 |
| 2.23 | 9.68 | 207.28 |
| 2.22 | R | R |
| 2.21 | 7.34 | 213.81 |
| 2.20 | -11.91 | 245.23 |
| 2.19 | -12.45 | 244.30 |
| 2.18 | 7.92 | 211.09 |
| 2.17 | 8.23 | 188.47 |
| 2.16 | 4.30 | 3623.65 |
| 2.15 | R | R |
| 2.14 | R | R |
| 2.13 | R | R |
| 2.12 | 12.46 | 410.70 |
| 2.11 | -11.58 | 328.31 |
| 2.10 | 16.68 | 818.04 |
| 2.09 | R | R |
| 2.08 | R | R |
| 2.07 | -16.60 | 672.60 |
| 2.06 | -12.40 | 2061.65 |
| 2.05 | 12.02 | 500.92 |
| 2.04 | R | R |
| 2.03 | 3.45 | 2319.05 |
| 2.02 | R | R |
| 2.01 | -3.13 | 2520.44 |
| 2.00 | R | R |
| 1.99 | R | R |
| 1.98 | R | R |
| 1.97 | -6.25 | 1088.27 |
| 1.96 | R | R |
| 1.95 | R | R |
| 1.94 | R | R |
| 1.93 | R | R |
| 1.92 | R | R |
| 1.91 | R | R |
| 1.90 | 2.30 | 3109.78 |
| 1.89 | R | R |

LEEDS, ENGLAND

GEOGRAPHIC LATITUDE 53.82
GEOGRAPHIC LONGITUDE 358.45
EFFECTIVE VERTICAL CUTOFF RIGIDITY 2.25

| RIGIDITY (GV) | ASYMPTOTIC LAT | ASYMPTOTIC LONG | RIGIDITY (GV) | ASYMPTOTIC LAT | ASYMPTOTIC LONG |
|---|---|---|---|---|---|
| 20.00 | 24.40 | 46.49 | 2.15 | R | R |
| 15.00 | 12.82 | 48.42 | 2.14 | 7.96 | 778.75 |
| 10.00 | 2.18 | 49.92 | 2.13 | R | R |
| 9.00 | 1.66 | 51.06 | 2.12 | R | R |
| 8.00 | 1.62 | 53.55 | 2.11 | R | R |
| 7.00 | .69 | 58.67 | 2.10 | R | R |
| 6.00 | -3.99 | 67.84 | 2.09 | 9.04 | 1540.59 |
| 5.00 | -11.83 | 81.70 | 2.08 | 4.33 | 1224.99 |
| 4.00 | -10.22 | 96.52 | 2.07 | R | R |
| 3.00 | 5.67 | 145.68 | | | |
| 2.90 | 11.65 | 156.43 | | | |
| 2.80 | 16.80 | 169.28 | | | |
| 2.70 | 18.93 | 185.06 | | | |
| 2.60 | 15.30 | 206.04 | | | |
| 2.50 | -7.22 | 246.19 | | | |
| 2.49 | -12.79 | 254.84 | | | |
| 2.48 | -19.39 | 267.30 | | | |
| 2.47 | -25.45 | 288.64 | | | |
| 2.46 | -15.59 | 334.68 | | | |
| 2.45 | -5.75 | 587.41 | | | |
| 2.44 | 4.45 | 473.27 | | | |
| 2.43 | 8.70 | 726.13 | | | |
| 2.42 | -8.51 | 309.79 | | | |
| 2.41 | 10.16 | 516.60 | | | |
| 2.40 | R | R | | | |
| 2.39 | 3.62 | 864.57 | | | |
| 2.38 | 8.90 | 404.44 | | | |
| 2.37 | -2.74 | 514.35 | | | |
| 2.36 | R | R | | | |
| 2.35 | R | R | | | |
| 2.34 | R | R | | | |
| 2.33 | R | R | | | |
| 2.32 | 17.98 | 456.98 | | | |
| 2.31 | R | R | | | |
| 2.30 | -5.76 | 557.08 | | | |
| 2.29 | R | R | | | |
| 2.28 | -12.23 | 981.31 | | | |
| 2.27 | -2.15 | 618.97 | | | |
| 2.26 | -9.42 | 1626.14 | | | |
| 2.25 | R | R | | | |
| 2.24 | -11.45 | 1048.40 | | | |
| 2.23 | R | R | | | |
| 2.22 | -7.62 | 553.74 | | | |
| 2.21 | -3.71 | 2343.56 | | | |
| 2.20 | R | R | | | |
| 2.19 | 3.84 | 938.53 | | | |
| 2.18 | R | R | | | |
| 2.17 | R | R | | | |
| 2.16 | -12.11 | 2477.53 | | | |

KIEL, FRG

GEOGRAPHIC LATITUDE 54.33
GEOGRAPHIC LONGITUDE 10.13
EFFECTIVE VERTICAL CUTOFF RIGIDITY 2.33

| RIGIDITY (GV) | ASYMPTOTIC LAT | ASYMPTOTIC LONG |
|---|---|---|
| 20.00 | 23.81 | 56.86 |
| 15.00 | 12.50 | 58.69 |
| 10.00 | 2.25 | 60.51 |
| 9.00 | 1.69 | 61.84 |
| 8.00 | 1.49 | 64.59 |
| 7.00 | .24 | 70.01 |
| 6.00 | -4.72 | 79.53 |
| 5.00 | -12.12 | 94.12 |
| 4.00 | -9.50 | 110.31 |
| 3.00 | 10.86 | 168.03 |
| 2.90 | 16.45 | 183.57 |
| 2.80 | 17.50 | 204.51 |
| 2.70 | 6.23 | 233.06 |
| 2.69 | 3.85 | 236.70 |
| 2.68 | 1.11 | 240.63 |
| 2.67 | -2.04 | 244.96 |
| 2.66 | -5.66 | 249.85 |
| 2.65 | -9.81 | 255.58 |
| 2.64 | -14.54 | 262.63 |
| 2.63 | -19.74 | 271.92 |
| 2.62 | -24.83 | 285.38 |
| 2.61 | -26.97 | 307.18 |
| 2.60 | -11.89 | 345.99 |
| 2.59 | 11.42 | 91.79 |
| 2.58 | R | R |
| 2.57 | 1.15 | 75.01 |
| 2.56 | 11.12 | 59.46 |
| 2.55 | -5.80 | 357.74 |
| 2.54 | -12.51 | 317.78 |
| 2.53 | -.14 | 280.45 |
| 2.52 | 4.94 | 58.29 |
| 2.51 | 4.42 | 358.96 |
| 2.50 | 16.15 | 413.62 |
| 2.49 | 2.49 | 31.66 |
| 2.48 | -4.07 | 1062.20 |
| 2.47 | 17.15 | 69.28 |
| 2.46 | R | R |
| 2.45 | R | R |
| 2.44 | R | R |
| 2.43 | R | R |
| 2.42 | R | R |
| 2.41 | 8.93 | 1640.35 |
| 2.40 | R | R |
| 2.39 | -9.05 | 247.44 |
| 2.38 | 7.35 | 98.99 |
| 2.37 | R | R |
| 2.36 | -20.64 | 283.03 |
| 2.35 | -3.55 | 599.39 |
| 2.34 | 8.90 | 75.19 |
| 2.33 | .67 | 174.70 |
| 2.32 | R | R |
| 2.31 | 7.62 | 166.10 |
| 2.30 | 1.59 | 2347.27 |
| 2.29 | 13.06 | 1147.55 |
| 2.28 | 5.76 | 500.98 |
| 2.27 | R | R |
| 2.26 | R | R |
| 2.25 | R | R |
| 2.24 | 10.17 | 489.49 |
| 2.23 | 16.19 | 1885.75 |
| 2.22 | 11.02 | 887.66 |
| 2.21 | R | R |
| 2.20 | R | R |
| 2.19 | R | R |
| 2.18 | R | R |
| 2.17 | 13.67 | 4018.28 |
| 2.16 | R | R |

MOSCOW, USSR

GEOGRAPHIC LATITUDE 55.47
GEOGRAPHIC LONGITUDE 37.32
EFFECTIVE VERTICAL CUTOFF RIGIDITY 2.41

| RIGIDITY (GV) | ASYMPTOTIC LAT | ASYMPTOTIC LONG |
|---|---|---|
| 20.00 | 23.74 | 80.71 |
| 15.00 | 13.39 | 82.16 |
| 10.00 | 4.47 | 84.19 |
| 9.00 | 3.81 | 85.84 |
| 8.00 | 3.07 | 89.02 |
| 7.00 | .75 | 94.82 |
| 6.00 | -5.28 | 104.25 |
| 5.00 | -12.20 | 117.86 |
| 4.00 | -9.88 | 133.63 |
| 3.00 | 10.06 | 195.42 |
| 2.90 | 13.95 | 210.03 |
| 2.80 | 13.46 | 228.75 |
| 2.70 | 2.80 | 255.28 |
| 2.69 | .61 | 258.91 |
| 2.68 | -1.93 | 262.90 |
| 2.67 | -4.87 | 267.37 |
| 2.66 | -8.29 | 272.52 |
| 2.65 | -12.25 | 278.68 |
| 2.64 | -16.77 | 286.42 |
| 2.63 | -21.66 | 296.93 |
| 2.62 | -25.87 | 312.66 |
| 2.61 | -24.31 | 338.72 |
| 2.60 | 12.68 | 32.16 |
| 2.59 | 15.54 | 396.97 |
| 2.58 | 2.23 | 98.43 |
| 2.57 | 5.37 | 54.97 |
| 2.56 | -1.77 | 28.25 |
| 2.55 | -12.40 | 335.58 |
| 2.54 | 2.74 | 114.21 |
| 2.53 | 9.84 | 119.69 |
| 2.52 | 2.63 | 46.25 |
| 2.51 | 14.69 | 62.28 |
| 2.50 | 9.07 | 376.57 |
| 2.49 | R | R |
| 2.48 | R | R |
| 2.47 | R | R |
| 2.46 | R | R |
| 2.45 | R | R |
| 2.44 | R | R |
| 2.43 | R | R |
| 2.42 | R | R |
| 2.41 | R | R |
| 2.40 | -1.89 | 276.69 |
| 2.39 | -9.23 | 1033.98 |
| 2.38 | 2.53 | 373.88 |
| 2.37 | -5.65 | 633.21 |
| 2.36 | R | R |
| 2.35 | -2.41 | 165.77 |
| 2.34 | 12.43 | 137.81 |
| 2.33 | R | R |
| 2.32 | R | R |
| 2.31 | R | R |
| 2.30 | -11.95 | 731.92 |
| 2.29 | R | R |
| 2.28 | R | R |
| 2.27 | R | R |
| 2.26 | R | R |
| 2.25 | R | R |
| 2.24 | R | R |
| 2.23 | R | R |
| 2.22 | -12.64 | 266.03 |
| 2.21 | R | R |
| 2.20 | R | R |
| 2.19 | R | R |
| 2.18 | R | R |
| 2.17 | -10.61 | 1312.12 |
| 2.16 | R | R |

CLIMAX, USA

GEOGRAPHIC LATITUDE 39.37
GEOGRAPHIC LONGITUDE 253.82
EFFECTIVE VERTICAL CUTOFF RIGIDITY 2.95

| RIGIDITY (GV) | ASYMPTOTIC LAT | ASYMPTOTIC LONG | RIGIDITY (GV) | ASYMPTOTIC LAT | ASYMPTOTIC LONG |
|---|---|---|---|---|---|
| 20.00 | .96 | 290.84 | 2.96 | R | R |
| 15.00 | -11.70 | 293.37 | 2.95 | R | R |
| 10.00 | -23.20 | 297.61 | 2.94 | -12.35 | 278.74 |
| 9.00 | -23.78 | 299.82 | 2.93 | -2.55 | 2482.68 |
| 8.00 | -23.91 | 303.77 | 2.92 | R | R |
| 7.00 | -24.92 | 311.32 | 2.91 | -16.17 | 616.88 |
| 6.00 | -28.44 | 326.02 | 2.90 | R | R |
| 5.00 | -27.29 | 351.18 | 2.89 | -8.94 | 326.62 |
| 4.00 | -7.37 | 14.08 | 2.88 | R | R |
| 3.90 | -4.67 | 17.21 | 2.87 | .81 | 1275.88 |
| 3.80 | -1.53 | 21.11 | 2.86 | R | R |
| 3.70 | 2.34 | 26.13 | 2.85 | -14.38 | 715.84 |
| 3.60 | 7.38 | 32.82 | 2.84 | R | R |
| 3.50 | 14.15 | 42.32 | 2.83 | R | R |
| 3.40 | 22.71 | 57.84 | 2.82 | R | R |
| 3.30 | 27.37 | 90.03 | 2.81 | R | R |
| 3.29 | 26.53 | 95.03 | 2.80 | R | R |
| 3.28 | 25.13 | 100.46 | 2.79 | R | R |
| 3.27 | 23.00 | 106.38 | 2.78 | R | R |
| 3.26 | 19.93 | 112.84 | 2.77 | R | R |
| 3.25 | 15.66 | 119.99 | 2.76 | R | R |
| 3.24 | 9.83 | 128.17 | 2.75 | R | R |
| 3.23 | 2.05 | 138.27 | 2.74 | R | R |
| 3.22 | -7.80 | 152.93 | 2.73 | R | R |
| 3.21 | -15.71 | 181.88 | 2.72 | R | R |
| 3.20 | 1.99 | 576.61 | 2.71 | R | R |
| 3.19 | -16.75 | 246.45 | 2.70 | R | R |
| 3.18 | -3.66 | 279.21 | 2.69 | R | R |
| 3.17 | 9.09 | 156.60 | 2.68 | R | R |
| 3.16 | -5.81 | 490.95 | 2.67 | R | R |
| 3.15 | 15.84 | 180.77 | 2.66 | R | R |
| 3.14 | -2.42 | 561.01 | 2.65 | R | R |
| 3.13 | 11.66 | 170.08 | 2.64 | R | R |
| 3.12 | 8.23 | 234.42 | 2.63 | 13.20 | 1893.44 |
| 3.11 | R | R | 2.62 | R | R |
| 3.10 | R | R | 2.61 | R | R |
| 3.09 | R | R | 2.60 | R | R |
| 3.08 | R | R | 2.59 | -8.42 | 1988.15 |
| 3.07 | R | R | 2.58 | R | R |
| 3.06 | -7.75 | 277.11 | | | |
| 3.05 | -4.87 | 616.58 | | | |
| 3.04 | -14.56 | 1009.46 | | | |
| 3.03 | -15.92 | 322.63 | | | |
| 3.02 | -7.25 | 320.62 | | | |
| 3.01 | 10.89 | 480.96 | | | |
| 3.00 | -9.32 | 318.06 | | | |
| 2.99 | 11.54 | 851.15 | | | |
| 2.98 | 15.81 | 463.61 | | | |
| 2.97 | R | R | | | |

LOMNICKY STIT, CZECHOSLOVAKIA

GEOGRAPHIC LATITUDE 49.20
GEOGRAPHIC LONGITUDE 20.22
EFFECTIVE VERTICAL CUTOFF RIGIDITY 4.00

| RIGIDITY (GV) | ASYMPTOTIC LAT | ASYMPTOTIC LONG | RIGIDITY (GV) | ASYMPTOTIC LAT | ASYMPTOTIC LONG |
|---|---|---|---|---|---|
| 20.00 | 14.30 | 70.93 | 4.04 | R | R |
| 15.00 | 1.02 | 76.24 | 4.03 | R | R |
| 10.00 | -10.53 | 86.53 | 4.02 | R | R |
| 9.00 | -10.57 | 90.18 | 4.01 | R | R |
| 8.00 | -9.73 | 95.38 | 4.00 | R | R |
| 7.00 | -9.02 | 104.35 | 3.99 | R | R |
| 6.00 | -9.21 | 122.60 | 3.98 | R | R |
| 5.00 | 3.93 | 164.36 | 3.97 | R | R |
| 4.90 | 7.68 | 171.47 | 3.96 | R | R |
| 4.80 | 11.73 | 179.98 | 3.95 | R | R |
| 4.70 | 15.50 | 190.65 | 3.94 | R | R |
| 4.60 | 17.63 | 204.63 | 3.93 | R | R |
| 4.50 | 14.93 | 223.39 | 3.92 | R | R |
| 4.40 | -.32 | 249.60 | 3.91 | R | R |
| 4.39 | -3.15 | 253.09 | 3.90 | 13.77 | 79.58 |
| 4.38 | -6.31 | 256.95 | 3.89 | R | R |
| 4.37 | -9.85 | 261.29 | 3.88 | R | R |
| 4.36 | -13.76 | 266.36 | 3.87 | -6.17 | 743.35 |
| 4.35 | -18.03 | 272.51 | 3.86 | R | R |
| 4.34 | -22.49 | 280.37 | 3.85 | 9.05 | 459.08 |
| 4.33 | -26.65 | 291.06 | 3.84 | R | R |
| 4.32 | -29.01 | 306.46 | 3.83 | R | R |
| 4.31 | -25.03 | 329.08 | 3.82 | -1.30 | 160.41 |
| 4.30 | .62 | 4.44 | 3.81 | R | R |
| 4.29 | 15.17 | 94.64 | 3.80 | 9.50 | 557.34 |
| 4.28 | -15.70 | 177.39 | 3.79 | R | R |
| 4.27 | R | R | 3.78 | R | R |
| 4.26 | -5.56 | 6.47 | 3.77 | R | R |
| 4.25 | -16.58 | 359.83 | 3.76 | 22.11 | 484.52 |
| 4.24 | 2.30 | 189.47 | 3.75 | .14 | 516.66 |
| 4.23 | -1.44 | 339.36 | 3.74 | -4.95 | 171.90 |
| 4.22 | -10.50 | 301.31 | 3.73 | R | R |
| 4.21 | -14.64 | 318.83 | 3.72 | -7.07 | 231.65 |
| 4.20 | 23.97 | 90.62 | 3.71 | R | R |
| 4.19 | 4.09 | 107.84 | 3.70 | -1.69 | 523.81 |
| 4.18 | 5.85 | 201.10 | 3.69 | R | R |
| 4.17 | -3.23 | 10.06 | 3.68 | R | R |
| 4.16 | 4.82 | 353.48 | 3.67 | R | R |
| 4.15 | R | R | 3.66 | R | R |
| 4.14 | R | R | 3.65 | -3.20 | 152.12 |
| 4.13 | -5.72 | 197.60 | 3.64 | R | R |
| 4.12 | R | R | 3.63 | R | R |
| 4.11 | -4.75 | 19.29 | 3.62 | 15.98 | 490.28 |
| 4.10 | 12.74 | 129.68 | 3.61 | R | R |
| 4.09 | -5.68 | 152.95 | 3.60 | -1.85 | 365.30 |
| 4.08 | R | R | 3.59 | R | R |
| 4.07 | R | R | | | |
| 4.06 | R | R | | | |
| 4.05 | R | R | | | |

JUNGFRAUJOCH, SWITZERLAND

GEOGRAPHIC LATITUDE 46.55
GEOGRAPHIC LONGITUDE 7.98
EFFECTIVE VERTICAL CUTOFF RIGIDITY 4.63

| RIGIDITY (GV) | ASYMPTOTIC LAT | ASYMPTOTIC LONG | RIGIDITY (GV) | ASYMPTOTIC LAT | ASYMPTOTIC LONG | RIGIDITY (GV) | ASYMPTOTIC LAT | ASYMPTOTIC LONG |
|---|---|---|---|---|---|---|---|---|
| 20.00 | 11.54 | 62.43 | 4.63 | R | R | 4.14 | R | R |
| 15.00 | -2.89 | 69.93 | 4.62 | 18.48 | 93.84 | 4.13 | R | R |
| 10.00 | -14.31 | 86.40 | 4.61 | R | R | 4.12 | R | R |
| 9.00 | -13.26 | 91.77 | 4.60 | 5.85 | 137.94 | 4.11 | R | R |
| 8.00 | -10.76 | 98.58 | 4.59 | -14.81 | 343.46 | 4.10 | R | R |
| 7.00 | -7.56 | 109.48 | 4.58 | R | R | 4.09 | R | R |
| 6.00 | -2.61 | 132.97 | 4.57 | 16.83 | 48.04 | 4.08 | R | R |
| 5.50 | 6.04 | 158.15 | 4.56 | -4.25 | 125.92 | 4.07 | R | R |
| 5.40 | 9.11 | 166.04 | 4.55 | 8.43 | 186.55 | 4.06 | R | R |
| 5.30 | 12.58 | 176.01 | 4.54 | -4.98 | 305.76 | 4.05 | R | R |
| 5.20 | 15.78 | 189.44 | 4.53 | -7.82 | 305.02 | 4.04 | R | R |
| 5.10 | 16.20 | 209.12 | 4.52 | 10.73 | 55.94 | 4.03 | R | R |
| 5.00 | 3.55 | 241.02 | 4.51 | 10.66 | 131.93 | 4.02 | R | R |
| 4.99 | .40 | 245.60 | 4.50 | R | R | 4.01 | R | R |
| 4.98 | -3.37 | 250.76 | 4.49 | 3.45 | 143.48 | 4.00 | R | R |
| 4.97 | -7.88 | 256.77 | 4.48 | 11.50 | 66.39 | 3.99 | R | R |
| 4.96 | -13.22 | 264.18 | 4.47 | 16.96 | 430.98 | 3.98 | R | R |
| 4.95 | -19.35 | 274.10 | 4.46 | 16.92 | 99.78 | 3.97 | R | R |
| 4.94 | -25.51 | 289.11 | 4.45 | -8.48 | 237.32 | 3.96 | R | R |
| 4.93 | -27.25 | 315.22 | 4.44 | R | R | 3.95 | 3.19 | 552.79 |
| 4.92 | 3.81 | 8.11 | 4.43 | R | R | 3.94 | R | R |
| 4.91 | 3.76 | 137.16 | 4.42 | R | R | | | |
| 4.90 | R | R | 4.41 | R | R | | | |
| 4.89 | -8.48 | 343.84 | 4.40 | R | R | | | |
| 4.88 | 19.83 | 55.96 | 4.39 | R | R | | | |
| 4.87 | -10.20 | 304.37 | 4.38 | R | R | | | |
| 4.86 | 13.47 | 54.52 | 4.37 | R | R | | | |
| 4.85 | 17.60 | 56.07 | 4.36 | R | R | | | |
| 4.84 | R | R | 4.35 | R | R | | | |
| 4.83 | R | R | 4.34 | R | R | | | |
| 4.82 | -4.93 | 141.03 | 4.33 | R | R | | | |
| 4.81 | 10.54 | 39.89 | 4.32 | R | R | | | |
| 4.80 | R | R | 4.31 | 14.31 | 899.64 | | | |
| 4.79 | R | R | 4.30 | R | R | | | |
| 4.78 | R | R | 4.29 | 21.01 | 461.84 | | | |
| 4.77 | R | R | 4.28 | R | R | | | |
| 4.76 | R | R | 4.27 | R | R | | | |
| 4.75 | R | R | 4.26 | R | R | | | |
| 4.74 | R | R | 4.25 | R | R | | | |
| 4.73 | R | R | 4.24 | R | R | | | |
| 4.72 | R | R | 4.23 | R | R | | | |
| 4.71 | R | R | 4.22 | R | R | | | |
| 4.70 | R | R | 4.21 | R | R | | | |
| 4.69 | R | R | 4.20 | R | R | | | |
| 4.68 | R | R | 4.19 | R | R | | | |
| 4.67 | 23.08 | 79.69 | 4.18 | R | R | | | |
| 4.66 | -12.39 | 344.27 | 4.17 | R | R | | | |
| 4.65 | R | R | 4.16 | R | R | | | |
| 4.64 | 1.56 | 3.04 | 4.15 | R | R | | | |

# Australian Neutron Monitor Data for the 16 February 1984 Event

by

A.G. Fenton, K.B.Fenton and J.E. Humble
Physics Department, University of Tasmania
G.P.O. Box 252C, Hobart, Tasmania, Australia 7001

Details of the neutron monitor network operated by the University of Tasmania in February 1984 are given in Table 1. Data obtained by these monitors on 15 and 16 February are tabulated in Tables 2 to 7 in the format suggested by Shea et al. (1985) as later modified by Shea et al. (1987, in preparation). In the modified format adopted here the columns headed TD refer to time accuracy and status of the data. In the present tabulations, all data have time accuracy better than 1 minute (the first zero) and no instrumental difficulties were experienced (the second zero).

Table 1. Neutron Monitor Network Operated by the University of Tasmania

| Location | Type of Monitor | Geographic Lat | Geographic Long | Altitude meters | Cutoff Rigidity GV |
|---|---|---|---|---|---|
| Mawson | 12-NM-57 | S67.30 | E 62.88 | sea level | 0.22 |
| Mt. Wellington | 6-NM-64 | 42.92 | 147.23 | 725 | 1.89 |
| Hobart | 12-NM-57 | 42.90 | 147.33 | sea level | 1.89 |
| Hobart | 9-NM-64 | 42.90 | 147.33 | sea level | 1.89 |
| Brisbane | 9-NM-64 | 27.42 | 153.08 | sea level | 7.24 |
| Darwin | 9-NM-64 | 12.42 | 130.87 | sea level | 14.07 |

The onset of the Ground Level Event (GLE) is assumed to occur during the timing interval which first attains 2 $\sigma$ above the pre-event level. The latter is chosen to be the period 0800-0900 UT on 16 February. $\sigma$ is calculated from the scatter of the 12 5-minute recordings registered during that period. According to this criterion, onset was observed in the interval 0905-0910 UT at all monitors for which 5-minute recording was in use. The same criterion, applied to 1-minute intervals, reveals that onset was observed by the Hobart IGY type monitor during the interval 0907-0908 UT, and at Mawson during 0906-0907 UT.

At Mawson the intensity rose to its peak value within three minutes of onset, reaching a level of 60.6% above the pre-event level during 0909-0910 UT. In the Hobart area the peak was reached several minutes later during the 0915-0920 UT, with Mt. Wellington registering a 16.9% increase and the IQSY monitor at sea level reaching 15.6%. The 1-minute data obtained by the smaller Hobart IGY monitor showed multiple peaks during the interval 0914 to 0924 UT.

The increase was short-lived, and was essentially ended by 1100 UT. The average intensity for the hour 1000-1100 UT was significantly greater than the pre-event level at both Mawson and Hobart. The last 5 minute value $\geq 2\ \sigma$ above the pre-event level at Mawson was that for 1015-1020 UT. In the Hobart area the last 5-minute values to be $\geq 2\ \sigma$ above the pre-event levels occurred at different times at the three monitors. For the Hobart IQSY monitor the last value to be $\geq 2\ \sigma$ above the pre-event level occurred during 0955-1000 UT, while the IGY type monitor which operates by the side of the IQSY instrument was already below the 2 $\sigma$ level by that time, but was $\geq 2\ \sigma$ above the pre-event level during 1015-1020 and 1040-1045 UT. The Mt. Wellington monitor, which is approximately 7 km west of the Hobart observatory, had 5 minute values $\geq 2\ \sigma$ above the pre-event level during 1005-1010 and 1055-1100 UT. These observations suggest that the flare particles did not uniformly illuminate the Hobart area.

No statistically significant increase was discernable in the short-period data recorded at Brisbane. However, the count total recorded by the Brisbane monitor for the hour 0900-1000 UT shows an approximately 1% increase over the count total for the previous hour (Table 6). No increase at all was seen at Darwin (Table 7), and the evidence therefore suggests that the spectrum for this event extended up to at least 7 GV but did not reach 14 GV.

## REFERENCES

SHEA, M.A.
D.F. SMART,
M. WADA and
A. INOUE

"A suggested standardised format for Cosmic Ray Ground Level Data," **Proc 19th Int. Cos. Ray. Conf., 5**, 510-513.

TABLE 2

MAWSON LATITUDE -67.60 LONGITUDE 62.88 ALTITUDE 0 M
MAWSON INSTRUMENT 12NM57 ICY NEUTRON MONITOR
MAWSON STANDARD PRESSURE 990.0 (MB) COEFFICIENT -0.739 % / (MB)
MAWSON PRE-INCREASE BASELINE TIME INTERVAL 84 02 16 080000-090000 UT
MAWSON PRE-INCREASE AVERAGE COUNTING RATE 9.78 COUNTS PER SECOND

| STATION | YY | MM | DD | MIN | TIME (UT) INTERVAL | CODE TD | UNCOR. | PRES. (mb) | COR. | % INC. |
|---|---|---|---|---|---|---|---|---|---|---|
| MAWSON | 84 | 02 | 15 | 60 | 000000-010000 | 00 | 9.87 | 989.1 | 9.80 | 0.2 |
| MAWSON | 84 | 02 | 15 | 60 | 010000-020000 | 00 | 9.88 | 989.4 | 9.84 | 0.6 |
| MAWSON | 84 | 02 | 15 | 60 | 020000-030000 | 00 | 9.87 | 989.2 | 9.81 | 0.3 |
| MAWSON | 84 | 02 | 15 | 60 | 030000-040000 | 00 | 9.90 | 989.0 | 9.83 | 0.5 |
| MAWSON | 84 | 02 | 15 | 60 | 040000-050000 | 00 | 9.96 | 989.1 | 9.89 | 1.1 |
| MAWSON | 84 | 02 | 15 | 60 | 050000-060000 | 00 | 9.87 | 989.4 | 9.82 | 0.4 |
| MAWSON | 84 | 02 | 15 | 60 | 060000-070000 | 00 | 9.80 | 989.7 | 9.77 | -0.1 |
| MAWSON | 84 | 02 | 15 | 60 | 070000-080000 | 00 | 9.81 | 990.0 | 9.81 | 0.3 |
| MAWSON | 84 | 02 | 15 | 60 | 080000-090000 | 00 | 9.80 | 989.8 | 9.78 | 0.0 |
| MAWSON | 84 | 02 | 15 | 60 | 090000-100000 | 00 | 9.96 | 989.5 | 9.92 | 1.4 |
| MAWSON | 84 | 02 | 15 | 60 | 100000-110000 | 00 | 9.88 | 989.0 | 9.81 | 0.3 |
| MAWSON | 84 | 02 | 15 | 60 | 110000-120000 | 00 | 10.04 | 988.7 | 9.95 | 1.7 |
| MAWSON | 84 | 02 | 15 | 60 | 120000-130000 | 00 | 9.97 | 988.3 | 9.85 | 0.7 |
| MAWSON | 84 | 02 | 15 | 60 | 130000-140000 | 00 | 10.01 | 987.7 | 9.84 | 0.6 |
| MAWSON | 84 | 02 | 15 | 60 | 140000-150000 | 00 | 10.08 | 987.0 | 9.86 | 0.8 |
| MAWSON | 84 | 02 | 15 | 60 | 150000-160000 | 00 | 10.10 | 986.4 | 9.83 | 0.5 |
| MAWSON | 84 | 02 | 15 | 60 | 160000-170000 | 00 | 10.12 | 986.0 | 9.82 | 0.4 |
| MAWSON | 84 | 02 | 15 | 60 | 170000-180000 | 00 | 10.28 | 985.0 | 9.90 | 1.3 |
| MAWSON | 84 | 02 | 15 | 60 | 180000-190000 | 00 | 10.15 | 984.0 | 9.71 | -0.7 |
| MAWSON | 84 | 02 | 15 | 60 | 190000-200000 | 00 | 10.40 | 983.6 | 9.92 | 1.4 |
| MAWSON | 84 | 02 | 15 | 60 | 200000-210000 | 00 | 10.47 | 982.6 | 9.91 | 1.4 |
| MAWSON | 84 | 02 | 15 | 60 | 210000-220000 | 00 | 10.49 | 982.2 | 9.90 | 1.2 |
| MAWSON | 84 | 02 | 15 | 60 | 220000-230000 | 00 | 10.49 | 981.9 | 9.88 | 1.0 |
| MAWSON | 84 | 02 | 15 | 60 | 230000-240000 | 00 | 10.60 | 981.3 | 9.94 | 1.6 |
| MAWSON | 84 | 02 | 16 | 60 | 000000-010000 | 00 | 10.51 | 980.8 | 9.82 | 0.4 |
| MAWSON | 84 | 02 | 16 | 60 | 010000-020000 | 00 | 10.42 | 980.7 | 9.73 | -0.6 |
| MAWSON | 84 | 02 | 16 | 60 | 020000-030000 | 00 | 10.77 | 980.5 | 10.04 | 2.7 |
| MAWSON | 84 | 02 | 16 | 60 | 030000-040000 | 00 | 10.45 | 980.5 | 9.74 | -0.4 |
| MAWSON | 84 | 02 | 16 | 60 | 040000-050000 | 00 | 10.70 | 980.4 | 9.97 | 1.9 |
| MAWSON | 84 | 02 | 16 | 60 | 050000-060000 | 00 | 10.70 | 980.1 | 9.95 | 1.7 |
| MAWSON | 84 | 02 | 16 | 60 | 060000-070000 | 00 | 10.63 | 980.1 | 9.88 | 1.0 |
| MAWSON | 84 | 02 | 16 | 60 | 070000-080000 | 00 | 10.47 | 980.3 | 9.75 | -0.3 |
| MAWSON | 84 | 02 | 16 | 05 | 080000-080500 | 00 | 10.13 | 980.6 | 9.45 | -3.3 |
| MAWSON | 84 | 02 | 16 | 05 | 080500-081000 | 00 | 10.24 | 980.6 | 9.55 | -2.3 |
| MAWSON | 84 | 02 | 16 | 05 | 081000-081500 | 00 | 10.56 | 980.7 | 9.86 | 0.8 |
| MAWSON | 84 | 02 | 16 | 05 | 081500-082000 | 00 | 10.67 | 980.7 | 9.96 | 1.8 |
| MAWSON | 84 | 02 | 16 | 05 | 082000-082500 | 00 | 10.77 | 980.7 | 10.06 | 2.8 |
| MAWSON | 84 | 02 | 16 | 05 | 082500-083000 | 00 | 10.88 | 980.8 | 10.16 | 3.9 |
| MAWSON | 84 | 02 | 16 | 05 | 083000-083500 | 00 | 10.29 | 980.8 | 9.62 | -1.7 |
| MAWSON | 84 | 02 | 16 | 05 | 083500-084000 | 00 | 10.19 | 980.8 | 9.52 | -2.7 |
| MAWSON | 84 | 02 | 16 | 05 | 084000-084500 | 00 | 10.67 | 980.8 | 9.97 | 1.9 |
| MAWSON | 84 | 02 | 16 | 05 | 084500-085000 | 00 | 10.24 | 980.9 | 9.57 | -2.1 |
| MAWSON | 84 | 02 | 16 | 05 | 085000-085500 | 00 | 10.67 | 980.9 | 9.97 | 2.0 |
| MAWSON | 84 | 02 | 16 | 05 | 085500-090000 | 00 | 10.35 | 980.9 | 9.67 | -1.1 |
| MAWSON | 84 | 02 | 16 | 05 | 090000-090500 | 00 | 10.93 | 980.9 | 10.22 | 4.5 |
| MAWSON | 84 | 02 | 16 | 01 | 090500-090600 | 00 | 11.20 | 980.9 | 10.47 | 7.1 |
| MAWSON | 84 | 02 | 16 | 01 | 090600-090700 | 00 | 13.33 | 980.9 | 12.47 | 27.5 |
| MAWSON | 84 | 02 | 16 | 01 | 090700-090800 | 00 | 14.13 | 980.9 | 13.21 | 35.1 |
| MAWSON | 84 | 02 | 16 | 01 | 090800-090900 | 00 | 16.00 | 980.9 | 14.96 | 53.0 |
| MAWSON | 84 | 02 | 16 | 01 | 090900-091000 | 00 | 16.80 | 980.9 | 15.71 | 60.6 |
| MAWSON | 84 | 02 | 16 | 01 | 091000-091100 | 00 | 16.53 | 980.9 | 15.46 | 58.1 |
| MAWSON | 84 | 02 | 16 | 01 | 091100-091200 | 00 | 15.73 | 980.9 | 14.71 | 50.4 |
| MAWSON | 84 | 02 | 16 | 01 | 091200-091300 | 00 | 16.00 | 980.9 | 14.96 | 53.0 |
| MAWSON | 84 | 02 | 16 | 01 | 091300-091400 | 00 | 14.13 | 980.9 | 13.21 | 35.1 |
| MAWSON | 84 | 02 | 16 | 01 | 091400-091500 | 00 | 15.73 | 980.9 | 14.71 | 50.4 |

Table 2 continued

| STATION | YY | MM | DD | MIN | TIME (UT) INTERVAL | CODE TD | UNCOR. | PRES. (mb) | COR. | % INC. |
|---|---|---|---|---|---|---|---|---|---|---|
| MAWSON | 84 | 02 | 16 | 01 | 091500-091600 | 00 | 14.93 | 980.9 | 13.96 | 42.8 |
| MAWSON | 84 | 02 | 16 | 01 | 091600-091700 | 00 | 13.87 | 980.9 | 12.96 | 32.6 |
| MAWSON | 84 | 02 | 16 | 01 | 091700-091800 | 00 | 14.13 | 980.9 | 13.21 | 35.1 |
| MAWSON | 84 | 02 | 16 | 01 | 091800-091900 | 00 | 14.40 | 980.9 | 13.46 | 37.7 |
| MAWSON | 84 | 02 | 16 | 01 | 091900-092000 | 00 | 13.60 | 980.9 | 12.72 | 30.0 |
| MAWSON | 84 | 02 | 16 | 01 | 092000-092100 | 00 | 13.60 | 980.9 | 12.72 | 30.0 |
| MAWSON | 84 | 02 | 16 | 01 | 092100-092200 | 00 | 12.80 | 980.9 | 11.97 | 22.4 |
| MAWSON | 84 | 02 | 16 | 01 | 092200-092300 | 00 | 12.53 | 980.9 | 11.72 | 19.8 |
| MAWSON | 84 | 02 | 16 | 01 | 092300-092400 | 00 | 13.07 | 980.9 | 12.22 | 24.9 |
| MAWSON | 84 | 02 | 16 | 01 | 092400-092500 | 00 | 12.80 | 980.9 | 11.97 | 22.4 |
| MAWSON | 84 | 02 | 16 | 01 | 092500-092600 | 00 | 13.33 | 980.9 | 12.47 | 27.5 |
| MAWSON | 84 | 02 | 16 | 01 | 092600-092700 | 00 | 12.53 | 980.9 | 11.72 | 19.8 |
| MAWSON | 84 | 02 | 16 | 01 | 092700-092800 | 00 | 11.47 | 980.9 | 10.72 | 9.6 |
| MAWSON | 84 | 02 | 16 | 01 | 092800-092900 | 00 | 12.00 | 980.9 | 11.22 | 14.7 |
| MAWSON | 84 | 02 | 16 | 01 | 092900-093000 | 00 | 12.27 | 980.9 | 11.47 | 17.3 |
| MAWSON | 84 | 02 | 16 | 01 | 093000-093100 | 00 | 12.00 | 980.9 | 11.22 | 14.7 |
| MAWSON | 84 | 02 | 16 | 01 | 093100-093200 | 00 | 12.00 | 980.9 | 11.22 | 14.7 |
| MAWSON | 84 | 02 | 16 | 01 | 093200-093300 | 00 | 12.27 | 980.9 | 11.47 | 17.3 |
| MAWSON | 84 | 02 | 16 | 01 | 093300-093400 | 00 | 11.20 | 980.9 | 10.47 | 7.1 |
| MAWSON | 84 | 02 | 16 | 01 | 093400-093500 | 00 | 11.73 | 980.9 | 10.97 | 12.2 |
| MAWSON | 84 | 02 | 16 | 01 | 093500-093600 | 00 | 12.00 | 980.9 | 11.22 | 14.7 |
| MAWSON | 84 | 02 | 16 | 01 | 093600-093700 | 00 | 12.80 | 980.9 | 11.97 | 22.4 |
| MAWSON | 84 | 02 | 16 | 01 | 093700-093800 | 00 | 11.47 | 980.9 | 10.72 | 9.6 |
| MAWSON | 84 | 02 | 16 | 01 | 093800-093900 | 00 | 11.20 | 980.9 | 10.47 | 7.1 |
| MAWSON | 84 | 02 | 16 | 01 | 093900-094000 | 00 | 11.20 | 980.9 | 10.47 | 7.1 |
| MAWSON | 84 | 02 | 16 | 01 | 094000-094100 | 00 | 11.20 | 980.9 | 10.47 | 7.1 |
| MAWSON | 84 | 02 | 16 | 01 | 094100-094200 | 00 | 10.40 | 980.9 | 9.72 | -0.6 |
| MAWSON | 84 | 02 | 16 | 01 | 094200-094300 | 00 | 11.20 | 980.9 | 10.47 | 7.1 |
| MAWSON | 84 | 02 | 16 | 01 | 094300-094400 | 00 | 12.00 | 980.9 | 11.22 | 14.7 |
| MAWSON | 84 | 02 | 16 | 01 | 094400-094500 | 00 | 11.20 | 980.9 | 10.47 | 7.1 |
| MAWSON | 84 | 02 | 16 | 01 | 094500-094600 | 00 | 12.80 | 980.9 | 11.97 | 22.4 |
| MAWSON | 84 | 02 | 16 | 01 | 094600-094700 | 00 | 11.47 | 980.9 | 10.72 | 9.6 |
| MAWSON | 84 | 02 | 16 | 01 | 094700-094800 | 00 | 11.73 | 980.9 | 10.97 | 12.2 |
| MAWSON | 84 | 02 | 16 | 01 | 094800-094900 | 00 | 10.93 | 980.9 | 10.22 | 4.5 |
| MAWSON | 84 | 02 | 16 | 01 | 094900-095000 | 00 | 11.73 | 980.9 | 10.97 | 12.2 |
| MAWSON | 84 | 02 | 16 | 01 | 095000-095100 | 00 | 10.67 | 980.9 | 9.97 | 2.0 |
| MAWSON | 84 | 02 | 16 | 01 | 095100-095200 | 00 | 11.73 | 980.9 | 10.97 | 12.2 |
| MAWSON | 84 | 02 | 16 | 01 | 095200-095300 | 00 | 12.00 | 980.9 | 11.22 | 14.7 |
| MAWSON | 84 | 02 | 16 | 01 | 095300-095400 | 00 | 12.00 | 980.9 | 11.22 | 14.7 |
| MAWSON | 84 | 02 | 16 | 01 | 095400-095500 | 00 | 10.13 | 980.9 | 9.47 | -3.1 |
| MAWSON | 84 | 02 | 16 | 01 | 095500-095600 | 00 | 11.47 | 980.9 | 10.72 | 9.6 |
| MAWSON | 84 | 02 | 16 | 01 | 095600-095700 | 00 | 10.93 | 980.9 | 10.22 | 4.5 |
| MAWSON | 84 | 02 | 16 | 01 | 095700-095800 | 00 | 11.20 | 980.9 | 10.47 | 7.1 |
| MAWSON | 84 | 02 | 16 | 01 | 095800-095900 | 00 | 10.67 | 980.9 | 9.97 | 2.0 |
| MAWSON | 84 | 02 | 16 | 01 | 095900-100000 | 00 | 11.47 | 980.9 | 10.72 | 9.6 |
| MAWSON | 84 | 02 | 16 | 05 | 100000-100500 | 00 | 11.47 | 981.0 | 10.73 | 9.7 |
| MAWSON | 84 | 02 | 16 | 05 | 100500-101000 | 00 | 10.88 | 981.0 | 10.18 | 4.1 |
| MAWSON | 84 | 02 | 16 | 05 | 101000-101500 | 00 | 10.93 | 981.0 | 10.23 | 4.6 |
| MAWSON | 84 | 02 | 16 | 05 | 101500-102000 | 00 | 11.15 | 981.0 | 10.43 | 6.6 |
| MAWSON | 84 | 02 | 16 | 05 | 102000-102500 | 00 | 10.72 | 981.0 | 10.03 | 2.6 |
| MAWSON | 84 | 02 | 16 | 05 | 102500-103000 | 00 | 10.93 | 981.0 | 10.23 | 4.6 |
| MAWSON | 84 | 02 | 16 | 05 | 103000-103500 | 00 | 10.61 | 981.0 | 9.93 | 1.5 |
| MAWSON | 84 | 02 | 16 | 05 | 103500-104000 | 00 | 10.77 | 981.0 | 10.08 | 3.1 |
| MAWSON | 84 | 02 | 16 | 05 | 104000-104500 | 00 | 10.88 | 981.0 | 10.18 | 4.1 |
| MAWSON | 84 | 02 | 16 | 05 | 104500-105000 | 00 | 10.93 | 981.0 | 10.23 | 4.6 |
| MAWSON | 84 | 02 | 16 | 05 | 105000-105500 | 00 | 10.93 | 981.0 | 10.23 | 4.6 |
| MAWSON | 84 | 02 | 16 | 05 | 105500-110000 | 00 | 10.35 | 981.0 | 9.68 | -1.0 |
| MAWSON | 84 | 02 | 16 | 60 | 110000-120000 | 00 | 10.76 | 981.0 | 10.06 | 2.9 |
| MAWSON | 84 | 02 | 16 | 60 | 120000-130000 | 00 | 10.65 | 980.8 | 9.95 | 1.7 |
| MAWSON | 84 | 02 | 16 | 60 | 130000-140000 | 00 | 10.72 | 980.6 | 10.00 | 2.3 |

TABLE 3

MTWELLNGTN LATITUDE -42.92 LONGITUDE 147.23 ALTITUDE 725 M
MTWELLNGTN INSTRUMENT 6NM64 IQSY NEUTRON MONITOR
MTWELLNGTN STANDARD PRESSURE 696.0 (MM/HG) COEFFICIENT -0.985 % / (MM)
MTWELLNGTN PRE-INCREASE BASELINE TIME INTERVAL 84 02 16 080000-090000 UT
MTWELLNGTN PRE-INCREASE AVERAGE COUNTING RATE 116.02 COUNTS PER SECOND

| STATION | YY | MM | DD | MIN | TIME (UT) INTERVAL | CODE TD | UNCOR. | PRES. (MM) | COR. | % INC. |
|---|---|---|---|---|---|---|---|---|---|---|
| MTWELLNGTN | 84 | 02 | 15 | 60 | 000000-010000 | 00 | 114.28 | 696.1 | 114.39 | -1.4 |
| MTWELLNGTN | 84 | 02 | 15 | 60 | 010000-020000 | 00 | 115.73 | 695.7 | 115.39 | -0.5 |
| MTWELLNGTN | 84 | 02 | 15 | 60 | 020000-030000 | 00 | 116.27 | 695.3 | 115.47 | -0.5 |
| MTWELLNGTN | 84 | 02 | 15 | 60 | 030000-040000 | 00 | 116.69 | 694.9 | 115.44 | -0.5 |
| MTWELLNGTN | 84 | 02 | 15 | 60 | 040000-050000 | 00 | 117.05 | 694.7 | 115.56 | -0.4 |
| MTWELLNGTN | 84 | 02 | 15 | 60 | 050000-060000 | 00 | 117.65 | 694.3 | 115.70 | -0.3 |
| MTWELLNGTN | 84 | 02 | 15 | 60 | 060000-070000 | 00 | 117.94 | 693.7 | 115.30 | -0.6 |
| MTWELLNGTN | 84 | 02 | 15 | 60 | 070000-080000 | 00 | 118.08 | 693.3 | 114.98 | -0.9 |
| MTWELLNGTN | 84 | 02 | 15 | 60 | 080000-090000 | 00 | 118.61 | 692.9 | 115.05 | -0.8 |
| MTWELLNGTN | 84 | 02 | 15 | 60 | 090000-100000 | 00 | 118.90 | 692.8 | 115.21 | -0.7 |
| MTWELLNGTN | 84 | 02 | 15 | 60 | 100000-110000 | 00 | 118.44 | 692.7 | 114.65 | -1.2 |
| MTWELLNGTN | 84 | 02 | 15 | 60 | 110000-120000 | 00 | 119.72 | 692.7 | 115.89 | -0.1 |
| MTWELLNGTN | 84 | 02 | 15 | 60 | 120000-130000 | 00 | 119.29 | 692.7 | 115.47 | -0.5 |
| MTWELLNGTN | 84 | 02 | 15 | 60 | 130000-140000 | 00 | 118.51 | 692.7 | 114.72 | -1.1 |
| MTWELLNGTN | 84 | 02 | 15 | 60 | 140000-150000 | 00 | 118.26 | 692.6 | 114.36 | -1.4 |
| MTWELLNGTN | 84 | 02 | 15 | 60 | 150000-160000 | 00 | 119.11 | 692.4 | 114.96 | -0.9 |
| MTWELLNGTN | 84 | 02 | 15 | 60 | 160000-170000 | 00 | 119.79 | 691.9 | 115.05 | -0.8 |
| MTWELLNGTN | 84 | 02 | 15 | 60 | 170000-180000 | 00 | 120.71 | 691.6 | 115.59 | -0.4 |
| MTWELLNGTN | 84 | 02 | 15 | 60 | 180000-190000 | 00 | 120.89 | 691.5 | 115.65 | -0.3 |
| MTWELLNGTN | 84 | 02 | 15 | 60 | 190000-200000 | 00 | 120.78 | 691.5 | 115.55 | -0.4 |
| MTWELLNGTN | 84 | 02 | 15 | 60 | 200000-210000 | 00 | 120.21 | 691.7 | 115.23 | -0.7 |
| MTWELLNGTN | 84 | 02 | 15 | 60 | 210000-220000 | 00 | 119.11 | 692.1 | 114.62 | -1.2 |
| MTWELLNGTN | 84 | 02 | 15 | 60 | 220000-230000 | 00 | 119.18 | 692.3 | 114.92 | -1.0 |
| MTWELLNGTN | 84 | 02 | 15 | 60 | 230000-240000 | 00 | 120.00 | 692.5 | 115.93 | -0.1 |
| MTWELLNGTN | 84 | 02 | 16 | 60 | 000000-010000 | 00 | 119.43 | 692.5 | 115.38 | -0.6 |
| MTWELLNGTN | 84 | 02 | 16 | 60 | 010000-020000 | 00 | 120.07 | 692.4 | 115.89 | -0.1 |
| MTWELLNGTN | 84 | 02 | 16 | 60 | 020000-030000 | 00 | 120.00 | 692.5 | 115.93 | -0.1 |
| MTWELLNGTN | 84 | 02 | 16 | 60 | 030000-040000 | 00 | 119.75 | 692.5 | 115.69 | -0.3 |
| MTWELLNGTN | 84 | 02 | 16 | 60 | 040000-050000 | 00 | 119.93 | 692.6 | 115.98 | 0.0 |
| MTWELLNGTN | 84 | 02 | 16 | 60 | 050000-060000 | 00 | 119.32 | 692.8 | 115.62 | -0.3 |
| MTWELLNGTN | 84 | 02 | 16 | 60 | 060000-070000 | 00 | 119.43 | 693.1 | 116.07 | 0.0 |
| MTWELLNGTN | 84 | 02 | 16 | 60 | 070000-080000 | 00 | 118.86 | 693.5 | 115.97 | 0.0 |
| MTWELLNGTN | 84 | 02 | 16 | 05 | 080000-080500 | 00 | 115.63 | 693.9 | 113.26 | -2.4 |
| MTWELLNGTN | 84 | 02 | 16 | 05 | 080500-081000 | 00 | 118.19 | 694.0 | 115.88 | -0.1 |
| MTWELLNGTN | 84 | 02 | 16 | 05 | 081000-081500 | 00 | 119.47 | 694.1 | 117.25 | 1.1 |
| MTWELLNGTN | 84 | 02 | 16 | 05 | 081500-082000 | 00 | 115.63 | 694.1 | 113.48 | -2.2 |
| MTWELLNGTN | 84 | 02 | 16 | 05 | 082000-082500 | 00 | 121.17 | 694.2 | 119.04 | 2.6 |
| MTWELLNGTN | 84 | 02 | 16 | 05 | 082500-083000 | 00 | 119.47 | 694.3 | 117.48 | 1.3 |
| MTWELLNGTN | 84 | 02 | 16 | 05 | 083000-083500 | 00 | 116.48 | 694.3 | 114.55 | -1.3 |
| MTWELLNGTN | 84 | 02 | 16 | 05 | 083500-084000 | 00 | 119.89 | 694.4 | 118.02 | 1.7 |
| MTWELLNGTN | 84 | 02 | 16 | 05 | 084000-084500 | 00 | 116.91 | 694.5 | 115.19 | -0.7 |
| MTWELLNGTN | 84 | 02 | 16 | 05 | 084500-085000 | 00 | 116.48 | 694.6 | 114.88 | -1.0 |
| MTWELLNGTN | 84 | 02 | 16 | 05 | 085000-085500 | 00 | 117.76 | 694.6 | 116.15 | 0.1 |
| MTWELLNGTN | 84 | 02 | 16 | 05 | 085500-090000 | 00 | 118.61 | 694.7 | 117.10 | 0.9 |
| MTWELLNGTN | 84 | 02 | 16 | 05 | 090000-090500 | 00 | 116.48 | 694.8 | 115.11 | -0.8 |
| MTWELLNGTN | 84 | 02 | 16 | 05 | 090500-091000 | 00 | 122.03 | 694.9 | 120.71 | 4.0 |
| MTWELLNGTN | 84 | 02 | 16 | 05 | 091000-091500 | 00 | 136.11 | 694.9 | 134.64 | 16.0 |
| MTWELLNGTN | 84 | 02 | 16 | 05 | 091500-092000 | 00 | 136.96 | 695.0 | 135.62 | 16.9 |
| MTWELLNGTN | 84 | 02 | 16 | 05 | 092000-092500 | 00 | 133.97 | 695.1 | 132.79 | 14.5 |
| MTWELLNGTN | 84 | 02 | 16 | 05 | 092500-093000 | 00 | 130.13 | 695.2 | 129.11 | 11.3 |
| MTWELLNGTN | 84 | 02 | 16 | 05 | 093000-093500 | 00 | 130.56 | 695.2 | 129.54 | 11.6 |
| MTWELLNGTN | 84 | 02 | 16 | 05 | 093500-094000 | 00 | 122.88 | 695.3 | 122.04 | 5.2 |
| MTWELLNGTN | 84 | 02 | 16 | 05 | 094000-094500 | 00 | 126.72 | 695.4 | 125.97 | 8.6 |
| MTWELLNGTN | 84 | 02 | 16 | 05 | 094500-095000 | 00 | 125.01 | 695.4 | 124.28 | 7.1 |
| MTWELLNGTN | 84 | 02 | 16 | 05 | 095000-095500 | 00 | 124.59 | 695.5 | 123.97 | 6.9 |

Table 3 continued

| STATION | YY | MM | DD | MIN | TIME (UT) INTERVAL | CODE TD | UNCOR. | PRES. (MM) | COR. | % INC. |
|---|---|---|---|---|---|---|---|---|---|---|
| MTWELLNGTN | 84 | 02 | 16 | 05 | 095500-100000 | 00 | 120.75 | 695.6 | 120.27 | 3.7 |
| MTWELLNGTN | 84 | 02 | 16 | 05 | 100000-100500 | 00 | 120.32 | 695.6 | 119.85 | 3.3 |
| MTWELLNGTN | 84 | 02 | 16 | 05 | 100500-101000 | 00 | 121.60 | 695.7 | 121.24 | 4.5 |
| MTWELLNGTN | 84 | 02 | 16 | 05 | 101000-101500 | 00 | 121.17 | 695.8 | 120.93 | 4.2 |
| MTWELLNGTN | 84 | 02 | 16 | 05 | 101500-102000 | 00 | 120.75 | 695.8 | 120.51 | 3.9 |
| MTWELLNGTN | 84 | 02 | 16 | 05 | 102000-102500 | 00 | 116.48 | 695.9 | 116.37 | 0.3 |
| MTWELLNGTN | 84 | 02 | 16 | 05 | 102500-103000 | 00 | 120.75 | 696.0 | 120.75 | 4.1 |
| MTWELLNGTN | 84 | 02 | 16 | 05 | 103000-103500 | 00 | 117.76 | 696.0 | 117.76 | 1.5 |
| MTWELLNGTN | 84 | 02 | 16 | 05 | 103500-104000 | 00 | 118.19 | 696.1 | 118.30 | 2.0 |
| MTWELLNGTN | 84 | 02 | 16 | 05 | 104000-104500 | 00 | 119.47 | 696.1 | 119.58 | 3.1 |
| MTWELLNGTN | 84 | 02 | 16 | 05 | 104500-105000 | 00 | 115.63 | 696.1 | 115.74 | -0.2 |
| MTWELLNGTN | 84 | 02 | 16 | 05 | 105000-105500 | 00 | 113.07 | 696.2 | 113.29 | -2.4 |
| MTWELLNGTN | 84 | 02 | 16 | 05 | 105500-110000 | 00 | 121.60 | 696.2 | 121.84 | 5.0 |
| MTWELLNGTN | 84 | 02 | 16 | 60 | 110000-120000 | 00 | 116.05 | 696.5 | 116.63 | 0.5 |
| MTWELLNGTN | 84 | 02 | 16 | 60 | 120000-130000 | 00 | 114.88 | 696.9 | 115.90 | -0.1 |
| MTWELLNGTN | 84 | 02 | 16 | 60 | 130000-140000 | 00 | 114.31 | 697.3 | 115.78 | -0.2 |
| MTWELLNGTN | 84 | 02 | 16 | 60 | 140000-150000 | 00 | 113.64 | 697.7 | 115.55 | -0.4 |
| MTWELLNGTN | 84 | 02 | 16 | 60 | 150000-160000 | 00 | 113.17 | 698.0 | 115.42 | -0.5 |
| MTWELLNGTN | 84 | 02 | 16 | 60 | 160000-170000 | 00 | 112.39 | 698.3 | 114.97 | -0.9 |
| MTWELLNGTN | 84 | 02 | 16 | 60 | 170000-180000 | 00 | 112.68 | 698.5 | 115.48 | -0.5 |
| MTWELLNGTN | 84 | 02 | 16 | 60 | 180000-190000 | 00 | 111.93 | 698.7 | 114.95 | -0.9 |
| MTWELLNGTN | 84 | 02 | 16 | 60 | 190000-200000 | 00 | 111.96 | 699.3 | 115.66 | -0.3 |
| MTWELLNGTN | 84 | 02 | 16 | 60 | 200000-210000 | 00 | 110.47 | 700.1 | 115.02 | -0.9 |
| MTWELLNGTN | 84 | 02 | 16 | 60 | 210000-220000 | 00 | 110.29 | 700.7 | 115.52 | -0.4 |
| MTWELLNGTN | 84 | 02 | 16 | 60 | 220000-230000 | 00 | 109.72 | 701.3 | 115.60 | -0.4 |
| MTWELLNGTN | 84 | 02 | 16 | 60 | 230000-240000 | 00 | 109.55 | 701.7 | 115.87 | -0.1 |

TABLE 4

HOBART LATITUDE -42.90 LONGITUDE 147.22 ALTITUDE 0 M
HOBART INSTRUMENT IGY NEUTRON MONITOR
HOBART STANDARD PRESSURE 1012.5 (MB) COEFFICIENT -0.739 % / (MB)
HOBART PRE-INCREASE BASELINE TIME INTERVAL 84 02 16 080000-090000 UT
HOBART PRE-INCREASE AVERAGE COUNTING RATE 8.05 COUNTS PER SECOND

| STATION | YY | MM | DD | MIN | TIME (UT) INTERVAL | CODE TD | UNCOR. | PRES. (mb) | COR. | % INC. |
|---|---|---|---|---|---|---|---|---|---|---|
| HOBART | 84 | 02 | 15 | 60 | 000000-010000 | 00 | 8.39 | 1006.5 | 8.03 | -0.3 |
| HOBART | 84 | 02 | 15 | 60 | 010000-020000 | 00 | 8.41 | 1005.5 | 7.98 | -0.8 |
| HOBART | 84 | 02 | 15 | 60 | 020000-030000 | 00 | 8.52 | 1004.3 | 8.01 | -0.4 |
| HOBART | 84 | 02 | 15 | 60 | 030000-040000 | 00 | 8.50 | 1003.7 | 7.96 | -1.1 |
| HOBART | 84 | 02 | 15 | 60 | 040000-050000 | 00 | 8.59 | 1003.2 | 8.02 | -0.4 |
| HOBART | 84 | 02 | 15 | 60 | 050000-060000 | 00 | 8.68 | 1002.4 | 8.05 | 0.1 |
| HOBART | 84 | 02 | 15 | 60 | 060000-070000 | 00 | 8.60 | 1001.7 | 7.94 | -1.3 |
| HOBART | 84 | 02 | 15 | 60 | 070000-080000 | 00 | 8.69 | 1001.2 | 8.00 | -0.6 |
| HOBART | 84 | 02 | 15 | 60 | 080000-090000 | 00 | 8.62 | 1000.7 | 7.90 | -1.8 |
| HOBART | 84 | 02 | 15 | 60 | 090000-100000 | 00 | 8.76 | 1000.4 | 8.01 | -0.4 |
| HOBART | 84 | 02 | 15 | 60 | 100000-110000 | 00 | 8.80 | 1000.2 | 8.04 | -0.2 |
| HOBART | 84 | 02 | 15 | 60 | 110000-120000 | 00 | 8.69 | 1000.3 | 7.94 | -1.3 |
| HOBART | 84 | 02 | 15 | 60 | 120000-130000 | 00 | 8.82 | 1000.4 | 8.06 | 0.2 |
| HOBART | 84 | 02 | 15 | 60 | 130000-140000 | 00 | 8.64 | 1000.5 | 7.91 | -1.7 |
| HOBART | 84 | 02 | 15 | 60 | 140000-150000 | 00 | 8.69 | 1000.7 | 7.97 | -1.0 |
| HOBART | 84 | 02 | 15 | 60 | 150000-160000 | 00 | 8.82 | 1000.5 | 8.07 | 0.3 |
| HOBART | 84 | 02 | 15 | 60 | 160000-170000 | 00 | 8.59 | 1000.1 | 7.83 | -2.6 |
| HOBART | 84 | 02 | 15 | 60 | 170000-180000 | 00 | 8.71 | 999.7 | 7.92 | -1.5 |
| HOBART | 84 | 02 | 15 | 60 | 180000-190000 | 00 | 8.75 | 999.5 | 7.95 | -1.3 |
| HOBART | 84 | 02 | 15 | 60 | 190000-200000 | 00 | 8.78 | 999.6 | 7.98 | -0.8 |
| HOBART | 84 | 02 | 15 | 60 | 200000-210000 | 00 | 8.82 | 1000.1 | 8.05 | 0.0 |
| HOBART | 84 | 02 | 15 | 60 | 210000-220000 | 00 | 8.71 | 1000.5 | 7.97 | -0.9 |
| HOBART | 84 | 02 | 15 | 60 | 220000-230000 | 00 | 8.76 | 1000.7 | 8.03 | -0.2 |
| HOBART | 84 | 02 | 15 | 60 | 230000-240000 | 00 | 8.62 | 1000.5 | 7.89 | -2.0 |
| HOBART | 84 | 02 | 16 | 60 | 000000-010000 | 00 | 8.94 | 1000.4 | 8.18 | 1.6 |
| HOBART | 84 | 02 | 16 | 60 | 010000-020000 | 00 | 8.84 | 1000.3 | 8.07 | 0.3 |
| HOBART | 84 | 02 | 16 | 60 | 020000-030000 | 00 | 8.76 | 1000.2 | 8.00 | -0.6 |
| HOBART | 84 | 02 | 16 | 60 | 030000-040000 | 00 | 8.64 | 1000.4 | 7.90 | -1.8 |
| HOBART | 84 | 02 | 16 | 60 | 040000-050000 | 00 | 8.73 | 1000.7 | 8.00 | -0.6 |
| HOBART | 84 | 02 | 16 | 60 | 050000-060000 | 00 | 8.69 | 1001.1 | 7.99 | -0.7 |
| HOBART | 84 | 02 | 16 | 60 | 060000-070000 | 00 | 8.62 | 1001.5 | 7.95 | -1.2 |
| HOBART | 84 | 02 | 16 | 60 | 070000-080000 | 00 | 8.57 | 1002.2 | 7.94 | -1.3 |
| HOBART | 84 | 02 | 16 | 05 | 080000-080500 | 00 | 8.69 | 1002.7 | 8.09 | 0.5 |
| HOBART | 84 | 02 | 16 | 05 | 080500-081000 | 00 | 8.48 | 1002.8 | 7.89 | -1.9 |
| HOBART | 84 | 02 | 16 | 05 | 081000-081500 | 00 | 8.59 | 1002.8 | 7.99 | -0.7 |
| HOBART | 84 | 02 | 16 | 05 | 081500-082000 | 00 | 8.75 | 1002.9 | 8.15 | 1.2 |
| HOBART | 84 | 02 | 16 | 05 | 082000-082500 | 00 | 8.48 | 1003.0 | 7.91 | -1.8 |
| HOBART | 84 | 02 | 16 | 05 | 082500-083000 | 00 | 8.80 | 1003.1 | 8.21 | 2.0 |
| HOBART | 84 | 02 | 16 | 05 | 083000-083500 | 00 | 8.80 | 1003.2 | 8.22 | 2.1 |
| HOBART | 84 | 02 | 16 | 05 | 083500-084000 | 00 | 8.80 | 1003.3 | 8.22 | 2.2 |
| HOBART | 84 | 02 | 16 | 05 | 084000-084500 | 00 | 8.37 | 1003.4 | 7.83 | -2.7 |
| HOBART | 84 | 02 | 16 | 05 | 084500-085000 | 00 | 8.80 | 1003.5 | 8.23 | 2.3 |
| HOBART | 84 | 02 | 16 | 05 | 085000-085500 | 00 | 8.48 | 1003.6 | 7.94 | -1.3 |
| HOBART | 84 | 02 | 16 | 05 | 085500-090000 | 00 | 8.43 | 1003.7 | 7.90 | -1.9 |
| HOBART | 84 | 02 | 16 | 05 | 090000-090500 | 00 | 8.37 | 1003.8 | 7.85 | -2.4 |
| HOBART | 84 | 02 | 16 | 01 | 090500-090600 | 00 | 8.00 | 1003.8 | 7.50 | -6.8 |
| HOBART | 84 | 02 | 16 | 01 | 090600-090700 | 00 | 9.33 | 1003.8 | 8.75 | 8.8 |
| HOBART | 84 | 02 | 16 | 01 | 090700-090800 | 00 | 9.60 | 1003.9 | 9.01 | 11.9 |
| HOBART | 84 | 02 | 16 | 01 | 090800-090900 | 00 | 9.07 | 1003.9 | 8.51 | 5.7 |
| HOBART | 84 | 02 | 16 | 01 | 090900-091000 | 00 | 9.33 | 1003.9 | 8.76 | 8.8 |
| HOBART | 84 | 02 | 16 | 01 | 091000-091100 | 00 | 9.60 | 1003.9 | 9.01 | 11.9 |
| HOBART | 84 | 02 | 16 | 01 | 091100-091200 | 00 | 9.60 | 1003.9 | 9.01 | 11.9 |
| HOBART | 84 | 02 | 16 | 01 | 091200-091300 | 00 | 9.33 | 1004.0 | 8.77 | 8.9 |
| HOBART | 84 | 02 | 16 | 01 | 091300-091400 | 00 | 9.33 | 1004.0 | 8.77 | 8.9 |
| HOBART | 84 | 02 | 16 | 01 | 091400-091500 | 00 | 9.87 | 1004.0 | 9.27 | 15.1 |

Table 4 continued

| STATION | YY | MM | DD | MIN | TIME (UT) INTERVAL | CODE TD | UNCOR. | PRES. (mb) | COR. | % INC. |
|---|---|---|---|---|---|---|---|---|---|---|
| HOBART | 84 | 02 | 16 | 01 | 091500-091600 | 00 | 9.87 | 1004.0 | 9.27 | 15.1 |
| HOBART | 84 | 02 | 16 | 01 | 091600-091700 | 00 | 9.33 | 1004.0 | 8.77 | 8.9 |
| HOBART | 84 | 02 | 16 | 01 | 091700-091800 | 00 | 9.87 | 1004.1 | 9.27 | 15.2 |
| HOBART | 84 | 02 | 16 | 01 | 091800-091900 | 00 | 9.87 | 1004.1 | 9.27 | 15.2 |
| HOBART | 84 | 02 | 16 | 01 | 091900-092000 | 00 | 9.33 | 1004.1 | 8.77 | 9.0 |
| HOBART | 84 | 02 | 16 | 01 | 092000-092100 | 00 | 9.07 | 1004.1 | 8.52 | 5.9 |
| HOBART | 84 | 02 | 16 | 01 | 092100-092200 | 00 | 9.33 | 1004.1 | 8.77 | 9.0 |
| HOBART | 84 | 02 | 16 | 01 | 092200-092300 | 00 | 9.60 | 1004.2 | 9.03 | 12.2 |
| HOBART | 84 | 02 | 16 | 01 | 092300-092400 | 00 | 10.40 | 1004.2 | 9.78 | 21.5 |
| HOBART | 84 | 02 | 16 | 01 | 092400-092500 | 00 | 9.60 | 1004.2 | 9.03 | 12.2 |
| HOBART | 84 | 02 | 16 | 01 | 092500-092600 | 00 | 9.33 | 1004.2 | 8.78 | 9.1 |
| HOBART | 84 | 02 | 16 | 01 | 092600-092700 | 00 | 8.53 | 1004.2 | 8.03 | -0.3 |
| HOBART | 84 | 02 | 16 | 01 | 092700-092800 | 00 | 8.80 | 1004.3 | 8.28 | 2.9 |
| HOBART | 84 | 02 | 16 | 01 | 092800-092900 | 00 | 9.07 | 1004.3 | 8.53 | 6.0 |
| HOBART | 84 | 02 | 16 | 01 | 092900-093000 | 00 | 9.33 | 1004.3 | 8.78 | 9.2 |
| HOBART | 84 | 02 | 16 | 01 | 093000-093100 | 00 | 9.07 | 1004.3 | 8.53 | 6.0 |
| HOBART | 84 | 02 | 16 | 01 | 093100-093200 | 00 | 9.07 | 1004.3 | 8.53 | 6.0 |
| HOBART | 84 | 02 | 16 | 01 | 093200-093300 | 00 | 8.00 | 1004.4 | 7.54 | -6.4 |
| HOBART | 84 | 02 | 16 | 01 | 093300-093400 | 00 | 9.33 | 1004.4 | 8.79 | 9.2 |
| HOBART | 84 | 02 | 16 | 01 | 093400-093500 | 00 | 9.07 | 1004.4 | 8.54 | 6.1 |
| HOBART | 84 | 02 | 16 | 01 | 093500-093600 | 00 | 8.27 | 1004.4 | 7.79 | -3.2 |
| HOBART | 84 | 02 | 16 | 01 | 093600-093700 | 00 | 9.07 | 1004.4 | 8.54 | 6.1 |
| HOBART | 84 | 02 | 16 | 01 | 093700-093800 | 00 | 8.53 | 1004.5 | 8.04 | -0.1 |
| HOBART | 84 | 02 | 16 | 01 | 093800-093900 | 00 | 8.00 | 1004.5 | 7.54 | -6.3 |
| HOBART | 84 | 02 | 16 | 01 | 093900-094000 | 00 | 8.27 | 1004.5 | 7.79 | -3.2 |
| HOBART | 84 | 02 | 16 | 01 | 094000-094100 | 00 | 9.87 | 1004.5 | 9.30 | 15.6 |
| HOBART | 84 | 02 | 16 | 01 | 094100-094200 | 00 | 8.53 | 1004.5 | 8.04 | -0.1 |
| HOBART | 84 | 02 | 16 | 01 | 094200-094300 | 00 | 8.80 | 1004.6 | 8.30 | 3.1 |
| HOBART | 84 | 02 | 16 | 01 | 094300-094400 | 00 | 8.53 | 1004.6 | 8.05 | 0.0 |
| HOBART | 84 | 02 | 16 | 01 | 094400-094500 | 00 | 8.80 | 1004.6 | 8.30 | 3.1 |
| HOBART | 84 | 02 | 16 | 01 | 094500-094600 | 00 | 9.87 | 1004.6 | 9.31 | 15.7 |
| HOBART | 84 | 02 | 16 | 01 | 094600-094700 | 00 | 8.80 | 1004.7 | 8.31 | 3.2 |
| HOBART | 84 | 02 | 16 | 01 | 094700-094800 | 00 | 8.27 | 1004.7 | 7.80 | -3.0 |
| HOBART | 84 | 02 | 16 | 01 | 094800-094900 | 00 | 9.07 | 1004.7 | 8.56 | 6.4 |
| HOBART | 84 | 02 | 16 | 01 | 094900-095000 | 00 | 9.33 | 1004.7 | 8.81 | 9.5 |
| HOBART | 84 | 02 | 16 | 01 | 095000-095100 | 00 | 9.60 | 1004.7 | 9.06 | 12.6 |
| HOBART | 84 | 02 | 16 | 01 | 095100-095200 | 00 | 9.07 | 1004.8 | 8.57 | 6.4 |
| HOBART | 84 | 02 | 16 | 01 | 095200-095300 | 00 | 8.80 | 1004.8 | 8.31 | 3.3 |
| HOBART | 84 | 02 | 16 | 01 | 095300-095400 | 00 | 8.80 | 1004.8 | 8.31 | 3.3 |
| HOBART | 84 | 02 | 16 | 01 | 095400-095500 | 00 | 8.80 | 1004.8 | 8.31 | 3.3 |
| HOBART | 84 | 02 | 16 | 01 | 095500-095600 | 00 | 8.53 | 1004.8 | 8.06 | 0.2 |
| HOBART | 84 | 02 | 16 | 01 | 095600-095700 | 00 | 8.27 | 1004.9 | 7.82 | -2.9 |
| HOBART | 84 | 02 | 16 | 01 | 095700-095800 | 00 | 8.80 | 1004.9 | 8.32 | 3.4 |
| HOBART | 84 | 02 | 16 | 01 | 095800-095900 | 00 | 8.27 | 1004.9 | 7.82 | -2.9 |
| HOBART | 84 | 02 | 16 | 01 | 095900-100000 | 00 | 9.60 | 1004.9 | 9.08 | 12.8 |
| HOBART | 84 | 02 | 16 | 05 | 100000-100500 | 00 | 9.01 | 1005.0 | 8.53 | 6.0 |
| HOBART | 84 | 02 | 16 | 05 | 100500-101000 | 00 | 8.80 | 1005.1 | 8.33 | 3.5 |
| HOBART | 84 | 02 | 16 | 05 | 101000-101500 | 00 | 8.59 | 1005.2 | 8.14 | 1.1 |
| HOBART | 84 | 02 | 16 | 05 | 101500-102000 | 00 | 8.96 | 1005.3 | 8.50 | 5.6 |
| HOBART | 84 | 02 | 16 | 05 | 102000-102500 | 00 | 8.80 | 1005.4 | 8.35 | 3.8 |
| HOBART | 84 | 02 | 16 | 05 | 102500-103000 | 00 | 8.43 | 1005.5 | 8.00 | -0.6 |
| HOBART | 84 | 02 | 16 | 05 | 103000-103500 | 00 | 8.53 | 1005.6 | 8.11 | 0.8 |
| HOBART | 84 | 02 | 16 | 05 | 103500-104000 | 00 | 8.91 | 1005.7 | 8.47 | 5.3 |
| HOBART | 84 | 02 | 16 | 05 | 104000-104500 | 00 | 8.96 | 1005.8 | 8.53 | 6.0 |
| HOBART | 84 | 02 | 16 | 05 | 104500-105000 | 00 | 8.64 | 1005.9 | 8.23 | 2.3 |
| HOBART | 84 | 02 | 16 | 05 | 105000-105500 | 00 | 8.64 | 1006.0 | 8.23 | 2.3 |
| HOBART | 84 | 02 | 16 | 05 | 105500-110000 | 00 | 8.43 | 1006.1 | 8.04 | -0.1 |
| HOBART | 84 | 02 | 16 | 60 | 110000-120000 | 00 | 8.50 | 1006.7 | 8.14 | 1.2 |
| HOBART | 84 | 02 | 16 | 60 | 120000-130000 | 00 | 8.37 | 1007.5 | 8.07 | 0.3 |
| HOBART | 84 | 02 | 16 | 60 | 130000-140000 | 00 | 8.21 | 1008.2 | 7.96 | -1.1 |

TABLE 5

HOBART LATITUDE -42.90 LONGITUDE 147.33 ALTITUDE 0 M
HOBART INSTRUMENT 9NM64 IQSY NEUTRON MONITOR
HOBART STANDARD PRESSURE 1012.5 (MB) COEFFICIENT -0.739 % / (MB)
HOBART PRE-INCREASE BASELINE TIME INTERVAL 84 02 16 080000-090000 UT
HOBART PRE-INCREASE AVERAGE COUNTING RATE 90.86 COUNTS PER SECOND

| STATION | YY | MM | DD | MIN | TIME (UT) INTERVAL | CODE TD | UNCOR. | PRES. (mb) | COR. | % INC. |
|---|---|---|---|---|---|---|---|---|---|---|
| HOBART | 84 | 02 | 15 | 60 | 000000-010000 | 00 | 94.58 | 1006.5 | 90.48 | -0.4 |
| HOBART | 84 | 02 | 15 | 60 | 010000-020000 | 00 | 95.50 | 1005.5 | 90.69 | -0.2 |
| HOBART | 84 | 02 | 15 | 60 | 020000-030000 | 00 | 95.93 | 1004.3 | 90.29 | -0.6 |
| HOBART | 84 | 02 | 15 | 60 | 030000-040000 | 00 | 96.57 | 1003.7 | 90.49 | -0.4 |
| HOBART | 84 | 02 | 15 | 60 | 040000-050000 | 00 | 96.43 | 1003.2 | 90.02 | -0.9 |
| HOBART | 84 | 02 | 15 | 60 | 050000-060000 | 00 | 97.21 | 1002.4 | 90.22 | -0.7 |
| HOBART | 84 | 02 | 15 | 60 | 060000-070000 | 00 | 97.71 | 1001.7 | 90.21 | -0.7 |
| HOBART | 84 | 02 | 15 | 60 | 070000-080000 | 00 | 97.92 | 1001.2 | 90.08 | -0.9 |
| HOBART | 84 | 02 | 15 | 60 | 080000-090000 | 00 | 98.20 | 1000.7 | 90.00 | -0.9 |
| HOBART | 84 | 02 | 15 | 60 | 090000-100000 | 00 | 98.28 | 1000.4 | 89.87 | -1.1 |
| HOBART | 84 | 02 | 15 | 60 | 100000-110000 | 00 | 98.63 | 1000.2 | 90.06 | -0.9 |
| HOBART | 84 | 02 | 15 | 60 | 110000-120000 | 00 | 98.35 | 1000.3 | 89.87 | -1.1 |
| HOBART | 84 | 02 | 15 | 60 | 120000-130000 | 00 | 98.77 | 1000.4 | 90.32 | -0.6 |
| HOBART | 84 | 02 | 15 | 60 | 130000-140000 | 00 | 98.28 | 1000.5 | 89.94 | -1.0 |
| HOBART | 84 | 02 | 15 | 60 | 140000-150000 | 00 | 97.99 | 1000.7 | 89.81 | -1.2 |
| HOBART | 84 | 02 | 15 | 60 | 150000-160000 | 00 | 97.85 | 1000.5 | 89.55 | -1.5 |
| HOBART | 84 | 02 | 15 | 60 | 160000-170000 | 00 | 98.13 | 1000.1 | 89.54 | -1.5 |
| HOBART | 84 | 02 | 15 | 60 | 170000-180000 | 00 | 99.20 | 999.7 | 90.25 | -0.7 |
| HOBART | 84 | 02 | 15 | 60 | 180000-190000 | 00 | 99.34 | 999.5 | 90.24 | -0.7 |
| HOBART | 84 | 02 | 15 | 60 | 190000-200000 | 00 | 99.13 | 999.6 | 90.12 | -0.8 |
| HOBART | 84 | 02 | 15 | 60 | 200000-210000 | 00 | 99.06 | 1000.1 | 90.38 | -0.5 |
| HOBART | 84 | 02 | 15 | 60 | 210000-220000 | 00 | 98.42 | 1000.5 | 90.07 | -0.9 |
| HOBART | 84 | 02 | 15 | 60 | 220000-230000 | 00 | 98.92 | 1000.7 | 90.66 | -0.2 |
| HOBART | 84 | 02 | 15 | 60 | 230000-240000 | 00 | 98.70 | 1000.5 | 90.33 | -0.6 |
| HOBART | 84 | 02 | 16 | 60 | 000000-010000 | 00 | 98.77 | 1000.4 | 90.32 | -0.6 |
| HOBART | 84 | 02 | 16 | 60 | 010000-020000 | 00 | 99.13 | 1000.3 | 90.58 | -0.3 |
| HOBART | 84 | 02 | 16 | 60 | 020000-030000 | 00 | 99.48 | 1000.2 | 90.84 | 0.0 |
| HOBART | 84 | 02 | 16 | 60 | 030000-040000 | 00 | 98.92 | 1000.4 | 90.45 | -0.4 |
| HOBART | 84 | 02 | 16 | 60 | 040000-050000 | 00 | 98.70 | 1000.7 | 90.46 | -0.4 |
| HOBART | 84 | 02 | 16 | 60 | 050000-060000 | 00 | 98.56 | 1001.1 | 90.60 | -0.3 |
| HOBART | 84 | 02 | 16 | 60 | 060000-070000 | 00 | 98.35 | 1001.5 | 90.67 | -0.2 |
| HOBART | 84 | 02 | 16 | 60 | 070000-080000 | 00 | 97.99 | 1002.2 | 90.81 | -0.1 |
| HOBART | 84 | 02 | 16 | 05 | 080000-080500 | 00 | 94.72 | 1002.7 | 88.10 | -3.0 |
| HOBART | 84 | 02 | 16 | 05 | 080500-081000 | 00 | 98.99 | 1002.8 | 92.14 | 1.4 |
| HOBART | 84 | 02 | 16 | 05 | 081000-081500 | 00 | 98.13 | 1002.8 | 91.35 | 0.5 |
| HOBART | 84 | 02 | 16 | 05 | 081500-082000 | 00 | 97.28 | 1002.9 | 90.62 | -0.3 |
| HOBART | 84 | 02 | 16 | 05 | 082000-082500 | 00 | 96.43 | 1003.0 | 89.89 | -1.1 |
| HOBART | 84 | 02 | 16 | 05 | 082500-083000 | 00 | 96.43 | 1003.1 | 89.96 | -1.0 |
| HOBART | 84 | 02 | 16 | 05 | 083000-083500 | 00 | 98.99 | 1003.2 | 92.41 | 1.7 |
| HOBART | 84 | 02 | 16 | 05 | 083500-084000 | 00 | 98.13 | 1003.3 | 91.68 | 0.9 |
| HOBART | 84 | 02 | 16 | 05 | 084000-084500 | 00 | 95.57 | 1003.4 | 89.36 | -1.7 |
| HOBART | 84 | 02 | 16 | 05 | 084500-085000 | 00 | 96.43 | 1003.5 | 90.22 | -0.7 |
| HOBART | 84 | 02 | 16 | 05 | 085000-085500 | 00 | 98.13 | 1003.6 | 91.89 | 1.1 |
| HOBART | 84 | 02 | 16 | 05 | 085500-090000 | 00 | 98.99 | 1003.7 | 92.75 | 2.1 |
| HOBART | 84 | 02 | 16 | 05 | 090000-090500 | 00 | 95.57 | 1003.8 | 89.62 | -1.4 |
| HOBART | 84 | 02 | 16 | 05 | 090500-091000 | 00 | 100.69 | 1003.9 | 94.49 | 4.0 |
| HOBART | 84 | 02 | 16 | 05 | 091000-091500 | 00 | 107.52 | 1004.0 | 100.97 | 11.1 |
| HOBART | 84 | 02 | 16 | 05 | 091500-092000 | 00 | 111.79 | 1004.1 | 105.06 | 15.6 |
| HOBART | 84 | 02 | 16 | 05 | 092000-092500 | 00 | 108.37 | 1004.2 | 101.93 | 12.2 |
| HOBART | 84 | 02 | 16 | 05 | 092500-093000 | 00 | 105.81 | 1004.3 | 99.59 | 9.6 |
| HOBART | 84 | 02 | 16 | 05 | 093000-093500 | 00 | 105.81 | 1004.4 | 99.67 | 9.7 |
| HOBART | 84 | 02 | 16 | 05 | 093500-094000 | 00 | 103.25 | 1004.5 | 97.33 | 7.1 |
| HOBART | 84 | 02 | 16 | 05 | 094000-094500 | 00 | 103.25 | 1004.6 | 97.40 | 7.2 |
| HOBART | 84 | 02 | 16 | 05 | 094500-095000 | 00 | 98.13 | 1004.7 | 92.64 | 2.0 |
| HOBART | 84 | 02 | 16 | 05 | 095000-095500 | 00 | 100.69 | 1004.8 | 95.12 | 4.7 |

Table 5 continued

| STATION | YY | MM | DD | MIN | TIME (UT) INTERVAL | CODE TD | UNCOR. | PRES. (mb) | COR. | % INC. |
|---|---|---|---|---|---|---|---|---|---|---|
| HOBART | 84 | 02 | 16 | 05 | 095500-100000 | 00 | 100.69 | 1004.9 | 95.19 | 4.8 |
| HOBART | 84 | 02 | 16 | 05 | 100000-100500 | 00 | 98.13 | 1005.0 | 92.84 | 2.2 |
| HOBART | 84 | 02 | 16 | 05 | 100500-101000 | 00 | 98.99 | 1005.1 | 93.72 | 3.1 |
| HOBART | 84 | 02 | 16 | 05 | 101000-101500 | 00 | 98.99 | 1005.2 | 93.79 | 3.2 |
| HOBART | 84 | 02 | 16 | 05 | 101500-102000 | 00 | 98.99 | 1005.3 | 93.86 | 3.3 |
| HOBART | 84 | 02 | 16 | 05 | 102000-102500 | 00 | 97.28 | 1005.4 | 92.31 | 1.6 |
| HOBART | 84 | 02 | 16 | 05 | 102500-103000 | 00 | 99.84 | 1005.5 | 94.81 | 4.3 |
| HOBART | 84 | 02 | 16 | 05 | 103000-103500 | 00 | 96.43 | 1005.6 | 91.63 | 0.8 |
| HOBART | 84 | 02 | 16 | 05 | 103500-104000 | 00 | 97.28 | 1005.7 | 92.51 | 1.8 |
| HOBART | 84 | 02 | 16 | 05 | 104000-104500 | 00 | 98.13 | 1005.8 | 93.39 | 2.8 |
| HOBART | 84 | 02 | 16 | 05 | 104500-105000 | 00 | 97.28 | 1005.9 | 92.65 | 2.0 |
| HOBART | 84 | 02 | 16 | 05 | 105000-105500 | 00 | 96.43 | 1006.0 | 91.90 | 1.1 |
| HOBART | 84 | 02 | 16 | 05 | 105500-110000 | 00 | 98.99 | 1006.1 | 94.41 | 3.9 |
| HOBART | 84 | 02 | 16 | 60 | 110000-120000 | 00 | 95.22 | 1006.7 | 91.22 | 0.4 |
| HOBART | 84 | 02 | 16 | 60 | 120000-130000 | 00 | 94.51 | 1007.5 | 91.08 | 0.2 |
| HOBART | 84 | 02 | 16 | 60 | 130000-140000 | 00 | 93.30 | 1008.2 | 90.38 | -0.5 |
| HOBART | 84 | 02 | 16 | 60 | 140000-150000 | 00 | 93.08 | 1008.8 | 90.57 | -0.3 |
| HOBART | 84 | 02 | 16 | 60 | 150000-160000 | 00 | 92.02 | 1009.5 | 90.00 | -0.9 |
| HOBART | 84 | 02 | 16 | 60 | 160000-170000 | 00 | 91.95 | 1009.8 | 90.13 | -0.8 |
| HOBART | 84 | 02 | 16 | 60 | 170000-180000 | 00 | 91.45 | 1010.5 | 90.11 | -0.8 |
| HOBART | 84 | 02 | 16 | 60 | 180000-190000 | 00 | 90.95 | 1011.7 | 90.42 | -0.5 |
| HOBART | 84 | 02 | 16 | 60 | 190000-200000 | 00 | 90.67 | 1012.7 | 90.80 | -0.1 |
| HOBART | 84 | 02 | 16 | 60 | 200000-210000 | 00 | 89.53 | 1013.6 | 90.26 | -0.7 |
| HOBART | 84 | 02 | 16 | 60 | 210000-220000 | 00 | 88.75 | 1014.4 | 90.00 | -0.9 |
| HOBART | 84 | 02 | 16 | 60 | 220000-230000 | 00 | 88.68 | 1015.5 | 90.66 | -0.2 |
| HOBART | 84 | 02 | 16 | 60 | 230000-240000 | 00 | 88.39 | 1016.3 | 90.91 | 0.1 |

TABLE 6

BRISBANE LATITUDE -27.42 LONGITUDE 153.08 ALTITUDE 0 M
BRISBANE INSTRUMENT IQSY NEUTRON MONITOR
BRISBANE STANDARD PRESSURE 1010.0 (MB) COEFFICIENT -0.739 % / (MB)
BRISBANE PRE-INCREASE BASELINE TIME INTERVAL 84 02 16 080000-090000 UT
BRISBANE PRE-INCREASE AVERAGE COUNTING RATE 76.36 COUNTS PER SECOND

| STATION | YY | MM | DD | MIN | TIME (UT) INTERVAL | CODE TD | UNCOR. | PRES. (mb) | COR. | % INC. |
|---|---|---|---|---|---|---|---|---|---|---|
| BRISBANE | 84 | 02 | 15 | 60 | 000000-010000 | 00 | 77.65 | 1006.2 | 75.50 | -1.1 |
| BRISBANE | 84 | 02 | 15 | 60 | 010000-020000 | 00 | 78.44 | 1005.7 | 75.98 | -0.5 |
| BRISBANE | 84 | 02 | 15 | 60 | 020000-030000 | 00 | 79.29 | 1005.1 | 76.47 | 0.1 |
| BRISBANE | 84 | 02 | 15 | 60 | 030000-040000 | 00 | 79.22 | 1004.3 | 75.95 | -0.5 |
| BRISBANE | 84 | 02 | 15 | 60 | 040000-050000 | 00 | 80.00 | 1003.5 | 76.25 | -0.1 |
| BRISBANE | 84 | 02 | 15 | 60 | 050000-060000 | 00 | 80.14 | 1003.0 | 76.10 | -0.3 |
| BRISBANE | 84 | 02 | 15 | 60 | 060000-070000 | 00 | 80.64 | 1003.3 | 76.74 | 0.5 |
| BRISBANE | 84 | 02 | 15 | 60 | 070000-080000 | 00 | 80.50 | 1003.9 | 76.95 | 0.8 |
| BRISBANE | 84 | 02 | 15 | 60 | 080000-090000 | 00 | 79.50 | 1004.3 | 76.22 | -0.2 |
| BRISBANE | 84 | 02 | 15 | 60 | 090000-100000 | 00 | 79.08 | 1004.9 | 76.15 | -0.3 |
| BRISBANE | 84 | 02 | 15 | 60 | 100000-110000 | 00 | 79.29 | 1005.3 | 76.58 | 0.3 |
| BRISBANE | 84 | 02 | 15 | 60 | 110000-120000 | 00 | 79.00 | 1005.2 | 76.25 | -0.1 |
| BRISBANE | 84 | 02 | 15 | 60 | 120000-130000 | 00 | 79.36 | 1005.1 | 76.54 | 0.2 |
| BRISBANE | 84 | 02 | 15 | 60 | 130000-140000 | 00 | 79.36 | 1004.9 | 76.42 | 0.1 |
| BRISBANE | 84 | 02 | 15 | 60 | 140000-150000 | 00 | 79.36 | 1004.5 | 76.20 | -0.2 |
| BRISBANE | 84 | 02 | 15 | 60 | 150000-160000 | 00 | 79.57 | 1003.7 | 75.95 | -0.5 |
| BRISBANE | 84 | 02 | 15 | 60 | 160000-170000 | 00 | 80.21 | 1003.1 | 76.23 | -0.2 |
| BRISBANE | 84 | 02 | 15 | 60 | 170000-180000 | 00 | 79.64 | 1003.1 | 75.69 | -0.9 |
| BRISBANE | 84 | 02 | 15 | 60 | 180000-190000 | 00 | 79.29 | 1003.3 | 75.46 | -1.2 |
| BRISBANE | 84 | 02 | 15 | 60 | 190000-200000 | 00 | 79.64 | 1003.5 | 75.91 | -0.6 |
| BRISBANE | 84 | 02 | 15 | 60 | 200000-210000 | 00 | 79.22 | 1003.8 | 75.67 | -0.9 |
| BRISBANE | 84 | 02 | 15 | 60 | 210000-220000 | 00 | 79.22 | 1004.0 | 75.78 | -0.8 |
| BRISBANE | 84 | 02 | 15 | 60 | 220000-230000 | 00 | 79.15 | 1004.3 | 75.88 | -0.6 |
| BRISBANE | 84 | 02 | 15 | 60 | 230000-240000 | 00 | 79.15 | 1004.3 | 75.88 | -0.6 |
| BRISBANE | 84 | 02 | 16 | 60 | 000000-010000 | 00 | 79.50 | 1004.3 | 76.22 | -0.2 |
| BRISBANE | 84 | 02 | 16 | 60 | 010000-020000 | 00 | 79.86 | 1004.1 | 76.45 | 0.1 |
| BRISBANE | 84 | 02 | 16 | 60 | 020000-030000 | 00 | 80.07 | 1003.9 | 76.54 | 0.2 |
| BRISBANE | 84 | 02 | 16 | 60 | 030000-040000 | 00 | 81.00 | 1003.3 | 77.08 | 0.9 |
| BRISBANE | 84 | 02 | 16 | 60 | 040000-050000 | 00 | 81.07 | 1003.1 | 77.04 | 0.9 |
| BRISBANE | 84 | 02 | 16 | 60 | 050000-060000 | 00 | 81.14 | 1002.9 | 76.99 | 0.8 |
| BRISBANE | 84 | 02 | 16 | 60 | 060000-070000 | 00 | 81.21 | 1002.8 | 77.00 | 0.8 |
| BRISBANE | 84 | 02 | 16 | 60 | 070000-080000 | 00 | 81.00 | 1002.9 | 76.86 | 0.6 |
| BRISBANE | 84 | 02 | 16 | 60 | 080000-090000 | 00 | 80.36 | 1003.1 | 76.36 | 0.0 |
| BRISBANE | 84 | 02 | 16 | 60 | 090000-100000 | 00 | 81.07 | 1003.3 | 77.15 | 1.0 |
| BRISBANE | 84 | 02 | 16 | 60 | 100000-110000 | 00 | 79.79 | 1003.5 | 76.04 | -0.4 |
| BRISBANE | 84 | 02 | 16 | 60 | 110000-120000 | 00 | 80.28 | 1003.7 | 76.63 | 0.4 |
| BRISBANE | 84 | 02 | 16 | 60 | 120000-130000 | 00 | 79.93 | 1003.9 | 76.41 | 0.1 |
| BRISBANE | 84 | 02 | 16 | 60 | 130000-140000 | 00 | 80.07 | 1003.5 | 76.32 | -0.1 |
| BRISBANE | 84 | 02 | 16 | 60 | 140000-150000 | 00 | 80.28 | 1003.0 | 76.24 | -0.2 |
| BRISBANE | 84 | 02 | 16 | 60 | 150000-160000 | 00 | 80.50 | 1002.4 | 76.10 | -0.3 |
| BRISBANE | 84 | 02 | 16 | 60 | 160000-170000 | 00 | 81.00 | 1002.0 | 76.35 | 0.0 |
| BRISBANE | 84 | 02 | 16 | 60 | 170000-180000 | 00 | 81.00 | 1001.9 | 76.29 | -0.1 |
| BRISBANE | 84 | 02 | 16 | 60 | 180000-190000 | 00 | 80.92 | 1001.9 | 76.22 | -0.2 |
| BRISBANE | 84 | 02 | 16 | 60 | 190000-200000 | 00 | 80.50 | 1002.2 | 75.99 | -0.5 |
| BRISBANE | 84 | 02 | 16 | 60 | 200000-210000 | 00 | 80.14 | 1002.8 | 75.99 | -0.5 |
| BRISBANE | 84 | 02 | 16 | 60 | 210000-220000 | 00 | 80.43 | 1003.5 | 76.65 | 0.4 |
| BRISBANE | 84 | 02 | 16 | 60 | 220000-230000 | 00 | 80.07 | 1003.9 | 76.54 | 0.2 |
| BRISBANE | 84 | 02 | 16 | 60 | 230000-240000 | 00 | 80.07 | 1004.0 | 76.60 | 0.3 |

TABLE 7

DARWIN LATITUDE -12.42 LONGITUDE 130.87 ALTITUDE 0 M
DARWIN INSTRUMENT 9NM64 IQSY NEUTRON MONITOR
DARWIN STANDARD PRESSURE 1008.0 (MB) COEFFICIENT -0.739 % / (MB)
DARWIN PRE-INCREASE BASELINE TIME INTERVAL 84 02 16 080000-090000 UT
DARWIN PRE-INCREASE AVERAGE COUNTING RATE 58.29 COUNTS PER SECOND

| STATION | YY | MM | DD | MIN | TIME (UT) INTERVAL | CODE TD | UNCOR. | PRES. (mb) | COR. | % INC. |
|---|---|---|---|---|---|---|---|---|---|---|
| DARWIN | 84 | 02 | 15 | 60 | 000000-010000 | 00 | 60.84 | 1001.0 | 57.77 | -0.9 |
| DARWIN | 84 | 02 | 15 | 60 | 010000-020000 | 00 | 61.08 | 1000.8 | 57.92 | -0.6 |
| DARWIN | 84 | 02 | 15 | 60 | 020000-030000 | 00 | 61.19 | 1000.2 | 57.76 | -0.9 |
| DARWIN | 84 | 02 | 15 | 60 | 030000-040000 | 00 | 61.94 | 999.2 | 58.04 | -0.4 |
| DARWIN | 84 | 02 | 15 | 60 | 040000-050000 | 00 | 62.36 | 998.4 | 58.09 | -0.3 |
| DARWIN | 84 | 02 | 15 | 60 | 050000-060000 | 00 | 62.65 | 997.7 | 58.06 | -0.4 |
| DARWIN | 84 | 02 | 15 | 60 | 060000-070000 | 00 | 62.44 | 997.3 | 57.69 | -1.0 |
| DARWIN | 84 | 02 | 15 | 60 | 070000-080000 | 00 | 62.83 | 997.4 | 58.09 | -0.3 |
| DARWIN | 84 | 02 | 15 | 60 | 080000-090000 | 00 | 62.36 | 997.9 | 57.88 | -0.7 |
| DARWIN | 84 | 02 | 15 | 60 | 090000-100000 | 00 | 61.90 | 998.7 | 57.79 | -0.9 |
| DARWIN | 84 | 02 | 15 | 60 | 100000-110000 | 00 | 61.94 | 999.5 | 58.17 | -0.2 |
| DARWIN | 84 | 02 | 15 | 60 | 110000-120000 | 00 | 61.08 | 999.9 | 57.54 | -1.3 |
| DARWIN | 84 | 02 | 15 | 60 | 120000-130000 | 00 | 61.76 | 1000.3 | 58.34 | 0.1 |
| DARWIN | 84 | 02 | 15 | 60 | 130000-140000 | 00 | 60.87 | 1000.7 | 57.67 | -1.1 |
| DARWIN | 84 | 02 | 15 | 60 | 140000-150000 | 00 | 61.05 | 1000.3 | 57.67 | -1.1 |
| DARWIN | 84 | 02 | 15 | 60 | 150000-160000 | 00 | 61.55 | 999.5 | 57.80 | -0.8 |
| DARWIN | 84 | 02 | 15 | 60 | 160000-170000 | 00 | 61.87 | 998.6 | 57.71 | -1.0 |
| DARWIN | 84 | 02 | 15 | 60 | 170000-180000 | 00 | 62.08 | 998.3 | 57.79 | -0.9 |
| DARWIN | 84 | 02 | 15 | 60 | 180000-190000 | 00 | 61.76 | 998.5 | 57.57 | -1.2 |
| DARWIN | 84 | 02 | 15 | 60 | 190000-200000 | 00 | 62.01 | 998.7 | 57.89 | -0.7 |
| DARWIN | 84 | 02 | 15 | 60 | 200000-210000 | 00 | 61.44 | 999.3 | 57.61 | -1.2 |
| DARWIN | 84 | 02 | 15 | 60 | 210000-220000 | 00 | 61.19 | 1000.1 | 57.72 | -1.0 |
| DARWIN | 84 | 02 | 15 | 60 | 220000-230000 | 00 | 61.37 | 1000.9 | 58.23 | -0.1 |
| DARWIN | 84 | 02 | 15 | 60 | 230000-240000 | 00 | 60.69 | 1001.9 | 58.02 | -0.5 |
| DARWIN | 84 | 02 | 16 | 60 | 000000-010000 | 00 | 60.48 | 1002.7 | 58.16 | -0.2 |
| DARWIN | 84 | 02 | 16 | 60 | 010000-020000 | 00 | 60.52 | 1002.3 | 58.02 | -0.5 |
| DARWIN | 84 | 02 | 16 | 60 | 020000-030000 | 00 | 60.73 | 1001.6 | 57.92 | -0.6 |
| DARWIN | 84 | 02 | 16 | 60 | 030000-040000 | 00 | 60.84 | 1001.1 | 57.81 | -0.8 |
| DARWIN | 84 | 02 | 16 | 60 | 040000-050000 | 00 | 62.01 | 1000.1 | 58.49 | 0.3 |
| DARWIN | 84 | 02 | 16 | 60 | 050000-060000 | 00 | 62.15 | 998.9 | 58.11 | -0.3 |
| DARWIN | 84 | 02 | 16 | 60 | 060000-070000 | 00 | 62.54 | 998.1 | 58.13 | -0.3 |
| DARWIN | 84 | 02 | 16 | 60 | 070000-080000 | 00 | 62.83 | 998.2 | 58.44 | 0.3 |
| DARWIN | 84 | 02 | 16 | 60 | 080000-090000 | 00 | 62.44 | 998.7 | 58.29 | 0.0 |
| DARWIN | 84 | 02 | 16 | 60 | 090000-100000 | 00 | 62.08 | 999.7 | 58.39 | 0.2 |
| DARWIN | 84 | 02 | 16 | 60 | 100000-110000 | 00 | 61.72 | 1000.6 | 58.44 | 0.3 |
| DARWIN | 84 | 02 | 16 | 60 | 110000-120000 | 00 | 61.65 | 1001.5 | 58.76 | 0.8 |
| DARWIN | 84 | 02 | 16 | 60 | 120000-130000 | 00 | 61.69 | 1002.4 | 59.19 | 1.5 |
| DARWIN | 84 | 02 | 16 | 60 | 130000-140000 | 00 | 61.19 | 1002.6 | 58.80 | 0.9 |
| DARWIN | 84 | 02 | 16 | 60 | 140000-150000 | 00 | 61.58 | 1002.2 | 59.00 | 1.2 |
| DARWIN | 84 | 02 | 16 | 60 | 150000-160000 | 00 | 61.69 | 1001.7 | 58.88 | 1.0 |
| DARWIN | 84 | 02 | 16 | 60 | 160000-170000 | 00 | 62.08 | 1001.5 | 59.17 | 1.5 |
| DARWIN | 84 | 02 | 16 | 60 | 170000-180000 | 00 | 62.54 | 1001.5 | 59.61 | 2.3 |
| DARWIN | 84 | 02 | 16 | 60 | 180000-190000 | 00 | 62.36 | 1001.6 | 59.48 | 2.0 |
| DARWIN | 84 | 02 | 16 | 60 | 190000-200000 | 00 | 62.08 | 1001.8 | 59.30 | 1.7 |
| DARWIN | 84 | 02 | 16 | 60 | 200000-210000 | 00 | 61.51 | 1002.3 | 58.97 | 1.2 |
| DARWIN | 84 | 02 | 16 | 60 | 210000-220000 | 00 | 61.23 | 1003.1 | 59.05 | 1.3 |
| DARWIN | 84 | 02 | 16 | 60 | 220000-230000 | 00 | 60.73 | 1003.8 | 58.87 | 1.0 |
| DARWIN | 84 | 02 | 16 | 60 | 230000-240000 | 00 | 60.69 | 1004.0 | 58.93 | 1.1 |

# Relativistic Solar Cosmic Rays on 16 February 1984

by

M.A. Pomerantz, J.W. Bieber and C.H. Tsao
Bartol Research Foundation of The Franklin Institute
University of Delaware, Newark, Delaware 19716, USA

The 37th ground level enhancement (GLE) observed since Forbush discovered solar cosmic rays in 1942 (Forbush, 1946) was produced by a flare beyond the west limb of the Sun on 16 February 1984. This event was especially noteworthy because it displayed the greatest anisotropy observed thus far throughout its entire duration of about one hour.

Extensive analysis reported elsewhere has yielded a number of important results concerning the acceleration and transport of particles with magnetic rigidities above 1 GV through the solar corona from the flare site to the foot of the interplanetary magnetic field line that connected the Sun and the Earth at the time of the GLE (separated by approximately 70°) and then through the interplanetary medium (Pomerantz et al., 1984; Bieber et al., 1985a, 1985b). In this report we present the high time resolution data (2-minute averages) recorded by the Bartol neutron monitor network comprising four stations: Thule, Greenland; Newark, Delaware; McMurdo and South Pole Stations, Antarctica.

Figure 1 shows the sharp spike representing the 16 February 1984 GLE in the context of the galactic cosmic ray background which was generally disturbed throughout the transit of solar Active Region 4408 across the visible disk. The 2-minute data are plotted on an expanded scale in Figure 2.

A real breakthrough in the observation of relativistic solar cosmic rays was achieved through the acquisition of data with a time resolution of 10 seconds by a recorder system developed at the University of Maryland for studies of the magnetospheric cusp at the South Pole Station. Figure 3, which displays a scatter among the points that is entirely compatible with the expected statistical uncertainties, shows no structure in the intensity profile.

## Acknowledgements

We are indebted to Ted Rosenberg for making it possible to extract the ultra-high time resolution data. This research was supported by the National Science Foundation's Division of Atmospheric Research under grant ATM-8303758 and Division of Polar Programs under grant DPP-8300544.

## REFERENCES

BIEBER, J.W., P.A. EVENSON and M.A. POMERANTZ — 1985a — "Exponential Anisotropy of Solar Cosmic Rays," to appear in **Proc., 19th Int'l. Cosmic Ray Conf.**, La Jolla, CA, Paper No. SH 3.2-1.

BIEBER, J.W., P.A. EVENSON and M.A. POMERANTZ — 1985b — "Coronal and Interplanetary Focused Transport of Solar Cosmic Rays," to be submitted to **J. Geophys. Res.**

FORBUSH, S.E. — 1946 — "Three Unusual Cosmic-Ray Increases Possibly Due to Charged Particles from the Sun," **Phys. Rev., 70**, 771.

POMERANTZ, M.A., J.W. BIEBER and P.A. EVENSON — 1984 — "The Remarkable Anisotropic Relativistic Solar Particle Event of 16 February 1984," **Proc., Int'l. Symposium on Cosmic Ray Modulation in the Heliosphere**, Morioka, Japan. pp. 437.

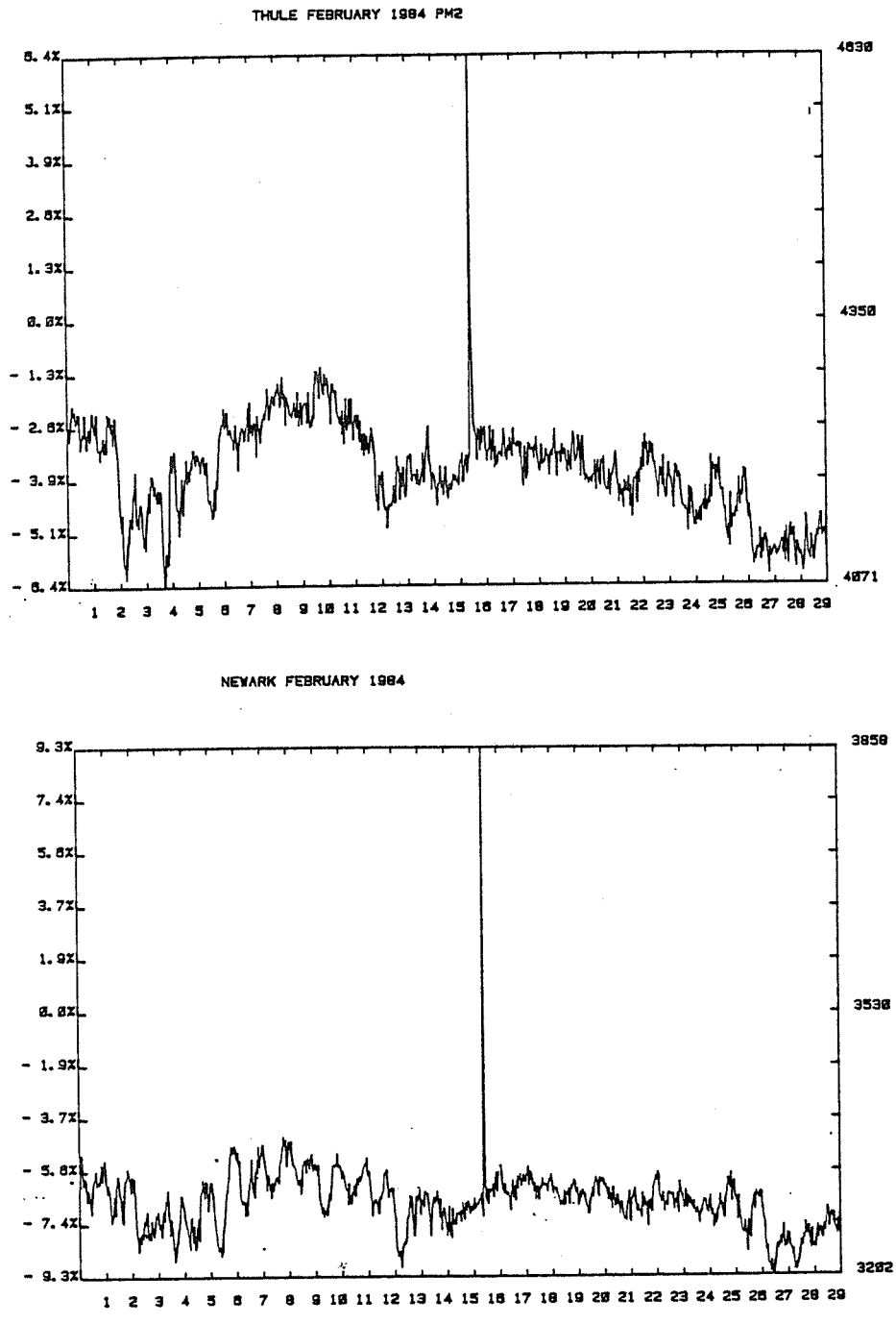


Figure 1a

Hourly average intensities at two northern hemisphere neutron monitor stations, Thule and Newark. The sharp spikes represent the 16 February 1984 GLE. The fluctuations, including the enhanced diurnal variation at Newark, are associated with the transit of region 4408 across the solar disk.

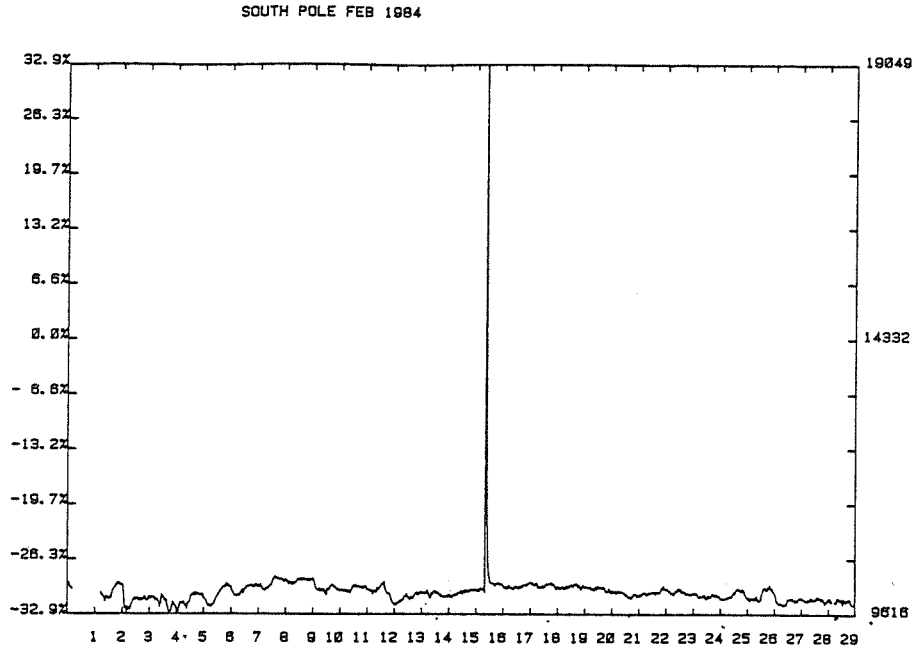


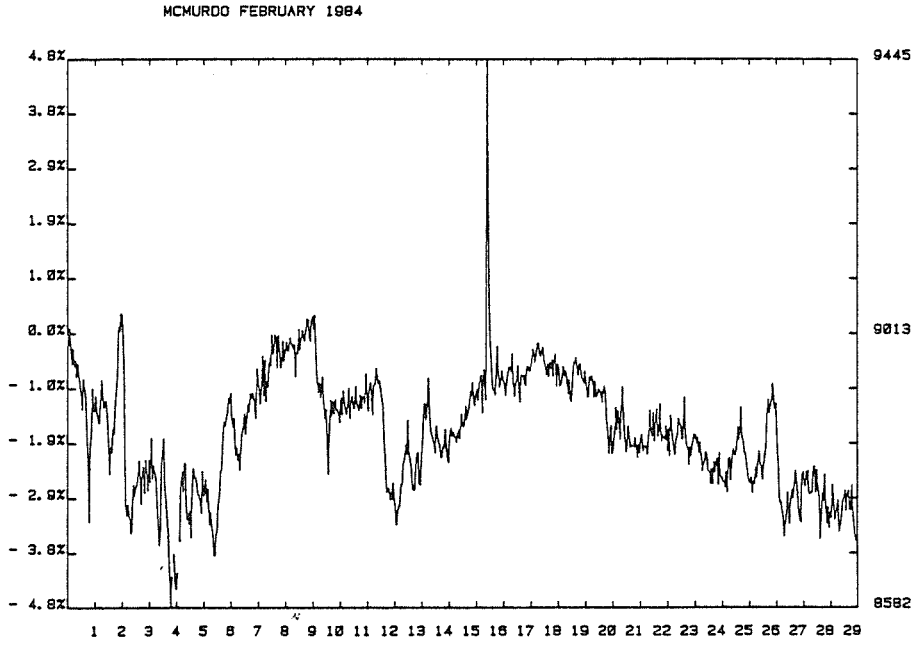


Figure 1b

Hourly average intensities at two southern hemisphere neutron monitor stations, South Pole and McMurdo. Note that the scales in both (a) and (b) differ, each being such that the highest value of the ordinate corresponds with the hourly average of the GLE, expressed in percent of the monthly mean intensity.

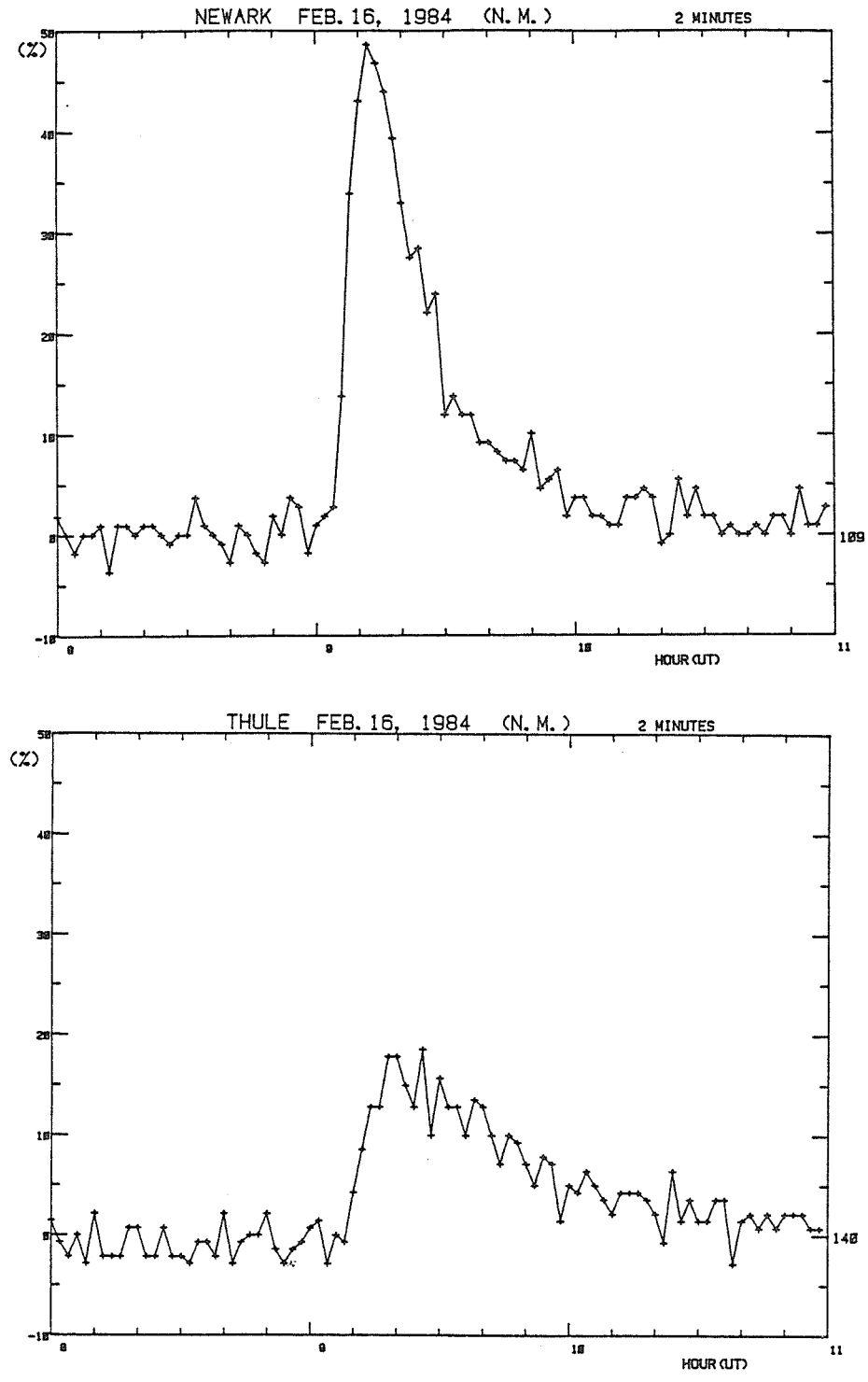


Figure 2a

The 16 February 1984 GLE as observed at Thule and Newark. The data points are 2-minute averages of the percentage differences from the pre-flare mean.

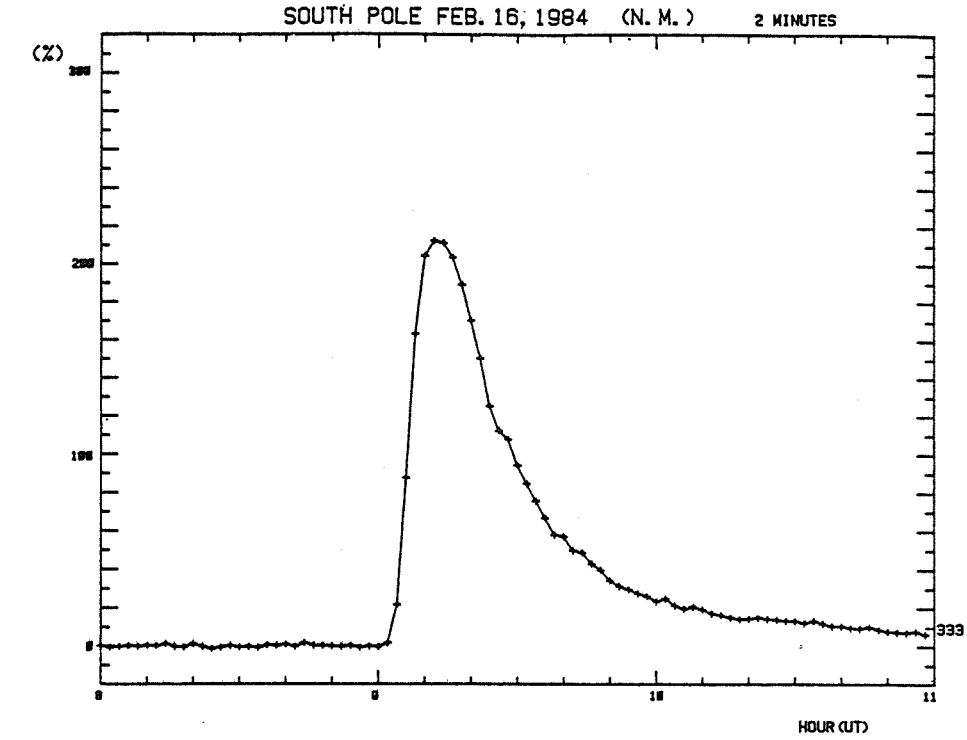


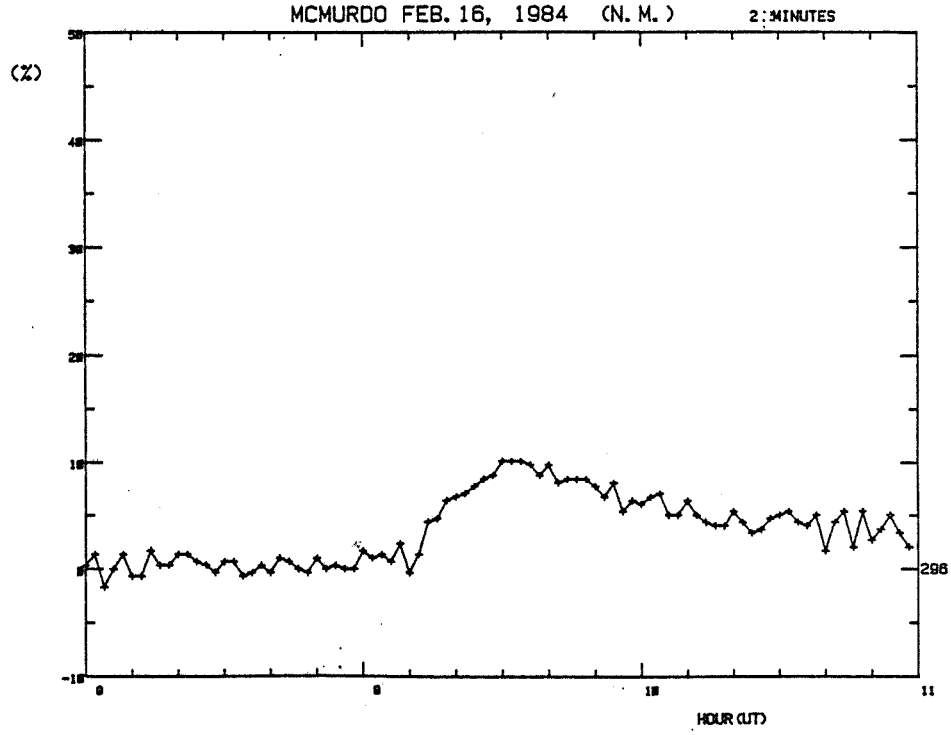


Figure 2b

The 16 February 1984 GLE at McMurdo and South Pole Stations. The fact that the South Pole neutron monitor is the world's most sensitive detector of relativistic solar cosmic rays is clearly evident.

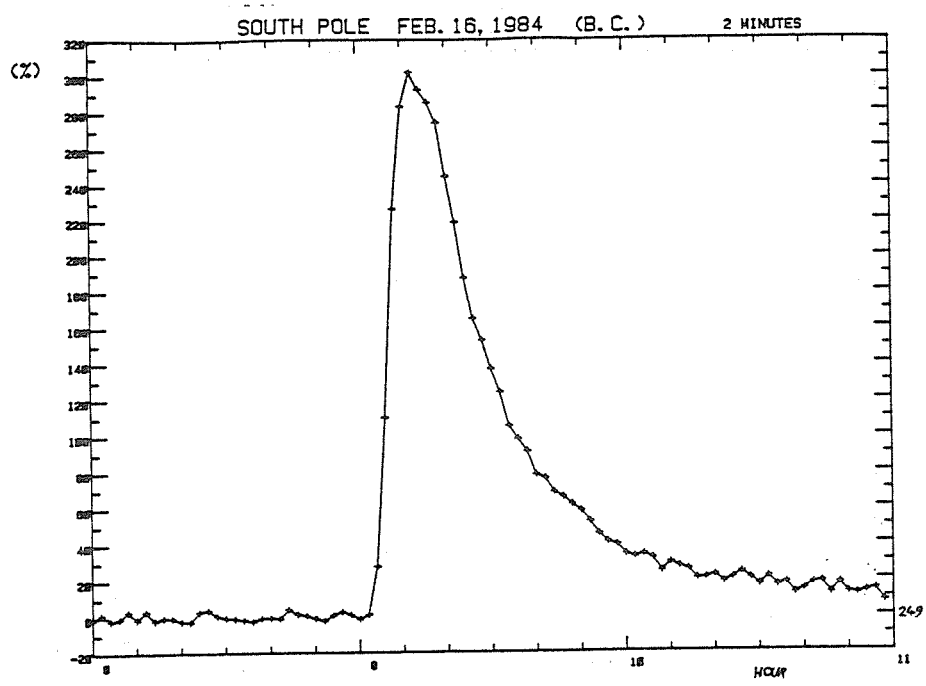


Figure 3a

Observations with the so-called "bare counters" (B.C.) at South Pole. This unshielded detector, which responds to atmospheric neutrons rather than tothose emanating from a local Pb producer, is sensitive to primary particles with slightly lower energies than is the standard "pile" sensor [cf. Figure 2b].

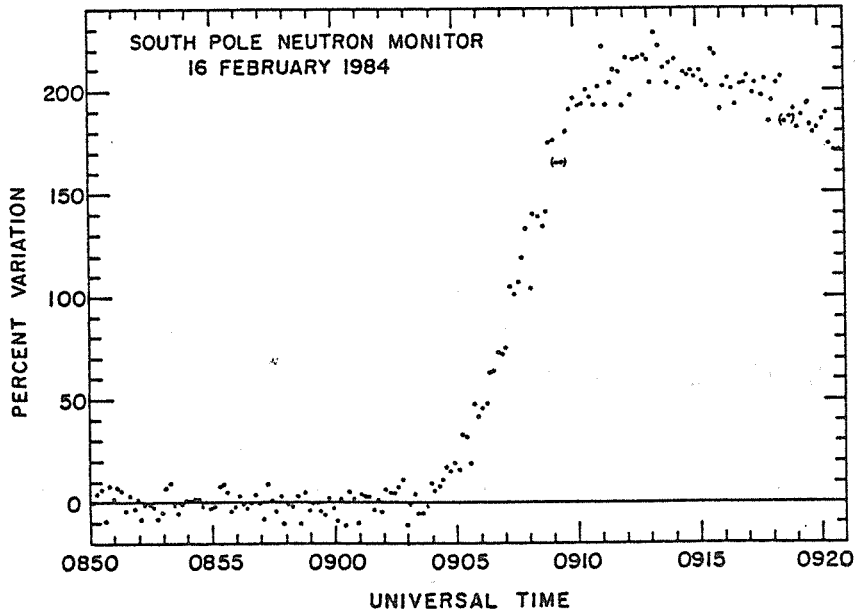


Figure 3b

GLE observations of unprecendented precision. The points represent 10 second averages, as recorded with the University of Maryland magnetospheric cusp data logging system at South Pole Station.

BARTOL RESEARCH FOUNDATION OF THE FRANKLIN INSTITUTE
UNIVERSITY OF DELAWARE
NEWARK, DELAWARE 19716 U.S.A.

THULE STATION — STANDARD PRESSURE : 754 mm HG

GEOGRAPHIC COORDINATES 76.5N, 68.7W — ALTITUDE 44 M
EFFICIENCY RELATIVE TO JAN 1965 = 1.000 — REAL COUNTS = 100 TIMES TABULATED COUNTS

PRESSURE DATA(2 MINUTES)

| YEAR | DAY (ZULU) | HOUR (UT) | 1 31 | 3 33 | 5 35 | 7 37 | 9 39 | 11 41 | 13 43 | 15 45 | 17 47 | 19 49 | 21 51 | 23 53 | 25 55 | 27 57 | 29 59 | MEAN |
|---|---|---|---|---|---|---|---|---|---|---|---|---|---|---|---|---|---|---|
| 1984 | 47 | 8 | 7548 | 7548 | 7548 | 7548 | 7549 | 7549 | 7549 | 7549 | 7549 | 7549 | 7549 | 7549 | 7549 | 7549 | 7549 | |
| | | | 7549 | 7548 | 7548 | 7549 | 7549 | 7549 | 7549 | 7549 | 7549 | 7550 | 7550 | 7550 | 7550 | 7550 | 7550 | 7549 |
| 1984 | 47 | 9 | 7550 | 7550 | 7550 | 7550 | 7550 | 7551 | 7551 | 7551 | 7551 | 7551 | 7551 | 7551 | 7551 | 7551 | 7551 | |
| | | | 7551 | 7551 | 7551 | 7551 | 7551 | 7551 | 7551 | 7551 | 7552 | 7552 | 7552 | 7552 | 7552 | 7552 | 7552 | 7551 |
| 1984 | 47 | 10 | 7552 | 7552 | 7552 | 7552 | 7552 | 7552 | 7552 | 7552 | 7552 | 7552 | 7552 | 7552 | 7553 | 7553 | 7553 | |
| | | | 7553 | 7553 | 7553 | 7553 | 7553 | 7553 | 7553 | 7553 | 7552 | 7552 | 7552 | 7552 | 7552 | 7552 | 7552 | 7552 |

GEOGRAPHIC COORDINATES 76.5N, 68.7W — ALTITUDE 44 M
EFFICIENCY RELATIVE TO JAN 1965 = 1.000 — REAL COUNTS = 100 TIMES TABULATED COUNTS

UNCORRECTED NEUTRON MONITOR DATA(2 MINUTES)

| YEAR | DAY (ZULU) | HOUR (UT) | 1 31 | 3 33 | 5 35 | 7 37 | 9 39 | 11 41 | 13 43 | 15 45 | 17 47 | 19 49 | 21 51 | 23 53 | 25 55 | 27 57 | 29 59 | SUM |
|---|---|---|---|---|---|---|---|---|---|---|---|---|---|---|---|---|---|---|
| 1984 | 47 | 8 | 141 | 138 | 136 | 139 | 135 | 142 | 136 | 136 | 136 | 140 | 140 | 136 | 136 | 140 | 136 | |
| | | | 136 | 135 | 138 | 138 | 136 | 142 | 135 | 138 | 139 | 139 | 142 | 136 | 135 | 136 | 138 | 4130 |
| 1984 | 47 | 9 | 140 | 140 | 135 | 139 | 138 | 144 | 151 | 156 | 156 | 163 | 163 | 159 | 156 | 164 | 152 | |
| | | | 160 | 156 | 156 | 152 | 158 | 156 | 152 | 148 | 152 | 151 | 148 | 146 | 150 | 148 | 140 | 4529 |
| 1984 | 47 | 10 | 145 | 144 | 147 | 146 | 143 | 142 | 144 | 144 | 144 | 143 | 142 | 138 | 147 | 140 | 143 | |
| | | | 140 | 140 | 143 | 143 | 135 | 140 | 142 | 139 | 142 | 139 | 142 | 142 | 142 | 139 | 139 | 4259 |

BARTOL RESEARCH FOUNDATION OF THE FRANKLIN INSTITUTE
UNIVERSITY OF DELAWARE
NEWARK, DELAWARE 19716 U.S.A.

NEWARK STATION — STANDARD PRESSURE : 760 mm HG

GEOGRAPHIC COORDINATES 39.7N, 75.7W — ALTITUTE 50 M
EFFICIENCY RELATIVE TO JUL 1964 = 1.000 — REAL COUNTS = 100 TIMES TABULATED COUNTS

PRESSURE DATA(2 MINUTES)

| YEAR | DAY (ZULU) | HOUR (UT) | 1 31 | 3 33 | 5 35 | 7 37 | 9 39 | 11 41 | 13 43 | 15 45 | 17 47 | 19 49 | 21 51 | 23 53 | 25 55 | 27 57 | 29 59 | MEAN |
|---|---|---|---|---|---|---|---|---|---|---|---|---|---|---|---|---|---|---|
| 1984 | 47 | 8 | 7588 | 7588 | 7588 | 7588 | 7589 | 7589 | 7589 | 7589 | 7590 | 7590 | 7590 | 7590 | 7590 | 7591 | 7591 | |
| | | | 7591 | 7591 | 7591 | 7592 | 7592 | 7592 | 7592 | 7592 | 7592 | 7593 | 7594 | 7594 | 7594 | 7594 | 7595 | 7591 |
| 1984 | 47 | 9 | 7595 | 7595 | 7595 | 7595 | 7595 | 7595 | 7595 | 7595 | 7595 | 7595 | 7595 | 7595 | 7595 | 7595 | 7595 | |
| | | | 7595 | 7595 | 7596 | 7596 | 7597 | 7597 | 7597 | 7597 | 7597 | 7597 | 7597 | 7597 | 7598 | 7599 | 7599 | 7596 |
| 1984 | 47 | 10 | 7599 | 7599 | 7599 | 7599 | 7600 | 7600 | 7600 | 7601 | 7601 | 7601 | 7602 | 7602 | 7602 | 7603 | 7603 | |
| | | | 7604 | 7604 | 7604 | 7604 | 7605 | 7605 | 7605 | 7605 | 7605 | 7605 | 7605 | 7605 | 7605 | 7606 | 7606 | 7603 |

NEWARK STATION — STANDARD PRESSURE : 760 mm HG

GEOGRAPHIC COORDINATES 39.7N, 75.7W — ALTITUTE 50 M
EFFICIENCY RELATIVE TO JUL 1964 = 1.000 — REAL COUNTS = 100 TIMES TABULATED COUNTS

UNCORRECTED NEUTRON MONITOR DATA(2 MINUTES)

| YEAR | DAY (ZULU) | HOUR (UT) | 1 31 | 3 33 | 5 35 | 7 37 | 9 39 | 11 41 | 13 43 | 15 45 | 17 47 | 19 49 | 21 51 | 23 53 | 25 55 | 27 57 | 29 59 | SUM |
|---|---|---|---|---|---|---|---|---|---|---|---|---|---|---|---|---|---|---|
| 1984 | 47 | 8 | 112 | 110 | 108 | 110 | 110 | 111 | 106 | 111 | 111 | 110 | 111 | 111 | 110 | 109 | 110 | |
| | | | 110 | 114 | 111 | 110 | 109 | 107 | 111 | 110 | 108 | 107 | 112 | 110 | 114 | 113 | 107 | 3303 |
| 1984 | 47 | 9 | 111 | 112 | 113 | 125 | 147 | 157 | 163 | 161 | 158 | 153 | 146 | 140 | 141 | 134 | 136 | |
| | | | 123 | 125 | 122 | 122 | 119 | 119 | 118 | 117 | 117 | 116 | 120 | 114 | 115 | 116 | 111 | 3871 |
| 1984 | 47 | 10 | 113 | 113 | 111 | 111 | 110 | 110 | 113 | 113 | 114 | 113 | 108 | 109 | 115 | 111 | 114 | |
| | | | 111 | 111 | 109 | 110 | 108 | 108 | 109 | 108 | 110 | 110 | 108 | 113 | 109 | 109 | 111 | 3322 |

BARTOL RESEARCH FOUNDATION OF THE FRANKLIN INSTITUTE
UNIVERSITY OF DELAWARE
NEWARK, DELAWARE 19716 U.S.A.

McMURDO STATION — STANDARD PRESSURE : 730 mm HG

GEOGRAPHIC COORDINATES 77.9S, 166.6E — ALTITUDE 48 M
EFFICIENCY RELATIVE TO DEC 1964 = 1.000 — REAL COUNTS = 100 TIMES TABULATED COUNTS

PRESSURE DATA(2 MINUTES)

| YEAR | DAY (ZULU) | HOUR (UT) | 1 31 | 3 33 | 5 35 | 7 37 | 9 39 | 11 41 | 13 43 | 15 45 | 17 47 | 19 49 | 21 51 | 23 53 | 25 55 | 27 57 | 29 59 | MEAN |
|---|---|---|---|---|---|---|---|---|---|---|---|---|---|---|---|---|---|---|
| 1984 | 47 | 8 | 7326 | 7326 | 7326 | 7326 | 7326 | 7326 | 7326 | 7326 | 7326 | 7326 | 7326 | 7326 | 7325 | 7325 | 7326 | |
| | | | 7326 | 7326 | 7326 | 7326 | 7327 | 7327 | 7327 | 7327 | 7327 | 7327 | 7327 | 7327 | 7327 | 7327 | 7327 | 7326 |
| 1984 | 47 | 9 | 7327 | 7327 | 7327 | 7327 | 7327 | 7327 | 7327 | 7327 | 7327 | 7327 | 7327 | 7327 | 7327 | 7327 | 7327 | |
| | | | 7327 | 7327 | 7327 | 7327 | 7327 | 7326 | 7326 | 7326 | 7326 | 7327 | 7327 | 7327 | 7327 | 7327 | 7327 | 7327 |
| 1984 | 47 | 10 | 7327 | 7327 | 7327 | 7327 | 7327 | 7327 | 7327 | 7327 | 7327 | 7327 | 7327 | 7327 | 7327 | 7326 | 7326 | |
| | | | 7326 | 7326 | 7326 | 7326 | 7326 | 7326 | 7326 | 7326 | 7326 | 7326 | 7326 | 7326 | 7326 | 7325 | 7325 | 7326 |

McMURDO STATION — STANDARD PRESSURE : 730 mm HG

GEOGRAPHIC COORDINATES 77.9S, 166.6E — ALTITUDE 48 M
EFFICIENCY RELATIVE TO DEC 1964 = 1.000 — REAL COUNTS = 100 TIMES TABULATED COUNTS

UNCORRECTED NEUTRON MONITOR DATA(2 MINUTES)

| YEAR | DAY (ZULU) | HOUR (UT) | 1 31 | 3 33 | 5 35 | 7 37 | 9 39 | 11 41 | 13 43 | 15 45 | 17 47 | 19 49 | 21 51 | 23 53 | 25 55 | 27 57 | 29 59 | SUM |
|---|---|---|---|---|---|---|---|---|---|---|---|---|---|---|---|---|---|---|
| 1984 | 47 | 8 | 289 | 293 | 284 | 289 | 293 | 287 | 287 | 294 | 290 | 290 | 293 | 293 | 291 | 290 | 288 | |
| | | | 291 | 291 | 287 | 288 | 289 | 287 | 292 | 290 | 288 | 287 | 291 | 288 | 289 | 288 | 288 | 8685 |
| 1984 | 47 | 9 | 293 | 291 | 292 | 290 | 295 | 287 | 292 | 301 | 302 | 307 | 308 | 309 | 311 | 313 | 314 | |
| | | | 318 | 318 | 318 | 317 | 314 | 317 | 312 | 313 | 313 | 313 | 311 | 308 | 312 | 304 | 307 | 9200 |
| 1984 | 47 | 10 | 306 | 308 | 309 | 303 | 303 | 307 | 303 | 301 | 300 | 300 | 304 | 301 | 298 | 299 | 302 | |
| | | | 303 | 304 | 301 | 300 | 303 | 294 | 301 | 304 | 295 | 304 | 296 | 299 | 304 | 299 | 295 | 9046 |

BARTOL RESEARCH FOUNDATION OF THE FRANKLIN INSTITUTE
UNIVERSITY OF DELAWARE
NEWARK, DELAWARE 19716 U.S.A.

SOUTH POLE STATION — STANDARD PRESSURE : 510 mm HG

GEOGRAPHIC COORDINATES 90.0S — ALTITUTE 2820 M
EFFICIENCY RELATIVE TO FEB 1977 = 1.000 — REAL COUNTS = 100 TIMES TABULATED COUNTS

PRESSURE DATA(2 MINUTES)

| YEAR | DAY (ZULU) | HOUR (UT) | 1 31 | 3 33 | 5 35 | 7 37 | 9 39 | 11 41 | 13 43 | 15 45 | 17 47 | 19 49 | 21 51 | 23 53 | 25 55 | 27 57 | 29 59 | MEAN |
|---|---|---|---|---|---|---|---|---|---|---|---|---|---|---|---|---|---|---|
| 1984 | 47 | 8 | 5103 | 5103 | 5103 | 5103 | 5103 | 5103 | 5103 | 5103 | 5103 | 5103 | 5103 | 5103 | 5103 | 5103 | 5103 | |
| | | | 5103 | 5103 | 5103 | 5103 | 5103 | 5103 | 5103 | 5103 | 5103 | 5103 | 5104 | 5104 | 5104 | 5104 | 5104 | 5103 |
| 1984 | 47 | 9 | 5104 | 5104 | 5104 | 5104 | 5104 | 5104 | 5104 | 5104 | 5104 | 5103 | 5103 | 5103 | 5103 | 5103 | 5103 | |
| | | | 5103 | 5103 | 5103 | 5103 | 5103 | 5103 | 5103 | 5103 | 5103 | 5103 | 5103 | 5103 | 5103 | 5103 | 5103 | 5103 |
| 1984 | 47 | 10 | 5103 | 5103 | 5103 | 5103 | 5103 | 5103 | 5103 | 5103 | 5103 | 5103 | 5103 | 5103 | 5103 | 5103 | 5103 | |
| | | | 5103 | 5103 | 5103 | 5103 | 5103 | 5103 | 5103 | 5102 | 5102 | 5102 | 5102 | 5102 | 5102 | 5102 | 5102 | 5103 |

SOUTH POLE STATION — STANDARD PRESSURE : 510 mm HG

GEOGRAPHIC COORDINATES 90.0S — ALTITUTE 2820 M
EFFICIENCY RELATIVE TO FEB 1977 = 1.000 — REAL COUNTS = 100 TIMES TABULATED COUNTS

UNCORRECTED NEUTRON MONITOR DATA(2 MINUTES)

| YEAR | DAY (ZULU) | HOUR (UT) | 1 31 | 3 33 | 5 35 | 7 37 | 9 39 | 11 41 | 13 43 | 15 45 | 17 47 | 19 49 | 21 51 | 23 53 | 25 55 | 27 57 | 29 59 | SUM |
|---|---|---|---|---|---|---|---|---|---|---|---|---|---|---|---|---|---|---|
| 1984 | 47 | 8 | 333 | 329 | 331 | 333 | 331 | 333 | 332 | 336 | 331 | 330 | 336 | 331 | 327 | 330 | 333 | |
| | | | 330 | 331 | 329 | 334 | 333 | 335 | 331 | 338 | 333 | 333 | 332 | 331 | 333 | 330 | 332 | 9961 |
| 1984 | 47 | 9 | 330 | 338 | 403 | 623 | 872 | 1009 | 1036 | 1032 | 1007 | 959 | 897 | 830 | 747 | 704 | 690 | |
| | | | 645 | 613 | 583 | 553 | 525 | 521 | 498 | 494 | 474 | 463 | 446 | 436 | 430 | 423 | 419 | 19000 |
| 1984 | 47 | 10 | 410 | 415 | 403 | 397 | 401 | 396 | 389 | 385 | 381 | 379 | 380 | 381 | 379 | 378 | 376 | |
| | | | 376 | 372 | 376 | 371 | 367 | 367 | 364 | 363 | 366 | 361 | 358 | 357 | 356 | 358 | 354 | 11316 |

# Turku Neutron Monitor Data for the 16 February 1984 Event

by

Jarmo Torsti
University of Turku
Department of Physical Sciences
SF-20500 Turku 50, Finland

We present the Turku double neutron monitor data for the 16 February 1984 event. Table 1 contains the 30-second data between 0700-1200 UT corresponding to the mean neutron energy 50 MeV, and about 10 GeV in free space. Table 2 contains the hourly data in four multiplicity categories according to the energy:

| Category | Mean Sea Level Energy GeV | Mean Energy in Free Space GeV |
|---|---|---|
| I | about 0.05 | 10 |
| II | about 0.15 | 20 |
| III | about 0.50 | 50 |
| IV | about 1.5 | 100 |

Table 1. Turku 30 Second Data for 16 February 1984 0700-1200 UT.

Counting rate per second

| STATION | YY | MM | DD | MIN | TIME SPAN | | UNCOR. | PRES. | COR. | % INC. |
|---|---|---|---|---|---|---|---|---|---|---|
| TURKU | 84 | 2 | 16 | 1 | 700- 701 | 1 | 5.70 | 1039.9 | 6.79 | 7.0 |
| | | | | | | 2 | 4.90 | 1039.9 | 5.84 | -8.0 |
| TURKU | 84 | 2 | 16 | 1 | 701- 702 | 1 | 5.50 | 1039.9 | 6.55 | 3.3 |
| | | | | | | 2 | 5.47 | 1039.9 | 6.51 | 2.6 |
| TURKU | 84 | 2 | 16 | 1 | 702- 703 | 1 | 4.87 | 1039.9 | 5.80 | -8.6 |
| | | | | | | 2 | 5.03 | 1039.9 | 6.00 | -5.5 |
| TURKU | 84 | 2 | 16 | 1 | 703- 704 | 1 | 5.20 | 1039.9 | 6.20 | -2.4 |
| | | | | | | 2 | 5.77 | 1039.9 | 6.87 | 8.3 |
| TURKU | 84 | 2 | 16 | 1 | 704- 705 | 1 | 6.07 | 1039.9 | 7.23 | 13.9 |
| | | | | | | 2 | 5.70 | 1039.9 | 6.79 | 7.0 |
| TURKU | 84 | 2 | 16 | 1 | 705- 706 | 1 | 5.37 | 1039.9 | 6.40 | 0.8 |
| | | | | | | 2 | 5.70 | 1039.9 | 6.79 | 7.0 |
| TURKU | 84 | 2 | 16 | 1 | 706- 707 | 1 | 5.33 | 1039.9 | 6.36 | 0.1 |
| | | | | | | 2 | 5.77 | 1039.9 | 6.87 | 8.3 |
| TURKU | 84 | 2 | 16 | 1 | 707- 708 | 1 | 5.23 | 1039.9 | 6.24 | -1.7 |
| | | | | | | 2 | 5.37 | 1039.9 | 6.40 | 0.8 |
| TURKU | 84 | 2 | 16 | 1 | 708- 709 | 1 | 4.80 | 1039.9 | 5.72 | -9.9 |
| | | | | | | 2 | 5.83 | 1039.9 | 6.95 | 9.5 |
| TURKU | 84 | 2 | 16 | 1 | 709- 710 | 1 | 5.03 | 1039.9 | 6.00 | -5.5 |
| | | | | | | 2 | 5.37 | 1039.9 | 6.40 | 0.8 |
| TURKU | 84 | 2 | 16 | 1 | 710- 711 | 1 | 5.20 | 1040.0 | 6.20 | -2.3 |
| | | | | | | 2 | 5.23 | 1040.0 | 6.24 | -1.7 |
| TURKU | 84 | 2 | 16 | 1 | 711- 712 | 1 | 6.20 | 1040.0 | 7.39 | 16.5 |
| | | | | | | 2 | 5.53 | 1040.0 | 6.60 | 3.9 |
| TURKU | 84 | 2 | 16 | 1 | 712- 713 | 1 | 4.90 | 1040.0 | 5.84 | -8.0 |
| | | | | | | 2 | 4.83 | 1040.0 | 5.76 | -9.2 |
| TURKU | 84 | 2 | 16 | 1 | 713- 714 | 1 | 5.37 | 1040.0 | 6.40 | 0.8 |
| | | | | | | 2 | 4.63 | 1040.0 | 5.52 | -13.0 |
| TURKU | 84 | 2 | 16 | 1 | 714- 715 | 1 | 5.53 | 1040.0 | 6.60 | 3.9 |
| | | | | | | 2 | 4.83 | 1040.0 | 5.76 | -9.2 |
| TURKU | 84 | 2 | 16 | 1 | 715- 716 | 1 | 5.33 | 1039.9 | 6.36 | 0.2 |
| | | | | | | 2 | 5.40 | 1039.9 | 6.44 | 1.4 |
| TURKU | 84 | 2 | 16 | 1 | 716- 717 | 1 | 4.70 | 1039.9 | 5.60 | -11.7 |
| | | | | | | 2 | 5.17 | 1039.9 | 6.16 | -3.0 |
| TURKU | 84 | 2 | 16 | 1 | 717- 718 | 1 | 5.13 | 1039.9 | 6.12 | -3.6 |
| | | | | | | 2 | 4.87 | 1039.9 | 5.80 | -8.6 |
| TURKU | 84 | 2 | 16 | 1 | 718- 719 | 1 | 5.73 | 1039.9 | 6.83 | 7.7 |
| | | | | | | 2 | 5.57 | 1039.9 | 6.64 | 4.5 |
| TURKU | 84 | 2 | 16 | 1 | 719- 720 | 1 | 5.57 | 1039.9 | 6.64 | 4.5 |
| | | | | | | 2 | 4.90 | 1039.9 | 5.84 | -8.0 |
| TURKU | 84 | 2 | 16 | 1 | 720- 721 | 1 | 5.77 | 1040.0 | 6.87 | 8.3 |
| | | | | | | 2 | 4.83 | 1040.0 | 5.76 | -9.2 |

Table 1. continued

| STATION | YY | MM | DD | MIN | TIME SPAN | | Counting rate per second | UNCOR. PRES. | COR. | % INC. |
|---|---|---|---|---|---|---|---|---|---|---|
| TURKU | 84 | 2 | 16 | 1 | 721- 722 | 1 | | 5.07 1040.0 | 6.04 | -4.8 |
| | | | | | | 2 | | 6.00 1040.0 | 7.15 | 12.7 |
| TURKU | 84 | 2 | 16 | 1 | 722- 723 | 1 | | 5.17 1040.0 | 6.16 | -3.0 |
| | | | | | | 2 | | 5.23 1040.0 | 6.24 | -1.7 |
| TURKU | 84 | 2 | 16 | 1 | 723- 724 | 1 | | 5.50 1040.0 | 6.56 | 3.3 |
| | | | | | | 2 | | 5.23 1040.0 | 6.24 | -1.7 |
| TURKU | 84 | 2 | 16 | 1 | 724- 725 | 1 | | 5.33 1040.0 | 6.36 | 0.2 |
| | | | | | | 2 | | 5.80 1040.0 | 6.91 | 8.9 |
| TURKU | 84 | 2 | 16 | 1 | 725- 726 | 1 | | 4.87 1040.0 | 5.80 | -8.6 |
| | | | | | | 2 | | 5.73 1040.0 | 6.84 | 7.7 |
| TURKU | 84 | 2 | 16 | 1 | 726- 727 | 1 | | 5.23 1040.0 | 6.24 | -1.7 |
| | | | | | | 2 | | 5.80 1040.0 | 6.92 | 9.0 |
| TURKU | 84 | 2 | 16 | 1 | 727- 728 | 1 | | 5.03 1040.0 | 6.00 | -5.4 |
| | | | | | | 2 | | 5.93 1040.0 | 7.08 | 11.5 |
| TURKU | 84 | 2 | 16 | 1 | 728- 729 | 1 | | 5.20 1040.0 | 6.20 | -2.3 |
| | | | | | | 2 | | 5.20 1040.0 | 6.20 | -2.3 |
| TURKU | 84 | 2 | 16 | 1 | 729- 730 | 1 | | 5.43 1040.0 | 6.48 | 2.1 |
| | | | | | | 2 | | 4.73 1040.0 | 5.64 | -11.1 |
| TURKU | 84 | 2 | 16 | 1 | 730- 731 | 1 | | 5.60 1040.0 | 6.68 | 5.2 |
| | | | | | | 2 | | 4.70 1040.0 | 5.60 | -11.7 |
| TURKU | 84 | 2 | 16 | 1 | 731- 732 | 1 | | 4.83 1040.0 | 5.76 | -9.2 |
| | | | | | | 2 | | 5.57 1040.0 | 6.64 | 4.6 |
| TURKU | 84 | 2 | 16 | 1 | 732- 733 | 1 | | 5.80 1040.0 | 6.92 | 9.0 |
| | | | | | | 2 | | 5.57 1040.0 | 6.64 | 4.6 |
| TURKU | 84 | 2 | 16 | 1 | 733- 734 | 1 | | 5.20 1040.0 | 6.20 | -2.3 |
| | | | | | | 2 | | 4.73 1040.0 | 5.64 | -11.1 |
| TURKU | 84 | 2 | 16 | 1 | 734- 735 | 1 | | 5.73 1040.0 | 6.84 | 7.7 |
| | | | | | | 2 | | 5.20 1040.0 | 6.20 | -2.3 |
| TURKU | 84 | 2 | 16 | 1 | 735- 736 | 1 | | 5.37 1040.1 | 6.40 | 0.8 |
| | | | | | | 2 | | 5.87 1040.1 | 7.00 | 10.2 |
| TURKU | 84 | 2 | 16 | 1 | 736- 737 | 1 | | 5.10 1040.1 | 6.08 | -4.2 |
| | | | | | | 2 | | 5.30 1040.1 | 6.32 | -0.4 |
| TURKU | 84 | 2 | 16 | 1 | 737- 738 | 1 | | 5.73 1040.1 | 6.84 | 7.7 |
| | | | | | | 2 | | 5.03 1040.1 | 6.00 | -5.4 |
| TURKU | 84 | 2 | 16 | 1 | 738- 739 | 1 | | 4.80 1040.1 | 5.73 | -9.8 |
| | | | | | | 2 | | 4.93 1040.1 | 5.88 | -7.3 |
| TURKU | 84 | 2 | 16 | 1 | 739- 740 | 1 | | 5.47 1040.1 | 6.52 | 2.7 |
| | | | | | | 2 | | 5.13 1040.1 | 6.12 | -3.5 |
| TURKU | 84 | 2 | 16 | 1 | 740- 741 | 1 | | 4.80 1040.0 | 5.72 | -9.8 |
| | | | | | | 2 | | 5.57 1040.0 | 6.64 | 4.6 |
| TURKU | 84 | 2 | 16 | 1 | 741- 742 | 1 | | 5.07 1040.0 | 6.04 | -4.8 |
| | | | | | | 2 | | 4.77 1040.0 | 5.68 | -10.4 |
| TURKU | 84 | 2 | 16 | 1 | 742- 743 | 1 | | 5.50 1040.0 | 6.56 | 3.3 |
| | | | | | | 2 | | 4.83 1040.0 | 5.76 | -9.2 |
| TURKU | 84 | 2 | 16 | 1 | 743- 744 | 1 | | 4.90 1040.0 | 5.84 | -7.9 |
| | | | | | | 2 | | 5.03 1040.0 | 6.00 | -5.4 |
| TURKU | 84 | 2 | 16 | 1 | 744- 745 | 1 | | 5.90 1040.0 | 7.04 | 10.9 |
| | | | | | | 2 | | 5.10 1040.0 | 6.08 | -4.2 |
| TURKU | 84 | 2 | 16 | 1 | 745- 746 | 1 | | 6.07 1040.0 | 7.23 | 14.0 |
| | | | | | | 2 | | 4.27 1040.0 | 5.09 | -19.8 |
| TURKU | 84 | 2 | 16 | 1 | 746- 747 | 1 | | 5.07 1040.0 | 6.04 | -4.8 |
| | | | | | | 2 | | 5.70 1040.0 | 6.80 | 7.1 |
| TURKU | 84 | 2 | 16 | 1 | 747- 748 | 1 | | 5.73 1040.0 | 6.84 | 7.7 |
| | | | | | | 2 | | 4.87 1040.0 | 5.80 | -8.6 |
| TURKU | 84 | 2 | 16 | 1 | 748- 749 | 1 | | 4.67 1040.0 | 5.57 | -12.3 |
| | | | | | | 2 | | 4.90 1040.0 | 5.84 | -7.9 |
| TURKU | 84 | 2 | 16 | 1 | 749- 750 | 1 | | 5.37 1040.0 | 6.40 | 0.8 |
| | | | | | | 2 | | 4.77 1040.0 | 5.68 | -10.4 |
| TURKU | 84 | 2 | 16 | 1 | 750- 751 | 1 | | 5.67 1040.0 | 6.76 | 6.4 |
| | | | | | | 2 | | 6.30 1040.0 | 7.51 | 18.3 |
| TURKU | 84 | 2 | 16 | 1 | 751- 752 | 1 | | 5.53 1040.0 | 6.60 | 3.9 |
| | | | | | | 2 | | 5.43 1040.0 | 6.48 | 2.1 |
| TURKU | 84 | 2 | 16 | 1 | 752- 753 | 1 | | 5.67 1040.0 | 6.76 | 6.4 |
| | | | | | | 2 | | 5.33 1040.0 | 6.36 | 0.2 |
| TURKU | 84 | 2 | 16 | 1 | 753- 754 | 1 | | 5.03 1040.0 | 6.00 | -5.5 |
| | | | | | | 2 | | 5.57 1040.0 | 6.64 | 4.6 |
| TURKU | 84 | 2 | 16 | 1 | 754- 755 | 1 | | 4.63 1040.0 | 5.52 | -13.0 |
| | | | | | | 2 | | 5.13 1040.0 | 6.12 | -3.6 |
| TURKU | 84 | 2 | 16 | 1 | 755- 756 | 1 | | 6.00 1039.9 | 7.15 | 12.7 |
| | | | | | | 2 | | 5.00 1039.9 | 5.96 | -6.1 |

Table 1. continued

Counting rate per second

| STATION | YY | MM | DD | MIN | TIME SPAN | | UNCOR. | PRES. | COR. | % INC. |
|---|---|---|---|---|---|---|---|---|---|---|
| TURKU | 84 | 2 | 16 | 1 | 756- 757 | 1 | 4.83 | 1039.9 | 5.76 | -9.2 |
| | | | | | | 2 | 4.80 | 1039.9 | 5.72 | -9.9 |
| TURKU | 84 | 2 | 16 | 1 | 757- 758 | 1 | 5.43 | 1039.9 | 6.48 | 2.0 |
| | | | | | | 2 | 4.67 | 1039.9 | 5.56 | -12.4 |
| TURKU | 84 | 2 | 16 | 1 | 758- 759 | 1 | 4.77 | 1039.9 | 5.68 | -10.5 |
| | | | | | | 2 | 5.73 | 1039.9 | 6.83 | 7.7 |
| TURKU | 84 | 2 | 16 | 1 | 759- 800 | 1 | 5.87 | 1039.9 | 6.99 | 10.2 |
| | | | | | | 2 | 4.80 | 1039.9 | 5.72 | -9.9 |
| TURKU | 84 | 2 | 16 | 1 | 800- 801 | 1 | 5.40 | 1039.9 | 6.44 | 1.4 |
| | | | | | | 2 | 5.90 | 1039.9 | 7.03 | 10.8 |
| TURKU | 84 | 2 | 16 | 1 | 801- 802 | 1 | 5.20 | 1039.9 | 6.20 | -2.4 |
| | | | | | | 2 | 5.53 | 1039.9 | 6.59 | 3.9 |
| TURKU | 84 | 2 | 16 | 1 | 802- 803 | 1 | 5.80 | 1039.9 | 6.91 | 8.9 |
| | | | | | | 2 | 5.77 | 1039.9 | 6.87 | 8.3 |
| TURKU | 84 | 2 | 16 | 1 | 803- 804 | 1 | 5.60 | 1039.9 | 6.67 | 5.2 |
| | | | | | | 2 | 5.63 | 1039.9 | 6.71 | 5.8 |
| TURKU | 84 | 2 | 16 | 1 | 804- 805 | 1 | 5.57 | 1039.9 | 6.63 | 4.5 |
| | | | | | | 2 | 5.73 | 1039.9 | 6.83 | 7.7 |
| TURKU | 84 | 2 | 16 | 1 | 805- 806 | 1 | 6.23 | 1040.0 | 7.43 | 17.1 |
| | | | | | | 2 | 6.17 | 1040.0 | 7.35 | 15.8 |
| TURKU | 84 | 2 | 16 | 1 | 806- 807 | 1 | 5.60 | 1040.0 | 6.68 | 5.2 |
| | | | | | | 2 | 5.70 | 1040.0 | 6.79 | 7.0 |
| TURKU | 84 | 2 | 16 | 1 | 807- 808 | 1 | 5.73 | 1040.0 | 6.83 | 7.7 |
| | | | | | | 2 | 4.80 | 1040.0 | 5.72 | -9.9 |
| TURKU | 84 | 2 | 16 | 1 | 808- 809 | 1 | 5.57 | 1040.0 | 6.64 | 4.5 |
| | | | | | | 2 | 5.03 | 1040.0 | 6.00 | -5.5 |
| TURKU | 84 | 2 | 16 | 1 | 809- 810 | 1 | 6.67 | 1040.0 | 7.95 | 25.2 |
| | | | | | | 2 | 5.37 | 1040.0 | 6.40 | 0.8 |
| TURKU | 84 | 2 | 16 | 1 | 810- 811 | 1 | 5.17 | 1039.9 | 6.16 | -3.0 |
| | | | | | | 2 | 5.60 | 1039.9 | 6.67 | 5.2 |
| TURKU | 84 | 2 | 16 | 1 | 811- 812 | 1 | 4.63 | 1039.9 | 5.52 | -13.0 |
| | | | | | | 2 | 5.00 | 1039.9 | 5.96 | -6.1 |
| TURKU | 84 | 2 | 16 | 1 | 812- 813 | 1 | 5.13 | 1039.9 | 6.12 | -3.6 |
| | | | | | | 2 | 5.33 | 1039.9 | 6.36 | 0.2 |
| TURKU | 84 | 2 | 16 | 1 | 813- 814 | 1 | 5.23 | 1039.9 | 6.24 | -1.7 |
| | | | | | | 2 | 5.27 | 1039.9 | 6.28 | -1.1 |
| TURKU | 84 | 2 | 16 | 1 | 814- 815 | 1 | 5.87 | 1039.9 | 6.99 | 10.2 |
| | | | | | | 2 | 4.67 | 1039.9 | 5.56 | -12.4 |
| TURKU | 84 | 2 | 16 | 1 | 815- 816 | 1 | 5.33 | 1039.9 | 6.36 | 0.2 |
| | | | | | | 2 | 5.20 | 1039.9 | 6.20 | -2.4 |
| TURKU | 84 | 2 | 16 | 1 | 816- 817 | 1 | 5.77 | 1039.9 | 6.87 | 8.3 |
| | | | | | | 2 | 4.60 | 1039.9 | 5.48 | -13.6 |
| TURKU | 84 | 2 | 16 | 1 | 817- 818 | 1 | 5.00 | 1039.9 | 5.96 | -6.1 |
| | | | | | | 2 | 5.47 | 1039.9 | 6.52 | 2.7 |
| TURKU | 84 | 2 | 16 | 1 | 818- 819 | 1 | 5.30 | 1039.9 | 6.32 | -0.5 |
| | | | | | | 2 | 5.33 | 1039.9 | 6.36 | 0.2 |
| TURKU | 84 | 2 | 16 | 1 | 819- 820 | 1 | 5.20 | 1039.9 | 6.20 | -2.4 |
| | | | | | | 2 | 5.40 | 1039.9 | 6.44 | 1.4 |
| TURKU | 84 | 2 | 16 | 1 | 820- 821 | 1 | 5.20 | 1039.9 | 6.20 | -2.4 |
| | | | | | | 2 | 5.00 | 1039.9 | 5.96 | -6.1 |
| TURKU | 84 | 2 | 16 | 1 | 821- 822 | 1 | 5.53 | 1039.9 | 6.59 | 3.9 |
| | | | | | | 2 | 4.97 | 1039.9 | 5.92 | -6.7 |
| TURKU | 84 | 2 | 16 | 1 | 822- 823 | 1 | 5.30 | 1039.9 | 6.32 | -0.5 |
| | | | | | | 2 | 5.30 | 1039.9 | 6.32 | -0.5 |
| TURKU | 84 | 2 | 16 | 1 | 823- 824 | 1 | 5.93 | 1039.9 | 7.07 | 11.4 |
| | | | | | | 2 | 5.20 | 1039.9 | 6.20 | -2.4 |
| TURKU | 84 | 2 | 16 | 1 | 824- 825 | 1 | 5.63 | 1039.9 | 6.71 | 5.8 |
| | | | | | | 2 | 6.03 | 1039.9 | 7.19 | 13.3 |
| TURKU | 84 | 2 | 16 | 1 | 825- 826 | 1 | 5.27 | 1040.0 | 6.28 | -1.1 |
| | | | | | | 2 | 5.67 | 1040.0 | 6.75 | 6.4 |
| TURKU | 84 | 2 | 16 | 1 | 826- 827 | 1 | 5.17 | 1040.0 | 6.16 | -3.0 |
| | | | | | | 2 | 5.17 | 1040.0 | 6.16 | -3.0 |
| TURKU | 84 | 2 | 16 | 1 | 827- 828 | 1 | 5.20 | 1040.0 | 6.20 | -2.3 |
| | | | | | | 2 | 5.57 | 1040.0 | 6.64 | 4.5 |
| TURKU | 84 | 2 | 16 | 1 | 828- 829 | 1 | 5.50 | 1040.0 | 6.56 | 3.3 |
| | | | | | | 2 | 5.53 | 1040.0 | 6.60 | 3.9 |
| TURKU | 84 | 2 | 16 | 1 | 829- 830 | 1 | 5.80 | 1040.0 | 6.91 | 8.9 |
| | | | | | | 2 | 4.93 | 1040.0 | 5.88 | -7.3 |
| TURKU | 84 | 2 | 16 | 1 | 830- 831 | 1 | 5.33 | 1040.0 | 6.36 | 0.2 |
| | | | | | | 2 | 5.43 | 1040.0 | 6.48 | 2.1 |

Table 1. continued

| STATION | YY | MM | DD | MIN | TIME SPAN | | Counting rate per second UNCOR. | PRES. | COR. | % INC. |
|---|---|---|---|---|---|---|---|---|---|---|
| TURKU | 84 | 2 | 16 | 1 | 831- 832 | 1 | 4.83 | 1040.0 | 5.76 | -9.2 |
| | | | | | | 2 | 5.43 | 1040.0 | 6.48 | 2.1 |
| TURKU | 84 | 2 | 16 | 1 | 832- 833 | 1 | 5.03 | 1040.0 | 6.00 | -5.4 |
| | | | | | | 2 | 5.47 | 1040.0 | 6.52 | 2.7 |
| TURKU | 84 | 2 | 16 | 1 | 833- 834 | 1 | 5.73 | 1040.0 | 6.84 | 7.7 |
| | | | | | | 2 | 5.20 | 1040.0 | 6.20 | -2.3 |
| TURKU | 84 | 2 | 16 | 1 | 834- 835 | 1 | 4.70 | 1040.0 | 5.60 | -11.7 |
| | | | | | | 2 | 5.23 | 1040.0 | 6.24 | -1.7 |
| TURKU | 84 | 2 | 16 | 1 | 835- 836 | 1 | 5.73 | 1040.0 | 6.84 | 7.7 |
| | | | | | | 2 | 5.60 | 1040.0 | 6.68 | 5.2 |
| TURKU | 84 | 2 | 16 | 1 | 836- 837 | 1 | 5.30 | 1040.0 | 6.32 | -0.4 |
| | | | | | | 2 | 5.03 | 1040.0 | 6.00 | -5.4 |
| TURKU | 84 | 2 | 16 | 1 | 837- 838 | 1 | 4.13 | 1040.0 | 4.93 | -22.3 |
| | | | | | | 2 | 5.93 | 1040.0 | 7.08 | 11.5 |
| TURKU | 84 | 2 | 16 | 1 | 838- 839 | 1 | 5.03 | 1040.0 | 6.00 | -5.4 |
| | | | | | | 2 | 5.63 | 1040.0 | 6.72 | 5.8 |
| TURKU | 84 | 2 | 16 | 1 | 839- 840 | 1 | 5.47 | 1040.0 | 6.52 | 2.7 |
| | | | | | | 2 | 5.63 | 1040.0 | 6.72 | 5.8 |
| TURKU | 84 | 2 | 16 | 1 | 840- 841 | 1 | 5.53 | 1040.0 | 6.60 | 4.0 |
| | | | | | | 2 | 4.90 | 1040.0 | 5.84 | -7.9 |
| TURKU | 84 | 2 | 16 | 1 | 841- 842 | 1 | 6.17 | 1040.0 | 7.35 | 15.9 |
| | | | | | | 2 | 5.43 | 1040.0 | 6.48 | 2.1 |
| TURKU | 84 | 2 | 16 | 1 | 842- 843 | 1 | 4.60 | 1040.0 | 5.49 | -13.6 |
| | | | | | | 2 | 5.43 | 1040.0 | 6.48 | 2.1 |
| TURKU | 84 | 2 | 16 | 1 | 843- 844 | 1 | 5.50 | 1040.0 | 6.56 | 3.3 |
| | | | | | | 2 | 4.50 | 1040.0 | 5.37 | -15.5 |
| TURKU | 84 | 2 | 16 | 1 | 844- 845 | 1 | 4.77 | 1040.0 | 5.68 | -10.5 |
| | | | | | | 2 | 5.10 | 1040.0 | 6.08 | -4.2 |
| TURKU | 84 | 2 | 16 | 1 | 845- 846 | 1 | 5.03 | 1040.0 | 6.00 | -5.4 |
| | | | | | | 2 | 5.40 | 1040.0 | 6.44 | 1.4 |
| TURKU | 84 | 2 | 16 | 1 | 846- 847 | 1 | 4.93 | 1040.0 | 5.88 | -7.3 |
| | | | | | | 2 | 5.30 | 1040.0 | 6.32 | -0.4 |
| TURKU | 84 | 2 | 16 | 1 | 847- 848 | 1 | 5.37 | 1040.0 | 6.40 | 0.8 |
| | | | | | | 2 | 5.83 | 1040.0 | 6.96 | 9.6 |
| TURKU | 84 | 2 | 16 | 1 | 848- 849 | 1 | 5.23 | 1040.0 | 6.24 | -1.7 |
| | | | | | | 2 | 5.03 | 1040.0 | 6.00 | -5.4 |
| TURKU | 84 | 2 | 16 | 1 | 849- 850 | 1 | 5.73 | 1040.0 | 6.84 | 7.7 |
| | | | | | | 2 | 4.53 | 1040.0 | 5.41 | -14.8 |
| TURKU | 84 | 2 | 16 | 1 | 850- 851 | 1 | 5.77 | 1040.0 | 6.87 | 8.3 |
| | | | | | | 2 | 5.63 | 1040.0 | 6.72 | 5.8 |
| TURKU | 84 | 2 | 16 | 1 | 851- 852 | 1 | 4.97 | 1040.0 | 5.92 | -6.7 |
| | | | | | | 2 | 5.57 | 1040.0 | 6.64 | 4.6 |
| TURKU | 84 | 2 | 16 | 1 | 852- 853 | 1 | 5.20 | 1040.0 | 6.20 | -2.3 |
| | | | | | | 2 | 5.37 | 1040.0 | 6.40 | 0.8 |
| TURKU | 84 | 2 | 16 | 1 | 853- 854 | 1 | 5.23 | 1040.0 | 6.24 | -1.7 |
| | | | | | | 2 | 5.77 | 1040.0 | 6.87 | 8.3 |
| TURKU | 84 | 2 | 16 | 1 | 854- 855 | 1 | 4.93 | 1040.0 | 5.88 | -7.3 |
| | | | | | | 2 | 6.33 | 1040.0 | 7.55 | 18.9 |
| TURKU | 84 | 2 | 16 | 1 | 855- 856 | 1 | 5.30 | 1040.0 | 6.32 | -0.5 |
| | | | | | | 2 | 5.93 | 1040.0 | 7.07 | 11.4 |
| TURKU | 84 | 2 | 16 | 1 | 856- 857 | 1 | 5.90 | 1040.0 | 7.03 | 10.8 |
| | | | | | | 2 | 5.07 | 1040.0 | 6.04 | -4.8 |
| TURKU | 84 | 2 | 16 | 1 | 857- 858 | 1 | 5.30 | 1040.0 | 6.32 | -0.5 |
| | | | | | | 2 | 4.97 | 1040.0 | 5.92 | -6.7 |
| TURKU | 84 | 2 | 16 | 1 | 858- 859 | 1 | 4.87 | 1040.0 | 5.80 | -8.6 |
| | | | | | | 2 | 5.53 | 1040.0 | 6.60 | 3.9 |
| TURKU | 84 | 2 | 16 | 1 | 859- 900 | 1 | 4.33 | 1040.0 | 5.17 | -18.6 |
| | | | | | | 2 | 5.73 | 1040.0 | 6.83 | 7.7 |
| TURKU | 84 | 2 | 16 | 1 | 900- 901 | 1 | 5.03 | 1040.0 | 6.00 | -5.5 |
| | | | | | | 2 | 5.60 | 1040.0 | 6.68 | 5.2 |
| TURKU | 84 | 2 | 16 | 1 | 901- 902 | 1 | 6.00 | 1040.0 | 7.15 | 12.7 |
| | | | | | | 2 | 4.70 | 1040.0 | 5.60 | -11.7 |
| TURKU | 84 | 2 | 16 | 1 | 902- 903 | 1 | 5.47 | 1040.0 | 6.52 | 2.7 |
| | | | | | | 2 | 5.90 | 1040.0 | 7.03 | 10.8 |
| TURKU | 84 | 2 | 16 | 1 | 903- 904 | 1 | 3.87 | 1040.0 | 4.61 | -27.4 |
| | | | | | | 2 | 4.97 | 1040.0 | 5.92 | -6.7 |
| TURKU | 84 | 2 | 16 | 1 | 904- 905 | 1 | 5.57 | 1040.0 | 6.64 | 4.5 |
| | | | | | | 2 | 4.97 | 1040.0 | 5.92 | -6.7 |
| TURKU | 84 | 2 | 16 | 1 | 905- 906 | 1 | 5.27 | 1040.0 | 6.28 | -1.1 |
| | | | | | | 2 | 5.20 | 1040.0 | 6.20 | -2.3 |

Table 1. continued

Counting rate per second

| STATION | YY | MM | DD | MIN | TIME SPAN | | UNCOR. | PRES. | COR. | % INC. |
|---|---|---|---|---|---|---|---|---|---|---|
| TURKU | 84 | 2 | 16 | 1 | 906- 907 | 1 | 5.87 | 1040.0 | 6.99 | 10.2 |
| | | | | | | 2 | 5.80 | 1040.0 | 6.91 | 8.9 |
| TURKU | 84 | 2 | 16 | 1 | 907- 908 | 1 | 6.27 | 1040.0 | 7.47 | 17.7 |
| | | | | | | 2 | 5.73 | 1040.0 | 6.83 | 7.7 |
| TURKU | 84 | 2 | 16 | 1 | 908- 909 | 1 | 6.47 | 1040.0 | 7.71 | 21.4 |
| | | | | | | 2 | 6.30 | 1040.0 | 7.51 | 18.3 |
| TURKU | 84 | 2 | 16 | 1 | 909- 910 | 1 | 7.03 | 1040.0 | 8.38 | 32.1 |
| | | | | | | 2 | 6.17 | 1040.0 | 7.35 | 15.8 |
| TURKU | 84 | 2 | 16 | 1 | 910- 911 | 1 | 6.07 | 1040.0 | 7.23 | 13.9 |
| | | | | | | 2 | 6.57 | 1040.0 | 7.83 | 23.3 |
| TURKU | 84 | 2 | 16 | 1 | 911- 912 | 1 | 6.73 | 1040.0 | 8.03 | 26.5 |
| | | | | | | 2 | 7.33 | 1040.0 | 8.74 | 37.7 |
| TURKU | 84 | 2 | 16 | 1 | 912- 913 | 1 | 6.57 | 1040.0 | 7.83 | 23.3 |
| | | | | | | 2 | 6.53 | 1040.0 | 7.79 | 22.7 |
| TURKU | 84 | 2 | 16 | 1 | 913- 914 | 1 | 5.97 | 1040.0 | 7.11 | 12.1 |
| | | | | | | 2 | 6.97 | 1040.0 | 8.30 | 30.8 |
| TURKU | 84 | 2 | 16 | 1 | 914- 915 | 1 | 6.20 | 1040.0 | 7.39 | 16.4 |
| | | | | | | 2 | 5.93 | 1040.0 | 7.07 | 11.4 |
| TURKU | 84 | 2 | 16 | 1 | 915- 916 | 1 | 6.23 | 1040.0 | 7.43 | 17.1 |
| | | | | | | 2 | 5.80 | 1040.0 | 6.91 | 8.9 |
| TURKU | 84 | 2 | 16 | 1 | 916- 917 | 1 | 7.03 | 1040.0 | 8.38 | 32.1 |
| | | | | | | 2 | 6.07 | 1040.0 | 7.23 | 13.9 |
| TURKU | 84 | 2 | 16 | 1 | 917- 918 | 1 | 6.53 | 1040.0 | 7.79 | 22.7 |
| | | | | | | 2 | 6.30 | 1040.0 | 7.51 | 18.3 |
| TURKU | 84 | 2 | 16 | 1 | 918- 919 | 1 | 5.70 | 1040.0 | 6.80 | 7.1 |
| | | | | | | 2 | 5.73 | 1040.0 | 6.83 | 7.7 |
| TURKU | 84 | 2 | 16 | 1 | 919- 920 | 1 | 6.03 | 1040.0 | 7.19 | 13.3 |
| | | | | | | 2 | 6.50 | 1040.0 | 7.75 | 22.1 |
| TURKU | 84 | 2 | 16 | 1 | 920- 921 | 1 | 4.60 | 1040.0 | 5.48 | -13.6 |
| | | | | | | 2 | 5.40 | 1040.0 | 6.44 | 1.4 |
| TURKU | 84 | 2 | 16 | 1 | 921- 922 | 1 | 5.10 | 1040.0 | 6.08 | -4.2 |
| | | | | | | 2 | 5.60 | 1040.0 | 6.68 | 5.2 |
| TURKU | 84 | 2 | 16 | 1 | 922- 923 | 1 | 6.13 | 1040.0 | 7.31 | 15.2 |
| | | | | | | 2 | 6.17 | 1040.0 | 7.35 | 15.8 |
| TURKU | 84 | 2 | 16 | 1 | 923- 924 | 1 | 5.73 | 1040.0 | 6.83 | 7.7 |
| | | | | | | 2 | 5.60 | 1040.0 | 6.68 | 5.2 |
| TURKU | 84 | 2 | 16 | 1 | 924- 925 | 1 | 6.70 | 1040.0 | 7.99 | 25.8 |
| | | | | | | 2 | 6.30 | 1040.0 | 7.51 | 18.3 |
| TURKU | 84 | 2 | 16 | 1 | 925- 926 | 1 | 6.27 | 1040.0 | 7.47 | 17.7 |
| | | | | | | 2 | 6.07 | 1040.0 | 7.23 | 13.9 |
| TURKU | 84 | 2 | 16 | 1 | 926- 927 | 1 | 7.03 | 1040.0 | 8.38 | 32.1 |
| | | | | | | 2 | 5.77 | 1040.0 | 6.87 | 8.3 |
| TURKU | 84 | 2 | 16 | 1 | 927- 928 | 1 | 5.47 | 1040.0 | 6.52 | 2.7 |
| | | | | | | 2 | 6.13 | 1040.0 | 7.31 | 15.2 |
| TURKU | 84 | 2 | 16 | 1 | 928- 929 | 1 | 6.07 | 1040.0 | 7.23 | 13.9 |
| | | | | | | 2 | 5.63 | 1040.0 | 6.72 | 5.8 |
| TURKU | 84 | 2 | 16 | 1 | 929- 930 | 1 | 6.27 | 1040.0 | 7.47 | 17.7 |
| | | | | | | 2 | 6.30 | 1040.0 | 7.51 | 18.3 |
| TURKU | 84 | 2 | 16 | 1 | 930- 931 | 1 | 5.77 | 1040.0 | 6.87 | 8.3 |
| | | | | | | 2 | 6.07 | 1040.0 | 7.23 | 13.9 |
| TURKU | 84 | 2 | 16 | 1 | 931- 932 | 1 | 6.30 | 1040.0 | 7.51 | 18.3 |
| | | | | | | 2 | 5.10 | 1040.0 | 6.08 | -4.2 |
| TURKU | 84 | 2 | 16 | 1 | 932- 933 | 1 | 5.50 | 1040.0 | 6.56 | 3.3 |
| | | | | | | 2 | 5.30 | 1040.0 | 6.32 | -0.5 |
| TURKU | 84 | 2 | 16 | 1 | 933- 934 | 1 | 5.33 | 1040.0 | 6.36 | 0.2 |
| | | | | | | 2 | 5.13 | 1040.0 | 6.12 | -3.6 |
| TURKU | 84 | 2 | 16 | 1 | 934- 935 | 1 | 5.40 | 1040.0 | 6.44 | 1.4 |
| | | | | | | 2 | 5.50 | 1040.0 | 6.56 | 3.3 |
| TURKU | 84 | 2 | 16 | 1 | 935- 936 | 1 | 6.27 | 1040.0 | 7.47 | 17.7 |
| | | | | | | 2 | 6.70 | 1040.0 | 7.99 | 25.8 |
| TURKU | 84 | 2 | 16 | 1 | 936- 937 | 1 | 5.60 | 1040.0 | 6.68 | 5.2 |
| | | | | | | 2 | 5.93 | 1040.0 | 7.07 | 11.4 |
| TURKU | 84 | 2 | 16 | 1 | 937- 938 | 1 | 5.57 | 1040.0 | 6.64 | 4.5 |
| | | | | | | 2 | 5.30 | 1040.0 | 6.32 | -0.5 |
| TURKU | 84 | 2 | 16 | 1 | 938- 939 | 1 | 6.40 | 1040.0 | 7.63 | 20.2 |
| | | | | | | 2 | 5.97 | 1040.0 | 7.11 | 12.1 |
| TURKU | 84 | 2 | 16 | 1 | 939- 940 | 1 | 5.07 | 1040.0 | 6.04 | -4.8 |
| | | | | | | 2 | 5.23 | 1040.0 | 6.24 | -1.7 |
| TURKU | 84 | 2 | 16 | 1 | 940- 941 | 1 | 5.57 | 1039.9 | 6.63 | 4.5 |
| | | | | | | 2 | 5.73 | 1039.9 | 6.83 | 7.7 |

Table 1. continued

| STATION | YY | MM | DD | MIN | TIME SPAN | | Counting rate per second | UNCOR. | PRES. | COR. | % INC. |
|---|---|---|---|---|---|---|---|---|---|---|---|
| TURKU | 84 | 2 | 16 | 1 | 941- 942 | 1 | | 5.37 | 1039.9 | 6.40 | 0.8 |
| | | | | | | 2 | | 4.87 | 1039.9 | 5.80 | -8.6 |
| TURKU | 84 | 2 | 16 | 1 | 942- 943 | 1 | | 5.27 | 1039.9 | 6.28 | -1.1 |
| | | | | | | 2 | | 5.77 | 1039.9 | 6.87 | 8.3 |
| TURKU | 84 | 2 | 16 | 1 | 943- 944 | 1 | | 5.70 | 1039.9 | 6.79 | 7.0 |
| | | | | | | 2 | | 5.33 | 1039.9 | 6.36 | 0.1 |
| TURKU | 84 | 2 | 16 | 1 | 944- 945 | 1 | | 5.70 | 1039.9 | 6.79 | 7.0 |
| | | | | | | 2 | | 5.73 | 1039.9 | 6.83 | 7.7 |
| TURKU | 84 | 2 | 16 | 1 | 945- 946 | 1 | | 5.90 | 1039.9 | 7.03 | 10.8 |
| | | | | | | 2 | | 6.43 | 1039.9 | 7.67 | 20.8 |
| TURKU | 84 | 2 | 16 | 1 | 946- 947 | 1 | | 6.13 | 1039.9 | 7.31 | 15.2 |
| | | | | | | 2 | | 5.33 | 1039.9 | 6.36 | 0.1 |
| TURKU | 84 | 2 | 16 | 1 | 947- 948 | 1 | | 6.00 | 1039.9 | 7.15 | 12.7 |
| | | | | | | 2 | | 5.47 | 1039.9 | 6.51 | 2.6 |
| TURKU | 84 | 2 | 16 | 1 | 948- 949 | 1 | | 5.63 | 1039.9 | 6.71 | 5.8 |
| | | | | | | 2 | | 6.20 | 1039.9 | 7.39 | 16.4 |
| TURKU | 84 | 2 | 16 | 1 | 949- 950 | 1 | | 5.10 | 1039.9 | 6.08 | -4.2 |
| | | | | | | 2 | | 6.07 | 1039.9 | 7.23 | 13.9 |
| TURKU | 84 | 2 | 16 | 1 | 950- 951 | 1 | | 5.00 | 1039.9 | 5.96 | -6.1 |
| | | | | | | 2 | | 5.57 | 1039.9 | 6.63 | 4.5 |
| TURKU | 84 | 2 | 16 | 1 | 951- 952 | 1 | | 5.90 | 1039.9 | 7.03 | 10.8 |
| | | | | | | 2 | | 5.90 | 1039.9 | 7.03 | 10.8 |
| TURKU | 84 | 2 | 16 | 1 | 952- 953 | 1 | | 5.53 | 1039.9 | 6.59 | 3.9 |
| | | | | | | 2 | | 5.47 | 1039.9 | 6.51 | 2.6 |
| TURKU | 84 | 2 | 16 | 1 | 953- 954 | 1 | | 5.93 | 1039.9 | 7.07 | 11.4 |
| | | | | | | 2 | | 5.77 | 1039.9 | 6.87 | 8.3 |
| TURKU | 84 | 2 | 16 | 1 | 954- 955 | 1 | | 5.43 | 1039.9 | 6.48 | 2.0 |
| | | | | | | 2 | | 5.23 | 1039.9 | 6.24 | -1.7 |
| TURKU | 84 | 2 | 16 | 1 | 955- 956 | 1 | | 5.00 | 1039.9 | 5.96 | -6.1 |
| | | | | | | 2 | | 5.10 | 1039.9 | 6.08 | -4.3 |
| TURKU | 84 | 2 | 16 | 1 | 956- 957 | 1 | | 5.63 | 1039.9 | 6.71 | 5.8 |
| | | | | | | 2 | | 5.73 | 1039.9 | 6.83 | 7.6 |
| TURKU | 84 | 2 | 16 | 1 | 957- 958 | 1 | | 5.77 | 1039.9 | 6.87 | 8.3 |
| | | | | | | 2 | | 5.23 | 1039.9 | 6.24 | -1.8 |
| TURKU | 84 | 2 | 16 | 1 | 958- 959 | 1 | | 5.27 | 1039.9 | 6.28 | -1.1 |
| | | | | | | 2 | | 5.30 | 1039.9 | 6.32 | -0.5 |
| TURKU | 84 | 2 | 16 | 1 | 959-1000 | 1 | | 4.83 | 1039.9 | 5.76 | -9.3 |
| | | | | | | 2 | | 6.13 | 1039.9 | 7.31 | 15.1 |
| TURKU | 84 | 2 | 16 | 1 | 1000-1001 | 1 | | 5.73 | 1039.9 | 6.83 | 7.6 |
| | | | | | | 2 | | 5.53 | 1039.9 | 6.59 | 3.9 |
| TURKU | 84 | 2 | 16 | 1 | 1001-1002 | 1 | | 5.47 | 1039.9 | 6.51 | 2.6 |
| | | | | | | 2 | | 5.70 | 1039.9 | 6.79 | 7.0 |
| TURKU | 84 | 2 | 16 | 1 | 1002-1003 | 1 | | 5.50 | 1039.9 | 6.55 | 3.3 |
| | | | | | | 2 | | 5.73 | 1039.9 | 6.83 | 7.6 |
| TURKU | 84 | 2 | 16 | 1 | 1003-1004 | 1 | | 5.33 | 1039.9 | 6.36 | 0.1 |
| | | | | | | 2 | | 5.33 | 1039.9 | 6.36 | 0.1 |
| TURKU | 84 | 2 | 16 | 1 | 1004-1005 | 1 | | 5.80 | 1039.9 | 6.91 | 8.9 |
| | | | | | | 2 | | 5.53 | 1039.9 | 6.59 | 3.9 |
| TURKU | 84 | 2 | 16 | 1 | 1005-1006 | 1 | | 5.40 | 1039.9 | 6.43 | 1.4 |
| | | | | | | 2 | | 6.10 | 1039.9 | 7.27 | 14.5 |
| TURKU | 84 | 2 | 16 | 1 | 1006-1007 | 1 | | 6.17 | 1039.9 | 7.35 | 15.7 |
| | | | | | | 2 | | 5.20 | 1039.9 | 6.20 | -2.4 |
| TURKU | 84 | 2 | 16 | 1 | 1007-1008 | 1 | | 5.60 | 1039.9 | 6.67 | 5.1 |
| | | | | | | 2 | | 5.63 | 1039.9 | 6.71 | 5.7 |
| TURKU | 84 | 2 | 16 | 1 | 1008-1009 | 1 | | 4.77 | 1039.9 | 5.68 | -10.5 |
| | | | | | | 2 | | 5.67 | 1039.9 | 6.75 | 6.4 |
| TURKU | 84 | 2 | 16 | 1 | 1009-1010 | 1 | | 5.90 | 1039.9 | 7.03 | 10.7 |
| | | | | | | 2 | | 5.30 | 1039.9 | 6.31 | -0.5 |
| TURKU | 84 | 2 | 16 | 1 | 1010-1011 | 1 | | 5.57 | 1039.9 | 6.63 | 4.5 |
| | | | | | | 2 | | 5.97 | 1039.9 | 7.11 | 12.0 |
| TURKU | 84 | 2 | 16 | 1 | 1011-1012 | 1 | | 5.17 | 1039.9 | 6.16 | -3.0 |
| | | | | | | 2 | | 6.33 | 1039.9 | 7.55 | 18.9 |
| TURKU | 84 | 2 | 16 | 1 | 1012-1013 | 1 | | 5.73 | 1039.9 | 6.83 | 7.6 |
| | | | | | | 2 | | 5.33 | 1039.9 | 6.35 | 0.1 |
| TURKU | 84 | 2 | 16 | 1 | 1013-1014 | 1 | | 6.17 | 1039.9 | 7.35 | 15.8 |
| | | | | | | 2 | | 5.80 | 1039.9 | 6.91 | 8.9 |
| TURKU | 84 | 2 | 16 | 1 | 1014-1015 | 1 | | 5.43 | 1039.9 | 6.47 | 2.0 |
| | | | | | | 2 | | 5.33 | 1039.9 | 6.35 | 0.1 |
| TURKU | 84 | 2 | 16 | 1 | 1015-1016 | 1 | | 5.13 | 1039.8 | 6.12 | -3.7 |
| | | | | | | 2 | | 6.17 | 1039.8 | 7.35 | 15.7 |

Table 1. continued

| STATION | YY | MM | DD | MIN | TIME SPAN | | Counting rate per second UNCOR. | PRES. | COR. | % INC. |
|---|---|---|---|---|---|---|---|---|---|---|
| TURKU | 84 | 2 | 16 | 1 | 1016-1017 | 1 | 5.13 | 1039.8 | 6.12 | -3.7 |
| | | | | | | 2 | 5.07 | 1039.8 | 6.04 | -4.9 |
| TURKU | 84 | 2 | 16 | 1 | 1017-1018 | 1 | 5.00 | 1039.8 | 5.96 | -6.2 |
| | | | | | | 2 | 5.23 | 1039.8 | 6.23 | -1.8 |
| TURKU | 84 | 2 | 16 | 1 | 1018-1019 | 1 | 5.43 | 1039.8 | 6.47 | 2.0 |
| | | | | | | 2 | 4.90 | 1039.8 | 5.84 | -8.0 |
| TURKU | 84 | 2 | 16 | 1 | 1019-1020 | 1 | 5.83 | 1039.8 | 6.95 | 9.5 |
| | | | | | | 2 | 5.23 | 1039.8 | 6.23 | -1.8 |
| TURKU | 84 | 2 | 16 | 1 | 1020-1021 | 1 | 5.57 | 1039.8 | 6.63 | 4.5 |
| | | | | | | 2 | 5.07 | 1039.8 | 6.04 | -4.9 |
| TURKU | 84 | 2 | 16 | 1 | 1021-1022 | 1 | 6.20 | 1039.8 | 7.39 | 16.4 |
| | | | | | | 2 | 5.20 | 1039.8 | 6.19 | -2.4 |
| TURKU | 84 | 2 | 16 | 1 | 1022-1023 | 1 | 5.93 | 1039.8 | 7.07 | 11.4 |
| | | | | | | 2 | 5.57 | 1039.8 | 6.63 | 4.5 |
| TURKU | 84 | 2 | 16 | 1 | 1023-1024 | 1 | 5.53 | 1039.8 | 6.59 | 3.9 |
| | | | | | | 2 | 5.10 | 1039.8 | 6.08 | -4.3 |
| TURKU | 84 | 2 | 16 | 1 | 1024-1025 | 1 | 4.73 | 1039.8 | 5.64 | -11.2 |
| | | | | | | 2 | 5.47 | 1039.8 | 6.51 | 2.6 |
| TURKU | 84 | 2 | 16 | 1 | 1025-1026 | 1 | 6.03 | 1039.8 | 7.19 | 13.2 |
| | | | | | | 2 | 5.27 | 1039.8 | 6.27 | -1.2 |
| TURKU | 84 | 2 | 16 | 1 | 1026-1027 | 1 | 5.40 | 1039.8 | 6.43 | 1.3 |
| | | | | | | 2 | 5.40 | 1039.8 | 6.43 | 1.3 |
| TURKU | 84 | 2 | 16 | 1 | 1027-1028 | 1 | 4.83 | 1039.8 | 5.76 | -9.3 |
| | | | | | | 2 | 6.03 | 1039.8 | 7.19 | 13.2 |
| TURKU | 84 | 2 | 16 | 1 | 1028-1029 | 1 | 6.27 | 1039.8 | 7.46 | 17.6 |
| | | | | | | 2 | 5.60 | 1039.8 | 6.67 | 5.1 |
| TURKU | 84 | 2 | 16 | 1 | 1029-1030 | 1 | 5.07 | 1039.8 | 6.03 | -4.9 |
| | | | | | | 2 | 5.70 | 1039.8 | 6.79 | 6.9 |
| TURKU | 84 | 2 | 16 | 1 | 1030-1031 | 1 | 5.17 | 1039.8 | 6.15 | -3.1 |
| | | | | | | 2 | 5.17 | 1039.8 | 6.15 | -3.1 |
| TURKU | 84 | 2 | 16 | 1 | 1031-1032 | 1 | 5.60 | 1039.8 | 6.67 | 5.1 |
| | | | | | | 2 | 5.47 | 1039.8 | 6.51 | 2.6 |
| TURKU | 84 | 2 | 16 | 1 | 1032-1033 | 1 | 4.97 | 1039.8 | 5.91 | -6.8 |
| | | | | | | 2 | 5.13 | 1039.8 | 6.11 | -3.7 |
| TURKU | 84 | 2 | 16 | 1 | 1033-1034 | 1 | 5.73 | 1039.8 | 6.83 | 7.6 |
| | | | | | | 2 | 5.57 | 1039.8 | 6.63 | 4.4 |
| TURKU | 84 | 2 | 16 | 1 | 1034-1035 | 1 | 5.00 | 1039.8 | 5.95 | -6.2 |
| | | | | | | 2 | 5.10 | 1039.8 | 6.07 | -4.3 |
| TURKU | 84 | 2 | 16 | 1 | 1035-1036 | 1 | 5.83 | 1039.7 | 6.95 | 9.4 |
| | | | | | | 2 | 4.80 | 1039.7 | 5.72 | -10.0 |
| TURKU | 84 | 2 | 16 | 1 | 1036-1037 | 1 | 5.23 | 1039.7 | 6.23 | -1.8 |
| | | | | | | 2 | 5.80 | 1039.7 | 6.91 | 8.8 |
| TURKU | 84 | 2 | 16 | 1 | 1037-1038 | 1 | 5.83 | 1039.7 | 6.95 | 9.4 |
| | | | | | | 2 | 5.63 | 1039.7 | 6.71 | 5.7 |
| TURKU | 84 | 2 | 16 | 1 | 1038-1039 | 1 | 5.33 | 1039.7 | 6.35 | 0.0 |
| | | | | | | 2 | 6.43 | 1039.7 | 7.66 | 20.7 |
| TURKU | 84 | 2 | 16 | 1 | 1039-1040 | 1 | 5.17 | 1039.7 | 6.15 | -3.1 |
| | | | | | | 2 | 5.03 | 1039.7 | 5.99 | -5.6 |
| TURKU | 84 | 2 | 16 | 1 | 1040-1041 | 1 | 5.87 | 1039.7 | 6.98 | 10.0 |
| | | | | | | 2 | 5.40 | 1039.7 | 6.43 | 1.2 |
| TURKU | 84 | 2 | 16 | 1 | 1041-1042 | 1 | 5.37 | 1039.7 | 6.39 | 0.6 |
| | | | | | | 2 | 5.87 | 1039.7 | 6.98 | 10.0 |
| TURKU | 84 | 2 | 16 | 1 | 1042-1043 | 1 | 4.80 | 1039.7 | 5.71 | -10.0 |
| | | | | | | 2 | 5.47 | 1039.7 | 6.51 | 2.5 |
| TURKU | 84 | 2 | 16 | 1 | 1043-1044 | 1 | 5.20 | 1039.7 | 6.19 | -2.5 |
| | | | | | | 2 | 5.97 | 1039.7 | 7.10 | 11.9 |
| TURKU | 84 | 2 | 16 | 1 | 1044-1045 | 1 | 5.17 | 1039.7 | 6.15 | -3.1 |
| | | | | | | 2 | 5.83 | 1039.7 | 6.94 | 9.4 |
| TURKU | 84 | 2 | 16 | 1 | 1045-1046 | 1 | 5.40 | 1039.7 | 6.43 | 1.3 |
| | | | | | | 2 | 5.47 | 1039.7 | 6.51 | 2.5 |
| TURKU | 84 | 2 | 16 | 1 | 1046-1047 | 1 | 6.10 | 1039.7 | 7.26 | 14.4 |
| | | | | | | 2 | 4.83 | 1039.7 | 5.75 | -9.4 |
| TURKU | 84 | 2 | 16 | 1 | 1047-1048 | 1 | 5.27 | 1039.7 | 6.27 | -1.2 |
| | | | | | | 2 | 4.93 | 1039.7 | 5.87 | -7.5 |
| TURKU | 84 | 2 | 16 | 1 | 1048-1049 | 1 | 4.97 | 1039.7 | 5.91 | -6.9 |
| | | | | | | 2 | 6.53 | 1039.7 | 7.78 | 22.5 |
| TURKU | 84 | 2 | 16 | 1 | 1049-1050 | 1 | 4.50 | 1039.7 | 5.36 | -15.6 |
| | | | | | | 2 | 5.43 | 1039.7 | 6.47 | 1.9 |
| TURKU | 84 | 2 | 16 | 1 | 1050-1051 | 1 | 5.90 | 1039.7 | 7.02 | 10.6 |
| | | | | | | 2 | 4.73 | 1039.7 | 5.63 | -11.2 |

Table 1. continued

| STATION | YY | MM | DD | MIN | TIME SPAN | Counting rate per second | UNCOR. | PRES. | COR. | % INC. |
|---|---|---|---|---|---|---|---|---|---|---|
| TURKU | 84 | 2 | 16 | 1 | 1051-1052 | 1 | 5.60 | 1039.7 | 6.66 | 5.0 |
| | | | | | | 2 | 5.37 | 1039.7 | 6.39 | 0.6 |
| TURKU | 84 | 2 | 16 | 1 | 1052-1053 | 1 | 5.20 | 1039.7 | 6.19 | -2.5 |
| | | | | | | 2 | 4.97 | 1039.7 | 5.91 | -6.9 |
| TURKU | 84 | 2 | 16 | 1 | 1053-1054 | 1 | 5.60 | 1039.7 | 6.66 | 5.0 |
| | | | | | | 2 | 5.20 | 1039.7 | 6.19 | -2.5 |
| TURKU | 84 | 2 | 16 | 1 | 1054-1055 | 1 | 5.83 | 1039.7 | 6.94 | 9.4 |
| | | | | | | 2 | 5.57 | 1039.7 | 6.63 | 4.4 |
| TURKU | 84 | 2 | 16 | 1 | 1055-1056 | 1 | 5.37 | 1039.6 | 6.39 | 0.6 |
| | | | | | | 2 | 4.40 | 1039.6 | 5.24 | -17.5 |
| TURKU | 84 | 2 | 16 | 1 | 1056-1057 | 1 | 4.73 | 1039.6 | 5.63 | -11.3 |
| | | | | | | 2 | 4.90 | 1039.6 | 5.83 | -8.1 |
| TURKU | 84 | 2 | 16 | 1 | 1057-1058 | 1 | 5.90 | 1039.6 | 7.02 | 10.6 |
| | | | | | | 2 | 5.03 | 1039.6 | 5.99 | -5.6 |
| TURKU | 84 | 2 | 16 | 1 | 1058-1059 | 1 | 5.40 | 1039.6 | 6.43 | 1.2 |
| | | | | | | 2 | 5.53 | 1039.6 | 6.58 | 3.7 |
| TURKU | 84 | 2 | 16 | 1 | 1059-1100 | 1 | 5.47 | 1039.6 | 6.51 | 2.5 |
| | | | | | | 2 | 5.90 | 1039.6 | 7.02 | 10.6 |
| TURKU | 84 | 2 | 16 | 1 | 1100-1101 | 1 | 5.40 | 1039.6 | 6.43 | 1.2 |
| | | | | | | 2 | 4.87 | 1039.6 | 5.79 | -8.8 |
| TURKU | 84 | 2 | 16 | 1 | 1101-1102 | 1 | 5.80 | 1039.6 | 6.90 | 8.7 |
| | | | | | | 2 | 5.27 | 1039.6 | 6.27 | -1.3 |
| TURKU | 84 | 2 | 16 | 1 | 1102-1103 | 1 | 5.57 | 1039.6 | 6.62 | 4.4 |
| | | | | | | 2 | 5.63 | 1039.6 | 6.70 | 5.6 |
| TURKU | 84 | 2 | 16 | 1 | 1103-1104 | 1 | 6.17 | 1039.6 | 7.34 | 15.6 |
| | | | | | | 2 | 5.13 | 1039.6 | 6.11 | -3.8 |
| TURKU | 84 | 2 | 16 | 1 | 1104-1105 | 1 | 5.37 | 1039.6 | 6.39 | 0.6 |
| | | | | | | 2 | 5.43 | 1039.6 | 6.47 | 1.9 |
| TURKU | 84 | 2 | 16 | 1 | 1105-1106 | 1 | 6.20 | 1039.6 | 7.38 | 16.2 |
| | | | | | | 2 | 5.13 | 1039.6 | 6.11 | -3.8 |
| TURKU | 84 | 2 | 16 | 1 | 1106-1107 | 1 | 5.67 | 1039.6 | 6.74 | 6.2 |
| | | | | | | 2 | 5.40 | 1039.6 | 6.43 | 1.2 |
| TURKU | 84 | 2 | 16 | 1 | 1107-1108 | 1 | 4.97 | 1039.6 | 5.91 | -6.9 |
| | | | | | | 2 | 4.57 | 1039.6 | 5.43 | -14.4 |
| TURKU | 84 | 2 | 16 | 1 | 1108-1109 | 1 | 5.27 | 1039.6 | 6.27 | -1.3 |
| | | | | | | 2 | 5.30 | 1039.6 | 6.31 | -0.6 |
| TURKU | 84 | 2 | 16 | 1 | 1109-1110 | 1 | 4.70 | 1039.6 | 5.59 | -11.9 |
| | | | | | | 2 | 4.83 | 1039.6 | 5.75 | -9.4 |
| TURKU | 84 | 2 | 16 | 1 | 1110-1111 | 1 | 5.00 | 1039.6 | 5.95 | -6.3 |
| | | | | | | 2 | 5.27 | 1039.6 | 6.27 | -1.3 |
| TURKU | 84 | 2 | 16 | 1 | 1111-1112 | 1 | 5.37 | 1039.6 | 6.39 | 0.6 |
| | | | | | | 2 | 5.07 | 1039.6 | 6.03 | -5.0 |
| TURKU | 84 | 2 | 16 | 1 | 1112-1113 | 1 | 4.43 | 1039.6 | 5.28 | -16.9 |
| | | | | | | 2 | 5.27 | 1039.6 | 6.27 | -1.3 |
| TURKU | 84 | 2 | 16 | 1 | 1113-1114 | 1 | 6.33 | 1039.6 | 7.54 | 18.7 |
| | | | | | | 2 | 5.47 | 1039.6 | 6.50 | 2.5 |
| TURKU | 84 | 2 | 16 | 1 | 1114-1115 | 1 | 4.50 | 1039.6 | 5.35 | -15.6 |
| | | | | | | 2 | 5.10 | 1039.6 | 6.07 | -4.4 |
| TURKU | 84 | 2 | 16 | 1 | 1115-1116 | 1 | 5.00 | 1039.6 | 5.95 | -6.3 |
| | | | | | | 2 | 5.10 | 1039.6 | 6.07 | -4.4 |
| TURKU | 84 | 2 | 16 | 1 | 1116-1117 | 1 | 6.13 | 1039.6 | 7.30 | 15.0 |
| | | | | | | 2 | 6.00 | 1039.6 | 7.14 | 12.5 |
| TURKU | 84 | 2 | 16 | 1 | 1117-1118 | 1 | 5.23 | 1039.6 | 6.23 | -1.9 |
| | | | | | | 2 | 5.80 | 1039.6 | 6.90 | 8.7 |
| TURKU | 84 | 2 | 16 | 1 | 1118-1119 | 1 | 5.53 | 1039.6 | 6.58 | 3.7 |
| | | | | | | 2 | 4.80 | 1039.6 | 5.71 | -10.0 |
| TURKU | 84 | 2 | 16 | 1 | 1119-1120 | 1 | 5.47 | 1039.6 | 6.50 | 2.5 |
| | | | | | | 2 | 5.30 | 1039.6 | 6.31 | -0.7 |
| TURKU | 84 | 2 | 16 | 1 | 1120-1121 | 1 | 5.97 | 1039.6 | 7.10 | 11.8 |
| | | | | | | 2 | 5.53 | 1039.6 | 6.58 | 3.7 |
| TURKU | 84 | 2 | 16 | 1 | 1121-1122 | 1 | 6.03 | 1039.6 | 7.18 | 13.1 |
| | | | | | | 2 | 5.40 | 1039.6 | 6.42 | 1.2 |
| TURKU | 84 | 2 | 16 | 1 | 1122-1123 | 1 | 5.80 | 1039.6 | 6.90 | 8.7 |
| | | | | | | 2 | 5.73 | 1039.6 | 6.82 | 7.5 |
| TURKU | 84 | 2 | 16 | 1 | 1123-1124 | 1 | 5.43 | 1039.6 | 6.46 | 1.8 |
| | | | | | | 2 | 5.67 | 1039.6 | 6.74 | 6.2 |
| TURKU | 84 | 2 | 16 | 1 | 1124-1125 | 1 | 5.40 | 1039.6 | 6.42 | 1.2 |
| | | | | | | 2 | 5.13 | 1039.6 | 6.11 | -3.8 |
| TURKU | 84 | 2 | 16 | 1 | 1125-1126 | 1 | 5.40 | 1039.6 | 6.42 | 1.2 |
| | | | | | | 2 | 4.60 | 1039.6 | 5.47 | -13.8 |

Table 1. continued

| STATION | YY | MM | DD | MIN | TIME SPAN | Counting rate per second | UNCOR. | PRES. | COR. | % INC. |
|---|---|---|---|---|---|---|---|---|---|---|
| TURKU | 84 | 2 | 16 | 1 | 1126-1127 | 1 | 4.33 | 1039.6 | 5.15 | -18.8 |
| | | | | | | 2 | 5.23 | 1039.6 | 6.23 | -1.9 |
| TURKU | 84 | 2 | 16 | 1 | 1127-1128 | 1 | 4.87 | 1039.6 | 5.79 | -8.8 |
| | | | | | | 2 | 5.30 | 1039.6 | 6.30 | -0.7 |
| TURKU | 84 | 2 | 16 | 1 | 1128-1129 | 1 | 5.43 | 1039.6 | 6.46 | 1.8 |
| | | | | | | 2 | 4.83 | 1039.6 | 5.75 | -9.4 |
| TURKU | 84 | 2 | 16 | 1 | 1129-1130 | 1 | 4.27 | 1039.6 | 5.08 | -20.0 |
| | | | | | | 2 | 4.53 | 1039.6 | 5.39 | -15.0 |
| TURKU | 84 | 2 | 16 | 1 | 1130-1131 | 1 | 5.17 | 1039.5 | 6.14 | -3.2 |
| | | | | | | 2 | 5.47 | 1039.5 | 6.50 | 2.4 |
| TURKU | 84 | 2 | 16 | 1 | 1131-1132 | 1 | 6.00 | 1039.5 | 7.14 | 12.4 |
| | | | | | | 2 | 5.97 | 1039.5 | 7.10 | 11.8 |
| TURKU | 84 | 2 | 16 | 1 | 1132-1133 | 1 | 5.63 | 1039.5 | 6.70 | 5.5 |
| | | | | | | 2 | 5.30 | 1039.5 | 6.30 | -0.7 |
| TURKU | 84 | 2 | 16 | 1 | 1133-1134 | 1 | 5.03 | 1039.5 | 5.99 | -5.7 |
| | | | | | | 2 | 5.10 | 1039.5 | 6.07 | -4.4 |
| TURKU | 84 | 2 | 16 | 1 | 1134-1135 | 1 | 5.80 | 1039.5 | 6.90 | 8.7 |
| | | | | | | 2 | 5.57 | 1039.5 | 6.62 | 4.3 |
| TURKU | 84 | 2 | 16 | 1 | 1135-1136 | 1 | 6.10 | 1039.5 | 7.25 | 14.3 |
| | | | | | | 2 | 4.80 | 1039.5 | 5.71 | -10.1 |
| TURKU | 84 | 2 | 16 | 1 | 1136-1137 | 1 | 5.50 | 1039.5 | 6.54 | 3.0 |
| | | | | | | 2 | 6.00 | 1039.5 | 7.13 | 12.4 |
| TURKU | 84 | 2 | 16 | 1 | 1137-1138 | 1 | 5.20 | 1039.5 | 6.18 | -2.6 |
| | | | | | | 2 | 5.43 | 1039.5 | 6.46 | 1.8 |
| TURKU | 84 | 2 | 16 | 1 | 1138-1139 | 1 | 5.83 | 1039.5 | 6.94 | 9.3 |
| | | | | | | 2 | 5.67 | 1039.5 | 6.74 | 6.2 |
| TURKU | 84 | 2 | 16 | 1 | 1139-1140 | 1 | 5.27 | 1039.5 | 6.26 | -1.3 |
| | | | | | | 2 | 6.47 | 1039.5 | 7.69 | 21.1 |
| TURKU | 84 | 2 | 16 | 1 | 1140-1141 | 1 | 5.67 | 1039.4 | 6.74 | 6.1 |
| | | | | | | 2 | 5.63 | 1039.4 | 6.70 | 5.5 |
| TURKU | 84 | 2 | 16 | 1 | 1141-1142 | 1 | 5.30 | 1039.4 | 6.30 | -0.7 |
| | | | | | | 2 | 5.50 | 1039.4 | 6.54 | 3.0 |
| TURKU | 84 | 2 | 16 | 1 | 1142-1143 | 1 | 5.17 | 1039.4 | 6.14 | -3.2 |
| | | | | | | 2 | 5.40 | 1039.4 | 6.42 | 1.1 |
| TURKU | 84 | 2 | 16 | 1 | 1143-1144 | 1 | 5.43 | 1039.4 | 6.46 | 1.8 |
| | | | | | | 2 | 5.63 | 1039.4 | 6.70 | 5.5 |
| TURKU | 84 | 2 | 16 | 1 | 1144-1145 | 1 | 5.00 | 1039.4 | 5.94 | -6.4 |
| | | | | | | 2 | 6.07 | 1039.4 | 7.21 | 13.6 |
| TURKU | 84 | 2 | 16 | 1 | 1145-1146 | 1 | 5.77 | 1039.4 | 6.85 | 8.0 |
| | | | | | | 2 | 5.20 | 1039.4 | 6.18 | -2.6 |
| TURKU | 84 | 2 | 16 | 1 | 1146-1147 | 1 | 5.43 | 1039.4 | 6.46 | 1.7 |
| | | | | | | 2 | 4.80 | 1039.4 | 5.70 | -10.1 |
| TURKU | 84 | 2 | 16 | 1 | 1147-1148 | 1 | 5.33 | 1039.4 | 6.34 | -0.1 |
| | | | | | | 2 | 4.80 | 1039.4 | 5.70 | -10.1 |
| TURKU | 84 | 2 | 16 | 1 | 1148-1149 | 1 | 6.17 | 1039.4 | 7.33 | 15.5 |
| | | | | | | 2 | 5.80 | 1039.4 | 6.89 | 8.6 |
| TURKU | 84 | 2 | 16 | 1 | 1149-1150 | 1 | 5.60 | 1039.4 | 6.66 | 4.9 |
| | | | | | | 2 | 4.60 | 1039.4 | 5.47 | -13.9 |
| TURKU | 84 | 2 | 16 | 1 | 1150-1151 | 1 | 4.93 | 1039.4 | 5.86 | -7.6 |
| | | | | | | 2 | 4.77 | 1039.4 | 5.67 | -10.7 |
| TURKU | 84 | 2 | 16 | 1 | 1151-1152 | 1 | 5.90 | 1039.4 | 7.01 | 10.5 |
| | | | | | | 2 | 4.77 | 1039.4 | 5.67 | -10.7 |
| TURKU | 84 | 2 | 16 | 1 | 1152-1153 | 1 | 5.67 | 1039.4 | 6.73 | 6.1 |
| | | | | | | 2 | 5.40 | 1039.4 | 6.42 | 1.1 |
| TURKU | 84 | 2 | 16 | 1 | 1153-1154 | 1 | 5.10 | 1039.4 | 6.06 | -4.5 |
| | | | | | | 2 | 5.60 | 1039.4 | 6.66 | 4.9 |
| TURKU | 84 | 2 | 16 | 1 | 1154-1155 | 1 | 5.17 | 1039.4 | 6.14 | -3.3 |
| | | | | | | 2 | 5.23 | 1039.4 | 6.22 | -2.0 |
| TURKU | 84 | 2 | 16 | 1 | 1155-1156 | 1 | 5.60 | 1039.4 | 6.66 | 4.9 |
| | | | | | | 2 | 5.43 | 1039.4 | 6.46 | 1.7 |
| TURKU | 84 | 2 | 16 | 1 | 1156-1157 | 1 | 5.43 | 1039.4 | 6.46 | 1.7 |
| | | | | | | 2 | 5.47 | 1039.4 | 6.50 | 2.4 |
| TURKU | 84 | 2 | 16 | 1 | 1157-1158 | 1 | 5.67 | 1039.4 | 6.74 | 6.1 |
| | | | | | | 2 | 4.67 | 1039.4 | 5.55 | -12.6 |
| TURKU | 84 | 2 | 16 | 1 | 1158-1159 | 1 | 4.93 | 1039.4 | 5.86 | -7.6 |
| | | | | | | 2 | 5.20 | 1039.4 | 6.18 | -2.6 |
| TURKU | 84 | 2 | 16 | 1 | 1159-1200 | 1 | 6.00 | 1039.4 | 7.13 | 12.4 |
| | | | | | | 2 | 6.03 | 1039.4 | 7.17 | 13.0 |
| TURKU | 84 | 2 | 16 | 1 | 1200-1201 | 1 | 5.13 | 1039.4 | 6.10 | -3.9 |
| | | | | | | 2 | 5.53 | 1039.4 | 6.58 | 3.6 |

Table 1. continued

Counting rate per second

| STATION | YY | MM | DD | MIN | TIME SPAN | | UNCOR. | PRES. | COR. | % INC. |
|---|---|---|---|---|---|---|---|---|---|---|
| TURKU | 84 | 2 | 16 | 1 | 1201-1202 | 1 | 5.87 | 1039.4 | 6.97 | 9.8 |
| | | | | | | 2 | 5.37 | 1039.4 | 6.38 | 0.5 |
| TURKU | 84 | 2 | 16 | 1 | 1202-1203 | 1 | 5.73 | 1039.4 | 6.81 | 7.3 |
| | | | | | | 2 | 5.03 | 1039.4 | 5.98 | -5.8 |
| TURKU | 84 | 2 | 16 | 1 | 1203-1204 | 1 | 5.90 | 1039.4 | 7.01 | 10.5 |
| | | | | | | 2 | 5.20 | 1039.4 | 6.18 | -2.6 |
| TURKU | 84 | 2 | 16 | 1 | 1204-1205 | 1 | 5.43 | 1039.4 | 6.46 | 1.7 |
| | | | | | | 2 | 6.23 | 1039.4 | 7.41 | 16.7 |
| TURKU | 84 | 2 | 16 | 1 | 1205-1206 | 1 | 5.63 | 1039.4 | 6.70 | 5.5 |
| | | | | | | 2 | 5.33 | 1039.4 | 6.34 | -0.1 |
| TURKU | 84 | 2 | 16 | 1 | 1206-1207 | 1 | 5.90 | 1039.4 | 7.01 | 10.5 |
| | | | | | | 2 | 4.87 | 1039.4 | 5.78 | -8.9 |
| TURKU | 84 | 2 | 16 | 1 | 1207-1208 | 1 | 5.27 | 1039.4 | 6.26 | -1.4 |
| | | | | | | 2 | 5.60 | 1039.4 | 6.66 | 4.9 |
| TURKU | 84 | 2 | 16 | 1 | 1208-1209 | 1 | 5.60 | 1039.4 | 6.66 | 4.9 |
| | | | | | | 2 | 5.77 | 1039.4 | 6.85 | 8.0 |
| TURKU | 84 | 2 | 16 | 1 | 1209-1210 | 1 | 4.63 | 1039.4 | 5.51 | -13.2 |
| | | | | | | 2 | 5.40 | 1039.4 | 6.42 | 1.1 |
| TURKU | 84 | 2 | 16 | 1 | 1210-1211 | 1 | 6.00 | 1039.4 | 7.13 | 12.3 |
| | | | | | | 2 | 5.63 | 1039.4 | 6.69 | 5.5 |
| TURKU | 84 | 2 | 16 | 1 | 1211-1212 | 1 | 4.80 | 1039.4 | 5.70 | -10.1 |
| | | | | | | 2 | 5.13 | 1039.4 | 6.10 | -3.9 |
| TURKU | 84 | 2 | 16 | 1 | 1212-1213 | 1 | 5.10 | 1039.4 | 6.06 | -4.5 |
| | | | | | | 2 | 5.90 | 1039.4 | 7.01 | 10.5 |
| TURKU | 84 | 2 | 16 | 1 | 1213-1214 | 1 | 5.33 | 1039.4 | 6.34 | -0.1 |
| | | | | | | 2 | 5.57 | 1039.4 | 6.62 | 4.2 |
| TURKU | 84 | 2 | 16 | 1 | 1214-1215 | 1 | 5.20 | 1039.4 | 6.18 | -2.6 |
| | | | | | | 2 | 5.23 | 1039.4 | 6.22 | -2.0 |
| TURKU | 84 | 2 | 16 | 1 | 1215-1216 | 1 | 5.50 | 1039.3 | 6.53 | 3.0 |
| | | | | | | 2 | 5.53 | 1039.3 | 6.57 | 3.6 |
| TURKU | 84 | 2 | 16 | 1 | 1216-1217 | 1 | 4.57 | 1039.3 | 5.43 | -14.5 |
| | | | | | | 2 | 5.80 | 1039.3 | 6.89 | 8.6 |
| TURKU | 84 | 2 | 16 | 1 | 1217-1218 | 1 | 5.47 | 1039.3 | 6.49 | 2.3 |
| | | | | | | 2 | 5.33 | 1039.3 | 6.34 | -0.2 |
| TURKU | 84 | 2 | 16 | 1 | 1218-1219 | 1 | 6.33 | 1039.3 | 7.52 | 18.5 |
| | | | | | | 2 | 5.60 | 1039.3 | 6.65 | 4.8 |
| TURKU | 84 | 2 | 16 | 1 | 1219-1220 | 1 | 4.50 | 1039.3 | 5.35 | -15.8 |
| | | | | | | 2 | 4.47 | 1039.3 | 5.31 | -16.4 |
| TURKU | 84 | 2 | 16 | 1 | 1220-1221 | 1 | 5.20 | 1039.3 | 6.18 | -2.7 |
| | | | | | | 2 | 5.93 | 1039.3 | 7.05 | 11.1 |
| TURKU | 84 | 2 | 16 | 1 | 1221-1222 | 1 | 5.30 | 1039.3 | 6.30 | -0.8 |
| | | | | | | 2 | 5.83 | 1039.3 | 6.93 | 9.2 |
| TURKU | 84 | 2 | 16 | 1 | 1222-1223 | 1 | 5.43 | 1039.3 | 6.45 | 1.7 |
| | | | | | | 2 | 5.47 | 1039.3 | 6.49 | 2.3 |
| TURKU | 84 | 2 | 16 | 1 | 1223-1224 | 1 | 5.47 | 1039.3 | 6.49 | 2.3 |
| | | | | | | 2 | 5.70 | 1039.3 | 6.77 | 6.7 |
| TURKU | 84 | 2 | 16 | 1 | 1224-1225 | 1 | 5.50 | 1039.3 | 6.53 | 2.9 |
| | | | | | | 2 | 5.03 | 1039.3 | 5.98 | -5.8 |
| TURKU | 84 | 2 | 16 | 1 | 1225-1226 | 1 | 5.77 | 1039.3 | 6.85 | 7.9 |
| | | | | | | 2 | 5.43 | 1039.3 | 6.45 | 1.7 |
| TURKU | 84 | 2 | 16 | 1 | 1226-1227 | 1 | 6.30 | 1039.3 | 7.48 | 17.9 |
| | | | | | | 2 | 5.37 | 1039.3 | 6.37 | 0.4 |
| TURKU | 84 | 2 | 16 | 1 | 1227-1228 | 1 | 5.43 | 1039.3 | 6.45 | 1.7 |
| | | | | | | 2 | 4.90 | 1039.3 | 5.82 | -8.3 |
| TURKU | 84 | 2 | 16 | 1 | 1228-1229 | 1 | 4.77 | 1039.3 | 5.66 | -10.8 |
| | | | | | | 2 | 5.67 | 1039.3 | 6.73 | 6.0 |
| TURKU | 84 | 2 | 16 | 1 | 1229-1230 | 1 | 5.83 | 1039.3 | 6.93 | 9.1 |
| | | | | | | 2 | 5.37 | 1039.3 | 6.37 | 0.4 |
| TURKU | 84 | 2 | 16 | 1 | 1230-1231 | 1 | 6.47 | 1039.2 | 7.68 | 21.0 |
| | | | | | | 2 | 5.17 | 1039.2 | 6.13 | -3.3 |
| TURKU | 84 | 2 | 16 | 1 | 1231-1232 | 1 | 5.17 | 1039.2 | 6.13 | -3.3 |
| | | | | | | 2 | 5.57 | 1039.2 | 6.61 | 4.1 |
| TURKU | 84 | 2 | 16 | 1 | 1232-1233 | 1 | 5.90 | 1039.2 | 7.01 | 10.4 |
| | | | | | | 2 | 6.33 | 1039.2 | 7.52 | 18.5 |
| TURKU | 84 | 2 | 16 | 1 | 1233-1234 | 1 | 5.80 | 1039.2 | 6.89 | 8.5 |
| | | | | | | 2 | 5.17 | 1039.2 | 6.13 | -3.3 |
| TURKU | 84 | 2 | 16 | 1 | 1234-1235 | 1 | 5.07 | 1039.2 | 6.02 | -5.2 |
| | | | | | | 2 | 5.27 | 1039.2 | 6.25 | -1.5 |
| TURKU | 84 | 2 | 16 | 1 | 1235-1236 | 1 | 4.83 | 1039.2 | 5.74 | -9.6 |
| | | | | | | 2 | 5.43 | 1039.2 | 6.45 | 1.6 |

Table 1. continued

| STATION | YY | MM | DD | MIN | TIME SPAN | | Counting rate per second UNCOR. | PRES. | COR. | % INC. |
|---|---|---|---|---|---|---|---|---|---|---|
| TURKU | 84 | 2 | 16 | 1 | 1236-1237 | 1 | 5.40 | 1039.2 | 6.41 | 1.0 |
| | | | | | | 2 | 5.93 | 1039.2 | 7.04 | 11.0 |
| TURKU | 84 | 2 | 16 | 1 | 1237-1238 | 1 | 5.97 | 1039.2 | 7.08 | 11.6 |
| | | | | | | 2 | 5.03 | 1039.2 | 5.97 | -5.9 |
| TURKU | 84 | 2 | 16 | 1 | 1238-1239 | 1 | 4.63 | 1039.2 | 5.50 | -13.4 |
| | | | | | | 2 | 5.37 | 1039.2 | 6.37 | 0.4 |
| TURKU | 84 | 2 | 16 | 1 | 1239-1240 | 1 | 5.33 | 1039.2 | 6.33 | -0.3 |
| | | | | | | 2 | 5.37 | 1039.2 | 6.37 | 0.4 |
| TURKU | 84 | 2 | 16 | 1 | 1240-1241 | 1 | 5.57 | 1039.1 | 6.61 | 4.1 |
| | | | | | | 2 | 4.93 | 1039.1 | 5.85 | -7.8 |
| TURKU | 84 | 2 | 16 | 1 | 1241-1242 | 1 | 4.93 | 1039.1 | 5.85 | -7.8 |
| | | | | | | 2 | 5.23 | 1039.1 | 6.21 | -2.2 |
| TURKU | 84 | 2 | 16 | 1 | 1242-1243 | 1 | 5.00 | 1039.1 | 5.93 | -6.5 |
| | | | | | | 2 | 5.40 | 1039.1 | 6.41 | 1.0 |
| TURKU | 84 | 2 | 16 | 1 | 1243-1244 | 1 | 5.13 | 1039.1 | 6.09 | -4.0 |
| | | | | | | 2 | 5.60 | 1039.1 | 6.65 | 4.7 |
| TURKU | 84 | 2 | 16 | 1 | 1244-1245 | 1 | 5.43 | 1039.1 | 6.45 | 1.6 |
| | | | | | | 2 | 6.30 | 1039.1 | 7.48 | 17.8 |
| TURKU | 84 | 2 | 16 | 1 | 1245-1246 | 1 | 5.10 | 1039.1 | 6.05 | -4.7 |
| | | | | | | 2 | 5.10 | 1039.1 | 6.05 | -4.7 |
| TURKU | 84 | 2 | 16 | 1 | 1246-1247 | 1 | 4.33 | 1039.1 | 5.14 | -19.0 |
| | | | | | | 2 | 5.13 | 1039.1 | 6.09 | -4.0 |
| TURKU | 84 | 2 | 16 | 1 | 1247-1248 | 1 | 5.60 | 1039.1 | 6.64 | 4.7 |
| | | | | | | 2 | 5.87 | 1039.1 | 6.96 | 9.7 |
| TURKU | 84 | 2 | 16 | 1 | 1248-1249 | 1 | 5.50 | 1039.1 | 6.53 | 2.8 |
| | | | | | | 2 | 5.63 | 1039.1 | 6.68 | 5.3 |
| TURKU | 84 | 2 | 16 | 1 | 1249-1250 | 1 | 5.30 | 1039.1 | 6.29 | -0.9 |
| | | | | | | 2 | 5.33 | 1039.1 | 6.33 | -0.3 |
| TURKU | 84 | 2 | 16 | 1 | 1250-1251 | 1 | 4.83 | 1039.1 | 5.73 | -9.7 |
| | | | | | | 2 | 5.10 | 1039.1 | 6.05 | -4.7 |
| TURKU | 84 | 2 | 16 | 1 | 1251-1252 | 1 | 5.00 | 1039.1 | 5.93 | -6.6 |
| | | | | | | 2 | 6.40 | 1039.1 | 7.59 | 19.6 |
| TURKU | 84 | 2 | 16 | 1 | 1252-1253 | 1 | 5.50 | 1039.1 | 6.52 | 2.8 |
| | | | | | | 2 | 5.27 | 1039.1 | 6.25 | -1.6 |
| TURKU | 84 | 2 | 16 | 1 | 1253-1254 | 1 | 5.17 | 1039.1 | 6.13 | -3.4 |
| | | | | | | 2 | 5.23 | 1039.1 | 6.21 | -2.2 |
| TURKU | 84 | 2 | 16 | 1 | 1254-1255 | 1 | 5.43 | 1039.1 | 6.45 | 1.5 |
| | | | | | | 2 | 5.47 | 1039.1 | 6.48 | 2.2 |
| TURKU | 84 | 2 | 16 | 1 | 1255-1256 | 1 | 5.67 | 1039.0 | 6.72 | 5.9 |
| | | | | | | 2 | 5.07 | 1039.0 | 6.01 | -5.3 |
| TURKU | 84 | 2 | 16 | 1 | 1256-1257 | 1 | 4.87 | 1039.0 | 5.77 | -9.1 |
| | | | | | | 2 | 5.43 | 1039.0 | 6.44 | 1.5 |
| TURKU | 84 | 2 | 16 | 1 | 1257-1258 | 1 | 5.80 | 1039.0 | 6.88 | 8.4 |
| | | | | | | 2 | 5.50 | 1039.0 | 6.52 | 2.8 |
| TURKU | 84 | 2 | 16 | 1 | 1258-1259 | 1 | 5.13 | 1039.0 | 6.09 | -4.1 |
| | | | | | | 2 | 5.33 | 1039.0 | 6.33 | -0.3 |
| TURKU | 84 | 2 | 16 | 1 | 1259-1300 | 1 | 5.60 | 1039.0 | 6.64 | 4.7 |
| | | | | | | 2 | 5.00 | 1039.0 | 5.93 | -6.6 |

Table 2. Turku Neutron Monitor Hourly Data in Four Multiplicity Categories (see text).

CATEGORY I (mean neutron energy 50 MeV at sea level)

Counting rates per hour

| STATION | YY | MM | DD | TIME SPAN | UNCOR. | PRES. | COR. | % INC. |
|---|---|---|---|---|---|---|---|---|
| TURKU | 84 | 2 | 46 | 12-13 | 31221 | 1040.9 | 37678.3 | -0.6 |
| TURKU | 84 | 2 | 46 | 13-14 | 31002 | 1041.0 | 37435.0 | -1.3 |
| TURKU | 84 | 2 | 46 | 14-15 | 31216 | 1041.0 | 37695.5 | -0.6 |
| TURKU | 84 | 2 | 46 | 15-16 | 31250 | 1041.0 | 37745.1 | -0.5 |
| TURKU | 84 | 2 | 46 | 16-17 | 31194 | 1041.0 | 37681.6 | -0.6 |
| TURKU | 84 | 2 | 46 | 18-17 | - | - | - | - |
| TURKU | 84 | 2 | 46 | 18-19 | 30889 | 1041.5 | 37401.0 | -1.4 |
| TURKU | 84 | 2 | 46 | 19-20 | 31210 | 1041.3 | 37758.0 | -0.4 |
| TURKU | 84 | 2 | 46 | 20-21 | 31057 | 1041.5 | 37619.1 | -0.8 |
| TURKU | 84 | 2 | 46 | 21-22 | 31153 | 1041.4 | 37714.3 | -0.5 |
| TURKU | 84 | 2 | 46 | 22-23 | 31233 | 1041.4 | 37794.3 | -0.3 |
| TURKU | 84 | 2 | 46 | 23-24 | 30856 | 1041.4 | 37340.1 | -1.5 |
| TURKU | 84 | 2 | 47 | 0- 1 | 31300 | 1041.1 | 37830.9 | -0.2 |
| TURKU | 84 | 2 | 47 | 1- 2 | 31181 | 1040.8 | 37615.3 | -0.8 |
| TURKU | 84 | 2 | 47 | 2- 3 | 31736 | 1040.5 | 38229.0 | 0.8 |
| TURKU | 84 | 2 | 47 | 3- 4 | 31539 | 1040.2 | 37929.8 | 0.0 |
| TURKU | 84 | 2 | 47 | 4- 5 | 31372 | 1039.8 | 37642.0 | -0.7 |
| TURKU | 84 | 2 | 47 | 5- 6 | 31680 | 1039.8 | 38007.2 | 0.2 |
| TURKU | 84 | 2 | 47 | 6- 7 | 31521 | 1039.9 | 37839.9 | -0.2 |
| TURKU | 84 | 2 | 47 | 7- 8 | 31415 | 1039.9 | 37712.7 | -0.5 |
| TURKU | 84 | 2 | 47 | 8- 9 | 31602 | 1040.0 | 37943.6 | 0.1 |
| TURKU | 84 | 2 | 47 | 9-10 | 34108 | 1039.9 | 40938.6 | 8.0 |
| TURKU | 84 | 2 | 47 | 10-11 | 32161 | 1039.6 | 38549.5 | 1.7 |
| TURKU | 84 | 2 | 47 | 11-12 | 31913 | 1039.4 | 38200.4 | 0.7 |
| TURKU | 84 | 2 | 47 | 12-13 | 31935 | 1039.0 | 38148.9 | 0.6 |
| TURKU | 84 | 2 | 47 | 13-14 | 32116 | 1038.6 | 38276.1 | 0.9 |
| TURKU | 84 | 2 | 47 | 14-15 | 31793 | 1038.6 | 37882.5 | -0.1 |
| TURKU | 84 | 2 | 47 | 15-16 | 32139 | 1038.5 | 38268.7 | 0.9 |
| TURKU | 84 | 2 | 47 | 16-17 | 32065 | 1038.4 | 38156.7 | 0.6 |
| TURKU | 84 | 2 | 47 | 17-18 | 32002 | 1038.1 | 38036.3 | 0.3 |
| TURKU | 84 | 2 | 47 | 18-19 | 31860 | 1038.0 | 37826.6 | -0.2 |
| TURKU | 84 | 2 | 47 | 19-20 | 31964 | 1037.9 | 37928.4 | 0.0 |
| TURKU | 84 | 2 | 47 | 20-21 | 31968 | 1037.7 | 37909.4 | 0.0 |
| TURKU | 84 | 2 | 47 | 21-22 | 32020 | 1037.5 | 37919.0 | 0.0 |
| TURKU | 84 | 2 | 47 | 22-23 | 32202 | 1037.4 | 38121.5 | 0.5 |
| TURKU | 84 | 2 | 47 | 23-24 | 32004 | 1037.2 | 37826.5 | -0.2 |
| TURKU | 84 | 2 | 48 | 0- 1 | 32039 | 1036.9 | 37811.5 | -0.3 |
| TURKU | 84 | 2 | 48 | 1- 2 | 32127 | 1036.7 | 37876.2 | -0.1 |
| TURKU | 84 | 2 | 48 | 2- 3 | 32263 | 1036.6 | 38014.7 | 0.2 |
| TURKU | 84 | 2 | 48 | 3- 4 | 32567 | 1036.6 | 38361.9 | 1.2 |
| TURKU | 84 | 2 | 48 | 4- 5 | 32598 | 1036.4 | 38369.7 | 1.2 |
| TURKU | 84 | 2 | 48 | 5- 6 | 32551 | 1036.3 | 38294.6 | 1.0 |
| TURKU | 84 | 2 | 48 | 6- 7 | 32288 | 1036.5 | 38013.6 | 0.2 |
| TURKU | 84 | 2 | 48 | 7- 8 | 32587 | 1036.5 | 38374.4 | 1.2 |
| TURKU | 84 | 2 | 48 | 8- 9 | 32260 | 1036.5 | 37993.7 | 0.2 |
| TURKU | 84 | 2 | 48 | 9-10 | 31733 | 1036.4 | 37349.4 | -1.5 |
| TURKU | 84 | 2 | 48 | 10-11 | 32951 | 1036.3 | 38749.6 | 2.2 |
| TURKU | 84 | 2 | 48 | 11-12 | 32349 | 1036.2 | 38032.9 | 0.3 |
| TURKU | 84 | 2 | 48 | 12-13 | 32503 | 1036.1 | 38194.1 | 0.7 |
| TURKU | 84 | 2 | 48 | 13-14 | 32685 | 1036.1 | 38394.7 | 1.3 |
| TURKU | 84 | 2 | 48 | 14-15 | 32200 | 1036.0 | 37816.3 | -0.3 |
| TURKU | 84 | 2 | 48 | 15-16 | 32509 | 1036.1 | 38192.4 | 0.7 |
| TURKU | 84 | 2 | 48 | 16-17 | 32071 | 1036.3 | 37714.7 | -0.5 |
| TURKU | 84 | 2 | 48 | 17-18 | 32390 | 1036.2 | 38067.9 | 0.4 |
| TURKU | 84 | 2 | 48 | 18-19 | 32352 | 1036.2 | 38038.6 | 0.3 |
| TURKU | 84 | 2 | 48 | 19-20 | 31943 | 1036.4 | 37598.8 | -0.8 |
| TURKU | 84 | 2 | 48 | 20-21 | 32478 | 1036.3 | 38208.7 | 0.8 |
| TURKU | 84 | 2 | 48 | 21-22 | 31749 | 1036.4 | 37361.8 | -1.5 |
| TURKU | 84 | 2 | 48 | 22-23 | 32129 | 1036.5 | 37826.4 | -0.2 |
| TURKU | 84 | 2 | 48 | 23-24 | 31901 | 1036.4 | 37553.6 | -1.0 |
| TURKU | 84 | 2 | 49 | 0- 1 | 32140 | 1036.5 | 37850.2 | -0.2 |
| TURKU | 84 | 2 | 49 | 1- 2 | 32455 | 1036.4 | 38197.0 | 0.7 |
| TURKU | 84 | 2 | 49 | 2- 3 | 32378 | 1036.4 | 38102.0 | 0.5 |
| TURKU | 84 | 2 | 49 | 3- 4 | 32105 | 1036.5 | 37806.8 | -0.3 |
| TURKU | 84 | 2 | 49 | 4- 5 | 32269 | 1036.4 | 37978.1 | 0.2 |

Table 2. continued

CATEGORY II (mean neutron energy 150 MeV at sea level)

Counting rates per hour

| STATION | YY | MM | DD | TIME SPAN | UNCOR. | PRES. | COR. | % INC. |
|---|---|---|---|---|---|---|---|---|
| TURKU | 84 | 2 | 46 | 12-13 | 12192 | 1040.9 | 14859.9 | -0.6 |
| TURKU | 84 | 2 | 46 | 13-14 | 12207 | 1041.0 | 14886.9 | -0.4 |
| TURKU | 84 | 2 | 46 | 14-15 | 12085 | 1041.0 | 14738.9 | -1.4 |
| TURKU | 84 | 2 | 46 | 15-16 | 11924 | 1041.0 | 14545.8 | -2.7 |
| TURKU | 84 | 2 | 46 | 16-17 | 11985 | 1041.0 | 14621.5 | -2.2 |
| TURKU | 84 | 2 | 46 | 18-17 | - | - | - | - |
| TURKU | 84 | 2 | 46 | 18-19 | 12018 | 1041.5 | 14698.2 | -1.7 |
| TURKU | 84 | 2 | 46 | 19-20 | 11965 | 1041.3 | 14620.2 | -2.2 |
| TURKU | 84 | 2 | 46 | 20-21 | 12160 | 1041.5 | 14878.7 | -0.5 |
| TURKU | 84 | 2 | 46 | 21-22 | 11858 | 1041.4 | 14501.0 | -3.0 |
| TURKU | 84 | 2 | 46 | 22-23 | 11992 | 1041.4 | 14657.7 | -2.0 |
| TURKU | 84 | 2 | 46 | 23-24 | 11942 | 1041.4 | 14597.2 | -2.4 |
| TURKU | 84 | 2 | 47 | 0- 1 | 12158 | 1041.1 | 14842.8 | -0.7 |
| TURKU | 84 | 2 | 47 | 1- 2 | 12170 | 1040.8 | 14826.9 | -0.8 |
| TURKU | 84 | 2 | 47 | 2- 3 | 12158 | 1040.5 | 14790.3 | -1.1 |
| TURKU | 84 | 2 | 47 | 3- 4 | 12286 | 1040.2 | 14919.7 | -0.2 |
| TURKU | 84 | 2 | 47 | 4- 5 | 12370 | 1039.8 | 14985.8 | 0.2 |
| TURKU | 84 | 2 | 47 | 5- 6 | 12398 | 1039.8 | 15017.5 | 0.4 |
| TURKU | 84 | 2 | 47 | 6- 7 | 12193 | 1039.9 | 14779.1 | -1.2 |
| TURKU | 84 | 2 | 47 | 7- 8 | 12204 | 1039.9 | 14792.5 | -1.1 |
| TURKU | 84 | 2 | 47 | 8- 9 | 12320 | 1040.0 | 14935.4 | -0.1 |
| TURKU | 84 | 2 | 47 | 9-10 | 13625 | 1039.9 | 16511.5 | 10.4 |
| TURKU | 84 | 2 | 47 | 10-11 | 12726 | 1039.6 | 15400.8 | 3.0 |
| TURKU | 84 | 2 | 47 | 11-12 | 12373 | 1039.4 | 14952.7 | 0.0 |
| TURKU | 84 | 2 | 47 | 12-13 | 12529 | 1039.0 | 15107.8 | 1.0 |
| TURKU | 84 | 2 | 47 | 13-14 | 12417 | 1038.6 | 14937.3 | -0.1 |
| TURKU | 84 | 2 | 47 | 14-15 | 12450 | 1038.6 | 14973.3 | 0.1 |
| TURKU | 84 | 2 | 47 | 15-16 | 12577 | 1038.5 | 15115.5 | 1.1 |
| TURKU | 84 | 2 | 47 | 16-17 | 12673 | 1038.4 | 15219.5 | 1.8 |
| TURKU | 84 | 2 | 47 | 17-18 | 12586 | 1038.1 | 15097.2 | 1.0 |
| TURKU | 84 | 2 | 47 | 18-19 | 12576 | 1038.0 | 15068.1 | 0.8 |
| TURKU | 84 | 2 | 47 | 19-20 | 12587 | 1037.9 | 15072.2 | 0.8 |
| TURKU | 84 | 2 | 47 | 20-21 | 12574 | 1037.7 | 15047.1 | 0.6 |
| TURKU | 84 | 2 | 47 | 21-22 | 12613 | 1037.5 | 15071.3 | 0.8 |
| TURKU | 84 | 2 | 47 | 22-23 | 12595 | 1037.4 | 15044.1 | 0.6 |
| TURKU | 84 | 2 | 47 | 23-24 | 12690 | 1037.2 | 15132.8 | 1.2 |
| TURKU | 84 | 2 | 48 | 0- 1 | 12410 | 1036.9 | 14775.6 | -1.2 |
| TURKU | 84 | 2 | 48 | 1- 2 | 12763 | 1036.7 | 15179.2 | 1.5 |
| TURKU | 84 | 2 | 48 | 2- 3 | 12640 | 1036.6 | 15024.4 | 0.5 |
| TURKU | 84 | 2 | 48 | 3- 4 | 12784 | 1036.6 | 15190.2 | 1.6 |
| TURKU | 84 | 2 | 48 | 4- 5 | 12559 | 1036.4 | 14912.4 | -0.3 |
| TURKU | 84 | 2 | 48 | 5- 6 | 12447 | 1036.3 | 14771.1 | -1.2 |
| TURKU | 84 | 2 | 48 | 6- 7 | 12557 | 1036.5 | 14912.5 | -0.3 |
| TURKU | 84 | 2 | 48 | 7- 8 | 12687 | 1036.5 | 15070.3 | 0.8 |
| TURKU | 84 | 2 | 48 | 8- 9 | 12704 | 1036.5 | 15092.7 | 0.9 |
| TURKU | 84 | 2 | 48 | 9-10 | 12748 | 1036.4 | 15135.1 | 1.2 |
| TURKU | 84 | 2 | 48 | 10-11 | 12882 | 1036.3 | 15280.4 | 2.2 |
| TURKU | 84 | 2 | 48 | 11-12 | 12700 | 1036.2 | 15061.1 | 0.7 |
| TURKU | 84 | 2 | 48 | 12-13 | 12685 | 1036.1 | 15034.6 | 0.5 |
| TURKU | 84 | 2 | 48 | 13-14 | 12667 | 1036.1 | 15007.8 | 0.4 |
| TURKU | 84 | 2 | 48 | 14-15 | 12656 | 1036.0 | 14992.2 | 0.3 |
| TURKU | 84 | 2 | 48 | 15-16 | 12840 | 1036.1 | 15215.0 | 1.7 |
| TURKU | 84 | 2 | 48 | 16-17 | 12636 | 1036.3 | 14988.4 | 0.2 |
| TURKU | 84 | 2 | 48 | 17-18 | 12751 | 1036.2 | 15115.9 | 1.1 |
| TURKU | 84 | 2 | 48 | 18-19 | 12675 | 1036.2 | 15031.8 | 0.5 |
| TURKU | 84 | 2 | 48 | 19-20 | 12579 | 1036.4 | 14935.7 | -0.1 |
| TURKU | 84 | 2 | 48 | 20-21 | 12530 | 1036.3 | 14868.9 | -0.6 |
| TURKU | 84 | 2 | 48 | 21-22 | 12630 | 1036.4 | 14991.9 | 0.3 |
| TURKU | 84 | 2 | 48 | 22-23 | 12653 | 1036.5 | 15027.1 | 0.5 |
| TURKU | 84 | 2 | 48 | 23-24 | 12698 | 1036.4 | 15078.7 | 0.8 |
| TURKU | 84 | 2 | 49 | 0- 1 | 12558 | 1036.5 | 14918.3 | -0.2 |
| TURKU | 84 | 2 | 49 | 1- 2 | 12531 | 1036.4 | 14877.0 | -0.5 |
| TURKU | 84 | 2 | 49 | 2- 3 | 12777 | 1036.4 | 15166.8 | 1.4 |
| TURKU | 84 | 2 | 49 | 3- 4 | 12539 | 1036.5 | 14895.1 | -0.4 |
| TURKU | 84 | 2 | 49 | 4- 5 | 12579 | 1036.4 | 14933.5 | -0.1 |

Table 2. continued

CATEGORY III (mean neutron energy 500 MeV at sea level)

Counting rates per hour

| STATION | YY | MM | DD | TIME SPAN | UNCOR. | PRES. | COR. | % INC. |
|---|---|---|---|---|---|---|---|---|
| TURKU | 84 | 2 | 46 | 12-13 | 8548 | 1040.9 | 10407.1 | 0.1 |
| TURKU | 84 | 2 | 46 | 13-14 | 8523 | 1041.0 | 10383.8 | -0.1 |
| TURKU | 84 | 2 | 46 | 14-15 | 8482 | 1041.0 | 10333.1 | -0.6 |
| TURKU | 84 | 2 | 46 | 15-16 | 8342 | 1041.0 | 10164.3 | -2.2 |
| TURKU | 84 | 2 | 46 | 16-17 | 8519 | 1041.0 | 10380.5 | -0.1 |
| TURKU | 84 | 2 | 46 | 18-17 | - | - | - | - |
| TURKU | 84 | 2 | 46 | 18-19 | 8427 | 1041.5 | 10294.7 | -0.9 |
| TURKU | 84 | 2 | 46 | 19-20 | 8510 | 1041.3 | 10386.8 | 0.0 |
| TURKU | 84 | 2 | 46 | 20-21 | 8347 | 1041.5 | 10200.8 | -1.8 |
| TURKU | 84 | 2 | 46 | 21-22 | 8424 | 1041.4 | 10288.7 | -1.0 |
| TURKU | 84 | 2 | 46 | 22-23 | 8393 | 1041.4 | 10245.8 | -1.4 |
| TURKU | 84 | 2 | 46 | 23-24 | 8536 | 1041.4 | 10421.8 | 0.3 |
| TURKU | 84 | 2 | 47 | 0- 1 | 8414 | 1041.1 | 10260.6 | -1.3 |
| TURKU | 84 | 2 | 47 | 1- 2 | 8616 | 1040.8 | 10482.8 | 0.9 |
| TURKU | 84 | 2 | 47 | 2- 3 | 8459 | 1040.5 | 10277.9 | -1.1 |
| TURKU | 84 | 2 | 47 | 3- 4 | 8528 | 1040.2 | 10345.9 | -0.4 |
| TURKU | 84 | 2 | 47 | 4- 5 | 8576 | 1039.8 | 10377.8 | -0.1 |
| TURKU | 84 | 2 | 47 | 5- 6 | 8543 | 1039.8 | 10334.9 | -0.5 |
| TURKU | 84 | 2 | 47 | 6- 7 | 8507 | 1039.9 | 10298.3 | -0.9 |
| TURKU | 84 | 2 | 47 | 7- 8 | 8429 | 1039.9 | 10206.5 | -1.8 |
| TURKU | 84 | 2 | 47 | 8- 9 | 8676 | 1040.0 | 10504.9 | 1.1 |
| TURKU | 84 | 2 | 47 | 9-10 | 8976 | 1039.9 | 10866.3 | 4.6 |
| TURKU | 84 | 2 | 47 | 10-11 | 8749 | 1039.6 | 10577.1 | 1.8 |
| TURKU | 84 | 2 | 47 | 11-12 | 8555 | 1039.4 | 10326.1 | -0.6 |
| TURKU | 84 | 2 | 47 | 12-13 | 8709 | 1039.0 | 10489.8 | 0.9 |
| TURKU | 84 | 2 | 47 | 13-14 | 8691 | 1038.6 | 10442.5 | 0.5 |
| TURKU | 84 | 2 | 47 | 14-15 | 8752 | 1038.6 | 10514.8 | 1.2 |
| TURKU | 84 | 2 | 47 | 15-16 | 8837 | 1038.5 | 10608.6 | 2.1 |
| TURKU | 84 | 2 | 47 | 16-17 | 8726 | 1038.4 | 10468.1 | 0.7 |
| TURKU | 84 | 2 | 47 | 17-18 | 8799 | 1038.1 | 10543.4 | 1.5 |
| TURKU | 84 | 2 | 47 | 18-19 | 8744 | 1038.0 | 10465.0 | 0.7 |
| TURKU | 84 | 2 | 47 | 19-20 | 8775 | 1037.9 | 10495.1 | 1.0 |
| TURKU | 84 | 2 | 47 | 20-21 | 8743 | 1037.7 | 10452.2 | 0.6 |
| TURKU | 84 | 2 | 47 | 21-22 | 8617 | 1037.5 | 10286.8 | -1.0 |
| TURKU | 84 | 2 | 47 | 22-23 | 8649 | 1037.4 | 10320.9 | -0.7 |
| TURKU | 84 | 2 | 47 | 23-24 | 8875 | 1037.2 | 10572.4 | 1.7 |
| TURKU | 84 | 2 | 48 | 0- 1 | 8732 | 1036.9 | 10386.3 | -0.1 |
| TURKU | 84 | 2 | 48 | 1- 2 | 8842 | 1036.7 | 10503.5 | 1.1 |
| TURKU | 84 | 2 | 48 | 2- 3 | 8663 | 1036.6 | 10284.9 | -1.0 |
| TURKU | 84 | 2 | 48 | 3- 4 | 8908 | 1036.6 | 10574.0 | 1.8 |
| TURKU | 84 | 2 | 48 | 4- 5 | 8815 | 1036.4 | 10456.5 | 0.6 |
| TURKU | 84 | 2 | 48 | 5- 6 | 8970 | 1036.3 | 10633.5 | 2.3 |
| TURKU | 84 | 2 | 48 | 6- 7 | 8820 | 1036.5 | 10464.3 | 0.7 |
| TURKU | 84 | 2 | 48 | 7- 8 | 8786 | 1036.5 | 10424.3 | 0.3 |
| TURKU | 84 | 2 | 48 | 8- 9 | 8803 | 1036.5 | 10448.5 | 0.5 |
| TURKU | 84 | 2 | 48 | 9-10 | 8812 | 1036.4 | 10451.4 | 0.6 |
| TURKU | 84 | 2 | 48 | 10-11 | 8689 | 1036.3 | 10296.8 | -0.9 |
| TURKU | 84 | 2 | 48 | 11-12 | 8626 | 1036.2 | 10219.2 | -1.7 |
| TURKU | 84 | 2 | 48 | 12-13 | 8887 | 1036.1 | 10523.4 | 1.3 |
| TURKU | 84 | 2 | 48 | 13-14 | 8681 | 1036.1 | 10274.5 | -1.1 |
| TURKU | 84 | 2 | 48 | 14-15 | 8939 | 1036.0 | 10577.2 | 1.8 |
| TURKU | 84 | 2 | 48 | 15-16 | 8599 | 1036.1 | 10180.1 | -2.0 |
| TURKU | 84 | 2 | 48 | 16-17 | 8739 | 1036.3 | 10356.1 | -0.3 |
| TURKU | 84 | 2 | 48 | 17-18 | 8761 | 1036.2 | 10375.1 | -0.2 |
| TURKU | 84 | 2 | 48 | 18-19 | 8873 | 1036.2 | 10512.0 | 1.2 |
| TURKU | 84 | 2 | 48 | 19-20 | 8800 | 1036.4 | 10437.6 | 0.4 |
| TURKU | 84 | 2 | 48 | 20-21 | 8593 | 1036.3 | 10187.4 | -2.0 |
| TURKU | 84 | 2 | 48 | 21-22 | 8778 | 1036.4 | 10408.7 | 0.2 |
| TURKU | 84 | 2 | 48 | 22-23 | 8793 | 1036.5 | 10431.4 | 0.4 |
| TURKU | 84 | 2 | 48 | 23-24 | 8695 | 1036.4 | 10313.8 | -0.7 |
| TURKU | 84 | 2 | 49 | 0- 1 | 8851 | 1036.5 | 10504.4 | 1.1 |
| TURKU | 84 | 2 | 49 | 1- 2 | 8882 | 1036.4 | 10532.5 | 1.4 |
| TURKU | 84 | 2 | 49 | 2- 3 | 8540 | 1036.4 | 10128.3 | -2.5 |
| TURKU | 84 | 2 | 49 | 3- 4 | 8818 | 1036.5 | 10462.8 | 0.7 |
| TURKU | 84 | 2 | 49 | 4- 5 | 8726 | 1036.4 | 10349.3 | -0.4 |

Table 2. continued

CATEGORY IV (mean neutron energy 1500 MeV at sea level)

Counting rates per hour

| STATION | YY | MM | DD | TIME SPAN | UNCOR. | PRES. | COR. | % INC. |
|---|---|---|---|---|---|---|---|---|
| TURKU | 84 | 2 | 46 | 12-13 | 908 | 1040.9 | 1121.8 | -1.3 |
| TURKU | 84 | 2 | 46 | 13-14 | 914 | 1041.0 | 1130.1 | -0.6 |
| TURKU | 84 | 2 | 46 | 14-15 | 818 | 1041.0 | 1011.3 | -11.1 |
| TURKU | 84 | 2 | 46 | 15-16 | 910 | 1041.0 | 1125.5 | -1.0 |
| TURKU | 84 | 2 | 46 | 16-17 | 931 | 1041.0 | 1151.6 | 1.3 |
| TURKU | 84 | 2 | 46 | 18-17 | - | - | - | - |
| TURKU | 84 | 2 | 46 | 18-19 | 902 | 1041.5 | 1118.4 | -1.6 |
| TURKU | 84 | 2 | 46 | 19-20 | 888 | 1041.3 | 1100.2 | -3.2 |
| TURKU | 84 | 2 | 46 | 20-21 | 915 | 1041.5 | 1135.3 | -0.2 |
| TURKU | 84 | 2 | 46 | 21-22 | 876 | 1041.4 | 1086.2 | -4.5 |
| TURKU | 84 | 2 | 46 | 22-23 | 909 | 1041.4 | 1126.4 | -0.9 |
| TURKU | 84 | 2 | 46 | 23-24 | 878 | 1041.4 | 1088.1 | -4.3 |
| TURKU | 84 | 2 | 47 | 0- 1 | 933 | 1041.1 | 1154.7 | 1.6 |
| TURKU | 84 | 2 | 47 | 1- 2 | 957 | 1040.8 | 1181.7 | 3.9 |
| TURKU | 84 | 2 | 47 | 2- 3 | 1020 | 1040.5 | 1257.7 | 10.6 |
| TURKU | 84 | 2 | 47 | 3- 4 | 883 | 1040.2 | 1086.8 | -4.4 |
| TURKU | 84 | 2 | 47 | 4- 5 | 882 | 1039.8 | 1082.8 | -4.8 |
| TURKU | 84 | 2 | 47 | 5- 6 | 964 | 1039.8 | 1183.3 | 4.1 |
| TURKU | 84 | 2 | 47 | 6- 7 | 992 | 1039.9 | 1218.2 | 7.1 |
| TURKU | 84 | 2 | 47 | 7- 8 | 907 | 1039.9 | 1114.1 | -2.0 |
| TURKU | 84 | 2 | 47 | 8- 9 | 911 | 1040.0 | 1119.1 | -1.6 |
| TURKU | 84 | 2 | 47 | 9-10 | 975 | 1039.9 | 1197.4 | 5.3 |
| TURKU | 84 | 2 | 47 | 10-11 | 947 | 1039.6 | 1161.1 | 2.1 |
| TURKU | 84 | 2 | 47 | 11-12 | 895 | 1039.4 | 1095.8 | -3.6 |
| TURKU | 84 | 2 | 47 | 12-13 | 956 | 1039.0 | 1167.8 | 2.7 |
| TURKU | 84 | 2 | 47 | 13-14 | 901 | 1038.6 | 1097.9 | -3.4 |
| TURKU | 84 | 2 | 47 | 14-15 | 926 | 1038.6 | 1127.8 | -0.8 |
| TURKU | 84 | 2 | 47 | 15-16 | 909 | 1038.5 | 1106.6 | -2.7 |
| TURKU | 84 | 2 | 47 | 16-17 | 964 | 1038.4 | 1172.5 | 3.1 |
| TURKU | 84 | 2 | 47 | 17-18 | 941 | 1038.1 | 1143.0 | 0.5 |
| TURKU | 84 | 2 | 47 | 18-19 | 959 | 1038.0 | 1163.6 | 2.3 |
| TURKU | 84 | 2 | 47 | 19-20 | 937 | 1037.9 | 1136.3 | -0.1 |
| TURKU | 84 | 2 | 47 | 20-21 | 953 | 1037.7 | 1154.6 | 1.5 |
| TURKU | 84 | 2 | 47 | 21-22 | 973 | 1037.5 | 1177.1 | 3.5 |
| TURKU | 84 | 2 | 47 | 22-23 | 907 | 1037.4 | 1096.9 | -3.5 |
| TURKU | 84 | 2 | 47 | 23-24 | 956 | 1037.2 | 1154.0 | 1.5 |
| TURKU | 84 | 2 | 48 | 0- 1 | 970 | 1036.9 | 1169.1 | 2.8 |
| TURKU | 84 | 2 | 48 | 1- 2 | 958 | 1036.7 | 1153.2 | 1.4 |
| TURKU | 84 | 2 | 48 | 2- 3 | 981 | 1036.6 | 1180.2 | 3.8 |
| TURKU | 84 | 2 | 48 | 3- 4 | 908 | 1036.6 | 1092.0 | -4.0 |
| TURKU | 84 | 2 | 48 | 4- 5 | 907 | 1036.4 | 1089.9 | -4.1 |
| TURKU | 84 | 2 | 48 | 5- 6 | 963 | 1036.3 | 1156.5 | 1.7 |
| TURKU | 84 | 2 | 48 | 6- 7 | 1012 | 1036.5 | 1216.4 | 7.0 |
| TURKU | 84 | 2 | 48 | 7- 8 | 978 | 1036.5 | 1175.7 | 3.4 |
| TURKU | 84 | 2 | 48 | 8- 9 | 949 | 1036.5 | 1141.1 | 0.4 |
| TURKU | 84 | 2 | 48 | 9-10 | 939 | 1036.4 | 1128.3 | -0.8 |
| TURKU | 84 | 2 | 48 | 10-11 | 943 | 1036.3 | 1132.2 | -0.4 |
| TURKU | 84 | 2 | 48 | 11-12 | 994 | 1036.2 | 1192.9 | 4.9 |
| TURKU | 84 | 2 | 48 | 12-13 | 936 | 1036.1 | 1122.7 | -1.3 |
| TURKU | 84 | 2 | 48 | 13-14 | 880 | 1036.1 | 1055.0 | -7.2 |
| TURKU | 84 | 2 | 48 | 14-15 | 911 | 1036.0 | 1092.0 | -4.0 |
| TURKU | 84 | 2 | 48 | 15-16 | 940 | 1036.1 | 1127.1 | -0.9 |
| TURKU | 84 | 2 | 48 | 16-17 | 938 | 1036.3 | 1126.0 | -1.0 |
| TURKU | 84 | 2 | 48 | 17-18 | 943 | 1036.2 | 1131.2 | -0.5 |
| TURKU | 84 | 2 | 48 | 18-19 | 930 | 1036.2 | 1116.0 | -1.9 |
| TURKU | 84 | 2 | 48 | 19-20 | 950 | 1036.4 | 1141.6 | 0.4 |
| TURKU | 84 | 2 | 48 | 20-21 | 975 | 1036.3 | 1170.9 | 3.0 |
| TURKU | 84 | 2 | 48 | 21-22 | 959 | 1036.4 | 1152.3 | 1.3 |
| TURKU | 84 | 2 | 48 | 22-23 | 1009 | 1036.5 | 1212.6 | 6.7 |
| TURKU | 84 | 2 | 48 | 23-24 | 945 | 1036.4 | 1135.6 | -0.1 |
| TURKU | 84 | 2 | 49 | 0- 1 | 941 | 1036.5 | 1131.4 | -0.5 |
| TURKU | 84 | 2 | 49 | 1- 2 | 934 | 1036.4 | 1122.2 | -1.3 |
| TURKU | 84 | 2 | 49 | 2- 3 | 981 | 1036.4 | 1178.5 | 3.7 |
| TURKU | 84 | 2 | 49 | 3- 4 | 944 | 1036.5 | 1135.0 | -0.2 |
| TURKU | 84 | 2 | 49 | 4- 5 | 910 | 1036.4 | 1093.4 | -3.8 |

# Neutron Monitor Observations at Mt. Washington and Durham During the Ground Level Event of 16 February 1984

by

J.A. Lockwood and J. LaBonte
Space Science Center
University of New Hampshire
Durham, New Hampshire 03824 USA

In the morning of 16 February 1984 the solar cosmic ray ground level event (GLE) recorded by many stations in the worldwide network of neutron monitors (NM) was also seen at Mt. Washington (altitude = 1900 m; geographic position: N44°18' W71°18'; vertical cutoff rigidity = 1.24 GV) and at Durham (altitude sea level; geographic position: N43°06' W75°50'; vertical cutoff rigidity = 1.41 GV). In Tables 1 and 2 we show the 5 minute pressure-corrected counting rates for the two NMs (barometric pressure coefficient is 0.97%/mm Hg). The percentage increase at Mt. Washington and Durham are ∿75% and 42.9% respectively. The counting rate versus time profiles shown in Figures 1 and 2 exhibit a rapid rise to maximum, a relatively large maximum, and decay to background in about 90 minutes.

The GLE on 16 February 1984 has a similar signature to that of the GLE on 7 May 1978 for which it was shown that:

a.) the propagation of the solar particles was nearly scatter free between the Sun and the Earth (Debrunner et al., 1984);

b.) the flare particles at the Sun had relatively easy access to the footpoint of the magnetic field line connecting the Sun and the Earth (Lockwood and Debrunner, 1986).

The interesting feature of this GLE is that the source of the particles was not on the visible disk of the Sun. Analyses of radioheliograph data and solar synoptic charts indicate two active regions beyond the West limb of the Sun at W95 (Region 4410) and at W130 (Region 4408). From the solar coronal propagation model for solar flare protons (Lockwood and Debrunner, 1986) and the solar wind speed information, we inferred that the active region at W130 could be a source for the solar flare protons seen at Earth early on 16 February 1984. Since the pitch angle distributions and energy spectra of the GLEs on 16 February 1984 and on 7 May 1978 are similar (Debrunner et al., 1985; Lockwood and Debrunner, 1986), the NM and spacecraft data for both the 16 February 1984 GLEs can also be used to study the acceleration of the solar flare protons, their coronal propagation and their injection into the interplanetary medium.

## ACKNOWLEDGEMENTS

This research was supported by the National Science Foundation, Grant Number ATM-832-4486.

## REFERENCES

DEBRUNNER, H., E. FLUCKIGER, J.A. LOCKWOOD, and R.E. McGUIRE 1984 **J. Geophys. Res.**, 89, 769.

DEBRUNNER, H., E. FLUCKIGER, J.A. LOCKWOOD, and R.E. McGUIRE 1985 **Proc. 19th Int. Cosmic Ray Conf.**, 4, 317.

LOCKWOOD, J.A. and H. DEBRUNNER 1986 **J. Geophys. Res.** (to be published).

Table 1. 5-minute pressure corrected neutron monitor counting rate for Mt. Washington on 16 February 1984 in Eastern Standard Time (EST -- add 5 hours to get UT).

MTW FEB 16 FIVE MINUTE COUNTS FOR 1984

| TIME | COUNT | TIME | COUNT | TIME | COUNT | TIME | COUNT | TIME | COUNT | TIME | COUNT |
|---|---|---|---|---|---|---|---|---|---|---|---|
| 5 | 183.0 | 415 | 316.0 | 825 | 185.0 | 1235 | 184.0 | 1645 | 183.0 | 2055 | 187.0 |
| 10 | 184.0 | 420 | 323.0 | 830 | 186.0 | 1240 | 181.0 | 1650 | 190.0 | 2100 | 184.0 |
| 15 | 187.0 | 425 | 299.0 | 835 | 186.0 | 1245 | 191.0 | 1655 | 193.0 | 2105 | 185.0 |
| 20 | 184.0 | 430 | 266.0 | 840 | 183.0 | 1250 | 189.0 | 1700 | 187.0 | 2110 | 184.0 |
| 25 | 183.0 | 435 | 249.0 | 845 | 187.0 | 1255 | 187.0 | 1705 | 189.0 | 2115 | 188.0 |
| 30 | 184.0 | 440 | 230.0 | 850 | 185.0 | 1300 | 187.0 | 1710 | 188.0 | 2120 | 183.0 |
| 35 | 186.0 | 445 | 222.0 | 855 | 186.0 | 1305 | 187.0 | 1715 | 187.0 | 2125 | 189.0 |
| 40 | 182.0 | 450 | 214.0 | 900 | 186.0 | 1310 | 186.0 | 1720 | 185.0 | 2130 | 183.0 |
| 45 | 188.0 | 455 | 201.0 | 905 | 186.0 | 1315 | 189.0 | 1725 | 184.0 | 2135 | 187.0 |
| 50 | 185.0 | 500 | 200.0 | 910 | 187.0 | 1320 | 188.0 | 1730 | 185.0 | 2140 | 181.0 |
| 55 | 185.0 | 505 | 201.0 | 915 | 185.0 | 1325 | 190.0 | 1735 | 184.0 | 2145 | 186.0 |
| 100 | 183.0 | 510 | 196.0 | 920 | 183.0 | 1330 | 186.0 | 1740 | 186.0 | 2150 | 185.0 |
| 105 | 181.0 | 515 | 195.0 | 925 | 187.0 | 1335 | 186.0 | 1745 | 188.0 | 2155 | 185.0 |
| 110 | 190.0 | 520 | 195.0 | 930 | 186.0 | 1340 | 186.0 | 1750 | 182.0 | 2200 | 184.0 |
| 115 | 184.0 | 525 | 192.0 | 935 | 182.0 | 1345 | 191.0 | 1755 | 188.0 | 2205 | 189.0 |
| 120 | 181.0 | 530 | 196.0 | 940 | 186.0 | 1350 | 187.0 | 1800 | 187.0 | 2210 | 183.0 |
| 125 | 182.0 | 535 | 193.0 | 945 | 183.0 | 1355 | 189.0 | 1805 | 192.0 | 2215 | 183.0 |
| 130 | 184.0 | 540 | 192.0 | 950 | 183.0 | 1400 | 187.0 | 1810 | 186.0 | 2220 | 188.0 |
| 135 | 185.0 | 545 | 191.0 | 955 | 185.0 | 1405 | 186.0 | 1815 | 188.0 | 2225 | 185.0 |
| 140 | 185.0 | 550 | 188.0 | 1000 | 186.0 | 1410 | 185.0 | 1820 | 185.0 | 2230 | 184.0 |
| 145 | 187.0 | 555 | 191.0 | 1005 | 185.0 | 1415 | 186.0 | 1825 | 187.0 | 2235 | 186.0 |
| 150 | 185.0 | 600 | 190.0 | 1010 | 183.0 | 1420 | 185.0 | 1830 | 182.0 | 2240 | 187.0 |
| 155 | 192.0 | 605 | 185.0 | 1015 | 185.0 | 1425 | 185.0 | 1835 | 187.0 | 2245 | 184.0 |
| 200 | 182.0 | 610 | 183.0 | 1020 | 183.0 | 1430 | 183.0 | 1840 | 188.0 | 2250 | 188.0 |
| 205 | 186.0 | 615 | 189.0 | 1025 | 184.0 | 1435 | 187.0 | 1845 | 189.0 | 2255 | 184.0 |
| 210 | 182.0 | 620 | 191.0 | 1030 | 184.0 | 1440 | 187.0 | 1850 | 181.0 | 2300 | 186.0 |
| 215 | 187.0 | 625 | 188.0 | 1035 | 186.0 | 1445 | 186.0 | 1855 | 186.0 | 2305 | 183.0 |
| 220 | 183.0 | 630 | 188.0 | 1040 | 185.0 | 1450 | 186.0 | 1900 | 189.0 | 2310 | 181.0 |
| 225 | 184.0 | 635 | 187.0 | 1045 | 183.0 | 1455 | 184.0 | 1905 | 184.0 | 2315 | 185.0 |
| 230 | 186.0 | 640 | 186.0 | 1050 | 184.0 | 1500 | 187.0 | 1910 | 186.0 | 2320 | 188.0 |
| 235 | 183.0 | 645 | 185.0 | 1055 | 183.0 | 1505 | 189.0 | 1915 | 187.0 | 2325 | 187.0 |
| 240 | 186.0 | 650 | 189.0 | 1100 | 182.0 | 1510 | 187.0 | 1920 | 187.0 | 2330 | 185.0 |
| 245 | 185.0 | 655 | 185.0 | 1105 | 187.0 | 1515 | 189.0 | 1925 | 183.0 | 2335 | 183.0 |
| 250 | 183.0 | 700 | 187.0 | 1110 | 184.0 | 1520 | 190.0 | 1930 | 186.0 | 2340 | 186.0 |
| 255 | 185.0 | 705 | 185.0 | 1115 | 183.0 | 1525 | 185.0 | 1935 | 187.0 | 2345 | 184.0 |
| 300 | 186.0 | 710 | 184.0 | 1120 | 184.0 | 1530 | 187.0 | 1940 | 189.0 | 2350 | 189.0 |
| 305 | 185.0 | 715 | 187.0 | 1125 | 186.0 | 1535 | 187.0 | 1945 | 184.0 | 2355 | 187.0 |
| 310 | 187.0 | 720 | 186.0 | 1130 | 188.0 | 1540 | 187.0 | 1950 | 188.0 | 2400 | 187.0 |
| 315 | 187.0 | 725 | 187.0 | 1135 | 184.0 | 1545 | 188.0 | 1955 | 187.0 | | |
| 320 | 185.0 | 730 | 189.0 | 1140 | 186.0 | 1550 | 187.0 | 2000 | 185.0 | | |
| 325 | 187.0 | 735 | 183.0 | 1145 | 188.0 | 1555 | 187.0 | 2005 | 189.0 | | |
| 330 | 187.0 | 740 | 184.0 | 1150 | 187.0 | 1600 | 186.0 | 2010 | 188.0 | | |
| 335 | 187.0 | 745 | 186.0 | 1155 | 185.0 | 1605 | 189.0 | 2015 | 183.0 | | |
| 340 | 181.0 | 750 | 182.0 | 1200 | 188.0 | 1610 | 187.0 | 2020 | 186.0 | | |
| 345 | 179.0 | 755 | 183.0 | 1205 | 188.0 | 1615 | 189.0 | 2025 | 189.0 | | |
| 350 | 182.0 | 800 | 183.0 | 1210 | 189.0 | 1620 | 186.0 | 2030 | 184.0 | | |
| 355 | 185.0 | 805 | 187.0 | 1215 | 185.0 | 1625 | 189.0 | 2035 | 187.0 | | |
| 400 | 182.0 | 810 | 187.0 | 1220 | 186.0 | 1630 | 186.0 | 2040 | 185.0 | | |
| 405 | 183.0 | 815 | 186.0 | 1225 | 185.0 | 1635 | 186.0 | 2045 | 185.0 | | |
| 410 | 239.0 | 820 | 183.0 | 1230 | 186.0 | 1640 | 187.0 | 2050 | 186.0 | | |

Table 2. 5-minute pressure corrected neutron monitor counting rate for Durham on 16 February 1984 in Eastern Standard Time (EST -- add 5 hours to get UT).

DUR FEB 16 FIVE MINUTE COUNTS FOR 1984

| TIME | COUNT | TIME | COUNT | TIME | COUNT | TIME | COUNT | TIME | COUNT | TIME | COUNT |
|---|---|---|---|---|---|---|---|---|---|---|---|
| 5 | 175.0 | 415 | 260.0 | 825 | 174.0 | 1235 | 178.0 | 1645 | 174.0 | 2055 | 177.0 |
| 10 | 175.0 | 420 | 265.0 | 830 | 176.0 | 1240 | 174.0 | 1650 | 174.0 | 2100 | 175.0 |
| 15 | 174.0 | 425 | 254.0 | 835 | 174.0 | 1245 | 177.0 | 1655 | 175.0 | 2105 | 176.0 |
| 20 | 176.0 | 430 | 231.0 | 840 | 174.0 | 1250 | 176.0 | 1700 | 177.0 | 2110 | 176.0 |
| 25 | 176.0 | 435 | 213.0 | 845 | 175.0 | 1255 | 175.0 | 1705 | 177.0 | 2115 | 176.0 |
| 30 | 176.0 | 440 | 202.0 | 850 | 176.0 | 1300 | 179.0 | 1710 | 177.0 | 2120 | 175.0 |
| 35 | 175.0 | 445 | 194.0 | 855 | 175.0 | 1305 | 177.0 | 1715 | 176.0 | 2125 | 177.0 |
| 40 | 174.0 | 450 | 190.0 | 900 | 172.0 | 1310 | 176.0 | 1720 | 174.0 | 2130 | 178.0 |
| 45 | 177.0 | 455 | 189.0 | 905 | 176.0 | 1315 | 178.0 | 1725 | 178.0 | 2135 | 175.0 |
| 50 | 173.0 | 500 | 182.0 | 910 | 175.0 | 1320 | 176.0 | 1730 | 177.0 | 2140 | 176.0 |
| 55 | 176.0 | 505 | 180.0 | 915 | 176.0 | 1325 | 179.0 | 1735 | 175.0 | 2145 | 177.0 |
| 100 | 176.0 | 510 | 182.0 | 920 | 176.0 | 1330 | 174.0 | 1740 | 176.0 | 2150 | 175.0 |
| 105 | 176.0 | 515 | 181.0 | 925 | 176.0 | 1335 | 176.0 | 1745 | 176.0 | 2155 | 178.0 |
| 110 | 174.0 | 520 | 180.0 | 930 | 175.0 | 1340 | 176.0 | 1750 | 177.0 | 2200 | 176.0 |
| 115 | 174.0 | 525 | 177.0 | 935 | 176.0 | 1345 | 177.0 | 1755 | 174.0 | 2205 | 177.0 |
| 120 | 175.0 | 530 | 178.0 | 940 | 176.0 | 1350 | 176.0 | 1800 | 176.0 | 2210 | 179.0 |
| 125 | 174.0 | 535 | 176.0 | 945 | 175.0 | 1355 | 178.0 | 1805 | 176.0 | 2215 | 177.0 |
| 130 | 175.0 | 540 | 177.0 | 950 | 176.0 | 1400 | 177.0 | 1810 | 175.0 | 2220 | 173.0 |
| 135 | 176.0 | 545 | 175.0 | 955 | 175.0 | 1405 | 177.0 | 1815 | 175.0 | 2225 | 177.0 |
| 140 | 174.0 | 550 | 177.0 | 1000 | 177.0 | 1410 | 176.0 | 1820 | 177.0 | 2230 | 180.0 |
| 145 | 176.0 | 555 | 176.0 | 1005 | 173.0 | 1415 | 178.0 | 1825 | 175.0 | 2235 | 177.0 |
| 150 | 174.0 | 600 | 177.0 | 1010 | 175.0 | 1420 | 177.0 | 1830 | 176.0 | 2240 | 173.0 |
| 155 | 175.0 | 605 | 175.0 | 1015 | 176.0 | 1425 | 176.0 | 1835 | 174.0 | 2245 | 177.0 |
| 200 | 175.0 | 610 | 175.0 | 1020 | 176.0 | 1430 | 176.0 | 1840 | 177.0 | 2250 | 177.0 |
| 205 | 173.0 | 615 | 176.0 | 1025 | 175.0 | 1435 | 174.0 | 1845 | 176.0 | 2255 | 177.0 |
| 210 | 176.0 | 620 | 173.0 | 1030 | 175.0 | 1440 | 177.0 | 1850 | 176.0 | 2300 | 176.0 |
| 215 | 174.0 | 625 | 176.0 | 1035 | 175.0 | 1445 | 172.0 | 1855 | 177.0 | 2305 | 174.0 |
| 220 | 174.0 | 630 | 176.0 | 1040 | 176.0 | 1450 | 177.0 | 1900 | 177.0 | 2310 | 174.0 |
| 225 | 175.0 | 635 | 178.0 | 1045 | 177.0 | 1455 | 178.0 | 1905 | 177.0 | 2315 | 174.0 |
| 230 | 174.0 | 640 | 175.0 | 1050 | 172.0 | 1500 | 178.0 | 1910 | 176.0 | 2320 | 174.0 |
| 235 | 176.0 | 645 | 177.0 | 1055 | 178.0 | 1505 | 175.0 | 1915 | 175.0 | 2325 | 176.0 |
| 240 | 177.0 | 650 | 175.0 | 1100 | 176.0 | 1510 | 179.0 | 1920 | 176.0 | 2330 | 176.0 |
| 245 | 173.0 | 655 | 178.0 | 1105 | 175.0 | 1515 | 175.0 | 1925 | 175.0 | 2335 | 174.0 |
| 250 | 173.0 | 700 | 173.0 | 1110 | 173.0 | 1520 | 174.0 | 1930 | 177.0 | 2340 | 174.0 |
| 255 | 175.0 | 705 | 175.0 | 1115 | 178.0 | 1525 | 177.0 | 1935 | 177.0 | 2345 | 175.0 |
| 300 | 174.0 | 710 | 176.0 | 1120 | 176.0 | 1530 | 176.0 | 1940 | 177.0 | 2350 | 175.0 |
| 305 | 175.0 | 715 | 176.0 | 1125 | 175.0 | 1535 | 177.0 | 1945 | 178.0 | 2355 | 177.0 |
| 310 | 175.0 | 720 | 176.0 | 1130 | 176.0 | 1540 | 175.0 | 1950 | 177.0 | 2400 | 176.0 |
| 315 | 175.0 | 725 | 176.0 | 1135 | 175.0 | 1545 | 177.0 | 1955 | 176.0 | | |
| 320 | 174.0 | 730 | 176.0 | 1140 | 177.0 | 1550 | 177.0 | 2000 | 176.0 | | |
| 325 | 174.0 | 735 | 175.0 | 1145 | 176.0 | 1555 | 175.0 | 2005 | 178.0 | | |
| 330 | 175.0 | 740 | 177.0 | 1150 | 175.0 | 1600 | 178.0 | 2010 | 177.0 | | |
| 335 | 176.0 | 745 | 176.0 | 1155 | 174.0 | 1605 | 176.0 | 2015 | 176.0 | | |
| 340 | 174.0 | 750 | 176.0 | 1200 | 175.0 | 1610 | 176.0 | 2020 | 175.0 | | |
| 345 | 175.0 | 755 | 175.0 | 1205 | 176.0 | 1615 | 176.0 | 2025 | 174.0 | | |
| 350 | 174.0 | 800 | 176.0 | 1210 | 174.0 | 1620 | 177.0 | 2030 | 175.0 | | |
| 355 | 173.0 | 805 | 177.0 | 1215 | 174.0 | 1625 | 177.0 | 2035 | 178.0 | | |
| 400 | 174.0 | 810 | 176.0 | 1220 | 176.0 | 1630 | 177.0 | 2040 | 176.0 | | |
| 405 | 175.0 | 815 | 175.0 | 1225 | 177.0 | 1635 | 173.0 | 2045 | 175.0 | | |
| 410 | 202.0 | 820 | 177.0 | 1230 | 177.0 | 1640 | 175.0 | 2050 | 174.0 | | |

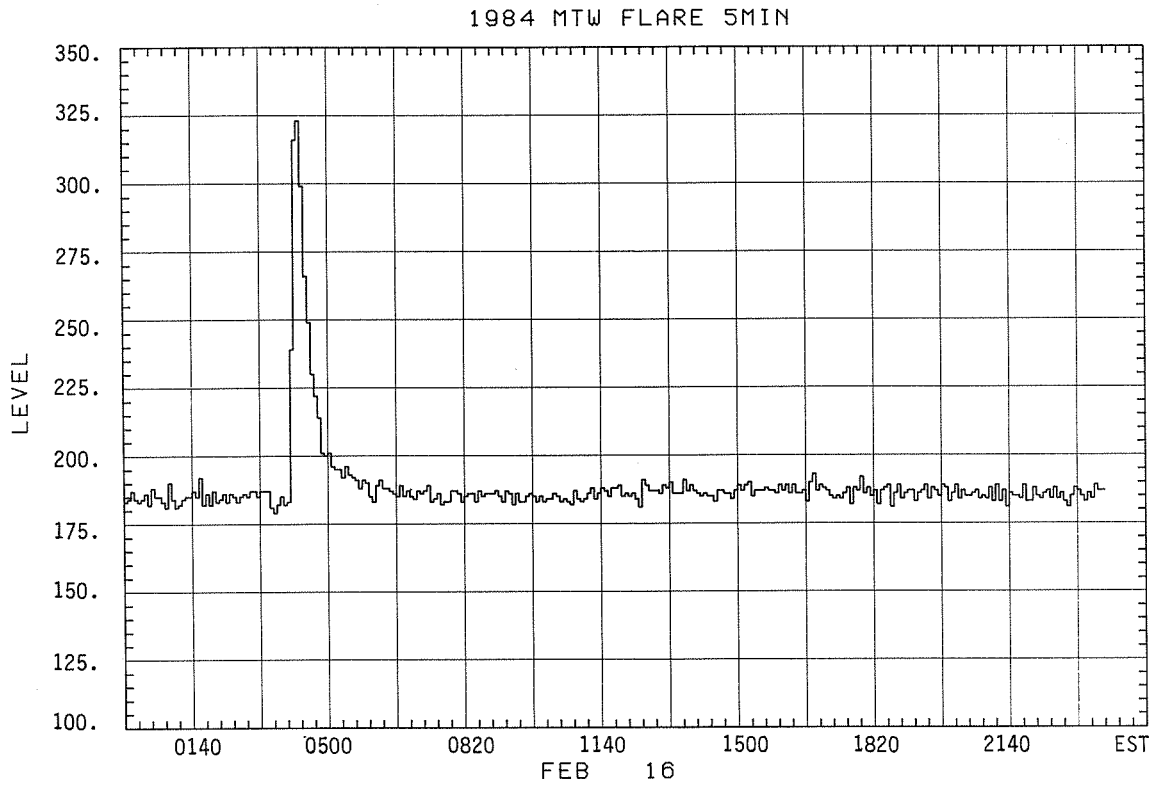


Fig. 1 5-minute pressure corrected neutron monitor counting rate for Mt. Washington on 16 February 1984 in Eastern Standard Time (EST -- add 5 hours to get UT).

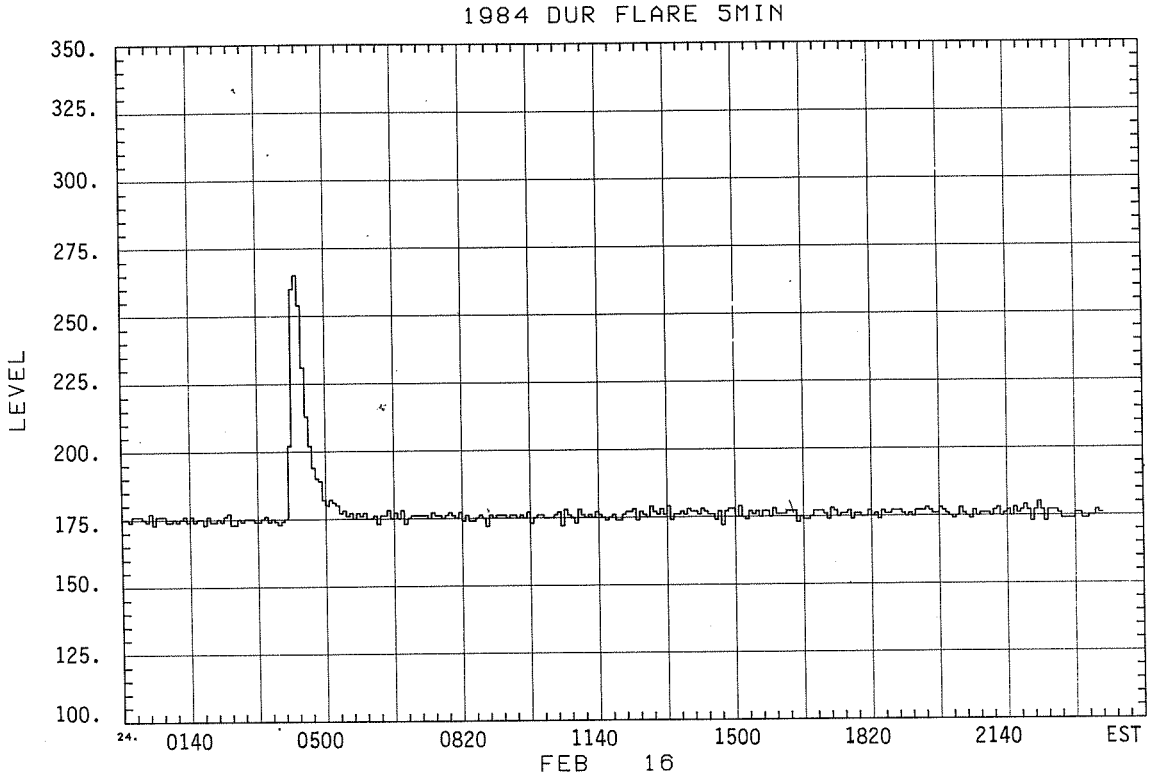


Fig 2. 5-minute pressure corrected neutron monitor counting rate for Durham on 16 February 1984 in Eastern Standard Time (EST -- add 5 hours to get UT).

# The Response of the Neutron Monitors at Jungfraujoch, Kerguelen and Terre Adelie to the 16 February 1984 Relativistic Solar Particle Event

by

H. Debrunner, E. Fluckiger, F. Golliez, M. Schubnell, and G. Sebor
Physikalisches Institut, Universitat Bern, Sidlerstrasse 5
3012 Bern, Switzerland

and

J.-P. Legrand, G. Casarrubios, D. Fouassier, P. Kossa, M. Lambrecht,
C. Mottais, and A. Zuntini
Territoire des Terres Australes et Antarctiques Francaises
75017 Paris-27, France
and
Centre National de la Recherche Scientifique
Institut National d'Astronomie et de Geophysique
94107 Saint Maur, France

This report contains the neutron monitor data from Jungfraujoch, Kerguelen, and Terre Adelie for the time period 15 February 1984, 0000 UT to 16 February 1984, 2400 UT.

The station and detector parameters are listed in Table 1. Please note that due to special experiments carried out in February 1984 the cosmic ray data for Jungfraujoch given in this report are based on two monitor sections only. The neutron monitor data are compiled according to the standardized format for cosmic ray ground-level event data suggested by Shea et al. (1985). The time interval from 0800-0900 UT on 16 February 1984 was used as the period of reference to calculate the relative count rates. The numerical values are given in Tables 2, 3 and 4. The pressure corrected relative counting rates of the three stations are also plotted in Figures 1, 2 and 3.

Table 1. Station and Detector Data

| | Jungfraujoch | Kerguelen | Terre Adelie |
|---|---|---|---|
| Geographic latitude | N46.55 | S49.35 | S66.67 |
| Geographic longitude | E07.98 | E70.22 | E140.02 |
| Altitude | 3550 m | 33 m | 35 m |
| Effective vertical cutoff rigidity for Epoch 1980.0 (Shea et al., 1983) | 4.63 GV | 1.14 GV | 0.00 GV |
| Station identification | JUN1 | POR2 | DUM2 |
| Instrument | 3 x 6IGY (2 x 6IGY)* | 3 x 6-NM-64 | 3 x 3-NM-64 |
| Average pressure corrected counting rate per hour (February 1984) | 545,980 (367,415)* | 739,320 | 395,180 |
| Standard barometric pressure | 482 mm Hg | 750 mm Hg | 740 mm Hg |
| Standard barometric coefficient | 0.96 %/mm Hg | 1.01 %/mm Hg | 0.99 %/mm Hg |

*Due to special experiments carried out in February 1984 the cosmic ray data for Jungfraujoch given in this report are based on two monitor sections only.

**Acknowledgments**

This work has been supported by the Swiss National Foundation, grants NF 2.811-0.83 and 2.206-0.84, by Territoire des Terres Australes et Antarctiques Francaises and by the French Centre National de Recherche Scientifique.

## REFERENCES

SHEA, M.A. D.F. SMART and L.C. GENTILE 1983 **18th International Cosmic Ray Conference, Bangalore, India, Conference Papers, 3, 411.**

SHEA, M.A. D.F. SMART M. WADA and A. INOUE 1985 **19th International Cosmic Ray Conference, La Jolla, California Conference Papers, 5, 510.**

Table 2. Data of the neutron monitor Jungfraujoch for the time period 15 February 1984, 0000 UT to 16 February 1984, 2400 UT

| STATION | YY | MM | DD | MIN | TIME SPAN (UT) | DATA CODE | UNCOR. (CPS) | PRES. (MMHG) | COR. (CPS) | % INC. |
|---|---|---|---|---|---|---|---|---|---|---|
| JUN1 | 84 | 2 | 15 | 60 | 0000-0100 | 0 | 96.75 | 487.9 | 102.39 | -0.8 |
| JUN1 | 84 | 2 | 15 | 60 | 0100-0200 | 0 | 96.89 | 487.5 | 102.15 | -1.0 |
| JUN1 | 84 | 2 | 15 | 60 | 0200-0300 | 0 | 97.20 | 486.8 | 101.78 | -1.4 |
| JUN1 | 84 | 2 | 15 | 60 | 0300-0400 | 0 | 97.97 | 485.9 | 101.71 | -1.5 |
| JUN1 | 84 | 2 | 15 | 60 | 0400-0500 | 0 | 98.37 | 485.3 | 101.54 | -1.6 |
| JUN1 | 84 | 2 | 15 | 60 | 0500-0600 | 0 | 99.00 | 484.8 | 101.70 | -1.5 |
| JUN1 | 84 | 2 | 15 | 60 | 0600-0700 | 0 | 99.52 | 484.9 | 102.33 | -0.9 |
| JUN1 | 84 | 2 | 15 | 60 | 0700-0800 | 0 | 100.13 | 484.9 | 102.96 | -0.3 |
| JUN1 | 84 | 2 | 15 | 60 | 0800-0900 | 0 | 99.98 | 484.9 | 102.80 | -0.4 |
| JUN1 | 84 | 2 | 15 | 60 | 0900-1000 | 0 | 99.89 | 485.0 | 102.81 | -0.4 |
| JUN1 | 84 | 2 | 15 | 60 | 1000-1100 | 0 | 99.65 | 485.1 | 102.66 | -0.5 |
| JUN1 | 84 | 2 | 15 | 60 | 1100-1200 | 0 | 99.24 | 485.5 | 102.63 | -0.6 |
| JUN1 | 84 | 2 | 15 | 60 | 1200-1300 | 0 | 98.69 | 485.9 | 102.45 | -0.7 |
| JUN1 | 84 | 2 | 15 | 60 | 1300-1400 | 0 | 99.01 | 486.1 | 102.98 | -0.2 |
| JUN1 | 84 | 2 | 15 | 60 | 1400-1500 | 0 | 98.76 | 486.2 | 102.83 | -0.4 |
| JUN1 | 84 | 2 | 15 | 60 | 1500-1600 | 0 | 98.60 | 486.3 | 102.76 | -0.5 |
| JUN1 | 84 | 2 | 15 | 60 | 1600-1700 | 0 | 98.84 | 486.3 | 103.01 | -0.2 |
| JUN1 | 84 | 2 | 15 | 60 | 1700-1800 | 0 | 98.47 | 486.3 | 102.62 | -0.6 |
| JUN1 | 84 | 2 | 15 | 60 | 1800-1900 | 0 | 98.16 | 486.3 | 102.30 | -0.9 |
| JUN1 | 84 | 2 | 15 | 60 | 1900-2000 | 0 | 98.73 | 486.3 | 102.89 | -0.3 |
| JUN1 | 84 | 2 | 15 | 60 | 2000-2100 | 0 | 98.16 | 486.3 | 102.29 | -0.9 |
| JUN1 | 84 | 2 | 15 | 60 | 2100-2200 | 0 | 98.69 | 486.4 | 102.95 | -0.3 |
| JUN1 | 84 | 2 | 15 | 60 | 2200-2300 | 0 | 98.81 | 486.3 | 102.98 | -0.2 |
| JUN1 | 84 | 2 | 15 | 60 | 2300-2400 | 0 | 99.01 | 486.3 | 103.18 | 0.0 |
| JUN1 | 84 | 2 | 16 | 60 | 0000-0100 | 0 | 98.46 | 486.2 | 102.51 | -0.7 |
| JUN1 | 84 | 2 | 16 | 60 | 0100-0200 | 0 | 98.83 | 486.0 | 102.70 | -0.5 |
| JUN1 | 84 | 2 | 16 | 60 | 0200-0300 | 0 | 98.86 | 485.8 | 102.54 | -0.7 |
| JUN1 | 84 | 2 | 16 | 60 | 0300-0400 | 0 | 99.77 | 485.6 | 103.28 | 0.1 |
| JUN1 | 84 | 2 | 16 | 60 | 0400-0500 | 0 | 99.26 | 485.5 | 102.65 | -0.6 |
| JUN1 | 84 | 2 | 16 | 60 | 0500-0600 | 0 | 99.45 | 485.4 | 102.75 | -0.5 |
| JUN1 | 84 | 2 | 16 | 60 | 0600-0700 | 0 | 99.18 | 485.5 | 102.57 | -0.6 |
| JUN1 | 84 | 2 | 16 | 5 | 0700-0705 | 0 | 97.88 | 485.7 | 101.42 | -1.7 |
| JUN1 | 84 | 2 | 16 | 5 | 0705-0710 | 0 | 97.71 | 485.5 | 101.05 | -2.1 |
| JUN1 | 84 | 2 | 16 | 5 | 0710-0715 | 0 | 97.44 | 485.4 | 100.68 | -2.5 |
| JUN1 | 84 | 2 | 16 | 5 | 0715-0720 | 0 | 99.42 | 485.6 | 102.92 | -0.3 |
| JUN1 | 84 | 2 | 16 | 5 | 0720-0725 | 0 | 99.34 | 485.6 | 102.83 | -0.4 |
| JUN1 | 84 | 2 | 16 | 5 | 0725-0730 | 0 | 99.18 | 485.5 | 102.57 | -0.6 |
| JUN1 | 84 | 2 | 16 | 5 | 0730-0735 | 0 | 99.70 | 485.6 | 103.20 | 0.0 |
| JUN1 | 84 | 2 | 16 | 5 | 0735-0740 | 0 | 100.01 | 485.6 | 103.52 | 0.3 |
| JUN1 | 84 | 2 | 16 | 5 | 0740-0745 | 0 | 98.08 | 485.6 | 101.53 | -1.6 |
| JUN1 | 84 | 2 | 16 | 5 | 0745-0750 | 0 | 99.96 | 485.5 | 103.38 | 0.2 |
| JUN1 | 84 | 2 | 16 | 5 | 0750-0755 | 0 | 98.51 | 485.3 | 101.68 | -1.5 |
| JUN1 | 84 | 2 | 16 | 5 | 0755-0800 | 0 | 100.54 | 485.6 | 104.07 | 0.8 |
| JUN1 | 84 | 2 | 16 | 5 | 0800-0805 | 0 | 100.30 | 485.5 | 103.73 | 0.5 |
| JUN1 | 84 | 2 | 16 | 5 | 0805-0810 | 0 | 99.36 | 485.5 | 102.76 | -0.4 |
| JUN1 | 84 | 2 | 16 | 5 | 0810-0815 | 0 | 99.77 | 485.6 | 103.27 | 0.1 |
| JUN1 | 84 | 2 | 16 | 5 | 0815-0820 | 0 | 99.69 | 485.4 | 103.00 | -0.2 |
| JUN1 | 84 | 2 | 16 | 5 | 0820-0825 | 0 | 99.80 | 485.6 | 103.31 | 0.1 |
| JUN1 | 84 | 2 | 16 | 5 | 0825-0830 | 0 | 99.84 | 485.6 | 103.35 | 0.1 |
| JUN1 | 84 | 2 | 16 | 5 | 0830-0835 | 0 | 99.55 | 485.4 | 102.86 | -0.4 |
| JUN1 | 84 | 2 | 16 | 5 | 0835-0840 | 0 | 98.63 | 485.7 | 102.20 | -1.0 |
| JUN1 | 84 | 2 | 16 | 5 | 0840-0845 | 0 | 100.92 | 485.7 | 104.57 | 1.3 |
| JUN1 | 84 | 2 | 16 | 5 | 0845-0850 | 0 | 99.65 | 485.7 | 103.26 | 0.0 |
| JUN1 | 84 | 2 | 16 | 5 | 0850-0855 | 0 | 99.96 | 485.4 | 103.28 | 0.1 |
| JUN1 | 84 | 2 | 16 | 5 | 0855-0900 | 0 | 99.48 | 485.7 | 103.08 | -0.1 |
| JUN1 | 84 | 2 | 16 | 1 | 0900-0901 | 0 | 99.68 | 485.8 | 103.39 | 0.2 |
| JUN1 | 84 | 2 | 16 | 1 | 0901-0902 | 0 | 97.50 | 485.6 | 100.93 | -2.2 |
| JUN1 | 84 | 2 | 16 | 1 | 0902-0903 | 0 | 100.57 | 485.4 | 103.90 | 0.7 |
| JUN1 | 84 | 2 | 16 | 1 | 0903-0904 | 0 | 98.75 | 485.6 | 102.22 | -1.0 |
| JUN1 | 84 | 2 | 16 | 1 | 0904-0905 | 0 | 100.35 | 485.6 | 103.88 | 0.6 |
| JUN1 | 84 | 2 | 16 | 1 | 0905-0906 | 0 | 99.00 | 485.6 | 102.48 | -0.7 |
| JUN1 | 84 | 2 | 16 | 1 | 0906-0907 | 0 | 99.43 | 485.6 | 102.93 | -0.3 |
| JUN1 | 84 | 2 | 16 | 1 | 0907-0908 | 0 | 106.47 | 485.6 | 110.21 | 6.8 |

Table 2. Cont.

| STATION | YY | MM | DD | MIN | TIME SPAN (UT) | DATA CODE | UNCOR. (CPS) | PRES. (MMHG) | COR. (CPS) | % INC. |
|---|---|---|---|---|---|---|---|---|---|---|
| JUN1 | 84 | 2 | 16 | 1 | 0908-0909 | 0 | 101.75 | 485.6 | 105.33 | 2.0 |
| JUN1 | 84 | 2 | 16 | 1 | 0909-0910 | 0 | 102.65 | 485.6 | 106.26 | 2.9 |
| JUN1 | 84 | 2 | 16 | 1 | 0910-0911 | 0 | 102.87 | 485.6 | 106.48 | 3.2 |
| JUN1 | 84 | 2 | 16 | 1 | 0911-0912 | 0 | 102.08 | 485.6 | 105.67 | 2.4 |
| JUN1 | 84 | 2 | 16 | 1 | 0912-0913 | 0 | 102.68 | 485.7 | 106.40 | 3.1 |
| JUN1 | 84 | 2 | 16 | 1 | 0913-0914 | 0 | 105.03 | 485.7 | 108.83 | 5.4 |
| JUN1 | 84 | 2 | 16 | 1 | 0914-0915 | 0 | 103.15 | 485.7 | 106.88 | 3.5 |
| JUN1 | 84 | 2 | 16 | 1 | 0915-0916 | 0 | 100.55 | 485.5 | 103.99 | 0.7 |
| JUN1 | 84 | 2 | 16 | 1 | 0916-0917 | 0 | 104.12 | 485.6 | 107.78 | 4.4 |
| JUN1 | 84 | 2 | 16 | 1 | 0917-0918 | 0 | 104.42 | 485.6 | 108.09 | 4.7 |
| JUN1 | 84 | 2 | 16 | 1 | 0918-0919 | 0 | 102.40 | 485.7 | 106.10 | 2.8 |
| JUN1 | 84 | 2 | 16 | 1 | 0919-0920 | 0 | 103.20 | 485.7 | 106.93 | 3.6 |
| JUN1 | 84 | 2 | 16 | 1 | 0920-0921 | 0 | 104.50 | 485.7 | 108.28 | 4.9 |
| JUN1 | 84 | 2 | 16 | 1 | 0921-0922 | 0 | 102.57 | 485.7 | 106.28 | 3.0 |
| JUN1 | 84 | 2 | 16 | 1 | 0922-0923 | 0 | 103.40 | 485.7 | 107.14 | 3.8 |
| JUN1 | 84 | 2 | 16 | 1 | 0923-0924 | 0 | 102.27 | 485.6 | 105.86 | 2.6 |
| JUN1 | 84 | 2 | 16 | 1 | 0924-0925 | 0 | 103.98 | 485.7 | 107.74 | 4.4 |
| JUN1 | 84 | 2 | 16 | 1 | 0925-0926 | 0 | 103.02 | 485.6 | 106.64 | 3.3 |
| JUN1 | 84 | 2 | 16 | 1 | 0926-0927 | 1 | | | | |
| JUN1 | 84 | 2 | 16 | 1 | 0927-0928 | 0 | 102.78 | 485.7 | 106.50 | 3.2 |
| JUN1 | 84 | 2 | 16 | 1 | 0928-0929 | 0 | 101.97 | 485.7 | 105.65 | 2.4 |
| JUN1 | 84 | 2 | 16 | 1 | 0929-0930 | 0 | 101.35 | 485.7 | 105.01 | 1.7 |
| JUN1 | 84 | 2 | 16 | 5 | 0930-0935 | 0 | 101.37 | 485.7 | 105.04 | 1.8 |
| JUN1 | 84 | 2 | 16 | 5 | 0935-0940 | 0 | 100.78 | 485.6 | 104.32 | 1.1 |
| JUN1 | 84 | 2 | 16 | 5 | 0940-0945 | 0 | 100.97 | 485.7 | 104.62 | 1.4 |
| JUN1 | 84 | 2 | 16 | 5 | 0945-0950 | 0 | 100.96 | 485.7 | 104.61 | 1.3 |
| JUN1 | 84 | 2 | 16 | 5 | 0950-0955 | 0 | 101.02 | 485.6 | 104.58 | 1.3 |
| JUN1 | 84 | 2 | 16 | 5 | 0955-1000 | 0 | 101.64 | 485.7 | 105.32 | 2.0 |
| JUN1 | 84 | 2 | 16 | 5 | 1000-1005 | 0 | 100.37 | 485.7 | 104.00 | 0.8 |
| JUN1 | 84 | 2 | 16 | 5 | 1005-1010 | 0 | 98.97 | 485.6 | 102.45 | -0.7 |
| JUN1 | 84 | 2 | 16 | 5 | 1010-1015 | 0 | 100.33 | 485.7 | 103.96 | 0.7 |
| JUN1 | 84 | 2 | 16 | 5 | 1015-1020 | 0 | 101.22 | 485.5 | 104.68 | 1.4 |
| JUN1 | 84 | 2 | 16 | 5 | 1020-1025 | 0 | 100.61 | 485.5 | 104.04 | 0.8 |
| JUN1 | 84 | 2 | 16 | 5 | 1025-1030 | 0 | 99.98 | 485.6 | 103.50 | 0.3 |
| JUN1 | 84 | 2 | 16 | 5 | 1030-1035 | 0 | 100.23 | 485.7 | 103.85 | 0.6 |
| JUN1 | 84 | 2 | 16 | 5 | 1035-1040 | 0 | 100.95 | 485.7 | 104.60 | 1.3 |
| JUN1 | 84 | 2 | 16 | 5 | 1040-1045 | 0 | 100.13 | 485.7 | 103.75 | 0.5 |
| JUN1 | 84 | 2 | 16 | 5 | 1045-1050 | 0 | 100.97 | 485.7 | 104.62 | 1.4 |
| JUN1 | 84 | 2 | 16 | 5 | 1050-1055 | 0 | 100.39 | 485.3 | 103.62 | 0.4 |
| JUN1 | 84 | 2 | 16 | 5 | 1055-1100 | 0 | 100.85 | 485.6 | 104.39 | 1.1 |
| JUN1 | 84 | 2 | 16 | 5 | 1100-1105 | 0 | 100.85 | 485.5 | 104.29 | 1.0 |
| JUN1 | 84 | 2 | 16 | 5 | 1105-1110 | 0 | 101.31 | 485.5 | 104.77 | 1.5 |
| JUN1 | 84 | 2 | 16 | 5 | 1110-1115 | 0 | 100.71 | 485.5 | 104.15 | 0.9 |
| JUN1 | 84 | 2 | 16 | 5 | 1115-1120 | 0 | 100.78 | 485.5 | 104.22 | 1.0 |
| JUN1 | 84 | 2 | 16 | 5 | 1120-1125 | 0 | 101.10 | 485.4 | 104.45 | 1.2 |
| JUN1 | 84 | 2 | 16 | 5 | 1125-1130 | 0 | 99.44 | 485.5 | 102.84 | -0.4 |
| JUN1 | 84 | 2 | 16 | 5 | 1130-1135 | 0 | 99.95 | 485.4 | 103.27 | 0.0 |
| JUN1 | 84 | 2 | 16 | 5 | 1135-1140 | 0 | 100.95 | 485.5 | 104.40 | 1.1 |
| JUN1 | 84 | 2 | 16 | 5 | 1140-1145 | 0 | 100.13 | 485.4 | 103.45 | 0.2 |
| JUN1 | 84 | 2 | 16 | 5 | 1145-1150 | 0 | 100.63 | 485.3 | 103.87 | 0.6 |
| JUN1 | 84 | 2 | 16 | 5 | 1150-1155 | 0 | 101.56 | 485.2 | 104.73 | 1.5 |
| JUN1 | 84 | 2 | 16 | 5 | 1155-1200 | 0 | 100.73 | 485.4 | 104.07 | 0.8 |
| JUN1 | 84 | 2 | 16 | 60 | 1200-1300 | 0 | 100.68 | 485.3 | 103.92 | 0.7 |
| JUN1 | 84 | 2 | 16 | 60 | 1300-1400 | 0 | 100.51 | 485.2 | 103.64 | 0.4 |
| JUN1 | 84 | 2 | 16 | 60 | 1400-1500 | 0 | 100.96 | 485.1 | 104.01 | 0.8 |
| JUN1 | 84 | 2 | 16 | 60 | 1500-1600 | 0 | 100.84 | 485.2 | 103.98 | 0.7 |
| JUN1 | 84 | 2 | 16 | 60 | 1600-1700 | 0 | 100.58 | 485.2 | 103.72 | 0.5 |
| JUN1 | 84 | 2 | 16 | 60 | 1700-1800 | 0 | 100.29 | 485.3 | 103.52 | 0.3 |
| JUN1 | 84 | 2 | 16 | 60 | 1800-1900 | 0 | 100.36 | 485.4 | 103.69 | 0.4 |
| JUN1 | 84 | 2 | 16 | 60 | 1900-2000 | 0 | 100.23 | 485.4 | 103.56 | 0.3 |
| JUN1 | 84 | 2 | 16 | 60 | 2000-2100 | 0 | 99.97 | 485.4 | 103.29 | 0.1 |
| JUN1 | 84 | 2 | 16 | 60 | 2100-2200 | 0 | 99.37 | 485.3 | 102.57 | -0.6 |
| JUN1 | 84 | 2 | 16 | 60 | 2200-2300 | 0 | 100.31 | 485.2 | 103.44 | 0.2 |
| JUN1 | 84 | 2 | 16 | 60 | 2300-2400 | 0 | 99.75 | 485.2 | 102.86 | -0.3 |

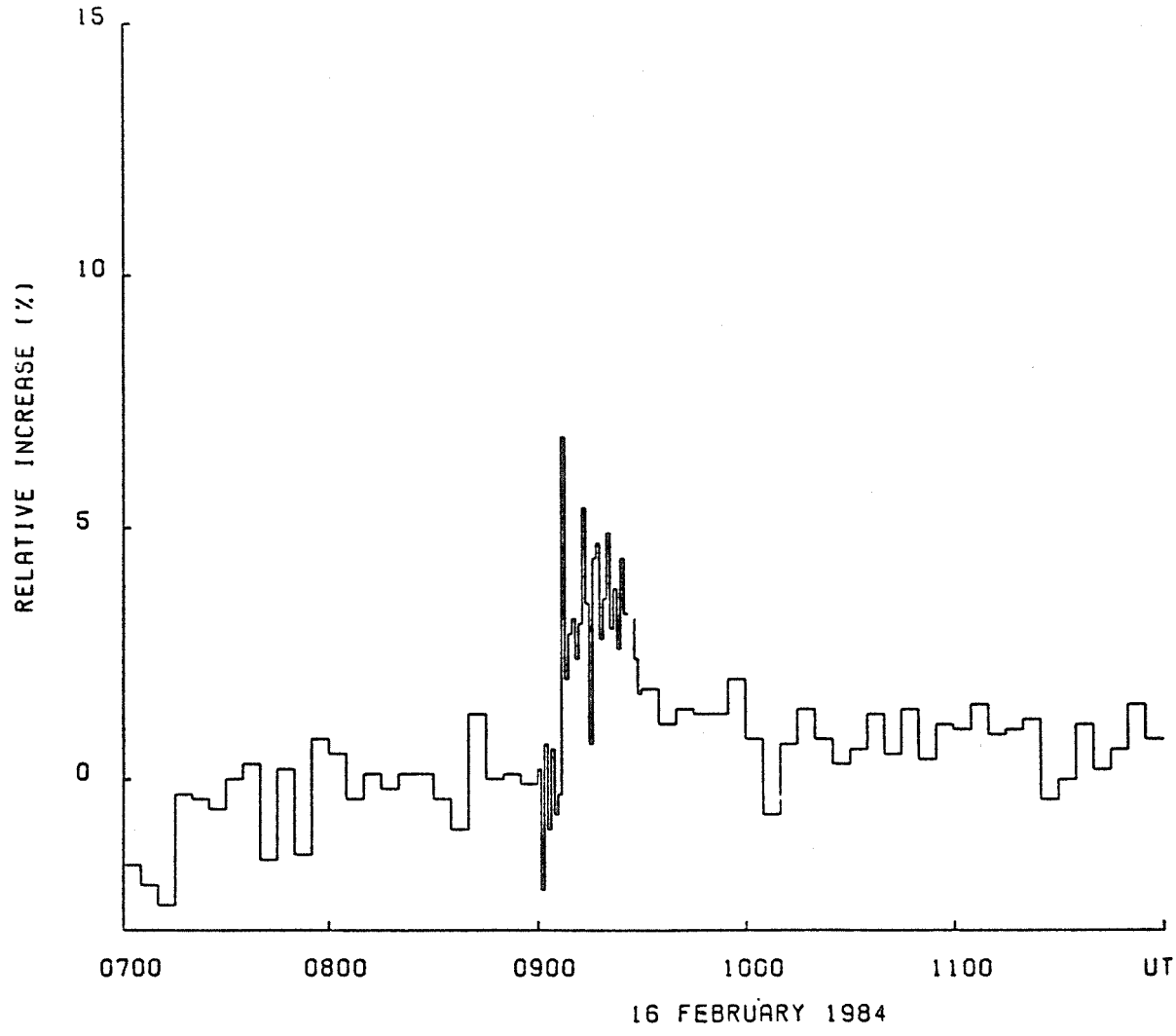


Figure 1. Relative increase of the pressure corrected cosmic ray intensity recorded by the Jungfraujoch neutron monitor for the 16 February 1984 ground-level event.

Table 3. Data of the neutron monitor Kerguelen for the time period 15 February 1984, 0000 UT to 16 February 1984, 2400 UT

| STATION | YY | MM | DD | MIN | TIME SPAN (UT) | DATA CODE | UNCOR. (CPS) | PRES. (MMHG) | COR. (CPS) | % INC. |
|---|---|---|---|---|---|---|---|---|---|---|
| POR2 | 84 | 2 | 15 | 60 | 0000-0100 | 0 | 192.78 | 756.8 | 206.44 | 0.1 |
| POR2 | 84 | 2 | 15 | 60 | 0100-0200 | 0 | 191.33 | 757.4 | 206.00 | -0.1 |
| POR2 | 84 | 2 | 15 | 60 | 0200-0300 | 0 | 189.44 | 758.1 | 205.56 | -0.4 |
| POR2 | 84 | 2 | 15 | 60 | 0300-0400 | 0 | 187.89 | 758.8 | 205.22 | -0.5 |
| POR2 | 84 | 2 | 15 | 60 | 0400-0500 | 0 | 187.33 | 759.4 | 205.89 | -0.2 |
| POR2 | 84 | 2 | 15 | 60 | 0500-0600 | 0 | 186.33 | 760.0 | 206.00 | -0.1 |
| POR2 | 84 | 2 | 15 | 60 | 0600-0700 | 0 | 185.22 | 760.3 | 205.56 | -0.4 |
| POR2 | 84 | 2 | 15 | 60 | 0700-0800 | 0 | 185.11 | 760.6 | 206.33 | 0.0 |
| POR2 | 84 | 2 | 15 | 60 | 0800-0900 | 0 | 184.33 | 761.1 | 206.11 | -0.1 |
| POR2 | 84 | 2 | 15 | 60 | 0900-1000 | 0 | 184.11 | 761.5 | 206.78 | 0.2 |
| POR2 | 84 | 2 | 15 | 60 | 1000-1100 | 0 | 184.44 | 761.6 | 207.33 | 0.5 |
| POR2 | 84 | 2 | 15 | 60 | 1100-1200 | 0 | 184.56 | 761.7 | 207.56 | 0.6 |
| POR2 | 84 | 2 | 15 | 60 | 1200-1300 | 0 | 183.44 | 761.8 | 206.67 | 0.2 |
| POR2 | 84 | 2 | 15 | 60 | 1300-1400 | 0 | 183.33 | 762.2 | 207.44 | 0.6 |
| POR2 | 84 | 2 | 15 | 60 | 1400-1500 | 0 | 181.89 | 762.6 | 206.33 | 0.0 |
| POR2 | 84 | 2 | 15 | 60 | 1500-1600 | 0 | 181.00 | 763.1 | 206.56 | 0.1 |
| POR2 | 84 | 2 | 15 | 60 | 1600-1700 | 0 | 181.00 | 763.2 | 206.89 | 0.3 |
| POR2 | 84 | 2 | 15 | 60 | 1700-1800 | 0 | 181.00 | 763.1 | 206.56 | 0.1 |
| POR2 | 84 | 2 | 15 | 60 | 1800-1900 | 0 | 181.11 | 762.6 | 205.78 | -0.2 |
| POR2 | 84 | 2 | 15 | 60 | 1900-2000 | 0 | 182.78 | 762.4 | 207.00 | 0.3 |
| POR2 | 84 | 2 | 15 | 60 | 2000-2100 | 0 | 182.33 | 762.1 | 205.78 | -0.2 |
| POR2 | 84 | 2 | 15 | 60 | 2100-2200 | 0 | 183.11 | 761.7 | 206.00 | -0.1 |
| POR2 | 84 | 2 | 15 | 60 | 2200-2300 | 0 | 184.00 | 761.5 | 206.78 | 0.2 |
| POR2 | 84 | 2 | 15 | 60 | 2300-2400 | 0 | 183.78 | 761.4 | 206.11 | -0.1 |
| POR2 | 84 | 2 | 16 | 60 | 0000-0100 | 0 | 184.11 | 761.5 | 206.67 | 0.2 |
| POR2 | 84 | 2 | 16 | 60 | 0100-0200 | 0 | 184.11 | 761.1 | 206.00 | -0.1 |
| POR2 | 84 | 2 | 16 | 60 | 0200-0300 | 0 | 185.33 | 760.7 | 206.56 | 0.1 |
| POR2 | 84 | 2 | 16 | 60 | 0300-0400 | 0 | 185.56 | 760.2 | 205.78 | -0.2 |
| POR2 | 84 | 2 | 16 | 60 | 0400-0500 | 0 | 187.11 | 760.0 | 207.00 | 0.3 |
| POR2 | 84 | 2 | 16 | 60 | 0500-0600 | 0 | 187.00 | 759.5 | 205.78 | -0.2 |
| POR2 | 84 | 2 | 16 | 60 | 0600-0700 | 0 | 187.33 | 759.4 | 205.78 | -0.2 |
| POR2 | 84 | 2 | 16 | 5 | 0700-0705 | 0 | 187.48 | 758.9 | 204.93 | -0.7 |
| POR2 | 84 | 2 | 16 | 5 | 0705-0710 | 0 | 186.26 | 758.9 | 203.60 | -1.3 |
| POR2 | 84 | 2 | 16 | 5 | 0710-0715 | 0 | 188.35 | 758.7 | 205.47 | -0.4 |
| POR2 | 84 | 2 | 16 | 5 | 0715-0720 | 0 | 191.23 | 758.6 | 208.40 | 1.0 |
| POR2 | 84 | 2 | 16 | 5 | 0720-0725 | 0 | 187.86 | 758.5 | 204.53 | -0.9 |
| POR2 | 84 | 2 | 16 | 5 | 0725-0730 | 0 | 190.12 | 758.6 | 207.20 | 0.4 |
| POR2 | 84 | 2 | 16 | 5 | 0730-0735 | 0 | 191.29 | 758.5 | 208.27 | 1.0 |
| POR2 | 84 | 2 | 16 | 5 | 0735-0740 | 0 | 187.74 | 758.5 | 204.40 | -0.9 |
| POR2 | 84 | 2 | 16 | 5 | 0740-0745 | 0 | 190.01 | 758.4 | 206.67 | 0.2 |
| POR2 | 84 | 2 | 16 | 5 | 0745-0750 | 0 | 191.66 | 758.5 | 208.67 | 1.2 |
| POR2 | 84 | 2 | 16 | 5 | 0750-0755 | 0 | 190.68 | 758.5 | 207.60 | 0.6 |
| POR2 | 84 | 2 | 16 | 5 | 0755-0800 | 0 | 192.64 | 758.5 | 209.73 | 1.7 |
| POR2 | 84 | 2 | 16 | 5 | 0800-0805 | 0 | 187.93 | 758.4 | 204.40 | -0.9 |
| POR2 | 84 | 2 | 16 | 5 | 0805-0810 | 0 | 186.83 | 758.4 | 203.20 | -1.5 |
| POR2 | 84 | 2 | 16 | 5 | 0810-0815 | 0 | 189.52 | 758.4 | 206.13 | -0.1 |
| POR2 | 84 | 2 | 16 | 5 | 0815-0820 | 0 | 189.28 | 758.4 | 205.87 | -0.2 |
| POR2 | 84 | 2 | 16 | 5 | 0820-0825 | 0 | 189.52 | 758.4 | 206.13 | -0.1 |
| POR2 | 84 | 2 | 16 | 5 | 0825-0830 | 0 | 191.49 | 758.4 | 208.27 | 1.0 |
| POR2 | 84 | 2 | 16 | 5 | 0830-0835 | 0 | 189.78 | 758.2 | 206.00 | -0.1 |
| POR2 | 84 | 2 | 16 | 5 | 0835-0840 | 0 | 191.31 | 758.3 | 207.87 | 0.8 |
| POR2 | 84 | 2 | 16 | 5 | 0840-0845 | 0 | 190.27 | 758.2 | 206.53 | 0.1 |
| POR2 | 84 | 2 | 16 | 5 | 0845-0850 | 0 | 191.19 | 758.3 | 207.73 | 0.7 |
| POR2 | 84 | 2 | 16 | 5 | 0850-0855 | 0 | 189.66 | 758.2 | 205.87 | -0.2 |
| POR2 | 84 | 2 | 16 | 5 | 0855-0900 | 0 | 191.13 | 758.2 | 207.47 | 0.6 |
| POR2 | 84 | 2 | 16 | 5 | 0900-0905 | 0 | 191.75 | 758.2 | 208.13 | 0.9 |
| POR2 | 84 | 2 | 16 | 5 | 0905-0910 | 0 | 200.67 | 758.1 | 217.60 | 5.5 |
| POR2 | 84 | 2 | 16 | 5 | 0910-0915 | 0 | 211.33 | 758.0 | 228.93 | 11.0 |
| POR2 | 84 | 2 | 16 | 5 | 0915-0920 | 0 | 211.30 | 757.9 | 228.67 | 10.8 |
| POR2 | 84 | 2 | 16 | 5 | 0920-0925 | 0 | 207.60 | 757.9 | 224.67 | 8.9 |
| POR2 | 84 | 2 | 16 | 5 | 0925-0930 | 0 | 202.79 | 757.9 | 219.47 | 6.4 |
| POR2 | 84 | 2 | 16 | 5 | 0930-0935 | 0 | 202.71 | 757.7 | 218.93 | 6.1 |
| POR2 | 84 | 2 | 16 | 5 | 0935-0940 | 0 | 201.84 | 757.7 | 218.00 | 5.7 |
| POR2 | 84 | 2 | 16 | 5 | 0940-0945 | 0 | 203.45 | 757.7 | 219.73 | 6.5 |

Table 3. Cont.

| STATION | YY | MM | DD | MIN | TIME SPAN (UT) | DATA CODE | UNCOR. (CPS) | PRES. (MMHG) | COR. (CPS) | % INC. |
|---|---|---|---|---|---|---|---|---|---|---|
| POR2 | 84 | 2 | 16 | 5 | 0945-0950 | 0 | 201.15 | 757.8 | 217.47 | 5.4 |
| POR2 | 84 | 2 | 16 | 5 | 0950-0955 | 0 | 197.74 | 757.9 | 214.00 | 3.7 |
| POR2 | 84 | 2 | 16 | 5 | 0955-1000 | 0 | 198.11 | 757.9 | 214.40 | 3.9 |
| POR2 | 84 | 2 | 16 | 5 | 1000-1005 | 0 | 194.54 | 757.9 | 210.53 | 2.1 |
| POR2 | 84 | 2 | 16 | 5 | 1005-1010 | 0 | 196.93 | 758.0 | 213.33 | 3.4 |
| POR2 | 84 | 2 | 16 | 5 | 1010-1015 | 0 | 194.64 | 758.1 | 211.07 | 2.3 |
| POR2 | 84 | 2 | 16 | 5 | 1015-1020 | 0 | 194.22 | 758.0 | 210.40 | 2.0 |
| POR2 | 84 | 2 | 16 | 5 | 1020-1025 | 0 | 194.03 | 758.1 | 210.40 | 2.0 |
| POR2 | 84 | 2 | 16 | 5 | 1025-1030 | 0 | 194.42 | 757.9 | 210.40 | 2.0 |
| POR2 | 84 | 2 | 16 | 5 | 1030-1035 | 0 | 194.54 | 757.9 | 210.53 | 2.1 |
| POR2 | 84 | 2 | 16 | 5 | 1035-1040 | 0 | 192.71 | 757.7 | 208.13 | 0.9 |
| POR2 | 84 | 2 | 16 | 5 | 1040-1045 | 0 | 195.37 | 757.6 | 210.80 | 2.2 |
| POR2 | 84 | 2 | 16 | 5 | 1045-1050 | 0 | 195.07 | 757.5 | 210.27 | 1.9 |
| POR2 | 84 | 2 | 16 | 5 | 1050-1055 | 0 | 197.37 | 757.4 | 212.53 | 3.0 |
| POR2 | 84 | 2 | 16 | 5 | 1055-1100 | 0 | 196.21 | 757.3 | 211.07 | 2.3 |
| POR2 | 84 | 2 | 16 | 5 | 1100-1105 | 0 | 195.00 | 756.9 | 208.93 | 1.3 |
| POR2 | 84 | 2 | 16 | 5 | 1105-1110 | 0 | 195.25 | 756.9 | 209.20 | 1.4 |
| POR2 | 84 | 2 | 16 | 5 | 1110-1115 | 0 | 195.25 | 756.9 | 209.20 | 1.4 |
| POR2 | 84 | 2 | 16 | 5 | 1115-1120 | 0 | 196.57 | 756.8 | 210.40 | 2.0 |
| POR2 | 84 | 2 | 16 | 5 | 1120-1125 | 0 | 194.52 | 756.7 | 208.00 | 0.8 |
| POR2 | 84 | 2 | 16 | 5 | 1125-1130 | 0 | 196.03 | 756.5 | 209.20 | 1.4 |
| POR2 | 84 | 2 | 16 | 5 | 1130-1135 | 0 | 196.28 | 756.5 | 209.47 | 1.5 |
| POR2 | 84 | 2 | 16 | 5 | 1135-1140 | 0 | 195.42 | 756.3 | 208.13 | 0.9 |
| POR2 | 84 | 2 | 16 | 5 | 1140-1145 | 0 | 197.80 | 756.3 | 210.67 | 2.1 |
| POR2 | 84 | 2 | 16 | 5 | 1145-1150 | 0 | 197.18 | 756.3 | 210.00 | 1.8 |
| POR2 | 84 | 2 | 16 | 5 | 1150-1155 | 0 | 196.05 | 756.3 | 208.80 | 1.2 |
| POR2 | 84 | 2 | 16 | 5 | 1155-1200 | 0 | 195.55 | 756.3 | 208.27 | 1.0 |
| POR2 | 84 | 2 | 16 | 60 | 1200-1300 | 0 | 197.00 | 756.0 | 209.22 | 1.4 |
| POR2 | 84 | 2 | 16 | 60 | 1300-1400 | 0 | 196.11 | 755.7 | 207.56 | 0.6 |
| POR2 | 84 | 2 | 16 | 60 | 1400-1500 | 0 | 199.11 | 755.0 | 209.33 | 1.5 |
| POR2 | 84 | 2 | 16 | 60 | 1500-1600 | 0 | 199.78 | 754.5 | 209.00 | 1.3 |
| POR2 | 84 | 2 | 16 | 60 | 1600-1700 | 0 | 198.56 | 754.3 | 207.22 | 0.5 |
| POR2 | 84 | 2 | 16 | 60 | 1700-1800 | 0 | 198.00 | 753.9 | 206.00 | -0.1 |
| POR2 | 84 | 2 | 16 | 60 | 1800-1900 | 0 | 201.33 | 752.5 | 206.33 | 0.0 |
| POR2 | 84 | 2 | 16 | 60 | 1900-2000 | 0 | 202.44 | 751.8 | 206.22 | 0.0 |
| POR2 | 84 | 2 | 16 | 60 | 2000-2100 | 0 | 203.44 | 750.9 | 205.44 | -0.4 |
| POR2 | 84 | 2 | 16 | 60 | 2100-2200 | 0 | 208.00 | 748.9 | 205.67 | -0.3 |
| POR2 | 84 | 2 | 16 | 60 | 2200-2300 | 0 | 210.11 | 747.9 | 205.56 | -0.4 |
| POR2 | 84 | 2 | 16 | 60 | 2300-2400 | 0 | 210.67 | 747.7 | 205.78 | -0.2 |

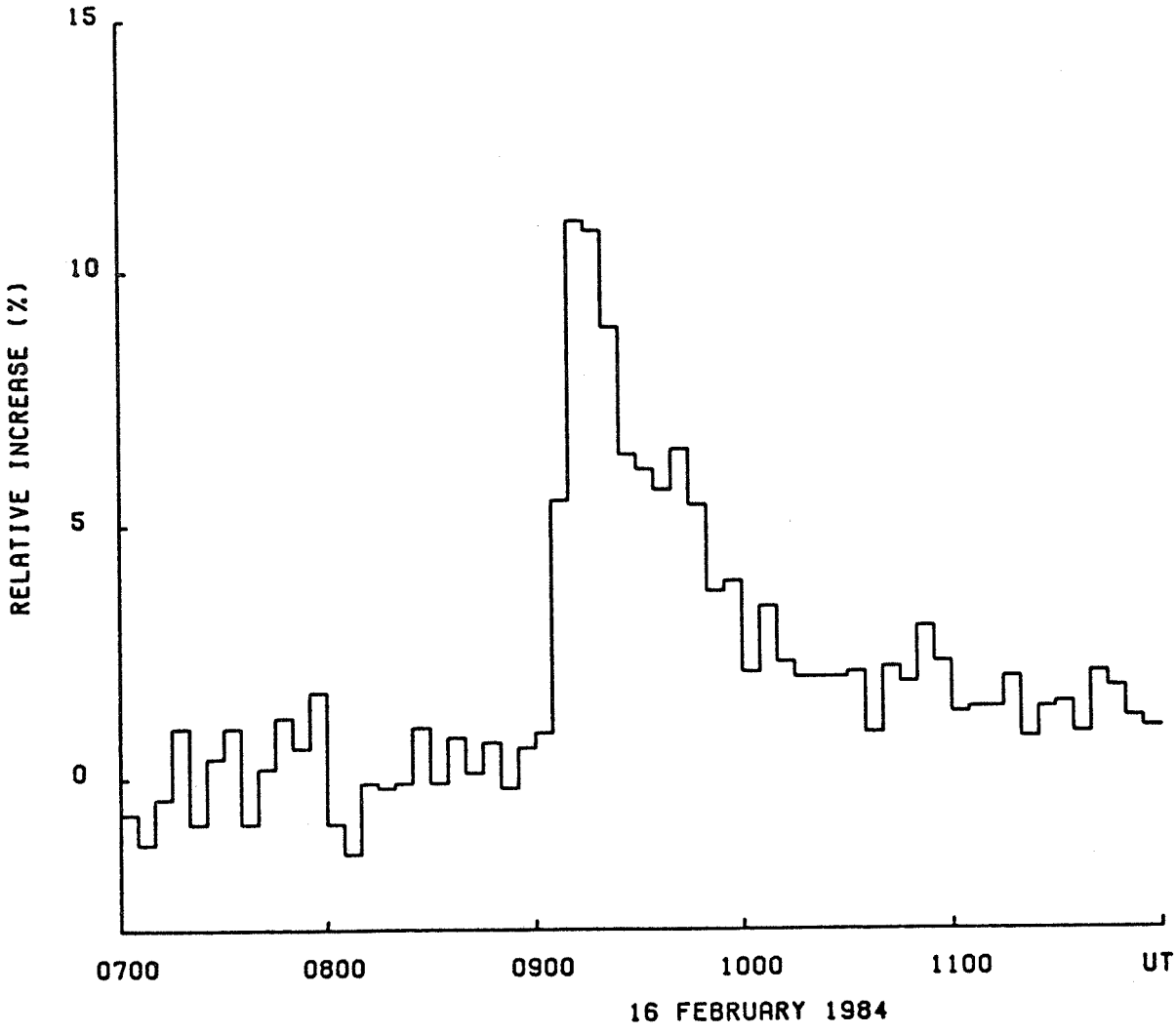


Figure 2. Relative increase of the pressure corrected cosmic ray intensity recorded by the Kerguelen neutron monitor for the 16 February 1984 ground-level event.

Table 4. Data of the neutron monitor Terre Adelie for the time period 15 February 1984, 0000 UT to 16 February 1984, 2400 UT

| STATION | YY | MM | DD | MIN | TIME SPAN (UT) | DATA CODE | UNCOR. (CPS) | PRES. (MMHG) | COR. (CPS) | % INC. |
|---|---|---|---|---|---|---|---|---|---|---|
| DUM2 | 84 | 2 | 15 | 60 | 0000-0100 | 0 | 104.33 | 745.2 | 109.83 | -0.7 |
| DUM2 | 84 | 2 | 15 | 60 | 0100-0200 | 0 | 103.94 | 745.2 | 109.39 | -1.1 |
| DUM2 | 84 | 2 | 15 | 60 | 0200-0300 | 0 | 104.33 | 745.1 | 109.67 | -0.8 |
| DUM2 | 84 | 2 | 15 | 60 | 0300-0400 | 0 | 104.89 | 744.9 | 109.89 | -0.6 |
| DUM2 | 84 | 2 | 15 | 60 | 0400-0500 | 0 | 104.83 | 744.8 | 109.83 | -0.7 |
| DUM2 | 84 | 2 | 15 | 60 | 0500-0600 | 0 | 105.28 | 744.8 | 110.28 | -0.3 |
| DUM2 | 84 | 2 | 15 | 60 | 0600-0700 | 0 | 105.72 | 744.9 | 110.78 | 0.2 |
| DUM2 | 84 | 2 | 15 | 60 | 0700-0800 | 0 | 104.83 | 745.0 | 110.00 | -0.5 |
| DUM2 | 84 | 2 | 15 | 60 | 0800-0900 | 0 | 105.06 | 744.8 | 110.06 | -0.5 |
| DUM2 | 84 | 2 | 15 | 60 | 0900-1000 | 0 | 104.78 | 744.8 | 109.78 | -0.7 |
| DUM2 | 84 | 2 | 15 | 60 | 1000-1100 | 0 | 105.06 | 744.8 | 110.11 | -0.4 |
| DUM2 | 84 | 2 | 15 | 60 | 1100-1200 | 0 | 105.11 | 744.7 | 109.94 | -0.6 |
| DUM2 | 84 | 2 | 15 | 60 | 1200-1300 | 0 | 105.00 | 744.5 | 109.67 | -0.8 |
| DUM2 | 84 | 2 | 15 | 60 | 1300-1400 | 0 | 105.33 | 744.2 | 109.61 | -0.9 |
| DUM2 | 84 | 2 | 15 | 60 | 1400-1500 | 0 | 106.00 | 743.6 | 109.78 | -0.7 |
| DUM2 | 84 | 2 | 15 | 60 | 1500-1600 | 0 | 106.72 | 743.2 | 110.11 | -0.4 |
| DUM2 | 84 | 2 | 15 | 60 | 1600-1700 | 0 | 106.83 | 742.4 | 109.22 | -1.2 |
| DUM2 | 84 | 2 | 15 | 60 | 1700-1800 | 0 | 106.94 | 742.3 | 109.28 | -1.2 |
| DUM2 | 84 | 2 | 15 | 60 | 1800-1900 | 0 | 107.83 | 741.7 | 109.50 | -1.0 |
| DUM2 | 84 | 2 | 15 | 60 | 1900-2000 | 0 | 108.50 | 741.0 | 109.39 | -1.1 |
| DUM2 | 84 | 2 | 15 | 60 | 2000-2100 | 0 | 109.11 | 740.4 | 109.44 | -1.0 |
| DUM2 | 84 | 2 | 15 | 60 | 2100-2200 | 0 | 109.56 | 739.9 | 109.39 | -1.1 |
| DUM2 | 84 | 2 | 15 | 60 | 2200-2300 | 0 | 110.00 | 739.6 | 109.50 | -1.0 |
| DUM2 | 84 | 2 | 15 | 60 | 2300-2400 | 0 | 110.56 | 739.2 | 109.56 | -0.9 |
| DUM2 | 84 | 2 | 16 | 60 | 0000-0100 | 0 | 111.89 | 738.7 | 110.39 | -0.2 |
| DUM2 | 84 | 2 | 16 | 60 | 0100-0200 | 0 | 111.28 | 738.6 | 109.61 | -0.9 |
| DUM2 | 84 | 2 | 16 | 60 | 0200-0300 | 0 | 112.17 | 738.6 | 110.39 | -0.2 |
| DUM2 | 84 | 2 | 16 | 60 | 0300-0400 | 0 | 112.50 | 738.3 | 110.56 | 0.0 |
| DUM2 | 84 | 2 | 16 | 60 | 0400-0500 | 0 | 112.50 | 738.1 | 110.28 | -0.3 |
| DUM2 | 84 | 2 | 16 | 60 | 0500-0600 | 0 | 112.39 | 738.1 | 110.22 | -0.3 |
| DUM2 | 84 | 2 | 16 | 60 | 0600-0700 | 0 | 112.89 | 738.1 | 110.67 | 0.1 |
| DUM2 | 84 | 2 | 16 | 5 | 0700-0705 | 0 | 114.49 | 737.9 | 112.13 | 1.4 |
| DUM2 | 84 | 2 | 16 | 5 | 0705-0710 | 0 | 112.83 | 738.1 | 110.73 | 0.1 |
| DUM2 | 84 | 2 | 16 | 5 | 0710-0715 | 0 | 112.06 | 738.0 | 109.87 | -0.7 |
| DUM2 | 84 | 2 | 16 | 5 | 0715-0720 | 0 | 111.86 | 738.0 | 109.67 | -0.8 |
| DUM2 | 84 | 2 | 16 | 5 | 0720-0725 | 0 | 111.88 | 738.1 | 109.80 | -0.7 |
| DUM2 | 84 | 2 | 16 | 5 | 0725-0730 | 0 | 113.40 | 738.2 | 111.40 | 0.7 |
| DUM2 | 84 | 2 | 16 | 5 | 0730-0735 | 0 | 112.00 | 738.3 | 110.13 | -0.4 |
| DUM2 | 84 | 2 | 16 | 5 | 0735-0740 | 0 | 113.15 | 738.3 | 111.27 | 0.6 |
| DUM2 | 84 | 2 | 16 | 5 | 0740-0745 | 0 | 110.96 | 738.2 | 109.00 | -1.4 |
| DUM2 | 84 | 2 | 16 | 5 | 0745-0750 | 0 | 111.91 | 738.2 | 109.93 | -0.6 |
| DUM2 | 84 | 2 | 16 | 5 | 0750-0755 | 0 | 112.81 | 738.3 | 110.93 | 0.3 |
| DUM2 | 84 | 2 | 16 | 5 | 0755-0800 | 0 | 111.39 | 738.3 | 109.53 | -1.0 |
| DUM2 | 84 | 2 | 16 | 5 | 0800-0805 | 0 | 112.00 | 738.3 | 110.13 | -0.4 |
| DUM2 | 84 | 2 | 16 | 5 | 0805-0810 | 0 | 112.68 | 738.3 | 110.80 | 0.2 |
| DUM2 | 84 | 2 | 16 | 5 | 0810-0815 | 0 | 113.76 | 738.3 | 111.87 | 1.2 |
| DUM2 | 84 | 2 | 16 | 5 | 0815-0820 | 0 | 114.92 | 738.3 | 113.00 | 2.2 |
| DUM2 | 84 | 2 | 16 | 5 | 0820-0825 | 0 | 111.05 | 738.3 | 109.20 | -1.3 |
| DUM2 | 84 | 2 | 16 | 5 | 0825-0830 | 0 | 111.91 | 738.2 | 109.93 | -0.6 |
| DUM2 | 84 | 2 | 16 | 5 | 0830-0835 | 0 | 112.00 | 738.3 | 110.13 | -0.4 |
| DUM2 | 84 | 2 | 16 | 5 | 0835-0840 | 0 | 111.87 | 738.3 | 110.00 | -0.5 |
| DUM2 | 84 | 2 | 16 | 5 | 0840-0845 | 0 | 113.02 | 738.3 | 111.13 | 0.5 |
| DUM2 | 84 | 2 | 16 | 5 | 0845-0850 | 0 | 112.23 | 738.4 | 110.47 | -0.1 |
| DUM2 | 84 | 2 | 16 | 5 | 0850-0855 | 0 | 111.26 | 738.3 | 109.40 | -1.1 |
| DUM2 | 84 | 2 | 16 | 5 | 0855-0900 | 0 | 112.84 | 738.4 | 111.07 | 0.4 |
| DUM2 | 84 | 2 | 16 | 5 | 0900-0905 | 0 | 111.19 | 738.3 | 109.33 | -1.1 |
| DUM2 | 84 | 2 | 16 | 5 | 0905-0910 | 0 | 113.58 | 738.4 | 111.80 | 1.1 |
| DUM2 | 84 | 2 | 16 | 5 | 0910-0915 | 0 | 117.99 | 738.4 | 116.13 | 5.0 |
| DUM2 | 84 | 2 | 16 | 5 | 0915-0920 | 0 | 119.07 | 738.4 | 117.20 | 6.0 |
| DUM2 | 84 | 2 | 16 | 5 | 0920-0925 | 0 | 119.56 | 738.5 | 117.80 | 6.5 |
| DUM2 | 84 | 2 | 16 | 5 | 0925-0930 | 0 | 117.44 | 738.4 | 115.60 | 4.5 |
| DUM2 | 84 | 2 | 16 | 5 | 0930-0935 | 0 | 118.61 | 738.5 | 116.87 | 5.7 |
| DUM2 | 84 | 2 | 16 | 5 | 0935-0940 | 0 | 118.95 | 738.5 | 117.20 | 6.0 |

Table 4. Cont.

| STATION | YY | MM | DD | MIN | TIME SPAN (UT) | DATA CODE | UNCOR. (CPS) | PRES. (MMHG) | COR. (CPS) | % INC. |
|---|---|---|---|---|---|---|---|---|---|---|
| DUM2 | 84 | 2 | 16 | 5 | 0940-0945 | 0 | 117.28 | 738.6 | 115.67 | 4.6 |
| DUM2 | 84 | 2 | 16 | 5 | 0945-0950 | 0 | 116.54 | 738.6 | 114.93 | 3.9 |
| DUM2 | 84 | 2 | 16 | 5 | 0950-0955 | 0 | 116.13 | 738.6 | 114.53 | 3.6 |
| DUM2 | 84 | 2 | 16 | 5 | 0955-1000 | 0 | 115.41 | 738.7 | 113.93 | 3.0 |
| DUM2 | 84 | 2 | 16 | 5 | 1000-1005 | 0 | 116.58 | 738.8 | 115.20 | 4.2 |
| DUM2 | 84 | 2 | 16 | 5 | 1005-1010 | 0 | 114.55 | 738.8 | 113.20 | 2.4 |
| DUM2 | 84 | 2 | 16 | 5 | 1010-1015 | 0 | 114.37 | 738.9 | 113.13 | 2.3 |
| DUM2 | 84 | 2 | 16 | 5 | 1015-1020 | 0 | 116.33 | 738.9 | 115.07 | 4.0 |
| DUM2 | 84 | 2 | 16 | 5 | 1020-1025 | 0 | 115.74 | 739.0 | 114.60 | 3.6 |
| DUM2 | 84 | 2 | 16 | 5 | 1025-1030 | 0 | 114.77 | 738.9 | 113.53 | 2.7 |
| DUM2 | 84 | 2 | 16 | 5 | 1030-1035 | 0 | 114.10 | 738.9 | 112.87 | 2.1 |
| DUM2 | 84 | 2 | 16 | 5 | 1035-1040 | 0 | 114.91 | 738.9 | 113.67 | 2.8 |
| DUM2 | 84 | 2 | 16 | 5 | 1040-1045 | 0 | 114.84 | 738.9 | 113.60 | 2.7 |
| DUM2 | 84 | 2 | 16 | 5 | 1045-1050 | 0 | 113.36 | 738.9 | 112.13 | 1.4 |
| DUM2 | 84 | 2 | 16 | 5 | 1050-1055 | 0 | 111.63 | 739.0 | 110.53 | -0.1 |
| DUM2 | 84 | 2 | 16 | 5 | 1055-1100 | 0 | 114.82 | 738.8 | 113.47 | 2.6 |
| DUM2 | 84 | 2 | 16 | 5 | 1100-1105 | 0 | 113.61 | 739.1 | 112.60 | 1.8 |
| DUM2 | 84 | 2 | 16 | 5 | 1105-1110 | 0 | 113.54 | 739.1 | 112.53 | 1.8 |
| DUM2 | 84 | 2 | 16 | 5 | 1110-1115 | 0 | 113.74 | 739.1 | 112.73 | 1.9 |
| DUM2 | 84 | 2 | 16 | 5 | 1115-1120 | 0 | 112.28 | 739.2 | 111.40 | 0.7 |
| DUM2 | 84 | 2 | 16 | 5 | 1120-1125 | 0 | 112.22 | 739.2 | 111.33 | 0.7 |
| DUM2 | 84 | 2 | 16 | 5 | 1125-1130 | 0 | 112.69 | 739.2 | 111.80 | 1.1 |
| DUM2 | 84 | 2 | 16 | 5 | 1130-1135 | 0 | 112.60 | 739.1 | 111.60 | 0.9 |
| DUM2 | 84 | 2 | 16 | 5 | 1135-1140 | 0 | 112.40 | 739.1 | 111.40 | 0.7 |
| DUM2 | 84 | 2 | 16 | 5 | 1140-1145 | 0 | 112.80 | 739.1 | 111.80 | 1.1 |
| DUM2 | 84 | 2 | 16 | 5 | 1145-1150 | 0 | 111.66 | 739.1 | 110.67 | 0.1 |
| DUM2 | 84 | 2 | 16 | 5 | 1150-1155 | 0 | 113.27 | 739.1 | 112.27 | 1.5 |
| DUM2 | 84 | 2 | 16 | 5 | 1155-1200 | 0 | 113.34 | 739.1 | 112.33 | 1.6 |
| DUM2 | 84 | 2 | 16 | 60 | 1200-1300 | 0 | 112.44 | 739.0 | 111.22 | 0.6 |
| DUM2 | 84 | 2 | 16 | 60 | 1300-1400 | 0 | 111.94 | 739.1 | 110.83 | 0.2 |
| DUM2 | 84 | 2 | 16 | 60 | 1400-1500 | 0 | 112.22 | 739.1 | 111.11 | 0.5 |
| DUM2 | 84 | 2 | 16 | 60 | 1500-1600 | 0 | 111.11 | 739.3 | 110.28 | -0.3 |
| DUM2 | 84 | 2 | 16 | 60 | 1600-1700 | 0 | 111.28 | 739.2 | 110.39 | -0.2 |
| DUM2 | 84 | 2 | 16 | 60 | 1700-1800 | 0 | 110.94 | 739.3 | 110.11 | -0.4 |
| DUM2 | 84 | 2 | 16 | 60 | 1800-1900 | 0 | 110.89 | 739.6 | 110.33 | -0.2 |
| DUM2 | 84 | 2 | 16 | 60 | 1900-2000 | 0 | 111.06 | 739.8 | 110.72 | 0.1 |
| DUM2 | 84 | 2 | 16 | 60 | 2000-2100 | 0 | 110.17 | 740.1 | 110.28 | -0.3 |
| DUM2 | 84 | 2 | 16 | 60 | 2100-2200 | 0 | 110.22 | 740.5 | 110.61 | 0.0 |
| DUM2 | 84 | 2 | 16 | 60 | 2200-2300 | 0 | 109.56 | 740.5 | 110.06 | -0.5 |
| DUM2 | 84 | 2 | 16 | 60 | 2300-2400 | 0 | 110.22 | 740.7 | 110.94 | 0.3 |

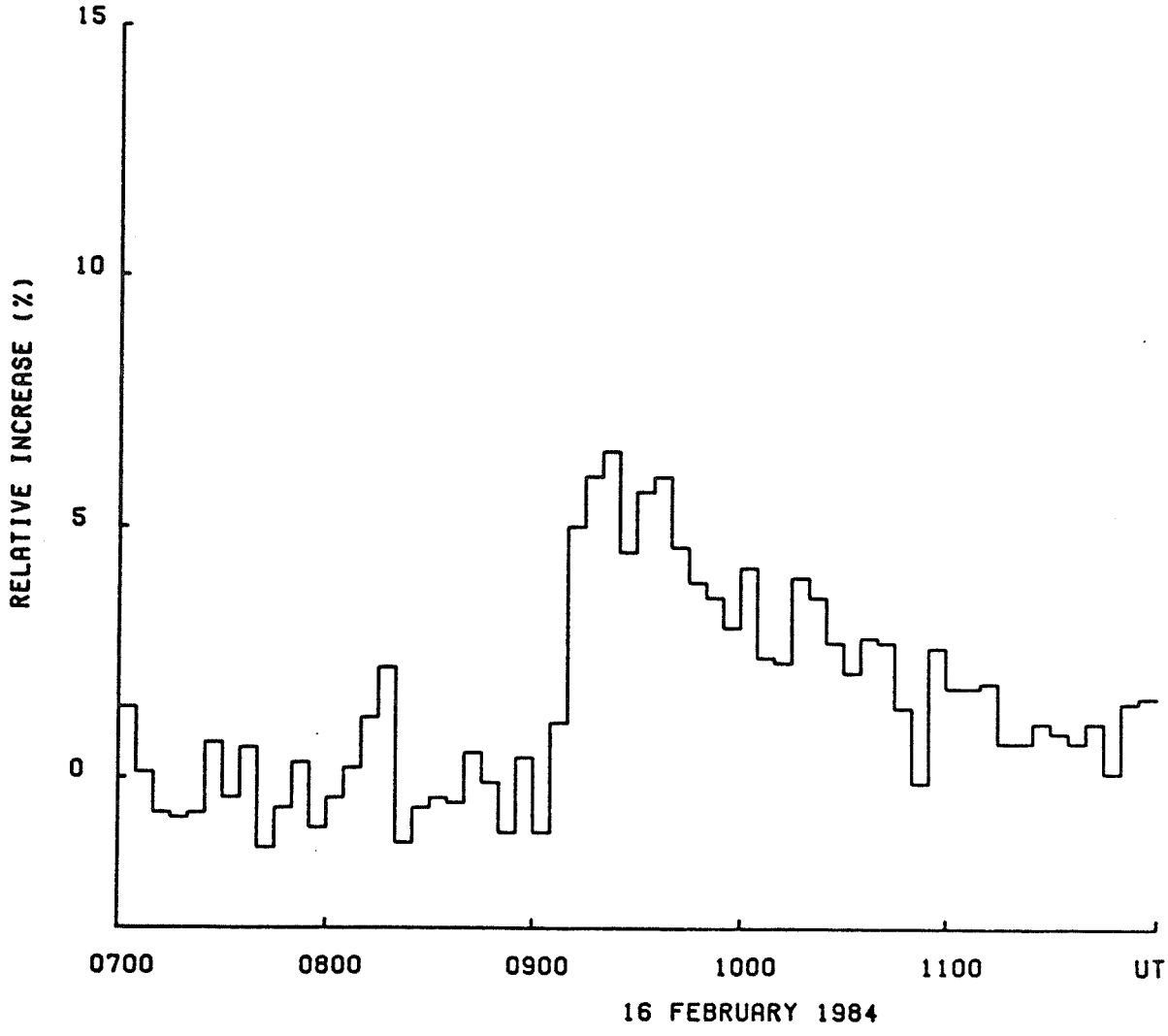


Figure 3. Relative increase of the pressure corrected cosmic ray intensity recorded by the Terre Adelie neutron monitor for the 16 February 1984 ground-level event.

# Solar Cosmic Ray Flare on 16 February 1984 Recorded by the Siberian and Far East Neutron Monitor Stations

by

N.P. Chirkov, A.T. Filippov and A.M. Novikov
Institute of Cosmophysical Research and Aeronomy, Yakutsk Branch
Siberian Department of the USSR Academy of Sciences, Yakutsk, USSR

and

A.V. Sergeev
Siberian Institute of Terrestrial Magnetism, Ionosphere and Radio Wave Propagation, Siberian Department of the USSR Academy of Sciences, Irkutsk, USSR

and

V.K. Korotkov
Northeast Complex Research Institute
Far East Scientific Center of the USSR Academy of Sciences
Magadan, USSR

and

V.L. Yanchukovsky
Institute of Geology and Geophysics
Siberian Department of the USSR Academy of Sciences
Novosibirsk, USSR

On 16 February 1984 the Siberian network of neutron supermonitor stations recorded the solar cosmic ray flare. The geographical coordinates and energy characteristics of the stations are given in Table 1. Statistical errors of apparatus measurements in an hour regime are also given

Table 1. Siberian Network of Neutron Supermonitor Stations

| Station Name | Rigidity (GV) | Geographic Coordinates Lat | Long | Sigma (Percent) |
|---|---|---|---|---|
| Tixie Bay | 0.52 | N71.6 | E129.0 | 0.17 |
| Magadan | 2.16 | 62.0 | 151.0 | 0.14 |
| Novosibirsk | 2.85 | 54.8 | 83.0 | 0.25 |
| Irkutsk | 3.74 | 52.5 | 104.0 | 0.18 |

The 5-minute data for the period 0700-1300 UT on 16 February 1984 for the stations are given in the following tables.

**Tixie Bay Station**
Neutron Supermonitor 12 NM 64
5-min data corrected for barometric effect
Count in impulses; scaling factor 100
**16 February 1984**

| Minutes | 05 | 10 | 15 | 20 | 25 | 30 | 35 | 40 | 45 | 50 | 55 | 60 |
|---|---|---|---|---|---|---|---|---|---|---|---|---|
| Hour (UT) | | | | | | | | | | | | |
| 0700-0800 | 264 | 265 | 266 | 269 | 267 | 263 | 264 | 270 | 267 | 266 | 268 | 267 |
| 0800-0900 | 264 | 265 | 265 | 271 | 267 | 268 | 270 | 265 | 268 | 271 | 271 | 263 |
| 0900-1000 | 268 | 264 | 267 | 269 | 269 | 272 | 266 | 275 | 269 | 275 | 276 | 280 |
| 1000-1100 | 275 | 272 | 270 | 272 | 275 | 274 | 270 | 269 | 271 | 265 | 267 | 276 |
| 1100-1200 | 272 | 268 | 271 | 271 | 269 | 268 | 267 | 268 | 270 | --- | 271 | 268 |
| 1200-1300 | 268 | 268 | 266 | 270 | 272 | 271 | 264 | 267 | 272 | 272 | 268 | 269 |

**Irkutsk Station**
Neutron Supermonitor 18 NM 64
5-min data corrected for barometric effect
Count in impulses; scaling coefficient 100
**16 February 1984**

| Minutes | 05 | 10 | 15 | 20 | 25 | 30 | 35 | 40 | 45 | 50 | 55 | 60 |
|---|---|---|---|---|---|---|---|---|---|---|---|---|
| Hour (UT) | | | | | | | | | | | | |
| 0700-0800 | 771 | 774 | 771 | 766 | 778 | 778 | 770 | 773 | 770 | 785 | 786 | 782 |
| 0800-0900 | 781 | 781 | 776 | 785 | 786 | 774 | 786 | 796 | 774 | 770 | 780 | 782 |
| 0900-1000 | 767 | 789 | 808 | 807 | 793 | 791 | 793 | 793 | 780 | 795 | 775 | 780 |
| 1000-1100 | 784 | 788 | 787 | 775 | 780 | 771 | 773 | 777 | 777 | 771 | 767 | 775 |
| 1100-1200 | 775 | 772 | 766 | 771 | 768 | 780 | 783 | 775 | 777 | 774 | 779 | 774 |
| 1200-1300 | 769 | 786 | 770 | 776 | 772 | 774 | 769 | 769 | 772 | 781 | 776 | 779 |

**Novosibirsk Station**
Neutron Supermonitor 18 NM 64
5-min data corrected for barometric effect
Count in impulses; scaling coefficient 128
**16 February 1984**

| Minutes | 05 | 10 | 15 | 20 | 25 | 30 | 35 | 40 | 45 | 50 | 55 | 60 |
|---|---|---|---|---|---|---|---|---|---|---|---|---|
| Hour (UT) | | | | | | | | | | | | |
| 0700-0800 | 173 | 171 | 175 | 174 | 178 | 175 | 172 | 184 | 178 | 176 | 175 | 176 |
| 0800-0900 | 177 | 173 | 178 | 175 | 180 | 175 | 179 | 176 | 174 | 175 | 177 | 175 |
| 0900-1000 | 181 | 179 | 183 | 188 | 184 | 179 | 178 | 178 | 178 | 180 | 180 | 179 |
| 1000-1100 | 178 | 177 | 178 | 180 | 175 | 179 | 178 | 179 | 177 | 178 | 178 | 177 |
| 1100-1200 | 175 | 175 | 176 | 175 | 177 | 174 | 179 | 183 | 178 | 176 | 173 | 175 |
| 1200-1300 | 174 | 179 | 174 | 175 | 173 | 174 | 176 | 177 | 180 | 181 | 174 | 183 |

**Magadan Station**
Neutron Supermonitor 18 NM 64
5-min data corrected for barometric effect
Count in impulses; scaling coefficient 64
**16 February 1984**

| Minutes | 05 | 10 | 15 | 20 | 25 | 30 | 35 | 40 | 45 | 50 | 55 | 60 |
|---|---|---|---|---|---|---|---|---|---|---|---|---|
| Hour (UT) | | | | | | | | | | | | |
| 0700-0800 | 645 | 642 | 650 | 646 | 637 | 650 | 649 | 645 | 649 | 647 | 642 | 641 |
| 0800-0900 | 638 | 651 | 646 | 648 | 644 | 646 | 646 | 643 | 642 | 641 | 647 | 643 |
| 0900-1000 | 641 | 687 | 717 | 725 | 704 | 694 | 691 | 688 | 674 | 668 | 665 | 669 |
| 1000-1100 | 661 | 661 | 662 | 661 | 654 | 660 | 659 | 663 | 657 | 658 | 659 | 644 |
| 1100-1200 | 649 | 649 | 652 | 647 | 643 | 655 | 647 | 651 | 651 | 654 | 649 | 651 |
| 1200-1300 | 649 | 654 | 645 | 651 | 642 | 650 | 654 | 655 | 654 | 646 | 644 | 647 |

# The 16 February 1984 Event Registered By The Rome Neutron Monitor

by

N. Iucci and M. Parisi
Dipartimento di Fisica, Universita "La Sapienza"
Piazzale A. Moro, 2, 00185 Roma, Italy

and

C. Signorini, M. Storini, G. Villoresi, and N.L. Zangrilli
Istituto di Fisica dello Spazio Interplanetario del C.N.R.
Reparto Raggi Cosmici, Dipartimento de Fisica
Universita "La Sapienza"
Piazzale A. Moro, 2, 00185 Roma, Italy

The 16 February 1984 cosmic ray increase observed at the high-latitude neutron monitor stations (see for instance SGD, 1984a) is probably due to the arrival at the Earth of relativistic solar cosmic rays originating on the invisible hemisphere of the Sun (about W95 (SGD, 1984b)); a type-IV radio emission is observed (SGD, 1984c; Solnechnye Dannye, 1984) to begin at about 0900 UT.

The Rome neutron monitor station is located at sea level at N41.9 E12.5. Generally, the Rome data are not affected by solar cosmic rays because it has the threshold rigidity of 6.32 GV. But there are some exceptions, as with 7 May 1978 event (Shea et al., 1979).

The data for the February 1984 event are shown in Figure 1. In panel (a) the hourly values for 15-17 February are plotted in percent of the daily average counting rate of 15 February. In panel (b) the 10-minute data for the interval 0705-1155 UT on 16 February are plotted in percent of the intensity recorded in the 0700-0800 UT time interval. The data are pressure corrected to 762.3 mm Hg (mean pressure in the interval 0905-0915 UT of 16 February).

The hourly pressure-corrected data of the Rome neutron monitor and barometric pressure for the year 1984 are given in Iucci et al., 1985 together with the daily section ratios. The 5-minute data for the time interval 0700-1200 UT of 16 February are reported here in Tables I and II.

For this event there is not a clear evidence of flare particle contribution to the Rome 12-NM-64 counting-rate at any time scale. The amplitude of the maximum increase, observed between 0905 UT and 0915 UT, is about three standard deviations.

**Acknowledgements**

We are indebted to our electronic staff (F. Re and F. Signoretti) for their careful work.

## REFERENCES

| | | |
|---|---|---|
| IUCCI, N., et al. | 1985 | **IFSI Report-85-13**, Frascati, Italy. |
| SGD | 1984a | **Solar Geophysical Data**, 476 Part I, April 1984, U.S. Department of Commerce (Boulder, CO, USA 80303), 102-105. |
| SGD | 1984b | **Solar Geophysical Data**, 476 Part II, April 1984, U.S. Department of Commerce (Boulder, CO, USA 80303), 118. |
| SGD | 1984c | **Solar Geophysical Data**, 476 Part I, April 1984, U.S. Department of Commerce (Boulder, CO, USA 80303), 99. |
| SHEA, M.A., et al. | 1979 | **16th Int. Cosmic Ray Conference**, 5, 226, Kyoto, Japan. |
| SOLNECHNYE DANNYE | 1984 | **Solnechnye Dannye, No. 2**, 70, USSR Academy of Sciences, Leningrad, USSR. |

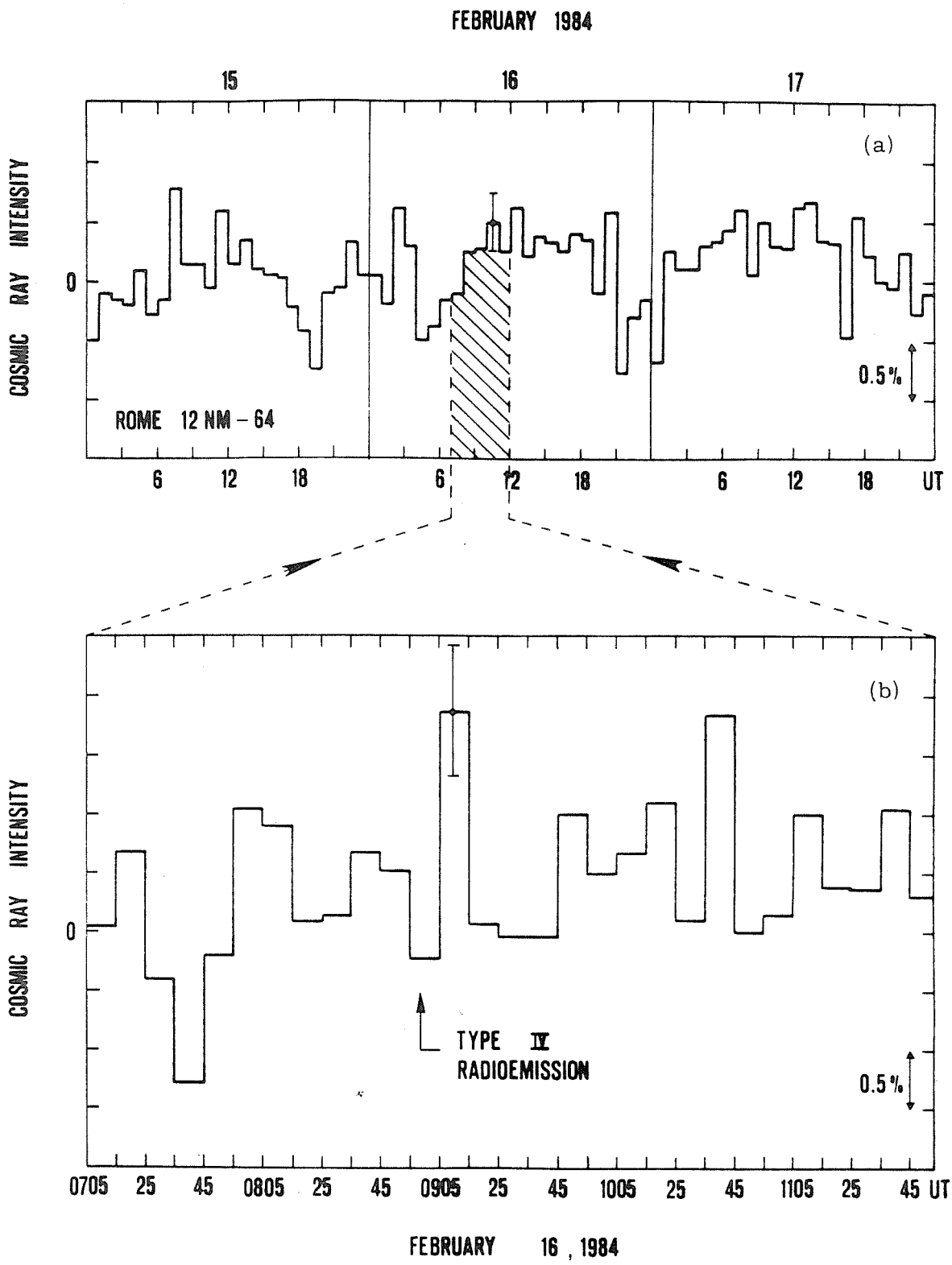


Fig. 1. Data for the February 1984 cosmic ray event:
(a) hourly values for 15-17 February plotted in percent of the daily average counting rate of 15 February;
(b) 10-minute data for the interval 0705-1155 UT on 16 February plotted in percent of the intensity recorded in the 0700-0800 UT time interval. Data are pressure corrected to 762.3 mm Hg.

TABLE I: Rome 5-minute pressure corrected data to 762.3 mmHg ( pressure coefficient = 0.94%/mmHg ); scaling factor = 10.

February 16, 1984

| UT | 00-05 | 05-10 | 10-15 | 15-20 | 20-25 | 25-30 | 30-35 | 35-40 | 40-45 | 45-50 | 50-55 | 55-60 |
|---|---|---|---|---|---|---|---|---|---|---|---|---|
| 07-08 | 3090 | 3079 | 3076 | 3108 | 3085 | 3104 | 3023 | 3014 | 3060 | 3074 | 3065 | 3134 |
| 08-09 | 3083 | 3085 | 3122 | 3036 | 3123 | 3083 | 3079 | 3085 | 3108 | 3087 | 3097 | 3069 |
| 09-10 | 3069 | 3136 | 3131 | 3084 | 3072 | 3063 | 3087 | 3055 | 3095 | 3099 | 3114 | 3091 |
| 10-11 | 3092 | 3115 | 3079 | 3106 | 3113 | 3077 | 3081 | 3155 | 3111 | 3084 | 3068 | 3084 |
| 11-12 | 3078 | 3122 | 3092 | 3075 | 3102 | 3053 | 3122 | 3099 | 3118 | 3083 | 3087 | 3034 |



TABLE II: Rome 5-minute barometric data in units of mB.

February 16, 1984

| UT | 00-05 | 05-10 | 10-15 | 15-20 | 20-25 | 25-30 | 30-35 | 35-40 | 40-45 | 45-50 | 50-55 | 55-60 |
|---|---|---|---|---|---|---|---|---|---|---|---|---|
| 07-08 | 1016.28 | 1016.34 | 1016.35 | 1016.33 | 1016.27 | 1016.26 | 1016.28 | 1016.26 | 1016.26 | 1016.28 | 1016.27 | 1016.26 |
| 08-09 | 1016.23 | 1016.27 | 1016.31 | 1016.32 | 1016.32 | 1016.31 | 1016.30 | 1016.27 | 1016.30 | 1016.26 | 1016.16 | 1016.17 |
| 09-10 | 1016.24 | 1016.31 | 1016.33 | 1016.34 | 1016.37 | 1016.37 | 1016.36 | 1016.35 | 1016.31 | 1016.27 | 1016.23 | 1016.21 |
| 10-11 | 1016.20 | 1016.23 | 1016.25 | 1016.22 | 1016.16 | 1016.07 | 1015.97 | 1015.84 | 1015.73 | 1015.69 | 1015.71 | 1015.74 |
| 11-12 | 1015.78 | 1015.79 | 1015.77 | 1015.71 | 1015.63 | 1015.59 | 1015.56 | 1015.51 | 1015.45 | 1015.43 | 1015.42 | 1015.39 |

# The Solar Flare of 16 February 1984 as Recorded at SANAE, Hermanus, Potchefstroom and Tsumeb

by

P.H. Stoker
Potchefstroom University for Christian Higher Education
Department of Physics
Potchefstroom 2520, Republic of South Africa

Table 1. Cosmic Ray Neutron Monitor Data for 16 February 1984
Real Counts 10 Times Tabulated Values

10-minute SANAE Data Corrected to 987.2 mb
5-minute Potchefstroom Data Corrected to 652.4 mm Hg
10-minute Hermanus Data Corrected to 760.0 mm Hg
5-minute Tsumeb Data Corrected to 660.0 mm Hg

Full Hourly Values (e.g., 2200) = total of 10 minute counts from 2110-2160

| Time | SANAE | | Potchefstroom | | Hermanus | | Tsumeb | |
|---|---|---|---|---|---|---|---|---|
| UT | 10-min | Hourly | 5-min | Hourly | 10-min | Hourly | 5-min | Hourly |
| 0805 | | | 1670 | | | | 9620 | |
| 0810 | | | 1700 | | 7010 | | 9640 | |
| 0815 | | | 1700 | | | | 9680 | |
| 0820 | | | 1630 | | 7070 | | 9680 | |
| 0825 | | | 1650 | | | | 9660 | |
| 0830 | | | 1640 | | 6930 | | 9740 | |
| 0835 | | | 1640 | | | | ---- | |
| 0840 | | | 1640 | | 6990 | | 9710 | |
| 0845 | | | 1660 | | | | 9570 | |
| 0850 | 2240 | | 1630 | | 6980 | | 9550 | |
| 0855 | | | 1670 | | | | 9640 | |
| 0900 | 2250 | 4490 | 1710 | 19940 | 7040 | 42020 | 9650 | 115780 |
| 0905 | | | 1690 | | | | 9740 | |
| 0910 | 2250 | | 1660 | | 7110 | | 9730 | |
| 0915 | | | 1660 | | | | 9790 | |
| 0920 | 3770 | | 1690 | | 7130 | | 9790 | |
| 0925 | | | 1670 | | | | 9780 | |
| 0930 | 3270 | | 1710 | | 7130 | | 9750 | |
| 0935 | | | 1670 | | | | 9720 | |
| 0940 | 2700 | | 1700 | | 7100 | | 9700 | |
| 0945 | | | 1640 | | | | 9710 | |
| 0950 | 2500 | | 1660 | | 7100 | | 9680 | |
| 0955 | | | 1620 | | | | 9690 | |
| 1000 | 2410 | 17200 | 1680 | 20050 | 7120 | 42690 | 9760 | 116840 |
| 1005 | | | 1650 | | | | 9740 | |
| 1010 | 2350 | | 1650 | | 7060 | | 9690 | |
| 1015 | | | 1680 | | | | 9710 | |
| 1020 | 2320 | | 1700 | | 7080 | | 9710 | |
| 1025 | | | 1640 | | | | 9790 | |
| 1030 | 2330 | | 1660 | | 7100 | | 9730 | |
| 1035 | | | 1650 | | | | 9650 | |
| 1040 | 2320 | | 1670 | | 7090 | | 9770 | |
| 1045 | | | 1670 | | | | 9680 | |
| 1050 | 2320 | | 1680 | | 7090 | | 9770 | |
| 1055 | | | 1660 | | | | 9710 | |
| 1100 | 2310 | 13950 | 1680 | 19990 | 7020 | 42440 | 9830 | 116780 |
| 1105 | | | 1650 | | | | 9650 | |
| 1110 | 2300 | | 1660 | | 7010 | | 9750 | |
| 1115 | | | 1690 | | | | 9710 | |
| 1120 | 2290 | | 1700 | | 7130 | | 9700 | |
| 1125 | | | 1690 | | | | 9780 | |
| 1130 | 2290 | | 1670 | | 7140 | | 9610 | |
| 1135 | | | 1700 | | | | 9680 | |
| 1140 | 2270 | | 1640 | | 7050 | | 9720 | |
| 1145 | | | 1680 | | | | 9770 | |
| 1150 | 2280 | | 1640 | | 7110 | | 9730 | |
| 1155 | | | 1640 | | | | 9760 | |
| 1200 | 2250 | 13680 | 1650 | 20010 | 7160 | 42600 | 9800 | 116660 |

| Time UT | SANAE | | Potchefstroom | | Hermanus | | Tsumeb | |
|---|---|---|---|---|---|---|---|---|
| 1205 | | | 1700 | | | | 9790 | |
| 1210 | 2250 | | 1680 | | 7080 | | 9840 | |
| 1215 | | | 1680 | | | | 9740 | |
| 1220 | 2280 | | 1670 | | 7160 | | 9740 | |
| 1225 | | | 1640 | | | | 9690 | |
| 1230 | 2300 | | 1680 | | 7080 | | 9760 | |
| 1235 | | | 1700 | | | | 9740 | |
| 1240 | 2250 | | 1630 | | 7070 | | 9690 | |
| 1245 | | | 1670 | | | | 9810 | |
| 1250 | 2320 | | 1670 | | 7080 | | 9710 | |
| 1255 | | | 1690 | | | | 9820 | |
| 1300 | 2250 | 13650 | 1700 | 20110 | 7130 | 42600 | 9950 | 117280 |
| 1305 | | | 1640 | | | | 9790 | |
| 1310 | 2330 | | 1650 | | 7050 | | 9780 | |
| 1315 | | | 1680 | | | | 9690 | |
| 1320 | ---- | | 1680 | | 7080 | | 9690 | |
| 1325 | | | 1680 | | | | 9810 | |
| 1330 | 2300 | | 1670 | | 7110 | | 9850 | |
| 1335 | | | 1660 | | | | 9800 | |
| 1340 | 2290 | | 1660 | | 7080 | | 9760 | |
| 1345 | | | 1650 | | | | 9740 | |
| 1350 | 2300 | | 1700 | | 7120 | | 9740 | |
| 1355 | | | 1650 | | | | 9760 | |
| 1400 | 2290 | 13810 | 1660 | 19980 | 7130 | 42570 | 9880 | 117290 |
| 1405 | | | | | | | | |
| 1410 | 2270 | | | | | | | |
| 1415 | | | | | | | | |
| 1420 | 2230 | | | | | | | |
| 1425 | | | | | | | | |
| 1430 | ---- | | | | | | | |
| 1435 | | | | | | | | |
| 1440 | 2260 | | | | | | | |
| 1445 | | | | | | | | |
| 1450 | 2290 | | | | | | | |
| 1455 | | | | | | | | |
| 1500 | 2260 | 13570 | | | | | | |
| 1505 | | | | | | | | |
| 1510 | 2290 | | | | | | | |
| 1515 | | | | | | | | |
| 1520 | 2250 | | | | | | | |
| 1525 | | | | | | | | |
| 1530 | 2270 | | | | | | | |
| 1535 | | | | | | | | |
| 1540 | 2230 | | | | | | | |
| 1545 | | | | | | | | |
| 1550 | 2320 | | | | | | | |
| 1555 | | | | | | | | |
| 1600 | 2260 | 13620 | | | | | | |

# Stratospheric Measurements of Solar Protons in February and April 1984

by

G.A. Basilevskaya and Yu.I. Stozhkov
P.N. Lebedev Physical Institute of the Academy of
Sciences of the USSR, Leninsky Prospect, 53
117924, Moscow, USSR

and

T.N. Charakhchyan
Institute of Nuclear Physics
Moscow State University
119899, Moscow, USSR

Solar proton measurements are made daily by a cosmic ray intensity sounding of the polar stratosphere (Murmansk region (cutoff rigidity 0.6 GV) and Mirny, Antarctica (cutoff rigidity 0.03 GV) (Shea and Smart, 1975)). The detector consists of 2 Geiger counters (the wall thickness is 0.05 G/cm$^2$ steel) arranged as a telescope interlayed by a 2 G/cm$^2$ thick aluminum plate. The proton energy is determined by the absorption in the residual atmosphere under the assumption of constant solar proton flux during the time of measurement. The nuclear interaction also is taken into account (Bazilevskaya and Makhmutov, 1983).

In Table 1 the data on stratospheric measurements during the solar proton events of 16 February 1984 and 26 April 1984 are presented. Unfortunately, the proton intensity increase began after the routine radiosonde flight on 16 February 1984. So it was detected in Murmansk only on 17 February. The heights of the radiosondes in Mirny were not adequate for this event. In April the counting rate of a single upper counter includes some contribution of X-rays originating from auroral electron precipitation. The enhanced counting rate of a single counter also was registered in Murmansk before the solar proton event commencement: 20 April 0655 UT - 0710 UT, 21 April 0650 UT - 0715 UT and 22 April 0655 UT - 0730 UT. Only the telescope data on the solar proton events are presented in the Table and in the Figure.

TABLE 1. Solar Proton Measurements in the Stratosphere in February and April 1984

| Date 1984 | Time UT | Location | Energy Interval MeV | Power Law Integral Spectral Index | Solar Proton Flux ($E \geq 150$ MeV) $cm^{-2}s^{-1}sr^{-1}$ | Symbol |
|---|---|---|---|---|---|---|
| 17 Feb | 0650-0715 | Murmansk | 80-160 | 3.5 | 0.06 | • |
| 17 Feb | 1035-1055 | Murmansk | 90-160 | 3.4 | 0.06 | x |
| 26 Apr | 0630-0700 | Murmansk | 110-210 | 4.5 | 0.2 | • |
| 26 Apr | 0820-0845 | Mirny | 120-280 | 8.5 | 0.3 | o |
| 26 Apr | 1050-1110 | Murmansk | 210-250 | 5.3 | - | x |
| 26 Apr | 1330-1430 | Mirny | 70-190 | 5.8 | 0.3 | + |
| 26 Apr | 1535-1555 | Murmansk | 345-390 | 6.0 | - | |
| 27 Apr | 0650-0715 | Murmansk | 75-155 | 3.7 | 0.06 | ▲ |
| 27 Apr | 0825-0840 | Mirny | 120-150 | 5.4 | 0.02 | ■ |
| 27 Apr | 0940-0955 | Murmansk | 100-150 | 4.5 | 0.03 | ▼ |
| 27 Apr | 1210-1240 | Murmansk | 75-135 | 3.5 | - | □ |

Figure 1 shows the integral energy spectra measured in the stratosphere. The symbols in the Table and the Figure are identical.

## REFERENCES

BAZILEVSKAYA, G.A. and V.S. MAKHMUTOV 1983 "Determination of the Absolute Fluxes of Solar Protons with E>100 MeV from Measurements in the Stratosphere and with Neutron Monitors," Geomagn. and Aeronom., 23, No. 3, 305-308.

SHEA, M.A. and D.F. SMART 1975 "Asymptotic Directions and Vertical Cutoff Rigidities for Selected Cosmic-Ray Stations as Calculated Using the International Geomagnetic Reference Field Model Appropriate for Epoch 1975.0, AFCRL-TR-75-0247.

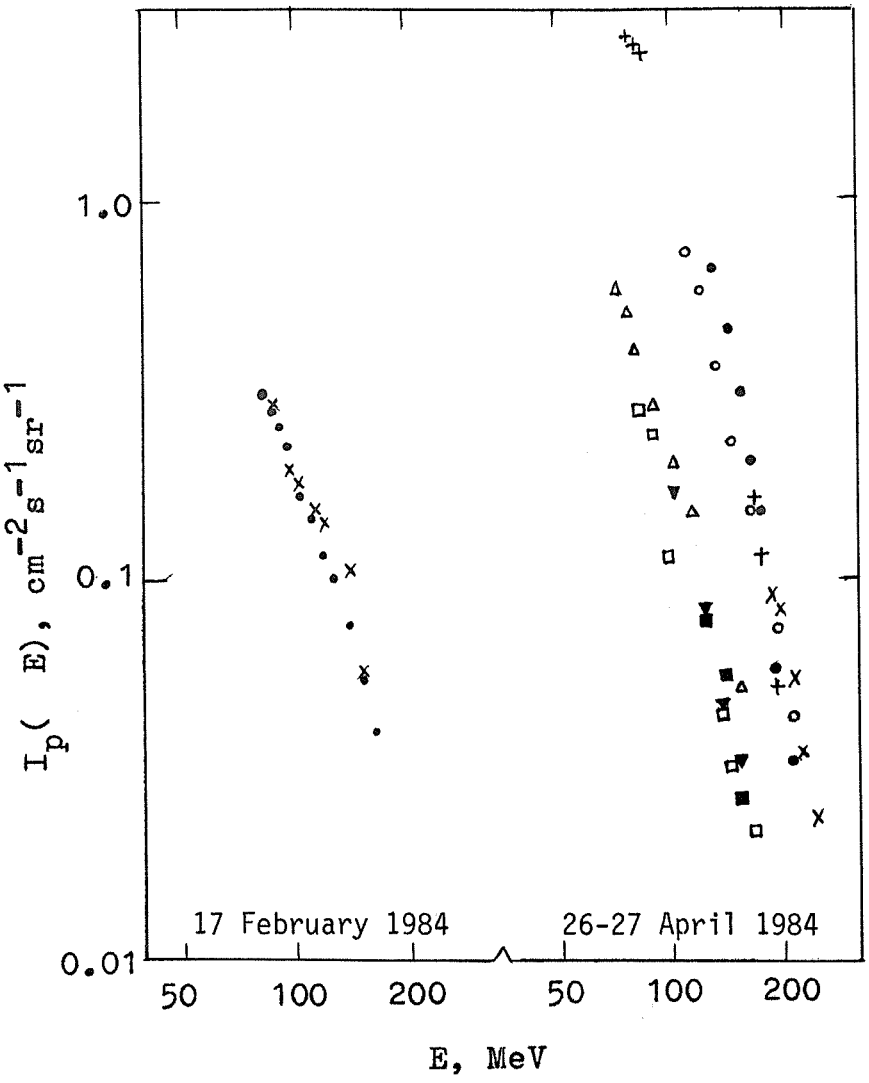


Fig. 1. Integral energy spectra of solar protons in the stratosphere. The symbols are the same as in Table 1.

## February - May 1984 Cosmic Ray Events Observed in Yakutsk

by

G.V. Skripin, G.V. Shafer, A.N. Prikhodko,
N.M. Belomestnova and S.V. Kholtosunova
Institute of Cosmophysical Research and Aeronomy
Lenin Ave., 31, 677891, Yakutsk, USSR

Tables 1-4 present the hourly pressure corrected values of cosmic ray intensity from the 6-NM-64 neutron supermonitor and the ASK-1 ionization chamber in Yakutsk (N62.0 E129.7; sea level) on 12-21 February and 22 April - 4 May 1984.

In the first period the cosmic ray flare was detected only by the neutron supermonitor. Table 5 gives the 15-minute pressure corrected data for 16 February, 0715-1245 UT. The intensity began to increase at 0845 UT and reached its maximum value of approximately 10 percent at 0915 UT, then it decayed for about 2.5 hours.

The 24 April solar event was seen both in the neutron and muon components as a Forbush decrease.

A sharp decrease of intensity began on 26 April at 1700 UT and lasted approximately 13-14 hours. The decrease value was about 7.5 percent and about 2.8 percent in the neutron and muon component, respectively. The neutron monitor data on the previous day showed a sharp decrease of about 2.0 percent.

Table 1. Hourly cosmic ray intensity data from the 6-NM-64 neutron supermonitor in Yakutsk on 12-21 February 1984 (0.01%). Pressure corrected.

| Hour (UT) | February 1984 12 | 13 | 14 | 15 | 16 | 17 | 18 | 19 | 20 | 21 |
|---|---|---|---|---|---|---|---|---|---|---|
| 0100 | -105 | -226 | -31 | -163 | -63 | -37 | -42 | 68 | -5 | -74 |
| 0200 | -26 | -105 | -68 | -105 | -26 | 16 | 53 | 79 | 58 | -68 |
| 0300 | -15 | -147 | -100 | -105 | -37 | 79 | 84 | 89 | 79 | -63 |
| 0400 | -15 | -132 | -58 | -26 | -5 | 105 | 0 | 89 | 110 | -68 |
| 0500 | -100 | -68 | -68 | -132 | -32 | 0 | 100 | 32 | 110 | -16 |
| 0600 | -21 | -168 | -58 | -137 | -37 | 5 | 94 | 63 | 79 | -105 |
| 0700 | -32 | -174 | -121 | -100 | -5 | 174 | 94 | 105 | 42 | -184 |
| 0800 | -26 | -242 | -42 | -47 | -5 | 63 | 63 | 85 | 79 | -16 |
| 0900 | 26 | -189 | -21 | -189 | -32 | 42 | 10 | 37 | 68 | -21 |
| 1000 | -105 | -226 | -105 | -163 | 400 | 16 | 21 | 32 | 53 | -42 |
| 1100 | -89 | -226 | -95 | -89 | 179 | 32 | 32 | 58 | 5 | -89 |
| 1200 | -115 | -184 | -100 | -89 | 79 | -16 | 32 | 95 | 100 | -58 |
| 1300 | -110 | -215 | -116 | -153 | 16 | 10 | 10 | 53 | -37 | 5 |
| 1400 | -174 | -184 | -132 | -95 | -16 | -5 | 0 | 16 | -47 | -32 |
| 1500 | -142 | -195 | -147 | -121 | -21 | -32 | -42 | 42 | -32 | -68 |
| 1600 | -184 | -195 | -116 | -137 | 0 | -47 | -68 | -47 | -16 | -63 |
| 1700 | -216 | -200 | -121 | -121 | -121 | -53 | -58 | -63 | 26 | -95 |
| 1800 | -284 | -247 | -95 | -100 | -74 | -63 | -21 | 10 | -16 | -95 |
| 1900 | -263 | -221 | -79 | -137 | -110 | 26 | -47 | 47 | -68 | -74 |
| 2000 | -305 | -232 | -89 | -74 | -79 | -58 | -16 | 42 | -47 | -42 |
| 2100 | -289 | -163 | -68 | -37 | -32 | -26 | -58 | 32 | -95 | -174 |
| 2200 | -358 | -179 | -26 | -95 | -26 | -10 | -42 | 189 | -10 | -168 |
| 2300 | -237 | -105 | -42 | -121 | -16 | 5 | 10 | 10 | 10 | -110 |
| 2400 | -158 | -94 | -16 | -100 | -16 | 5 | 10 | 53 | -74 | -116 |
| Mean | -138 | -184 | -80 | -110 | 2 | 10 | 13 | 51 | 16 | -76 |

Table 2. Hourly cosmic ray intensity data of the ASK-1 ionization chamber in Yakutsk for 12-21 February 1984 (0.01%). Pressure and ionization burst corrected.

| February 1984 12 | 13 | 14 | 15 | 16 | 17 | 18 | 19 | 20 | 21 |
|---|---|---|---|---|---|---|---|---|---|
| 363 | 324 | 383 | 394 | 414 | 450 | 442 | 449 | 435 | 494 |
| 352 | 357 | 353 | 404 | 437 | 407 | 426 | 459 | 480 | 489 |
| 409 | 366 | 405 | 432 | 441 | 439 | 468 | 468 | 471 | 418 |
| 366 | 370 | 397 | 402 | 463 | 437 | 462 | 516 | 477 | 488 |
| 406 | 378 | 372 | 402 | 445 | 458 | 472 | 453 | 505 | 473 |
| 377 | 352 | 376 | 411 | 391 | 455 | 477 | 479 | 518 | 431 |
| 388 | 336 | 415 | 417 | 436 | 447 | 460 | 433 | 487 | 491 |
| 375 | 339 | 382 | 408 | 427 | 463 | 464 | 464 | 507 | 459 |
| 384 | 329 | 452 | 343 | 420 | 442 | 443 | 463 | 506 | 485 |
| 369 | 323 | 387 | 388 | 390 | 458 | 444 | 478 | 454 | 453 |
| 349 | 312 | 430 | 391 | 405 | 444 | 466 | 462 | 510 | 493 |
| 333 | 329 | 422 | 361 | 407 | 399 | 448 | 424 | 521 | 451 |
| 349 | 320 | 387 | 369 | 403 | 457 | 462 | 428 | 456 | 483 |
| 348 | 327 | 373 | 414 | 409 | 412 | 439 | 426 | 462 | 459 |
| 290 | 328 | 381 | 385 | 409 | 404 | 433 | 476 | 430 | 452 |
| 321 | 328 | 387 | 403 | 423 | 437 | 412 | 476 | 465 | 447 |
| 316 | 325 | 383 | 395 | 407 | 414 | 432 | 454 | 407 | 483 |
| 304 | 355 | 365 | 403 | 420 | 441 | 416 | 468 | 430 | 453 |
| 309 | 330 | 410 | 401 | 377 | 450 | 416 | 452 | 449 | 427 |
| 279 | 327 | 412 | 398 | 402 | 433 | 442 | 461 | 474 | 443 |
| 285 | 349 | 396 | 394 | 389 | 436 | 429 | 461 | 473 | 428 |
| 297 | 355 | 445 | 403 | 433 | 409 | 446 | 475 | 475 | 434 |
| 284 | 371 | 439 | 415 | 419 | 430 | 437 | 509 | 453 | 450 |
| 318 | 381 | 399 | 432 | 389 | 425 | 433 | 509 | 446 | 390 |
| 340 | 342 | 398 | 399 | 415 | 435 | 445 | 464 | 470 | 457 |

Table 3. Hourly cosmic ray intensity data of the 6-NM-64 neutron supermonitor in Yakutsk on 22 April - 4 May 1984 (0.01%). Pressure corrected.

| Hour (UT) | April 1984 22 | 23 | 24 | 25 | 26 | 27 | 28 | 29 | 30 | May 1984 01 | 02 | 03 | 04 |
|---|---|---|---|---|---|---|---|---|---|---|---|---|---|
| 0100 | 37 | 116 | 147 | 253 | --- | -389 | -642 | -500 | -437 | -326 | -153 | -163 | -10 |
| 0200 | -21 | 163 | 174 | 253 | --- | -542 | -610 | -547 | -405 | -368 | -247 | -174 | 16 |
| 0300 | -53 | 153 | 195 | 242 | --- | -663 | -589 | -457 | -453 | -416 | -200 | -253 | -58 |
| 0400 | 74 | 137 | 105 | 332 | -63 | -726 | -574 | -532 | -379 | -463 | -158 | -305 | -105 |
| 0500 | 195 | 163 | 195 | 263 | --- | -742 | -400 | -616 | -374 | -489 | -121 | -379 | -121 |
| 0600 | 195 | 137 | 163 | 279 | -100 | -695 | -710 | -668 | -337 | -453 | -189 | -284 | -205 |
| 0700 | 158 | 174 | 163 | 226 | -184 | -668 | -658 | -700 | -463 | -447 | -163 | -226 | -237 |
| 0800 | 210 | 184 | 195 | 279 | -105 | -621 | --- | -584 | -437 | -432 | -321 | -263 | -216 |
| 0900 | 153 | 168 | 226 | 158 | 5 | -689 | -800 | -705 | -395 | -363 | -132 | -263 | -289 |
| 1000 | 137 | 189 | 174 | 153 | -63 | -595 | -674 | -710 | -358 | -484 | - 79 | -337 | -195 |
| 1100 | 179 | 174 | 210 | 68 | -16 | -605 | -747 | -595 | -342 | -353 | -158 | -358 | -216 |
| 1200 | 110 | 168 | 216 | 68 | -10 | -537 | -621 | -579 | -384 | -458 | -068 | -332 | -253 |
| 1300 | 68 | 142 | 132 | 89 | -5 | -521 | -658 | -579 | -295 | -447 | -200 | -289 | -221 |
| 1400 | 121 | 205 | 184 | 5 | 5 | -600 | -616 | -563 | -389 | -500 | -368 | -247 | -258 |
| 1500 | 79 | 153 | 126 | 63 | -45 | -489 | -631 | -495 | -347 | -405 | -363 | -258 | -237 |
| 1600 | 153 | 163 | 195 | 63 | 0 | -679 | -663 | -500 | -358 | -432 | -405 | -232 | -247 |
| 1700 | 126 | 47 | 242 | 5 | -74 | -595 | -632 | -521 | -479 | -316 | -389 | -242 | -226 |
| 1800 | 174 | 147 | 216 | -26 | -195 | -647 | -505 | -416 | -474 | -332 | -347 | -242 | -226 |
| 1900 | 126 | 137 | 163 | -68 | -163 | -579 | -584 | -495 | -526 | -410 | -268 | -232 | -205 |
| 2000 | 89 | 153 | 184 | -74 | -410 | -537 | -558 | -410 | -542 | -368 | -253 | -179 | -221 |
| 2100 | 79 | 147 | 226 | -121 | -426 | -405 | -553 | -400 | -468 | -289 | -163 | -132 | -258 |
| 2200 | 147 | 105 | 195 | -37 | -521 | -463 | -568 | -442 | -463 | -337 | -079 | -84 | -163 |
| 2300 | 142 | 121 | 216 | -68 | -389 | -437 | -510 | -521 | -474 | -242 | -126 | 21 | -221 |
| 2400 | 68 | 184 | 232 | --- | -526 | -437 | -547 | -526 | -474 | -221 | -221 | 5 | -95 |
| Mean | 114 | 151 | 186 | 104 | -163 | -522 | -611 | -544 | -419 | -390 | -215 | -227 | -186 |

Table 4. Hourly cosmic ray intensity data of the ASK-1 ionization chamber in Yakutsk on 20 April - 5 May 1984 (0.01%). Pressure and ionization bursts corrected.

| Hour (UT) | April 1984 20 | 21 | 22 | 23 | 24 | 25 | 26 | 27 | 28 | 29 | 30 | May 1984 01 | 02 | 03 | 04 | 05 |
|---|---|---|---|---|---|---|---|---|---|---|---|---|---|---|---|---|
| 0100 | 87 | 119 | 160 | 140 | 96 | 66 | 102 | -83 | -93 | 19 | 1 | 66 | 78 | 16 | 48 | 33 |
| 0200 | 115 | 154 | 148 | 121 | 101 | 85 | 94 | -95 | -76 | -6 | 2 | 49 | 85 | 11 | 42 | 20 |
| 0300 | 75 | 151 | 149 | 137 | 117 | 70 | 98 | -143 | -116 | -6 | 16 | 12 | 81 | 4 | 28 | 37 |
| 0400 | 129 | 148 | 184 | 131 | 73 | 88 | 105 | -160 | -70 | 9 | 15 | 48 | 55 | 5 | -17 | 21 |
| 0500 | 132 | 170 | 158 | 146 | 116 | 70 | 99 | -183 | -106 | -54 | 32 | 8 | 57 | -3 | -20 | 14 |
| 0600 | 100 | 185 | 171 | 170 | 89 | 105 | 96 | -208 | -91 | -46 | 16 | 0 | 45 | 6 | 3 | 29 |
| 0700 | 99 | 202 | 157 | 156 | 113 | 107 | 93 | -182 | -103 | -49 | -19 | -20 | 61 | 3 | -61 | 42 |
| 0800 | 108 | 176 | 174 | 136 | 103 | 90 | 79 | -171 | -113 | -81 | 31 | 1 | 25 | -6 | -21 | 36 |
| 0900 | 124 | 173 | 155 | 162 | 61 | 43 | 100 | -160 | -128 | -33 | -5 | -21 | 26 | -20 | -50 | 12 |
| 1000 | 116 | 165 | 133 | 140 | 85 | 27 | 107 | -124 | -135 | -38 | 1 | 7 | 54 | -37 | -19 | 10 |
| 1100 | 94 | 178 | 146 | 155 | 59 | 67 | 102 | -109 | -110 | -78 | 24 | -25 | 5 | -16 | -34 | 37 |
| 1200 | 86 | 153 | 128 | 158 | 74 | 58 | 81 | -112 | -104 | -66 | 20 | -4 | 35 | -24 | -15 | 28 |
| 1300 | 71 | 167 | 128 | 119 | 54 | 71 | 99 | -130 | -123 | -51 | 19 | 1 | 18 | -28 | 3 | 20 |
| 1400 | 56 | 141 | 109 | 142 | 45 | 43 | 105 | -159 | -69 | 6 | 38 | -15 | -10 | -17 | -19 | 26 |
| 1500 | 82 | 138 | 133 | 141 | 77 | 71 | 84 | -147 | -93 | -31 | 27 | 36 | -3 | -30 | 3 | 28 |
| 1600 | 56 | 149 | 136 | 198 | 30 | 87 | 102 | -181 | -19 | -7 | 23 | 10 | -38 | -20 | 20 | -9 |
| 1700 | 76 | 177 | 155 | 135 | 61 | 94 | 112 | -145 | -11 | 1 | 4 | 33 | -24 | -39 | 7 | 21 |
| 1800 | 76 | 148 | 111 | 119 | 14 | 80 | 111 | -141 | -7 | 1 | 25 | 53 | -12 | -6 | 32 | 50 |
| 1900 | 70 | 136 | 111 | 132 | 32 | 79 | 72 | -139 | -2 | 17 | 18 | 39 | 3 | -4 | -5 | 14 |
| 2000 | 60 | 132 | 104 | 102 | 49 | 87 | 46 | -74 | 21 | -7 | 15 | 46 | 16 | 10 | -18 | 11 |
| 2100 | 72 | 130 | 141 | 130 | 35 | 105 | -15 | -54 | 20 | 27 | 17 | 51 | 14 | 13 | 21 | 28 |
| 2200 | 88 | 123 | 120 | 112 | 49 | 85 | -44 | -84 | 19 | 26 | -21 | 86 | -8 | 20 | 8 | 48 |
| 2300 | 106 | 157 | 102 | 107 | 81 | 99 | -53 | -84 | 20 | -7 | 52 | 80 | 27 | 43 | -8 | 57 |
| 2400 | 119 | 154 | 98 | 108 | 88 | 102 | -96 | -83 | 9 | 23 | 59 | 74 | -7 | 38 | 20 | 40 |
| Mean | 92 | 155 | 138 | 137 | 71 | 78 | 70 | -131 | -62 | -18 | 17 | 26 | 24 | -3 | -2 | 27 |

Table 5. The 15-min pressure corrected data (%) of the 6-NM-64 neutron supermonitor on 16 February 1984 0715-1245 UT in Yakutsk.

| Minute | 15 | 30 | 45 | 60 |
|---|---|---|---|---|
| Hour (UT) | | | | |
| 0700 | 0.16 | 0.70 | 0.17 | 0.56 |
| 0800 | -0.35 | 0.15 | -0.40 | 4.60 |
| 0900 | 9.96 | 6.82 | 2.74 | 4.08 |
| 1000 | 1.30 | 1.75 | 1.70 | 1.61 |
| 1100 | 1.57 | 0.22 | -1.50 | 0.52 |
| 1200 | 0.96 | 0.45 | -0.48 | --- |

# Cosmic Ray Variations at Alma Ata During the Solar Events in February and April 1984

by

V.P. Antonova and A.G. Zusmanovich
Institute of Ionosphere of Academy of Sciences of Kazakh SSR
480069, Alma Ata, USSR

We present the neutron component of the cosmic ray intensity recorded at the high altitude station of the Institute of Ionosphere of Academy of Sciences Kazakh SSR. The station coordinates are N43°15' E76°55', altitude 3340 m. The cut-off rigidity is 6.69 GV. The instrument is a Super Neutron Monitor 18 NM-64 having a counting rate of about $4.5 \times 10^6$ impulses per hour. The median barometric pressure is 675 mb. The hourly and 5-minute values of the neutron component intensity are recorded. The scaling factor is 512 for all presented data.

## Period 12-21 February 1984

The corrected hourly cosmic ray neutron component data are presented in Table 1 and shown in Figure 1.

Table 1. Alma Ata Cosmic Ray Data for 12-21 February 1984 (corrected for pressure)

| | February 1984 | | | | | | | | | |
|---|---|---|---|---|---|---|---|---|---|---|
| Day | 12 | 13 | 14 | 15 | 16 | 17 | 18 | 19 | 20 | 21 |
| Hour (UT) | | | | | | | | | | |
| 0100 | 9099 | 8956 | 9014 | 9027 | 9022 | 9063 | 9093 | 9071 | 9118 | 9039 |
| 0200 | 9103 | 8987 | 9018 | 9008 | 9013 | 9074 | 9099 | 9080 | 9121 | 9035 |
| 0300 | 9133 | 9058 | 9069 | 9015 | 9039 | 9077 | 9112 | 9082 | 9126 | 9048 |
| 0400 | 9137 | 9008 | 9087 | 9047 | 9050 | 9098 | 9136 | 9084 | 9132 | 9067 |
| 0500 | 9141 | 9009 | 9118 | 9070 | 9078 | 9133 | 9133 | 9100 | 9130 | 9040 |
| 0600 | 9140 | 9037 | 9154 | 9067 | 9082 | 9135 | 9164 | 9097 | 9115 | 9032 |
| 0700 | 9158 | 9034 | 9142 | 9054 | 9085 | 9139 | 9161 | 9109 | 9134 | 9037 |
| 0800 | 9143 | 9029 | 9109 | 9058 | 9069 | 9137 | 9157 | 9119 | 9129 | 9065 |
| 0900 | 9118 | 9022 | 9090 | 9058 | 9084 | 9133 | 9146 | 9118 | 9188 | 9052 |
| 1000 | 9104 | 9069 | 9065 | 9058 | 9112 | 9104 | 9160 | 9098 | 9178 | 9091 |
| 1100 | 9091 | 9100 | 9066 | 9048 | 9074 | 9104 | 9141 | 9104 | 9168 | 9112 |
| 1200 | 9090 | 9114 | 9089 | 9024 | 9069 | 9111 | 9130 | 9112 | 9165 | 9103 |
| 1300 | 9079 | 9120 | 9085 | 9014 | 9056 | 9108 | 9124 | 9110 | 9068 | 9111 |
| 1400 | 9042 | 9092 | 9079 | 9021 | 9054 | 9090 | 9119 | 9076 | 9050 | 9137 |
| 1500 | 9003 | 9075 | 9059 | 9020 | 9062 | 9069 | 9126 | 9127 | 9036 | 9123 |
| 1600 | 8929 | 9078 | 9069 | 9015 | 9051 | 9066 | 9131 | 9147 | 9033 | 9119 |
| 1700 | 8873 | 9052 | 9046 | 9018 | 9044 | 9056 | 9124 | 9124 | 9097 | 9078 |
| 1800 | 8868 | 9052 | 9032 | 9014 | 9035 | 9066 | 9095 | 9116 | 9046 | 9060 |
| 1900 | 8851 | 9032 | 9033 | 9029 | 9033 | 9061 | 9094 | 9186 | 9060 | 9037 |
| 2000 | 8853 | 9046 | 9027 | 9028 | 9033 | 9064 | 9067 | 9176 | 9072 | 9036 |
| 2100 | 8849 | 9027 | 9038 | 9014 | 9033 | 9059 | 9074 | 9089 | 9038 | 9041 |
| 2200 | 8882 | 9006 | 9033 | 9027 | 9022 | 9058 | 9078 | 9123 | 9031 | 9037 |
| 2300 | 8906 | 8997 | 9057 | 9028 | 9047 | 9047 | 9079 | 9135 | 9058 | 9023 |
| 2400 | 8951 | 9000 | 9021 | 9018 | 9044 | 9058 | 9085 | 9090 | 9030 | 9018 |

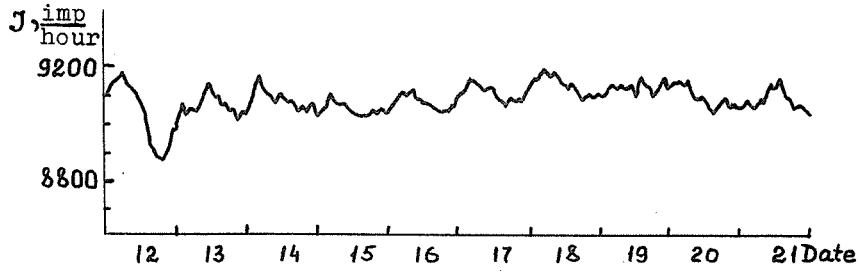


Fig. 1. Corrected hourly neutron monitor data from Alma Ata for the period 12-21 February 1984 are shown.

During this period we observed a weak decrease of the cosmic ray intensity on 12 February and the cosmic ray event on 16 February after 0900 UT. The increase was not observed in the hourly data but was clearly observed in the 5-minute data (Table 2, Figure 2).

Table 2. Alma Ata Cosmic Ray 5-minute Data for 16 February 1984
(corrected for pressure)

| Minutes | 05 | 10 | 15 | 20 | 25 | 30 | 35 | 40 | 45 | 50 | 55 | 60 |
|---|---|---|---|---|---|---|---|---|---|---|---|---|
| Hour (UT) | | | | | | | | | | | | |
| 0800 | 754.3 | 756.2 | 756.2 | 756.2 | 753.3 | 754.3 | 756.2 | 759.0 | 755.2 | 755.2 | 751.4 | 755.2 |
| 0900 | 755.8 | 758.7 | 753.9 | 757.8 | 754.9 | 754.8 | 757.8 | 755.8 | 753.9 | 757.8 | 759.7 | 753.0 |
| 1000 | 756.4 | 760.2 | 763.1 | 761.2 | 762.2 | 758.3 | 755.4 | 758.3 | 757.3 | 759.3 | 756.4 | 756.4 |
| 1100 | 755.4 | 750.7 | 755.6 | 758.5 | 757.5 | 753.6 | 756.5 | 757.5 | 754.6 | 755.6 | 754.6 | 755.6 |
| 1200 | 755.6 | 754.6 | 755.6 | 753.6 | 755.6 | 753.6 | 755.6 | 756.5 | 754.6 | 755.6 | 754.6 | 756.5 |

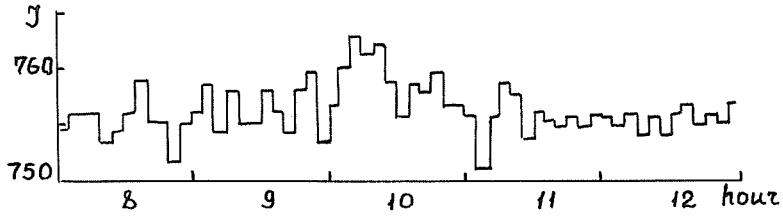


Fig. 2. Corrected 5-minute data from Alma Ata for the period 0800-1200 UT on 16 February are shown.

**Period 20 April - 4 May 1984**

The hourly data for this period are presented in Table 3 and Figure 3.

TABLE 3. Data for 20 April to 4 May 1984

(corrected for pressure; efficiency 110.9 percent)

| Day | April 1984 20 | 21 | 22 | 23 | 24 | 25 | 26 | 27 | 28 | 29 | 30 | May 1984 01 | 02 | 03 | 04 |
|---|---|---|---|---|---|---|---|---|---|---|---|---|---|---|---|
| Hour (UT) | | | | | | | | | | | | | | | |
| 0100 | 8780 | 8846 | 8889 | 8859 | 8900 | 9011 | 8952 | 8614 | 8433 | 8477 | 8570 | 8538 | 8699 | 8736 | 8871 |
| 0200 | 8769 | 8870 | 8902 | 8868 | 8905 | 9001 | 8950 | 8584 | 8401 | 8459 | 8558 | 8562 | 8732 | 8730 | 8915 |
| 0300 | 8788 | 8874 | 8915 | 8902 | 8904 | 9005 | 8979 | 8525 | 8380 | 8470 | 8559 | 8595 | 8781 | 8719 | 8871 |
| 0400 | 8805 | 8898 | 8933 | 8923 | 8925 | 9027 | 8994 | 8435 | 8381 | 8461 | 8620 | 8589 | 8769 | 8690 | 8854 |
| 0500 | 8840 | 8913 | 8963 | 8924 | 8926 | 9008 | 8959 | 8405 | 8377 | 8485 | 8623 | 8595 | 8773 | 8642 | 8801 |
| 0600 | 8876 | 8917 | 8961 | 8906 | 8952 | 9027 | 8920 | 8391 | 8365 | 8488 | 8623 | 8592 | 8777 | 8639 | 8753 |
| 0700 | 7792 | 8926 | 8970 | 8910 | 8914 | 9008 | 8927 | 8385 | 8358 | 8467 | 8608 | 8593 | 8814 | 8627 | 8724 |
| 0800 | 8888 | 8939 | 8960 | 8918 | 8922 | 8922 | 8942 | 8388 | 8348 | 8466 | 8598 | 8607 | 8833 | 8642 | 8643 |
| 0900 | 8887 | 8947 | 8969 | 8910 | 8911 | 8897 | 8969 | 8367 | 8340 | 8451 | 8616 | 8586 | 8856 | 8640 | 8627 |
| 1000 | 8877 | 8945 | 8940 | 8910 | 8945 | 8878 | 9000 | 8374 | 8341 | 8441 | 8620 | 8582 | 8837 | 8625 | 8620 |
| 1100 | 8890 | 8935 | 8933 | 8907 | 8955 | 8870 | 8967 | 8364 | 8332 | 8473 | 8615 | 8603 | 8828 | 8641 | 8664 |
| 1200 | 8893 | 8920 | 8928 | 8907 | 8963 | 8887 | 8969 | 8381 | 8345 | 8475 | 8628 | 8590 | 8837 | 8609 | 8645 |
| 1300 | 8885 | 8917 | 8905 | 8915 | 8962 | 8898 | 8937 | 8401 | 8340 | 8491 | 8626 | 8611 | 8781 | 8606 | 8680 |
| 1400 | 8850 | 8919 | 8899 | 8895 | 8966 | 8918 | 8949 | 8445 | 8362 | 8497 | 8636 | 8608 | 9693 | 8607 | 8683 |
| 1500 | 8830 | 8896 | 8873 | 8859 | 8961 | 8992 | 8950 | 8454 | 8367 | 8516 | 8650 | 8619 | 8655 | 8641 | 8698 |
| 1600 | 8841 | 8897 | 8875 | 8864 | 8953 | 8987 | 8960 | 8480 | 8383 | 8536 | 8623 | 8633 | 8607 | 8626 | 8703 |
| 1700 | 8830 | 8883 | 8867 | 8862 | 8945 | 8980 | 8953 | 8461 | 8384 | 8543 | 8579 | 8645 | 8607 | 8623 | 8710 |
| 1800 | 8821 | 8843 | 8876 | 8873 | 8985 | 8938 | 8860 | 8437 | 8426 | 8568 | 8566 | 8680 | 8608 | 8612 | 8717 |
| 1900 | 8808 | 8854 | 8882 | 8875 | 8994 | 8899 | 8801 | 8458 | 8459 | 8587 | 8531 | 8683 | 8648 | 8630 | 8721 |
| 2000 | 8792 | 8845 | 8856 | 8873 | 8989 | 8916 | 8711 | 8457 | 8460 | 8597 | 8524 | 8728 | 8665 | 8655 | 8712 |
| 2100 | 8826 | 8818 | 8869 | 8883 | 8965 | 8922 | 8656 | 8487 | 8470 | 8607 | 8514 | 8696 | 8676 | 8689 | 8726 |
| 2200 | 8833 | 8836 | 8853 | 8892 | 8972 | 8933 | 8594 | 8500 | 8476 | 8591 | 8528 | 8680 | 8692 | 8740 | 8735 |
| 2300 | 8840 | 8857 | 8862 | 8904 | 8971 | 8930 | 8577 | 8504 | 8478 | 8594 | 8539 | 8675 | 8708 | 8797 | 8724 |
| 2400 | 8831 | 8878 | 8864 | 8903 | 8991 | 8962 | 8587 | 8495 | 8486 | 8580 | 8552 | 8683 | 8725 | 8847 | 8733 |

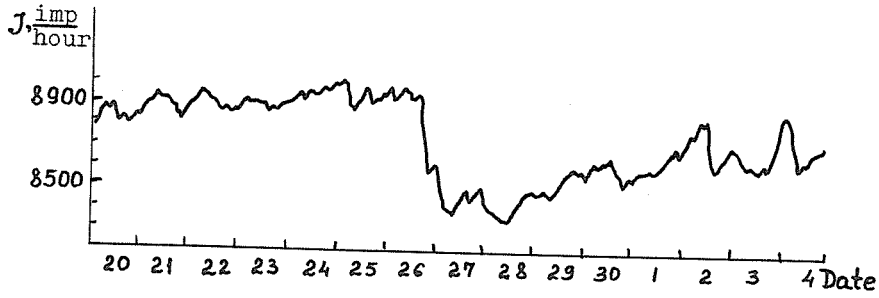


Fig. 3. Corrected hourly neutron monitor data from Alma Ata for the period 20 April - 4 May 1984 are shown.

The clearly expressed Forbush effect begins on 26 April and has a maximum decrease of 6.5 percent. The large fluctuations of cosmic ray intensity connected with the decreasing of the solar and geomagnetic activity are observed during 2 - 4 May 1984.

## Galactic Cosmic Rays During the Period 20 April-4 May 1984

by

Martin A. Pomerantz
Bartol Research Foundation of The Franklin Institute
University of Delaware, Newark, Delaware 19716, USA

There were no unusual time variations in the galactic cosmic ray intensity during the transit of solar Active Region 4474 across the visible disk. A classical Forbush decrease, clearly representing the arrival of a shock produced by the 24 April solar flare, commenced on 26 April.

The intensity profiles at the four stations comprising the Bartol neutron monitor network were essentially similar. Hence only the data from McMurdo Station, Antarctica, are plotted in Figure 1.

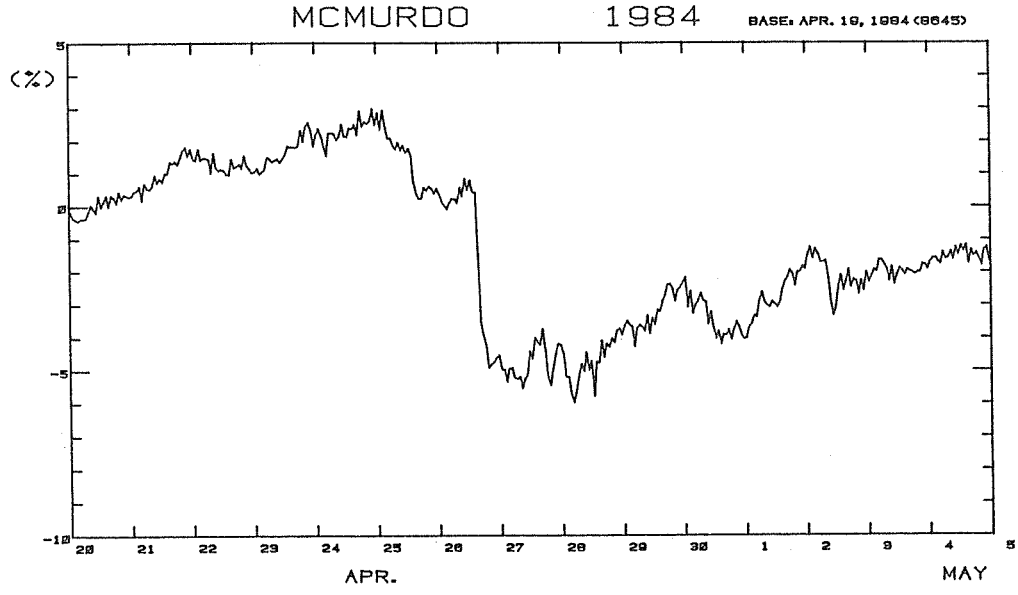


Figure 1

# Cosmic Ray Variations in April and May 1984 according to the Novosibirsk Neutron Component Data and Neutron Multiplicity of Local Generation

by

V.L. Yanchukovsky and R.Z. Khisamov
Institute of Geology and Geophysics, Siberian Branch, USSR
Academy of Sciences, Novosibirsk, USSR

At the end of April and the beginning of May 1984 the Novosibirsk cosmic ray station observed a Forbush decrease (FD) in cosmic rays. This FD made up 8 percent of the summary count of the neutron supermonitor (NSM).

Figure 1 shows variations for the summary intensity and for intensities of different neutron multiplicities of the local generation (from m $\geq$ 1 to m $\geq$ 6) in the monitor NM 64 from 20 April to 5 May 1984. The data were obtained by a NSM with 4 sections and corrected for the barometer effect.

The Novosibirsk station has geographic coordinates N55.0 E82.9 and geomagnetic cut-off rigidity R=2.91 GV. The mean square deviations sigma are shown for each channel in Figure 1. The averaging intervals equal one hour for the summary count for m $\geq$1 and m $\geq$2; 2 hours for m $\geq$3; 4 hours for m $\geq$4 and m $\geq$5; and 6 hours for m $\geq$6. During the experiment the intensity was observed to decrease for multiplicities up to m $\geq$6.

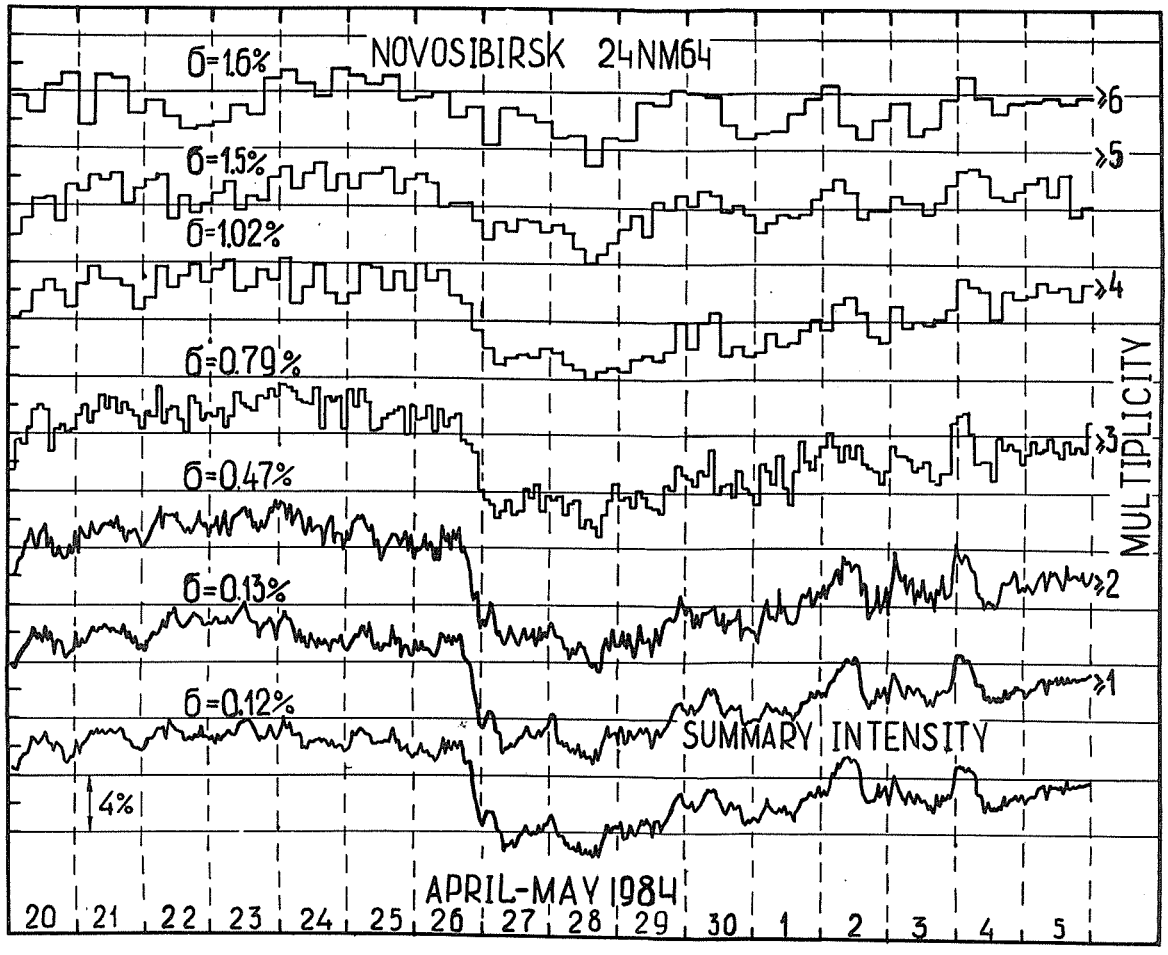


Fig. 1. Novosibirsk neutron supermonitor data for 20 April - 5 May 1984 are shown. Standard deviations for the summary intensity and different neutron multiplicities m $\geq$1 to m $\geq$6 are included.

# Cosmic Ray Observations at Khabarovsk During the Disturbed Periods in February and April 1984

by

S.F. Rezaeva and A.P. Sidorenko
Department of Physics of Near-Terrestrial Space
NESCRI, Khabarovsk, USSR

Hourly and mean diurnal data of cosmic ray intensity for 26 February - 5 March and 20 April - 4 May 1984 are presented in the tables. These data are corrected for atmospheric pressure under P=1000 mb and barometric coefficient 0.0071%/mb. The mean diurnal total (of three sections) intensity for the same periods is shown in the figures.

Table 1. Cosmic Ray Intensities for 26 February - 5 March 1984

| | February 1984 | | | | March 1984 | | | | | Hourly |
|---|---|---|---|---|---|---|---|---|---|---|
| Day | 26 | 27 | 28 | 29 | 01 | 02 | 03 | 04 | 05 | Means |
| Hour (UT) | | | | | | | | | | |
| 0100 | 6452 | 6461 | 6454 | 6515 | 6463 | 6509 | 6519 | 6526 | 6572 | 6497 |
| 0200 | 6496 | 6454 | 6510 | 6550 | 6508 | 6531 | 6498 | 6550 | 6548 | 6516 |
| 0300 | 6471 | 6457 | 6518 | 6535 | 6496 | 6508 | 6504 | 6565 | 6550 | 6512 |
| 0400 | 6477 | 6461 | 6546 | 6541 | 6506 | --- | 6516 | 6539 | 6545 | 6516 |
| 0500 | 6500 | 6484 | 6556 | 6533 | 6497 | --- | 6507 | 6539 | 6570 | 6523 |
| 0600 | 6504 | 6503 | 6566 | 6536 | 6485 | --- | 6519 | 6564 | 6530 | 6526 |
| 0700 | 6473 | 6447 | 6544 | 6511 | 6504 | --- | 6489 | 6547 | 6565 | 6510 |
| 0800 | 6483 | 6481 | 6508 | 6536 | 6490 | --- | 6473 | 6559 | 6560 | 6511 |
| 0900 | 6472 | 6502 | 6520 | 6555 | 6453 | 6504 | 6485 | 6548 | 6560 | 6511 |
| 1000 | 6460 | 6458 | 6520 | 6538 | 6444 | 6499 | 6472 | 6558 | 6552 | 6500 |
| 1100 | 6475 | 6423 | 6532 | 6551 | 6433 | 6501 | 6494 | 6541 | 6569 | 6502 |
| 1200 | 6429 | 6436 | 6476 | 6544 | 6444 | 6482 | 6485 | 6534 | 6545 | 6486 |
| 1300 | 6442 | 6441 | 6489 | 6523 | 6432 | 6475 | 6496 | 6581 | 6552 | 6492 |
| 1400 | 6413 | 6409 | 6523 | 6518 | 6494 | 6496 | 6509 | 6526 | 6573 | 6496 |
| 1500 | 6413 | 6398 | 6483 | 6540 | 6497 | 6497 | 6511 | 6535 | 6559 | 6493 |
| 1600 | 6466 | 6383 | 6506 | 6542 | 6475 | 6487 | 6527 | 6537 | 6573 | 6500 |
| 1700 | 6417 | 6392 | 6476 | 6510 | 6491 | 6510 | 6502 | 6556 | 6550 | 6489 |
| 1800 | 6444 | 6383 | 6499 | 6518 | 6455 | 6501 | 6539 | 6527 | 6553 | 6491 |
| 1900 | 6439 | 6376 | 6522 | 6503 | 6471 | 6456 | 6524 | 6513 | 6541 | 6483 |
| 2000 | 6483 | 6409 | 6485 | 6503 | 6458 | 6488 | 6480 | 6524 | 6519 | 6483 |
| 2100 | 6482 | 6471 | 6498 | 6498 | 6496 | 6469 | 6503 | 6513 | 6501 | 6492 |
| 2200 | 6474 | 6452 | 6527 | 6488 | 6510 | 6457 | 6529 | 6510 | 6527 | 6497 |
| 2300 | 6502 | 6458 | 6517 | 6481 | 6501 | 6467 | 6506 | 6516 | 6537 | 6498 |
| 2400 | 6456 | 6465 | 6513 | 6482 | 6492 | 6489 | 6524 | 6531 | 6556 | 6501 |
| Daily Means | 6463 | 6442 | 6512 | 6523 | 6479 | 6491 | 6505 | 6539 | 6550 | 6500 |

Table 2. Cosmic Ray Intensities for 20 April - 4 May 1984

| Day | April 1984 20 | 21 | 22 | 23 | 24 | 25 | 26 | 27 | 28 | 29 | 30 | May 1984 01 | 02 | 03 | 04 | Hourly Means |
|---|---|---|---|---|---|---|---|---|---|---|---|---|---|---|---|---|
| Hour (UT) | | | | | | | | | | | | | | | | |
| 0100 | 6449 | --- | --- | 6547 | 6507 | 6562 | 6518 | --- | 6158 | 6192 | 6279 | 6300 | 6388 | 6386 | 6476 | 6397 |
| 0200 | 6468 | --- | --- | 6543 | 6521 | 6577 | 6506 | 6331 | 6154 | 6203 | 6323 | 6307 | 6419 | 6342 | 6434 | 6394 |
| 0300 | 6432 | --- | --- | 6541 | 6529 | 6556 | 6500 | 6164 | 6153 | 6195 | 6323 | 6287 | 6406 | 6337 | 6398 | 6371 |
| 0400 | 6445 | --- | --- | --- | 6551 | 6518 | 6531 | 6147 | 6123 | 6167 | 6278 | 6285 | 6393 | 6281 | 6323 | 6337 |
| 0500 | 6473 | --- | --- | --- | 6502 | 6563 | 6502 | 6093 | 6112 | 6154 | 6279 | 6276 | 6392 | --- | 6345 | 6336 |
| 0600 | 6481 | --- | --- | --- | 6574 | 6498 | 6488 | 6119 | 6099 | 6150 | 6277 | 6258 | 6402 | --- | 6323 | 6334 |
| 0700 | 6507 | --- | --- | --- | 6503 | 6536 | 6513 | 6120 | 6102 | 6122 | 6262 | 6293 | 6399 | 6281 | 6334 | 6331 |
| 0800 | 6482 | --- | --- | --- | 6549 | 6490 | 6470 | 6138 | 6090 | 6145 | 6284 | 6261 | 6395 | 6287 | 6323 | 6326 |
| 0900 | 6479 | --- | --- | 6502 | 6549 | 6481 | 6463 | 6147 | 6108 | 6189 | 6290 | 6271 | 6376 | 6308 | 6332 | 6346 |
| 1000 | --- | --- | --- | 6525 | 6522 | 6451 | 6492 | 6205 | 6127 | 6171 | 6316 | 6268 | 6410 | 6288 | 6314 | 6341 |
| 1100 | --- | --- | --- | 6511 | 6530 | 6464 | 6483 | 6237 | 6129 | 6168 | 6325 | 6299 | 6389 | 6274 | 6339 | 6346 |
| 1200 | --- | --- | --- | 6538 | 6516 | 6463 | 6481 | 6188 | 6193 | 6199 | 6314 | 6274 | 6400 | 6302 | 6348 | 6351 |
| 1300 | --- | --- | --- | 6492 | 6505 | 6449 | 6469 | 6185 | 6163 | 6220 | 6337 | 6303 | 6342 | 6306 | 6327 | 6342 |
| 1400 | --- | --- | --- | 6499 | 6527 | 6506 | 6453 | 6158 | 6183 | 6230 | 6330 | 6302 | 6325 | 6315 | 6321 | 6346 |
| 1500 | --- | --- | --- | 6479 | 6490 | 6497 | 6457 | 6148 | 6186 | 6277 | 6282 | 6323 | 6300 | 6321 | 6337 | 6341 |
| 1600 | --- | --- | --- | 6472 | 6488 | 6487 | 6451 | 6144 | 6198 | 6301 | 6258 | 6374 | 6316 | 6326 | 6360 | 6350 |
| 1700 | --- | --- | --- | 6477 | 6521 | 6489 | 6403 | 6178 | 6201 | 6294 | 6226 | 6332 | 6309 | 6321 | 6347 | 6342 |
| 1800 | --- | --- | --- | 6459 | 6517 | 6478 | 6394 | 6218 | 6214 | 6258 | 6248 | 6336 | 6323 | 6326 | 6367 | 6345 |
| 1900 | --- | --- | --- | 6480 | 6509 | 6482 | 6309 | 6221 | 6170 | 6278 | 6246 | 6357 | 6357 | 6334 | 6355 | 6342 |
| 2000 | --- | --- | --- | 6528 | 6499 | 6471 | 6265 | 6258 | 6223 | 6283 | 6243 | 6339 | 6367 | 6369 | 6365 | 6351 |
| 2100 | --- | --- | --- | 6478 | 6503 | 6455 | 6246 | 6254 | 6211 | 6283 | 6284 | 6326 | 6365 | 6403 | 6349 | 6346 |
| 2200 | --- | --- | --- | 6509 | 6496 | 6514 | 6249 | 6223 | 6215 | 6285 | 6255 | 6317 | 6379 | 6439 | 6345 | 6352 |
| 2300 | --- | --- | --- | 6497 | 6543 | 6484 | 6255 | 6205 | 6198 | 6280 | 6265 | 6326 | 6383 | 6466 | 6385 | 6357 |
| 2400 | --- | --- | --- | 6526 | 6546 | --- | --- | 6153 | 6213 | 6303 | 6294 | 6374 | 6394 | 6470 | 6376 | 6355 |
| Daily Means | 6468 | --- | --- | 6505 | 6521 | 6499 | 6430 | 6185 | 6164 | 6223 | 6284 | 6308 | 6372 | 6340 | 6356 | 6358 |

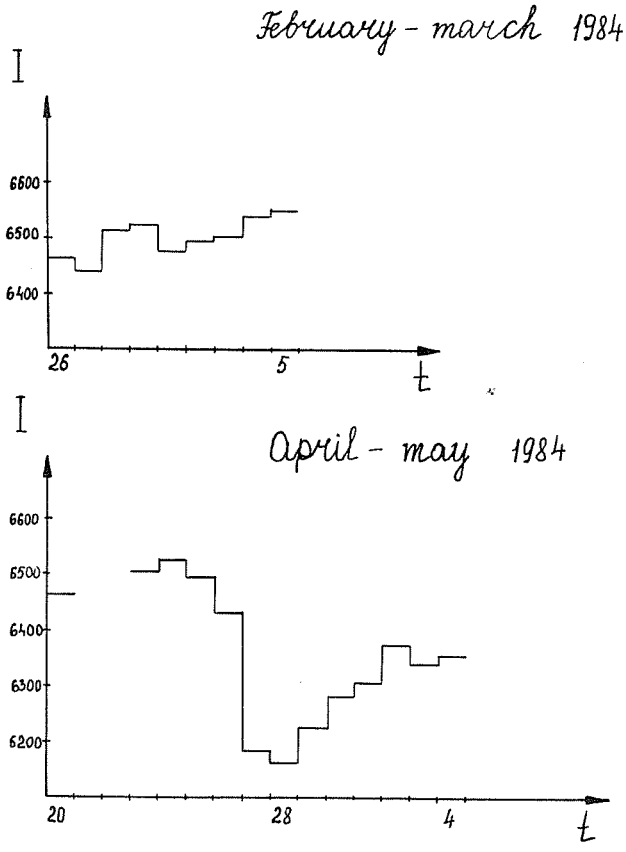


Fig. 1. The mean diurnal total intensity for a.) 26 February - 5 March 1984 and b.) 20 April - 4 May 1984 are shown.

# Cosmic Ray Intensity Variations From the ASK-1 Ionization Chamber at Tixie Bay during the February, April and May 1984 Solar Events

by

V.I. Ipatyev, A.M. Novikov and G.V. Shafer
Institute of Cosmophysical Research and Aeronomy
Lenin Avenue, 31, 677891, Yakutsk, USSR

We present the hourly cosmic ray intensities from the ASK-1 ionization chamber at Tixie Bay (N71.6 E129.0, sea level) for the two periods of 12-21 February and 20 April - 5 May 1984 associated with solar events. These data are pressure corrected ionization burst data.

ASK-1 is a spherical ionization chamber of 950 liters volume, filled with 10 atmospheres of spectral Argon. It is a continuous monitoring instrument since January 1976.

The data are presented in percent from the mean compensated ionization current of cosmic rays $I_0=1.79X10^7$ ion pairs/s in the chamber volume. A detailed description of the ionization chamber, its parameters and data treatment are given in the monograph by Shafer and Shafer (1984).

The solar cosmic ray flares on 16 February and 24 April were not detected by the ionization chamber, but in the second period a large Forbush effect was recorded (see Figure 1). On 26 April at 1700 UT a rapid decrease began and lasted for 13 hours. Then a subsequent gradual decrease continued with large fluctuations up to 1500 UT on 28 April. The amplitude of the Forbush effect in intensity minimum was about 3.5 percent. At the recovery phase on 2 May one more decrease of small amplitude was observed.

Table 1. Hourly Corrected Cosmic Ray Intensity from the ASK-1 Ionization Chamber at Tixie Bay for 12-21 February 1984 (0.01 percent).

| | February 1984 | | | | | | | | | |
|---|---|---|---|---|---|---|---|---|---|---|
| Day | 12 | 13 | 14 | 15 | 16 | 17 | 18 | 19 | 20 | 21 |
| Hour (UT) | | | | | | | | | | |
| 0100 | 447 | 416 | 475 | 512 | 485 | 516 | 483 | 529 | 582 | 511 |
| 0200 | 454 | 455 | 421 | 489 | 493 | 497 | 443 | 512 | 544 | 542 |
| 0300 | 465 | 462 | 447 | 489 | 509 | 480 | 481 | 579 | 613 | 535 |
| 0400 | 488 | 458 | 441 | 487 | 572 | 467 | 495 | 555 | 548 | 567 |
| 0500 | 471 | 505 | 477 | 496 | 588 | 486 | 500 | 531 | 554 | 508 |
| 0600 | 491 | 454 | 467 | 487 | 523 | 513 | 491 | 519 | 575 | 500 |
| 0700 | 490 | 461 | 458 | 492 | 483 | 477 | 544 | 586 | 594 | 541 |
| 0800 | 476 | 438 | 491 | 503 | 484 | 494 | 508 | 550 | 563 | 544 |
| 0900 | 482 | 454 | 489 | 528 | 521 | 459 | 513 | 565 | 553 | 542 |
| 1000 | 504 | 431 | 447 | 486 | 496 | 461 | 506 | 571 | 535 | 562 |
| 1100 | 487 | 374 | 472 | 486 | 479 | 495 | 528 | 551 | 520 | 566 |
| 1200 | 447 | 409 | 465 | 478 | 522 | 454 | 548 | 544 | 547 | 558 |
| 1300 | 455 | 396 | 510 | 468 | 471 | 469 | 509 | 540 | 497 | 544 |
| 1400 | 457 | 395 | 488 | 460 | 530 | 436 | 514 | 561 | 528 | 577 |
| 1500 | 448 | 380 | 497 | 458 | 481 | 458 | 524 | 528 | 535 | 538 |
| 1600 | 450 | 392 | 468 | 504 | 455 | 473 | 488 | 522 | 528 | 535 |
| 1700 | 419 | 352 | 481 | 497 | 450 | 430 | 512 | 523 | 516 | 524 |
| 1800 | 417 | 423 | 463 | 510 | 462 | 451 | 481 | 551 | 492 | 527 |
| 1900 | 402 | 398 | 501 | 556 | 478 | 477 | 506 | 542 | 537 | 525 |
| 2000 | 404 | 414 | 485 | 483 | 483 | 454 | 523 | 519 | 538 | 540 |
| 2100 | 405 | 430 | 542 | 485 | 473 | 458 | 519 | 551 | 544 | 504 |
| 2200 | 378 | 402 | 470 | 499 | 488 | 454 | 557 | 586 | 526 | 497 |
| 2300 | 400 | 432 | 450 | 452 | 485 | 445 | 531 | 540 | 544 | 501 |
| 2400 | 417 | 434 | 441 | 478 | 490 | 484 | 517 | 544 | 519 | 487 |
| Mean | 448 | 422 | 473 | 491 | 496 | 470 | 512 | 546 | 543 | 532 |

Table 2. Hourly Corrected Cosmic Ray Intensity from the ASK-1 Ionization Chamber at Tixie Bay for 20 April - 5 May 1984 (0.01 percent).

| Day | April 1984 20 | 21 | 22 | 23 | 24 | 25 | 26 | 27 | 28 | 29 | 30 | May 1984 01 | 02 | 03 | 04 | 05 |
|---|---|---|---|---|---|---|---|---|---|---|---|---|---|---|---|---|
| Hour (UT) | | | | | | | | | | | | | | | | |
| 0100 | 215 | 132 | 210 | 261 | 127 | 163 | 222 | 134 | --- | 37 | 117 | 110 | 136 | 44 | 121 | 148 |
| 0200 | 218 | 139 | 183 | 260 | 156 | 197 | 223 | 120 | --- | 65 | 112 | 100 | 124 | 50 | 150 | 148 |
| 0300 | 215 | 138 | 198 | 254 | 147 | 201 | 247 | 101 | --- | 71 | 95 | 83 | 117 | 53 | 139 | 162 |
| 0400 | 202 | 149 | 220 | 258 | 134 | 194 | 246 | 101 | --- | 42 | 90 | 78 | 122 | 54 | 140 | 165 |
| 0500 | 200 | 140 | 237 | 227 | 158 | 235 | 255 | 67 | --- | 13 | 101 | 80 | 66 | 64 | 114 | 185 |
| 0600 | 216 | 164 | 245 | 218 | 180 | 224 | 267 | 34 | --- | 90 | 110 | 82 | 85 | 19 | 118 | 159 |
| 0700 | 199 | 144 | 239 | 214 | 188 | 224 | 259 | 48 | --- | 1 | 133 | 61 | 92 | 6 | 116 | 114 |
| 0800 | 223 | 163 | 258 | 221 | 193 | 226 | 253 | 129 | --- | 20 | 127 | 45 | 75 | 23 | 108 | 147 |
| 0900 | 225 | 150 | 262 | 214 | 197 | 221 | 265 | 119 | --- | 33 | 104 | 45 | 81 | 29 | 84 | 154 |
| 1000 | 238 | 155 | 259 | 185 | 206 | 211 | 289 | 113 | --- | 29 | 130 | 69 | 99 | 42 | 105 | 142 |
| 1100 | 241 | 165 | 270 | 206 | 189 | 207 | 298 | 108 | --- | 28 | 107 | 64 | 81 | 24 | 107 | 156 |
| 1200 | 207 | 142 | 252 | 188 | 187 | 178 | 279 | 76 | --- | 20 | 111 | 61 | 81 | 72 | 119 | 145 |
| 1300 | 216 | 155 | 267 | 155 | 140 | 196 | 290 | 71 | --- | 46 | 109 | 67 | 37 | 71 | 120 | 145 |
| 1400 | 187 | 166 | 259 | 186 | 177 | 233 | 323 | 73 | --- | 82 | 106 | 79 | 22 | 50 | 139 | 159 |
| 1500 | 172 | 183 | 245 | 136 | 161 | 212 | 324 | 42 | --- | 1 | 110 | 86 | 9 | 53 | 122 | 169 |
| 1600 | 179 | 188 | 272 | 179 | 160 | 210 | 330 | 68 | --- | 29 | 97 | 82 | 24 | 41 | 136 | 171 |
| 1700 | 152 | 183 | 253 | 170 | 160 | 229 | 364 | 5 | --- | 35 | 114 | 80 | 10 | 73 | 133 | 178 |
| 1800 | 144 | 183 | 279 | 160 | 183 | 199 | 326 | 7 | --- | 47 | 79 | 97 | 6 | 72 | 139 | 161 |
| 1900 | 125 | 167 | 266 | 162 | 175 | 195 | 303 | 48 | --- | 27 | 91 | 117 | 3 | 70 | 138 | 181 |
| 2000 | 110 | 184 | 249 | 162 | 172 | 202 | 292 | 43 | --- | 21 | 114 | 124 | 8 | 87 | 158 | 137 |
| 2100 | 107 | 186 | 257 | 159 | 142 | 193 | 209 | 62 | --- | 38 | 87 | 108 | 11 | 91 | 153 | 150 |
| 2200 | 118 | 202 | 251 | 158 | 165 | 219 | 190 | 66 | --- | 52 | 94 | 114 | 24 | 95 | 140 | 170 |
| 2300 | 97 | 195 | 241 | 134 | 168 | 218 | 164 | 14 | --- | 67 | 116 | 121 | 21 | 110 | 171 | 165 |
| 2400 | 122 | 199 | 248 | 124 | 175 | 247 | 155 | 58 | --- | 58 | 115 | 119 | 49 | 124 | 150 | 145 |
| Mean | 180 | 165 | 247 | 191 | 168 | 210 | 266 | 71 | --- | 16 | 107 | 86 | 56 | 59 | 130 | 158 |

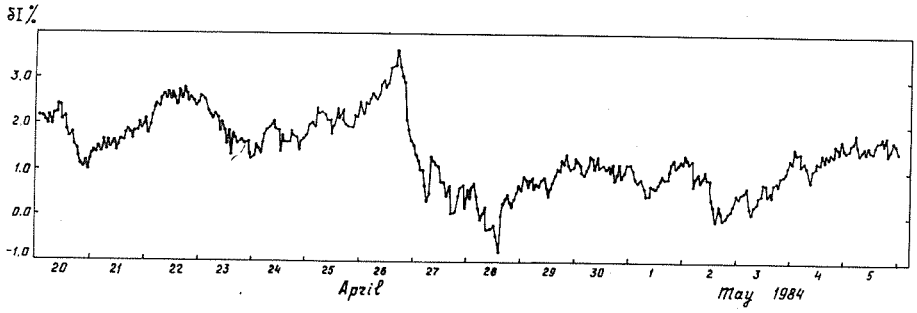


Fig. 1. A large Forbush decrease is seen beginning on 26 April in the ASK-1 ionization chamber data at Tixie Bay.

## REFERENCES

SHAFER, G.V. and Yu.G. SHAFER 1984 Pretsizionnye nabludeniya kosmicheskikh luchei v Yakutske Novosibirsk, **Nauka**, 732 p. (in Russian).

# The 16 February and 24 April 1984 Solar-Terrestrial Events:

## The Ionospheric Observations

by

Richard Thompson
IPS Radio and Space Services
P.O. Box 702
Darlinghurst NSW 2010
Australia

One of the most important justifications for synoptic observations of the Sun-Earth environment is the ability to examine unusual and sometimes unexpected events in that environment. The two events studied in this report are examples.

The first event started at around 0915 UT on 16 February with a sharp rise in the particle flux and did not end until around 1330 UT on 17 February. The source of the proton event appears to have been Region 4408 which crossed the West limb of the Sun on 13 February. This region was growing rapidly as it crossed the limb and had already produced two M class flares.

The second event studied in this report started around 1330 UT on 25 April and ended 2 May at 0855 UT. The initial cause of the event was the very large flare from Region 4474 late on 24 April. The long duration of the event was probably due to a sequence of flares produced by this region in subsequent days.

The following papers illustrate the wide variety of techniques and locations used to observe the ionospheric phenomena associated with these two events. This variety can be seen in the following table.

| Authors | Type of Observation | Location | Events |
|---|---|---|---|
| Ohshio, Ohtani and Terajima | VLF circuits | Tokyo (Japan) | 16 Feb |
| Mori et al. | VLF and HF circuits | Tokyo (Japan) | 16 Feb |
| Koizumi and Ohshio | Ionosonde | Japanese stations | 16 Feb |
| Kainuma et al. | HF doppler measurements | Japan | 16 Feb |
| Sugiuchi et al. | VLF circuits | Japan | 16 Feb |
| Krishnaswamy et al.* | Riometer, magnetometer | South Pole | 16 Feb |
| Klekociuk | VLF circuits | | 16 Feb |
| Ulyev and Shirochkov | Riometer | Arctic and Antarctic stations | 16 Feb, 24 Apr |
| Wilkinson | Ionosonde | Global ionosondes | 16 Feb, 24 Apr |
| Brunelli et al. | Neutron Monitors, riometer magnetometer, ionosonde, VLF circuits, auroral spectra | Kola Peninsula (East USSR) | 16 Feb, 24 Apr |
| Belyaev et al. | Ionosonde | Sverdlovsk (Central USSR) | 16 Feb, 24 Apr |
| Kuznetsov et al. | Ionosonde, magnetometer | Novosibirsk (Central USSR) | 16 Feb, 24 Apr |
| Maksimov et al. | Ionosonde | Khabarovsk (West USSR) | 16 Feb, 24 Apr |
| Atanasijevic and Balster | VLF circuit | Nijmegen (Netherlands) | 24 Apr |
| Ohshio et al. | Ionosonde, HF, LF and VLF circuits | Japan | 24 Apr |

*Krishnaswamy et al. paper was moved to the Geomagnetic Section (see page 327 and following).

# SPA's Observed at Inubo During February 6-March 5, 1984

by

Mitsuo Ohshio
Radio Research Laboratory
4-2-1 Nukui-Kita, Koganei, Tokyo 184, Japan

and

Akira Ohtani and Yoshiko Terajima
Inubo Radio Wave Observatory, Radio Research Laboratory
9961 Tennodai, Choshi, Chiba 288, Japan

This report gives sudden phase anomalies (SPA's) which appeared on any of the five circuits of long-distance propagating VLF radio waves received at Inubo Radio Wave Observatory (35°42.2' N, 140°51.5' E), Radio Research Laboratory, Japan during February 6-March 5, 1984 as a period to be interested in (Table 2). The parameters of the five circuits concerned are listed in Table 1. The five circuits concerned are useful for detecting SPA's

Table 1. Parameters for the circuits of the available long-distance propagating VLF radio waves.

| Transmitting Stations | | | | | | Arc Distance |
|---|---|---|---|---|---|---|
| Name | Call Sign | Location (Geographic Coordinates) | | Frequency (kHz) | Radiation Power (kW) | to Inubo (Mm) |
| Rugby | GBR | 52°22' N | 001°11' W | 16.0 | 60 | 9.55 |
| La Reunion | Ω/LR | 20°58' S | 055°17' E | 13.6 | 10 | 10.97 |
| North West Cape | NWC | 21°49' S | 114°10' E | 22.3 | 1000 | 6.99 |
| Haiku | Ω/H | 21°24' N | 157°50' W | 13.6 | 10 | 6.10 |
| North Dakota | Ω/ND | 46°22' N | 098°21' W | 13.6 | 10 | 9.14 |

with a longitudinal width of 262°50' (about 3/4 of the circumference of the earth).

171 SPA events observed under the above-described condition are given in Table 2. In the table, notes for reading off are as follows:
(1) A blank box represents no phenomenon.
(2) An oblique line represents no observation.
(3) The letter E or D with parentheses attached to a time denotes that the time concerned is earlier or more delayed than the given time, respectively.
(4) An asterisk shows a multi-peak event.
(5) The figure 0 denotes a null SPA effect, i.e., an SPA in the case of no change in phase in spite of any variation in amplitude. It is found at the event on February 18 on the GBR circuit.
(6) Unfortunately, there was no observational period owing to an interruption of electric current at Inubo due to a snow-laden accident of a power-transmission line near Inubo during the period from 1511 U.T. on February 17 till 1225 U.T. on February 18, 1984. In the interval, three SPA events on February 17 and six ones on February 18 were observed on any of the five circuits of long-distance propagating VLF radio waves from Aldra (Ω/N, 66°25' N, 013°09' E, 11.3 kHz, 10 kW, 7.81 Mm, in conformity to the order of the parameters in Table 1), La Reunion (11.3 kHz), North West Cape, Haiku (11.3 kHz), and North Dakota (11.3 kHz) (cf. Table 1) to Toyokawa (34.83° N, 137.37° E), the Research Institute of Atmospherics, Nagoya University, Japan.
(7) In Table 2, SPA's till March 5, 1984 are given as described at the beginning of this report. However, SPA's till March 4, 1984 are apparently given there, because there were no phenomena on March 5, 1984.

The SPA's observed at Inubo during February 6-March 5, 1984 had the following features.
(i) Occurrence frequency, $N$ and
(ii) Magnitude, $\Delta\phi$
Here, 'occurrence frequency' in the case that a positive SPA was observed even on only one circuit is decided to be unity, i.e., $N(\Delta\phi > 0^{\circ}) = 1$ and 'magnitude' means the maximum deviation of an SPA from the quiet value.

According to the observational data, $N(\Delta\phi > 0^{\circ}$, Dec. 1983) = 23 and $N(\Delta\phi > 0^{\circ}$, Jun. 1984) = 16. The former was small together with $N(\Delta\phi > 0^{\circ}$, Nov. 1983) = 12. The latter truly expressed a case typical for small occurrence frequencies which the months in 1984 after June showed. On the contrary, the data indicate that the occurrence frequencies for the months lying between the above-described two groups of months were large in a group, i.e., $N(\Delta\phi > 0^{\circ}$, Jan.-May 1984) = 91, 179, 106, 123, and 151. Particularly, $N(\Delta\phi > 0^{\circ}$, Feb. 1984) = 179 showed the maximum value during the months. As described in the above item (6), if SPA's during the interruption of electric current at Inubo had been observed likewise at Toyokawa, $N$ = 188 could have been obtained.

Next, when the occurrence frequencies in the cases that all the SPA's on all the avilable circuits except no phenomena attained their values above 50 and 100 degrees are expressed as $N(\Delta\phi \geq 50^0)$ and $N(\Delta\phi \geq 100^0)$, respectively (,although the condition is severe and rough), $N(\Delta\phi \geq 50^0$, Dec. 1983-Jun. 1984) = 3, 4, 6, 3, 6, 11, and 0 and $N(\Delta\phi \geq 100^0$, Dec. 1983-Jun. 1984) = 0, 1, 0, 0, 2, 3, and 0 were recorded. During these seven months, the period during Jan.-May 1984 during which $N(\Delta\phi > 0^0)$'s were large was not prominent in both the occurrence frequencies. It will be pointed out, however, that May 1984 had both the relatively large occurrence frequencies for these seven months in terms of a single month.

Generally, in the case of a comparison in terms of a single month it could be concluded that relatively small and much SPA's appeared in February 1984 in comparison with the three months preceding February and the four months following February. It will be concluded that events at about 0325 on 10th, about 0249 on 11th, about 0216 on 22nd, about 0205 and about 0358 on 24th, and about 0326 on 25th (,where a number of four figures represent the time of the maximum SPA value, $t_m$ in U.T. and an ordinal number represents a date in February 1984) were outstanding in February 1984, a phase deviation per unit propagational distance (e.g., 1 Mm), $\Delta\phi_D$ being considered. Further, during the period concerned in March, i.e., during March 1-5 $N(\Delta\phi > 0^0) = 29$, $N(\Delta\phi \geq 50^0) = 0$, and $N(\Delta\phi \geq 100^0) = 0$ were obtained. On the other hand, although the period corresponded to 16.1 % of the whole March, $N(\Delta\phi > 0^0$, Mar. 1-5, 1984)/$N(\Delta\phi > 0^0$, Mar. 1984) = 27.4 % was obtained. It could be concluded, therefore, that relatively small and much SPA's appeared also during this short period in the same way as during the whole February.

(iii) Shape in time variation

Generally, a large SPA is caused by a large solar X-ray flare and the follow of the former to the latter time variation is good in this case [Ohshio, 1978]. It is assumed, therefore, that both have nearly equal times in each start, maximum, and end. Here, times spent for increasing stage and decreasing one are represented by $\tau_i$ and $\tau_d$, respectively.

An event to have $t_m \fallingdotseq 0216$ U.T. on February 22 and to take $\tau_i \fallingdotseq 49$ min. and $\tau_d \fallingdotseq 136$ min. and another event to have $t_m \fallingdotseq 0204$ U.T. on February 24 and to take $\tau_i \fallingdotseq 40$ min. and $\tau_d > 97$ min. formed a slow increasing type. However, the relation between the maximum enhanced solar X-ray flare radiation flux [SGD, 1984] which caused these two SPA phenomena and $\tau_d/\tau_i$ was found to be commonplace [Ohshio, 1978]. The seven large SPA events other than these two events (which occurred on February 10, 11, 19, 24, 25, 27, and 29 and which included the above-described five outstanding SPA events) took shape in combination with monotonous increase in a broad sense and monotonous decrease in a broad sense. This shape occupies the maximum ratio (37 %) among shapes in time variation in enhanced solar X-ray flare radiation flux [Ohshio, 1978]. It is generally discussed that there were no SPA's to show any peculiar shapes in time variation in the period concerned at least for large SPA events.

## References


Ohshio, M. 1978 Ionospheric *D* region Disturbances Caused by Solar X-ray Flares, pp. 1-346, Planning and Support Division, Radio Res. Labs., Tokyo, June 1978.

SGD 1984 Solar-Geophysical Data, comprehensive reports, No. 480 Part II, pp. 52-56, U.S. Dept. of Commerce, National Oceanic and Atmospheric Administration, National Environmental Satellite, Data, and Information Service, National Geophysical Data Center, Boulder, Colo., Aug. 1984.

Table 2. SPA's observed at Inubo during February 6-March 5, 1984 (a).

| Date | GBR-16.0kHz | | | | LA REUNION-13.6kHz | | | | NWC-22.3kHz | | | | HAIKU-13.6kHz | | | | N.DAKOTA-13.6kHz | | | |
|---|---|---|---|---|---|---|---|---|---|---|---|---|---|---|---|---|---|---|---|---|
| | UNIVERSAL TIME | | | PA | UNIVERSAL TIME | | | PA | UNIVERSAL TIME | | | PA | UNIVERSAL TIME | | | PA | UNIVERSAL TIME | | | PA |
| | START | END | MAX | (DEG) | START | END | MAX | (DEG) | START | END | MAX | (DEG) | START | END | MAX | (DEG) | START | END | MAX | (DEG) |
| 6 | 0423 | 0449 | 0440 | 12 | 0430 | 0644 | 0438 | 62 | 0431 | 0722 | 0436 | 42 | 0431 | 0613 | 0438 | 16 | 0431 | 0448 | 0438 | 8 |
| 6 | | | | | 2326 | 0016 | 2340 | 17 | 2325 | 0019 | 2348 | 46 | 2326 (D) | 0020 (D) | 2348 | 44 | 2327 (D) | 0018 (D) | 2348 | 24 |
| 7 | | | | | 0019 | 0048 | 0026 | 9 | 0020 | 0050 | 0026 | 14 | 0020 (E) | 0118 | 0025 | 17 | 0018 (E) | 0110 | 0027 | 14 |
| 7 | 0424 | 0440 | 0431 | 13 | 0407 | 0607 | 0432 | 7 | 0408 | 0608 | 0430 | 10 | | | | | | | | |
| 7 | 0633 | 0710 | 0643 | 13 | 0638 | 0706 | 0647 | 4 | | | | | | | | | | | | |
| 7 | | | | | 0852 | 0924 | 0857 | 16 | 0852 | 0916 | 0856 | 10 | | | | | | | | |
| 7 | | | | | 1028 | 1122 | 1035 | 19 | | | | | | | | | | | | |
| 7 | | | | | 2230 | 2253 | 2240 | 4 | 2231 | 2309 | 2241 | 17 | 2229 | 2323 | 2243 | 37 | 2232 | 2300 | 2244 | 18 |
| 8 | | | | | 0126 | 0232 | 0138 | 22 | 0125 | 0217 | 0134 | 26 | 0127 | 0229 | 0136 | 16 | 0127 | 0157 | 0136 | 14 |
| 8 | | | | | 0254 | 0406 | 0318 | 35 | 0256 | 0409 | 0316 | 39 | 0256 | 0411 | 0320 | 22 | 0258 | 0417 | 0320 | 24 |
| 8 | | | | | 0409 | 0428 | 0416 | 4 | 0410 | 0428 | 0414 | 4 | 0411 | 0433 | 0414 | 12 | 0410 | 0424 | 0417 | 6 |
| 8 | 0458 | 0422 | 0406 | 12 | 0458 | 0446 | 0408 | 9 | 0459 | 0442 | 0409 | 7 | | | | | | | | |
| 8 | | | | | 0732 | 0936 | 0744 | 77 | 0732 | 0858 | 0744 | 44 | | | | | | | | |
| 9 | | | | | | | | | | | | | 0038 | 0040 | 0043 | 3 | | | | |
| 9 | | | | | | | | | 0041 | 0146 | 0102 | 31 | 0041 | 0148 | 0101 | 22 | 0042 | 0147 | 0100 | 12 |
| 9 | | | | | 0412 | 0436 | 0419 | 7 | 0412 | 0440 | 0418 | 4 | | | | | | | | |
| 9 | | | | | 0437 | 0610 | 0446 | 4 | | | | | 0438 | 0446 | 0448 | 8 | | | | |
| 9 | | | | | 0614 | 0716 | 0623 | 21 | 0616 | 0717 | 0622 | 14 | | | | | | | | |
| 9 | | | | | 0936 | 1026 | 0952 | 12* | | | | | | | | | | | | |
| 9 | | | | | 1133 | 1209 | 1144 | 13 | | | | | | | | | | | | |
| 9 | | | | | | | | | 2336 | 0042 | 0000 | 10 | 2338 | 0030 | 0000 | 7 | | | | |
| 10 | 0136 | 0206 | 0143 | 12 | 0137 | 0248 | 0149 | 41 | 0136 | 0240 | 0147 | 48 | 0138 | 0252 | 0149 | 26 | 0140 | 0219 | 0149 | 13 |
| 10 | 0306 | 0413 | 0324 | 70 | 0304 | 0400 | 0325 | 235 | 0255 | 0426 | 0323 | 162 | 0306 | 0407 | 0325 | 114 | 0304 | 0440 | 0325 | 61 |
| 10 | 0414 | 0430 | 0421 | 14 | | | | | 0412 | 0447 | 0418 | 4 | | | | | | | | |
| 10 | | | | | 0802 | 0822 | 0809 | 4 | 0803 | 0838 | 0810 | 7 | | | | | | | | |
| 10 | 1031 | 1041 | 1034 | 23 | 1033 | 1147 | 1038 | 90 | 1033 | 1040 | 1037 | 18 | | | | | | | | |
| 10 | | | | | 1254 | 1312 | 1301 | 4 | | | | | | | | | | | | |
| 10 | 2247 | 2330 | 2254 | 28 | 2240 | 2327 | 2246 | 13 | 2241 | 2326 | 2241 | 37 | 2240 | 2346 | 2253 | 49 | 2242 | 2323 | 2251 | 19 |
| 11 | | | | | 0127 | 0230 (D) | 0144 | 17 | 0126 | 0227 (D) | 0140 | 18 | 0127 | 0230 | 0140 | 11 | 0128 | 0200 | 0139 | 9 |
| 11 | 0238 | 0316 | 0248 | 29 | 0238 (E) | 0342 (D) | 0250 | 174 | 0238 (E) | 0342 (D) | 0248 | 132 | 0240 | 0443 | 0250 | 97 | 0239 | 0442 | 0249 | 79 |
| 11 | | | | | 0342 (E) | 0430 | 0349 | 23 | 0342 (E) | 0433 (D) | 0347 | 18 | | | | | | | | |
| 11 | | | | | 0430 | 0444 (D) | 0437 | 12 | 0431 | 0454 (D) | 0436 | 7 | | | | | | | | |
| 11 | | | | | 0444 (E) | 0522 | 0459 | 14 | 0454 (E) | 0524 | 0459 | 13 | | | | | | | | |
| 11 | | | | | 0528 | 0546 | 0532 | 6 | 0528 | 0546 | 0532 | 6 | | | | | | | | |
| 11 | | | | | 0631 | 0722 | 0653 | 26* | 0632 | 0736 | 0652 | 20* | | | | | | | | |
| 11 | | | | | 0824 | 0857 | 0832 | 10 | | | | | | | | | | | | |
| 11 | | | | | 0903 | 0920 | 0907 | 9 | 0903 | 0917 | 0906 | 8 | | | | | | | | |
| 11 | | | | | 2242 | 2348 | 2300 | 24* | 2240 | 0014 | 2300 | 80* | 2238 | 0014 | 2300 | 95* | 2243 | 2335 | 2300 | 38* |
| 12 | 0013 | 0032 | 0018 | 9 | 0017 | 0035 | 0021 | 16 | 0017 | 0047 | 0021 | 27 | 0017 | 0112 | 0021 | 28 | 0013 | 0108 | 0020 | 13 |
| 12 | | | | | 0246 | 0310 | 0251 | 4 | 0247 | 0306 | 0248 | 4 | 0248 | 0309 | 0250 | 4 | 0244 | 0310 | 0248 | 6 |
| 12 | | | | | 0316 | 0340 | 0322 | 14 | 0317 | 0335 | 0322 | 14 | 0318 | 0342 | 0322 | 7 | 0318 | 0340 | 0323 | 6 |
| 12 | | | | | 0340 | 0453 | 0358 | 28 | 0342 | 0442 | 0358 | 22 | 0342 | 0432 | 0358 | 11 | | | | |
| 12 | | | | | 0442 | 0647 | 0440 | 28 | 0420 | 0640 | 0441 | 21 | | | | | | | | |
| 12 | 0916 | 0948 | 0918 | 10 | 0916 | 1018 | 0922 | 86 | 0916 | 0952 | 0920 | 35 | | | | | | | | |
| 12 | | | | | 1042 | 1132 | 1106 | 11 | | | | | | | | | | | | |
| 12 | 1702 | 1807 | 1740 | 43 | | | | | | | | | | | | | | | | |
| 13 | | | | | 0702 | 0735 | 0710 | 4 | 0700 | 0721 | 0710 | 6 | | | | | | | | |
| 13 | | | | | 0800 | 0908 | 0828 | 41 | 0801 | 0844 | 0824 | 24 | | | | | | | | |
| 14 | | | | | 0139 | 0309 | 0146 | 36 | 0137 | 0240 | 0144 | 42 | 0139 | 0248 | 0145 | 23 | 0137 | 0222 | 0143 | 26 |
| 14 | | | | | | | | | 0313 | 0348 | 0321 | 4 | 0314 | 0340 | 0321 | 3 | | | | |

Table 2. *continued* (b).

| Date | GBR-16.0kHz | | | | LA REUNION-13.6kHz | | | | NWC-22.3kHz | | | | HAIKU-13.6kHz | | | | N.DAKOTA-13.6kHz | | | |
|---|---|---|---|---|---|---|---|---|---|---|---|---|---|---|---|---|---|---|---|---|
| | UNIVERSAL TIME | | | PA | UNIVERSAL TIME | | | PA | UNIVERSAL TIME | | | PA | UNIVERSAL TIME | | | PA | UNIVERSAL TIME | | | PA |
| | START | END | MAX | (DEG) | START | END | MAX | (DEG) | START | END | MAX | (DEG) | START | END | MAX | (DEG) | START | END | MAX | (DEG) |
| 14 | | | | | | | | | 0204 | 0227 | 0208 | 6 | | | | | | | | |
| 16 | | | | | | | | | 0224 | 0312 | 0231 | 16 | | | | | | | | |
| 16 | | | | | 0737 | 0856 | 0745 | 42* | 0738 | 0857 | 0744 | 26* | | | | | | | | |
| 16 | | | | | | | | | | | | | 2156 | 2248 | 2202 | 21 | 2156 | 2248 | 2205 | 16 |
| 17 | | | | | | | | | 0014 | 0126 | 0104 | 10 | 0016 | 0147 | 0106 | 6 | 0012 | 0112 | 0103 | 14 |
| 17 | | | | | 0604 | 0730 | 0620 | 41 | 0601 | 0718 | 0618 | 35 | | | | | | | | |
| 17 | 1152 | 1300 | 1159 | 16 | 1150 | 1252 | 1200 | 43 | | | | | | | | | | | | |
| 18 | | | | 0 | 2240 | 2320 | 2247 | 12 | 2240 | 2330 | 2246 | 42 | 2239 | 2350 | 2247 | 61 | 2238 | 2354 | 2247 | 48 |
| 19 | | | | | | | | | 0028 | 0043 | 0035 | 6 | 0029 | 0048 | 0032 | 4 | 0026 | 0111 | 0036 | 14 |
| 19 | | | | | 0157 | 0224 | 0200 | 6 | 0157 | 0228 | 0200 | 8 | 0157 | 0230 | 0200 | 4 | | | | |
| 19 | 0237 | 0356 | 0257 | 39 | 0234 | 0450 | 0257 | 138 | 0233 | 0428 | 0250 | 112 | 0236 | 0401 | 0257 | 70 | 0237 | 0336 | 0250 | 58 |
| 19 | | | | | 0720 | 0833 | 0730 | 37 | 0721 | 0827 | 0728 | 16 | | | | | | | | |
| 19 | | | | | | | | | 2359 | 0020 | 0003 | 7 | 2359 | 0029 | 0004 | 6 | | | | |
| 20 | 0031 | 0128 | 0040 | 26 | 0031 | 0130 | 0038 | 41 | 0031 | 0146 | 0038 | 62 | 0029 | 0149 | 0038 | 54 | 0032 | 0136 | 0039 | 38 |
| 20 | | | | | | | | | 0150 | 0212 | 0154 | 4 | 0150 | 0216 | 0154 | 3 | | | | |
| 20 | | | | | 0433 | 0506 | 0441 | 12 | 0432 | 0506 | 0440 | 10 | 0433 | 0456 | 0446 | 13 | | | | |
| 20 | 0602 | 0644 | 0618 | 17 | 0600 | 0632 | 0618 | 9* | 0602 | 0638 | 0617 | 8* | | | | | | | | |
| 20 | 0644 | 0804 | 0642 | 22 | 0643 | 0829 | 0756 | 56 | 0642 | 0816 | 0756 | 39 | 0644 | 0709 | 0747 | 7 | | | | |
| 20 | | | | | 0947 | 1040 | 0957 | 23 | | | | | | | | | | | | |
| 20 | | | | | 1148 | 1210 | 1157 | 6 | | | | | | | | | | | | |
| 20 | | | | | | | | | | | | | 2332 | 0032 | 2346 | 13 | | | | |
| 21 | | | | | | | | | | | | | 0035 | 0149 | 0049 | 20 | | | | |
| 21 | | | | | 0200 | 0245 | 0211 | 10 | | | | | 0201 | 0246 | 0206 | 8 | 0202 | 0226 | 0206 | 6 |
| 21 | | | | | 0251 | 0316 | 0256 | 4 | | | | | 0257 | 0312 | 0255 | 2 | | | | |
| 21 | | | | | 0414 | 0638 | 0604 | 11 | | | | | | | | | | | | |
| 21 | | | | | 0644 | 0717 | 0650 | 6 | | | | | | | | | | | | |
| 21 | | | | | 0732 (E) | 0801 (D) | 0743 | 8 | | | | | | | | | | | | |
| 21 | | | | | 0801 | 0850 | 0808 | 31 | 0800 | 0846 | 0809 | 17 | | | | | | | | |
| 21 | | | | | 0904 | 0929 | 0909 | 14 | | | | | | | | | | | | |
| 21 | | | | | 1046 | 1153 | 1053 | 42 | | | | | | | | | | | | |
| 21 | | | | | | | | | 2316 | 2330 | 2318 | 4 | 2316 | 2332 | 2318 | 1 | | | | |
| 21 | | | | | | | | | 2332 | 2357 | 2340 | 7 | 2333 | 0000 | 2338 | 4 | 2331 | 0008 | 2337 | 9 |
| 22 | | | | | | | | | | | | | 0036 | 0053 | 0043 | 4 | | | | |
| 22 | | | | | 0014 | 0107 | 0059 | 8 | 0053 | 0112 | 0054 | 12 | 0014 | 0116 | 0059 | 7 | 0014 | 0116 | 0059 | 8 |
| 22 | 0127 | 0332 | 0214 | 39 | 0127 | 0432 | 0216 | 165 | 0120 | 0414 | 0215 | 126 | 0120 | 0354 | 0215 | 111 | 0127 | 0356 | 0216 | 74 |
| 22 | | | | | 0449 | 0534 | 0401 | 10 | 0411 | 0414 | 0401 | 8 | | | | | | | | |
| 22 | 0610 | 0641 | 0618 | 17 | 0611 | 0633 | 0620 | 7 | 0612 | 0631 | 0616 | 6 | | | | | | | | |
| 22 | 0641 | 0700 | 0645 | 7 | 0636 | 0700 | 0646 | 9 | 0637 | 0657 | 0641 | 1 | | | | | | | | |
| 22 | | | | | 0704 | 0722 | 0708 | 6 | 0704 | 0726 | 0709 | 1 | | | | | | | | |
| 22 | 0808 | 0842 | 0818 | 16 | 0808 | 0906 | 0819 | 71 | 0808 | 0858 | 0818 | 38 | | | | | | | | |
| 22 | | | | | 1017 | 1052 | 1027 | 9 | | | | | | | | | | | | |
| 22 | | | | | | | | | 2342 | 0006 (D) | 2357 | 45 | 2357 | 0005 | 2356 | 3 | 2352 | 0007 (D) | 2356 | 6 |
| 22 | 0006 | 0038 | 0010 | 13 | | | | | 0006 (E) | 0050 | 0008 | 35 | 0006 | 0042 | 0010 | 16 | 0007 (E) | 0028 | 0011 | 14 |
| 23 | | | | | | | | | 0018 | 0118 | 0104 | 11 | 0018 | 0122 | 0106 | 6 | | | | |
| 23 | 0127 | 0220 | 0142 | 12 | | | | | 0125 | 0218 | 0140 | 33 | 0126 | 0218 | 0136 | 14 | 0126 | 0203 | 0138 | 7 |
| 23 | | | | | 0246 | 0310 | 0252 | 10 | 0246 | 0307 | 0250 | 11 | 0247 | 0308 | 0252 | 1 | 0246 | 0316 | 0253 | 6 |
| 23 | | | | | 0539 | 0617 | 0547 | 13 | 0540 | 0615 | 0546 | 14 | | | | | | | | |
| 23 | | | | | 0628 | 0712 | 0634 | 14 | 0628 | 0707 | 0634 | 13 | | | | | | | | |
| 23 | | | | | 0742 | 0816 | 0747 | 9 | | | | | | | | | | | | |
| 23 | | | | | 0856 | 0940 | 0900 | 7 | | | | | | | | | | | | |

Table 2. *continued* (c).

| Date | GBR-16.0kHz | | | | LA REUNION-13.6kHz | | | | NWC-22.3kHz | | | | HAIKU-13.6kHz | | | | N.DAKOTA-13.6kHz | | | |
|---|---|---|---|---|---|---|---|---|---|---|---|---|---|---|---|---|---|---|---|---|
| | UNIVERSAL TIME | | | PA | UNIVERSAL TIME | | | PA | UNIVERSAL TIME | | | PA | UNIVERSAL TIME | | | PA | UNIVERSAL TIME | | | PA |
| | START | END | MAX | (DEG) | START | END | MAX | (DEG) | START | END | MAX | (DEG) | START | END | MAX | (DEG) | START | END | MAX | (DEG) |
| 23 | | | | | 1312 | 1343 | 1320 | 9 | | | | | | | | | | | | |
| 23 | | | | | | | | | 2320 | 0008 | 2336 | 11 | 2322 | 0006 | 2335 | 9 | 2320 | 2358 | 2332 | 11 |
| 24 | | | | | | | | | 0011 | 0030 | 0015 | 7 | 0012 | 0034 | 0016 | ✓ | | | | |
| 24 | 0106 | (D) 0124 | 0112 | 16 | 0104 | 0123 | 0111 | 22 | 0103 | (D) 0134 | 0111 | 29 | 0106 | (D) 0125 | 0111 | 19 | 0106 | 0124 | 0112 | 18 |
| 24 | (E) 0124 | 0323 | 0206 | 71 | 0124 | 0341 | 0204 | 125 | (E) 0134 | 0340 | 0205 | 88 | (E) 0125 | 0330 | 0206 | 76 | 0124 | 0340 | 0205 | 85 |
| 24 | 0341 | 0400 | 0348 | 53 | 0341 | 0448 | 0358 | 168 | 0340 | 0416 | 0356 | 93 | 0341 | 0414 | 0356 | 73 | 0343 | 0422 | 0358 | 54 |
| 24 | | | | | 0644 | (D) 0706 | 0640 | 17 | 0642 | (D) 0701 | 0650 | 14 | | | | | | | | |
| 24 | 0707 | 0747 | 0712 | 29 | (E) 0706 | 0812 | 0713 | 80 | (E) 0704 | 0849 | 0712 | 56 | | | | | | | | |
| 24 | | | | | 0850 | 0920 | 0900 | 10 | | | | | | | | | | | | |
| 24 | | | | | | | | | 2233 | 2254 | 2238 | 6 | 2233 | 2248 | 2240 | 7 | | | | |
| 24 | 2336 | 0018 | 2352 | 28 | 2335 | 0026 | 2346 | 13 | 2332 | 0046 | 2356 | 27 | 2336 | 0100 | 2352 | 22 | 2336 | 0024 | 2350 | 8 |
| 24 | | | | | | | | | 0140 | 0152 | 0146 | 8 | 0139 | 0156 | 0146 | 4 | 0138 | 0158 | 0142 | 7 |
| 24 | | | | | 0147 | 0239 | 0208 | 14 | 0146 | 0211 | 0210 | 30 | 0146 | 0248 | 0208 | 11 | 0148 | 0233 | 0210 | 12 |
| 24 | 0312 | 0440 | 0326 | 70 | 0310 | 0409 | 0326 | 188 | 0310 | 0420 | 0325 | 131 | 0310 | 0426 | 0326 | 108 | 0310 | 0430 | 0326 | 89 |
| 24 | | | | | 0426 | 0446 | 0437 | 7 | 0431 | 0446 | 0437 | ✓ | | | | | | | | |
| 24 | | | | | 0914 | 0946 | 0922 | 13 | | | | | | | | | | | | |
| 24 | 1003 | 1041 | 1032 | 32 | | | | | | | | | | | | | | | | |
| 24 | | | | | | | | | 2232 | 2306 | 2242 | 6 | 2233 | 2307 | 2242 | 4 | | | | |
| 26 | 0110 | 0152 | 0120 | 8 | | | | | 0107 | 0201 | 0120 | 16 | 0107 | 0216 | 0119 | 11 | | | | |
| 26 | | | | | 0413 | 0448 | 0418 | 6 | 0413 | 0442 | 0419 | ✓ | | | | | | | | |
| 26 | | | | | 1240 | 1400 | 1300 | 28 | | | | | | | | | | | | |
| 26 | | | | | | | | | | | | | 2334 | 2356 | 2339 | 3 | | | | |
| 27 | | | | | | | | | | | | | 0022 | 0110 | 0033 | 8 | | | | |
| 27 | 0216 | 0248 | 0220 | 22 | 0207 | 0243 | 0220 | 14 | | | | | 0207 | 0256 | 0220 | 11 | | | | |
| 27 | | | | | 0727 | 0829 | 0738 | 14 | 0730 | 0806 | 0738 | 6 | | | | | | | | |
| 27 | 0852 | 0950 | 0900 | 24 | 0852 | 1101 | 0901 | 108 | 0853 | 0854 | 0904 | 61 | | | | | | | | |
| 27 | | | | | | | | | 2102 | 2150 | 2116 | 47 | 2102 | 2242 | 2116 | 83 | 2103 | 2246 | 2118 | 69 |
| 28 | | | | | | | | | 0122 | 0200 | 0131 | ✓ | | | | | | | | |
| 28 | | | | | 0703 | 0721 | 0710 | 4 | 0703 | 0721 | 0709 | 4 | | | | | | | | |
| 28 | | | | | 0721 | 0623 | 0744 | 20 | 0722 | 0621 | 0742 | 16 | | | | | | | | |
| 28 | | | | | 0724 | 0826 | 0738 | 10 | 0723 | 0757 | 0736 | 7 | | | | | | | | |
| 28 | | | | | | | | | | | | | 2050 | 2118 | 2048 | 14 | | | | |
| 28 | | | | | | | | | 2203 | 2300 | 2225 | 11 | 2203 | 2316 | 2225 | 23 | 2206 | 2330 | 2224 | 22 |
| 29 | 0222 | 0258 | 0238 | 6 | 0223 | 0316 | 0248 | 7 | 0224 | 0310 | 0247 | 9 | 0223 | 0303 | 0247 | 3 | 0222 | 0302 | 0246 | 6 |
| 29 | 0330 | 0403 | 0343 | 12 | 0329 | 0412 | 0341 | 8 | 0331 | 0407 | 0340 | 8 | 0330 | 0408 | 0340 | 4 | 0332 | 0418 | 0341 | 12 |
| 29 | 0739 | 0751 | 0744 | 13 | | | | | | | | | | | | | | | | |
| 29 | 0758 | 0856 | 0802 | 31 | 0757 | 0825 | 0800 | ✓ | | | | | | | | | | | | |
| 29 | 1006 | 1144 | 1026 | 31 | | | | | | | | | | | | | | | | |
| 29 | 1125 | 1206 | 1140 | 17 | 1124 | 1208 | 1149 | 17* | | | | | | | | | | | | |
| 29 | | | | | | | | | | | | | 2131 | 2144 | 2136 | ✓ | 2131 | 2140 | 2136 | 13 |
| 29 | | | | | 2141 | 2232 | 2156 | 16 | | | | | 2144 | (D) 2234 | 2154 | 89 | 2140 | (D) 2234 | 2144 | 119 |
| 29 | | | | | | | | | 2234 | 2330 | 2239 | 9 | (E) 2234 | 2342 | 2237 | 21 | (E) 2236 | 2330 | 2238 | 20 |
| 1 | | | | | | | | | 0010 | 0030 | 0016 | 4 | 0009 | 0037 | 0017 | 4 | | | | |
| 1 | | | | | | | | | 0046 | 0130 | 0104 | 7 | 0044 | 0124 | 0104 | 4 | | | | |
| 1 | 0147 | 0212 | 0144 | 9 | 0147 | 0218 | 0146 | 14 | 0147 | 0230 | 0142 | 14 | 0147 | 0226 | 0142 | 8 | 0147 | 0218 | 0143 | 8 |
| 1 | 0232 | 0310 | 0236 | 36 | 0232 | 0344 | 0238 | 82 | 0232 | 0355 | 0237 | 81 | 0232 | 0348 | 0238 | 70 | 0232 | 0335 | 0237 | 46 |
| 1 | | | | | 0438 | 0442 | 0442 | ✓ | 0438 | 0443 | 0443 | ✓ | | | | | | | | |
| 1 | | | | | 0442 | 0447 | 0401 | 16 | 0444 | 0438 | 0401 | 12 | | | | | | | | |
| 1 | 0731 | 0808 | 0736 | 19 | 0729 | 0840 | 0737 | 47 | 0729 | 0824 | 0735 | 18 | | | | | | | | |
| 1 | | | | | 0847 | 1044 | 1022 | 8 | | | | | | | | | | | | |

Table 2. *continued* (d).

| Date | GBR-16.0kHz | | | | LA REUNION-13.6kHz | | | | NWC-22.3kHz | | | | HAIKU-13.6kHz | | | | N.DAKOTA-13.6kHz | | | |
|---|---|---|---|---|---|---|---|---|---|---|---|---|---|---|---|---|---|---|---|---|
| | UNIVERSAL TIME | | | PA | UNIVERSAL TIME | | | PA | UNIVERSAL TIME | | | PA | UNIVERSAL TIME | | | PA | UNIVERSAL TIME | | | PA |
| | START | END | MAX | (DEG) | START | END | MAX | (DEG) | START | END | MAX | (DEG) | START | END | MAX | (DEG) | START | END | MAX | (DEG) |
| 1 | | | | | | | | | | | | | 2117 | 2137 | 2122 | 9 | | | | |
| 1 | | | | | | | | | | | | | 2137 | 2144 | 2140 | ↓ | | | | |
| 1 | | | | | | | | | | | | | 2224 | 2247 | 2233 | 6 | | | | |
| 1 | | | | | | | | | 2336 | 2357 | 2340 | 10 | 2336 | 2354 | 2346 | 6 | | | | |
| 2 | | | | | | | | | 0007 | 0034 | 0013 | 4 | 0008 | 0040 | 0014 | 3 | | | | |
| 2 | | | | | 0312 | 0343 | 0316 | 8 | 0311 | 0346 | 0318 | 10 | 0312 | 0348 | 0319 | ↓ | | | | |
| 2 | | | | | 0357 | 0426 | 0403 | 4 | 0352 | 0426 | 0402 | 6 | | | | | | | | |
| 2 | 0434 | 0444 | 0436 | 26 | 0434 | 0444 | 0440 | 82 | 0434 | 0448 | 0438 | 76 | 0434 | 0447 | 0440 | 32 | 0434 | 0442 | 0438 | 28 |
| 2 | 0637 | 0647 | 0640 | 16 | 0635 | 0738 | 0641 | 18 | 0635 | 0726 | 0639 | 14 | | | | | | | | |
| 2 | | | | | 0806 | 0918 | 0814 | 35 | 0806 | 0906 | 0814 | 12 | | | | | | | | |
| 2 | | | | | 1006 | 1128 | 1014 | 41 | | | | | | | | | | | | |
| 2 | | | | | 1240 | 1404 | 1256 | 37 | | | | | | | | | | | | |
| 2 | | | | | | | | | | | | | 1946 | 2016 | 2004 | 13 | | | | |
| 3 | | | | | | | | | 0021 | 0120 | 0041 | 16 | 0021 | 0116 | 0040 | 10 | | | | |
| 3 | | | | | 0136 | 0240 | 0144 | 18 | 0134 | 0234 | 0144 | 8 | 0136 | 0238 | 0146 | 7 | | | | |
| 3 | | | | | 0404 | 0432 | 0411 | 4 | 0404 | 0437 | 0409 | 6 | | | | | | | | |
| 3 | | | | | | | | | | | | | 2201 | 2235 | 2206 | 7 | 2201 | 2228 | 2204 | 11 |
| 4 | | | | | | | | | 0014 | 0110 | 0030 | 10 | 0014 | 0114 | 0028 | ↓ | | | | |
| 4 | | | | | | | | | 0146 | 0227 | 0203 | ↓ | 0146 | 0222 | 0203 | 3 | | | | |
| 4 | | | | | | | | | 0403 | 0441 | 0411 | ↓ | | | | | | | | |
| 4 | 0444 | 0602 | 0442 | 7 | 0444 | 0624 | 0442 | 12 | 0440 | 0630 | 0442 | 11 | | | | | | | | |
| | | | | | | | | | | | | | | | | | | | | |
| | | | | | | | | | | | | | | | | | | | | |
| | | | | | | | | | | | | | | | | | | | | |
| | | | | | | | | | | | | | | | | | | | | |

Note: Notes for reading off are given in the items (1)-(7) in the text.

SWF's and SES's detected at Hiraiso during the period from February 6 to March 6, 1984

by

H. Mori, C. Nemoto, T. Ishii, and C. Ouchi
Hiraiso Solar Terrestrial Research Center, Radio Research Laboratory
Nakaminato, Ibaraki 311-12, Japan

This report summarizes sudden ionospheric disturbances ( SID ) observed at Hiraiso during the period from February 6 to March 6, 1984. The SID phenomena reported here are : (1) short wave fadeout ( SWF ) detected by the amplitude recording of HF radio signals, and (2) sudden enhancement of signal ( SES ) by the observation of the amplitude of the Loran C pulse signals. Parameters of the propagation circuits are shown in Table 1. Figure 1 illustrates the time of maximum and the maximum deviation from the quiet level of each of detected SID phenomena. In the figure, it could be discussed that outstanding SID's occurred on February 10, 11, 17, 18, 19, 22, 24, 25, 27, and 29, i.e., mainly in the third quarter of this period. The collapse of simultaneity for their occurrence in the same event would be ascribed to the directivity of circuits, the occupation of latitude as the whole circuit, the sensitivity for their appearance, and so on.

Table 1. Parameters of circuits monitoring SID's at Hiraiso.

| TYPE OF SID | TRANSMISSION | | | | RECEPTION | DISTANCE (km) |
|---|---|---|---|---|---|---|
| | STATION | GEOGRAPHIC COORDINATES | FREQUENCY | RADIATION POWER(kW) | | |
| SES | IWOJIMA | 24°48'N 141°20'E | 100 kHz | 4000 | HIRAISO 36°22'N 140°38'E | 1290 |
| SWF | SHEPPARTON | 36°20'S 145°25'E | 15 MHz | 100 | | 8100 |
| | KAUAI | 22°00'N 159°46'W | 15 MHz | 10 | | 5910 |
| | FORT COLLINS | 40°41'N 105°02'W | 15 MHz | 10 | | 9150 |

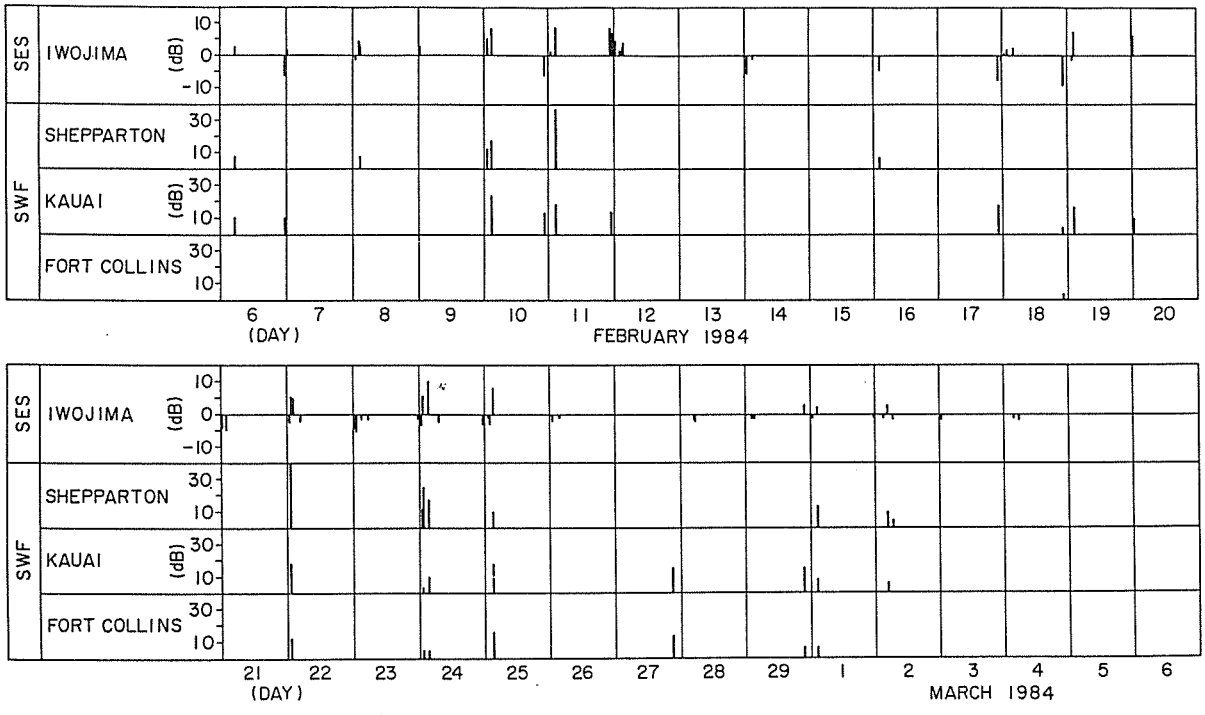


Fig. 1. The maximum values and the times(U.T.) of maximum of SES's and SWF's detected by Hiraiso Solar Terrestrial Research Center, RRL, Japan, during the period from February 6 to March 6, 1984.

It could be concluded that a part of Japan or the whole Japan was covered with SID at those times, since SID's other than SWF and SES, i.e., SPA [Ohshio, Ohtani, & Terajima, 1985] and/or SIF (sudden increase of $f_{min}$) [Koizumi & Ohshio, 1985] appeared on the very times.

During February 6 to March 6, solar activity was low to moderate. The significant solar active regions appearing in the period were SESC-assigned region Nos 4413, 4421, and 4423, where most of the flares causing these SID's occurred. Here SESC is an abbreviation of Space Environment Services Center, which is at Boulder, Colo., U.S.A.

## References


Koizumi, T. and M. Ohshio 1985 Ionospheric Activity Observed by Vertical Sounding at Japanese Stations During February 6 — March 6, 1984, this issue.

Ohshio, M., A. Ohtani, and Y. Terajima 1985 SPA's Observed at Inubo During February 6 — March 5, 1984, this issue.

PRF-SGD 1984 Preliminary report and Forecast of Solar Geophysical Data, SESC PRF 441 — 445, U.S. Dept. of Commerce, National Oceanic and Atmospheric Administration, Environmental Research Laboratories, Space Environment Services Center, Boulder, Colo., 14 February — 13 March.

# Ionospheric Activity Observed by Vertical Sounding at Japanese Stations During February 6-March 6, 1984

by

Tokuji Koizumi and Mitsuo Ohshio
Radio Research Laboratory
4-2-1 Nukui-Kita, Koganei, Tokyo 184, Japan

In order to know ionospheric states from ionospheric vertical routine observations, it seems to be possible to understand their general conditions well by noticing the daily deviation from their average variation in $f_oF2$, $f_{min}$, and $E_s$ as parameters analyzed. This report describes the results to have investigated the aspect of variations in $f_oF2$ and $f_{min}$, based on the data of ionospheric vertical routine observation at intervals of 15 minutes made at the five Japanese ionospheric sounding stations, Wakkanai (45°23.5' N, 141°41.2' E), Akita (39°43.5' N, 140°08.0' E), Kokubunji (Tokyo) (35°42.4' N, 139°29.3' E), Yamagawa (31°12.1' N, 130°37.1' E), and Okinawa (26° 16.9' N, 127°48.4' E) during February 6-March 6, 1984.

The consecutively daily variations in the maximum value of $f_oF2$ within a day at the above-described five stations are shown in Figure 1. Generally, the variation in $f_oF2$ relates to geomagnetic variations and depends a great deal on its related region (latitude), season, and local time. So that, the consecutively daily variation in $\Sigma K$ index for a day at Kakioka (36.23° N, 140.18° E in geographical coordinates and 26.2°, 207.3° in geomagnetic ones) is also given. The correspondence to these two parameters with each other indicated neither so much disturbed geomagnetic field nor strong ionospheric storms during the period. The consecutively daily variations in the maximum value of $f_oF2$ within a day among observational stations were similar mutually at Akita, Kokubunji (Tokyo), and Yamagawa, while had no similar cases in some days at Wakkanai and Okinawa. The latter seems to be ascribed to regional character at both the stations. In the figure, a time zone where a spread $F$ phenomenon with its duration above 3 hours appeared is marked as a qualitative aim. These spread $F$ phenomena supported that there were no world-wide ionospheric disturbances covering the whole Japan, because many of the phenomena appeared only in the northern Japan and there were some cases where the phenomena did not occur at these five stations simultaneously, that is, because these spread $F$ phenomena distributed locally.

In the same way as the case of $f_oF2$, the consecutively daily variations in the maximum value of $f_{min}$ within a day at the five stations are shown in Figure 2. The figure shows that the consecutively daily variations at the five stations had a good correspondence mutually for several cases during the period. The magnitude of $f_{min}$ can be considered to be an index to express the amount of electron density in the lower ionosphere through the amount of absorption of radio waves there. The figure indicates that high values of $f_{min}$ occurred on February 10, 11, 18, 22, 24, and 25 and that they were higher than the average value during the period together with the five stations. None of $f_{min}$'s for these six days had a good correlation with $\Sigma K$ index at Kakioka (cf. Figure 1), so it is understood that the enhancement of electron density in the lower ionosphere due to the arrival of charged particles was not remarkable on each day.

In order to investigate the aspect which the high value of $f_{min}$ as the maximum value within a day assumed within that day, for the six days when that $f_{min}$ showed a high value as pointed out in Figure 2, the values of $f_{min}$, $f_oE$, $f_bE_s$, and $f_oF1$ were extracted from an $f$-plot at intervals of 15 minutes and their diurnal variations for these five stations are shown in Figure 3. In the figure, $f_{min}$ to have had a value higher than the median of this month in each time is shown by black. The figure indicates that the times which the maximum values of $f_{min}$ within a day occupied agreed with one another at the five stations for the six events, except that the time of the maximum value of $f_{min}$ at Akita on February 18 was more delayed than those times at the other four stations by 45 minutes. By virtue of the above result, it is found that during the period the events in which the maximum value of $f_{min}$ within a day was remarkably large agreed mutually both temporally and locally.

It is obvious from the black parts in Figure 3, however, that the aspect of variations in $f_{min}$ higher than the median in a whole day including its maximum value was different in terms of both event and locality. That is, it is supposed that the aspect of its variations on February 10, 22, and 25 originated in the enhancement of electron density in the lower ionosphere caused by a solar X-ray flare with a short duration ($\lesssim$ 2-3 h.) and with a large amount of flux in comparison with its surrounding fluxes, that the aspect on February 24 by two successive solar X-ray flares with nearly the same flux with each other about 2 hours apart, and that the aspect on February 18 by a solar X-ray flare with a long duration ($>$ 12 h.) and with a medium-scale flux. It is presumed from the aspect of variations in $f_{min}$ higher than the median on February 11 that a compound event that an SID with a short duration ($\lesssim$ 1 h.) occurred, while an ionospheric winter anomaly occurred continuously was formed. The February 10 event is also enough to make an event compound with a small-scale ionospheric winter anomaly having influenced only $f_{min}$ at Wakkanai presume. These presumptions are consistent with time variations in solar X-ray flare radiation flux [SGD, 1984], reports at Wakkanai and Akita Radio Wave Observatories [Monthly Reports, 1984], and sudden phase anomalies (SPA's) detected at Inubo (35°42.2' N, 140°51.5' E) [Ohshio *et al.*, 1985]. Thus, Figure 3 to show the aspect of variations in $f_{min}$ higher than the median in a whole day clearly, provided a precise information enough to be able to investigate also the cause of the enhancement of $f_{min}$.

## References

Monthly Reports 1984 Monthly Reports on IUWDS Geoalert and Presto Messages, Western Pacific Regional Warning Center, Radio Research Laboratories, Japan, March 9, 1984.

Ohshio, M., A. Ohtani, and 1985 SPA's Observed at Inubo During February 6-March 5, 1984, this issue.

Y. Terajima

SGD 1984 Solar-Geophysical Data, comprehensive reports, No. 480 Part II, pp. 52-56, U.S. Dept. of Commerce, National Oceanic and Atmospheric Administration, National Environmental Satellite, Data, and Information Service, National Geophysical Data Center, Boulder, Colo., Aug. 1984.

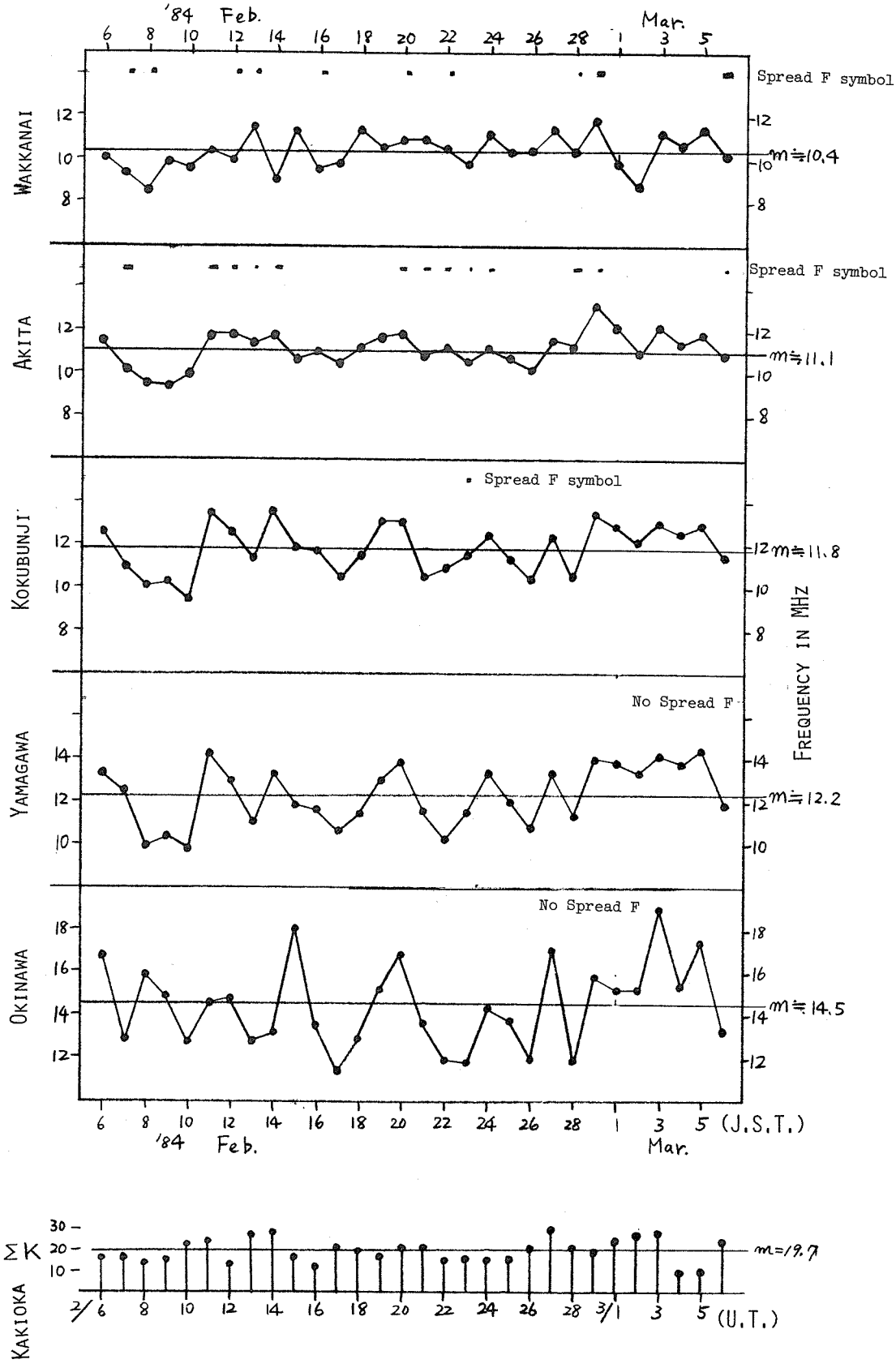


Fig. 1. Consecutively daily variations (in J.S.T. = U.T. + 9 h.) in the maximum value of $f_oF2$ (MHz) within a day observed at the five Japanese ionospheric sounding stations, Wakkanai, Akita, Kokubunji (Tokyo), Yamagawa, and Okinawa and those in $\Sigma K$ for a day (in U.T.) at Kakioka, Japan during February 6-March 6, 1984. The letter m represents an average value in the period. A time zone where a spread $F$ phenomenon with its duration above 3 hours appeared is shown in a black and tiny rectangle at each station.

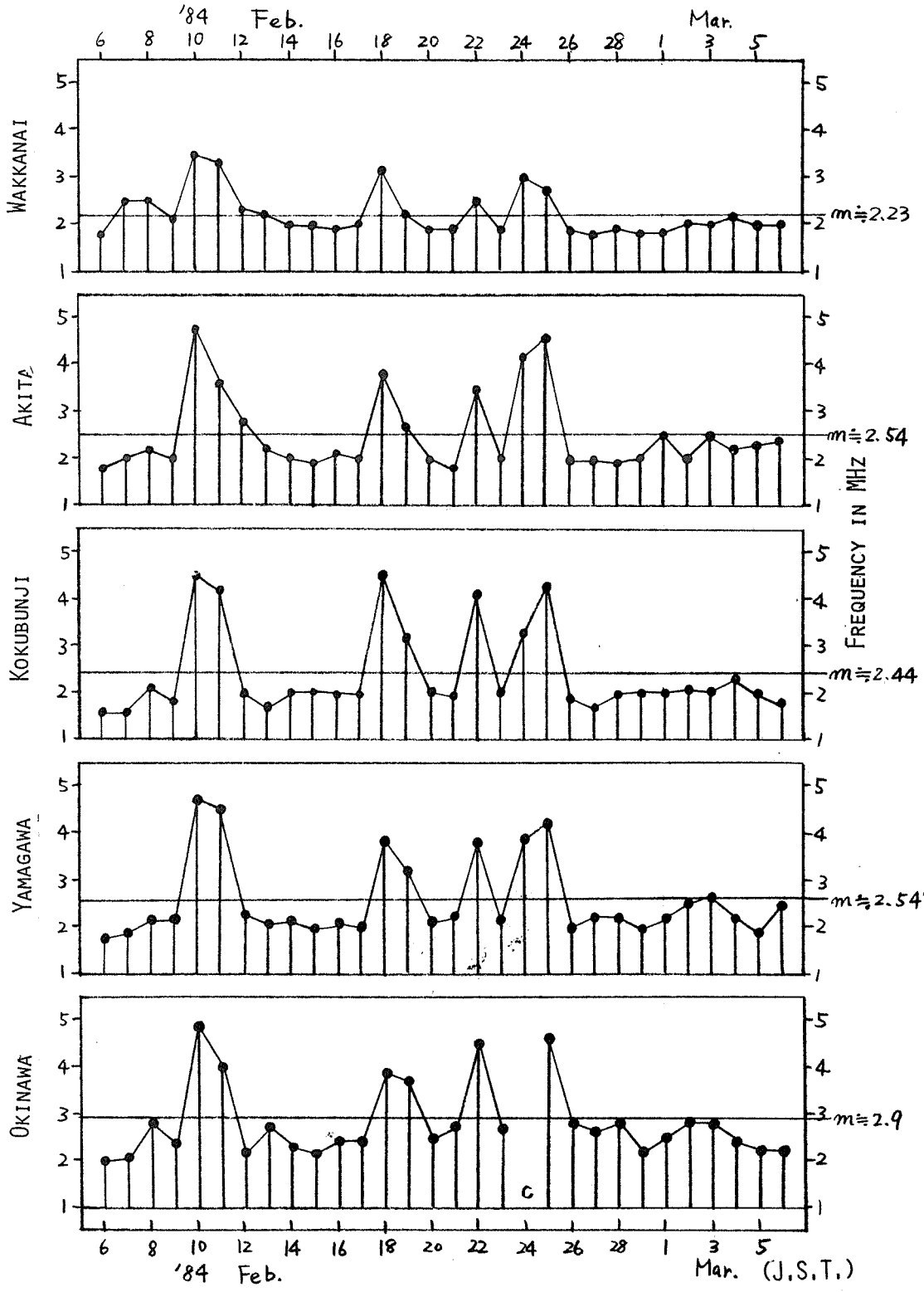


Fig. 2. Consecutively daily variations (in J.S.T. = U.T. + 9 h.) in the maximum value of *fmin* (MHz) within a day observed at the five Japanese ionospheric sounding stations, Wakkanai, Akita, Kokubunji (Tokyo), Yamagawa, and Okinawa during February 6-March 6, 1984. The letter m represents an average value in the period.

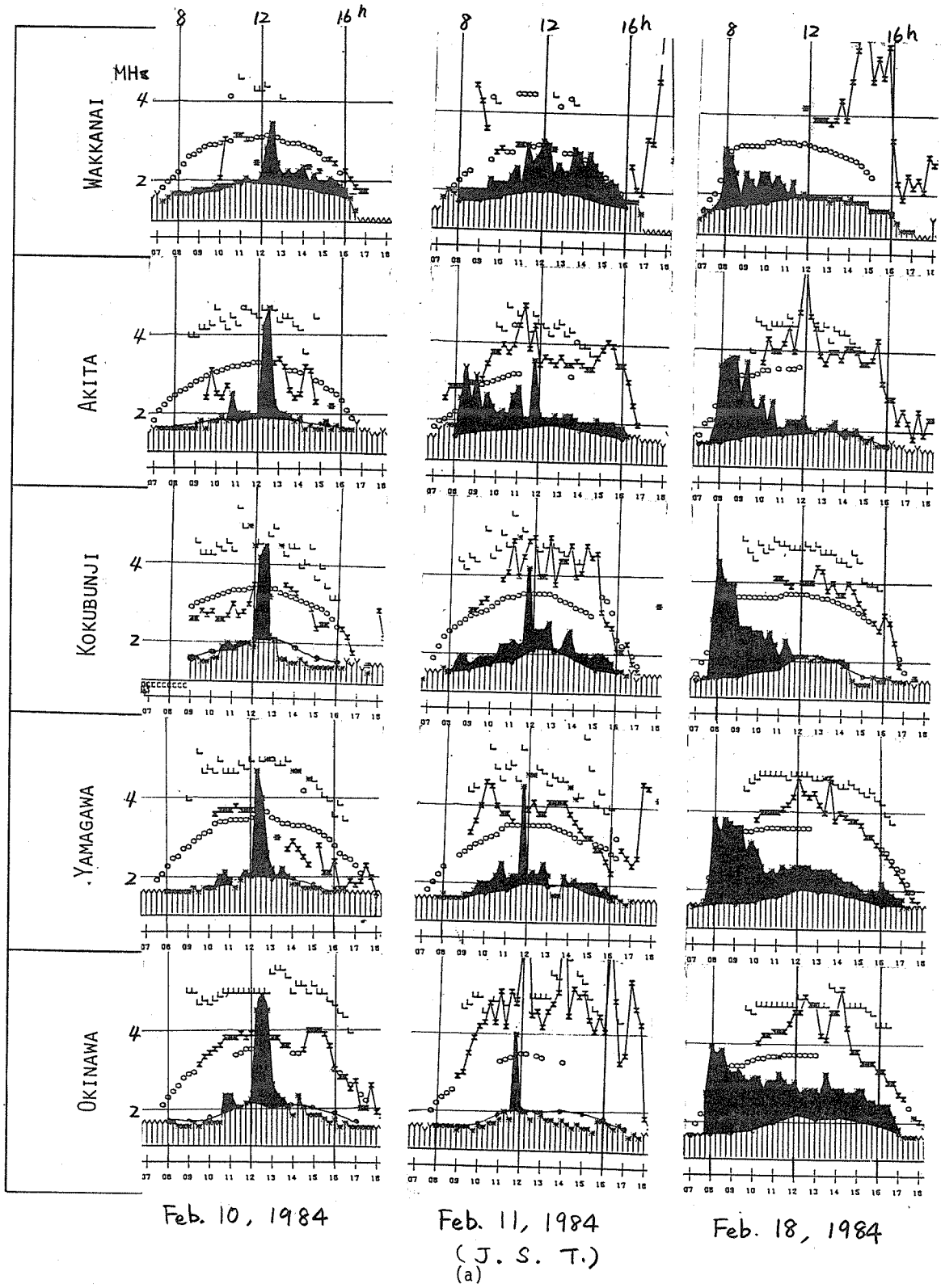


Fig. 3. Diurnal variations (in J.S.T. = U.T. + 9 h.) at intervals of 15 minutes of $f_{min}$ (a vertical segment of a line), $f_0E$ (a circle), $f_bE_s$ (the mark X with a segment of a line binding the letters), and $f_0F1$ (a circle, an asterisk, and the letter L) (each in MHz) observed at the five Japanese ionospheric sounding stations, Wakkanai, Akita, Kokubunji (Tokyo), Yamagawa, and Okinawa for the six days, February 10, 11, 18 (a), 22, 24, and 25 (b), 1984. The part of $f_{min}$ to have had a value higher than the median of this month is shown by black.

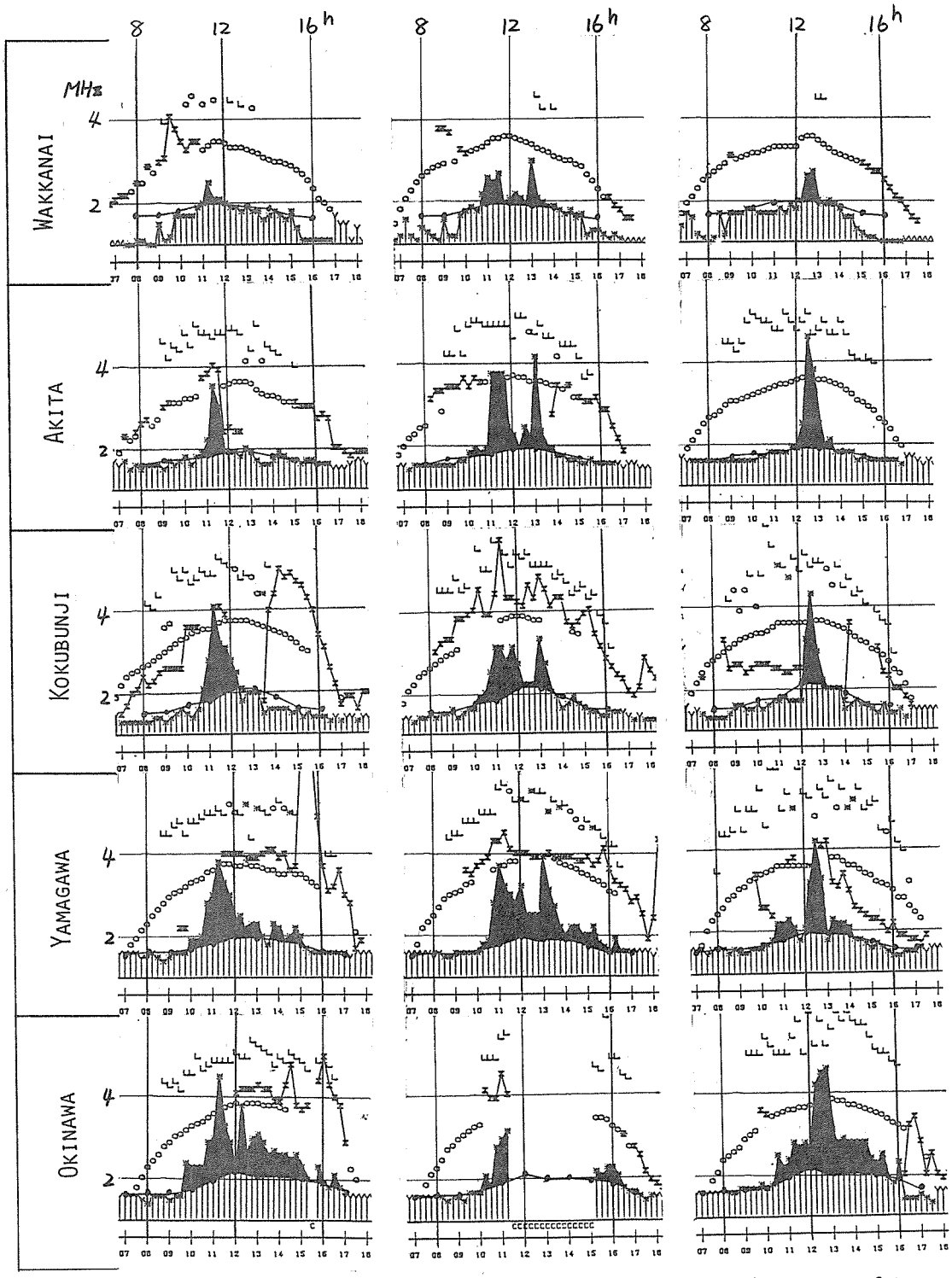


Feb. 22, 1984 Feb. 24, 1984 (J. S. T.) Feb. 25, 1984

Fig. 3(b)

# Solar flare effects on HF Doppler measurements during February 7 - 11, 1984

by

S. Kainuma, T. Kikuchi, A. Suzuki

Radio Research Laboratory
4-2-1 Nukui-Kita, Koganei
Tokyo 184, Japan

and

Y. Echizenya

Akita Radio Wave Observatory
Radio Research Laboratory
6-1 Tegata-Sumiyoshi, Akita
Akita 010, Japan

This report describes the sudden frequency deviations (SFD) caused by the solar flares on the Japanese HF standard signals, JJY (Nazaki, 36.18°N, 139.85°E) received at Akita, Japan (39.73°N, 140.14°E). The Doppler frequency measurements are made at frequencies of 2.5, 5, 8, 10, 15 MHz and the recording is made on the digital magnetic tape with a sampling rate of 1/10 sec.

Figures 1 and 2 show plots of the Doppler frequency deviations observed during the period of February 7 - 11, 1984. These figures include various types of frequency deviations; a positive single impulse (Fig. 1(a)), a positive impulse followed by a decrease (Fig. 1(b)), positive double peaks followed by a decrease (Fig. 1(c)), and oscillatory SFD (Fig. 2) (refer to Chen and Villard, 1963; Donnelly, 1967). Fig. 2 indicates a correlation between the SFD and the 9.5 GHz solar radio flux observed at Hiraiso (36.37°N, 140.63°E). It should be noted that the peaks coincide with each other as pointed with the arrows.

## References

Chan, K. L., and O. G. Villard, Jr. 1963 Sudden frequency deviations induced by solar flares, J. Geophys. Res., 68, 3197-3224.

Donnelly, R. F. 1967 The solar flare radiations responsible for sudden frequency deviations, J. Geophys. Res., 72, 5247-5256.

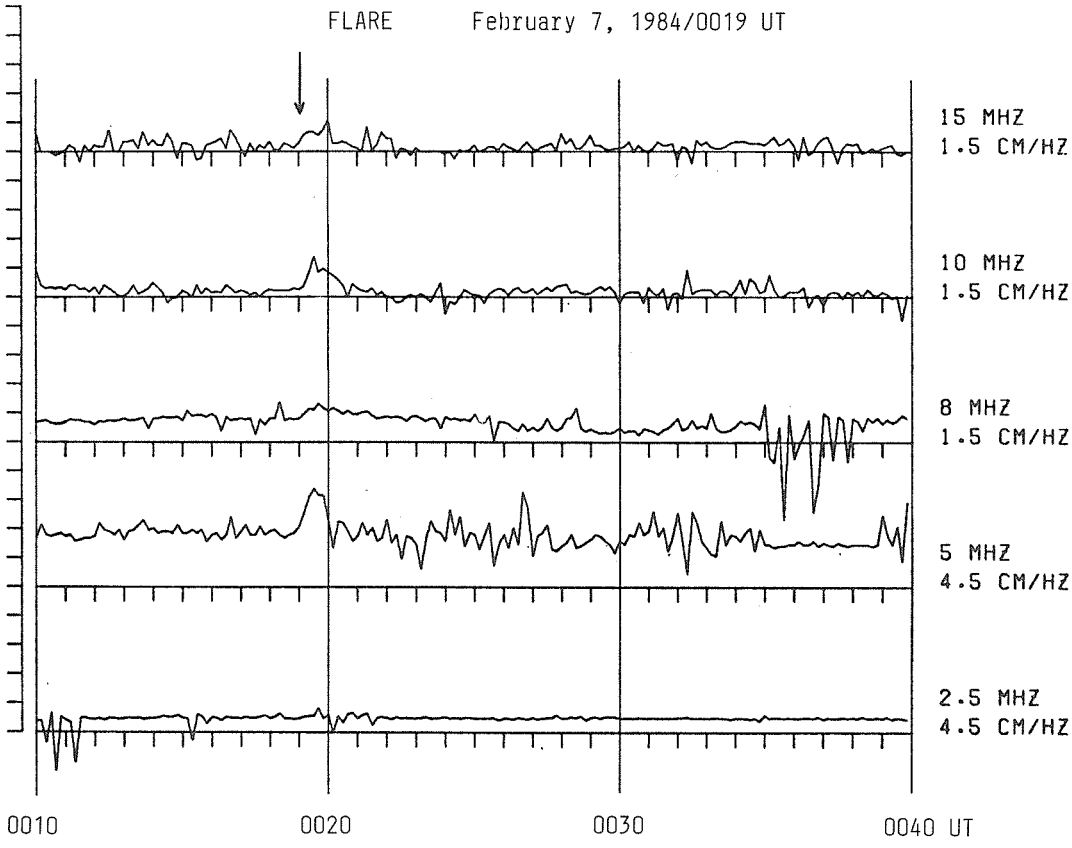
FLARE
February 7, 1984/0019 UT
15 MHZ
1.5 CM/HZ
10 MHZ
1.5 CM/HZ
8 MHZ
1.5 CM/HZ
5 MHZ
4.5 CM/HZ
2.5 MHZ
4.5 CM/HZ
0010
0020
0030
0040 UT

(a)

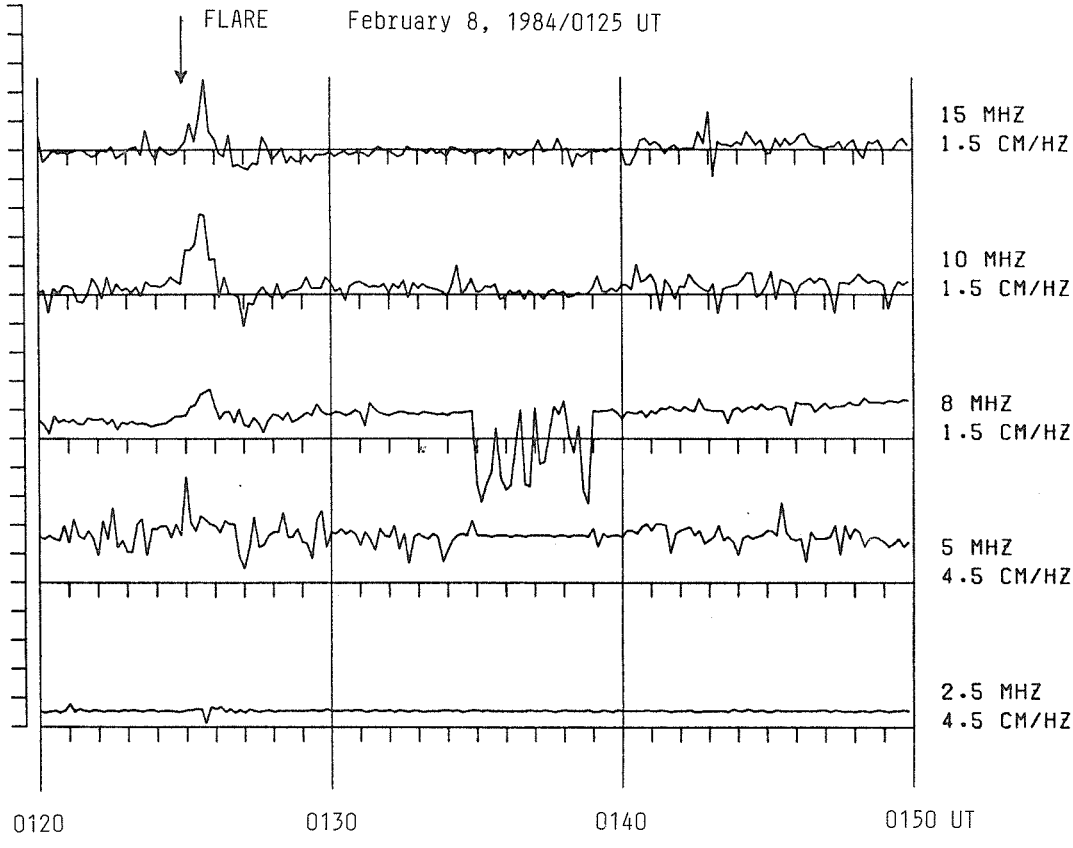
FLARE
February 8, 1984/0125 UT
15 MHZ
1.5 CM/HZ
10 MHZ
1.5 CM/HZ
8 MHZ
1.5 CM/HZ
5 MHZ
4.5 CM/HZ
2.5 MHZ
4.5 CM/HZ
0120
0130
0140
0150 UT

(b)

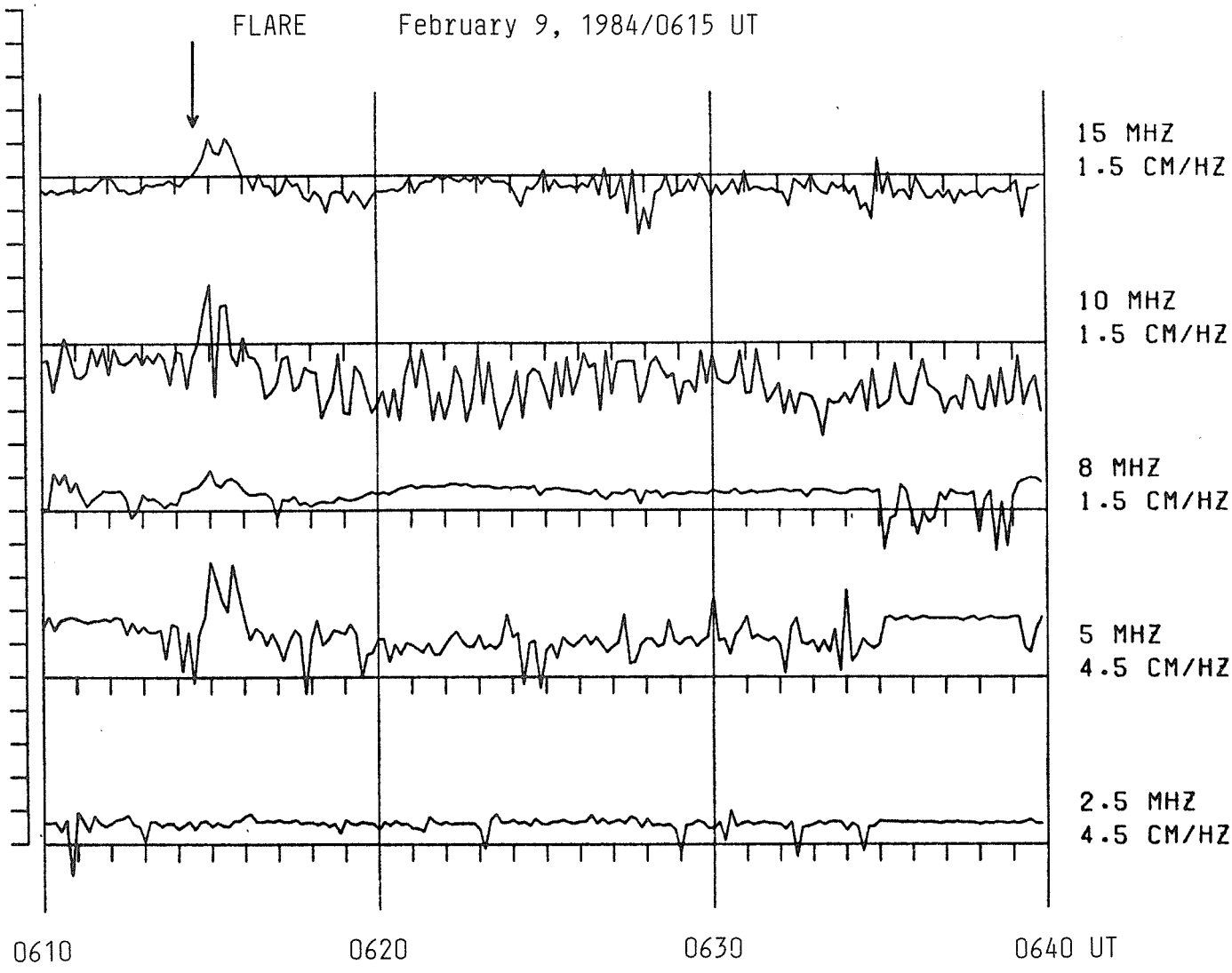


(c)

Fig. 1 Sudden frequency deviations (SFD's) observed on the JJY-Akita path. The SFD's consist of a positive single impulse (a), a positive impulse followed by a decrease (b) and positive double peaks followed by a decrease (c).

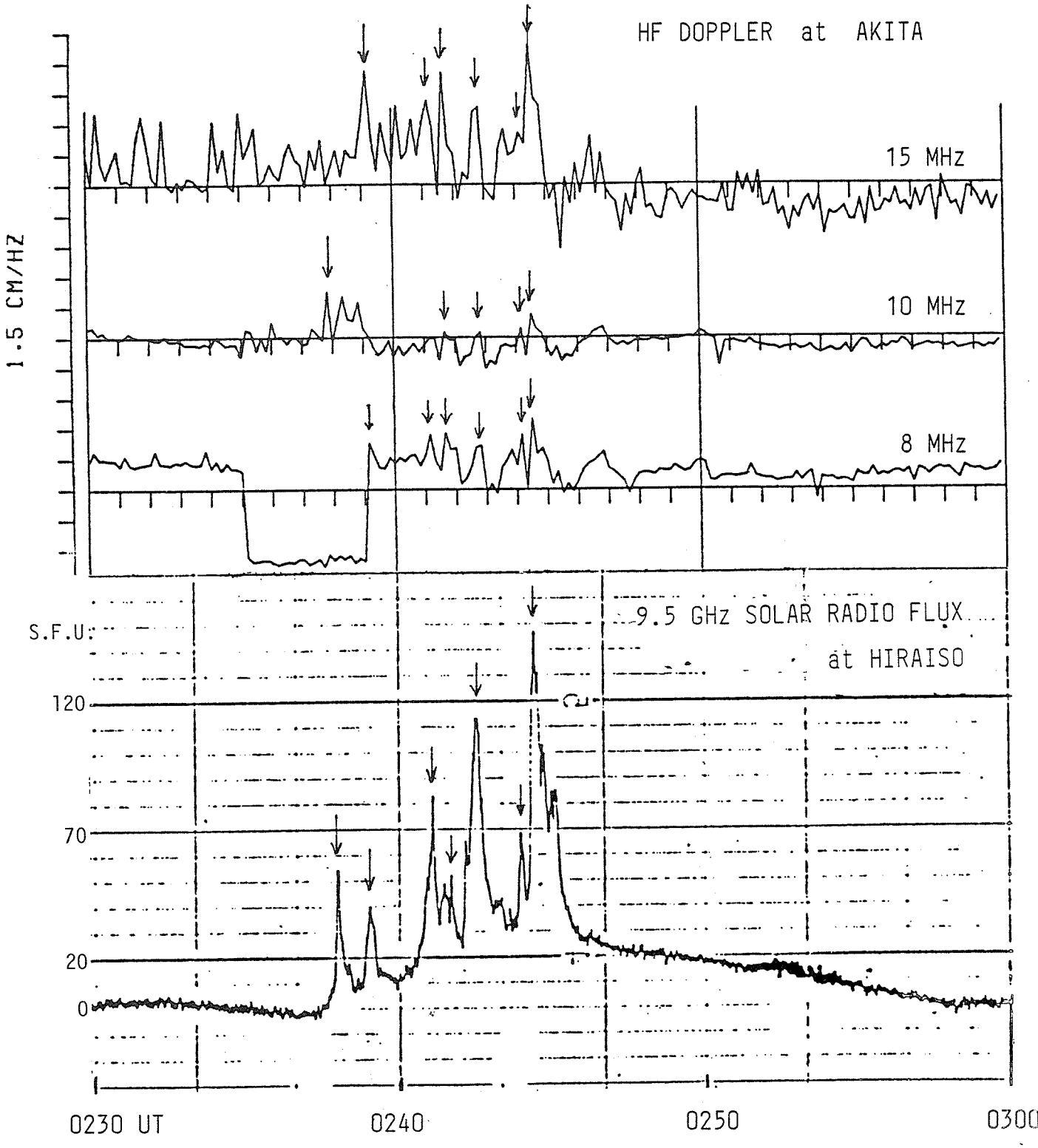


Fig. 2 Oscillatory SFD observed on the JJY-Akita path on February 11, 1984, along with the 9.5 GHz solar radio flux observed at Hiraiso. A good coincidence is observed between the peaks as pointed with the arrows.

# Sudden phase anomaly due to solar protons on February 16, 1984

by

H. Sugiuchi, A. Ohtani

Inubo Radio Wave Observatory
Radio Research Laboratory
9961 Tennodai, Choshi
Chiba 288, Japan

and

T. Kikuchi

Radio Research Laboratory
4-2-1 Nukui-Kitamachi, Koganei
Tokyo 184, Japan

The VLF radio signals, Omega ALDRA (13.6 kHz, Norway, 66.42°N, 13.13°E), GBR (16.0 kHz, U.K., 52.37°N, 1.18°W), and Omega NORTH DAKOTA (13.6 kHz, U.S.A., 46.37°N, 98.33°W) have been received at Inubo, Japan (35.7°N, 140.86°E), to detect the ionospheric disturbances caused by the energetic particles injected at the time of solar proton events and geomagnetic storms. The ALDRA-Inubo path traverses the auroral zone of $< 68°$ corrected geomagnetic latitude (CGL), while the GBR- and N.DAKOTA-Inubo paths traverse the regions of $< 65°$ CGL and $< 63°$ CGL, respectively. The phase and amplitude of the VLF signals are measured with the phase tracking VLF receivers and the cesium-beam frequency standard.

Fig. 1 shows sudden phase advances and amplitude decreases of the VLF signals starting at 0910 UT, February 16, 1984. Of the three signals, the ALDRA signal is most severely disturbed, because the path traverses the outer edge of the polar cap region. The phase advance of the ALDRA signal amounts to 190 degrees.

Fig. 2 shows the proton flux with E = 16 - 34 MeV detected by the GMS satellite on the geostationary orbit, along with the phase deviations of the ALDRA and N.DAKOTA signals. It is observed that the proton flux increases considerably, in correspondence to the phase advance on the ALDRA signal. The geostationary satellite well detects the increase in the solar proton flux, although the satellite is inside the magnetosphere. Therefore, the time history of the proton flux detected by the GMS satellite agrees with that of the phase deviations of the ALDRA signal (Kikuchi et al., 1985).

The distinct features of this solar proton event are the abrupt onset and short duration as shown in Fig. 1. The VLF phase anomalies in Fig. 1 have a similar shape to the sudden phase anomaly due to solar X-ray radiation. The data obtained on the low latitude path (not shown) indicates no occurrence of solar flares at the time of this event.

Reference

Kikuchi, T. A. Ohtani, and S. Isozaki 1985 Solar-terrestrial disturbances of June-September 1982 IV. Ionospheriuc disturbances 8. Propagation disturbances of VLF radio waves on the trans-polar paths, J. Radio Res. Lab., in press.

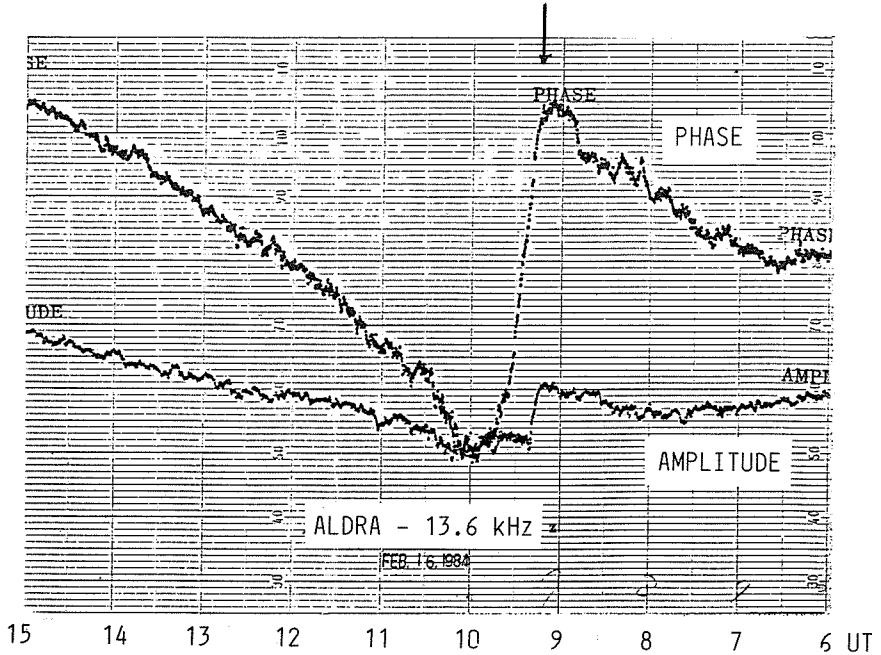


(a)

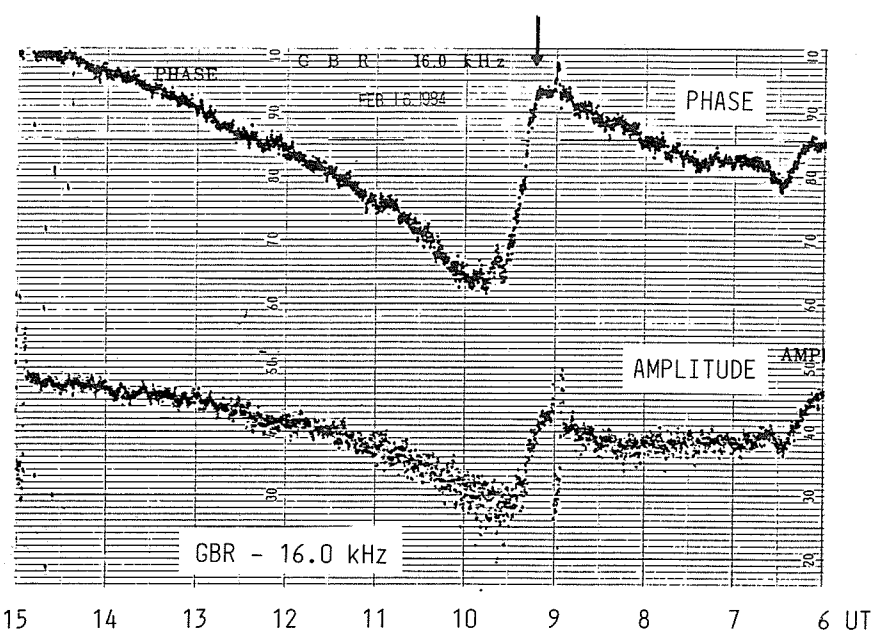


(b)

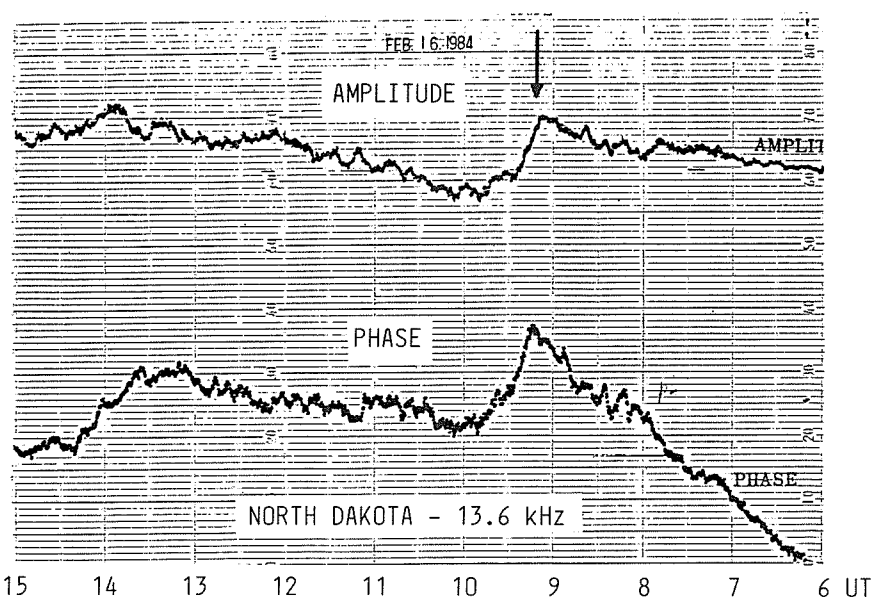


(c)

Fig.1 Abrupt phase advances and amplitude decreases observed on the Omega ALDRA (a), GBR (b), and Omega NORTH DAKOTA (c) signals at the time of the solar proton event on February 16, 1984.

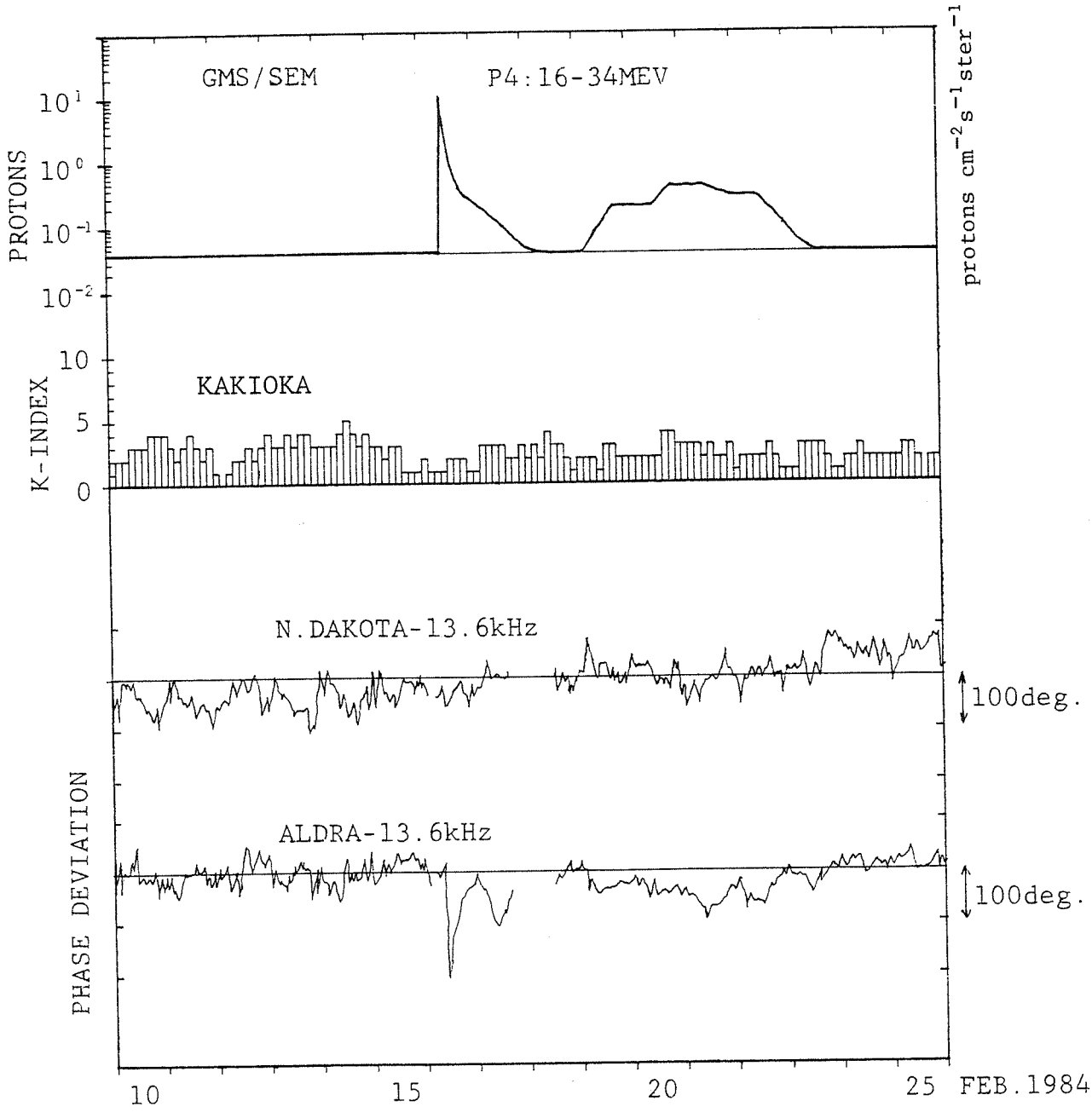


Fig.2 Correlation between the VLF phase advance and the solar proton flux (E = 16 - 34 MeV) detected by the GMS satellite on the geostationary orbit.

## VLF Propagation Observations During the GLE of 16 February 1984

by

A. Klekociuk
Physics Department, University of Tasmania
G.P.O. Box 252C, Hobart, Tasmania, Australia 7001

Recordings of the signal strength of the 22.3 kHz transmissions from the U.S. Navy communication station NWC at North West Cape, Western Australia (S21.8 E114.2) are made using a total power receiver with an effective time constant of 2 seconds. Observations are also conducted of the 13.0 kHz transmissions from the Omega navigation station G, Victoria (S38.5 E147.0), using a phase-tracking Tracor receiver with a time-constant of 15 seconds referenced to a Rubidium frequency standard. The outputs from both receivers are recorded using slow-speed chart recorders. The observing sites (with NOAA designations GN for the NWC measurements, and LE for the Omega measurements) are located near Hobart, Tasmania (S42.8 E147.4); the orientations of the two propagation paths are illustrated in Figure 1.

The sections of the NWC chart recordings between 0700 UT and 1100 UT for 14-18 February 1984 inclusive, are presented in Figure 2. The SID associated with the C2.3 X-ray flare on 16 February is readily apparent. This provides an indication of the sensitivity of the propagation path to ionospheric disturbances at this time. There is a small signal enhancement near 0915 UT on this day. Satellite observations do not indicate the occurrence of a significant concurrent increase in the solar X-ray flux. The VLF signal enhancement may reflect the increased flux of corpuscular radiation associated with the GLE. As shown in Figure 1, the NWC propagation path was fully illuminated, while the Omega propagation path was entering the terminator.

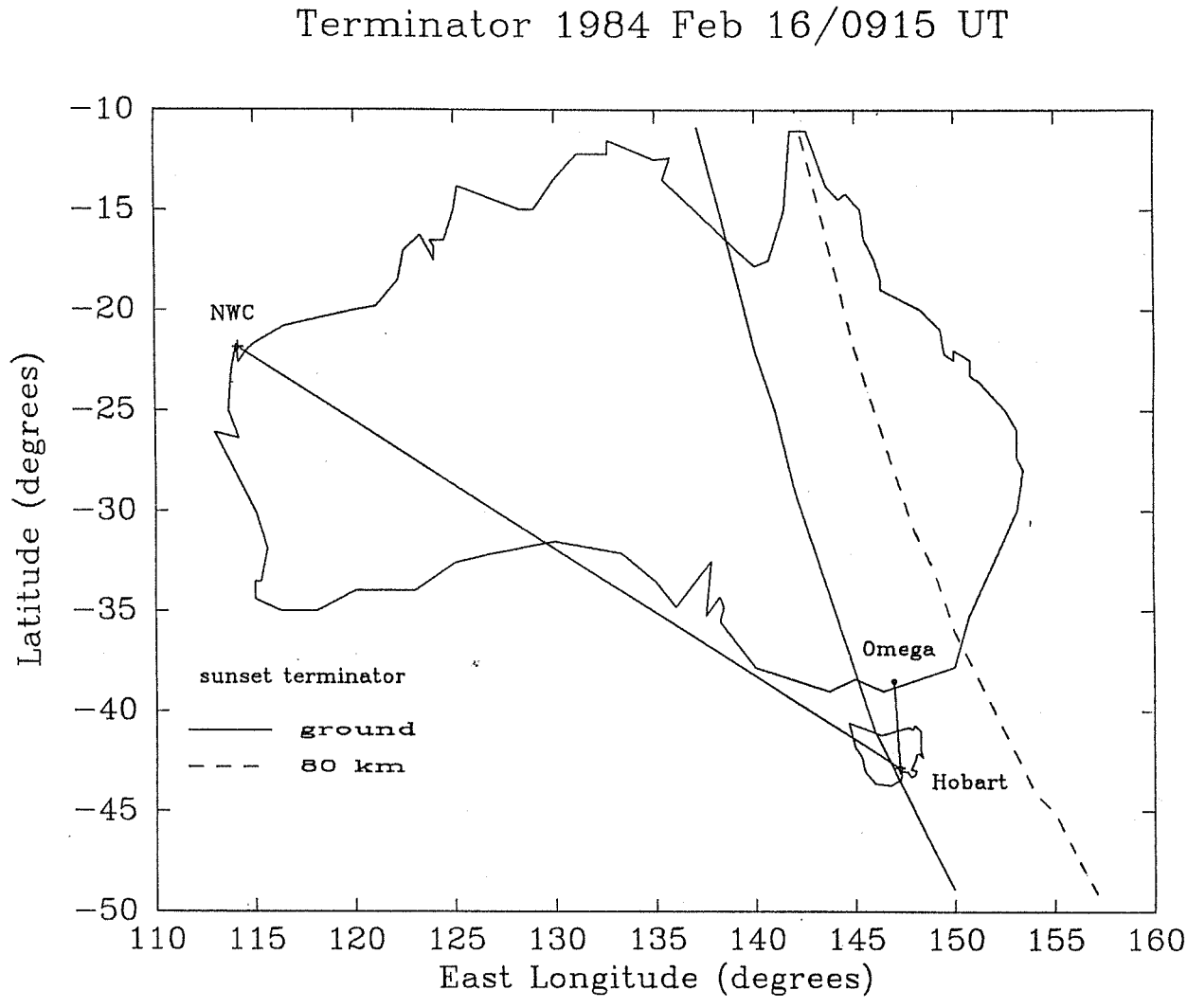


Fig. 1. The orientation of the propagation paths between Hobart and the NWC and the Omega G transmitters. The location for the sunset terminator at the ground and for a height of 80 km (within the daytime D region) are also illustrated.

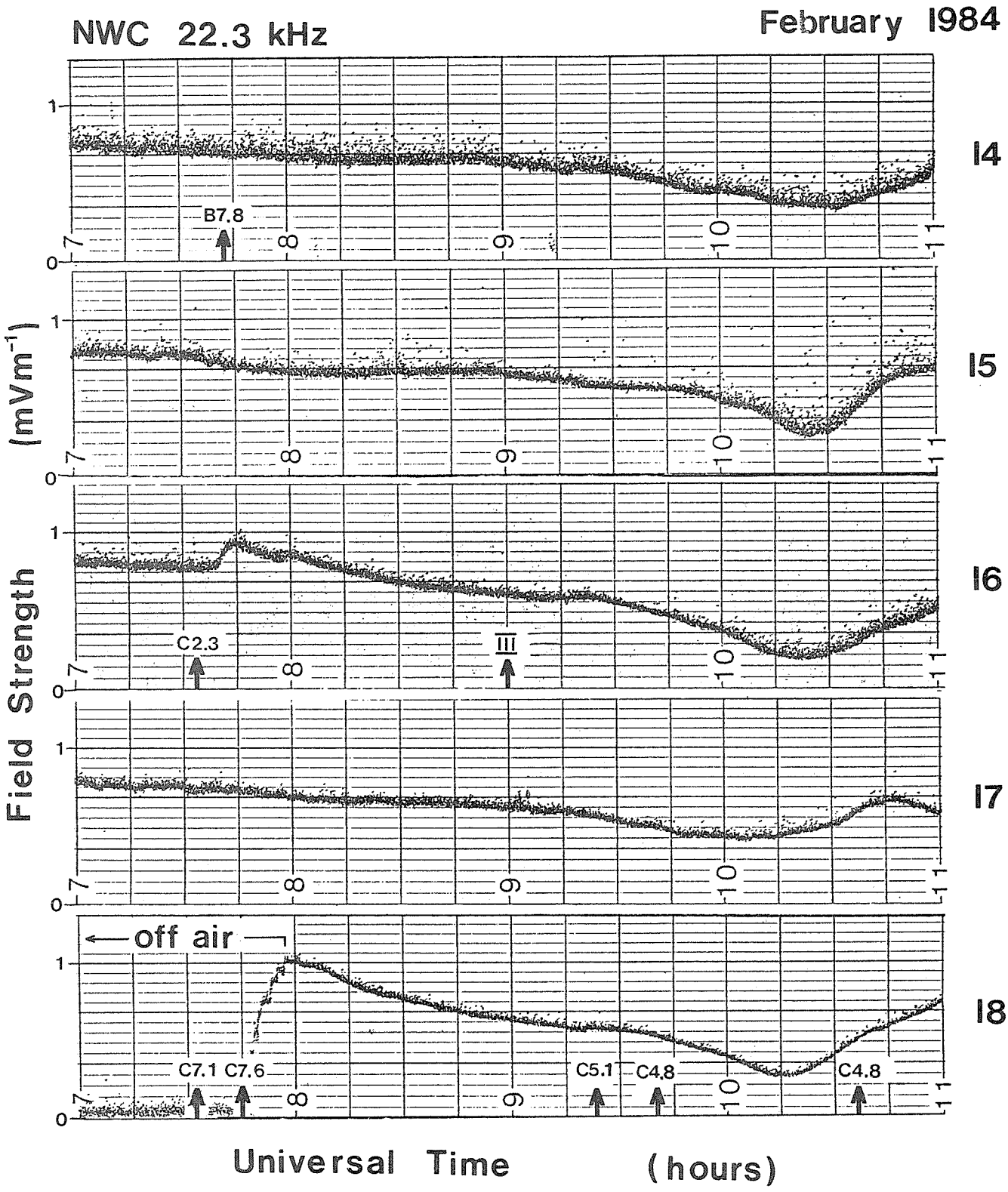


Fig. 2. Sections of the chart recordings of NWC for 14-18 February inclusive. The commencement times for 1-8A X-ray flares are indicated together with their peak flux using the NOAA/SESC classification scheme. The occurrence of Type III solar radio bursts on 16 February is also indicated.

The nighttime propagation behavior of NWC for 15-19 February inclusive is presented in Figure 3. Two modes are dominant in the Earth-ionosphere cavity during the night, and their mutual interference is responsible for the dusk effects between 1000 and 1130 UT and the dawn effects after 1900 UT. There is no evidence for any gross changes in the propagation characteristics associated with the satellite particle events on 16 and 19 February.

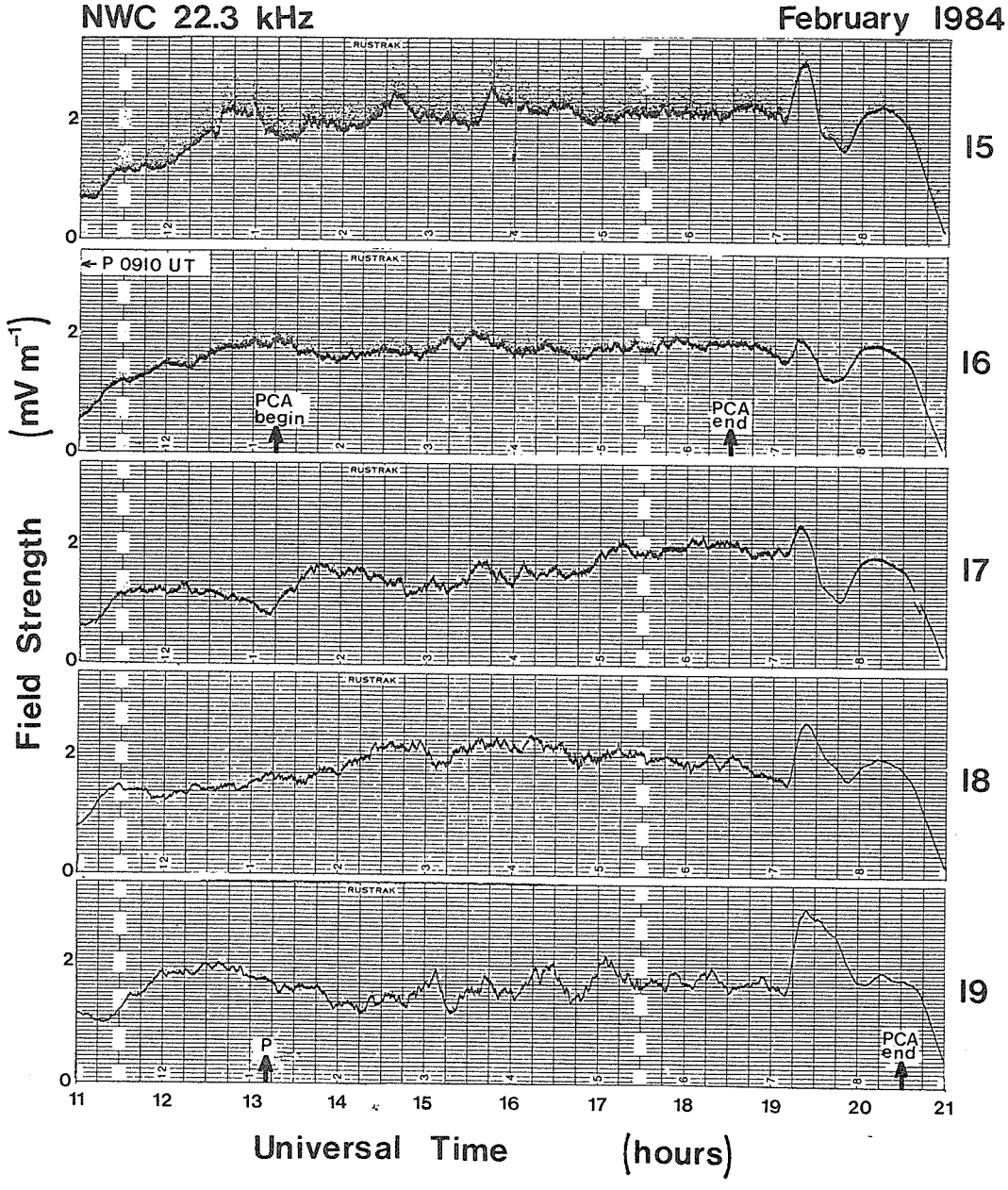


Fig. 3. NWC field strength recordings for nighttime propagation from 15-19 February inclusive. The onset times of 10 MeV satellite proton events ('P') and PCA event times are indicated.

The Omega receiver records for 15-19 February inclusive are presented in Figure 4. Because the propagation distance is small, the ground wave is dominant. This makes the propagation path relatively insensitive to changing ionospheric conditions One SPA event associated with the major flare of 17 February is identified. Nighttime disturbances are apparent on 16 and 18 February.

The particle, X-ray, and radio data have been obtained from **Solar-Geophysical Data** (SGD, 1984).

REFERENCES

SGD 1984 **Solar-Geophysical Data** 475 and 476 Part 1, and 480 Part II, U.S. Department of Commerce (Boulder, Colorado, USA 80303).

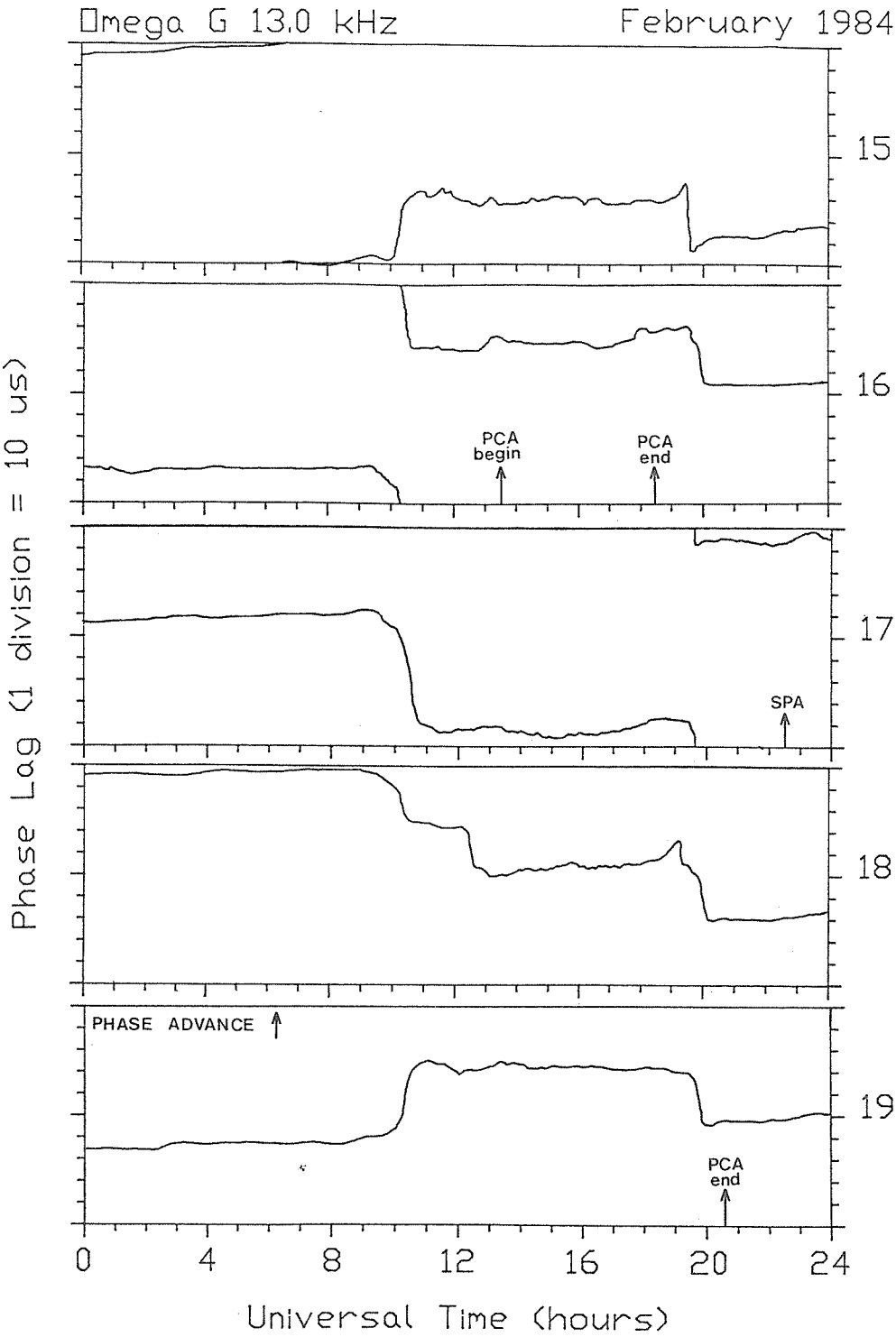


Fig. 4. Omega G phase recordings from 15-19 February inclusive. One Sudden Phase Anomaly (SPA) associated with an X2/2B flare on 17 February is indicated. The occurrence times of PCA events are also noted.

# Polar Cap Absorption (PCA) Events in February and April-May 1984 By Riometer Data at the Soviet Arctic and Antarctic Stations

by

V.A. Ulyev and A.V. Shirochkov
The Arctic and Antarctic Research Institute (AARI)
191104, Leningrad, USSR

## Introduction

Three PCA events which took place in February and April-May 1984 are analyzed using riometer data from 8 Soviet stations in both the Arctic and Antarctic. A description of the main ionospheric effects during these events is given. The data are presented in the same way as Driatsky (1974) and Shirochkov (1977).

The temporal absorption variations at our stations during the PCA events of 16-18 February (PCA event 1), 18-25 February (PCA event 2) and 25 April - 4 May (PCA event 3) are presented in Figures 1 and 2.

The upper panel of each Figure contains data from the Northern Hemisphere, while the lower one presents data for the Southern Hemisphere. Data of Antarctic stations should be regarded as preliminary only. Note the different ordinate scale, being equal to 2 dB in Figure 1 and 4 dB in Figure 2. All data are obtained by riometers operating at 32 MHz.

The thick abscissa axes in both Figures indicate periods when the Sun zenith angles at the observation sites were greater than 90°. The time scale for both Figures is the same, equal to 4 hours. The time of observations is given in the Universal Time (UT).

Details concerning our observational sites are given in Table 1 (see WDC-B, 1978). As previously shown in Driatsky et al. (1982), the stations located at invariant latitudes greater than 70° are called stations in the center of the polar cap, whereas other stations are called stations in the auroral zone.

Table 1. Positions and Riometer Frequencies of the 8 Arctic and Antarctic Stations.

| Station | Geographic Latitude | Geographic Longitude | Corrected Geomagnetic Latitude | Zone | Riometer Frequency MHz |
|---|---|---|---|---|---|
| NP (North Pole) | N80.30 | E185.50 | N75.80 | center | 32 |
| Heiss | N80.60 | E58.00 | N74.57 | center | 32 |
| Dixon | N73.50 | E80.40 | N67.67 | auroral | 32 |
| Amderma | N69.80 | E61.70 | N63.90 | auroral | 32 |
| Novolazarevskaya | S70.77 | E11.82 | S62.33 | auroral | 32 |
| Molodezhnaya | S67.57 | E45.87 | S66.50 | auroral | 32 |
| Mirny | S66.50 | E93.00 | S77.32 | center | 32 |
| Vostok | S78.45 | E106.87 | S83.23 | center | 30 |

Other tables contain data on different effects concurrent with the PCA events.

## General Description of the PCA Events

The description of the PCA events is given in the following order: a) temporal and latitudinal effects of the absorption distribution; b) day-to-night ratio in measured absorption; c) midday recovery effect; d) north-south asymmetry; and e) an increase due to the Sudden Storm Commencement (SSC) influence. All of these effects are described by means of the corresponding parameters which are presented in the tables. A brief analysis of each of these effects is given after each table.

## Temporal Variations of the Absorption

Temporal variations are considered for the whole PCA duration. The main characteristics are: date and time of the beginning, maximum, and the end of the event; maximum of the absorption, its intensity; the duration of the event; duration and nature of the rise and decrease stages, as well as a ratio of these durations. An absorption intensity is evaluated in certain units, depending on the maximum absorption magnitude, as proposed by Driatsky (1974). We evaluated the ratio of the durations of the rise ($T_{rise}$) and decrease ($T_{decrease}$) of the absorption by:

$$K_D = T_{decrease}/T_{rise}$$

Parameters of temporal absorption variations were taken from one of the central polar cap stations, where the ionosphere was illuminated by the Sun continuously during the whole duration of the PCA events or during at least its greater part. Table 2 contains these data for the PCA events considered.

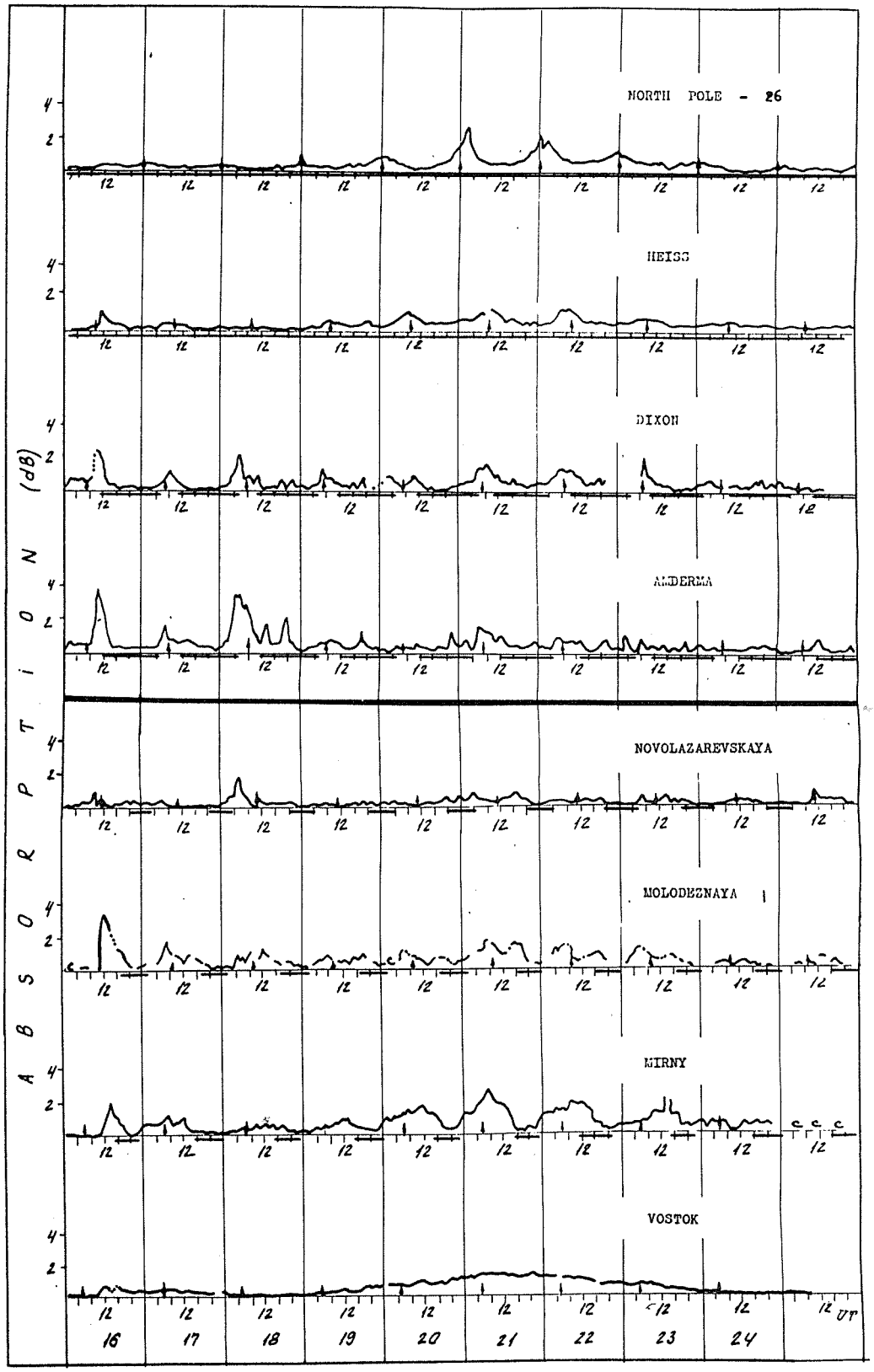


Fig. 1. PCA variations during the period 16-25 February 1984.

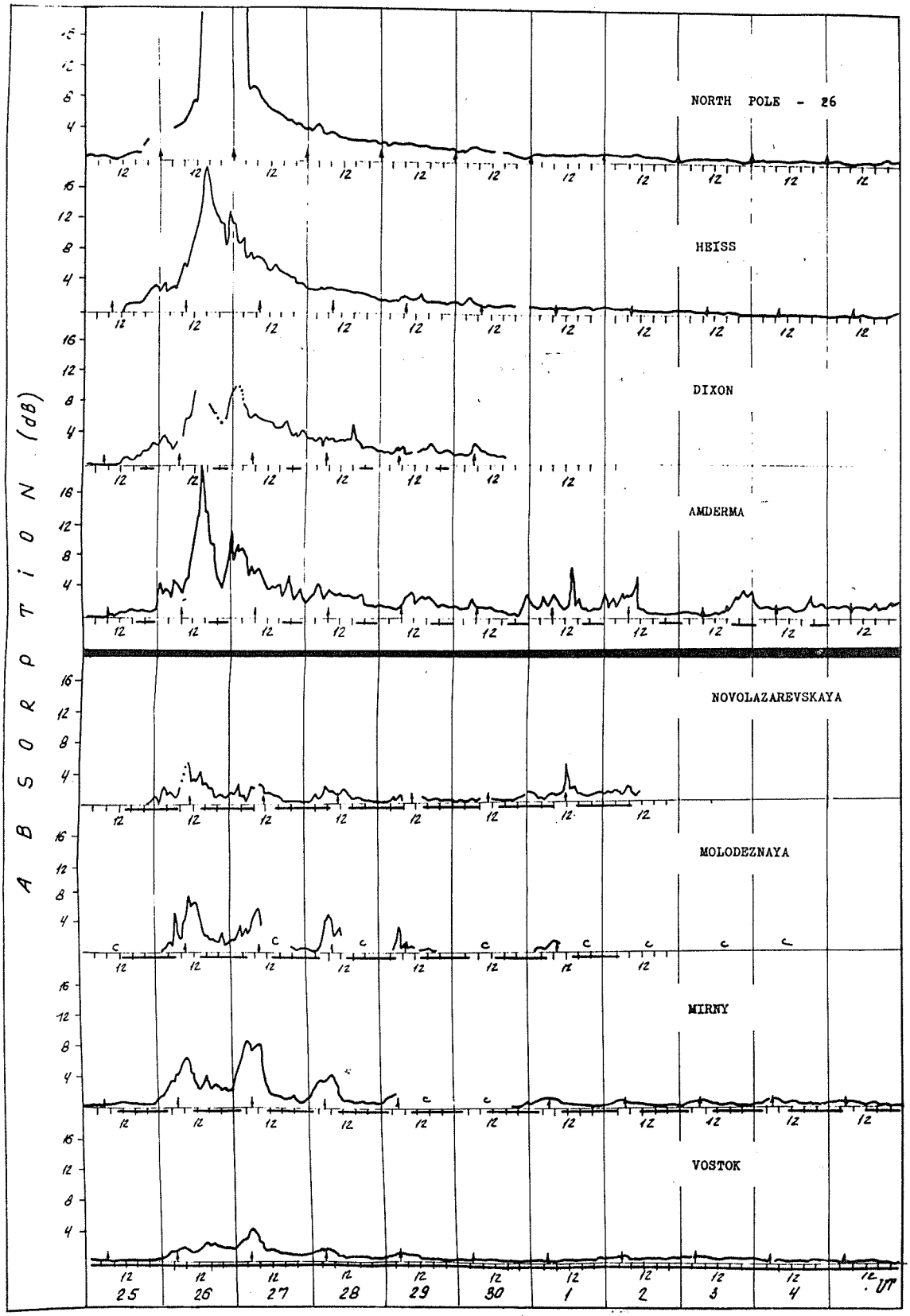


Fig. 2. PCA variations during the period 25 April - 4 May 1984.

Table 2. Characteristics of the PCA Events

| PCA | Date | Station | Start Date | UT | Max Date | UT | End Date | UT | Max Abs. dB | Int. | Dur. Day | $T_{rise}$ Day | $K_D$ $T_{decrease}/T_{rise}$ |
|---|---|---|---|---|---|---|---|---|---|---|---|---|---|
| 1 | 16-18 Feb 1984 | Vostok | 16 Feb | 1000 | 16 Feb | 1200 | 18 Feb | 1200 | 0.8 | 1 | 2 | 0.1 | 13 |
| 2 | 18-24 Feb 1984 | Vostok | 18 Feb | 0000 | 21 Feb | 0800 | 24 Feb | 1000 | 1.3 | 1 | 6 | 3.3 | 0.93 |
| 3 | 25 Apr 4 May 1984 | Heiss | 25 Apr | 1400 | 26 Apr | 1500 | 04 May | 1000 | 20 | 4 | 9 | 1.0 | 7.9 |
| | | Heiss | | | 25 Apr | 2200 | | | 3.5 | | | | |
| | | Heiss | | | 26 Apr | 2300 | | | 1.3 | | | | |

Conclusions can be made from this information. PCA event 1 is characterized by a very fast rise stage and by a very slow decrease stage. The temporal variations of the absorption can be described by the power law. Together with comparatively low absorption values and large $K_D$ ratio, it is a manifestation of the PCA events caused by relatively weak flares occurring on the western part of the Sun's limb.

For PCA event 3 the rise of the absorption is as long as 24 hours with the $K_D$ ratio being equal to 7.9. Such parameters of the amplitude-temporal variation are characteristic of the PCA events caused by the flares occurring near the central meridian. Two additional maxima of the absorption are recorded during PCA event 3; one at the rise stage and another at the decrease stage. The second increase has an abrupt peak form. We can attribute this type of temporal absorption variation to the influence of the solar cosmic ray fluxes reaching the Earth with a shock wave.

## Latitudinal Distribution of the Absorption

We introduce an artificial index for the description of the latitudinal variations of absorption during the PCA events for a fixed period of time (UT):

$$K_L = A_{HL}/A_{LL}$$

where $A_{HL}$ is the absorption at a high latitude riometer station, and $A_{LL}$ is the absorption at a low latitude riometer station.

Values for corresponding pairs of stations for the PCA events considered are given in Table 3.

Table 3. Latitude Variations of Absorption for the Arctic and Antarctic Stations.

| | | | | $K_L$ | | | | | |
|---|---|---|---|---|---|---|---|---|---|
| | | | | Arctic | | | Antarctic | | |
| PCA | Date | UT | PCA Phase | NP-Heiss | Heiss-Dixon | Dixon-Amderma | Vostok-Mirny | Mirny-Molod. | Molod.-Novol. |
| 1 | 16 Feb | 1200 | max | 0.45 | 0.95 | 1.1 | 0.5 | 1.5 | 5.0 |
| 2 | 21 Feb | 0800 | max | 0.5 | 0.49 | 0.6 | 0.45 | 1.40 | 8.0 |
| 3 | 26 Apr | 1500 | max | 1.0 | | | 0.58 | 2.0 | 1.0 |
| | 26 Apr | 0800 | rise | 0.95 | 1.15 | 1.1 | 0.25 | 1.0 | 1.3 |
| | 27 Apr | 0800 | decrease | 1.2 | 1.15 | 1.05 | 0.50 | 1.3 | 3.0 |
| | 28 Apr | 0800 | decrease | 1.2 | 1.0 | 1.0 | 0.50 | 1.9 | 2.1 |

One can see that $K_L < 1$ for the Northern Hemisphere stations during PCA events 1 and 2. This can be attributed to different levels of solar illumination at various latitudes. Besides, there is some superposition of auroral absorption on the PCA at stations located in the auroral zone. An unusual effect can be seen in the Antarctica: the magnitude of the absorption in Mirny ( $\Lambda$ = 76.°8) is greater than it is at Vostok station ( $\Lambda$ =84.3°). This effect can also be explained by an uneven illumination of the central polar cap region by solar cosmic ray fluxes.

During PCA event 3 the absorption intensity was approximately equal to the same value throughout the northern polar region due to the enhanced geomagnetic activity at the time of a PCA event. At the same time in the Antarctica, the Mirny absorption value was greater than at Vostok due to the difference in the illumination by the Sun. For other PCA events, absorption latitudinal distribution in Antarctica was normal, decreasing with a decrease of invariant latitude due to geomagnetic cut-off.

## Day-to-Night Variations of the Absorption

This kind of absorption variation during PCA events is caused by the changes of the lower ionosphere illumination by the Sun from daytime to nighttime conditions (Driatsky, 1974).

Usually these variations are characterized by the $K_{DN}$ index: $K_{DN} = A_D/A_N$ where $A_D$ is the absorption value under daytime conditions and $A_N$ is the absorption value under nighttime conditions. The $K_{DN}$ index is determined for the same time period, therefore either $A_D$ value or $A_N$ value must be approximated.

The calculated values of the $K_{DN}$ index for the PCA events considered are given in Table 4. These $K_{DN}$ index values were calculated for local midnight, which corresponds to 1200 UT for the North Pole Station, whereas for the other stations it corresponds to 2000-2100 UT.

Table 4. Day-to-Night Variations of Absorption for the Antarctic and Antarctic Stations

| PCA | Date | UT | PCA phase | $K_{DN}$ Arctic NP | Heiss | Dixon | Amderma | Antarctic Novol. | Molod. | Mirny | Vostok |
|---|---|---|---|---|---|---|---|---|---|---|---|
| 1 | 16 Feb 2000 | | decrease | | 1.5 | | | | | | |
| 2 | 20 Feb 2000 | | rise | | 3.1 | | | | 3.2 | 3.0 | |
| | 21 Feb 2000 | | max | 4.0 | 3.2 | | | | 4.1 | 3.4 | |
| | 20 Feb 2000 | | decrease | 3.1 | 2.6 | | | | 3.0 | 3.1 | |
| 3 | 26 Apr 2000 | | decrease | | | | | 5.1 | | | |
| | 27 Apr 2000 | | decrease | | | | | 5.0 | | 5.3 | 2.2 |
| | 28 Apr 2000 | | decrease | | | | | | | 6.5 | 1.6 |

The $K_{DN}$ values were relatively low (1.5-2.2) during PCA event 3 at the Vostok station. The $K_{DN}$ values during PCA event 1 at Heiss Island also were low. This means that the lower ionosphere above these stations was only partially illuminated by the Sun.

In all other cases the $K_{DN}$ index has its usual value (Driatsky, 1974). Note that during PCA event 2 the $K_{DN}$ index values were lower than during PCA event 3. This can be attributed to the softer energetic spectra of solar cosmic rays during PCA event 2.

## Midday Recovery Effects

This effect is a notable decrease of the absorption near the local noon during PCA events. The main feature of such an effect is a depth or magnitude of an absorption decrease which can be expressed by the equation:

$$K_{MDR} = 2\,Amin/(A_b+A_e)$$

where $A_b$ is the absorption value at the beginning of the effect, $A_{min}$ is the absorption value at the maximum of the effect, and $A_e$ is the absorption value at the end of the effect. Calculated values of the $K_{MDR}$ index are given in Table 5.

Table 5. Midday Recovery Effects.

| PCA | Date | UT | PCA Phase | $K_{MDR}$ Antarctic Novolazarevskaya | Molodezhnaya |
|---|---|---|---|---|---|
| 2 | 21 Feb | 1200 | max | 0.67 | 0.47 |
| | 22 Feb | 1100 | decrease | | 0.65 |

Midday recovery effects are observed during PCA event 2 at the auroral stations only. This is explained by the soft energetic spectra of the solar cosmic rays (SCR) which caused this PCA event (Gottingen, 1984). On the other hand, the absence of this effect at high-latitude stations such as Mirny indicates SCR spectra are not of a soft kind. We failed to find any traces of midday recovery effects at the Northern Hemisphere stations. It is probably explained by several factors, including any increase in the Sun illumination during the daytime. One suggests that the solar cosmic energetic spectra were comparatively hard during PCA events 1 and 3, and this is why we could not see any midday recovery effects at this time. An increased level of geomagnetic activity can be another reason for the situation, preventing midday recovery effects disclosure. We could not identify an absorption decrease as midday recovery effects at auroral stations in Antarctica on 26, 28 and 29 April near the local noon for the same reason.

## Absorption Increase Due to SSC Effects

Sometimes smooth absorption variations during the PCA events are disrupted by some impulsive increase of absorption, closely correlating with an SSC impulse or with a sudden increase of geomagnetic activity level (Driatsky, 1974; Driatsky, et al., 1982). Such an effect numerically can be expressed by:

$$K_{SSC} = A_{PC}/A_{AZ}$$

where $A_{PC}$ is the absorption value in the center of the polar cap during the appearance of the SSC impulse, and $A_{AZ}$ is the absorption value in the auroral zone during the SSC impulse occurrence. When $K_{SSC}>1$, it means that the SSC-influenced absorption increase is caused by the solar cosmic ray fluxes, which arrived with a shock wave. When $K_{SSC}<1$, it means that such an effect is caused by the fluxes of magnetic particles. Results of the $K_{SSC}$ index estimation are given in Table 6.

Table 6. Absorption Increase Due to SSC Effects

| PCA | Date | UT | Geomagnetic Activity | $K_{SSC}$ Arctic Heiss-Dixon | Heiss-Amderma |
|---|---|---|---|---|---|
| 2 | 20 Feb | 1600 | SSC-impulse | | |
| 3 | 26 Apr | 0000 | $K_p$=5 | 1.4 | 1.3 |

Though an SSC impulse occurred during PCA event 2 no changes of absorption intensity were recorded. During PCA events 1 and 3 (Driatsky, et al., 1982) no SSC impulses were found, but there was a short-lived absorption increase during PCA event 3 at the stations of the Northern Hemisphere on 26-27 April 1984. Similar effects were not observed in the Southern Hemisphere. This situation can be attributed to the influence of the Sun's illumination difference in the Northern and Southern Hemispheres as well as to a possible high degree of solar cosmic ray fluxes anisotropy in the interplanetary space, which might cause an enhanced SCR precipitation above the northern polar region only. This evidence leads us to suggest that a sudden absorption increase on 26-27 April 1984 is caused by SCR fluxes with soft energetic spectra and with anisotropic pitch-angle distribution.

## North-South Asymmetry in the Absorption

Asymmetry in absorption is characterized by significantly different values of absorption at magnetically conjugate points (Shirochkov, 1977; Logatchev, 1983). Numerically this effect can be described by the equation

$$K_{AS}=A_N/A_S$$

where $A_N$ is the absorption value at any station in the Northern Hemisphere and $A_S$ is the absorption value at a conjugate station in the Southern Hemisphere, taken at the same time.

The comparison was made for such pairs as the North Pole station (or Heiss Island) and Mirny Obsaervatory, Dixon Islands (or Amderma) and Molodeznaya. Both pairs are not truly conjugate, therefore our evaluations of the asymmetry effects are approximate.

There is a strong absorption asymmetry during the absorption maxima for all three types of PCA events (see Table 7).

Table 7. North-South Asymmetry in the Absorption

| PCA | Date | UT | PCA Phase | $K_{AS}$ NP-Mirny | Heiss-Mirny | Dixon-Molodezh. | Amderma-Molodezhn. |
|---|---|---|---|---|---|---|---|
| 1 | 16 Feb | 1200 | max | 0.25 | | 0.5 | |
| 2 | 21 Feb | 0800 | max | | 0.5 | | |
| 3 | 26 Apr | 1500 | max | | 5.0 | | 6.0 |
| | 26 Apr | 0800 | increase | 1.05 | | | |
| | 27 Apr | 0800 | decrease | | 1.0 | | |
| | 28 Apr | 0800 | decrease | | 0.95 | | |
| | 26 Apr | 2300 | SSC-peak | | >10.0 | | >10.0 |

The difference in the illumination regime for the Northern and Southern Hemispheres causes different $K_{AS}$ index values during PCA events 1 and 2. During PCA event 3, under similar Sun's illumination con-

ditions in both hemispheres, we have almost equal absorption values at the considered pairs of stations. In our opinion it is a strong evidence of the solar cosmic ray fluxes isotropic pitch-angle distribution in the interplanetary space.

As mentioned above, there is a strong and opposite North-South asymmetry of these effects as the midday recovery of absorption and SSC-influenced absorption increase.

## General Conclusions

We have shown that the PCA events in February and April-May 1984 are accompanied by the following effects: a) day-to-night absorption variations; b) midday recovery of absorption; c) SSC-influenced absorption increase; and d) North-South asymmetry in absorption intensity. Some numerical evaluations of these effects were made. On the basis of these evaluations one can draw preliminary conclusions:

1. PCA event 1 (16-18 February 1984) was caused by a small solar flare occurring in the western part of the Sun's Limb. Solar cosmic ray fluxes from such a flare have a rather hard type of energetic spectra.

2. PCA event 2 (18-25 February 1984) was caused by several small solar flares in the eastern part of the Sun's Limb. Solar cosmic ray fluxes from such flares have a rather soft type of energetic spectra and isotropic pitch-angle distribution in the interplanetary space.

3. PCA event 3 (25 April - 4 May 1984) was caused by several stong solar flares near the Sun's central meridian. Solar cosmic ray fluxes from such flares have a rather hard type of energetic spectra and isotropic pitch-angle distribution in the interplanetary space. There was a short-lived impulsive absorption increase during PCA event 3 caused by an SCR accompanying a shock wave. These solar cosmic rays have a soft type of energetic spectra and the anisotropic pitch-angle distribution.

## REFERENCES


DRIATSKY, V.M. 1974 **The nature of the anomalous absorption of cosmic radio emission in the lower ionosphere at high latitudes,** Hydromet Publishing House, Leningrad, USSR, p 224 (in Russian).

DRIATSKY, V.M V.A. ULYEV and A.V. SHIROCHKOV 1982 "Polar cap absorption events in September and November of 1977 at the soviet arctic and antarctic stations", **Report UAG-83, Part II,** pp. 295-303.

GOTTINGEN 1984 "Monthly geomagnetic planetary indices" (February, April, May), International Service Geomagnetic Indices, Institut fur Geophysik, Gottingen, Federal Republic of Germany.

LOGATCHEV, Y.I. 1983 **The Catalogue of SPE for 1970-1979,** Moscow, Nauka, 171 p. (in Russian).

SHIROCHKOV, A.V. 1977 "North-South asymmetry in asbsorption magnitude of the PCA", **Geomagnetism and Aeronomia, vol. 17,** pp. 445-449 (in Russian).

ULYEV, V.A. 1977 "Relation of midday recovery effect onset during PCA to flare longitude", **Trudy AANII, Vol. 350,** pp. 84-88 (in Russian).

WDC-B 1978 **Ionosphere catalogue of data for 1957-1977,** Report of the World Data Center (WDC-B), Moscow (in Russian).

# Daily Ionospheric Indices During February and April 1984

by

P.J. Wilkinson
IPS Radio and Space Services
P.O. Box 702
Darlinghurst, NSW 2010, Australia

ABSTRACT

Daily ionospheric indices for the Northern and Southern Hemispheres for periods in February and April 1984, are presented together with a few brief comments on the mid-latiude ionosphere, based on the indices.

## Introduction

Daily ionospheric indices are calculated using hourly foF2 data from a selection of ionospheric stations in both hemispheres. The method used to obtain the indices is described in more detail in Wilkinson (1983 and 1984). Daily indices are similar to IF2, IG and the Australian T indices and can be used to express the gross effects of ionospheric disturbances over large regions of the globe.

Seasonal differences in the F2 region response to geomagnetic activity are taken into account by calculating two hemispheric indices separately. Generally the summer hemisphere index responds more markedly to ionospheric storm effects than the winter index.

Indices are calculated using a 50% trimmed mean of all available data in a 24 hour period and the process is repeated every six hours, producing a 24 hour sliding daily index. The standard deviation of the mean is also calculated as an estimate of the spread in likely index values for a hemisphere.

In general, when the F2 region is undisturbed, the daily indices for the Northern Hemisphere, "$I_n$", and the Southern Hemisphere, "$I_S$", will not be significantly different and $\sigma_S$ and $\sigma_n$ (the standard deviations of the mean indices) will tend to their minimum values. In other words, there is less variation in foF2, and hence in the F2 region, between remote locations. This is equivalent to saying that the local F2 region is close to the average F2 region used as the basis for the indices.

When the ionosphere is disturbed, two effects occur. The F2 region responds more at high latitudes than at low latitudes resulting in increase in $\sigma_I$ for both hemispheres. As an ionospheric storm may first enhance the foF2 values recorded, before the more typical reduction in foF2, the first effect the storm has on the indices may be seen as an increase in I, or more often, an increase in $\sigma_I$ . The following depression in foF2 will have more effect in the summer hemisphere and will result in reductions of the summer index with respect to the winter index.

## The Data

Indices calculated for two periods centered on 16 February and 24 April are displayed in the accompanying figures. The mean Northern Hemisphere index is plotted at the centre of the 24 hour period to which it refers and the Southern Hemisphere index is plotted to the right of it. Both indices appear with error bars that are twice the standard deviation of the mean index.

Bearing in mind the ideas outlined in the previous section, some brief comments are made on the two periods based on the daily ionospheric indices.

## 13-22 February 1984

Two storm sudden commencements (SSC), accompanied by increases in geomagnetic activity as measured by both Kp and Dst, are included in this period.

Before the first SSC at 1505 UT on 12 February 1984, Dst is already negative, indicating a developing or developed ring current. Within 24 hours of the SSC, Dst decreases below -40 nT where it remains on the 13 February. During this period the Southern Hemisphere index, $I_S$, is depressed as is $I_n$ to a smaller extent. Dst then increases slowly to be above -20 nT on 16 February.

By the 16 February the Northern Hemisphere index has recovered to just below pre-storm levels and $\sigma_n$ is smaller, showing the ionosphere is less disturbed. However, $I_S$ is significantly higher than $I_n$ and continues to increase above pre-storm levels. The enhancement is probably not related to solar fluxes as the Ottawa 2800 MHz flux reaches its lowest level for the interval at this time. It is not possible to speculate further without inspecting the individual station data -- which is outside the objectives of this note.

The enhanced condition persists through the 17 February until $I_s$ drops to the same level as $I_n$. Magnetic activity again increases during this period and Dst drops below -20 nT. The second SSC at 1550 UT on 20 February is followed by a small drop in Dst that has little direct effect on the hemispheric indices, although the $\sigma_n$ increases are consistent with the Northern Hemisphere being more disturbed than the South. Both $I_s$ and $I_n$ are enhanced on 21 February, which may be a positive ionospheric storm effect in both hemispheres. Again, it is unlikely to be a result of solar flux changes.

20-29 April 1984

Disturbed magnetic conditions, beginning with an SSC on the 17 April, precede the start of this period. The Dst index is generally within $\pm$ 10 nT of 0 nT on 20 April, when $I_n$ and to a lesser extent $I_s$ show small depressions. This is followed on 22-23 April by a very quiet period with $I_s$ and $I_n$ equal, and $\sigma_s$ and $\sigma_n$ taking their lowest values for the two intervals.

The 24 April is therefore a slightly disturbed period following a particularly quiet day. As magnetic activity increases, $I_s$ drops below $I_n$. First $\sigma_s$ increases, then $\sigma_n$ increases, rapidly overtaking $\sigma_s$. The ionosphere is therefore becoming progressively more disturbed in both hemispheres.

Activity then increases on the 24 and 25 April before a more rapid increase on 26 April, when Dst decreases below -50 nT and does not return above -30 nT for the rest of the period considered. The sharp increase in activity is accompanied by a drop in $I_n$ followed later by a lesser drop in $I_s$. Both indices become equal, at below pre-storm levels, on the 27 April. By this time the Ottawa 2800 MHz flux has increased from 123 flux units on 20 April to 180 flux units on 28 April, suggesting the ionosphere is again controlled more by magnetic activity than solar fluxes.

## Conclusions

The daily ionospheric indices show that the hemispheric ionosphere was disturbed several times during the two periods displayed in Figures 1 and 2. In Figure 1 the specific day of interest, 16 February, is situated in a post-ionospheric storm period when the two hemispheres may be responding differently, the summer hemisphere being enhanced above pre-storm levels. The second period, Figure 2, is preceded by an ionospherically quiet period and precedes an ionospheric disturbance that persists for some days.

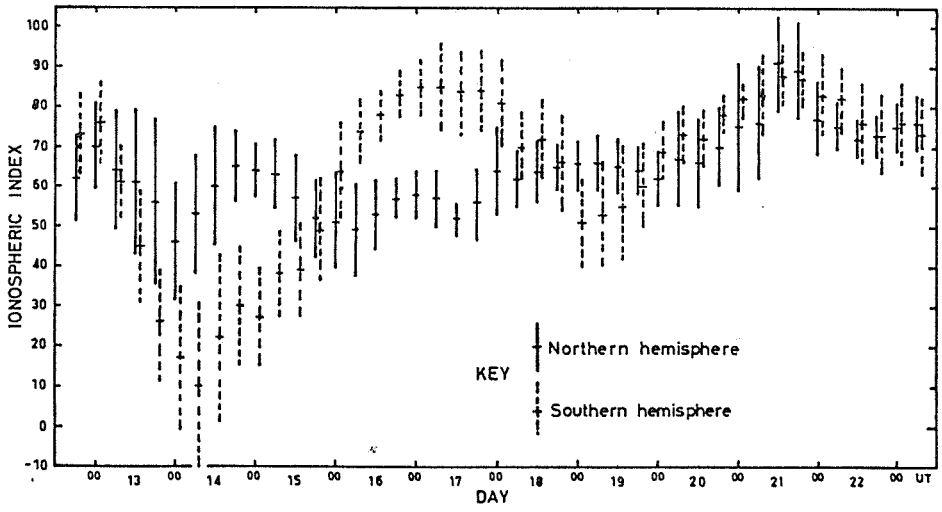


Fig. 1. Daily ionospheric indices for the period 13 to 22 February 1984.

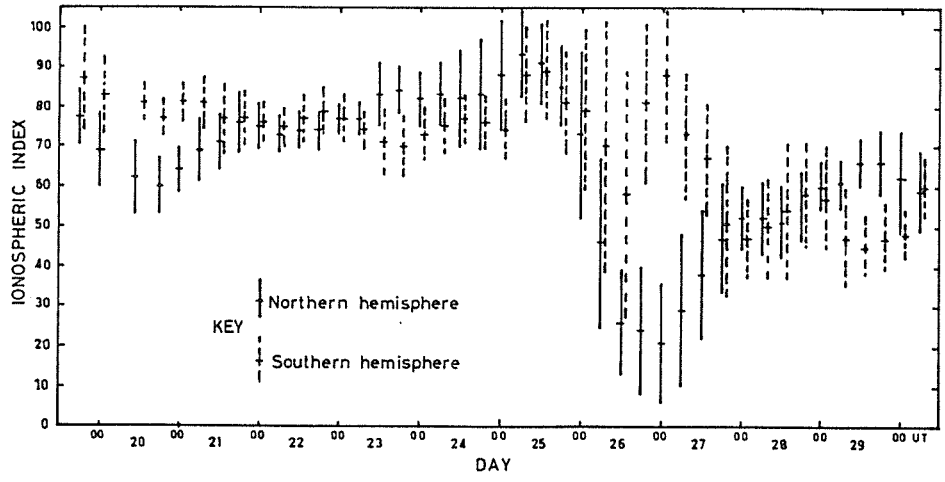


Fig. 2. Daily ionospheric indices for the period 20 to 29 April 1984.

REFERENCES


WILKINSON, P.J. 1983 "Ionospheric indices for monthly and daily use," Proc ICAP-83, 268.

WILKINSON, P.J. 1984 "Daily indices,", presented at Meudon STP meeting, 1984.

# Auroral Zone Geophysical Phenomena Associated With the Major Solar Proton Events on 16 February and 24 April 1984

by

B.E. Brunelli, G.P. Beloglazova, N.I. Fedorova,
V.Ya. Gorelov, V.P. Kozelov, R.S. Kukushkina,
L.L. Lazutin, N.V. Shulgina, G.F. Totunova,
E.V. Vashenyuk and N.V. Volkov
Polar Geophysical Institute of Academy of
Sciences of the USSR, Apatity, Murmansk region
USSR, 184200

## Introduction

This report presents the results of observations at the stations of the Polar Geophysical Institute on the Kola peninsula during the periods of time related to the solar proton events on 16 February and 24 April 1984. The report includes the data of the neutron monitor and riometer at Apatity (L=5.0), the riometer, geomagnetic H-component records and spectral measurements of aurora at Loparskaya (L=5.2), the ionosonde at Murmansk (L=5.4) and VLF propagation path Aldra (L=5.6) - Apatity.

## The 16 February 1984 Event

Figure 1 presents hourly count rates of the neutron monitor at Apatity.

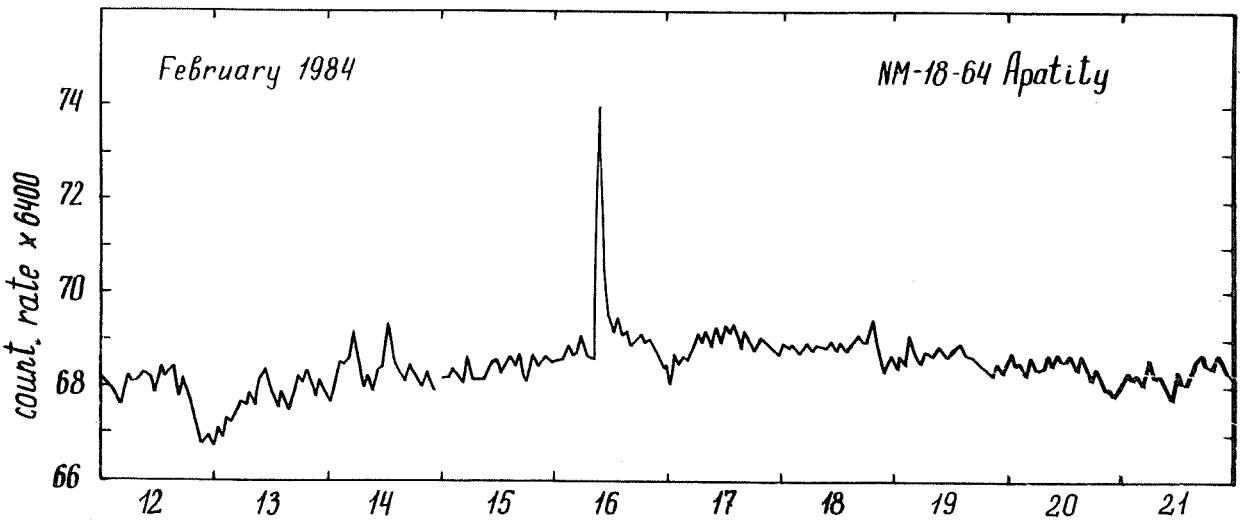


Fig. 1. Hourly count rates of the neutron monitor at Apatity from 12 to 21 February 1984.

The event on 16 February originated during rather quiet interplanetary conditions. The increase caused by the behind-the-West-limb flare was very sharp and shortlived. Its duration was about 4 hours, and the amplitude was 12.5 percent according to the 5-minute data. Variations of ionospheric absorption and H-component records at Loparskaya are given in Figures 2 and 3, respectively. Almost all occasions of absorption in Figure 2 have auroral origin since they correlate with the magnetic disturbances. Nevertheless, the event on 16 February originated during a perfectly quiet geomagnetic field and thus it was totally caused by solar particles. Figure 4 shows the event on 16 February on a larger scale from the 32 MHz riometer data and the 5-minute count rates of the neutron monitor at Apatity.

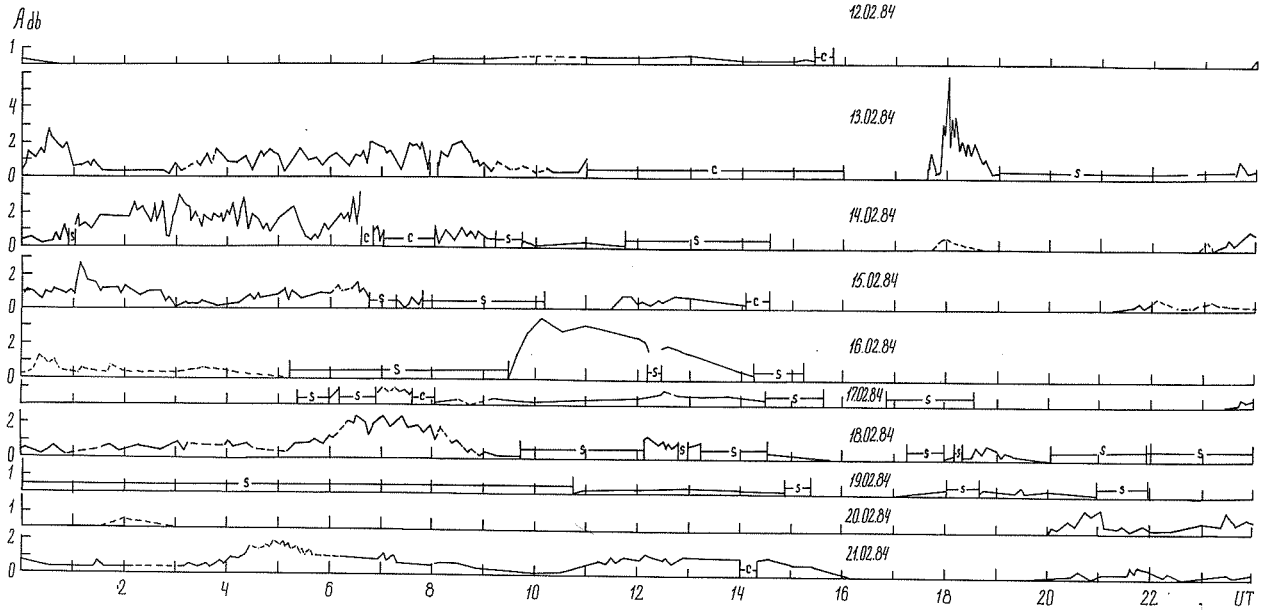


Fig. 2. Riometer absorption records from 12 to 21 February 1984 (Loparskaya 32 MHz).

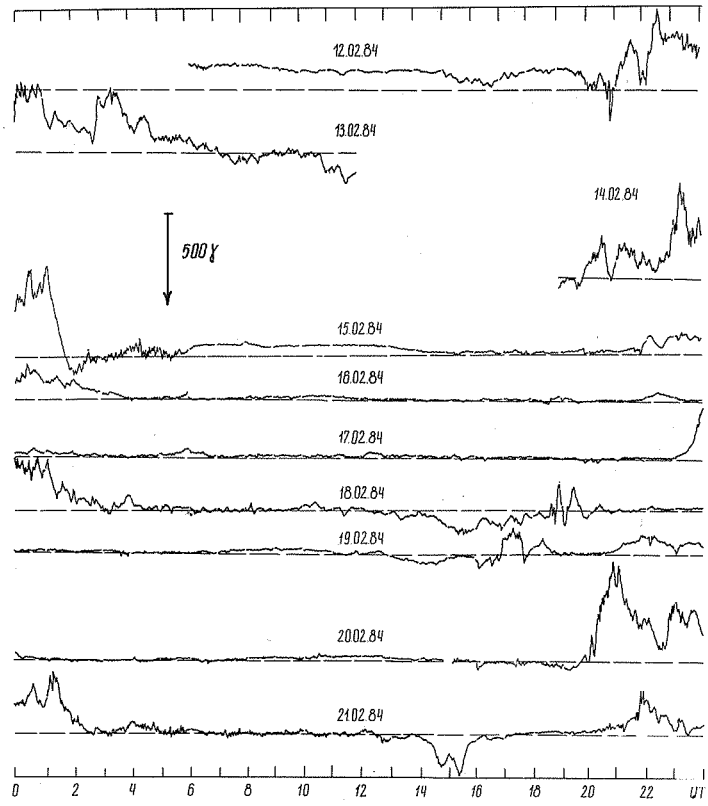


Fig. 3. H-component geomagnetic field records from 12 to 21 February 1984 (Loparskaya).

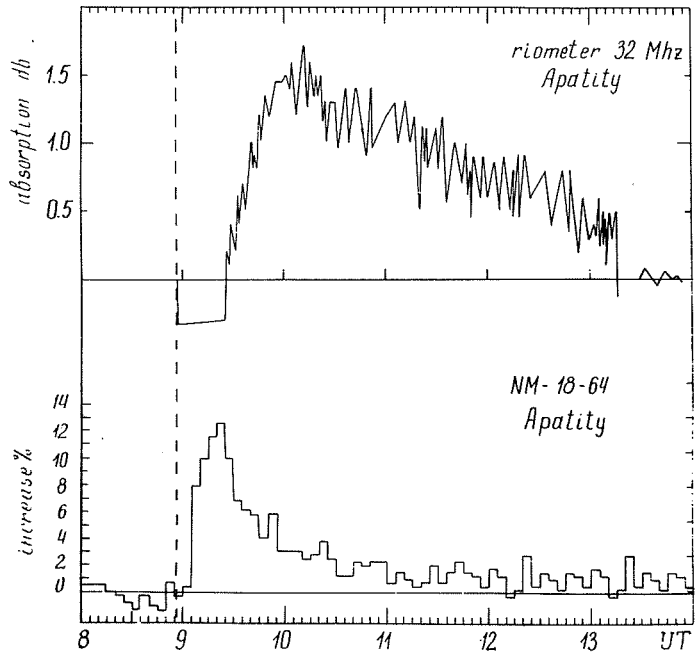


Fig. 4. The riometer 32 MHz records and the 5-min data of the neutron monitor at Apatity for the event on 16 February. The dotted line shows the starting time of a decametric radio burst.

The beginning of absorption was preceded by the decametric component of a solar radio burst (negative values of absorption). It started at 0857±1 minute and is marked in Figure 4 by the dotted line. At the neutron monitor the increase started between 0905 and 0910 UT, and the maximum was reached at about 0920 UT. The most remarkable feature of this event was the nearly equal duration of the increase at the neutron monitor and the riometer absorption. Usually, the time scale increases for relativistic and low energy solar protons differs greatly. Borovkov et al. (1984) suggested that the observed features of the 16 February event could be explained by the local generation of solar cosmic rays near the footpoint of the interplanetary field line leading to the Earth. Such a process might be initiated by the coronal shock propagating from the flare site through the corona.

Figure 5 presents the results of the VLF phase measuring over the Aldra-Apatity path (Figure 6). It is situated well inside the auroral zone ($L \geq 5$) and its length equals 880 km. The phase decrease relative to the "ideal" curve observed during all days except 16 February were caused by auroral particle precipitation. The phase anomaly that started at 0915 UT on 16 February during a quiet geomagnetic field without doubt was related to penetrating solar protons. The maximum of this anomaly was observed at 0955 UT and had the value of 10 microseconds. The appropriate decrease of the reflecting layer was 10-12 km relative to the normal midday level. This allowed us to get the estimates of electron concentration at the level 50 km (about 200-300 $cm^{-3}$) and the energy of the penetrating solar protons (approximately 30 MeV). The period of recovery to the normal conditions continued until 0400 UT on 17 February.

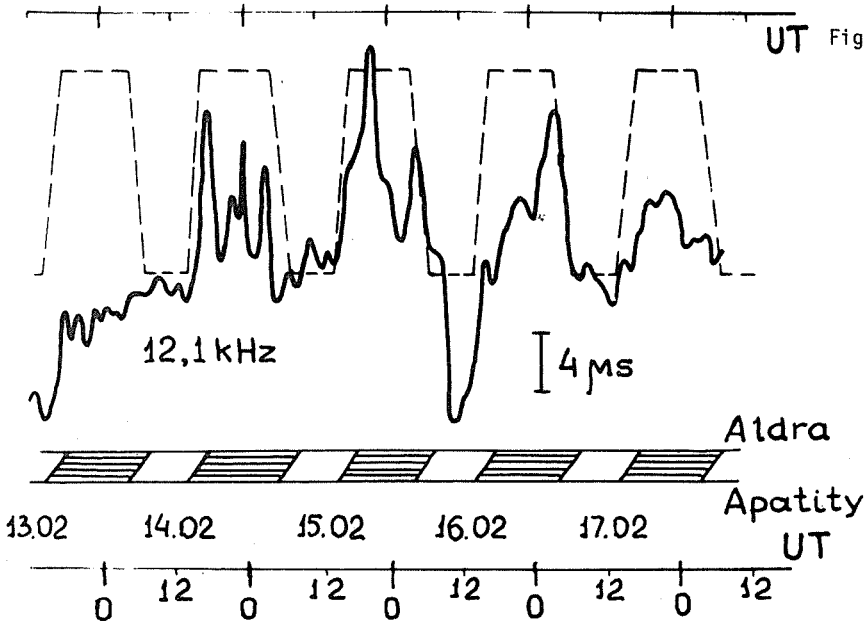


Fig. 5. VLF phase diurnal variation on the Aldra-Apatity path. The dotted line shows the "ideal" diurnal variation of the VLF phase. Luminosity conditions are also shown.

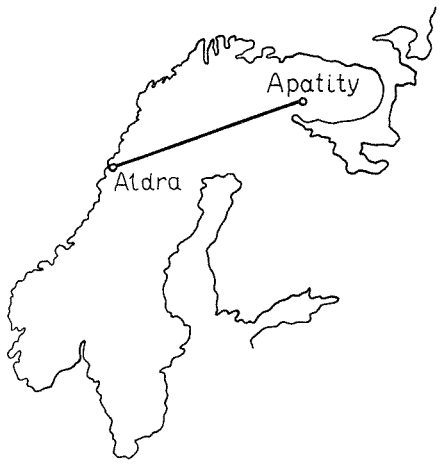


Fig. 6. The Aldra-Apatity VLF path.

Figure 7 shows the f-plots from the ionosphere sounding at Murmansk. Moderate disturbances which correlate with the magnetic activity are observed during the entire period from 13 to 21 February. It is remarkable that during the event on 16 February no observable variations were recorded.

Figure 8 gives the intensity of various auroral emissions measured at Loparskaya with the meridional spectograph C-180-S. An analogous device with an image amplifier was used for refinement of the data when the intensity was weak. The main auroral emissions: 3914A $N2^+$, 5577A (Oxygen 1), 6300A (Oxygen 1), and the H-alpha are given without subtracting the night sky luminosity. The observations were made during a moon period and not always under good weather conditions. And this, naturally, affected the accuracy of the data. Generally, the behavior of different emissions and spectral characteristics of precipitating auoral particles were typical for the magnetic activity observed simultaneously.

## The 24 April 1984 Event

Figure 9 shows the plot of hourly count rates of the neutron monitor at Apatity. There was no observable increase in the relativistic cosmic rays due to a powerful X12 flare at 2356 UT on 24 April. The event on 24 April, as the one just considered on 16 February, originated during quiet interplantary conditions, but it was followed by a Forbush decrease that began at about 1200 UT on 26 April. The recovery of the intensity did not reach the pre-decreased level until 6 May. Figures 10 and 11 present the riometer absorption data and the records of the geomagnetic H-component at Loparskaya, respectively. As one can see from comparison of Figures 10 and 11, some cases of absorption before the event correlate with magnetic disturbances and therefore are caused by aurora. At the period just after the solar flare and until the midday on 25 April there was no absorption, perhaps due to a low intensity of solar protons. Further, however, the absorption had started. It certainly was caused by solar particles in spite of isolated auroral bursts. The maximum of this absorption was reached near the midday on 26 April coinciding with the start of the Forbush decrease. Then the absorption slowly decreased until the end of the day 30 April when a new auroral activity arose.

Figure 12 gives f-plots from the Murmansk ionosonde data. During the period 21 to 26 April only weak variations of foF2 and fmin were observed. But at early hours on 26 April when the intensity of solar particles increased significantly the blackout started and it continued until the end of day 28 April. The periods of full absorption also were observed during the following days, but they were perhaps due to strong auroral precipitations.

## REFERENCES

BOROVKOV, L.P., E.V. VASHENYUK and L.L. LAZUTIN 1984 "Izvestiya Academii Nauk USSR", **seriya fizcheskaya, v. 48,** N 11, 2174 (sov., in Russian).

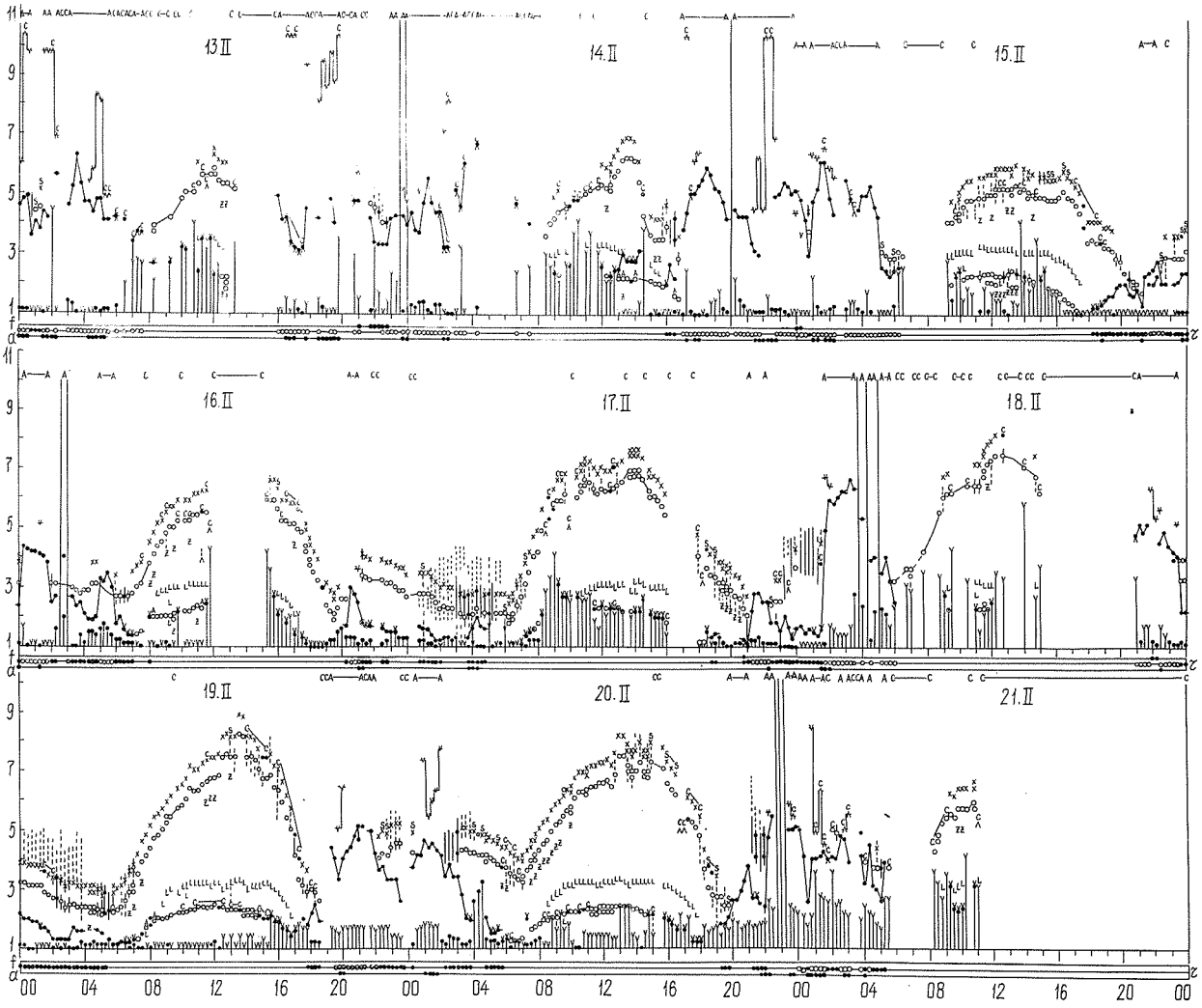


Fig. 7. f-plots from 13 to 21 February 1984 (ionosonde at Murmansk).

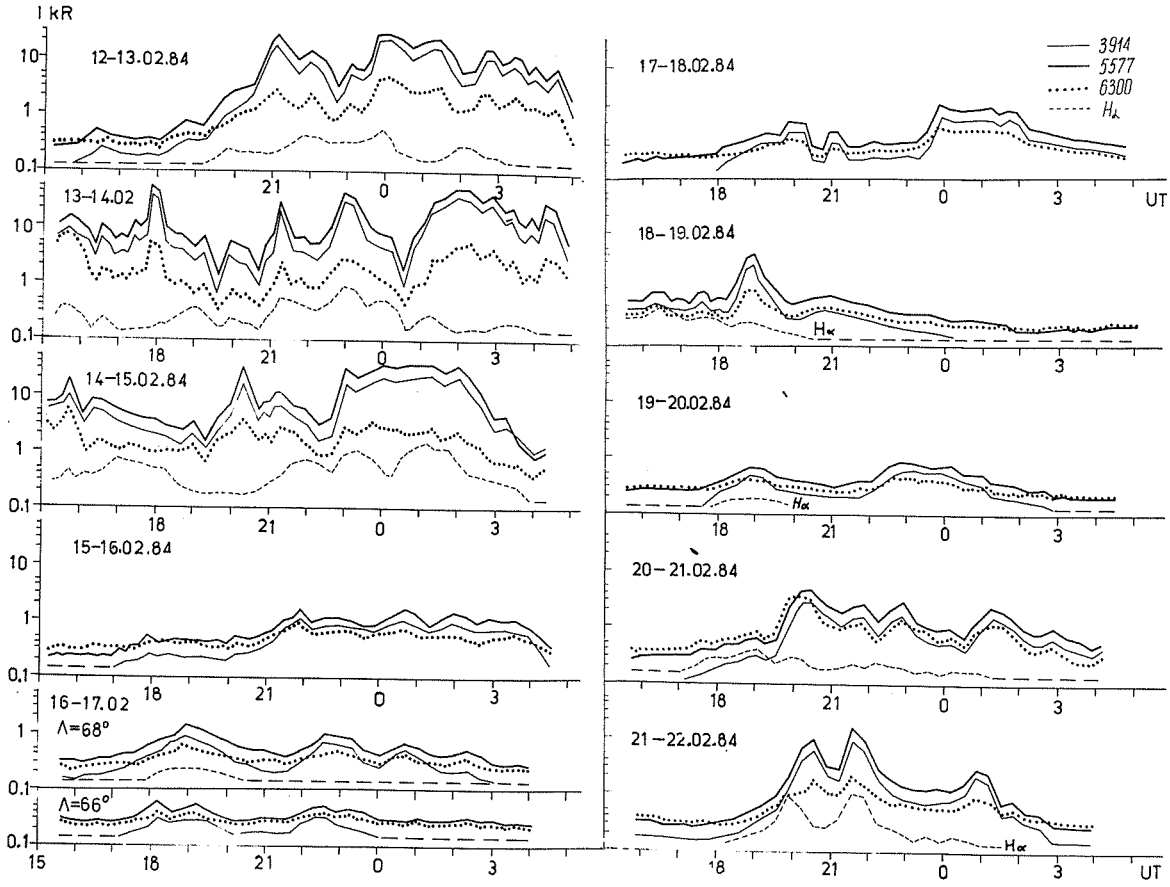


Fig. 8. The intensity of various auroral emissions, log $I_{KR}$ (Loparskaya).

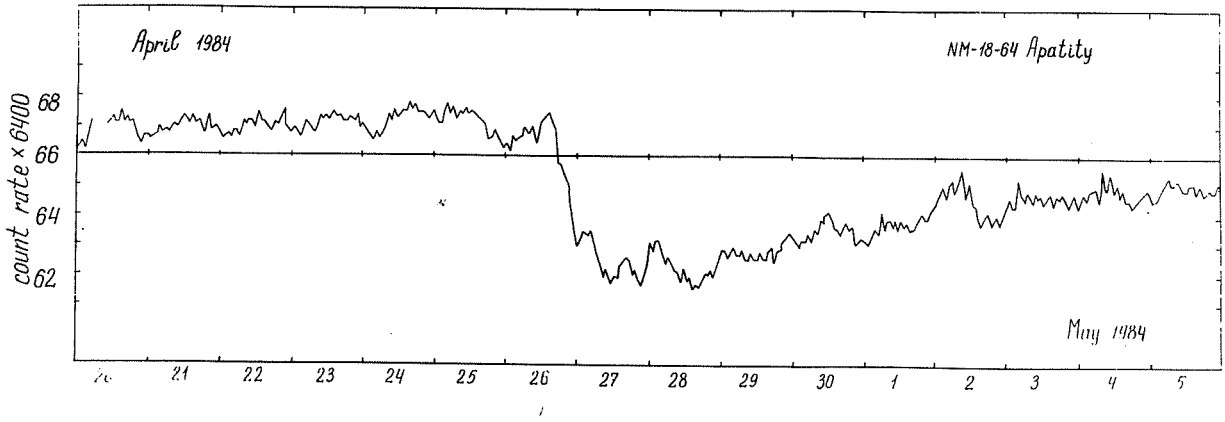


Fig. 9. Hourly count rates of the neutron monitor at Apatity from 20 April to 5 May 1984.

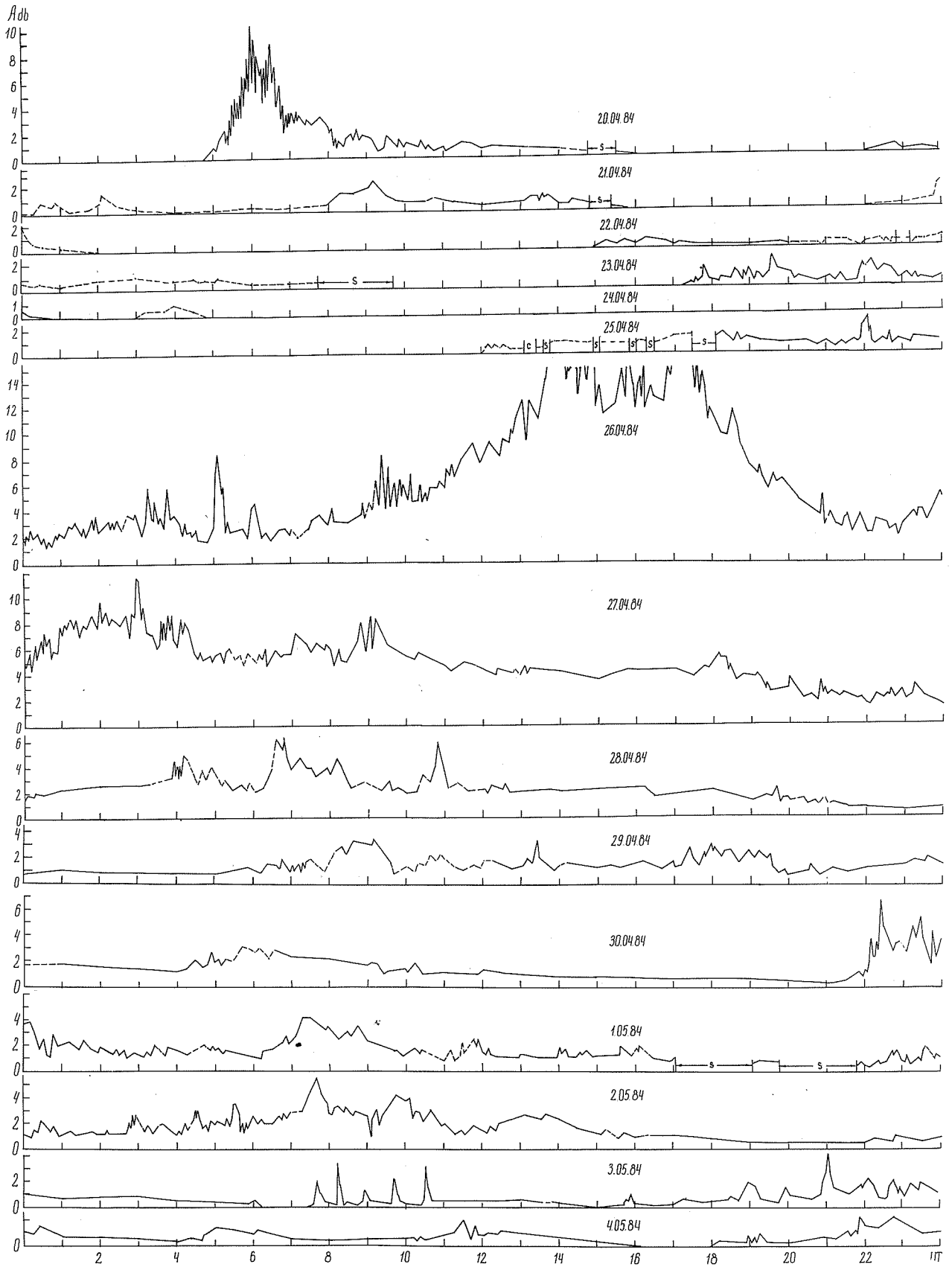


Fig. 10. Riometer absorption records from 20 April to 4 May 1984 (Loparskaya 32 MHz).

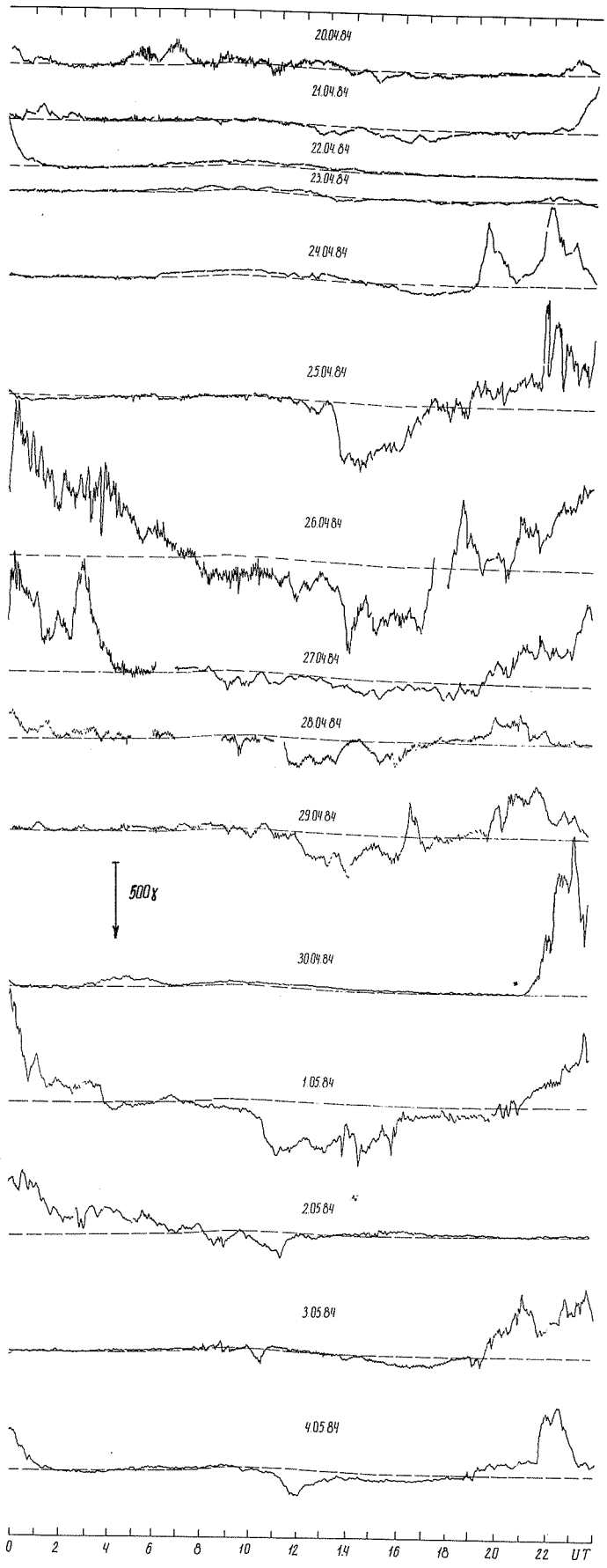


Fig.11. H-component geomagnetic field records since 20 April to 04 May, 1984 (Loparskaya).

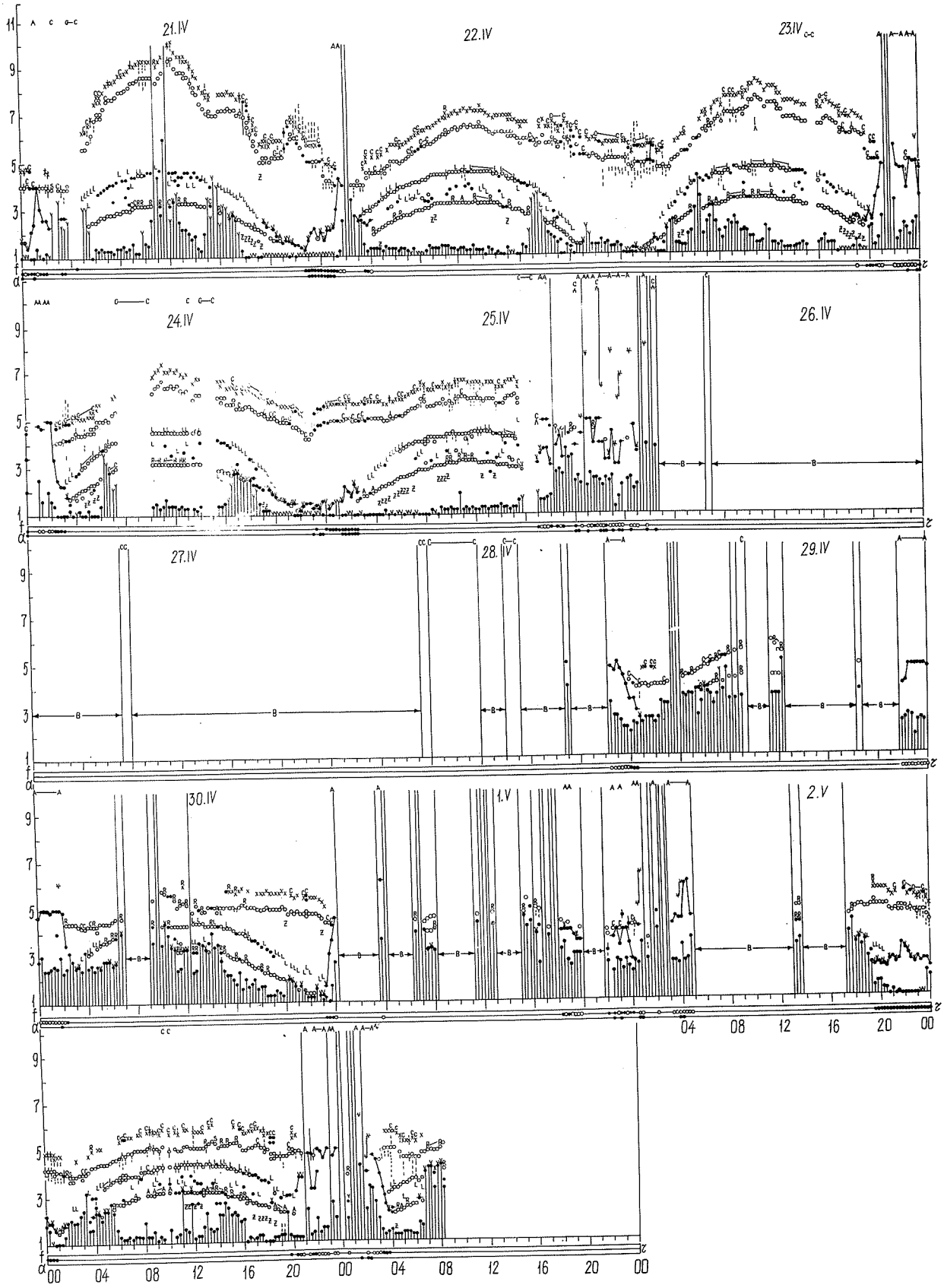


Fig. 12. f-plots from 21 April to 4 May 1984 (ionosonde at Murmansk).

# The Phenomena in the Ionosphere on 16 February and 24 April 1984 Observed at Sverdlovsk (Arty) Station (N56°26' E58°34')

by

V.A. Belyaev, M.V. Levin and V.F. Zakharchenko
Institute of Geophysics, The Urals Science Center
USSR Academy of Sciences, Amundsen Street, 100
Sverdlovsk 620147, USSR



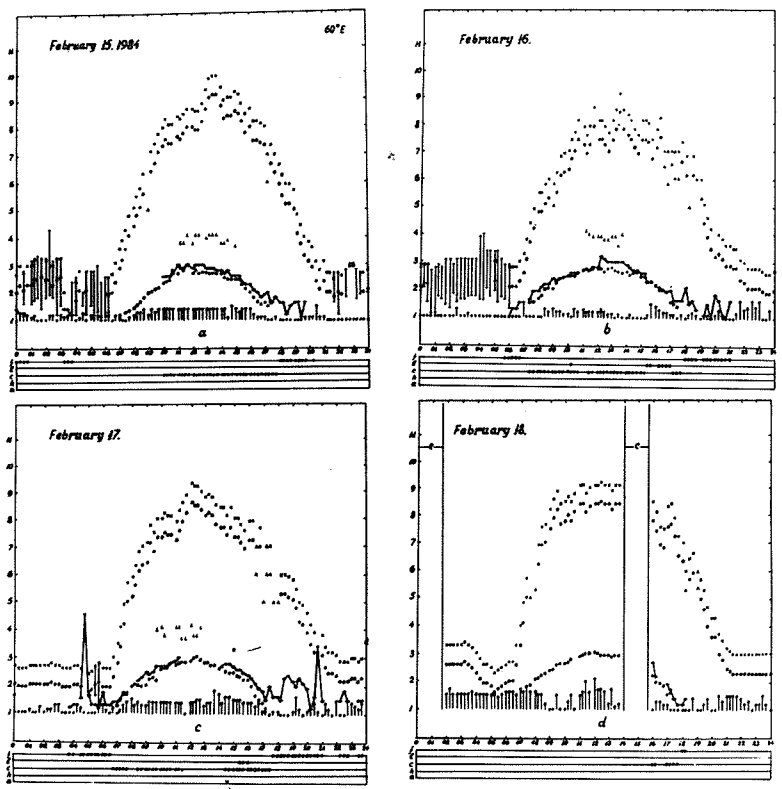


Fig. 1. f-plots for 15-18 February 1984 at Sverdlovsk (Arty).

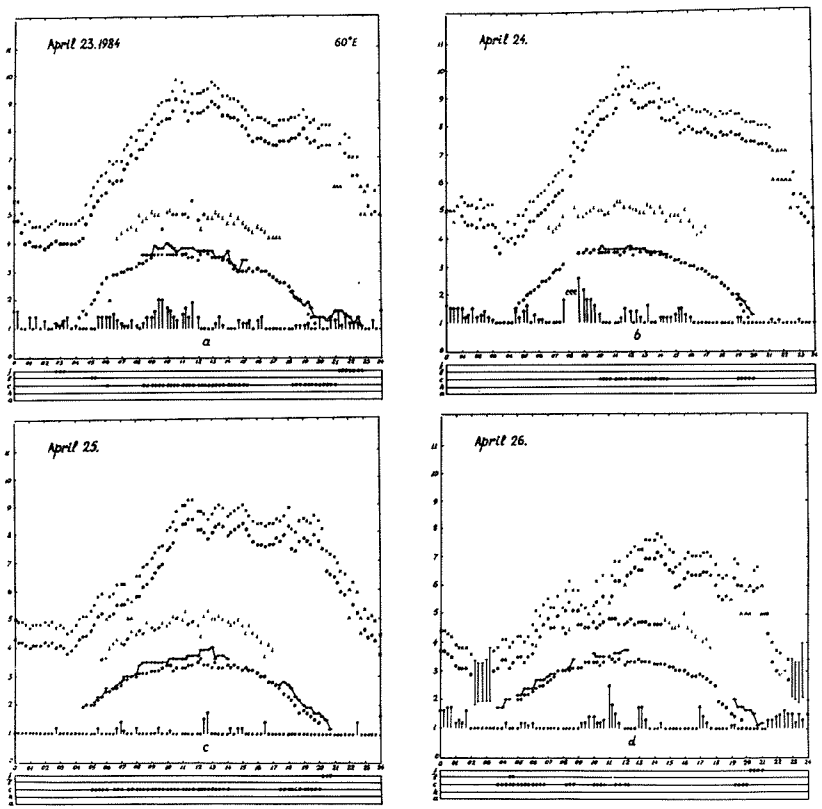


Fig. 2. f-plots for 23-26 April 1984 at Sverdlovsk (Arty).

# Ionospheric Parameters and Geomagnetic Variations in February and April 1984 from Novosibirsk Data

by

V.V. Kuznetsov, V.T. Levadny, I.I. Nesterova,
N.I. Izrayleva, I.V. Pavlova and V.V. Plotkin
Institute of Geology and Geophysics, Siberian Branch, USSR
Academy of Sciences, Novosibirsk, USSR

The vertical incidence sounding of the ionosphere is carried out at Novosibirsk (N55.0 E82.9) by an automatic ionosphere station (AIS). The results of the soundings on 12-17 February and 25-30 April 1984 are presented as standard f-plots made according to the rules of the URSI Handbook on Ionogram Interpretation and Reduction (Figures 1 and 2).

The geomagnetic data obtained during 24-28 April 1984 are presented as magnetograms (Figure 3).

## 12-17 February 1984 Period

Figure 1 shows the diffusion in the F-region for the period 12-17 February 1984 at night from 2000 LT to 0700 LT. On 16 February, foF2 fell sharply to 1.5 MHz.

## 24-30 April 1984 Period

On 25 April 1984 at 0615 LT a sudden ionospheric disturbance (SID) was recorded. At 0630 LT the radiowave absorption in the lower ionosphere increased (fmin = 4.2 MHz). At the same time (on 25 April at 0600 LT or 0000 UT) the magnetograms show a magnetic bay variation of the D and H components.

The negative ionosphere disturbance began on 26 April 1984 at 2200 LT (there were no ionospheric data on 27 April during 0000-0600 LT).

On 27 April 1984 the electron concentration of the F2-region was lower than that of the F1-region (the condition G: foF2 < foF1). The maximum deviation $\Delta$ foF2 was 35-40 percent. The restoration phase of the ionospheric disturbance lasted until 30 April. This ionospheric disturbance proceeded against the background of a moderate magnetic storm with a sudden commencement. The magnetic storm started on 25 April 1984 at 0000 UT and was over on 30 April 1984 at 1700 UT. The maximum values of the D, H and Z components were 186 nT, 167 nT and 86 nT, respectively. The active magnetic storm period was observed between 1300 UT on 25 April and 0100 UT on 27 April 1984.

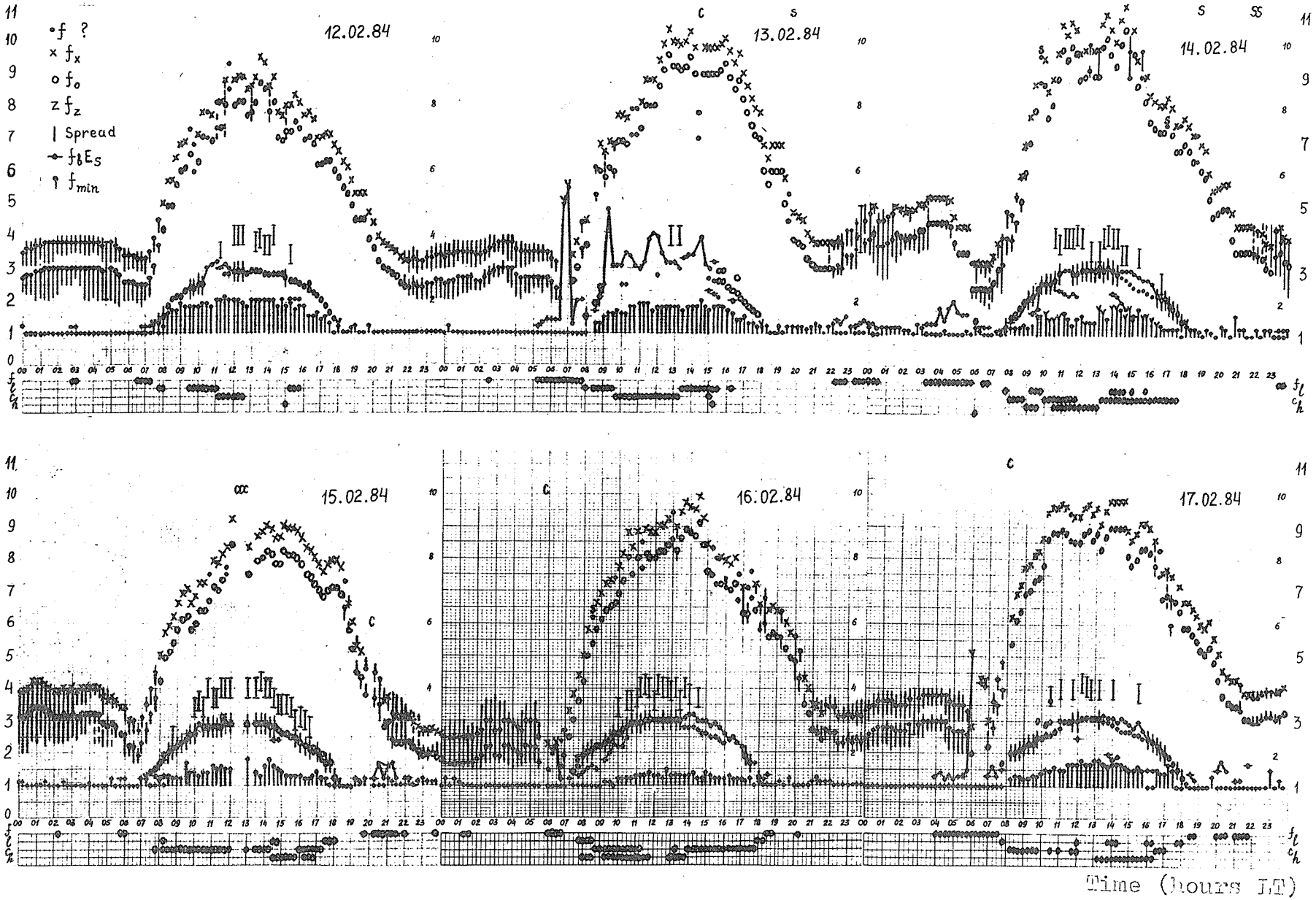


Fig. 1. f-plots from Novosibirsk for the period 12-17 February 1984.

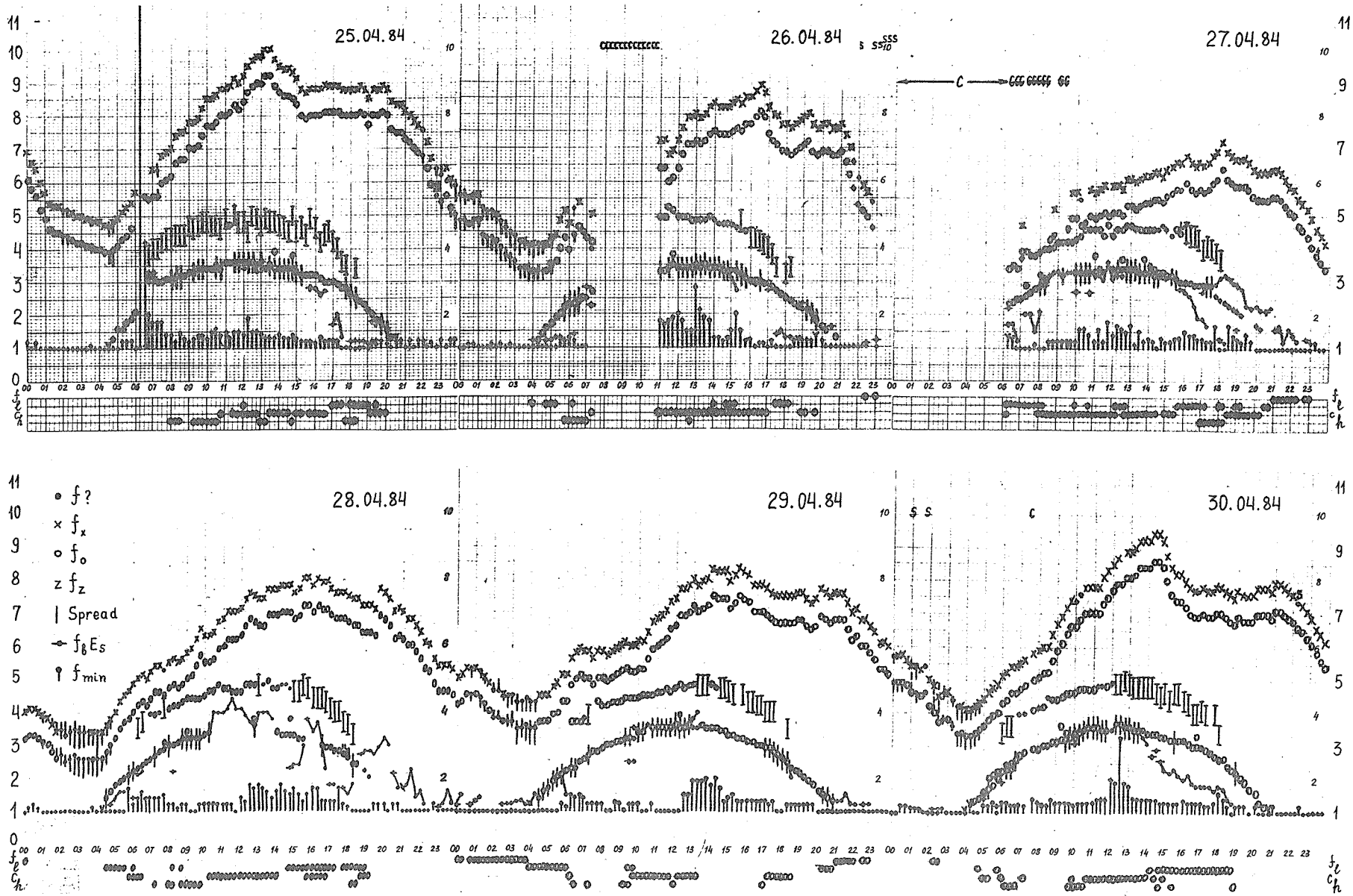


Fig. 2. f-plots from Novosibirsk for the period 25-30 April 1984.

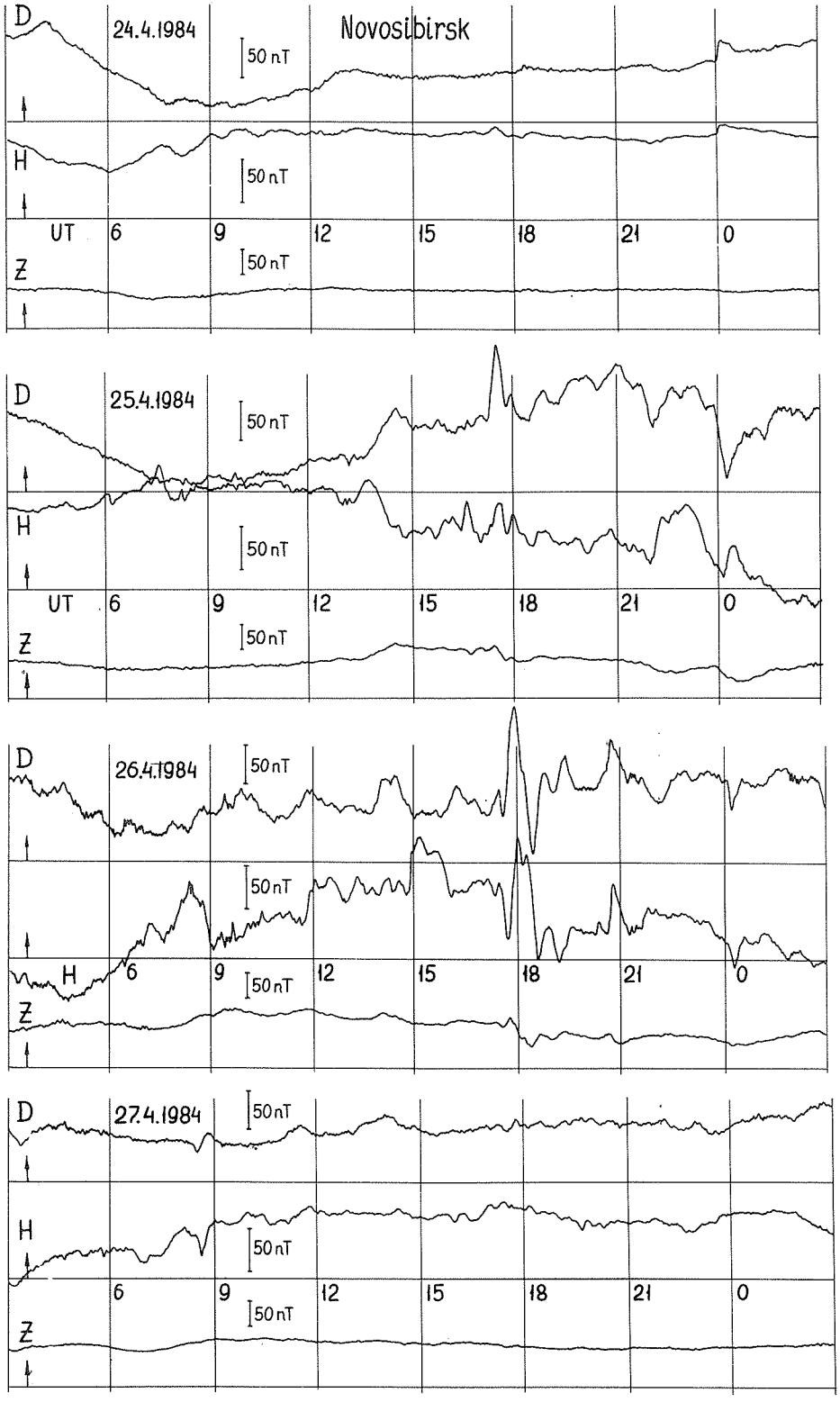


Fig. 3. Magnetograms from Novosibirsk for the period 24-28 April 1984.

# Standard Ionospheric Observations at Khabarovsk in February and April 1984

by

V.S. Maksimov, N.D.Pogorelova and T.F. Kudiakova
Department of Physics of Near-Terrestrial Space
NESCRI, Khabarovsk, USSR

These ionospheric data were obtained by an SP-3 ionosonde at Khabarovsk (geomagnetic coordinates: N39 E200). Standard f-plots, characterizing the general picture of ionospheric phenomena during the active periods in February and April 1984, as well as E-plots and the curves of the F-region effective heights are shown in the figures.

Editor's Note: All the graphs in this paper were printed from microfilm copy sent to the data center. We apologize for the poor copy of some of the graphs. The original microfilm is available from us. Please contact the data center if you require larger versions of these graphs or a copy of the original microfilm.

Khabarovsk E-graphs for the period 12-20 February 1984:

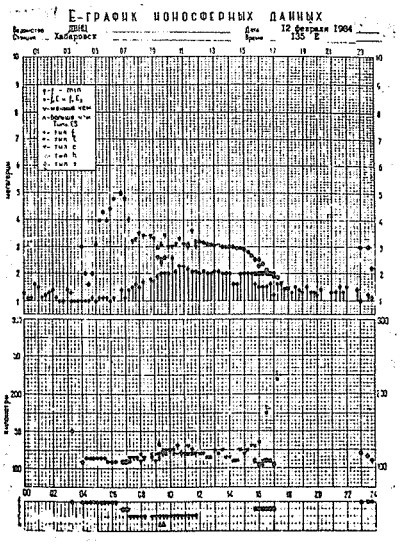


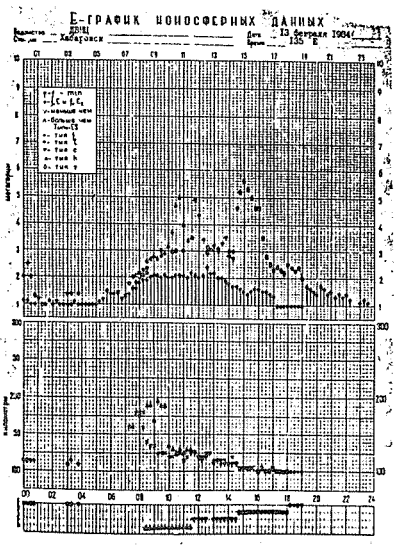


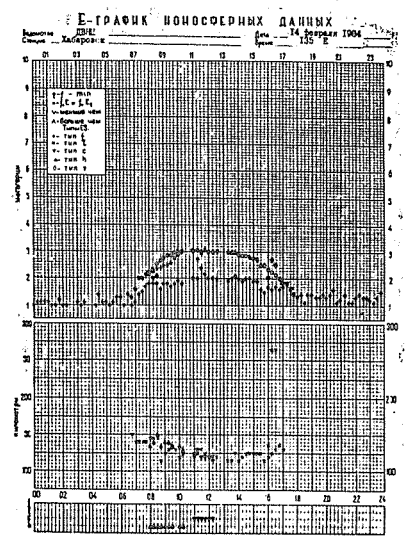


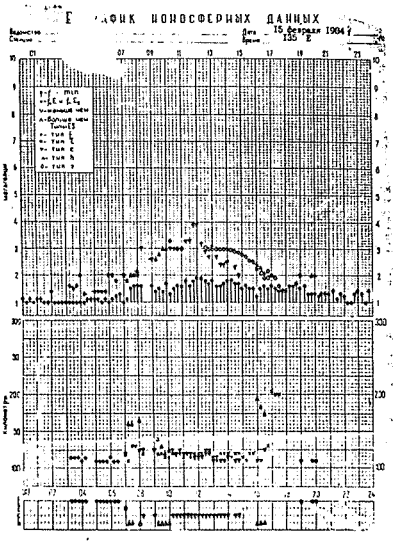


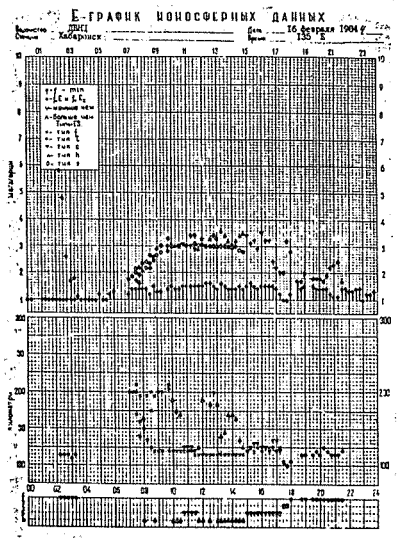


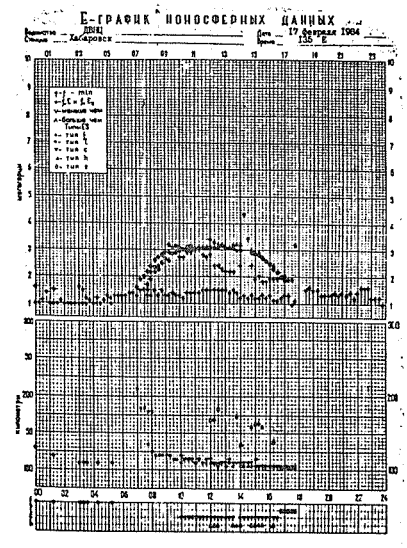


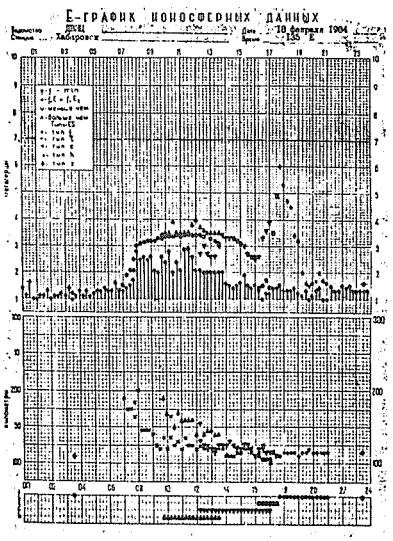


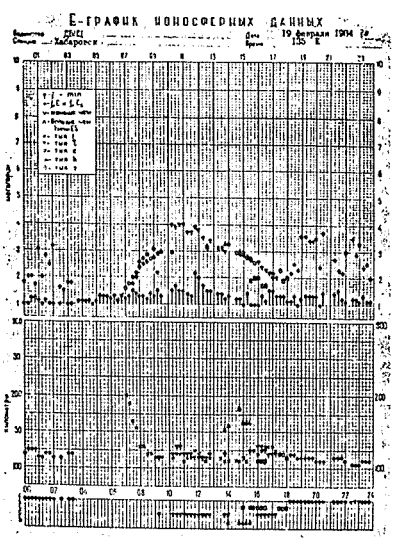


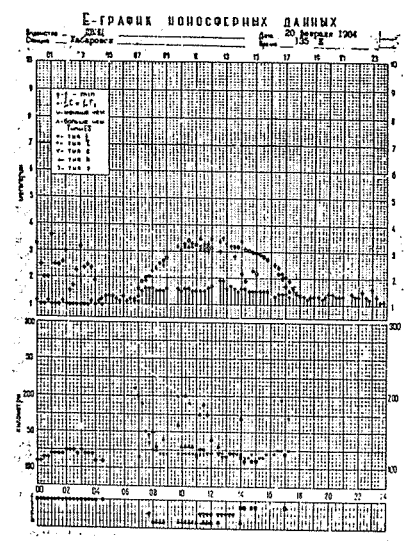

Khabarovsk F-graphs for the period 12-20 February 1994:

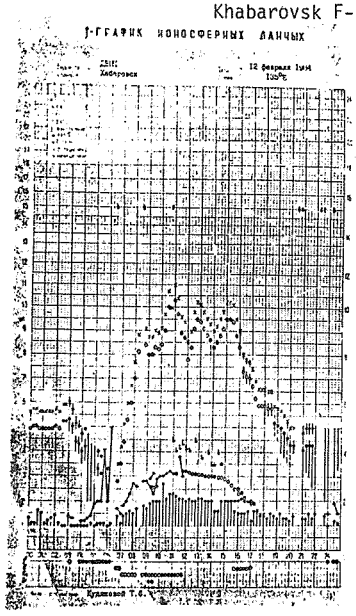


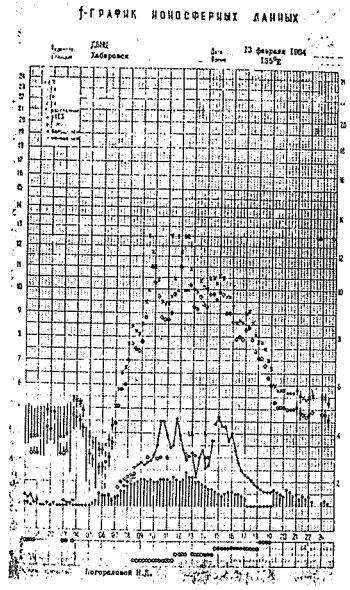


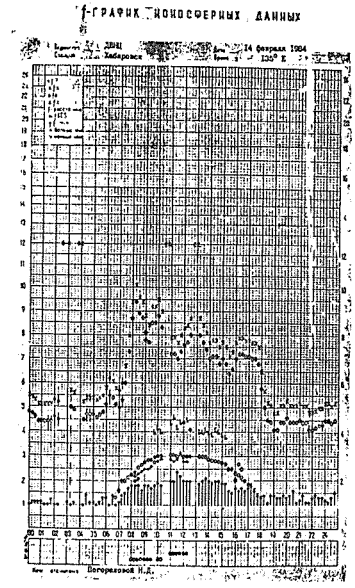


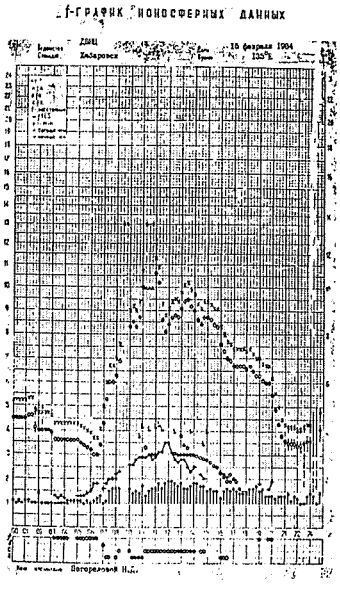


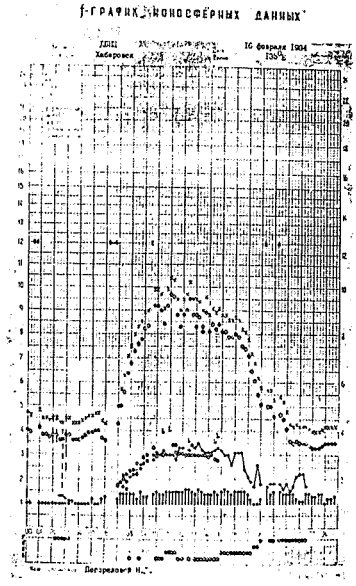


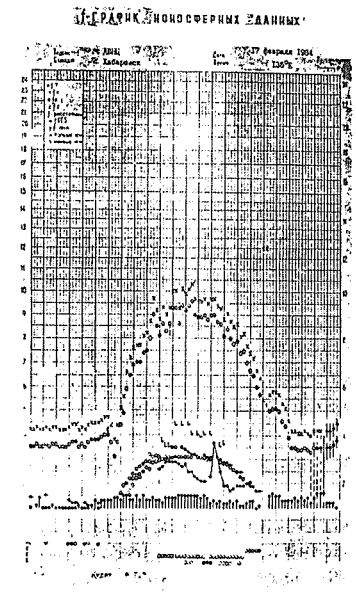


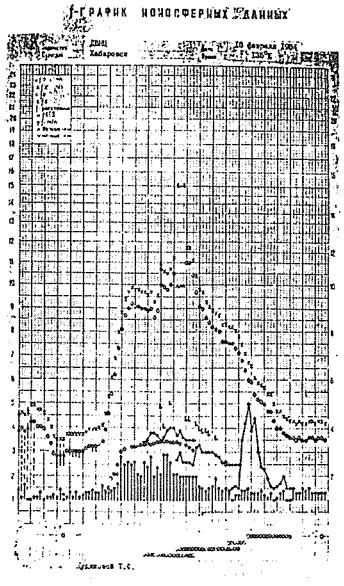


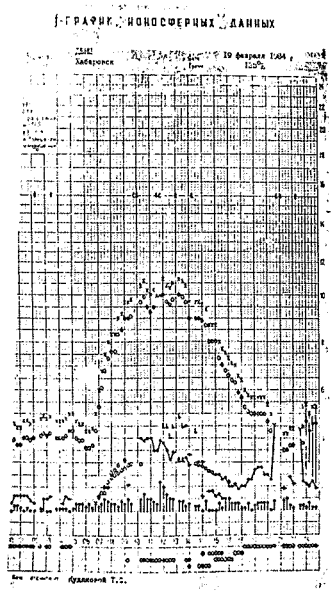


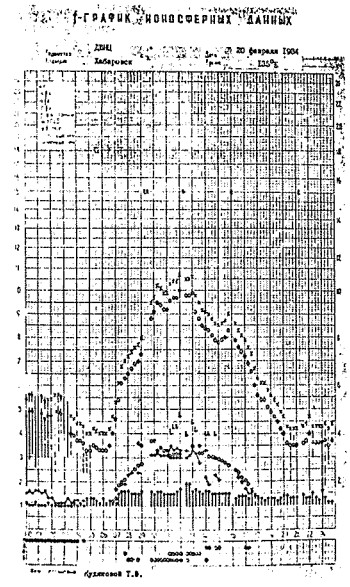

Khabarovsk E-graphs for the period 20 April - 4 May 1984:

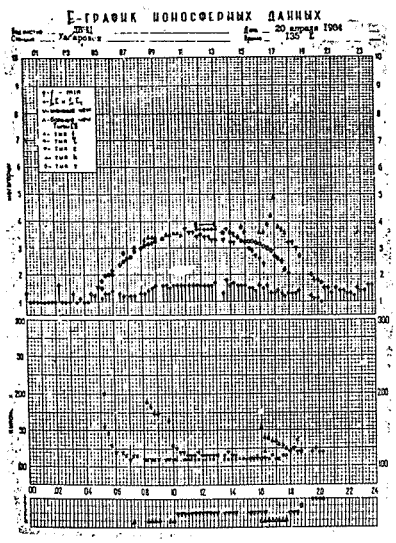


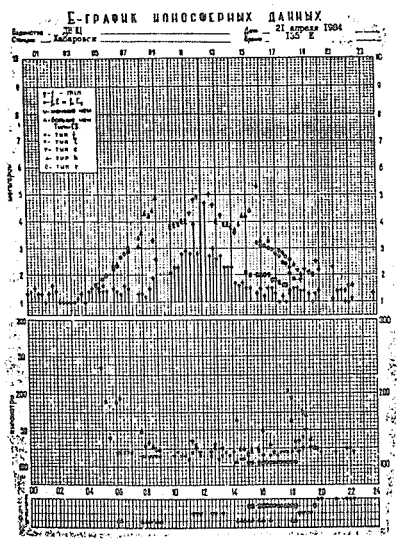


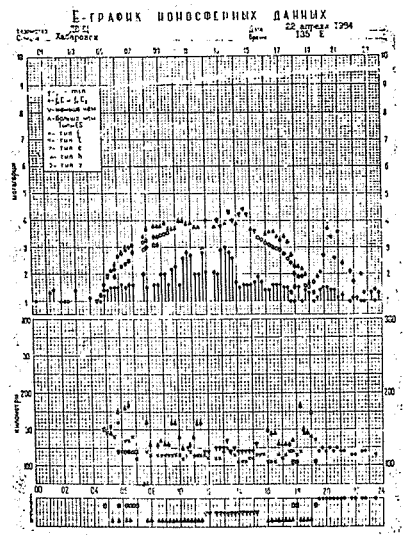


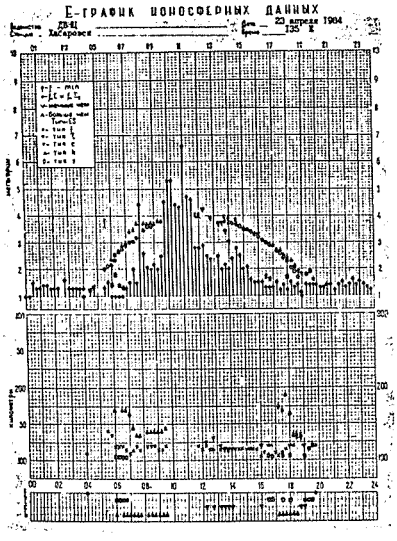


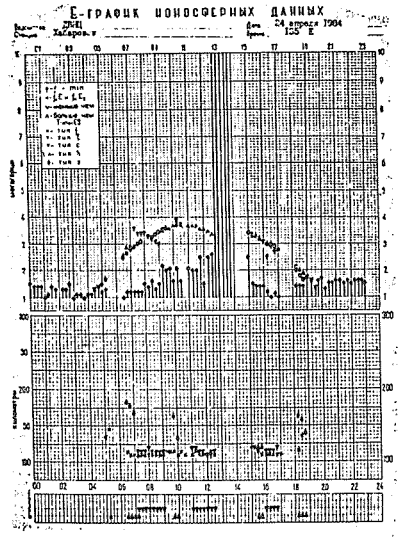


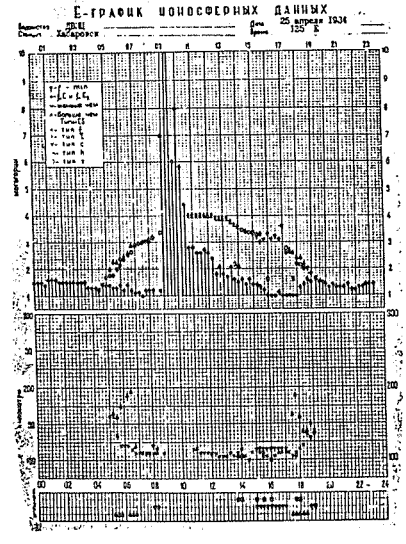


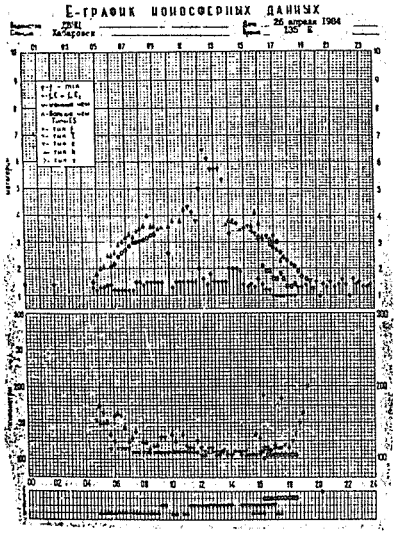


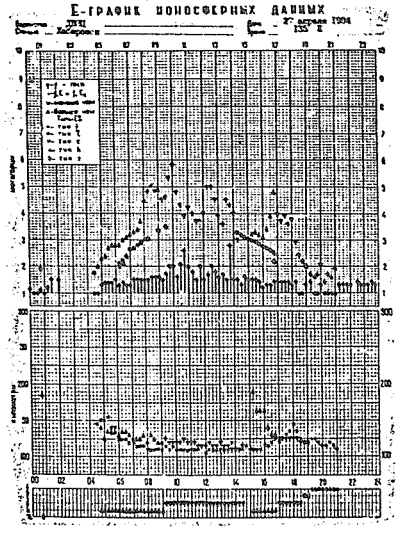


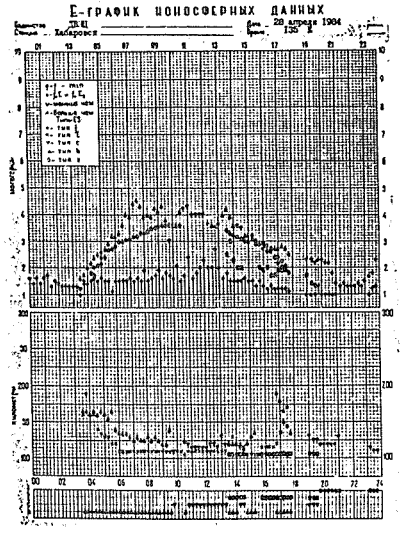

Khabarovsk E-graphs for the period 20 April - 4 May 1984 continued:

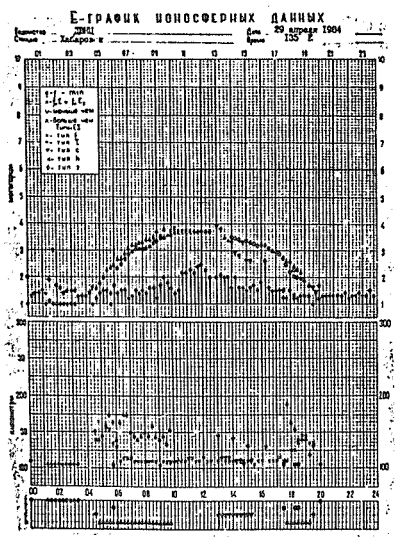


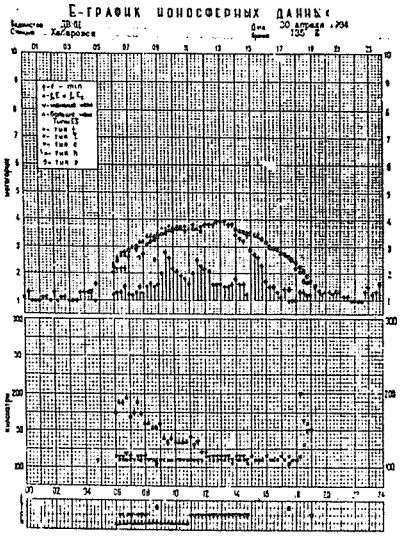


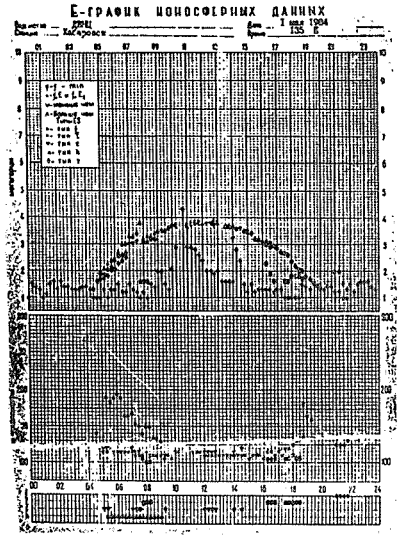


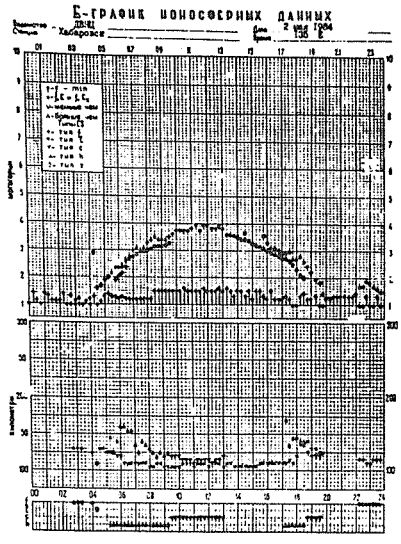


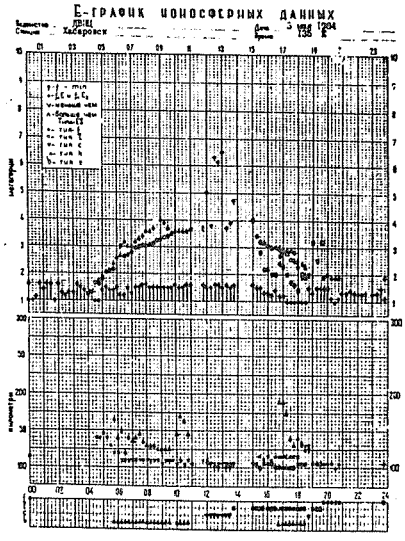


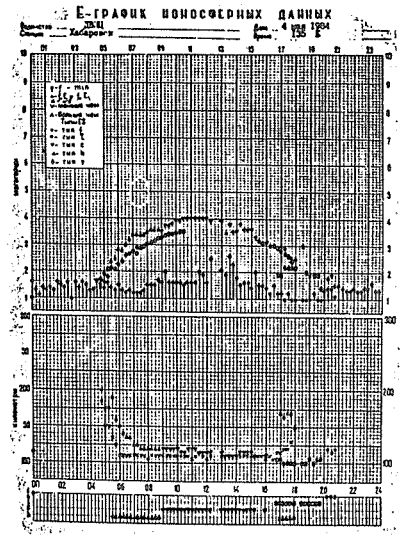

Khabarovsk F-graphs for the period 20 April - 4 May 1984:

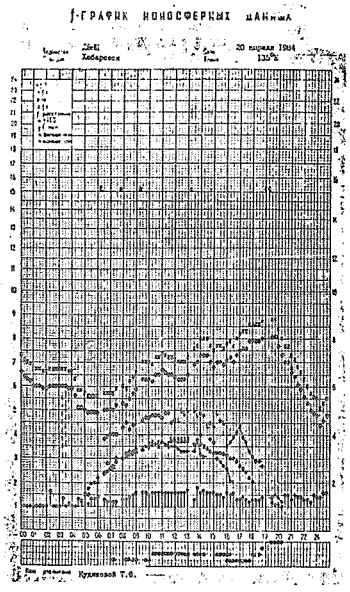


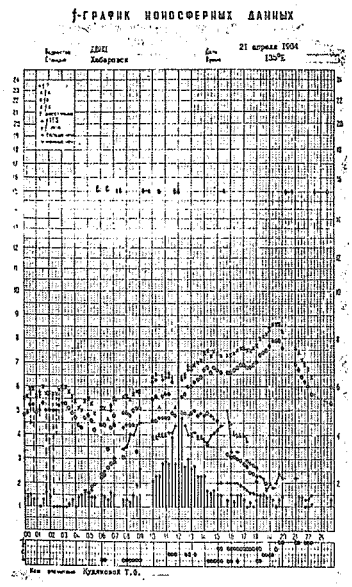


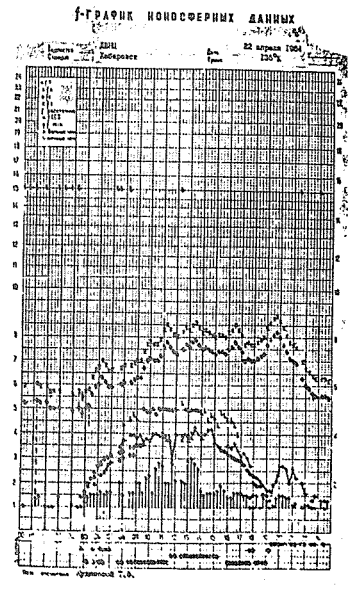


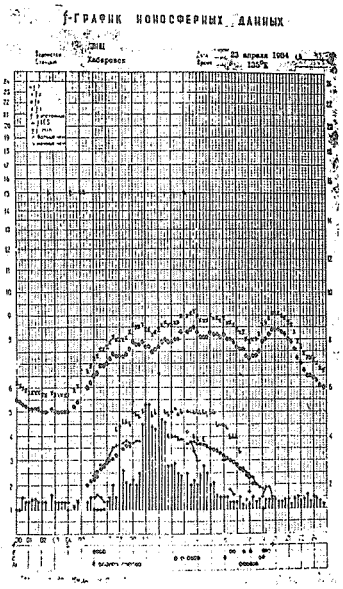


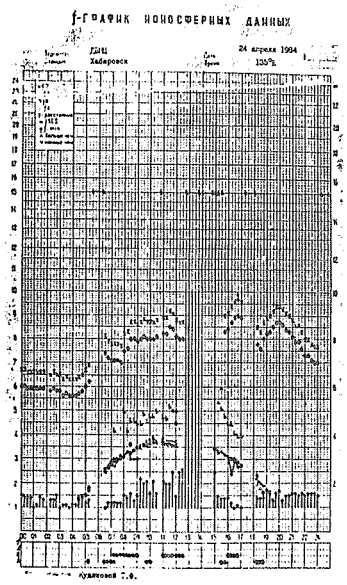


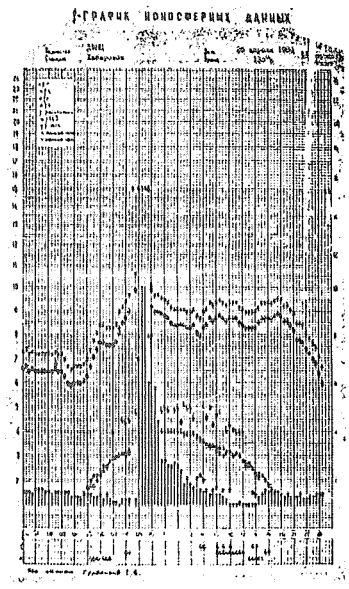


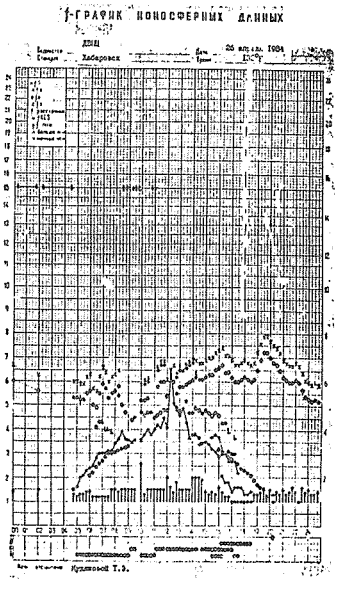


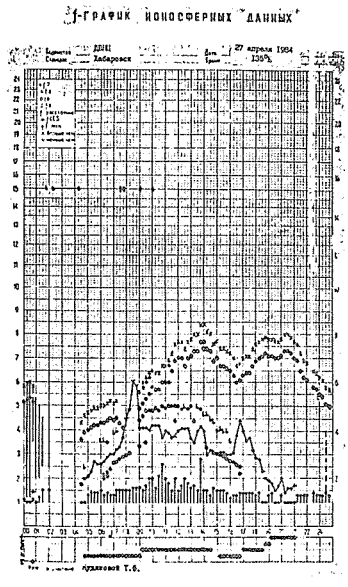


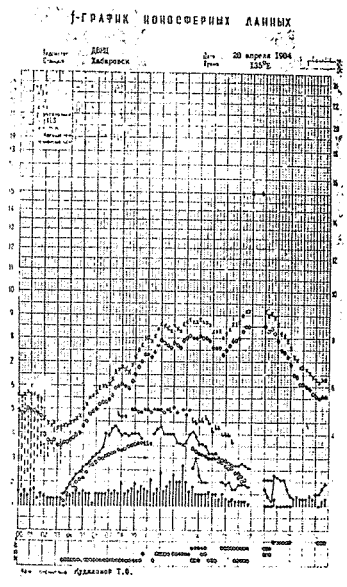

Khabarovsk F-graphs for the period 20 April - 4 May 1984 continued:

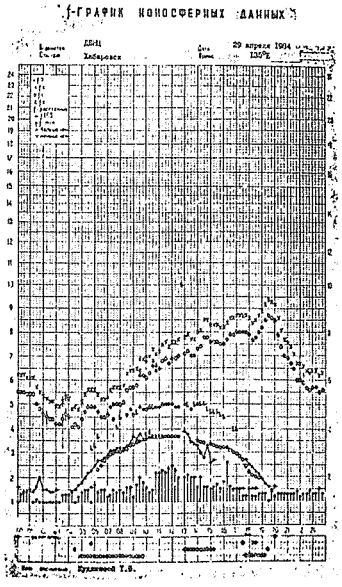


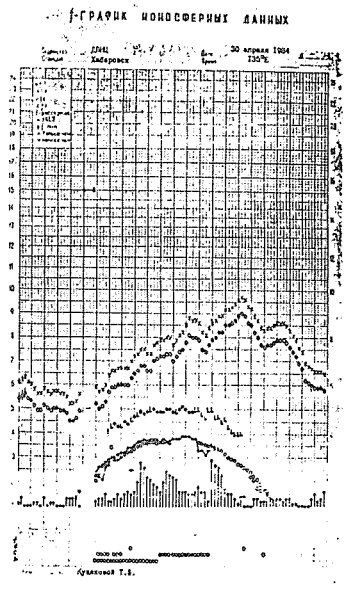


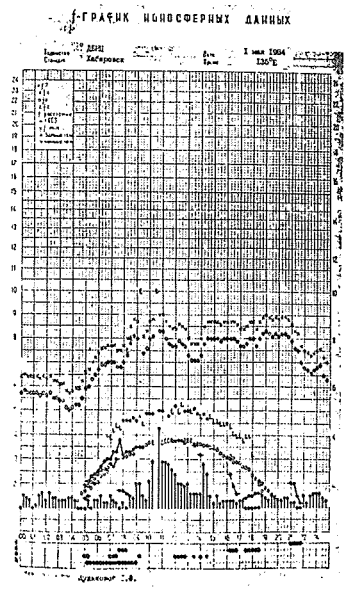


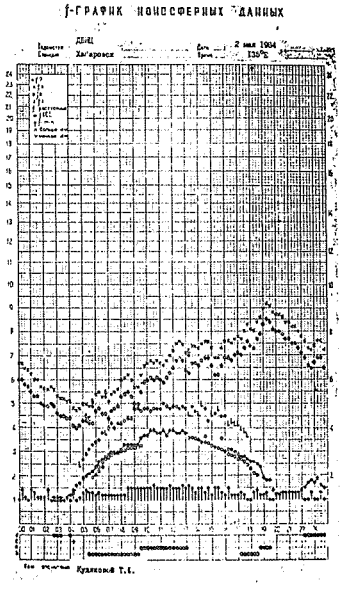


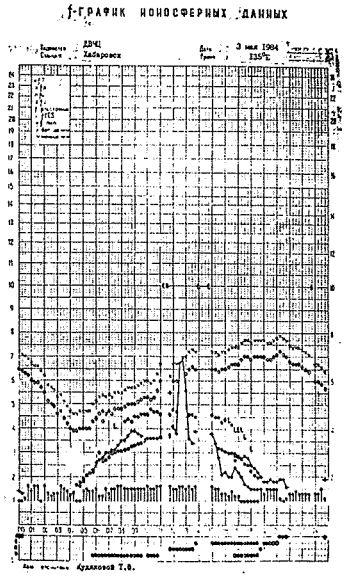


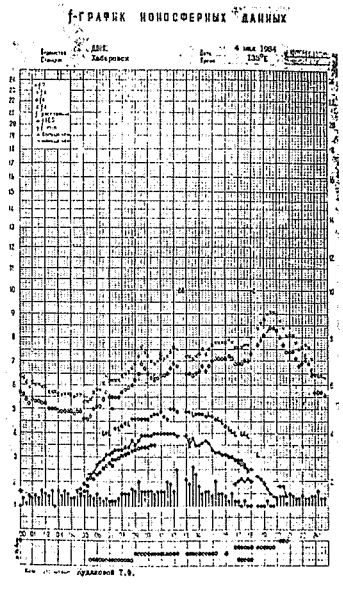

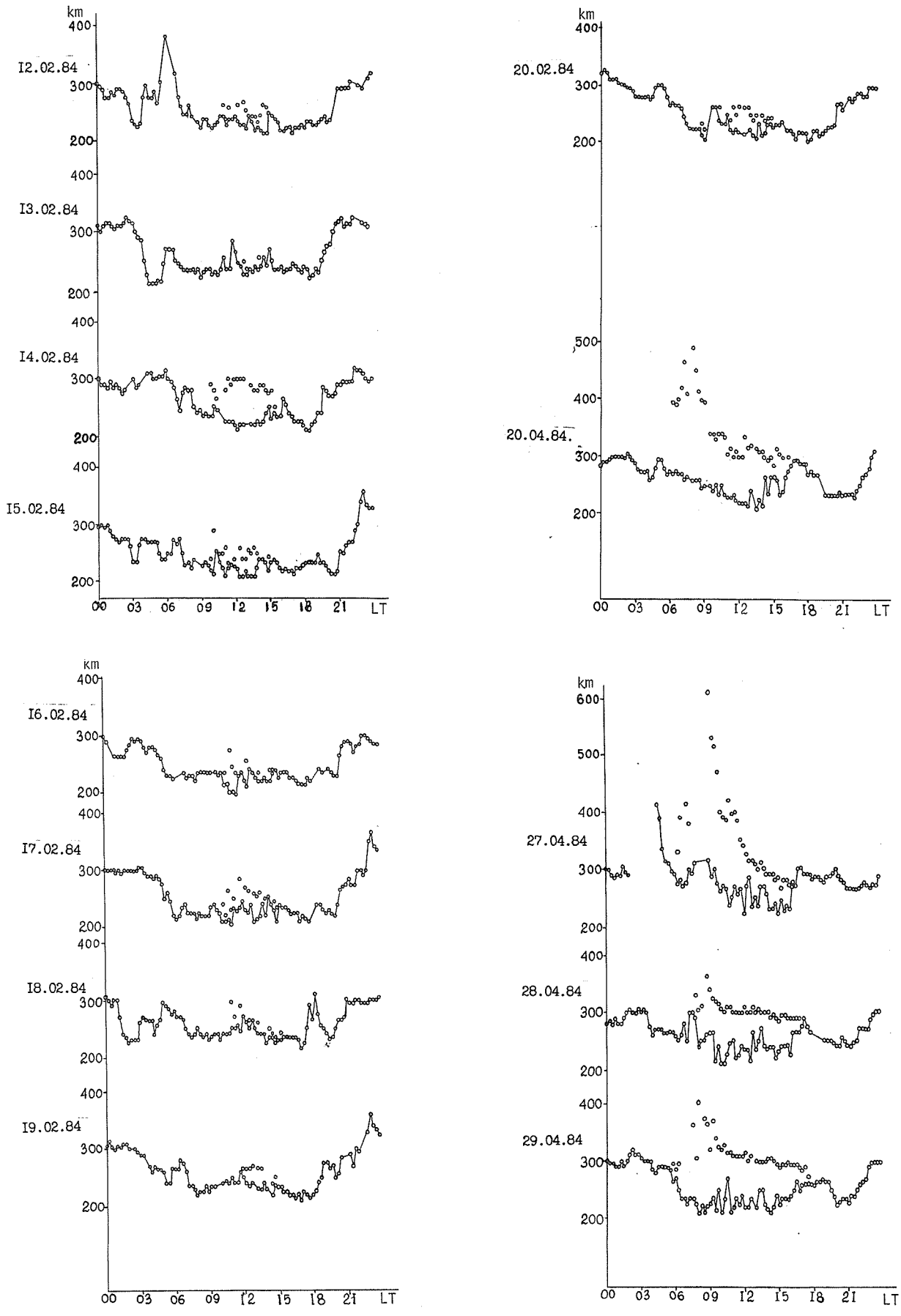


h-graphs ionospheric data -- Curves of the F-region effective height from Khabarovsk for the periods 12-20 February and 20 April - 4 May 1984.

h-graphs continued

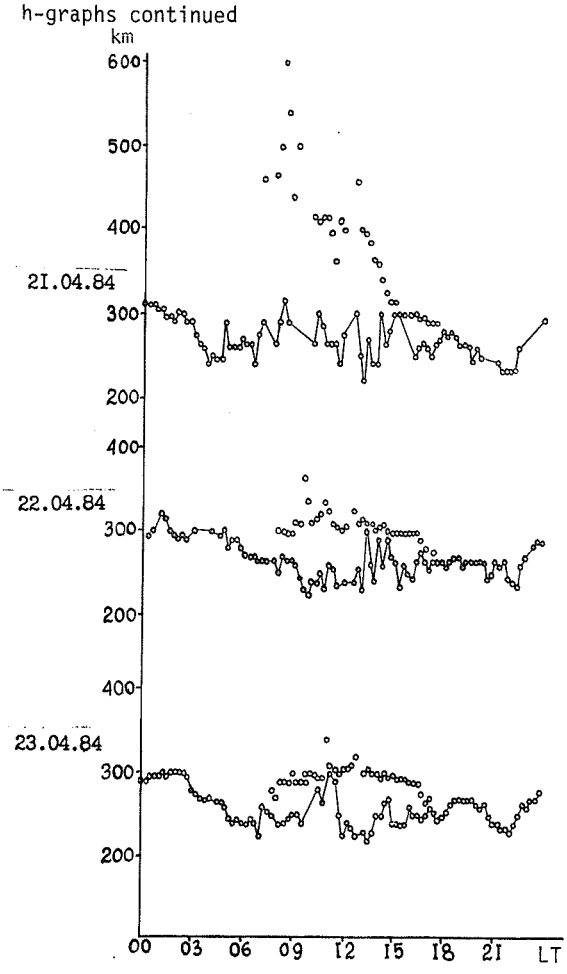


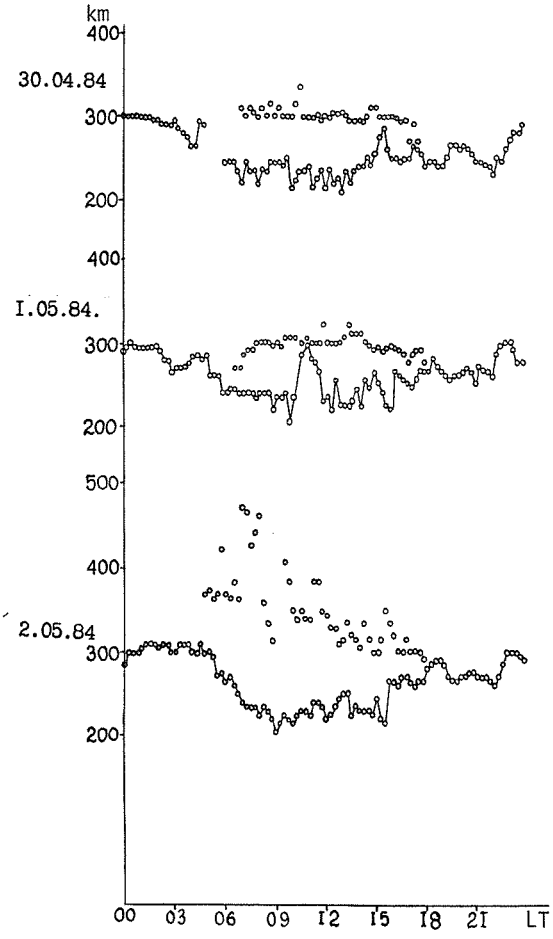


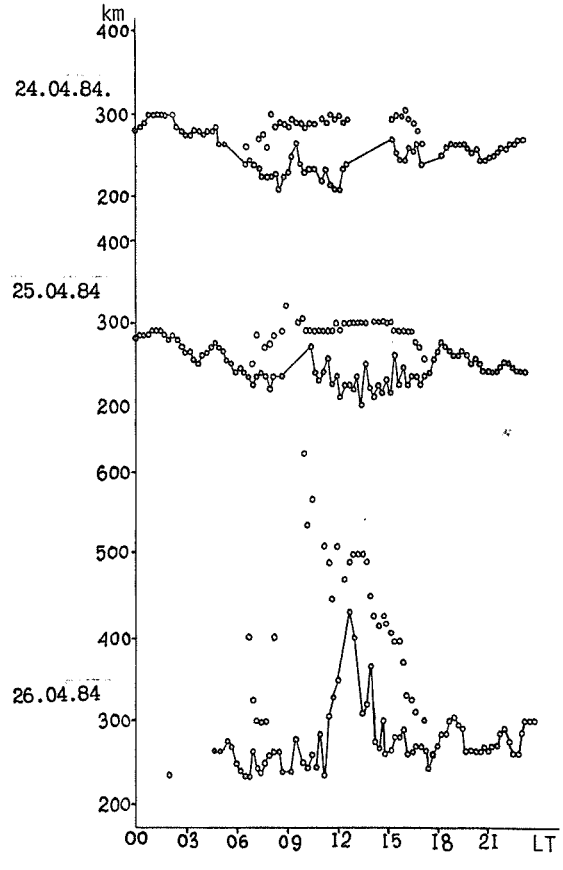


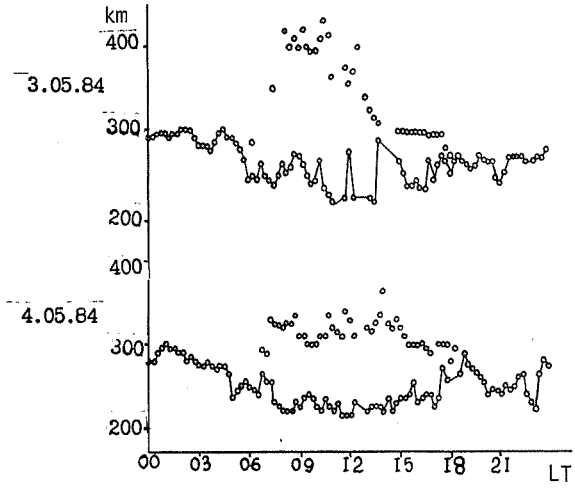

Khabarovsk Neutron Monitor Data for 26 February - 5 March 1984

| Hour UT | 1984 February 26 | 27 | 28 | 29 | 1984 March 01 | 02 | 03 | 04 | 05 | Hourly Average |
|---|---|---|---|---|---|---|---|---|---|---|
| 0100 | 6452 | 6461 | 6454 | 6515 | 6463 | 6509 | 6519 | 6526 | 6572 | 6497 |
| 0200 | 6496 | 6454 | 6510 | 6550 | 6508 | 6531 | 6498 | 6550 | 6548 | 6516 |
| 0300 | 6471 | 6457 | 6518 | 6535 | 6496 | 6508 | 6504 | 6565 | 6550 | 6512 |
| 0400 | 6477 | 6461 | 6546 | 6541 | 6506 | --- | 6516 | 6539 | 6545 | 6516 |
| 0500 | 6500 | 6484 | 6556 | 6533 | 6497 | --- | 6507 | 6539 | 6570 | 6523 |
| 0600 | 6504 | 6503 | 6566 | 6536 | 6485 | --- | 6519 | 6564 | 6530 | 6526 |
| 0700 | 6473 | 6447 | 6544 | 6511 | 6504 | --- | 6489 | 6547 | 6565 | 6510 |
| 0800 | 6483 | 6481 | 6508 | 6536 | 6490 | --- | 6473 | 6559 | 6560 | 6511 |
| 0900 | 6472 | 6502 | 6520 | 6555 | 6453 | 6504 | 6485 | 6548 | 6560 | 6511 |
| 1000 | 6460 | 6458 | 6520 | 6538 | 6444 | 6499 | 6472 | 6558 | 6552 | 6500 |
| 1100 | 6475 | 6423 | 6532 | 6551 | 6433 | 6501 | 6494 | 6541 | 6569 | 6502 |
| 1200 | 6429 | 6436 | 6476 | 6544 | 6444 | 6482 | 6485 | 6534 | 6545 | 6486 |
| 1300 | 6442 | 6441 | 6489 | 6523 | 6432 | 6475 | 6496 | 6581 | 6552 | 6492 |
| 1400 | 6413 | 6409 | 6523 | 6518 | 6494 | 6496 | 6509 | 6526 | 6573 | 6496 |
| 1500 | 6413 | 6398 | 6483 | 6540 | 6497 | 6497 | 6511 | 6535 | 6559 | 6493 |
| 1600 | 6466 | 6383 | 6506 | 6542 | 6475 | 6487 | 6527 | 6537 | 6573 | 6500 |
| 1700 | 6417 | 6392 | 6476 | 6510 | 6491 | 6510 | 6502 | 6556 | 6550 | 6489 |
| 1800 | 6444 | 6383 | 6499 | 6518 | 6455 | 6501 | 6539 | 6527 | 6553 | 6491 |
| 1900 | 6439 | 6376 | 6522 | 6503 | 6471 | 6456 | 6524 | 6513 | 6541 | 6483 |
| 2000 | 6483 | 6409 | 6485 | 6503 | 6458 | 6488 | 6480 | 6524 | 6519 | 6483 |
| 2100 | 6482 | 6471 | 6498 | 6498 | 6496 | 6469 | 6503 | 6513 | 6501 | 6492 |
| 2200 | 6474 | 6452 | 6527 | 6488 | 6510 | 6457 | 6529 | 6510 | 6527 | 6497 |
| 2300 | 6502 | 6458 | 6517 | 6481 | 6501 | 6467 | 6506 | 6516 | 6537 | 6498 |
| 2400 | 6456 | 6465 | 6513 | 6482 | 6492 | 6489 | 6524 | 6531 | 6556 | 6501 |
| MEAN | 6463 | 6442 | 6512 | 6523 | 6479 | 6491 | 6505 | 6539 | 6550 | 6500 |

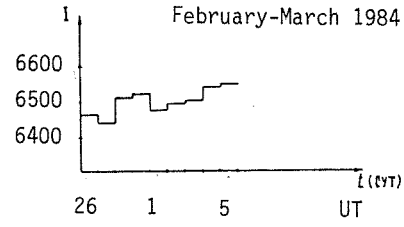


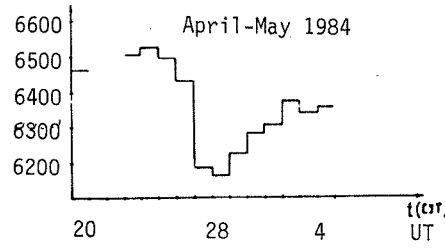


Khabarovsk Neutron Monitor Data for 20 April - 4 May 1984

| Hour UT | 1984 April 20 | 21 | 22 | 23 | 24 | 25 | 26 | 27 | 28 | 29 | 30 | 1984 May 01 | 02 | 03 | 04 | Hourly Average |
|---|---|---|---|---|---|---|---|---|---|---|---|---|---|---|---|---|
| 0100 | 6449 | --- | --- | 6547 | 6507 | 6562 | 6518 | --- | 6158 | 6192 | 6279 | 6300 | 6388 | 6386 | 6476 | 6397 |
| 0200 | 6468 | --- | --- | 6543 | 6521 | 6577 | 6506 | 6331 | 6154 | 6203 | 6323 | 6307 | 6419 | 6342 | 6434 | 6394 |
| 0300 | 6432 | --- | --- | 6541 | 6529 | 6556 | 6500 | 6164 | 6153 | 6195 | 6323 | 6287 | 6406 | 6337 | 6398 | 6371 |
| 0400 | 6445 | --- | --- | --- | 6551 | 6518 | 6531 | 6147 | 6123 | 6167 | 6278 | 6285 | 6393 | 6281 | 6323 | 6337 |
| 0500 | 6473 | --- | --- | --- | 6502 | 6563 | 6502 | 6093 | 6112 | 6154 | 6279 | 6276 | 6392 | --- | 6345 | 6336 |
| 0600 | 6481 | --- | --- | --- | 6574 | 6498 | 6488 | 6119 | 6099 | 6150 | 6277 | 6258 | 6402 | --- | 6323 | 6334 |
| 0700 | 6507 | --- | --- | --- | 6503 | 6536 | 6513 | 6120 | 6102 | 6122 | 6262 | 6293 | 6399 | 6281 | 6334 | 6331 |
| 0800 | 6482 | --- | --- | --- | 6549 | 6490 | 6470 | 6138 | 6090 | 6145 | 6284 | 6261 | 6395 | 6287 | 6323 | 6326 |
| 0900 | 6479 | --- | --- | 6502 | 6549 | 6481 | 6463 | 6147 | 6108 | 6189 | 6290 | 6271 | 6376 | 6308 | 6332 | 6346 |
| 1000 | --- | --- | --- | 6525 | 6522 | 6451 | 6492 | 6205 | 6127 | 6171 | 6316 | 6268 | 6410 | 6288 | 6314 | 6341 |
| 1100 | --- | --- | --- | 6511 | 6530 | 6464 | 6483 | 6237 | 6129 | 6168 | 6325 | 6299 | 6389 | 6274 | 6339 | 6346 |
| 1200 | --- | --- | --- | 6538 | 6516 | 6463 | 6481 | 6188 | 6193 | 6199 | 6314 | 6274 | 6400 | 6302 | 6348 | 6351 |
| 1300 | --- | --- | --- | 6492 | 6505 | 6449 | 6469 | 6185 | 6163 | 6220 | 6337 | 6303 | 6342 | 6306 | 6327 | 6342 |
| 1400 | --- | --- | --- | 6499 | 6527 | 6506 | 6453 | 6158 | 6183 | 6230 | 6330 | 6302 | 6325 | 6315 | 6321 | 6346 |
| 1500 | --- | --- | --- | 6479 | 6490 | 6497 | 6457 | 6148 | 6186 | 6277 | 6282 | 6323 | 6300 | 6321 | 6337 | 6341 |
| 1600 | --- | --- | --- | 6472 | 6488 | 6487 | 6451 | 6144 | 6198 | 6301 | 6258 | 6374 | 6316 | 6326 | 6360 | 6350 |
| 1700 | --- | --- | --- | 6477 | 6521 | 6489 | 6403 | 6178 | 6201 | 6294 | 6226 | 6332 | 6309 | 6321 | 6347 | 6342 |
| 1800 | --- | --- | --- | 6459 | 6517 | 6478 | 6394 | 6218 | 6214 | 6258 | 6248 | 6336 | 6323 | 6326 | 6367 | 6345 |
| 1900 | --- | --- | --- | 6480 | 6509 | 6482 | 6309 | 6221 | 6170 | 6278 | 6246 | 6357 | 6357 | 6334 | 6355 | 6342 |
| 2000 | --- | --- | --- | 6528 | 6499 | 6471 | 6265 | 6253 | 6223 | 6283 | 6243 | 6339 | 6367 | 6369 | 6365 | 6351 |
| 2100 | --- | --- | --- | 6476 | 6503 | 6455 | 6246 | 6254 | 6211 | 6283 | 6284 | 6326 | 6365 | 6403 | 6349 | 6346 |
| 2200 | --- | --- | --- | 6509 | 6496 | 6514 | 6249 | 6223 | 6215 | 6285 | 6255 | 6317 | 6379 | 6439 | 6345 | 6352 |
| 2300 | --- | --- | --- | 6497 | 6543 | 6484 | 6255 | 6205 | 6198 | 6280 | 6265 | 6326 | 6383 | 6466 | 6385 | 6357 |
| 2400 | --- | --- | --- | 6526 | 6546 | --- | --- | 6153 | 6213 | 6303 | 6294 | 6374 | 6394 | 6470 | 6376 | 6355 |
| MEAN | 6468 | --- | --- | 6505 | 6521 | 6499 | 6430 | 6185 | 6164 | 6223 | 6284 | 6308 | 6372 | 6340 | 6356 | 6358 |

# Sudden Ionospheric Disturbances Associated with the Region 4474 as Recorded at Nijmegen

by

I. Atanasijevic and H.A.M. Balster
Astronomical Institute, Faculty of Sciences
Nijmegen, The Netherlands

Since mid-1978 we have recorded, at the Astronomical Institute of the Faculty of Sciences, Nijmegen, the Netherlands, the amplitude of the fieldstrength and the relative phase of the time-signal transmitter HGB, frequency 75 kHz, located at Prangins, Switzerland, almost exactly 600 km south of Nijmegen. The very stable, narrow band (200 Hz) VLF receiver for fieldstrength recording was built by the electronics department of the faculty. For relative phase measurements use is made of a Hewlett-Packard 117A VLF comparator. Data on observed Sudden Ionospheric Disturbances (SID), i.e., on Sudden Enhancements of Signals (SES) and Sudden Phase Anomalies (SPA), are transmitted to the West European Regional Warning Center at the Paris-Meudon Observatory.

During the period from 20 April to 4 May 1984, a relatively large number of SID's was recorded at Nijmegen. According to data on SID's and H-alpha solar flares published in the SGD prompt reports, some of these were associated with flares which occurred in the Region 4474. On our recordings they are indicated by "4474". For the same period, data on SES's for a West-East path of about 480 km are available from recordings of the 60 kHz transmitter MSF, Rugby, Great Britain, made by H.A.M. Balster at his home near Nijmegen.

Table 1 is a list of SID's of importance 2 or more on a scale from 1- to 3+ recorded at Nijmegen from 20 April to 4 May 1984, associated with flares in the Region 4474.

Table 1. SID's of Importance $\geq 2$ Associated with the Region 4474 as Recorded at Nijmegen at 75 kHz.

| Date 1984 | Begin Time UT | Importance |
|---|---|---|
| 23 April | 1614 | 2 |
| 24 April | 1725 | 2 |
| 25 April | 0844 | 2 |
| | 1458 | 2 |
| 26 April | 0859 | 2 |
| | 1242 | 2+ |
| 27 April | 1351 | 2 |
| 29 April | 1400 | 2 |
| | 1434 | 2 |
| 30 April | 1149 | 3 |
| 2 May | 1608 | 2 |

## REFERENCES

SGD 1984 **Solar-Geophysical Data,** 477 Part I, May 1984, U.S. Department of Commerce (Boulder, Colorado, USA 80303).

SGD 1984 **Solar-Geophysical Data,** 478 Part I, June 1984, U.S. Department of Commerce (Boulder, Colorado, USA 80303).

SGD 1984 **Solar-Geophysical Data,** 479 Part I, July 1984, U.S. Department of Commerce (Boulder, Colorado, USA 80303).

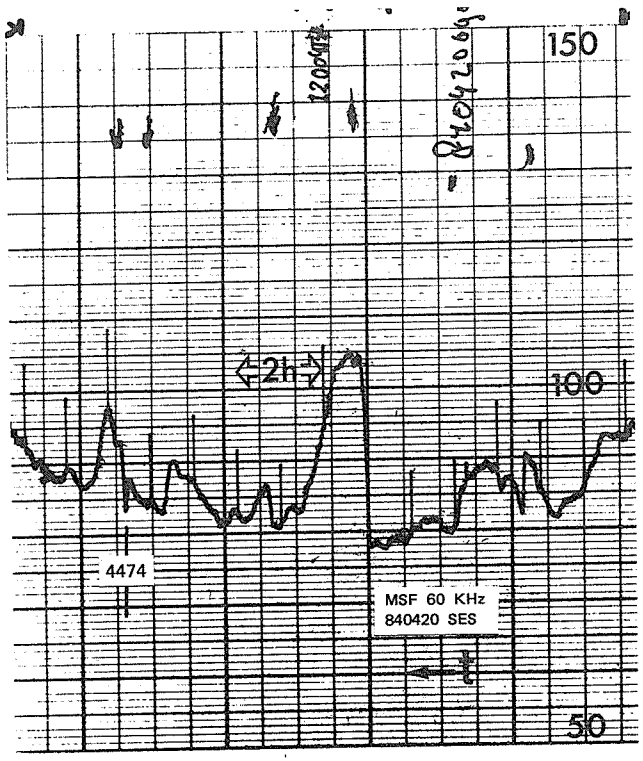


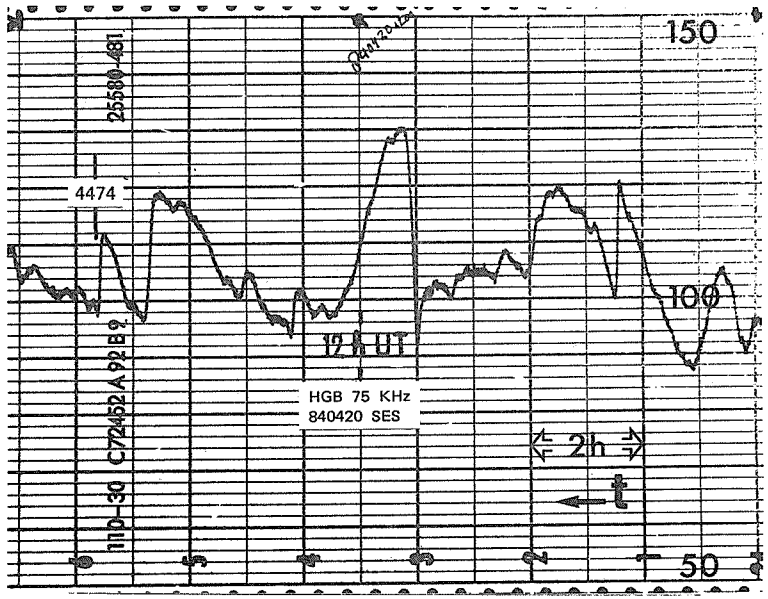


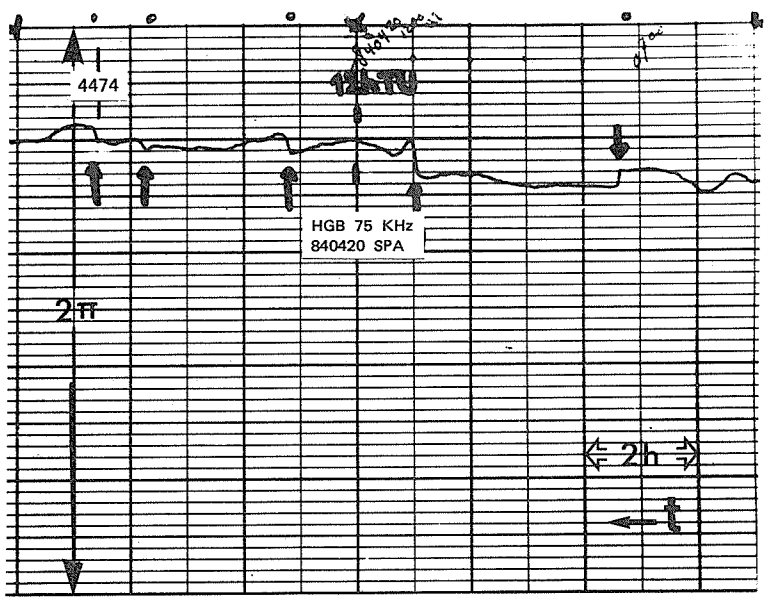


SIDs on 20 April 1984 recorded at Nijmegen.

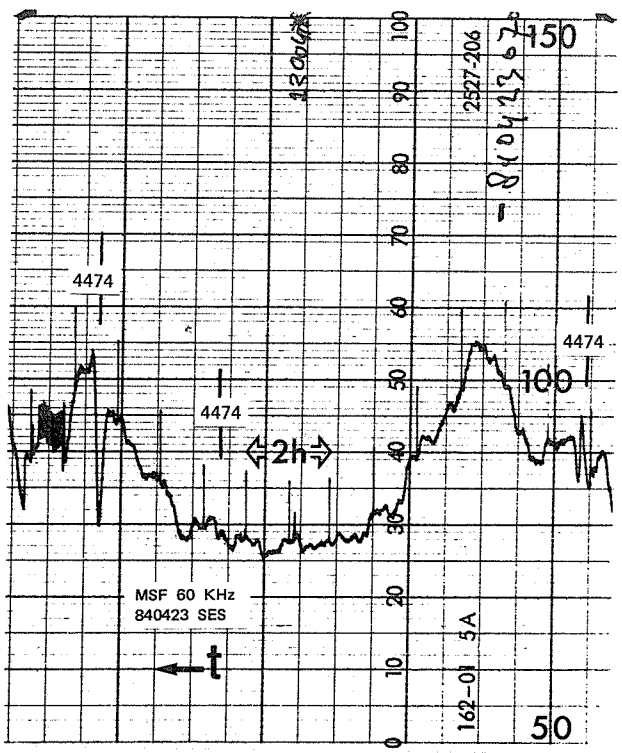


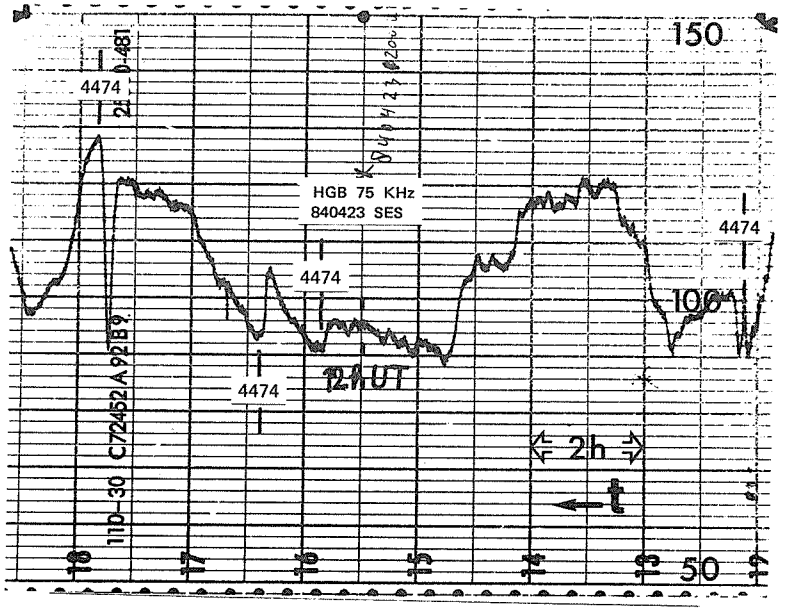


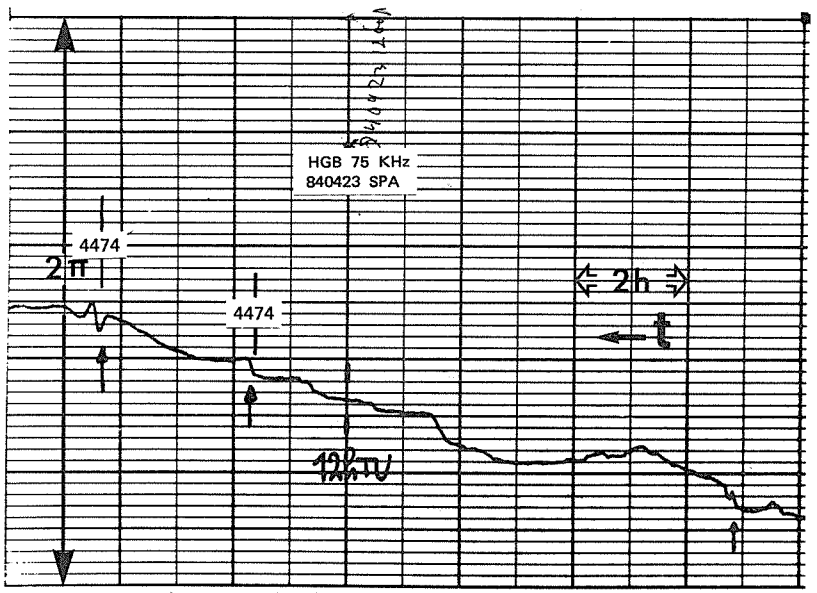


SIDs on 23 April 1984 recorded at Nijmegen.

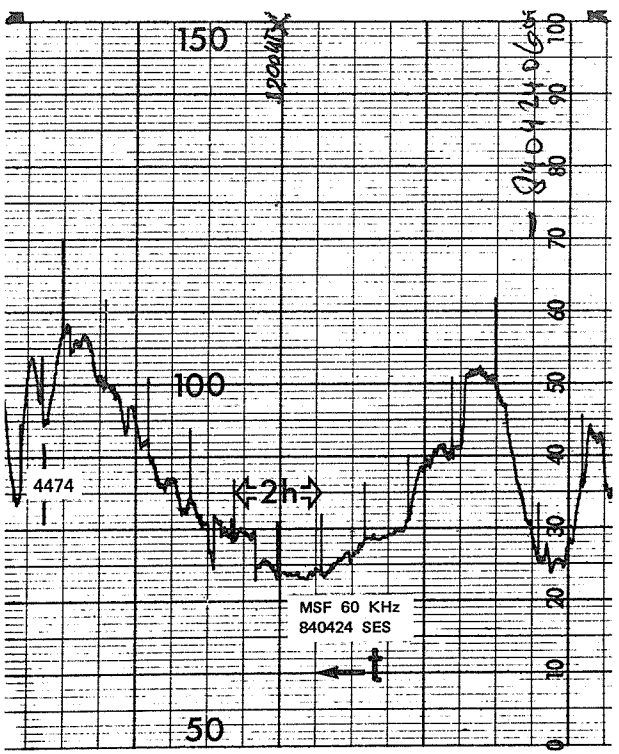


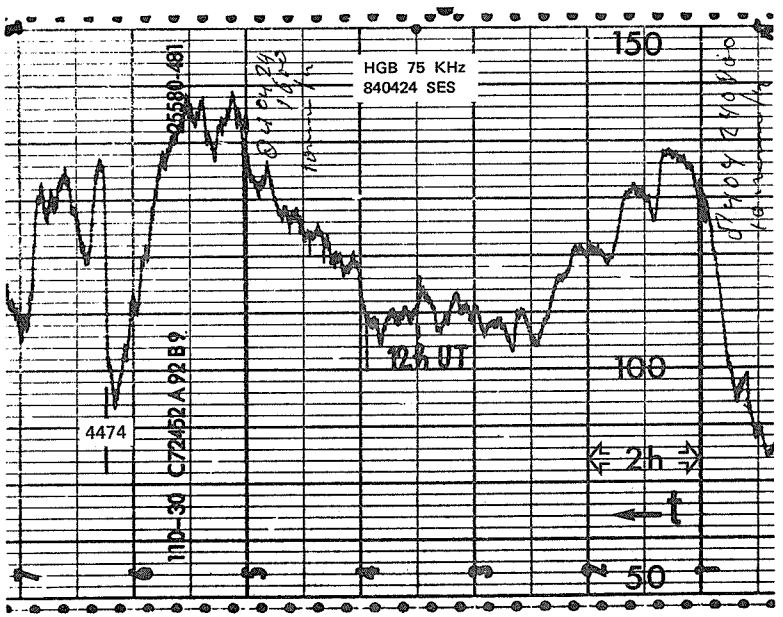


SIDs on 24 April 1984 recorded at Nijmegen.

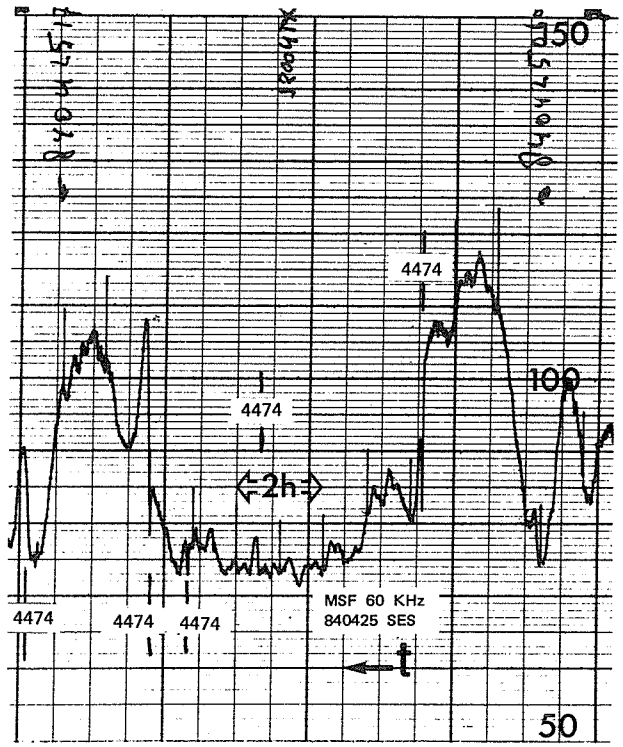


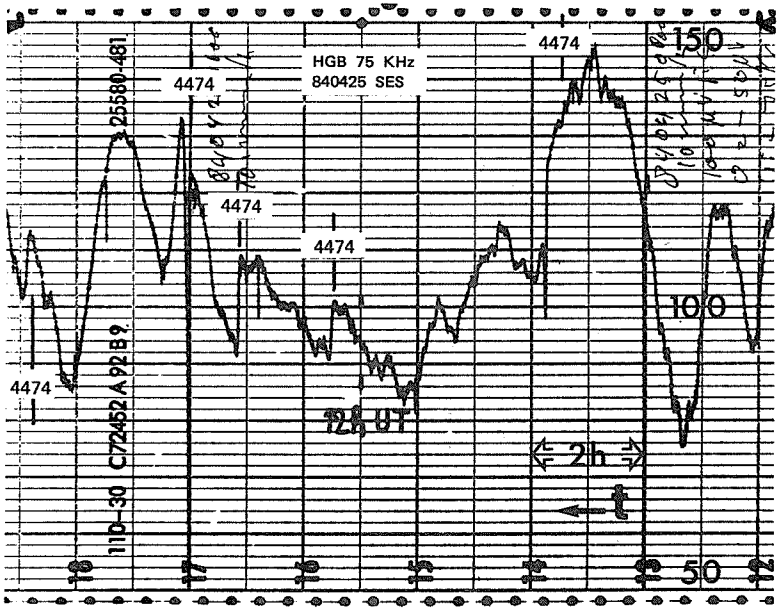


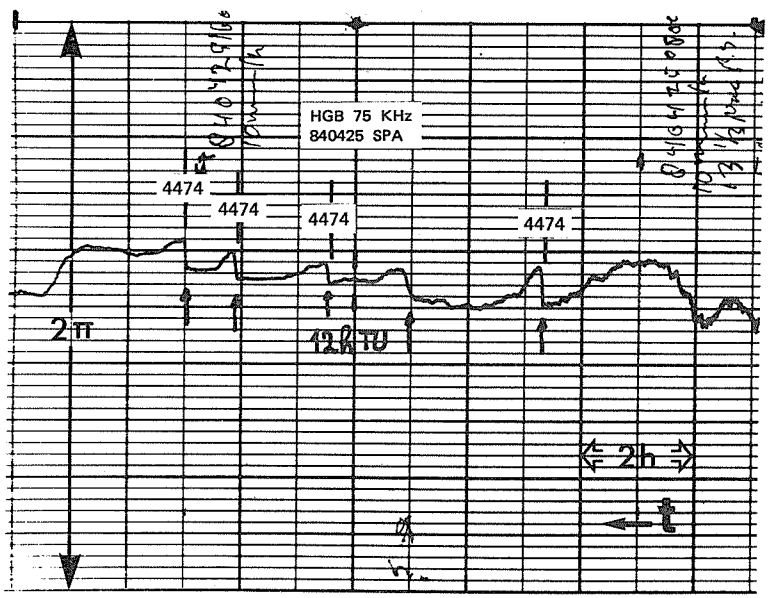


SIDs on 25 April 1984 recorded at Nijmegen.

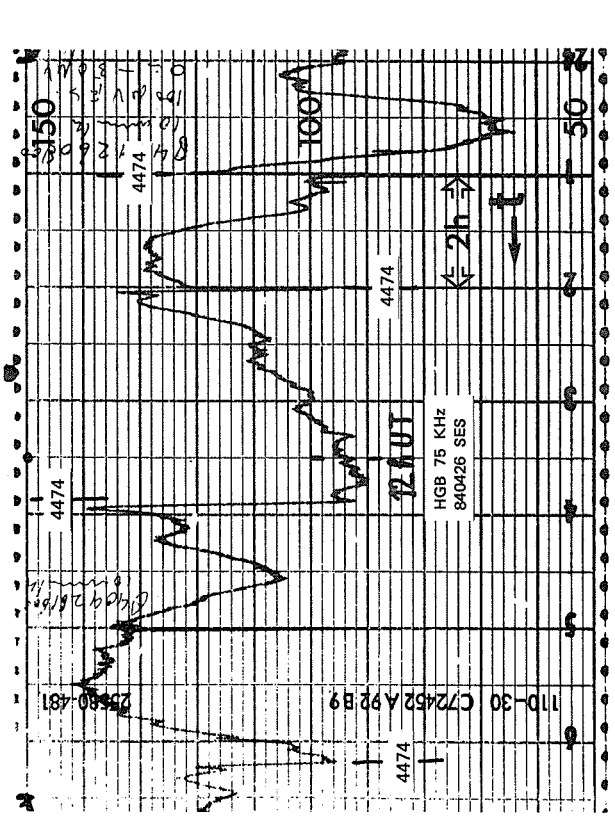


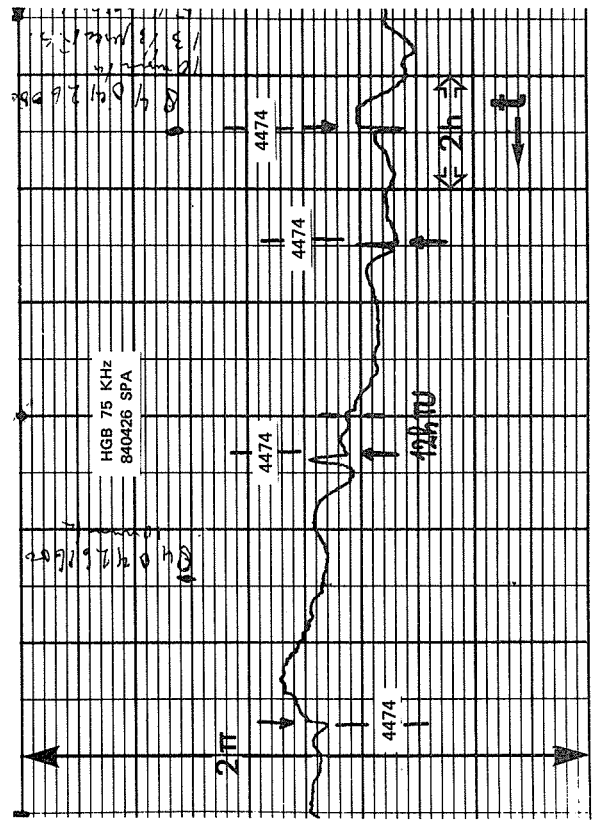


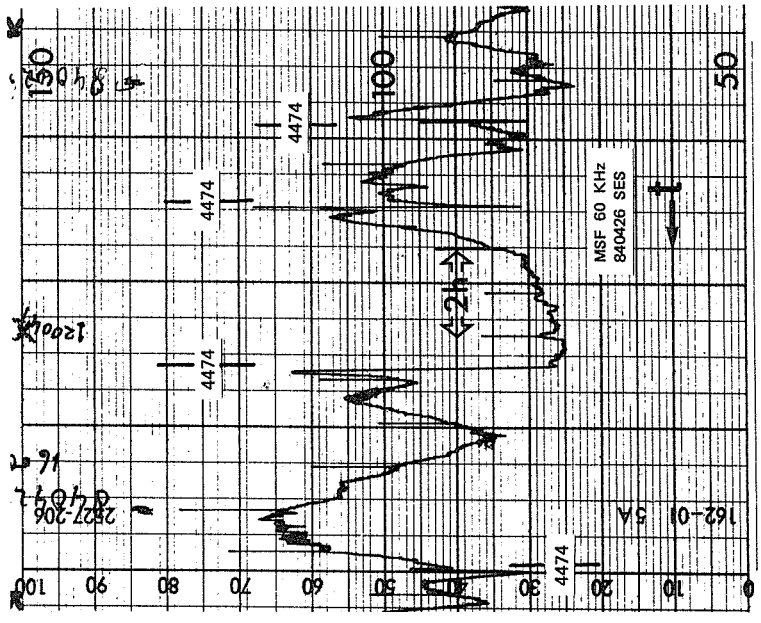


SIDs on 26 April 1984 recorded at Nijmegen.

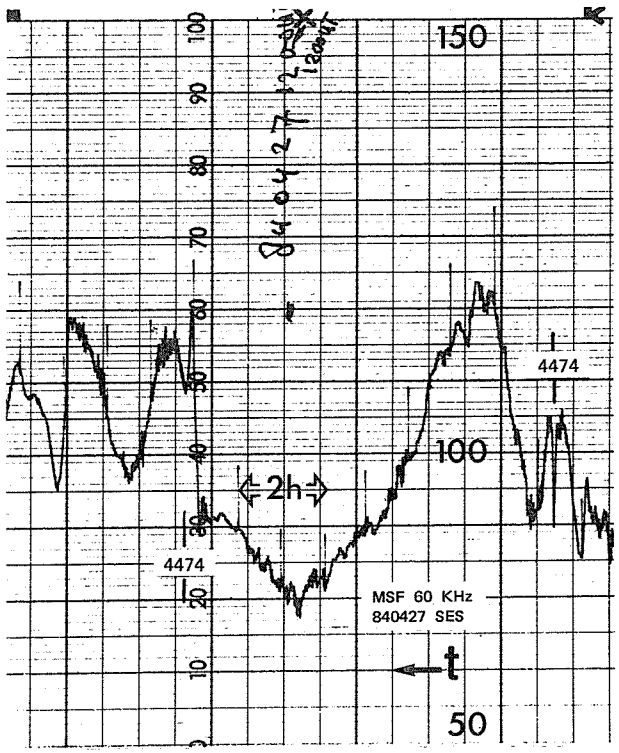


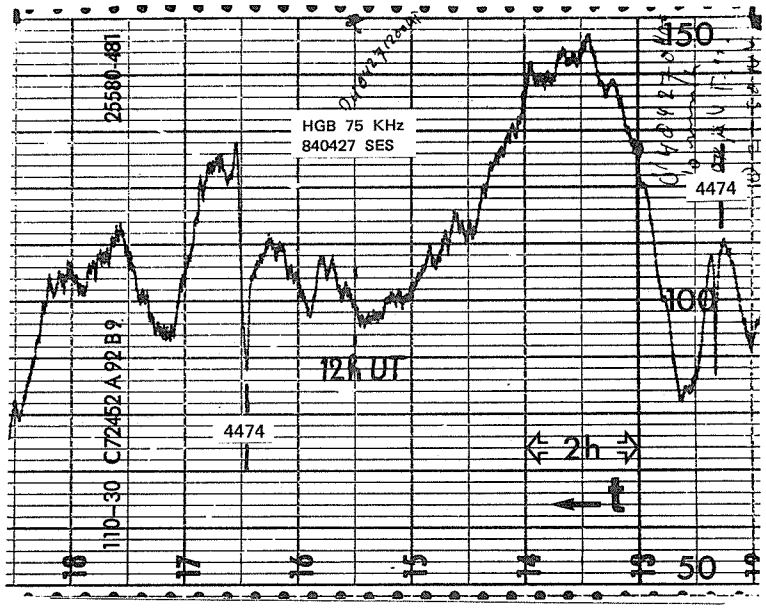


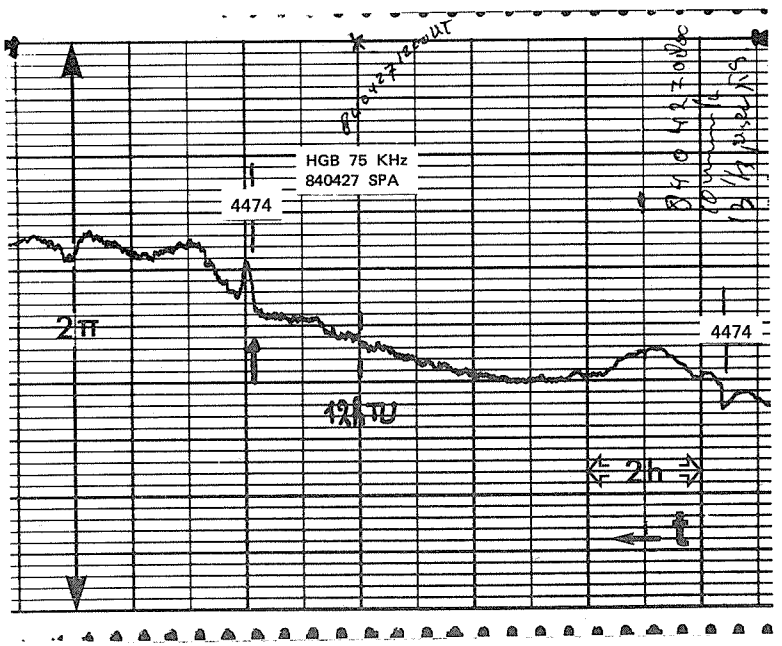


SIDs on 27 April 1984 recorded at Nijmegen.

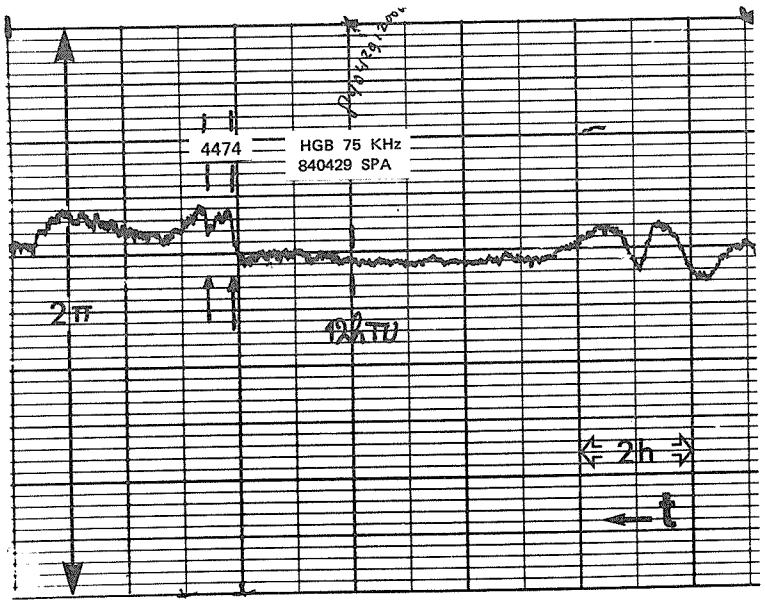


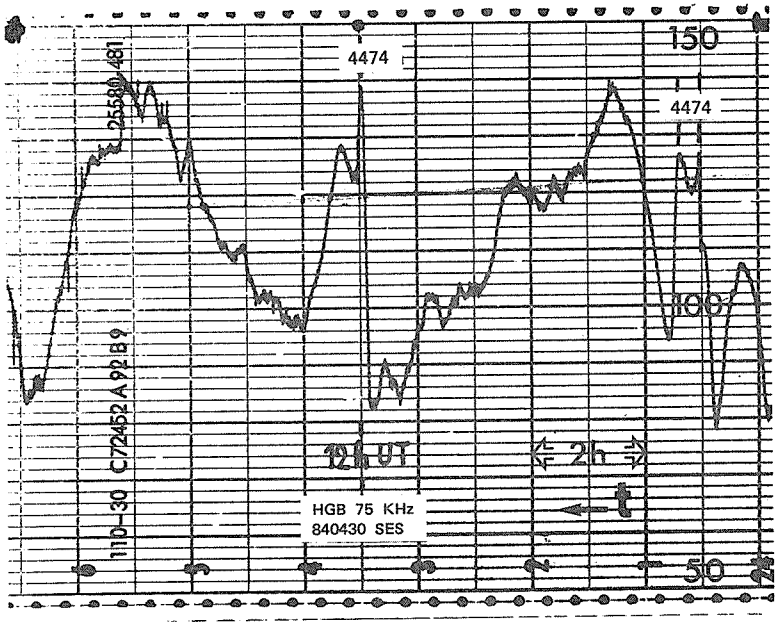


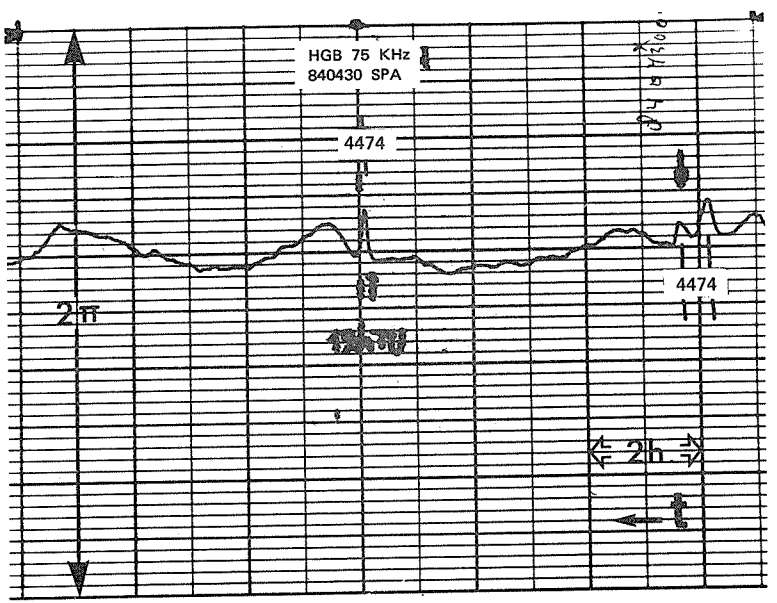


SIDs on 29 and 30 April 1984 recorded at Nijmegen.

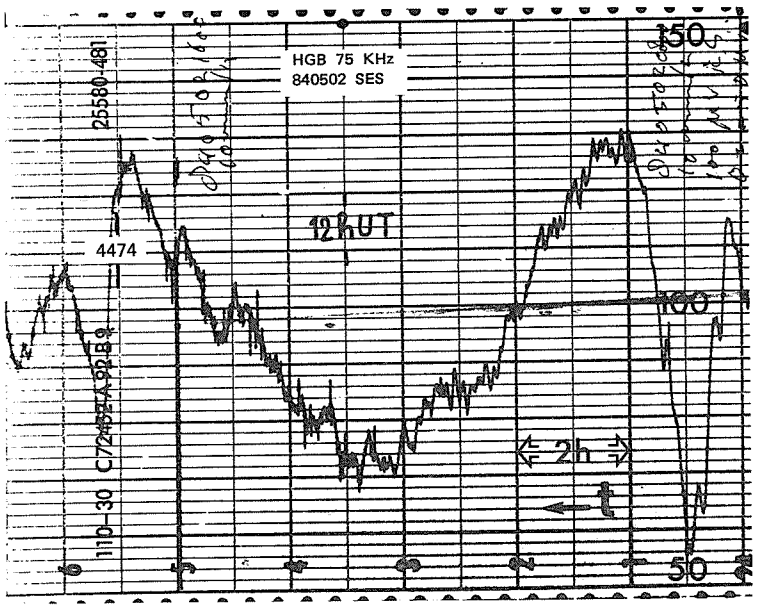


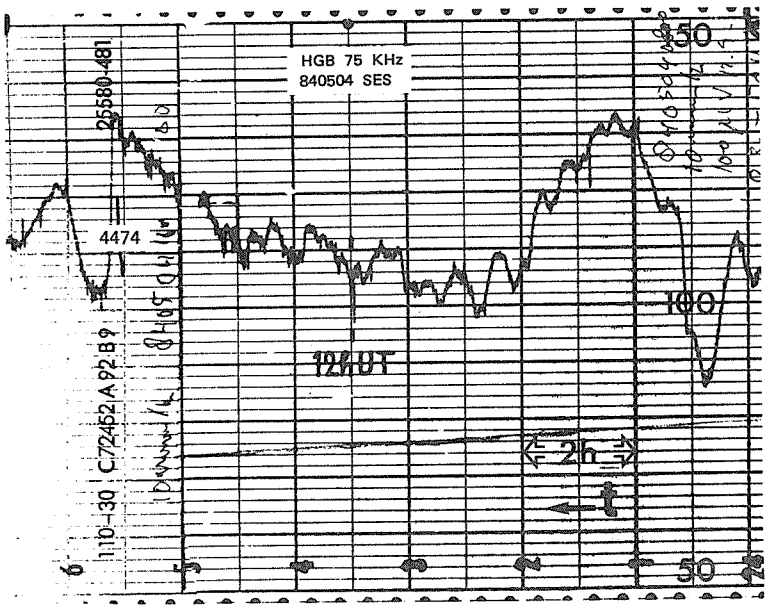


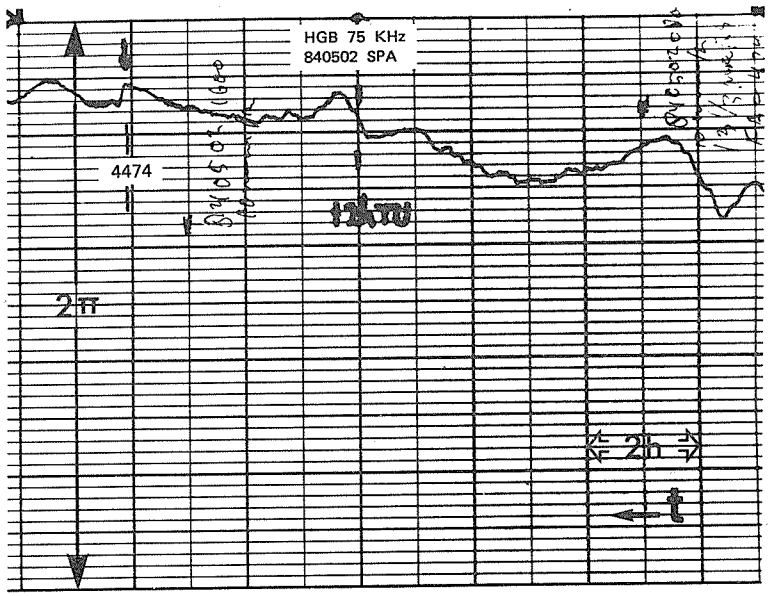


SIDs on 2 and 4 May 1984 recorded at Nijmegen.

# Comprehensive Results of Various Solar-Ionospheric Observations made by Radio Research Laboratory, Japan on April 24-27, 1984

by

M. Ohshio*, K. Ohbu**, H. Kumagai**, A. Ohtani***, H. Mori**, T. Ishii**, T. Koizumi*, S. Kainuma*, A. Suzuki*, T. Kikuchi*, H. Minakoshi*, and I. Nishimuta****

*Radio Research Laboratory
4-2-1 Nukui-Kita, Koganei, Tokyo 184, Japan
**Hiraiso Solar Terrestrial Research Center, Radio Research Laboratory
3601 Isozaki, Nakaminato, Ibaraki 311-12, Japan
***Inubo Radio Wave Observatory, Radio Research Laboratory
9961 Tennodai, Choshi, Chiba 288, Japan
****Yamagawa Radio Wave Observatory, Radio Research Laboratory
2719 Narikawa, Yamagawa, Ibusuki, Kagoshima 891-05, Japan

## 1. INTRODUCTION

Solar Terrestrial electromagnetic disturbance events in June, July, and December 1982 comprised one of the most conspicuous ones during the 21st solar cycle to have begun in June 1976. A large-scale solar terrestrial electromagnetic disturbance event 16 months after the above-described last event occurred in April 1984 when a smoothed monthly relative sunspot number was 50 (the minimum value was 12 in June 1976 and the maximum one was 165 in December 1979 in the cycle) [SGD, 1985]. That is, a region of sunspot activity with SESC-assigned No. 4474 which appeared at the east limb of the solar disk on April 21, grew up producing a number of flares and generated a large flare of X13/3B at 2356 U.T. on April 24. Here, SESC is an abbreviation of Space Environment Services Center, where is at Boulder, Colo., U.S.A. This region produced a solar radio burst of type IV with intensity 3 at the same time.

The Radio Research Laboratory, Japan carries on the routine observations at the seven stations shown in Table 1, besides various radio observations with a short period for the purpose of some study. Radio disturbances due

Table 1. Ionospheric routine observations conducted by the Radio Research Laboratory, Japan.

| Station | Geographic | | Geomagnetic | | Technical Method |
|---|---|---|---|---|---|
| | Latitude | Longitude | Latitude | Longitude | |
| Wakkanai | 45°23.5' N | 141°41.2' E | 35.3° | 206.5° | Ionospheric Vertical Sounding |
| Akita | 39°43.5' N | 140°08.0' E | 29.5° | 205.9° | " |
| Kokubunji (Tokyo) | 35°42.4' N | 139°29.3' E | 25.5° | 205.8° | " |
| Yamagawa | 31°12.1' N | 130°37.1' E | 20.4° | 198.3° | " |
| Okinawa | 26°16.9' N | 127°48.4' E | 15.3° | 196.0° | " |
| Hiraiso | 36°22.0' N | 140°37.5' E | 26.3° | 206.8° | Solar & HF, LF Radio Receiving |
| Inubo | 35°42.2' N | 140°51.5' E | 25.6° | 207.0° | VLF Radio Receiving |

to electromagnetic waves, high energy particles, and low energy plasma which the above-described large solar flare emitted were successfully detected by these various observational networks. But solar radio fluxes were directly detected.

This report presents observational results and some considerations for them as much as possible on solar-terrestrial physical problems of the event concerned laying stress on radio disturbances due to the occurrence of this large solar flare, detected at the Radio Research Laboratory, Japan, being supported by related phenomena detected at other organizations.

## 2. ELECTROMAGNETIC WAVE RADIATION

As described in 1., a solar flare is detected on the ground as solar radio bursts in the sense of family relation to solar agencies influencing the earth's electromagnetic phenomena. The time variation in their flux offers a useful information to analyze the time variation in solar extreme ultraviolet (EUV) flare fluxes which are closely related to solar radio burst flux in their radiation mechanism. Solar X-ray flares and the above-described solar EUV flares enhance anomalous ionization in the lower part and in the middle and upper parts of the ionosphere, respectively and produce various kinds of sudden ionospheric disturbances (S.I.D.'s).

First, the aspect of solar radio bursts themselves and next, aspects of various SID's are described.

### 2.1. Solar radio bursts

Major solar radio bursts associated with the 3B/X13 flare (S12E43) were observed at Hiraiso by the total flux

observations at four frequencies: 9500, 500, 200, and 100 MHz. Figure 1 shows the time variations in radio bursts at the four frequencies. The abscissa and ordinate show time in U.T. and logarithmic (except 100 MHz) radio flux density in S.F.U. (Solar Flux Unit, 1 S.F.U. = 1 x $10^{-22}$ $Wm^{-2}Hz^{-1}$), respectively. Since only the linear scale record was available for 100 MHz during this event, the record was far saturated around the burst peak at the frequency. The radio burst at 9500 MHz was composed of the first impulsive phase (2357-0052 U.T.) and the second gradual phase (0102-0405 U.T.). The radio bursts at other three lower frequencies were also composed of two phases: large impulsive peaks (before about 0018 U.T.) and their successive long-extended fluctuations. Start times, times of the maximum, durations, and peak flux densities of the bursts at the four frequencies are tabulated in Table 2. In the table, the duration of the first phase is shown at 9500 MHz. These values were one of

Table 2. Major solar radio bursts associated with the 3B/X13 flare at four frequencies observed at Hiraiso in April 1984.

| Frequency (MHz) | Start Time (U.T.) d. h. m. | Time of Maximum (U.T.) d. h. m. | Duration (min.) | Peak Flux Density (S.F.U.) |
|---|---|---|---|---|
| 9500 | 24 23 56.6 | ——— * | 55 | over 9000* |
| 500 | 24 23 59.3 | 25 00 00.4 | 128 | 77000 |
| 200 | 25 00 00 | 25 00 00.6 | 103 | 46000 |
| 100 | 25 00 01 | 25 00 01** | 109 | over 10000** |

Notes 1. The single asterisk means doubtful or unavailable due to saturation.
2. The values with the double asterisk were not obtained from the linear scale record (in Figure 1), but were partially available for this event from logarithmic record.

the largest ones at each frequency in this solar cycle.

One of the interesting features of the radio bursts is the fluctuations seen in the second phase at 500, 200, and 100 MHz. Peaks at 0048 U.T. (500 MHz), 0052 U.T. (200 MHz), and 0055 U.T. (100 MHz) correlated with one another, which suggested the outward movement of the matter emitted in the corona from the chromosphere. At the corresponding times, indeed, the filament eruption was observed at Hida Observatory (36°15' N, 137°18' E) [Kurokawa, 1985] and the strong type II (0000-0012 U.T.) and type IV (0000-0200 U.T.) bursts were detected by the radio spectrum observation at Nobeyama (35°56' N, 138°29' E). The decrease of the radio flux between the first and the second phases at 9500 MHz is considered to have been caused by the emitted matter which obscured the radio source area in the lower corona.

## 2.2. SPA

It is considered that the time variation in sudden phase anomaly (S.P.A.) reflects that in the enhanced radiation flux of solar X-ray flare relatively faithfully which is today well regarded as to be the greater part of cause for the occurrence of not only SPA but also SID's occurring in the lower ionosphere, because SPA is continuous in its record and does not fall into saturation. A large SPA is caused by a large solar X-ray flare and the follow of the former to the latter time variation is particularly good [Ohshio, 1978].

The SPA's of the event concerned are shown in Figure 2 which appeared in phase variation of the five circuits [Ohshio *et al.*, 1985a] of long-distance propagating VLF radio waves received at Inubo. The maximum value for the SPA's concerned occurred around 0007 U.T. (slightly different in circuits) on April 25. The subsolar point at that time was at (13°11' N, 178°15' E), so that it is expected that large and distinct SPA's appeared on the eastern and southern circuits to Inubo. In fact, large and distinct SPA's such as $\Delta\phi$ = 286, 302, and 297° were observed on Haiku-, North Dakota-, and North West Cape-Inubo circuits, respectively. The maximum observed value of SPA normalized to propagational distance $D$ = 1 Mm (= 1000 km), $\Delta\phi_{o,m,D}$ and the representative solar zenith angle, $\overline{\chi}$ on a circuit for the above-described three circuits were $\Delta\phi_{o,m,D}$ = 46.9, 33.0, and 42.5° and $\overline{\chi}$ = 26.1, 53.2, and 53.6°, respectively. It is discussed, therefore, that an SPA with the largest effect substantially occurred on Haiku-Inubo circuit.

The application of the above-described good follow to the SPA on Haiku-Inubo circuit which appeared most largely substantially admits that an interpolation of the record of solar X-ray (wavelength $\lambda$ = 0.1-0.8 nm) flare with no observational record (0002-0013 U.T. on April 25) due to saturation [Coffey and Wilkinson, 1984] can be made without gross error by means of a mere geometrical elongation of the portion with record in both the sides. Thereby, $F_m$($\lambda$ = 0.1-0.8 nm, $t_m$ = 0003.5 U.T., April 25, 1984) = 2.48 x $10^{-3}$ $Wm^{-2}$ was presumed, where $F_m$ and $t_m$ denote the maximum radiation flux and its time, respectively. By the use of the radiation flux immediately before the beginning of the flare concerned, $F_q$($\lambda$ = 0.1-0.8 nm, $t$ = 2352 U.T., Apr. 24, 1984) = 1.417 x $10^{-6}$ $Wm^{-2}$, $\Delta F_m$ = $F_m$ - $F_q$ = 2.48 x $10^{-3}$ $Wm^{-2}$ could be obtained. From the relation between $\Delta F_m$($\lambda$ = 0.1-0.8 nm, $t_m$) ($Wm^{-2}$) and observed phase advance of the maximum SPA normalized to both a propagational distance $D$ = 1 Mm and a representative solar zenith angle $\overline{\chi}$ = 0°, $\Delta\phi_{o,m,n}$(degrees $Mm^{-1}$ at $\overline{\chi}$ = 0°) [Ohshio *et al.*, 1985b], the calculated phase advance of the maximum SPA in the same normalization as that described above, $\Delta\phi_{t,m,n}$ = 60° was obtained. But, $\Delta\phi_{o,m,n}$ = 54.0° was reduced. Consequently, it is discussed that from the presumption of the maximum solar X-ray ($\lambda$ = 0.1-0.8 nm) radiation flux the calculated SPA was estimated with an excess error of 11 %. From the same presumption, $\Delta\phi_{t,m,n}$(North Dakota-, North West Cape-, and Rugby-Inubo)'s were estimated with excess errors of +14, -12, and -15 %, respectively. Here the geographic coordinates of these three stations are 46°22' N, 98°21' W; 21°49' S, 114°10' E; and 52°22' N, 1°11' W in written order [Ohshio *et al.*, 1985a]. Accordingly, it seems to be invalid to re-

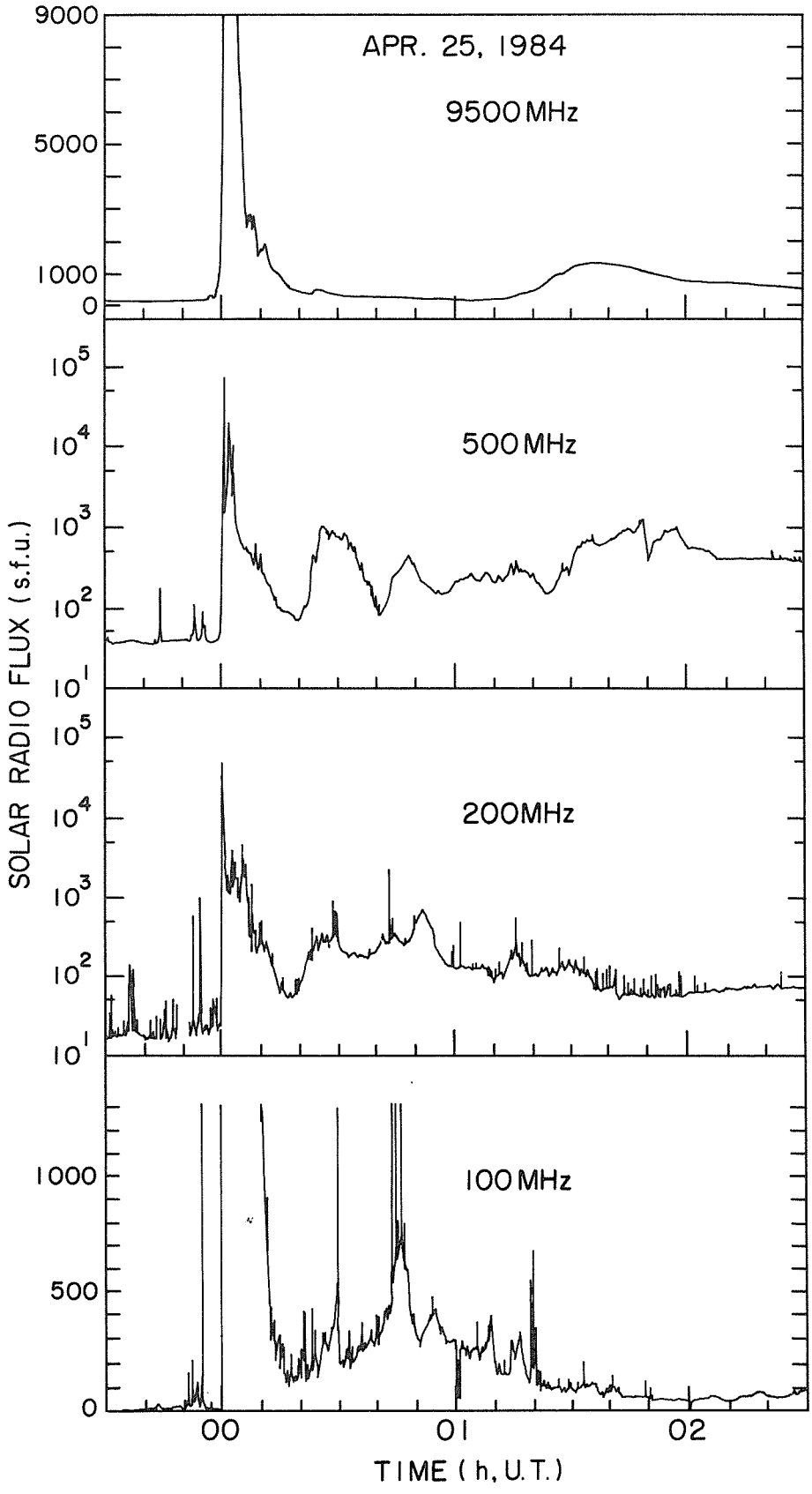


Fig. 1. Time variations in solar radio fluxes of bursts at the four frequencies associated with the large solar flare concerned on April 24-25, 1984 observed at Hiraiso. Note: s.f.u. = $1 \times 10^{-22}$ $Wm^{-2}Hz^{-1}$.

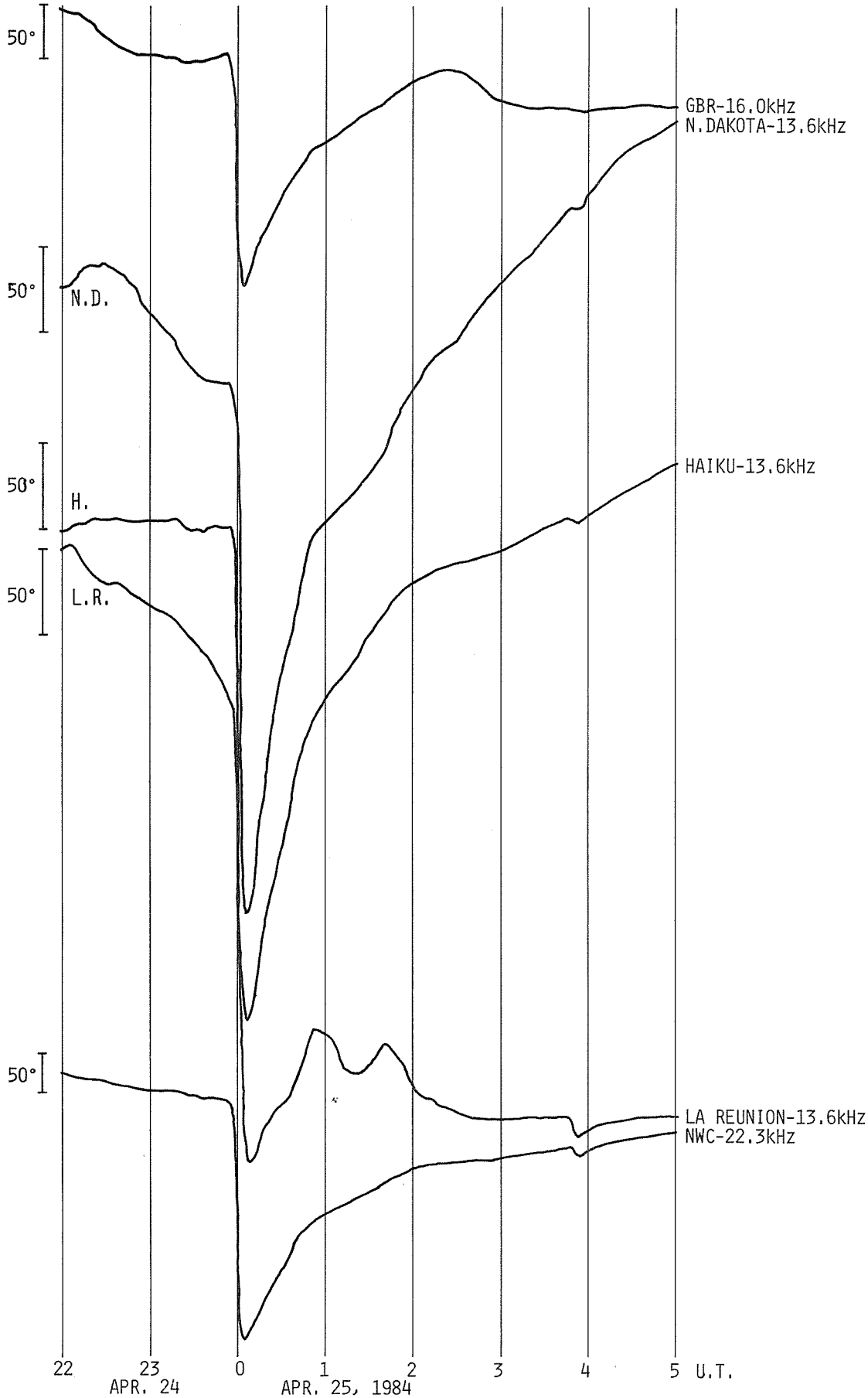


Fig. 2. Time variations in SPA's caused by the large solar flare concerned on April 24-25, 1984 observed at Inubo. Downward direction indicates the advance in phase.

duce the above-described value of the maximum radiation flux hastily, only in terms of the estimation on Haiku-Inubo circuit.

The maximum enhanced radiation flux of the solar X-ray (λ = 0.1-0.8 nm) flare concerned, $\Delta F_m \approx 2 \times 10^{-3}$ $Wm^{-2}$ was larger than those on August 2, 1972 and in June (4 events) and July (2 events) 1982 and was almost equal to those in the events on August 4 and 7, 1972 [Ohshio, 1974] and on December 15 and 17, 1982 [Ohshio *et al.*, 1985b]. Consequently, it is inferred that the solar X-ray flare having occurred on April 24-25, 1984 was, indeed, a giant solar X-ray flare in the largest class in the observational history of solar X-ray flare fluxes.

2.3. SES and SWF

SID's to have been detected at Hiraiso on April 25, 1984, i.e., sudden enhancement of signals (S.E.S.) and short wave fadeout (S.W.F.) are shown in Figure 3.

The figure (a) shows the time variation in phase of Loran C (100 kHz) radio waves which were transmitted at Tokachibuto (42°45' N, 143°43' E) and were received at Hiraiso. The figure shows that the phase advanced by about 340 degrees abruptly from about 2356 U.T. on April 24 when the X13/3B solar flare occurred, afterwards turned to its recovery, again began to advance from 0051 U.T. to attain about 120 degrees, and afterwards began to recover from 0112 U.T. slowly.

The figure (b) shows the time variations in SES's of Loran C radio waves which were transmitted at Tokachibuto and Iwojima (24°48' N, 141°20' E) and were received at Hiraiso. A comparison of the SES variation with the phase one on Tokachibuto-Hiraiso circuit indicates that the amplitude increased at the beginning of the advance in phase and conversely had a tendency to decrease abruptly when the phase advanced to some extent. The decrease continued till the phase advance attained its maximum, and afterwards the amplitude formed a dull maximum while the phase increased. On the other hand, the SES variation on Iwojima-Hiraiso circuit indicates a monotonous increase till the time of the maximum in phase (Tokachibuto-Hiraiso circuit) advance, and afterwards a monotonous decrease as the phase (Tokachibuto-Hiraiso circuit) increased. The relation between the time variation in SES and that in phase on Iwojima-Hiraiso circuit is unfortunately unknown, because of no observation in phase on that circuit at that time.

The figure (c) shows the time variation in electric field strength of a short wave (15 MHz) broadcast which was transmitted at Shepparton (36°20' S, 145°25' E) and was received at Hiraiso. The figure indicates that the strength began to go abruptly down around 0000 U.T. on April 25 accompanying the occurrence of the above-described flare, began to recover around 0030 U.T. after it sank below the limit of detection of the receiver, and again began to go abruptly down around 0100 U.T. to keep a level near the limit of detection. About the time the phase advance in Loran C radio waves was also in progress not so abruptly, as seen in the figure (a). Consequently, the second SID? seems to have occurred around 0100 U.T. However, neither solar X-ray flare on the observational record obtained by GOES (Geostationary Operational Environmental Satellite)-5 satellite [Coffey and Wilkinson, 1984] nor solar radio burst with 9.5 GHz on the observational record obtained at Hiraiso (cf. Figure 1) can be found around 0100 U.T. Accordingly, this phenomenon around 0100 U.T. shown in Figure 3 is difficult of solution at present.

2.4. SIF

The ionospheric vertical sounding as routine observation is carried on at intervals of 15 minutes at the five stations in Japan shown in Table 1. The aspect of sudden increase of $f_{min}$ (S.I.F.) caused by a solar flare is described for the three stations, Wakkanai, Kokubunji (Tokyo), and Okinawa in this report.

As shown in Figure 4, SIF's were observed around 1300 J.S.T. (= U.T. + 9 h.) on April 24 and around 0900 J.S.T. on April 25. In the case of April 24, SIF's increased remarkably and attained their maximum value simultaneously for these three stations. Particularly, the SIF reached blackout at Kokubunji. But this SIF event did not originate in the large solar flare which was the subject of present report. This SIF was caused by the solar X-ray flare with X1/2B, S10E55 in heliographic coordinates, 0339 (start), 0402 (maximum), and 0429 (end) U.T. on April 24, 1984 [PRF-SGD, 1984].

In the case of April 25, a blackout in SIF appeared during 0900-0930 J.S.T. for these three stations intensely and literally suddenly from the quiet level of $f_{min}$, without going through any remarkable level of SIF on its way to blackout level in terms of the observation at intervals of 15 minutes. This event is the very subject of present report. In detail, the blackout appeared at 0900 and 0915 J.S.T. at Okinawa and continued from 0900 even till 0930 J.S.T. at Kokubunji, while occurred only at 0915 J.S.T. at Wakkanai. The difference in the occurrence of blackout among stations will probably be ascribed to the fact that the nominal routine observation at 0900 J.S.T. in this case is practically carried on, shifting operational time slightly such as from 0859 J.S.T. at Wakkanai, 0900 J.S.T. at Kokubunji, and 0901 J.S.T. at Okinawa with duration of about 24 seconds, owing to the adoption of operational system of oblique sounding in addition to vertical sounding in Japan. Further, the quantitative comparison of $f_{min}$'s at different stations is difficult because of difference in both conditions of ionosonde and its S/N reflecting locality.

The SIF concerned is considered to have continued till 1115, 1215, and 1400 J.S.T. at Wakkanai, Kokubunji, and Okinawa, respectively.

2.5. SFD

The time variations in sudden frequency deviation (S.F.D.) caused by the large solar flare concerned while JJY signal with a frequency of 10 MHz emitted at Nazaki (36.18° N, 139.85° E) was received at Akita and the signals with frequencies of 10 and 8 MHz were received at Uji (34.89° N, 135.78° E) (Kyoto) are shown in Figure 5.

As shown in the figure, SFD was observed on JJY frequency received at Akita and Uji (10 MHz). The SFD began

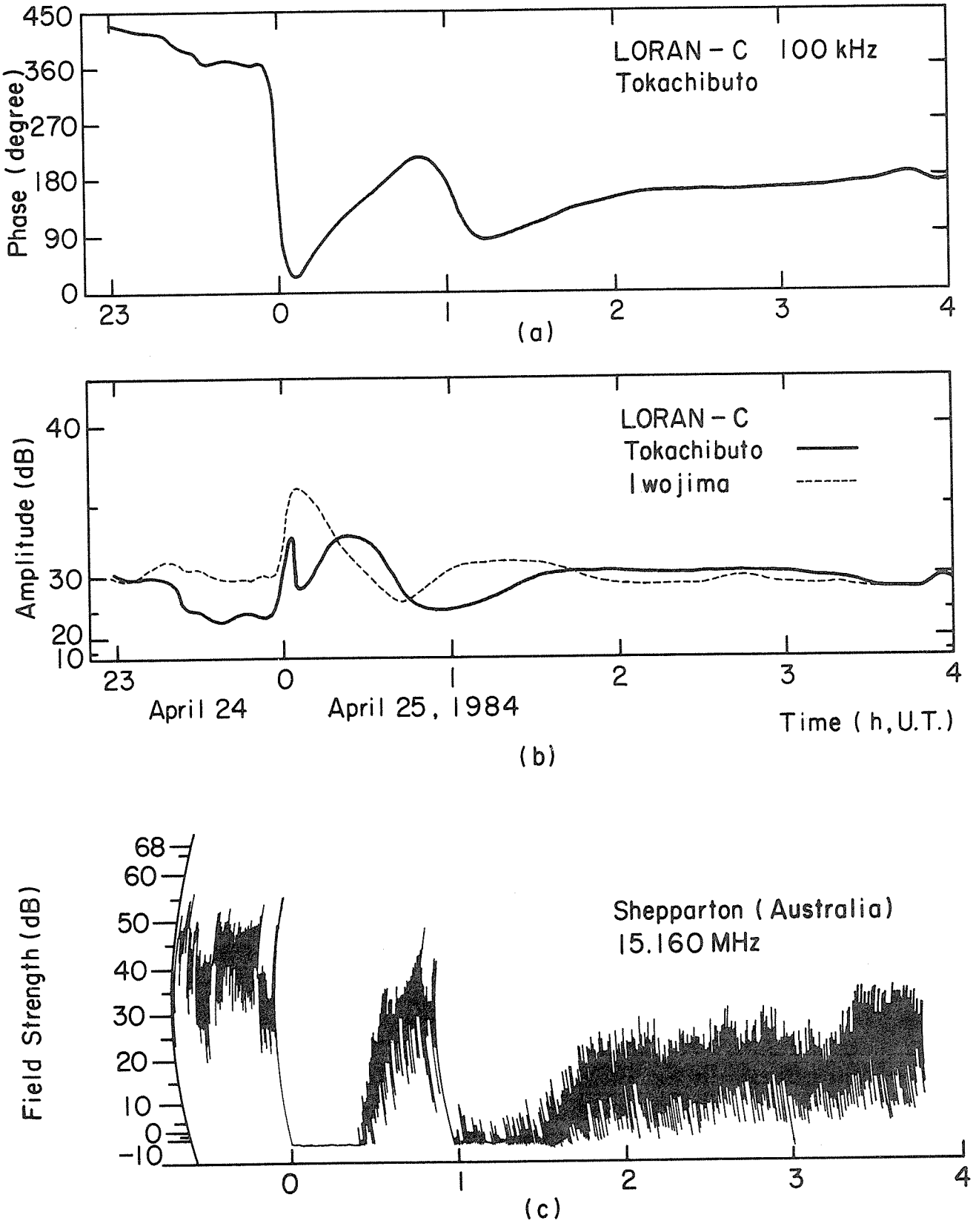


Fig. 3. Time variations in SES's (b), the phase accompanying the SES (a), and SWF (c) caused by the large solar flare concerned on April 24-25, 1984 observed at Hiraiso.

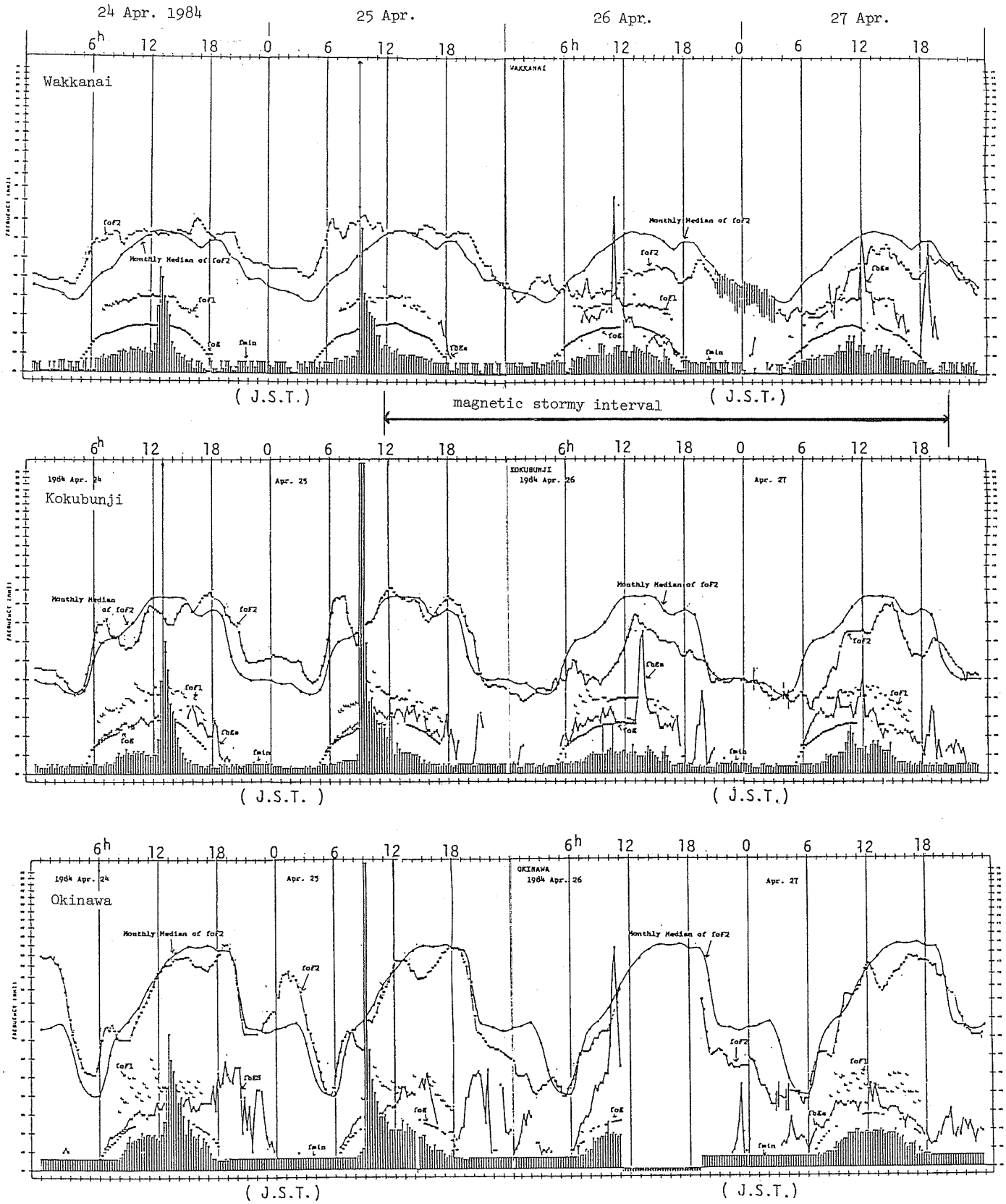


Fig. 4. Consecutively daily variations in $f_{min}$ (vertical lines) and $f_oF2$ (segments of curved lines and dots) together with its monthly median (smooth curves) observed at intervals of 15 min. at the three stations caused by the solar flare on April 24 and the large solar flare concerned on April 24-25, 1984 (see 2.4. in the text). SIF's and ionospheric storms are seen on April 24-25 and 26-27, respectively. A magnetic stormy interval is shown (see 4.1. in the text). Note: J.S.T. = U.T. + 9 h.

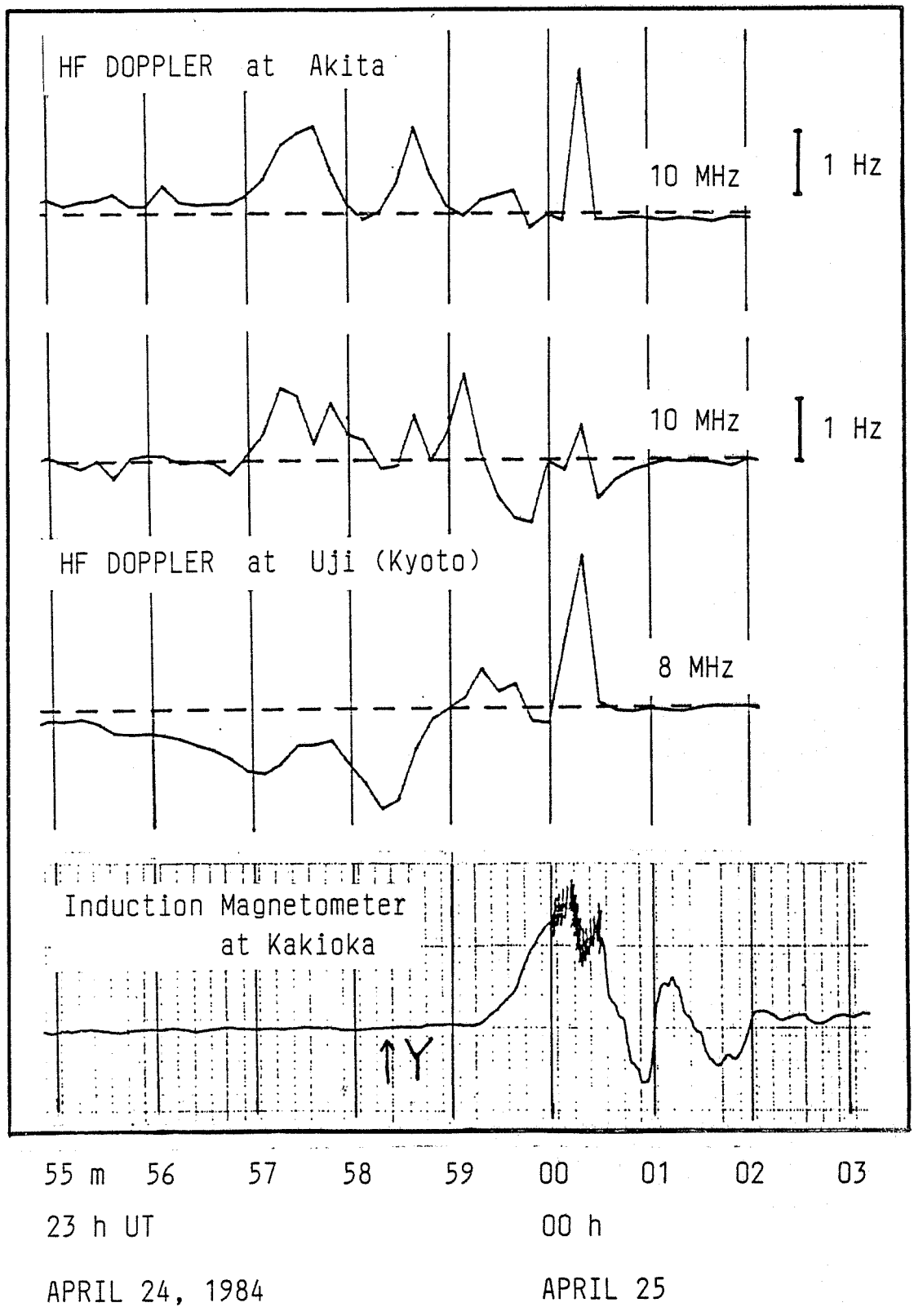


Fig. 5. Time variations in SFD's appearing on HF Doppler records obtained at the two stations and in Gsfe appearing on induction magnetograph obtained at Kakioka caused by the large solar flare concerned on April 24-25, 1984.

to increase at 2357 U.T. on April 24 and oscillated with a period of about one minute till the SFD disappeared at 0000 $30^{s}$ U.T. on April 25. On the other hand, a record of induction magnetometer at Kakioka (36.23° N, 140.18° E) indicated that, as shown in the lowest section of the figure, a geomagnetic solar flare effect (G.s.f.e.) occurred with beginning to oscillate at 2359 $15^{s}$ U.T. on April 24 and continued till 0002 U.T. on April 25. Also the oscillation had a period of about one minute.

The feature of the event concerned, as described above, is found in the fact that both SFD and Gsfe oscillated with a period of about one minute and that the beginning of oscillation was more delayed by about 2 minutes in the latter than in the former.

Some considerations for the event are as follows: it is possible that the period of about one minute might be ascribed to atmospheric oscillation due to atmospheric heating, geomagnetic pulsation due to oscillation of lines of magnetic force, etc. However, the geomagnetic pulsation as the cause is impossible due to the preceding of SFD and to the short period of geomagnetic pulsation (estimated at about 20 seconds in Japan). Further, the atmospheric oscillation as the cause is impossible due to no time difference in beginning of oscillations at Akita and Uji. On the other hand, it is inferred that the SFD event shown in Figure 5 might be attributed to solar electromagnetic wave radiations capable of ionizing the earth's neutral atmosphere, since a tiny variation with half a cycle can be found at a portion (2357-2358 U.T., see Figure 1) immediately before the large solar radio burst in the time variation in solar radio (9.5 GHz) flux.

In connection with the Gsfe shown in Figure 5, the fact that Gsfe began to oscillate by about 2 minutes later than SFD is considered to have been caused by the difference at beginning of effectively enhanced ionization at altitude where each SID occurred. That is, it is inferred that the effectively enhanced ionization at altitude where SFD occurred was realized by enhanced production of electrons in the *F* region due to the solar EUV flare which began to oscillate at the same time as the beginning of oscillation in solar radio (9.5 GHz) flux described above, and that SFD with sensitive response occurred at once. Here, the time variation in solar EUV flare flux is considered to have been similar to that in solar radio (GHz band) burst flux because of their same radiation mechanism.

On the other hand, the effectively enhanced ionization at altitude where Gsfe occurred is considered to have been realized by enhanced production of electrons in the lower *E* region due to the solar X-ray (wavelength 0.1-0.8 nm) flare and others. According to the observational data [Coffey and Wilkinson, 1984], solar X-ray radiation flux concerned began to increase suddenly at 2357 U.T. on April 24. But the calculation [Kikuchi and Ohshio, to be published] indicated that the enhanced production of electrons enough to begin to cause the Gsfe was realized by enhanced radiation flux at 2359 U.T.

### 2.6. SITEC

An enormous large sudden increase in ionospheric total electron content (S.I.T.E.C.) was observed just around 00 h. U.T. on April 25, 1984 at Hiraiso, Tokyo, and Yamagawa by means of Faraday rotation measurement of 136 MHz signal from a geostationary satellite, ETS (Engineering Test Satellite)-II. It is considered that this SITEC was induced by EUV and soft X-ray bursts emitted from the large solar flare (X13/3B) which occurred in a region with SESC-assigned No. 4474 (cf. 1.) (S12E43) at 2356 U.T. on April 24, 1984. Figure 6 shows the time variations in TEC observed at Hiraiso, Tokyo, and Yamagawa along with a solar radio (9.5 GHz) burst flux (cf. Figure 1), whose time variation is similar to the time variation in solar EUV burst flux which is considered to be a main cause of SITEC, observed at Hiraiso.

It is seen from the figure that the SITEC occurred at the onset of the solar radio (9.5 GHz) burst with its maximum flux of more than 9,000 S.F.U., instantaneously reached the maximum increment of about $1.3 \times 10^{17}$ elec. $m^{-2}$ (about 50 % of background TEC), and recovered in about 30 minutes. This value of SITEC was so large as to be several times higher than any of the maximum value of SITEC's which had been observed at Hiraiso during the period March 1979-August 1983 [Ogawa and Ohbu, 1984].

## 3. HIGH ENERGY PARTICLE EMISSION

Anomalous enhancement of ionization in the *D* region due to the precipitation of solar high energy particles emitted in occurrence of intense solar flares into the earth's polar cap regions is detected as phase advance on long-distance propagating VLF radio wave circuits. The phenomenon which is called polar cap phase anomaly (P.C.P.A.) as one of means detecting polar cap disturbances (P.C.D.'s), was detected on phase record of two omega circuits of long-distance propagating VLF radio waves received at Inubo through the auroral zone and the polar cap region, i.e., North Dakota (46°22' N, 98°21' W)-Inubo and Aldra (66°25' N, 13°09' E)-Inubo, respectively in connection with the occurrence of the large solar flare with X13/3B concerned.

Consecutively daily variations in phase deviation from the mean values at the same time (at intervals of 30 minutes) on the six quietest days in a month for the above-described both circuits are shown in the two sections of the bottom of Figure 7. According to the figure, the phase deviation began to advance from around 12 h. U.T. and attained the maximum value of advance showing above 200 degrees on April 26 for both circuits, and afterwards recovered on May 2 and 3 for North Dakota-Inubo circuit and Aldra-Inubo one, respectively. These beginning and maximum advance corresponded to the beginning and the maximum value of flux, respectively, of the time variation in solar proton emission flux with energy of 4.0-8.0 MeV which was observed by a Japanese artificial satellite, GMS/SEM (Geostationary Meteorological Satellite/Space Environment Monitor) and was plotted at intervals of 3 hours shown at the top section of the figure.

These phase deviations, therefore, are discussed to have been arisen from anomalous enhancement of ionization in the *D* region due to the precipitation of solar protons into the polar cap regions, associated with the large

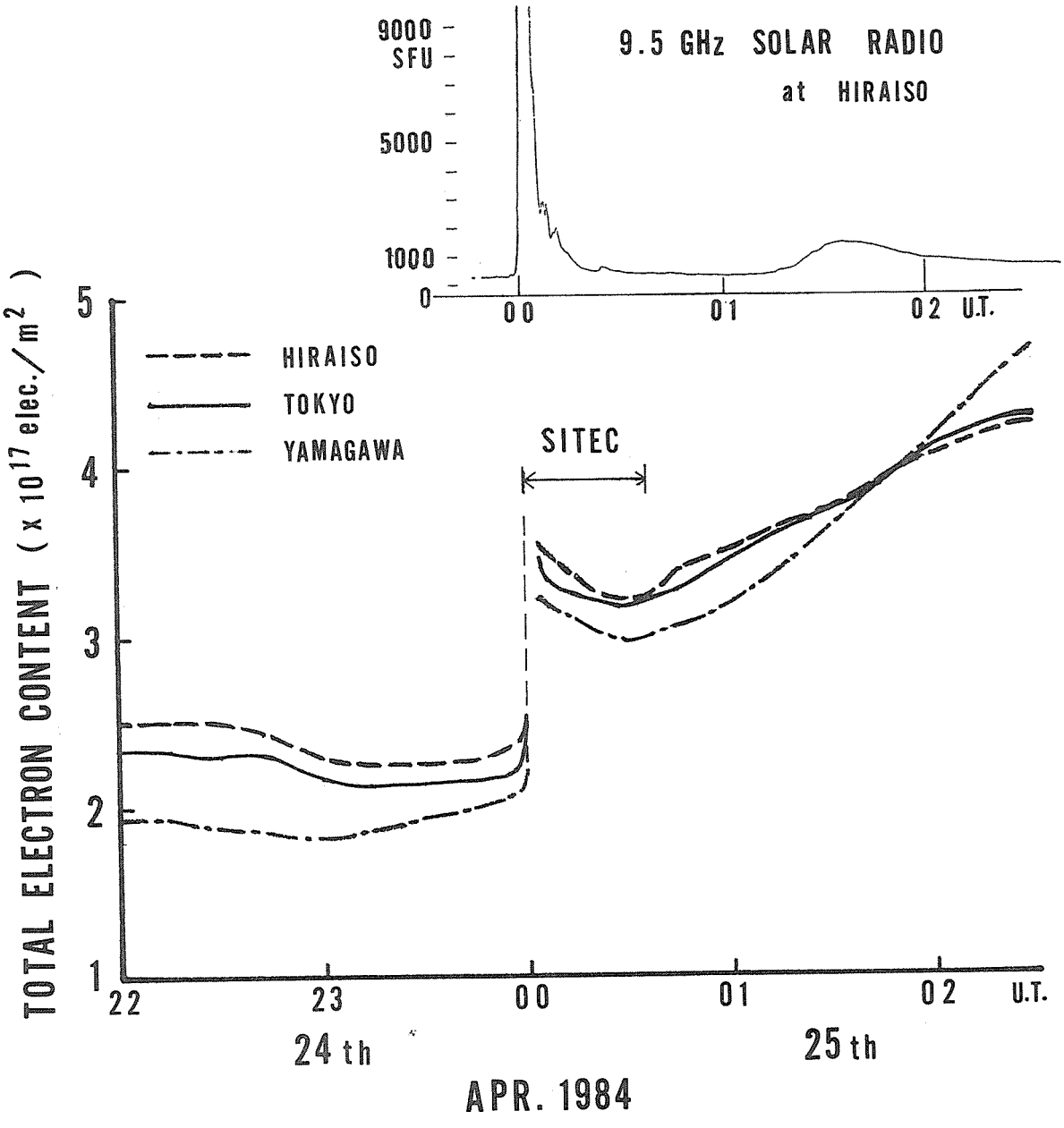


Fig. 6. Time variations in SITEC's appearing on TEC records obtained at the three stations, which were caused by the large solar flare concerned on April 24-25, 1984, and in a solar radio (9.5 GHz) burst flux observed at Hiraiso (reproduced from Fig. 1), which was associated with the same flare. Note: SFU = $1 \times 10^{-22}$ $Wm^{-2}Hz^{-1}$.

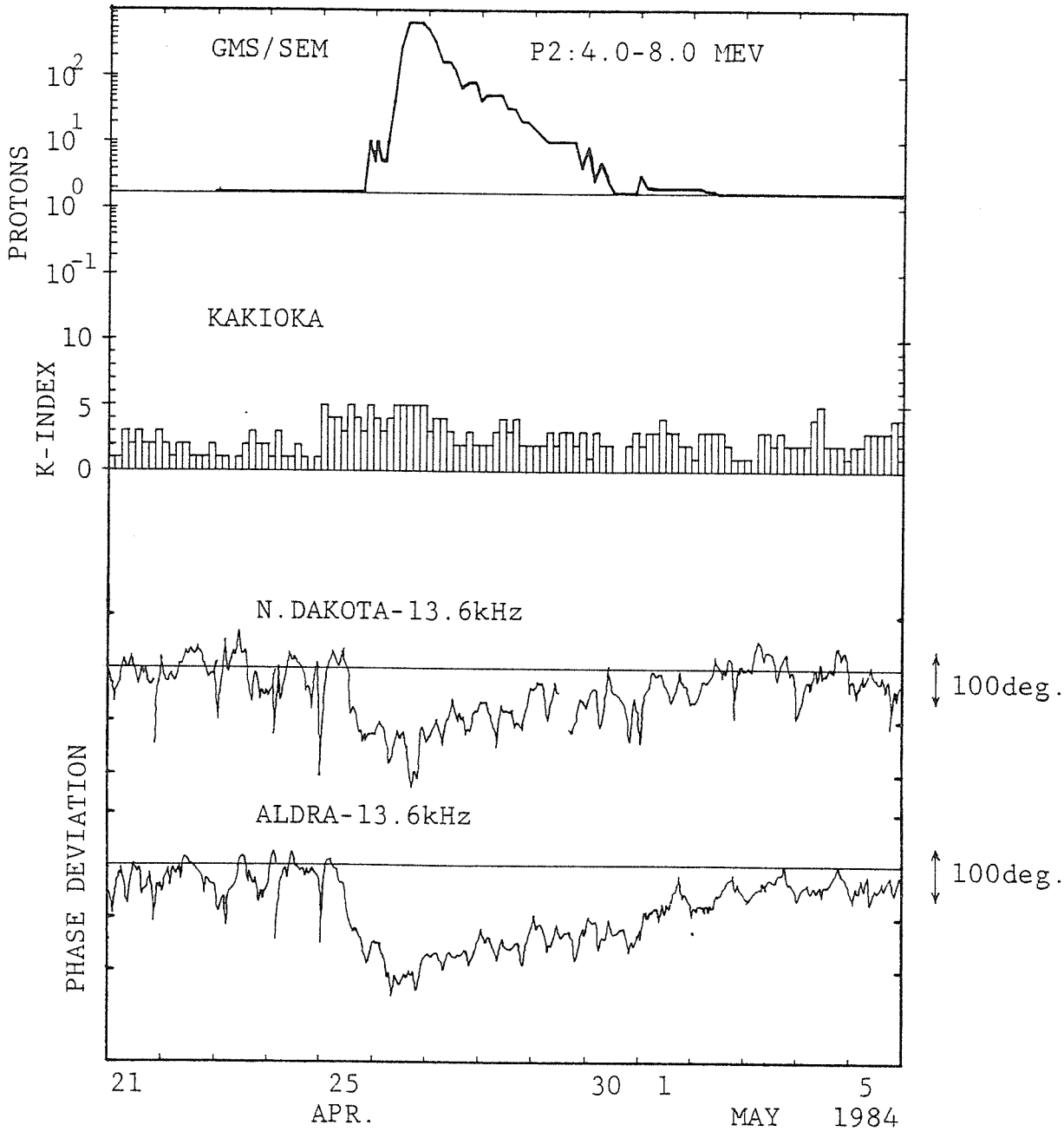


Fig. 7. Time variations in PCPA's appearing on consecutively daily variations in phase deviation (downward direction indicates the advance) from the mean values at the same time (at intervals of 30 min.) on the six quietest days in a month for the two VLF radio wave circuits to Inubo, together with time variations in solar proton (4.0-8.0 Mev) emission flux (protons $cm^{-2}s^{-1}ster^{-1}$), which is shown by having plotted at intervals of 3 h. extracted from raw data obtained at a Japanese satellite, GMS/SEM conducted by Meteorological Satellite Center and in $K$ indices at Kakioka, for a period including the PCPA event caused by the large solar flare concerned on April 24-25, 1984.

solar flare concerned with X13/3B. Thus, the proton event, indeed, was so large-scale that the maximum phase advance was above 200 degrees on both the circuits.

## 4. LOW ENERGY PLASMA FLOW

The low energy plasma here denotes a solar plasma with keV range energy to cause geomagnetic storms. As seen in the second section of Figure 7, $K$ indices at Kakioka (36.23$^{o}$ N, 140.18$^{o}$ E) increased suddenly from the 00-03 h. U.T. range on April 25. But the geomagnetic storm caused by the large solar flare concerned with X13/3B had its S SC at 1449 U.T. on April 26, its $\Delta H_{max}$ = 118 nT at 0015 U.T. on April 27, and its end at 12 h. U.T. on April 27 at Kakioka. The manifestation of a medium-scale geomagnetic storm in spite of the occurrence of so large a solar flare is primarily considered to have originated in the heliolongitudinal position of its occurrence on the solar disk, (S12E43).

Effects of the geomagnetic storm on various ionospheric observational items are described as follows.

### 4.1. $f_oF2$

As described in 2.4., two solar flares which began at 0339 U.T. on April 24 and at 2356 U.T. on April 24, 1984 brought about two geomagnetic storms whose times (day/hour (U.T.)) of beginning, maximum, and end along with $\Delta H_{max}$ observed at Kakioka (36.23$^{o}$ N, 140.18$^{o}$ E) were 25/02.5 h. with Sg, 26/0931, ——; 163 nT and 26/1449 with SS C, 27/0015, 27/12 h.; 118 nT, respectively. The dash denotes indistinctness owing to the beginning of the second storm before the complete recovery of the first one. Consequently, these two geomagnetic storms were consecutive without interval.

Thus, in terms of the time variation in $f_oF2$ shown in Figure 4 expressed in J.S.T. = U.T. + 9 h., a geomagnetic stormy interval was shown as a period from the beginning of the first storm till the end of the second one. In the figure, it is seen that $f_oF2$ was low all day long on April 26 (J.S.T.) during the geomagnetic stormy interval for each of the three stations, but that no observation was made at Okinawa during 1115-1900 J.S.T. owing to some ionosonde trouble. Further, a spread $F$ phenomenon ranging over about 6 hours occurred on April 26-27 (J.S.T.) at Wakkanai.

Anyhow, the ionospheric storm was not so strong in Japan, probably due to the medium-scale geomagnetic storms such as $\Delta H_{max}$ = 163 and 118 nT observed at Kakioka.

### 4.2. Total electron content and slab thickness

The time variations in ionospheric total electron content $N_t$ which was observed in Tokyo by the method described in 2.6. and in slab thickness $\tau$ which is defined as the ratio of $N_t$ and peak electron density are shown in Figure 8 together with $K_p$ indices for the geomagnetic disturbances. They are expressed as the ratio of deviation from the monthly median and the monthly median. The plot of $K_p$ indices indicates two big heaps: the earlier heap corresponds to the gradual geomagnetic storm beginning at 02.5 h. U.T. on April 25 and the later one to the storm with SSC at 1449 U.T. on April 26 due to the large solar flare concerned on April 24-25, 1984 (see 4.1. in the text).

The deviation of $N_t$ was not quite large and rather at random throughout the three days. Therefore, it is not easy to find distinct features related to the geomagnetic disturbances. On the other hand, the deviation of $\tau$ increased so much as to be more than 50 % with the increase in $K_p$. This large increase of $\tau$ can probably be considered to have corresponded to the increase in neutral gas temperature due to the geomagnetic disturbances [Kersley and Hosseinieh, 1976].

### 4.3. Electric field strength in HF radio wave circuits

Disturbances on long-distance propagating HF radio waves received at Hiraiso associated with the two geomagnetic storms described in 4.1. were as follows.

In Thule (76.60$^{o}$ N, 68.80$^{o}$W)-Hiraiso circuit (12 MHz) through the polar cap region, the electric field strength at the receiving site was below interference level from around 12 h. U.T. on April 25 till around 19 h. U.T. on May 2. In WWV (Fort Collins, 40$^{o}$41' N, 105$^{o}$02' W)-Hiraiso circuit (15 MHz) through the subauroral zone, the depression in electric field strength received and the reduction in receivable time interval occurred for April 26 and 27. On the other hand, no influence of the geomagnetic storms could be found out on both WWVH (Kauai, 22$^{o}$00' N, 159$^{o}$46' W)-Hiraiso circuit (15 MHz) situated in the middle and low latitudes and the transequatorial Shepparton (36$^{o}$20' S, 145$^{o}$25' E)-Hiraiso circuit (15 MHz).

From these facts described above, it could be discussed that the geomagnetic influence on the ionosphere did not reach low latitude regions so great a deal, taking into consideration together with the aspect of the deviation of $f_oF2$ from the monthly median (see Figure 4).

### 4.4. Phase deviation on VLF radio wave circuits

According to the second section from the top of Figure 7, the geomagnetic field in Japan was disturbed from 00 h. U.T. on April 25 till at least 12 h. U.T. on April 30 including effects of the two geomagnetic storms described in 4.1. Those effects did not appear remarkably in phase deviation on both the circuits shown in the two sections from the bottom of Figure 7.

Generally, the geomagnetic storm effect on phase on VLF radio wave circuits is easy to appear on North Dakota

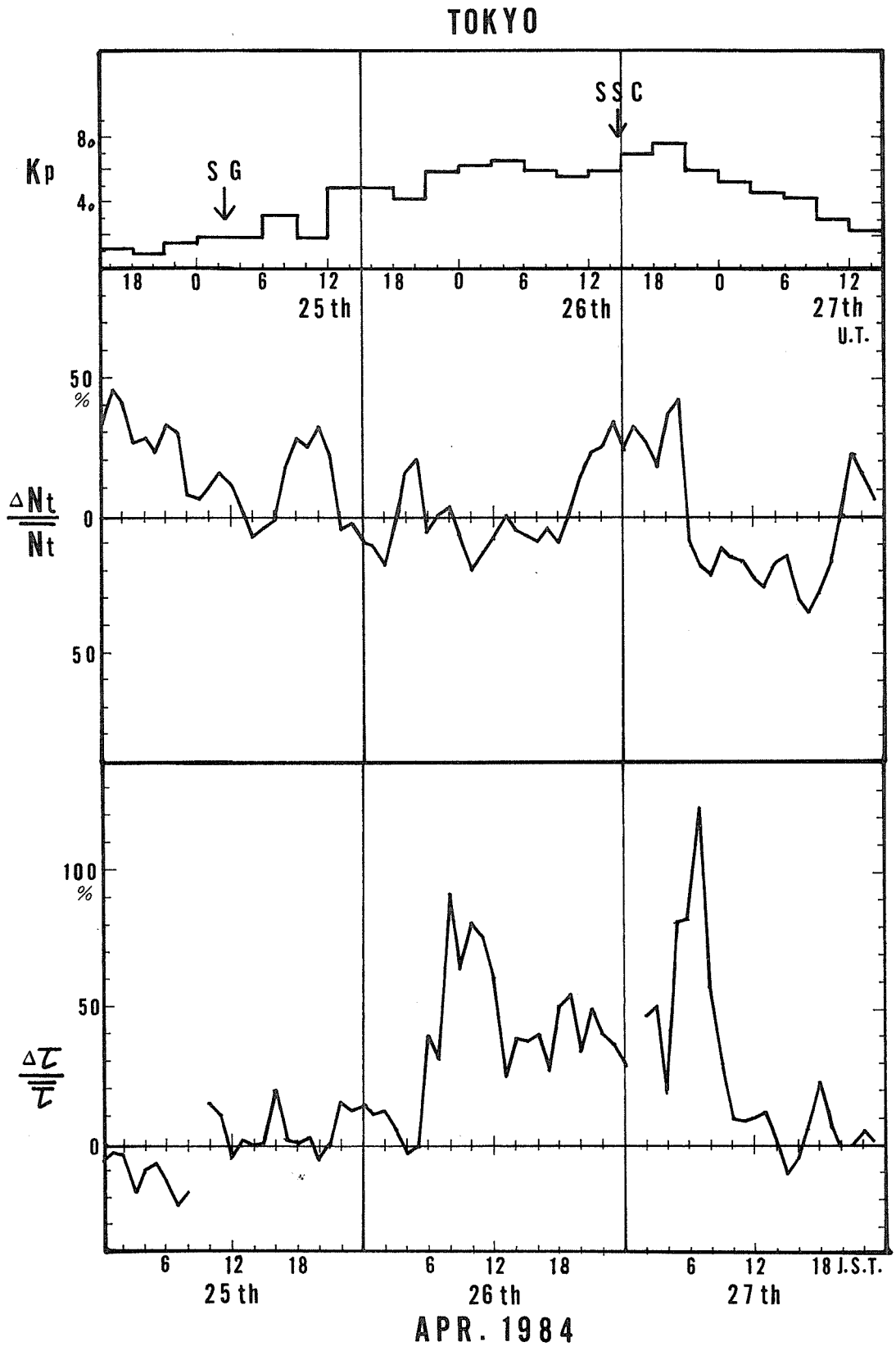


Fig. 8. Time variations in ionospheric total electron content $N_t$ and slab thickness $\tau$ observed in Tokyo together with $K_p$ indices during the geomagnetic disturbances on April 25-27, 1984, the latter half of which was caused by the large solar flare concerned on April 24-25, 1984 (see 4.1. in the text). The upper bar and the symbol $\Delta$ attached to each notation denote the monthly median and the deviation from it, respectively. SG and SSC indicate the beginning of the gradual geomagnetic storm and the storm sudden commencement, respectively.

($46^{o}22'$ N, $98^{o}21'$ W)-Inubo circuit. In the PCPA event (cf. 3. in the text) ranging from April 25 till at least April 30, however, the solar proton effect was so large that the reflecting altitude of VLF radio waves on that circuit lowered greatly. On account of this deep lowering, the precipitating charged particles associated with the geomagnetic storms could not attain the deeply modified reflecting altitude. Consequently, no geomagnetic storm effect is considered to have appeared on phase in VLF radio waves on North Dakota-Inubo circuit.

## 5. CONCLUSIONS

A large solar flare with X13/3B occurred at 2356 U.T. on April 24, 1984. Various observational results of its effects detected by various ionospheric observational networks conducted at Radio Research Laboratory, Japan were presented in this report together with some considerations for them.

Various large-scale SID's were observed. From an estimation of the maximum enhanced solar X-ray radiation flux concerned, it was known that the solar X-ray flare, together with the solar radio bursts was indeed gigantic. The SFD assumed a distinctly oscillatory aspect with a period of about one minute, which would suggest some oscillatory structure of solar ionizing agencies. Large-scale PCPA's were also detected. On the other hand, ionospheric disturbances associated with the geomagnetic storm caused by the solar flare concerned were not so intense.

## ACKNOWLEDGEMENTS

The authors express their hearty thanks to Kakioka Magnetic Observatory (geomagnetic informations) and Meteorological Satellite Center (solar proton flux informations) both of which belong to Japan Meteorological Agency. Ministry of Transport, Japan for their ready consent of the authors' using their valuable observational data. The authors deeply thank also Dr. M. Tsutsui, Radio Atmospheric Science Center, Kyoto University for his ready consent of the authors' using his valuable HF Doppler data.

## REFERENCES


| | | |
|---|---|---|
| Coffey, H. E. and D. C. Wilkinson | 1984 | Enlarged copied data of the time variations in solar X-ray radiation fluxes ($Wm^{-2}$) with wavelengths of 0.1-0.8 and 0.05-0.4 nm observed by GEOS 5, sent by their courtesy, July 1984. Their reduced size is published in Solar-Geophysical Data, comprehensive reports, No. 482 Part II, pp. 55-56, U.S. Dept. of Commerce, National Oceanic and Atmospheric Administration, National Environmental Satellite, Data, and Information Service, National Geophysical Data Center, Boulder, Colo., Oct. 1984. |
| Kersley, L. and H. H. Hosseinieh | 1976 | The Dependence of Ionospheric Slab Thickness on Geomagnetic Activity, J. Atmos. Terr. Phys., 38, pp. 1357-1360. |
| Kikuchi, T. and M. Ohshio | | to be published. |
| Kurokawa, H. | 1985 | Private communication to one of the authors (H. Kumagai). |
| Ogawa, T. and K. Ohbu | 1984 | Correlation of Sudden Increases in Total Electron Content to Solar Flare Microwave and Soft X-ray Bursts, STP Workshop, Paris, pp. 18-22, June 1984. |
| Ohshio, M. | 1974 | Solar-Terrestrial Disturbances of August 1972 4. Solar X-ray Flares and Their corresponding Sudden Ionospheric Disturbances, J. Radio Res. Labs., 21, pp. 311-340. |
| Ohshio, M. | 1978 | Ionospheric *D* region Disturbances Caused by Solar X-ray Flares, pp. 1-346, Planning and Support Division, Radio Res. Labs., Tokyo, June 1978. |
| Ohshio, M., A. Ohtani, and Y. Terajima | 1985a | SPA's Observed at Inubo During February 6-March 5, 1984, this issue. |
| Ohshio, M., Y. Terajima, and K. Ohtaka | 1985b | Solar-Terrestrial Disturbances of June-September 1982 IV. Ionospheric Disturbances 1. Solar X-ray Flares and Their Corresponding Sudden Ionospheric Disturbances, J. Radio Res. Lab. to be published. |
| PRF-SGD | 1984 | Preliminary Report and Forecast of Solar Geophysical Data, SESC PRF 452, U.S. Dept. of Commerce, National Oceanic and Atmospheric Administration, Environmental Res. Labs., Space Environment Services Center, Boulder, Colo., 1 May 1984. |
| SGD | 1985 | Solar-Geophysical Data, prompt reports, No. 485 Part I, pp. 9-10, U.S. Dept. of Commerce, Natioanl Oceanic and Atmospheric Administration, National Environmental Satellite, Data, and Information Service, National Geophysical Data Center, Boulder, Colo., Jan. 1985. |

# The 16 February and 24 April 1984 Solar-Terrestrial Events:

## The Geomagnetic Observations

by

Joe H. Allen
World Data Center A for Solar-Terrestrial Physics
NOAA E/GC2
325 Broadway, Boulder, Colorado U.S.A.

The papers showing geomagnetic variations during disturbed periods associated with solar activity in February and April 1984 display mangetograms recorded at standard magnetic observatories and special networks of stations. Some global coverage is achieved for both events although, as is often the case, most of the recording sites are in the Northern Hemisphere. High latitude observations from the South Pole Station were reported by Krishnaswamy et al. for the February event only. Numerous authors in papers covered both intervals (mainly from auroral zone sites). And only the April event was discussed by Harada (Japan) and Mukherjee et al. (India). The paper by Brunelli et al. in the Ionosphere Section of this UAG Report includes H-component magnetograms from Loparskaya in the Kola Peninsula near Murmansk.

In general, these papers do not attempt to relate magnetic activity events to specific solar phenomena. They simply present the record of time and amplitude variation of the magnetic field at given locations. However, it is notable that many papers include variations recorded by magnetometer arrays linked in common observing programs. Allen and co-authors used magnetograms from an extensive Scandanavian array and several arrays crossing North America. These records are collected by researchers involved in several independent programs but they kindly deposit copies of their data at NOAA's National Geophysical Data Center - World Data Center A for Solar-Terrestrial Physics. An attempt was made in that paper, because of the global coverage of the arrays, to relate the patterns of observed magnetic variations to the occurrence of substorms in the auroral zone and the effects of field-aligned currents at lower latitudes.

The impressive large solar flare observed at 2356 UT on 24 April 1984, was accompanied by magnetic effects reported as sfe's by Harada et al., and commented upon by Allen et al. At Honolulu the H-component stepped almost 50 nT in the positive direction on the hour/day change, remained near maximum offset for about 12 minutes, then began an hour-long decay to the quiet level. The event onset was missed at Guam because the magnetogram was changed around 0000 UT. Sitka also recorded substantial H and D changes. The June 1984 issue of **Solar-Geophysical Data** Part I contains the list of Principal Magnetic Storms for April 1984 (pp. 116-117). In it, College, Honolulu, Sitka and Gnangara reported Sudden Commencements near 0000 UT on 25 April. However, M. Sugiura has reviewed the Honolulu magnetograms (personal communication) and confirms that the recorded change there is not an SSC. This event may be the subject of further research or become better categorized.

| Authors | Type of Observation | Location | Events |
|---|---|---|---|
| Krishnaswamy et al. | Riometer and Magnetometer | South Pole | 16 Feb |
| Allen et al. | Magnetometers | Scandinavia and N. America | 16 Feb, 24 Apr |
| Loginov | Magnetometers | Kola Peninsula, USSR | 16 Feb, 24 Apr |
| Belyaev et al. | Magnetometer, Cosmic Rays | Sverdlovsk (Arty), USSR | 16 Feb, 24 Apr |
| Rusakova | Pulsations | Mid-latitude (Borok, USSR) | 16 Feb, 24 Apr |
| Molochuskin et al. | Magnetometer | Tixie, USSR | 16 Feb, 24 Apr |
| Danilov et al. | Magnetometers | Yakutsk, USSR | 16 Feb, 24 Apr |
| Mukherjee et al. | Magnetometer | Low latitude and equatorial (India) | 25-27 Apr |
| Harada et al. | Magnetometer | Japan | 24 Apr |

# Riometer and Magnetometer Data from South Pole for 16 February 1984

by

S. Krishnaswamy and T.J. Rosenberg
Institute for Physical Science and Technology
University of Maryland
College Park, Maryland 20742, USA

and

C.G. Maclennan and L.J. Lanzerotti
AT&T Bell Laboratories
Murray Hill, New Jersey 07974, USA

This report presents riometer and magnetometer data recorded by the University of Maryland digital data acquisition system at South Pole (L=13.8°, geomagnetic latitude = S78.5) on 16 February 1984.

The magnetic field measurements were made by Bell Laboratories fluxgate magnetometers which measure field variations (with frequencies less than 0.25 Hz) in the geomagnetic North-South (H), East-West (D) and vertical (Z) directions, with a noise level of 0.25 nanoTesla. Cosmic radio noise was measured by the University of Maryland riometers operating at frequencies of 30 MHz and 51.4 MHz with 200 kHz bandwidths, time constants of 0.25 seconds and noise levels of about 0.02 dB. The riometer antennas point toward the zenith and have half-power beamwidths of $\pm 30°$. The magnetometer and riometer data together with data from several other geophysical sensors (search coil micropulsation monitors and multichannel VLF detectors) are multiplexed, digitized and recorded on magnetic tape. The riometer and magnetometer outputs are sampled at 1-second intervals.

Figure 1 shows the cosmic noise absorption in dB at 30 MHz and 51.4 MHz, and the variations in nanoTeslas of the H, D and Z components of the geomagnetic field on 16 February 1984. The riometer voltage values were converted to absorption using a computer technique developed at the University of Maryland that we refer to as the Inflection Point Method (Krishnaswamy et al., 1985). In this method, the reference or background value (the so-called "quiet day curve" value) for a given sidereal time interval is taken to be the signal level corresponding to the inflection point on the high-signal side of the distribution of cosmic noise values for that interval. Quiet day curves were computed for the month of February for the two frequencies to produce the riometer absorption curves in Figure 1. The absorption values are believed to be accurate to within about 0.05 dB. The plot resolution for all the curves in the figure is 2 minutes.

The data show that the ionospheric absorption was essentially zero until about 0920 UT (0600 MLT) at which time the absorption increases dramatically due to the solar particle event. The absorption reaches a maximum of about 5 dB at 30 MHz and 2 dB at 51.4 MHz about one hour after the start of the absorption event and then decays gradually. There is still some residual absorption at 2400 UT (0.5 dB at 30 MHz, 0.2 dB at 51.4 MHz). The slowly varying absorption (PCA type) is caused mainly by solar protons; some of the more rapid variations may possibly be due to the effect of magnetospheric electron precipitation or solar electrons. Variations of the local magnetic field accompanied the absorption activity. Most prominent were the negative H bay of approximately 200 nT peaking near absorption maximum and the several cycles of almost 30-minute period fluctuations in D and Z that began just prior to the event and continued until the time of absorption maximum.

Table 1 gives the absorption values at selected times from 0930 UT to 2400 UT and also the ratio $r = A(30.0)/A(51.4)$ of the absorption at the two frequencies. In general, this ratio depends on the flux and the spectrum of the precipitating particles as well as on geometrical factors such as the amount of the antenna beam filled by the absorbing region. The ratio is in the range 2.53 to 2.91 and appears to reach its minimum value near the time of maximum absorption. A value of 2.94 is expected for a uniform absorbing region obeying an $f^{-n}$ dependence on frequency, where n=2. Measured values less than 2.94 (n<2), particularly during PCA events when the assumption of a uniform absorbing region is probably valid, are likely due to the height dependence of absorption that is related to the high energy proton spectrum. The last column gives the value of the exponent n. This lies in the range 1.72 to 1.98 and also has its minimum value near absorption maximum.

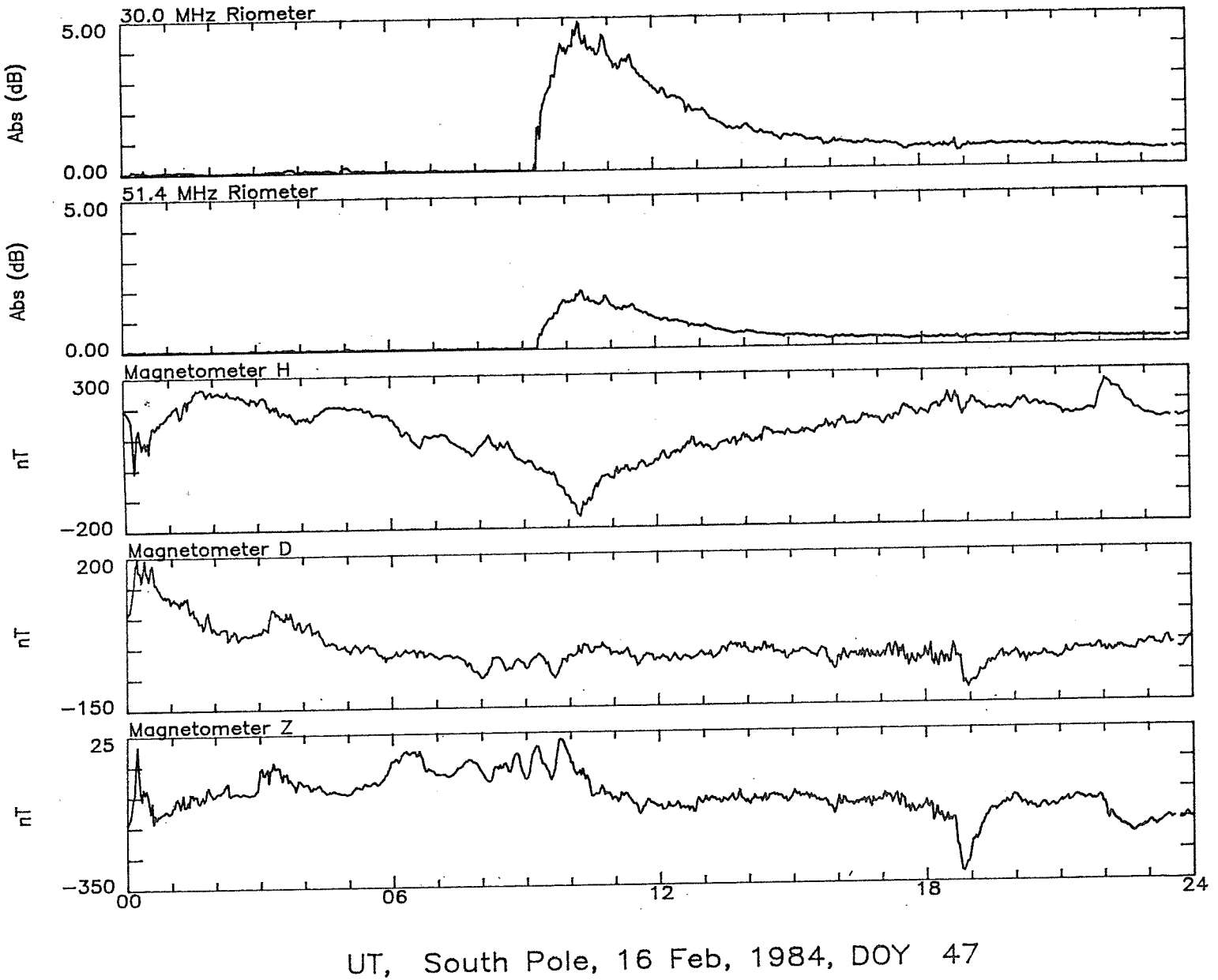


Fig. 1. Cosmic noise absorption in dB at 30 MHz and 51.4 MHz (upper two panels) and geomagnetic field variations in nanoTeslas (lower three panels) at South Pole on 16 February 1984.

Table 1. Cosmic Noise Absorption Values (1-min average), South Pole, 16 February 1984.

| Time UT | A(30 MHz) dB | A(51.4 MHz) dB | $\frac{A(30)}{A(51.4)}$ | n |
|---|---|---|---|---|
| 0930 | 2.05 | 0.78 | 2.63 | 1.80 |
| 1000 | 3.91 | 1.53 | 2.55 | 1.74 |
| 1030 | 4.86 | 1.92 | 2.53 | 1.72 |
| 1100 | 3.80 | 1.45 | 2.62 | 1.79 |
| 1200 | 2.72 | 0.99 | 2.75 | 1.88 |
| 1300 | 1.93 | 0.70 | 2.76 | 1.89 |
| 1400 | 1.35 | 0.49 | 2.76 | 1.89 |
| 1500 | 1.07 | 0.39 | 2.74 | 1.87 |
| 1600 | 0.82 | 0.29 | 2.83 | 1.93 |
| 1700 | 0.77 | 0.27 | 2.85 | 1.95 |
| 1800 | 0.67 | 0.24 | 2.79 | 1.91 |
| 1900 | 0.64 | 0.24 | 2.67 | 1.82 |
| 2000 | 0.71 | 0.27 | 2.63 | 1.80 |
| 2100 | 0.65 | 0.25 | 2.60 | 1.78 |
| 2200 | 0.64 | 0.22 | 2.91 | 1.98 |
| 2300 | 0.56 | 0.20 | 2.80 | 1.91 |
| 2400 | 0.53 | 0.20 | 2.65 | 1.81 |

**Acknowledgements**

The acquisition of these data at South Pole is made possible by financial and logistic support provided by the National Science Foundation Division of Polar Programs.

## REFERENCES

KRISHNASWAMY, S., D.L. DETRICK and T.J. ROSENBERG 1985 "The Inflection Point Method of Determining Riometer Quiet Day Curves", **Radio Science, 20**, 1, pp.123-136.

# Scandinavian and North American Geomagnetic Variations for the February and April 1984 Active Intervals

by

J.H. Allen and L.D. Morris
National Geophysical Data Center
World Data Center-A for Solar-Terrestrial Physics
NOAA E/GC2
325 Broadway, Boulder, Colorado 80303, USA

and

C. Sucksdorff and H. Nevanlina
Finnish Meteorological Institute
Department of Geophysics
Box 503
00101 Helsinki 10, Finland

This combined report covers magnetically active intervals in February and April 1984. Stacked magnetograms are included from the EISCAT magnetometer array in Scandinavia and the RGON array located mainly in North America. EISCAT is the European Incoherent Scatter Radar which is supported by a cross-like array of seven magnetometers that complement the existing network of standard magnetic observatories in that region. RGON is the Remote Geophysical Observing Network. Both arrays are similar to special magnetometer networks created for the IMS (International Magnetospheric Study: 1976-1979). Sucksdorff and Nevanlina describe the EISCAT array; Allen and Morris the RGON network. A brief discussion gives an overview of the magnetic variations as seen in these records and in standard magnetic activity indices.

We collectively acknowledge here the many individuals and institutions who cooperate to make available the EISCAT and RGON magnetic variations records used in this data report and who produce and disseminate the several magnetic activity indices used here.

## RGON Network

Figure 1 is a map and listing of the RGON magnetometer sites in 1984. The network is a cooperative effort between Danish (Greenland), Canadian, and U.S. scientists. Station names are grouped by chains: "Mid-Latitude", "East-West" and "Alaska". Mid-latitude sites extend from San Juan to Honolulu, E-W sites from Narssarssuaq to Anchorage, and Alaskan sites from Talkeetna to Mould Bay. They are operated by university research groups funded by the U.S. National Science Foundation. Other support is provided by the U.S. Geological Survey (USGS) and the National Oceanic and Atmospheric Administration (NOAA). Most RGON magnetometers are at special observing sites but some are located at standard magnetic observatories. Some magnetometers record data on site, and all relay data via NOAA-GOES satellite platforms to a central collection point at NOAA's Space Environment Services Center (SESC). These data are used in near-real-time by SESC to provide alerts about magnetic activity levels that may interfere with the operation of technological systems, e.g., satllites, electric power distribution, TV and hf-radio transmissions, aircraft and ship navigation, and geophysical surveys. The data are tranferred to NOAA's National Geophysical Data Center (NGDC) and World Data Center-A for Solar-Terrestrial Physics for archiving and to be used in retrospective analyses.

RGON instruments are tri-axial fluxgates with nominal 0.1 nT resolution. Some are oriented with the horizontal sensors aligned with geographic N-S and E-W (measuring X,Y,Z variations) while others have the horizontal sensors along and normal to the local magnetic meridian (measuring H,D,Z). Digital data are available in nearly real time from the Space Environment Laboratory Data Acquisition and Display System (SELDADS) as 1-minute or 5-minute averages. The 1-minute data are archived at NGDC. Stacked common-scale RGON plots used in this report are from 5-minute average data.

## EISCAT Magnetometer Cross

The Technical University of Braunschweig, BRD, installed seven fluxgate magnetometers in northern parts of Finland and Norway 1982-1983 to support observations made by the European Incoherent Scatter facility (EISCAT). The fluxgate magnetometers are of a new type developed by Hermann Luhr (1980) and manufactured by Co. Helatronix (Helatronic Type 2450). More than two years of recordings show that Luhr's pulse integrated system, giving all information directly in digital form, is very reliable.

The locations and start times of the stations are given in Table 1. Figure 2 shows the locations of the stations together with the permanent magnetic observatories nearby.

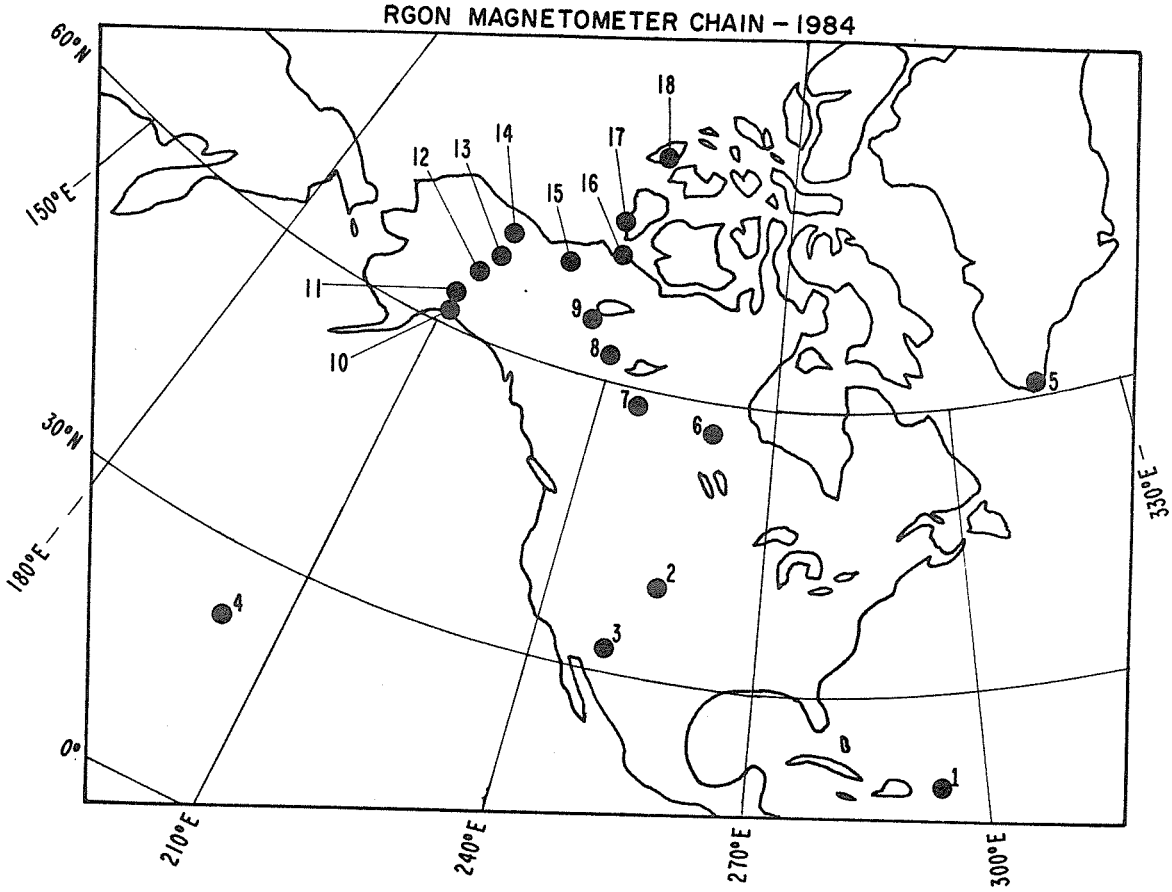


RGON MAGNETOMETERS - 1984

Mid-Latitude E-W Chain:

| | | | | |
|---|---|---|---|---|
| 1. | San Juan | (SJG) | 18.1 N | 293.8 E |
| 2. | Boulder | (BOU) | 40.1 | 254.8 |
| 3. | Tucson | (TUC) | 32.2 | 249.2 |
| 4. | Honolulu | (HON) | 21.3 | 202.0 |

East - West Chain:

| | | | | |
|---|---|---|---|---|
| 5. | Narssarssuaq | (NAQ) | 61.1 N | 314.8 E |
| 6. | Lynn Lake | (LYN) | 56.8 | 258.9 |
| 7. | Fort Smith | (FSM) | 58.0 | 246.0 |
| 8. | Fort Simpson | (FSP) | 61.8 | 238.8 |
| 9. | Norman Wells | (NOW) | 64.9 | 234.5 |
| 10. | Anchorage | (AMU) | 61.2 | 210.1 |

Alaska Chain:

| | | | | |
|---|---|---|---|---|
| 11. | Talkeetna | (TLK) | 62.3 N | 209.9 E |
| 12. | College | (CMO) | 64.9 | 212.2 |
| 13. | Fort Yukon | (FYU) | 66.6 | 214.7 |
| 14. | Arctic Village | (AVI) | 68.1 | 214.4 |
| 15. | Inuvik | (INK) | 68.2 | 226.7 |
| 16. | Cape Parry | (CPY) | 70.2 | 235.3 |
| 17. | Sachs Harbour | (SAH) | 72.0 | 235.0 |
| 18. | Mould Bay | (MBC) | 76.2 | 240.6 |

Fig. 1. Map and listing of the Remote Geophysical Observing Network (RGON) magnetometer sites in 1984.

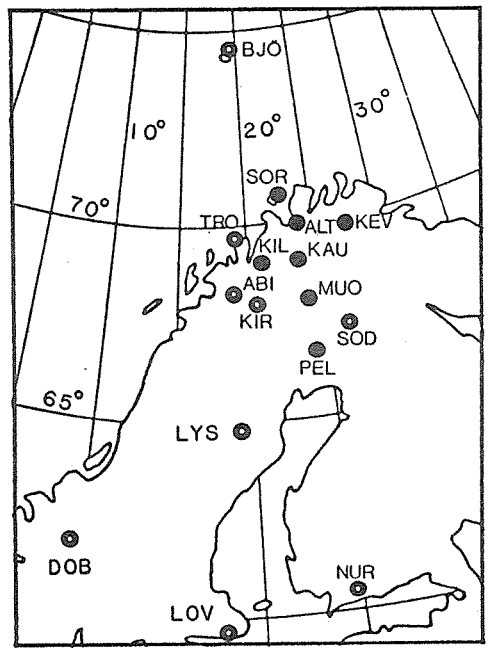


Fig. 2. The EISCAT magnetometers (spots) and magnetic observatories (circles) in North Scandinavia in 1984.

Table 1. Coordinates and Start Times of the EISCAT Magnetometers

| Station Name | Abbre-viation | Geographic Lat. °N | Geographic Long. °E | Corrected Geomagnetic Lat. °N | Corrected Geomagnetic Long. °E | Date Started Recording |
|---|---|---|---|---|---|---|
| Soroya | SOR | 70.54 | 22.22 | 67.30 | 107.90 | 82/09/15 |
| Alta | ALT | 69.86 | 22.96 | 66.62 | 107.81 | 82/09/17 |
| Kautokeino | KAU | 69.02 | 23.05 | 65.78 | 107.16 | 82/09/19 |
| Muonio | MUO | 68.01 | 23.53 | 64.73 | 106.66 | 82/09/23 |
| Pello | PEL | 66.90 | 24.08 | 63.56 | 106.02 | 82/09/09 |
| Kilpisjarvi | KIL | 69.05 | 20.70 | 65.98 | 105.45 | 83/06/19 |
| Kevo | KEV | 69.76 | 27.01 | 66.24 | 110.60 | 83/06/16 |

The magnetometers have been in continuous operation since the time of start given in Table 1. There are some interruptions in the recordings due to failures in electronics, too long a time without power in remote places, etc. As a rule, however, the gaps have lasted only a few days. Technicians from the Sodankyla Geophysical Observatory have succeeded in repairing the stations promptly. Also, in the data now in question there is a gap to be seen in the recording of the station Soroya: X and Y are missing on 24-27 April 1984, giving a straight line. Only the calibration signals can be seen.

The data produced by the EISCAT magnetometers are 20 second mean values of X, Y and Z. The time used is UT and is correct to about 1 second. X, Y and Z are given in units 0.1 nT. The data are available at the Finnish Meteorological Institute, Department of Geophysics, Box 503, SF-00101 Helsinki, in the form of merged tapes, where the stations follow each other so that there is always 20 minutes of data from one station, then the corresponding data from the next station, etc. The format used is the so-called "IAGA-format" given in **IAGA News** (Sucksdorff, 1981).

Plots similar to the enclosed ones are made regularly every day and distributed on microfiche to several institutes. The microfiche are made every three months. To save plotter time, two-minute mean values are used in drawing the plots.

During the days of the February event, RGON Alaska Chain sites Sachs Harbour (SAH) and Inuvik (INK) were not operating. In April, Sachs Harbour (SAH) and Cape Parry (CPY) were out of order.

## OVERVIEW OF MAGNETIC VARIATIONS

### February Interval:

On 14 February 1984, the EISCAT array recorded persistent negative H or X bays due to overhead substorm westward electrojets beginning around 0100 UT, during post-midnight (geomagnetic local time) hours, and lasting four to five hours. During this time the lower-latitude and western auroral zone RGON stations (COL, TLK, and ANC) recorded large positive H or X bays due to substorm eastward electrojets that started around 0300 UT. However, Cape Parry recorded an isolated, sharp onset negative bay at 0600 UT, comparable to those recorded in the X-component by the East-West Chain over Greenland and much of Canada.

Around 1100 UT, RGON stations from Greenland across Canada (now rotated into the post-midnight sector) recorded the start of the first of two large negative bays due to substorm westward electrojets while the EISCAT array showed positive eastward auroral electrojet bays. From about 2200 UT on the 14th through about 0200 UT on the 15th, EISCAT again recorded a large negative bay but during this event only the more eastern and poleward RGON sites (LYN, FSM and FSP) recorded positive bays and these were poorly defined. This disturbance lacked the high-frequency variations seen during the substorms early on the 14th.

Negative substorm bays beginning around 1000 UT on the 15th were recorded at College, Arctic Village, and Cape Parry (Fort Yukon is anomalously quiet) and at the high-latitude western sites of the East-West chain (College magnetograms are shown in both the Alaska and East-West chains). During this time, the EISCAT stations were undisturbed. About 2100 UT on the 15th, EISCAT recorded the start of negative bays that lasted until about 0400 UT on the 16th. RGON was generally undisturbed. Low-level negative bays of limited longitudinal extent were recorded by RGON around 1300 UT on the 16th while EISCAT was undisturbed. Similar conditions occurred on the 17th at 1000 UT.

Global sub-auroral zone magnetic variations as characterized by the Kp index musical note diagrams for February showed a sudden commencement in the latter half of the 12th with bursts of higher activity just after 0000 UT for the next three days, dropping to quiet levels around midday of the 15th. The provisional hourly equatorial Dst index began going negative around midday on the 10th, reaching a minimum of -54 nT from 2100-2200 UT, and recovering to a quiet time level just before midday on the 12th. A second 3-day period of negative Dst occurred from the 12th-15th, reaching a minimum of -64 nT from 0500-0600 UT on the 14th.

During the 14th and 15th, Boulder and Tucson RGON sites recorded moderate disturbances with the largest variations in the D component (field-aligned current responses). Declination changes at Boulder and Tucson are remarkably similar to the prevalent substorm horizontal component changes recorded by the N. American auroral zone stations during hours from 0000 UT to 1400 UT (local night time). That is, positive H or X bays during local evening hours in the auroral zone are matched by positive D changes at mid-latitude, consistent with an eastward auroral electrojet connected by field-aligned currents flowing out toward the magnetotail. Later, negative auroral zone H or X bays are matched by negative D changes at BOU and TUC, consistent with inward flowing field-aligned currents forming the westward auroral electrojet.

### April Interval:

Both EISCAT and RGON magnetometer arrays recorded relatively quiet conditions on 24 April 1984. We do not know what may have caused the sharp offsets in H and Z at Tucson (TUC) around 1400 UT on the 24th. The Kp chart shows a low level of activity and the daily average Dst was only 1 nT with low variance ($\pm$ 4). Dst began to increase at the start of the 25th and Kp reached 5+ by midday. Allen determined that the most disturbed 24-hours of this storm began with 2100 UT on the 25th and achieved a value of Ap* = 102. This was a much larger magnetic storm than that of the February period when Ap* reached only 44 for the 24-hour period beginning at 0300 UT on the 14th.

Beginning around 1300 UT on 25 April, the EISCAT array recorded a period of positive X lasting about 6 hours followed by some 12 hours of negative X variations lasting until around 0800 UT on the 26th. This pattern repeated during the latter half of the 26th through about 0500 UT on the 27th. These were days of continuing large variations during which the only "isolated" substorm to be clearly seen was the negative X bay with sharp onset around 0230 UT on the 27th.

On the 25th, Greenland, Canada and Alaska were magnetically rather quiet until around 1300 UT when a large negative bay began across N. America. The disturbed H or X and Z components seemed to respond earlier at more eastern and lower latitude sites while Mould Bay (MOB) remained undisturbed until the 26th. Narssarssuaq (NAQ) was the only RGON site to record positive X values. All others on the E-W Chain recorded large negative bays although the broken nature of the traces and the amplitude scale of the plots make it difficult to be sure of the pattern of variation at each location. The widespread positive Z recorded across N. America during these hours indicates the westward electrojet was below the lowest latitude auroral zone sites. Again, the predawn declination variations at Boulder (BOU) and Tucson (TUC) are similar to the N. American auroral zone horizontal changes.

The RGON plotted reference levels "float" from day to day with the value shown being the offset necessary to keep the component within its assigned area of the graph. To some extent, this obscures the fact of a substantial change in H at Honolulu (HON) from the end of the 24th to the start of the 25th (these are 5-min average plotted points). A check of the original Honolulu standard observatory magnetogram revealed a large deviation in H and D exactly at 0000 UT on 25 April. This is followed by a gradual magnetic storm main phase H depression which reaches minimum around 0415 UT on the 26th. Another impulse at HON was recorded around 1450 UT on the 26th.

In order to follow the midlatitude RGON magnetometer traces from the 25th to the 26th, it is necessary to note that the main phase H depression lowers the HON H-trace off the bottom of the plotting frame around 2000 UT on the 25th, after which it appears at the top of the frame. This shift persists during most of the 26th and 27th. The observatory 3-letter codes on the left side of the plotting frame only mark the normal position of each trace. Boulder (BOU) and Tucson (TUC) are consistently the most disturbed of the four midlatitude RGON sites during these events.

## REFERENCES


LUHR, H. 1980 "Das Impulsintegrationsverfaren. Ein Saturationskern-Magnetometer mit digitaler Messwertdarstellung", **Diss. Techn. Universitat Cardo-Wilhelmina zu Braunschweig,** Braunschweig, 81 p.

SUCKSDORFF, C. 1981 "Tape formats for geomagnetic data", **IAGA News No. 20**, p. 113.

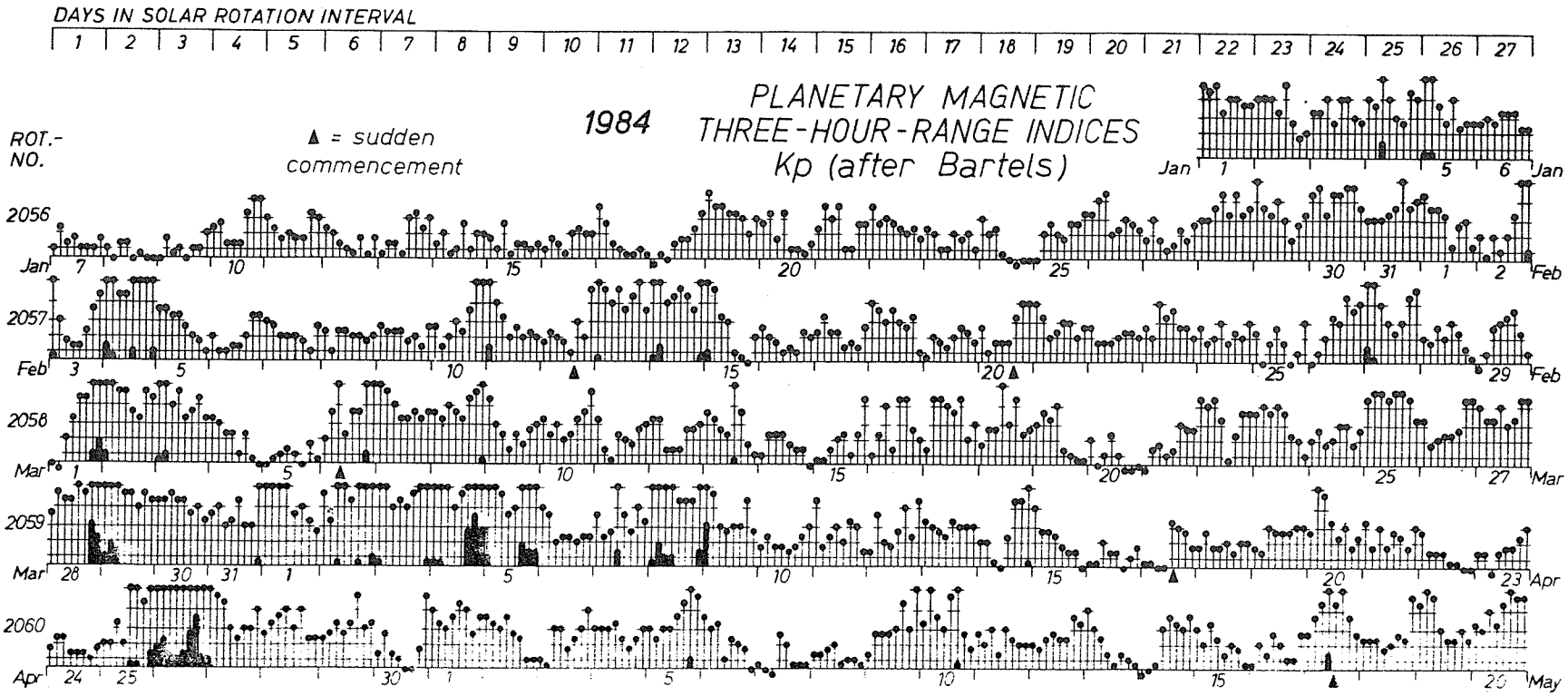




Hourly Equatorial Dst Values (Provisional)

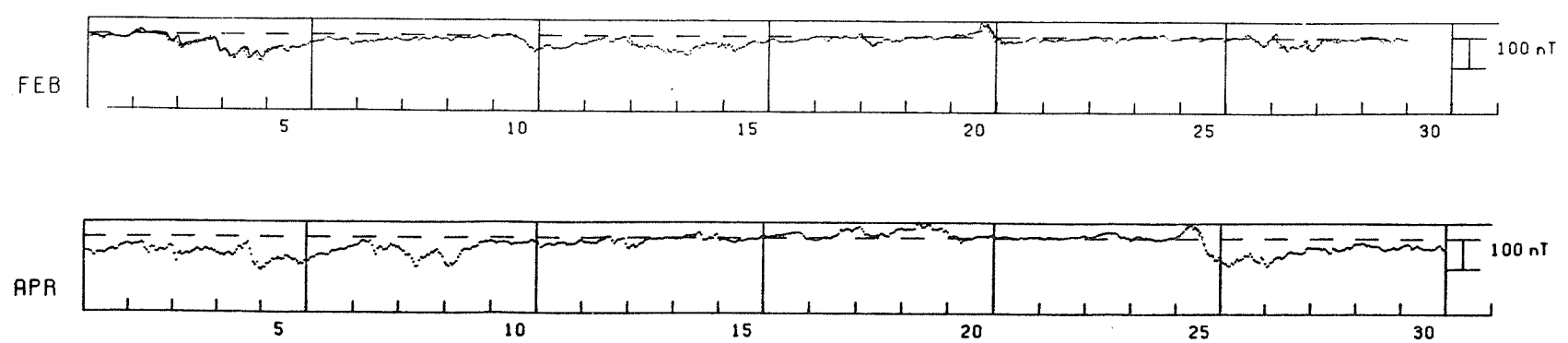

# EISCAT-MAGNETOMETER CROSS 1984-02-14

TWO-MINUTE MEAN VALUES,PRELIMINARY BASE VALUES

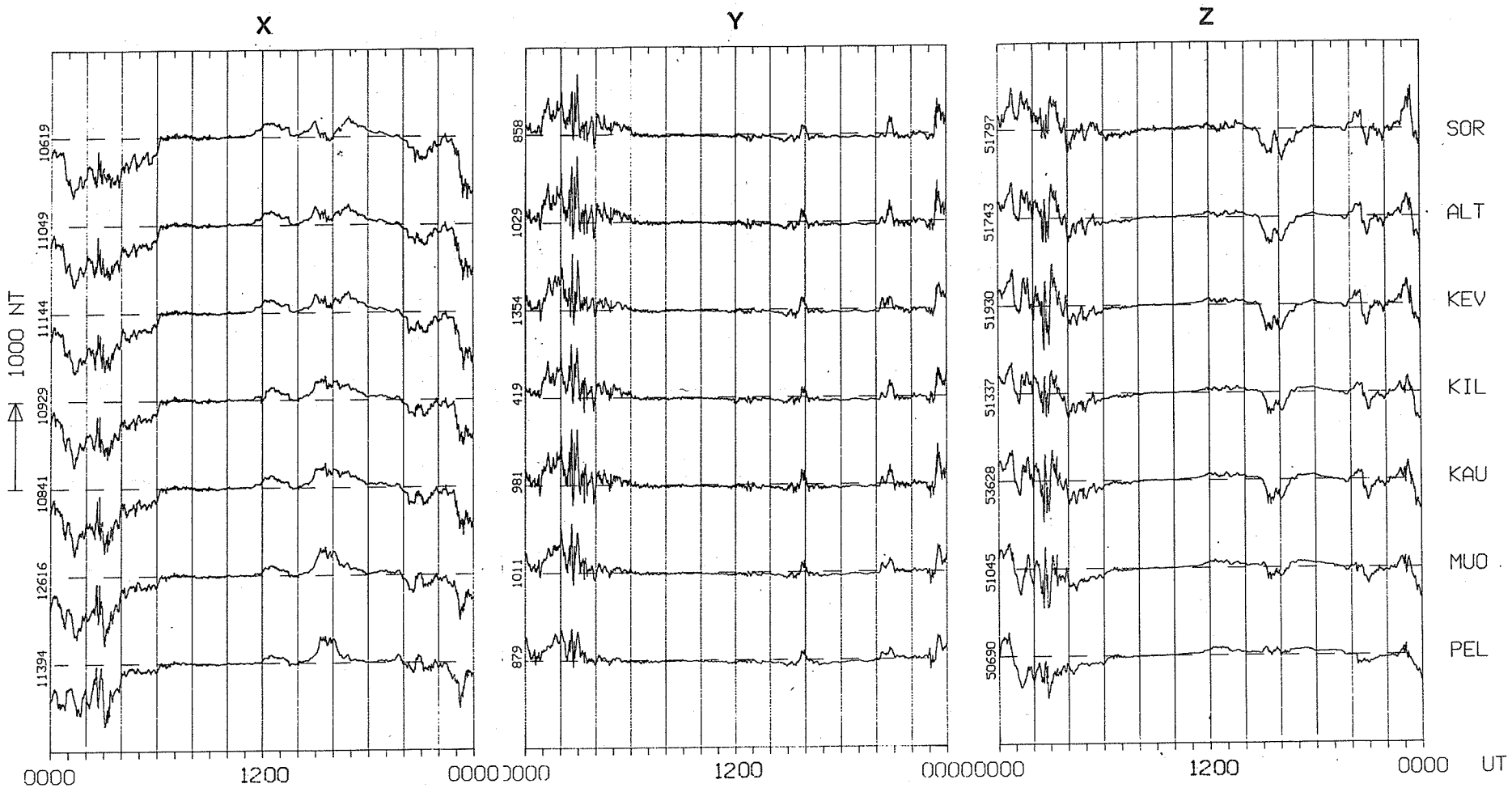

# EISCAT-MAGNETOMETER CROSS 1984-02-15

TWO-MINUTE MEAN VALUES,PRELIMINARY BASE VALUES

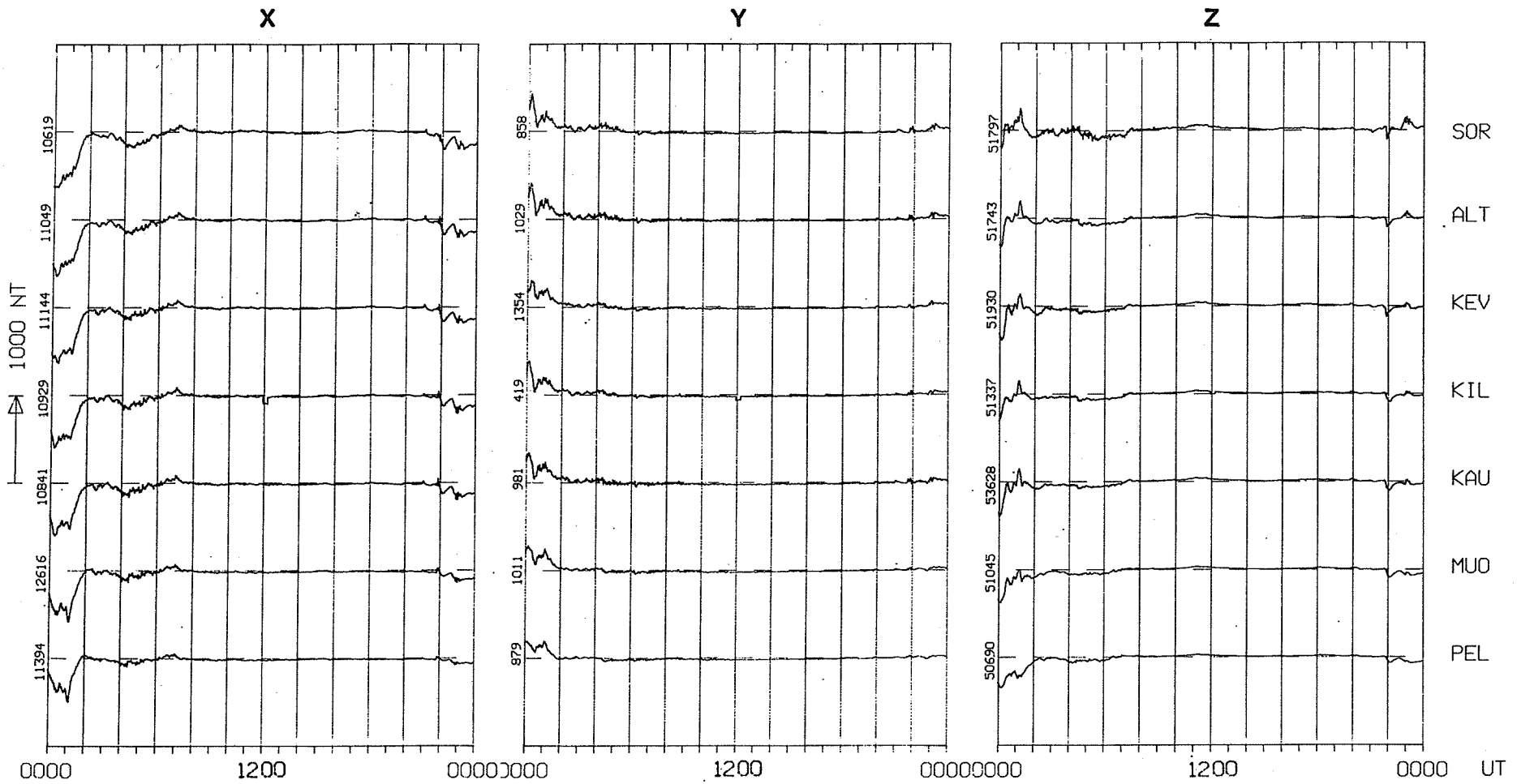

# EISCAT-MAGNETOMETER CROSS 1984-02-16

TWO-MINUTE MEAN VALUES,PRELIMINARY BASE VALUES

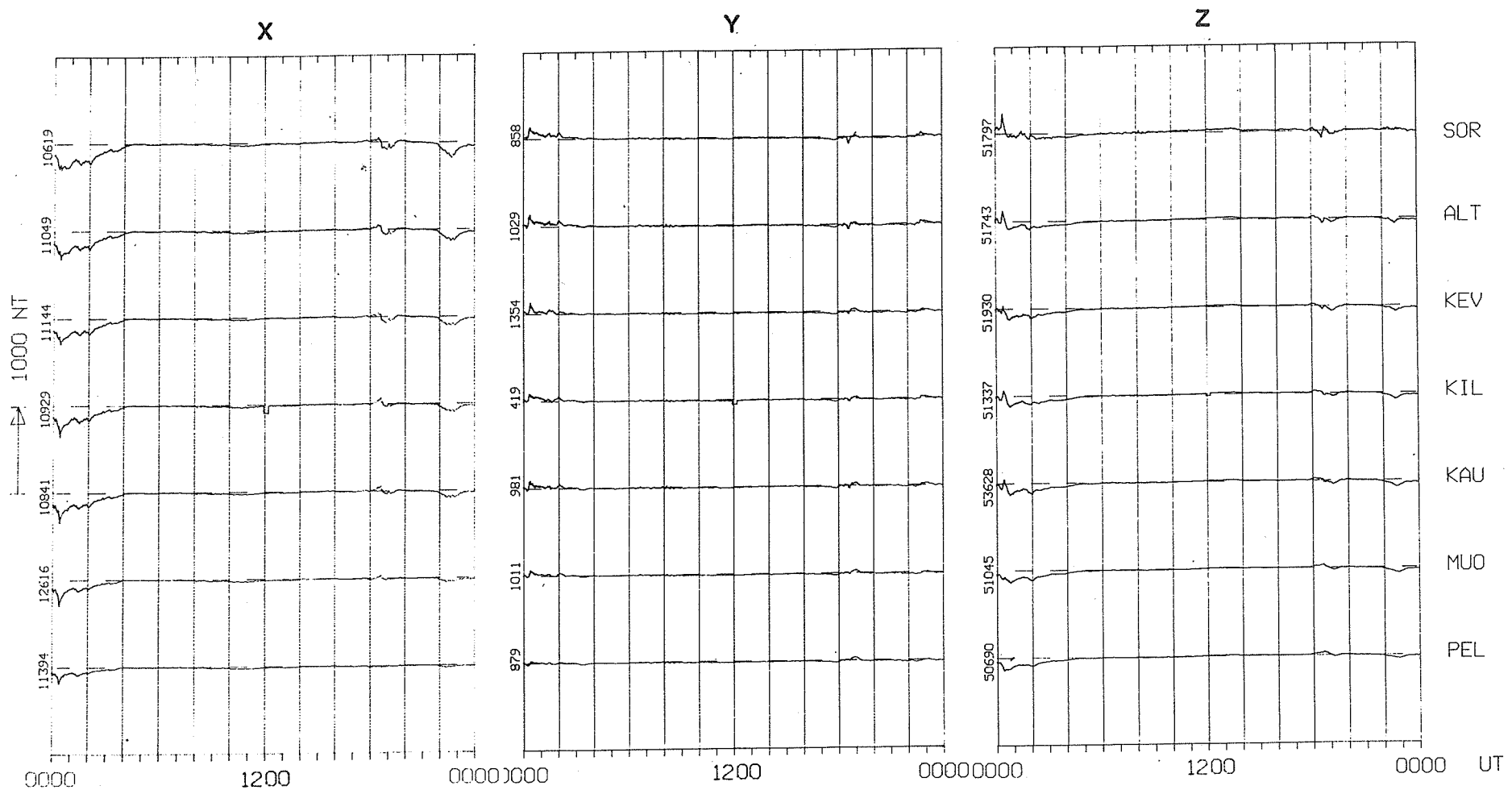

# EISCAT-MAGNETOMETER CROSS 1984-04-24

TWO-MINUTE MEAN VALUES,PRELIMINARY BASE VALUES

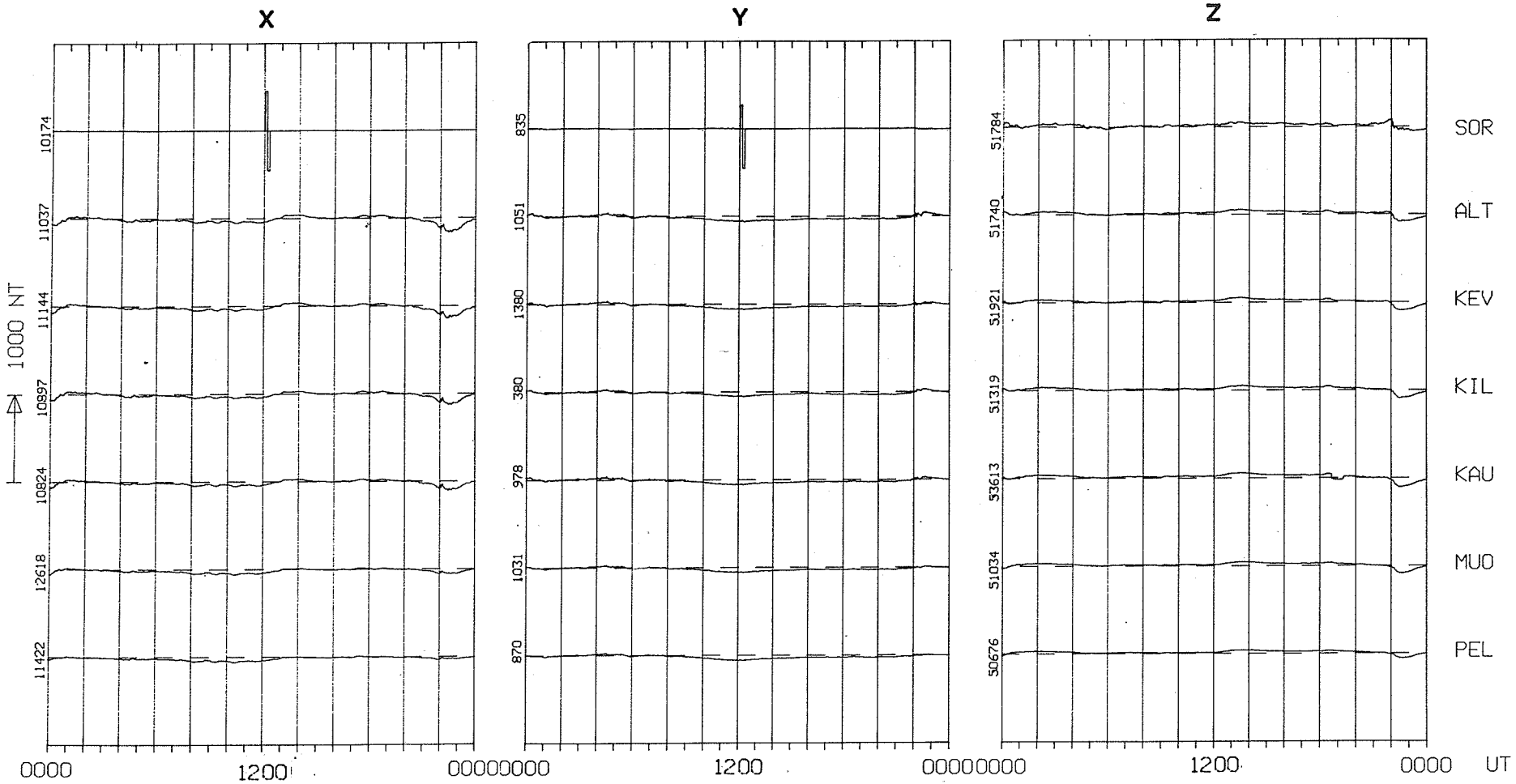

# EISCAT-MAGNETOMETER CROSS 1984-04-25

TWO-MINUTE MEAN VALUES,PRELIMINARY BASE VALUES

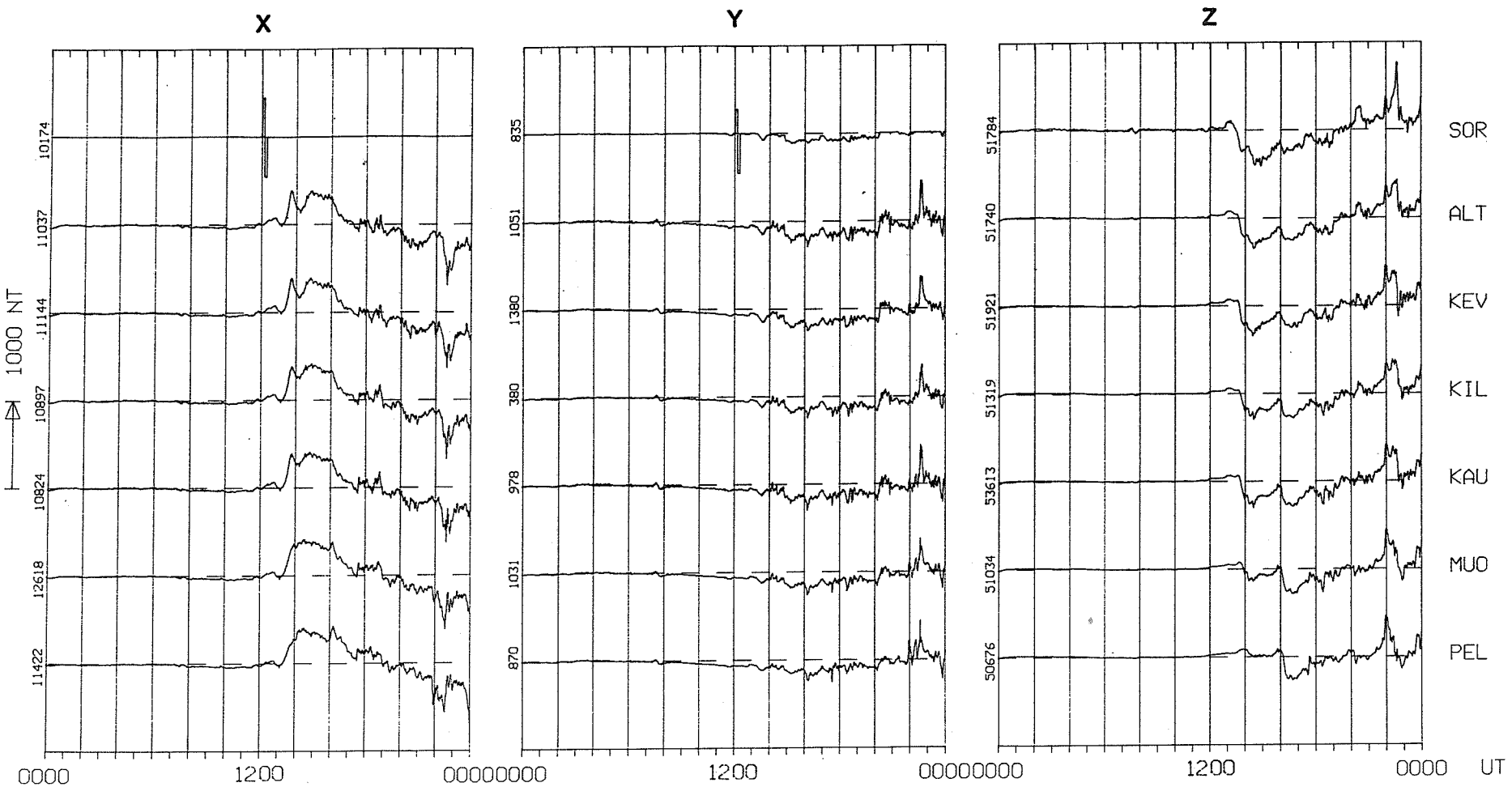

# EISCAT-MAGNETOMETER CROSS 1984-04-26

TWO-MINUTE MEAN VALUES,PRELIMINARY BASE VALUES

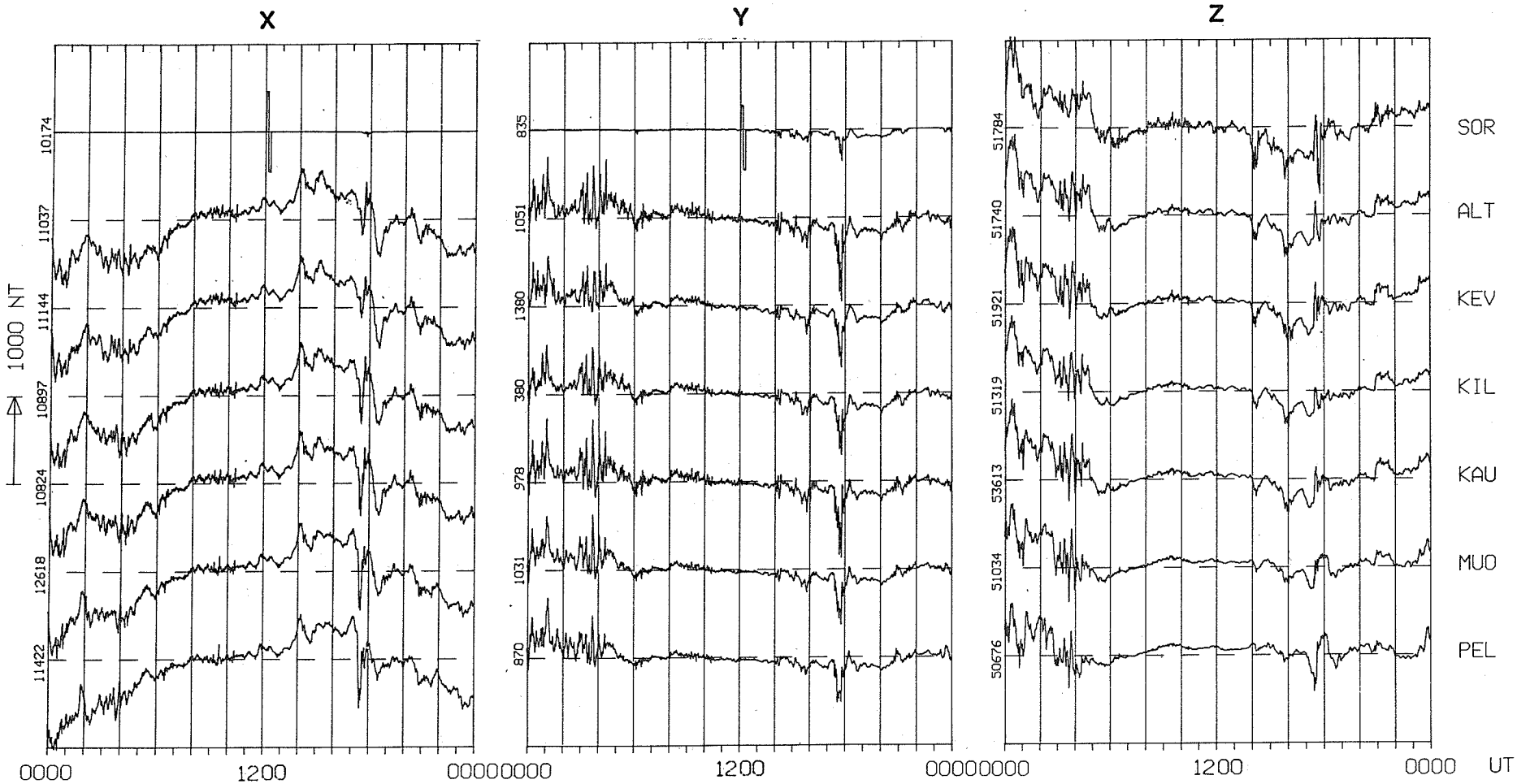

# EISCAT-MAGNETOMETER CROSS 1984-04-27

TWO-MINUTE MEAN VALUES,PRELIMINARY BASE VALUES

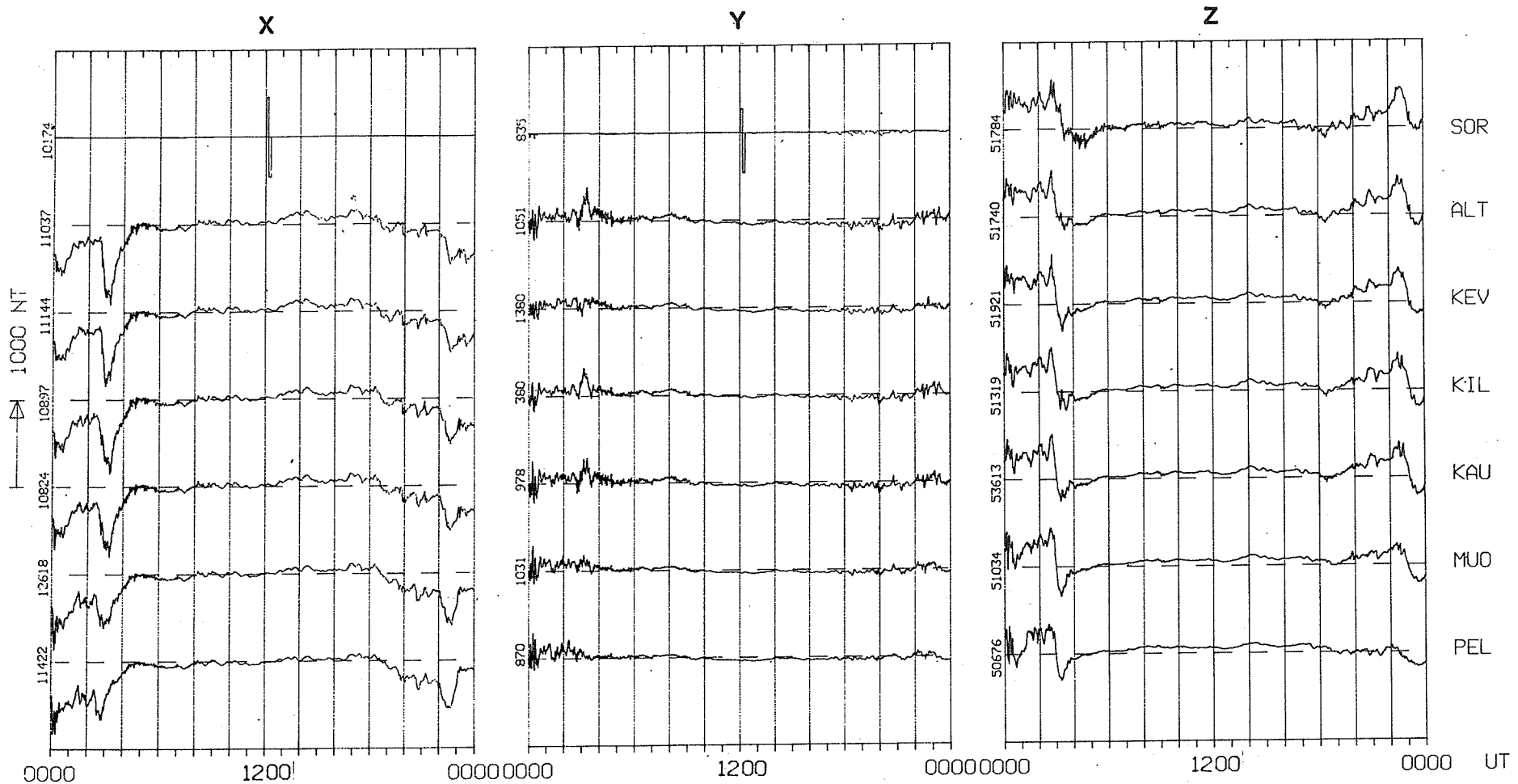


242 mm

# RGON MAGNETOGRAMS
14 February 1984

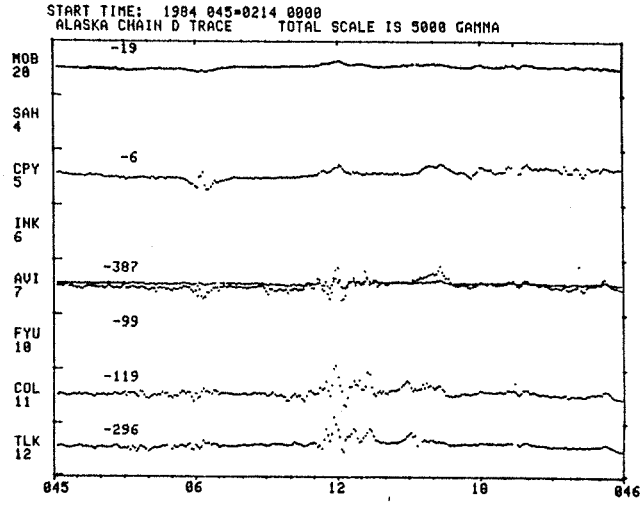


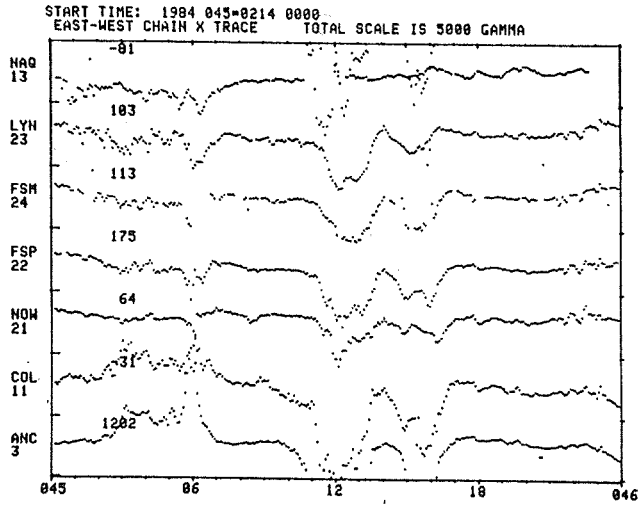


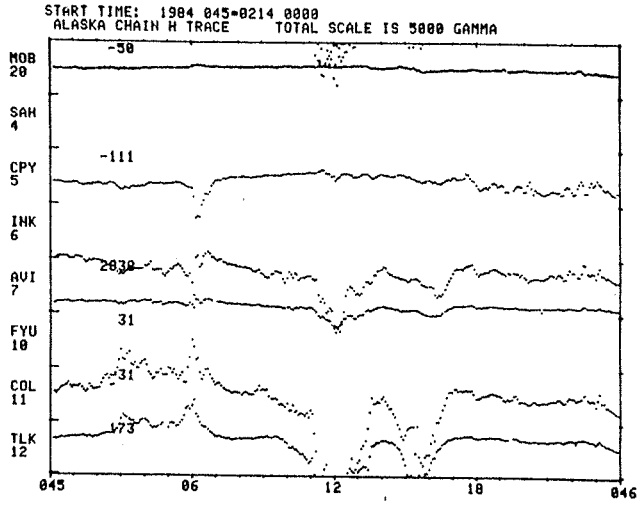


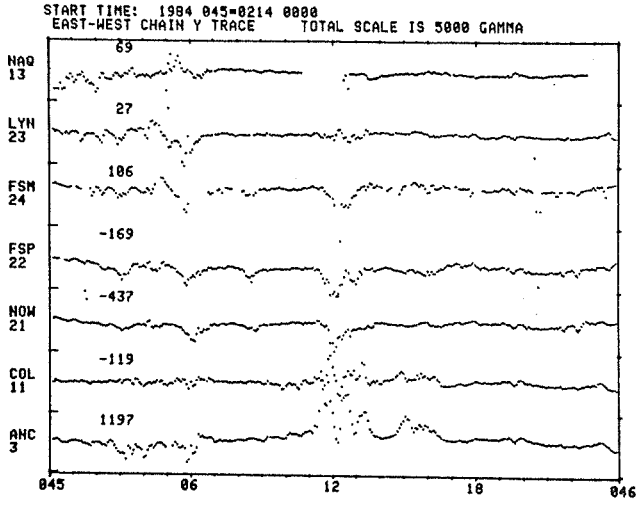


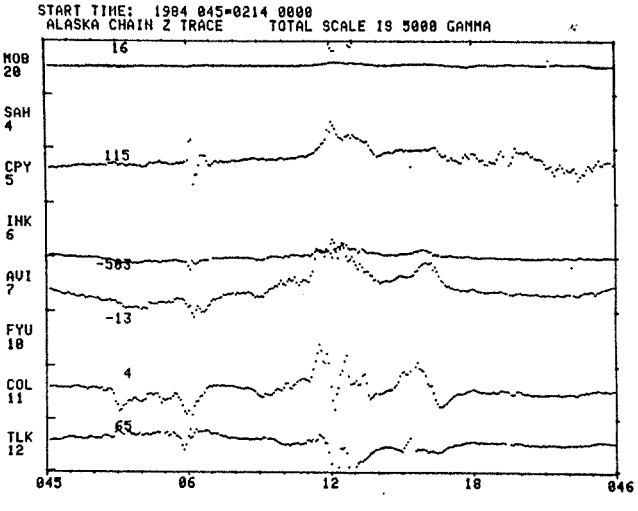


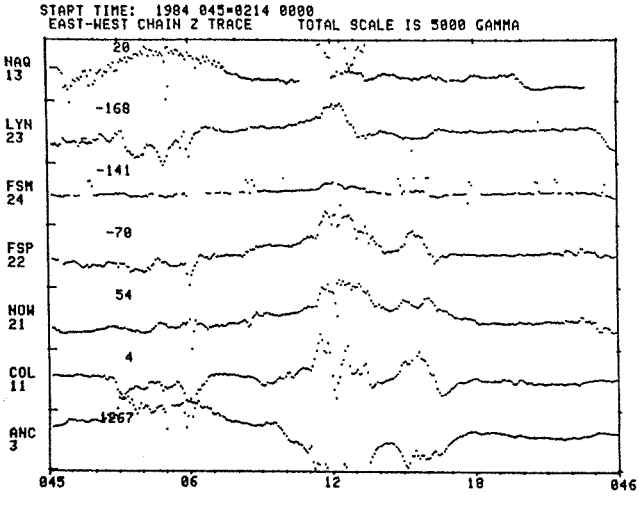

RGON MAGNETOGRAMS
15 February 1984

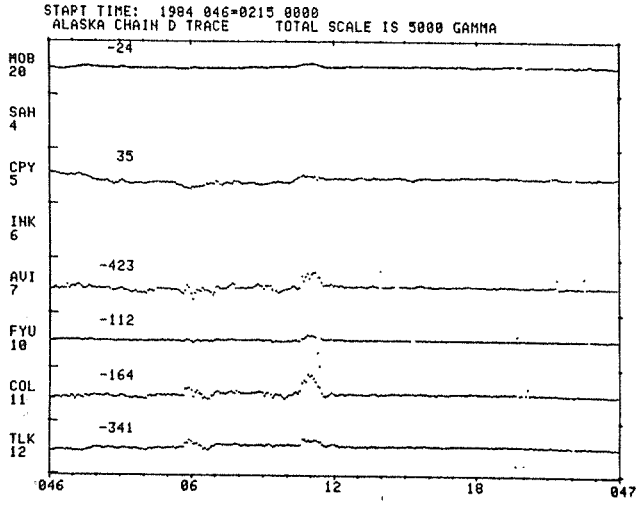


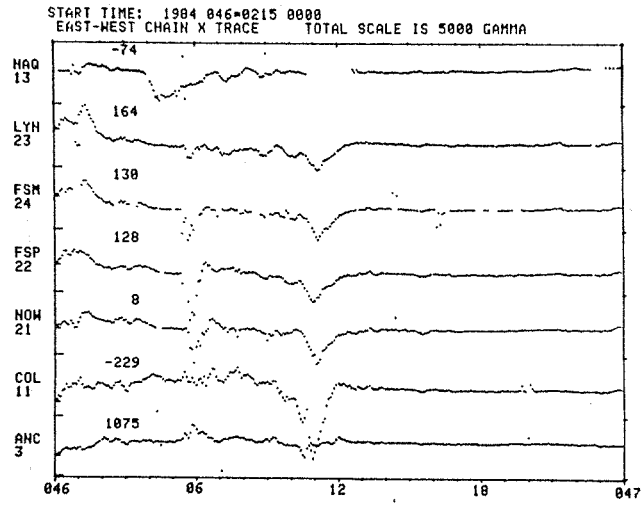


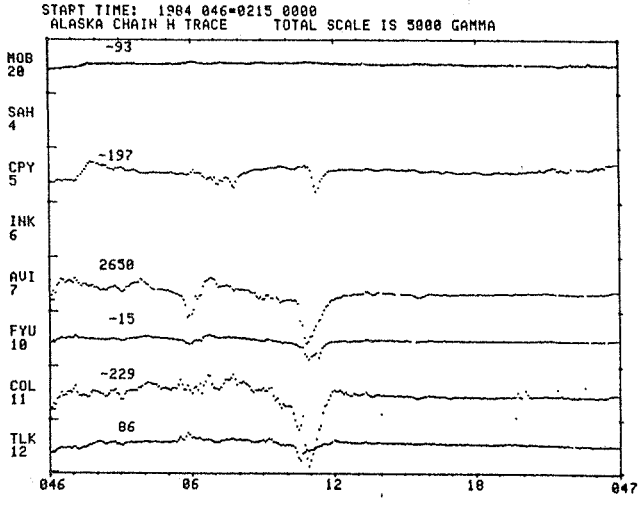


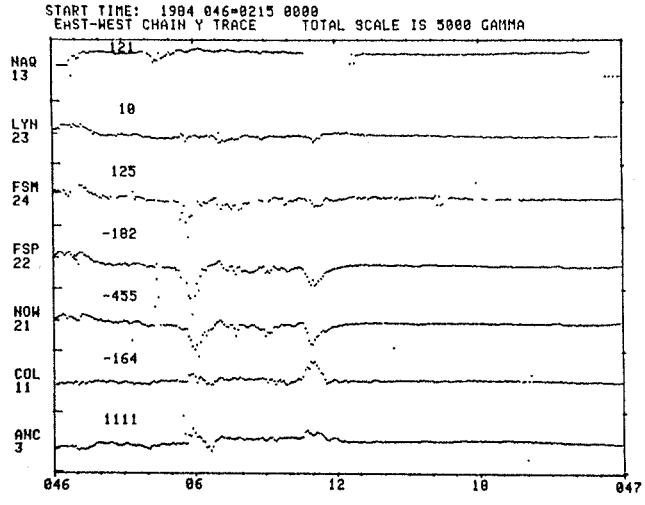


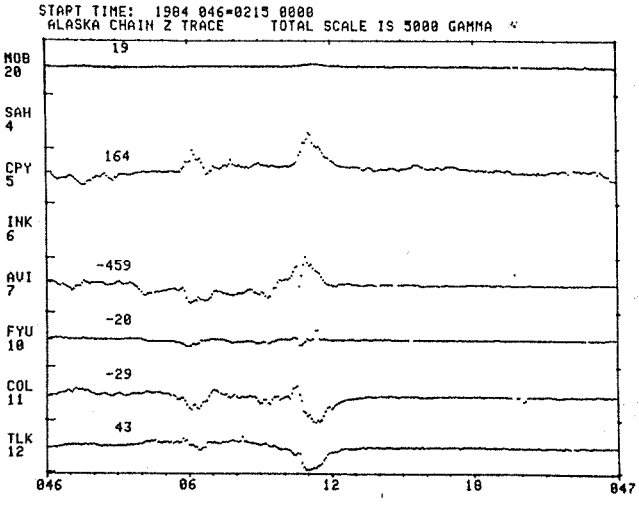


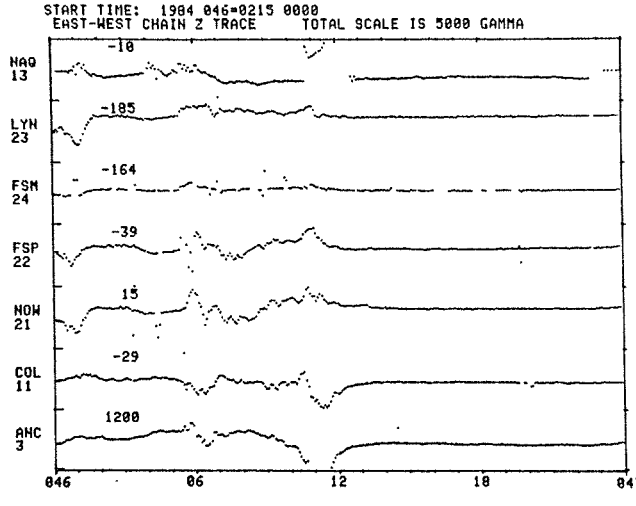

# RGON MAGNETOGRAMS
14-15 February 1984

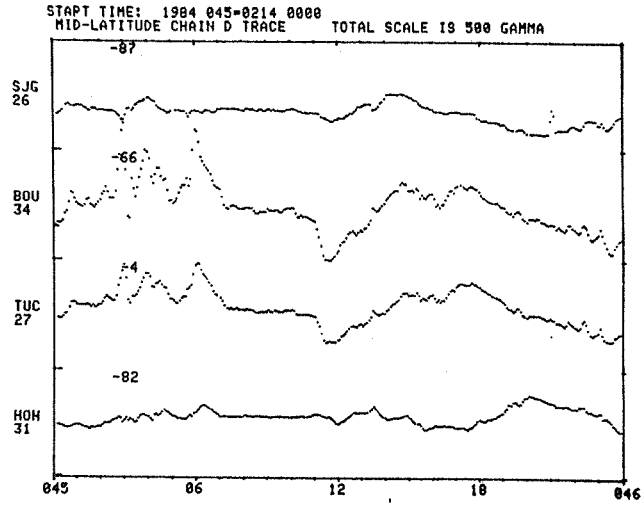


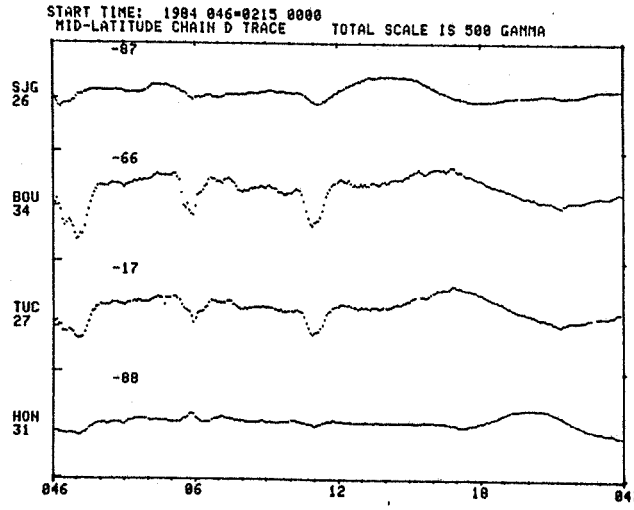


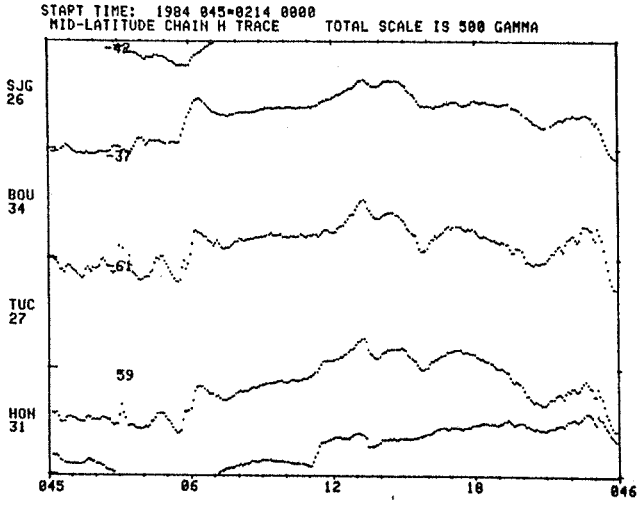


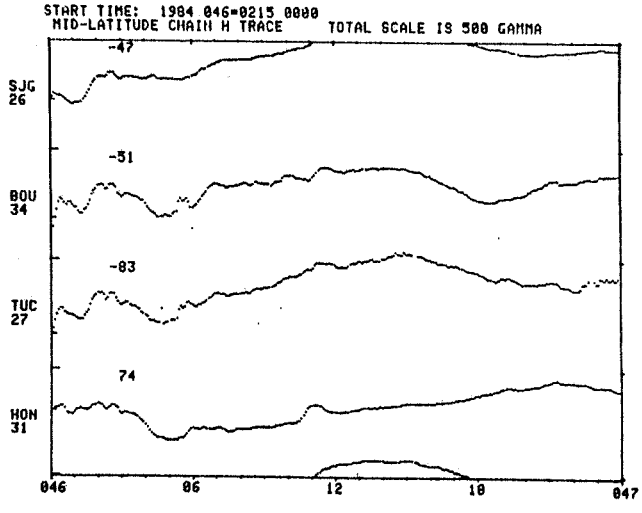


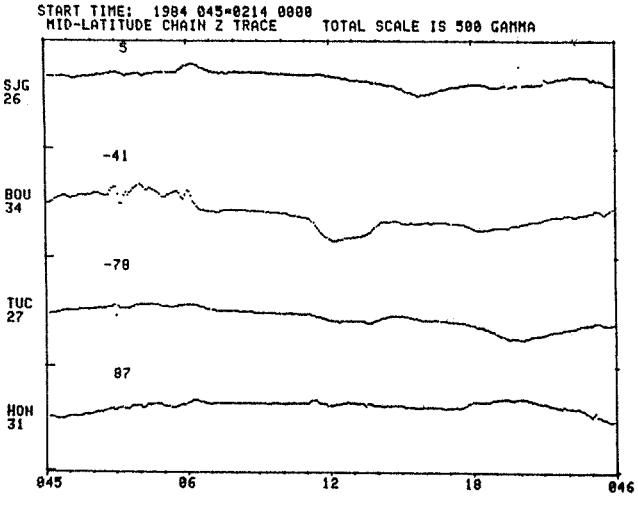


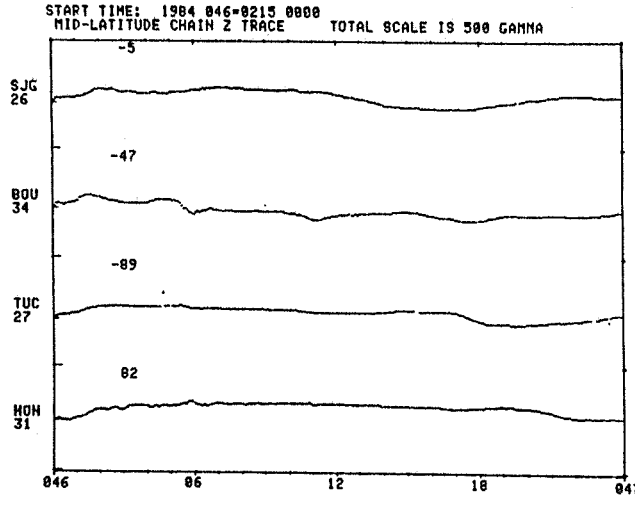

# RGON MAGNETOGRAMS
16 February 1984

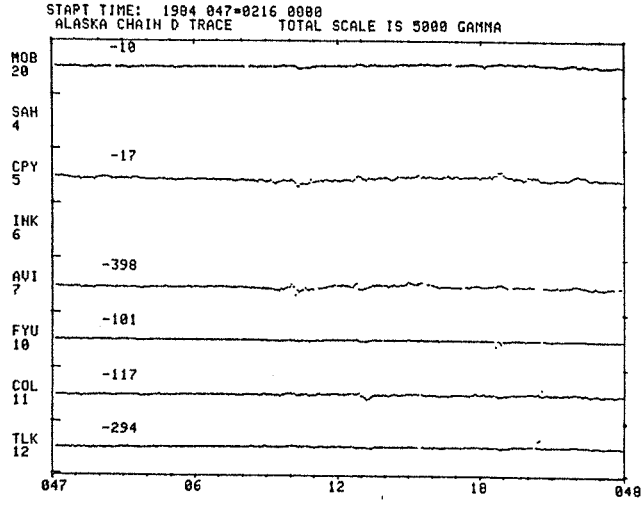


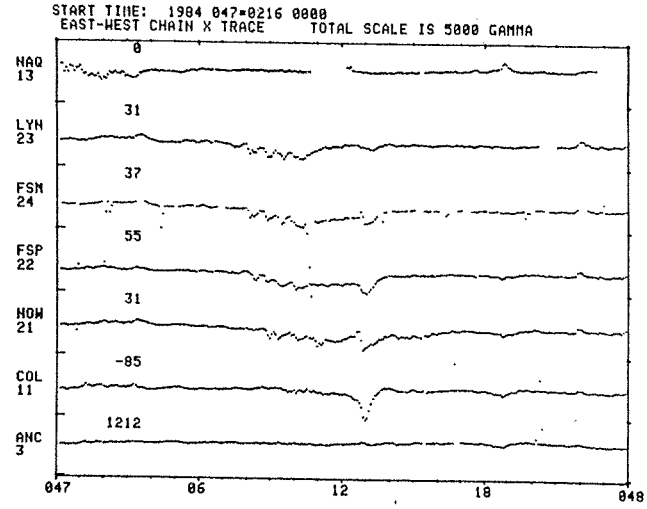


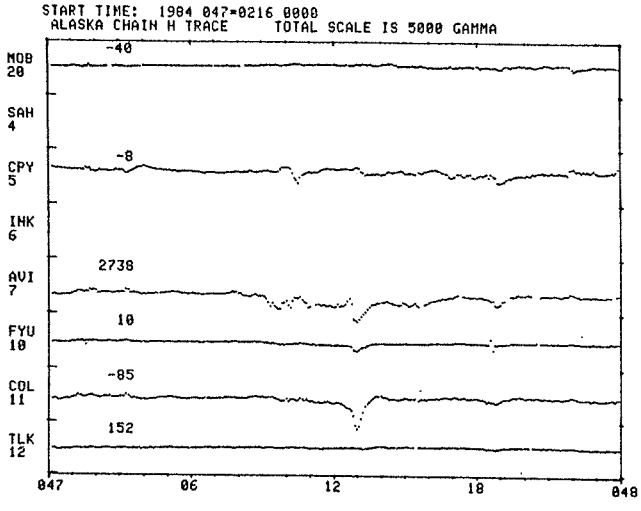


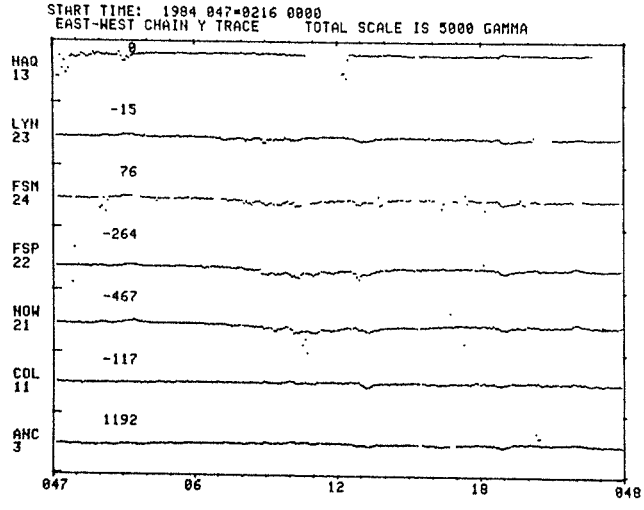


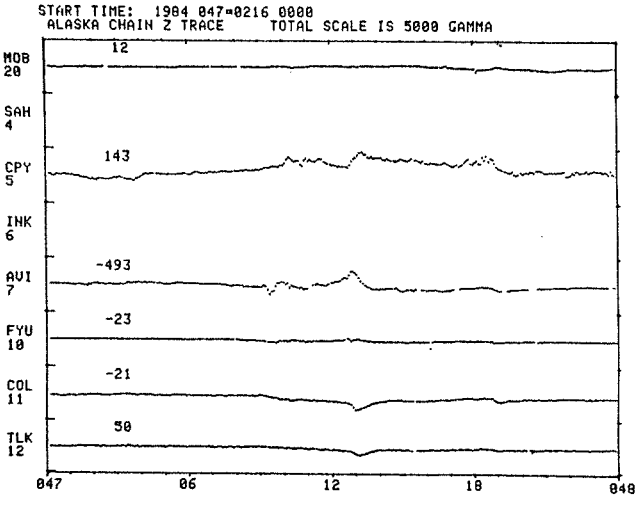


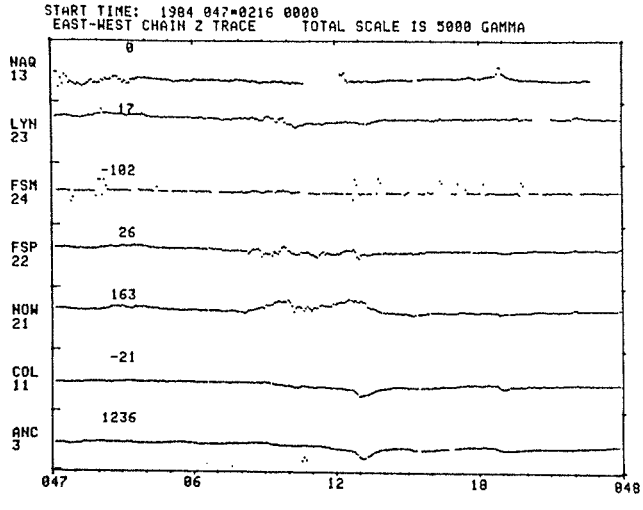

RGON MAGNETOGRAMS
17 February 1984

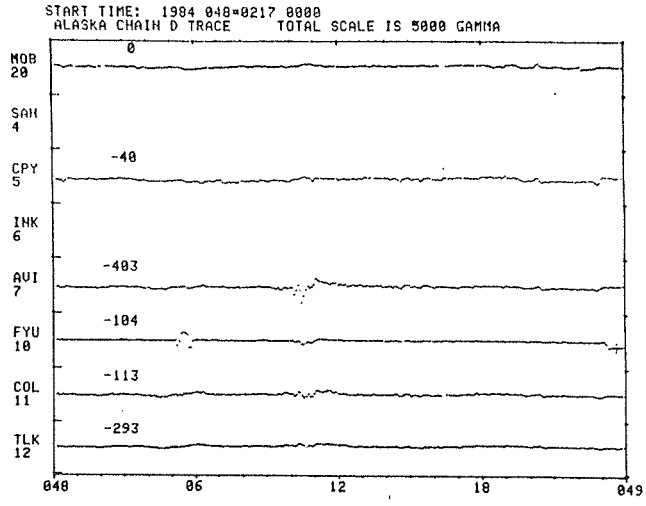


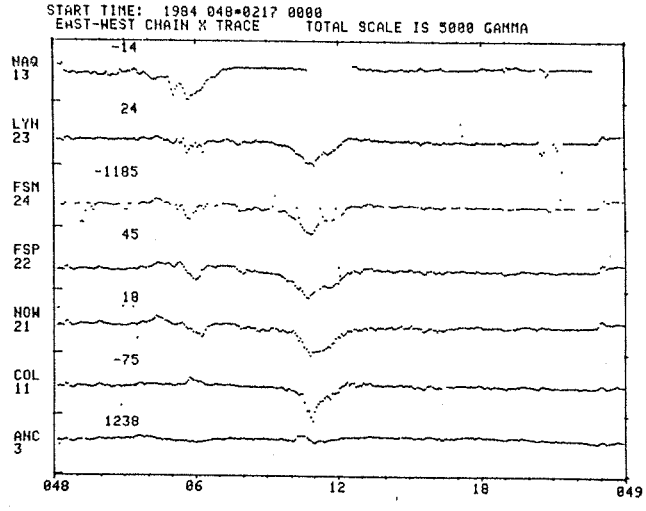


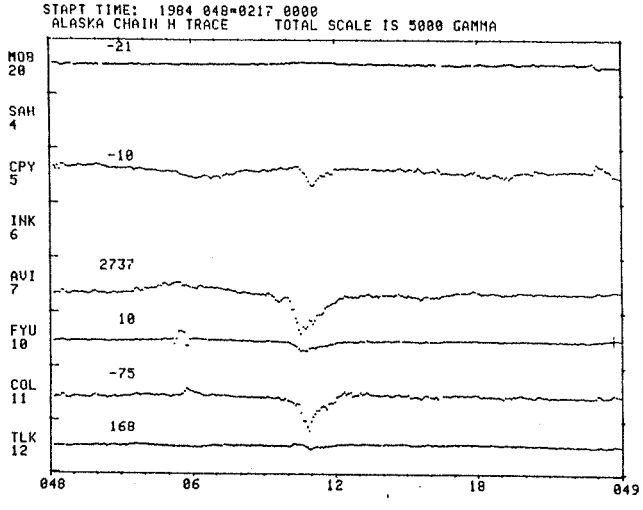


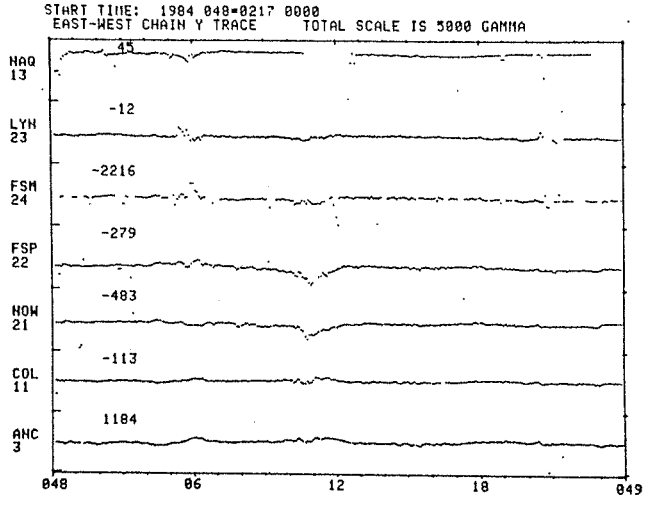


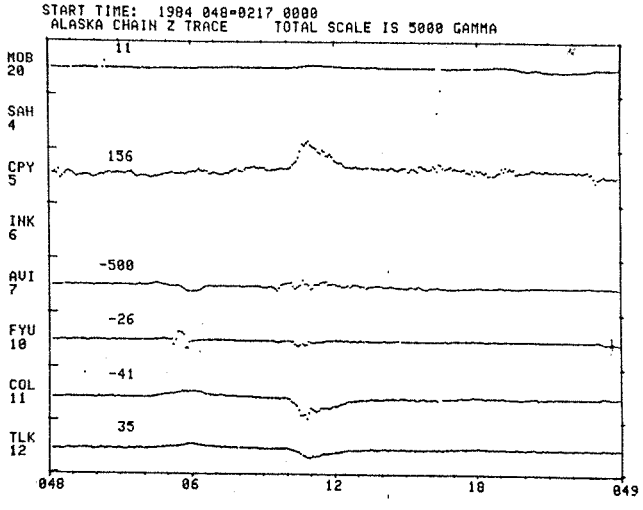


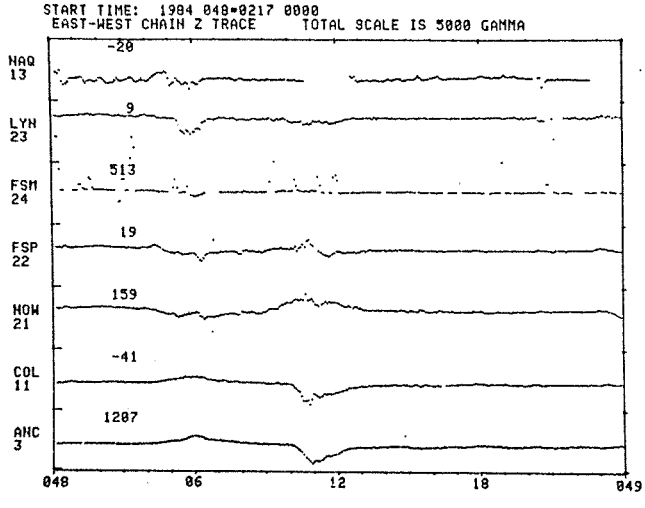

RGON MAGNETOGRAMS
16-17 February 1984

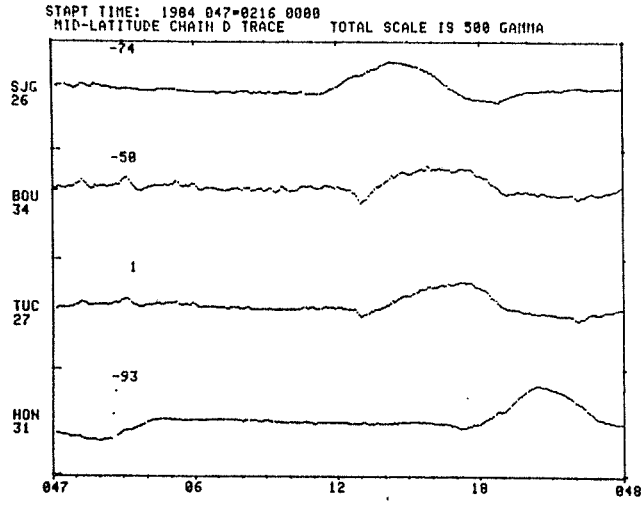


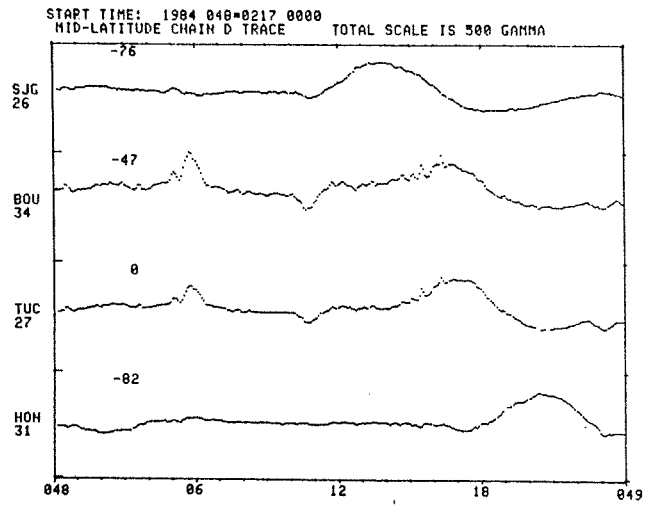


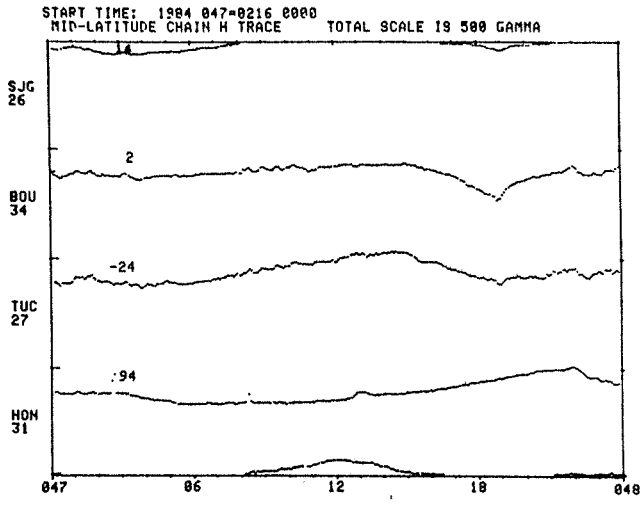


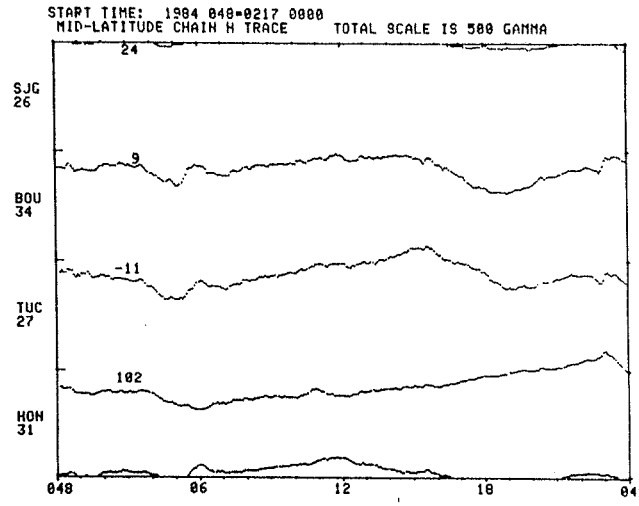


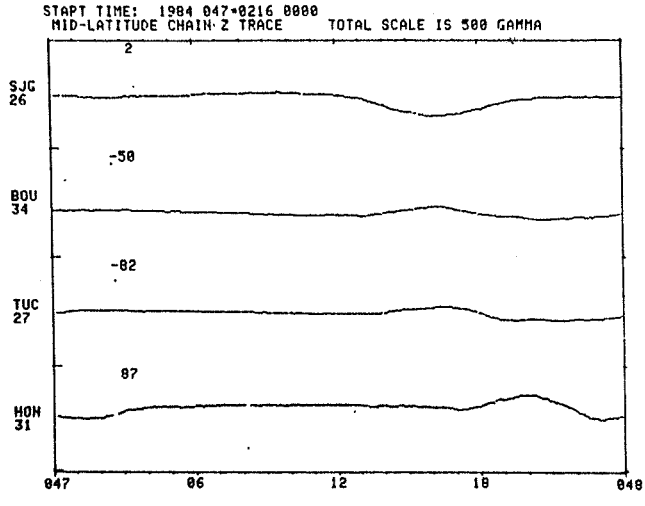


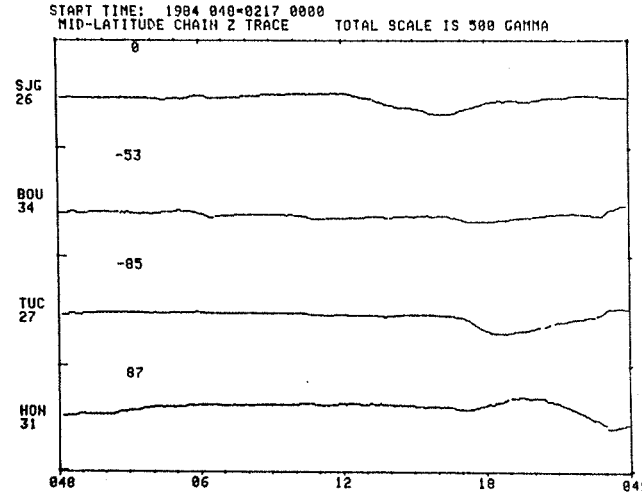

# RGON MAGNETOGRAMS
24 April 1984

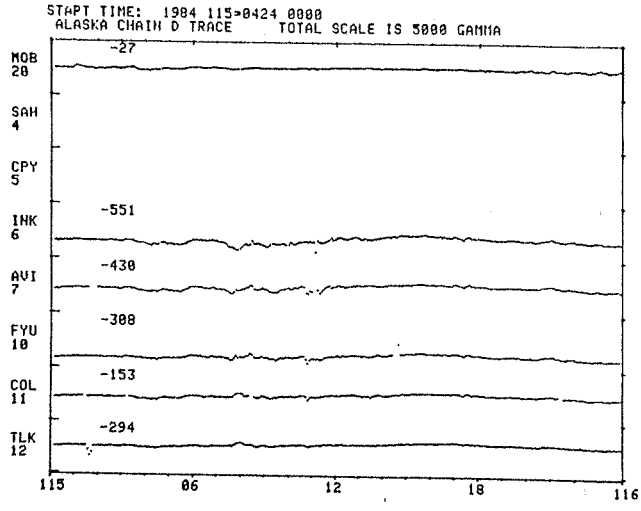


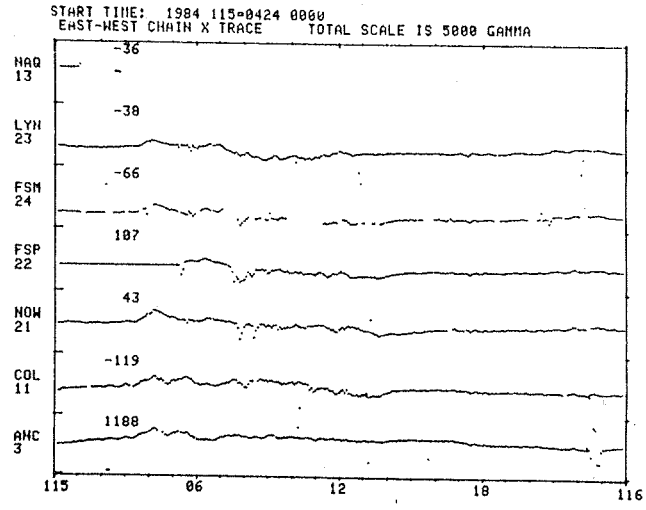


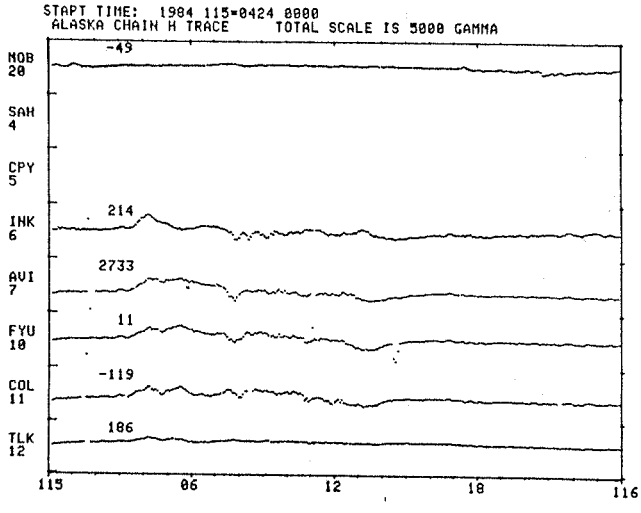


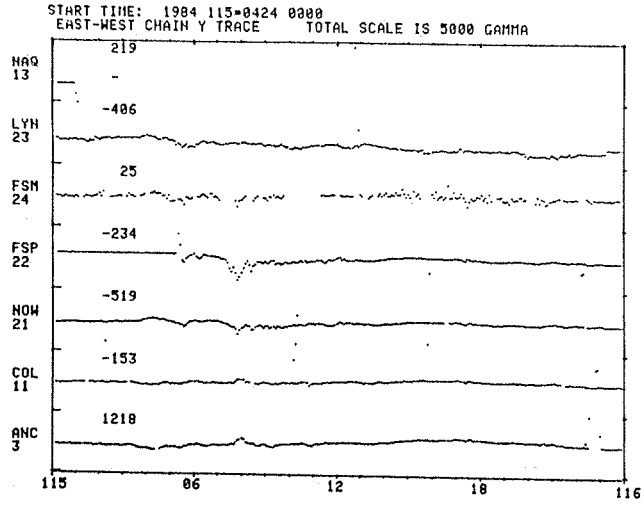


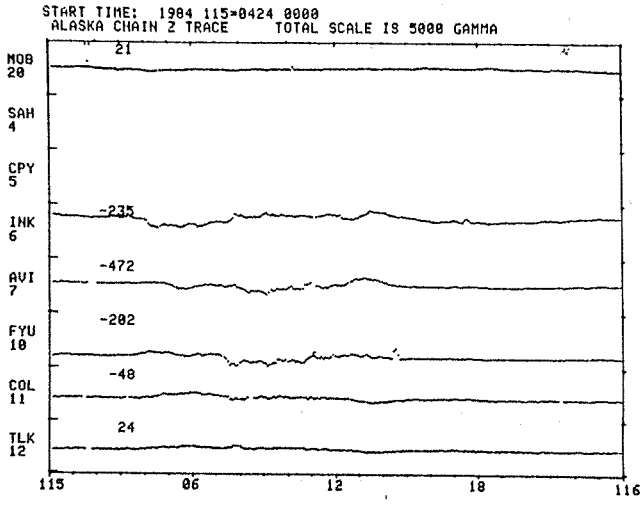


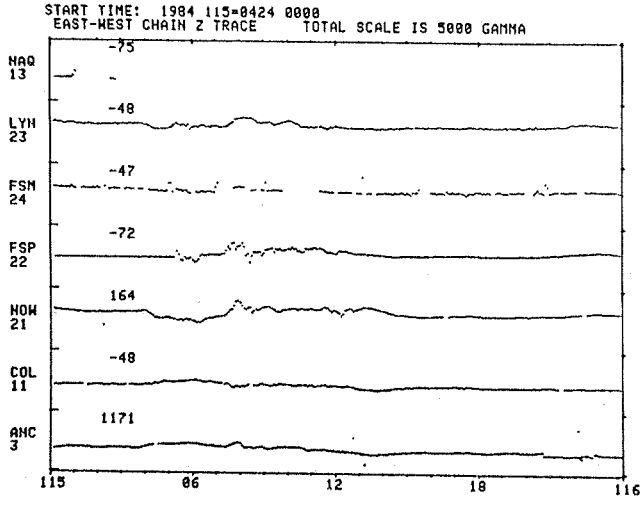

# RGON MAGNETOGRAMS
25 April 1984

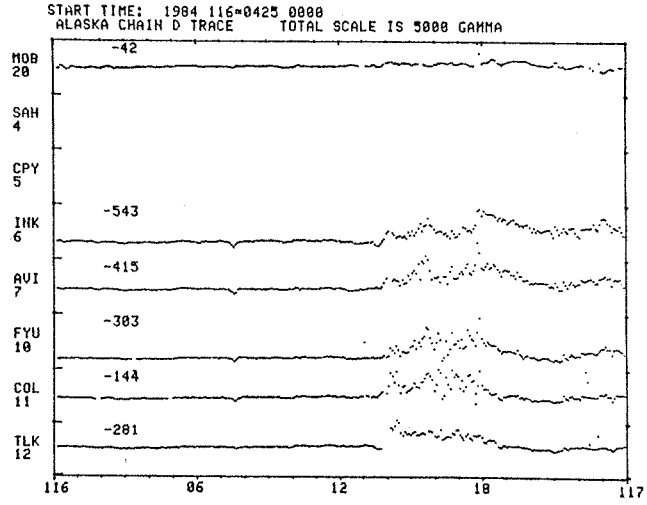


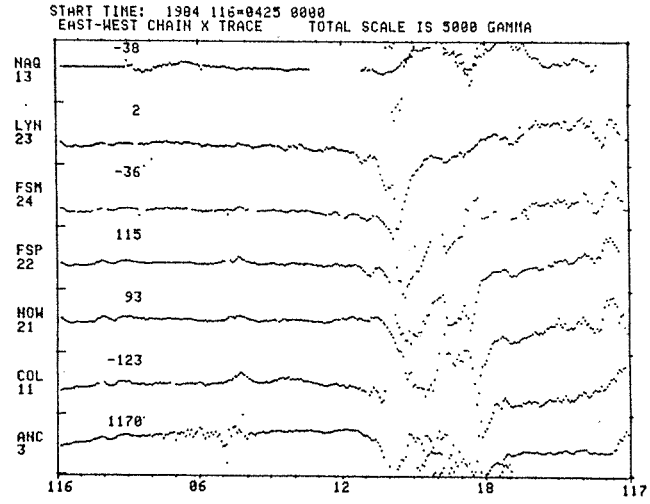


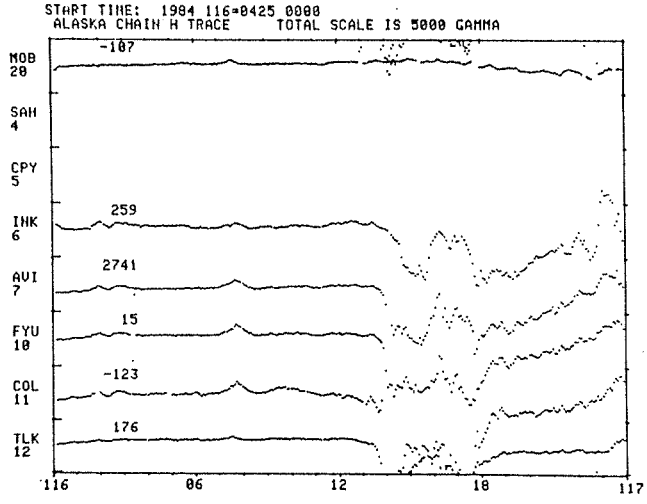


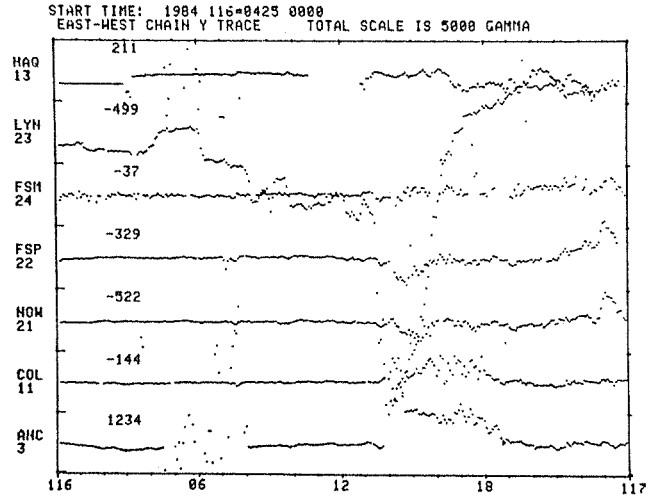


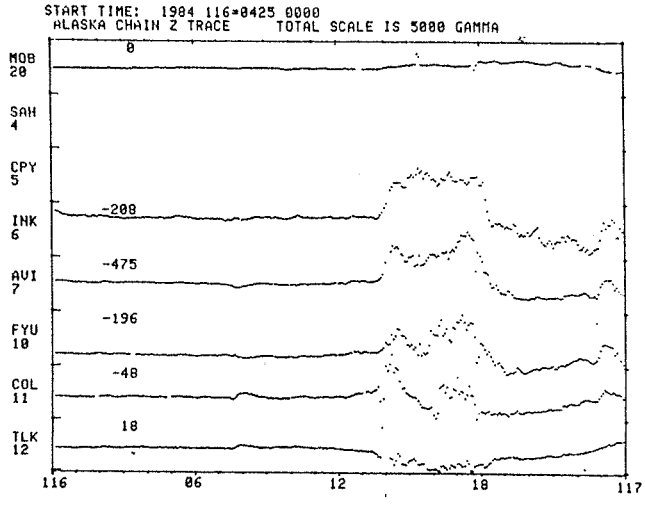


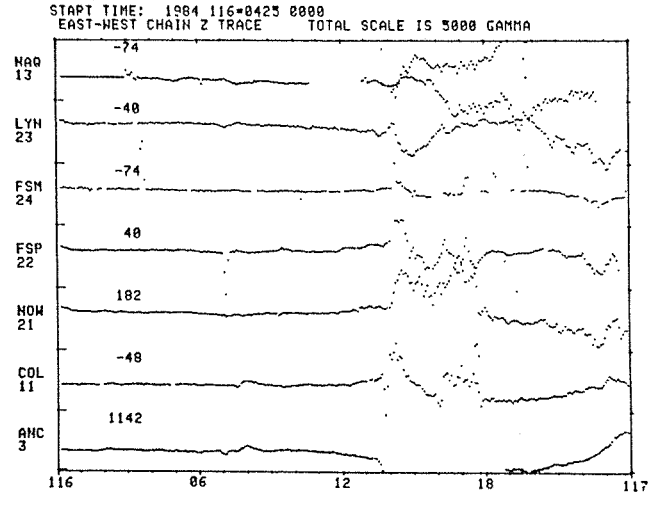

RGON MAGNETOGRAMS
24-25 April 1984

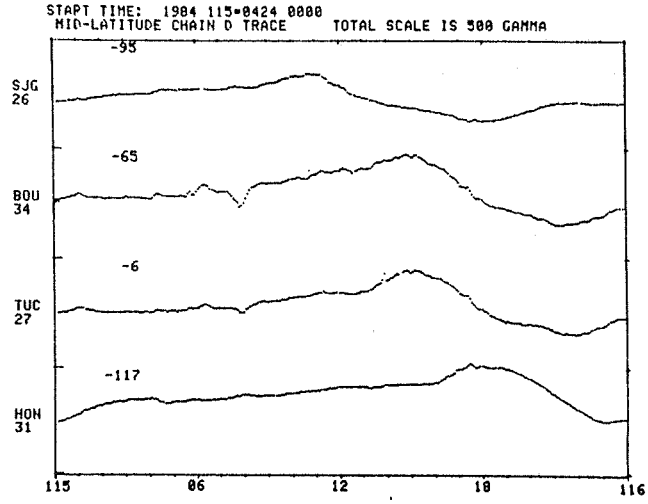


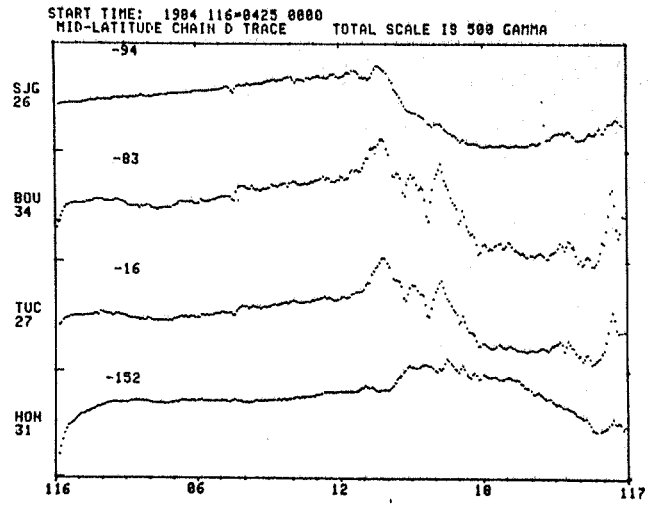


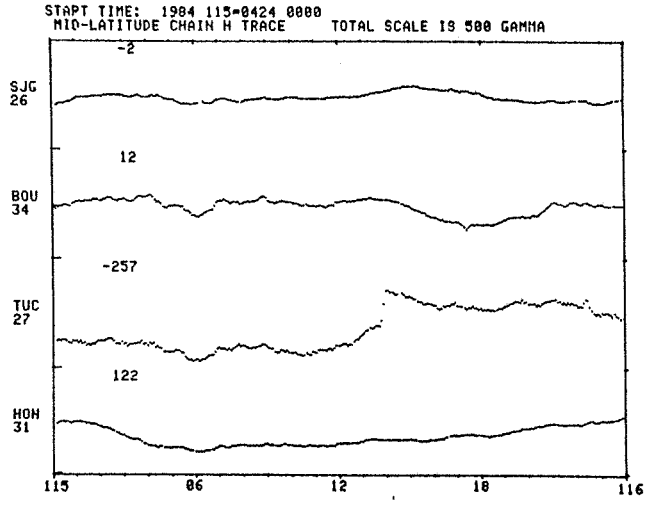


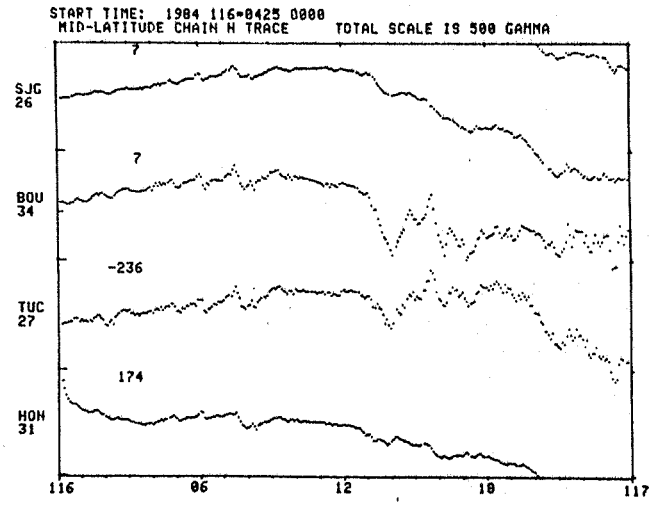


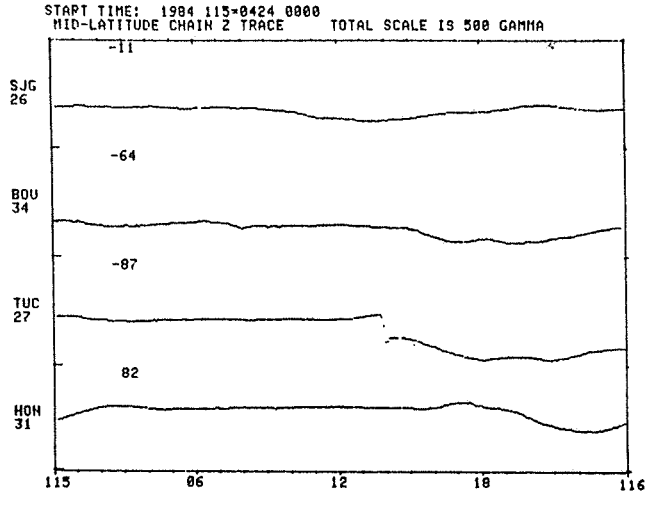


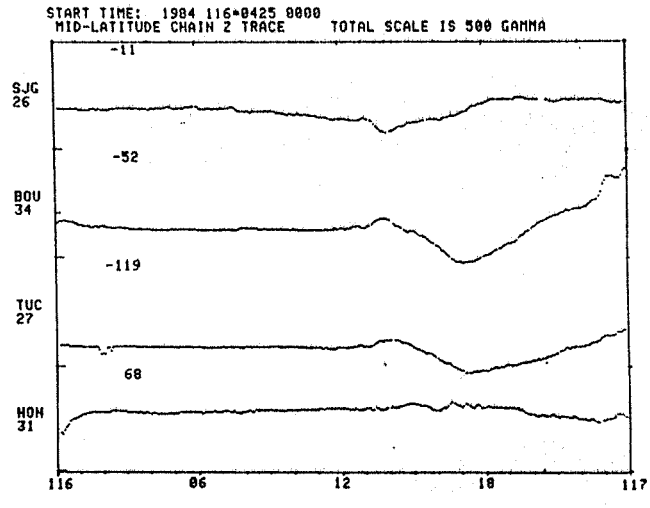

RGON MAGNETOGRAMS
26 April 1984

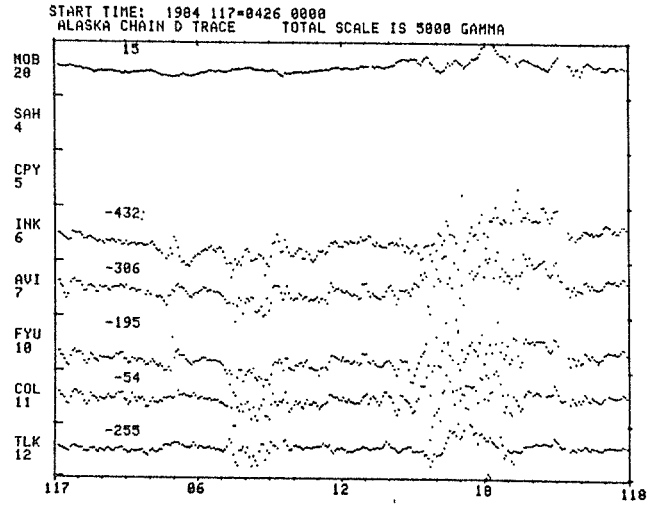


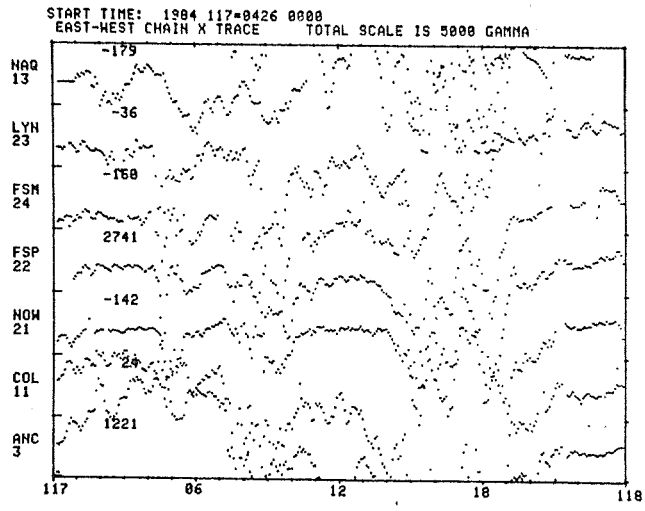


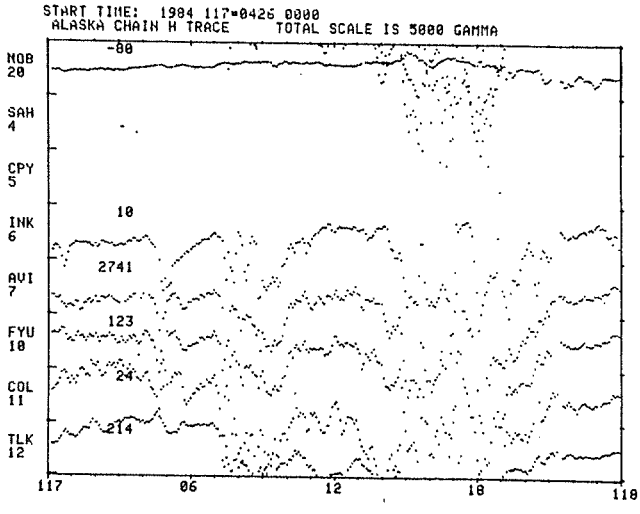


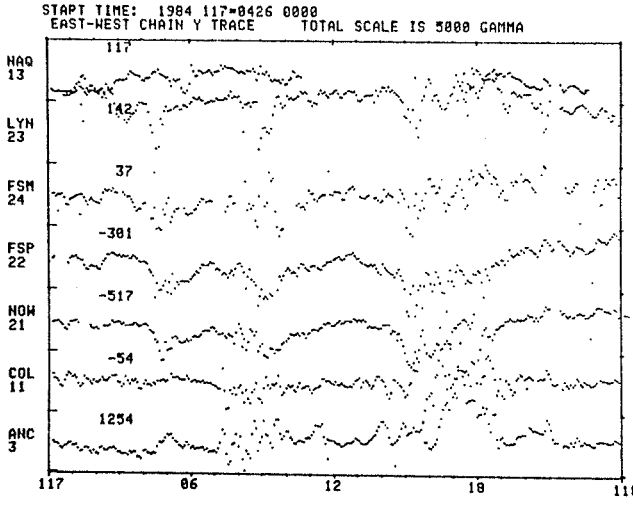


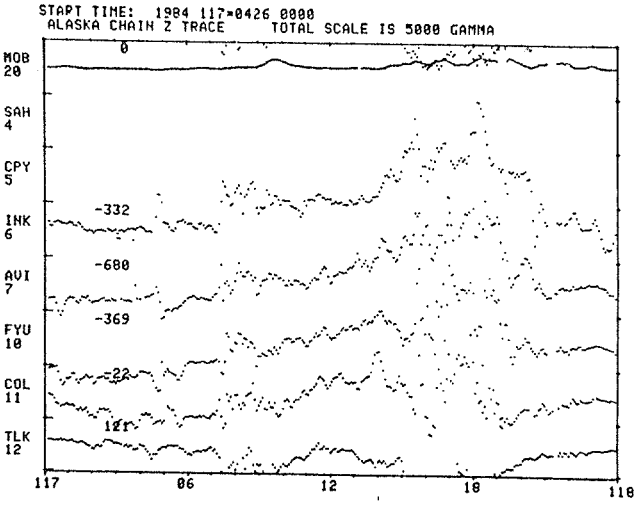


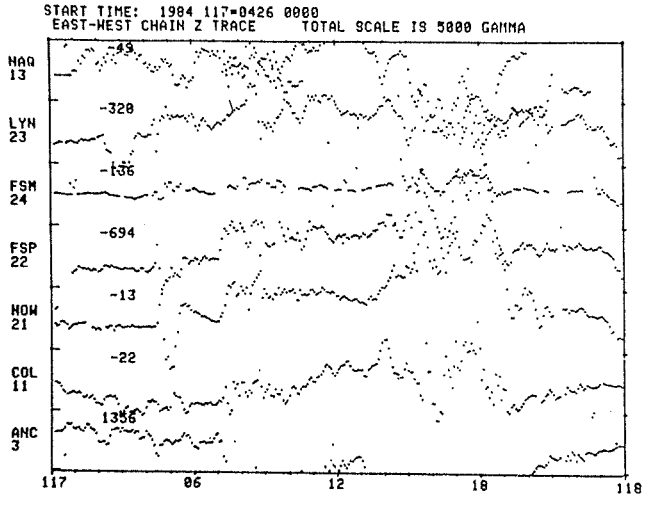

RGON MAGNETOGRAMS
27 April 1984

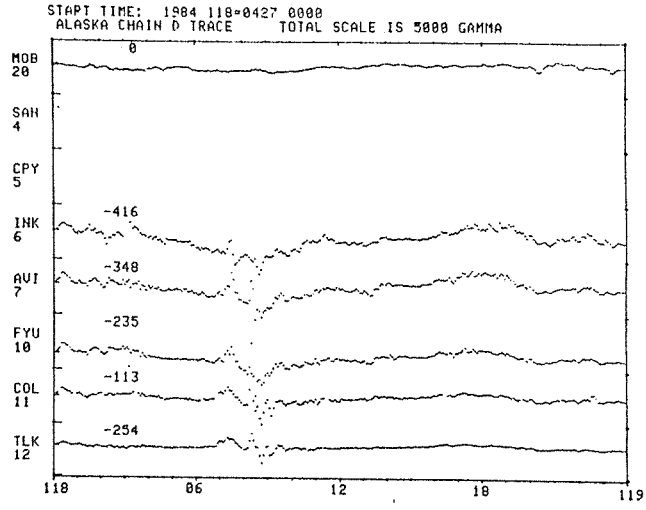


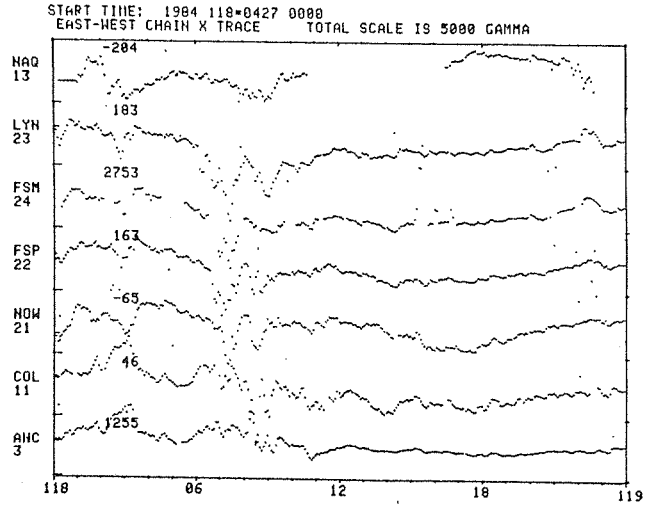


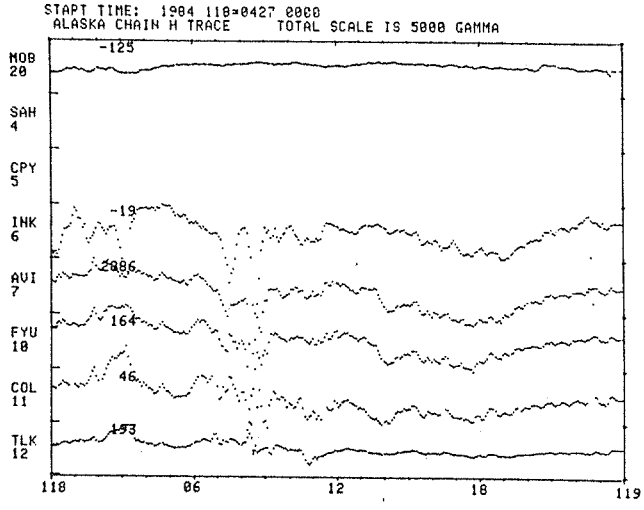


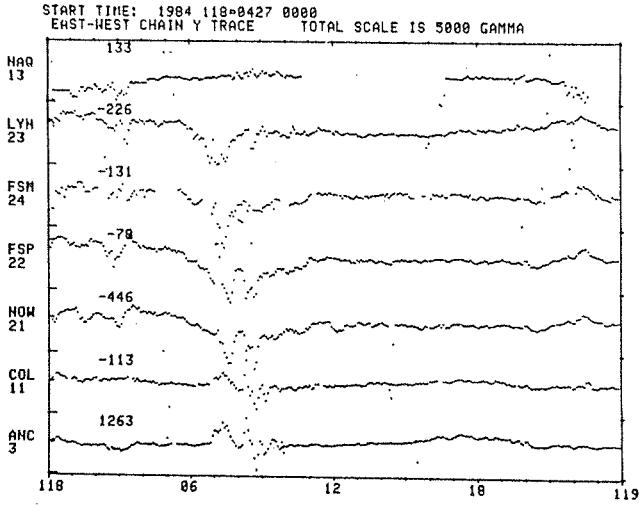


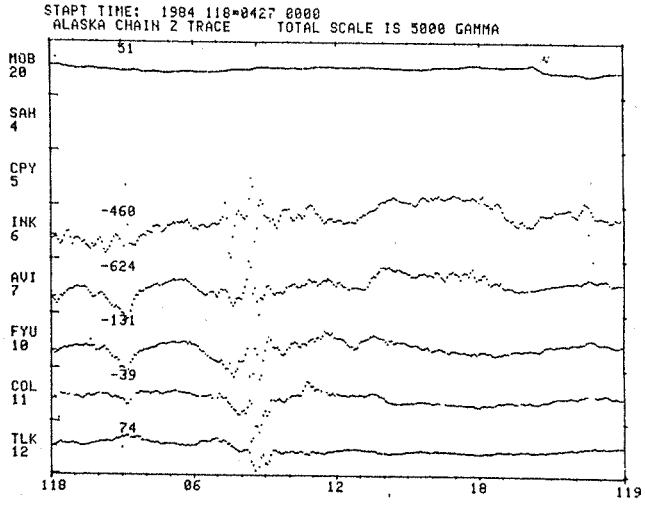


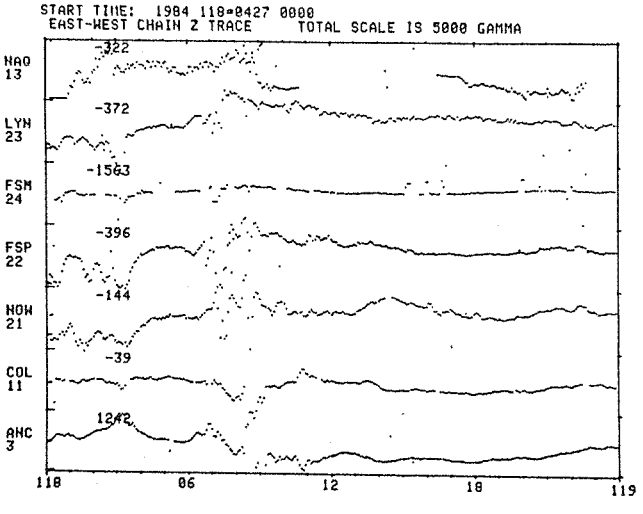

RGON MAGNETOGRAMS
26-27 April 1984

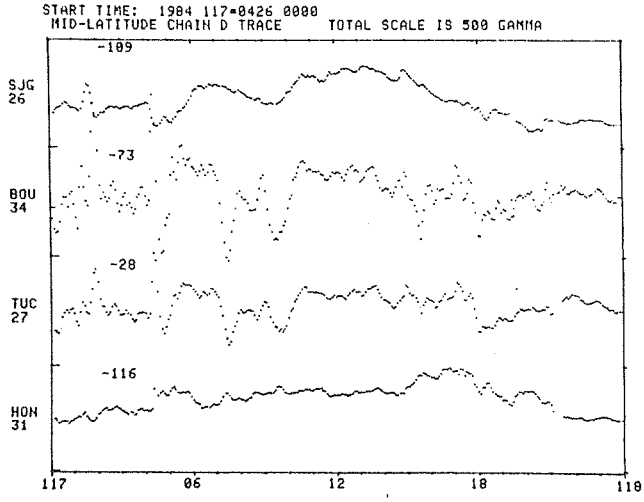


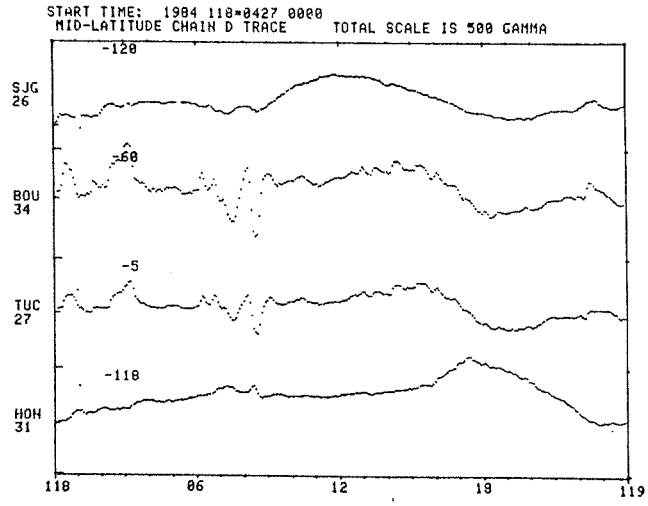


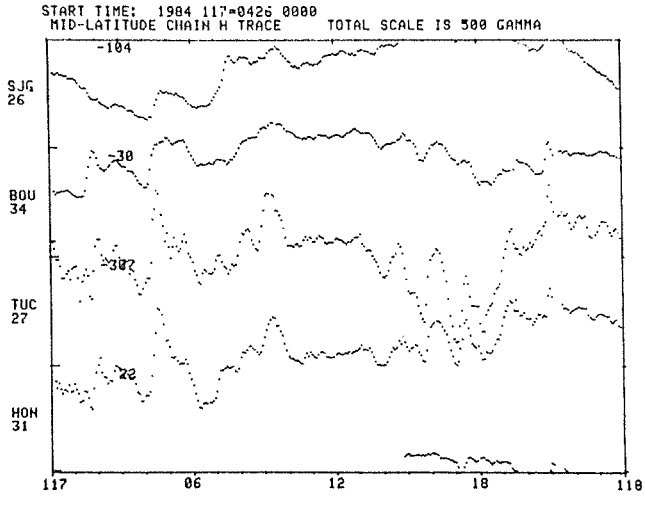


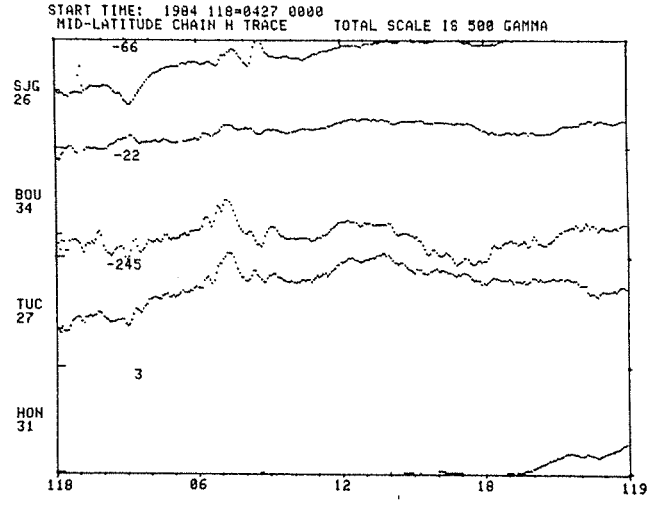


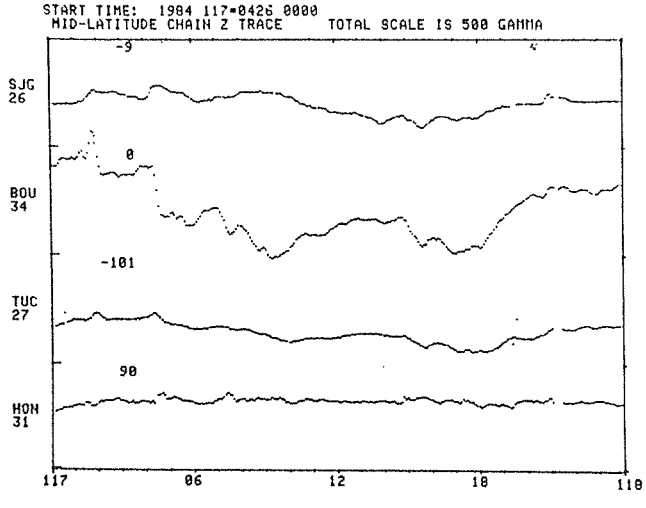


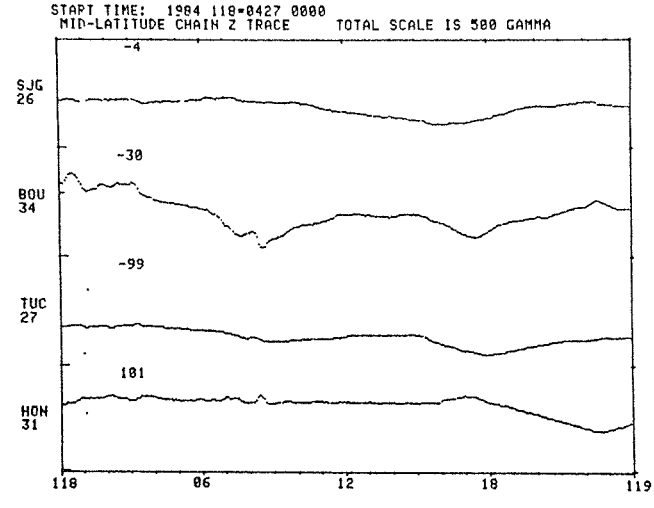

## Observations of the Geomagnetic Field at Kola Peninsula Stations

by

G.A. Loginov
Polar Geophysical Institute
Academy of Sciences of USSR
Murmansk, USSR

Figures 1 and 2 show normal-run H component magnetic records obtained from stations of the Kola Peninsula for the two intervals 12-21 February 1984 and 20 April - 4 May 1984 respectively.

Locations of the stations are given in Table 1.

TABLE 1.

| Station | Code | Geographic Latitude | Geographic Longitude |
|---|---|---|---|
| Rybachy | Rb | N70.0 | E32.0 |
| D. Zelentsy | DZ | 69.2 | 35.9 |
| Loparskaya | Lp | 68.6 | 33.3 |
| Lovozero | Lv | 68.0 | 35.1 |
| Krasnoshel'e | Ks | 67.4 | 36.9 |
| Boyarskaya | Br | 65.8 | 33.8 |

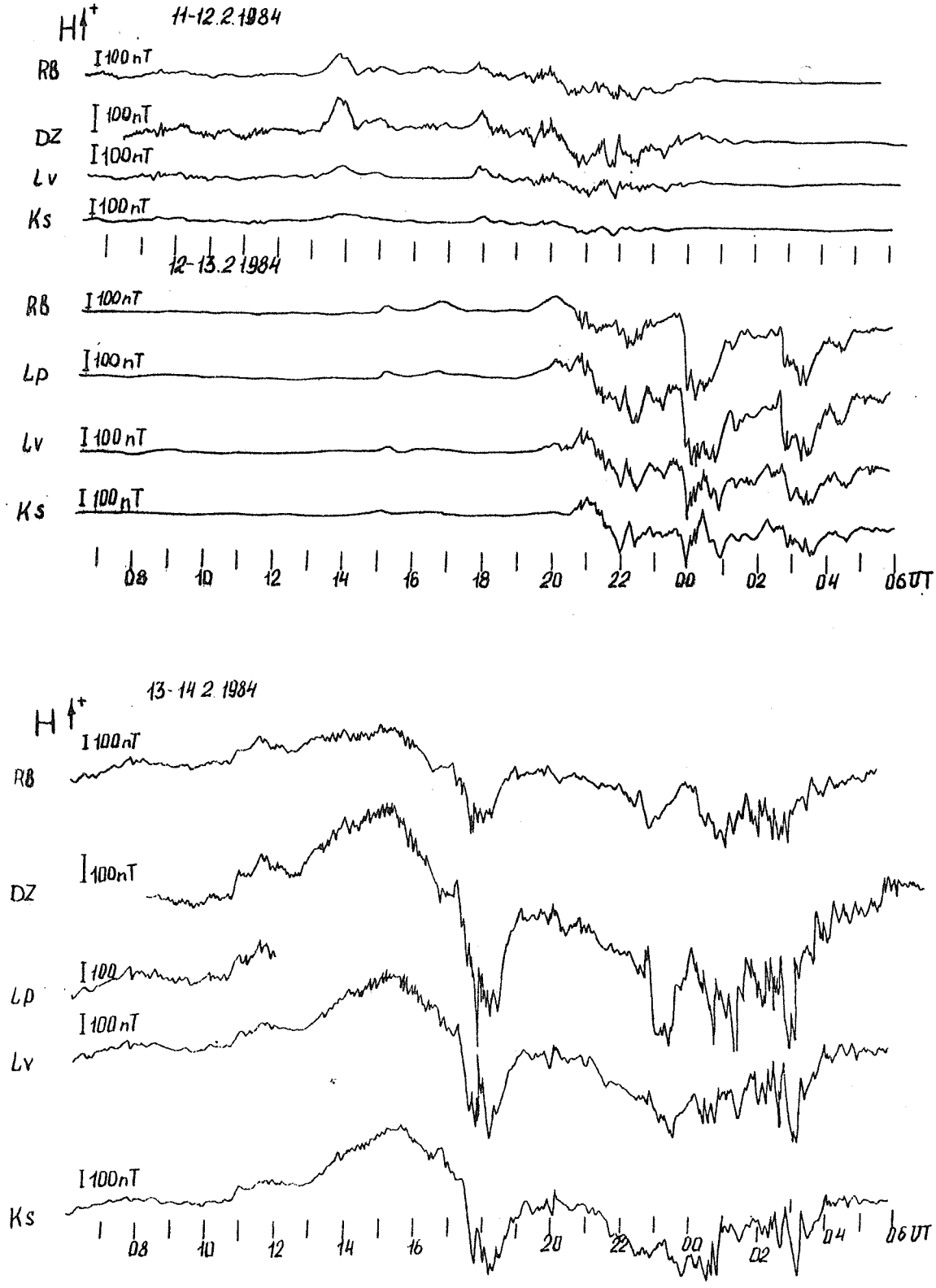


Fig. 1. Normal run H-component magnetograms obtained from the stations of the Kola Peninsula for the interval 12-21 February 1984.

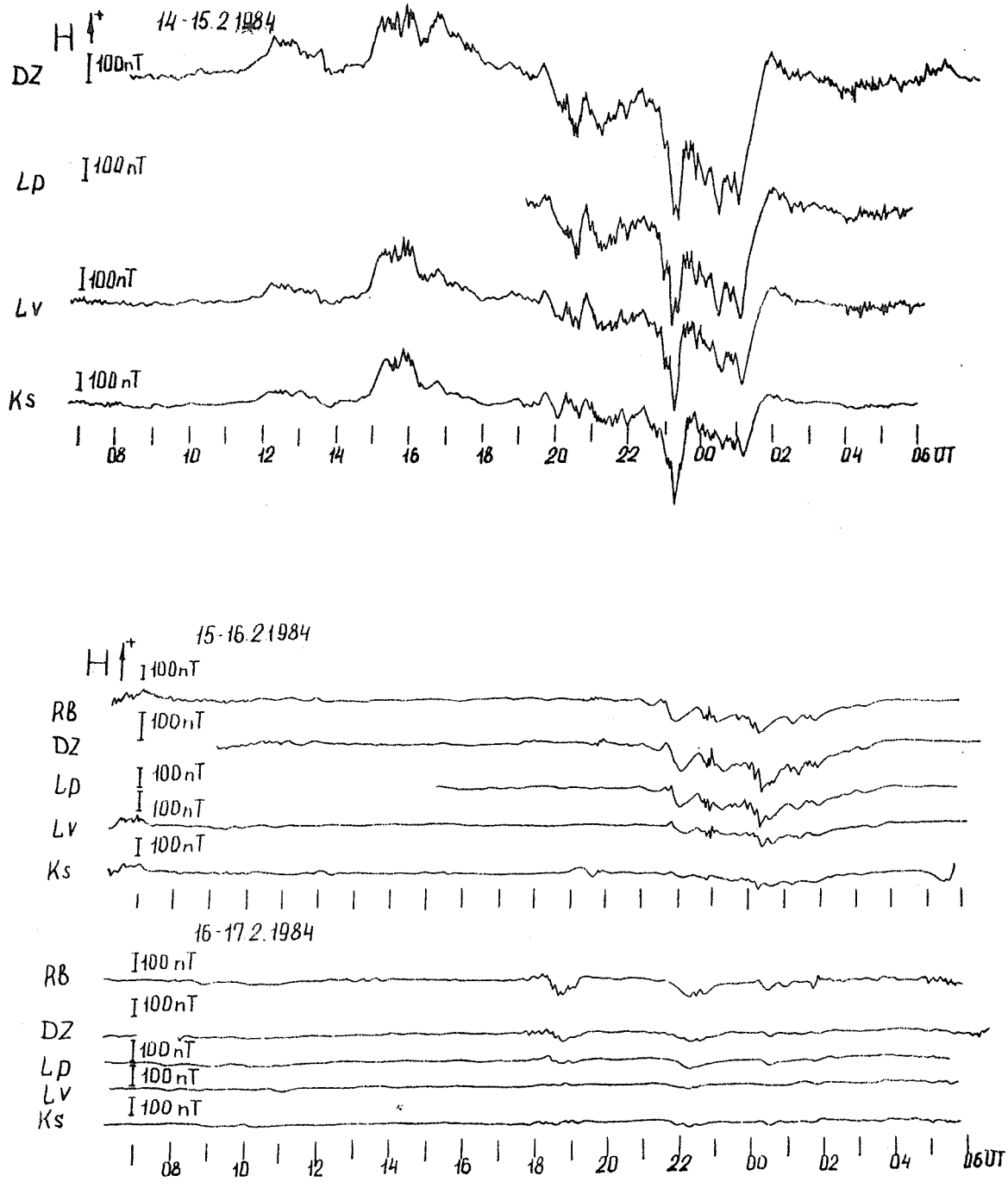


Fig. 1. continued

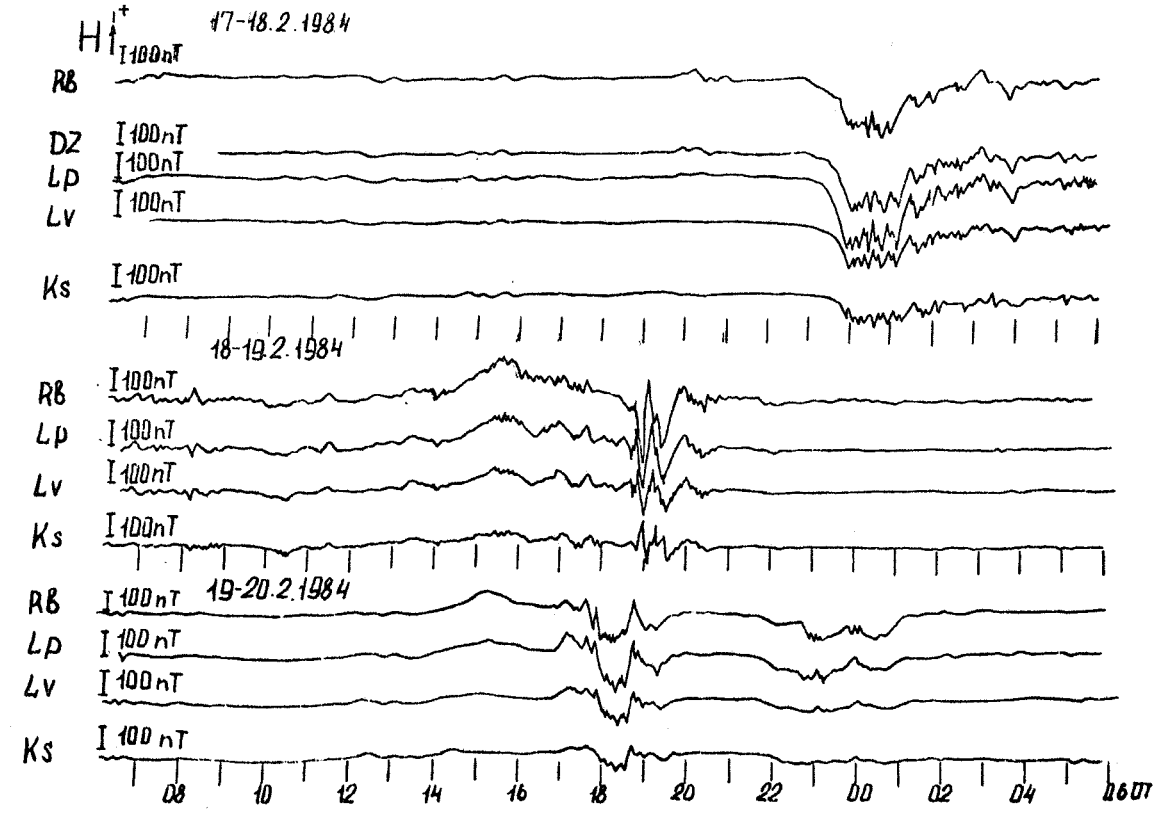


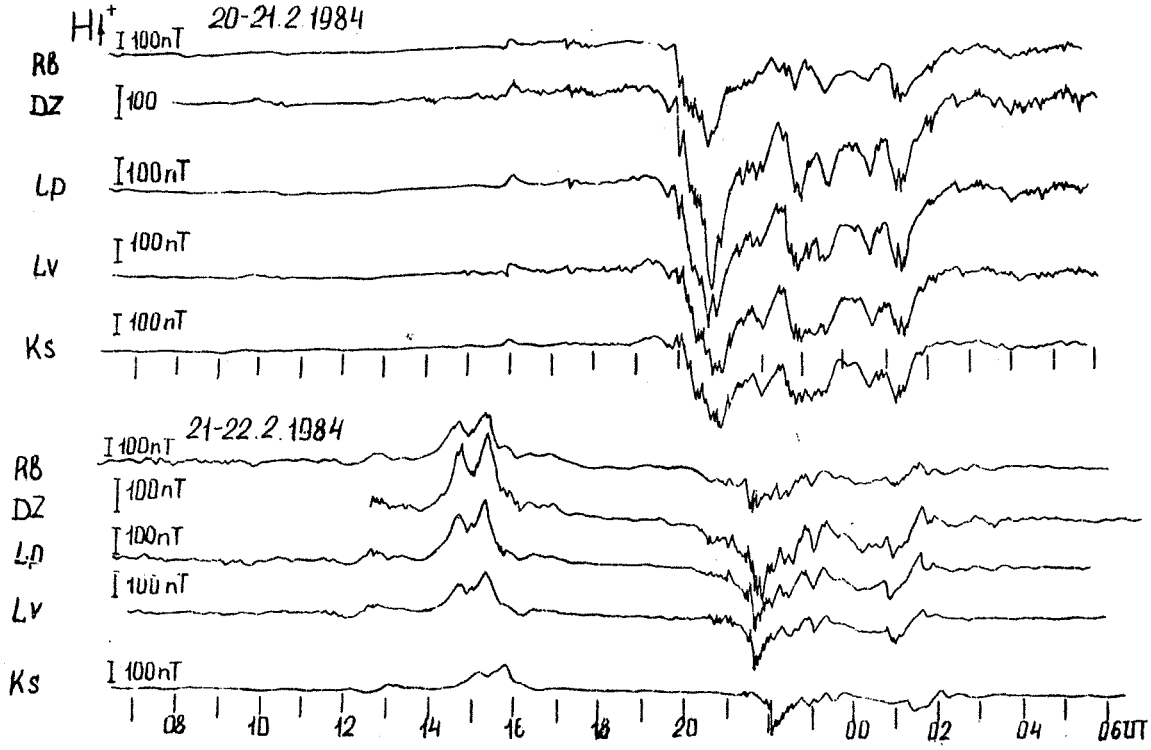


Fig. 1. continued

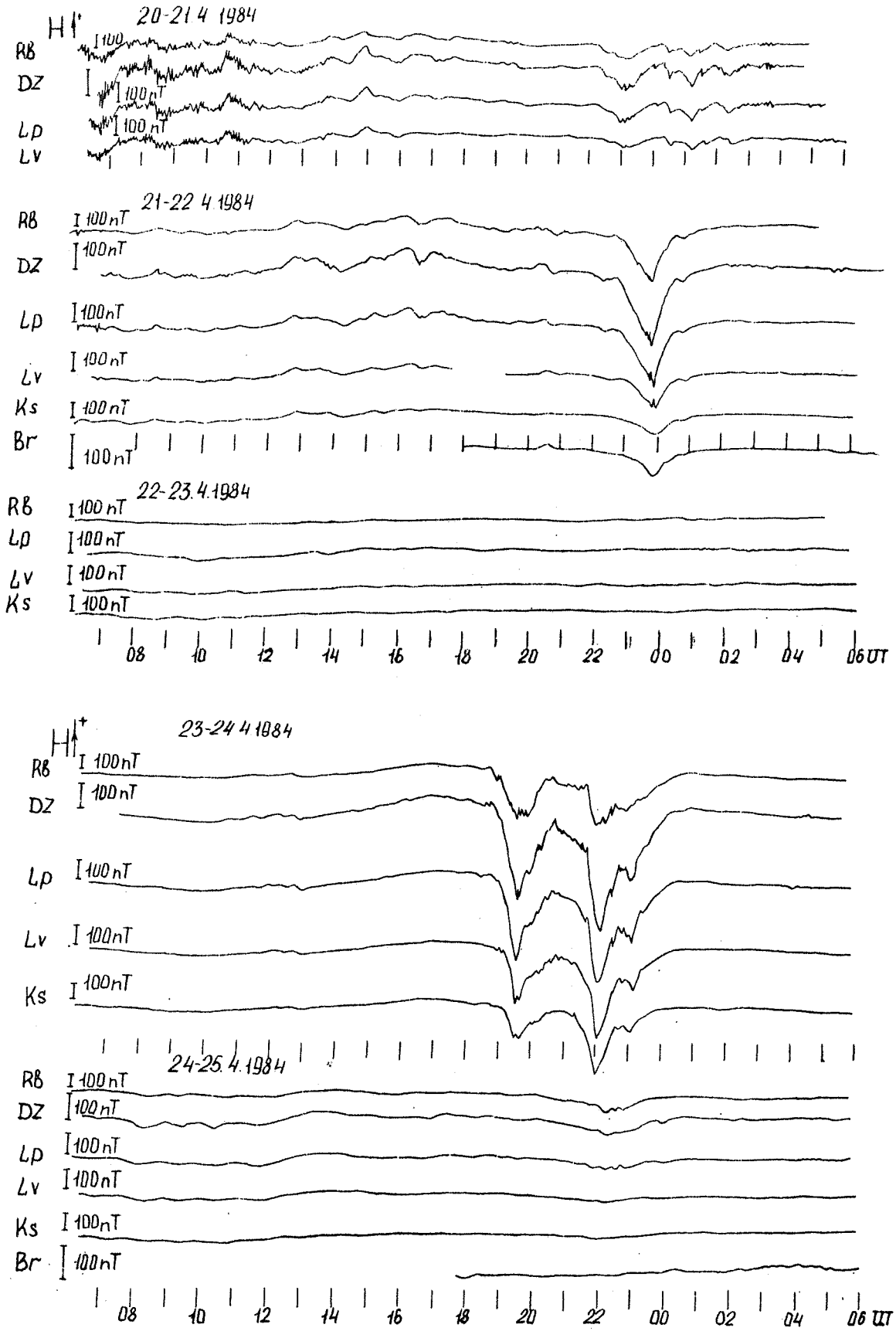


Fig. 2. Normal run H-component magnetograms obtained from the stations of the Kola Peninsula for the interval 20 April - 4 May 1984.

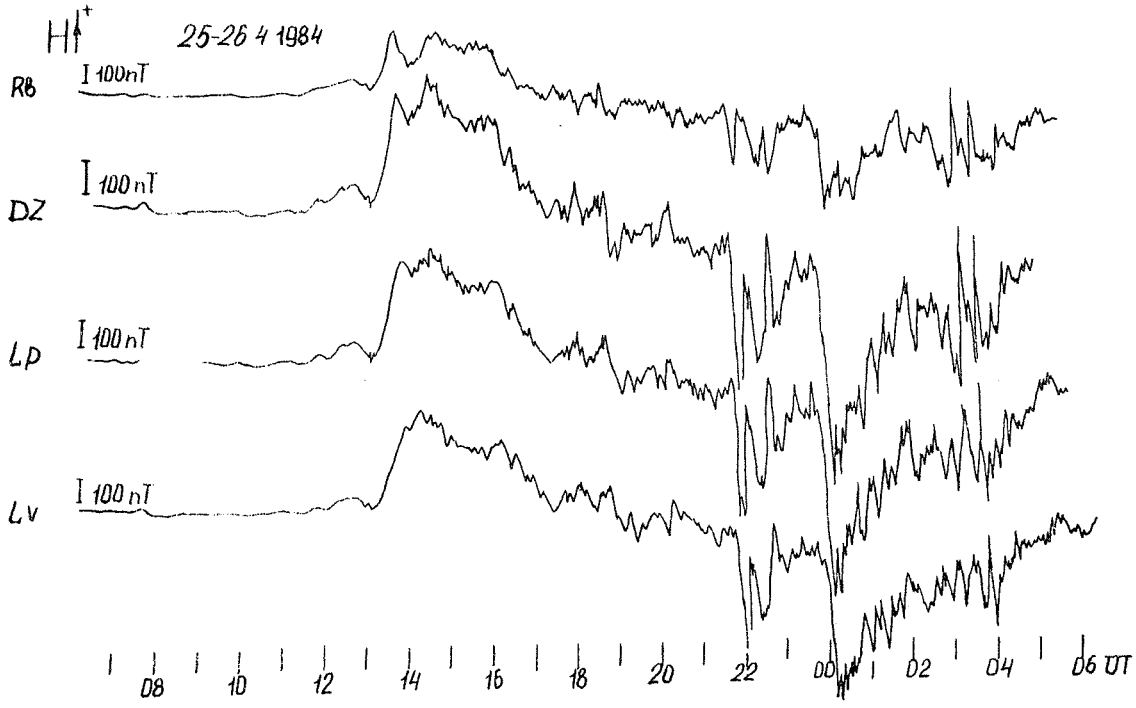


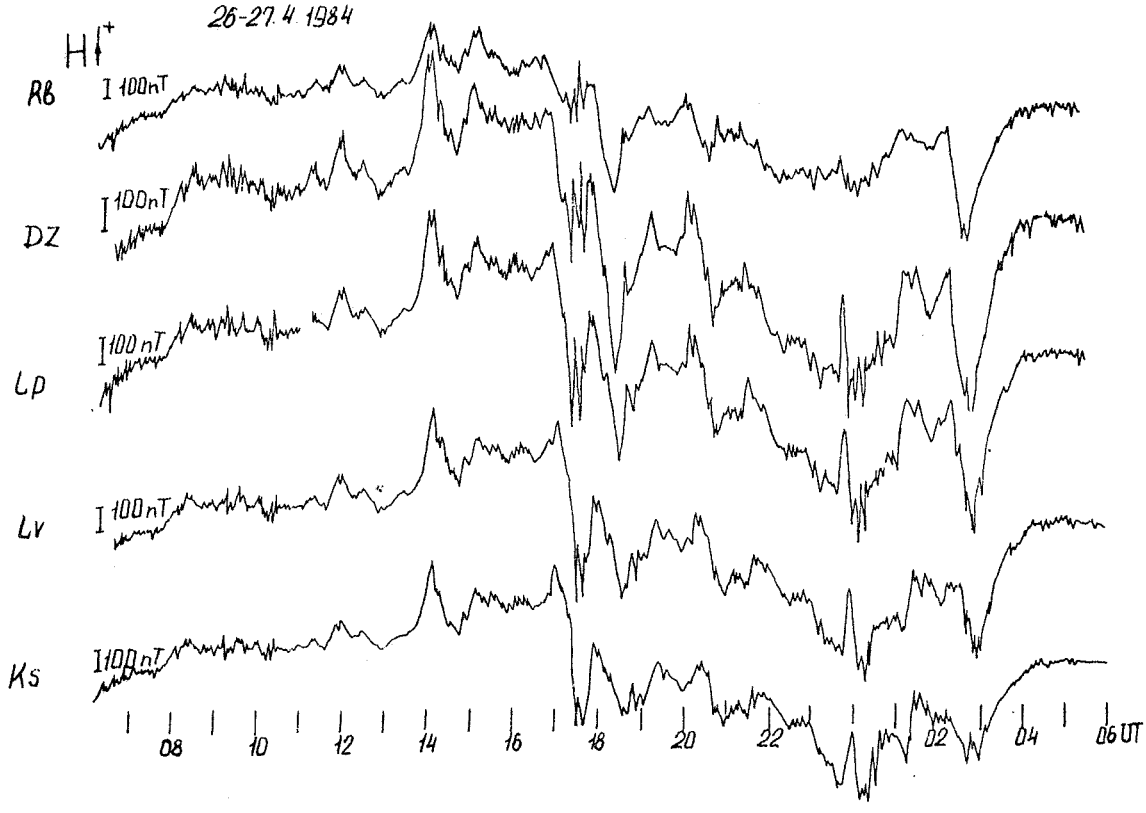


Fig. 2. continued

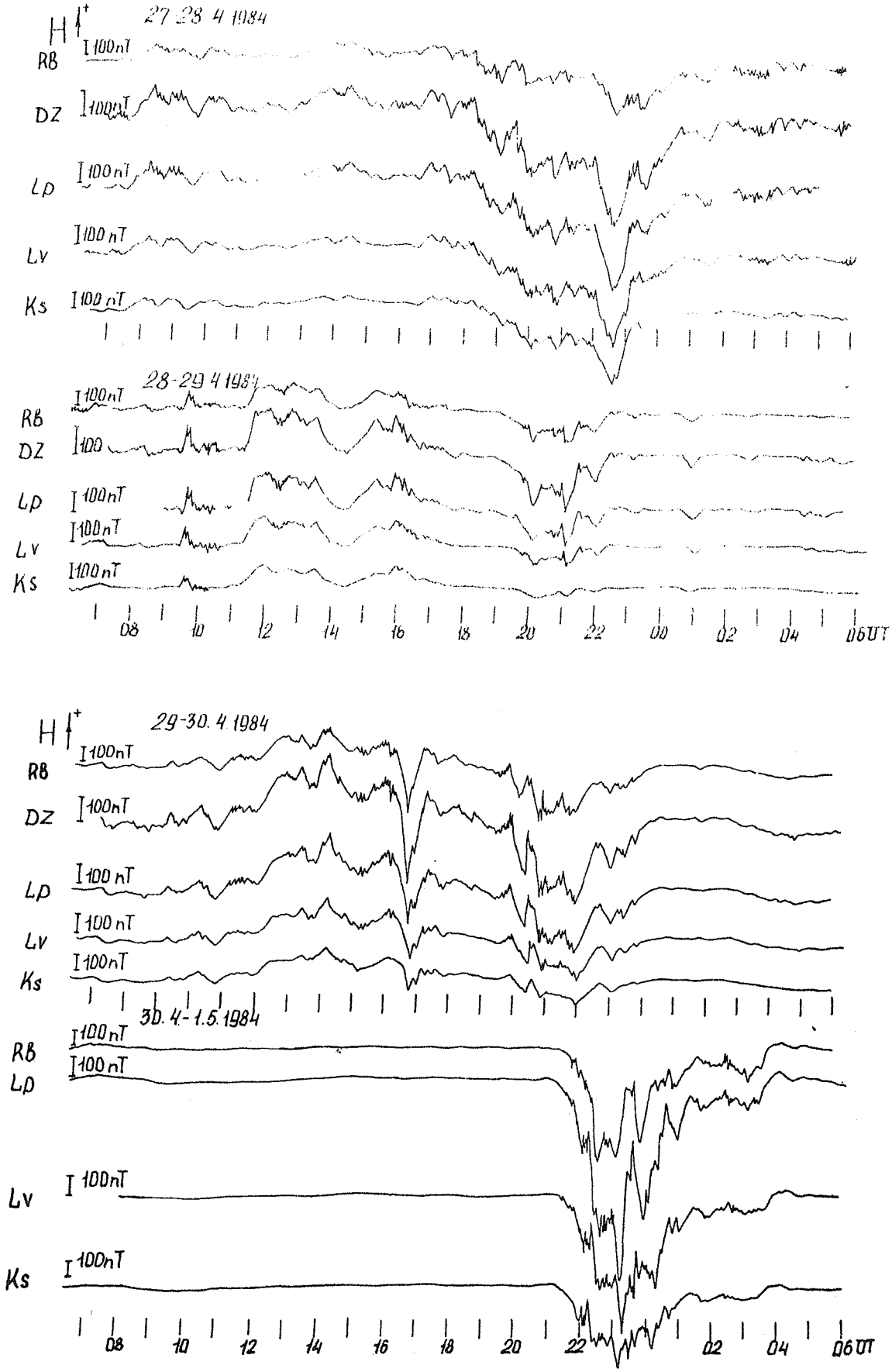


Fig. 2. continued

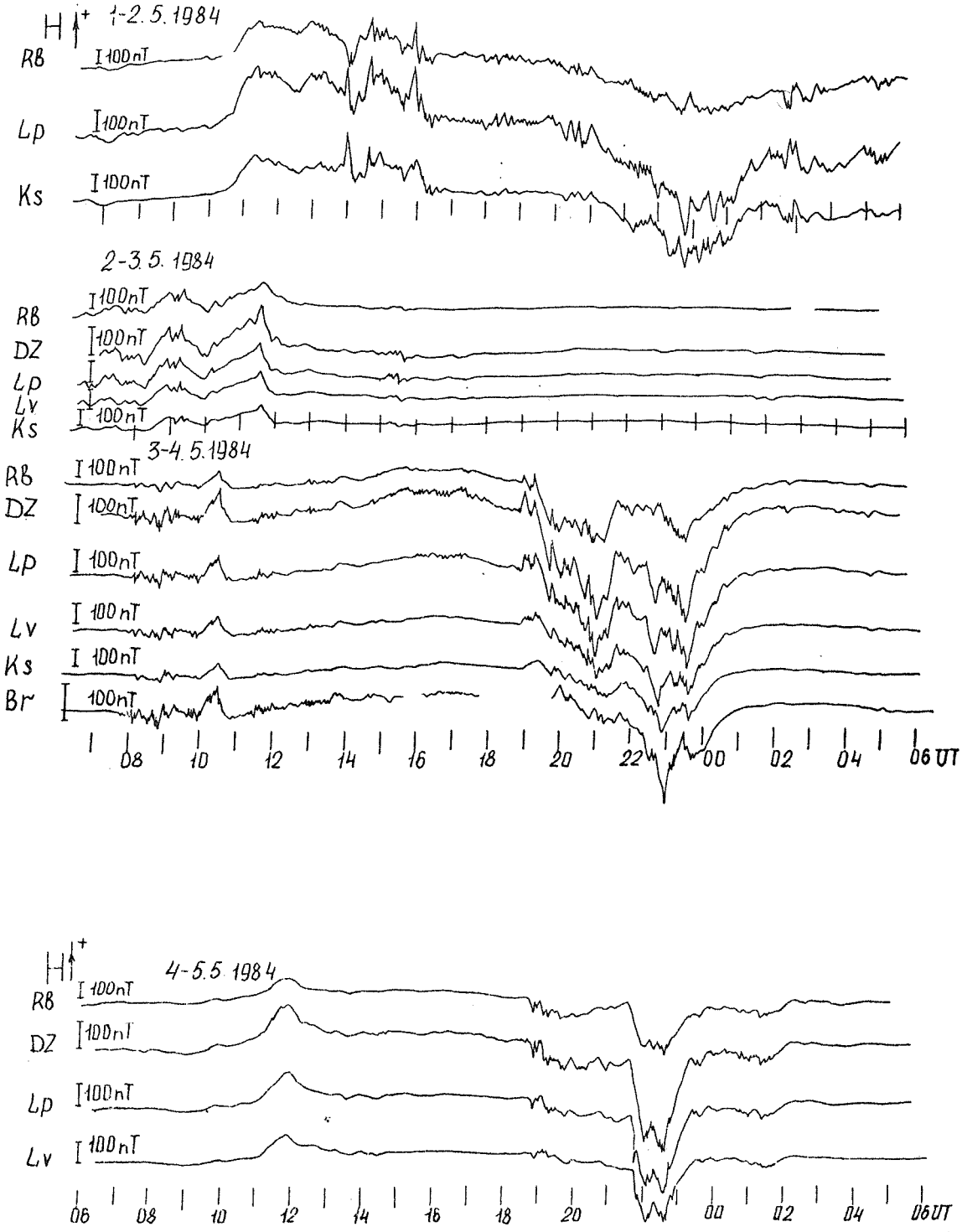


Fig. 2. continued

# Magnetic Field and Cosmic Rays Data During 12-21 February and 20 April - 4 May 1984 at Sverdlovsk (Arty) Station

by

V.A. Belyaev, L.N. Ivanova, V.A. Shapiro and B.L. Shirman
Sverdlovsk, USSR

The results obtained at Sverdlovsk (Arty) station (N56°26' E58°34') are presented. The cut-off rigidity of the cosmic rays station is 2.3 GeV.

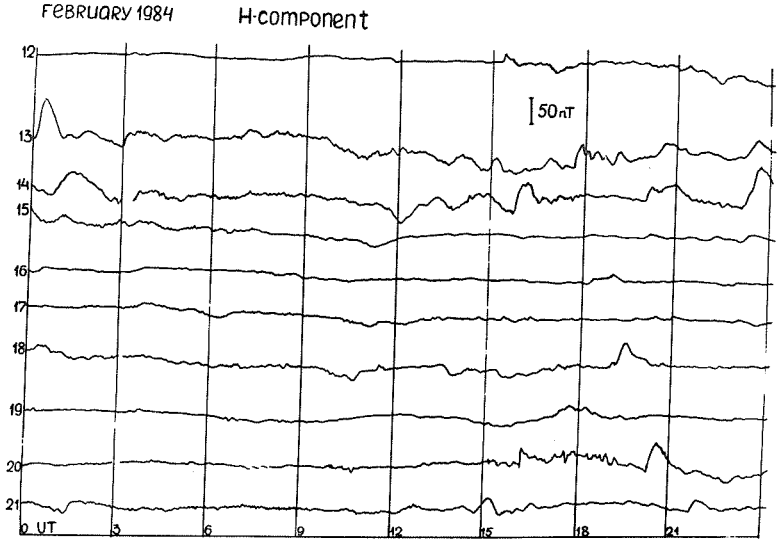


Fig. 1. The geomagnetic records of the H component at Arty during the period 12-21 February 1984.

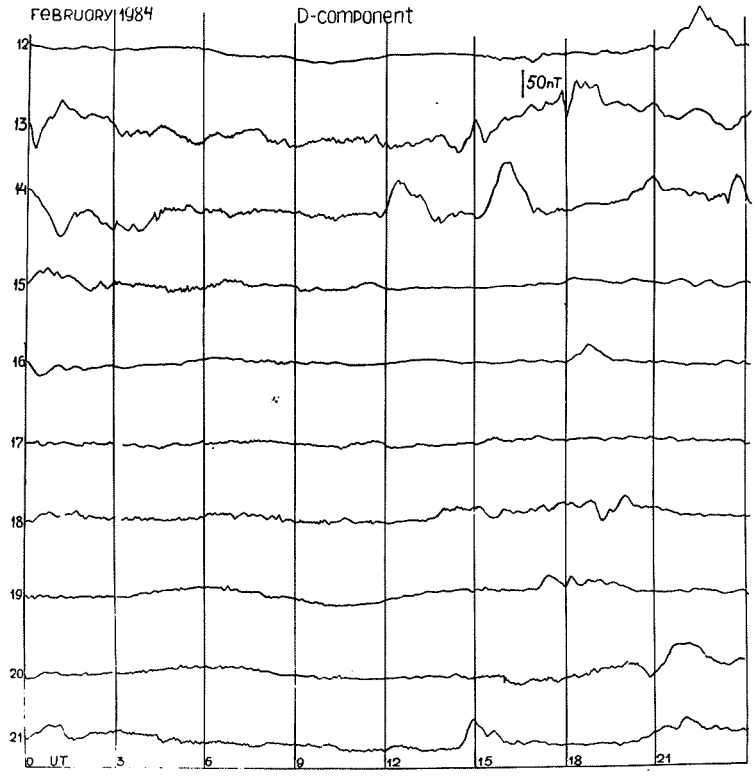


Fig. 2. The geomagnetic records of the D component at Arty during the period 12-21 February 1984.

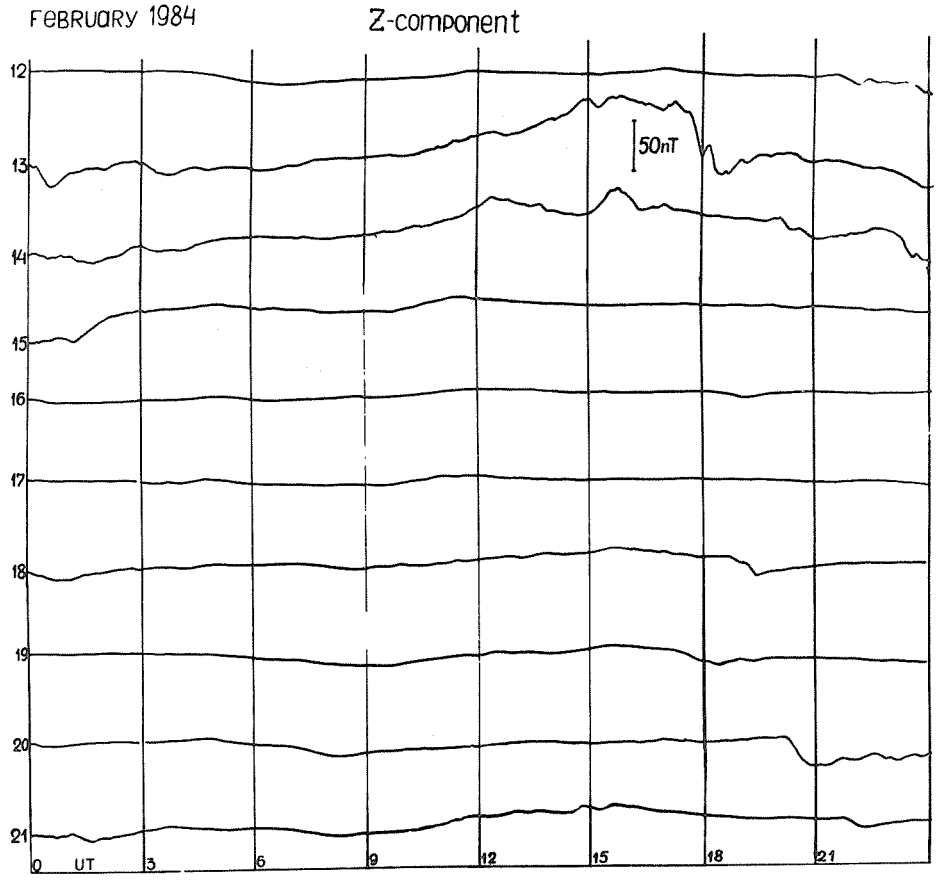


Fig. 3. The geomagnetic records of the Z component at Arty during the period 12-21 February 1984.

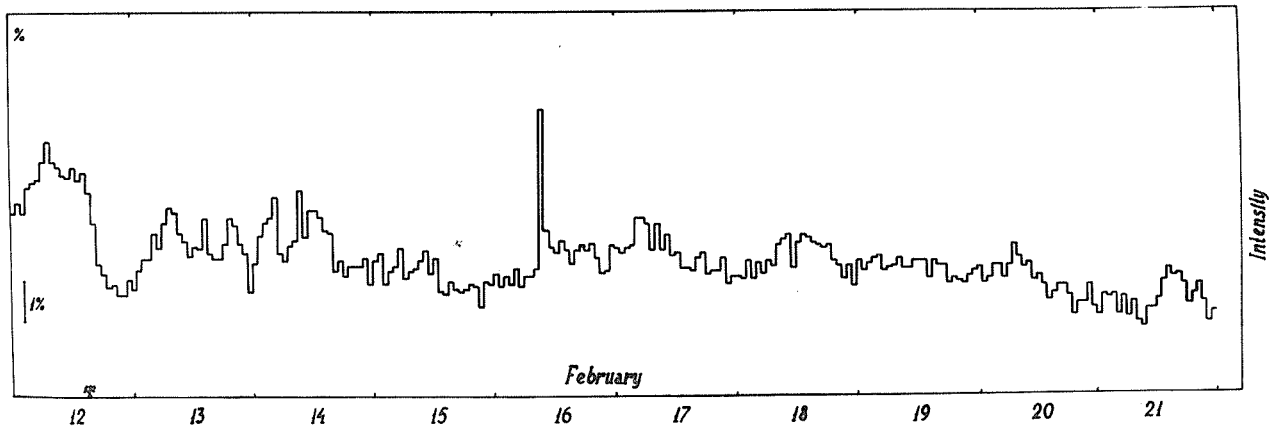


Fig 4. Hourly values of the neutron intensity observed during the period 12-21 February 1984. There is a 3.9 percent increase of cosmic rays intensity observed at 0900 UT.

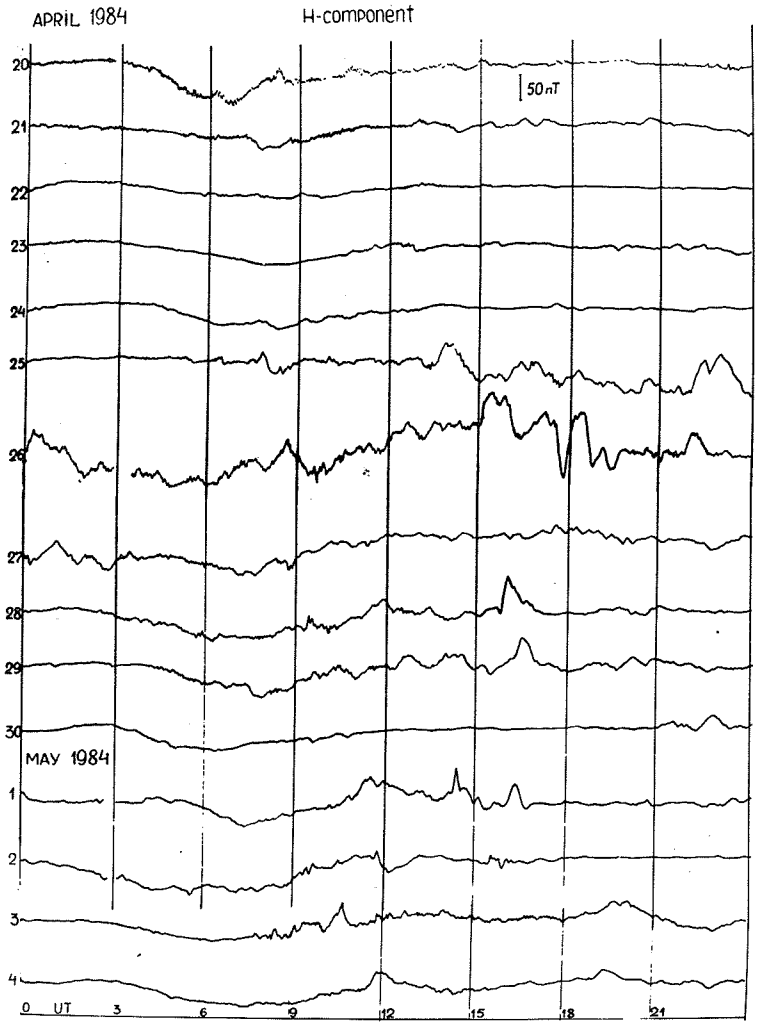


Fig. 5. The geomagnetic records of the H component at Arty during the period 20 April - 4 May 1984.

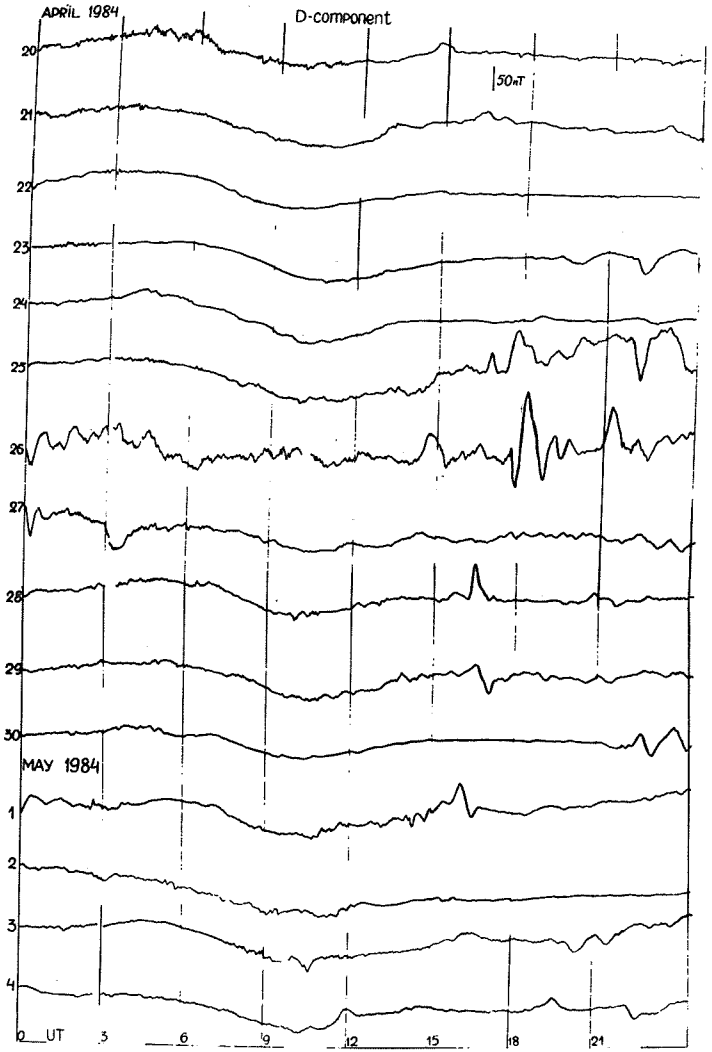


Fig. 6. The geomagnetic records of the D component at Arty during the period 20 April - 4 May 1984.

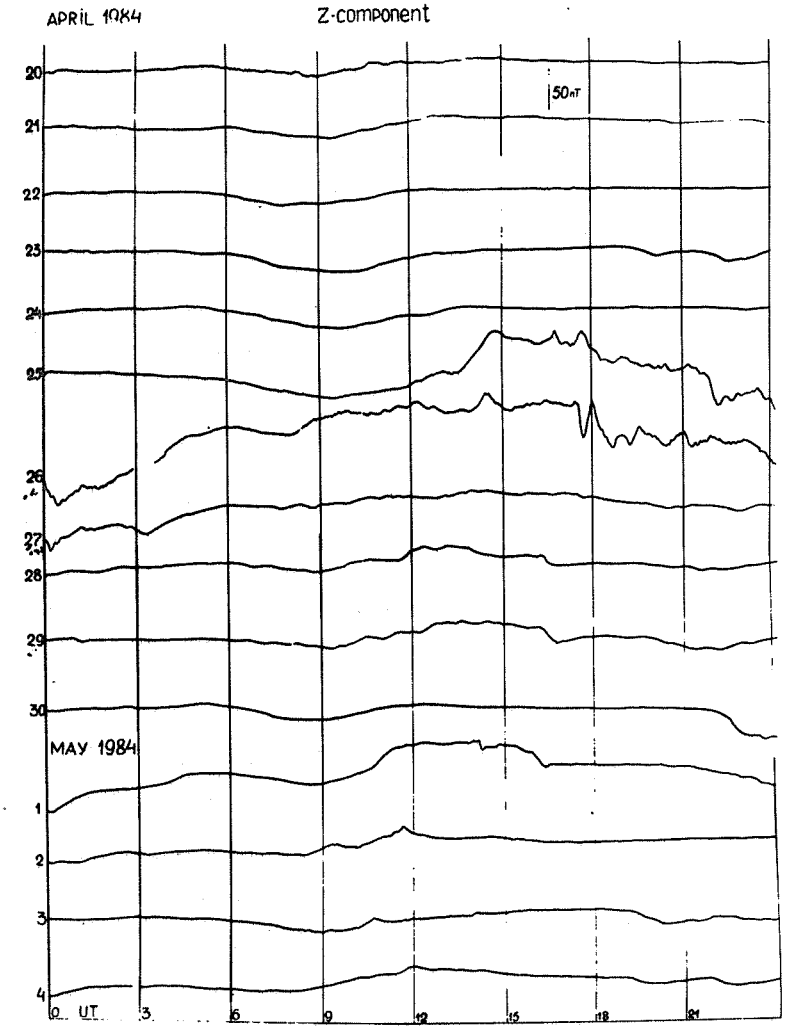


Fig. 7. The geomagnetic records of the Z component at Arty during the period 20 April - 4 May 1984.

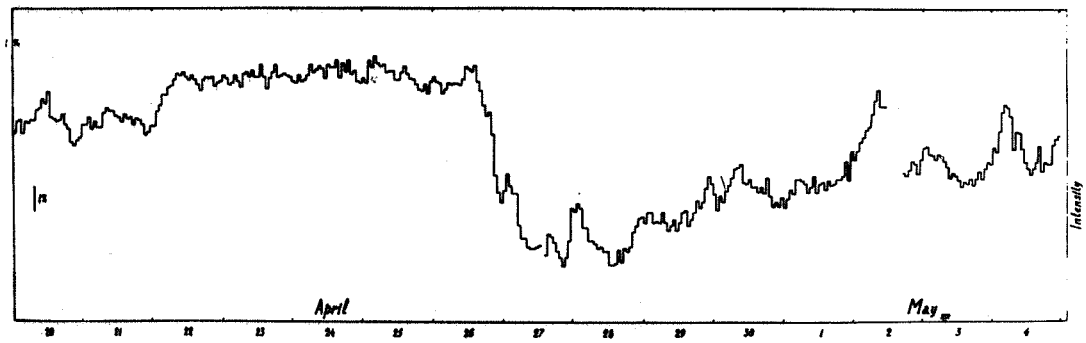


Fig. 8. The cosmic rays data for 20 April - 4 May 1984. A considerable Forbush decrease with an amplitude of 8 percent is seen.

# The Amplitude and Spectral Characteristics of Mid-latitude Geomagnetic Pulsations Pc2-4

by

T.B. Rusakova
Academy of Sciences of the USSR
Borok Observatory
Borok, USSR

This paper presents the power spectra and the average amplitudes of the Pc2-4 pulsations observed at the Geophysical Observatory Borok (N54.0 E113.4), USSR during 12-21 February and 20-27 April 1984 by the two components $H_X$ and $H_Y$. The data cover a period in the almost noon sector of the magnetosphere. The power spectra were deduced for the time interval when the predominant periods of steady magnetic pulsations Pc2-4 were observed. The recorders have a speed of 15 mm/min and sensitivity of $H_X$ = -.16 nT/mm and of $H_Y$ = 0.14 nT/mm.

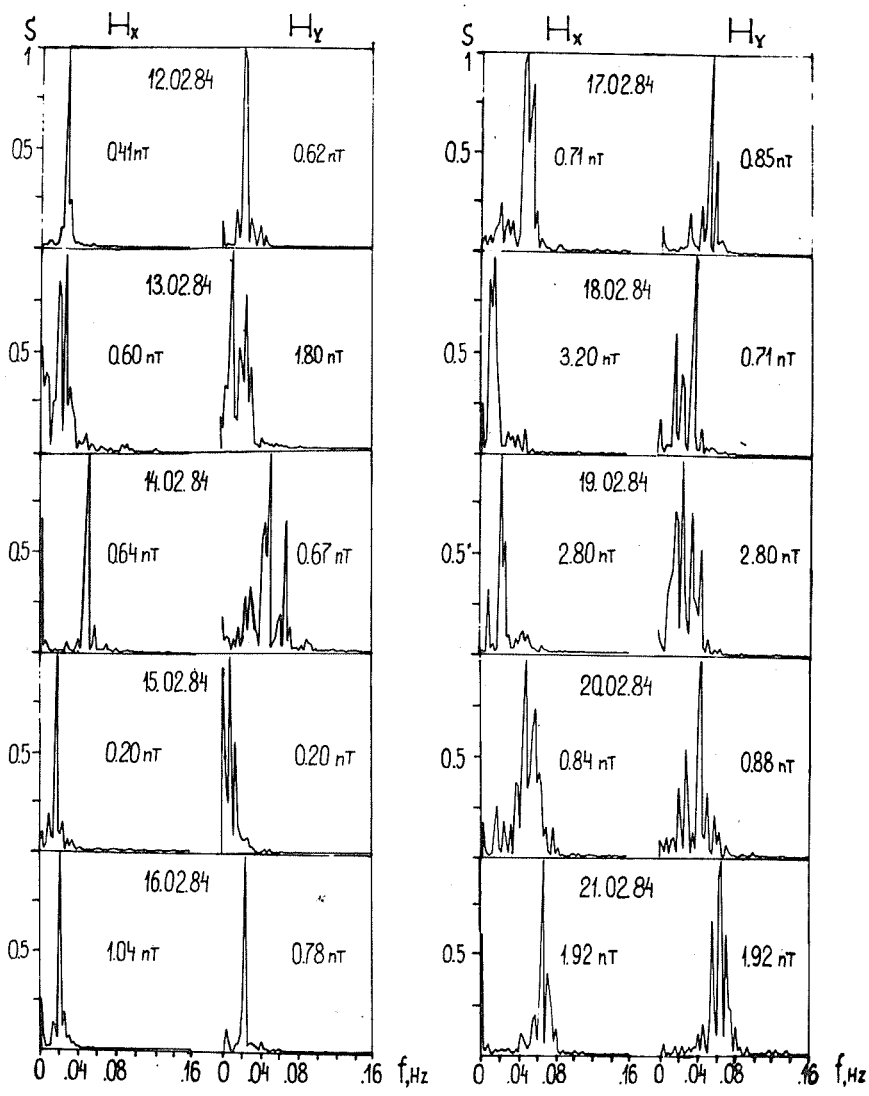


Fig. 1. The power spectra and average amplitudes of Pc2-4 pulsations from Borok are shown for the $H_X$ and $H_Y$ components for the period 12-21 February 1984. F = frequency. S = the normalized spectral density.

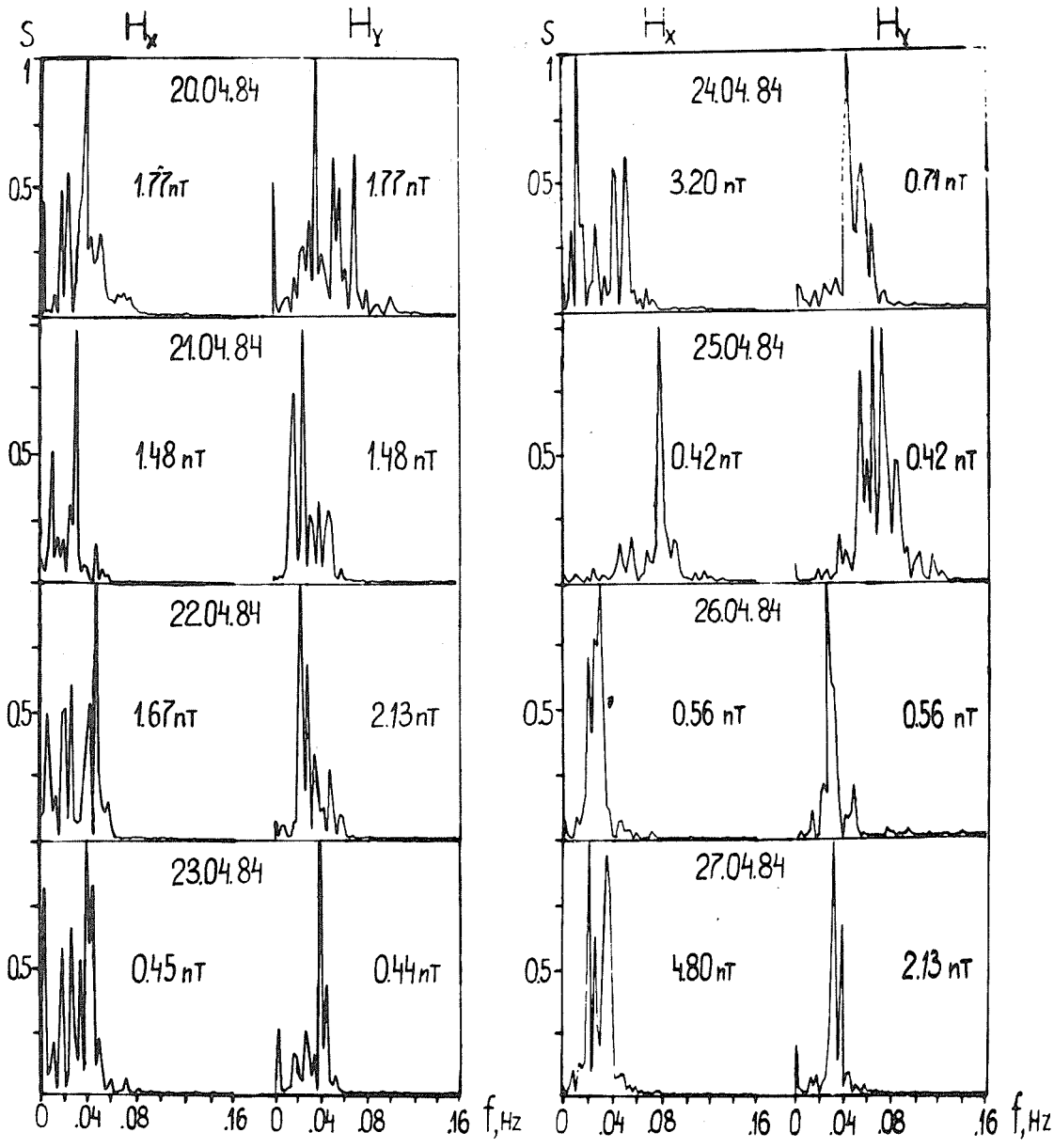


Fig. 2. The power spectra and average amplitudes of Pc2-4 pulsations from Borok are shown for the $H_x$ and $H_y$ components for the period 20-27 April 1984. F = frequency. S = the normalized spectral density.

# Time Variations of the Geomagnetic Field Measured at Tixie Observatory During February, April and May 1984

by

N.E. Molochushkin and A.M. Novikov
Polar Geocosmophysical Observatory "Tixie"
Tixie, USSR

Presented here are the traces of the H, Z, and D components of the geomagnetic field recorded at the Polar Geocosmophysical Observatory "Tixie" by its Bobrov magneto-variation station during 12-21 February and 20 April - 4 May 1984.

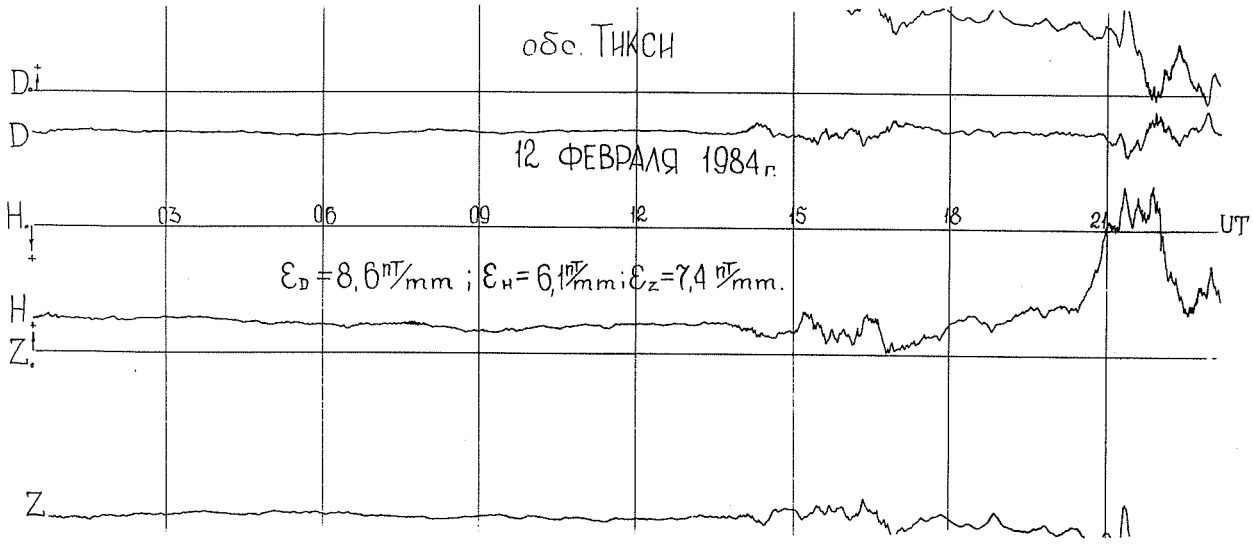


12 February 1984

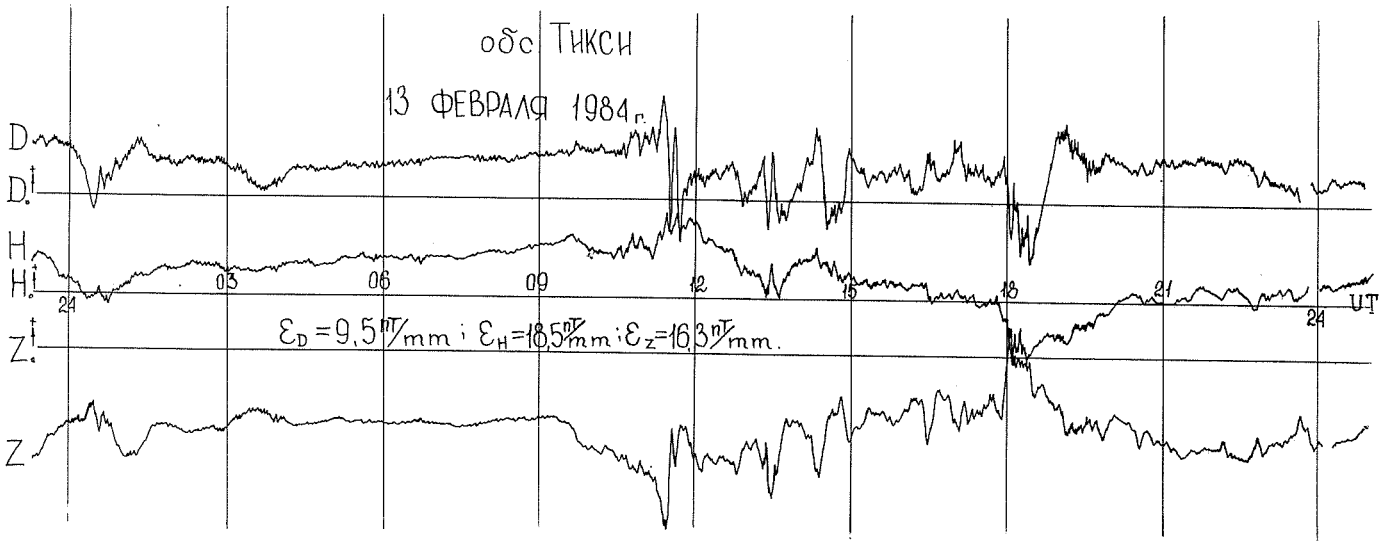


13 February 1984

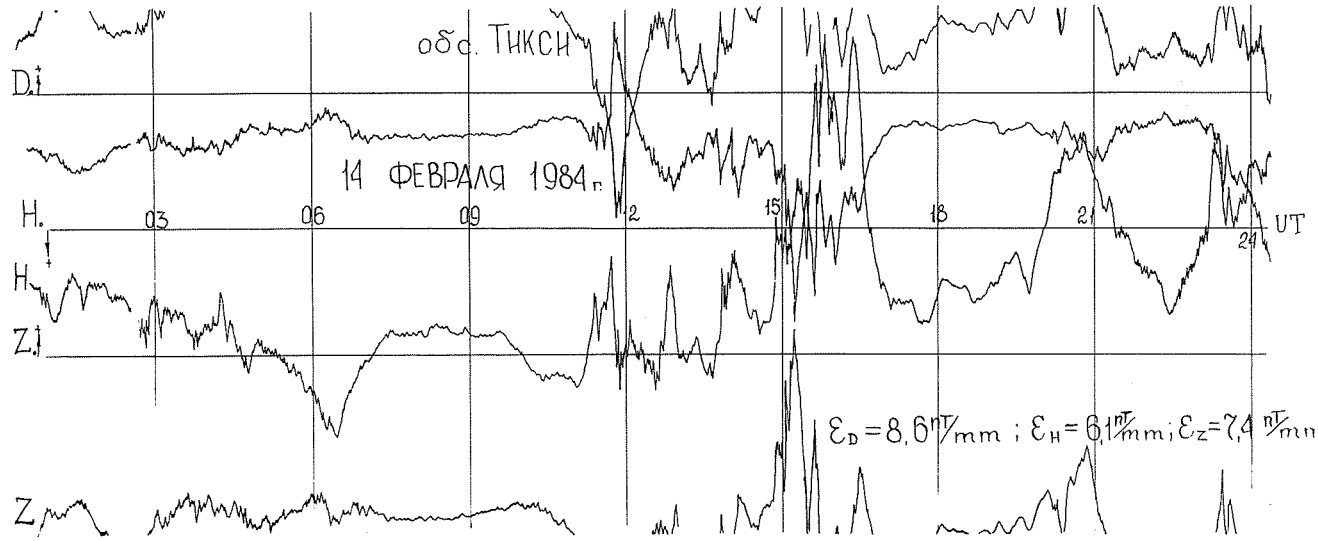


14 February 1984

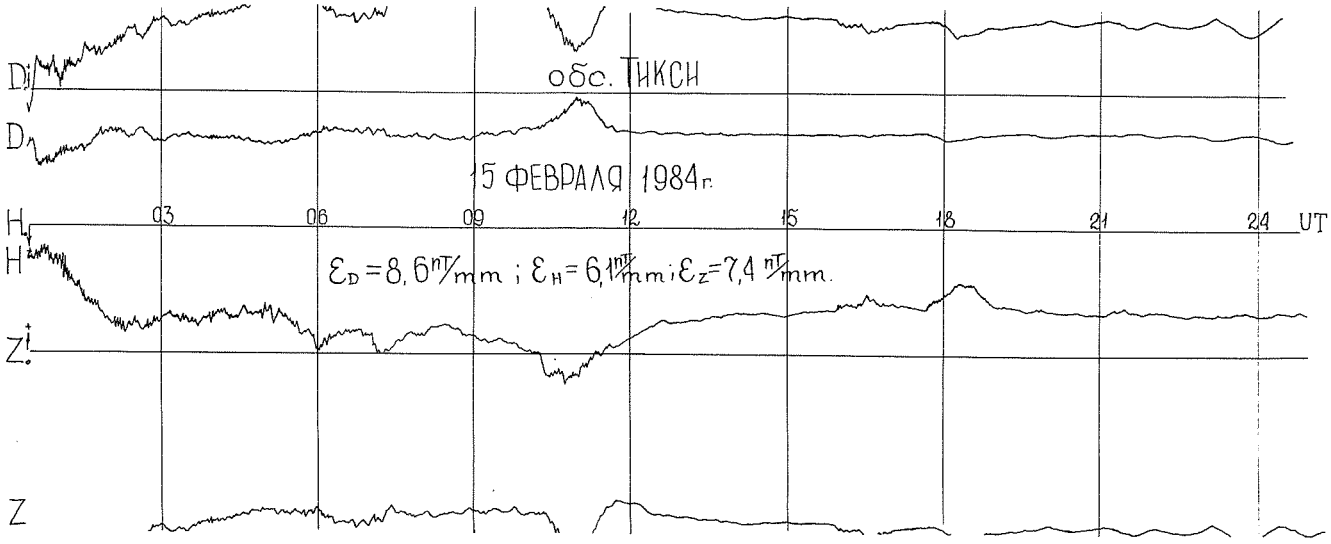


15 February 1984

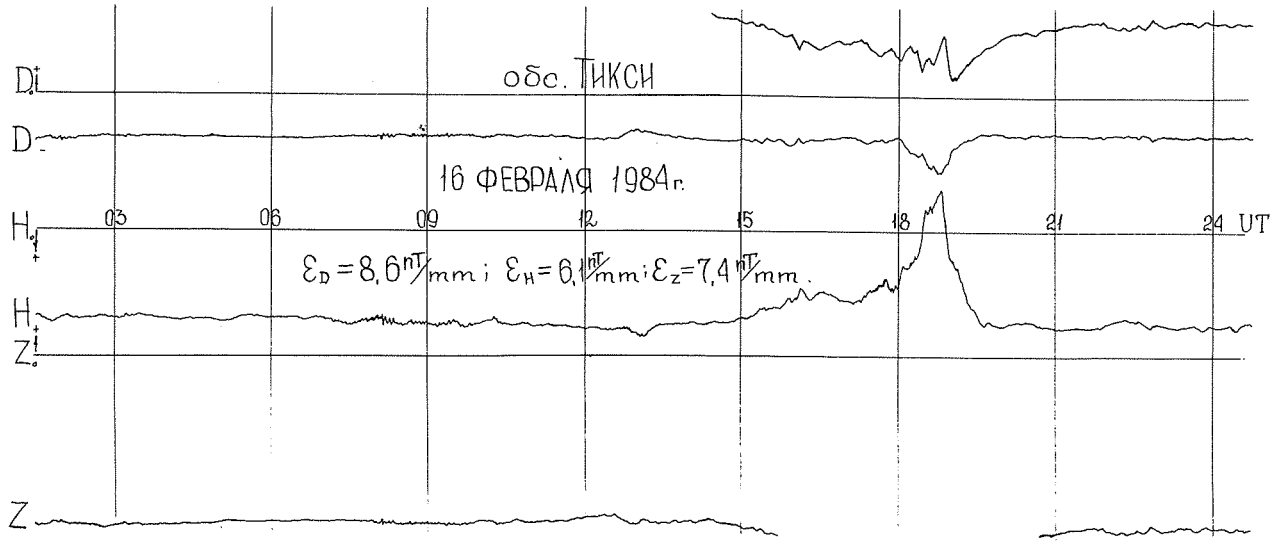


16 February 1984

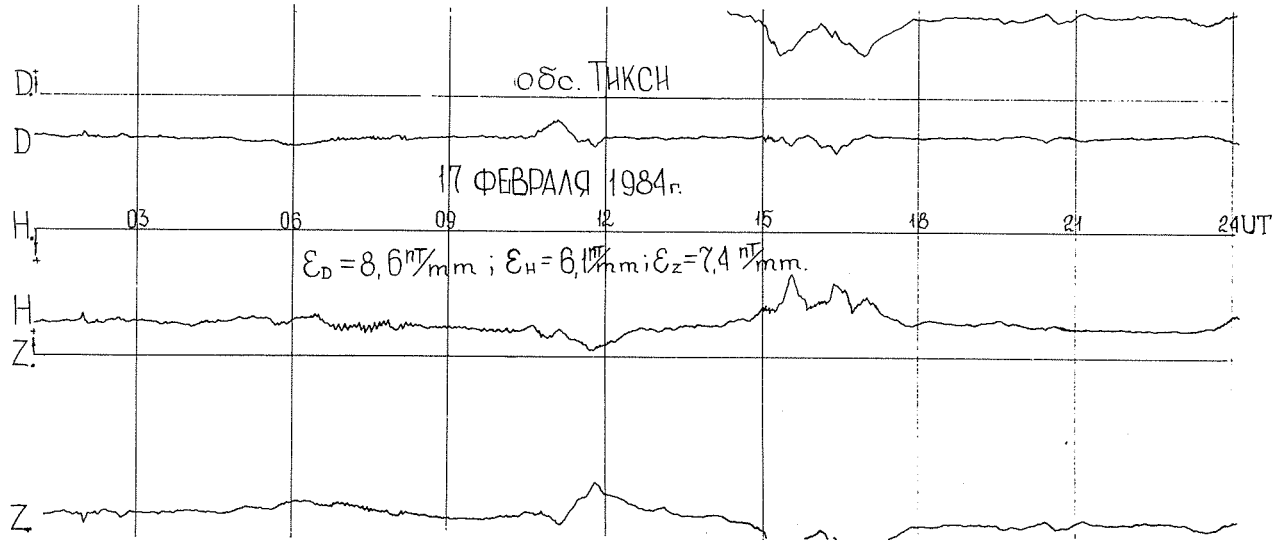


17 February 1984

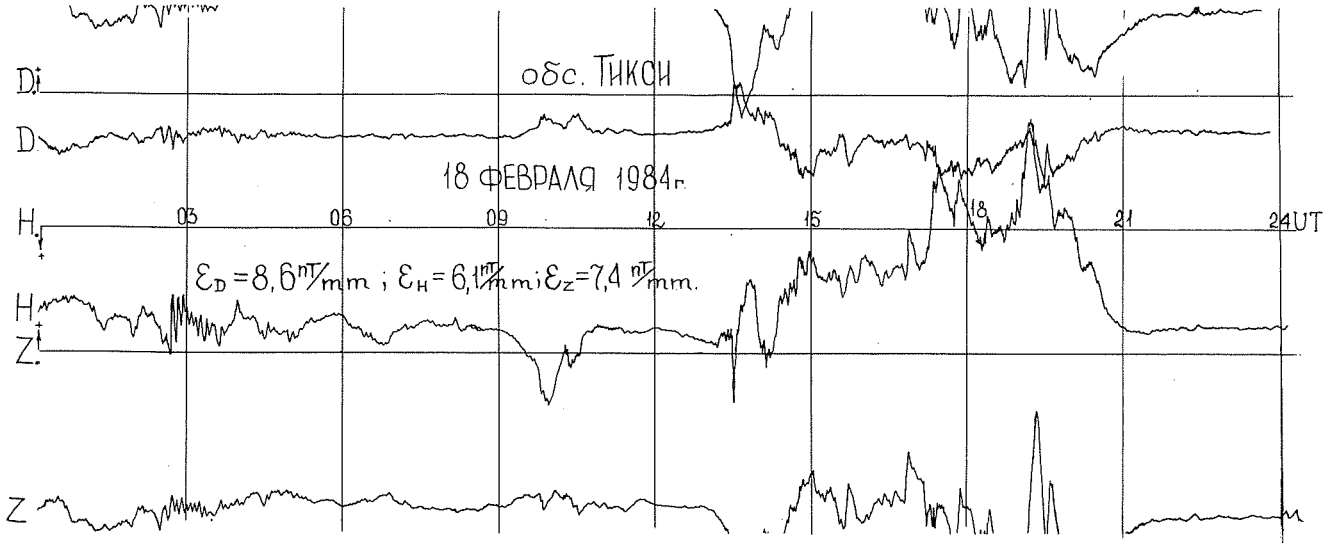


18 February 1984

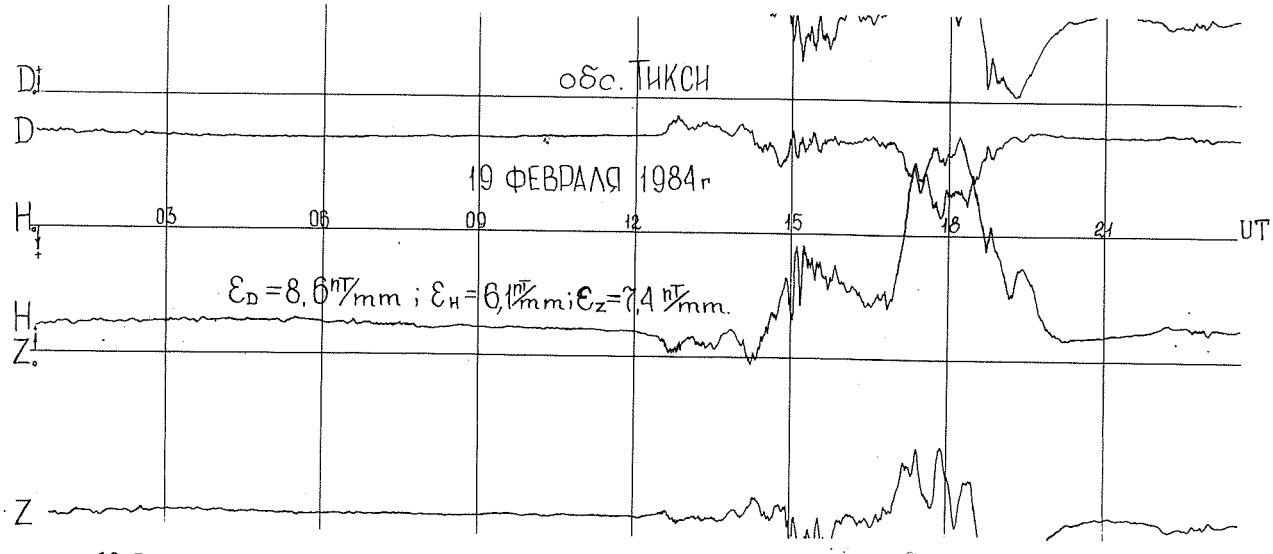


19 February 1984

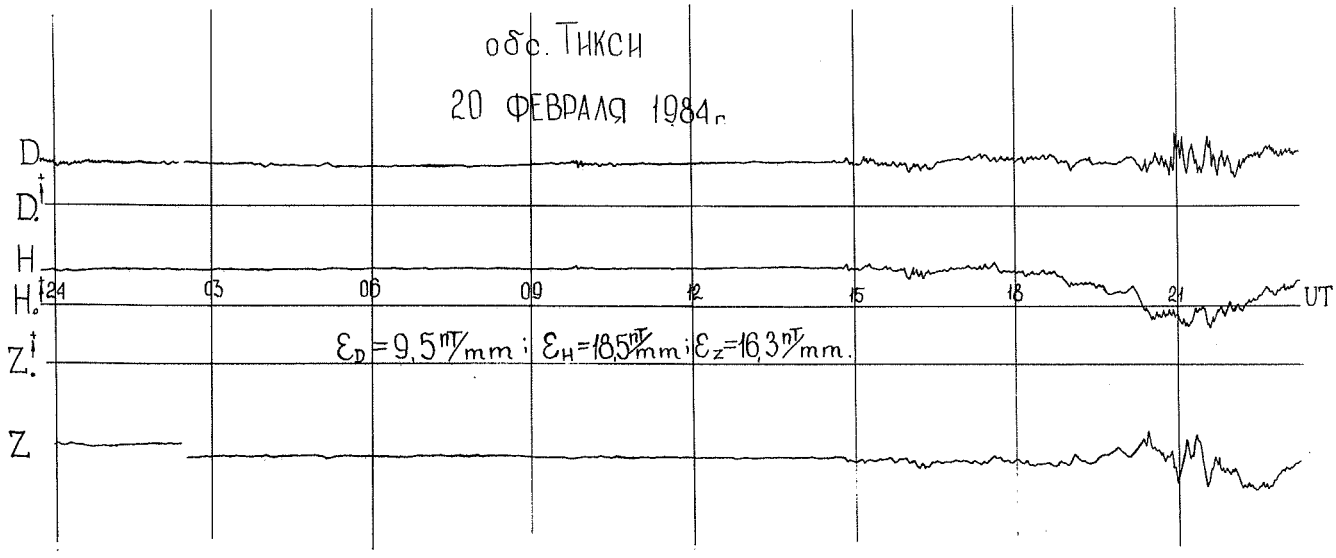


20 February 1984

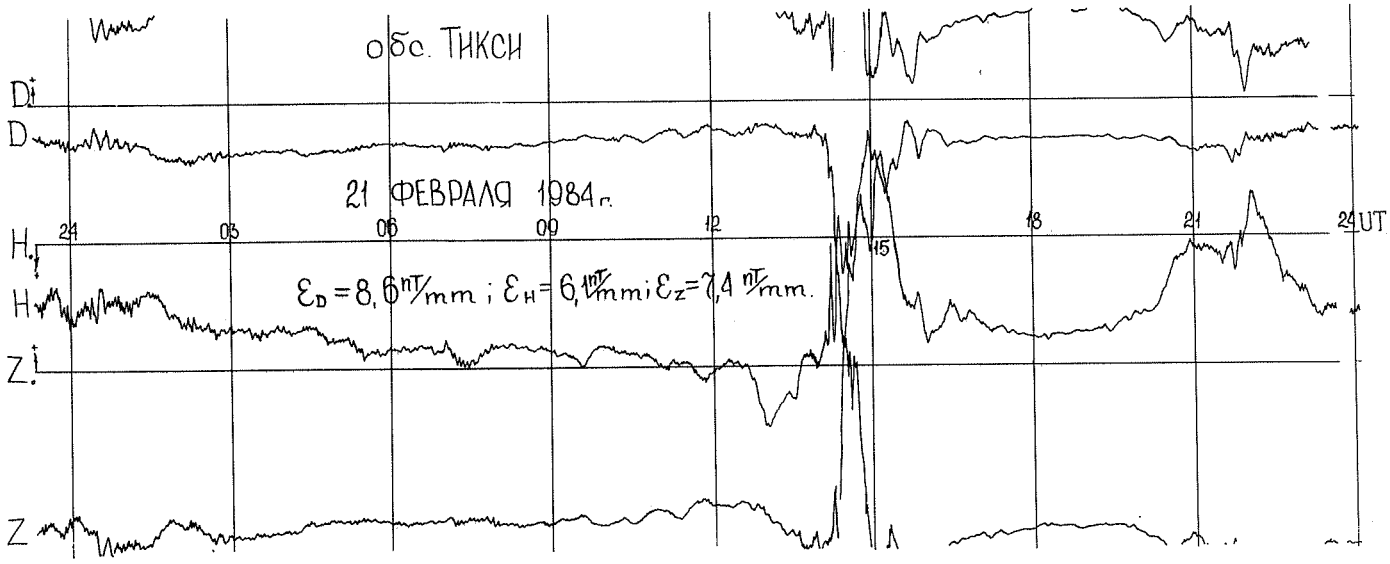


21 February 1984

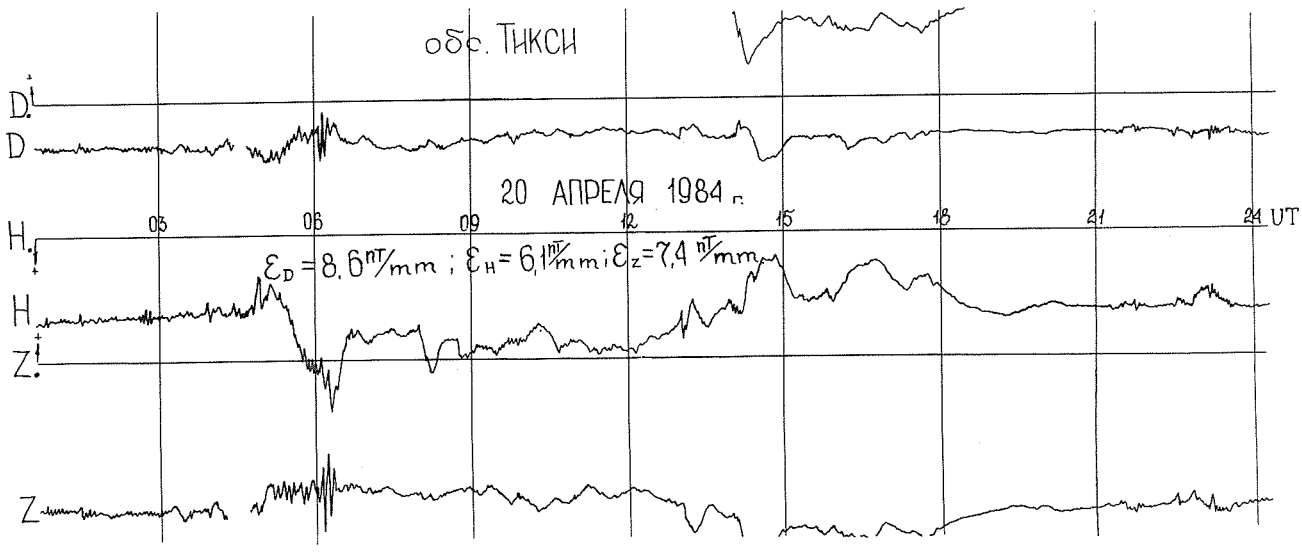


20 April 1984

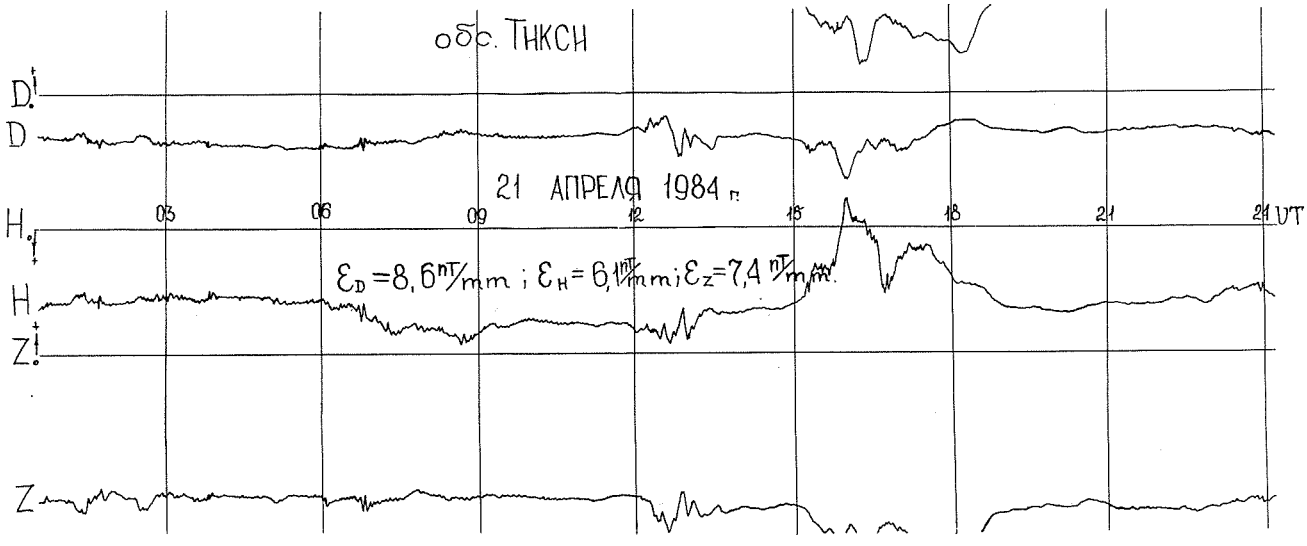


21 April 1984

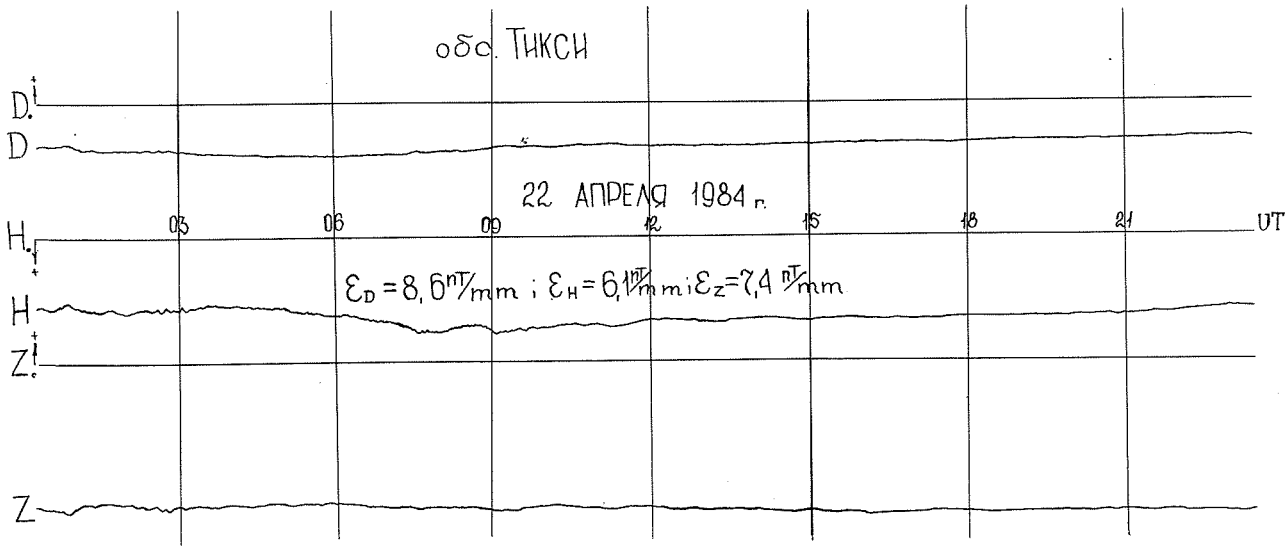


22 April 1934

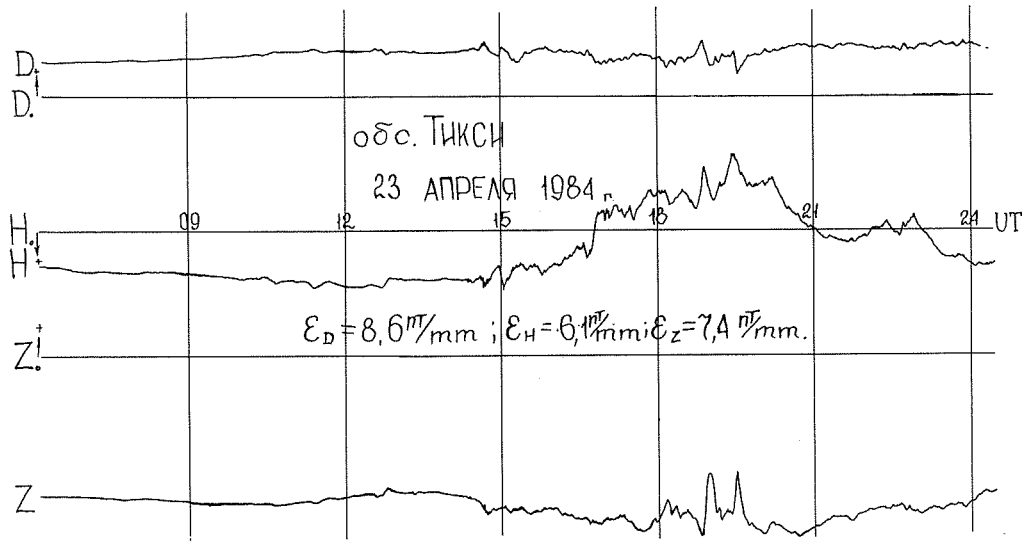


23 April 1984

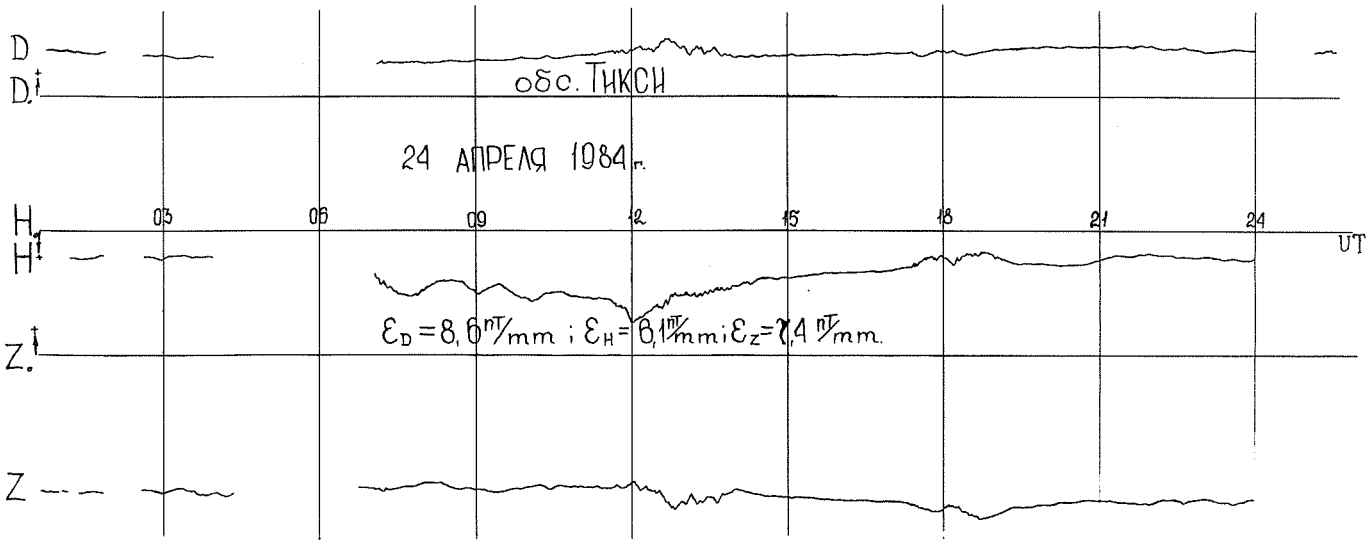


24 April 1984

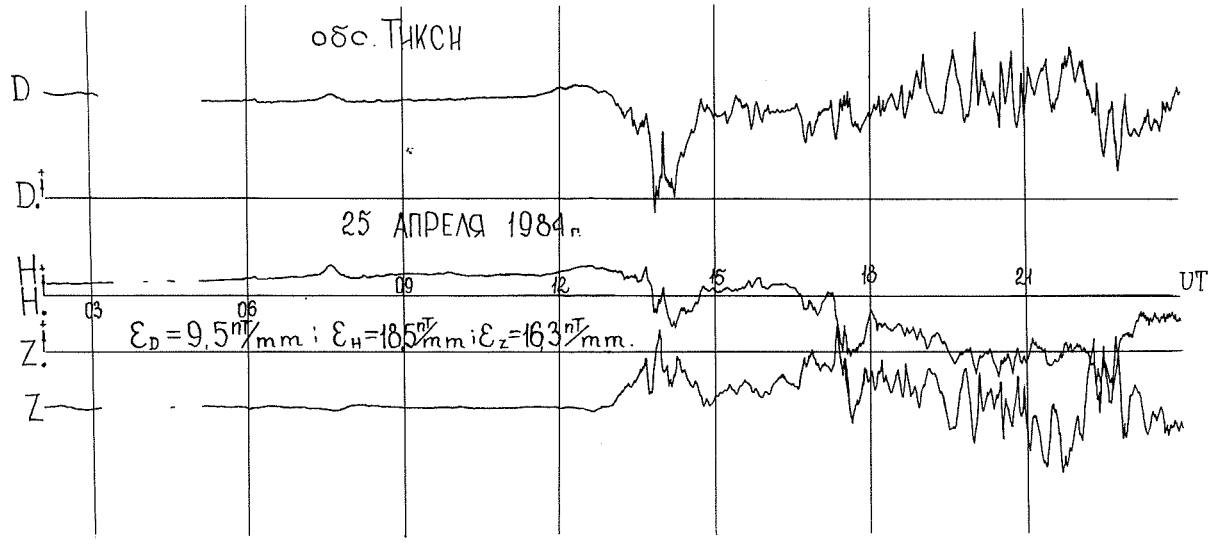


25 April 1984

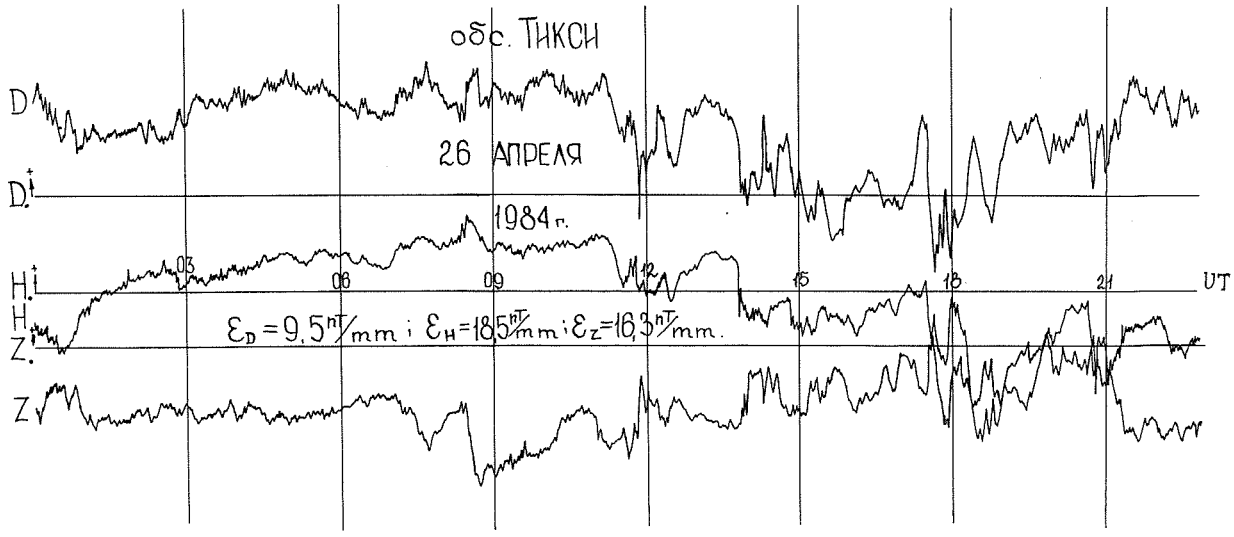


26 April 1984

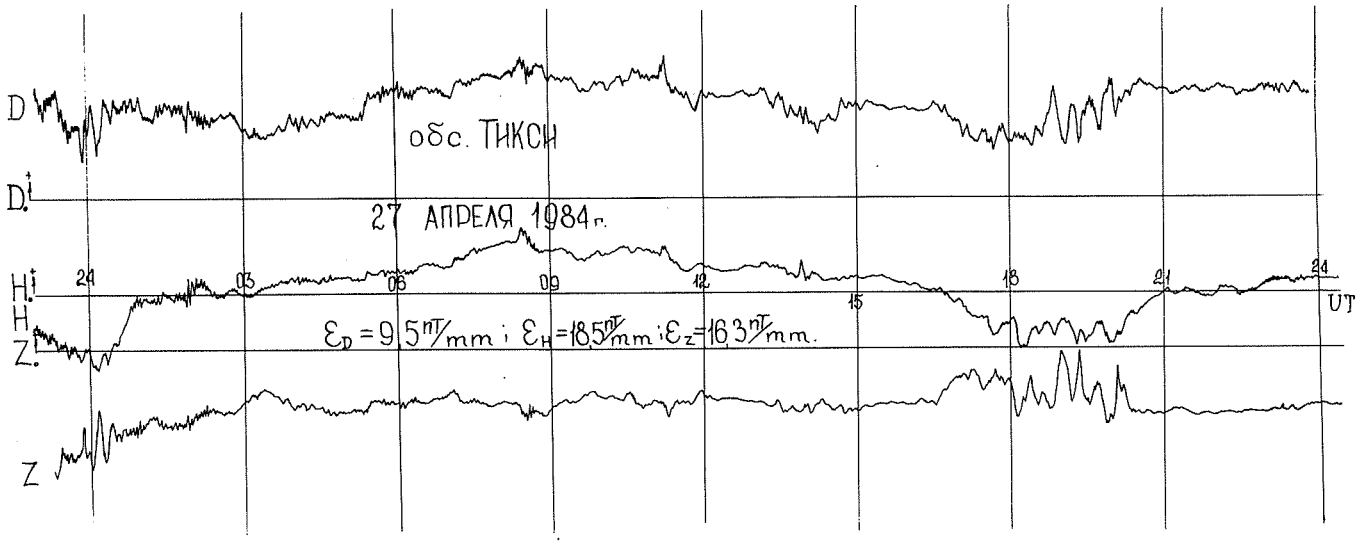


27 April 1984

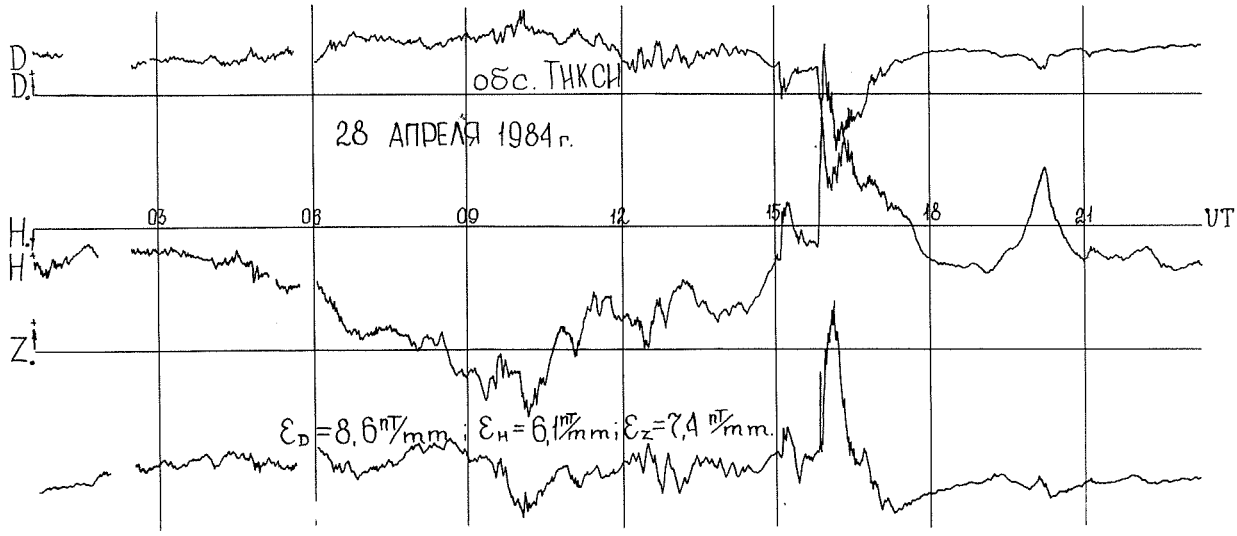


28 April 1984

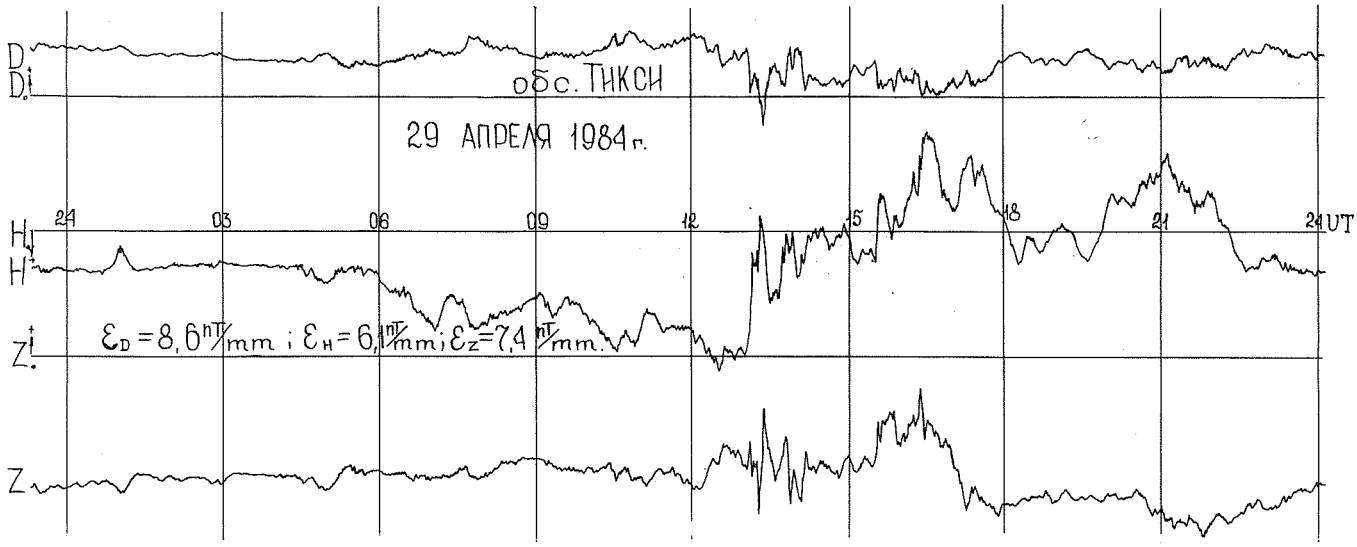


29 April 1984

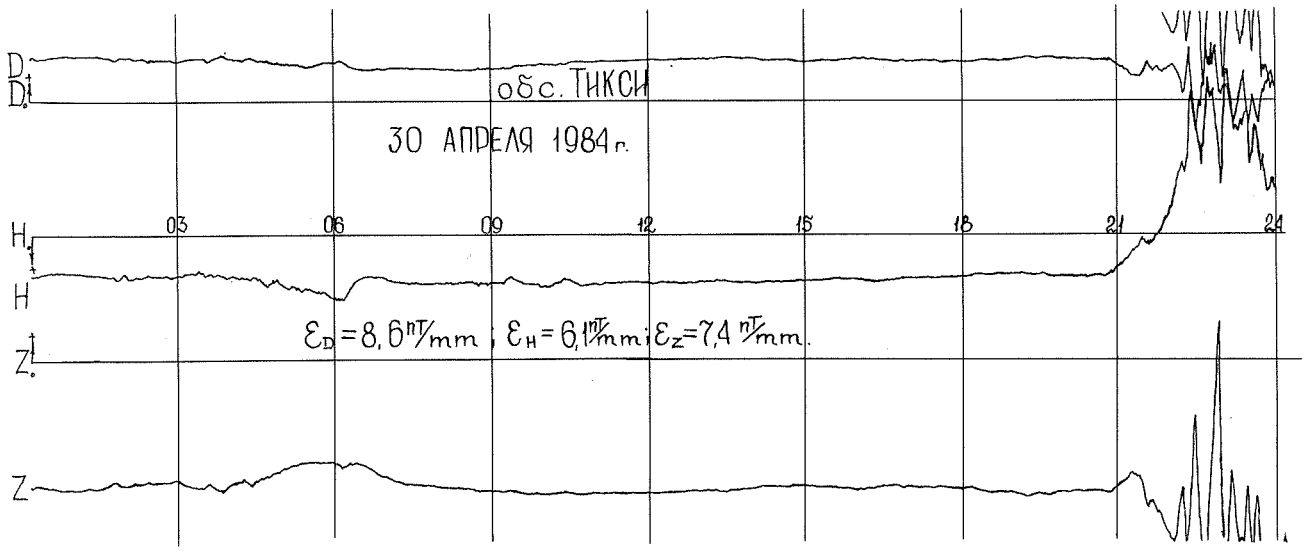


30 April 1984

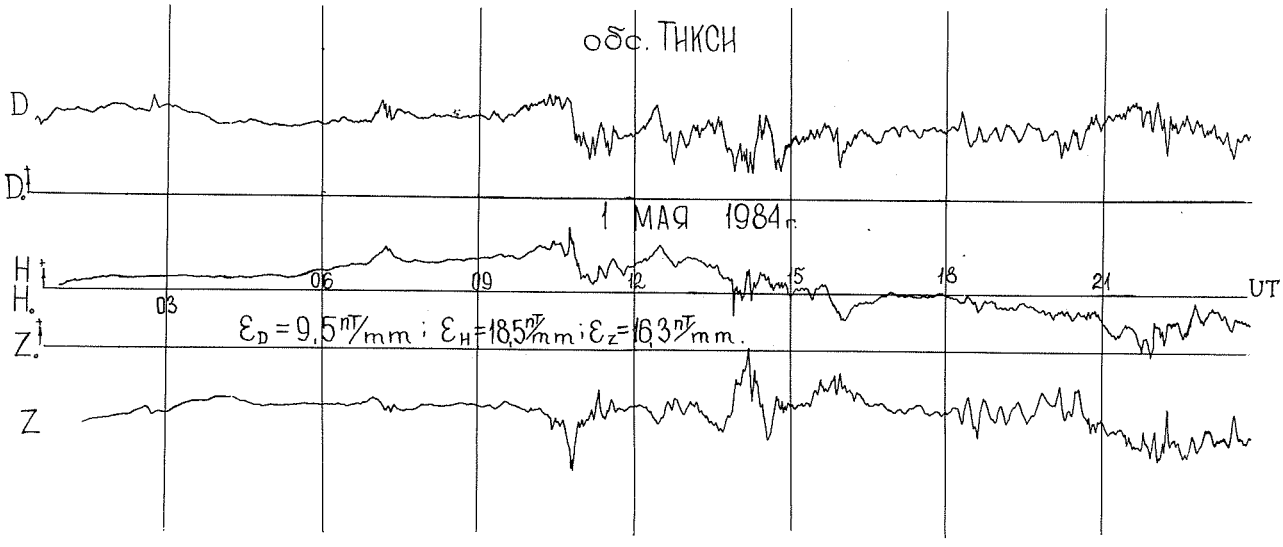


1 May 1984

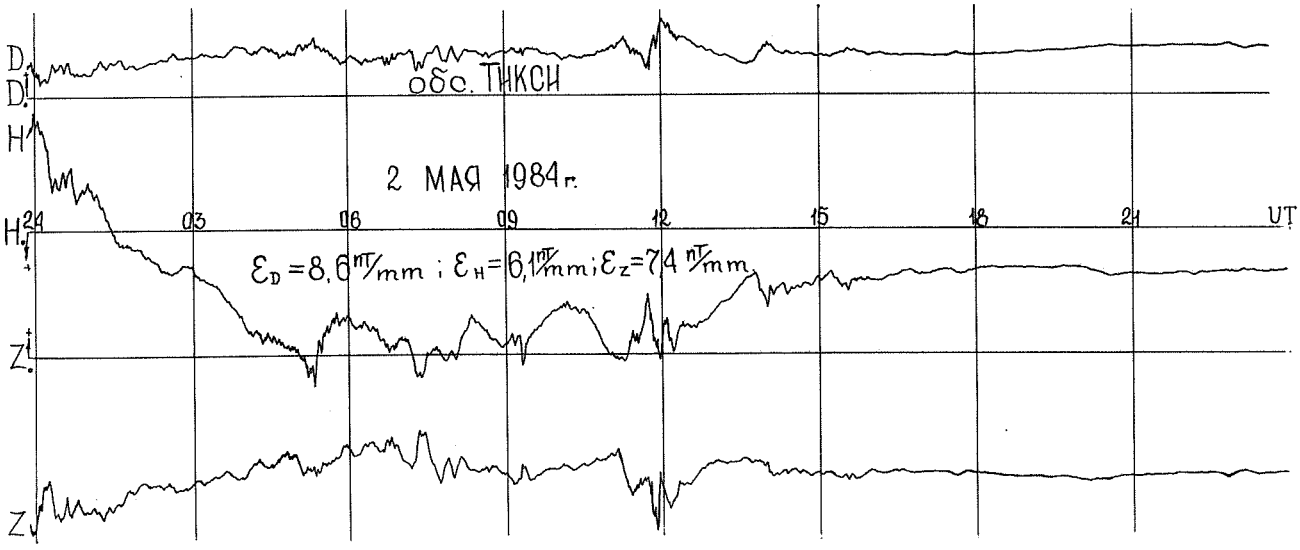


2 May 1984

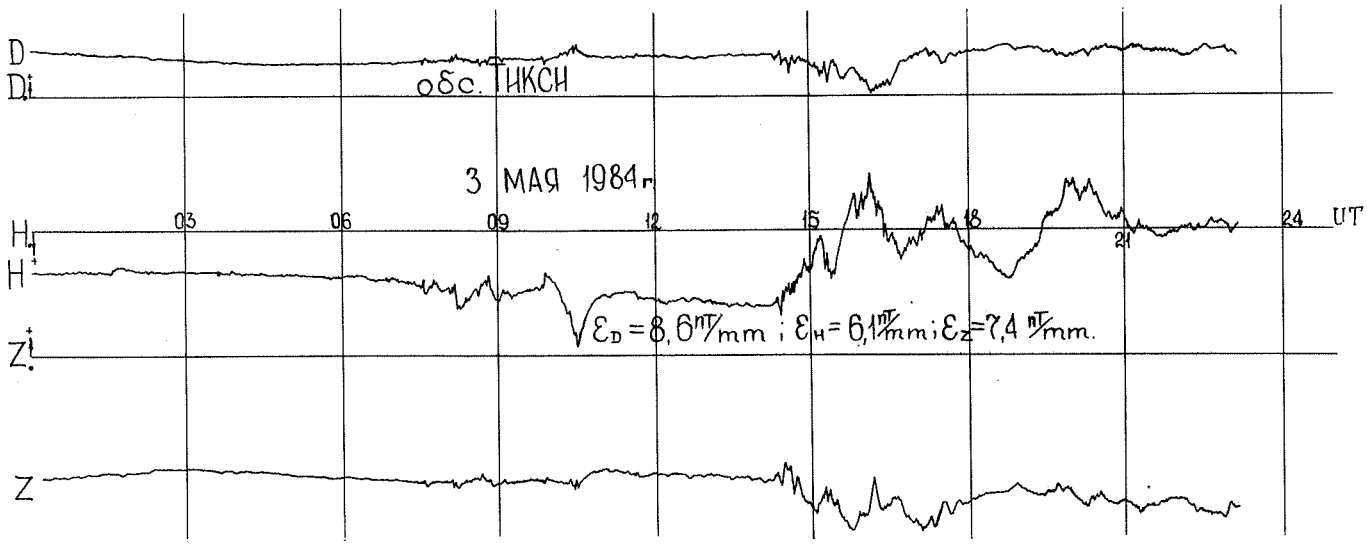


3 May 1984

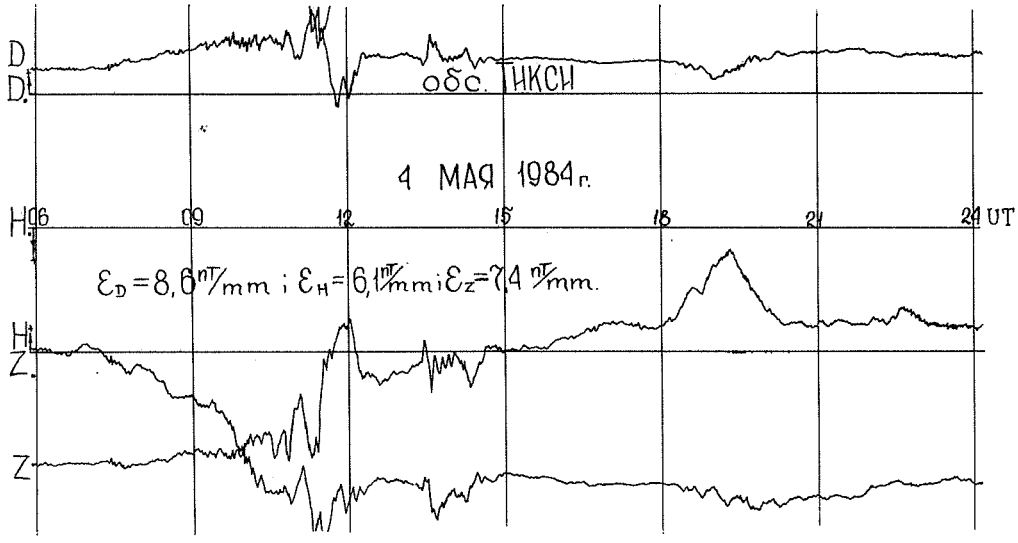


4 May 1984

# Geomagnetic Storms and Pulsations in Yakutsk

by

A.A. Danilov, A.V. Sobolev, and S.I. Solovyev
Institute of Cosmophysical Research and Aeronomy
Lenin Ave., 31, 677891 Yakutsk, USSR

In Yakutsk (N62°01' E129°43') we observe the geomagnetic field variations using three series of the quartz variometers with 0.4, 4 and 12 nT/mm divisions, respectively, and with recording speeds of 20 and 90 mm/h. The geomagnetic pulsations are observed with an induction magnetometer with 0.04-0.3 nT/mm and with recording speeds of 7.5 and 30 mm/min.

Tables 1 and 2 give the data on the storms and pulsations. All the storms show a gradual onset. The amplitude of the pulsations on the H-component is given in nanoteslas (nT).

Table 1. Geomagnetic Storms on 12-15 February and 25 April - 2 May 1984

| Onset | | End | | Amplitude nT | | | Character of | Active Period | | | |
|---|---|---|---|---|---|---|---|---|---|---|---|
| | | | | | | | | Onset | | End | |
| Date | UT | Date | UT | D | H | Z | Storm | Date | UT | Date | UT |
| 12 Feb | 1500 | 15 Feb | 1200 | 241 | 223 | 295 | Moderate | 13 Feb | 1100 | 13 Feb | 2100 |
| 25 Apr | 0700 | 29 Apr | 2400 | 300 | 355 | 402 | Large | 25 Apr | 1400 | 27 Apr | 0400 |
| 30 Apr | 2200 | 2 May | 1300 | 154 | 137 | 85 | Small | | | | |

Table 2a. Geomagnetic Pulsations in February 1984

| Date | Type | Onset UT | End UT | Period s | Amplitude |
|---|---|---|---|---|---|
| February | | | | | |
| 12 | Pc3 | 00 | 0300 | 20 | 0.4 |
| | Pc4 | 00 | 0110 | 60 | 0.4 |
| | Pc4 | 2030 | 24.. | 40-80 | 0.4 |
| | Pi1(B) | 1355 | 1359 | | 0.03 |
| | Pi1(C) | 2057 | 2452 | 5 | 0.1 |
| 13 | Pc4 | 00 | 24.. | 40-120 | 0.4-0.8 |
| | Pi2 | 1750 | 1900 | 50-160 | 2.5 |
| | Pc1 | 0944 | 11 | 2-4 | 0.05 |
| | Pi1(C) | 1730 | 20 | 6 | 0.5 |
| 14 | Pc4 | 00 | 07 | 40-80 | |
| | Pi2 | 1107 | 1113 | 70 | 1.2 |
| | Pi2 | 1117 | 1125 | 60 | 1.2 |
| | Pi2 | 1132 | 12 | 60 | 0.8 |
| | Pi2 | 1340 | 1353 | 40-80 | 2.0 |
| | Pi2 | 1442 | 1520 | 60 | 2.8 |
| | Pc3,4 | 2140 | 24.. | 20-120 | 0.8-1.2 |
| | Pc1 | 06 | 1040 | 3 | 0.07 |
| | Pi1(B) | 1344 | 1353 | | |
| | Pi1(B) | 1450 | 1456 | | |
| | Pi1(C) | 15 | 17 | 4 | 0.1 |
| 15 | Pc3 | 00 | 0830 | 30 | 0.6 |
| | Pc4 | 00 | 1130 | 60-120 | 1.2 |
| | Pi2 | 1740 | 19 | 80-100 | 0.8 |
| | Pi2 | 1944 | 2003 | 100 | 0.4 |
| | Pc3 | 1944 | 24.. | 30 | 0.3 |
| | Pc4 | 20 | 24.. | 60-120 | 1 |
| | Pc1 | 0539 | 0834 | 3 | 0.1 |
| 16 | Pc4 | 00 | 07 | 60 | |
| | Pc3 | 00 | 0230 | 25 | |
| | Pi2 | 1757 | 1806 | 70 | 0.4 |
| | Pc3 | 1950 | 24.. | 25 | 0.4 |
| | Pc1 | 0036 | 0154 | 0.8 | 0.08 |
| | Pc1 | 1823 | 1839 | 0.8 | 0.04 |
| | Pc1 | 2014 | 2023 | 0.8 | 0.12 |
| 17 | Pc4 | 00 | 0205 | 40-80 | 0.4 |
| | Pc3 | 0205 | 0640 | 40 | 0.4 |
| | Pi2 | 1459 | 1530 | 100 | 1.6 |
| | Pc3 | 20 | 24 | 40 | 0.4 |
| 18 | Pc4 | 00 | 08 | 60-80 | 0.4 |
| | Pi2 | 1011 | 1026 | 90 | 0.4 |
| | Pi2 | 1025 | 1027 | 120 | 0.4 |
| | Pi2 | 1307 | 1346 | 120 | 0.8 |
| | Pi2 | 1647 | 1702 | 120 | 0.8 |
| 18 | Pi2 | 1709 | 1722 | 60-120 | 0.8 |
| | Pi2 | 1740 | 1744 | 60 | 0.8 |
| | Pi2 | 1900 | 1905 | 60 | 1.2 |
| | Pc3 | 2130 | 24.. | 40 | 0.4 |
| | Pc1 | 06 | 07 | 4 | 0.06 |
| | Pi1(B) | 1330 | 1337 | | |
| | Pi1(B) | 1644 | 1647 | | 0.04 |
| | Pc1(B) | 1650 | 1654 | | 0.05 |
| | Pi1(B) | 1718 | 1722 | | 0.05 |
| 19 | Pc4 | 00 | 0810 | 80 | 1.2 |
| | Pc3 | 00 | 0810 | 30 | 0.4 |
| | Pi2 | 1225 | 1240 | 60 | 0.4 |
| | Pi2 | 1245 | 1252 | 120 | 0.4 |
| | Pi2 | 1700 | 1741 | 80 | 0.4 |
| | Pi2 | 1747 | 1759 | 70 | 0.4 |
| | Pc3 | 2120 | 24.. | 20 | 0.4 |
| | Pc1 | 0032 | 0203 | 1.4 | 0.1 |
| | Pi1(B) | 1230 | 1245 | | 0.2 |
| | Pi1(B) | 1248 | 1253 | | 0.05 |
| | Pi1(B) | 1659 | 1707 | | 0.2 |
| | Pi1(B) | 1711 | 1716 | | 0.05 |
| | Pi1(B) | 1733 | 1738 | | 0.05 |
| | Pi1(B) | 1747 | 1753 | | 0.05 |
| 20 | Pc4 | 00 | 0130 | 60 | 0.4 |
| | Pc3 | 0203 | 0805 | 20 | 1.2 |
| | Pi2 | 0950 | 1000 | 80 | 1.2 |
| | Pi2 | 1010 | 1013 | 80 | 0.4 |
| | Pi2 | 1037 | 1103 | 80 | 0.8 |
| | Pi2 | 1153 | 1601 | 120 | 0.8 |
| | Pi2 | 1603 | 1625 | 120 | 1.2 |
| | Pc4 | 1625 | 19 | 60-120 | 0.8 |
| | Pc3 | 1901 | 20 | 15 | 0.4 |
| | Pc4 | 20 | 24 | 60 | 0.4 |
| | Pc1 | 00 | 02 | 0.8 | 0.06 |
| | Pi1(B) | 1448 | 1454 | | 0.2 |
| | Pi1(B) | 1557 | 1616 | | 0.2 |
| 21 | Pc4 | 00 | 13 | 60-100 | 1.6 |
| | Pc3 | 00 | 08 | 20 | 0.6 |
| | Pi2 | 1333 | 1343 | 70 | 0.8 |
| | Pi2 | 1350 | 1510 | 80 | 0.8 |
| | Pi2 | 2020 | 2027 | 80 | 0.8 |
| | Pi2 | 2130 | 2145 | 80 | 1.2 |
| | Pc4 | 2230 | 24 | 60-100 | 0.4 |
| | Pi1(B) | 1336 | 1342 | | 0.04 |
| | Pi1(B) | 1412 | 1421 | | 0.04 |
| | Pi1(B) | 1431 | 1440 | | 0.2 |
| | Pc3 | 00 | 0540 | 20 | 0.8 |

Table 2b. Geomagnetic Pulsations in April - May 1984

| Date | Type | Onset UT | End UT | Period s | Amplitude |
|---|---|---|---|---|---|
| April | | | | | |
| 20 | Pi2 | 0743 | 0813 | 80 | 4 |
| | Pc3 | 1810 | 24 | 40 | 2 |
| | Pc4 | 2000 | 24 | 80-120 | 2 |
| | Pc1 | No record | | | |
| | Pi1 | No record | | | |
| 21 | Pc3 | 0015 | 08 | 40 | 1.2 |
| | Pc4 | 02 | 08 | 60-80 | 6 |
| | Pi2 | 1213 | 1300 | 90 | 1.2 |
| | Pc3 | 1840 | 24 | 40 | 0.8 |
| | Pc4 | 2230 | 24 | 80 | 1.2 |
| | Pi1(B) | 1209 | 1212 | | 0.03 |
| | Pi1(B) | 1220 | 1224 | | 0.15 |
| | Pi1(B) | 1230 | 1236 | | |
| | Pi1(B) | 1253 | 1256 | | 0.15 |
| 22 | Pc4 | 0153 | 0915 | 100 | 3.2 |
| | Pc3 | 0153 | 0845 | 30 | 0.8 |
| | Pc3 | 1050 | 1130 | 30 | 0.4 |
| | Pc4 | 1050 | 1250 | 80 | 0.4 |
| | Pc4 | 2225 | 24.. | 50 | 1.2 |
| 23 | Pc4 | 00 | 0250 | 80 | 0.4 |
| | Pi2 | 1406 | 1412 | 120 | 0.8 |
| | Pi2 | 1416 | 1426 | 80 | 0.8 |
| | Pi2 | 1433 | 1446 | 100 | 1.6 |
| | Pi2 | 1453 | 1515 | 100 | 1.2 |
| | Pi2 | 1544 | 1600 | 100 | 0.4 |
| | Pi2 | 1632 | 1634 | 100 | 0.8 |
| | Pi1(B) | 1436 | 1441 | | 0.03 |
| | Pi1(B) | 1502 | 1511 | | 0.03 |
| 24 | Pc4 | 0030 | 08 | 80 | 0.4 |
| | Pc3 | 0300 | 0950 | 30 | 0.8 |
| | Pi2 | 1720 | 1732 | 110 | 1.6 |
| | Pi2 | 1736 | 1753 | 100 | 1.2 |
| | Pi2 | 1805 | 1824 | 100 | 1.2 |
| 25 | Pc3 | 0015 | 0042 | 20 | 0.4 |
| | Pc4 | 0042 | 0500 | 80-100 | 1.6 |
| | Pi2 | 0553 | 0601 | 80 | 2.4 |
| | Pi2 | 0606 | 0613 | 80 | 2 |
| | Pi2 | 0623 | 0631 | 100 | 2 |
| | Pc4 | 0715 | 1200 | 100 | 0.8 |
| | Pi2 | 1340 | 1420 | 80 | 0.8 |
| | Pi2 | 1626 | 1645 | 60 | 2 |
| | Pi2 | 1713 | | 80 | 4 |
| | Pc3 | 1713 | 24.. | 20 | 0.4 |
| | Pc4 | 1713 | 24.. | 80 | 1.2 |
| | Pi1(C) | 1309 | 1423 | 4* | 0.15 |
| | Pi1(C) | 16 | 24 | 8 | 0.50 |
| | Pi1(B) | 1629 | 1644 | | |
| 26 | Pc3 | 00 | 07 | 20 | 0.4 |
| | Pc4 | 00 | 07 | 80 | 1.2 |
| | Pi2 | 1345 | 1400 | 60 | 1.2 |
| | Pi1(C) | 1450 | 24 | 6 | 0.70 |
| | Pi1(B) | 1347 | 1354 | | 0.05 |
| 27 | Pc3 | 00 | 09 | 40 | 0.45 |
| | Pc4 | 00 | 09 | 80-100 | 0.25 |
| | Pi2 | 0803 | 0815 | 60 | 0.27 |
| | Pi2 | 0824 | 0845 | 40-70 | 0.45 |
| | Pi2 | 1635 | 1656 | 50 | 0.25 |
| | Pi2 | 1704 | 1714 | 60 | 0.3 |
| | Pi2 | 1727 | 1731 | 40 | 0.25 |
| | Pc3 | 1731 | 2020 | 15-40 | 0.2 |
| 27 | Pi1(B) | 1108 | 1113 | | 0.05 |
| | Pi1(B) | 1638 | 1643 | | 0.05 |
| | Pi1(B) | 1647 | 1650 | | 0.05 |
| | Pi1(C) | 1734 | 2028 | 6 | 0.25 |
| 28 | Pc3 | 00 | 08 | 40 | 1.2 |
| | Pc4 | 0540 | 1030 | 60-80 | 1.2 |
| | Pi2 | 1506 | 1515 | 40 | 1.2 |
| | Pi2 | 1547 | 1600 | 40 | 2.0 |
| | Pi1(B) | 1551 | 1603 | | 0.5 |
| | Pi1(C) | 1551 | 1720 | 4 | 0.1 |
| 29 | Pc3 | 00 | 11 | 40 | 2 |
| | Pi2 | 1313 | 1317 | 60 | 1.2 |
| | Pi2 | 1550 | 1555 | 40 | 0.8 |
| | Pi2 | 1557 | 1602 | 40 | 0.8 |
| | Pi2 | 1603 | 1607 | 40 | 0.8 |
| | Pi2 | 1608 | 1614 | 40 | 0.8 |
| | Pc3 | 1930 | 24 | 30 | 0.4 |
| | Pc1 | 0430 | 06 | 0.8-1.2 | 0.05 |
| | Pi1(B) | 1306 | 1310 | | 0.03 |
| | Pi1(B) | 1315 | 1320 | | 0.15 |
| | Pi1(B) | 1532 | 1536 | | 0.03 |
| | Pi1(B) | 1551 | 1554 | | 0.15 |
| | Pi1(B) | 1558 | 16 | | 0.15 |
| | Pi1(B) | 1604 | 1609 | | |
| | Pi1(C) | 16 | 1732 | 5 | 0.08 |
| | Pi1(C) | 2150 | 2400 | 5 | 0.06 |
| 30 | Pc3 | 0130 | 04 | 40 | 0.4 |
| | Pc4 | 04 | 06 | 40-60 | 0.4 |
| | Pc4 | 2015 | 24 | 60-120 | 0.4 |
| | Pc3 | 2230 | 24 | 40 | 0.4 |
| | Pi1(C) | 2150 | 2400 | 5 | 0.06 |
| May | | | | | |
| 1 | Pc4 | 02 | 04 | 40-80 | 0.4 |
| | Pi2 | 1037 | 1100 | 40-100 | 1.2 |
| | Pi2 | 1351 | 1415 | 50 | 2.4 |
| | Pi2 | 1450 | 1500 | 50 | 1.6 |
| | Pi1(C) | 1037 | 1130 | 6 | 0.10 |
| | Pi1(B) | 1351 | 1356 | | 0.30 |
| | Pi1(B) | 1359 | 1406 | | 0.15 |
| | Pi1(C) | 14 | 17 | 5 | 0.08 |
| 2 | Pc3,4 | 18 | 24 | 20-60 | 0.4 |
| | Pi2 | 1145 | 1153 | 60 | 3.2 |
| | Pc1 | 0930 | 1040 | 2 | 0.08 |
| | Pi1(C) | 1138 | 1210 | 4 | 0.06 |
| | Pc1 | 16 | 1633 | 0.8 | 0.06 |
| 3 | Pc3,4 | 00 | 0115 | 40-60 | 0.4 |
| | Pc3 | 0115 | 0505 | 15 | 0.8 |
| | Pi2 | 0733 | 0739 | 80 | 1.2 |
| | Pc4 | 15 | 24 | 80-100 | 1.6 |
| | Pc3 | 19 | 24.. | 30-45 | 0.8 |
| | Pi1(C) | 1415 | 16 | 5 | 0.10 |
| 4 | Pc3 | 00 | 04 | 40 | 0.4 |
| | Pc3 | 0230 | 0720 | 20 | 0.4 |
| | Pi2 | 1008 | 1016 | 50 | 1.2 |
| | Pi2 | 1026 | 1029 | 50 | 1.2 |
| | Pi2 | 1043 | 1051 | 50-80 | 1.2 |
| | Pi2 | 1103 | 1142 | 50 | 1.2 |
| | Pc3 | 1930 | 2150 | 40 | 1.2 |
| | Pc4 | 2150 | 24.. | 80 | 2.4 |
| | Pi1(C) | 1030 | 1140 | 4 | 0.07 |

# Low Latitude and Equatorial Geomagnetic Field Variations Observed during 25 and 27 April 1984

by

G.K. Mukherjee and G.K. Rangarajan
Indian Institute of Geomagnetism
Colaba, Bombay 400 005
India

The data and magnetograms used in this report are derived from seven magnetic observatories maintained by the Indian Institute of Geomagnetism, Colaba, Bombay. The details of the station coordinates and instrumentation have been reported earlier (Rangarajan, 1982). The period of study included only one disturbed day (26 April) and no international quiet days. Ap values were 33, 103 and 26 respectively on 25, 26 and 27 April. The equatorial Dst values were mostly negative during the interval, with largest negative value of -91 nT occurring at 0100 UT on 27 April. The solar parameters RI and flux at 2800 MHz showed large variations during the interval with their corresponding maximum reached on 26 and 27 April respectively.

During the period of interest, magnetic disturbances with gradual commencement were observed at the Indian magnetic observatories. The traces show great similarity between stations. The details of the statistics of the storm are given in Table 1. Figure 1 shows variations of the H-component of magnetic records during the interval 0000 UT 25 April to 0000 UT 27 April.

Table 1. Details of the April 1984 Geomagnetic Storms Recorded at the Indian Magnetic Stations

| 1984 25 April Begin UT | 27 April End UT | Maximum 3 h Index | K | Station | Range D ' | Range H nT | Range Z nT |
|---|---|---|---|---|---|---|---|
| 1400 | 0300 | 25(6) | 6 | Trivandrum | 7 | 144 | 104 |
| | | 26(6) | 6 | Annamalainagar | 7 | 135 | 58 |
| | | | | Alibag | 7 | 89 | 52 |
| | | | | Ujjain | 7 | 108 | 36 |
| | | | | Shillong | 4 | 102 | 25 |
| | | | | Jaipur | 9 | 91 | 42 |
| | | | | Gulmarg | 11 | 131 | 57 |

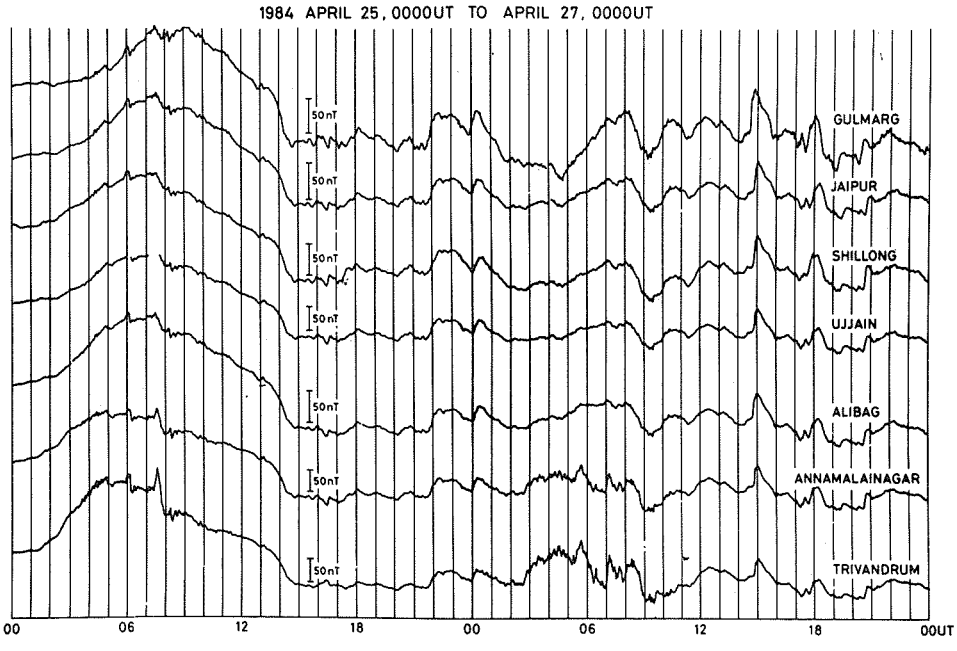


Fig. 1. H-component at Indian chain of geomagnetic observatories for the period 25-27 April 1984.

25 April

On this day many impulsive and large amplitude oscillations appear in the records of all stations. Distinctively, the impulse recorded at 0600 UT is seen at all Indian magnetic stations. In contrast, the positive impulse recorded at 0720 UT shows more enhancement in magnitude at the two equatorial stations Trivandrum and Annamalainagar as compared to the other low latitude stations. The enhancement is due to the signature of strong electrojet currents flowing in the ionosphere at the equatorial stations.

26 April

Strong DP2 fluctuations between 0300 UT and 1000 UT are recorded at Trivandrum and Annamalainagar but are absent on other low latitude magnetograms. Another interesting phenomenon is the recurrent bays recorded during the night -- three consecutive bays are recorded between 1400 and 2100 UT. The details of these significant positive bays are listed in Table 2. Note that the maximum change in H during the bay events are recorded at Gulmarg and the lowest values at Trivandrum.

Table 2. Details of the Significant Positive Bays Recorded at the Indian Magnetic Stations

| Date 1984 | Begin UT | Max UT | | H Amplitude* nT |
|---|---|---|---|---|
| April 26 | 1424 | 1504 | Trivandrum | 47 |
| | | | Annamalainagar | 60 |
| | | | Alibag | 50 |
| | | | Ujjain | 62 |
| | | | Shillong | 59 |
| | | | Jaipur | 51 |
| | | | Gulmarg | 77 |

*Amplitude calculated as the range (Maximum-Beginning)

REFERENCES

RANGARAJAN, G.K. 1982 "Low Latitude and Equatorial Geomagnetic Field Variations during September 1977," World Data Center A for Solar-Terrestrial Physics, **Report UAG-83, Part II Solar-Geophysical Activity Reports for September 7-24, 1977 and November 22, 1977**, J. McKinnon and J.V. Lincoln, ed., 456-460.

# Geomagnetic Variations in Japanese Area

by

Akira Harada, Masayuki Kuwashima and Tetsuya Uwai
Kakioka Magnetic Observatory
Kakioka 595, Yasato, Ibaraki, 315-01, Japan

Table 1. Symbols and Coordinates of the Stations

| Station | Symbol | Geographic Lat | Geographic Long | Geomagnetic Lat | Geomagnetic Long |
|---|---|---|---|---|---|
| Memambetsu | MMB | N43.9 | E144.2 | N34.2 | E209.7 |
| Kakioka | KAK | 36.2 | 140.2 | 26.2 | 207.3 |
| Kanoya | KNY | 31.4 | 130.9 | 20.7 | 199.4 |
| Chichijima | CBI | 27.2 | 142.3 | 17.4 | 210.3 |

Table 2. sfe Event on 24 April 1984

| Station | 24 April Begin UT | 25 April End UT | Maximum or Minimum on 25 April: H Time UT | H Amplitude nT | D Time UT | D Amplitude nT | Z Time UT | Z Amplitude nT |
|---|---|---|---|---|---|---|---|---|
| MMB | 2358 | 0105 | 0001 | -81 | 0004 | +34(+4.5) | 0013 | -20 |
| KAK | 2357 | 0037 | 0001 | -32 | 0006 | +42(+4.8) | 0014 | -33 |
| KNY | 2357 | 0100 | 0001 | -32 | 0002 | +59(+6.1) | 0002 | - 9 |

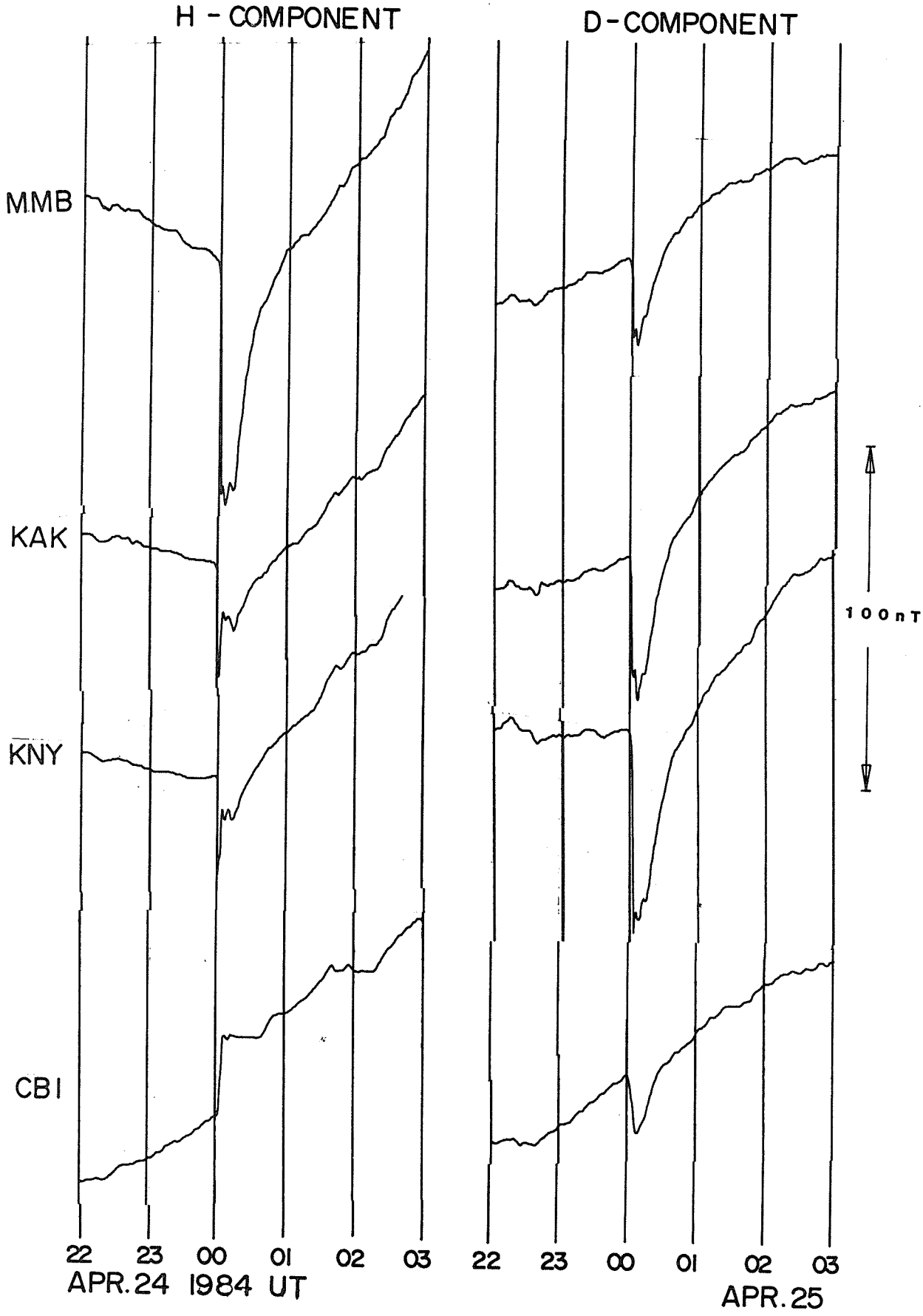


Fig. 1. sfe-associated magnetic variations at Japanese stations.

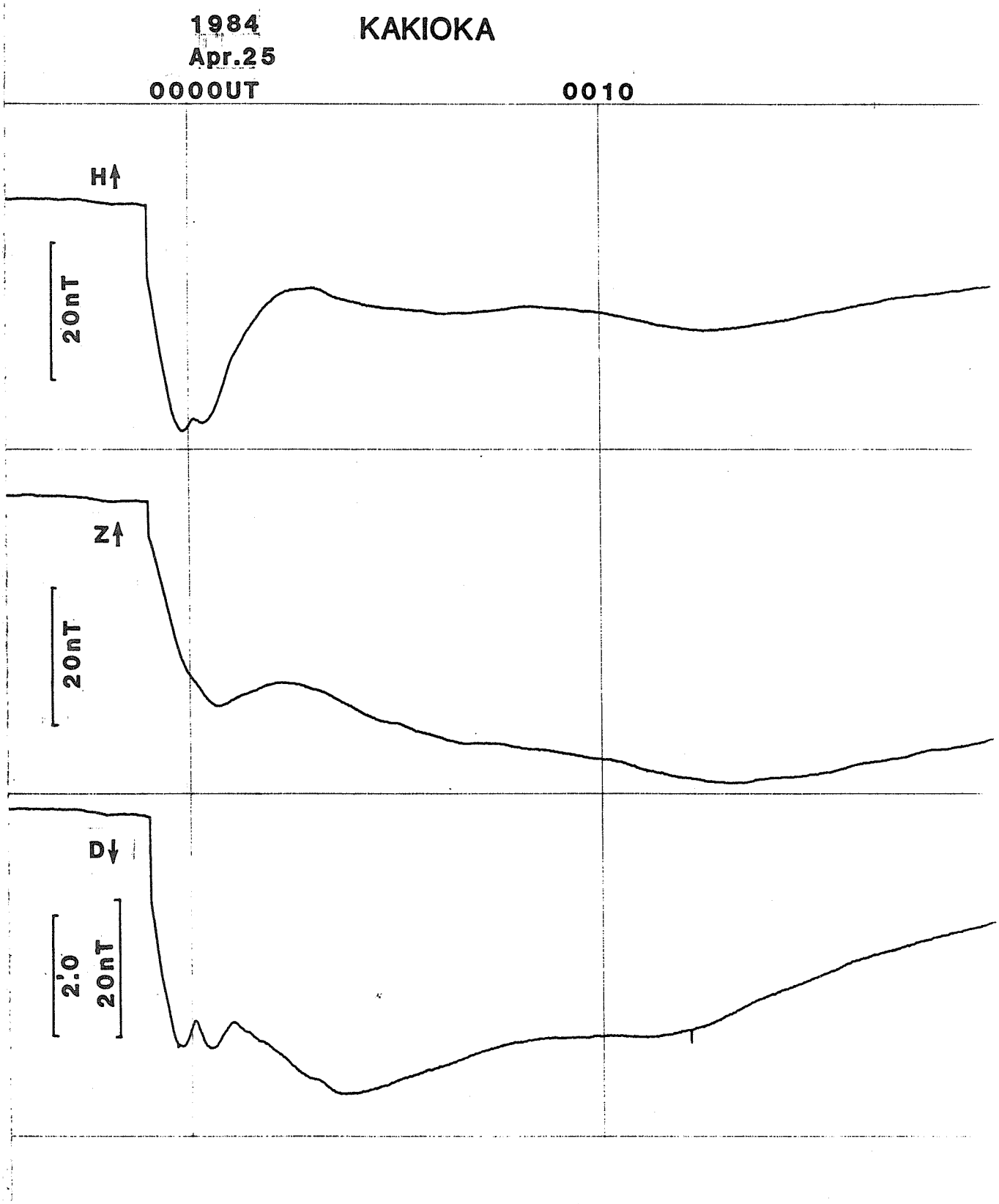


Fig. 2. Rapid-run magnetogram at Kakioka on 25 April 1984.

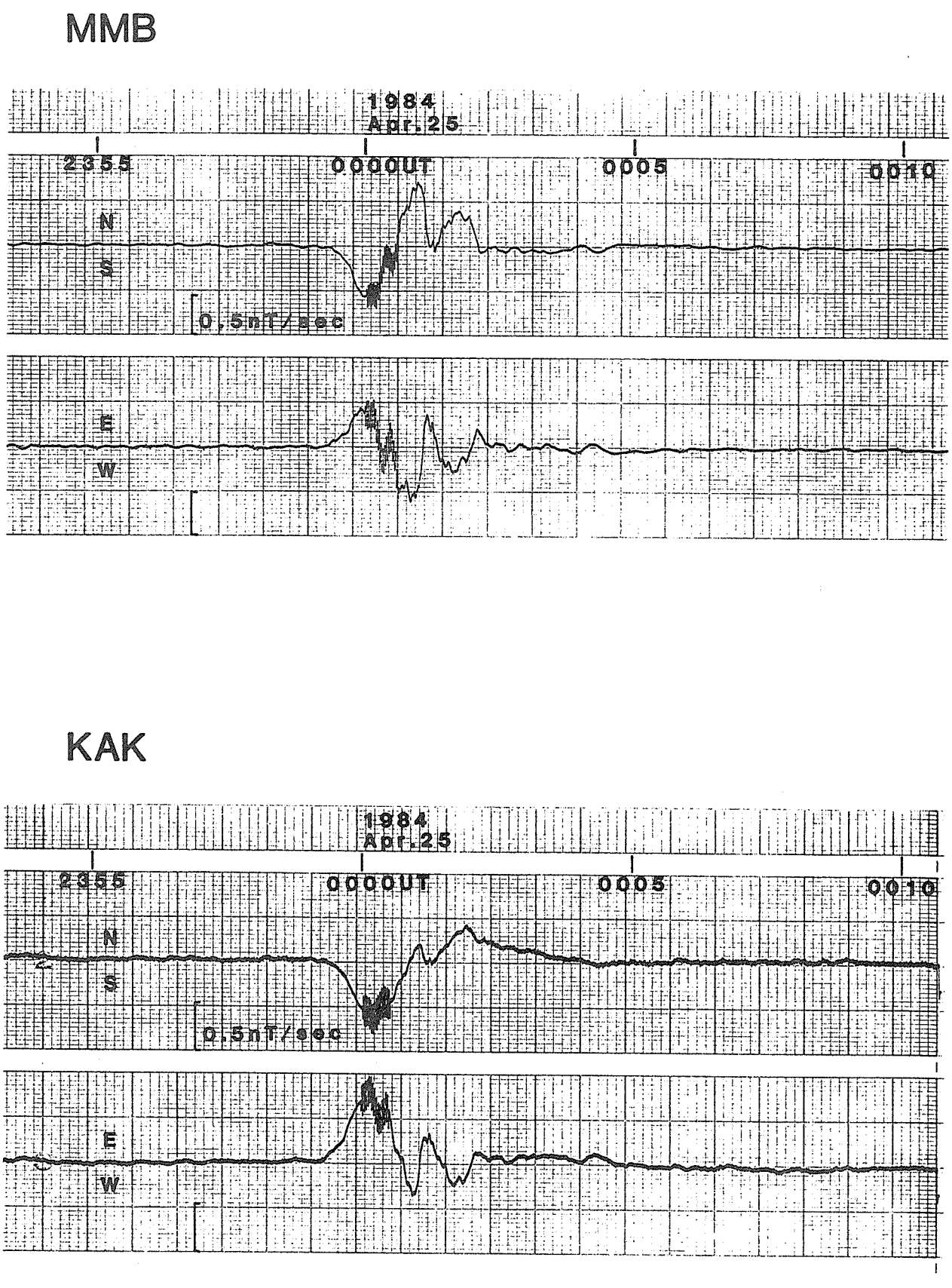


Fig. 3a. Shown here are induction magnetograms for 25 April 1984, at the Japanese stations MMB and KAK. The time mark of 0000 UT is superposed on each record.

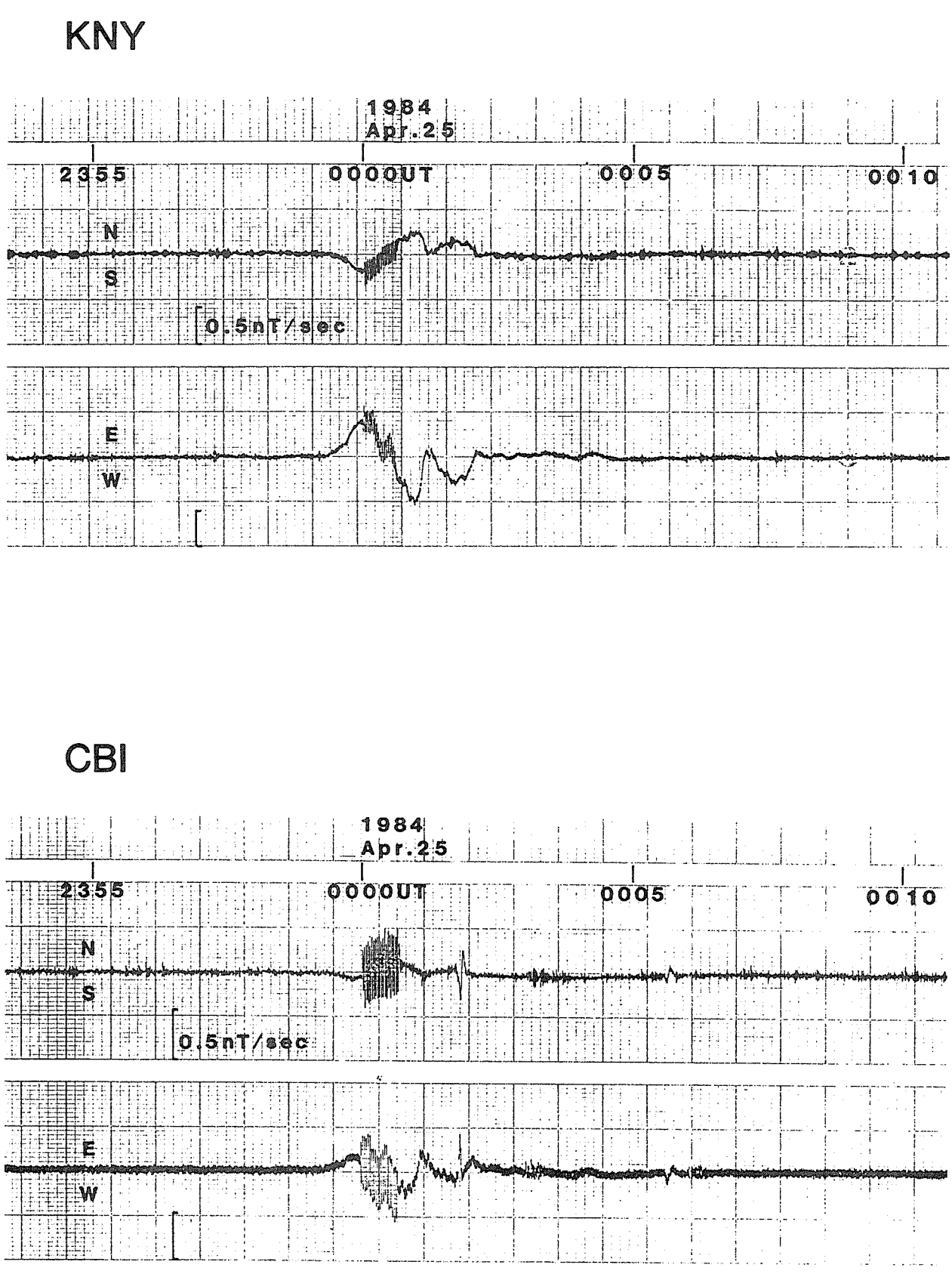


Fig. 3b. Shown here are induction magnetograms for 25 April 1984, at the Japanese stations KNY and CBI. The time mark of 0000 UT is superposed on each record.

# AUTHOR INDEX


| | Page |
|---|---|
| Abramov-Maksimov, V.E. | 78 |
| Alekseyev, N.V. | 152 |
| Allen, J.H. | 326, 330 |
| Antonova, V.P. | 233 |
| Atanasijevic, I. | 24, 303 |
| Aurass, H. | 58 |
| Avdyushin, S.I. | 140 |
| Baker,D.N. | 132 |
| Balster, H.A.M. | 24,303 |
| Basilevskaya, G.A. | 228 |
| Belian, R.D. | 132 |
| Beloglazova, G.P. | 279 |
| Belomestnova, N.M. | 230 |
| Belyaev, V.A. | 288, 363 |
| Bieber, J.W. | 184 |
| Blake, J.B. | 117 |
| Bobrovskaya, V.V. | 152 |
| Bogod, V.M. | 62 |
| Bohme, A. | 58 |
| Brautigam, D.H. | 123 |
| Brunelli, B.E. | 279 |
| Casarrubios, G. | 211 |
| Charakhchyan, T.N. | 228 |
| Chernov, G.P. | 88 |
| Chertok, I.M. | 49, 88 |
| Chirkov, N.P. | 221 |
| Chuchkov, E.A. | 103 |
| Cliver, E.W. | 55 |
| Coffey, H. | 1 |
| Comari, M. | 52, 97 |
| Danilov, A.A. | 378 |
| Darchieva, L.A. | 150 |
| Debrunner, H. | 211 |
| Echizenya, Y. | 258 |
| Enome, S. | 81 |
| Ermakov, S.I. | 103 |
| Fedorova, N.I. | 279 |
| Fenimore, E.E. | 101 |
| Fenton, A.G. | 173 |
| Fenton, K.B. | 173 |
| Filippov, A.T. | 221 |
| Fluckiger, E. | 211 |
| Fomichev, V.V. | 49, 88 |
| Fornasari, L. | 52, 97 |
| Fouassier, D. | 211 |
| Gentile, L.C. | 55, 155 |
| Gnezdilov, A.A. | 49, 88 |
| Golliez, F. | 211 |
| Gorelov, V. Ya. | 279 |
| Gorgutsa, R.V. | 49, 88 |
| Grigorov, N.L. | 152 |
| Gussenhoven, M.S. | 123 |
| Hanser, F.A. | 106 |
| Harada, A. | 383 |
| Hickey, J.R. | 146 |
| Hiei, E. | 4 |
| Higbie, P.R. | 132 |
| Hill, R.E. | 35 |
| Hruska, J. | 48 |
| Humble, J.E. | 173 |
| Ipatyev, V.I. | 240 |
| Irie, M. | 4 |
| Ishii, T. | 250, 312 |
| Iucci, N. | 223 |
| Ivanova, L.N. | 363 |
| Ivanova, T.A. | 150 |
| Izrayleva, N.I. | 289 |
| Kainuma, S. | 258, 312 |
| Kane, S.R. | 101 |
| Khisamov, R.Z. | 237 |
| Kholtosunova, S.V. | 230 |
| Kikuchi, T. | 258, 262, 312 |
| Klebesadel, R.W. | 101 |
| Klekociuk, A. | 265 |
| Koizumi, T. | 252, 312 |
| Kolasinski, W.A. | 117 |
| Kondratyeva, M.A. | 152 |
| Kontor, N.N. | 103 |
| Korotkov, V.K. | 221 |
| Korzhavin, A.N. | 62 |
| Kossa, P. | 211 |
| Kozelov, V.P. | 279 |
| Krishnaswamy, S. | 327 |
| Kruger, A. | 58 |
| Kudiakova, T.F. | 293 |
| Kukushkina, R.S. | 279 |
| Kumagai, H. | 312 |
| Kurths, J. | 58 |
| Kuwashima, M. | 383 |
| Kuznetsov, V.V. | 289 |
| Kyle, H.L. | 146 |
| LaBonte, J. | 207 |
| Lambrecht, M. | 211 |
| Lanzerotti, L.L. | 327 |
| Laros, J.G. | 101 |
| Lazutin,L.L. | 279 |
| Legrand, J.-P. | 211 |
| Levadny, V.T. | 289 |
| Levin, M.V. | 288 |
| Lockwood, J.A. | 207 |
| Loginov, G.A. | 355 |
| Lukina, T.N. | 150 |
| Maclennan, C.G. | 327 |
| Major, E.R. | 146 |
| Maksimov, V.S. | 293 |
| Markeev, A.K. | 49, 88 |
| Messerotti, M. | 52, 97 |
| Minakoshi, H. | 312 |
| Miyazawa, M. | 4 |
| Molochushkin, N.E. | 369 |
| Mori, H. | 250, 312 |
| Morozova, T.I. | 150 |
| Morris, L.D. | 330 |
| Mottais, C. | 211 |
| Mukherjee, G.K. | 381 |
| Mullen, E.G. | 123 |
| Natori, T. | 4 |
| Nazarova, M.N. | 140 |
| Nemoto, T. | 250 |
| Nesterova, I.I. | 289 |
| Nevanlina, H. | 330 |
| Nishimuta, I. | 312 |
| Nishio, M. | 81 |
| Nonino, M. | 52, 97 |
| Novikov, A.M. | 221, 240, 369 |
| Nymmik, R.A. | 152 |
| Oberhardt, M.R. | 123 |
| Ohbu, K. | 312 |
| Ohshio, M. | 244, 252, 312 |
| Ohtani, A. | 244, 262, 312 |
| Ouchi, C. | 250 |
| Parisi, M. | 223 |
| Pavlov, N.N. | 150 |
| Pavlova, I.V. | 289 |
| Pereslegina, N.V. | 103 |
| Pereyaslova, N.K. | 140 |
| Peterova, N.G. | 62, 78 |
| Petrenko, I.E. | 140 |
| Plotkin, V.V. | 289 |
| Pogorelova, N.D. | 293 |
| Pomerantz, M.A. | 184, 236 |
| Prikhodko, A.N. | 230 |

# AUTHOR INDEX


| | Page |
|---|---|
| Rangarajan, G.K. | 381 |
| Rezaeva, S.F. | 238 |
| Robinson, R. | 132 |
| Rosenberg, T.J. | 327 |
| Rubinshtein,I.A. | 150 |
| Rusakova, T.B. | 367 |
| Schubnell, M. | 211 |
| Sebor, G. | 211 |
| Sechinov, V.P. | 152 |
| Sellers, B. | 106 |
| Sergeev, A.V. | 221 |
| Shafer,G.V. | 230, 240 |
| Shapiro, V.A. | 363 |
| Shatilov, V.A. | 62 |
| Shea, M.A. | ix, 153, 155 |
| Shibasaki, K. | 81 |
| Shirman, B.L. | 363 |
| Shirochkov, A.V. | 269 |
| Shulgina, N.V. | 279 |
| Sidorenko, A.P. | 238 |
| Signorini, C. | 223 |
| Skripin, G.V. | 230 |
| Smart, D.F. | 155 |
| Sobolev, A.V. | 378 |
| Sofaly, K. | 132 |
| Solovyev, S.I. | 378 |
| Sosnovetz, E.N. | 150 |
| Stoker, P.H. | 226 |
| Storini, M. | 223 |
| Stozhkov, Yu.I. | 228 |
| Sucksdorff, C. | 330 |
| Sugiuchi, H. | 262 |
| Suzuki, T. | 312 |
| Suzuki, A. | 258 |
| Terajima, Y. | 244 |
| Thompson, R. | 243 |
| Torsti, J. | 192 |
| Totunova, G.F. | 279 |
| Tretyakova, Ch.A. | 152 |
| Tsao, C.H. | 184 |
| Tulupov, V.I. | 103 |
| Tverskaya, L.V. | 150 |
| Ulyev, V.A. | 269 |
| Uwai, T. | 383 |
| Vakulov, P.V. | 152 |
| Vashenyuk, E.V. | 279 |
| Vatrushin, S.M | 62, 78 |
| Villoresi, G. | 223 |
| Volkov, N.V. | 279 |
| Wells, G.D. | 10, 55 |
| Wilkinson, D.C. | 100 |
| Wilkinson, P.J. | 276 |
| Yamaguchi, K. | 4 |
| Yanchukovsky, V.L. | 221, 237 |
| Zakharchenko, V.F. | 288 |
| Zangrilli, N.L. | 223 |
| Zhuravlev, D.A. | 152 |
| Zlobec, P. | 52, 97 |
| Zuntini, A. | 211 |
| Zusmanovich, A.G. | 233 |


☆ U.S. GOVERNMENT PRINTING OFFICE: 1987—773 -002 /60526

## UAG SERIES OF REPORTS

Fewer than four UAG Reports are published at irregular intervals each year. Copies of these publications may be purchased through the NATIONAL GEOPHYSICAL DATA CENTER, Solar-Terrestrial Physics Division (E/GC2) 325 Broadway, Boulder, Colorado 80303, USA. A $3.00 handling charge per order will be added to single-copy price, if any, listed below. Please note, too, that some reports are available on microfiche only. Orders must include check or money order payable in U.S. currency to Commerce, NOAA/NGDC.

UAG- 1 IQSY NIGHT AIRGLOW DATA, by L.L. Smith, F.E. Roach, and J.M. McKennan, ESSA Aeronomy Laboratory Boulder, CO, July 1968, 305 pp, $1.75.

UAG- 2 A REEVALUATION OF SOLAR FLARES, 1964-1966, by Helen W. Dodson and E. Ruth Hedeman, McMath-Hulbert Observatory, University of Michigan, Pontiac, MI, August 1968, 28 pp.

UAG- 3 OBSERVATIONS OF JUPITER'S SPORADIC RADIO EMISSION IN THE RANGE 7.6-41 MHZ, 6 JULY 1966 THROUGH 8 SEPTEMBER 1968, by James W. Warwick and George A. Dulk, University of Colorado, Boulder, CO, October 1968, 35 pp.

UAG- 4 ABBREVIATED CALENDAR RECORD 1966-1967, by J. Virginia Lincoln, Hope I. Leighton and Dorothy K. Kropp, ESSA [now NOAA], Aeronomy and Space Data Center, Boulder, CO, January 1969, 170 pp.

UAG- 5 DATA ON SOLAR EVENT OF MAY 23, 1967, AND ITS GEOPHYSICAL EFFECTS, compiled by J. Virginia Lincoln, World Data Center A, Upper Atmosphere Geophysics, ESSA [now NOAA], Boulder, CO, February 1969, 120 pp.

UAG- 6 INTERNATIONAL GEOPHYSICAL CALENDARS 1957-1969, by A.H. Shapley and J. Virginia Lincoln, ESSA Research Laboratories [now NOAA], Boulder, CO, March 1969, 25 pp.

UAG- 7 OBSERVATIONS OF THE SOLAR ELECTRON CORONA: FEBRUARY 1964 - JANUARY 1968, by Richard T. Hansen, High Altitude Observatory, NCAR, Boulder, CO, and Kamuela, HI, October 1969, 12 pp.

UAG- 8 DATA ON SOLAR-GEOPHYSICAL ACTIVITY OCTOBER 24 - NOVEMBER 6, 1968, Parts 1 and 2, compiled by J. Virginia Lincoln, World Data Center A, Upper Atmosphere Geophysics, ESSA [now NOAA], Boulder, CO, March 1970, 312 pp, $1.75 (includes Parts 1 and 2).

UAG- 9 DATA ON COSMIC RAY EVENT OF NOVEMBER 18, 1968, AND ASSOCIATED PHENOMENA, compiled by J. Virginia Lincoln, World Data Center A, Upper Atmosphere Geophysics, ESSA [now NOAA], Boulder, CO, April 1970, 109 pp.

UAG-10 ATLAS OF IONOGRAMS, edited by A.H. Shapley, ESSA Research Laboratories [now NOAA], Boulder, CO, May 1970, 243 pp, $1.50.

UAG-11 [Superseded by UAG-30]

UAG-12 SOLAR-GEOPHYSICAL ACTIVITY ASSOCIATED WITH THE MAJOR GEOMAGNETIC STORM OF MARCH 8, 1970, Parts 1, 2 and 3, compiled by J. Virginia Lincoln and Dale B. Bucknam, World Data Center A, Upper Atmosphere Geophysics, ESSA [now NOAA], Boulder, CO, April 1971, 466 pp, $3.00 (includes 3 parts).

UAG-13 DATA ON THE SOLAR PROTON EVENT OF NOVEMBER 2, 1969, THROUGH THE GEOMAGNETIC STORM OF NOVEMBER 8-10, 1969, compiled by Dale B. Bucknam and J. Virginia Lincoln, World Data Center A, Upper Atmosphere Geophysics, ESSA [now NOAA], Boulder, CO, May 1971, 76 pp.

UAG-14 AN EXPERIMENTAL, COMPREHENSIVE FLARE INDEX AND ITS DERIVATION FOR 'MAJOR' FLARES, 1955-1969, by Helen W. Dodson and E. Ruth Hedeman, McMath-Hulbert Observatory, University of Michigan, Pontiac, MI, July 1971, 25 pp.

UAG-15 [Superseded by UAG-30]

UAG-16 TEMPORAL DEVELOPMENT OF THE GEOPHYSICAL DISTRIBUTION OF AURORAL ABSORPTION FOR 30 SUBSTORM EVENTS IN EACH OF IQSY (1964-65) AND IASY (1960), by F.T. Berkey, University of Alaska, Fairbanks, AK; V.M. Driatskiy, Arctic and Antarctic Research Institute, Leningrad, USSR; K. Henriksen, Auroral Observatory, Tromso, Norway; D.H. Jelly, Communications Research Center, Ottawa, Canada; T.I. Shchuka, Arctic and Antarctic Research Institute, Leningrad, USSR; A. Theander, Kiruna Geophysical Observatory, Kiruna, Sweden; and J. Yliniemi, University of Oulu, Oulu, Finland, September 1971, 131 pp, $1.50 (microfiche only).

UAG-17 IONOSPHERIC DRIFT VELOCITY MEASUREMENTS AT JICAMARCA, PERU (JULY 1967 - MARCH 1970), by Ben B. Balsley, NOAA Aeronomy Laboratory, Boulder, CO, and Ronald F. Woodman, Jicamarca Radar Observatory, Instituto Geofisico del Peru, Lima, Peru, October 1971, 45 pp, $1.50 (microfiche only).

UAG-18 A STUDY OF POLAR CAP AND AURORAL ZONE MAGNETIC VARIATIONS, by K. Kawasaki and S.-I. Akasofu, University of Alaska, Fairbanks, AK, June 1972, 21 pp.

UAG-19 REEVALUATION OF SOLAR FLARES 1967, by Helen W. Dodson and E. Ruth Hedeman, McMath-Hulbert Observatory, University of Michigan, Pontiac, MI, and Marta Rovira de Miceli, San Miguel Observatory, Argentina, June 1972, 15 pp.

UAG-20 [Superseded by UAG-30]

UAG-21 PRELIMINARY COMPILATION OF DATA FOR RETROSPECTIVE WORLD INTERVAL JULY 26 - AUGUST 14, 1972, by J. Virginia Lincoln and Hope I. Leighton, World Data Center A for Solar-Terrestrial Physics, NOAA, Boulder, CO, November 1972, 128 pp.

UAG-22 AURORAL ELECTROJET MAGNETIC ACTIVITY INDICES (AE) FOR 1970, by Joe Haskell Allen, National Geophysical and Solar-Terrestrial Data Center, Boulder, CO, November 1972, 146 pp.

UAG-23 U.R.S.I. HANDBOOK OF IONOGRAM INTERPRETATION AND REDUCTION, Second Edition, November 1972, edited by W.R. Piggott, Radio and Space Research Station, Slough, UK, and K. Rawer, Arbeitsgruppe fur Physikalische Weltraumforschung, Freiburg, GFR, November 1972, 324 pp, $1.75.

UAG-23A U.R.S.I. HANDBOOK OF IONOGRAM INTERPRETATION AND REDUCTION, Second Edition, Revision of Chapters 1-4, edited by W.R. Piggott, Radio and Space Research Station, Slough, UK, and K. Rawer, Arbeitsgruppe fur Physikalische Weltraumforschung, Freiburg, GFR, November 1972, 135 pp, $2.14.

UAG-24 DATA ON SOLAR-GEOPHYSICAL ACTIVITY ASSOCIATED WITH THE MAJOR GROUND LEVEL COSMIC RAY EVENTS OF 24 JANUARY AND 1 SEPTEMBER 1971, Parts 1 and 2, compiled by Helen E. Coffey and J. Virginia Lincoln, World Data Center A for Solar-Terrestrial Physics, NOAA, Boulder, CO, December 1972, 462 pp, $2.00 (includes Parts 1 and 2).

UAG-25 OBSERVATIONS OF JUPITER'S SPORADIC RADIO EMISSION IN THE RANGE 7.6-41 MHZ, 9 SEPTEMBER 1968 THROUGH 9 DECEMBER 1971, by James W. Warwick, George A. Dulk and David G. Swann, University of Colorado, Boulder, CO, February 1973, 35 pp.

UAG-26 DATA COMPILATION FOR THE MAGNETOSPHERICALLY QUIET PERIODS FEBRUARY 19-23 AND NOVEMBER 29 - DECEMBER 3, 1970, compiled by Helen E. Coffey and J. Virginia Lincoln, World Data Center A for Solar-Terrestrial Physics, NOAA, Boulder, CO, May 1973, 129 pp.

UAG-27 HIGH SPEED STREAMS IN THE SOLAR WIND, by D.S. Intriligator, University of Southern California, Los Angeles, CA, June 1973, 16 pp.

UAG-28 COLLECTED DATA REPORTS ON AUGUST 1972 SOLAR-TERRESTRIAL EVENTS, Parts 1, 2 and 3, edited by Helen E. Coffey, World Data Center A for Solar-Terrestrial Physics, NOAA, Boulder, CO, July 1973, 932 pp, $4.50.

UAG-29 AURORAL ELECTROJET MAGNETIC ACTIVITY INDICES AE(11) FOR 1968, by Joe Haskell Allen, Carl C. Abston and Leslie D. Morris, National Geophysical and Solar-Terrestrial Data Center, Boulder, CO, October 1973, 148 pp.

UAG-30 CATALOGUE OF DATA ON SOLAR-TERRESTRIAL PHYSICS, prepared by NOAA Environmental Data Service, Boulder, CO, October 1973, 317 pp, $1.75. Supersedes catalogs UAG-11, 15 and 20.

UAG-31 AURORAL ELECTROJET MAGNETIC ACTIVITY INDICES AE(11) FOR 1969, by Joe Haskell Allen, Carl C. Abston and Leslie D. Morris, National Geophysical and Solar-Terrestrial Data Center, Boulder, CO, February 1974, 142 pp.

UAG-32 SYNOPTIC RADIO MAPS OF THE SUN AT 3.3 MM FOR THE YEARS 1967-1969, by Earle B. Mayfield, Kennon P. White III, and Fred I. Shimabukuro, Aerospace Corp., El Segundo, CA, April 1974, 26 pp.

UAG-33 AURORAL ELECTROJET MAGNETIC ACTIVITY INDICES AE(10) FOR 1967, by Joe Haskell Allen, Carl C. Abston and Leslie D. Morris, National Geophysical and Solar-Terrestrial Data Center, Boulder, CO, May 1974, 142 pp.

UAG-34 ABSORPTION DATA FOR THE IGY/IGC AND IQSY, compiled and edited by A.H. Shapley, National Geophysical and Solar-Terrestrial Data Center, Boulder, CO; W.R. Piggott, Appleton Laboratory, Slough, UK; and K. Rawer, Arbeitsgruppe fur Physikalische Weltraumforschung, Freiburg, GFR, June 1974, 381 pp, $2.00.

UAG-35 [Superseded by UAG-92]

UAG-36 AN ATLAS OF EXTREME ULTRAVIOLET FLASHES OF SOLAR FLARES OBSERVED VIA SUDDEN FREQUENCY DEVIATIONS DURING THE ATM-SKYLAB MISSIONS, by R.F. Donnelly and E.L. Berger, NOAA Space Environment Laboratory; Lt. J.D. Busman, NOAA Commissioned Corps; B. Henson, NASA Marshall Space Flight Center; T.B. Jones, University of Leicester, UK; G.M. Lerfald, NOAA Wave Propagation Laboratory; K. Najita, University of Hawaii; W.M. Retallack, NOAA Space Environment Laboratory and W.J. Wagner, Sacramento Peak Observatory, October 1974, 95 pp.

UAG-37 AURORAL ELECTROJET MAGNETIC ACTIVITY INDICES AE(10) FOR 1966, by Joe Haskell Allen, Carl C. Abston and Leslie D. Morris, National Geophysical and Solar-Terrestrial Data Center, Boulder, CO, December 1974, 142 pp.

UAG-38 MASTER STATION LIST FOR SOLAR-TERRESTRIAL PHYSICS DATA AT WDC-A FOR SOLAR-TERRESTRIAL PHYSICS, by R.W. Buhmann, World Data Center A for Solar-Terrestrial Physics, Boulder, CO; Juan D. Roederer, University of Denver, Denver, CO; and M.A. Shea and D.F. Smart, Air Force Cambridge Research Laboratories, Hanscom AFB, MA, December 1974, 110 pp, $1.60.

UAG-39 AURORAL ELECTROJET MAGNETIC ACTIVITY INDICES AE(11) FOR 1971, by Joe Haskell Allen, Carl C. Abston and Leslie D. Morris, National Geophysical and Solar-Terrestrial Data Center, Boulder, CO, February 1975, 144 pp, $2.05.

UAG-40 H-ALPHA SYNOPTIC CHARTS OF SOLAR ACTIVITY FOR THE PERIOD OF SKYLAB OBSERVATIONS, MAY 1973 - MARCH 1974, by Patrick S. McIntosh, NOAA Space Environment Laboratory, Boulder, CO, February 1975, 32 pp.

UAG-41 H-ALPHA SYNOPTIC CHARTS OF SOLAR ACTIVITY DURING THE FIRST YEAR OF SOLAR CYCLE 20 OCTOBER 1964 - AUGUST 1965, by Patrick S. McIntosh, NOAA Space Environment Laboratory, Boulder, CO, and Jerome T. Nolte, American Science and Engineering, Inc., Cambridge, MA, March 1975, 25 pp.

UAG-42 OBSERVATIONS OF JUPITER'S SPORADIC RADIO EMISSION IN THE RANGE 7.6-80 MHZ, 10 DECEMBER 1971 THROUGH 21 MARCH 1975, by James W. Warwick, George A. Dulk and Anthony C. Riddle, University of Colorado, Boulder, CO, April 1975, 49 pp.

UAG-43 CATALOG OF OBSERVATION TIMES OF GROUND-BASED SKYLAB-COORDINATED SOLAR OBSERVING PROGRAMS, compiled by Helen E. Coffey, World Data Center A for Solar-Terrestrial Physics, NOAA, Boulder, CO, May 1975, 159 pp, $3.00.

UAG-44 SYNOPTIC MAPS OF SOLAR 9.1 CM MICROWAVE EMISSION FROM JUNE 1962 TO AUGUST 1973, by Werner Graf and Ronald N. Bracewell, Stanford University, Stanford, CA, May 1975, 183 pp, $2.55.

UAG-45 AURORAL ELECTROJET MAGNETIC ACTIVITY INDICES AE(11) FOR 1972, by Joe Haskell Allen, Carl C. Abston and Leslie D. Morris, National Geophysical and Solar-Terrestrial Data Center, Boulder, CO, May 1975, 144 pp, $1.50 (microfiche only).

UAG-46 INTERPLANETARY MAGNETIC FIELD DATA 1963-1964, by Joseph H. King, National Space Science Data Center, NASA Goddard Space Flight Center, Greenbelt, MD, June 1975, 382 pp, $2.95.

UAG-47 AURORAL ELECTROJET MAGNETIC ACTIVITY INDICES AE(11) FOR 1973, by Joe Haskell Allen, Carl C. Abston and Leslie D. Morris, National Geophysical and Solar-Terrestrial Data Center, Boulder, CO, June 1975, 144 pp, $1.50 (microfiche only).

UAG-48 [Superseded by UAG-48A]

UAG-48A SYNOPTIC OBSERVATIONS OF THE SOLAR CORONA DURING CARRINGTON ROTATIONS 1580-1596 (11 OCTOBER 1971 - 15 JANUARY 1973), [Re-issue of UAG-48 with quality images], by R.A. Howard, M.J. Koomen, D.J. Michels, R. Tousey, C.R. Detwiler, D.E. Roberts, R.T. Seal, and J.D. Whitney, U.S. Naval Research Laboratory, Washington, DC; and R.T. Hansen and S.F. Hansen, C.J. Garcia and E. Yasukawa, High Altitude Observatory, NCAR, Boulder, CO, February 1976, 200 pp, $4.27. Supersedes UAG-48.

UAG-49 [Superseded by UAG-92]

UAG-50 HIGH-LATITUDE SUPPLEMENT TO THE URSI HANDBOOK ON IONOGRAM INTERPRETATION AND REDUCTION, edited by W.R. Piggott, British Antarctic Survey, c/o Appleton Laboratory, Slough, UK, October 1975, 294 pp, $4.00.

UAG-51 SYNOPTIC MAPS OF SOLAR CORONAL HOLE BOUNDARIES DERIVED FROM HE II 304A SPECTROHELIOGRAMS FROM THE MANNED SKYLAB MISSIONS, by J.D. Bohlin and D.M. Rubenstein, U.S. Naval Research Laboratory, Washington, DC, November 1975, 30 pp.

UAG-52 EXPERIMENTAL COMPREHENSIVE SOLAR FLARE INDICES FOR CERTAIN FLARES, 1970-1974, by Helen W. Dodson and E. Ruth Hedeman, McMath-Hulbert Observatory, University of Michigan, Pontiac, MI, November 1975, 27 pp.

UAG-53 DESCRIPTION AND CATALOG OF IONOSPHERIC F-REGION DATA, JICAMARCA RADIO OBSERVATORY (NOVEMBER 1966 - APRIL 1969), by W.L. Clark and T.E. Van Zandt, NOAA Aeronomy Laboratory, Boulder, CO, and J.P. McClure, University of Texas at Dallas, Dallas, TX, April 1976, 10 pp.

UAG-54 [Superseded by UAG-85]

UAG-55 EQUIVALENT IONOSPHERIC CURRENT REPRESENTATIONS BY A NEW METHOD, ILLUSTRATED FOR 8-9 NOVEMBER 1969 MAGNETIC DISTURBANCES, by Y. Kamide, Cooperative Institute for Research in Environmental Sciences, University of Colorado, Boulder, CO; H.W. Kroehl, Data Studies Division, National Geophysical and Solar-Terrestrial Data Center, Boulder, CO; M. Kanamitsu, Advanced Study Program, National Center for Atmospheric Research, Boulder, CO; Joe Haskell Allen, Data Studies Division, National Geophysical and Solar-Terrestrial Data Center, Boulder, CO; and S.-I. Akasofu, Geophysical Institute, University of Alaska, Fairbanks, AK, April 1976, 91 pp, $1.50 (microfiche only).

UAG-56 ISO-INTENSITY CONTOURS OF GROUND MAGNETIC H PERTURBATIONS FOR THE DECEMBER 16-18, 1971, GEOMAGNETIC STORM, Y. Kamide, Cooperative Institute for Research in Environmental Sciences, University of Colorado, Boulder, CO, April 1976, 37 pp.

UAG-57 MANUAL ON IONOSPHERIC ABSORPTION MEASUREMENTS, edited by K. Rawer, Institut fur Physikalische Weltraumforschung, Freiburg, GFR, June 1976, 302 pp, $4.27.

UAG-58 ATS6 RADIO BEACON ELECTRON CONTENT MEASUREMENTS AT BOULDER, JULY 1974 - MAY 1975, by R.B. Fritz, NOAA Space Environment Laboratory, Boulder, CO, September 1976, 61 pp.

UAG-59 AURORAL ELECTROJET MAGNETIC ACTIVITY INDICES AE(11) FOR 1974, by Joe Haskell Allen, Carl C. Abston and Leslie D. Morris, National Geophysical and Solar-Terrestrial Data Center, Boulder, CO, December 1976, 144 pp, $2.16.

UAG-60 GEOMAGNETIC DATA FOR JANUARY 1976 [AE(7) INDICES AND STACKED MAGNETOGRAMS], by Joe Haskell Allen, Carl C. Abston and Leslie D. Morris, National Geophysical and Solar-Terrestrial Data Center, Boulder, CO, July 1977, 57 pp.

UAG-61 COLLECTED DATA REPORTS FOR STIP INTERVAL II 20 MARCH - 5 MAY 1976, edited by Helen E. Coffey and John A. McKinnon, World Data Center A for Solar-Terrestrial Physics, Boulder, CO, August 1977, 313 pp, $2.95.

UAG-62 GEOMAGNETIC DATA FOR FEBRUARY 1976 [AE(7) INDICES AND STACKED MAGNETOGRAMS], by Joe Haskell Allen, Carl C. Abston and Leslie D. Morris, National Geophysical and Solar-Terrestrial Data Center, Boulder, CO, September 1977, 55 pp.

UAG-63 GEOMAGNETIC DATA FOR MARCH 1976 [AE(7) INDICES AND STACKED MAGNETOGRAMS], by Joe Haskell Allen, Carl C. Abston and Leslie D. Morris, National Geophysical and Solar-Terrestrial Data Center, Boulder, CO, September 1977, 57 pp.

UAG-64 GEOMAGNETIC DATA FOR APRIL 1976 [AE(8) INDICES AND STACKED MAGNETOGRAMS], by Joe Haskell Allen, Carl C. Abston and Leslie D. Morris, National Geophysical and Solar-Terrestrial Data Center, Boulder, CO, February 1978, 55 pp.

UAG-65 THE INFORMATION EXPLOSION AND ITS CONSEQUENCES FOR DATA ACQUISITION, DOCUMENTATION, PROCESSING, by G.K. Hartmann, Max-Planck-Institut fur Aeronomie, Lindau, GFR, May 1978, 36 pp.

UAG-66 SYNOPTIC RADIO MAPS OF THE SUN AT 3.3 MM 1970-1973, by Earle B. Mayfield and Fred I. Shimabukuro, Aerospace Corp., El Segundo, CA, May 1978, 30 pp.

UAG-67 IONOSPHERIC D-REGION PROFILE DATA BASE, A COLLECTION OF COMPUTER-ACCESSIBLE EXPERIMENTAL PROFILES OF THE D AND LOWER E REGIONS, by L.F. McNamara, Ionospheric Prediction Service, Sydney, Australia, August 1978, 30 pp, $1.50 (microfiche only).

UAG-68 A COMPARATIVE STUDY OF METHODS OF ELECTRON DENSITY PROFILE ANALYSIS, by L.F. McNamara, Ionospheric Prediction Service, Sydney, Australia, August 1978, 30 pp, $1.50 (microfiche only).

UAG-69 SELECTED DISTURBED D-REGION ELECTRON DENSITY PROFILES. THEIR RELATION TO THE UNDISTURBED D REGION, by L.F. McNamara, Ionospheric Prediction Service, Sydney, Australia, October 1978, 50 pp, $1.50 (microfice only).

UAG-70 ANNOTATED ATLAS OF H-ALPHA SYNOPTIC CHARTS FOR SOLAR CYCLE 20 (1964-1974) CARRINGTON SOLAR ROTATIONS 1487-1616, by Patrick S. McIntosh, NOAA Space Environment Laboratory, Boulder, CO, February 1979, 327 pp, $3.50.

UAG-71 MAGNETIC POTENTIAL PLOTS OVER THE NORTHERN HEMISPHERE FOR 26-28 MARCH 1976, A.D. Richmond, NOAA Space Environment Laboratory, Boulder, CO; H.W. Kroehl, National Geophysical and Solar-Terrestrial Data Center, Boulder, CO; M.A. Henning, Lockheed Missiles and Space Co., Aurora, CO; and Y. Kamide, Kyoto Sangyo University, Kyoto, Japan, April 1979, 118 pp, $1.50.

UAG-72 ENERGY RELEASE IN SOLAR FLARES, PROCEEDINGS OF THE WORKSHOP ON ENERGY RELEASE IN FLARES, 26 FEBRUARY - 1 MARCH 1979, CAMBRIDGE, MASSACHUSETTS, U.S.A., edited by David M. Rust, American Science and Engineering, Inc., Cambridge, MA; and A. Gordon Emslie, Harvard-Smithsonian Center for Astrophysics, Cambridge, MA, July 1979, 68 pp, $1.50 (microfiche only).

UAG-73 AURORAL ELECTROJET MAGNETIC ACTIVITY INDICES AE(11-12) FOR JANUARY - JUNE 1975, by Joe Haskell Allen, Carl C. Abston, J.E. Salazar and J.A. McKinnon, National Geophysical and Solar-Terrestrial Data Center, NOAA, Boulder, CO, August 1979, 114 pp, $1.75 (microfiche only).

UAG-74 ATS-6 RADIO BEACON ELECTRON CONTENT MEASUREMENTS AT OOTACAMUND, INDIA, OCTOBER - JULY 1976, by S.D. Bouwer, K. Davies, R.F. Donnelly, R.N. Grubb, J.E. Jones and J.H. Taylor, NOAA Space Environment Laboratory, Boulder, CO; and R.G. Rastogi, M.R. Deshpande, H. Chandra and G. Sethia, Physical Research Laboratory, Ahmedabad, India, March 1980, 58 pp, $2.50.

UAG-75 THE ALASKA IMS MERIDIAN CHAIN: MAGNETIC VARIATIONS FOR 9 MARCH - 27 APRIL 1978, by H.W. Kroehl and G.P. Kosinski, National Geophysical and Solar-Terrestrial Data Center, Boulder, CO; S.-I. Akasofu, G.J. Romick, C.E. Campbell and G.K. Corrick, University of Alaska, Fairbanks, AK; and C.E. Hornback and A.M. Gray, NOAA Space Environment Laboratory, Boulder, CO, June 1980, 107 pp, $3.00.

UAG-76 AURORAL ELECTROJET MAGNETIC ACTIVITY INDICES AE(12) FOR JULY - DECEMBER 1975, by Joe Haskell Allen, Carl C. Abston, J.E. Salazar and J.A. McKinnon, National Geophysical and Solar-Terrestrial Data Center, NOAA, Boulder, CO, August 1980, 116 pp, $2.50.

UAG-77 SYNOPTIC SOLAR MAGNETIC FIELD MAPS FOR THE INTERVAL INCLUDING CARRINGTON ROTATIONS 1601-1680, MAY 5, 1973 - APRIL 26, 1979, by J. Harvey, B. Gillespie, P. Miedaner and C. Slaughter, Kitt Peak National Observatory, Tucson, AZ, August 1980, 66 pp, $2.50.

UAG-78 THE EQUATORIAL LATITUDE OF AURORAL ACTIVITY DURING 1972-1977, by N.R. Sheeley, Jr. and R.A. Howard, E.O. Hulbert Center for Space Research, U.S. Naval Research Laboratory, Washington, DC and B.S. Dandekar, Air Force Geophysics Laboratory, Hanscom AFB, MA, October 1980, 61 pp, $3.00.

UAG-79 SOLAR OBSERVATIONS DURING SKYLAB, APRIL 1973 - FEBRUARY 1974, I. CORONAL X-RAY STRUCTURE, II. SOLAR FLARE ACTIVITY, by J.M. Hanson, University of Michigan, Ann Arbor, MI; and E.C. Roelof and and R.E. Gold, The Johns Hopkins University, Laurel, MD, December 1980, 43 pp, $2.50.

UAG-80 EXPERIMENTAL COMPREHENSIVE SOLAR FLARE INDICES FOR 'MAJOR' AND CERTAIN LESSER FLARES, 1975-1979, compiled by Helen W. Dodson and E. Ruth Hedeman, The Johns Hopkins University, Laurel, MD, July 1981, 33 pp, $2.00.

UAG-81 EVOLUTIONARY CHARTS OF SOLAR ACTIVITY (CALCIUM PLAGES) AS FUNCTIONS OF HELIOGRAPHIC LONGITUDE AND TIME, 1964-1979, by E. Ruth Hedeman, Helen W. Dodson and Edmond C. Roelof, The Johns Hopkins University, Laurel, MD, August 1981, 103 pp, $4.00.

UAG-82 INTERNATIONAL REFERENCE IONOSPHERE - IRI 79, edited by J. Virginia Lincoln and Raymond O. Conkright, National Geophysical and Solar-Terrestrial Data Center, NOAA, Boulder, CO, November 1981, 243 pp, $4.50.

UAG-83 SOLAR-GEOPHYSICAL ACTIVITY REPORTS FOR SEPTEMBER 7-24, 1977 AND NOVEMBER 22, 1977, Parts 1 and 2, compiled by John A. McKinnon and J. Virginia Lincoln, World Data Center A for Solar-Terrestrial Physics, NOAA, Boulder, CO, February 1982, 553 pp, $10.00.

UAG-84 CATALOG OF AURORAL RADIO ABSORPTION DURING 1976-1979 AT ABISKO, SWEDEN, by J.K. Hargreaves, C.M. Taylor and J.M. Penman, Environmental Sciences Department, University of Lancaster, Lancaster, UK, July 1982, 69 pp, $3.00.

UAG-85 CATALOG OF IONOSPHERE VERTICAL SOUNDINGS DATA, edited by Raymond O. Conkright and H. Irene Brophy, National Geophysical Data Center, NOAA, Boulder, CO, July 1982, 107 pp. Supersedes UAG-54.

UAG-86 [Superseded by UAG-92]

UAG-87 CHANGES IN THE GLOBAL ELECTRIC FIELDS AND CURRENTS FOR MARCH 17-19, 1978, FROM SIX IMS MERIDIAN CHAINS OF MAGNETOMETERS, by Y. Kamide, Kyoto Sangyo University, Kyoto, Japan; H.W. Kroehl, National Geophysical Data Center, NOAA, Boulder, CO; and A.D. Richmond, NOAA Space Environment Laboratory, Boulder, CO, November 1982, 102 pp, $3.50.

UAG-88 NUMERICAL MODELING OF IONOSPHERIC PARAMETERS FROM GLOBAL IMS MAGNETOMETER DATA FOR THE CDAW-6 INTERVALS, by Y. Kamide, Kyoto Sangyo University, Kyoto, Japan; H.W. Kroehl, National Geophysical Data Center, NOAA, Boulder, CO; and B.A. Hausman, National Geophysical Data Center, NOAA, Boulder, CO, November 1983, 197 pp, $4.00.

UAG-89 ATMOSPHERIC HANDBOOK: ATMOSPHERIC DATA TABLES AVAILABLE ON COMPUTER TAPE, by V.E. Derr, NOAA Environmental Research Laboratories, Boulder, CO, July 1984, 56 pp.

UAG-90 EXPERIENCE WITH PROPOSED IMPROVEMENTS OF THE INTERNATIONAL REFERENCE IONOSPHERE (IRI): CONTRIBUTED PAPERS, MAINLY FROM THE URSI-COSPAR WORKSHOP HELD IN BUDAPEST IN 1980, edited by K. Rawer, University of Freiburg, Federal Republic of Germany, and C.M. Minnis, former Secretary General of URSI, Brussels, Belgium, May 1984, 233 pp, $6.00.

UAG-91 COMBINED CATALOG OF IONOSPHERE VERTICAL SOUNDINGS DATA, compiled by Raymond O. Conkright and Marcus O. Ertle, National Geophysical Data Center, NOAA, Boulder, CO, December 1984, 174 pp.

UAG-92 INTERNATIONAL CATALOG OF GEOMAGNETIC DATA, compiled by C.C. Abston, National Geophysical Data Center, NOAA, Boulder, CO; N.E. Papitashvili, Academy of Sciences of the USSR, World Data Center B2, Moscow, USSR; and V.O. Papitashvili, IZMIRAN, Moscow Region, USSR, August 1985, 291 pp. Supersedes UAG-35, 49, and 86.

UAG-93 IONOGRAM ANALYSIS WITH THE GENERALISED PROGRAM POLAN, by J.E. Titheridge, University of Auckland, New Zealand, December 1985, 194 pp.

UAG-94 THE SOLAR MAGNETIC FIELD--1976 THROUGH 1985: AN ATLAS OF PHOTOSPHERIC MAGNETIC FIELD OBSERVATIONS AND COMPUTED CORONAL MAGNETIC FIELDS FROM THE JOHN M. WILCOX SOLAR OBSERVATORY AT STANFORD, by J. Todd Hoeksema and Philip H. Scherrer, Center for Space Science and Astrophysics, Stanford University, Stanford, CA, January 1986, 370 pp, $9.00.

UAG-95 SUNSPOT NUMBERS: 1610-1985, (based on THE SUNSPOT-ACTIVITY IN THE YEARS 1610-1960, by Prof. M. Waldmeier, Copyright 1961, Swiss Federal Observatory, Zurich, Switzerland), revised by John A. McKinnon, National Geophysical Data Center, NOAA, Boulder, CO, January 1987, 112 pp, $10.00.

UAG-96 SOLAR-GEOPHYSICAL ACTIVITY REPORTS FOR STIP INTERVAL XV 12-21 February 1984 Ground-Level Event AND STIP INTERVAL XVI 20 April-4 May 1984 Forbush Decrease, compiled by Helen E. Coffey and Joe H. Allen, National Geophysical Data Center, NOAA, Boulder, CO, July 1987, 418 pp, $15.00.